Diels–Alder and Electrocyclic Strategies in Complex Molecule Synthesis

By Isuru Dissanayake Mudiyanselage

A thesis by conventional/publication format, submitted to attain the degree of Doctor of Philosophy

THE UNIVERSITY of ADELAIDE

School of Physical Sciences

Department of Chemistry

March 2023

Supervisor: Dr. Thomas Fallon

Table of Contents

Abstract

The central theme of this thesis can be considered the study and application of pericyclic reactions, specifically the Diels−Alder and electrocyclisation reaction towards the generation of complex functional molecules. Chapter 1 serves as a brief introduction to these two reactions recounting their respective history, current state and future directions.

A Diels–Alder (DA) methodology was developed for the synthesis of a synthetically challenging motif. It involved the synthesis of a 2,5-bis(*tert*-butyldimethylsilyloxy)furan diene capable of performing a DA cycloaddition followed by an aromatisation sequence to afford a variety of *para*-hydroquinones among other arenes. DA reactions primarily afford non-aromatic six-membered rings, however the 2,5-bis(*tert*-butyldimethylsilyloxy)furan diene has been engineered to undergo a facile aromatisation process after the [4+2] cycloaddition. It was therefore appropriate to conduct a non-comprehensive review on a variety of dienes that induce aromatisation after the DA reaction and their application in natural product total synthesis. This review is contained in Chapter 2 and acts as a literature preface for the peer-review published Diels–Alder methodology in Chapter 3 (authorship statement provided).

A great portion of the following synthetic work in this thesis utilises 1,3,5,7-cyclooctatetraene (COT) as the starting material. The oddity of using a bare annulene as a starting material inspired Chapter 4, which is a review focusing on total syntheses of natural products that begin with unfunctionalised annulenes: cyclobutadiene, benzene and COT.

Endiandric acids are a famous natural product family known for its unique skeletal structures, biological activity and specifically for their unique biosynthesis. Their biosynthesis involves a tetraene undergoing a beautiful 8π-electrocyclisation/6π-electrocyclisation/intramolecular Diels−Alder cascade to form structurally complex molecules. Multiple historical syntheses involved construction of the tetraene, which can be a challenging and lengthy task. Our group recognised alternative routes via COT that drastically shortened the step count to these fascinating products. In our third-generation methodology, kingianic acids A, B, D and endiandric acid M was synthesised via the lithium enolate of cyclooctatrienone (derived from COT), which is covered in Chapter 5. There are limitations to this methodology, encouraging the development of the next generation. At the end of Chapter 5, we report a successful proof-of-concept involving the creation of a bis-Bpin tetraene molecule that can potentially afford natural product related compounds.

Torquoselective electrocyclisations have been extensively developed for the 4π electrocyclic variant, however is very limited in 6π and 8π electrocyclisations. Certain bicyclo[4.2.0]octadiene related natural products have shown to possess low to mild levels of torquoselectivity during the electrocyclisation events of their biosynthesis. Chapter 6 is a purely computational study on the kinetics, thermodynamics and torquoselectivity of the biosynthetic cascade of bicyclo[4.2.0]octadiene related natural products. The understanding gained through these experiments inspired hypothetical compounds that have been computationally predicted to undertake fully torquoselective 8π electrocyclisations and aims to stimulate future endeavours in torquoselective electrocyclisations.

The supporting information for experimental chapters (3, 5 and 6) is provided in Chapter 7. References are provided at the end of each chapter. Numbering for compounds, figures, schemes and tables are done according to each chapter i.e., 3.5 (chapter.number). Colour is used in many figures, schemes and tables throughout the thesis to aid in their understanding and must be printed in colour if a physical copy is required.

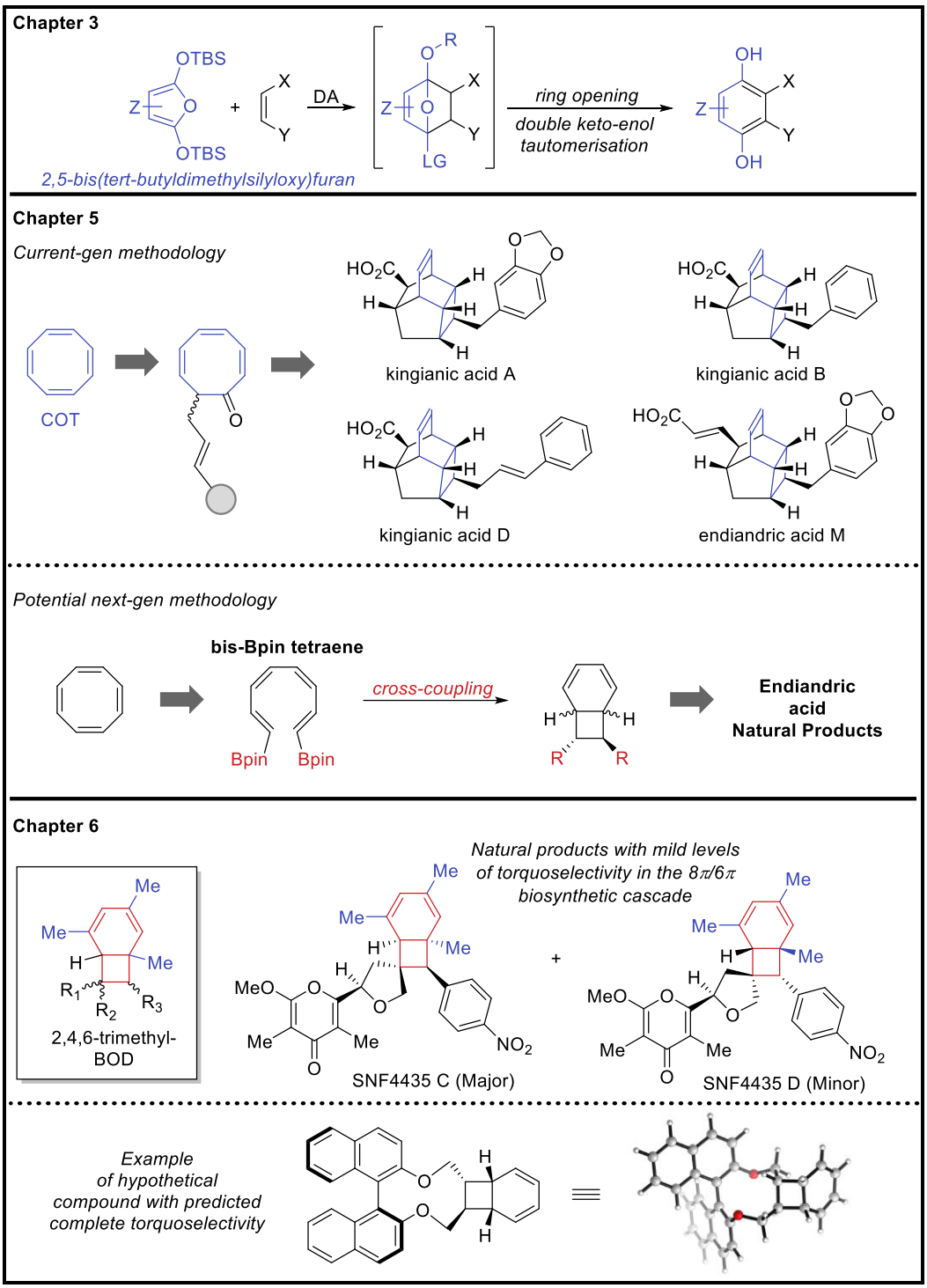

Visual abstract of all experimental chapters

Publications

1. Isuru Dissanayake, Jacob D. Hart, Emma C. Becroft, Christopher J. Sumby, and Christopher G. Newton. (2020). Bisketene Equivalents as Diels–Alder Dienes, *Journal of the American Chemical Society*, *142(31)*, 13328–13333. https://doi.org/10.1021/jacs.0c06306

Declaration

I certify that this work contains no material which has been accepted for the award of any other degree or diploma in my name, in any university or other tertiary institution and, to the best of my knowledge and belief, contains no material previously published or written by another person, except where due reference has been made in the text. In addition, I certify that no part of this work will, in the future, be used in a submission in my name, for any other degree or diploma in any university or other tertiary institution without the prior approval of the University of Adelaide and where applicable, any partner institution responsible for the joint award of this degree.

The author acknowledges that copyright of published works contained within the thesis resides with the copyright holder(s) of those works.

I give permission for the digital version of my thesis to be made available on the web, via the University's digital research repository, the Library Search and also through web search engines, unless permission has been granted by the University to restrict access for a period of time.

I acknowledge the support I have received for my research through the provision of an Australian Government Research Training Program Scholarship.

Signature:

Date: 03/03/2023

Acknowledgements

Firstly, my thanks are to my principal supervisor Dr. Thomas Fallon for his support, guidance and inspiration. I'd also like to extend this to Assistant Professor Christopher Newton (my past supervisor), with whom I published my first work under. To Associate Professor Jonathan George for his contributions towards my wider understanding of organic synthetic chemistry.

My thanks warmly go to members of the Fallon Research Group, past and present, with whom it has been a pleasure to study with. I'd also like to extend this to past and present George Research Group members, and past Newton Research Group members at the University of Adelaide.

My thanks also go to Professor Christopher Sumby for the single crystal X-ray analyses. Associate Professor Stephen Bell, I thank for his help in regards to postgraduate administrative tasks. Professor Hugh Harris for his role as co-supervisor. Associate Professor Martin Johnston for NMR use at Flinders University. Peter Apoefis, Matthew Bull and Philip Clements I thank for their technical support.

Abbreviations

%	percentage or percentage yield or weight by volume percentage
[O]	oxidation
Å	angstrom
Ac	acetyl
Acac	acetylacetonate
AIBN	azobisisobutyronitrile
aq.	aqueous
BINAP	2,2′-bis(diphenylphosphino)-1,1′-binaphthyl
BINOL	1,1’-bi-2-naphthol
BHT	butylated hydroxytoluene
BMIDA	N-methyliminodiacetic acid boronate ester
Bn	benzyl
BOD	bicyclo[4.2.0]octadiene
Bpin	pinacol boronate ester
br.	broad
cat.	Catalyst
CAN	ceric ammonium nitrate
CDI	1,1'-carbonyldiimidazole
COD	1,5-cyclooctadiene
COSY	correlation spectroscopy
COT	cyclooctatetraene
d	doublet
d.e.	diastereomeric excess
d.r.	diastereomeric ratio
DA	Diels−Alder
DBU	1,8-diazabicyclo[5.4.0]undec-7-ene
DCC	N,N′-dicyclohexylcarbodiimide
DCE	1,2-dichloroethane
DCM	dichloromethane
DDQ	2,3-dichloro-5,6-dicyano-1,4-benzoquinone
DFT	density functional theory
DIBAL-H	diisobutylaluminium hydride
DIPEA	N,N-diisopropylethylamine
DMAD	dimethyl acetylenedicarboxylate
DMAP	4-dimethylaminopyridine
DMF	dimethylformamide
DMPU	N, N′-dimethylpropyleneurea
DMSO	dimethyl sulfoxide
dppe	1,2-bis(diphenylphosphino)ethane
Ea	activation energy
EDC.HCl	1-ethyl-3-(3′-dimethylaminopropyl)carbodiimide · HCl
EDG	electron donating group
e.e.	enantiomeric excess
EI	electron impact
equiv.	equivalents
ESI	electrospray ionization
EWG	electron withdrawing group
g	grams
HMBC	heteronuclear multiple-bond correlation spectroscopy
HMDS	hexamethyldisilazane
HMPA	hexamethylphosphoramide

HOBt	hydroxybenzotriazole
HRMS	high-resolution mass spectrometry
HSQC	heteronuclear single-quantum correlation spectroscopy
hv	photochemical energy
HWE	Horner-Wadsworth-Emmons
Hz	hertz
IMDA	intramolecular Diels−Alder
IR	infrared
IUPAC	International Union of Pure and Applied Chemistry
J	coupling constant
Ka	association rate constant
kcal	kilocalories
kg	kilogram
kJ	kilojoules
kW	kilowatts
L	litre
LDA	lithium diisopropylamide
M	Molar or metal
m	multiplet
m.p.	melting point
M^+	molecular ion
MAD	methylaluminum bis (2, 6-di-t-butyl-4-methylphenoxide)
mbar	millibar
mCPBA	meta-chloroperoxybenzoic acid
mg	milligrams
MHz	megahertz
MIDA	methyliminodiacetic acid
min	minute
mL	millilitres
mmol	millimole
mol	mole
mol%	molar percentage
mol. sieves	molecular sieves
Ms	mesyl
MS	mass spectrometry
MTAD	4-methyl-1,2,4-triazoline-3,5-dione
NBS	N-bromosuccinamide
NHC	N-heterocyclic carbene
NMO	N-methylmorpholine N-oxide
NMR	nuclear magnetic resonance
NOESY	nuclear Overhauser effect spectroscopy
°	degrees
°C	degrees Celcius
p	pentet
Ph	phenyl
PIDA	(diacetoxyiodo)benzene
PMB-Cl	4-methoxybenzyl chloride
Ppm	parts per million
PTAD	4-phenyl-1,2,4-triazole-3,5-dione
q	quartet
RCDA	radical cation Diels-Alder
rel. G	relative Gibbs free energy
Rf	retention factor

RT	room temperature
s	second or singlet
sat.	saturated
SM	starting material
T	temperature
$t_{1/2}$	half-life
TBAF	tetra-n-butylammonium fluoride
TBDMS	tert-butyldimethylsilyl
TBS	tert-butyldimethylsilyl
TES	triethylsilyl
Tf	triflyl
THF	tetrahydrofuran
TIPB	1,3,5-triisopropylbenzene
TLC	thin layer chromatography
TMEDA	N,N,N′,N′-tetramethylethane-1,2-diamine
TMS	trimethylsilyl
TPAP	tetrapropylammonium perruthenate
Ts	tosyl
TS	transition state
UV	ultraviolet
V	volts
W	watts
w/v	weight by volume
Xphos	2-dicyclohexylphosphino-2′,4′,6′-triisopropylbiphenyl
Δ	heat
δ	chemical shift
µL	microlitres
µmol	micromole
µW	microwave

Chapter 1

Introduction

1.1 Introduction to pericyclic reactions and preamble

There are three recognised classes of organic synthetic reactions by transition state topology: linear, pericyclic and coarctate reactions (Figure 1.1).[1,2] The most common topology in synthesis is linear, where the transition state (**1.1** as an example) is acyclic. Pericyclic transition states (**1.2** as an example) involve a cyclic geometry, with reaction progression occurring in a concerted manner. The least common is the coarctate topology, where it is characterised by a figure eight-like transition state (**1.3** as an example).

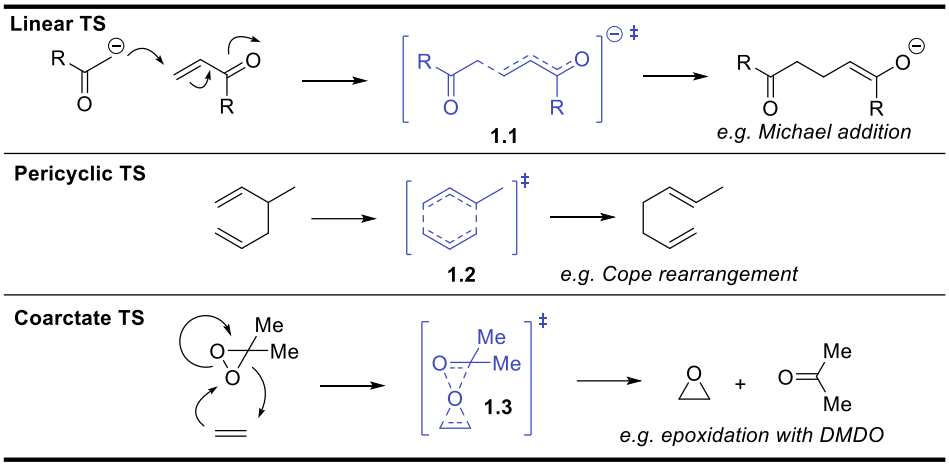

Figure 1.1: The three classes of synthetic reactions by transition state topology

Pericyclic reactions contain sub-classes, two of which are cycloadditions (specifically [4+2]) and electrocyclic reactions. These two are fundamental reactions underpinning the body of work in this thesis. The contents of the thesis aim to contribute to the study and application of these reactions. Broken into two main parts, the first develops a Diels–Alder methodology for the synthesis of a synthetically challenging motif and the later parts applies/studies electrocyclisations in a complex total synthesis setting. Therefore, it is appropriate for this first chapter to concisely introduce the history, current state, future and other important aspects of these reactions.

1.2 Diels-Alder reaction

The Diels–Alder (DA) reaction is one of the most powerful tools within an organic synthetic chemist's arsenal. Nearly 100 years of research since its introduction to the field, has led it to develop into the most powerful 6-membered ring forming annulation, capable of rapidly generating molecular complexity.

1.2.1 History

The earliest work on the study of the DA reaction was published in a series of 28 articles from 1928 to 1937, authored by Otto Diels and his student Kurt Alder (involved in the first 19 articles), which the reaction bears their joint names.[3,4] Their first publication detailed the correction to a study by Walter Albrecht in 1906.[5] Albrecht reported that the reaction between cyclopentadiene **1.4** and 1,4-benzoquinone **1.5** formed cyclopentadienequinone **1.6**, where the cyclopentadiene **1.4** added to the double bond of **1.5** through its methylene group, retaining its diene moiety. He also reported di-cyclopentadiene quinone **1.7** from the double addition of cyclopentadiene **1.4**. Hermann Staudinger hypothesized an alternative cyclobutane product **1.8** in 1912.[6]

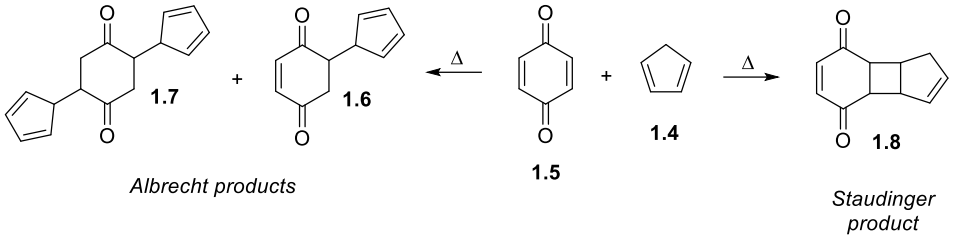

Scheme 1.1: Albrecht and Staudinger's postulated products from the thermal reaction between cyclopentadiene and 1,4-benzoquinone

Diels and Alder provided strong evidence to disprove both Albrecht and Staudinger's assertions. Structural comparison to N,N'-dicarboxyethyl-endomethylene tetrahydropyridazine **1.9** highlighted the possibility of a methylene bridge (highlighted in blue in Scheme 1.2A) from the thermal reaction between cyclopentadiene **1.4** and diethyl azodicarboxylate **1.10**. Euler and Josephson's work in 1920, involved the addition of 2 moles of isoprene **1.11** to 1 mole of 1,4-benzoquinone **1.5** to form compound **1.12**, illustrating the formation of bonds to the 1,4 position of the isoprene **1.11** (Scheme 1.2B).[7]

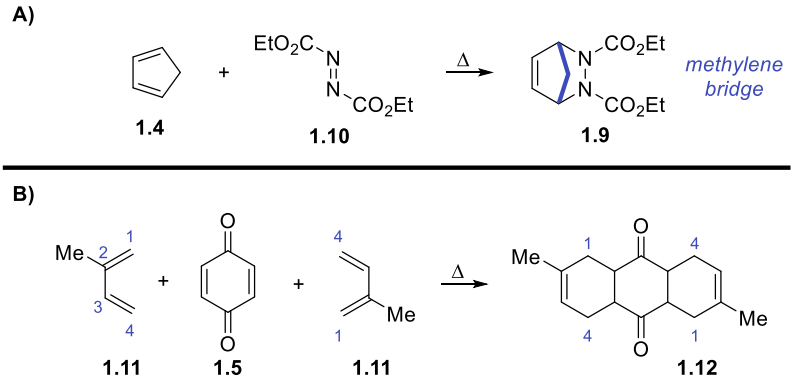

Scheme 1.2: A) Cycloaddition between cyclopentadiene and diethyl azodicarboxylate. B) Euler and Josephson's 1920 synthesis of anthracenedione 1.12

The authors therefore concluded the correct structures to be compound **1.12** instead of **1.6** and **1.13** instead of **1.7** (Scheme 1.3), which are further validated by additional experimentation. It was clear to Diels and Alder that the potential implication of this reaction is great, to the extent they explicitly reserved the right to study and apply this reaction. They postulated synthetic application towards more complex and valuable compounds such as natural products, as well as the reaction being involved in the biosynthesis of such natural products. Fast forward to 1950, well after their 28th and final article in their research series, they were deservedly awarded the Nobel chemistry prize "for their discovery and development of the diene synthesis".[8]

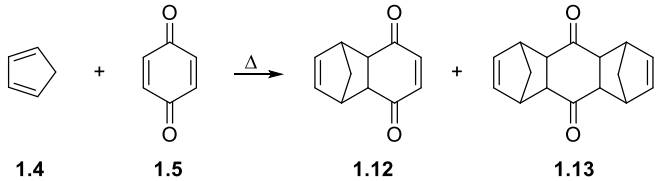

Scheme 1.3: Diels and Alder's product elucidation

A couple years later, Robert B. Woodward would publish his hallmark synthesis of cortisone **1.14** and cholesterol **1.15** showcasing the first instance of the Diels−Alder reaction in a total synthesis (Scheme 1.4).[9–13]

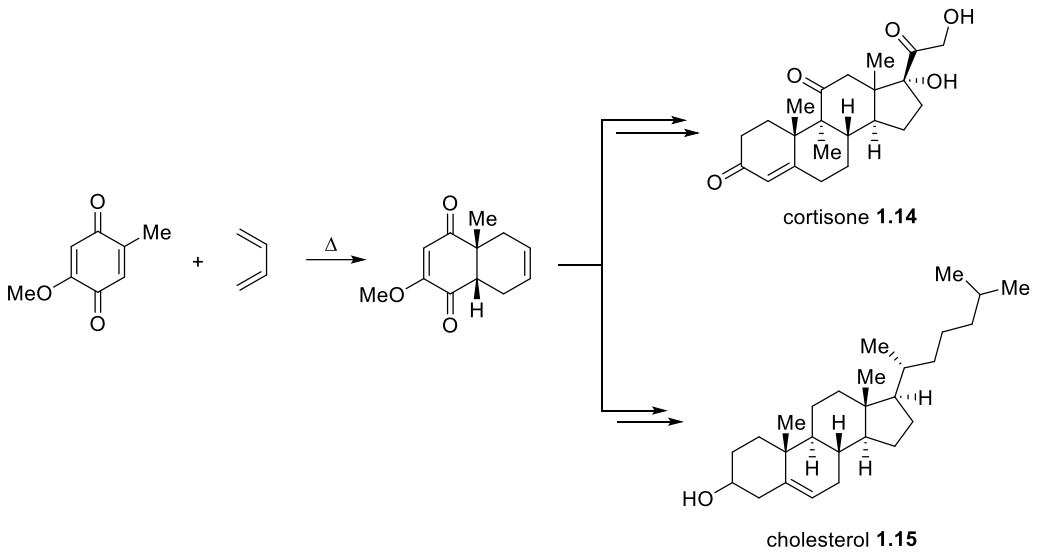

Scheme 1.4: Woodward's total synthesis of cortisone and cholesterol

1.2.2 Current state

1.2.2.1 Mechanism

Robert B. Woodward along with Thomas J. Katz, Roald Hoffmann, as well as many others have been instrumental in the elucidation of the Diels−Alder mechanism since the late 1930s.[14] The current consensus is the reaction undergoing a concerted [π4s + π2s] cycloaddition, proceeding through a cyclic transition state **1.16** (Scheme 1.5).[15–18] A high level of understanding on the mechanism of this reaction has currently been achieved, therefore it is apt for the following paragraphs within this section (1.2.2.1) to summarise this in order to render this thesis to be more accessible to the non-expert reader.

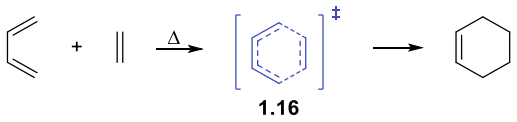

Scheme 1.5: Currently agreed transition state of a Diels−Alder reaction between a 1,3-diene and ethylene

Frontier molecular orbital (FMO) theory explains the facile nature of the interaction between a 4π electron system (diene) and 2π electron system (dienophile).[19] The overlap of the diene and dienophile orbitals is thermally allowed under the Woodward–Hoffmann rules.[20,21] In a normal demand DA, the electron donating group (EDG) on the diene raises the highest occupied molecular orbital (HOMO) and the electron withdrawing group (EWG) on the dienophile lowers the lowest unoccupied molecular orbital (LUMO) (Figure 1.2). In an inverse demand DA, the roles of the electronic effects of the substituent are exchanged, however still lead to the same outcome.

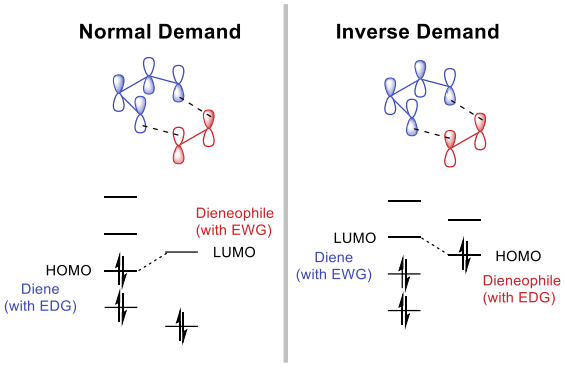

Figure 1.2: Orbital diagrams of normal and inverse Diels−Alder reactions

FMO theory additionally predicts the regioselectivity pattern of appropriately substituted systems.[22–24] In a more simplistic method, analysis of the resonance structures leads to the general *ortho-para* rule. In general, the carbon with the largest HOMO coefficient forms a bond with the carbon with the largest LUMO coefficient. See scheme 1.6 for a visual summary of all possible outcomes in a normal demand DA reaction.

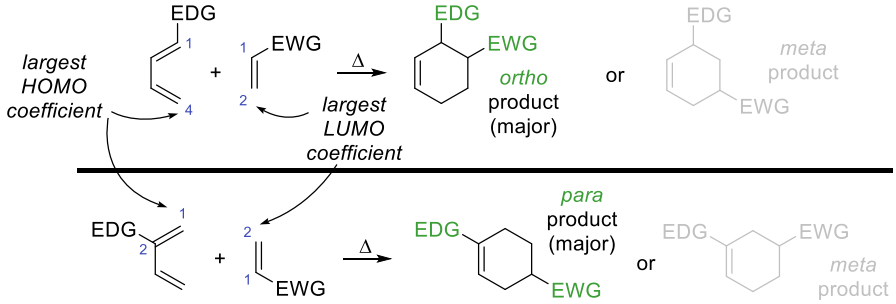

Scheme 1.6: General regioselectivity rules for normal demand DA reactions

Concerted Diels–Alder cycloadditions are stereospecific. Stereochemistry of the diene and dienophile is retained due to suprafacial interaction of the frontier orbitals (antarafacial is symmetry forbidden).[21] See scheme 1.7 for a visual summary on the outcomes of all possible diene and dienophile combinations.

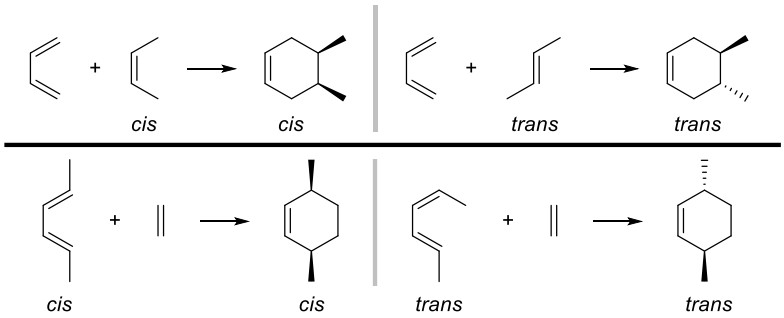

Scheme 1.7: General stereospecificity rules for the DA reaction

Diels–Alder reactions that form two stereocentres on the carbons that bond with each other leads to the possibility of two diastereomers. For this to occur, there must be at least one substituent on either end of a diene (C1 or C4 on diene **1.17**) and one substituent on the dienophile (C1 or C2 on dienophile **1.18**) (Scheme 1.8).

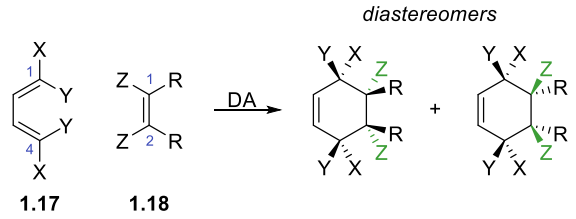

Scheme 1.8: Possible diastereomers from appropriately substituted dienes and dienophiles

Preference for a diastereomer can be predicted depending on the combination of diene and dienophile, leading to an *endo*/*exo* stereoselectivity model. Early work performed by Alder and Stein lead to an empirical rule known as the "Alder *endo* rule", dictating the endo product is favoured among dienophiles bearing unsaturated groups.[25,26] Secondary orbital interactions (SOIs), first postulated by Woodward and Hoffmann, explains that the orbital overlap of the diene C2 **1.4** and carbonyl carbon of the dienophile **1.19** induces selectivity of an *endo*-transition state (Scheme 1.9) providing a 98.5:1.5 ratio of diastereomers **1.20** and **1.21** and has been the widely accepted theory.[21,27–29] It's accurate in regards to DA reactions involving highly activated cyclic dienophiles under kinetically favoured thermal conditions, however is inconsistent with acyclic dienophiles.[30] *Exo*-selectivity often arises from the destabilising steric effects in the DA transition state as a result of bulky substituents.

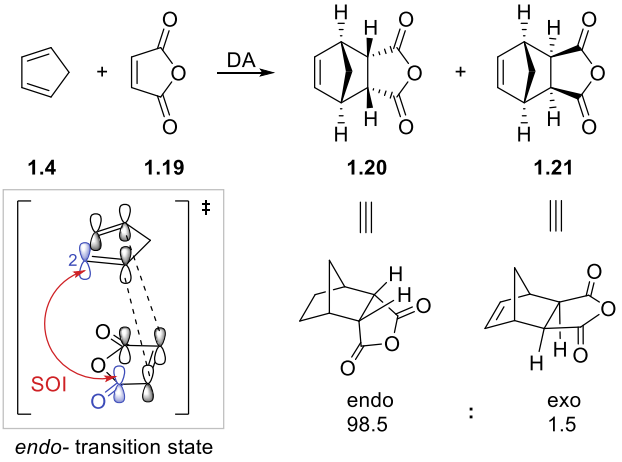

Scheme 1.9: Example of an *endo*-selective DA reaction with transition state showing SOI

1.2.2.2 State-of-Art

Over 38,000 research articles have been published that include the word "Diels–Alder" since 1928.[31] A whole field was created and careers flourished under the Diels-Alder reaction. Today, the application of the cycloaddition has become extremely diverse, possibly more so than what Diels and Alder originally envisioned, spawning different types of Diels−Alder reactions, all with their own growing areas.[32–34] Figure 1.3 highlights the main types of Diels−Alders with examples.

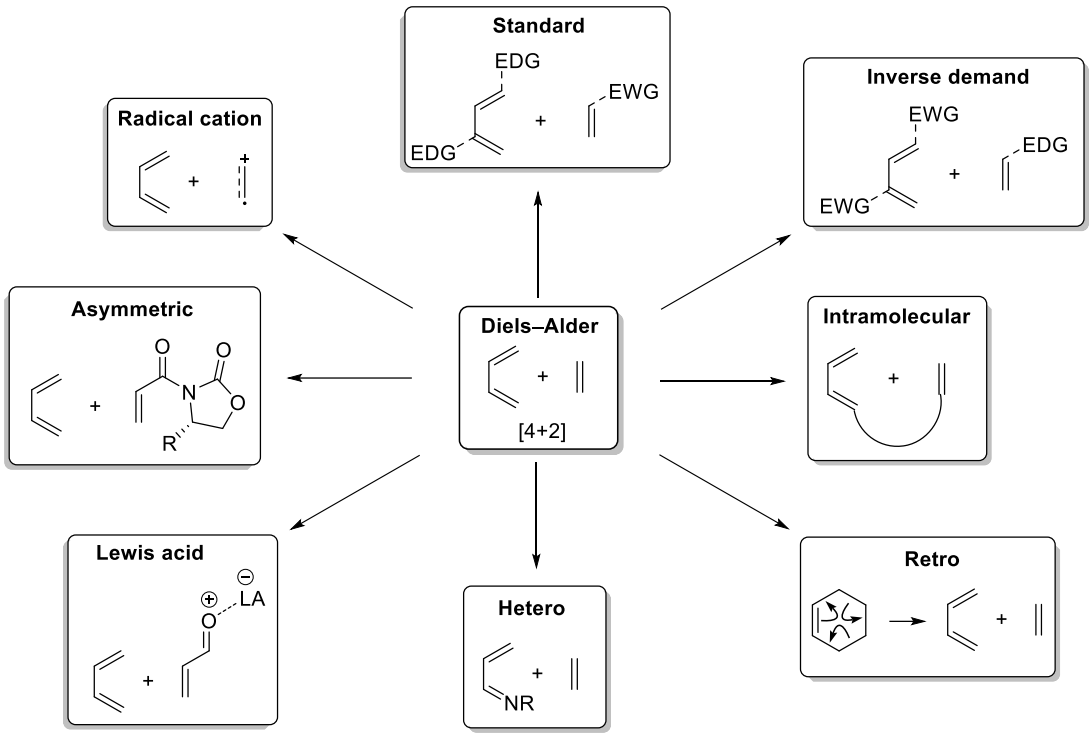

Figure 1.3: Sub-classes of the Diels–Alder reaction

Modern DA reactions are multifaceted due to the ever-growing requirement of synthesising increasingly intricate molecules efficiently. A notable example is Gaich's total synthesis of canataxpropellane **1.22**, where they carry out an asymmetric Diels–Alder with an in situ generated isobenzofuran diene **1.23** in the initial steps (Scheme 1.10).[35] The chiral silane **1.24** is responsible for inducing a DA transition state that is selective for compound **(–)-1.25** over **(+)-1.25** (1.5:1 d.r.) via steric effects.

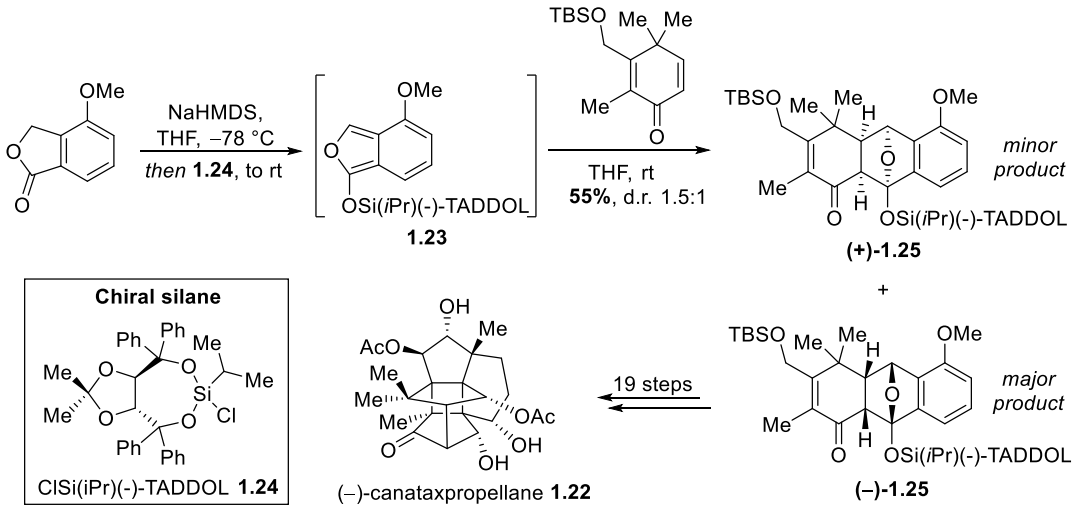

Scheme 1.10: Gaich's 2020 total synthesis of canataxpropellane

1.2.3 Future directions and Our work

Despite the immense advances in the Diels−Alder reaction, there are still undiscovered chemical reaction spaces and knowledge gaps to be filled.

The DA reaction and its retro variant have garnered interest from the biomedical and nanomedicine field due to their atom economy, reversibility and substituent retention.[36] These characteristics allow for it be an effective click reaction, allowing for delivery of active ingredients and release upon temperature manipulations (Scheme 1.11A). Use in polymer

chemistry has also been established and is growing due to its simplicity and scalability. Furan/maleimide coupling partners are well-established (Scheme 1.11B), however newer efforts are towards developing new reaction partners (anthracene, myrcene, eugenol, etc.).[37] The discovery of natural enzymes, Diels−Alderases, has brought immense intrigue to the organic chemistry community. Its research has been a multidisciplinary endeavour in regard to elucidating structures, mechanism and selectivity (Scheme 1.11C left).[38,39] Further study is required with potential applications in total synthesis chemistry and industry. Organocatalysis has already been recognised in Diels−Alder chemistry, however relatively recent work involving the IDPi catalyst and similar compounds have brought great progress in both enantioselective synthesis but also the construction of compounds that are not synthesisable by standard DA methods (Scheme 1.11C right).[40–42]

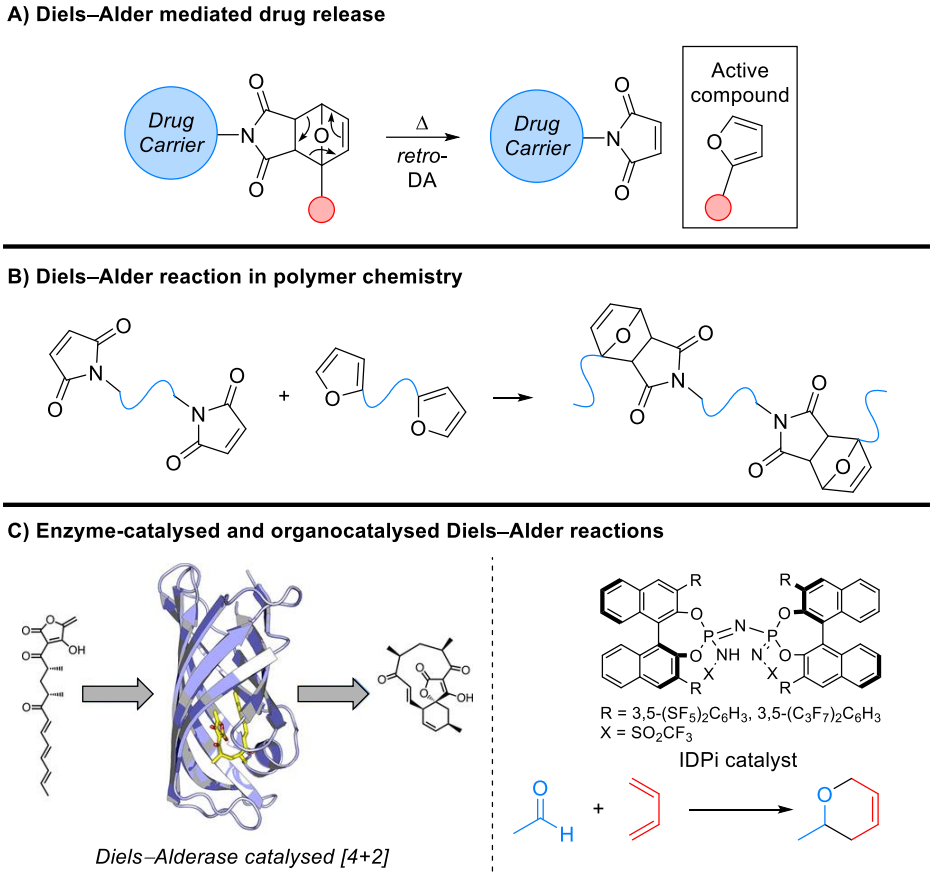

Scheme 1.11: A) Example of drug delivery via a retro DA process. B) Polymerisation via the reaction between a diene and dienophile chain. C) Example of both enzyme and organocatalysis in the DA reaction.

Our work with the Diels−Alder reaction looked at expanding its synthetic utility. It traditionally affords cycloalkene cycloadducts, however we have developed a methodology that delivers aromatic rings. Specifically, 2,5-bis(*tert*-butyldimethylsilyloxy)furan diene derivatives were developed, capable of undergoing a [4+2] and facile aromatisation sequence to give afford a variety of *para*-hydroquinones among other arenes. This project constitutes chapter 3 in this thesis, where chapter 2 acts as a literature preface, providing a non-comprehensive review on a variety of dienes that induce aromatisation after the DA reaction and their application in natural product total synthesis.

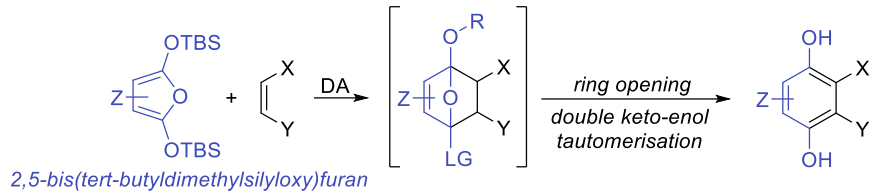

Scheme 1.12: Diels–Alder methodology involving 2,5-bis(*tert*-butyldimethylsilyloxy)furan dienes to synthesise a variety of *para*-hydroquinones

1.3 Electrocyclic reactions

Electrocyclisations are rearrangements where ring-opening or closing events occur under photochemical or thermal conditions, and the net result is a loss of one π bond and gain of one σ bond or vice versa.[43,44]

1.3.1 History

The Nazarov cyclisation is one of the earliest examples of an electrocyclic reaction, elucidated by Ivan N. Nazarov in 1941 (not the first report of a Nazarov cyclisation).[45–47] The reaction involves a divinyl ketone **1.26** undergoing an acid-promoted cationic 4π electrocyclic ring closure to yield a cyclopentenone **1.27** (Scheme 1.13).[48,49] The 4π electrocyclic ring closing event is conrotatory under thermal conditions (intermediate **1.28**), hence the *trans* relationship between the two R groups (intermediate **1.29**). This relationship is then destroyed by the elimination reaction providing intermediate **1.30** which then tautomerises to **1.27**.

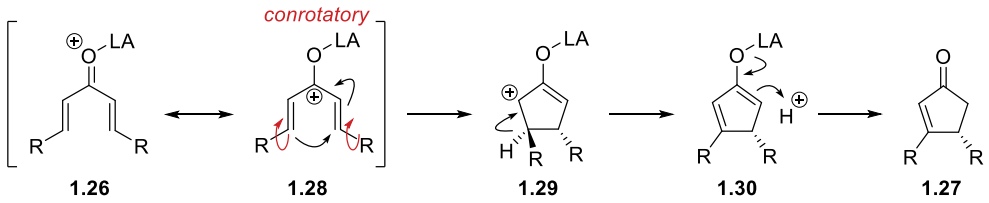

Scheme 1.13: General mechanism of Nazarov cyclisation

It was only until Robert B. Woodward and Roald Hoffman's hallmark work in the 1960s on the Woodward-Hoffman rules for pericyclic reactions that the stereochemical outcome of electrocyclisations were understood.[50]

Interestingly, Elias J. Corey's 1963 total synthesis of dihydrocostunolide **1.31** reports an electrocyclic reaction.[51,52] It proceeded via a photochemically allowed 6π conrotatory ring opening of compound **1.32** followed by a thermally allowed 6π disrotatory ring closing of intermediate **1.33** affording compound **1.34**. Despite a well-defined example of stereoselection, Corey offered no explanation of the stereochemical outcomes at the time.

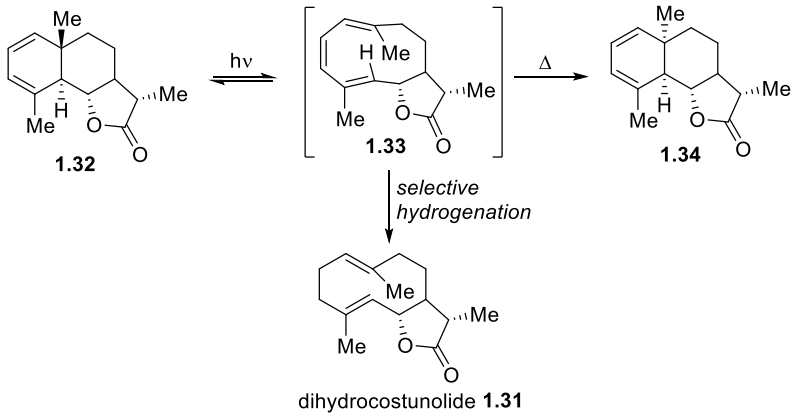

Scheme 1.14: Corey's 1963 total synthesis of dihydrocostunolide

1.3.2 Current state

1.3.2.1 Mechanism

The Woodward−Hoffman selection rules are well-established and accurately predict the *cis*/*trans* geometry of the product through determining whether the reaction proceeds through a conrotatory or disrotatory mechanism. General rules for determining the rotation based on the number of π electrons and whether the reaction was thermally or photochemically induced is summarised in table 1.1.

No. of π electrons	Thermally allowed	Photochemically allowed
4n	Conrotatory	Disrotatory
4n+2	Disrotatory	Conrotatory

Table 1.1: Summarised selectivity rules for thermal and photochemical electrocyclic reactions.

1.3.2.2 Applications in total synthesis

Electrocyclisations are ubiquitous in nature. A notable example is the biosynthesis of vitamin D3 **1.35**, where a photochemically promoted 6π conrotatory ring opening of 7-dehydrocholesterol **1.36** is then followed by a [1,7]-hydride shift from **1.37** (Scheme 1.15).

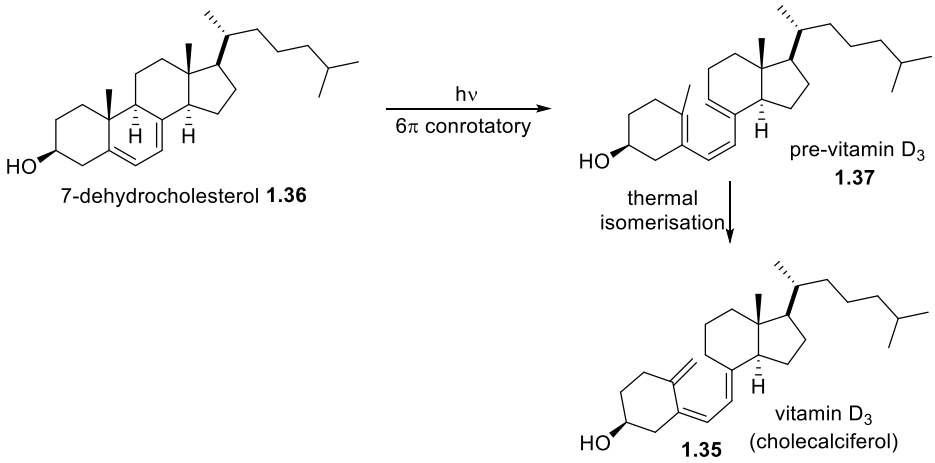

Scheme 1.15: Biosynthesis of vitamin D3

Biosyntheses that include electrocyclisations have been performed in synthetic laboratory settings. Seminal work by K.C. Nicolaou in his biomimetic approaches to endiandric acids involve the synthesis of a linear Z,Z,Z,Z tetraene **1.38**, from the semi-hydrogenation of **1.39**, where an 8π/6π electrocyclisation cascade occurs to yield a bicyclo[4.2.0]octadiene (BOD) molecule **1.40**.[53–57]

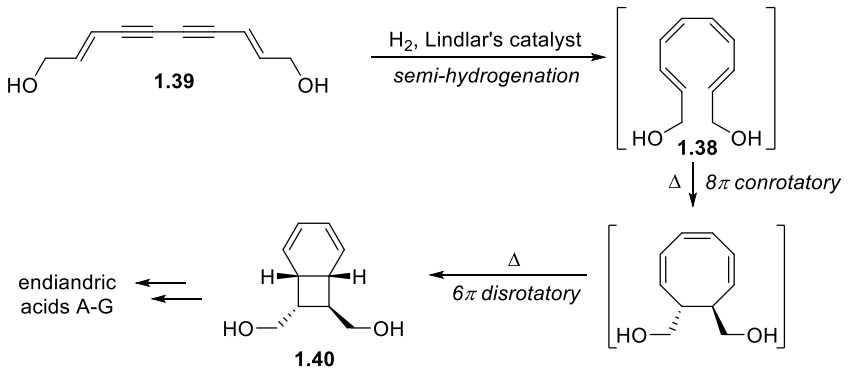

Scheme 1.16: Biomimetic 8π/6π electrocyclisation cascade in Nicolaou's total synthesis of endiandric acids A-G

1.3.3 Future directions and Our work

Electrocyclisations continue to be a staple in natural product total synthesis with growing attention towards its asymmetric variants.

1.3.3.1 Total synthesis

Nicolaou's synthesis of endiandric acids utilised a unique 8π/6π cascade of a linear tetraene to deliver BOD compounds. Our work focuses on the *anti*-1,2-difunctionalisation of cyclooctatetraene (COT), whereby the 8π is skipped and the 6π directly affords a BOD molecule, therefore providing a more efficient sequence to BODs. Chapter 5 constitutes this methodology, where we apply it to the synthesis of a few endiandric acid derivatives (Scheme 1.17). Due to the oddity of using a bare annulene (COT in this case) as a starting material, we felt it apt to write a review focusing on total syntheses of natural products that begin with unfunctionalised annulenes: cyclobutadiene, benzene and COT. This review is held in chapter 4 which also serves as a barrier separating chapters involving Diels−Alders from the electrocyclic related chapters that will follow.

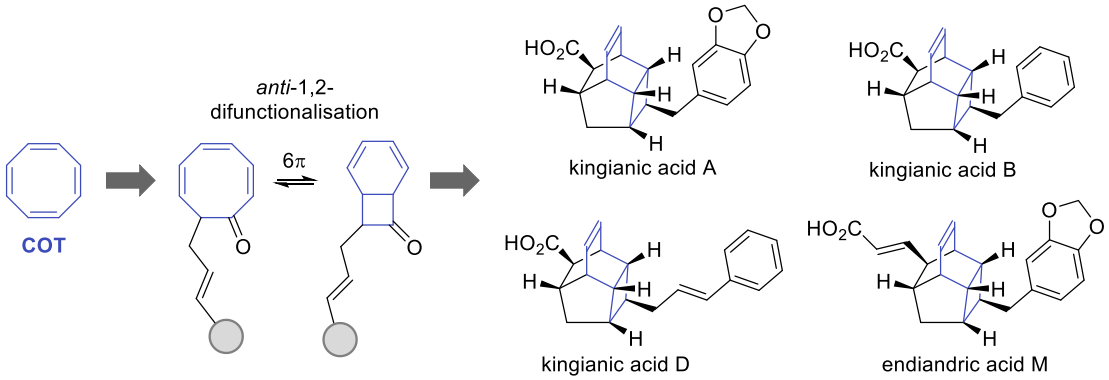

Scheme 1.17: Preview of project in chapter 5 involving the total synthesis of endiandric acid natural products from cyclooctatetraene

1.3.3.2 Torquoselectivity

Torquoselectivity may arise from bias towards inward or outward rotation of substituents in conrotatory or disrotatory mechanisms. This is another level of selectivity in electrocyclisations unrelated to the Woodward−Hoffman rules. Hexatriene **1.41** has two possible directions for a thermal disrotatory 6π giving two possible products, **1.42** and **1.43**, that are enantiomers of each other. Similarly, for a photochemical conrotatory 6π, the two possible products, **1.44** and **1.45**, are enantiomers of each other.

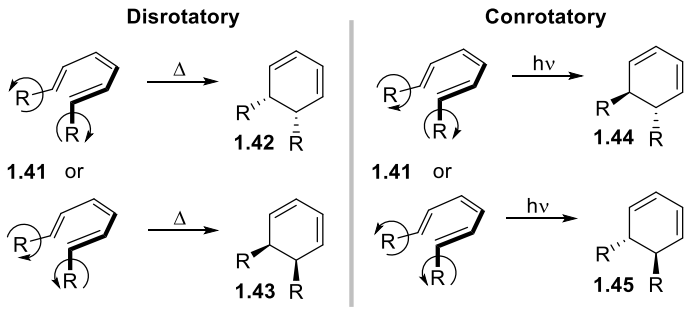

Scheme 1.18: Possible torquoselectivity in 6π electrocyclic ring closing

Some Torquoselective methods have been developed, with selective driving forces often occurring from steric strain, electronic properties of substituents, chiral catalysts, induction

from neighbouring stereocentres (becomes a case of diastereoselectivity) and axial to tetrahedral chirality transfer.[58]

Torquoselectivity is therefore a major target of research and is a major theme in Chapter 6. Torquoselective electrocyclisations have been extensively developed for the 4π electrocyclic variant, however is very limited in 6π and 8π electrocyclisations. Certain bicyclo[4.2.0]octadiene related natural products have shown to possess low to mild levels of torquoselectivity during the electrocyclisation events of their 8π/6π biosynthetic cascade (Scheme 1.19). The project in chapter 6 is a purely computational study on the kinetics, thermodynamics and torquoselectivity of the biosynthetic cascade of bicyclo[4.2.0]octadiene related natural products. The understanding gained through these experiments inspired hypothetical compounds that have been computationally predicted to undertake fully torquoselective 8π electrocyclisations and aims to stimulate future endeavours in torquoselective electrocyclisations.

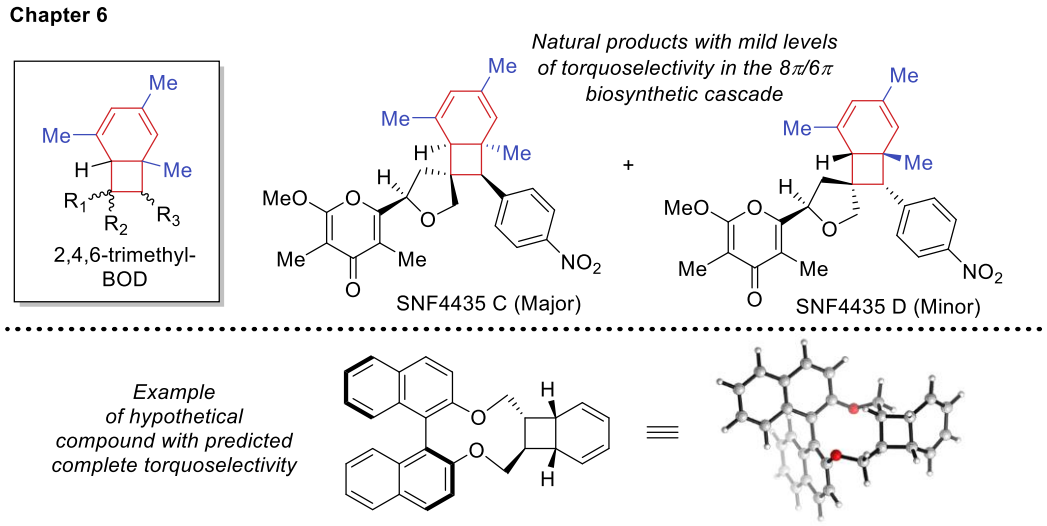

Scheme 1.19: Preview of project in chapter 6 looking at torquoselectivity in the biosynthesis of natural products

1.4 References

[1] R. Herges, *Angew. Chem. Int. Ed. Eng.***1994**, *33*, 255–276.
[2] R. Herges, *J. Chem. Inf. Model.* **1994**, *34*, 91–102.
[3] O. Diels, K. Alder, *Justus Liebigs Ann. Chem.* **1928**, *460*, 98–122.
[4] "Diels–Alder reaction," can be found under https://en.wikipedia.org/wiki/Diels%E2%80%93Alder_reaction, **2022**.
[5] W. Albrecht, *Justus Liebigs Ann. Chem.* **1906**, *348*, 31–49.
[6] H. Staudinger, *Die Ketene*, F. Enke, Stuttgart, **1912**.
[7] H. v. Euler, K. O. Josephson, *Ber. Dtsch. chem. Ges. (A and B Series)* **1920**, *53*, 822–826.
[8] NobelPrize.org, "The Nobel Prize in Chemistry 1950," can be found under https://www.nobelprize.org/prizes/chemistry/1950/summary/, **2023**.
[9] R. B. Woodward, F. Sondheimer, D. Taub, K. Heusler, W. M. McLamore, *J. Am. Chem. Soc.* **1951**, *73*, 2403–2404.
[10] R. B. Woodward, F. Sondheimer, D. Taub, *J. Am. Chem. Soc.* **1951**, *73*, 3547–3548.
[11] R. B. Woodward, F. Sondheimer, D. Taub, *J. Am. Chem. Soc.* **1951**, *73*, 3548–3548.
[12] R. B. Woodward, F. Sondheimer, D. Taub, *J. Am. Chem. Soc.* **1951**, *73*, 4057–4057.

[13] R. B. Woodward, F. Sondheimer, D. Taub, K. Heusler, W. M. McLamore, *J. Am. Chem. Soc.* **1952**, *74*, 4223–4251.
[14] K. N. Houk, F. Liu, Z. Yang, J. I. Seeman, *Angew. Chem. Int. Ed.* **2021**, *60*, 12660–12681.
[15] M. J. S. Dewar, Santiago. Olivella, J. J. P. Stewart, *J. Am. Chem. Soc.* **1986**, *108*, 5771–5779.
[16] J. J. Gajewski, K. B. Peterson, J. R. Kagel, *J. Am. Chem. Soc.* **1987**, *109*, 5545–5546.
[17] K. N. Houk, Y. Tsong. Lin, F. K. Brown, *J. Am. Chem. Soc.* **1986**, *108*, 554–556.
[18] E. Goldstein, B. Beno, K. N. Houk, *J. Am. Chem. Soc.* **1996**, *118*, 6036–6043.
[19] K. N. Houk, *Acc Chem Res* **1975**, *8*, 361–369.
[20] R. Hoffmann, R. B. Woodward, *Acc Chem Res* **1968**, *1*, 17–22.
[21] R. B. Woodward, R. Hoffmann, *Angew. Chem. Int. Ed. Eng.***1969**, *8*, 781–853.
[22] S. D. Kahn, C. F. Pau, L. E. Overman, W. J. Hehre, *J. Am. Chem. Soc.* **1986**, *108*, 7381–7396.
[23] K. N. Houk, *J. Am. Chem. Soc.* **1973**, *95*, 4092–4094.
[24] I. Fleming, F. L. Gianni, T. Mah, *Tetrahedron Lett.* **1976**, *17*, 881–884.
[25] K. Alder, G. Stein, *Justus Liebigs Ann. Chem.* **1935**, *515*, 185–200.
[26] K. Alder, G. Stein, *Justus Liebigs Ann. Chem.* **1934**, *514*, 1–33.
[27] L. M. Stephenson, D. E. Smith, S. P. Current, *J. Org. Chem.* **1982**, *47*, 4170–4171.
[28] J. M. Mellor, C. F. Webb, *J. Chem. Soc., Perkin Trans. 2* **1974**, 17–22.
[29] Y. Kobuke, T. Sugimoto, J. Furukawa, T. Fueno, *J. Am. Chem. Soc.* **1972**, *94*, 3633–3635.
[30] K. N. Houk, L. J. Luskus, *J. Am. Chem. Soc.* **1971**, *93*, 4606–4607.
[31] A research topic search of SciFinder-n conducted in Jan 2022 produced around 38000 research literature references containing the concept "Diels–Alder," **n.d.**
[32] T. J. Brocksom, J. Nakamura, M. L. Ferreira, U. Brocksom, *J Braz Chem Soc* **2001**, *12*, 597–622.
[33] M. Gregoritza, F. P. Brandl, *Eur. J. Pharm. Biopharm.* **2015**, *97*, 438–453.
[34] J. A. Norton, *Chem. Rev.* **1942**, *31*, 319–523.
[35] F. Schneider, K. Samarin, S. Zanella, T. Gaich, *Science (1979)* **2020**, *367*, 676–681.
[36] A. Oluwasanmi, C. Hoskins, *Int. J. Pharm.* **2021**, *604*, 120727.
[37] B. Briou, B. Améduri, B. Boutevin, *Chem. Soc. Rev.* **2021**, *50*, 11055–11097.
[38] M. J. Byrne, N. R. Lees, L.-C. Han, M. W. van der Kamp, A. J. Mulholland, J. E. M. Stach, C. L. Willis, P. R. Race, *J. Am. Chem. Soc.* **2016**, *138*, 6095–6098.
[39] K. Watanabe, *J. Nat. Med.* **2021**, *75*, 434–447.
[40] S. Ghosh, J. E. Erchinger, R. Maji, B. List, *J. Am. Chem. Soc.* **2022**, *144*, 6703–6708.
[41] L. Liu, H. Kim, Y. Xie, C. Farès, P. S. J. Kaib, R. Goddard, B. List, *J. Am. Chem. Soc.* **2017**, *139*, 13656–13659.
[42] T. Gatzenmeier, M. Turberg, D. Yepes, Y. Xie, F. Neese, G. Bistoni, B. List, *J. Am. Chem. Soc.* **2018**, *140*, 12671–12676.
[43] P. Muller, *Pure and Applied Chemistry* **1994**, *66*, 1077–1184.
[44] V. Gold, Ed. , *The IUPAC Compendium of Chemical Terminology*, International Union Of Pure And Applied Chemistry (IUPAC), Research Triangle Park, NC, **2019**.
[45] I. N. Nazarov, I. I. Zaretskaya, *Izv. Akad. Nauk. SSSR Ser. Khim.* **1941**, *0*, 211–224.
[46] D. Vorländer, M. Schroedter, *Ber. Dtsch. chem. Ges.* **1903**, *36*, 1490–1497.
[47] A. T. Blomquist, C. S. Marvel, *J. Am. Chem. Soc.* **1933**, *55*, 1655–1662.
[48] C. W. Shoppee, R. E. Lack, *J. Chem. Soc. C* **1969**, *0*, 1346–1349.
[49] C. W. Shoppes, B. J. A. Cooke, *J. Chem. Soc. Perkin 1* **1972**, 2271.
[50] R. B. Woodward, R. Hoffmann, *J. Am. Chem. Soc.* **1965**, *87*, 395–397.

[51] E. J. Corey, A. G. Hortmann, *J. Am. Chem. Soc.* **1963**, *85*, 4033–4034.
[52] E. J. Corey, A. G. Hortmann, *J. Am. Chem. Soc.* **1965**, *87*, 5736–5742.
[53] K. C. Nicolaou, N. A. Petasis, R. E. Zipkin, J. Uenishi, *J. Am. Chem. Soc.* **1982**, *104*, 5555–5557.
[54] K. C. Nicolaou, N. A. Petasis, J. Uenishi, R. E. Zipkin, *J. Am. Chem. Soc.* **1982**, *104*, 5557–5558.
[55] K. C. Nicolaou, N. A. Petasis, R. E. Zipkin, *J. Am. Chem. Soc.* **1982**, *104*, 5560–5562.
[56] K. C. Nicolaou, R. E. Zipkin, N. A. Petasis, *J. Am. Chem. Soc.* **1982**, *104*, 5558–5560.
[57] K. C. Nicolaou, N. A. Petasis, **1984**, pp. 155–173.
[58] S. Thompson, A. G. Coyne, P. C. Knipe, M. D. Smith, *Chem. Soc. Rev.* **2011**, *40*, 4217.

Chapter 2

Dienes in the Diels−Alder reaction that facilitate subsequent aromatisation of the newly formed ring

2.1 Opening remarks

The Diels–Alder (DA) reaction is one of the most powerful tools within an organic synthetic chemist's arsenal. Nearly 100 years of research since its introduction to the field, has led it to develop into the most powerful 6-membered ring forming annulation, capable of rapidly generating molecular complexity.

Early PhD work under Assistant Professor Christopher Newton focused on the development of a bis-silyl furan diene **2.1** that can undergo a tandem Diels−Alder, deprotection and tautomerisation that yields a *para*-hydroquinone **2.2** or *para*-quinone **2.3**, depending on the oxidation of the dienophile **2.4**. Typical Diels−Alder (DA) reactions don't form aromatic 6-membered rings, however by implementing appropriate functionality on either the diene and/or dienophile can allow for this. Therefore, it is apt for this chapter to be a non-comprehensive review on classes of functionalised dienes that synthesise arenes in a total synthesis setting.

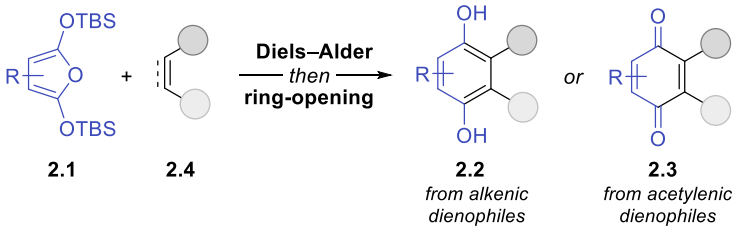

Scheme 2.1: Chapter 2 Diels−Alder methodology visual abstract

2.2 The archetypal Diels−Alder reaction

The Diels−Alder in its simplest form yields a cyclohexene molecule **2.5** from a 1,3-butadiene **2.6** and ethylene **2.7** molecule. This transformation alone is quite powerful since the reaction can conceptually help access most natural compounds due to the abundancy of six-membered rings. However, this simple form of DA cannot directly access aromatic six-membered rings which are also prolific. Approaches do exist where formation of the cycloadduct is followed by the addition of an oxidant (commonly DDQ), oxidising the ring to an aromatic **2.8**.[1–3] Although important as a reaction class, redox manipulations can cause issues in synthesis, namely generation of free radicals, formation of undesired products and incompatibility with the substrate.

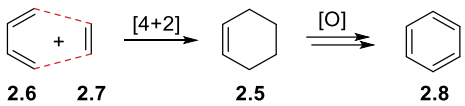

Scheme 2.2: Simplified Diels−Alder reaction and subsequent oxidation to an aromatic

Through certain types of dienes, addition of acid, base or thermal conditions can enable rearrangement of the cycloadduct to form a benzene ring. Pyrones **2.9**, pyridazine **2.10**, furans **2.11**, and other appropriately substituted acyclic dienes **2.12** undergoing a DA can rearrange to form a substituted aromatic ring **2.8** (Figure 2.1, blue highlights indicate the reactive diene moiety). They will be explored in their respective sections with any notable reactivities and mechanisms summarised as well as their use in total synthesis. Ultimately, this review will serve as a guide for this unique form of DA reactions, as well as inspiration for future projects.

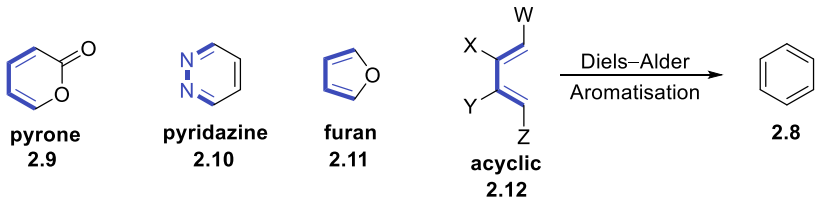

Figure 2.1: Pyrones, pyridazines, furans and acyclic dienes in the synthesis of aromatic compounds

2.3 Pyrone dienes

2.3.1 Introduction

2-Pyrone **2.9**, is an unsaturated six-membered cyclic lactone. It's use as a diene was discovered by Otto Diels and Kurt Alder's in 1931, during their period of Diels−Alder investigations.[4] Methyl coumalate **2.13** and maleic anhydride **2.14** in refluxing toluene undergoes a [4+2] cycloaddition whereby extrusion of carbon dioxide from compound **2.15** occurs by a retro [4+2] yielding a hexadiene intermediate **2.16**, which subsequently undergoes another Diels−Alder with a second equivalent of maleic anhydride to afford compound **2.17**.

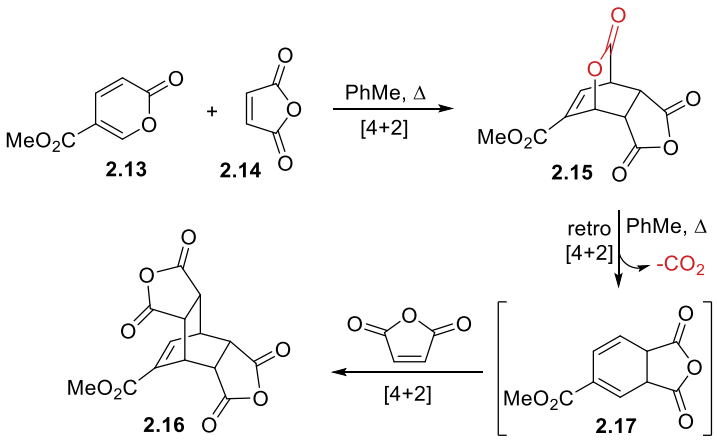

Scheme 2.3: Diels and Alder's preliminary work with methyl coumalate

It was only till the 1970s that the use of 2-pyrones **2.9** as dienes in the Diels−Alder was more extensively utilised.[5–7] It's well documented that 2-pyrones **2.9** with alkynic dienophiles **2.18** form lactone bridged, 1,4-cyclohexadiene intermediates **2.19** that thermodynamically and kinetically undergo facile loss of carbon dioxide through a retro Diels−Alder reaction to synthesise arenes **2.8** (Scheme 2.4). This can also occur with alkenic dienophiles **2.20** which possess a leaving group that can eliminate (see intermediate **2.21**) to form intermediate **2.19** and give an arene **2.8**.

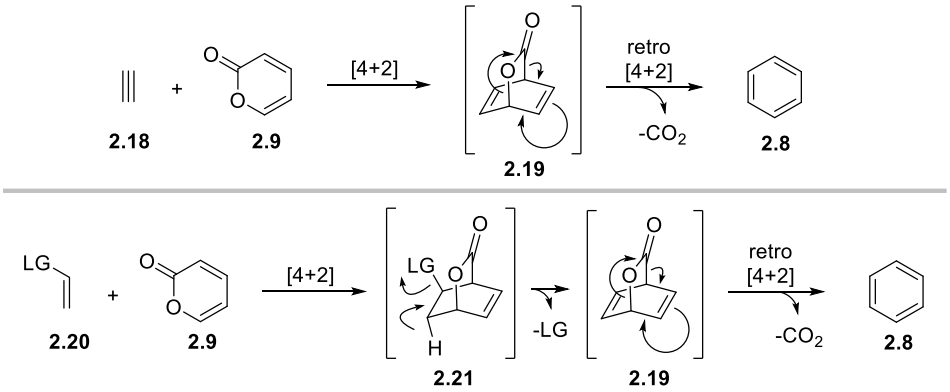

Scheme 2.4: Reaction mechanism of 2-pyrone diene undergoing DA/aromatisation cascade to furnish arenes

The tunability of the electronic properties of 2-pyrones is also synthetically advantageous, following the same selectivity rules as standard Diels−Alder reactions. 2-pyrone dienes participate in inverse electron demand DA (IEDDA) reactions. Scheme 2.5 shows the electron density of 2-pyrone **2.9** to be large at C3 and C5 and deficient at C4 and C6. Highly polarised

2-pyrones and dienophiles **2.22** proceed in a stepwise fashion (see intermediate **2.23**) in contrast to the conventional concerted mechanism.[8,9]

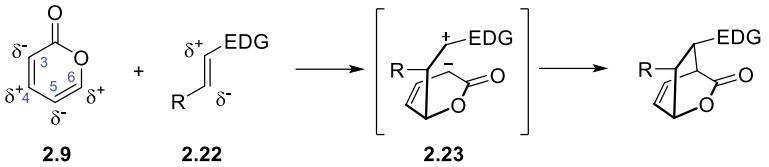

2.9 **2.22** **2.23**

Scheme 2.5: Step-wise mechanism of 2-pyrone IEDDA reaction

The following sections highlight three select examples of 2-pyrone diene DA reactions in the key step of natural product total syntheses.

2.3.2 Nitidine

Guitián's 1992 formal synthesis of nitidine **2.24**, an anti-leukemia agent, was prepared from the intermolecular Diels−Alder between 2-pyrone and aryne.[10] They synthesise a tricyclic pyrone **2.25**, possessing stabilisation from an ethyl ester, which reacts with the corresponding aryne from the thermal decomposition of diazonium 2-carboxylate **2.26**, furnishing the skeletal ring structure **2.27**. Sequential steps of removing the ester and transforming the cyclic amide into an imide provided nitidine **2.24**. An interesting observation is that the reaction evolves three moles of a gaseous molecule (two CO_2 molecules and one N_2), which may provide an easier purification. Previous syntheses were inefficient in constructing the tetracyclic skeleton core, where the common strategy was to connect the A/B ring fragment with the D ring in sequential one bond forming reactions per step and also some using expensive transition metal catalysis (gold and palladium).[11–15] Guitián's strategy is invariably more efficient in forming ring C in one step.

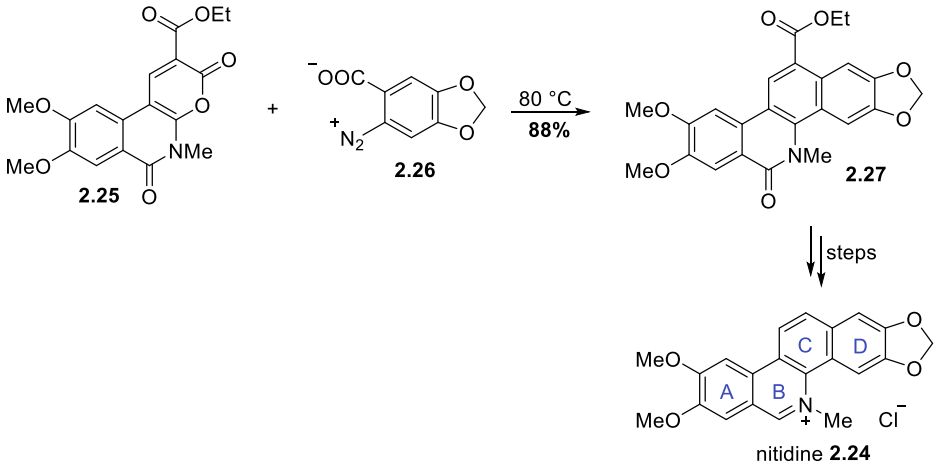

Scheme 2.6: Total synthesis of nitidine

2.3.3 Haouamine A

Haouamine A **2.28** was synthesised by Baran et al. through an intramolecular 2-pyrone Diels-Alder in 2006.[16] Microwave irradiation of compound **2.29** furnishes the bent arene macrocycle and thereby providing the full heptacyclic framework with high atropselectivity (10:1 in favour of **2.28**). Immediate global deacetylation with potassium carbonate after carbon dioxide evolution (see intermediate **2.30**) imparts the desired natural product **2.28**. Following formal syntheses intersected this synthesis at intermediate **2.29**, highlighting the practicality of the 2-pyrone DA reaction.[17,18]

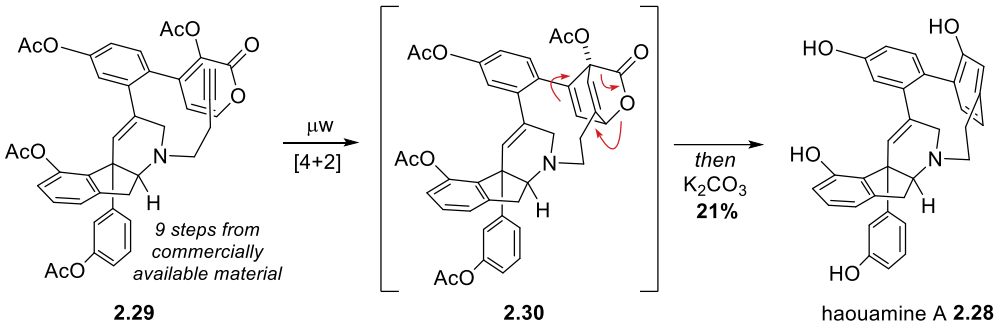

Scheme 2.7: Baran's 2006 total synthesis of haouamine A

Baran later removed the highly atroposelective 2-pyrone DA reaction for an alternative strategy to access atrop-haouamine A **2.31** as well as for improved scalability.[19] Compound **2.32** tosyl group was converted to the primary iodide and then Boc deprotection and heating with Hünig's base delivered macrocycles **2.33** and **2.34** in a 1.45:1 mixture. Additional aromatisation and demethylation steps gave the corresponding haouamine A **2.28** and atrop-haouamine A **2.31**. The new method is useful for accessing the atropisomer, however the additional oxidation step is undesirable. Work by Chen in 2020 showcase a formal synthesis exclusively intersecting compound **2.33** from the selective oxidation of cyclohexene **2.35**.[20] In terms of quickly forming the macrocycle of haouamine A **2.28** with the correct oxidation state/atropselectivity, using the 2-pyrone DA reaction methodology is more appropriate.

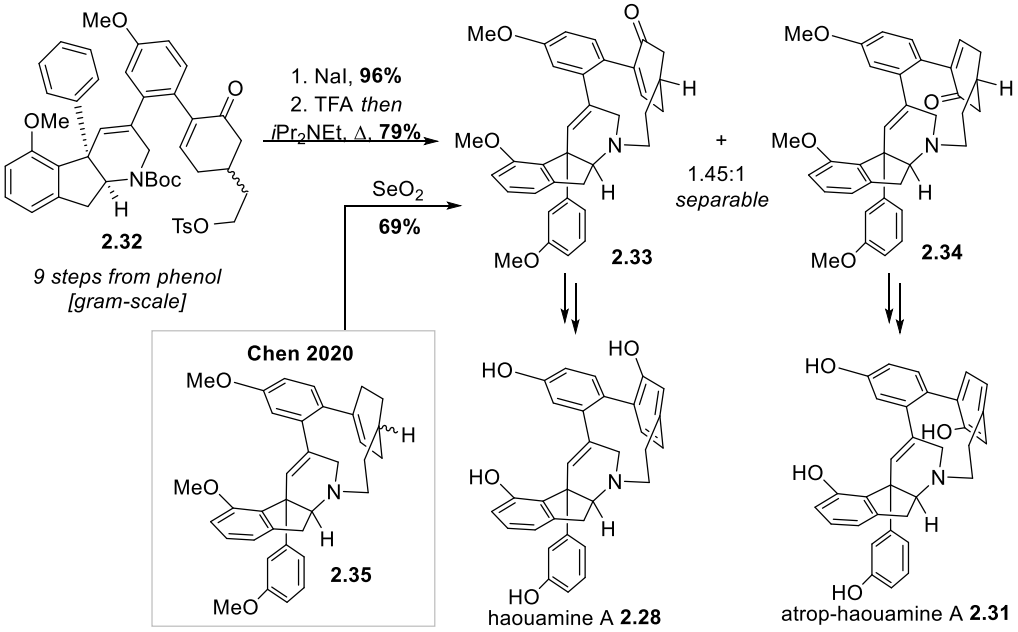

Scheme 2.8: Baran's 2009 total synthesis of haouamine A and its atropisomer with Chen's 2020 formal synthesis

2.3.4 Cavicularin

Another cyclophane natural product, (±)-cavicularin **2.36**, was synthesised by Beaudry et al. in 2013.[21] Substrate **2.37** was heated to 240 °C via microwave irradiation undergoing the intramolecular [4+2] (intermediate **2.38**) followed by subsequent loss of phenylsufinic acid (intermediate **2.39**) and carbon dioxide producing intermediate **2.40**. The order of the phenylsufinic acid and carbon dioxide eliminations is unknown and inconsequential. Standard boron tribromide mediated demethylation conditions yielded (±)-cavicularin **2.36** in 80% yield. The two previous total syntheses involved an acetylenic dienophile, however this synthesis utilised an alkenic dienophile with an electron withdrawing group (PhO_2S-) that enables aromatisation from its extrusion.

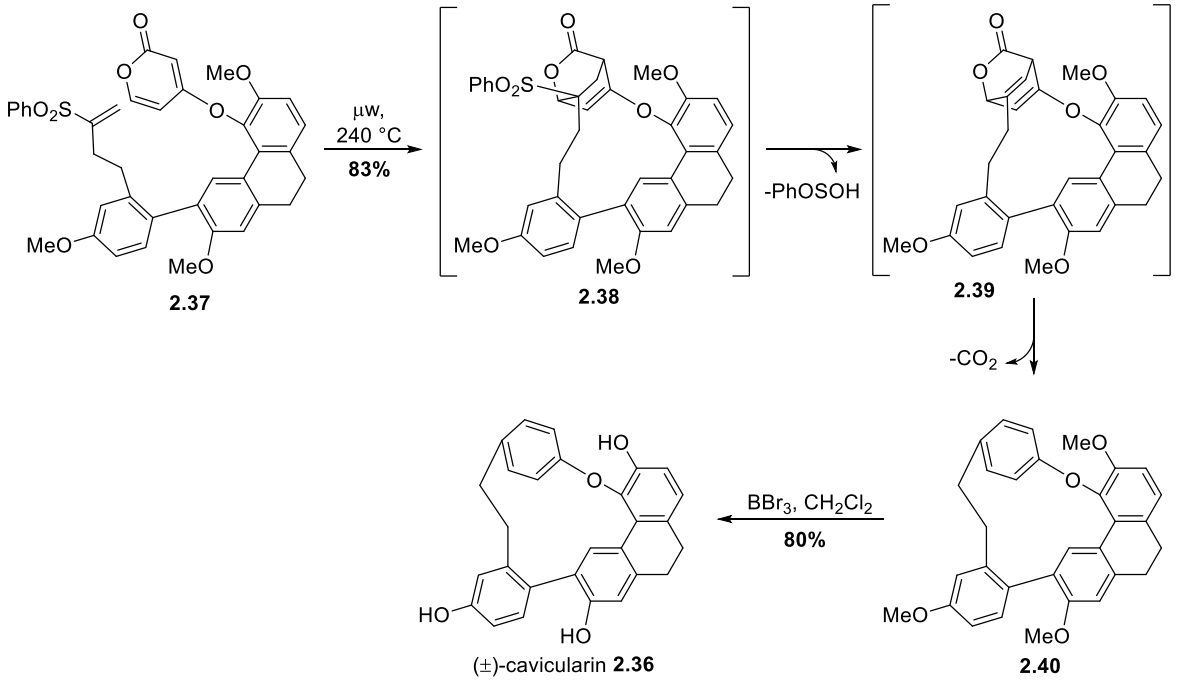

Scheme 2.9: Beaudry's 2013 total synthesis of (±)-cavicularin

Substrates with alternative dienophiles were also tested, however gave undesired outcomes. Isomeric vinyl sulfone **2.41** yielded the undesired regioisomer **2.42**, influenced by the electronic properties of the dienophile. Alkyne substrate **2.43** furnished a mixture of regioisomers **2.40** and **2.42** (2.2:1), owing to a lack of electronic activation.

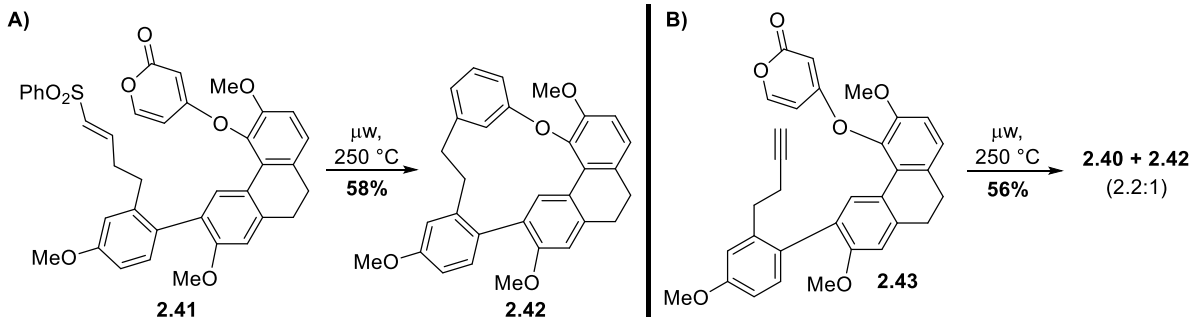

Scheme 2.10: A) DA with Isomeric vinyl sulfone 2.41. B) DA with Alkyne substrate 2.43

In 2014, the Beaudry group improved upon their previous synthesis, performing it enantio- and regioselectively using a chinchona-based thiourea organocatalyst **2.44**.[22] The catalyst was developed by the Deng group, where mechanistic studies have indicated the hydrogen bond donor and acceptor motifs raise the HOMO of the diene and lower the LUMO of the dienophile, and also orientating them to be *exo* selective (see Figure 2.2).[23]

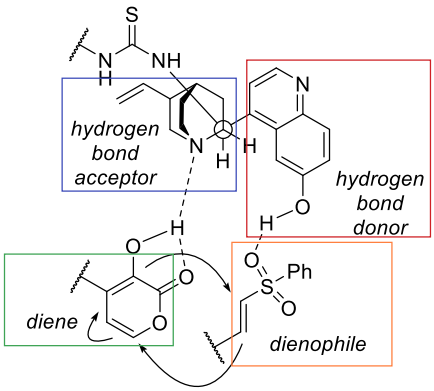

Figure 2.2: Proposed mode of action of bifunctional organocatalyst

Compound **2.46** was subjected to mild thermal conditions with organocatalyst **2.44** to regioselectively form intermediate **2.47** with an enantiomeric ratio of 89:11. End game chemistry to furnish (+)-cavicularin **2.36** proceeded without erosion of enantiopurity. This is the first and only reported case of an organocatalysed enantioselective intramolecular 2-pyrone Diels−Alder reaction.

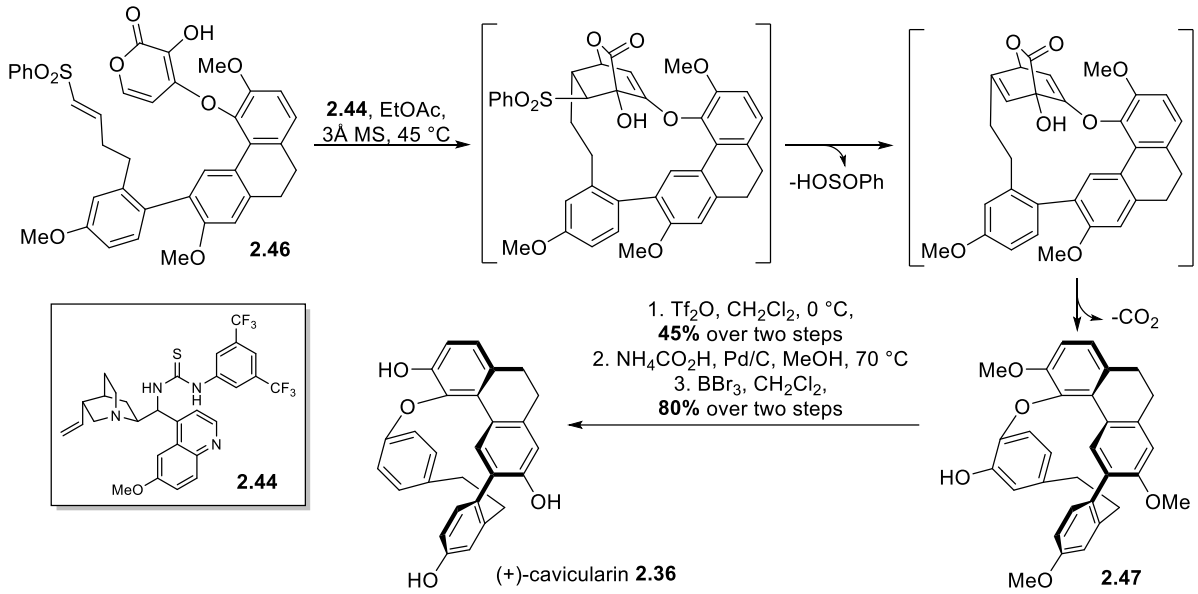

Scheme 2.11: Beaudry's 2014 enantioselective total synthesis of (+)-cavicularin

2.4 Pyridazine dienes

2.4.1 Introduction

Pyridazine (1,2-diazine) **2.10**, is a heterocycle with a 1,2-nitrogen moiety in its aromatic ring. It can be considered analogous to pyrone in that it evolves nitrogen gas instead of carbon dioxide after undergoing the retro [4+2] to yield an arene (Scheme 2.12).

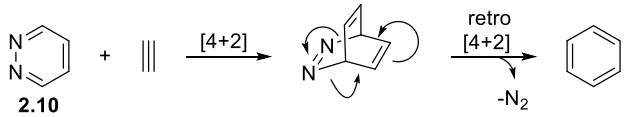

Scheme 2.12:

The earliest reported works surrounding the pyridazine Diels-Alder was in 1972. Neunhoeffer and Werner reported the intermolecular Diels-Alder reaction between a pyridazine dicarboxylate **2.48** and ynamine **2.49**.[24] [4+2] cycloaddition followed by loss of dinitrogen furnished 1-diethylamino-2-methyl-benzene carboxylate **2.50**.

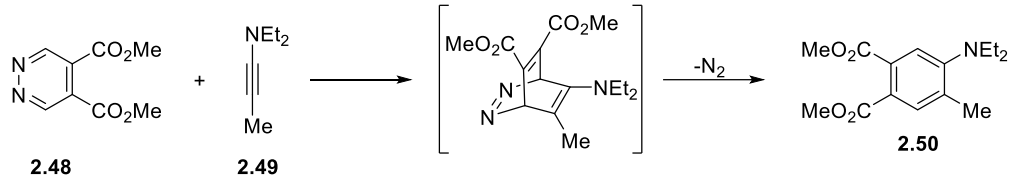

2.48 2.49 2.50

Scheme 2.13: Neunhoeffer and Werner's 1972 work with pyridazines

Jojima, Takeshiba and Konotsune, in the same year, published an intramolecular pyridazine Diels-Alder reaction.[25] Intramolecular [4+2] cycloaddition of phenoxy pyridazine substrate **2.51**, then subsequent nitrogen and hydrogen chloride gas extrusion yielded xanthene in a fair 54% yield.

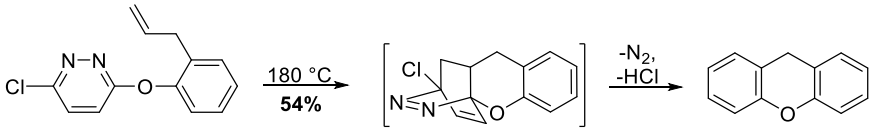

2.51 2.52

Scheme 2.14: Jojima, Takeshiba and Konotsune's 1972 work with pyridazines

Pyridazine dienes follow the same conventions as hydrocarbon dienes in the Diels−Alder (i.e. regioselectivity, etc.). However, an interesting feature of this diene is that it can undergo thermal cycloadditions despite possessing aromatic character. Computational energy calculations of DA reactions of benzene and aza aromatic compounds (AACs) with ethylene were performed by Rios-Gutierrez and Perez et al. in 2019 (Figure 2.3).[26] The [4+2] cycloaddition with benzene **2.8** presented a relatively high activation energy of 36.3 kcal/mol compared to 1,4-butadiene **2.53** (27.5 kcal/mol). However, an increase in the number of nitrogen atoms in an aromatic ring, going from pyridine **2.54** to tetrazine **2.56**, decreases the activation energy as well as increase the exothermicity of the reaction (Figure 2.3). An increase in the number of nitrogen nuclei decreases ring electron density, thereby decreasing the aromatic character of the AACs and therefore why pyridazines can undergo thermal DA reactions. The increase in nitrogen atoms also changes the mechanism of the DA reaction from a normal to an inverse demand. Therefore the electron withdrawing nitrogen atoms significantly lower the LUMO coefficient of the diene, and explains why compounds **2.10**, **2.55** and **2.56** are more reactive than butadiene **2.53**.

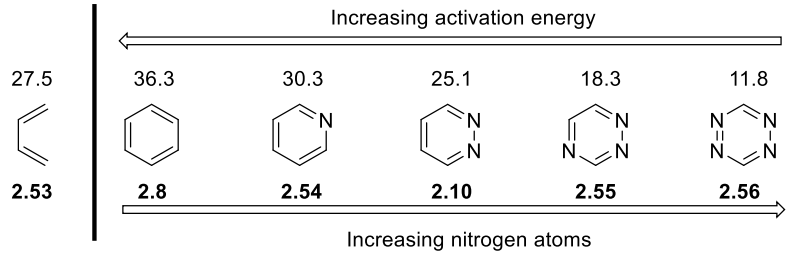

Figure 2.3: DA reactivity of aza aromatic compounds and 1,3-butadiene as dienes reacting with ethylene (dienophile)

Unfortunately, pyridazine has seen limited use in the total synthesis of natural products to form arenes. Instead, it has been typically used to form pyrroles, through a tetrazine **2.56**→1,2-diazine **2.10**→pyrrole pathway strategy.[27–30] Two total syntheses involving pyridazine Diels-Alder strategies will be explored.

2.4.2 CC-1065

Antitumour, antibiotic CC-1065 **2.57** (duocarmycin family), isolated from *Streptomyces zelensis*, was synthesised by the Boger group in 1987.[31–33] Its synthesis involved the peptide

coupling between three fragments, two of which is PDE-I **2.58**, a phosphodiesterase inhibitor from *Streptomyces* strain MD769-C6. A prior study by Boger et al. in 1984 established a methodology in constructing indoline ring systems via an intramolecular pyridazine Diels−Alder reaction.[34] Under prolonged harsh thermal conditions, substrate **2.59** underwent the aza Diels−Alder yielding indoline **2.60** in 87% yield. Another 9 steps were required to install the indole moiety and other functionalities to yield PDE-I **2.58**. PDE-I was dimerised making PDE-I dimer **2.61**, which is the right-hand fragment of CC-1065 **2.57** (shown in blue), and therefore utilised in its the total synthesis. Construction of a 4,6,7-substituted indoline **2.60** is a challenge and even more so for the odd structure of a substituted tetrahydro-pyrollo-indole **2.58**. Standard electrophilic aromatic substitutions or transition metal cross-couplings would not be able to install these unusual substitution patterns on these heteroaromatics, however the Diels−Alder reaction in this instance was successful. Use of pyridazine dienes may be advantageous for synthetic products bearing unique heteroaromatics, however limitations on applying this style of DA reaction would be on the starting material synthesis of the diene and dienophile partner, which may not be trivial.

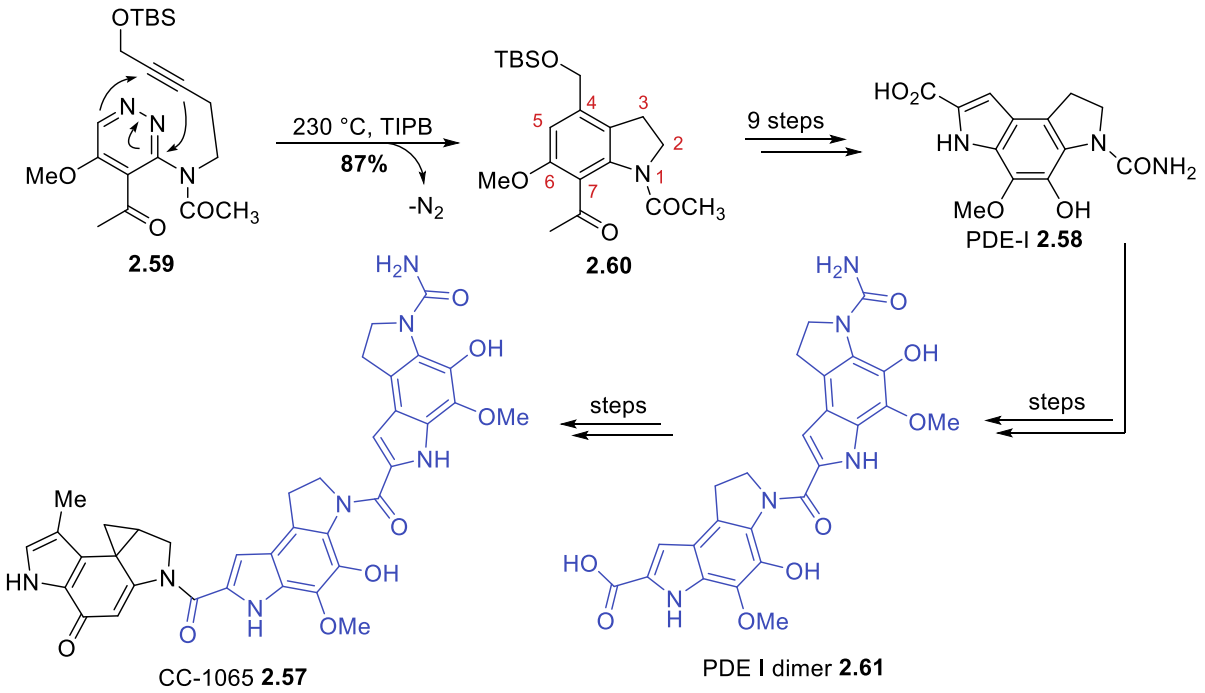

Scheme 2.15: Boger's 1987 total synthesis of CC-1065

2.4.3 Cuparene

Cuparene **2.62** and herbertene **2.63** are sesquiterpene natural products. Despite possessing relatively simple chemical structures they have been popular synthetic targets in the organic synthetic community. They are both regioisomers of each other, with the only difference being the position of the methyl on the benzene ring (ortho or para). If a synthetic route to these products begins from the aromatic ring (compounds **2.64** or **2.65**), installation of the cyclopentane ring can only access one of the products (i.e., **2.64**→**2.62** and **2.65**→**2.63** only, Figure 2.4). Therefore, there has been interest for the sake of synthetic economy to develop a divergent strategy.

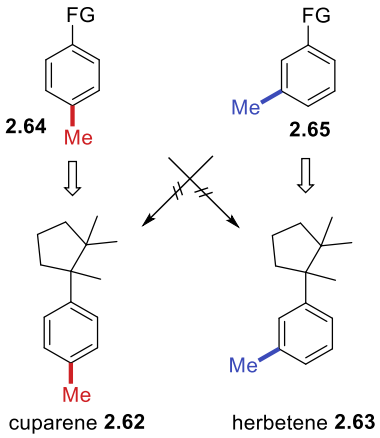

Figure 2.4: Strategy for cuparene and herbertene synthesis

Ho started with the isomerisation of terminal alkyne of substrate **2.66** to an allene **2.67**, which underwent the intramolecular [4+2] **2.68**, dinitrogen extrusion and isomerisation of the alkene into the benzene ring, yielding dihydroisobenzofuran **2.69**. Desymmetrisation by oxidation, allowing separation of the regioisomers **2.70** and **2.71**, is followed by lactone opening and then decarboxylation to produce either cuparene **2.62** or herbertene **2.63**. [35,36] While the intramolecular aza [4+2] cycloaddition is an entertaining transformation due to the three proposed intermediates enroute to **2.69**, it takes more than 8 steps to synthesise **2.66** to reach the key step and is an unnecessarily complicated synthesis of a very simple product.

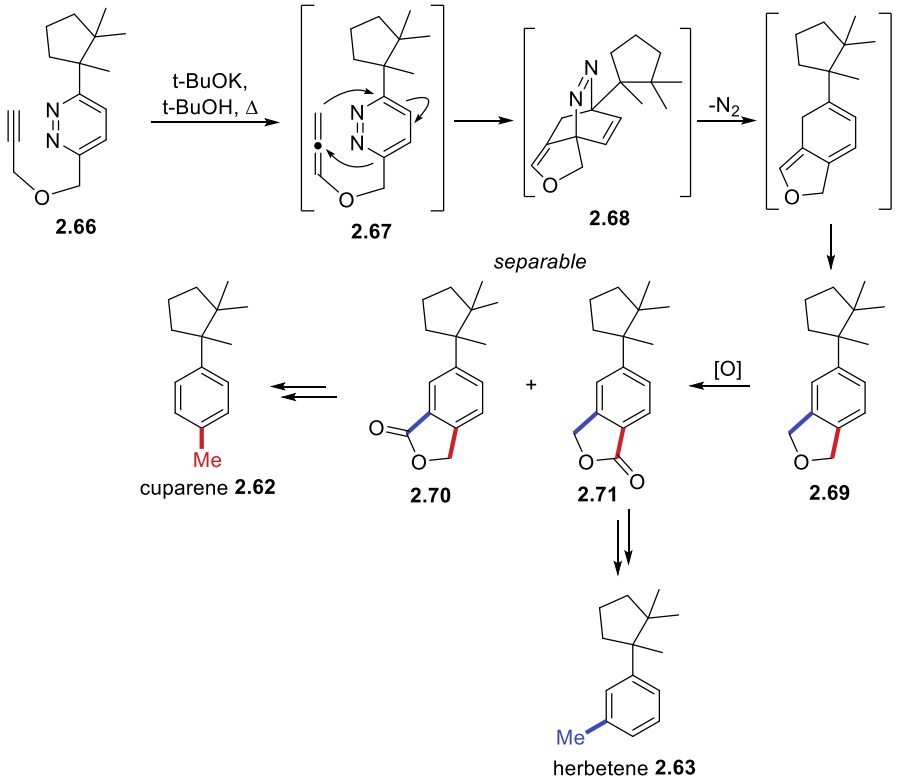

Scheme 2.16: Ho's synthesis of cuparene and herbertene

2.5 Furan dienes

2.5.1 Introduction

Furans **2.11**, a 5-membered heterocyclic compound possessing a lone oxygen atom, have been extensively researched as a diene in the Diels−Alder reaction since the early work of Diels and Alder.[37,38] It's weak aromatic character allows for [4+2] cycloadditions with reactive dienophiles, furnishing 7-oxabicyclo[2.2.1]heptanes **2.72**.

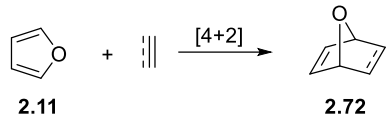

2.11 2.72

Scheme 2.17: Cycloadduct of a furan diene

Although capable of undergoing intermolecular Diels−Alder reactions, intramolecular Diels-Alder of furans (IMDAF) have provided access to complex cycloadducts at comparatively lower thermal conditions with inactivated [39–41] dienophiles. In a typical IMDAF, compound **2.73** undergoes an intramolecular DA (see **2.74**) followed by ring-opening of the oxygen bridge (see **2.75**) and then alcohol elimination to furnish the aromatic product **2.76**.

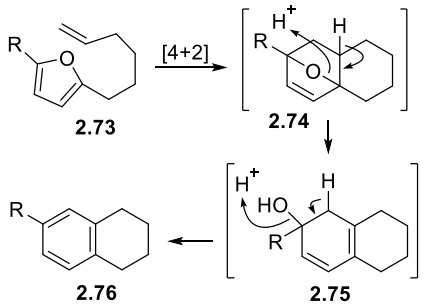

2.73 2.74 2.75 2.76

Scheme 2.18: Typical intramolecular Diels−Alder of furans (IMDAF)

Furan diene DA reactions have been reported to be reversible, converting some of the initial kinetically favoured *endo* cycloadducts to the thermodynamically favoured *exo* cycloadducts.[42–44] However, aromatisation destroys the stereochemistry of the cycloadduct, and therefore no consideration needs to be taken on *endo*/*exo* selectivity in this instance.

Six articles displaying applications to or towards the total synthesis of natural products will be highlighted.

2.5.2 Gilvocarcins

Suzuki et al. published impressive total syntheses of two natural products of the gilvocarcin family in 1994.[45] A key step was the benzyne-furan cycloaddition involving 2-methoxyfuran **2.77** undergoing a regiochemical cycloaddition with pre-benzyne compound **2.78**. They correctly theorised that the alkoxy substituent (-OBn) would act as an electron withdrawing group via inductive effect, providing head-to-head cycloaddition (see intermediate **2.79**). Additionally, this provided prerequisite functionality that mapped well onto the eventual natural products (specifically the methoxy group). The naphthol intermediate **2.80** was used to furnish either gilvocarcin M **2.81** or V **2.82** after additional steps.

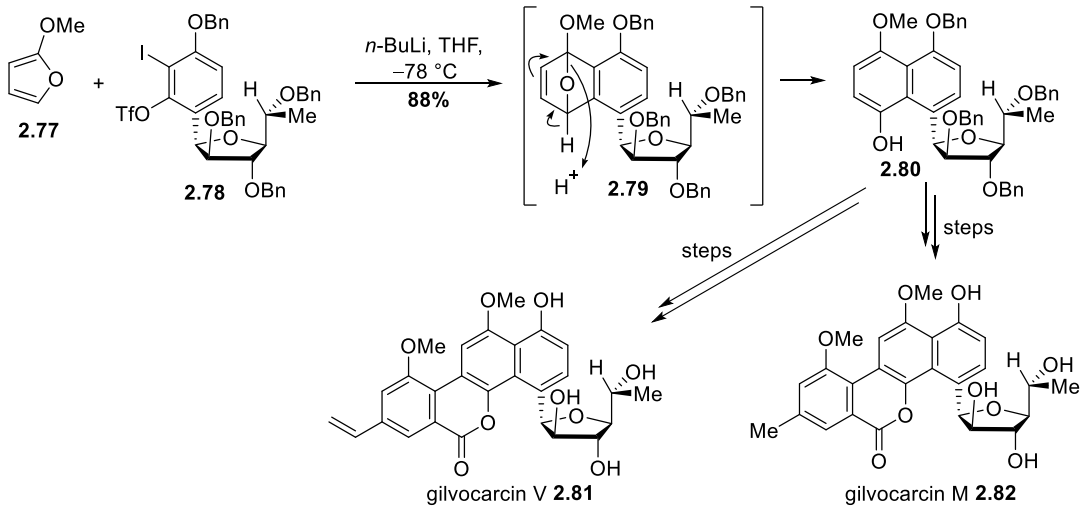

Scheme 2.19: Suzuki's 1994 total synthesis of gilvocarcin V and M

2.5.3 *C*-aryl glycosides

Martin group adopted a similar strategy for accessing major classes of *C*-aryl glycosides such as kidamycin **2.83**.[46] Furan glycoside substrate **2.84** underwent a [4+2] with in situ generated benzyne **2.85** to form intermediate **2.86**. Isolated intermediate **2.86** underwent an acid-catalysed rearrangement to *C*-aryl glycoside derivative **2.87**. The use of a Diels−Alder to construct a complex naphthalene is acceptable here, however, having separate cycloaddition and aromatisation steps is inefficient, where they could easily be telescoped.

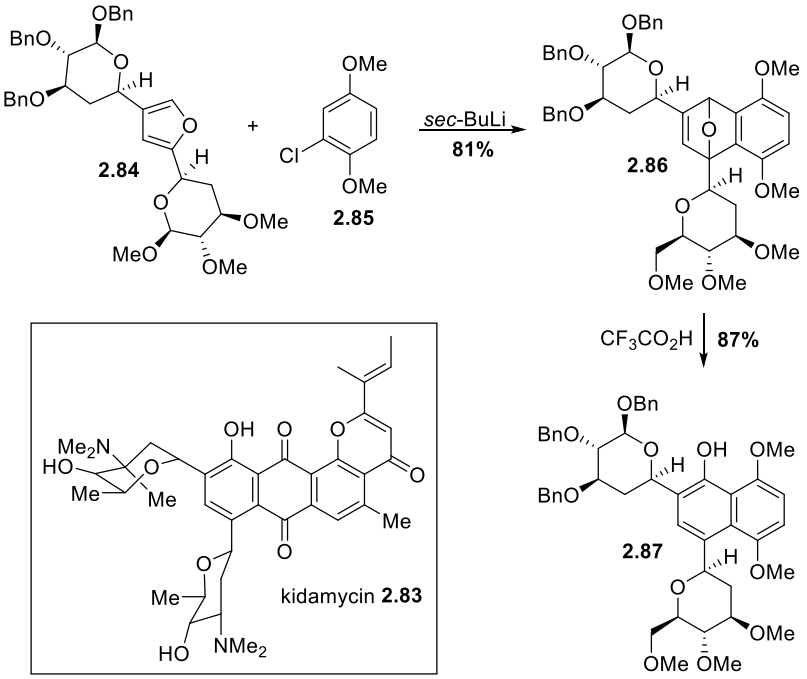

Scheme 2.20: Synthesis of a *C*-aryl glycoside model

2.5.4 Vinaxanthone

An early building block in the synthesis of vinaxanthone **2.88** was synthesised via an intermolecular Diels−Alder between furan **2.89** and disubstituted alkyne **2.90**.[47] The reaction boasted very high regioselectivity provided by the high polarisation between the -OTBS and -OPiv groups of diene **2.89** and the ketone on dienophile **2.90** acting as the dominant activating group. Cycloadduct **2.91** was made in 96% yield, where consequent acid-mediated aromatisation to **2.92** and then pivaloyl group migration yielded highly substituted arene **2.93**. It was apt to apply this DA reaction to construct a complex, highly oxidated arene, which otherwise would be difficult to synthesise via substitution or cross-coupling. It is unusual for

the TBS group on compound **2.91** to survive the acidic conditions, and the pivaloyl migrating, however these events are insignificant to the overall synthesis. Similar to section 2.5.3, the aromatisation step could be combined with the [4+2] cycloaddition in a one-pot procedure.

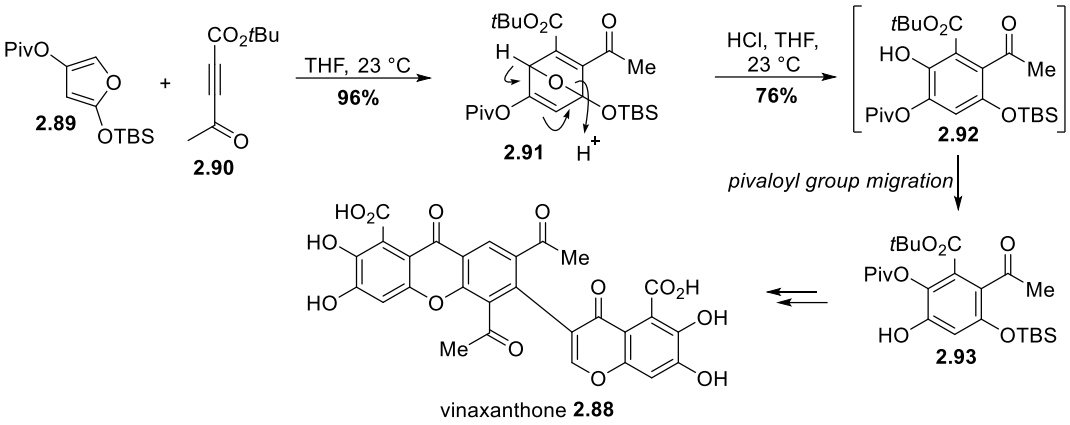

Scheme 2.21: Total synthesis of vinaxanthone via an intermolecular Diels−Alder furan diene reaction

2.5.5 Sparstolonin B

The Yu et al. synthesis of sparstolonin B **2.94** utilised a unique furan diene **2.95**.[48] [4+2] cycloaddition of DMAD **2.96** to the diene **2.95** is consequently followed by treatment of acid to initiate rearrangement and aromatisation yielding substrate biphenyl ether **2.97**. A further eight steps installing the last two rings and functional groups furnished sparstolonin B **2.94**. The reaction mechanism of the rearrangement/aromatisation is proposed to go through oxetane ring intermediates **2.98** or **2.99**, and then a retro [2+2] releasing formaldehyde. The previous aromatisation events involve the loss of a proton or alcohol, but this synthesis involves a carbon-containing leaving group, which is inspiring.

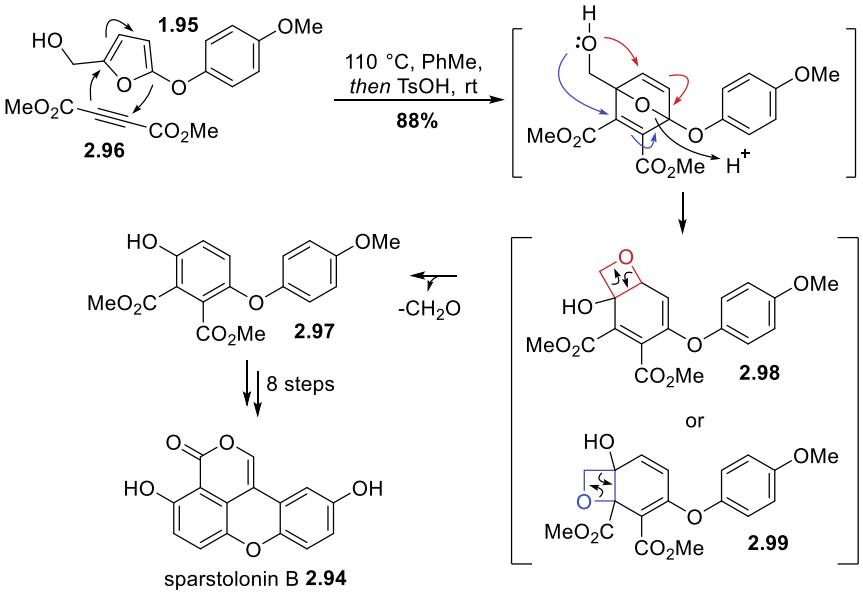

Scheme 2.22: Yu's total synthesis of Sparstolonin B

2.5.6 Benthaminin I

In the synthesis of benthaminin I **2.100** by Chahboun et al., a Lewis acid-catalysed Diels−Alder of a furan **2.101** and methyl propiolate **2.102** generated intermediate **2.103** with complete regioselectivity.[49] This transformation provides the necessary functional groups for installing the remaining methyl group (from ester) and fused furan ring (alcohol group). The extra five

steps to afford benthaminin I **2.100** from compound **2.103** is inelegant, where having a more complex diene and/or dienophile may make the synthesis more attractive.

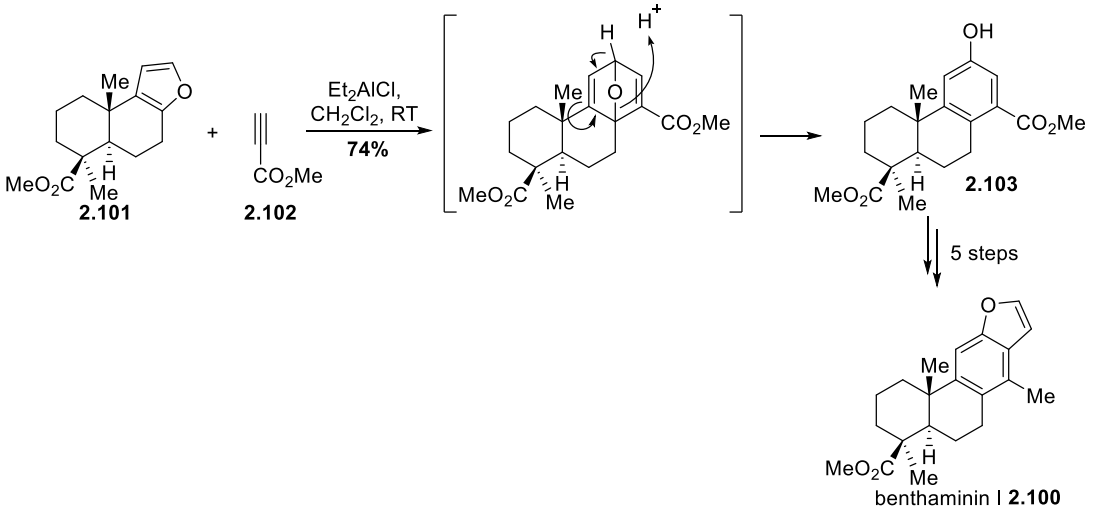

Scheme 2.23: Chahboun's total synthesis of Benthaminin I

2.5.7 8-Hydroxyphenanthridines

Gunderson group have developed a methodology to synthesis 8-hydroxyphenanthridines **2.104**, the framework of a family of natural products (e.g., anhydrolycorinium chloride **2.105** and oxoassoanine **2.106**), through a microwave assisted IMDAF/aromatisation sequence.[50] Compound **2.107** undergoes heating at 180 °C to furnish compound **2.108** that maps onto 8-hydroxyphenanthridine **2.104** related products. It is notable that both diene and dienophile partners have no significant activating groups, therefore requiring harsh thermal conditions. Despite the extremely elevated temperatures, compound **2.108** is synthesised in a very good yield of 87% (descriptive language for yields, i.e., very good yield, follow Vogel's 1996 ed. Textbook[51] and is used throughout this thesis). 8-hydroxyphenanthridine **2.104** scaffolds are possible to be synthesised by cross-coupling reactions, however DA reactions offers an alternative with no transition metal catalysis.

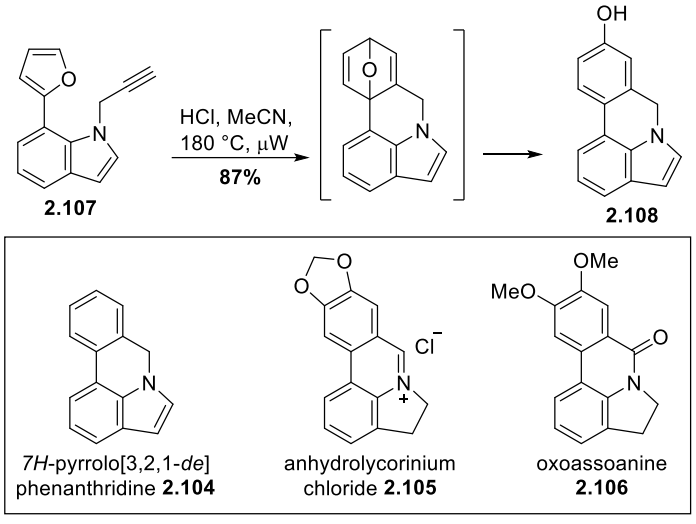

Scheme 2.24: Synthesis of 8-hydroxyphenanthridine framework via microwave assisted IMDAF/aromatisation sequence

2.6 Acyclic dienes

2.6.1 Introduction

Cyclic dienes **2.107** are generally more reactive in the Diels−Alder than their acyclic counterparts due to the locked *s-cis* conformation that is required for a [4+2] cycloaddition transition state. Acyclic dienes can either be *s-cis* **2.108** or *s-trans* **2.109**, but only undergo a DA reaction with the *s-cis* **2.108** conformer. However, established acyclic dienes such as Danishefsky's diene **2.110** still prove useful, often promoting regiospecific additions, such as the case with methacrolein **2.111** selectively furnishing cyclohexenone **2.113** (Figure 2.5B).[52] The following three total syntheses highlight the use of a symmetrical and unsymmetrical dienes that can undergo subsequent aromatisation after a [4+2] cycloaddition.

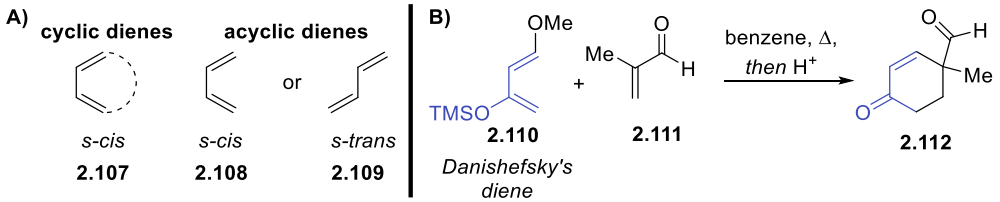

Figure 2.5: A) Conformation of cyclic and acyclic dienes. B) DA with Danishefsky's diene and maleic anhydride

2.6.2 Ismine

One of the earliest constructions of a benzene ring via a Diels−Alder reaction was reported by Hill and Carlson in 1964.[53] 1,4-diacetoxybutadiene **2.113** underwent a [4+2] cycloaddition with 3,4-methylenedioxy-β-nitrostyrene **2.114**, followed by elimination of both acetoxy groups (see intermediate **2.115**) to form arene **2.116**. An additional four steps to install the methylene alcohol and amine furnished ismine **2.117**. Diene **2.113** would be very accessible to make and use in a wide variety of natural products/complex molecule synthesis, however it is wasted here on a very simple natural product that can be readily made by an aryl-aryl cross-coupling.

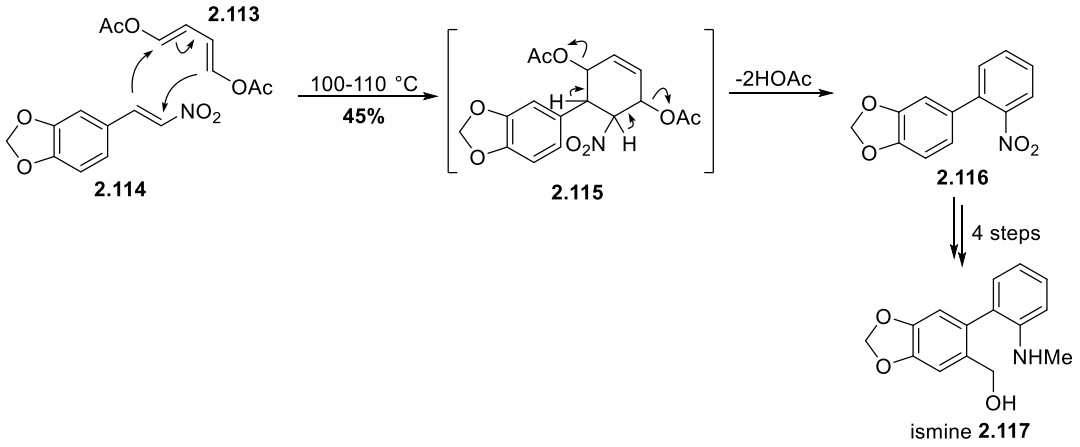

Scheme 2.25: 1964 total synthesis of ismine

2.6.3 Kwanzoquinone C

In the synthesis of kwanzoquinone C **2.118**, Tietze et al. synthesised a tetrasubstituted 1,3 butadiene **2.119**.[54] Reaction with bromo-quinone **2.120** followed by subsequent additions of acid and then base, eliminated HBr and ethanol, respectively, to form compound **2.121**. Diene **2.119** is a highly engineered molecule capable of regioselective addition (when temperatures of −10 °C is maintained), similar to Danishefsky's diene **2.110**. The acid/base sequence for selective elimination of leaving groups could be altered to arrive at different products and therefore bring greater versatility to this diene **2.120**.

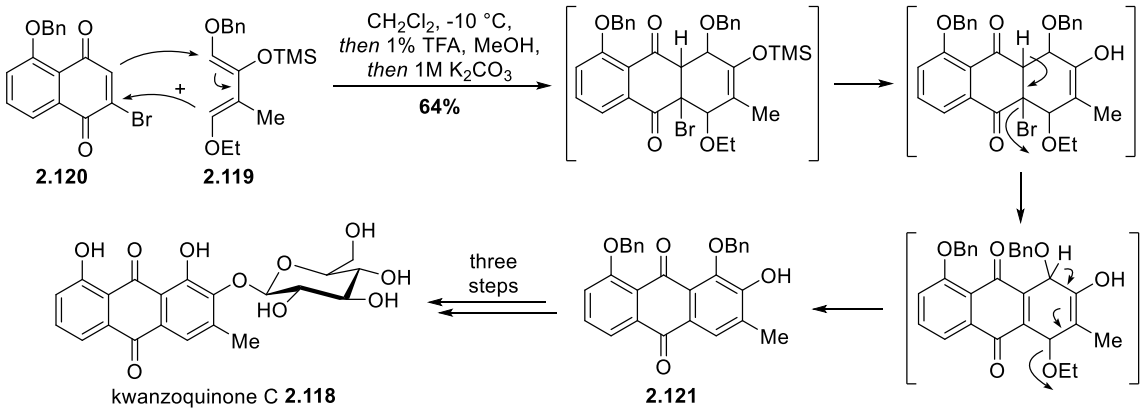

Scheme 2.26: Tietze's synthesis of kwanzoquinone C

Anthraquinone **2.122** was also synthesised with a similar diene. By changing the benzyl to a methyl group on the diene **2.123**, it allowed the methoxy to act as a leaving group and therefore facilitated aromatisation after the [4+2] cycloaddition to compound **2.124**. Only acid was required to force elimination/aromatisation providing an arene **2.124** with a different substitution pattern to compound **2.121**.

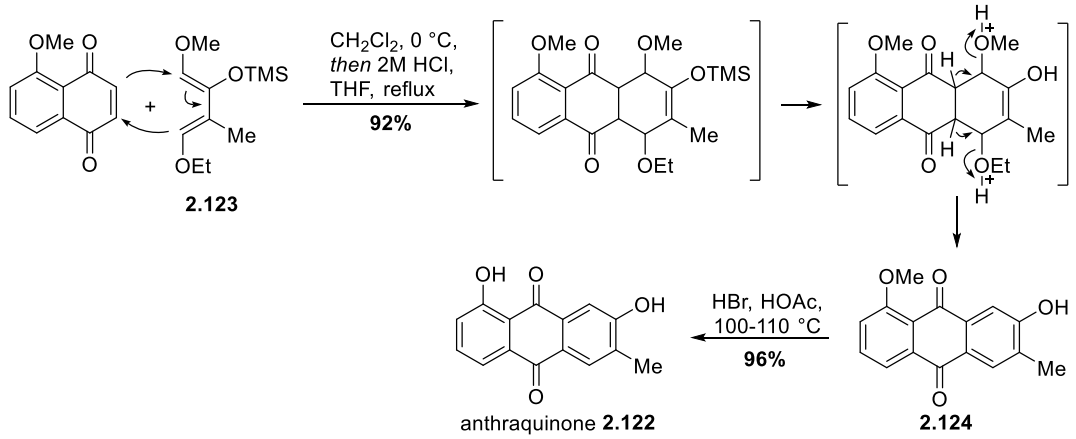

Scheme 2.27: Tietze's synthesis of anthraquinone

2.7 Conclusions and Future Perspectives

We wished to highlight functionalised dienes that will allow aromatisation after cycloaddition, to go beyond the conventional utility of the Diels−Alder reaction and showcase its extra capabilities. The presented diverse (however, noncomprehensive) examples of total syntheses that employ these exciting dienes offers an alternative method of building benzene rings. Whole arene moieties are often installed or the starting substrate of a total synthesis, however highly substituted benzenes may be too difficult to add or synthesise by orthodox means depending on the substituents and the substitution pattern. Limitations do exist for the dienes highlighted, where many total synthesis examples require harsh forcing conditions of highly elevated temperatures or too engineered and are not applicable to a wider variety of aromatic scaffolds. Further research in developing methods that use Lewis-acid catalysts and organocatalysts may solve these issues. The development of new dienes may be unnecessary, where dedicating efforts towards new creative strategies to implement them may be more productive. Natural product total synthesis is not the only test for the applicability of this class of reaction. Fabrication of designed molecules for use in medicinal or materials chemistry stand to benefit and possibly prove more important than the classic total synthesis.

2.8 References

[1] A. Rammohan, A. F. Khasanov, D. S. Kopchuk, D. Gunasekar, G. v. Zyryanov, O. N. Chupakhin, *Nat Prod Bioprospect* **2022**, *12*, 12.

[2] M. A. Filatov, A. v. Cheprakov, *Tetrahedron* **2011**, *67*, 3559–3566.

[3] H. Li, Y. Qiu, C. Zhao, Z. Yuan, X. Xie, X. She, *Chem Asian J* **2014**, *9*, 1274–1277.

[4] O. Diels, K. Alder, *Justus Liebigs Ann. Chem.* **1931**, *490*, 257–266.

[5] J. A. Reed, C. L. Schilling, R. F. Tarvin, T. A. Rettig, J. K. Stille, *J. Org. Chem.* **1969**, *34*, 2188–2192.

[6] Q. Cai, *Chin J Chem* **2019**, *37*, 946–976.

[7] G. Huang, C. Kouklovsky, A. Torre, *Chemistry – A European Journal* **2021**, *27*, 4760–4788.

[8] J. Sauer, R. Sustmann, *Angew. Chem. Int. Ed. Eng.***1980**, *19*, 779–807.

[9] R. Gompper, *Angew. Chem. Int. Ed. Eng.***1969**, *8*, 312–327.

[10] D. Perez, E. Guitian, L. Castedo, *J. Org. Chem.* **1992**, *57*, 5911–5917.

[11] M. HANAOKA, H. YAMAGISHI, M. MARUTANI, C. MUKAI, *Chem Pharm Bull (Tokyo)* **1987**, *35*, 2348–2354.

[12] M. Hanaoka, H. Yamagishi, M. Marutani, C. Mukai, *Tetrahedron Lett.* **1984**, *25*, 5169–5172.

[13] M. Cushman, L. Cheng, *J. Org. Chem.* **1978**, *43*, 286–288.

[14] T. Enomoto, A.-L. Girard, Y. Yasui, Y. Takemoto, *J. Org. Chem.* **2009**, *74*, 9158–9164.

[15] M. Blanchot, D. A. Candito, F. Larnaud, M. Lautens, *Org. Lett.* **2011**, *13*, 1486–1489.

[16] P. S. Baran, N. Z. Burns, *J. Am. Chem. Soc.* **2006**, *128*, 3908–3909.

[17] A. Fürstner, J. Ackerstaff, *Chem. Commun.* **2008**, 2870.

[18] T. Taniguchi, H. Zaimoku, H. Ishibashi, *J. Org. Chem.* **2009**, *74*, 2624–2626.

[19] N. Z. Burns, I. N. Krylova, R. N. Hannoush, P. S. Baran, *J. Am. Chem. Soc.* **2009**, *131*, 9172–9173.

[20] K. H. (Kenny) Park, A. Rizzo, D. Y.-K. Chen, *Chem. Sci.* **2020**, *11*, 8132–8137.

[21] P. Zhao, C. M. Beaudry, *Org. Lett.* **2013**, *15*, 402–405.

[22] P. Zhao, C. M. Beaudry, *Angew. Chem. Int. Ed.* **2014**, *53*, 10500–10503.

[23] Y. Wang, H. Li, Y.-Q. Wang, Y. Liu, B. M. Foxman, L. Deng, *J. Am. Chem. Soc.* **2007**, *129*, 6364–6365.

[24] H. Neunhoeffer, G. Werner, *Tetrahedron Lett.* **1972**, *13*, 1517–1518.

[25] T. JOJIMA, H. TAKESHIBA, T. KONOTSUNE, *Chem Pharm Bull (Tokyo)* **1972**, *20*, 2191–2203.

[26] L. R. Domingo, M. Ríos-Gutiérrez, P. Pérez, *Org Biomol Chem* **2020**, *18*, 292–304.

[27] J. S. Oakdale, D. L. Boger, *Org. Lett.* **2010**, *12*, 1132–1134.

[28] A. Hamasaki, J. M. Zimpleman, I. Hwang, D. L. Boger, *J. Am. Chem. Soc.* **2005**, *127*, 10767–10770.

[29] D. L. Boger, R. S. Coleman, J. S. Panek, D. Yohannes, *J. Org. Chem.* **1984**, *49*, 4405–4409.

[30] D. L. Boger, J. Hong, *J. Am. Chem. Soc.* **2001**, *123*, 8515–8519.

[31] D. L. Boger, R. S. Coleman, *J. Org. Chem.* **1986**, *51*, 3250–3252.

[32] D. L. Boger, R. S. Coleman, *J. Am. Chem. Soc.* **1987**, *109*, 2717–2727.

[33] D. L. Boger, R. S. Coleman, *J. Am. Chem. Soc.* **1988**, *110*, 1321–1323.

[34] D. L. Boger, R. S. Coleman, *J. Org. Chem.* **1984**, *49*, 2240–2245.

[35] T.-L. Ho, M.-H. Chang, *J. Chem. Soc. Perkin 1* **1999**, 2479–2482.

[36] T.-L. Ho, M. Hua Chang, *Tetrahedron Lett.* **1994**, *35*, 4819–4822.

[37] O. Diels, K. Alder, *Justus Liebigs Ann. Chem.* **1931**, *490*, 243–257.

[38] O. Diels, S. Olsen, *J. Prakt. Chem.* **1940**, *156*, 285–314.
[39] G. Appendino, J. Hoflack, P. J. de Clercq, G. Chiari, M. Calleri, *Tetrahedron* **1988**, *44*, 4605–4618.
[40] B. H. Lipshutz, *Chem. Rev.* **1986**, *86*, 795–819.
[41] A. Padwa, A. C. Flick, **2013**, pp. 1–41.
[42] R. C. Boutelle, B. H. Northrop, *J. Org. Chem.* **2011**, *76*, 7994–8002.
[43] C. Toncelli, D. C. De Reus, F. Picchioni, A. A. Broekhuis, *Macromol Chem Phys* **2012**, *213*, 157–165.
[44] V. Froidevaux, M. Borne, E. Laborbe, R. Auvergne, A. Gandini, B. Boutevin, *RSC Adv* **2015**, *5*, 37742–37754.
[45] T. Hosoya, E. Takashiro, T. Matsumoto, K. Suzuki, *J. Am. Chem. Soc.* **1994**, *116*, 1004–1015.
[46] D. E. Kaelin, O. D. Lopez, S. F. Martin, *J. Am. Chem. Soc.* **2001**, *123*, 6937–6938.
[47] A. Axelrod, A. M. Eliasen, M. R. Chin, K. Zlotkowski, D. Siegel, *Angew. Chem. Int. Ed.* **2013**, *52*, 3421–3424.
[48] X. Tang, L. Tong, M. Yao, Q. Liang, X. Wang, H. Yu, *Synlett* **2017**, *28*, 1187–1190.
[49] S. Mahdjour, M. Harche-Kaid, A. Haidour, R. Chahboun, E. Alvarez-Manzaneda, *Org. Lett.* **2016**, *18*, 5964–5967.
[50] H. S. Gulbrandsen, H. Serigstad, M. Lovell Read, I. Joos, L.-L. Gundersen, *European J. Org. Chem.* **2019**, *2019*, 6044–6052.
[51] A. I. Vogel, *Vogel's Textbook of Practical Organic Chemistry*, Prentice Hall, London, **1996**.
[52] S. Danishefsky, T. Kitahara, *J. Am. Chem. Soc.* **1974**, *96*, 7807–7808.
[53] R. K. Hill, R. M. Carlson, *Tetrahedron Lett.* **1964**, *5*, 1157–1160.
[54] L. F. Tietze, K. M. Gericke, C. Güntner, *European J. Org. Chem.* **2006**, *2006*, 4910–4915.

Chapter 3

Bisketene Equivalents as Diels–Alder Dienes

3.1 Introduction

para-Hydroquinones (*p*-HQ) and their substituted derivatives are common motifs in many biologically and structurally fascinating molecules (Figure 3.1A).[1–7] Notably, these motifs are inherently oxidatively sensitive, converting into their corresponding quinone derivatives under mild conditions as well as being mildly acidic (Figure 3.1B).

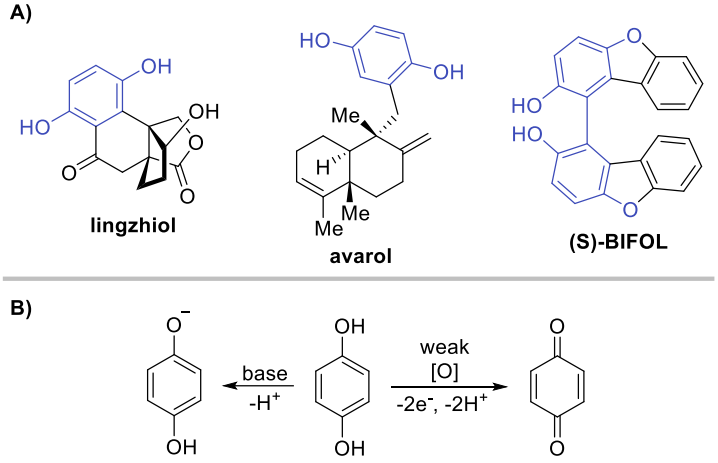

Figure 3.1: A) Select *para*-hydroquinone containing molecules. B) *para*-Hydroquinone sensitivity to basic and oxidative conditions

Therefore, the synthesis of complex hydroquinones typically incorporates two general strategies: iterative functionalisation of an aromatic in a lower oxidation state that will eventually undergo selective redox state adjustment into the desired *p*-HQ or a simple protecting group strategy (Figure 3.2).[8–10] Both approaches invariably introduce challenges in terms of success and/or step count in difficult settings.[11,12]

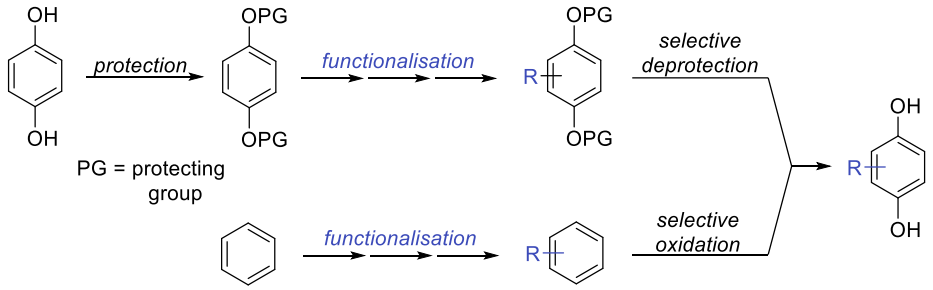

Figure 3.2: Typical approaches to accessing substituted *para*-hydroquinones

For example, in Trost's total synthesis of (+)-frondosin A **3.1**, the final deprotection to form the target compound from **3.2** proved challenging.[13] Initial attempts involving BBr_3 or sodium ethanethiolate resulted in decomposition and mono-deprotection, respectively. The method ultimately employed was an oxidation/reduction sequence involving ceric ammonium nitrate, followed by sodium dithionite, however this only proceeded in moderate yield (Scheme 3.1).

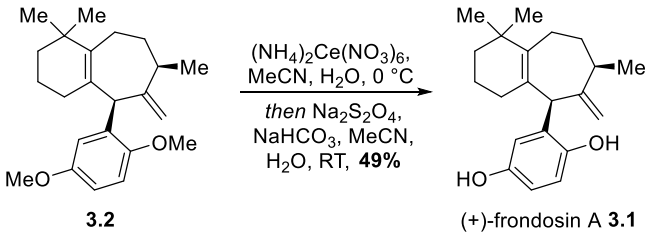

Scheme 3.1: Deprotection to yield (+)-frondosin A

Strategies such as the Hauser–Kraus (HK) annulation and the Moore rearrangement are distinguished in efficiently accessing *p*-HQs (Figure 3.3). The HK annulation is an anionic Michael–Dieckmann condensation that form dihydroxynaphthalenes **3.3** from isobenzofuranones **3.4** and olefinic Michael acceptors **3.5** (Figure 3.3A).[14–16] The Moore rearrangement is initiated from the 4π electrocyclic ring opening of a cyclobutenone–alkyne **3.6**, where a radical cyclisation and then subsequent hydrogen abstractions can form either *p*-HQ **3.7** or *p*-benzoquinones (*p*-BQs) **3.8** (Figure 3.3B).[17–20] Limitations of these established methods involve harsh conditions necessary for substrate preparation and/or cyclisation (e.g. strong base, organolithium nucleophiles, high temperatures), therefore limiting generality. This highlights the need for more general, convergent, non-oxidative strategies that deliver *p*-HQs in unprotected form.

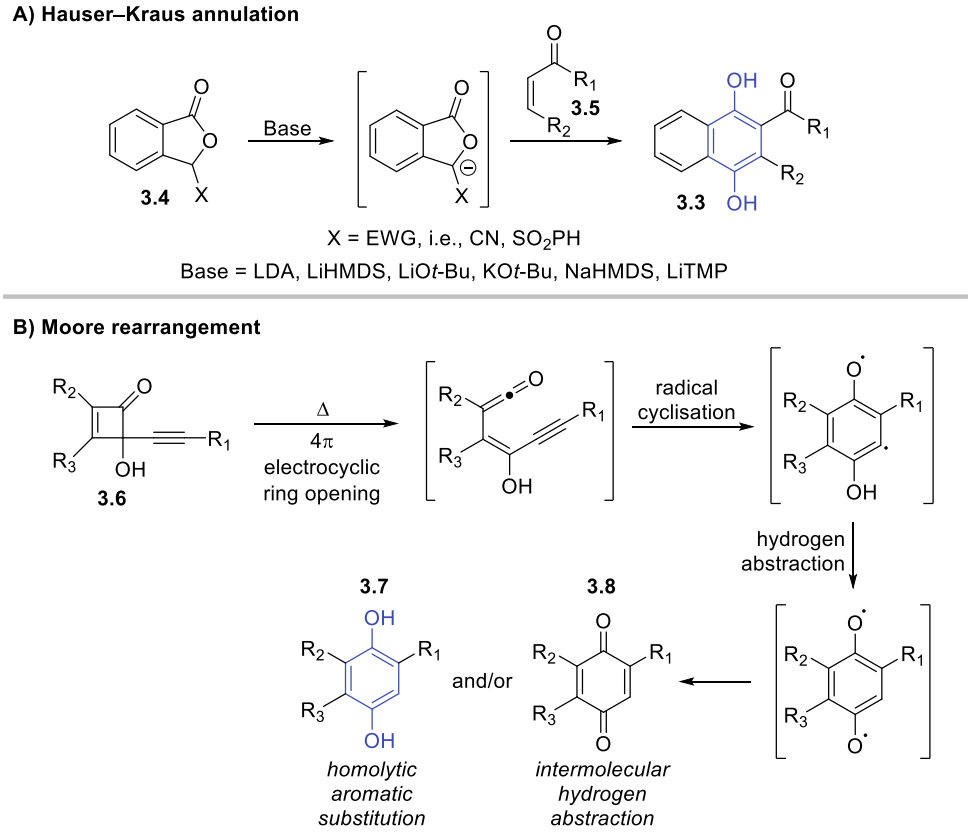

Figure 3.3: A) Generalisation of Hauser–Kraus annulations. B) Generalisation of Moore rearrangement towards p-HQs

Para-hydroquinone **3.9** can be retrosynthetically disconnected via a Diels–Alder (DA) transform through their respective bis-keto tautomer **3.10** (Figure 3.4). This reveals 1,3-butadiene-1,4-dione **3.11** as a diene. Ketenes themselves are unsuitable partners for the DA reaction, providing (formally) [2+2] cycloadducts, thus necessitating masking of this functionality during cycloaddition.[21–24] For DA approaches to *para*-hydroquinones to be of most synthetic value, the masked ketenes must be highly reactive towards cycloaddition, readily accessible, and the DA reaction/ketone unmasking should be achievable in one-pot, either via a domino sequence of reactions, or through the sequential addition of reagents.

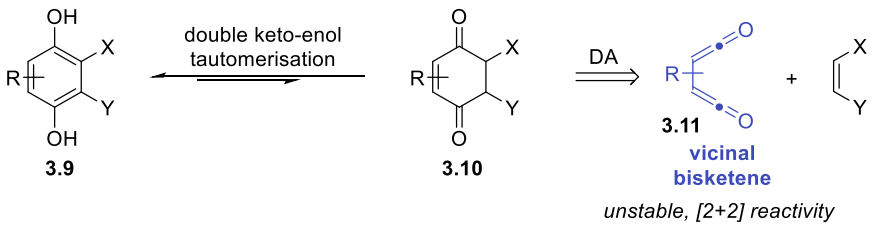

Figure 3.4: DA disconnection of p-HQs (this work)

With respect to the development of a 1,3-butadiene-1,4-dione **3.11** synthetic equivalent, an appropriately functionalised 2,5-substituted furan **3.12** represents a potential candidate.[25] Cycloaddition forming oxygen-bridged bicyclic **3.13** would be followed by facile ring opening and then tautomerisation to the para-hydroquinone **3.14**. Chan and co-workers in 1980 have developed a simple 2,5-bis(trimethylsilyloxy)furan diene **3.15**, capable of undergoing this DA/ring-opening/tautomerization sequence, with the addition of sodium fluoride for aromatisation.[26] However, the diene has been described as "very sensitive to moisture and air", limiting its use and development.[27–33]

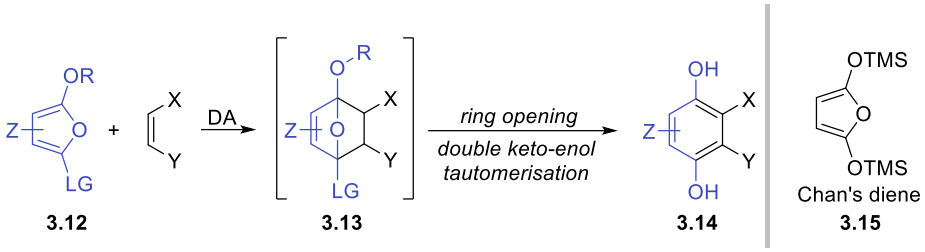

Scheme 3.2: Proposed masked ketene approach to para-hydroquinones via a DA/aromatisation sequence

The development and application of a 2,5-bis(*tert*-butyldimethylsilyloxy)furan diene **3.16**, is the subject of the publication in this chapter.[34]

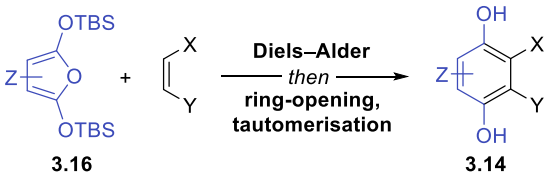

Figure 3.5: 2,5-bis(*tert*-butyldimethylsilyloxy)furan diene

3.2 Authorship Statement

Statement of Authorship

Title of Paper	Masked Bisketenes as Diels–Alder Dienes
Publication Status	■ Published ☐ Accepted for Publication ☐ Submitted for Publication ☐ Unpublished and Unsubmitted work written in manuscript style
Publication Details	*J. Am. Chem. Soc.* **2020**, 142, 31, 13328–13333. DOI: 10.1021/jacs.0c06306

Principal Author

Name of Principal Author (Candidate)	Isuru Dissanayake
Contribution to the Paper	Performed majority of experimental work, data acquisition and interpretation, aided in writing supporting information
Overall percentage (%)	[redacted] 40%
Certification:	This paper reports on original research I conducted during the period of my Higher Degree by Research candidature and is not subject to any obligations or contractual agreements with a third party that would constrain its inclusion in this thesis. I am the primary author of this paper.
Signature	Date 15/06/2020

Co-Author Contributions

By signing the Statement of Authorship, each author certifies that:

i. the candidate's stated contribution to the publication is accurate (as detailed above);

ii. permission is granted for the candidate in include the publication in the thesis; and

iii. the sum of all co-author contributions is equal to 100% less the candidate's stated contribution.

Name of Co-Author	Christopher G. Newton
Contribution to the Paper	Overall project supervisor, performed some experimental work, data acquisition and interpretation, wrote the manuscript, edited supporting information and acted as corresponding author
Signature	Date 15-06-2020

Name of Co-Author	Jacob D. Hart
Contribution to the Paper	Contributed greatly to experimental work, data acquisition and interpretation, aided in writing supporting information
Signature	Date 15/6/20

Name of Co-Author	Emma C. Becroft		
Contribution to the Paper	Aided (during summer internship) in experimental work, data acquisition and interpretation		
Signature		Date	17/6/20

Name of Co-Author	Christopher J. Sumby		
Contribution to the Paper	Performed X-ray crystallography, processed/refined crystallographic data		
Signature		Date	17/6/20

3.3 Manuscript - Bisketene Equivalents as Diels–Alder Dienes

JACS
JOURNAL OF THE AMERICAN CHEMICAL SOCIETY
pubs.acs.org/JACS
Communication

Bisketene Equivalents as Diels–Alder Dienes

Isuru Dissanayake,[‡] Jacob D. Hart,[‡] Emma C. Becroft, Christopher J. Sumby, and Christopher G. Newton*

Cite This: J. Am. Chem. Soc. 2020, 142, 13328–13333
Read Online
ACCESS | Metrics & More | Article Recommendations | Supporting Information

ABSTRACT: 2,5-Bis(*tert*-butyldimethylsilyloxy)furans are established as vicinal bisketene equivalents for application as dienes in the Diels–Alder reaction. Cycloaddition with olefinic dienophiles, under exceptionally mild conditions, enables convergent access to highly substituted *para*-hydroquinones in unprotected form via a one-pot Diels–Alder/ring-opening/tautomerization sequence. The synthesis of *para*-benzoquinones from acetylenic dienophiles, including benzynes, is also demonstrated, and 2,5-bis(*tert*-butyldimethylsilyloxy)pyrroles are established as competent dienes for the synthesis of *para*-iminoquinones. Application in natural product synthesis enables gram-scale access to the neuroprotective agent (±)-indanostatin.

The *para*-hydroquinone (*p*-HQ) motif is embedded within a diverse array of pharmaceuticals,[1] natural products,[2,3] synthetic reagents,[4] and ligand families[5] (Figure 1a). Traditional approaches toward the synthesis of highly substituted derivatives typically involve multistep functionalization sequences, initiated from either an aromatic in a lower oxidation state or a simple protected *p*-HQ (Figure 1b).[6] Selective redox state adjustment[7,8] or protecting group removal[9] can be challenging to achieve in these contexts, highlighting the need for more convergent, nonoxidative strategies that deliver *p*-HQs in unprotected form. Although a small number of such strategies have been developed, most notably the Hauser–Kraus reaction of annulated furanones,[10] and Moore rearrangement of γ-hydroxy-cyclobutenones,[11] the harsh conditions necessary for substrate preparation and/or cyclization limits generality (e.g., strong base, organolithium nucleophiles, high temperatures).

p-HQs can be retrosynthetically disconnected via a Diels–Alder (DA) transform through their bis-keto tautomer to reveal vicinal bisketenes as synthons (Figure 1c). The pronounced instability of this motif,[12] coupled with the propensity of ketenes to undergo [2 + 2] cycloadditions with olefins,[13] necessitates the development of a bisketene equivalent to realize the proposed strategy. In principle, a variety of appropriately 2,5-difunctionalized furans may enable direct access to *p*-HQs under redox-neutral conditions via a DA/ring-opening/tautomerization sequence.[14] The feasibility of such an approach was demonstrated by Chan and coworkers in 1980 through DA reactions of simple 2,5-bis(trimethylsilyloxy)furans, followed by NaF promoted aromatization.[15] The authors described 2,5-bis(trimethylsilyloxy)furans as "*very sensitive to moisture and air*", noting that the rate of autoxidation increased with additional substitution on the furan backbone.[16] Consequently it appears the challenges associated with substrate stability, combined with a proclivity for users to employ strong acids to promote cycloadduct aromatization,[17] have discouraged efforts to further develop this strategy.[18,19]

In an attempt to address these limitations we initiated reaction development with a systematic stability study[20] of pertinent 2,5-difunctionalized furans (Figure 2a; see Supporting Information for additional details). In alignment with the findings of Chan, 2,5-bis(trimethylsilyloxy)furan (**1**) rapidly decomposed when employing standard handling techniques. Assessment of related candidates revealed diene stability scales with silyl group size (compare **1**–**3**), arriving at 2,5-bis(*tert*-butyldimethylsilyloxy)furan (**3**) as a robust and conveniently accessed candidate. Introduction of alternate leaving groups was also explored. Methoxy-derivative **4**, prepared in three steps from commercial materials, exhibited a comparable stability profile relative to **3**. Finally, introduction of bromine (**5**) proved beneficial, resulting in the most stable of all substrates prepared.

The DA reactivities of furans **1**–**5** were benchmarked in PhMe using *N*-methylmaleimide (NMM) as the dienophile (Figure 2b). Bis(silyloxy)furans **1**, **2**, and **3** all reached completion within ∼200 min, exhibiting only a small rate retardation with increased silyl group size. Methoxy-derivative **4** proved 3–4 times more reactive, whereas bromide **5** performed the worst, with less than 50% conversion observed after 250 min. Overall, bis(*tert*-butyldimethylsilyloxy)furan (**3**) strikes the best balance between ease of synthesis, stability, and DA reactivity, and as such we elected to focus exclusively on its continued development.

Studies into the ring opening/tautomerization of DA adducts **6**-*endo* and **6**-*exo* revealed that simply stirring in MeOH promotes the desired aromatization event, avoiding the need for addition of an acid, or a fluoride source (Figure 2c). Moreover, conducting the DA reaction in MeOH enabled the

Received: June 11, 2020
Published: July 18, 2020

https://dx.doi.org/10.1021/jacs.0c06306
J. Am. Chem. Soc. 2020, 142, 13328–13333

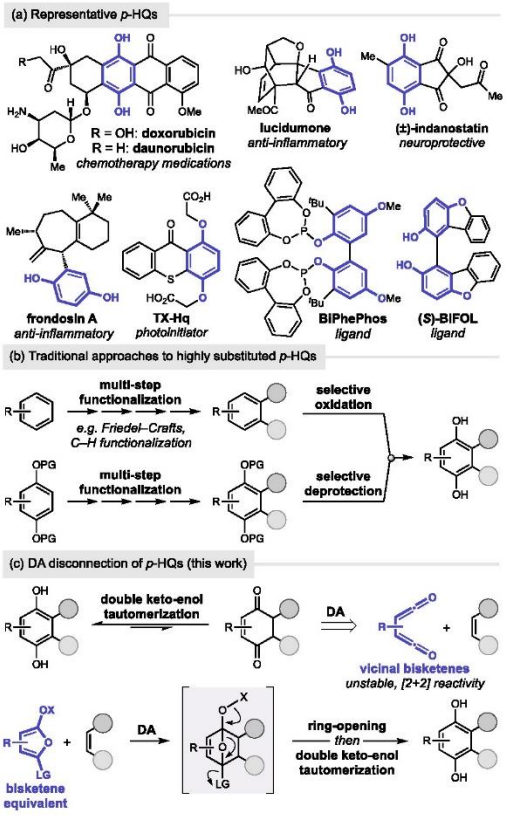

Figure 1. Motivation for reaction development. PG = protecting group, LG = leaving group.

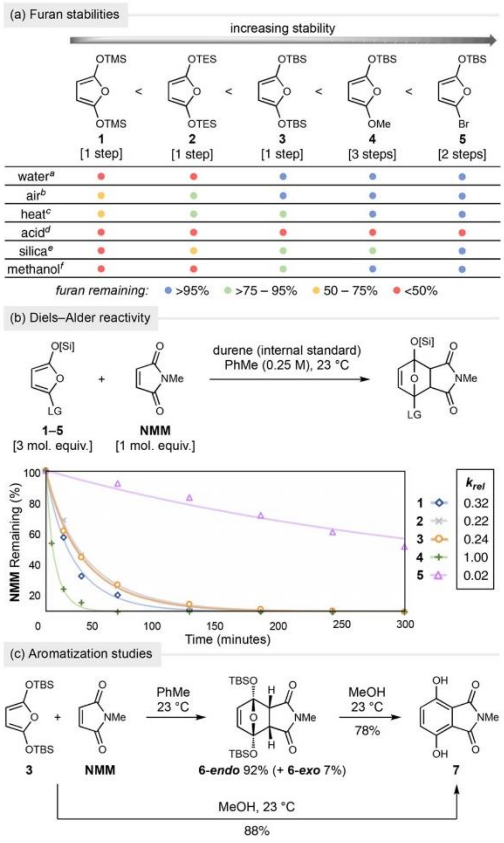

Figure 2. Development of a convenient vicinal bisketene equivalent. LG = leaving group. [a]0.025 M $(CD_3)_2CO/D_2O$ mixture (9:1) stirred for 1 h. [b]Compressed air bubbled through a 0.025 M $CDCl_3$ solution for 10 min. [c]Dilute C_6D_6 solution heated at 120 °C in a microwave reactor for 2 h. [d]0.10 M TFA solution in $CDCl_3$ stirred for 1 min. [e]1.0 mL of a 0.025 M $CDCl_3$ solution stirred with untreated silica (250 mg) for 2 h. [f]0.20 M $CDCl_3/CD_3OD$ mixture (1:4) stirred for 1 h.

synthesis of *p*-HQ **7** in 88% isolated yield, directly from furan **3**, via a one-pot DA/ring-opening/tautomerization cascade.

Having identified a suitable vicinal bisketene equivalent we investigated the scope of *p*-HQ formation (Table 1). With respect to diene structure the reaction appears general, and a library of furans (prepared directly from the corresponding cyclic anhydrides; see Supporting Information) were readily converted into *p*-HQs upon reaction with NMM in MeOH at 65 °C. In the case of monofunctionalized derivatives, methyl (**8**), allyl (**9**), and phenyl (**10**) functionality was well tolerated. More highly substituted five- and six-membered fused bicyclic furans also reacted smoothly (**11**–**15**), including steroid-inspired pentacyclic derivative **14**. The chemoselectivity of desilylation was highlighted through preparation of silyl enol ether **15** in 95% yield, and notably, no evidence for olefin migration was observed for all substrates screened. With more sterically demanding silylated intermediates, such as for indole **16** and biaryl **17**, the rate of MeOH promoted aromatization drops significantly. In these cases *p*-HQ formation can be expedited through addition of an acid additive. Extension to a one-pot double DA/double aromatization strategy provided the BiPhePhos ligand scaffold[5a] in 53% yield (**17**), creating opportunities for a highly convergent approach to a library of ligand derivatives. With less reactive dienophiles, the DA reaction is best conducted in an aprotic solvent (or neat) followed by addition of MeOH. Under these conditions, sulfone (**18**), ketone (**19**), ester (**20**), and aldehyde (**21**) activating groups were all tolerated. Finally, orientational selectivity of the cycloaddition event was demonstrated through coupling of unsymmetrical monofunctionalized dienes with methyl acrylate (**22** and **23**, up to 6:1 in favor of the expected *para*-isomer).

Exploratory studies from Chan and co-workers toward the synthesis of *para*-benzoquinones (*p*-BQ) from 2,5-bis-(trimethylsilyloxy)furans were hampered by competitive *p*-HQ formation.[15] Optimistic that the 2,5-bis(*tert*-butyl-dimethylsilyloxy)furan motif may be more well suited to *p*-BQ formation, we probed reactivity with acetylenic dienophiles (Table 2). Indeed, cycloaddition of several representative derivatives with dimethyl acetylenedicarboxylate (DMAD), followed by addition of TFA, provided *p*-BQs **24**–**26** in good to excellent yields (without any evidence for *p*-HQ formation). Encouraged by these results we evaluated benzynes as coupling partners. *ortho*-Iodotriflates were identified as suitable

https://dx.doi.org/10.1021/jacs.0c06306
J. Am. Chem. Soc. 2020, 142, 13328–13333

Table 1. Scope of *p*-HQ Formation

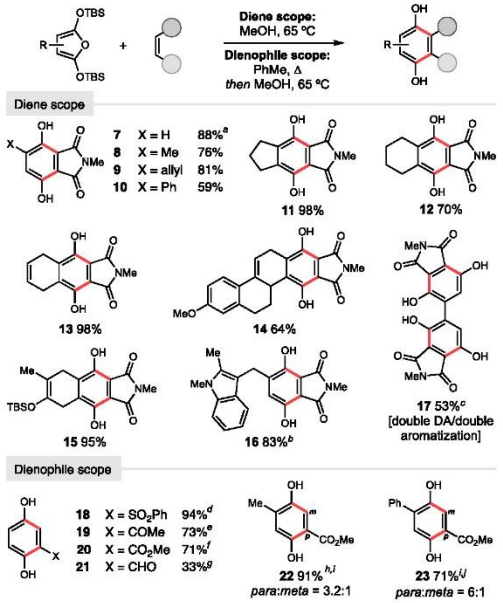

[a]DA at 23 °C. [b]Aromatization achieved by addition of TFA at 23 °C. [c]DA in PhMe at 23 °C, aromatization achieved by addition of H_2SO_4 at 23 °C. [d]80 °C. [e]60 °C. [f]111 °C. [g]50 °C. [h]DA neat at 23 °C. [i]Combined yield of isomers. [j]DA neat at 55 °C.

Table 2. Scope of *p*-BQ Formation

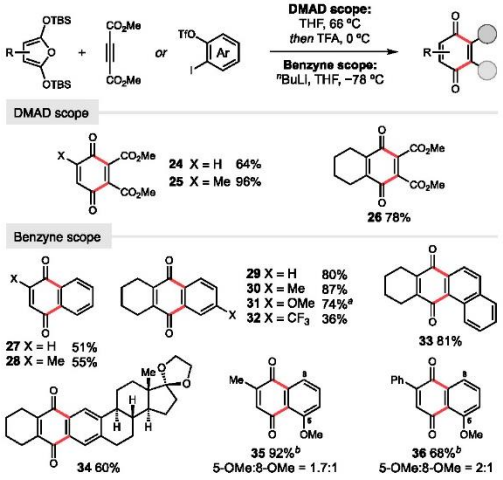

[a]Determined by ^{1}H NMR. [b]Combined yield of isomers.

precursors, enabling low temperature benzyne generation in the presence of our furans.[21] In contrast to the DMAD-derived cycloadducts, TFA addition is unnecessary, and intermediate desilylation can be achieved via a simple acidic workup. A brief diene screen revealed that increased steric bulk on the furan backbone resulted in improved yields (**27**–**29**). With respect to benzyne substitution, electron-rich substrates react exceptionally well (**30** and **31**); however, a significant reduction in yield was observed with incorporation of trifluoromethyl functionality (**32**). 1-Naphthyne is also a competent dienophile (**33**), as too are more complex steroid-derived benzynes (**34**). Although orientational selectivity[22] of the cycloaddition is not especially high in the case of **35** and **36** (up to 2:1), isomer separation can be achieved via standard flash chromatography, allowing ready access to the methoxy-naphthalene-1,4-dione fragment present in both doxo- and daunorubicin.[1]

The generality of our approach is highlighted through extension to 2,5-bis(*tert*-butyldimethylsilyloxy)pyrroles as synthetic equivalents of vicinal ketenimine-ketenes (Figure 3a). While these pyrrole derivatives are less stable than their

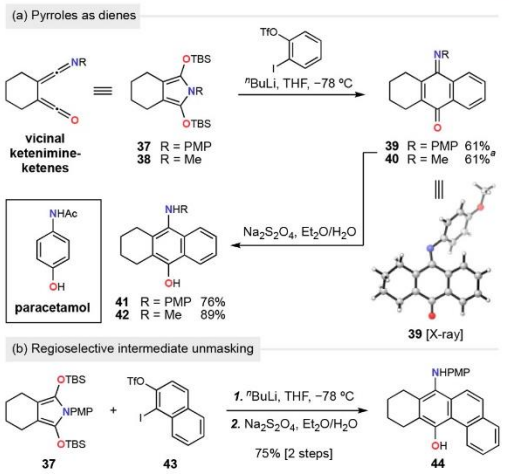

Figure 3. Bis(*tert*-butyldimethylsilyloxy)pyrroles as vicinal ketenimine-ketene equivalents. PMP = *para*-methoxyphenyl. [a]Determined by ^{1}H NMR.

corresponding furan congeners (see Supporting Information), they exhibit comparable reactivity with arynes.[23] Thus, reaction of aryl- and alkylated pyrroles **37** and **38** with benzyne provided *para*-iminoquinones (*p*-IQs) **39** and **40**, both in 61% yield. Notably, *p*-IQs feature within natural products,[24] and derivatives have been demonstrated as versatile intermediates for the synthesis of complex alkaloids[25] and BINOL derivatives.[26] Moreover, they serve as convenient precursors to the biologically relevant *para*-aminophenol motif (e.g., paracetamol)[27] via sodium dithionite promoted reduction (**41** and **42**). Further experiments demonstrated regioselective ring opening of unsymmetrical cycloadducts can be achieved (Figure 3b). In this example, a two-step reductive coupling of pyrrole **37** with 1-naphthyne (generated from *ortho*-iodotriflate **43**) provided phenanthrene **44** in 75% yield.

We became interested in the development of a cross-conjugated extension to further expand the synthetic potential of our methodology (Figure 4a).[28] In principle the simplest candidate, vinylfuran **45**, would enable a diene-transmissive double DA sequence, which if conducted with two different dienophiles leads to even more highly functionalized aromatics. The success of such a strategy is reliant upon both the inherent

https://dx.doi.org/10.1021/jacs.0c06306
J. Am. Chem. Soc. 2020, 142, 13328−13333

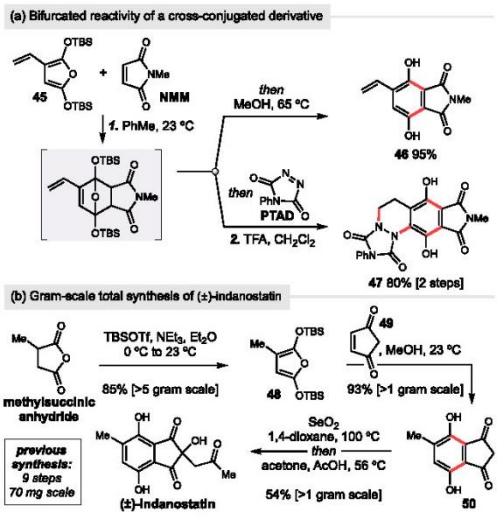

Figure 4. (a) Extension to a cross-conjugated derivative and (b) application of *p*-HQ formation in natural product synthesis.

diene site selectivity of **45** (cyclic versus semicyclic) and the relative rates of the first and second cycloadditions, both of which are difficult to infer from the diverging reactivity reported for related cross-conjugated furans.[29] Fortuitously, NMM reacted with complete selectivity for the (desired) cyclic diene site of **45**.[30] Moreover, the second DA reaction is markedly slower than the first, allowing not only a change in dienophile but also bifurcation of reactivity: addition of MeOH promoted aromatization to generate vinyl-substituted *p*-HQ **46**, whereas addition of 4-phenyl-1,2,4-triazole-3,5-dione (PTAD) enabled a hetero-Diels–Alder reaction. Although subsequent deprotection and aromatization can be achieved in excellent yield via in situ addition of TFA, in this particular case purification is simplified by a stepwise approach, yielding tetracyclic *p*-HQ **47** in 80% yield over two steps from **45**.

Finally, to demonstrate scalability of *p*-HQ formation, as well as the applicability of our methodology in natural product synthesis, we pursued the total synthesis of the neuroprotective agent (±)-indanostatin[3b] (Figure 4b). The marked base sensitivity of our envisioned dienophile, 1,3-cyclopentenedione (**49**), has precluded its application as a coupling partner in conceptually related anionic (formal) DA strategies toward *p*-HQs.[31] Pleasingly, methylfuran **48** (synthesized in one step from methylsuccinic anhydride) reacted smoothly with **49** in MeOH at room temperature, providing gram-scale quantities of *p*-HQ **50** in 93% yield, and without the need for chromatographic purification. A subsequent one-pot oxidation[32]/alkylation procedure (via the intermediate trione hydrate) yielded over 1 g of (±)-indanostatin in only three steps total (cf. nine steps for the previous total synthesis[31]).

In conclusion, we have established the 2,5-bis(*tert*-butyldimethylsilyloxy)furan motif as a general vicinal bisketene equivalent for application as a diene in the DA reaction. A mild, user-friendly protocol provides access to a variety of highly substituted *p*-HQs by reaction with olefinic dienophiles. In turn, employing acetylenic dienophiles provides efficient access to *p*-BQs, or *p*-IQs when 2,5-bis(*tert*-butyldimethylsilyloxy)pyrroles are utilized as dienes. While one can imagine employing more robust silyloxy substituents in attempts to further tweak furan stability, and indeed we anticipate in some cases this may provide improved results, generally speaking it appears the *tert*-butyldimethylsilyl functionality strikes an excellent balance between diene stabilization and ease of intermediate desilylation. In essence, the methodology disclosed herein represents a transform-based strategy[33] in which two C–C bonds of several *para*-quinone ring systems are made simultaneously via a cycloaddition event. This approach avoids the need for lengthy sequences of redox manipulations and/or functional group interconversions, both of which are commonplace in more classical structure-goal strategies.[33] As such, we believe the methodology developed herein has the potential to permit more step-economic syntheses of *para*-quinones, and a proof-of-principle application has been demonstrated through a gram-scale three-step total synthesis of (±)-indanostatin.

■ ASSOCIATED CONTENT

Supporting Information

The Supporting Information is available free of charge at https://pubs.acs.org/doi/10.1021/jacs.0c06306.

Crystal structure of **39** (CIF)

Experimental procedures and spectral data (PDF)

■ AUTHOR INFORMATION

Corresponding Author

Christopher G. Newton – *Department of Chemistry, The University of Adelaide, Adelaide, SA 5005, Australia;* orcid.org/0000-0002-8962-5917; Email: chris.newton@uga.edu

Authors

Isuru Dissanayake – *Department of Chemistry, The University of Adelaide, Adelaide, SA 5005, Australia*

Jacob D. Hart – *Department of Chemistry, The University of Adelaide, Adelaide, SA 5005, Australia*

Emma C. Becroft – *Department of Chemistry, The University of Adelaide, Adelaide, SA 5005, Australia*

Christopher J. Sumby – *Department of Chemistry, The University of Adelaide, Adelaide, SA 5005, Australia;* orcid.org/0000-0002-9713-9599

Complete contact information is available at: https://pubs.acs.org/10.1021/jacs.0c06306

Author Contributions

‡I.D. and J.D.H. contributed equally to this work.

Notes

The authors declare no competing financial interest.

■ ACKNOWLEDGMENTS

This work was supported by an Australian Research Council Discovery Early Career Award for C.G.N. (DE180100462). Financial support from the University of Adelaide is gratefully acknowledged. We thank Associate Professor David Huang (University of Adelaide) for assistance with rate calculations.

■ REFERENCES

(1) Minotti, G.; Menna, P.; Salvatorelli, E.; Cairo, G.; Gianni, L. Anthracyclines: Molecular Advances and Pharmacologic Develop-

ments in Antitumor Activity and Cardiotoxicity. *Pharmacol. Rev.* **2004**, *56*, 185.
(2) Select reviews: (a) Marcos, I. S.; Conde, A.; Moro, R. F.; Basabe, P.; Diez, D.; Urones, J. G. Quinone/Hydroquinone Sesquiterpenes. *Mini-Rev. Org. Chem.* **2010**, *7*, 230. (b) Sunassee, S. N.; Davies-Coleman, M. T. Cytotoxic and antioxidant marine prenylated quinones and hydroquinones. *Nat. Prod. Rep.* **2012**, *29*, 513.
(3) Representative examples: (a) Yan, Y.-M.; Zhang, H.-X.; Liu, H.; Wang, Y.; Wu, J.-B.; Li, Y.-P.; Cheng, Y.-X. (±)-Lucidumone, a COX-2 Inhibitory Caged Fungal Meroterpenoid from *Ganoderma Lucidum*. *Org. Lett.* **2019**, *21*, 8523. (b) Hayakawa, Y.; Kobayashi, T.; Izawa, M. Indanostatin, a New Neuroprotective Compound from *Streptomyces* sp. *J. Antibiot.* **2013**, *66*, 731. (c) Patil, A. D.; Freyer, A. J.; Killmer, L.; Offen, P.; Carte, B.; Jurewicz, A. J.; Johnson, R. K. Frondosins, Five New Sesquiterpene Hydroquinone Derivatives with Novel Skeletons from the Sponge *Dysidea Frondosa*: Inhibitors of Interleukin-8 Receptors. *Tetrahedron* **1997**, *53*, 5047.
(4) Karasu, F.; Arsu, N.; Jockusch, S.; Turro, N. J. Thioxanthone Hydroquinone-*O,O'*-diacetic Acid: Photoinitiator or Photostabilizer? *J. Org. Chem.* **2013**, *78*, 9161.
(5) (a) Billig, E.; Abatjoglou, A. G.; Bryant, D. R. Homogeneous Rhodium Carbonyl Compound-Phosphite Ligand Catalysts and Process for Olefin Hydroformylation. U.S. Patent 4,769,498, Sep. 6, 1988. (b) Sollewijn Gelpke, A. E.; Fraanje, J.; Goubitz, K.; Schenk, H.; Hiemstra, H. Resolution and Some Properties of (1,1')-Bi-(dibenzofuranyl)-2,2'-diol (BIFOL). *Tetrahedron* **1997**, *53*, 5899.
(6) Select reviews: (a) Akai, S.; Kita, Y. Recent Progress in the Synthesis of *p*-Quinones and *p*-Dihydroquinones Through Oxidation of Phenol Derivatives. A Review. *Org. Prep. Proced. Int.* **1998**, *30*, 603. (b) Weaver, M. G.; Pettus, T. R. R. Synthesis of *para*- and *ortho*-Quinones. In *Comprehensive Organic Synthesis II*, 2nd ed.; Knochel, P., Ed.; Elsevier: 2014; Vol. 7, p 373.
(7) (a) Behrman, E. J. The Persulfate Oxidation of Phenols and Arylamines (The Elbs and the Boyland−Sims Oxidations). *Organic Reactions* **1988**, 421. (b) Behrman, E. J. The Elbs and Boyland-Sims peroxydisulfate oxidations. *Beilstein J. Org. Chem.* **2006**, *2*, DOI: 10.1186/1860-5397-2-22.
(8) Representative examples: (a) Evans, J. C.; Klix, R. C.; Bach, R. D. Diels-Alder Approaches to Model Compounds Related to Fredericamycin A. *J. Org. Chem.* **1988**, *53*, 5519. (b) Lindsey, C. C.; Wu, K. L.; Pettus, T. R. R. Synthesis of Electron Deficient *5,6*-Aryloxy Spiroketals. *Org. Lett.* **2006**, *8*, 2365. (c) Wu, A.-H.; Hau, C.-K.; Wong, H. N. C. Synthesis of Enantiopure (*S,R,S*)- and (*R,S,R*)-1,4,5,8,9,16-Hexahydroxytetraphenylenes. *Adv. Synth. Catal.* **2007**, *349*, 601. (d) Gurung, S. K.; Kim, H. P.; Park, H. Inhibition of Prostaglandin E_2 Production by Synthetic Wogonin Analogs. *Arch. Pharmacal Res.* **2009**, *32*, 1503.
(9) Representative examples: (a) Gerencsér, J.; Keserü, G. M.; Macsári, I.; Nógrádi, M.; Kajtár-Peredy, M.; Szöllösy, Á. Synthesis of Isoplagiochin A. *J. Org. Chem.* **1997**, *62*, 3666. (b) Noda, Y.; Yasuda, M. Enantioselective Synthesis of (−)-(*R*)-Cordiachromene and (−)-(*R*)-Dictyochromenol Utilizing Intramolecular S_NAr Reaction. *Helv. Chim. Acta* **2012**, *95*, 1946. (c) Trost, B. M.; Hu, Y.; Horne, D. B. Total Synthesis of (+)-Frondosin A. Application of the Ru-Catalyzed [5 + 2] Cycloaddition. *J. Am. Chem. Soc.* **2007**, *129*, 11781.
(10) (a) Hauser, F. M.; Rhee, R. P. New Synthetic Methods for the Regioselective Annelation of Aromatic Rings: 1-Hydroxy-2,3-Disubstituted Naphthalenes and 1,4-Dihydroxy-2,3-Disubstituted Naphthalenes. *J. Org. Chem.* **1978**, *43*, 178. (b) Kraus, G. A.; Sugimoto, H. An annelation route to quionones. *Tetrahedron Lett.* **1978**, *19*, 2263. (c) Mal, D.; Pahari, P. Recent Advances in the Hauser Annulation. *Chem. Rev.* **2007**, *107*, 1892.
(11) (a) Karlsson, J. O.; Nguyen, V. N.; Foland, L. D.; Moore, H. W. (2-Alkynylethenyl)ketenes: A New Benzoquinone Synthesis. *J. Am. Chem. Soc.* **1985**, *107*, 3392. (b) Perri, S. T.; Foland, L. D.; Decker, O. H. W.; Moore, H. W. Synthesis of Benzoquinones and Annulated Derivatives from Conjugated Ketenes. *J. Org. Chem.* **1986**, *51*, 3067. (c) Moore, H. W.; Decker, O. H. W. Conjugated Ketenes: New Aspects of Their Synthesis and Selected Utility for the Synthesis of Phenols, Hydroquinones, and Quinones. *Chem. Rev.* **1986**, *86*, 821. (d) Nguyen, T. V. Convenient Access to Hydroquinone and Quinone Derivatives from Cyclobutenedione Units. *Aust. J. Chem.* **2010**, *63*, 1309.
(12) (a) Allen, A. D.; Ma, J.; McAllister, M. A.; Tidwell, T. T.; Zhao, D.-C. New Tricks from an Old Dog: Bisketenes after 90 Years. *Acc. Chem. Res.* **1995**, *28*, 265. (b) Tidwell, T. T. Ketene Chemistry after 100 Years: Ready for a New Century. *Eur. J. Org. Chem.* **2006**, *2006*, 563.
(13) (a) Hyatt, J. A.; Raynolds, P. W. Ketene Cycloadditions. In *Organic Reactions*; Paquette, L. A., Ed.; John Wiley and Sons, Inc.: New York, 1994; Vol. *45*, p 159. (b) Mackay, E. G.; Newton, C. G. Masked Ketenes as Dienophiles in the Diels−Alder Reaction. *Aust. J. Chem.* **2016**, *69*, 1365.
(14) Review on the DA chemistry of substituted furans: Bur, S.; Padwa, A. [4 + 2] Cycloaddition Chemistry of Substituted Furans. In *Methods and Applications of Cycloaddition Reactions in Organic Syntheses*; Nishiwaki, N., Ed.; John Wiley & Sons, Inc: 2014; p 355.
(15) Brownbridge, P.; Chan, T. H. Chemistry of 2,5-Bis-(trimethylsiloxy) Furans. I: Preparation and Diels-Alder Reactions. *Tetrahedron Lett.* **1980**, *21*, 3423.
(16) Chan reports that, in the presence of water, 2,5-bis(trimethylsilyloxy)furans hydrolyze to the corresponding succinic acid and, in the presence of oxygen, they form the corresponding bis(trimethylsilyl) maleate.
(17) Le Vézouët, R.; White, A. J. P.; Burrows, J. N.; Barrett, A. G. M. Synthetic studies on the CDEF ring system of lactonamycin. *Tetrahedron* **2006**, *62*, 12252.
(18) Simple derivatives of 2,5-bis(trimethylsilyloxy)furans have been applied in a handful of DA reactions. For a comprehensive list, see: (a) Troll, T.; Schmid, K. Darstellung und reaktionen von 1,3-bis-(trimethylsiloxy)-isobenzofuranen. *Tetrahedron Lett.* **1984**, *25*, 2981. (b) Seitz, G.; van Gemmern, R. [4 + 2] Cycloaddition of trimethylsilyloxy-substituted furans with tetrachlorocyclopropenes, a new preparation of cycloheptadienediones. *Chem. Ztg.* **1987**, *111*, 209. (c) Taguchi, T.; Hosoda, A.; Tomizawa, G.; Kawara, A.; Masuo, T.; Suda, Y.; Nakajima, M.; Kobayashi, Y. The Diels-Alder Reaction of 1-Phenylsulfonyl-3,3,3-trifluoropropene. *Chem. Pharm. Bull.* **1987**, *35*, 909. (d) Samoilova, R. I.; van Liemt, W.; Steggerda, W. F.; Lugtenburg, J.; Hoff, A. J.; Spoyalov, A. P.; Tyryshkin, A. M.; Gritzan, N. P.; Tsvetkov, Y. D. ENDOR and EPR Studies of Highly Isotopically ^{13}C-Enriched Ubiquinone Radicals. *J. Chem. Soc., Perkin Trans. 2* **1994**, *2*, 609. (e) Boullais, C.; Breton, J.; Nabedryk, E.; Mioskowski, C. Synthesis of Ubiquinones-3 Specifically Labelled with ^{13}C at C(5)- or C(6)- Positions. *Tetrahedron* **1997**, *53*, 2505. (f) Falcou, A.; Boullais, C. Synthesis of [2,3-$^{13}C_2$-2,5-cyclohexadienyl] Ubiquinone 3. *J. Labelled Compd. Radiopharm.* **1998**, *41*, 657. (g) van Liemt, W. B. S.; Steggerda, W. F.; Esmeijer, R.; Lugtenburg, J. Synthesis and Spectroscopic Characterisation of ^{13}C-Labelled Ubiquinone-0 and Ubiquinone-10. *Recl. Trav. Chim. Pays-Bas* **1994**, *113*, 153.
(19) For a comprehensive list of 2,5-bis(trimethylsilyloxy)furans being applied in non-DA settings, see: (a) Brownbridge, P.; Chan, T.-H. Chemistry of 2,5-Bis(trimethylsiloxy)furans. II: Reactions with Carbonyl Compounds and the Synthesis of 2,6-Diaryl-3,7-dioxabicyclo[3.3.0]octane-4,8-diones. *Tetrahedron Lett.* **1980**, *21*, 3427. (b) Brownbridge, P.; Chan, T.-H. Chemistry of 2,5-Bis(trimethylsiloxy)furans. III: Synthesis of γ-Hydroxybutenolides. *Tetrahedron Lett.* **1980**, *21*, 3431. (c) Frick, U.; Simchen, G. Reaktionen der Trialkylsilyl-trifluormethansulfonate, VIII. Synthese von *O*-(Trimethylsilyl)keten-*O,N*-acetalen, 2,5-Bis(trimethylsiloxy)-pyrrolen, -furanen, und -thiophenen. *Liebigs Ann.* **1987**, *1987*, 839. (d) Kates, M. J.; Schauble, J. H. Facile Conversion of Succinic to Maleic-Type Anhydrides, Thioanhydrides, and Imides. *J. Org. Chem.* **1995**, *60*, 6676. (e) Pohmakotr, M.; Yotapan, N.; Tuchinda, P.; Kuhakarn, C.; Reutrakul, V. Highly Diastereoselective Synthesis of β-Carboxy-γ-lactams and Their Ethyl Esters via Sc(OTf)$_3$-Catalyzed Imino Mukaiyama-Aldol Type Reaction of 2,5-Bis(trimethylsilyloxy)-furan with Imines. *J. Org. Chem.* **2007**, *72*, 5016. (f) Laws, S. W.;

https://dx.doi.org/10.1021/jacs.0c06306
J. Am. Chem. Soc. 2020, 142, 13328−13333

Howard, S. Y.; Mato, R.; Meng, S.; Fettinger, J. C.; Shaw, J. T. Organocatalytic Mukaiyama Mannich Reactions of 2,5-Bis-(trimethylsilyloxy)furan. *Org. Lett.* **2019**, *21*, 5073.
(20) Stability studies adapted from those originally disclosed by Sherburn and coworkers: Horvath, K. L.; Magann, N. L.; Sowden, M. J.; Gardiner, M. G.; Sherburn, M. S. Unlocking Acyclic π-Bond Rich Structure Space with Tetraethynylethylene−Tetravinylethylene Hybrids. *J. Am. Chem. Soc.* **2019**, *141*, 19746.
(21) Matsumoto, T.; Hosoya, T.; Katsuki, M.; Suzuki, K. New Efficient Protocol for Aryne Generation. Selective Synthesis of Differentially Protected 1,4,5-Naphthalenetriols. *Tetrahedron Lett.* **1991**, *32*, 6735.
(22) For a leading reference on the regioselectivity and orientational selectivity of arynes, see: Medina, J. M.; Mackey, J. L.; Garg, N. K.; Houk, K. N. The Role of Aryne Distortions, Steric Effects, and Charges in Regioselectivities of Aryne Reactions. *J. Am. Chem. Soc.* **2014**, *136*, 15798.
(23) Attempts to employ olefinic dienophiles have to date been unsuccessful.
(24) (a) Sun, H. H.; Sakemi, S.; Burres, N.; McCarthy, P. Isobatzellines A, B, C, and D. Cytotoxic and antifungal pyrroloquinoline alkaloids from the marine sponge *Batzella* sp. *J. Org. Chem.* **1990**, *55*, 4964. (b) Chang, L. C.; Otero-Quintero, S.; Hooper, J. N. A.; Bewley, C. A. Batzelline D and Isobatzelline E from the Indopacific Sponge *Zyzzya fuliginosa*. *J. Nat. Prod.* **2002**, *65*, 776.
(25) (a) Chuang, K. V.; Navarro, R.; Reisman, S. E. Benzoquinone-derived sulfinylimines as versatile intermediates for alkaloid synthesis: Total synthesis of (−)-3-demethoxyerythratidinone. *Chem. Sci.* **2011**, *2*, 1086. (b) Chuang, K. V.; Navarro, R.; Reisman, S. E. Short, Enantioselective Total Syntheses of (−)-8-Demethoxyrunanine and (−)-Cepharatines A, C, and D. *Angew. Chem., Int. Ed.* **2011**, *50*, 9447.
(26) Wang, J.-Z.; Zhou, J.; Xu, C.; Sun, H.; Kürti, L.; Xu, Q.-L. Symmetry in Cascade Chirality-Transfer Processes: A Catalytic Atroposelective Direct Arylation Approach to BINOL Derivatives. *J. Am. Chem. Soc.* **2016**, *138*, 5202.
(27) Bessems, J. G. M.; Vermeulen, N. P. E. Paracetamol (Acetaminophen)-Induced Toxicity: Molecular and Biochemical Mechanisms, Analogues and Protective Approaches. *Crit. Rev. Toxicol.* **2001**, *31*, 55.
(28) (a) Hopf, H.; Sherburn, M. S. Dendralenes Branch Out: Cross-Conjugated Oligoenes Allow the Rapid Generation of Molecular Complexity. *Angew. Chem., Int. Ed.* **2012**, *51*, 2298. (b) Newton, C. G.; Sherburn, M. S. Cross-Conjugation in Synthesis. In *Cross Conjugation: Modern Dendralene, Radialene and Fulvene Chemistry*; Hopf, H., Sherburn, M. S., Eds.; Wiley-VCH Verlag GmbH & Co. KGaA: Weinheim, 2016; p 413.
(29) (a) Mcnamara, J. M.; Kishi, Y. Practical asymmetric synthesis of aklavinone. *Tetrahedron* **1984**, *40*, 4685. (b) Eberbach, W.; Fritz, H.; Laber, N. A Simple Route to Furo[3,4-*b*]furans, Compounds with a New Diheteropentalene System. *Angew. Chem., Int. Ed. Engl.* **1988**, *27*, 568. (c) Fallon, T.; Willis, A. C.; Paddon-Row, M. N.; Sherburn, M. S. Furanodendralenes. *J. Org. Chem.* **2014**, *79*, 3185.
(30) Presumably the vinyl group of **45** prefers to adopt an unreactive *s-trans* conformation (as drawn), as a result of the bulky proximal *tert*-butyldimethylsilyl substituent.
(31) Wang, S.; Kraus, G. Annulations of 5-Phenylthiobutenolides and First Synthesis of (±)-Indanostatin. *Synlett* **2019**, *30*, 353.
(32) Teeters, W. O.; Shriner, R. L. A New Preparation of Ninhydrin. *J. Am. Chem. Soc.* **1933**, *55*, 3026.
(33) Corey, E. J.; Cheng, X.-M. *The Logic of Chemical Synthesis*; Wiley: 1995.

https://dx.doi.org/10.1021/jacs.0c06306
J. Am. Chem. Soc. 2020, 142, 13328−13333

3.4 Summary of personal contributions

This section constitutes a visual summary of personal contributions to the manuscript. Figures from the manuscript have been included in this section with minor changes.

Five select dienes were synthesised and tested for stability and reactivity to ascertain the optimal diene for further methodology development (Dienes **1-5** in figure 3.6A and B). Elucidation of mechanism in the Diels–Alder/aromatisation protocol was also undertaken (Figure 3.6C).

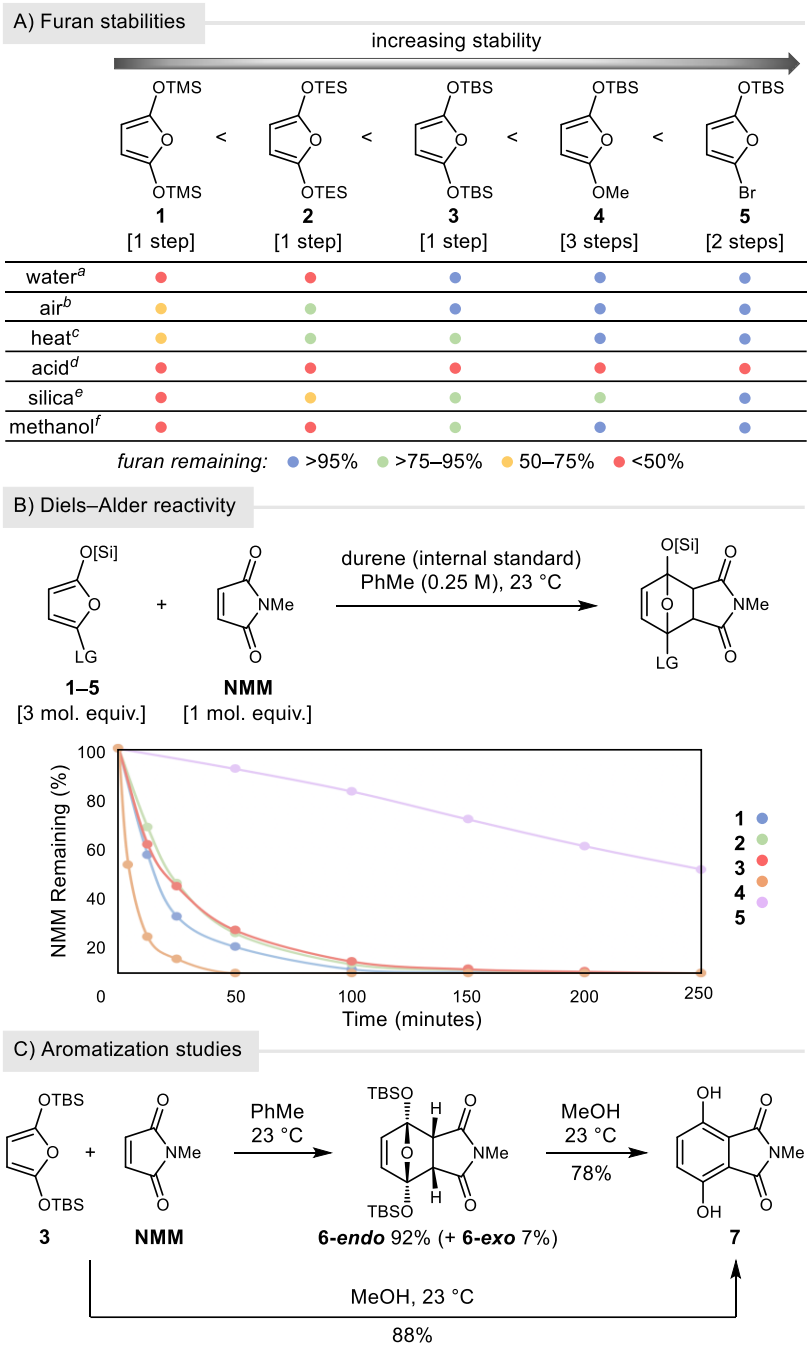

Figure 3.6: Furan stability, reactivity and mechanistic studies. ***Taken directly from manuscript.***

Major efforts to synthesise a diene scope and tests with a variety of dienophiles to furnish *para*-hydroquinones were lead personally (Compounds **7-23**, excluding **16** in figure 3.7). Some involvement occurred in synthesising *para*-benzoquinones (*p*-BQ) with benzynes, however were mainly completed by other authors.

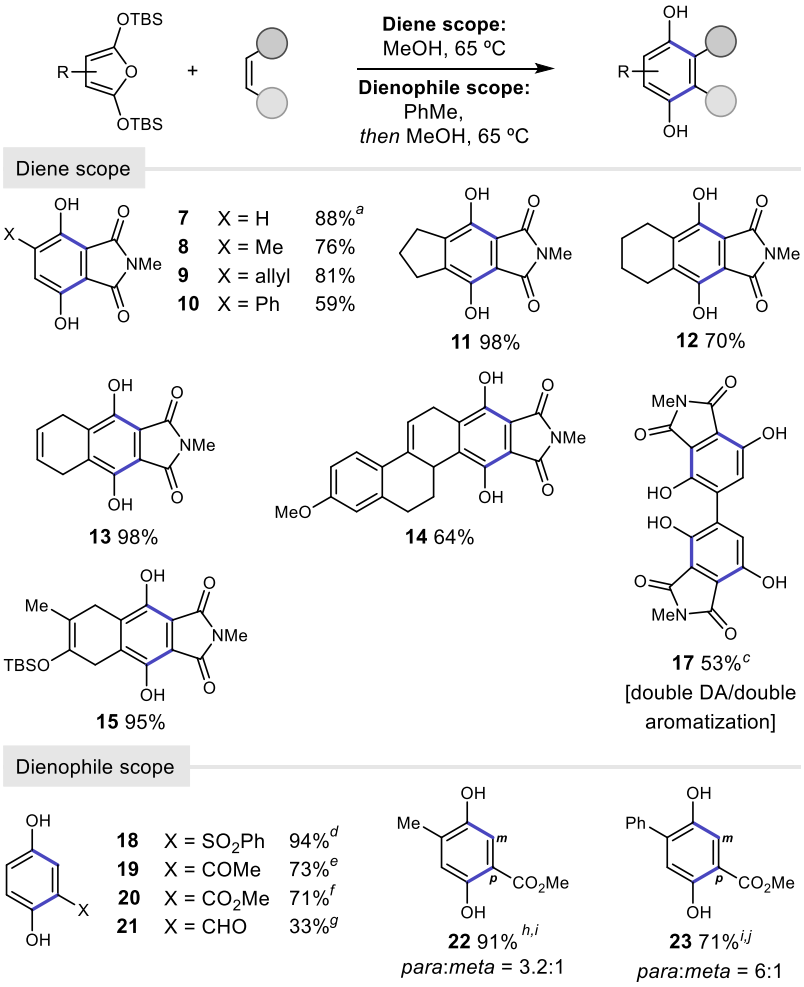

Figure 3.7: Scope of *p*-hydroquinone compound synthesis. *Taken directly from manuscript.*

The synthesis and reactions of the bifurcated reactive diene was done exclusively (Compounds **45**-**47** in figure 3.8A). Major contributions were conducted on the short total synthesis of (±)-indanostatin **51** (synthesised compounds **48**-**50** in figure 3.8B).

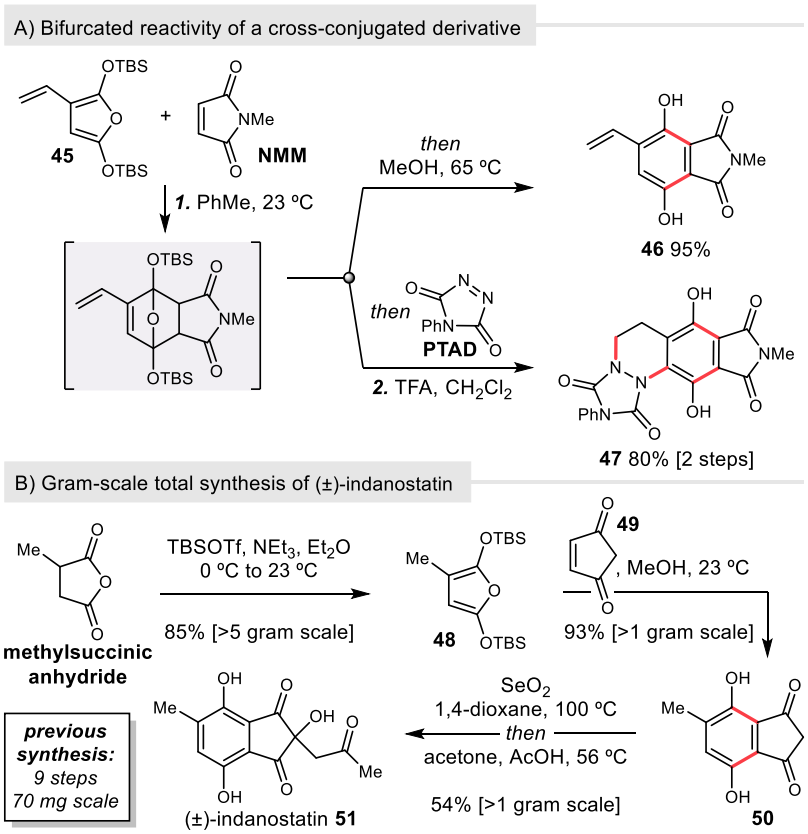

Figure 3.8: A) cross-conjugated diene derivative. B) Natural product synthesis of indanostatin. ***Taken directly from manuscript.***

3.5 Conclusion

In the development of a 1,3-butadiene-1,4-dione **3.11** synthetic equivalent, 2,5-Bis(*tert*-butyldimethylsilyloxy)furans **3.16** were established as suitable masked vicinal bisketenes for application as dienes in the Diels–Alder reaction (Figure 3.9A). A variety of highly substituted *p*-HQs **3.14** are readily accessible via a mild, user-friendly protocol. Venturing beyond our original scope, efficient access to *p*-BQs **3.17**, or *para*-iminoquinones (*p*-IQs) **3.18** when 2,5-bis(*tert*-butyldimethylsilyloxy) pyrroles **3.19** are utilized as dienes, were achieved with the use of acetylenic dienophiles instead of olefinic dienophiles (Figure 3.9B). Demonstrated utility and generality of our developed methodology has been shown through the syntheses of quinones relevant to pharmaceutical, natural product, catalysis and material fields, particularly through a proof-of-principle application of a gram-scale, three-step total synthesis of (±)-indanostatin **51**.

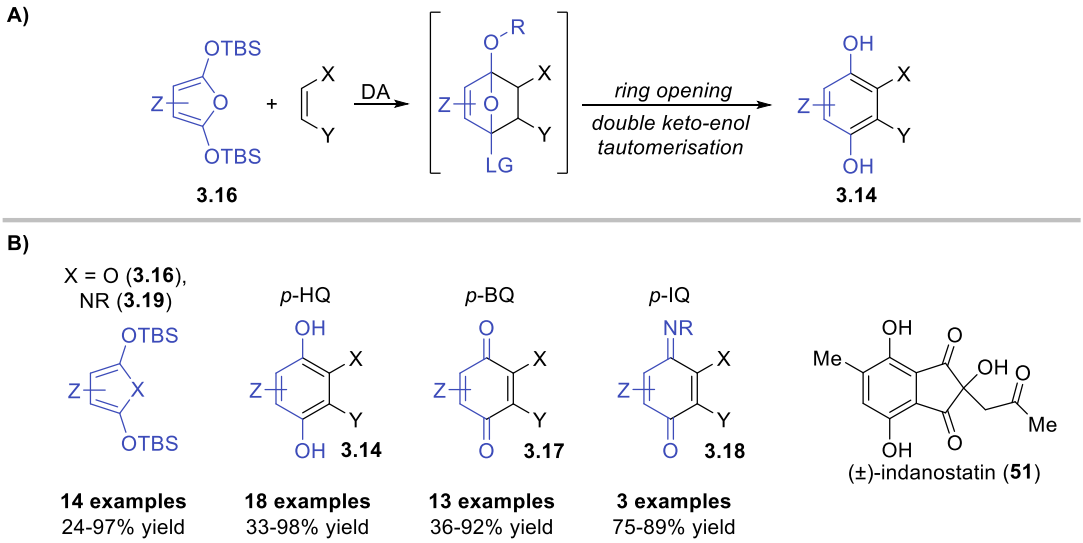

Figure 3.9: A) 2,5-Bis(*tert*-butyldimethylsilyloxy)furans (and derivatives) as suitable synthetic equivalents of 1,3-butadiene-1,4-dione. B) Overall scope of the developed methodology

3.6 Future directions

This project is considered a concluded story, however there were proposals to apply this methodology in complex total syntheses. Chromazonarol **3.20** and lingzhiol **3.21** were both viable targets, where we envisioned constructing the *para*-hydroquinone motif at a late stage of their respective syntheses (Scheme 3.3). Synthesis of intermediates **3.22** and **3.23** is a challenging task, but are manageable in a future standalone project.

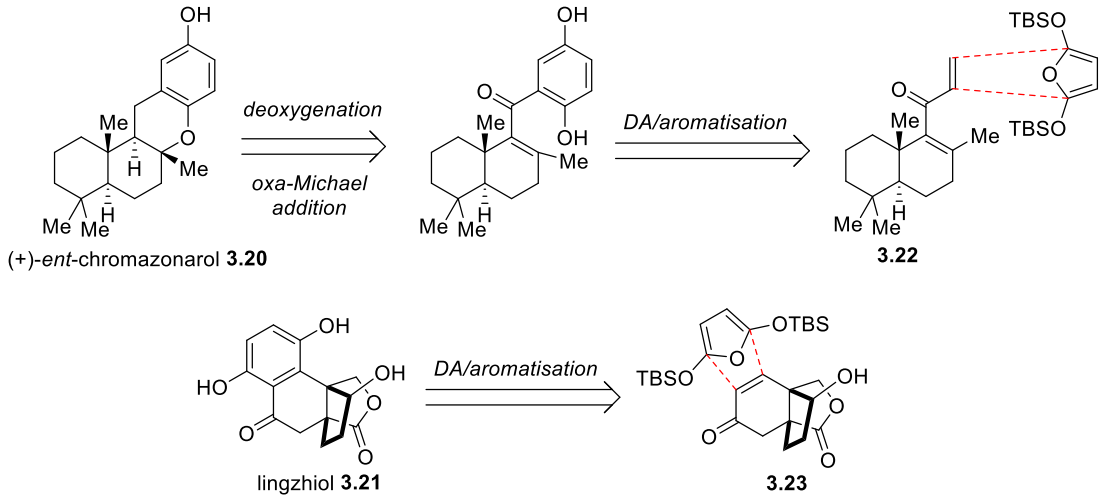

Scheme 3.3: Proposed retrosynthesis of chromazonarol and lingzhiol utilising our developed DA methodology

3.7 References

[1] D. Chen, H.-M. Liu, M.-M. Li, Y.-M. Yan, W.-D. Xu, X.-N. Li, Y.-X. Cheng, H.-B. Qin, *Chem. Commun.* **2015**, *51*, 14594–14596.

[2] Y.-M. Yan, J. Ai, L. Zhou, A. C. K. Chung, R. Li, J. Nie, P. Fang, X.-L. Wang, J. Luo, Q. Hu, F.-F. Hou, Y.-X. Cheng, *Org. Lett.* **2013**, *15*, 5488–5491.

[3] Y.-C. Shen, C.-H. Lu, R. Chakraborty, Y.-H. Kuo, *Nat Prod Res* **2003**, *17*, 83–89.

[4] J. An, D. F. Wiemer, *J. Org. Chem.* **1996**, *61*, 8775–8779.

[5] T. Ling, A. X. Xiang, E. A. Theodorakis, *Angew. Chem. Int. Ed.* **1999**, *38*, 3089–3091.

[6] J. Sakurai, T. Oguchi, K. Watanabe, H. Abe, S. Kanno, M. Ishikawa, T. Katoh, *Chemistry - A European Journal* **2008**, *14*, 829–837.

[7] A. E. Sollewijn Gelpke, J. Fraanje, K. Goubitz, H. Schenk, H. Hiemstra, *Tetrahedron* **1997**, *53*, 5899–5908.

[8] S. Akai, Y. Kita, *Org Prep Proced Int* **1998**, *30*, 603–629.

[9] E. J. Behrman, in *Organic Reactions*, John Wiley & Sons, Inc., Hoboken, NJ, USA, **1988**, pp. 421–511.

[10] E. J. Behrman, *Beilstein J. Org. Chem.* **2006**, *2*, DOI 10.1186/1860-5397-2-22.

[11] J. Gerencsér, G. M. Keserü, I. Macsári, M. Nógrádi, M. Kajtár-Peredy, Á. Szöllösy, *J. Org. Chem.* **1997**, *62*, 3666–3670.

[12] Y. Noda, M. Yasuda, *Helv. Chim. Acta.* **2012**, *95*, 1946–1952.

[13] B. M. Trost, Y. Hu, D. B. Horne, *J. Am. Chem. Soc.* **2007**, *129*, 11781–11790.

[14] F. M. Hauser, R. P. Rhee, *J. Org. Chem.* **1978**, *43*, 178–180.

[15] D. Mal, P. Pahari, *Chem. Rev.* **2007**, *107*, 1892–1918.

[16] G. A. Kraus, H. Sugimoto, *Tetrahedron Lett.* **1978**, *19*, 2263–2266.

[17] J. O. Karlsson, Nghi V. Nguyen, L. D. Foland, H. W. Moore, *J. Am. Chem. Soc.* **1985**, *107*, 3392–3393.

[18] S. T. Perri, L. D. Foland, O. H. W. Decker, H. W. Moore, *J. Org. Chem.* **1986**, *51*, 3067–3068.

[19] H. W. Moore, O. H. W. Decker, *Chem. Rev.* **1986**, *86*, 821–830.

[20] T. v. Nguyen, *Aust. J. Chem.* **2010**, *63*, 1309.

[21] A. D. Allen, J. Ma, M. A. McAllister, T. T. Tidwell, D. Zhao, *Acc. Chem. Res.* **1995**, *28*, 265–271.

[22] T. T. Tidwell, *European J. Org. Chem.* **2006**, *2006*, 563–576.

[23] J. A. Hyatt, P. W. Raynolds, in *Organic Reactions*, John Wiley & Sons, Inc., Hoboken, NJ, USA, **1994**, pp. 159–646.
[24] E. G. Mackay, C. G. Newton, *Aust. J. Chem.* **2016**, *69*, 1365.
[25] S. Bur, A. Padwa, in *Methods and Applications of Cycloaddition Reactions in Org. Synth.*, John Wiley & Sons, Inc., Hoboken, New Jersey, **2014**, pp. 355–406.
[26] P. Brownbridge, T.-H. Chan, *Tetrahedron Lett.* **1980**, *21*, 3423–3426.
[27] R. le Vézouët, A. J. P. White, J. N. Burrows, A. G. M. Barrett, *Tetrahedron* **2006**, *62*, 12252–12263.
[28] T. Taguchi, A. Hosoda, G. Tomizawa, A. Kawara, T. Masuo, Y. Suda, M. Nakajima, Y. Kobayashi, *Chem Pharm Bull (Tokyo)* **1987**, *35*, 909–912.
[29] R. I. Samoilova, W. van Liemt, W. F. Steggerda, J. Lugtenburg, A. J. Hoff, A. P. Spoyalov, A. M. Tyryshkin, N. P. Gritzan, Y. D. Tsvetkov, *Journal of the Chemical Society, Perkin Transactions 2* **1994**, 609.
[30] T. Troll, K. Schmid, *Tetrahedron Lett.* **1984**, *25*, 2981–2984.
[31] C. Boullais, J. Breton, E. Nabedryk, C. Mioskowski, *Tetrahedron* **1997**, *53*, 2505–2512.
[32] A. Falcou, C. Boullais, *J Labelled Comp Radiopharm* **1998**, *41*, 657–668.
[33] W. B. S. van Liemt, W. F. Steggerda, R. Esmeijer, J. Lugtenburg, *Recl. Trav. Chim. Pays-Bas* **1994**, *113*, 153–161.
[34] I. Dissanayake, J. D. Hart, E. C. Becroft, C. J. Sumby, C. G. Newton, *J. Am. Chem. Soc.* **2020**, *142*, 13328–13333.

Chapter 4

Annulenes as Starting Materials in the Total Synthesis of Natural Products

4.1 Opening remarks

This review summarises all past total syntheses that have used unsubstituted annulenes as a starting material or intermediate. Its aim is to highlight the unique strategies displayed to apply these molecules and their viability for future total synthesis targets.

4.2 Introduction

Annulenes are cyclic hydrocarbons containing the maximum amount of unsaturation. According to IUPAC naming conventions they are named as [*n*]annulene, where *n* is the number of carbons in the ring, however the first three are well-known as cyclobutadiene **4.1**, benzene **4.2** and cyclooctatetraene **4.3** (COT).[1,2] Annulenes have varying aromaticity, with **4.1**, **4.2** and **4.3** being anti-aromatic, aromatic and non-aromatic, respectively. This contributes to their unique reactivity and therefore influences their synthetic utility. Each annulene will have their own respective sections underlining their use in the total synthesis of natural products. *[10]*Annulene and above will not be mentioned since they are not involved in any reported syntheses that we are aware of.

Table 4.1: Annulenes of relevance to this review.

***[4]*annulene**	***[6]*annulene**	***[8]*annulene**
cyclobutadiene	benzene	cyclooctatetraene
 **4.1**	 **4.2**	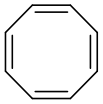 **4.3**
Anti-aromatic	aromatic	Non-aromatic

4.3 [*4*]Annulene

4.3.1 Structural and Chemical Characteristics of [*4*]annulene

Cyclobutadiene **4.1**, is the smallest of the annulenes, possessing a rectangular structure. Its 4π electrons are localised, making it anti-aromatic.[3,4] This incurs a heavy electronic penalty resulting in high reactivity and low stability, it however has been observed in a matrix at temperatures below 35 K.[5,6] One degradation pathway occurs via a Diels−Alder dimerization followed by electrocyclic ring-opening to afford **4.3** (Figure 4.1). This can be suppressed by inclusion in a host-guest complex or by complexation with iron tricarbonyl.[7–11] Cyclobutadieneiron tricarbonyl **4.4** was first synthesised by Pettit in 1965, from **4.3**.[9] Rosenblum and Gatsonis, two years later, reported a one-pot procedure from α-pyrone **4.5**.[10] Interestingly, the complex possesses some aromatic characteristics, undergoing Friedel-Crafts acylation and other substitution reactions through a mechanism that is identical to electrophilic aromatic substitutions.[12,13] Treatment with ceric ammonium nitrate releases **4.1**, which can then undergo cycloadditions. This compound offers an in-situ generation of cyclobutadiene bypassing its instability, making it available for synthetic utility. This protected form of cyclobutadiene has been used in several total synthesis campaigns.

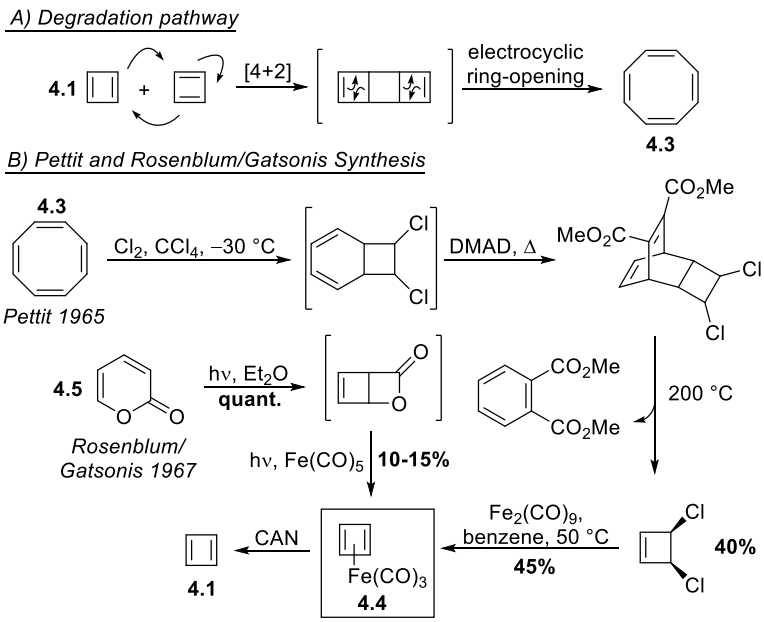

Figure 4.1: A) One degradation pathway of cyclobutadiene. B) Two viable syntheses of stabilised cyclobutadiene.

4.3.2 Asteriscanolide

Snapper has accomplished an impressive synthesis of asteriscanolide **4.6** using an ester cyclobutadieneiron tricarbonyl complex **4.7** (Scheme 4.1).[14] Asteriscanolide is a formidable target for total synthesis due to its unique 5/8/5 tricyclic structure containing three contiguous *syn* stereocentres. Photolysis of pyrone **4.8** is followed by heating in the presence of $Fe_2(CO)_9$ to form complex **4.7** in 64% yield. Subjection of complex **4.7** to lithium aluminium hydride with a Lewis acid resulted in full reduction of the ester to methyl **4.8** in 93% yield. *Para*-selective electrophilic aminomethylation proceeded in 50% yield. Installation of enantiopure cyclopentenol **4.10** in 50% yield sets the stage for the key transformations. Release of the cyclobutadiene **4.11** from iron tricarbonyl via heating with trimethylamine N-oxide lead to rapid [4+2] cycloaddition, forming cycloadduct **4.12** in 63% yield. Ring-opening metathesis, furnishing dialkenyl cyclobutane intermediate **4.14**, was followed by Cope rearrangement to form compound **4.15** in 74% yield. Over the course of two sequences, the tricyclic structure as well as two of the four stereocentres has been constructed. Other syntheses of this natural product required lengthier successive steps to build the rings or to install the final functionalities.[15–18] Snapper utilised complex **4.7** as the base from which fast addition of essential structures transpired. This culminated in the cyclobutadiene of **4.11** participating in a cycloaddition/ring-opening/ring-closing sequence over two steps, affording the majority of the structural challenges of **4.6**. It must also be noted where the cyclobutadiene ends up in the final product. The cyclobutadiene is conceptually cleaved in half with a two-carbon insertion in-between the alkenes on both sides to form the 1,4-cyclooctadiene in compound **4.15**. Installation of the remaining functionality over the course of three steps finally gave (+)-asteriscanolide **4.6** in 42% over three steps. Employing the antipode of compound **4.10** would prepare (−)-asteriscanolide.

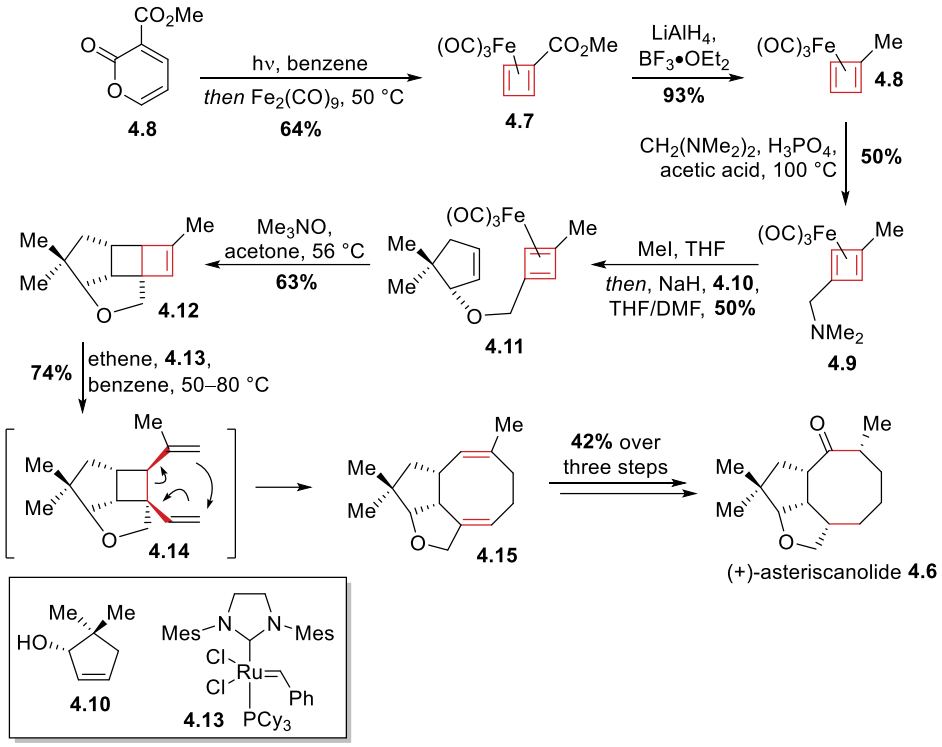

Scheme 4.1: Snapper's 2000 total synthesis of (+)-asteriscanolide

4.3.3 Pleocarpenene and Pleocarpenone

Ester cyclobutadieneiron tricarbonyl **4.7** was used again by Snapper in his 2006 total synthesis of pleocarpenene **4.16** and pleocarpenone **4.17** (Scheme 4.2).[19] Snapper adopted a similar strategy to his asteriscanolide synthesis, however instead of constructing an eight-membered ring, a seven-membered ring is his focus. Complex **4.7** was converted to alcohol **4.18** in 76% over three steps. Oxidation to **4.19** was followed by asymmetric reduction with (S)-B-Me-CBS-catalyst afforded enantioenriched alcohol **4.20** (96% yield and 92% e.e.). Olefin metathesis with methyl acrylate on the terminal alkene gave compound **4.21** in 94% yield. CAN oxidation to unmask the cyclobutadiene was then followed by [4+2] cycloaddition to give a separable diastereomeric mixture of compounds **α-4.22** and **β-4.22**. The antipode of the CBS catalyst from earlier would give the enantiomers of this mixture of diastereomers. Carrying on with **β-4.22**, conversion to bishydroxyl protected compound **4.23** proceeded in 87-89% over two steps. Cyclopropanation with ethyl diazoacetate catalysed by $Cu(acac)_2$ afforded compound **4.24** in 93-95% yield. Swern oxidation and then addition with methyl magnesium bromide provided compound **4.25** in 79-82% yield. Thermal ring expansion/opening to yield bicyclo[5.3.0]decane **4.26** followed in 76% yield.[20] Complex **4.7**, again, served as a great base to add functionality, eventually leading to **4.21**, setting the scene for the main transformation. The purpose of the key subsequent cycloaddition/cyclopropanation/thermal rearrangement strategy was to furnish a seven-membered ring with most of the prerequisite functionalities that map onto the natural products (e.g., stereochemistry and functional groups). The constituents of the cyclobutadiene ring have been split, becoming a part of the seven-membered ring. This highlights that by varying the number of carbons of the partner in the cycloaddition for cyclobutadiene, one could hypothetically construct any ring size above four-carbons. Pleocarpenene **4.16** was synthesised from compound **4.26** over four steps in 51% yield. Conversion to pleocarpenone **4.17** occurred through ozonolysis and epimerisation in 85% yield.

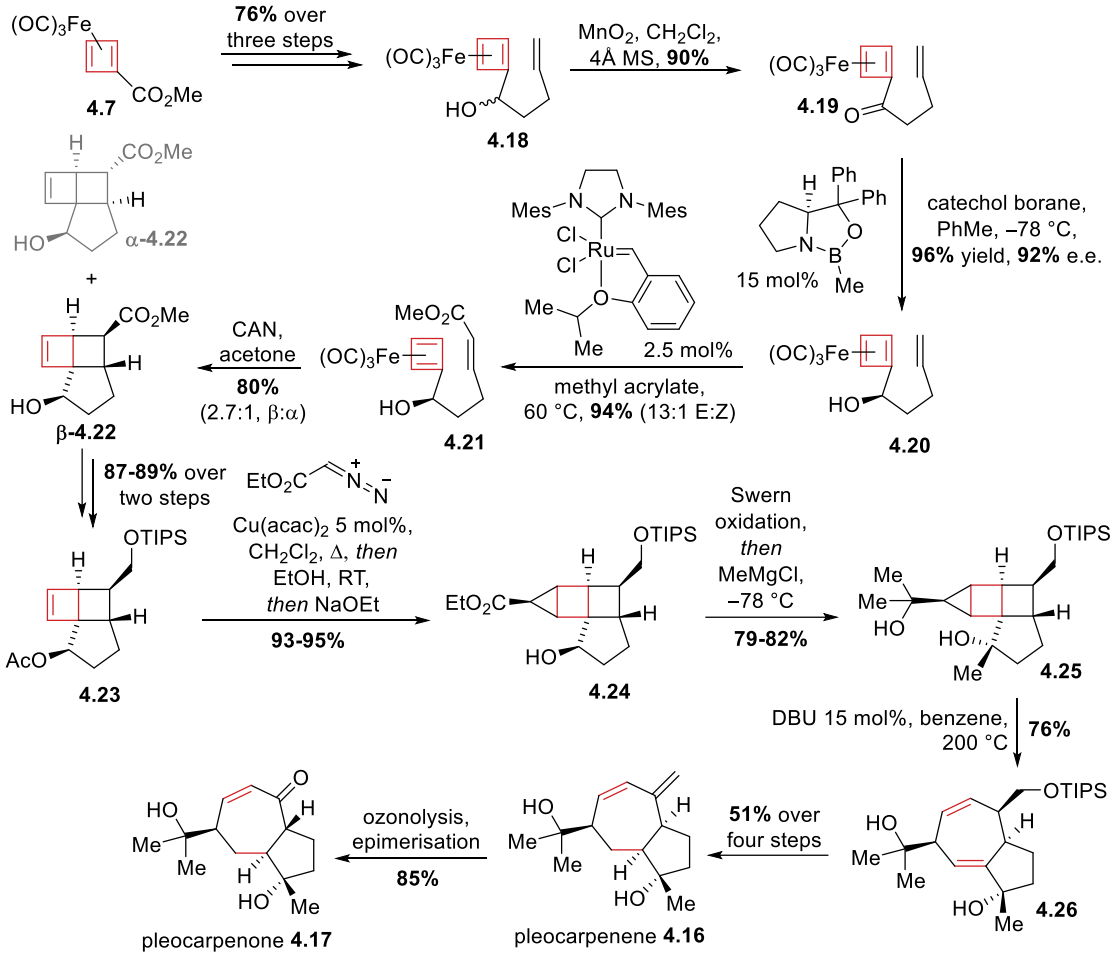

Scheme 4.2: Snapper's 2006 total synthesis of Pleocarpenene and Pleocarpenone

4.3.4 Ladderanes

Ladderanes are molecules containing multiple fused cyclobutane rings. It is a motif that is also present in natural products (Figure 4.2).

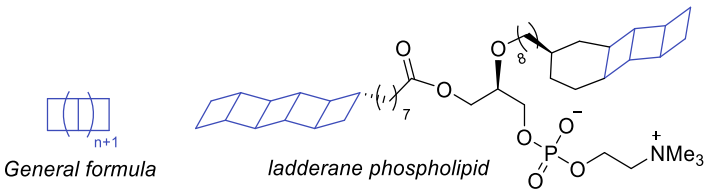

Figure 4.2: Example of ladderanes

Previous syntheses of ladderane containing natural products involved strategies where bonds are formed internally within larger ring structures to form multiple four-membered rings. In Corey's 1994 synthesis of pentacycloanammoxic ester **4.27** (will also be discussed more later in the chapter), several manipulations of COT amounted to what could be considered an informal double 4π electrocyclisation of COT to afford the [3]-ladderane **4.28**.[21] Burns effected a sulfoxide Ramberg–Bäcklund olefination of α-chlorosulfoxide **4.29** to yield bicyclohexane **4.30**, which was then dimerised to compound **4.31** eventually delivering **4.32**.[22] Compound **4.30** was employed again in the [2+2] cycloaddition with **4.33** to give **4.34.** With the core constructed, further transformations presented **4.35**. These past two syntheses highlighted the preference for a top-down approach versus the opposite strategy.

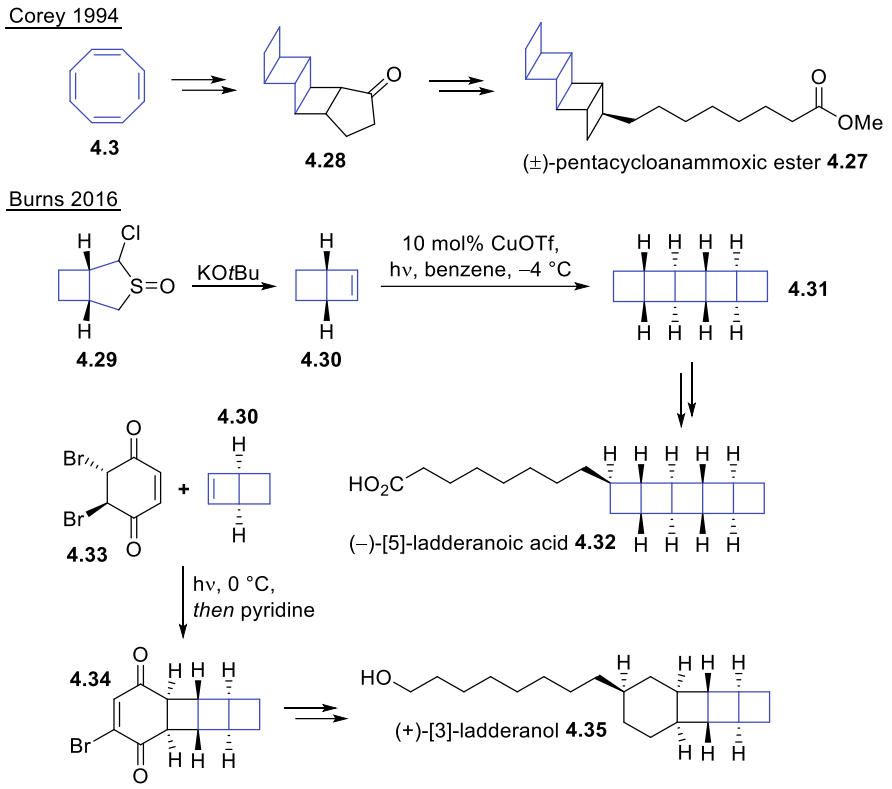

Figure 4.3: Previous total syntheses of ladderane natural products

Cyclobutadiene is an obvious building block for ladderane natural product total synthesis, however it has not been used in this capacity. Work by Mehta and Warrener (shown below) showcase its viability for constructing ladderanes and serves as inspiration for potential future ladderane natural product targets. Mehta in 1994, accomplished the first synthesis and characterisation of [9], [11] and [13]-ladderanes through the oligomerisation of 1,2-dicarbomethoxycyclobutadiene **4.36** (Scheme 4.3).[23] The reaction was a complicated mixture of five different lengths of ladderanes.

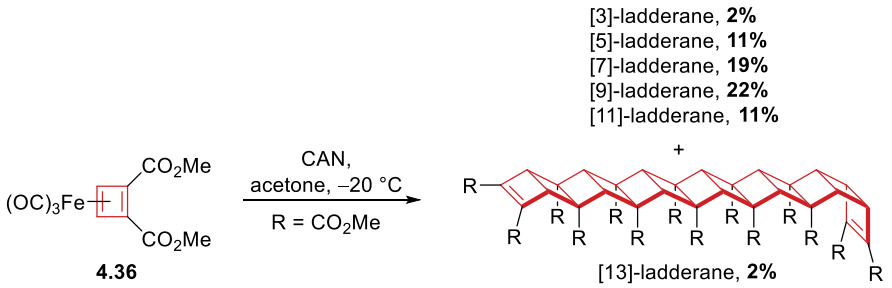

Scheme 4.3: Synthesis of [3], [5], [7], [9], [11] and [13]-ladderane

In the same year, Warrener performed a serial protocol of cyclobutadiene and DMAD **4.37** ruthenium-catalysed cycloadditions to form complex ladderanes (Scheme 4.4).[24] From starting material **4.39**, iterative cycloadditions over 5 steps eventually provide **4.42**.

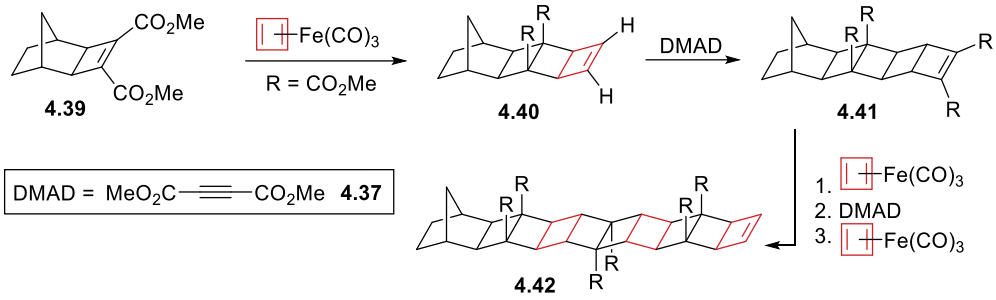

Scheme 4.4: Warrener's synthesis of complex ladderanes

4.4 [*6*]Annulene

4.4.1 Structural and Chemical Characteristics of [*6*]annulene

Out of all the annulenes, benzene is arguably the most distinguished. Currently well-established as a stable six-carbon ring containing conjugated π bonds (Figure 4.4), it had a long history of structurally elucidation[25–30] starting from its isolation[31–35] in the early 1800s to its confirmation in 1929 by Kathleen Lonsdale.[36,37] It is a planar ring with delocalised π orbitals which contribute to its aromaticity and reactivity.[38–42] It typically undergoes electrophilic aromatic substitutions and requires forcing conditions for hydrogenations and cycloadditions.[43,44] Benzene is a readily available feedstock to a variety of commodity chemicals with downstream applications in pharmaceuticals, agrochemicals and materials. However, unfunctionalised benzene itself has seen limited use in total syntheses of natural products.

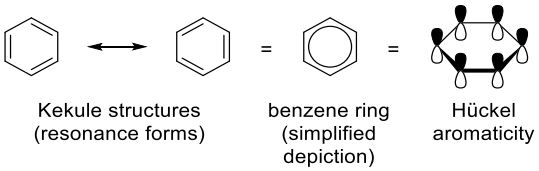

Figure 4.4: Structures of benzene

4.4.2 Pinitol

Motherwell's concise synthesis of pinitol **4.43** started from the temperature-controlled poly-dihydroxylation of benzene to favour the neo diastereomer formation.[45] Subsequent protection of the diols gave a mixture of **4.44**, **4.45** with the desired product **4.46** in 8% yield. Base-promoted ring closure formed epoxide **4.47** in 83% yield. Regiospecific ring-opening was followed by acidic workup to in situ deprotect delivering racemic pinitol **4.43** in 60% over two steps. Despite being a relatively small molecule, its synthetic challenge arises from its two *syn* and one *anti* diol relationship. The use of benzene may be convenient as it provides the core six-membered ring, however a major limitation are the poor yields of the regioselective dihydroxylations. It may be more effective to start from an aromatic starting material with an already higher oxidation state.

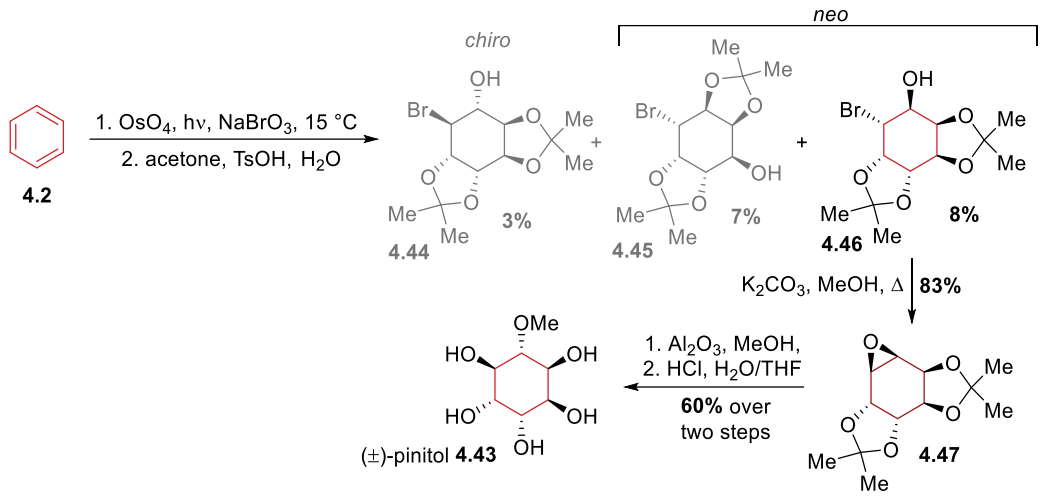

Scheme 4.5: Motherwell's 1997 total synthesis of (±)-pinitol

4.4.3 Sarlah's dearomative methodologies

4.4.3.1 Pancratistatin, lycoricidine and narciclasine

Sarlah has developed dearomative methodologies of benzene to access a variety of natural products. An enantioselective, dearomative 1,2-*trans*-carbonamination of benzene methodology was established and utilised in the total synthesis of pancratistatin **4.48**.[46] The mechanism of this strategy begins with the light-promoted *para*-cycloaddition between benzene **4.2** and MTAD **4.49** to give cycloadduct **4.50**. π-Complexation of the diene in **4.50** to the metal complex *anti* to the arenophile moiety forming **4.51**, is followed by subsequent oxidative addition to intermediate **4.52**. Transmetalation with an aryl metal reagent (ArM, refer to Scheme 4.6) furnished intermediate **4.53**, is followed by reductive elimination to afford complex **4.54**. Final π-decomplexation bears the product **4.55** and regenerates the transition metal catalyst.

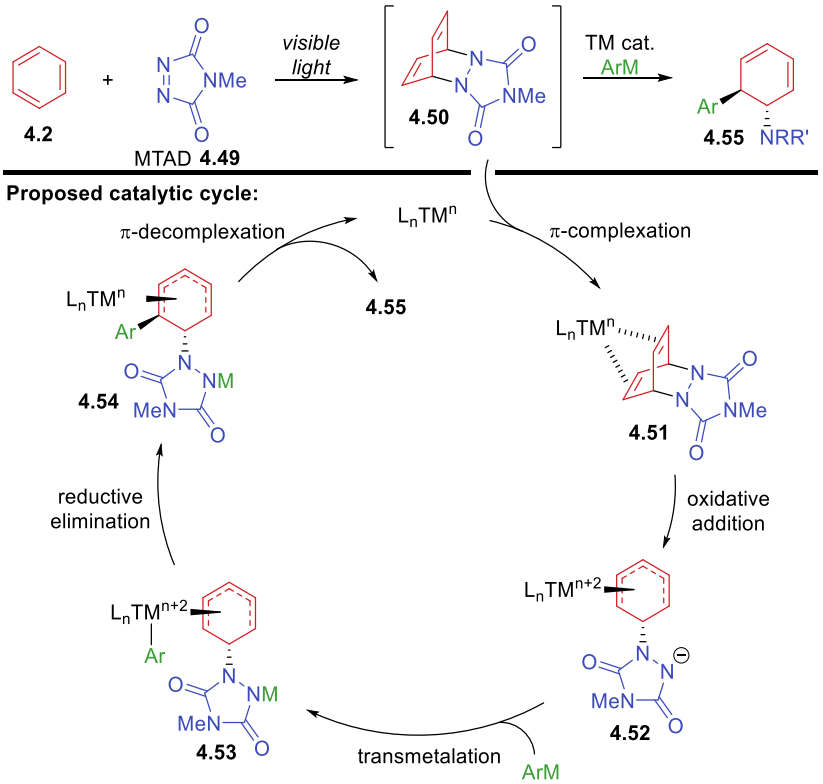

Scheme 4.6: General mechanism of enantioselective, dearomative carboamination of benzene

This reaction was performed in the first step in the total synthesis pancratistatin to deliver product **4.56** in 65% yield. *trans*-Dihydroxylation of the furthest olefin from the urazole nitrogen occurred in 74% yield, **4.57**. An Upjohn dihydroxylation of the remaining olefin afforded the *cis*-diol **4.58** in 91% yield. $LiAlH_4$ reduction of the urazole and immediate addition of Raney-cobalt under hydrogen atmosphere generates free amine compound **4.59** in 60% yield. Bromination, followed by carbonylation and amide cyclisation gave the corresponding 7-deoxypancratistatin **4.60** in 72% over two steps. Conversion to pancratistatin **4.48** was affected by the initial persilylation of all hydroxyls with HMDS, followed by cupration and oxidation with *t*BuOOH in 62% yield. The challenge of this natural product is constructing the *trans*, *cis*, *trans* stereochemical relationship on the cyclohexane ring. What Sarlah identified, is that its creation would be possible through an overall triple olefin-like difunctionalisation of benzene. This philosophy has been extrapolated to other total syntheses.

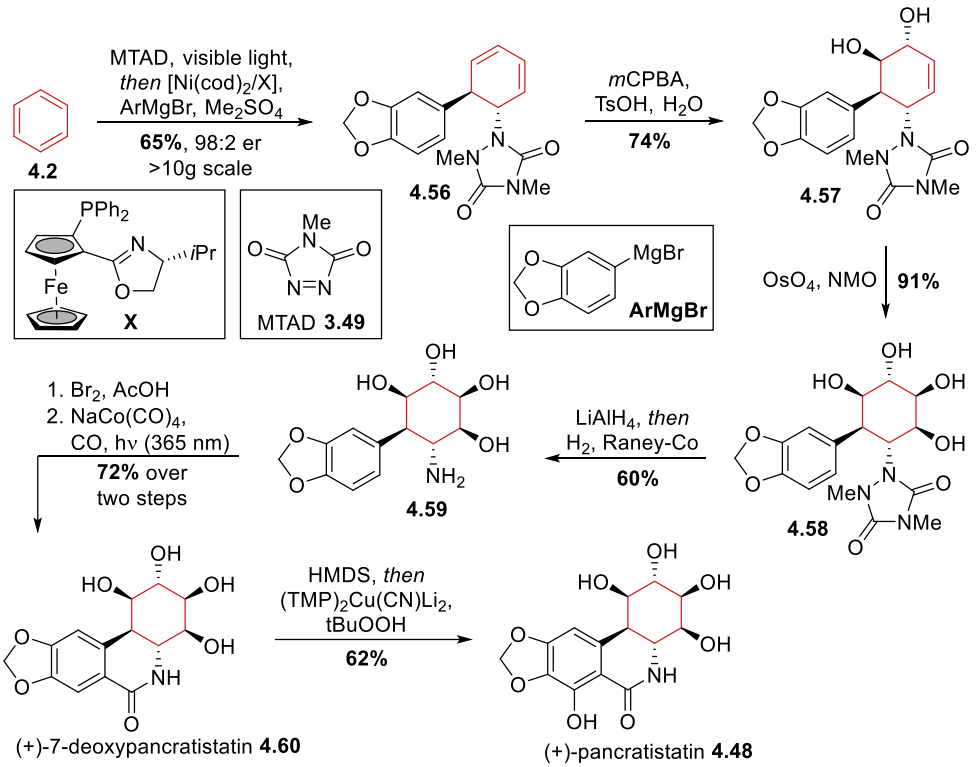

Scheme 4.7: Sarlah's 2017 total synthesis of (+)-pancratistatin

Sarlah employed the same dearomative strategy in his scalable route to lycoricidine **4.61** and narciclasine **4.62**.[47] These two natural products possess a similar structure to pancratistatins (**4.60** and **4.48**), but differ with its aminocyclitol core containing four contiguous stereocentres instead of six. Only an overall double olefin-like difunctionalisation of benzene strategy would be necessary. From compound **4.56** formation of the bromohydrin and parallel aryl bromination through two equivalences of NBS in THF/H_2O afforded compound **4.63** in 74% yield. Upjohn dihydroxylation and subsequent diol protection delivered compound **4.64** in 78% over two steps. Lithium-halogen exchange via *tert*-butyllithium and then nucleophilic acyl substitution gave the lactam **4.65** in 65% yield. Treatment with samarium iodide furnished lycoricidine **4.61** in 94% yield. The cupration/oxidation conditions stated earlier was repeated to form narciclasine **4.62** in 57% yield.

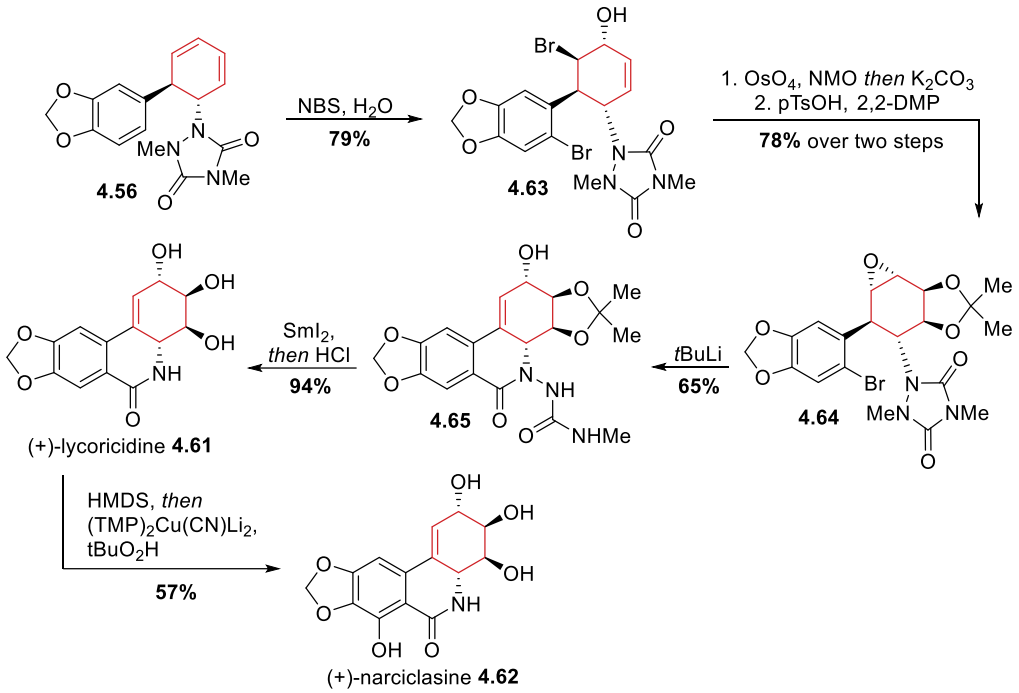

Scheme 4.8: Sarlah's 2019 total synthesis (+)-lycoricidine and (+)-narciclasine

4.4.3.2 Ribostamycin

Recently, Sarlah devised a copper-catalysed 1,2-hydroamination of benzene, which was applied to the total synthesis of ribostamycin **4.66**.[48] The proposed mechanism starts the same as the previous dearomative strategy with a light-promoted *para*-cycloaddition between benzene **4.2** and MTAD **4.49** to give cycloadduct **4.50**. π-complexation to cycloadduct **4.50** with a ligated copper(I) hydride species (L_nCu-H, Scheme 4.9) gives intermediate **4.67**. In the hydrocupration pathway, **4.67** undergoes hydrometallation *anti* to the arenophile moiety to intermediate **4.68**. β-elimination of bridgehead arenophile moiety delivers diene **4.69**. In the alternative allylic substitution pathway, complex **4.67** could undergo oxidative addition, forming species **4.70**, followed by reductive elimination to afford diene **4.69**. For both pathways, additional equivalent of silane regenerates the copper hydride species and releases the desired product **4.71**.

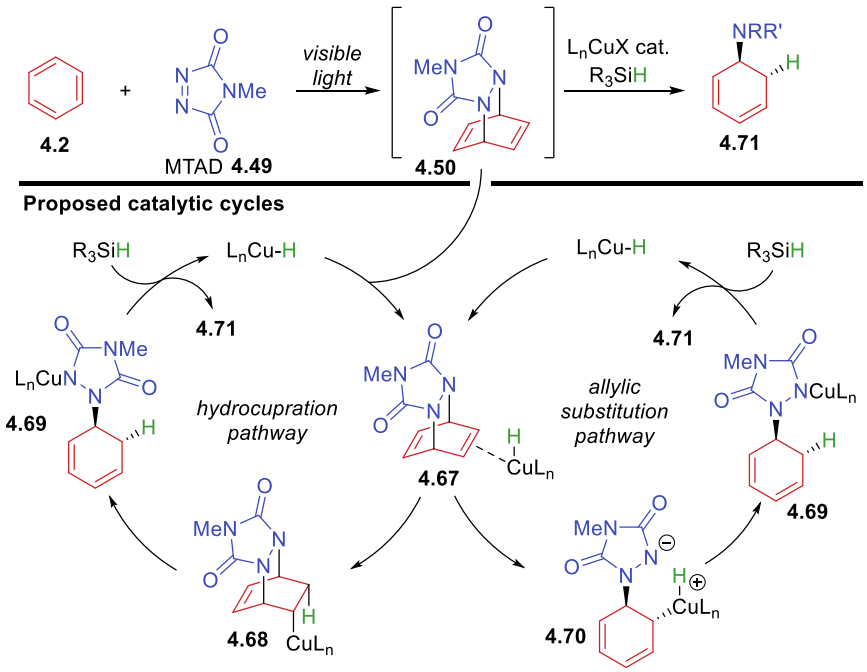

Scheme 4.9: General mechanism of enantioselective, dearomative hydroamination of benzene

Sensitive diene **4.71** was immediately Boc-protected and epoxidized by *m*CPBA in a 45% yield to give **4.72**. Base Boc-deprotection was followed by a *5-exo-tet* cyclisation yielding a secondary allylic alcohol that was proximately benzyl-protected to give urazole bridgehead **4.73** in 54% yield. Over three steps, installation of the semi-protected trans-1,2-diol and ribose moiety (R_1, Scheme 4.10) with β-selectivity occurred in 32% yield to deliver **4.74**. Chemoselective removal of the oxime, α-selective installation of the thioglycoside donor (R_2, Scheme 4.10) and the one-pot conversion of the urazole to provided cyclic diazene **4.75** in 31% yield over three steps. Double use of Pearlman's catalyst resulted in global removal of benzyl groups, and conversion of azides and the bridgehead diazine to amines to provide ribostamycin **4.66** in 91% yield as a tetraacetate salt. The structural challenges of this natural product are different to the aforementioned products in section 4.4.3.1, as it possesses five contiguous alternating stereocentres on the central six-membered ring that is connected to two different sugar motifs. Despite this, an olefin functionalisation approach was still utilised. The developed enantioselective dearomative hydroamination is derivative of the previous methodology, however is a remarkable improvement on previously established dearomative hydroamination conditions that produced inseparable mixtures, low yields and were racemic.[48] The general idea with all of Sarlah's dearomative reactions is to perform it in the opening step, setting up the initial desired stereocentres which helps direct the subsequent installations of future stereocentres. It must also be highlighted that the development of this methodology to furnish enantiopure, 1,2-*anti*-di-heterosubstituted cyclohexadienes has considerable implications for the syntheses of other molecular targets.

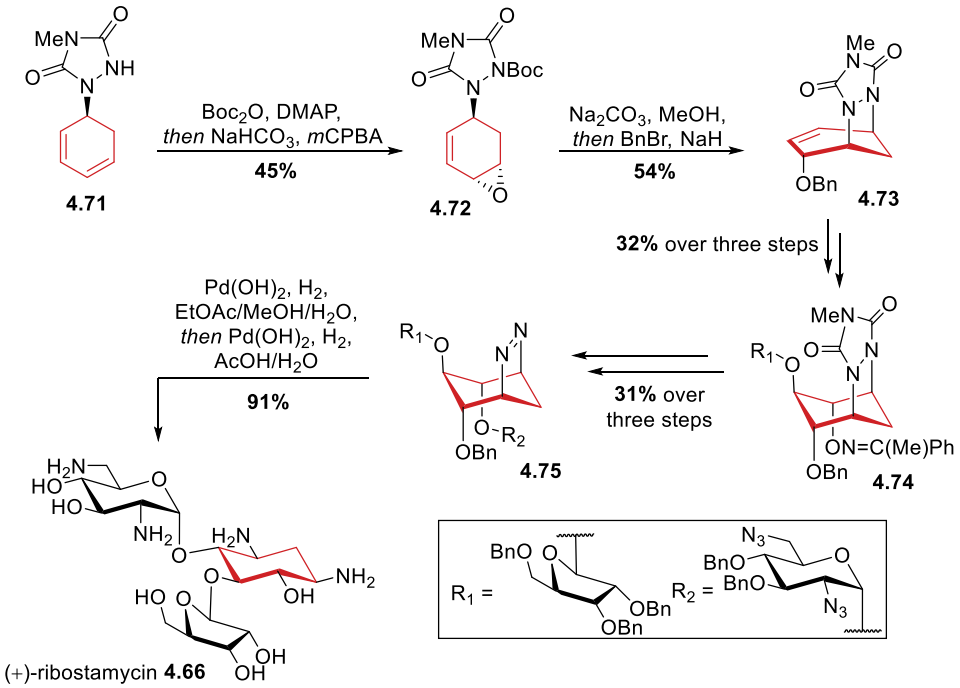

Scheme 4.10: Sarlah's 2022 total synthesis of (±)-ribostamycin

4.4.4 Chemoenzymatic dearomative methodologies

Gibson is credited with the first report of chemoenzymatic benzene **4.2** oxidation to afford *cis*-1,2-dihydrocatechol **4.76**.[49] This was possible due to a chemically induced mutation of *P. putida* that lacks a key dehydrogenase enzyme. Further research has led to genetic engineering of *E. coli* JM109 (pDTG601) to overexpress the toluene dioxygenase (TDO) enzyme (Figure 4.5B) for the oxidation of toluene **4.77** to **4.78**.[50] This reaction is highly scalable, producing kilograms to tonnes of catechols with exquisite regio-, stereo- and enantioselectivity. With

minor expansion beyond our initial scope, select total syntheses that begin from toluene derived catechols **4.78** are highlighted.

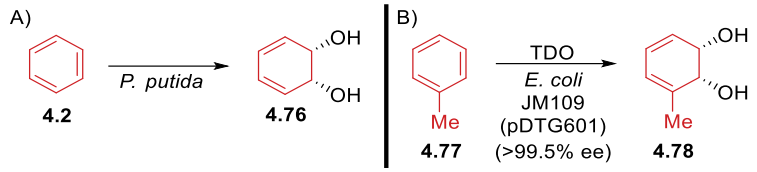

Figure 4.5: A) Chemoenzymatic oxidation of benzene to deliver *cis*-1,2-dihydrocatechol. B) Chemoenzymatic oxidation of toluene to deliver corresponding *cis*-1,2-dihydrocatechol

4.4.4.1 AB-ring system of *ent*-taxoids

Banwell in 1998 reported a sequence to synthesise the AB-ring systems of taxoids and *ent*-taxoids from toluene **4.77** (refer to paclitaxel **4.79** in Scheme 4.11).[51] Compound **4.80** was made from the acetylation of **4.78** with p-methoxybenzaldehyde dimethyl acetal. Diels−Alder reaction with α-chloroacrylonitrile, followed by hydrolysis afforded bicyclo[2.2.2]octene ketone **4.81** in 86% over two steps. Conversion to compound **4.82** occurred in eight steps to set the stage for the key step. Anionic oxy-Cope rearrangement of **4.82** to **4.83** proceeded in 90% yield. The AB-ring structure of *ent*-taxoids **4.84** was prepared in three steps from **4.83**. Paclitaxel **4.79** is a famous synthetic target due to its structural complexity (contains four rings, over ten stereocentres and high oxidation state) and importance to the pharmaceutical industry. Toluene derived catechol **4.80** serves as a useful platform to build bridged compounds via cycloaddition reactions, leading to more intricate bridged molecules like **4.84**. It must also be highlighted that toluene, over the course of 15 steps, has been cleaved and now constitutes a side of the AB ring system **4.84**.

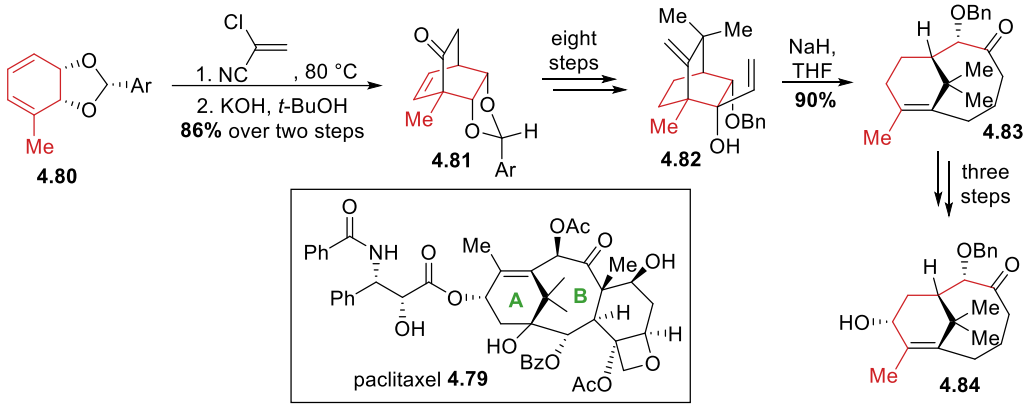

Scheme 4.11: Synthesis of the AB-ring system associated with *ent*-taxoids

4.4.4.2 (−)-connatusin A

Similar to **4.80**, compound **4.85** was also derived from toluene over two steps. A high-pressure Diels−Alder followed by dimethylation afforded **4.86** and another five steps gave compound **4.87**, setting the scene for the key transformation. A photochemically-promoted oxa-di-π-methane rearrangement of **4.87** gave tetracycle **4.88** in 95% yield (brsm). A final eight steps yielded connatusin A **4.89**.[52] The comparable approach of initially synthesising the bicyclo[2.2.2]octene through cycloaddition, differed with this key step effectively performing a ring contraction on the toluene skeleton instead of the cleavage in Scheme 4.11.

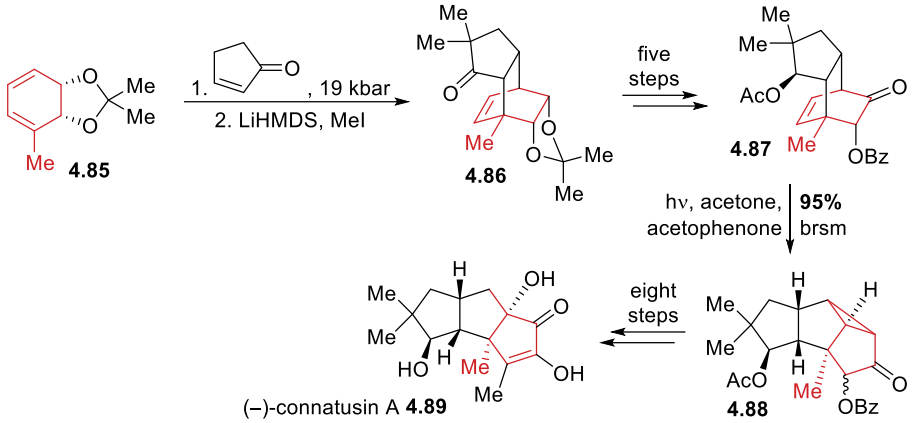

Scheme 4.12: Total synthesis of (−)-connatusin A

4.4.4.3 *ent*-rezishanone C

Compound **4.90** was accessed from **4.85** with similar α-chloroacrylonitrile DA conditions from scheme 4.11. A one-pot deprotection of the acetal and subsequent stereocentre inversion gave *trans*-diol compound **4.91** in 86% yield. A lengthy twenty steps furnished rezishanone C **4.92**.[53] This synthesis has maintained toluene's carbon skeletal structure but has saturated its bonds during the installation of functional groups.

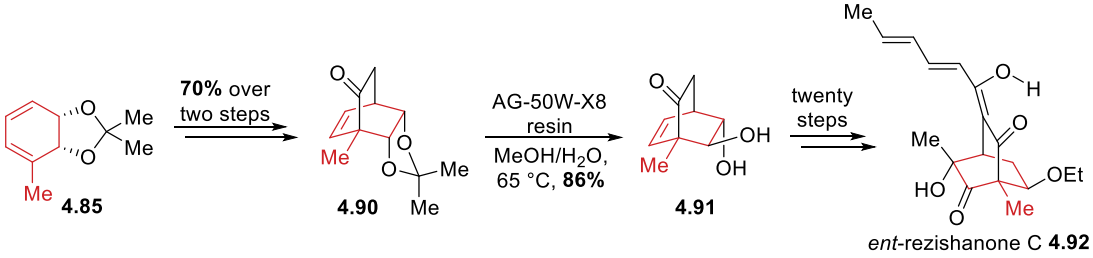

Scheme 4.13: Total synthesis of *ent*-rezishanone C

What all these selected total syntheses involving benzene (or toluene) highlight is the common strategy of the initial dearomative reaction. Due to the aromaticity of benzene, it is often limited to electrophilic substitutions which are reactions that have comparatively lower complexity building power (compared to cycloadditions, for example). By developing dearomative methodologies this issue is bypassed, opening further reaction possibilities.

4.5 [*8*]Annulene

4.5.1 Structural and Chemical Characteristics of [*8*]Annulene

1,3,5,7-cyclooctatetraene (COT) **4.3** was first synthesised by Richard Willstätter in 1905 from pseudopelletierine **4.93**.[54] Walter Reppe drastically improved its synthesis via a postulated [2+2+2+2] cycloaddition of acetylene **4.94** affording yields near 90%.[55] It is a conjugated eight-carbon ring system possessing 8π electrons, which fulfills the requirements for anti-aromaticity, but escapes it by adopting a tub-shaped conformation instead of planar.[56,57] The reactivity for COT is similar to ordinary polyenes and has been employed in some total syntheses.

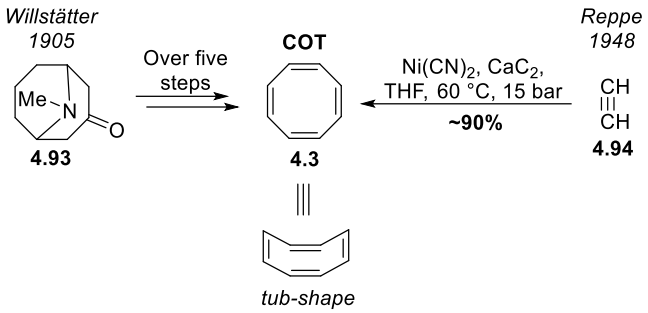

Figure 4.6: Few syntheses of COT

4.5.2 Roxaticin

D.A. Evans used COT to synthesise a fragment in his convergent synthesis of roxaticin (Scheme 4.14).[58] A Hg(II) catalysed *trans*-1,2-acetoxyation of COT **4.3** produced compound **4.95** in 88% yield. Removal of the acetate groups by $LiAlH_4$ was followed by oxidative ring fragmentation and alkene isomerisation to give unstable di-aldehyde **4.96** in 60%. Ester-aldehyde **4.97** was formed from triethylphosphonoacetate and the aldehyde reduced to an alcohol to give the ester-alcohol **4.98** in 60% over two steps. Nucleophilic substitution of the alcohol with bromide was then proceeded by heating with triethyl phosphite to furnish phosphonate **4.99** in 60% over two steps. Deprotonated **4.99** via LiHMDS was added to aldehyde **4.100** to provide compound **4.101** in 83% yield. Ester hydrolysis followed by macrolactonisation to close the macrocycle and then global deprotection yielded roxaticin **4.102** in 42% over three steps. In the synthesis of **4.99**, conversion of COT **4.3** to a linear polyene required reactions to be carried out in the omission of light to prevent undesirable isomerisations and polymerisations, which represents a limitation. However, the most difficult aspect in this synthesis was likely the installation of alcohol and methyl groups with the desired stereochemistry, whereas COT **4.3** provided easy access to a linear polyene rather than sequential homologation/metathesis steps to build it.

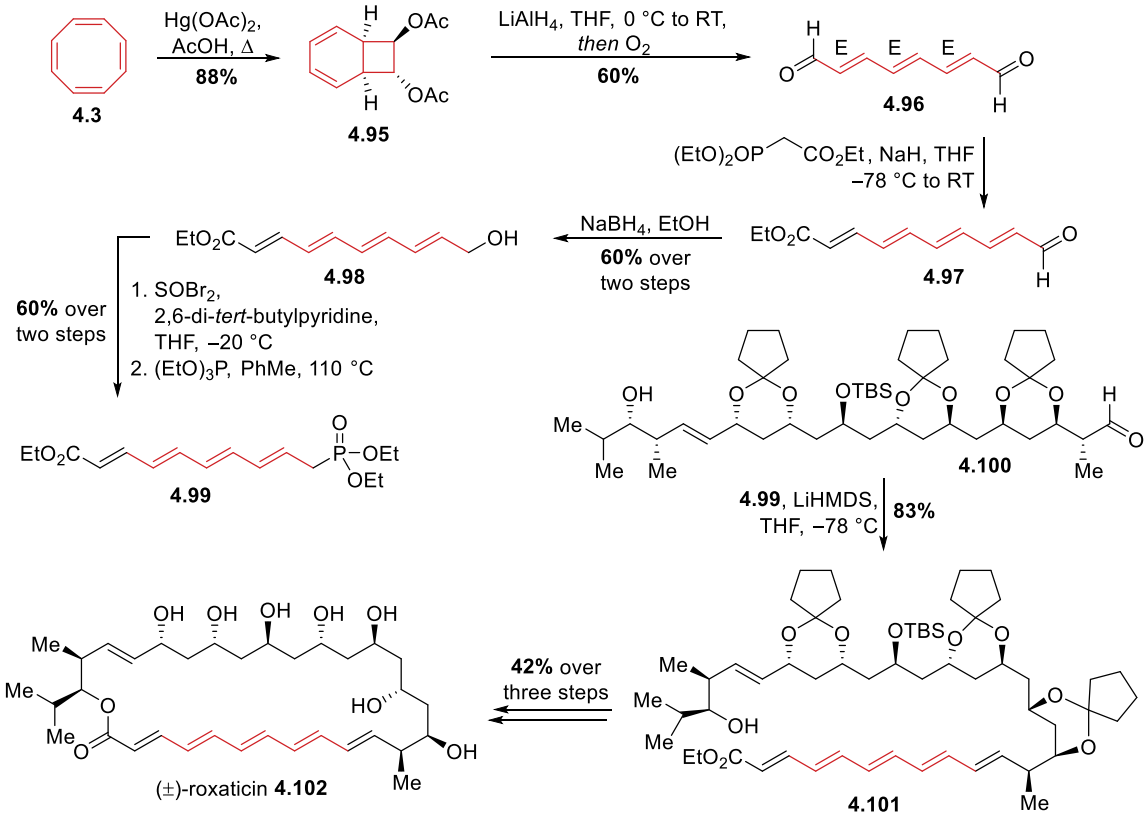

Scheme 4.14: Total synthesis of (±)-roxaticin

4.5.3 Pentacycloanammoxic ester

E.J. Corey published the total synthesis of pentacycloanammoxic ester **4.27**, a ladderane natural product.[21] The synthesis begins with the bromination of COT to give **4.103** and subsequent Diels−Alder reaction with DBAD **4.104** imparted compound **4.105** in 64% yield over two steps. Selective reduction of the olefin and elimination of the dibromide afforded cyclobutene **4.106** in 80% over two steps. An *exo*-selective [2+2] photocycloaddition with 2-cyclopentenone and then Cbz cleavage under Pd/C conditions furnished azo bridge ketone **4.107** in 40% (brsm) and 76% yield, respectively. Removal of the azo bridge to form [*3*]-ladderane was affected by initial protection of the ketone (91% yield) and followed by UV irradiation to produce pentacycle **4.108** in a low 6% yield. α-Diazo ketone **4.109** was made from two steps in 80% yield. Photo-Wolff rearrangement formed the butane methyl ester in 72% yield, which was reduced to the alcohol and then oxidised to the aldehyde by Swern oxidation in 80% yield over two steps. Stirring with triethylamine over six days epimerised the aldehyde to the preferred endo diastereomer **4.110** in a ratio of 7:1. Final manipulations of Wittig olefination, alkene reduction and esterification furnished (±)-pentacycloanammoxic ester **4.27**.

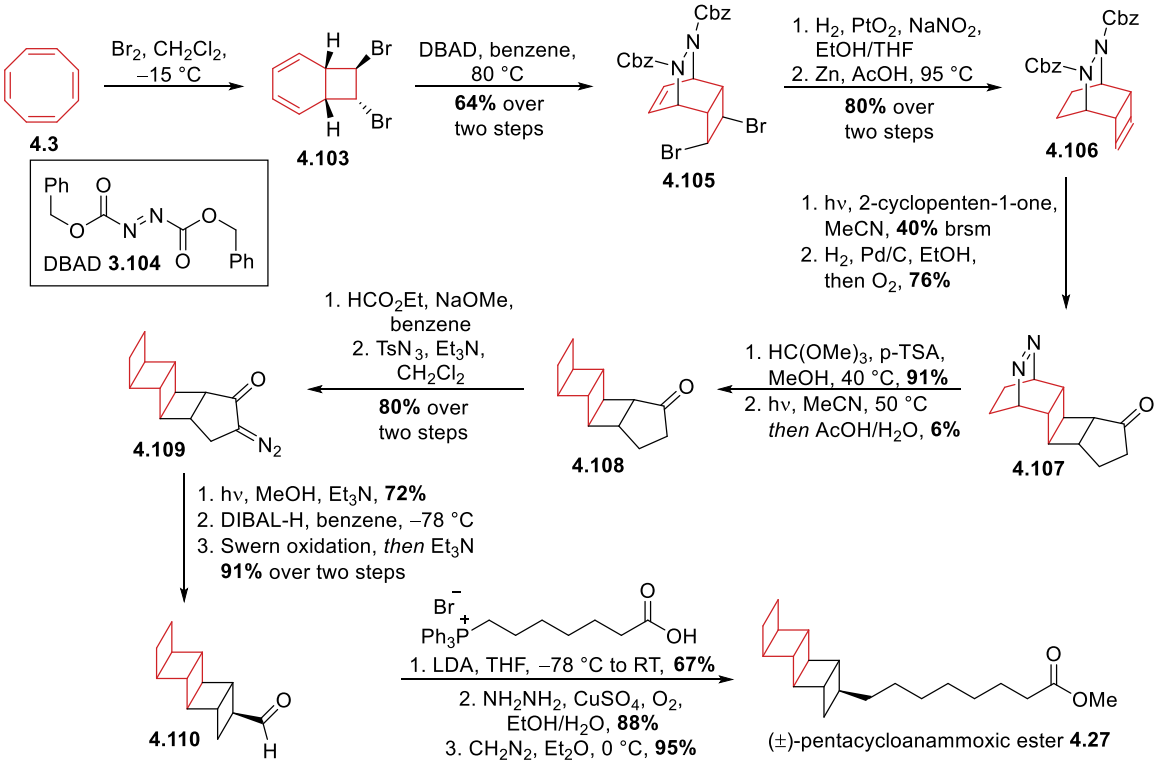

Scheme 4.15: Total synthesis of pentacycloanammoxic ester

The challenge of synthesising ladderane compounds is the formation of the ladderane moiety. It has already been discussed in Section 4.3.4 that top-down strategies have predominated ladderane natural product synthesis. To further elaborate, Corey has essentially performed a formal electrocyclic ring-closing of COT to create a molecule (cyclopentanone **4.108)** that is similar to synthon **4.111** over 9 steps. While it is a creative strategy, it is plagued by limitations of low yields on the nitrogen extrusion step, and no enantioselectivity. In 2006, Corey reported the improved enantioselective synthesis omitting the use of COT **4.3** (Figure 4.7B).[59] A [2+2] between cyclobutene **4.112** and cyclopentenone **4.113** delivered **4.114** in 78% yield. A further seven steps provided compound **4.115** which slightly differs from **4.111** by one unsaturation. COT **5.3** was possibly used because it already contains the right number of carbons for a [*3*]-ladderane, however its required manipulations were clearly limiting in terms of yield. This bottom-up approach was more advantageous for fruitful [*3*]-ladderane assembly and subsequent enantioselective imparting transformations leading to the asymmetric synthesis of (+)-pentacycloanammoxic ester **4.27**.

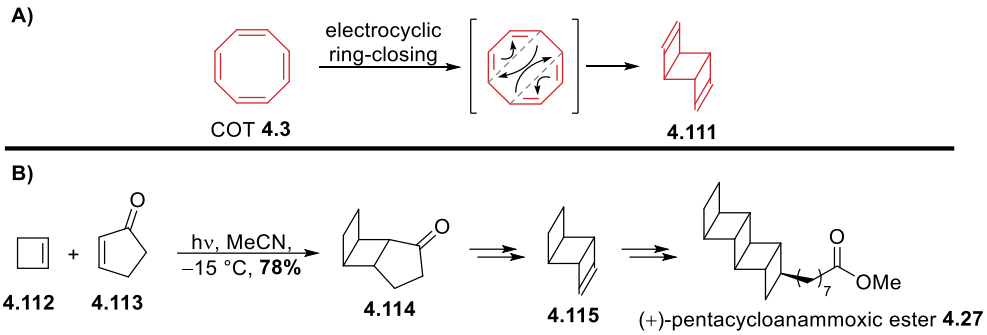

Figure 4.7: A) Electrocyclisation of COT to [*3*]-ladderene 4.111 B) Summary of enantioselective total synthesis of (+)- pentacycloanammoxic ester

4.5.4 β-Allose

Mehta made β-allose **4.116** in a lengthy sequence starting from COT **4.3**.[60] The synthesis starts from the formation of the lithium cyclooctatetraenide dianion **4.117** which was then treated with dimethyl carbamoyl chloride to deliver bicyclo[4.2.1]nona-2,4,7-trien-9-one **4.118**. Baeyer−Villiger oxidation formed bicyclic lactone **4.119** in 60% yield. Regio- and stereo-controlled dihydroxylation proceeded through catalytic osmium tetroxide followed by acetonide protection of the diols to give **4.120** in 75% over two steps. Ring opening of the lactone with $LiAlH_4$ and then TBS protection of the alcohol occurred in 43% yield over two steps to provide **4.121**. Ozonolysis and then rearrangement gave compound **4.122**. Oxidation of the lactol to lactone was then followed by lactone ring opening with methoxide and methylation of the alcohol with methyl iodide (**4.123** in 29% over four steps). A further eight steps furnished β-allose **4.116** in 10% yield. The purpose of the initial seven steps is to install four stereocentres on the left-side of COT **4.3** (end result is **4.121**). Ozonolysis removes the two carbons on the right-side of **4.121** and ensuing rearrangement of the molecule sets all desired stereocentres for the final product. Despite this captivating key step, the challenges of synthesising an allose sugar does not warrant such lengthy complex transformations. The unique structural and chemical characteristics of COT is not utilised to its extent here with other alternatives being more practical.

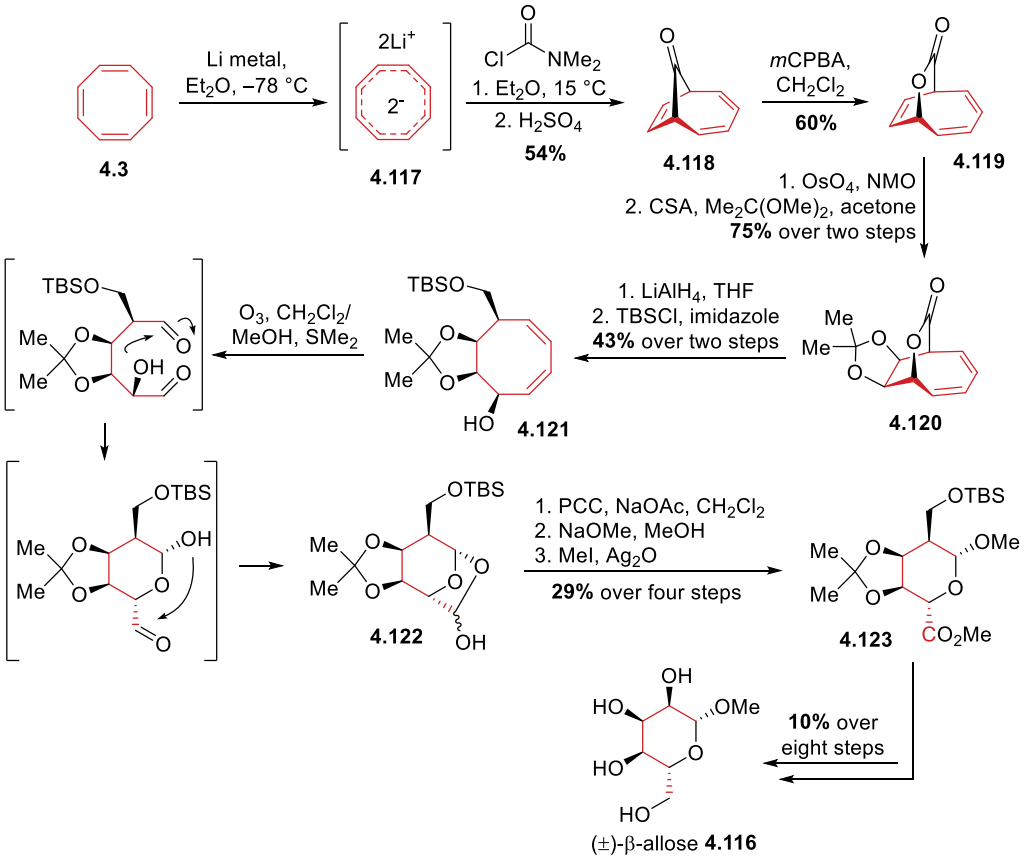

Scheme 4.16: Mehta's 2004 total synthesis of β-Allose

4.5.5 Endiandric acid derived natural products

Black postulated the biosynthesis of endiandric acid derivatives to arise from the 8π electrocyclisation/6π electrocyclisation/IMDA cascade starting from a linear tetraene molecule **4.124** (Scheme 4.17B).[61–64] This was later verified by Nicolaou in his hallmark four paper series on the total syntheses of endiandric acid natural products.[65–68] Nicolaou was also the first to notice that cyclooctatetraene **4.3** can undergo reactions with a variety of electrophiles such as bromine to furnish 1,2-disubstituted cyclooctatrienes **4.125**, which maps onto intermediate **4.126** in the biosynthesis (Scheme 4.17A).[69] This approach was marred with issues arising from competing ring-opening electrocyclisations (equilibrium with **4.127**, depending on the R group) and lengthy transformations required for synthetic utility and was ultimately abandoned for another strategy. Fallon devised formal *anti*-1,2-difunctionalisation methodologies of cyclooctatriene **4.3** that accessed these bicyclo[4.2.0]octadiene **4.128** related natural products (Scheme 4.17C). His 2020 paper began with the epoxidation of COT (forming **4.129**), followed by an *anti*-S_N2' ring opening using dodecyl cuprate that gave alcohol **4.130** in 96% yield.[70] A sequence of gold-catalysed vinyl transfer (forming **4.131**), Claisen rearrangement and 6π electrocyclisation presented BOD **4.132** in 48% over two steps. Simple olefination manipulations over two steps gave beilcyclone A **4.133** in 61%. Alternative olefinic conditions over three steps gave endiandric acid J **4.134** in 39%. His 2022 paper began with the rhodium-catalysed cyclopropanation of cyclooctatetraene in 72% yield (forming **4.135**), followed by nucleophilic ring-opening using piperonyl cuprate and then hydrolysis to the diacid **4.136** in 87% yield.[71] Decarboxylation and olefination transformations furnished kingianic acid A **4.137** in 14% yield over three steps. To date, these syntheses are the most concise in accessing the BOD structure **4.128**. COT **4.3** presents itself as the best starting material for the synthesis of these class of natural products because it directly intersects an already rapid structure generating biosynthesis. However, the cuprate chemistry developed in these methodologies are substrate specific and the synthesis of its reagents are non-trivial, limiting it use for the synthesis of other endiandric acid derivatives.

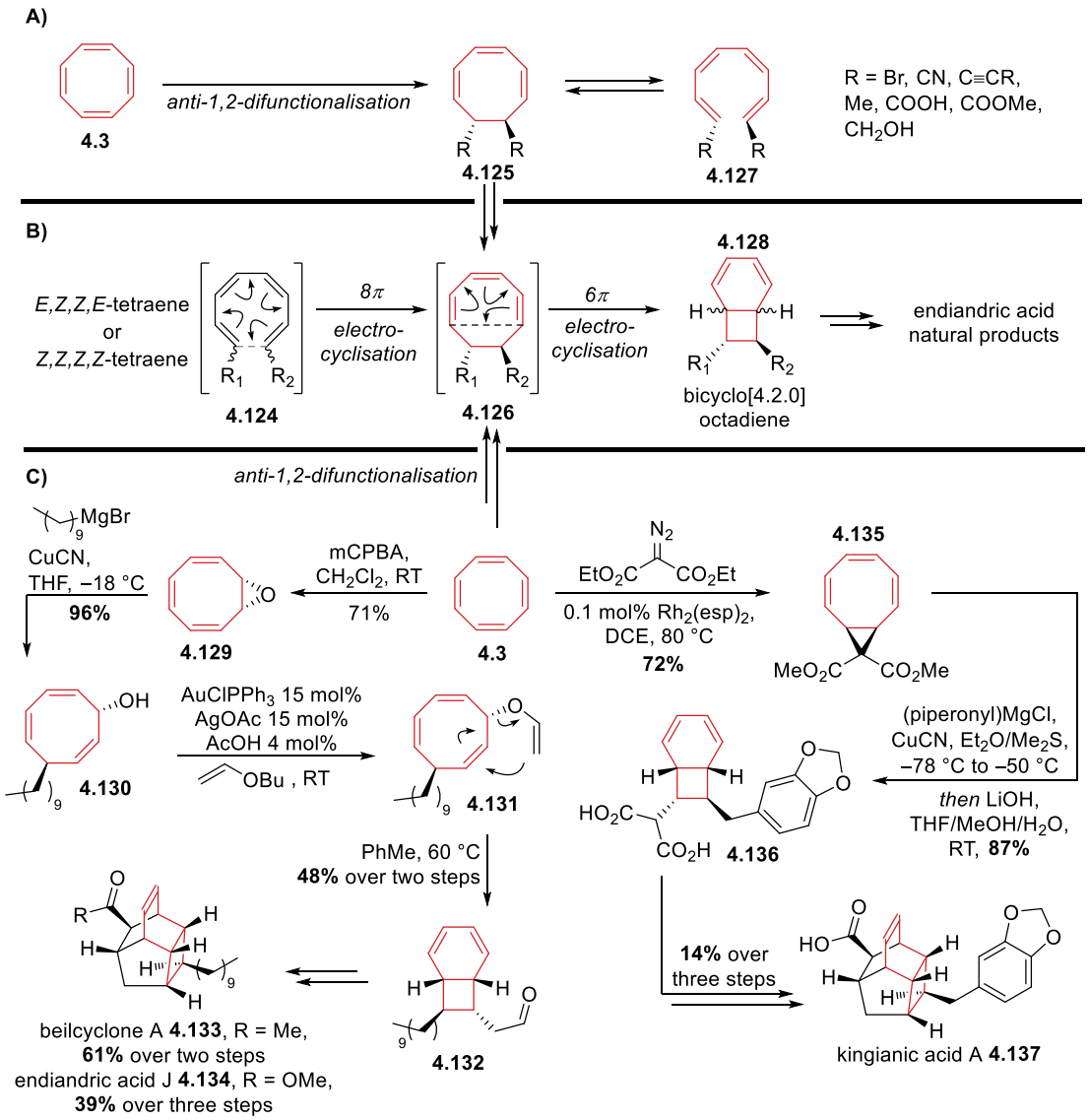

Scheme 4.17: A) Nicolaou's cyclooctatetraene approach B) Black's proposed biosynthesis of endiandric acid derivatives C) Fallon's syntheses of beilcyclone A, endiandric acid J and kingianic acid A from cyclooctatetraene

4.6 Conclusion

Annulenes have been thoroughly studied by researchers for their unique structural and chemical characteristics. They often constitute the core skeleton of several compounds and have been used pre-functionalised to have further synthetic utility, however is not a necessity. The total synthesis examples containing cyclobutadiene possess some functionality for stability, however its bare form also has potential. The use of benzene appears to mainly occur via dearomative methods involving oxygenations and cycloadditions and remains to be a key feedstock in many synthetic pursuits. Cyclooctatriene has been shown to be the most versatile among the three annulene classes in this chapter. It can undergo addition, cycloaddition, oxidation and cleavage reactions to deliver a plethora of natural products. Hopefully, this chapter has displayed simple unfunctionalised annulenes to be viable building blocks and to inspire future complex synthetic endeavours that apply them.

4.7 References

[1] Seyhan N. Eğe, *Organic Chemistry: Structure and Reactivity*, Prentice Hall Macmillan, **1994**.

[2] In *The IUPAC Compendium of Chemical Terminology*, International Union Of Pure And Applied Chemistry (IUPAC), Research Triangle Park, NC, **2014**.
[3] P. Senn, *J Chem Educ* **1992**, *69*, 819.
[4] H. Kollmar, V. Staemmler, *J. Am. Chem. Soc.* **1977**, *99*, 3583–3587.
[5] C. Y. Lin, A. Krantz, *J. Chem. Soc. Chem. Commun.* **1972**, 1111.
[6] R. J. S. Francis A. Carey, *Advanced Organic Chemistry: Part A: Structure and Mechanisms*, Springer Science & Business Media, **2007**.
[7] D. J. Cram, M. E. Tanner, R. Thomas, *Angew. Chem. Int. Ed. Eng.***1991**, *30*, 1024–1027.
[8] R. Pettit, J. Henery, *Org. Synth.* **1970**, *50*, 21.
[9] G. F. Emerson, L. Watts, R. Pettit, *J. Am. Chem. Soc.* **1965**, *87*, 131–133.
[10] Myron. Rosenblum, Christos. Gatsonis, *J. Am. Chem. Soc.* **1967**, *89*, 5074–5075.
[11] D. Seyferth, *Organometallics* **2003**, *22*, 2–20.
[12] J. D. Fitzpatrick, L. Watts, G. F. Emerson, R. Pettit, *J. Am. Chem. Soc.* **1965**, *87*, 3254–3255.
[13] L. Brener, J. S. McKennis, R. Pettit, *Org. Synth.* **1976**, *55*, 43.
[14] J. Limanto, M. L. Snapper, *J. Am. Chem. Soc.* **2000**, *122*, 8071–8072.
[15] Y. Liang, X. Jiang, Z.-X. Yu, *Chem. Commun.* **2011**, *47*, 6659.
[16] M. E. Krafft, Y. Y. Cheung, K. A. Abboud, *J. Org. Chem.* **2001**, *66*, 7443–7448.
[17] Y. Liang, X. Jiang, X.-F. Fu, S. Ye, T. Wang, J. Yuan, Y. Wang, Z.-X. Yu, *Chem Asian J* **2012**, *7*, 593–604.
[18] P. A. Wender, N. C. Ihle, C. R. D. Correia, *J. Am. Chem. Soc.* **1988**, *110*, 5904–5906.
[19] M. J. Williams, H. L. Deak, M. L. Snapper, *J. Am. Chem. Soc.* **2007**, *129*, 486–487.
[20] H. L. Deak, M. J. Williams, M. L. Snapper, *Org. Lett.* **2005**, *7*, 5785–5788.
[21] V. Mascitti, E. J. Corey, *J. Am. Chem. Soc.* **2004**, *126*, 15664–15665.
[22] J. A. M. Mercer, C. M. Cohen, S. R. Shuken, A. M. Wagner, M. W. Smith, F. R. Moss, M. D. Smith, R. Vahala, A. Gonzalez-Martinez, S. G. Boxer, N. Z. Burns, *J. Am. Chem. Soc.* **2016**, *138*, 15845–15848.
[23] G. Mehta, M. B. Viswanath, A. C. Kunwar, *J. Org. Chem.* **1994**, *59*, 6131–6132.
[24] R. N. Warrener, G. Abbenante, C. H. L. Kennard, *J. Am. Chem. Soc.* **1994**, *116*, 3645–3646.
[25] J. Dewar, *Proceedings of the Royal Society of Edinburgh* **1869**, *6*, 82–86.
[26] A. Ladenburg, *Ber. Dtsch. chem. Ges.* **1869**, *2*, 140–142.
[27] Aug. Kekulé, *Ann. Chem. Pharmacie* **1872**, *162*, 77–124.
[28] H. E. Armstrong, *J. Chem. Soc., Trans.* **1887**, *51*, 258–268.
[29] A. Baeyer, *Justus Liebigs Ann. Chem.* **1888**, *245*, 103–190.
[30] J. Thiele, *Justus Liebigs Ann. Chem.* **1899**, *306*, 87–142.
[31] C. B. Mansfield, *Ann. Chem. Pharmacie* **1849**, *69*, 162–180.
[32] Aug. Wilh. Hofmann, *Ann. Chem. Pharmacie* **1845**, *55*, 200–205.
[33] E. Mitscherlich, *Ann. Phar.* **1834**, *9*, 39–48.
[34] R. Kaiser, *Angew. Chem. Int. Ed. Eng.***1968**, *7*, 345–350.
[35] Michael Faraday, *Philos Trans R Soc Lond* **1825**, *115*, 440–466.
[36] K. Lonsdale, *Proceedings of the Royal Society of London. Series A, Containing Papers of a Mathematical and Physical Character* **1931**, *133*, 536–552.
[37] K. Lonsdale, *Proceedings of the Royal Society of London. Series A, Containing Papers of a Mathematical and Physical Character* **1929**, *123*, 494–515.
[38] E. Hückel, *Z. Phys.* **1933**, *83*, 632–668.
[39] E. Hückel, *Z. Phys.* **1932**, *76*, 628–648.
[40] E. Hückel, *Z. Phys.* **1931**, *72*, 310–337.

[41] E. Hückel, *Z. Phys.* **1931**, *70*, 204–286.
[42] D. L. Cooper, J. Gerratt, M. Raimondi, *Nature* **1986**, *323*, 699–701.
[43] LibreTexts, "18: Reactions of Aromatic Compounds," can be found under https://chem.libretexts.org/Bookshelves/Organic_Chemistry/Map%3A_Organic_Chemistry_(Wade)/18%3A_Reactions_of_Aromatic_Compounds, **2022**.
[44] D. R. Stranks, M. L. Heffernan, K. C. Lee Dow, P. T. McTigue, G. R. A. Withers, *Chemistry: A Structural View.*, Melbourne University Press., Carlton, Victoria, **1970**.
[45] P. M. J. Jung, W. B. Motherwell, A. S. Williams, *Chem. Commun.* **1997**, 1283–1284.
[46] L. W. Hernandez, J. Pospech, U. Klöckner, T. W. Bingham, D. Sarlah, *J. Am. Chem. Soc.* **2017**, *139*, 15656–15659.
[47] T. W. Bingham, L. W. Hernandez, D. G. Olson, R. L. Svec, P. J. Hergenrother, D. Sarlah, *J. Am. Chem. Soc.* **2019**, *141*, 657–670.
[48] C. N. Ungarean, P. Galer, Y. Zhang, K. S. Lee, J. M. Ngai, S. Lee, P. Liu, D. Sarlah, *Nat. Synth.* **2022**, *1*, 542–547.
[49] D. T. Gibson, J. R. Koch, C. L. Schuld, R. E. Kallio, *Biochemistry* **1968**, *7*, 3795–3802.
[50] G. J. Zylstra, L. P. Wackett, D. T. Gibson, *Appl Environ Microbiol* **1989**, *55*, 3162–3166.
[51] M. G. Banwell, P. Darmos, M. D. McLeod, D. C. R. Hockless, *Synlett* **1998**, *1998*, 897–899.
[52] D. J.-Y. D. Bon, M. G. Banwell, I. A. Cade, A. C. Willis, *Tetrahedron* **2011**, *67*, 8348–8352.
[53] Q. Yan, M. G. Banwell, M. L. Coote, R. Lee, A. C. Willis, *Chem Asian J* **2017**, *12*, 1480–1484.
[54] R. Willstätter, E. Waser, *Ber. Dtsch. chem. Ges.* **1911**, *44*, 3423–3445.
[55] W. Reppe, O. Schlichting, K. Klager, T. Toepel, *Justus Liebigs Ann. Chem.* **1948**, *560*, 1–92.
[56] H. S. KAUFMAN, I. FANKUCHEN, H. MARK, *Nature* **1948**, *161*, 165–165.
[57] P. M. Thomas, A. Weber, *J. Raman Spectrosc.* **1978**, *7*, 353–357.
[58] D. A. Evans, B. T. Connell, *J. Am. Chem. Soc.* **2003**, *125*, 10899–10905.
[59] V. Mascitti, E. J. Corey, *J. Am. Chem. Soc.* **2006**, *128*, 3118–3119.
[60] G. Mehta, K. Pallavi, *Tetrahedron Lett.* **2004**, *45*, 3865–3867.
[61] W. M. Bandaranayake, J. E. Banfield, D. St. C. Black, *J. Chem. Soc. Chem. Commun.* **1980**, 902.
[62] W. Bandaranayake, J. Banfield, D. Black, G. Fallon, B. Gatehouse, *Aust. J. Chem.* **1981**, *34*, 1655.
[63] W. Bandaranayake, J. Banfield, D. Black, G. Fallon, B. Gatehouse, *Aust. J. Chem.* **1982**, *35*, 567.
[64] J. Banfield, D. Black, D. Collins, B. Hyland, J. Lee, S. Pranowo, *Aust. J. Chem.* **1994**, *47*, 587.
[65] K. C. Nicolaou, N. A. Petasis, R. E. Zipkin, J. Uenishi, *J. Am. Chem. Soc.* **1982**, *104*, 5555–5557.
[66] K. C. Nicolaou, N. A. Petasis, J. Uenishi, R. E. Zipkin, *J. Am. Chem. Soc.* **1982**, *104*, 5557–5558.
[67] K. C. Nicolaou, R. E. Zipkin, N. A. Petasis, *J. Am. Chem. Soc.* **1982**, *104*, 5558–5560.
[68] K. C. Nicolaou, N. A. Petasis, R. E. Zipkin, *J. Am. Chem. Soc.* **1982**, *104*, 5560–5562.
[69] K. C. Nicolaou, N. A. Petasis, **1984**, pp. 155–173.
[70] O. Yahiaoui, A. Almass, T. Fallon, *Chem. Sci.* **2020**, *11*, 9421–9425.
[71] H. D. Patel, T. Fallon, *Org. Lett.* **2022**, *24*, 2276–2281.

Chapter 5

Total synthesis of Endiandria/Beilschmiedia derived bridged tetracyclic natural products via the lithium enolate of cyclooctatrienone

Authorship Declaration: All experimental synthesis, analysis and presentation of results within this chapter was conducted personally under the supervision of Dr Thomas Fallon

5.1 Introduction to the endiandria/beilschmiedia family of natural products

5.1.1 Isolation

Endiandria and *Beilschmiedia* are both genus of plants in the laurel family, Lauraceae. They are abundant sources of secondary metabolites that have been the focus of rigorous research in the organic chemistry community and are the only known source of endiandric acid derivatives.[1–11] Molecules within the endiandric acid family of natural products share a bicyclo[4.2.0]octadiene **5.1** structural moiety, where they can be assigned into one of three main groups: 13-carbon fused tetracycle **5.2**, 11-carbon bridged tetracycle **5.3** and 16-carbon pentacycle **5.4** (Figure 5.1).

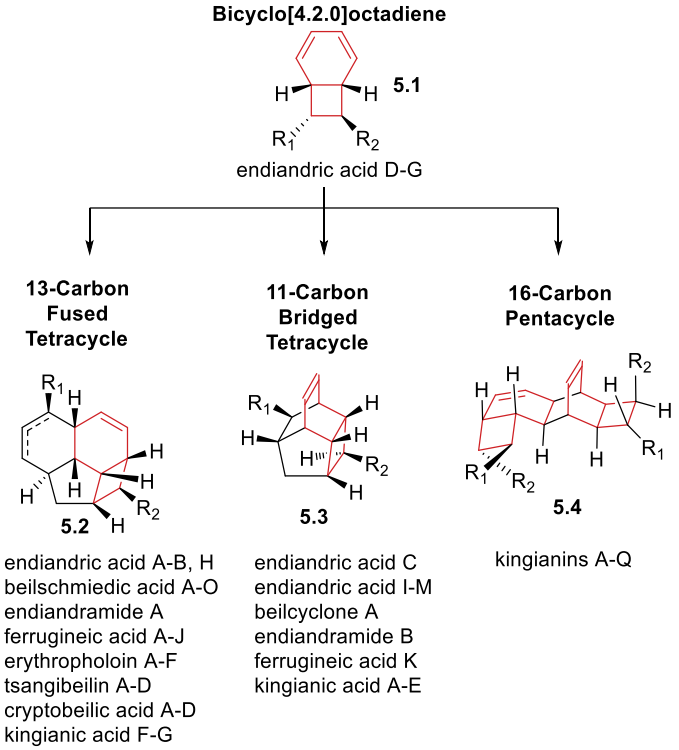

Figure 5.1: The entire isolated family of endiandric acid derivatives

5.1.2 Biosynthesis

In his early isolation work, Black postulated the biosynthesis of this family of natural products.[11–15] They proposed polyketides, which are also involved in the biosynthesis of 2-pyrone and flavonoid derivatives in the Lauraceae family, convert to E,Z,Z,E polyenes **5.5**. These polyenes contain a central tetraene moiety that undergo facile 8π electrocyclisation to form a cyclooctatriene ring **5.6**, which in turn undergoes a 6π electrocyclisation to yield a bicyclo[4.2.0]octadiene (BOD) structure **5.7**. Whether a 1,3-diene **5.7a** or alkene **5.7b** is *endo* with respect to the BOD, will influence the mode of the intramolecular Diels−Alder (IMDA) reaction and therefore the corresponding products (**5.2** and **5.3**, respectively). The products are isolated as racemates suggesting origins from achiral substrates and non-enzyme mediated pathways.

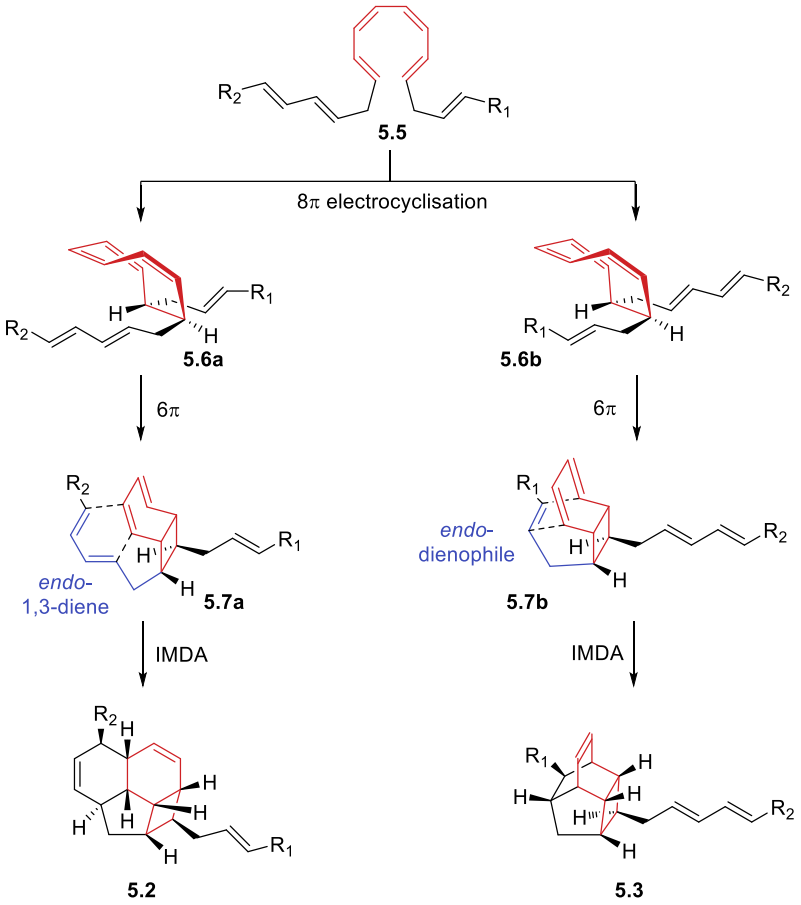

Scheme 5.1: Black's postulated biosynthesis of fused and bridged tetracyclic endiandric acids

The kingianins were first reported in 2011 by Litaudon, revealing a third possibility where an intermolecular Diels−Alder between two BOD molecules **5.1** forms a pentacyclic compound **5.4**, which constitutes the kingianin sub-family (Scheme 5.2).[16]

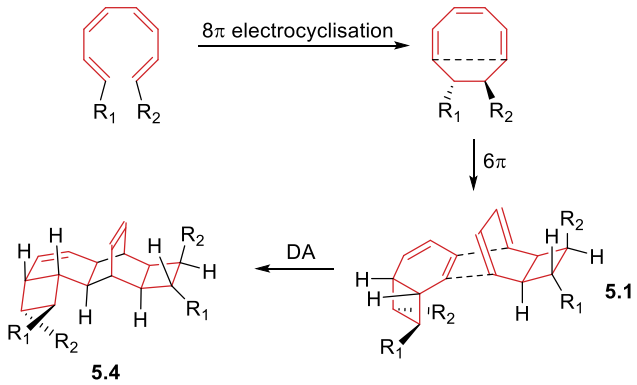

Scheme 5.2: Postulated biosynthesis of pentacyclic endiandric acids

5.1.3 Bioactivity

Extending beyond the structural and biosynthetic interest of this family, their biological activity has been studied for therapeutic potential. Select endiandric acid related natural products with notable bioactivity are outlined below.

5.1.3.1 Anti-cancer

A variety of endiandric acid derivatives were screened against anti-apoptotic proteins (Bcl-xL and Mcl-1), which are involved in cancer cell survival.[17–20] Ferrugineic acid B **5.8** exhibited the best binding affinity for Mcl-1 (85% inhibition at 100 μM), with ferrugineic C **5.9** having

the highest for Bcl-xL (93% inhibition at 100 μM).[7,10] The 13-carbon fused tetracyclic endiandric natural products had generally good binding affinity for Mcl-1. Kingianins G-L (**5.10**-**5.15**) were good inhibiting Bcl-xL, with kingianin G **5.10** with the best (K_i value of 2 ± 0 μM).[16] Pure enantiomers of the kingianins were separated by chiral prep HPLC. (−)-enantiomers were found to exhibit significantly higher binding affinities than their corresponding (+)-enantiomers, highlighted by (−)-kingianin K **5.15** (K_i value of 6.0 ± 0.2 μM) and (+)-kingianin K **5.15** (K_i value of 122 ± 45 μM).

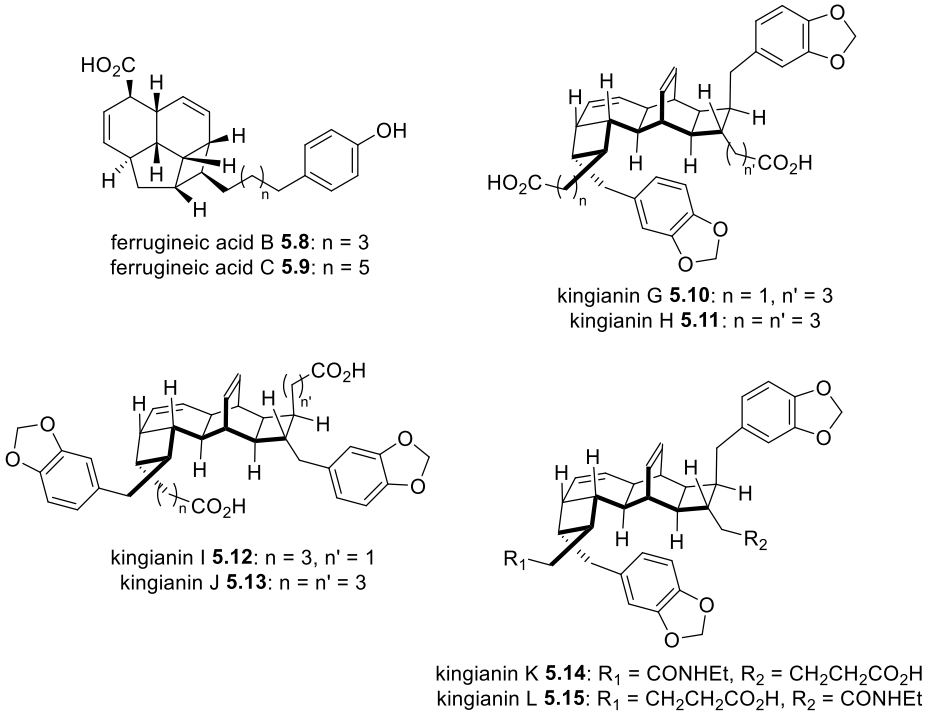

Figure 5.2: Structures of endiandric acid derivatives with anti-cancer properties

5.1.3.2 Cytotoxic

In regards to cytotoxic capabilities, beilschmiedic acids A, K, L, M, N (**5.16**-**5.20**) exhibited moderate activity against NCl-H460 human lung cancer cells (LC_{50} values of 5.5, 5.9, 4.4, 8.7, 6.1 μM, respectively).[8] Kingianic acid A **5.21** had poor IC_{50} against HT-29 (colorectal adenocarcinoma cell lines) and A549 (lung adenocarcinoma epithelial cell lines) of (35.0 ± 0.2 μM and 85.4 ± 0.2 μM, respectively).[10] Kingianic acid E **5.22** possessed moderate IC_{50} against A549 and HT-29 (15.36 ± 0.19 μM and 17.10 ± 0.11 μM, respectively).

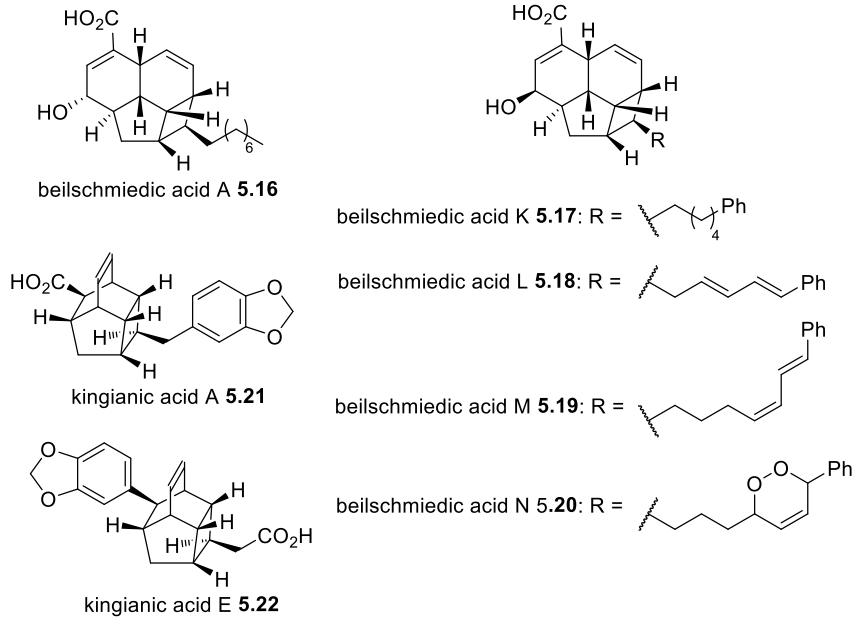

Figure 5.3: Structures of endiandric acid derivatives with cytotoxic properties

5.1.3.3 Anti-malarial

For anti-malaria, cryptobeilic acids A-D (**5.23**-**5.26**) and tsangibeilin B **5.27** have been reported to exhibit anti-plasmodial activity *in vitro* against *P. falciparum* NF54 (IC_{50} values of 17.7, 5.35, 14.0, 10.8 and 8.2 µM, respectively).[9]

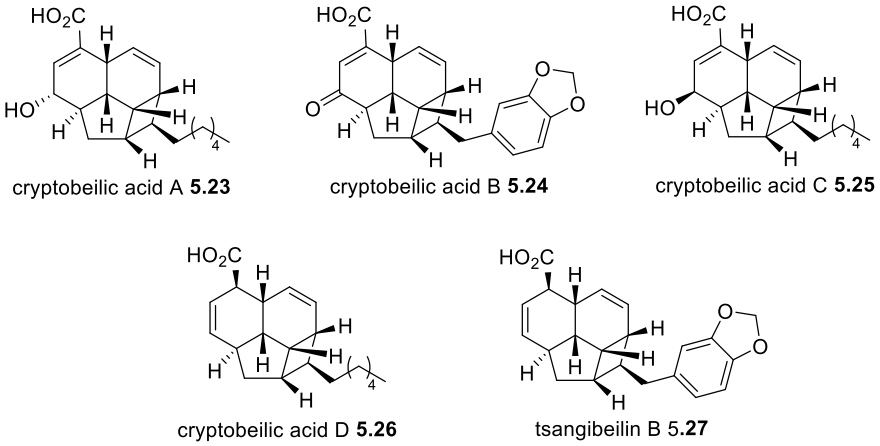

Figure 5.4: Structures of endiandric acid derivatives with anti-malarial properties

5.1.3.4 Anti-asthma and anti-inflammatory

Tested for anti-asthmatic/anti-inflammatory properties, endiandramide A **5.28** and B **5.29** possesses potent iNOS inhibitory activities (IC_{50} values of 9.59 and 16.40 µM, respectively).[5,6] Tsangibeilins A **5.30**, B **5.27**, D **5.31** and endiandric acids K **5.32**, L **5.33**, M **5.34** have moderate anti-inflammatory activity (IC_{50} values 30–96 µM). Endiandric acid H **5.35** and its synthetic derivatives have already been used in the production of medicament for the treatment of allergic, asthmatic disorders, or diseases that can be treated by inhibiting c-maf and NFAT.[21,22]

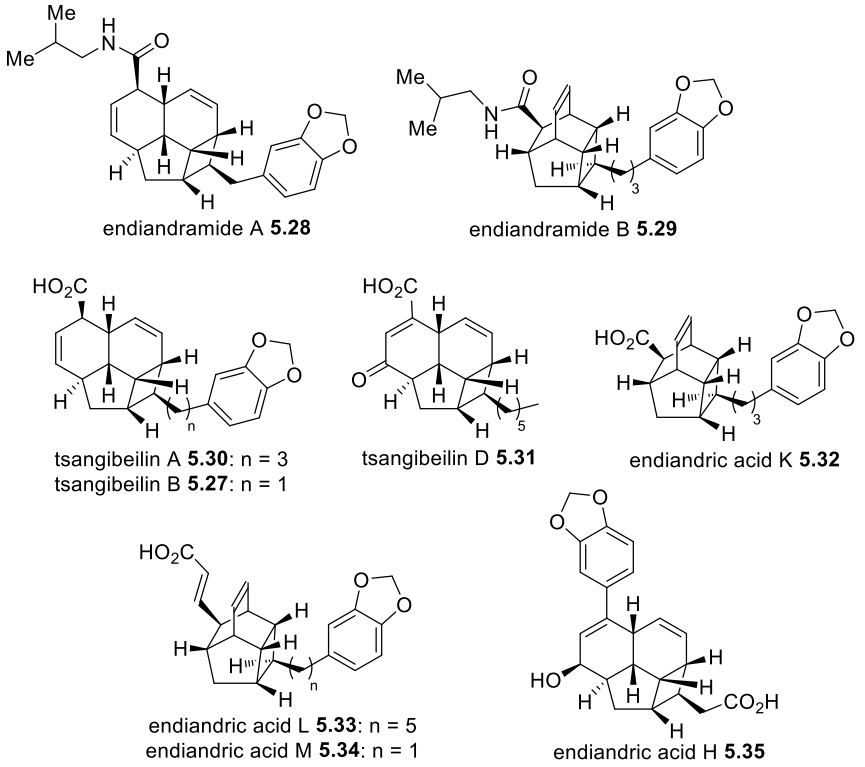

Figure 5.5: Structures of endiandric acid derivatives with anti-asthma and anti-inflammatory properties

5.1.3.5 Anti-microbial

Looking at anti-microbial activity, beilschmiedic acids A-C (**5.16**, **5.36**-**5.37**) were tested against *Bacillus subtillis*, *Micrococcus luteus* and *Streptococcus faecalis*.[2] Beilschmiedic acid C **5.37** was found to be the best against the three strains (minimum inhibitory concentrations (MICs) of 5.6, 0.7 and 22.7 µM, respectively). Beilschmiedic acid B **5.36** (MIC = 11.3 µM) and C **5.37** (MIC = 5.6 µM) were found to be more active than ampicillin **5.38** (MIC = 89.5 µM) against *B. subtillis*. Beilschmiedic acid C **5.37** was more effective than ampicillin **5.38** (MIC = 5.58 µM) against *M. luteus*. Beilschmiedic acids C **5.37** and I–O (**5.39**-**5.40**, **5.17**-**5.20**, **5.41**), exhibited potent anti-bacterial activity against methicillin-resistant *S. aureus* (MIC between 10-13 µg/mL).[8] Cryptobeilic acids A **5.23** and B **5.24** demonstrated anti-bacterial activity against *Escherichia coli* 6r3 (MIC of 10 and 20 µg/mL, respectively), which was moderate compared to ampicillin **5.38** (MIC = 5 µg/mL).[9] Erythrophloin C **5.42** displayed anti-tubercular activity against *Mycobacterium tuberculosis* (MIC = 50 µg/mL).[23]

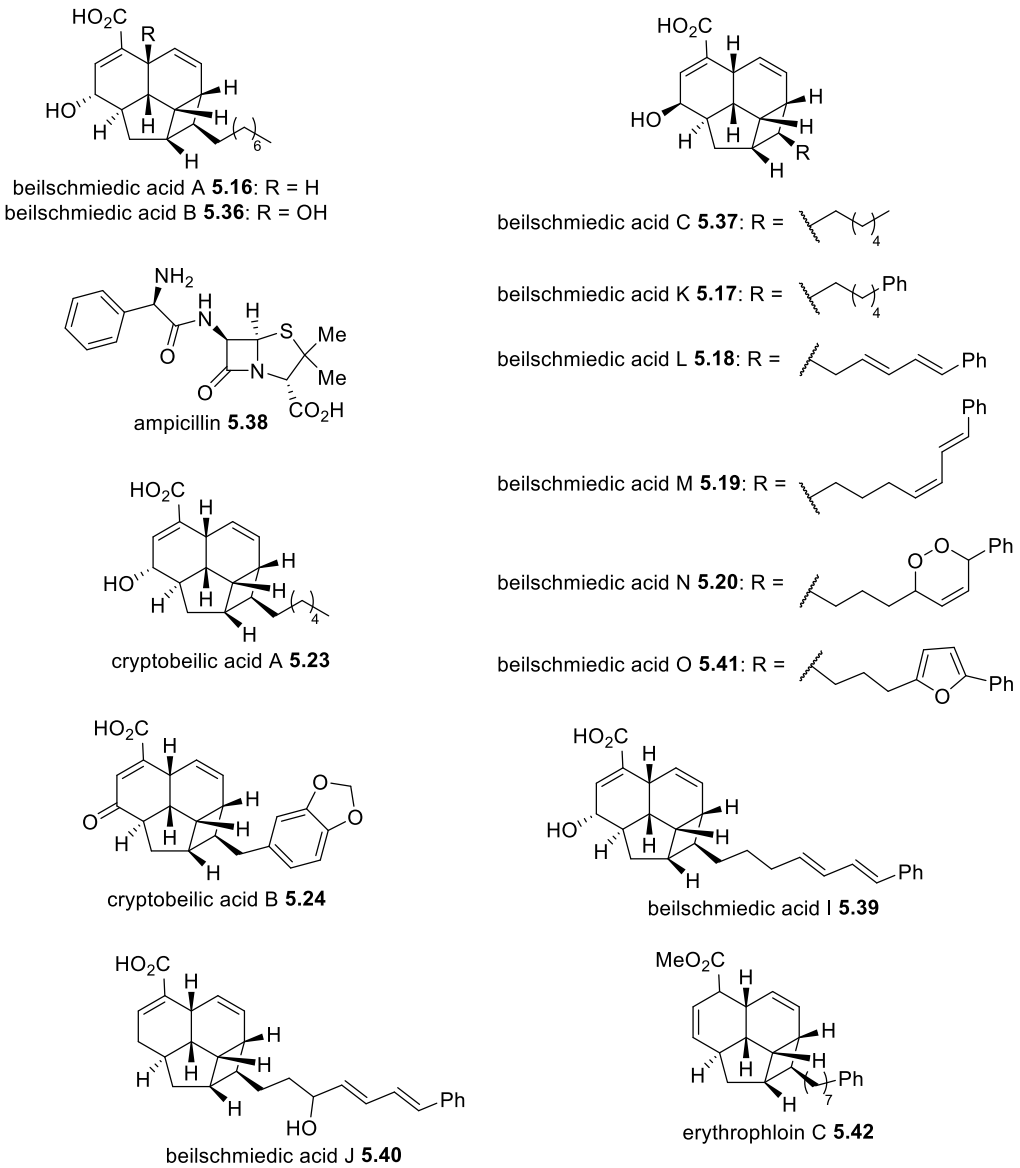

Figure 5.6: Structures of endiandric acid derivatives with anti-microbial properties

5.1.3.6 Anti- hyperglycaemic

For anti-hyperglycaemic capabilities, kingianin L **5.15** proved a more potent α-amylase inhibition activity (IC_{50} = 0.0008903 ± 0.5 mg/mL), compared to acarbose **5.43** (IC_{50} = 0.03 ± 0.01 mg/mL). kingianin M **5.44** shown better inhibition against α-glucosidase (IC_{50} = 0.11 ± 0.08 mg/mL), compared to acarbose **5.43** (IC_{50} = 1.81 ± 0.1 mg/mL).[24]

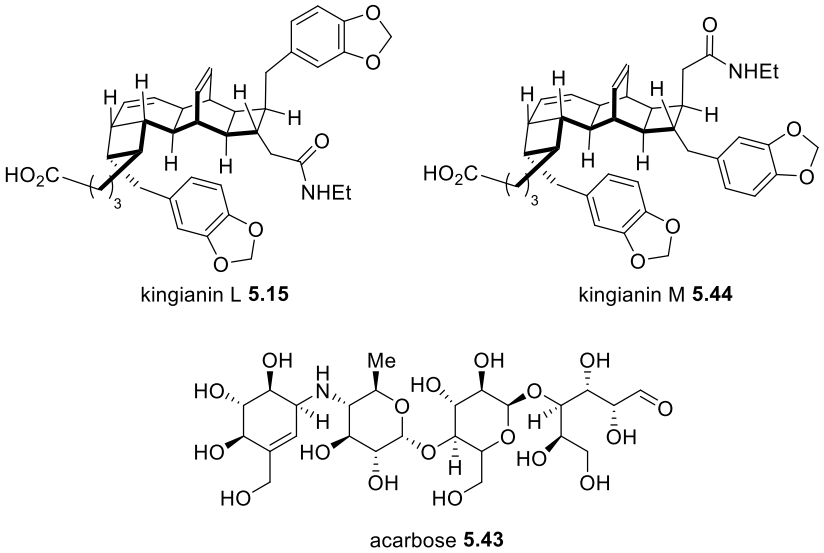

Figure 5.7: Structures of endiandric acid derivatives with anti- hyperglycaemic properties

It must be highlighted that the above biological testings have only been conducted on isolates, with no testing on synthetic material or analogues and represents a gap in knowledge that can be targeted.

5.2 Summary of all previous total syntheses

The combination of a scholarly interest in the biosynthesis of endiandric acid derivatives and their potential pharmaceutical value led to them becoming a target for total synthesis. All reported syntheses of this family of natural products are summarised within this section.

5.2.1 Nicolaou – endiandric acids A-G

K.C Nicolaou was the first to report total syntheses of members of this family of natural products. A series of four papers in 1982 detailed two approaches to accessing endiandric acids A-G (**5.45**-**5.51**).[25–28] The first two papers report an abiotic approach of selectively accessing individual products and the last two articles follow a biomimetic strategy, taking direct inspiration from Black's proposed biosynthesis, and consequently validating the hypothesis.

The abiotic synthesis began by subjecting decadiene-diyne-diol **5.52** (one step from 2-penten-4-yn-1-ol) to semi-hydrogenation conditions yielding an E,Z,Z,E tetraene diol **5.53** which collapsed into the BOD diol **5.54** through the 8π/6π cascade in 45-55% yield over two steps. Trapping the endo alcohol through an iodoetherification furnished alcohol **5.55**. Further manipulations of unmasking the alcohol **5.55** and its conversion to the nitrile **5.56** was to construct a molecule with two different functional handles for derivatisation, ultimately serving as the central intermediate. Endiandric acid D **5.48** was synthesised in eight steps from BOD **5.56**, with a further four steps to convert it into endiandric acid G **5.51**. DIBAL-H reduction of BOD **5.56** furnished aldehyde **5.57**, where choice of Horner−Wadsworth−Emmons (HWE) reagent leads to divergent pathways of either accessing the bridged or fused tetracycles. Installation of a methacrylate moiety through the HWE reaction was followed by the IMDA reaction (see intermediate **5.58**) to lock it into the bridged tetracycle. A further seven steps yielded endiandric acid C **5.47**. Alternatively, installation of the phenyl diene motif gave compound **5.59** which was further functionalised to fused tetracycles endiandric acid A **5.45** and endiandric acid B **5.46** in five and seven steps, respectively. Compound **5.59** was converted to aldehyde **5.60** (over four steps) providing access to endiandric acids E **5.49** and F **5.50**.

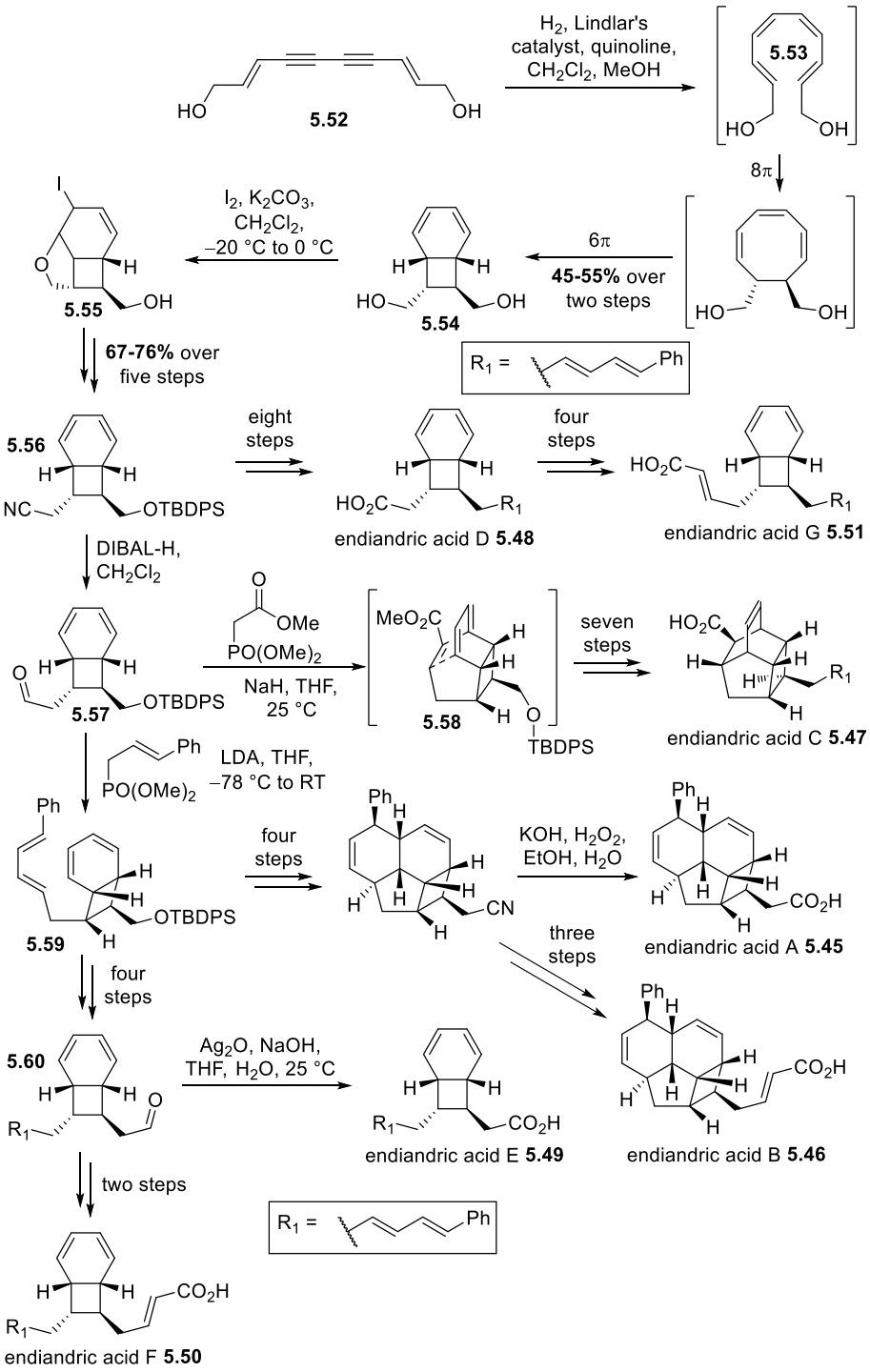

Scheme 5.3: Nicolaou's abiotic total synthesis of endiandric acids A-G

Polyenyne **5.61** (accessed in 13 steps) was semi-hydrogenated under the same earlier conditions, followed by heating in toluene at 100 °C to yield endiandric methyl ester A **5.62** in 30% yield. No observation of endiandric methyl ester D **5.63** and E **5.64** was made, however examination of the hydrogenation mixture revealed their presence and were subsequently isolated in 12% and 10%, respectively. No observation of the proposed cyclooctatrienes and conjugated tetraene gave early insight into the kinetics and thermodynamics of this cascade. Polyenyne **5.65** (accessed in 14 steps) was exposed to semi-hydrogenation giving isolated yields of 15% and 12% for endiandric methyl ester F **5.66** and G **5.67**, respectively. Semi-hydrogenation followed by consequential thermal conditions yielded a mixture of endiandric methyl ester B **5.68** and C **5.69** in 23% and 5% yield, respectively. This result highlighted the preference for the formation of the fused tetracycle **5.68** over the bridged **5.69** (ratio of 4.5:1, respectively) in instances where both modes of the IMDA reactions are possible.

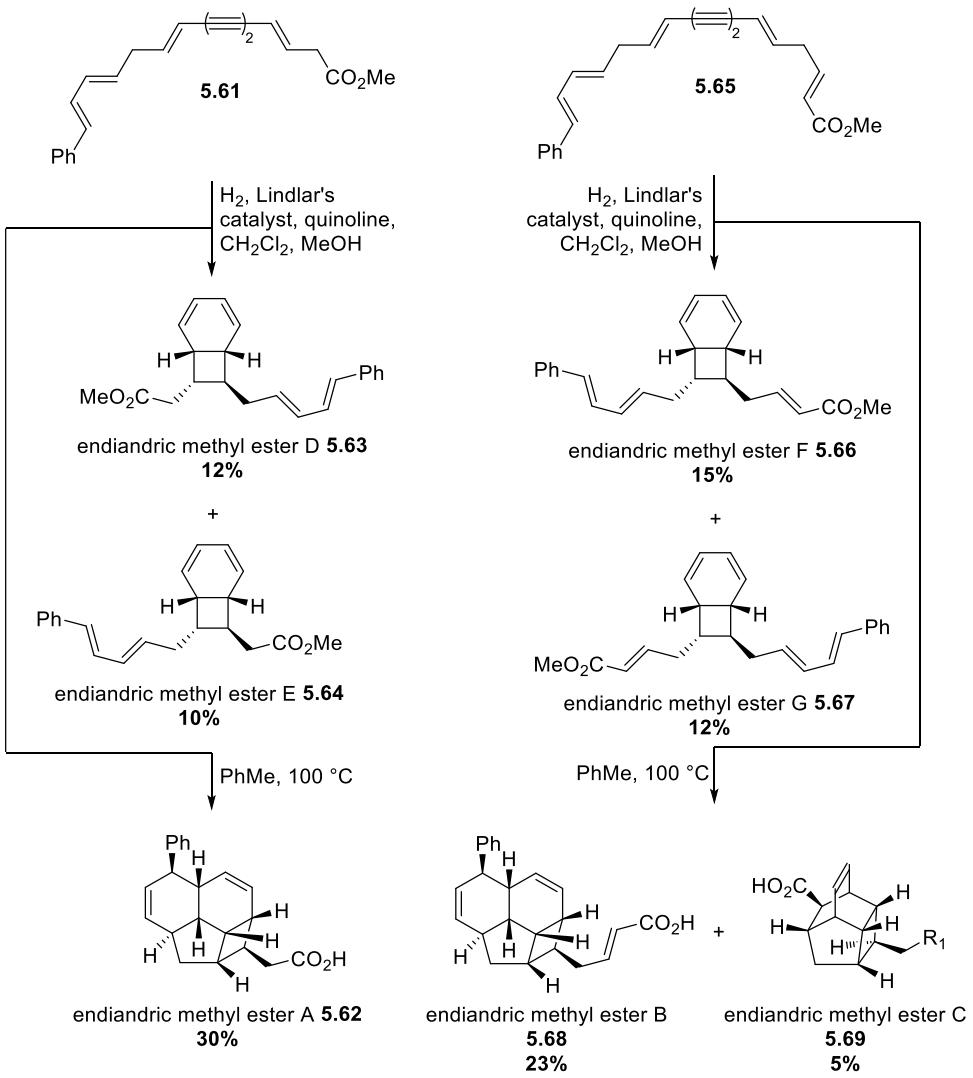

Scheme 5.4: Nicolaou's biomimetic total synthesis of endiandric esters A-G

Nicolaou's work represents a landmark in the application of pericyclic cascades in biomimetic total synthesis, however it has some shortcomings. The high step count and capricious semi-hydrogenation that only provided respectable and reproducible yields of 45-55% with an inaccessible "super" Lindlar catalyst (gifted by John Partridge at Roche inc.) have been major limitations of further utilisation of Nicolaou's methodology.[29]

5.2.2 Vosburg – cryptobeilic ethyl ester D

Vosburg in 2016 constructed E,Z,Z,E tetraene **5.70** from the Suzuki coupling of fragments **5.71** and **5.72** (both accessed from compound **5.73**) which succumbed to the cascade to form BOD **5.74** in 59% yield.[30] A further four steps to install the ethyl ester diene and perform the IMDA furnished cryptobeilic ethyl ester D **5.75** in 47% over four steps. An ester hydrolysis would afford the actual natural product: cryptobeilic acid D **5.26**.

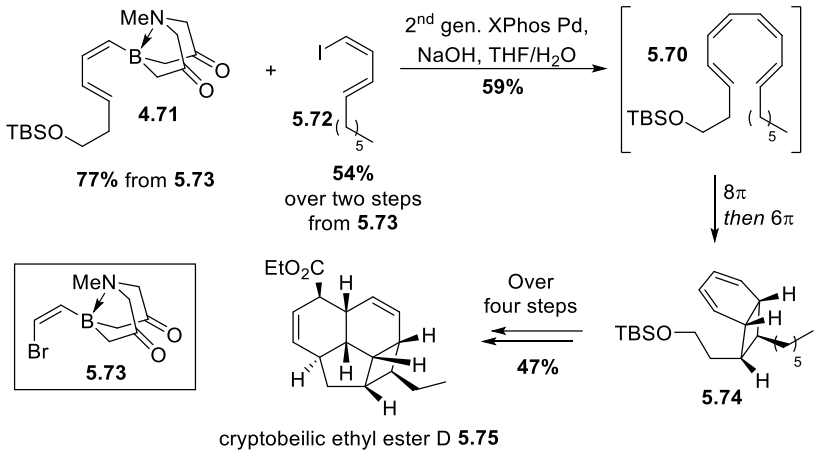

Scheme 5.5: Vosburg's total synthesis of cryptobeilic ethyl ester D

This strategy of cross-coupling two diene fragments (**5.71** and **5.72** in this case) has been commonly used in the synthesis of several BOD containing compounds.[31–34] The main drawbacks of this approach is the high step count of making the fragments and their substrate specific nature.

5.2.3 Sherburn and Lawrence – endiandric acid A, kingianic acid F, kingianin A, D and F

Sherburn and Lawrence's approach can be considered complementary to Nicolaou's biomimetic synthesis, focusing on the viability of a Z,Z,Z,Z-tetraene undergoing the biosynthetic cascade (instead of a E,Z,Z,E tetraene).[35] Tetryne molecule **5.76** (accessed from **5.77** in 48% over three steps) was converted to phenyl pentadiene tetryne **5.78** in 16% over two steps. Rieke zinc semi-hydrogenation afforded Z,Z,Z,Z tetraene **5.79** where subjection to thermal and deprotection conditions yielded fused tetracycle **5.80** in 22% over two steps. Conversion of the primary alcohol to the carboxylic acid via Ley oxidation gave endiandric acid A **5.45** in 86% yield. Under a similar protocol, an isosafrole fragment was coupled, forming compound **5.81**, followed by semi-hydrogenation to intermediate **5.82**. An 8π/6π/IMDA cascade, deprotection (to **5.83**) and oxidation presented kingianic acid E **5.22**.

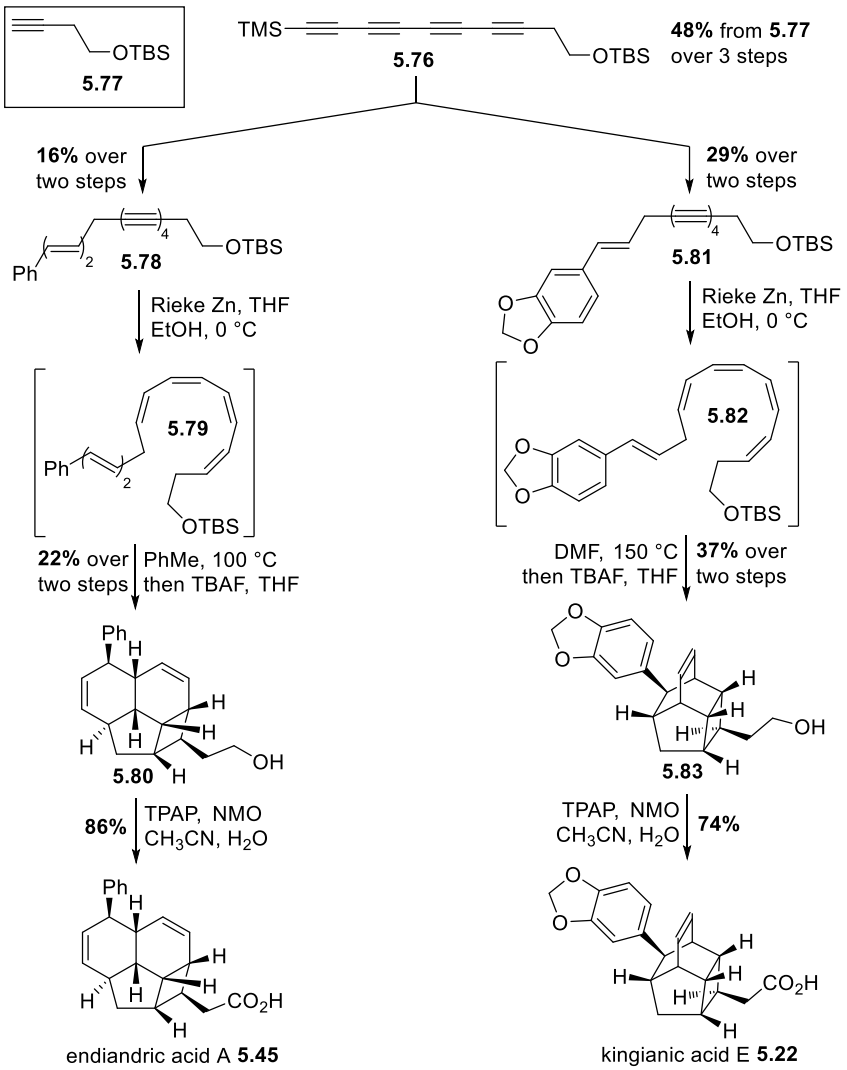

Scheme 5.6: Sherburn and Lawrence's total synthesis of endiandric acid A and kingianic acid E

Their kingianin synthesis began with the semi-hydrogenation of tetraene **5.84** (made in 22% yield over six steps), followed by an 8π/6π/IMDA cascade and deprotection to deliver a 1:1 separable mixture of BOD diastereomers **5.85** and **5.86** (Scheme 5.7). BOD diastereomer **5.85** was oxidised to the carboxylic acid and then underwent a radical cation intermolecular DA with Ledwith−Weitz salt **5.87** to afford the pentacyclic framework. Amide coupling gave kingianin A **5.88** and D **5.89** in a 10:3 mixture (17% yield over three steps). BOD diastereomer **5.86** was first subjected to Ledwith-Weitz salt **5.87** followed by oxidation and amide coupling to give kingianin F **5.90** in an 8:6 mixture with other products (37% over three steps).

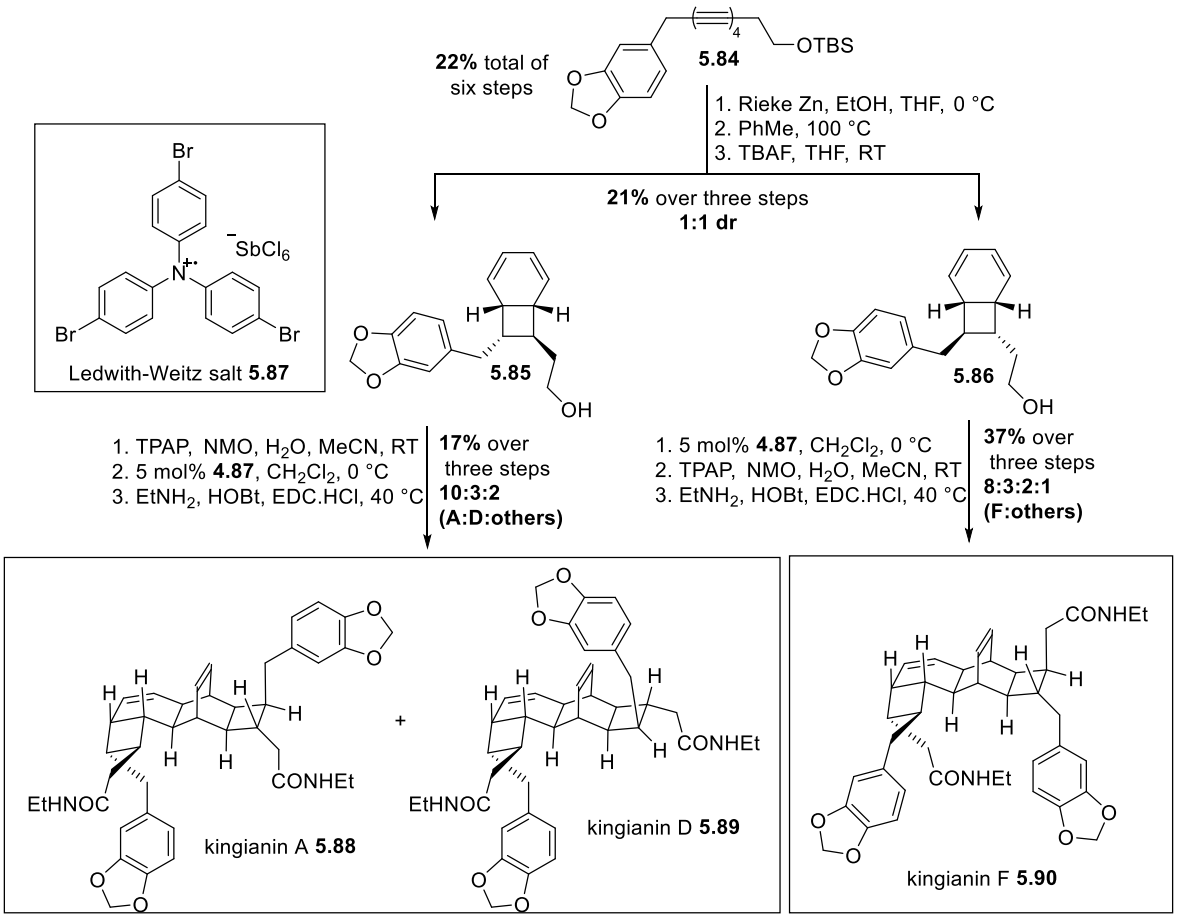

Scheme 5.7: Sherburn and Lawrence's total synthesis of kingianin A, D and F

5.2.4 Parker – kingianin A, D, F, H, J

In Parker's first synthesis of kingianin A, a mixture of BOD alcohols **5.91** and **5.92** were linked using adipoyl dichloride to give a mixture of C-2 symmetric dimer **5.93** and racemic substrate **5.94** (Scheme 5.8).[36] A radical cation DA (RCDA) reaction synthesised the desired product **5.95** in 34% yield and other product **5.96** in 39% yield. Pentacycle **5.95** was converted to kingianin A **5.88** in 26% over five steps. The reasoning behind this strategy was to selectively form pentacycle **5.95**. It was hypothesised that racemic substrate **5.94** wouldn't undergo the RCDA to form the *endo*-cycloadduct, however to their surprise, the *exo*-cycloadduct **5.96** was formed as the major.

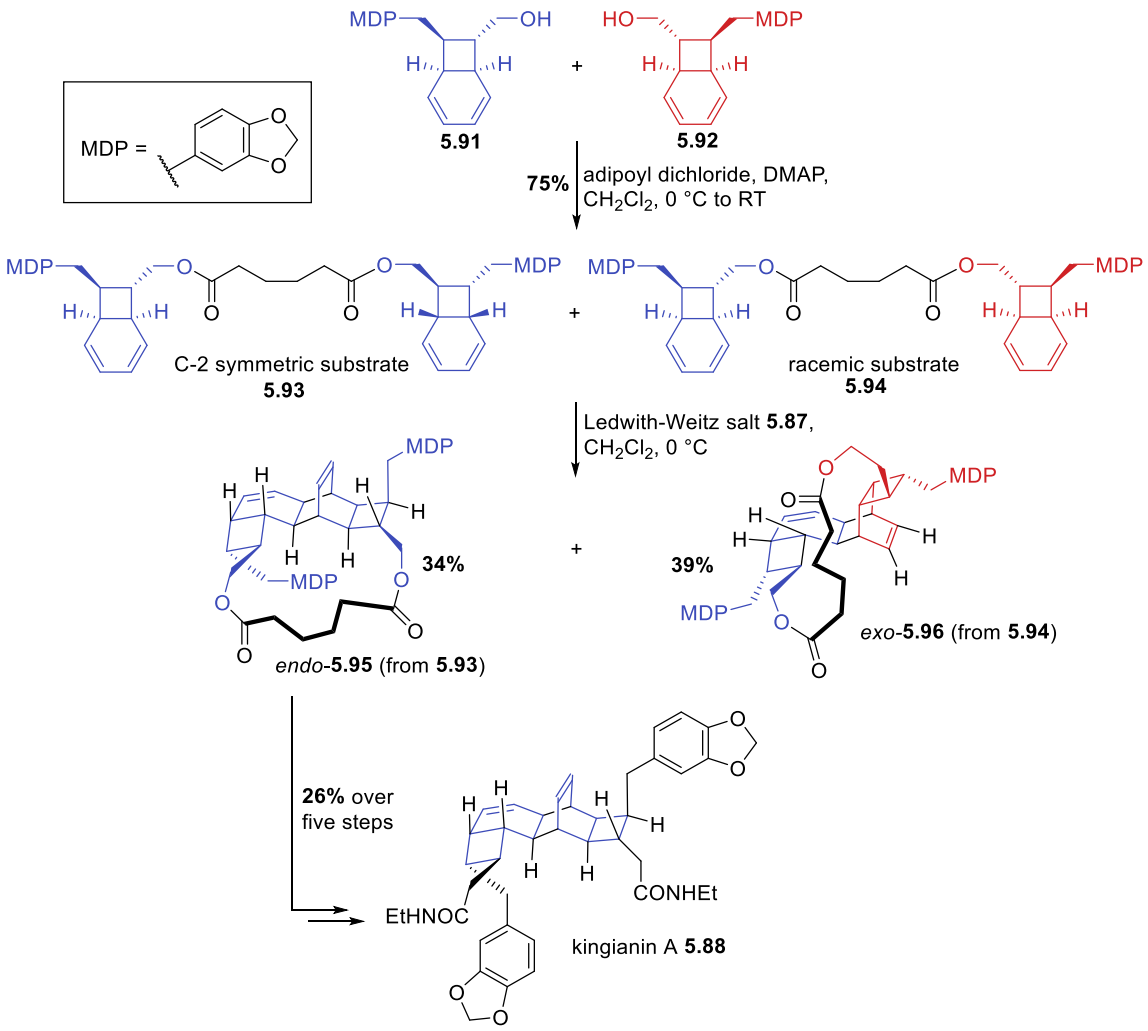

Scheme 5.8: Parker's 2013 total synthesis of kingianin A

Therefore, Parker subsequently chose to forgo the tether strategy when pursuing more kingianin natural products.[37] The alcohol BOD **5.91** underwent a RCDA, affording a separable mixture of pentacycles **5.97** and **5.98** (along with other compounds) in 37% and 18% yield, respectively (Scheme 5.9). Pentacycle **5.97** was converted over three steps into kingianin H **5.99** in 50% yield and pentacycle **5.98** was converted to kingianin D **5.100** in 32% over four steps.

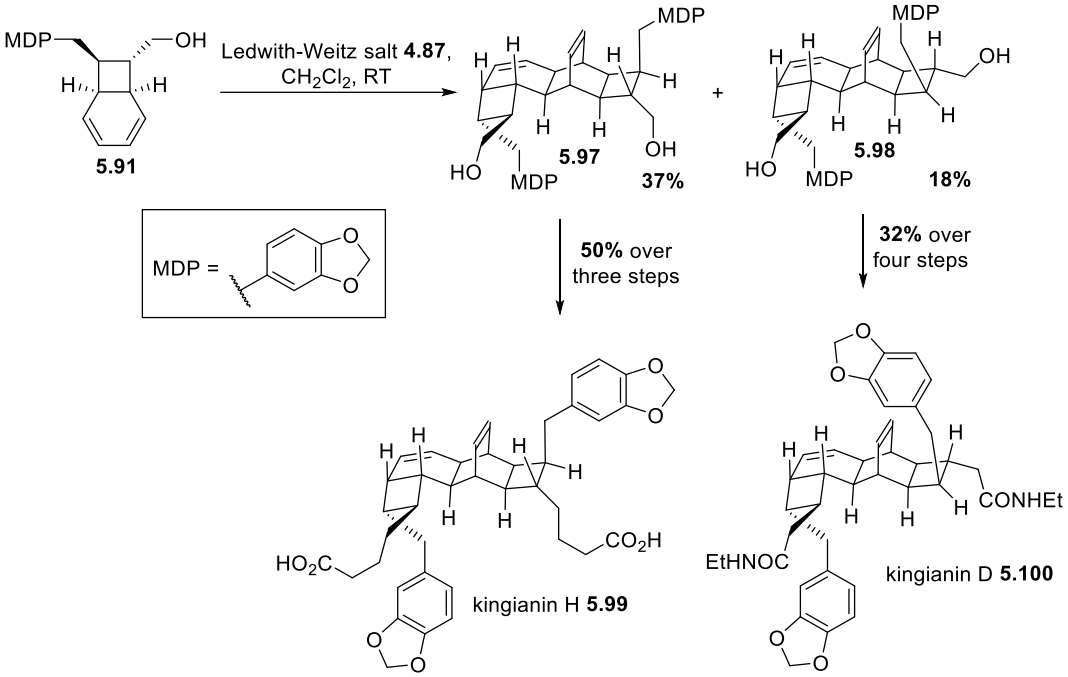

Scheme 5.9: Parker's 2014 total synthesis of kingianin D and H

Alcohol BOD **5.101** was converted to acetate **5.102** (in 89% yield) and then subjected to RCDA conditions followed by alcohol deprotection via $LiAlH_4$ to yield pentacycle **5.103** in 46% yield over two steps. Conversion to kingianin F **5.104** occurred in 28% over four steps or alternative access to kingianin J **5.105** happened in 6% over 8 steps.

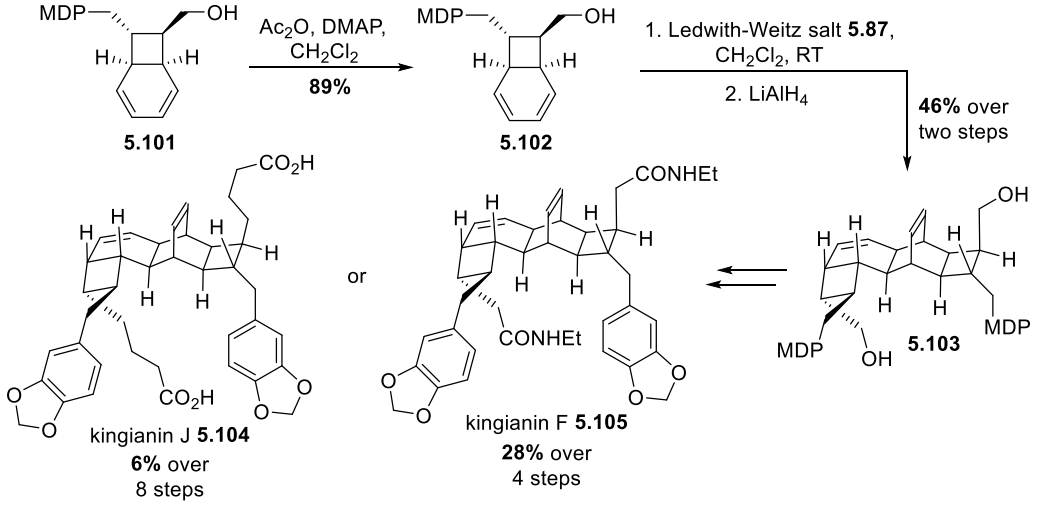

Scheme 5.9: Parker's 2014 total synthesis of kingianin F and J

5.2.5 Moses – kingianin A (formal)

Moses in 2014 reported a formal synthesis of kingianin A **5.88** which employs an electrochemically-mediated RCDA delivering pentacycle **5.97** from BOD **5.91** in 13% yield, intersecting Parker's previous syntheses.[38] The advantage of the electrochemical RCDA over the Ledwith−Weitz salt **5.87** is the ability to selectively form one pentacyclic species from a mixture of diastereomers without the complication of forming mixed dimeric species. This was owed to an intramolecular cyclisation of BOD **5.106** forming tricycle **5.107**.

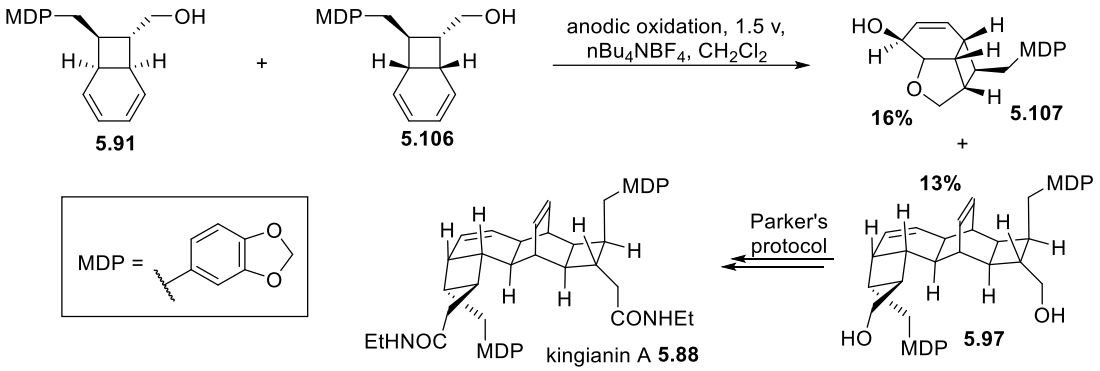

Scheme 5.10: Moses' 2014 formal total synthesis of kingianin A

5.2.6 Grieco – endiandric acid A

Grieco's synthesis of endiandric acid A is quite unique in how it completely disregards Black's proposed biosynthetic strategy.[39] Cyclohexenone **5.108** was synthesised in seven steps in 59% overall yield. A Lewis acid catalysed DA gave tricycle **5.109** followed by functionalisations to deliver compound **5.110** in 48% yield over four steps. A 4-exo-trig cyclisation presented the familiar tetracycle **5.111** in 65% yield. A further five steps of functionalisation afforded endiandric acid A **5.45** in 24% yield. The high step count in this purely abiotic total synthesis, supports Black's biosynthetic cascade to be the most efficient way to construct the skeletal cores of the endiandric acid family.

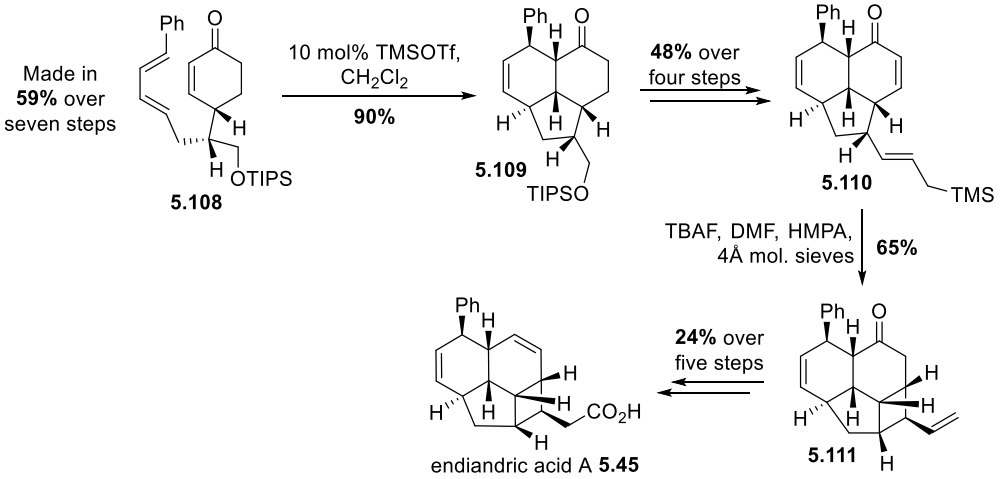

Scheme 5.11: Grieco's 1997 total synthesis of endiandric acid A

5.2.7 Lu – (−)-kingianin F

Recently, Lu developed a methodology on the enantioselective Diels−Alder reaction of cyclobutenones which was applied to the first reported enantioselective synthesis of an endiandric acid natural product.[40] Bicyclooctene **5.112** was synthesised by the enantioselective DA between cyclobutanone **5.113** and butadiene **5.114** in 93% yield and 93% enantiomeric excess. Over the course of five steps, removal of the ester and installation of the prerequisite substituents occurred in 30% yield providing compound **5.115**. A diastereoselective reduction of the enoate **5.115** to compound **5.116** proceeded in 99% yield and 12:1 diastereomeric ratio. Careful temperature-controlled manipulations to afford BOD **5.117** progressed in 48% yield over three steps. The Sherburn/Lawrence protocol stated earlier was applied here to finally deliver (−)-kingianin F **5.105** in 18% yield over three steps.

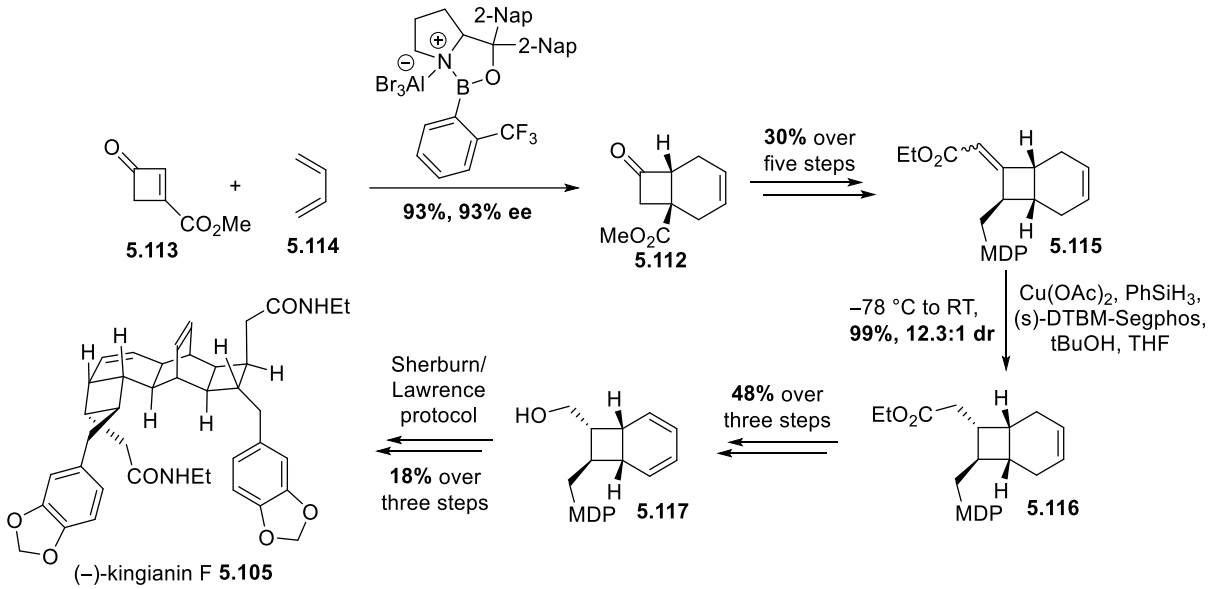

Scheme 5.12: Lu's 2021 enantioselective synthesis of (−)-kingianin F

Lu's synthesis represents a shift in dogma in terms of being able to access enantiopure BOD compounds that have otherwise been experimentally and theoretically shown to racemise during their synthesis (through reversibility in the 8π/6π cascade).[41–43] The main limitation of this methodology is the non-trivial diastereoselective reduction requiring a specialised ligand, which may not extrapolate well to other BOD substrates.

5.3 Aims

The general strategy to form endiandric acid derivatives (shown throughout section 5.2) is to synthesise a tetraene to then undergo Black's biosynthetic cascade, with the exception of a few notable cases (e.g., Grieco and Lu)[39,40]. Construction of the tetraene often involves cross-coupling or semi-hydrogenation chemistry, which aren't necessarily trivial, have high step counts and are substrate specific (Scheme 5.13). The Fallon group envisioned a methodology involving the *anti*-1,2-difunctionalisation of cyclooctatetraene **5.118** (COT) to intersect the biosynthesis, which would invariably be a more efficient synthesis of BOD compounds.

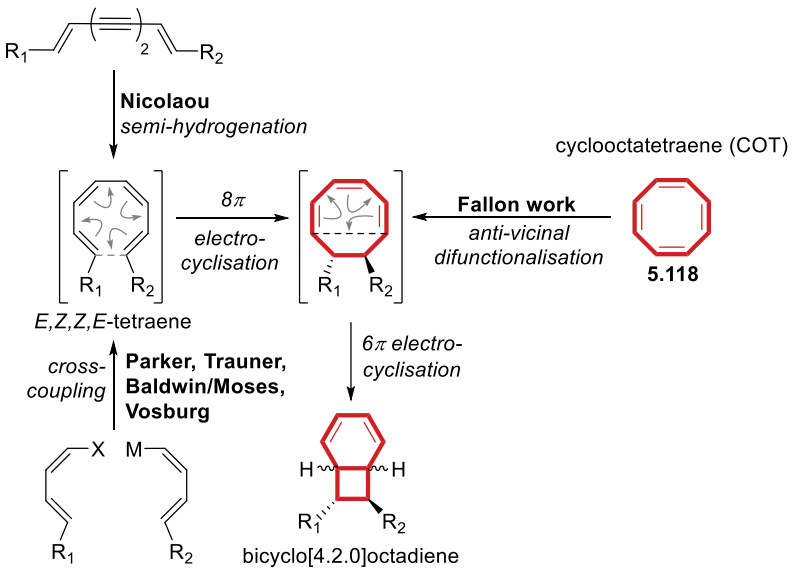

Scheme 5.13: Common methodologies to intersect Black's 8π/6π biosynthetic cascade and our own proposal via cyclooctatetraene

Nicolaou has already previously investigated this strategy during his hallmark total synthesis of endiandric acids A-G (Scheme 5.14).[29] COT **5.118** is known to undergo addition with electrophiles such as bromine to deliver 1,2-disubstituted cyclooctatrienes **5.119a** which are in equilibrium with the corresponding BOD **5.120a**.[44] The bromine addition product preferentially lies as the BOD **5.120a**, already delivering the desired BOD skeleton, however requires replacement of the bromine with a carbon substituent. A substitution reaction with KCN initially forms **5.120b** however equilibrates to **5.121b**, since it is thermodynamically favourable for the product to have extended conjugation.[45] The same outcome occurs when **5.120a** is reacted with acetylenic Grignard reagents to afford the linear tetraene **5.121c**.[46] The treatment of COT with alkali metals (Li, Na or K) provides a dianion that is capable of delivering 1,2-disubstituted cyclooctatrienes **5.119**, when quenched with a suitable electrophile. Quenching with methyl iodide affords **5.120d** in low yields, and addition of carbon dioxide preferentially gives the linear tetraene **5.121e**.[47,48] Conversion of acid **5.121e** to the ester derivative presented **5.120f** when the initially formed **5.121f** was heated to 80 °C. Further manipulations to arrive at a synthetically useful compound, such as **5.120g**, would eventually prove unattractive. Despite being a highly direct route, the overall low yields starting from **5.118** and the starting material expense would forcibly turn Nicolaou's attention to another strategy that would ultimately be used in his published total synthesis.[25–28]

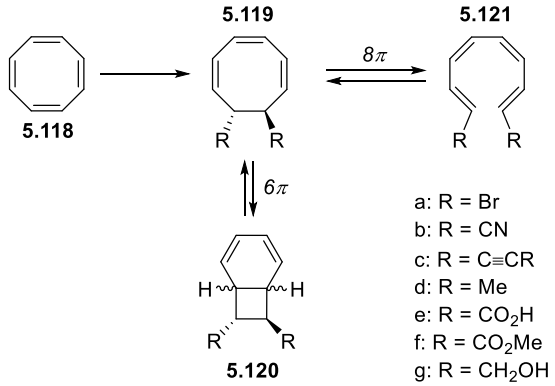

Scheme 5.14: Nicolaou's investigation on cyclooctatetraene derivatisation

5.3.1 Previous Fallon group approaches

To avoid the issues highlighted by Nicolaou, Fallon group devised indirect *anti*-1,2-difunctionalisation approaches. The first-generation strategy started with the epoxidation of COT **5.118** to give epoxide **5.122** in 71%, followed by an *anti*-S_N2' ring opening using dodecyl cuprate to provide alcohol **5.123** in 96% yield.[41] Subsequent gold-catalysed vinyl transfer, Claisen rearrangement (see intermediate **5.124**) and 6π electrocyclisation presented BOD **5.125** in 48% over two steps. Wittig olefination on the aldehyde handle with 1-(triphenylphosphoranylidene)-2-propanone followed by heating at 120 °C gave beilcyclone A **5.126** in 61% yield over two steps. Use of Ethyl triphenylphosphoranylideneacetate followed by heating afforded endiandric ethyl ester J (54% over two steps) which was then hydrolysed to the acid **5.127** in 72%. The alkylation/vinyl transfer/Claisen key step to form BOD **5.125** was inspired by Pineschi's work on stereoselective and enantioselective *anti*-S_N2' ring opening addition reactions on COT-epoxide **5.122**.[49,50] Pineschi observed that after esterification to form **5.128**, a [3,3]-ester transposition of **5.129** and subsequent 6π electrocyclisation furnished the corresponding BOD ester **5.130** (Scheme 5.15B). Enabling a Claisen rearrangement instead of a [3,3]-ester transposition would lead to intermediates relevant to endiandric acids.

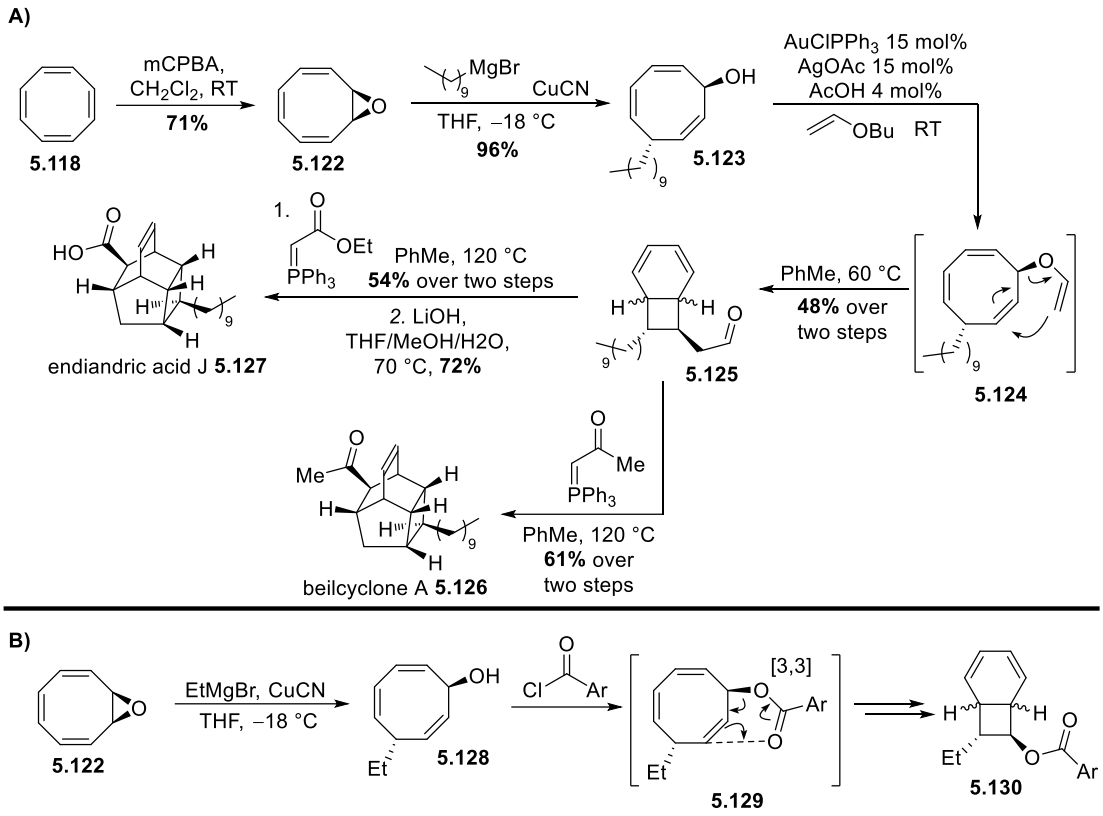

Scheme 5.15: A) Fallon's 2020 total synthesis of beilcyclone A and endiandric acid J. B) Pineschi's alkylation of COT-epoxide

However, the first-generation alkylation/vinyl transfer/Claisen method is still inefficient in constructing BOD compounds and therefore a more concise route was explored. In 2022, the second-generation method led with the rhodium-catalysed cyclopropanation of cyclooctatetraene **5.118** to deliver cyclopropane **5.131** in 72%. A 1,5-nucelophilic ring-opening using piperonyl cuprate was then followed by hydrolysis to the diacid **5.132** in 87% yield. Decarboxylation upon treatment with CDI afforded a N-acyl imidazole intermediate which was then reduced by DIBAL-H to the BOD **5.133** in 30% yield. Wittig olefination followed by reflux and hydrolysis furnished kingianic acid A **5.21** in 50% and 92% yield, respectively. This strategy impressively delivers a synthetically useful BOD for total synthesis in a rapid two steps. However, there are major drawbacks which limit its utility in further endiandric acid derivative synthesis. Synthesising organocuprate/copper reagents that are selective for 1,5-addition **5.134** is challenging, where the cuprate species formed may instead undergo 1,7- **5.135** and even 1,2-addition **5.136** (when cuprate has failed to form) (Scheme 5.16B).

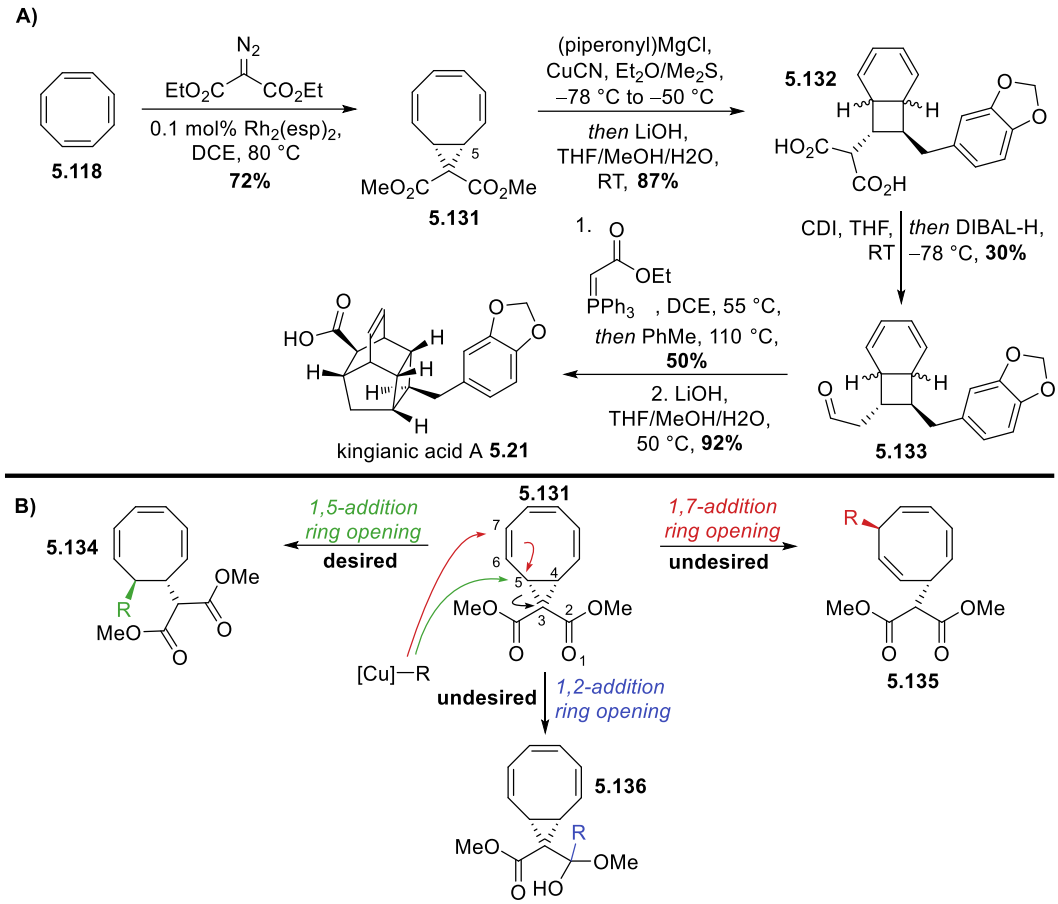

Scheme 5.16: A) Fallon's 2022 total synthesis of kingianic acid A. B) Selectivity issues of cuprate addition

These two approaches provide among the fastest generation of natural product relevant BOD intermediates to date, but are depend on cuprate chemistry which is difficult to perform and substrate specific. Therefore, it would be apt to develop a more user-friendly methodology, based on simple access to a central intermediate that serves as a point of divergence to several endiandric acid derivatives.

5.3.2 Current approach

5.3.2.1 Holmes' synthesis of cyclooctatrienone derivatives

We identified Holmes' work as another strategy towards the indirect *anti*-1,2-difunctionalisation of COT from which we envisioned a route to the synthesis of endiandric acid derivatives. Holmes reported the synthesis of a variety of cyclooctatrienone derivatives from COT-epoxide **5.122** (Scheme 5.17).[51] They found that the treatment of COT-epoxide **5.122** with LDA in a HMPA/THF solvent mix forms a stable COT lithium enolate **5.137** at −78 °C. The formation of COT lithium enolate **5.137** was postulated to arise from the deprotonation of C1 on **5.122** and then rearrangement to the enolate.[52] The HMPA/THF solvent mixture is responsible for stabilising the enolate anion to allow for the subsequent alkylation. Alkylation at the C8 position of **5.137** with a variety of electrophiles such as methyl iodide, ally bromide, bromoselenobenzene and bromine furnished substituted cyclooctatrienones **5.138a-d**, respectively.

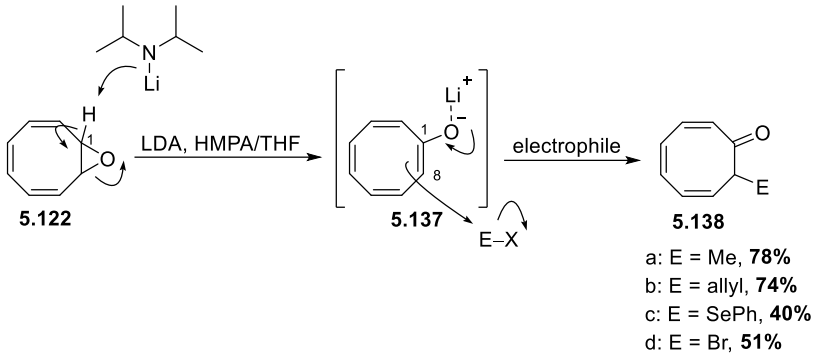

Scheme 5.17: Select examples from Holmes' COT lithium enolate alkylation work

Cyclooctatrienone **5.139** itself is found to be extremely unreactive for derivatisation at the C8 carbon via the enolate anion and is the motive for Holmes' study. The parent unsubstituted cyclooctatrienone **5.139** can be synthesised from the treatment of COT-epoxide **5.122** with LDA in THF solvent. Studies by Matsuda revealed nucleophilic addition of alkoxides to the carbonyl on **5.139** induces a ring contraction to cyclohexadiene compounds **5.140a-d**.[53] Roberts performed deuterium experiments on **5.139** by reacting it under forcing NaOD, D_2O conditions, incorporating deuterium atoms at the C2, C6, C7 and C8 positions on compound **5.141**.[54]

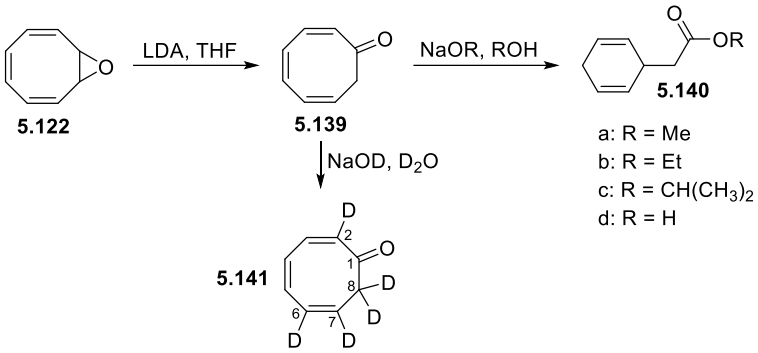

Scheme 5.18: Synthesis of unsubstituted cyclooctatrienone with studies by Matsuda and Roberts

Gund and Carpino have also shown under non-nucleophilic bases and a variety of electrophiles that cyclooctatrienone **5.139** was resistant to substitution.[55] Reactions with n-butyl nitrite, NBS and trimethylene thiotosylate all failed to synthesise their corresponding compounds (**5.142**, **5.138d** and **5.143**, respectively).

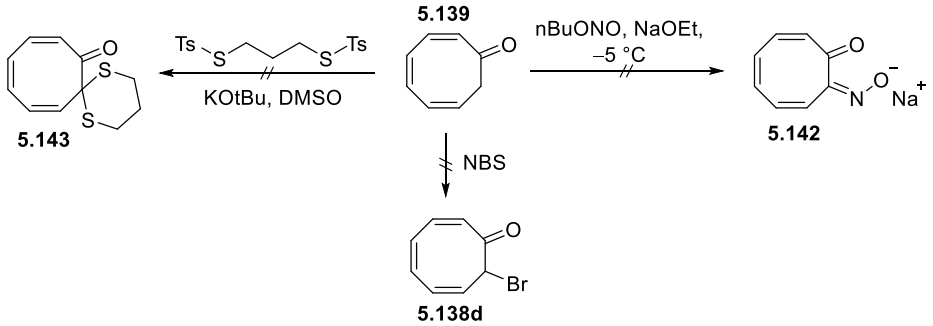

Scheme 5.19: Studies by Gund and Carpino on substituted cyclooctatrienone synthesis

One other known method for preparing cyclooctatriene derivatives is via the diazoalkane induced ring expansion of tropone **5.144**, however the substrate scope is very limited (Scheme 5.20).[56]

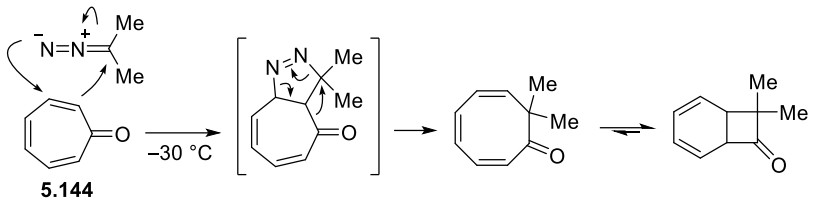

Scheme 5.20: Franck-Neumann's work on diazoalkane induced ring expansion of tropone

5.3.2.2 Our postulated third-generation total synthesis methodology

Taking inspiration from the synthesis of cyclooctatrienone **5.138b**, a derivative of an allylic electrophile should react with the cyclooctatrienone enolate **5.137** to furnish the corresponding compound **5.145.** Functionalisation of the ketone via homologation or 1,2-carbonyl addition/deoxygenation strategies should yield a BOD **5.146** that can undergo an IMDA to form bridged tetracyclic endiandric acid derivatives.

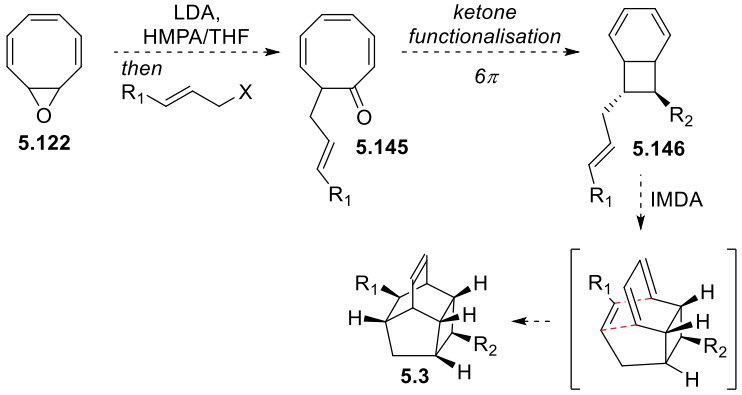

Scheme 5.21: Third-generation methodology for endiandric acid natural product synthesis

5.4 Methodology development

5.4.1 Synthesis of substituted cyclooctatrienones (installation of the first substituent)

We began with the successful synthesis of cyclooctatrienone ester **5.147** with ethyl (E)-5-bromopent-2-enoate as the electrophile in 52% yield (Scheme 5.22). It was theorised that compound **5.147** can easily undergo transformations highlighted in scheme 5.21 (ketone functionalisation followed by 6π/IMDA cascade) to deliver bridged tetracyclic acids such as kingianic acid A **5.21**.

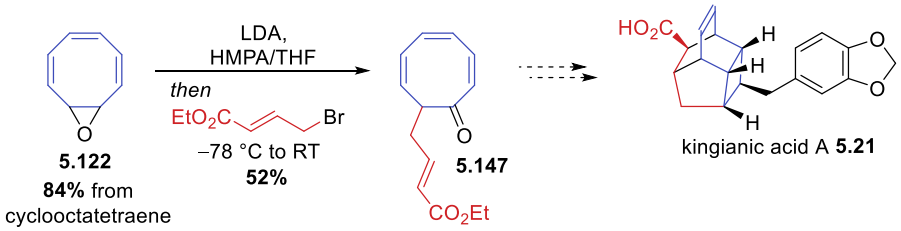

Scheme 5.22: Synthesis of cyclooctatrienone ester 5.147 via ethyl (E)-5-bromopent-2-enoate

Improvements in yield were accomplished by exchanging the bromo-electrophile with an iodo-electrophile, increasing it to 80% yield (Scheme 5.23).

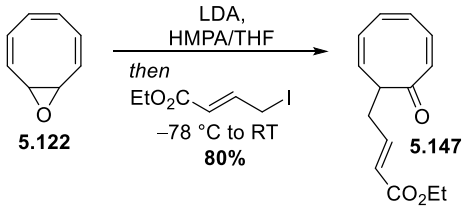

Scheme 5.23: Synthesis of cyclooctatrienone ester 5.147 via ethyl (E)-5-iodopent-2-enoate

HMPA is recognised as a toxic carcinogen, therefore a comparatively safer co-solvent, DMPU, was used with little difference, giving a yield of 76% (Scheme 5.24). We continued to use HMPA out of convenience, but these results highlight safer alternatives to HMPA are viable.

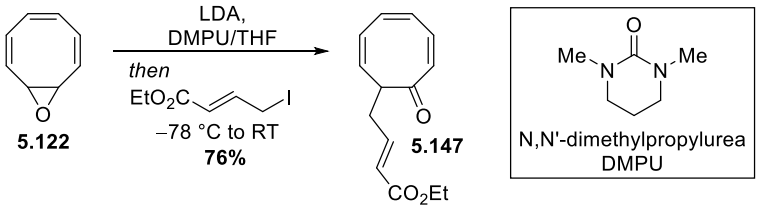

Scheme 5.24: Synthesis of cyclooctatrienone ester 5.147 via ethyl (E)-5-iodopent-2-enoate with DMPU as co-solvent

We also fostered an interest in accessing other bridged tetracycles that either relate to endiandric products or non-natural derivatives. Electrophile 1,3-Benzodioxole, 5-(3-bromo-1-propenyl)-, (*E*)- (ZCI) delivered good yields of 64% yield of cyclooctatrienone **5.148**, which maps on to kingianic acid E **5.22**. Extending beyond the endiandric acid family scope, (E)-cinnamyl iodide and 4-(bromomethyl)-2(5H)-furanone provided their corresponding products **5.149** and **5.150** in yields of 47% and 31%, respectively. 3-(Bromomethyl)-2,5-furandione regrettably furnished unsubstituted cyclooctatrienone **5.139**.

Table 5.1: Synthesis of cyclooctatrienones 5.148-5.150

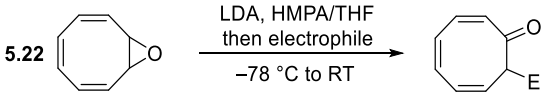

Entry	Electrophile	Result
1	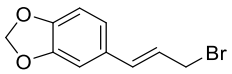	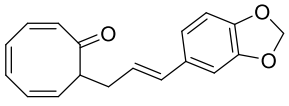 **5.148** **64%**
2	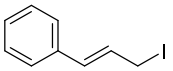	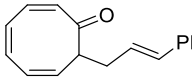 **5.149** **47%**
3	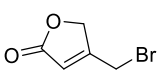	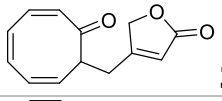 **5.150** **31%**
4	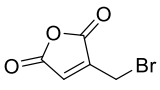	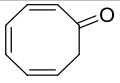 **5.139** (Sole product in crude NMR)

5.4.2 Installation of the second substituent via ketone functionalisation

5.4.2.1 Initial investigations

The ketone lends a suitable handle to functionalise and intersect intermediates in endiandric natural product synthesis. We proposed a nucleophilic addition to form alcohol **5.151** from

5.147 and then a deoxygenation to compound **5.152** would complete the formal *anti*-1,2-difunctionalisation of COT, and allow access to relevant natural products **5.153**. However, the 1,2-additions with Grignard reagents were unsuccessful. An alternative tactic by undertaking a Wittig olefination with (methoxymethyl)triphenylphosphonium chloride to produce compound **5.154** and then hydrolysis to aldehyde **5.155**, was also unsuccessful.

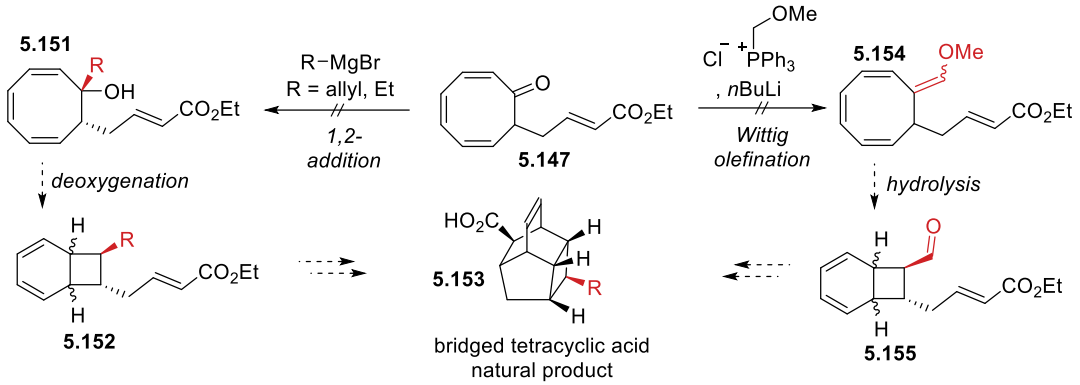

Scheme 5.25: Initial attempts at ketone functionalisation

We conjectured that Grignard addition to the ketone, forming **5.156**, is followed by a facile 8π ring-opening to tetraene **5.157** and then further rearrangements (Scheme 5.26). Wittig reagents that are formed under lithium base conditions generally enable betaine intermediate formation (see intermediate **5.158**), which is similar to the Grignard addition intermediate **5.156** and would undergo the same degradation process.

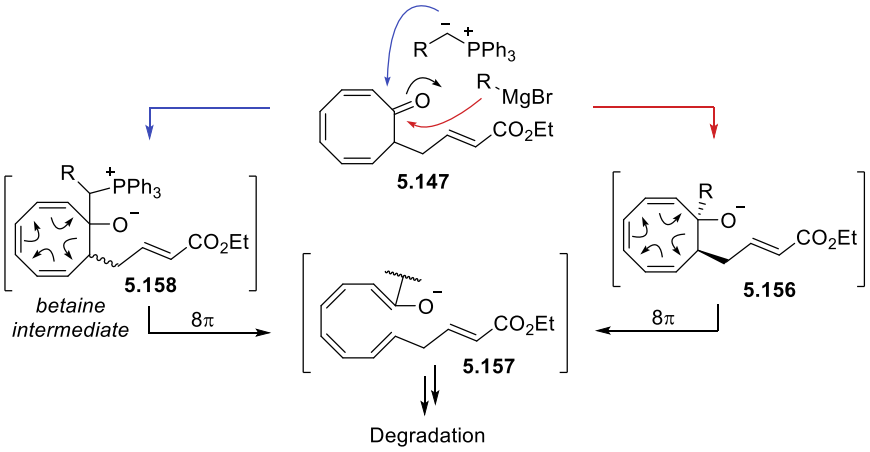

Scheme 5.26: Proposed mechanisms of degradation

Another proposed idea involving Wittig olefination to **5.159** with ethyl triphenylphosphoranylideneacetate followed by a diastereoselective alkene reduction to **5.160** (see Lu's work)[40] required highly specialised conditions to avoid diastereoselectivity and regioselectivity issues with other olefins and was disregarded.

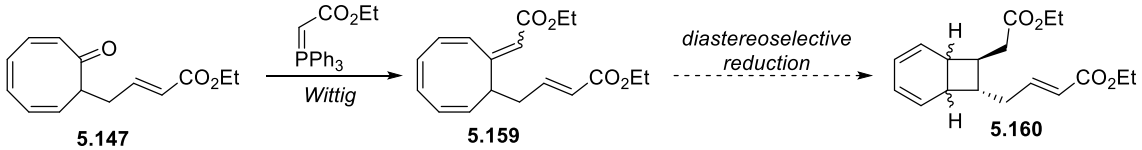

Scheme 5.27: Possible Wittig/diastereoselective reduction strategy

5.4.2.2 Alternative approach via initial formation of bridged tetracycle

The conjugated ketone in compound **5.147** is incompatible with transformations that can produce and maintain the desired BOD structure. This was solved by first performing the 6π

electrocyclisation/IMDA cascade, thereby removing conjugation and forming a robust bridged tetracycle, where the ketone is now safe to address. Cyclooctatrienone **5.147** was dissolved in degassed toluene (0.010 M) with a crystal of BHT and heated to 110 °C to afford ethyl ester tetracycle **5.161** in an excellent 90% yield (Scheme 5.28). The ketone in compound **5.161** should now be able to serve as a site of functionalisation to build relevant natural products **5.153**.

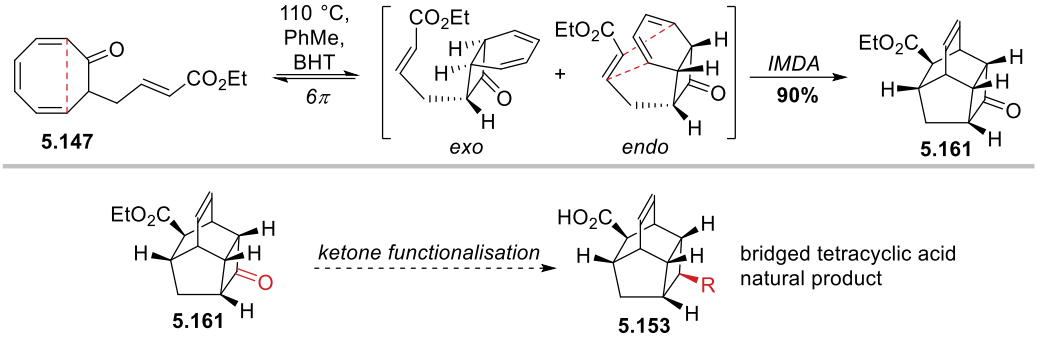

Scheme 5.28: Synthesis of ethyl ester tetracycle 5.161

The 1,3-benzodioxole **5.148** and phenyl cyclooctatrienone **5.149** required an elevated temperature of 150 °C to deliver their corresponding tetracycles **5.162** and **5.163** in 40% and 44% yield, respectively (Scheme 5.29).

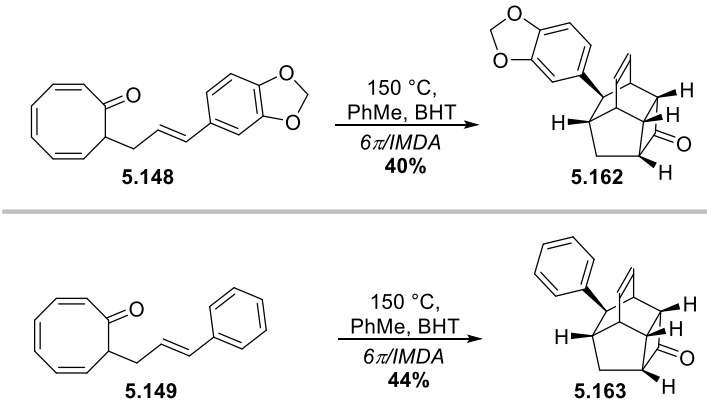

Scheme 5.29: Synthesis of 1,3-benzodioxole 5.162 and phenyl tetracycle 5.163

Heating furanone cyclooctatrienone **5.150** at 150 °C only gave degradation. There were no observable cycloaddition products by NMR analysis, with discouraging literature precedent also suggesting formation of **5.164** to be unlikely.[57,58] The initial 6π electrocyclisation to *endo*-**5.165** should be feasible, however there has been no previously reported IMDA reaction with a cyclic dienophile and 1,3-hexadiene in these substrate systems.

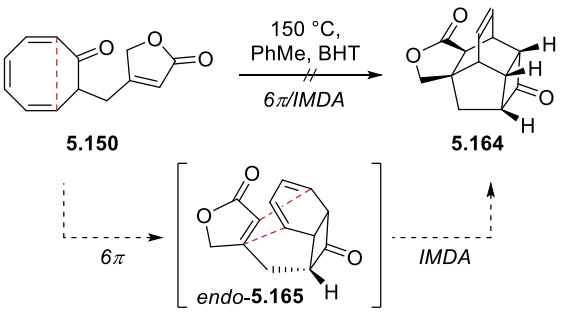

Scheme 5.30: Attempted synthesis of furanone tetracycle 5.164

5.4.2.3 Synthesis of the central intermediate for a divergent total synthesis

With compound **5.161** in hand, we wished to investigate the feasibility of the addition/deoxygenation tactic. Diastereoselective 1,2-addition with benzyl magnesium bromide to the outside face of the ketone furnished alcohol **5.166**, however subsequent attempts to deoxygenate were unsuccessful (Scheme 5.32). Barton−McCombie and triethylsilane-mediated deoxygenations had no effect on the alcohol. We postulated that the position of the alcohol was too sterically encumbered for it to be functionalised for removal. Deoxygenation also needs to be diastereoselective to afford the desired diastereomer **5.167** over **5.168**, and is difficult to control. This tactic was eventually discarded due to an unreactive alcohol and potential downstream stereoselectivity challenges.

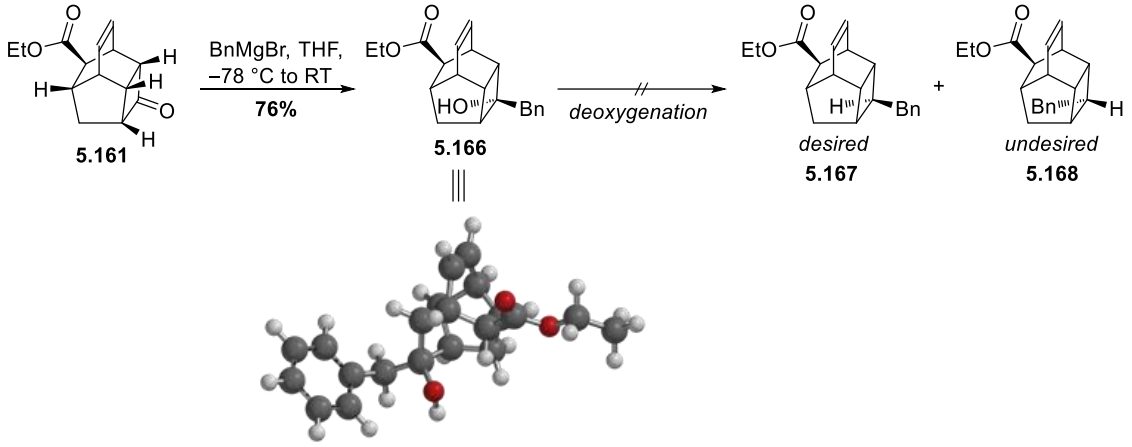

Scheme 5.32: Efforts on Grignard addition/deoxygenation of tetracycle 5.161

Instead, the one-carbon homologation protocol with (methoxymethyl)triphenylphosphonium chloride proved to be successful. Wittig olefination with the phosphonium reagent gave an E/Z mixture of compound **5.169** where subsequent treatment with an acid unmasked the methyl vinyl ether to present aldehyde **5.170**. The kinetic aldehyde **5.170** is under thermodynamic control in the presence of acid and eventually tautomerises to the thermodynamically favoured product **5.171** possessing the desired stereochemistry (see ^{1}H NMR spectra in Scheme 5.33). The aldehyde in compound **5.171** serves as a suitable functional handle, allowing for divergent synthesis to a variety of bridged tetracyclic endiandric natural products **5.153**, and serving as the central intermediate for this total synthesis project.

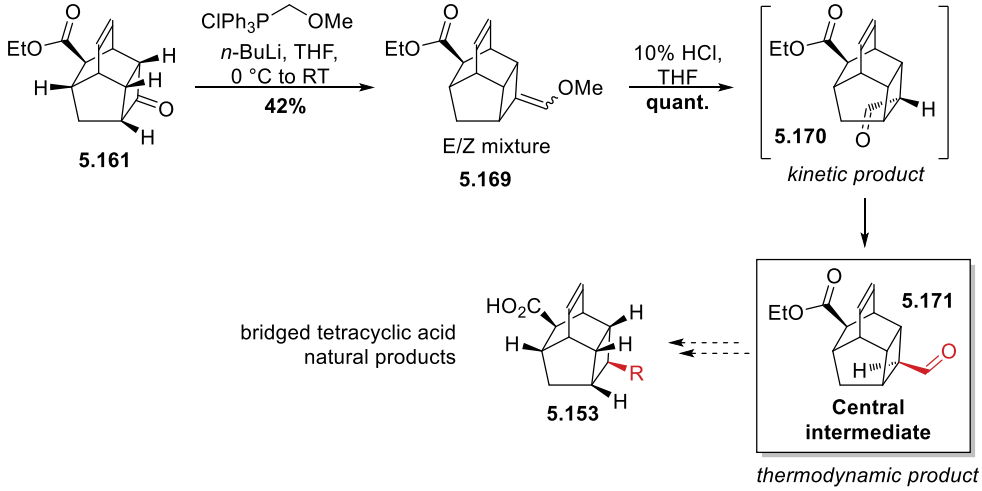

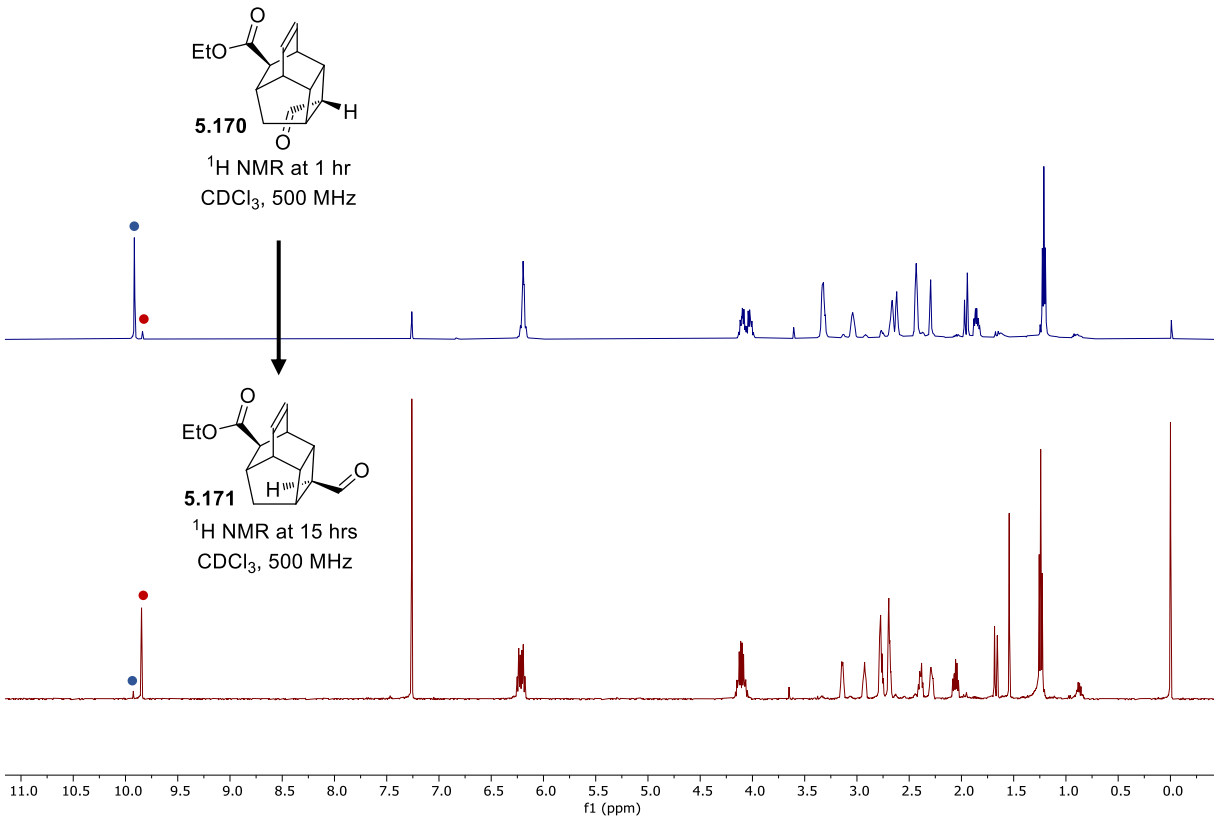

Scheme 5.33: Synthesis of aldehyde 5.171 via a one-carbon homologation protocol and ^{1}H NMR showing conversion of aldehyde 5.170 to 5.171 overtime

5.5 Total synthesis of kingianic acid A, B, D and endiandric acid M

With possession of the central intermediate **5.171** in hand, divergent total syntheses to a few bridged tetracyclic endiandric acids were accomplished. Treatment of aldehyde **5.171** with phenyl magnesium bromide gave alcohol **5.172** as a 1:1 mixture of diastereomers in 52% yield. This mixture was rendered inconsequential by subsequent triethylsilane-mediated deoxygenation and ester hydrolysis to yield kingianic acid B **5.173** in 56% yield over two steps (Scheme 5.34).

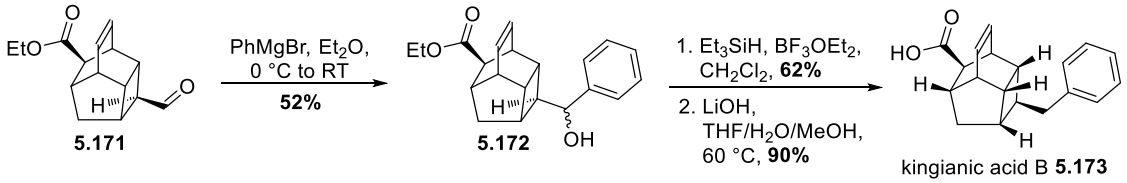

Scheme 5.34: Total synthesis of kingianic acid B

Extending beyond Grignard reagents, rhodium-catalysed 1,2-additions was used to add 3,4-methylenedioxyphenylboronic acid in 67% yield, followed by deoxygenation to **5.174** in 79% yield. Final ester hydrolysis provided kingianic acid A **5.21** in 99% yield.

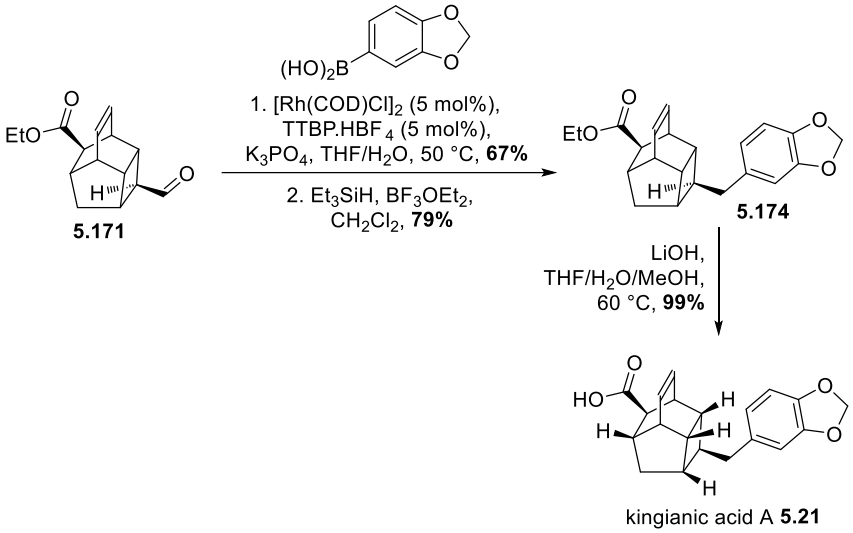

Scheme 5.35: Total synthesis of kingianic acid A

Alternative catalytic conditions were required to couple the less reactive trans-2-phenylvinylboronic acid, giving a humble 19% yield of alcohol **5.175** as a diastereomeric mixture. We attributed the low yield to competing proto-deboronation processes. Subsequent deoxygenation and ester hydrolysis in 97% and 71% yield, respectively, delivered the first synthesis of kingianic acid D **5.176**.

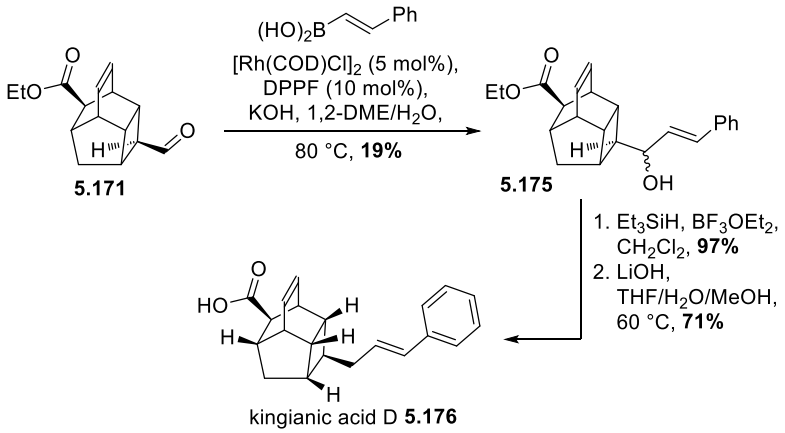

Scheme 5.36: Total synthesis of kingianic acid D

From kingianic ethyl ester A **5.174**, DIBAL-H reduction followed by Dess-Martin periodinane oxidation afforded aldehyde **5.177** in 64% yield over two steps. Wittig olefination with ethyl triphenylphosphoranylideneacetate followed by ester hydrolysis in 49% and quantitative yield, respectively, gave the first synthesis of endiandric acid M **5.178**.

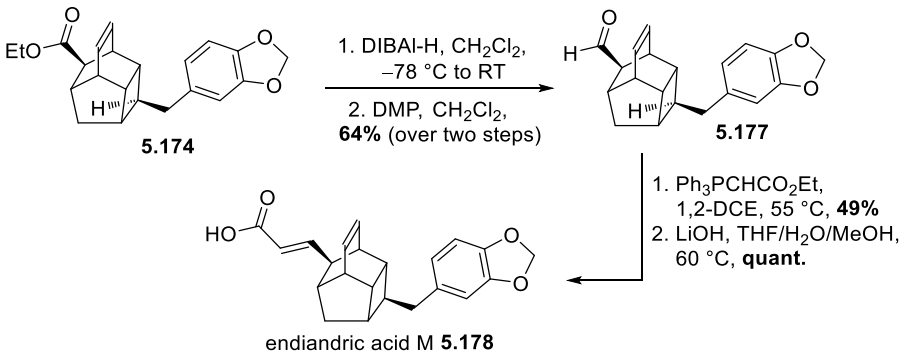

Scheme 5.37: Total synthesis of endiandric acid M

5.6 Additional work

5.6.1 Investigating modularity of synthetic intermediates

We conducted additional studies to assess the viability of functionalising our intermediates through simple functional group interconversions. We hoped to potentially access other endiandric natural products and their derivatives for future medicinal chemistry research.

5.6.1.1 Ethyl ester functional group interconversions

Global reduction of compound **5.161** with DIBAL-H followed by oxidation with Dess-Martin periodinane afforded aldehyde **5.179** in 46% over two steps (Scheme 5.38). Wittig olefination with ethyl triphenylphosphoranylideneacetate synthesises intermediate **5.180**, which can conceptually form endiandric acid L **5.181** and ferrugineic acid K **5.182**, and also served as a model for synthesising endiandric acid M **5.178**. Alternatively, ester hydrolysis of **5.161** in 50% yield to **5.183**, followed by amide coupling to **5.184** in 69% yield, delivers an amide that can be extrapolated to endiandramide B **5.29**.

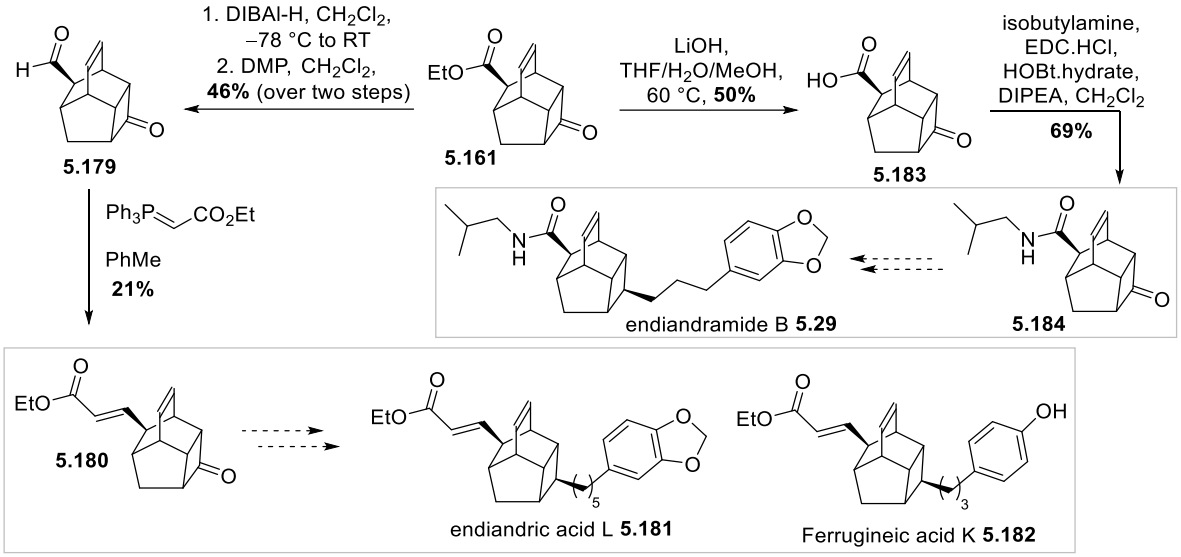

Scheme 5.38: Functional group interconversions on the ethyl ester of compound 5.161

5.6.1.2 Rhodium-catalysed 1,2-additions to aldehydes

The rhodium-catalysed 1,2-addition, deoxygenation reaction protocol used in the total synthesis (Scheme 5.39), provided a user-friendly avenue towards derivatives for possible medicinal chemistry applications.

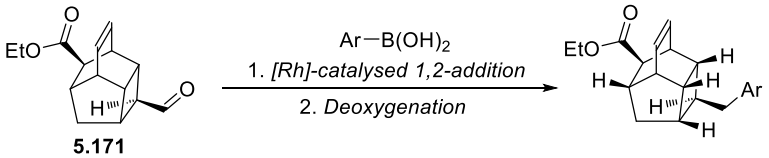

Scheme 5.39: General rhodium-catalysed 1,2-addition/deoxygenation reaction protocol

Methoxy **5.185** and fluoro phenyl **5.186** boronic acids were successfully coupled in quantitative and 82% yield, with subsequent deoxygenation proceeding smoothly in 92% and 85%, respectively (Table 5.2). The indole **5.187**, nitrile **5.188** and dimethylamine **5.189** coupled well in 77%, 41% and 56% yield, respectively. Unfortunately, attempted deoxygenation led to degradation for those substrates. The thiophene boronic acid **5.190** was unproductive.

Table 5.2: Summary of attempted rhodium-catalysed 1,2-addition/deoxygenation reaction protocol results

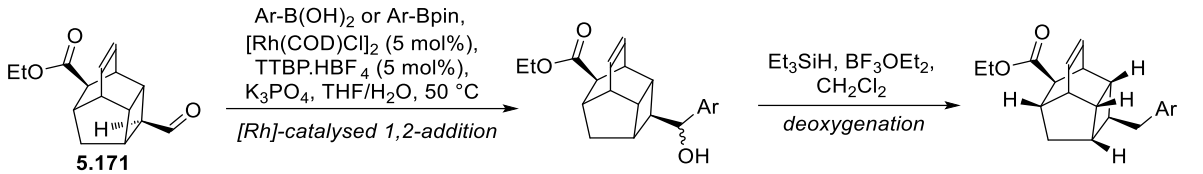

Entry	Aryl-boronic acid or Bpin	[Rh]-catalysed 1,2-addition results	Deoxygenation results
1	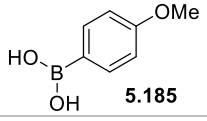 **5.185**	Quant. yield	92%
2	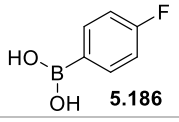 **5.186**	82%	85%
3	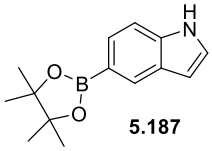 **5.187**	77%	Degradation
4	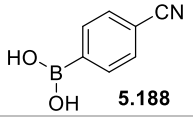 **5.188**	41%	Degradation
5	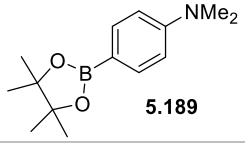 **5.189**	56%	Degradation
6	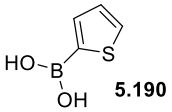 **5.190**	No reaction	N/A

5.6.2 Towards the synthesis of fused tetracyclic endiandric natural products

The current methodology focused on constructing the bridged tetracyclic class of endiandric natural products (**5.21**, **5.173**, **5.176** and **5.178**) as a result of the initial alkylation step using ethyl (E)-5-iodopent-2-enoate (Scheme 5.40). This methodology can be modified to target the fused tetracyclic variants via construction of cyclooctatrienone **5.191** derivatives. The 6π/IMDA cascade to compound **5.192** can be followed with the previous protocols to lend fused tetracyclic natural products **5.2**.

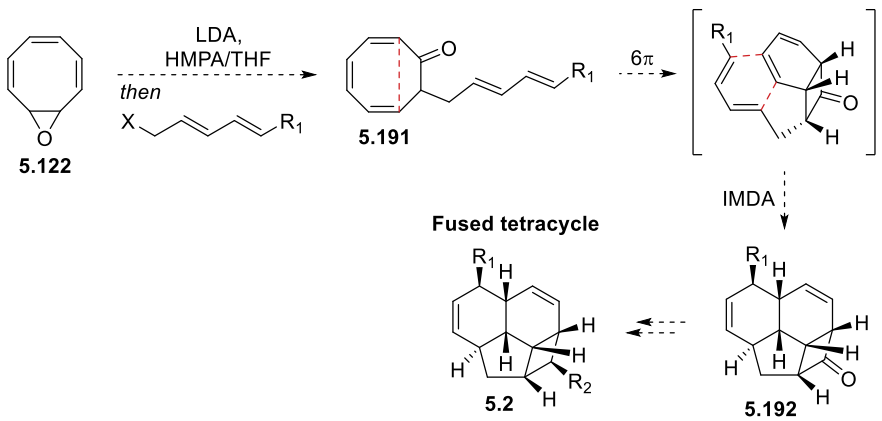

Scheme 5.40: Proposed synthesis of fused tetracyclic endiandric acids

Electrophile [(1E,3E)-5-bromo-1,3-pentadien-1-yl]benzene was used to make benzyl butadiene cyclooctatrienone **5.193** in 65% yield (Scheme 5.41). Subjection to thermal conditions at 110 °C in toluene with a crystal of BHT, yielded a rough 1:1:1 mixture (by NMR) of three compounds **5.194**-**5.196**. Two of the compounds afforded structures with characterisation data matching the fused **5.194** and bridged **5.195** tetracyclic molecules. In previous total syntheses where both fused and bridged compounds were possible, the fused compound has always predominated.[25,26]

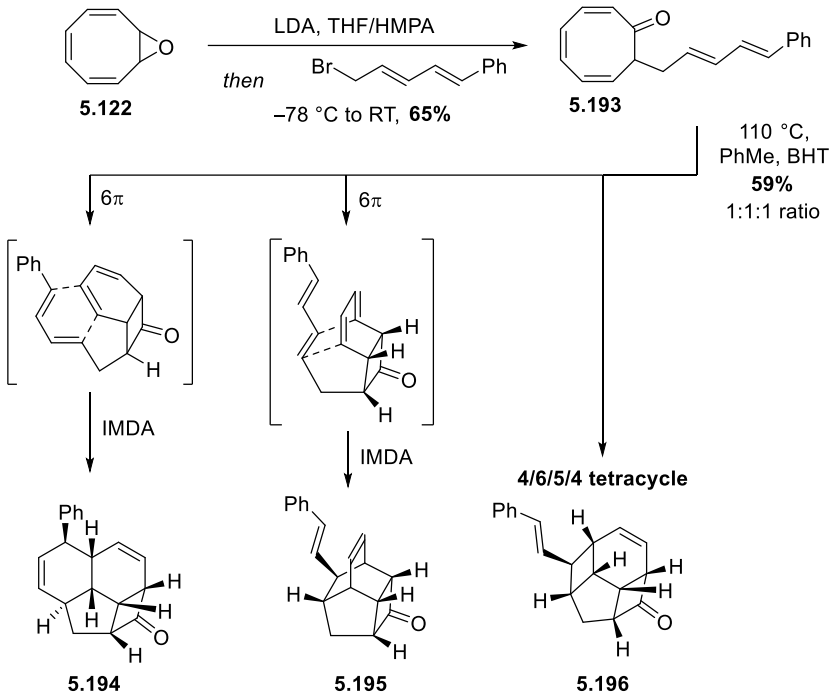

Scheme 5.41: Synthesis and thermal reaction of cyclooctatrienone 5.193

The third has been characterised as a highly unusual 4/6/5/4 tetracyclic compound **5.196**. The molecule was found to be quite unstable, rapidly degrading at room temperature overnight, making it difficult to obtain quality characterisation data. Its instability is possibly owed to the inherent ring strain of the 4/6/5/4 structure, which also has not been previously reported in literature. The exact mechanism of formation is currently unknown and difficult to elucidate due the compound's instability.

This methodology has potential to access fused tetracyclic endiandric acids such as endiandric acid A (Scheme 5.42), however is currently limited by the uncontrolled formation of undesired side-products.

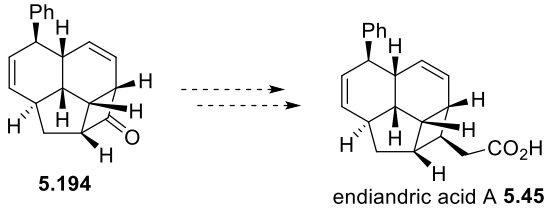

Scheme 5.42: Potential access to endiandric acid A via intermediate 5.195

5.7 Conclusion

In conclusion, we accomplished the total synthesis of kingianic acid A **5.21**, B **5.173**, D **5.176** and endiandric acid M **5.178** via our user-friendly third-generation methodology based on substituted cyclooctatrienones (Scheme 5.43). This methodology is limited to constructing the bridged tetracyclic sub-family of endiandric acids, however can provide easy access to all

reported bridged tetracycles (via central intermediate **5.171**), which previous literature syntheses are unable to do.

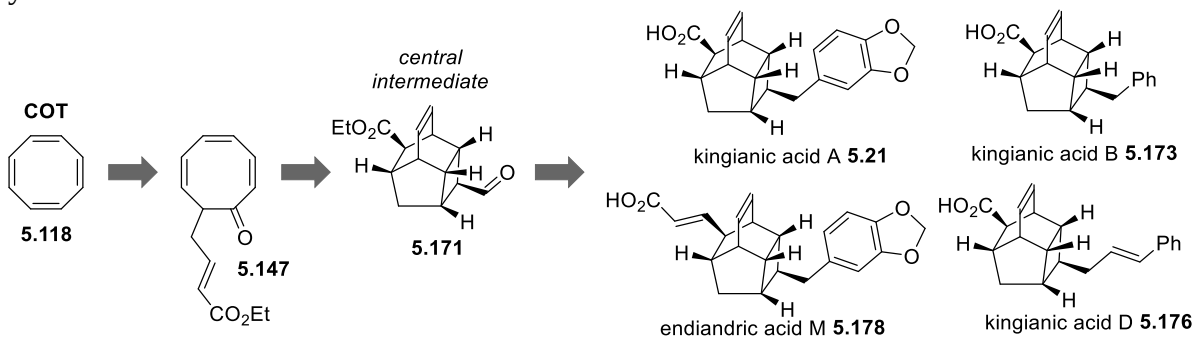

Scheme 5.43: Overview of third-generation methodology to access bridged tetracyclic endiandric acid natural products

5.8 Future directions

5.8.1 Towards asymmetric synthesis of endiandric acid natural products

We recognised an additional advantage of this methodology is the potential enantioselective synthesis of endiandric acid natural products. An asymmetric alkylation using chiral lithium amide bases can provide either cyclooctatrienone ***ent*-A 5.147** or ***ent*-B 5.147** which then can undergo the 6π/IMDA cascade to afford products ***ent*-A 5.161** or ***ent*-B 5.161,** respectively. Locking the cyclooctatrienones in the bridged tetracyclic structure would prevent racemisation.

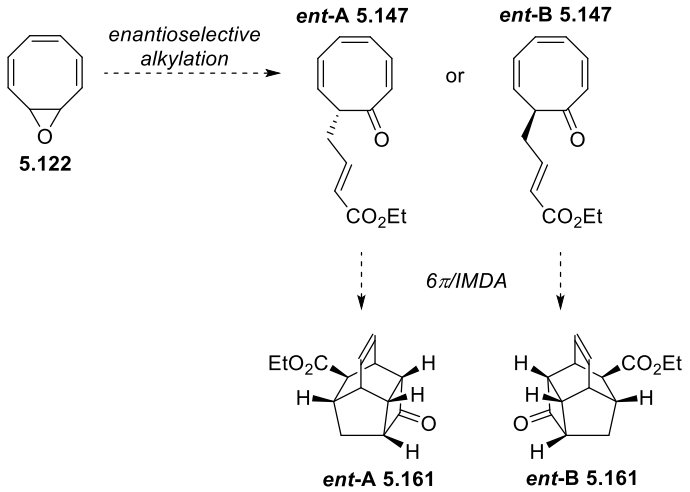

Scheme 5.44: Hypothesised enantioselective route to enantiopure endiandric acid derivatives

In our preliminary work, bis[(R)-1-phenylethyl]amine **5.197** was used to generate a chiral lithium amide which we anticipated would influence the face (*re* or *si*) of the nucleophilic substitution (see proposed transition state in Scheme 5.45). Disappointingly, the product **5.147** isolated gave no optical rotation. We imagined the high concentration of the HMPA co-solvent preferentially interacts with the lithium enolate over the chiral amide and therefore no chiral influence was imparted.

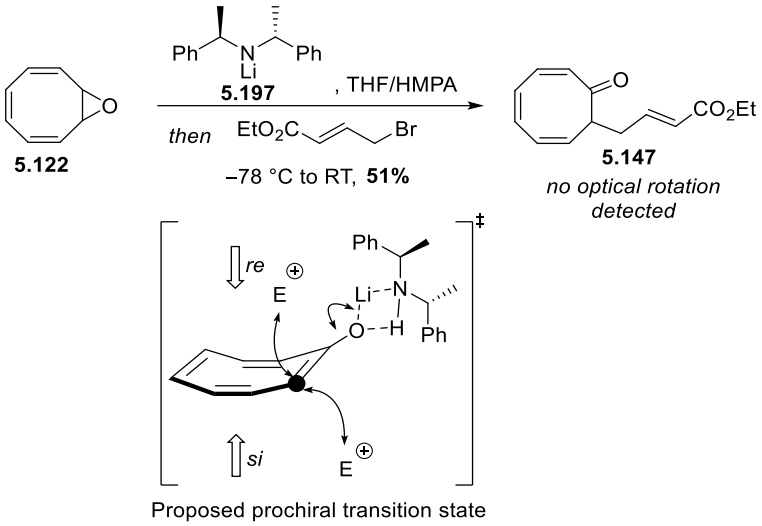

Scheme 5.45: Preliminary attempt at enantioselective alkylation with chiral lithium amide

Another possible reason for the unsuccessful enantioselectivity could be due to the ineffectiveness of the chiral amide **5.197** to provide a chiral pocket. Cyclooctatrienone lithium enolate could undergo alkene isomerisations shown in figure 7.11A. As a result there are four chemically equivalent quadrants of the cyclooctatrienone lithium enolate that needs to be considered instead of only the *re* and *si* faces (Figure 7.11B). Addition in either quadrants A and B (*re* face) or quadrants C and D (*si* face) would give racemic mixtures. Therefore, a chiral amide base has to be capable of simultaneously blocking the A and D quadrants or the B and C quadrants to achieve enantioselectivity, which is an unsolved challenge.

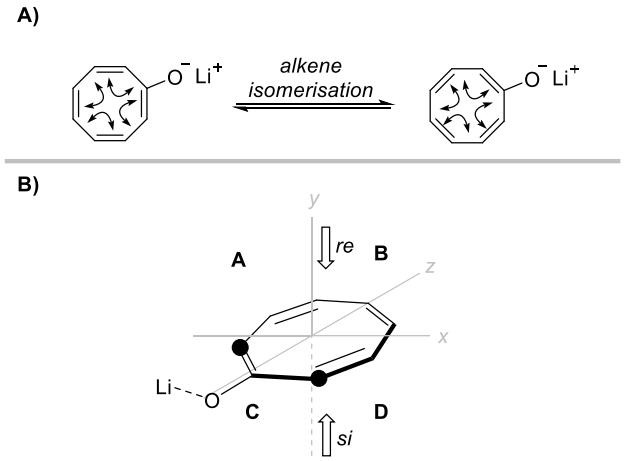

Figure 5.11: A) Alkene isomerisation of cyclooctatrienone lithium enolate. B) The four quadrants from which alkylation can occur

5.8.2 Synthesis of bis-Bpin tetraene – Next generation synthesis of bicyclo[4.2.0]octadiene compounds

The following is preliminary work on the potential next generation synthesis of BOD compounds in the Fallon group. Due to the shortness of this project, it has been included in this chapter instead of given its own.

5.8.2.1 Direct methods

The main work of this chapter described formal anti-1,2-difunctionalisations of COT for total synthesis purposes, however direct approaches have also been previously reported in literature. In Walter Reppe's 1948 work, the difunctionalisation of COT **5.118** with $Hg(OAc)_2$ yields an

anti-1,2 acetate bicyclo[4.2.0]octadiene (BOD) **5.198**.[44,59] Likewise, addition of chlorine yielded the dichloro BOD **5.199**. The dibromo BOD **5.120a**, made from the addition of bromine, is a noteworthy intermediate in nucleophilic substitutions to install carbon-centred substituents.[60] The reaction with potassium cyanide yielded a bis-nitrile linear tetraene **5.121b**, which is formed from a ring opening 6π/8π electrocyclisation cascade.[45]

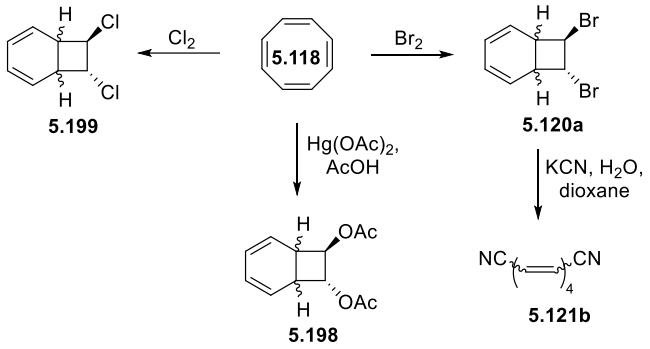

Scheme 5.46: Examples of the anti-1,2-difunctionalisations of COT

Heating **5.120a** with a variety of alkyne Grignard derivatives were reported to yield their corresponding tetraenes (Scheme 5.47).[46] The parent ethynyl magnesium bromide product was unisolable. Silyl-alkynes (R = e, f, g) interestingly existed as a mixture of the linear tetraene and BOD structure.[61] The styrenyl tetraene **5.200h** was also reported.[62]

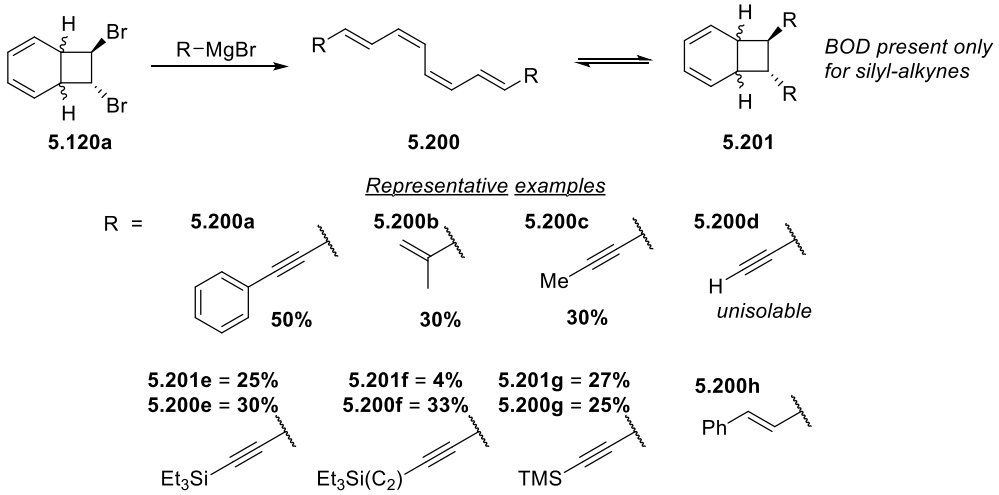

Scheme 5.47: Substitution of dibromo COT with Grignard reagents

5.8.2.2 Transition metal catalysed methods - Attempted diboration of COT via platinum catalysis

Diboration of alkenes is a powerful reaction leading to many useful synthetic intermediates. The reaction often uses bis(pinacolato)diborane as the borylating reagent and catalysed by a variety of metal catalysts (copper, platinum, rhodium, palladium, iridium, etc.) (Scheme 5.48A).[63–69] Non-catalytic methods have also been employed with carbonate salts.[70,71] A patent filed in 1999 described the platinum-catalysed diboration of COT **5.118**, to yield a mixture of the 1,2- **5.202** and 1,4-addition **5.203** products (Scheme 5.48B).[72] No yield or stereochemistry was stated. Repeating this reaction and acquiring 2D NMR data revealed the major compound to be a diborylated bicyclo[5.1.0]octa-2,4-diene compound **5.204** (Scheme 5.48C). Further attempts at transition metal catalysed diborations were unfruitful and was discontinued.

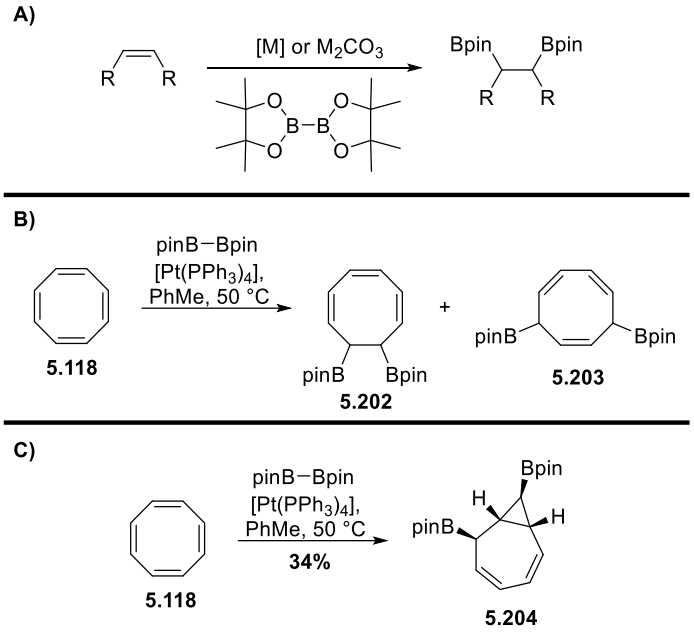

Scheme 5.48: A) Established alkene diboration methods. B) Patent's work with platinum catalysed diboration of COT. C) Our work with platinum catalysed diboration of COT

5.8.2.3 Methods via the cyclooctatetraene dianion

The cyclooctatetraene dianion **5.205** is a flat, aromatic compound with the formula of $(C_8H_8)^{2-}$. It can be synthesised by the addition of lithium, sodium, potassium or magnesium metal to a solution of cyclooctatetraene **5.118**.[73–78] Alternatively, it can be accessed from 1,5-cyclooctadiene **5.206** with *n*-butyllithium/TMEDA or potassium-naphthalene.[79,80] COT dianion **5.205** is a well-studied, reactive intermediate for nucleophilic addition to a variety of electrophiles (a few select examples are shown in Scheme 5.49). In Nicolaou's previous work synthesising intermediates that intersect endiandric acid derivatives, treatment of **5.205** with methyl iodide afforded BOD **5.207** and addition to CO_2 yielded di-carboxylic acid tetraene **5.208**.[29] The synthetic manipulations needed for these substrates to be used in total synthesis proved too cumbersome and was abandoned. Müllen's work in 1991, involved reactions with bis-electrophiles (such as **5.209**) in varying chain lengths, conformational mobility, and leaving groups.[81] Compound **5.209** undergoes nucleophilic substitution furnishing tricycle **5.210**. COT dianion **5.205** is not limited to carbon-centred electrophiles, reacting with chlorodiisopropylphosphine to afford bis-phosphine tetraene **5.211**.[82]

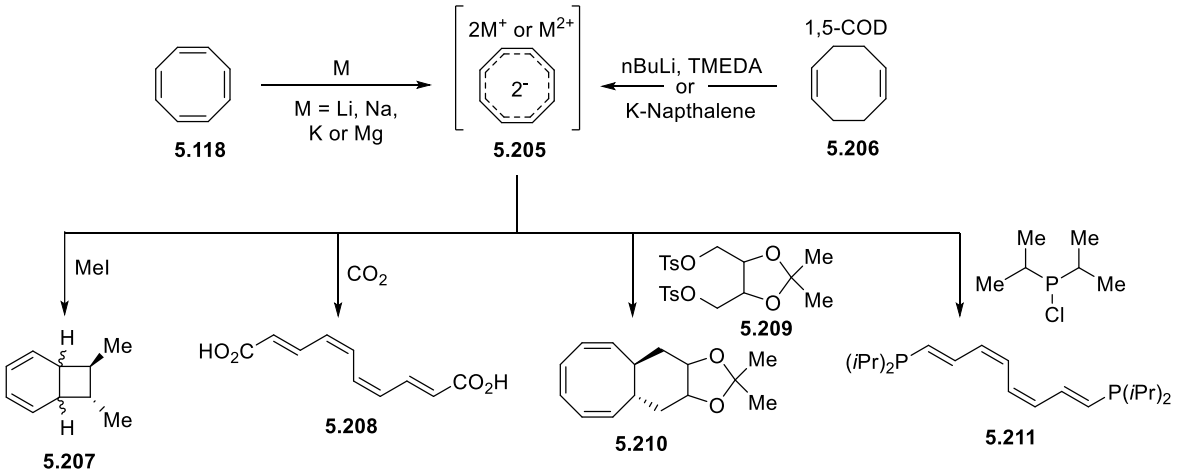

Scheme 5.49: Examples of 1,2-difunctionalisations of COT dianion

Cyclooctatetraene dianions can also undergo competitive 1,4-difunctionalisations, depending on the electrophile, representing a potential selectivity issue. Both dipotassium **5.212** and

dilithium **5.213** cyclooctatetraenides react with TMSCl to afford 1,4-bis(trimethylsilyl)cyclooctatriene **5.214** (Scheme 5.50).[83,84] Müllen reacted dilithium cyclooctatetraenide **5.213** with a variety of bis-electrophiles to afford 1,4-disubstituted cyclooctatrienes.[81] Bis-electrophiles **5.215** and **5.216** exclusively afforded 1,4-disubstituted products **5.217** and **5.218**, respectively. Biaryl bis-electrophile **5.219** gave a mixture of 1,4-**5.220** and 1,2-disubstituted **5.221** products.

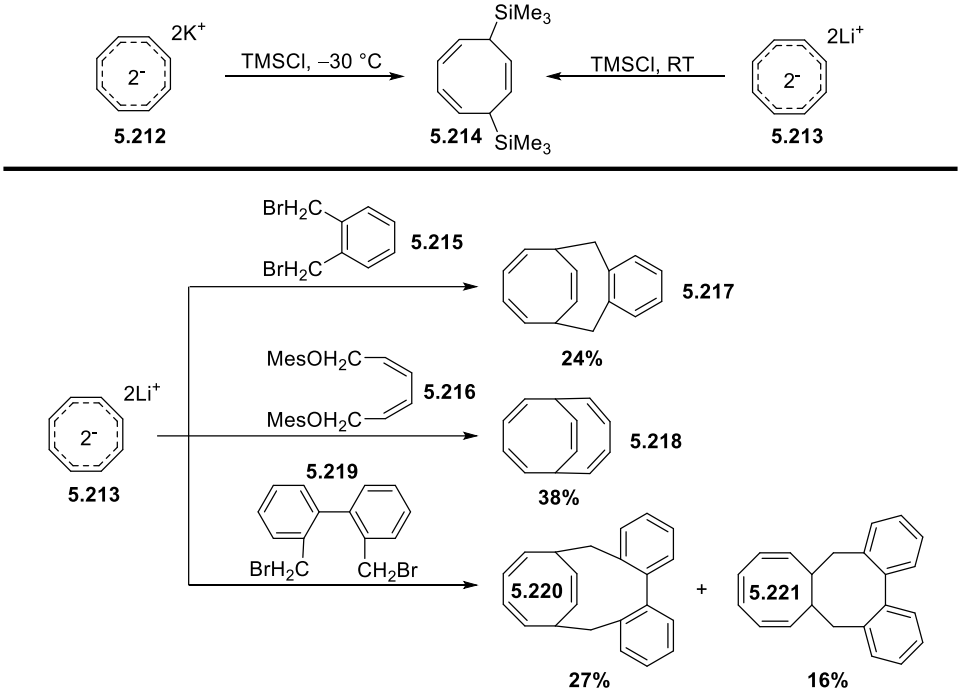

Scheme 5.50: Examples of 1,4-difunctionalisations of COT dianion

5.8.2.4 Aim

The COT dianion represents an excellent reagent for accessing *anti*-1,2-disubstituted cyclooctatrienes (and corresponding BOD products), however limited electrophile choice due to competing undesired reactivity has led to a lack of useful cyclooctatriene/BOD compounds. An electrophile that can install a functional handle would allow subsequent derivatisation to a variety of synthetically useful compounds. In 1991, Yu N. Bubnov reported the di-borylation of potassium cyclooctatetraenide dianion **5.212** to furnish linear E,Z,Z,E-1,8-bis(dipropylboryl)octatetraene **5.222** in quantitative yields, with chlorodipropylborane as the electrophile (Scheme 5.51).[85,86] It is presumed that the 1,2-adduct **5.223** is initially formed but a facile 8π electrocyclic ring opening occurs to form the thermodynamically favourable tetraene **5.222**.

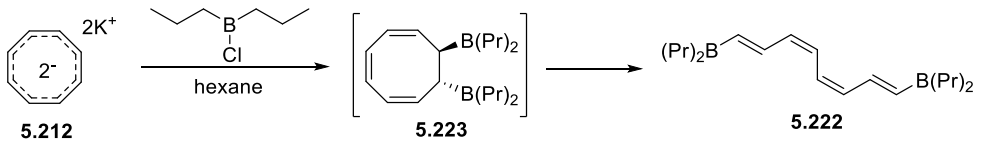

Scheme 5.51: Synthesis of E,Z,Z,E-1,8-bis(dipropylboryl)octatetraene 5.222

Taking direct inspiration, addition of a pinacolborane with an appropriate leaving group would provide a bis-Bpin tetraene **5.224** (Scheme 5.52).

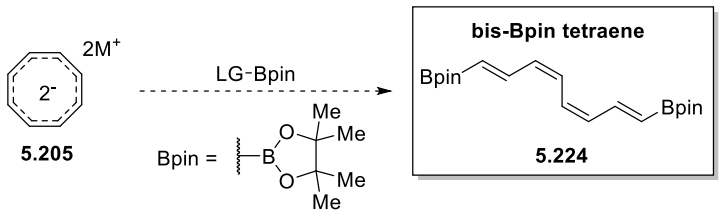

Scheme 5.52: Synthesis of bis-Bpin tetraene

Tetraene **5.224** would provide a better platform than **5.222** for convenient derivatisation through established cross-coupling chemistry. We envision a possible double palladium-catalysed Suzuki cross-coupling reaction with a variety of electrophiles (aryl, benzylic, etc.) would deliver a diverse set of bis-substituted tetraenes **5.225**, which may collapse into the cyclooctatriene **5.226** and then BOD **5.227**, depending on the type of substitution (Scheme 5.53).

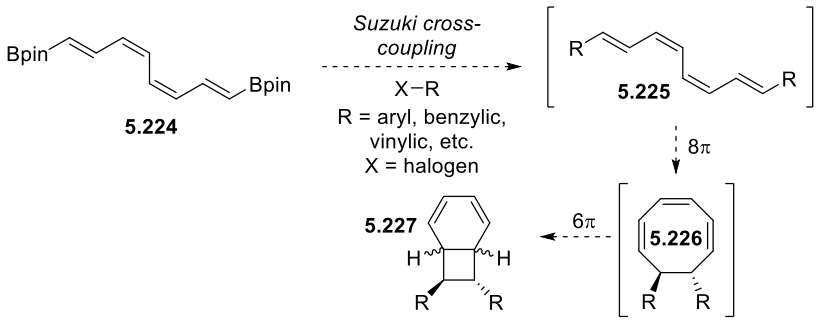

Scheme 5.53: Hypothesised synthetic utility of bis-Bpin tetraene

5.8.2.5 Synthesis of bis-Bpin tetraene

Initial efforts started with the lithium cyclooctatetraenide dianion to avoid handling the potassium metal. Addition of commercially available 2-isopropoxy-4,4,5,5-tetramethyl-1,3,2-dioxaborolane **5.228** was only met with degradation. Pinacolborane **5.229** provided trace amounts of **5.224**, however attempts at optimisation were unfruitful. We attributed these issues to the lithium cyclooctatetraenide dianion, since the choice of the counter metal ion can influence the selectivity.

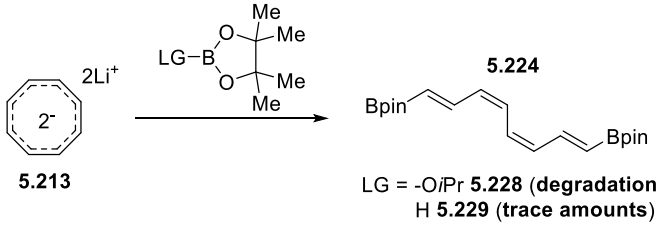

Scheme 5.54: Initial experiments with lithium cyclooctatetraenide dianion

Moving forward, potassium cyclooctatetraenide dianion **5.212** was used, due to its successful use in Bubnov's work. A solution of potassium cyclooctatetraenide dianion **5.212** in THF (0.5 M) was added to three equivalences of pinacolborane **5.229** (neat) at room temperature under inert atmosphere to yield a 1:1 mixture of the desired tetraene **5.224** and mono-Bpin cyclooctatriene **5.230** (Scheme 5.55). The mono-Bpin product **5.230** likely arises from a competing hydroboration reaction.

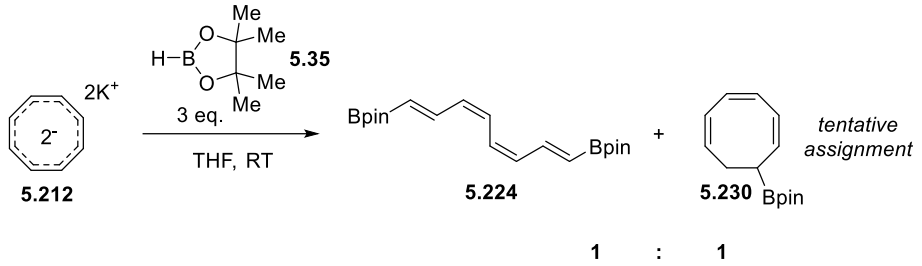

Scheme 5.55: Synthesis of tetraene 5.224 with mono-Bpin cyclooctatriene 5.230

Optimisation revealed a vast excess of pinacolborane **5.229** (>13 equivalences) was required to suppress the formation of the undesired cyclooctatriene **5.230** to deliver the desired tetraene **5.224** in a 93% crude yield (Scheme 5.56). The rate of addition must also be controlled where the blue/purple colour that appears upon addition of the potassium cyclooctatetraenide dianion solution must fully dissipate before adding more of the dianion solution. Purification involved dilution with hexane, filtration to remove salts and concentrating under reduced pressure. The product is a mixture of the tetraene **5.224** and minor amounts of an unremovable borane impurity. Purification by column chromatography degrades tetraene **5.224** and the impurity has similar solubilities in organic solvents ruling out recrystallisation. Nevertheless, the tetraene was used in subsequent cross-coupling reactions.

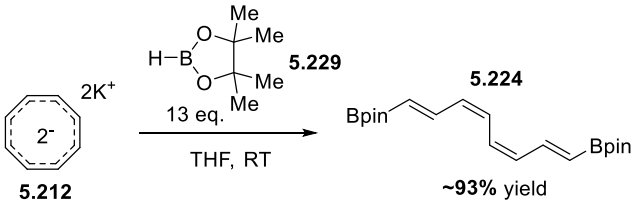

Scheme 5.56: Current optimised conditions for the synthesis of tetraene 5.224

Pinacolborane **5.229** is an odd choice for an electrophile, having a hydride as a leaving group. Its typical reactivity involves hydroboration of alkenes and alkynes in the presence of a catalyst, catalyst-free hydroboration of aldehydes, ketones and carboxylic acids, and borylations in C-H activation chemistry.[87] A paper by Singaram in 2011, describes the synthesis of alkyl, aryl, heteroaryl, vinyl and allylic pinacol boronic esters from the reaction between pinacolborane **5.229** and organomagnesium halides (Scheme 5.57).[88] This methodology is similar to our reaction where nucleophilic substitution to the pinacolborane leads to the hydride leaving.

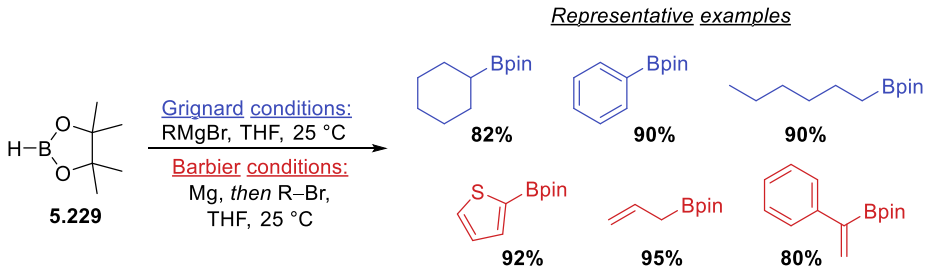

Scheme 5.57: Hydride as a leaving group in the reaction of pinacolborane with Grignard and Barbier reagents

Improving the synthesis of **5.224** may come from using other Bpin reagents that can serve as suitable electrophiles such as chloro- **5.231** and fluoro- **5.232** Bpin, which won't facilitate hydroborations (Figure 5.12). These halo-boranes are inspired by Bubnov's use of chlorodipropylborane.

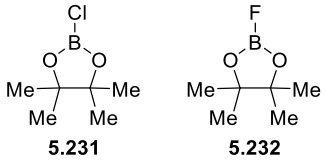

Figure 5.12: Possible reagents for the improved synthesis of tetraene 5.224

5.8.2.6 Suzuki cross-coupling with bis-Bpin tetraene

A few simple Suzuki cross coupling reactions were performed with bis-Bpin tetraene **5.224**. Reactions with phenyl bromide and benzyl bromide afforded their corresponding products **5.233** and **5.234** in 20% and 11%, respectively. These modest yields could be increased by improving the purity of bis-Bpin tetraene **5.224** and optimising the catalyst conditions. Compound **5.233** sits as the open tetraene, instead of undergoing the 8π/6π cascade to the BOD, in order to maintain the thermodynamically favourable conjugation between tetraene and terminal phenyl groups.

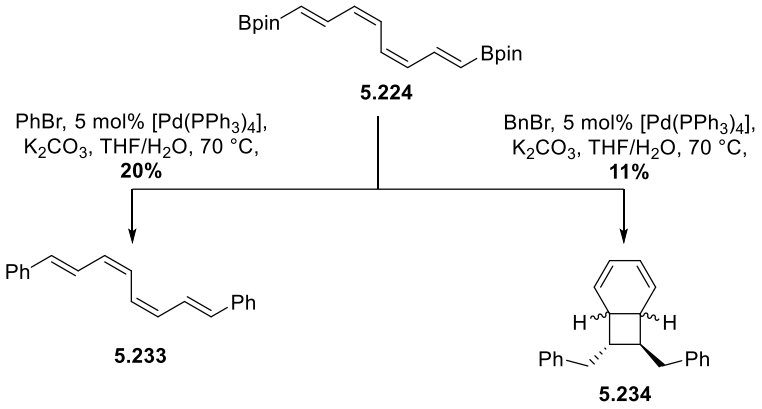

Scheme 5.58: Synthesis of tetraene 5.233 and BOD 5.234 via bis-Bpin tetraene 5.224

Attempts with allylic electrophiles such as allyl bromide and (E)-cinnamyl bromide were unsuccessful so far (Scheme 5.59). Allyl−vinyl cross-couplings are challenging and would likely need more specialised catalytic conditions. Once solved, compound **5.235** should provide convenient access to bridged scaffolds **5.236**.

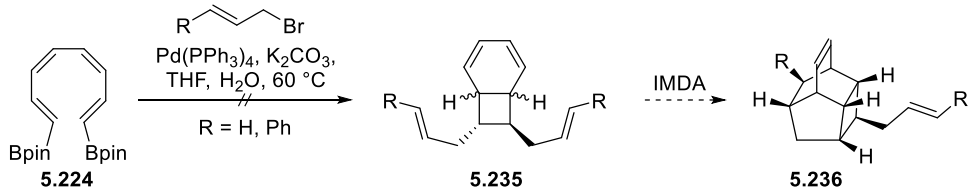

Scheme 5.59: Attempted synthesis of bis-allylic BODs

5.8.2.7 Conclusion and Future directions

With encouraging preliminary results, bis-Bpin tetraene **5.224** has potential to access multiple molecules of interest, however further optimisation of its synthesis and synthetic use is required. Possible future directions may involve functionalisation to give di-substituted tetraene **5.237** with a pinacol boronate ester and N-methyliminodiacetic acid boronate ester allowing for selective cross couplings (Scheme 5.60). To expand beyond the tested aryl and benzylic couplings, we would look to develop alkyl, vinyl and allylic couplings as well. Ultimately, this methodology can potentially access natural products in the endiandric acid family, and offers access to more derivatives for medicinal chemistry studies.

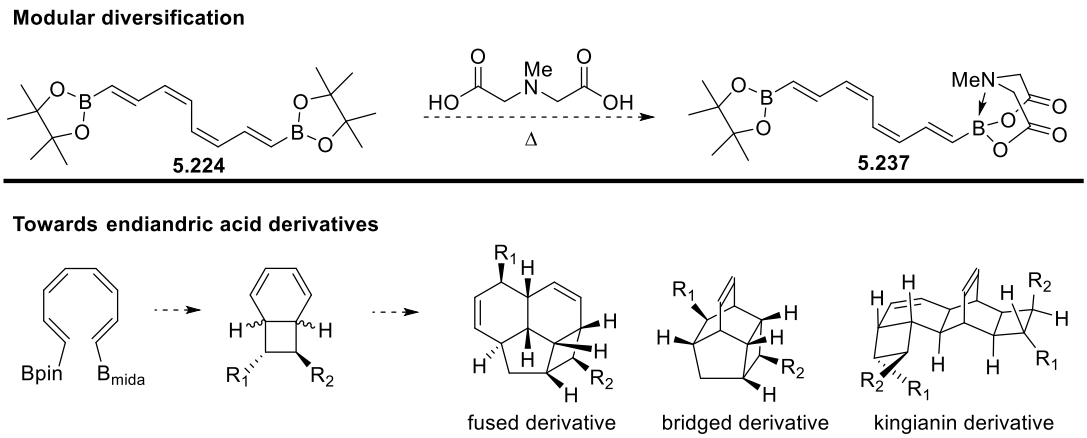

Scheme 5.60: Future directions for bis-Bpin tetraene 5.224

5.9 References

[1] B. Lenta, J. Chouna, P. Nkeng-Efouet, N. Sewald, *Biomolecules* **2015**, *5*, 910–942.

[2] J. R. Chouna, P. A. Nkeng-Efouet, B. N. Lenta, K. P. Devkota, B. Neumann, H.-G. Stammler, S. F. Kimbu, N. Sewald, *Phytochemistry* **2009**, *70*, 684–688.

[3] J. R. Chouna, P. Alango Nkeng-Efouet, B. Ndjakou Lenta, J. Duplex Wansi, B. Neumann, H.-G. Stammler, S. Fon Kimbu, N. Sewald, *Helv. Chim. Acta.* **2011**, *94*, 1071–1076.

[4] J. R. Chouna, P. A. Nkeng-Efouet, B. N. Lenta, J. D. Wansi, S. F. Kimbu, N. Sewald, *PhytoChem. Lett.* **2010**, *3*, 13–16.

[5] Y.-T. Huang, H.-S. Chang, G.-J. Wang, C.-H. Lin, I.-S. Chen, *Int J Mol Sci* **2012**, *13*, 16430–16443.

[6] Y.-T. Huang, H.-S. Chang, G.-J. Wang, M.-J. Cheng, C.-H. Chen, Y.-J. Yang, I.-S. Chen, *J Nat Prod* **2011**, *74*, 1875–1880.

[7] C. Apel, C. Gény, V. Dumontet, N. Birlirakis, F. Roussi, V. C. Pham, H. Doan Thi Mai, V. H. Nguyen, V. M. Chau, M. Litaudon, *J Nat Prod* **2014**, *77*, 1430–1437.

[8] R. B. Williams, S. M. Martin, J.-F. Hu, V. L. Norman, M. G. Goering, S. Loss, M. O'Neil-Johnson, G. R. Eldridge, C. M. Starks, *J Nat Prod* **2012**, *75*, 1319–1325.

[9] F. M. Talontsi, M. Lamshöft, J. O. Bauer, A. A. Razakarivony, B. Andriamihaja, C. Strohmann, M. Spiteller, *J Nat Prod* **2013**, *76*, 97–102.

[10] M. Azmi, C. Gény, A. Leverrier, M. Litaudon, V. Dumontet, N. Birlirakis, F. Guéritte, K. Leong, S. Halim, K. Mohamad, K. Awang, *Molecules* **2014**, *19*, 1732–1747.

[11] J. Banfield, D. Black, D. Collins, B. Hyland, J. Lee, S. Pranowo, *Aust. J. Chem.* **1994**, *47*, 587.

[12] J. Banfield, D. Black, D. Collins, B. Hyland, J. Lee, S. Pranowo, *Aust. J. Chem.* **1994**, *47*, 587.

[13] W. M. Bandaranayake, J. E. Banfield, D. St. C. Black, *J. Chem. Soc. Chem. Commun.* **1980**, 902.

[14] W. Bandaranayake, J. Banfield, D. Black, G. Fallon, B. Gatehouse, *Aust. J. Chem.* **1981**, *34*, 1655.

[15] W. Bandaranayake, J. Banfield, D. Black, G. Fallon, B. Gatehouse, *Aust. J. Chem.* **1982**, *35*, 567.

[16] A. Leverrier, K. Awang, F. Guéritte, M. Litaudon, *Phytochemistry* **2011**, *72*, 1443–1452.

[17] M. S. Davids, A. Letai, *J. Clin. Oncol.* **2012**, *30*, 3127–3135.

[18] G. Lessene, P. E. Czabotar, P. M. Colman, *Nat Rev Drug Discov* **2008**, *7*, 989–1000.

[19] P. S. Jeng, E. H. Cheng, *Nat Chem Biol* **2013**, *9*, 351–352.

[20] W. J. Placzek, J. Wei, S. Kitada, D. Zhai, J. C. Reed, M. Pellecchia, *Cell Death Dis* **2010**, *1*, e40–e40.

[21] Eder C., Kogler H., Haag-Richter S., *New Fused Tetracyclic Compounds, e.g., Endiandric Acid H Obtained from the Plant Beilschmieda Fulva, Are C-Maf and NFAT Inhibitors Useful for Treating Allergy or Asthma*, **2004**, DE 10235624 A1.

[22] Eder C., Kogler H., Haag-Richter S., *Endiandric Acid H and Its Derivatives, Process for Their Preparation and Use Thereof*, **2006**, US007019028B2.

[23] P.-S. Yang, M.-J. Cheng, C.-F. Peng, J.-J. Chen, I.-S. Chen, *J Nat Prod* **2009**, *72*, 53–58.

[24] N. Amirah Saad, S. Mohammad, M. Hafizi Abu Bakar, M. Tasyriq Che Omar, M. Litaudon, K. Awang, M. Nurul Azmi, *J Braz Chem Soc* **2022**, DOI 10.21577/0103-5053.20220067.

[25] K. C. Nicolaou, R. E. Zipkin, N. A. Petasis, *J. Am. Chem. Soc.* **1982**, *104*, 5558–5560.
[26] K. C. Nicolaou, N. A. Petasis, R. E. Zipkin, *J. Am. Chem. Soc.* **1982**, *104*, 5560–5562.
[27] K. C. Nicolaou, N. A. Petasis, J. Uenishi, R. E. Zipkin, *J. Am. Chem. Soc.* **1982**, *104*, 5557–5558.
[28] K. C. Nicolaou, N. A. Petasis, R. E. Zipkin, J. Uenishi, *J. Am. Chem. Soc.* **1982**, *104*, 5555–5557.
[29] K. C. Nicolaou, N. A. Petasis, **1984**, pp. 155–173.
[30] E. bin Go, S. P. Wetzler, L. J. Kim, A. Y. Chang, D. A. Vosburg, *Tetrahedron* **2016**, *72*, 3790–3794.
[31] K. A. Parker, Y.-H. Lim, *J. Am. Chem. Soc.* **2004**, *126*, 15968–15969.
[32] C. M. Beaudry, D. Trauner, *Org. Lett.* **2005**, *7*, 4475–4477.
[33] M. F. Jacobsen, J. E. Moses, R. M. Adlington, J. E. Baldwin, *Org. Lett.* **2005**, *7*, 2473–2476.
[34] K. A. Parker, Z. Wang, *Org. Lett.* **2006**, *8*, 3553–3556.
[35] S. L. Drew, A. L. Lawrence, M. S. Sherburn, *Chem. Sci.* **2015**, *6*, 3886–3890.
[36] H. N. Lim, K. A. Parker, *Org. Lett.* **2013**, *15*, 398–401.
[37] H. N. Lim, K. A. Parker, *J. Org. Chem.* **2014**, *79*, 919–926.
[38] J. C. Moore, E. S. Davies, D. A. Walsh, P. Sharma, J. E. Moses, *Chem. Commun.* **2014**, *50*, 12523–12525.
[39] S. May, P. Grieco, H.-H. Lee, *Synlett* **1997**, *1997*, 493–494.
[40] P. Yan, C. Zhong, J. Zhang, Y. Liu, H. Fang, P. Lu, *Angew. Chem. Int. Ed.* **2021**, *60*, 4609–4613.
[41] O. Yahiaoui, A. Almass, T. Fallon, *Chem. Sci.* **2020**, *11*, 9421–9425.
[42] H. D. Patel, T. Fallon, *Org. Lett.* **2022**, *24*, 2276–2281.
[43] R. Guo, B. P. Witherspoon, M. K. Brown, *Tetrahedron* **2022**, *122*, 132932.
[44] A. C. Cope, N. A. Nelson, D. S. Smith, *J. Am. Chem. Soc.* **1954**, *76*, 1100–1104.
[45] H. Hoever, *Tetrahedron Lett.* **1962**, *3*, 255–256.
[46] H. Straub, J. M. Rao, E. Müller, *Justus Liebigs Ann. Chem.* **1973**, *1973*, 1339–1351.
[47] D. A. Bak, K. Conrow, *J. Org. Chem.* **1966**, *31*, 3958–3965.
[48] T. S. Cantrell, *J. Am. Chem. Soc.* **1970**, *92*, 5480–5483.
[49] F. del Moro, P. Crotti, V. di Bussolo, F. Macchia, M. Pineschi, *Org. Lett.* **2003**, *5*, 1971–1974.
[50] M. Pineschi, F. del Moro, P. Crotti, F. Macchia, *European J. Org. Chem.* **2004**, *2004*, 4614–4620.
[51] P. A. Chaloner, A. B. Holmes, *J. Chem. Soc. Perkin 1* **1976**, 1838.
[52] A. C. Cope, B. D. Tiffany, *J. Am. Chem. Soc.* **1951**, *73*, 4158–4161.
[53] M. Ogawa, M. Takagi, T. Matsuda, *Chem. Lett.* **1972**, *1*, 527–530.
[54] C. Ganter, S. M. Pokras, J. D. Roberts, *J. Am. Chem. Soc.* **1966**, *88*, 4235–4237.
[55] P. H. Gund, Molecular Orbital Calculations And Attempted Synthesis Of Cyclooctatrienyne And 1,2-Cyclooctatriendione. Synthesis Of 3,3-Dichlorotricyclo(4.2.0.0(1,4))Oct-5-En-2-One, University of Massachusetts Amherst, **1967**.
[56] M. Franck-Neumann, *Tetrahedron Lett.* **1970**, *11*, 2143–2146.
[57] X. Li, S. J. Danishefsky, *J. Am. Chem. Soc.* **2010**, *132*, 11004–11005.
[58] M. Karthikeyan, R. Kamakshi, V. Sridar, B. S. R. Reddy, *Synth Commun* **2003**, *33*, 4199–4204.
[59] W. Reppe, O. Schlichting, K. Klager, T. Toepel, *Justus Liebigs Ann. Chem.* **1948**, *560*, 1–92.
[60] R. Huisgen, G. Boche, *Tetrahedron Lett.* **1965**, *6*, 1769–1774.

[61] S. J. Harris, D. R. M. Walton, *Tetrahedron* **1978**, *34*, 1037–1042.
[62] E. Müller, H. Straub, J. Madhusudana Rao, *Tetrahedron Lett.* **1970**, *11*, 773–776.
[63] X. Liu, *Synlett* **2003**, 2442–2443.
[64] L. T. Kliman, S. N. Mlynarski, J. P. Morken, *J. Am. Chem. Soc.* **2009**, *131*, 13210–13211.
[65] T. Ishiyama, M. Yamamoto, N. Miyaura, *Chem. Commun.* **1997**, 689–690.
[66] J. Hu, Y. Zhao, Z. Shi, *Nat Catal* **2018**, *1*, 860–869.
[67] M. Wang, S. Gao, M. Chen, *Org. Lett.* **2019**, *21*, 2151–2155.
[68] D. Fiorito, S. Keskin, J. M. Bateman, M. George, A. Noble, V. K. Aggarwal, *J. Am. Chem. Soc.* **2022**, *144*, 7995–8001.
[69] K. Toribatake, H. Nishiyama, *Angew. Chem. Int. Ed.* **2013**, *52*, 11011–11015.
[70] A. Bonet, C. Pubill-Ulldemolins, C. Bo, H. Gulyás, E. Fernández, *Angew. Chem. Int. Ed.* **2011**, *50*, 7158–7161.
[71] E. Davenport, E. Fernandez, *Chem. Commun.* **2018**, *54*, 10104–10107.
[72] S. M. Marcuccio, M. Rodopoulos, H. Weigold, P. Osvath, *Organoboron Derivatives and Process for Coupling Organic Compounds*, **1999**, WO1999-AU882.
[73] W. J. Evans, D. J. Wink, A. L. Wayda, D. A. Little, *J. Org. Chem.* **1981**, *46*, 3925–3928.
[74] G. Märkl, B. Alig, *J. Organomet. Chem.* **1984**, *273*, 1–29.
[75] H. J. Kablitz, R. Kallweit, G. Wilke, *J. Organomet. Chem.* **1972**, *44*, 49–50.
[76] W. Rutsch, A. Frey, M. Neuenschawander, P. Engel, *Helv. Chim. Acta.* **1979**, *62*, 718–739.
[77] H. Lehmkuhl, S. Kintopf, K. Mehler, *J. Organomet. Chem.* **1972**, *46*, 1–2.
[78] W. J. Richter, *Chem. Ber.* **1985**, *118*, 97–106.
[79] W. Gausing, G. Wilke, *Angew. Chem. Int. Ed. Eng.***1978**, *17*, 371–372.
[80] L. H. Simons, J. J. Lagowski, *Tetrahedron Lett.* **2002**, *43*, 1771–1773.
[81] P. Auchter-Krummel, G. Krummel, K. Müllen, J. Lex, *Chem. Ber.* **1991**, *124*, 2819–2831.
[82] G. Märkl, B. Alig, E. Eckl, *Tetrahedron Lett.* **1983**, *24*, 1955–1958.
[83] J. Rausch, C. Apostolidis, O. Walter, V. Lorenz, C. G. Hrib, L. Hilfert, M. Kühling, S. Busse, F. T. Edelmann, *New J. Chem.* **2015**, *39*, 7656–7666.
[84] N. C. Burton, F. G. N. Cloke, P. B. Hitchcock, H. C. de Lemos, A. A. Sameh, *J. Chem. Soc., Chem. Commun.* **1989**, 1462–1464.
[85] M. E. GURSKII, A. v. GEIDERIKH, A. v. IGNATENKO, YU. N. BUBNOV, *ChemInform* **2010**, *23*, no-no.
[86] M. E. Gurskii, A. v. Geiderikh, A. v. Ignatenko, Y. N. Bubnov, *Organometallic chemistry in the USSR* **1991**, *4*, 107.
[87] P. V. Ramachandran, J. S. Chandra, A. Ros, R. Fernández, J. M. Lassaletta, V. K. Aggarwal, D. J. Blair, E. L. Myers, in *Encyclopedia of Reagents for Organic Synthesis*, John Wiley & Sons, Ltd, Chichester, UK, **2017**, pp. 1–12.
[88] J. W. Clary, T. J. Rettenmaier, R. Snelling, W. Bryks, J. Banwell, W. T. Wipke, B. Singaram, *J. Org. Chem.* **2011**, *76*, 9602–9610.

Chapter 6

Computational studies on the kinetics, thermodynamics and torquoselectivity of the 8π/6π electrocyclisation cascade of bicyclo[4.2.0]octadiene related natural products

Authorship declaration: Majority of the computational modelling, analysis and presentation of results was conducted personally with early preliminary work conducted by Dr Thomas Fallon

6.1 Asymmetric electrocyclic reactions

Electrocyclic reactions are a class of pericyclic reaction where either a ring opening or closing event occurs, resulting in the net conversion of a π bond to a σ bond or σ bond to a π bond, respectively.[1,2] Torquoselectivity in electrocyclic reactions may arise from bias towards inward or outward rotation of the terminal substituents in conrotatory or disrotatory mechanisms, but without torquoselection, a racemic mixture arises (Figure 6.1).[3,4] This is another aspect of selectivity in electrocyclisations unrelated to the Woodward–Hoffman rules.

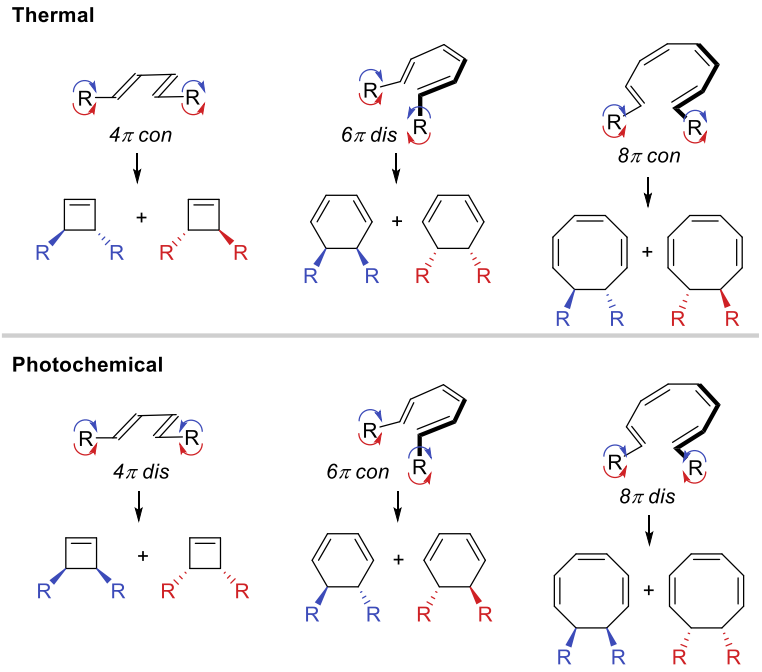

Figure 6.1: Enantiomers of thermal and photochemical 4π, 6π and 8π electrocyclisations

Asymmetric photochemical electrocyclisations are quite limited, however, there has been significant development in asymmetric thermal electrocyclisations.[5] In regards to thermal 4π electrocyclisations, the Nazarov cyclisation has many powerful substrate and catalyst-controlled asymmetric methods. Denmark et al. in the 1980s developed a chiral silane intermediate **6.1** that transferred asymmetry in the Nazarov cyclisation (Scheme 6.1).[6–8] Treatment of **6.1** with iron trichloride formed intermediate **6.2** from a torquoselective conrotatory 4π ring closure reaction (see intermediate **6.3**). Silane group elimination afforded tricycle **6.4** in 58% yield which maintained an enantiomeric excess of 88%. They reasoned that the intermediate cation tricycle favoured the C–Si σ bond lying perpendicular to the pentadienyl system (see **6.5**) instead of being equatorial (see **6.6**).

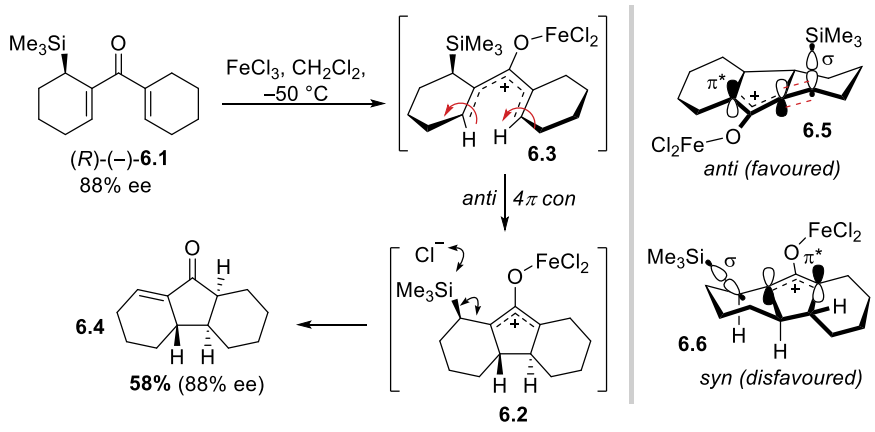

Scheme 6.1: Denmark's silicon chiral auxiliary

Rueping et al. employed a chiral Brønsted acids to an asymmetric Nazarov cyclisation (Scheme 6.2).[9] The BINOL phosphate catalyst coordinates with the cyclopentadienyl cation intermediate and impose torquoselection during the 4π ring closure.

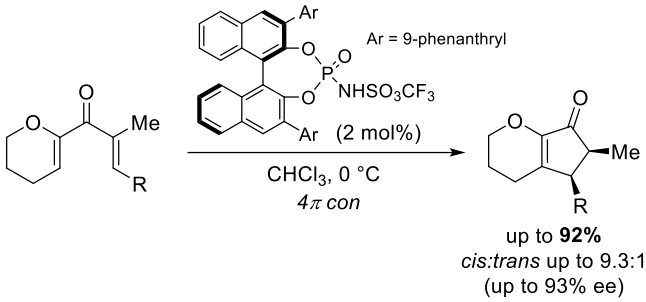

Scheme 6.2: BINOL phosphate catalysed asymmetric Nazarov cyclisation

Torquoselectivity in both 6π and 8π electrocyclisations are mainly substrate dependent and comparatively fewer in number than the 4π. Magomedov achieved a torquoselective 6π electrocyclisation with a camphor-derived compound **6.7** (Scheme 6.3).[10] The triene **6.8** is formed *in-situ* with the MAD Lewis acid and N-methylpyrrolidine (NMP), where the single diastereomeric outcome **6.9** is a result of the direction of the disrotatory 6π reducing the steric clash between the phenyl and bridgehead dimethyl groups (see **6.10** for disfavoured product).

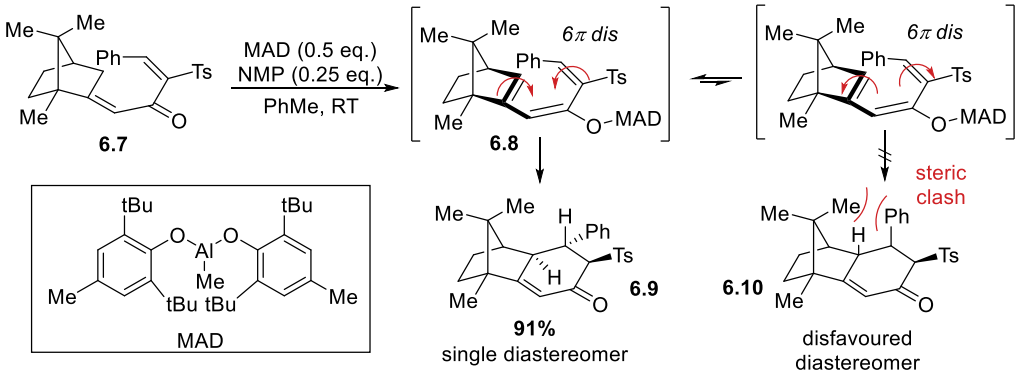

Scheme 6.3: Magomedov's Lewis acid-catalysed diastereoselective 6π electrocyclization

Paquette et al. performed the addition of two alkenyl anions (**6.11** and **6.12**) to a squarate ester **6.13**, which then undergoes a ring opening 4π electrocyclisation to generate charged octatetraenyl intermediates (Scheme 6.4).[11] The two possible chiral helical intermediates (**6.14** and **6.15**) are in equilibrium with each other, however the stereochemical outcome is dependent on the rates of their respective 8π electrocyclisations. The stereochemistry of the TBSO- group in intermediate **6.15** sterically clashes with the neighbouring cycloalkene and is destabilising the transition state. **6.14** minimises this steric clash and therefore the 8π electrocyclisation can proceed and give intermediate **6.16** with complete diastereoselectivity. Further rearrangement furnishes tetracycle **6.17** with 85% e.e.

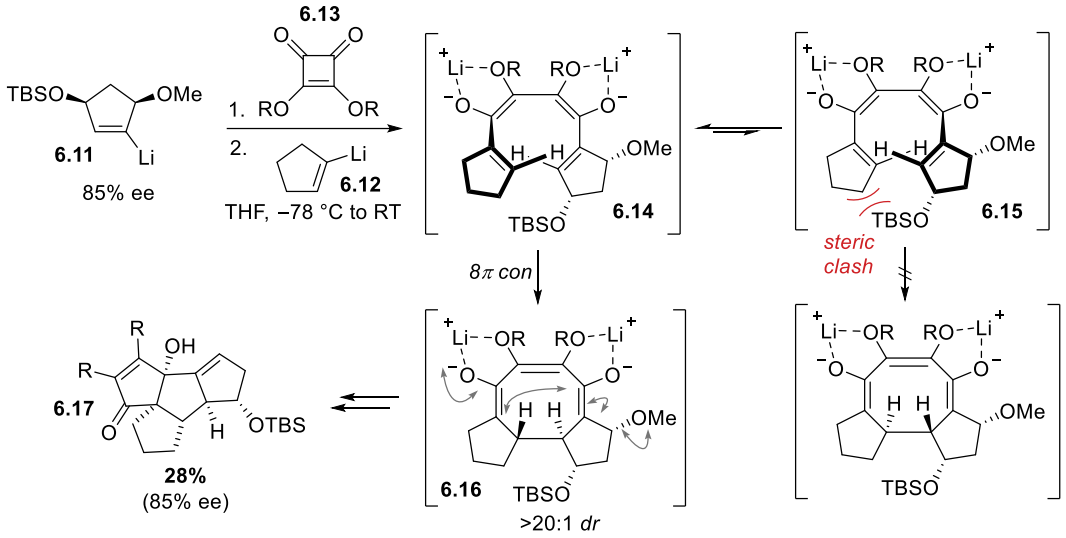

Scheme 6.4: Paquette's diastereoselective 8π electrocyclization

6π electrocyclic reactions often follow 8π electrocyclisations due to the formation of a cyclooctatriene bearing a triene with *cis*-stereochemistry which provides the prerequisite for the 6π to occur. Work by Suffert and Schreiner reported the synthesis of fenestradienes from a diastereoselective 8π/6π electrocyclic cascade.[12,13] They have conducted computational calculations that elucidate and support their experimental outcomes (Figure 6.2). Starting at tetraene **6.18** (n = 1 or 2), the first 8π transition states control the (R,R)- or (R,S)-diastereoselectivities in the cascade. The six-membered tetraene **6.18** (n=1) prefers the (R,R)-stereoisomer (5 kJ/mol lower than (R,S)-stereoisomer). Therefore, fenestradiene **6.19** (n=1) is the kinetic product from **6.18** (n=1). This preference is reversed for the seven-membered tetraene **6.18** (n=2), preferring the (R,S)- pathway (13 kJ/mol lower than (R,R)-stereoisomer). Interestingly, cyclooctatriene **6.20** is the thermodynamic product for **6.18** (n=1) and both the kinetic and thermodynamic product for **6.18** (n=2). It is postulated that the cycloalkane moieties are in their most stable conformations as cyclooctatrienes **6.20** as opposed to the high ring strains in their valence isomer fenestradienes **6.21**. This doesn't apply to cyclooctatriene **6.22** with (R,R)-configuration for both n = 1 or 2, due to unfavourable ring strain to the cycloalkane moiety. This work is currently the best illustration of a fully torquoselective 8π/6π electrocyclisation cascade in literature.

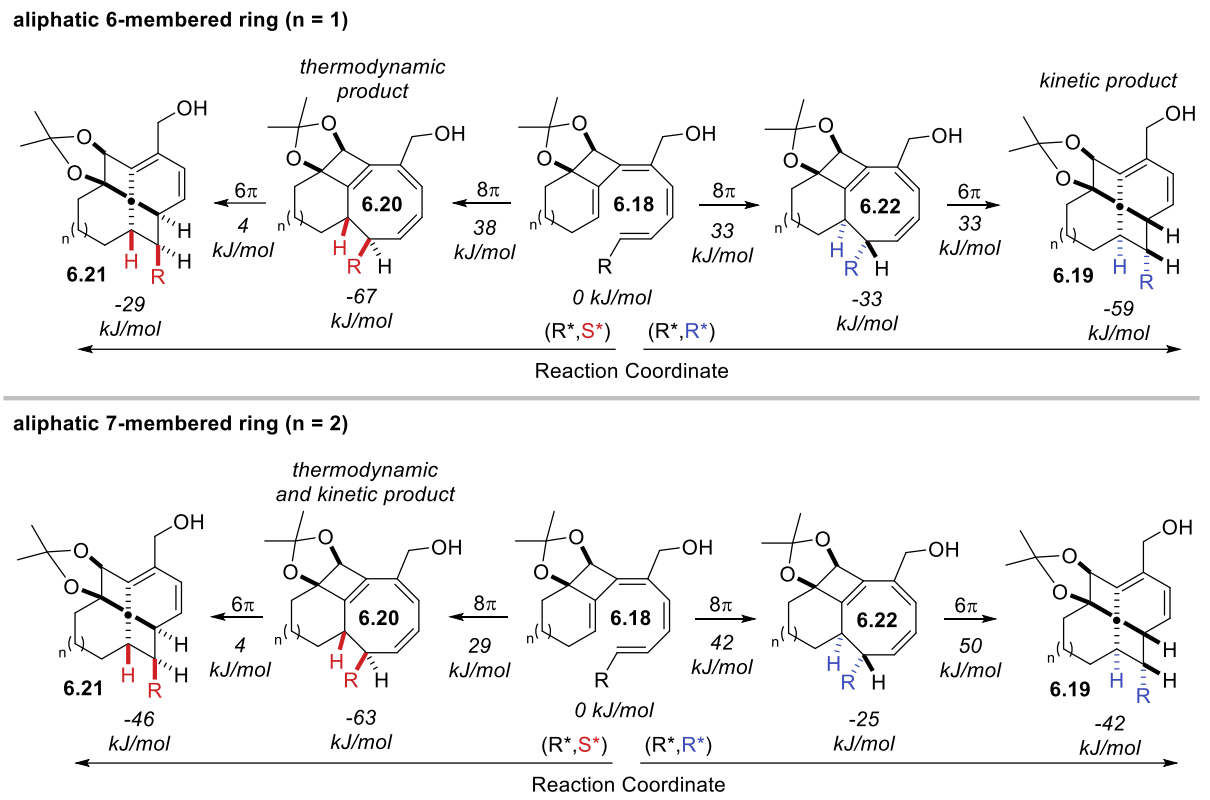

Figure 6.2: Gibbs free energy profile for the two possible stereochemical outcomes in the 8π/6π ring closing cascade for 6-membered tetraene 6.18 (n = 1) and 7-membered tetraene 6.18 (n = 2)

Torquoselective 8π/6π electrocyclisation cascades also appear in the biosynthesis of several natural products and are a key focus in this chapter.

6.2 2,4,6-trimethylbicyclo[4.2.0]octadiene related natural products

The biosynthesis of the endiandric acid family of natural products begin from a linear tetraene **6.23** that undergoes an 8π electrocyclisation to cyclooctatriene **6.24** and then a 6π electrocyclisation to afford a bicyclo[4.2.0]octadiene **6.25** (BOD) (Figure 6.3A).[14,15] Depending on the terminal substitutions of the BOD **6.26** (R_1 or R_2), an intramolecular Diels−Alder reaction (IMDA) can occur in one of two modes to furnish either the fused tetracycle **6.27** or bridged tetracycle **6.28** (Figure 6.3B). An intermolecular Diels−Alder reaction between two BODs can also occur to give pentacycle **6.29**. There is no torquoselectivity during the 8π electrocyclisation and therefore the final products are racemic. Torquoselectivity in the subsequent 6π electrocyclisation is generally minimal with both pathways often leading to mixtures of different natural products. All of these natural products are isolated as their racemates, which was one of the early clues to their non-enzymatic cascade pericyclic biosyntheses. It perhaps also highlights the inherent difficulty of enantio-torquoselective 8π electrocyclisations.

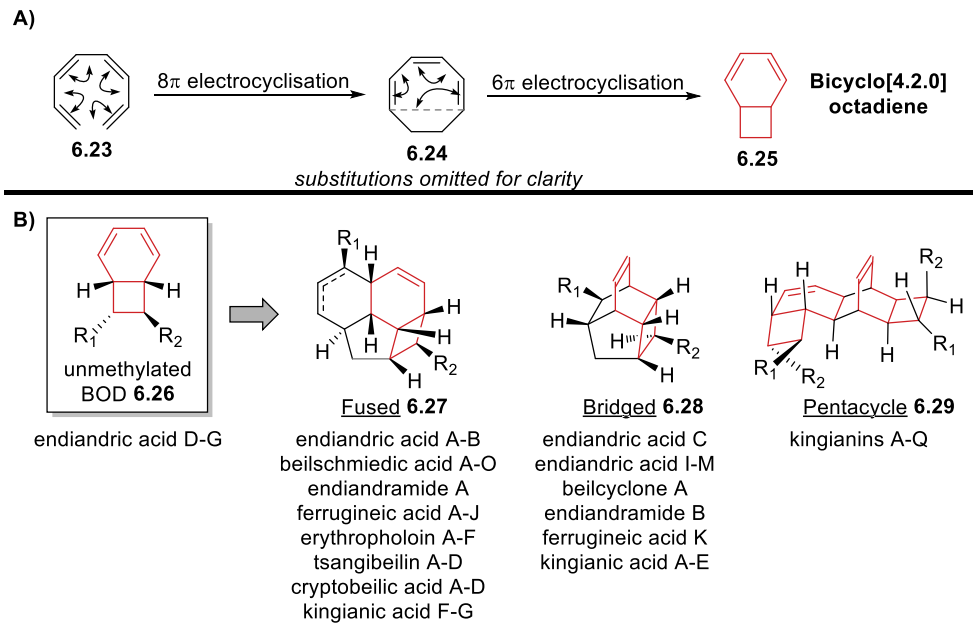

Figure 6.3: A) Biosynthetic pathway of bicyclo[4.2.0]octadiene synthesis with terminal substitutions omitted B) All reported endiandric acid derivatives with reference to their shared BOD moiety

Related to this family are a series of secondary metabolites that possess a 2,4,6-trimethylbicyclo[4.2.0]octadiene **6.30** core which are formed from a similar biosynthesis (8π/6π electrocyclisation cascade). Fascinatingly, the complex substitutions of all these molecules (compounds **6.31** to **6.40** in Figure 6.4) influence the non-enzymatically catalysed torquoselectivity of their electrocyclisations, leading to a selective preference of their respective stereoisomers. However, torquoselectivity is generally modest and diastereomer mixtures were obtained.

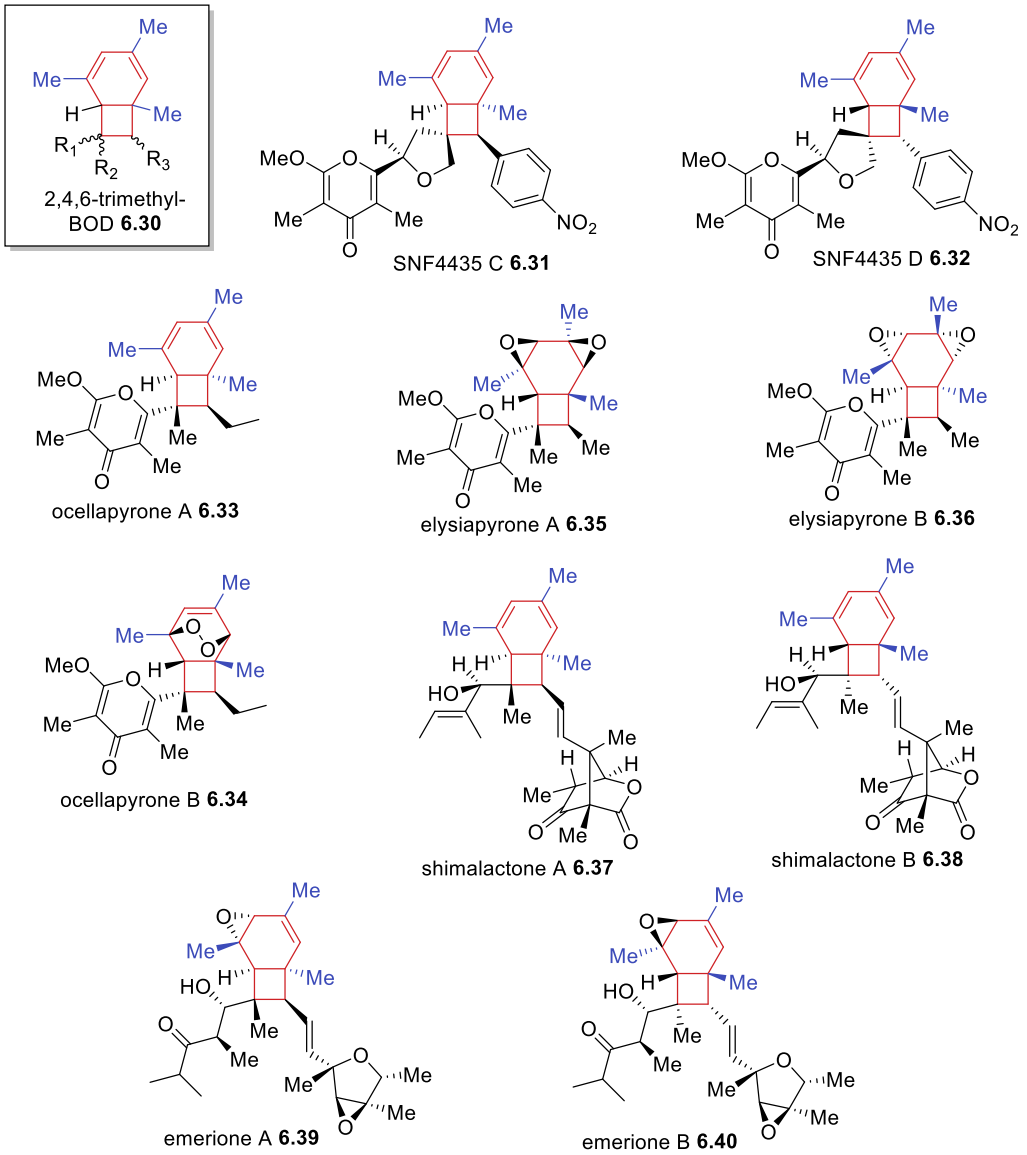

Figure 6.4: All reported 2,4,6-trimethylbicyclo[4.2.0]octadiene related natural products

6.2.1 Previous syntheses of 2,4,6-trimethylBOD related natural products

6.2.1.1 SNF4435 C and D

Parker (2004), Baldwin (2005) and Trauner (2005) have all accomplished total syntheses of SNF4435 C **6.31** and SNF4435 D **6.32**.[16–18] All have intersected compound **6.41** (either directly or from an in-situ alkene isomerisation) to yield similar outcomes. Parker accessed SNF4435 C **6.31** and D **6.32** in a 4:1 ratio. Baldwin undertook a biomimetic approach, reporting a 3.6:1 ratio of **6.31** and **6.32**, respectively. Trauner furnished **6.31** and **6.32** in a 3:1 ratio, respectively. It was highlighted that there had to be torquoselectivity in both the 8π and 6π electrocyclisation. There are two possible 8π transition states: $TS_{8\pi}$ **6.42** and **6.43**. $TS_{8\pi}$ **6.42** has its pyrone moiety pointing away from the aryl substituent whereas $TS_{8\pi}$ **6.42** is pointing towards it. The steric hindrance that arises in $TS_{8\pi}$ **6.42** is proposed to influence selectivity towards the $TS_{8\pi}$ that eventual affords SNF4435 C **6.31**. The 6π electrocyclisation is exclusively endo-selective with $TS_{6\pi}$ **6.44** and **6.45** leading to the corresponding natural products ("*endo*" denotes the aryl substituent facing the same direction as the cyclohexadiene moiety). The explanation of this outcome will be answered in a later section. Their isolation from natural sources yielded a rough 3:1 ratio, closely matching all previous laboratory syntheses and supports its non-enzymatic origin.

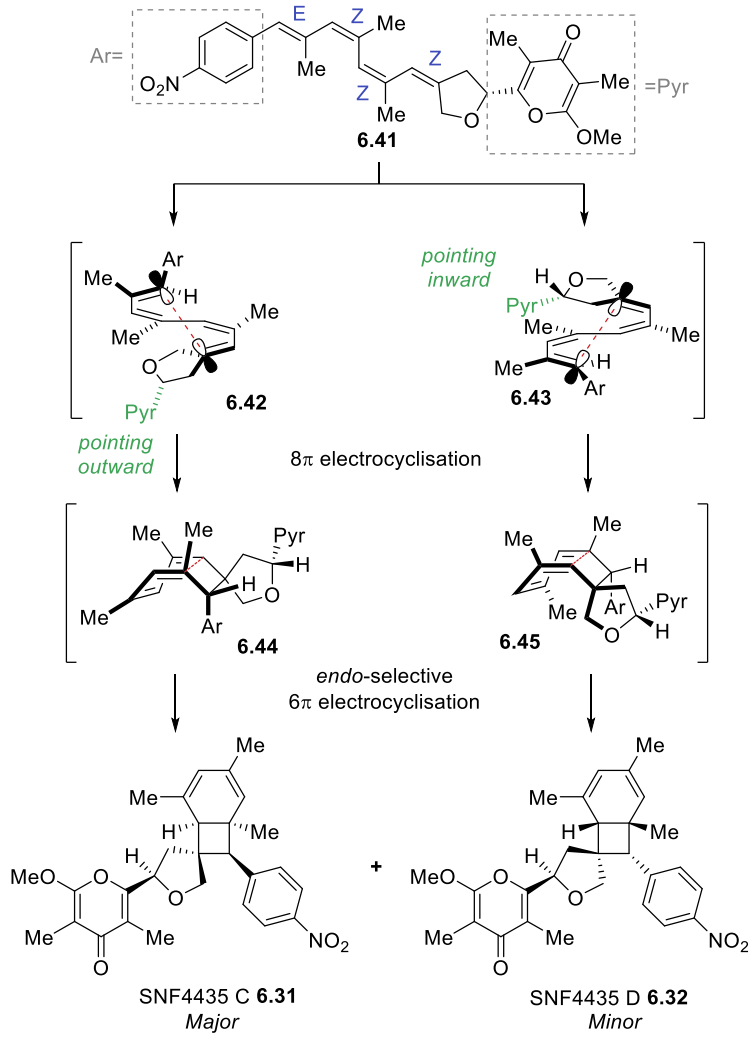

Scheme 6.5: Mechanistic pathway to SNF4435 C and D

6.2.1.2 Ocellapyrone A and B

Trauner (2005) and Adlington/Moses (2007) have both intersected compound **6.46** in their respective total syntheses of ocellapyrones.[19,20] In Trauner's synthesis, the alkene isomerisation to intermediate **6.47**, 8π electrocyclisation to cyclooctatrienes **6.48** and **6.49** and final 6π electrocyclisation was performed at 45 °C. Ocellapyrone A **6.33** and compound **6.50** was formed in a 1:9.8 ratio, respectively. Compound **6.50** was then converted to ocellapyrone B **6.34** via a [4+2] cycloaddition with singlet oxygen. At elevated temperatures of 150 °C, ocellapyrone A **6.33** was present but no **6.50**. This outcome was supported by Adlington/Moses where they applied temperatures of 120 °C on compound **6.46** to only furnish ocellapyrone A **6.33** with no compound **6.50**. It was postulated that **6.50** is likely to be the kinetic product in the 6π electrocyclisation but at high temperatures the reaction becomes reversible with equilibrium favouring the thermodynamically stable *exo* conformer, ocellapyrone A **6.33**. It must also be noted that no torquoselectivity occurs in the 8π electrocyclisation, therefore leading to racemic products.

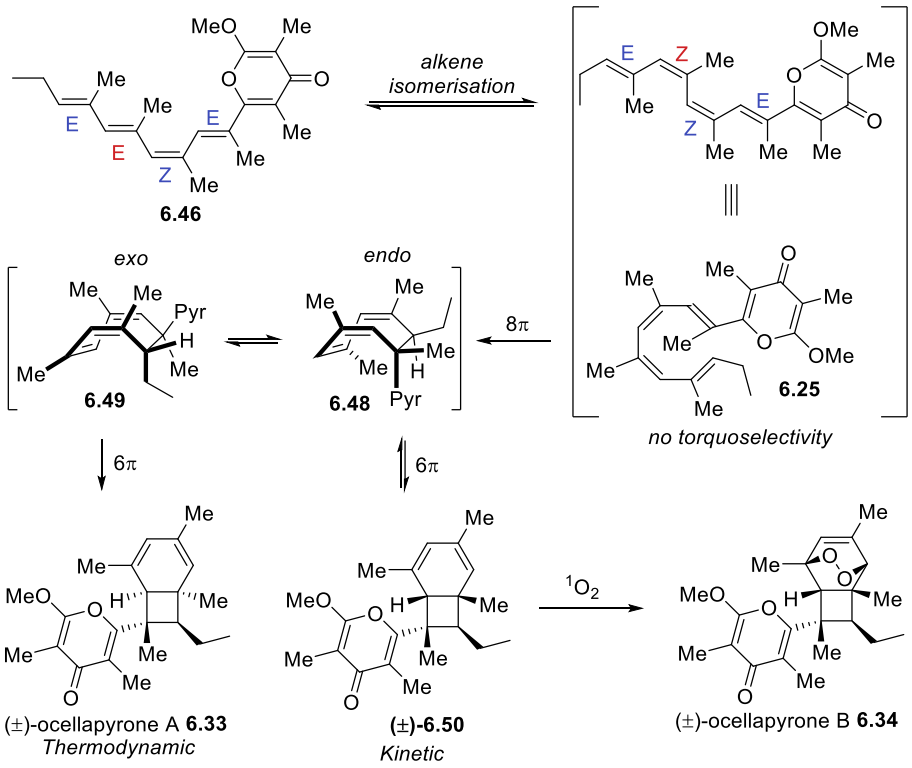

Scheme 6.6: Mechanistic pathway to ocellapyrone A and B

6.2.1.3 Elysiapyrone A and B

Elysiapyrone A **6.35** and B **6.36**, synthesised by Trauner (2005), have a similar 6π electrocyclisation selectivity to ocellapyrones (**6.33** and **6.34**).[21] The 8π electrocyclisation of compound **6.51** is not torquoselective, but at mild thermal conditions, there is a kinetic preference for the *endo* product **6.54** in the 6π electrocyclisation as opposed to the thermodynamically more stable *exo* **6.55** (ratio of 1.9:1). ("*endo*" denotes the pyrone substituent facing the same direction as the cyclohexadiene moiety)

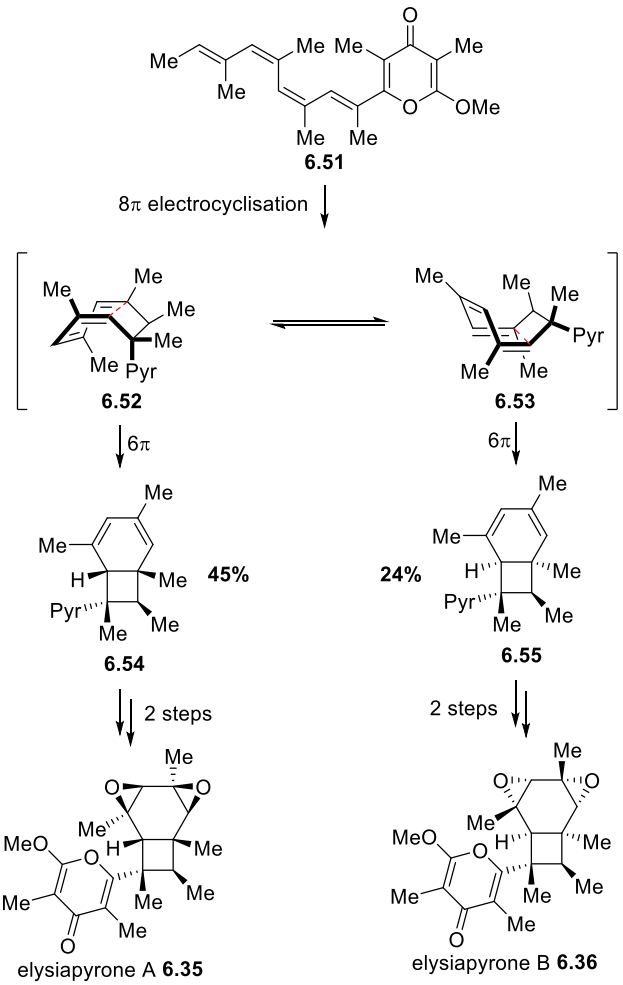

Scheme 6.7: Mechanistic pathway to Elysiapyrone A and B

6.2.1.4 Shimalactone A and B

Shimalactones A **6.37** and B **6.38** have been synthesised chemically by Trauner (2008) and chemoenzymatically by Fujii and Uchiyama (2020).[22,23] In Trauner's synthesis starting from compound **6.56**, the 8π electrocyclisation experiences torquoselectivity due to the steric clash between the two chiral terminal substituents on the tetraene (allyl alcohol and keto-lactone groups highlighted on **6.56**), with $TS_{8\pi}$ **6.57** being favoured over **6.58**. Similar to the SNF compounds, the 6π electrocyclisation is *endo*-selective ($TS_{6\pi}$ **6.59** and **6.60**) to furnish shimalactone A **6.37** and B **6.38** in a 5:1 ratio. ("*endo*" denotes the keto-lactone substituent facing the same direction as the cyclohexadiene moiety)

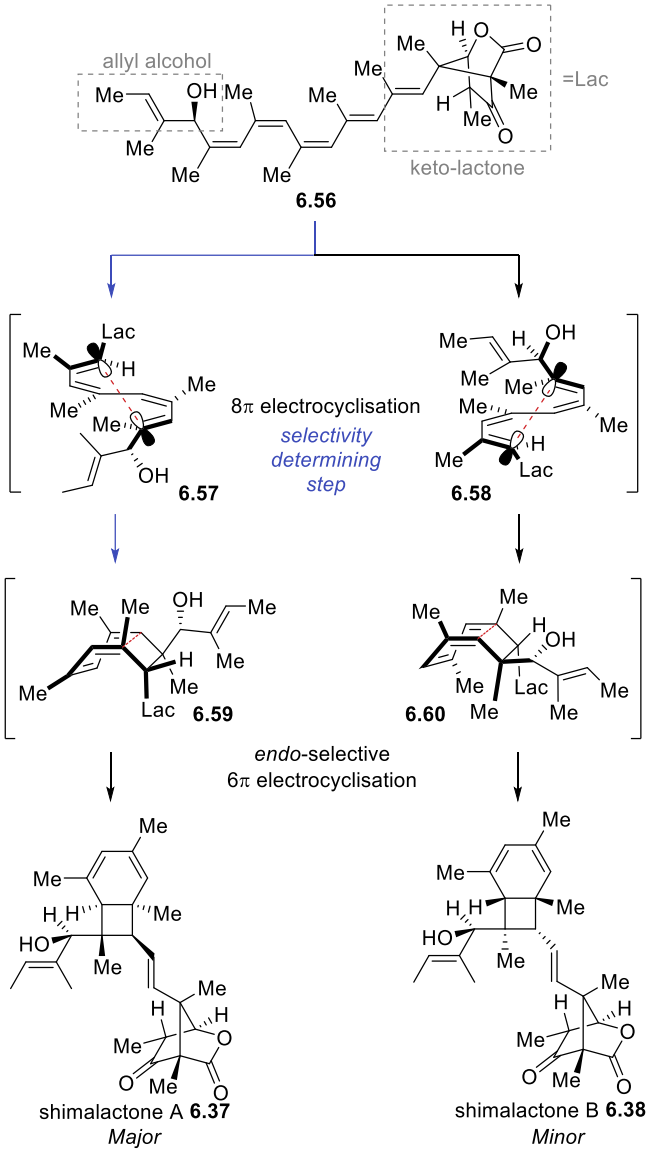

Scheme 6.8: Mechanistic pathway to shimalactone A and B

Fujii and Uchiyama reported an impressive biosynthesis study, where they identified and expressed a biosynthetic gene cluster to synthesise preshimalactone **6.61** and preshimalactone epoxide **6.62**. They confirmed the cascade to the natural products proceeded non-enzymatically from preshimalactone epoxide **6.62** where compound **6.56** is an intermediate. They also modelled the reaction pathway using DFT calculations of the 8π/6π electrocyclisation cascade, reporting $TS_{8\pi}$ **6.57** to be 15.1 kJ/mol lower than $TS_{8\pi}$ **6.58**, despite ground state shimalactone B **6.38** being 3.3 kJ/mol lower than **6.37**. This suggests the preference for shimalactone A **6.57** to be kinetically driven.

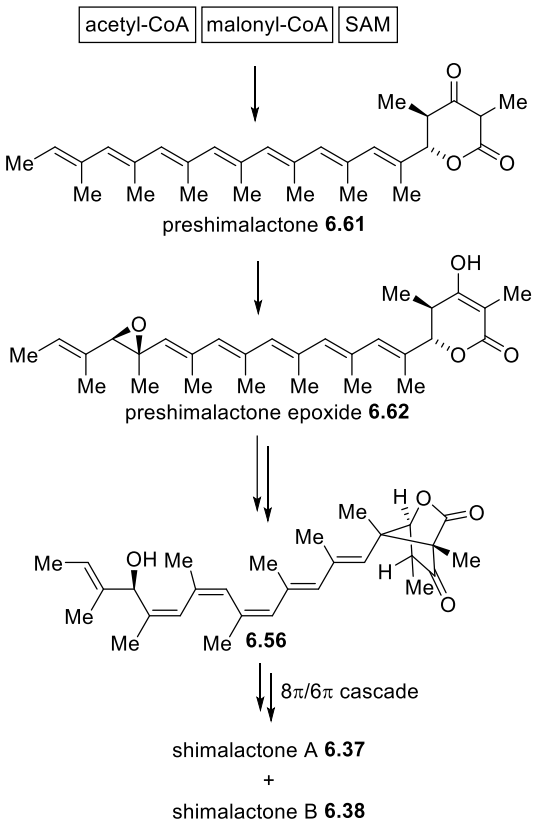

Scheme 6.9: Shimalactone biosynthesis starting from preshimalactone

6.2.1.5 Emerione A and B

Miller in 2022 published a bioinspired synthesis of emerione A **6.39** and B **6.40**.[24] The 8π electrocyclisation starting from compound **6.63** was unselective which was verified by their own computational calculations, with the $TS_{8\pi}$ and cyclooctatrienes of **6.64** and **6.65** to be isoenergetic. The 6π electrocyclisation was *endo*-selective. Their computational work calculated the *endo* $TS_{6\pi}$ of **6.64** and **6.65** (shown in Scheme 6.10A) to be 7.9 and 7.5 kJ/mol lower than the alternative *exo* $TS_{6\pi}$, respectively (see Scheme 6.11B for visual clarification on *exo*-6π product). It was postulated that there was "a strong and dominant steric penalty when the bridgehead methyl is *syn* to the vinyl dioxabicyclo[3.1.0]hexane moiety". The outcome is the preference for the product's bridgehead methyl being *trans* to the moiety, highlighted in green (compounds **6.66** and **6.67** in Scheme 6.10). This reasoning can be extrapolated to other syntheses involving *endo*-selective 6π electrocyclisations (SNF4435 C **6.31** and D **6.32**, and shimalactone A **6.37** and B **6.38**). *m*CPBA oxidations of **6.66** and **6.67** deliver emerione A **6.39** and B **6.40**, respectively.

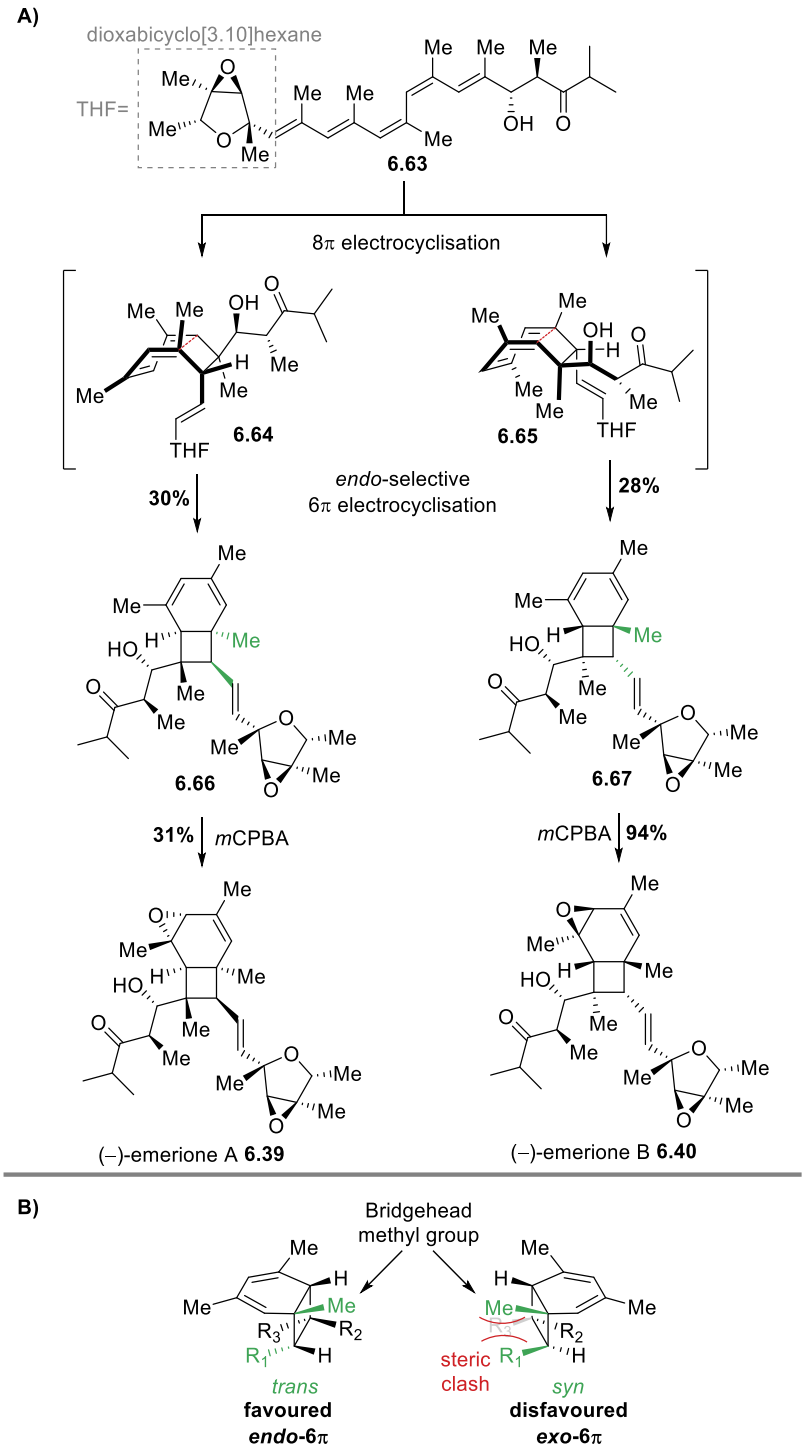

Scheme 6.10: A) Mechanistic pathway to emerione A and B. B) General graphic for *endo* and *exo* 6π products

6.3 General Aims

Developments in torquoselective 6π and 8π electrocyclisations have been limited to specific engineered substrates. The previous section highlighted substrates which provide low to mild levels of torquoselectivity in the 8π/6π electrocyclisation cascade in a total synthesis setting. Literature has already established the importance of the 2-methyl in terms of 6π torquoselectivity, however, understanding the role of all the methyl groups would give a complete picture on their effects on the kinetics and thermodynamics of the cascade (Figure 6.5A). There have been few attempts on the asymmetric synthesis of bicyclo[4.2.0]octadiene compounds and calculating the rate of reversibility of the 8π/6π cascade would be important for future endeavours (Figure 6.5B). Modelling the 8π/6π cascade of previously synthesised natural

products and engineered molecules that provide mild 8π torquoselectivity (Figure 6.5C) would give complementary insight and serve to test the computational methodology used. Finally, the 8π/6π cascade of several hypothetical substrates will be modelled to test their aptitude for 8π torquoselectivity (Figure 6.5D). By conducting a purely computational study on a selection of examples and models, we hope to fill knowledge gaps, elucidate a general pattern of the 8π/6π electrocyclisation cascade and ultimately offer insights for the development of asymmetric 8π electrocyclic reactions.

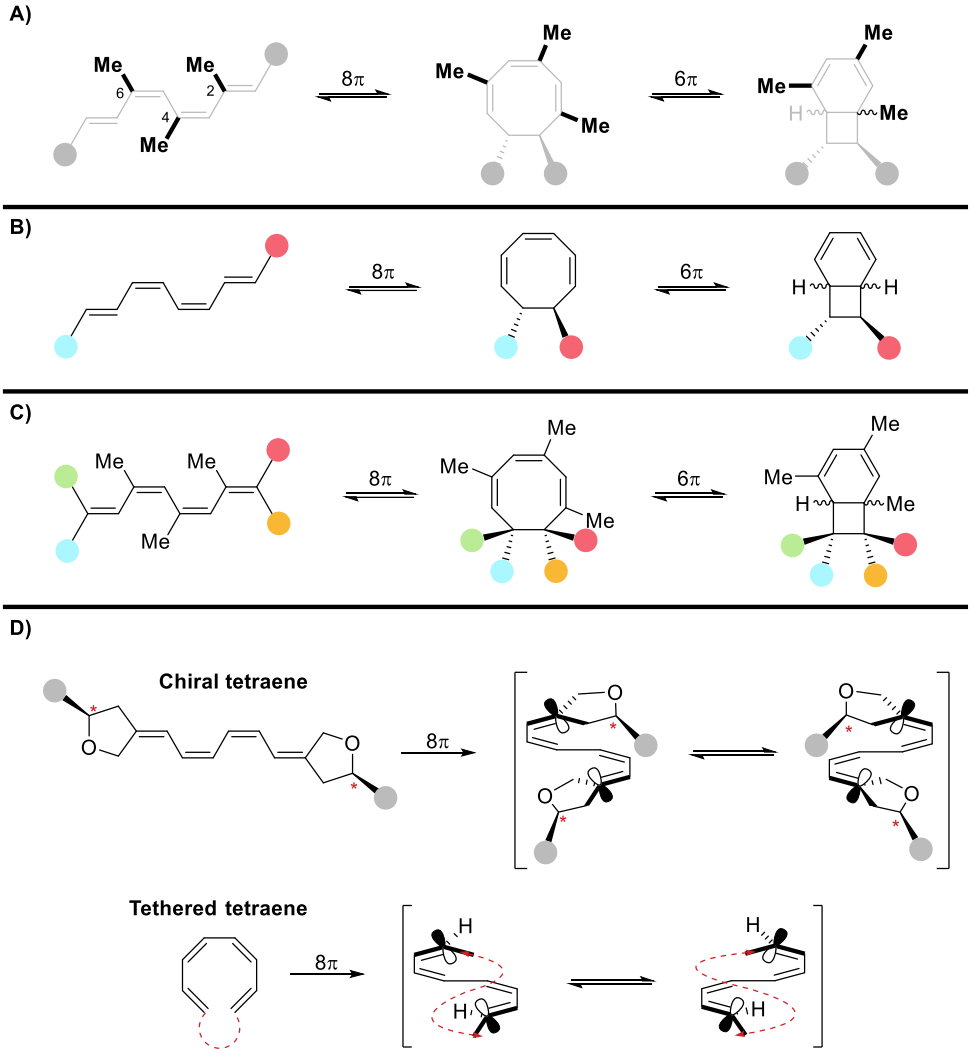

Figure 6.5: A) Observing the effects of methyl groups on the overall kinetics and thermodynamics in the 8π/6π cascade. B) Calculating the rate of reversibility of the 8π/6π cascade. C) Modelling the 8π/6π cascade of natural products and engineered molecules. D) Modelling the 8π/6π cascade of hypothetically 8π torquoselective substrates.

6.4 Results and Discussion

6.4.1 Effects of the methyl substitution on the 8π/6π cascade of 2,4,6-trimethylbicyclo[4.2.0]octadiene

To gain a complete understanding of the methyl group effects, we calculated the energy profile of the synthetic pathway from tetraene to BOD of various combinations of substituted tetraenes **6.68-6.77**, where the positions of the methyl groups directly correlate to the natural products (Figure 6.6). By isolating and having different combinations of methyl groups, we can identify their specific functions.

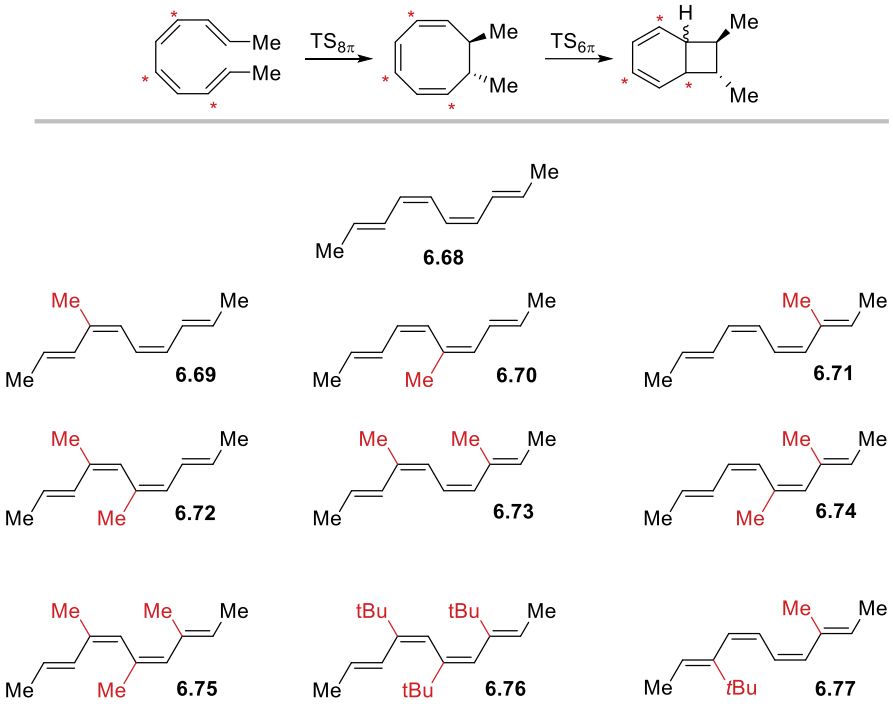

Figure 6.6: Entire scope for methyl tetraenes 6.68-6.77

This section can be considered complementary to Houk's computational work on terminal substituent effects on the 8π/6π cascade of 1,3,5,7-tetraenes (Figure 6.7).[25] Using M062X/6-31+G(d,p) computations, they reported the 6π electrocyclic ring closure is typically the rate determining step (RDS) of the cascade. For un- and mono-substituted tetraenes (**6.78-6.80**), the 8π is facile, but the 6π closure is slow and reversible. Di- and tri-substituted tetraenes (**6.68**, **6.81-6.85**) undergo facile 8π, however are less exergonic due to steric clash destabilising the cyclooctatriene. The subsequent 6π is kinetically facile and thermodynamically favourable due to release of steric hindrance when converted to the corresponding BOD. Tri- and tetra-substituted tetraenes (**6.84-6.86**) exclusively give the BOD structure. It was also highlighted that di- and tri-substituted tetraenes (**6.68**, **6.81-6.85**) can undergo diastereoselective 6π electrocyclisations.

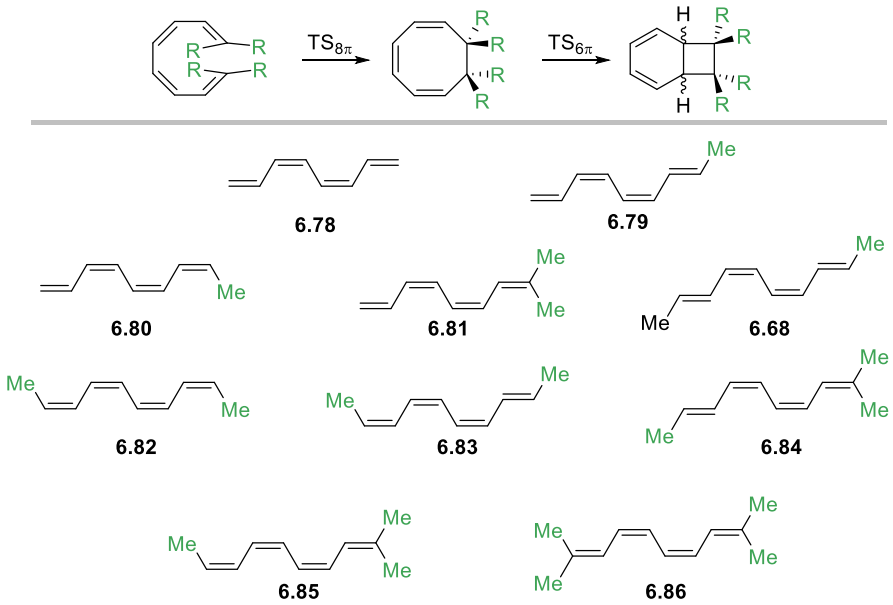

Figure 6.7: Houk's set of 1,3,5,7-octatetraenes

We started with tetraene **6.68**, using M062X functional and def2SVP basis set for geometry optimisations/frequency calculations and the same functional with def2TZVP basis set to calculate the single point energies (and used for all subsequent calculations within this chapter).[26–29] The numbers highlighted in blue are our values and red are Houk's values that have been converted from kcal/mol to kJ/mol (Scheme 6.11). Using the def2TZVP basis (vs 6-31+G(d,p)) gives similar results with somewhat elevated reaction barriers and predicts somewhat lower product stabilities. The **$TS_{6\pi}$** is the RDS (activation energy of 99.9 kJ/mol) and the BOD **6.88** is the thermodynamic sink (-15.1 kJ/mol) and has a high reverse barrier energy of 108.3 kJ/mol.

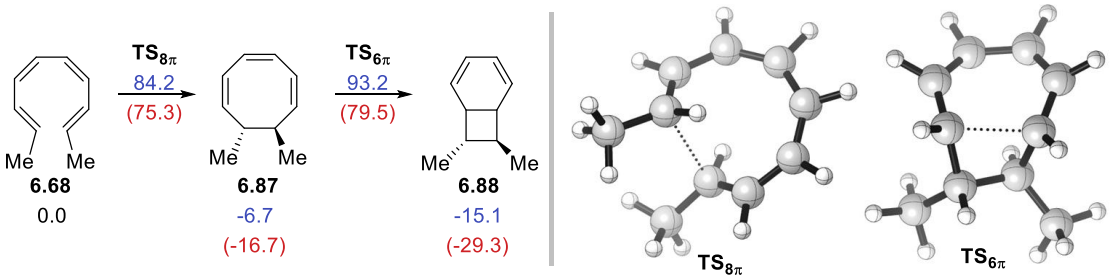

Scheme 6.11: Gibbs free energy profile (kJ/mol) and transition structures for the 8π/6π ring closure cascade of tetraene 6.68

Our next step is to add one methyl substituent in positions that correlate with the methylation pattern of the natural products to isolate their respective effects. There are three possibilities with a methyl group introduced at C6 (**6.69**), C4 (**6.70**) and C2 (**6.71**). The free energies of activation for 8π ($\Delta G^{\ddagger}_{8\pi}$) and 6π ($\Delta G^{\ddagger}_{6\pi}$) ring closure and the ground state energies for the 8π ($\Delta G_{8\pi}$) and 6π ($\Delta G_{6\pi}$) electrocyclization products for tetraenes **6.69**-**6.71** have been summarised in scheme 6.12. $\Delta G_{6\pi 1}$ (arising from $\Delta G^{\ddagger}_{6\pi 1}$) designates the unfavourable *syn* BOD and $\Delta G_{6\pi 2}$ (arising from $\Delta G^{\ddagger}_{6\pi 2}$) indicates the favourable *trans* BOD. All Gibbs free energies are reported in kJ/mol and were calculated using the tetraene precursor as the point of reference. In scheme 6.12 for the monomethyl tetraenes **6.69**-**6.71** calculated free energies, it is clear that the C2 methyl has the greatest effect on lowering the $\Delta G^{\ddagger}_{8\pi}$ (see tetraene **6.71**), with the C4 methyl in tetraene **6.70** having the least. The $\Delta G_{6\pi 2}$ of **6.71** is 10.8 kJ/mol lower than its $\Delta G_{6\pi 1}$ counterpart, whereas $\Delta G_{6\pi 2}$ **6.69** and **6.70** is 5.5 and 5.6 kJ/mol lower, respectively. Therefore, the C2 methyl group imparts the greatest influence on the thermodynamics. Oddly, the $\Delta G^{\ddagger}_{6\pi 2}$ of **6.69** and **6.71** are comparable to their $\Delta G^{\ddagger}_{6\pi 1}$ counterpart. $\Delta G^{\ddagger}_{6\pi 2}$ **6.70** is calculated to be 0.9 kJ/mol higher than $\Delta G^{\ddagger}_{6\pi 1}$ **6.63**, but can be considered isoenergetic.

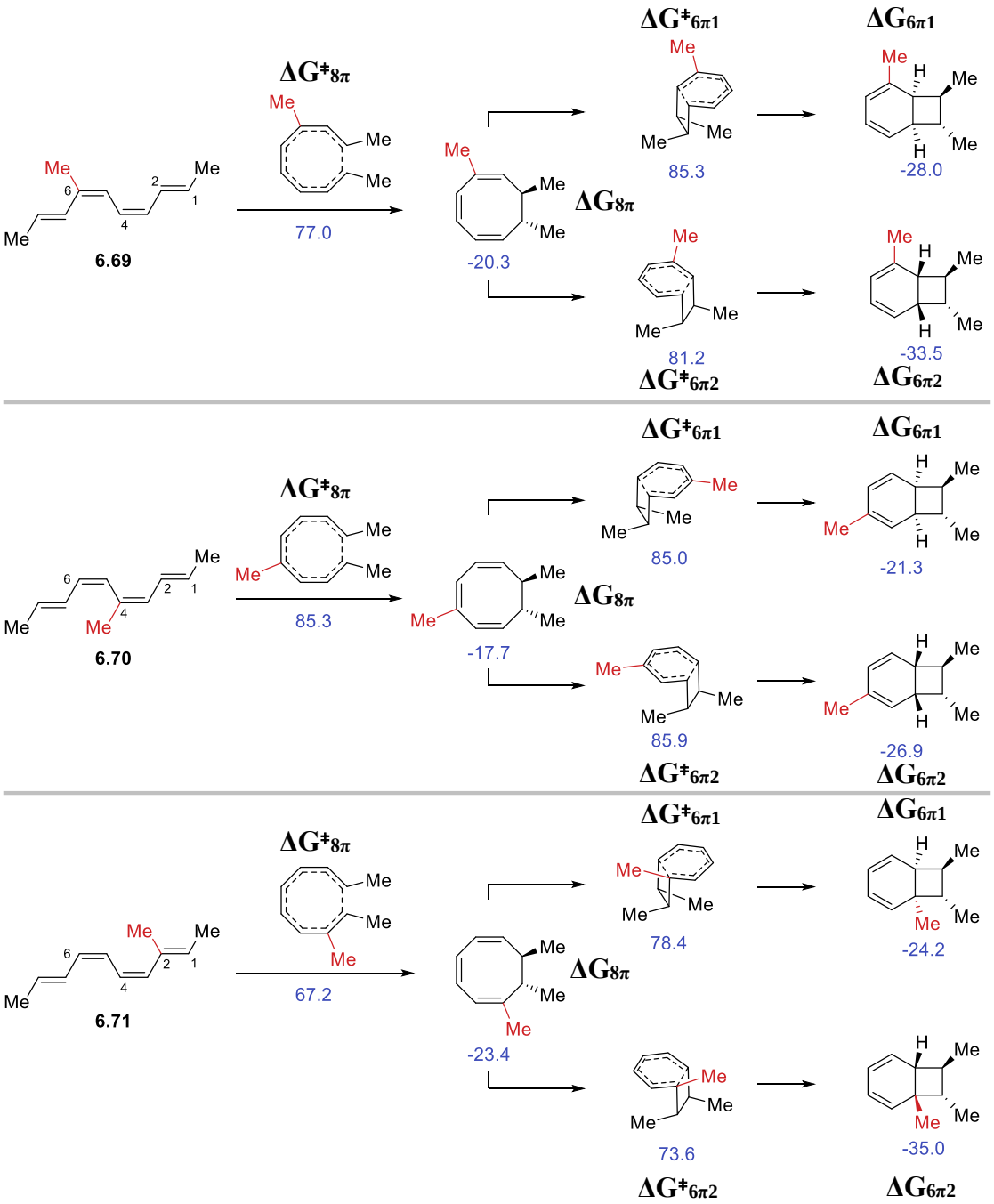

Scheme 6.12: Summary of computed activation and reaction free energies for 8π/6π cascade ring closures of dimethyl tetraenes 6.69-6.71

Moving on, we installed the second methyl substituent in positions that correlate with the natural products to observe potential synergetic behaviour. There are three possibilities with methyl groups at C6/C4 (**6.72**), C6/C2 (**6.73**) and C4/C2 (**6.74**). The free energies of activation for 8π ($\Delta G^{\ddagger}_{8\pi}$) and 6π ($\Delta G^{\ddagger}_{6\pi}$) ring closure and the ground state energies for the 8π ($\Delta G_{8\pi}$) and 6π ($\Delta G_{6\pi}$) electrocyclization products for tetraenes **6.72-6.74** have been summarised in scheme 6.13. The $\Delta G^{\ddagger}_{8\pi}$ of all dimethyl tetraenes **6.72-6.74** are generally lower in energy than the $\Delta G^{\ddagger}_{8\pi}$ of monomethyl tetraenes **6.69-6.71**, with the exception of **6.72**. The absence of the C2 methyl in tetraene **6.72** corresponded to a comparatively higher $\Delta G^{\ddagger}_{8\pi}$ of 76.2 kJ/mol, compared to tetraenes **6.73-6.74**. The $\Delta G_{6\pi 2}$ of **6.73** and **6.74** are roughly 10 kJ/mol lower than their $\Delta G_{6\pi 1}$ counterpart, whereas $\Delta G_{6\pi 2}$ **6.72** is only 5.8 kJ/mol lower. Although the C2 methyl still maintains the greatest influence, we are seeing additive effects from the other methyl groups when present.

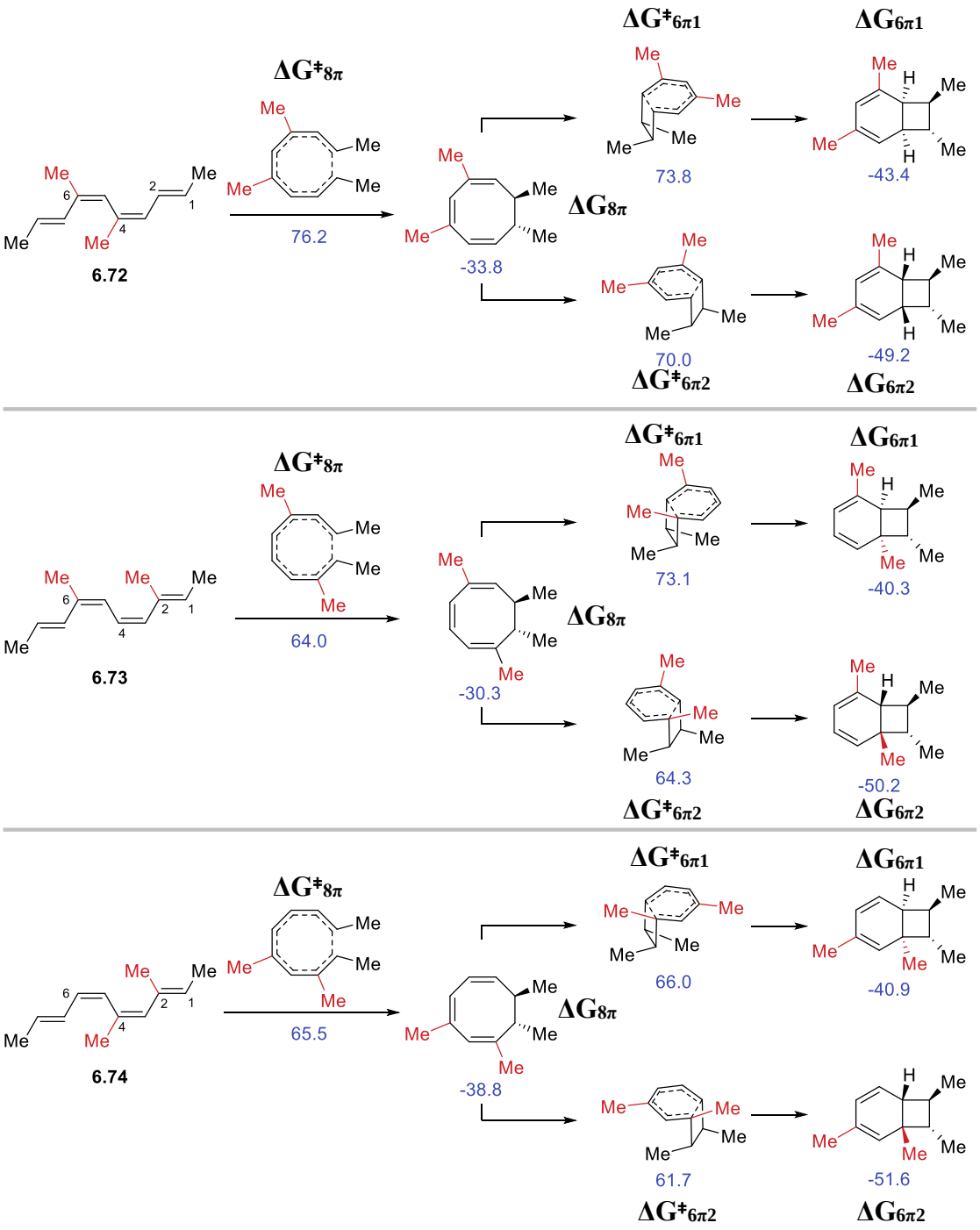

Scheme 6.13: Summary of computed activation and reaction free energies for 8π/6π cascade ring closures of dimethyl tetraenes 6.72-6.74

Finally, we modelled the full trimethyl tetraene **6.75**. In comparing tetraene **6.68** to **6.75**, the 8π is considerably more facile with a transition state barrier of 62.6 kJ/mol to reach cyclooctatriene **6.89** which is also more exergonic than **6.87** with an energy of -47.2 kJ/mol (Scheme 6.14)). **TS1$_{6\pi}$** is 7.8 kJ/mol higher than **TS2$_{6\pi}$** and the resulting **BOD 6.90** is 9.6 kJ/mol lower than **BOD 6.91**. The 6π to **6.90** is both more kinetically rapid and thermodynamically favourable than its diastereomer **6.91**. This was anticipated due to the favourable *trans* relationship between the terminal (on C1) and bridgehead methyl (on C2). Across the 8π/6π cascade ring closures in tetraenes **6.69-6.75**, the C2 methyl provides the greatest influence for lowering the 8π electrocyclisation activation energy as well as directing the cascade to the favoured **ΔG$_{6\pi2}$** product. However, the C4 and C6 methyl groups provide an additive effect on the thermodynamic stability of the **ΔG$_{6\pi2}$** product. Houk's previously stated trend of increasing the

number of substitutions leads to more rapid kinetics and favourable thermodynamics is documented in our work, when you move from unsubstituted tetraene **6.68** to monomethyl **6.69-6.71**, dimethyl **6.72-6.74** and finally trimethyl tetraene **6.75**.

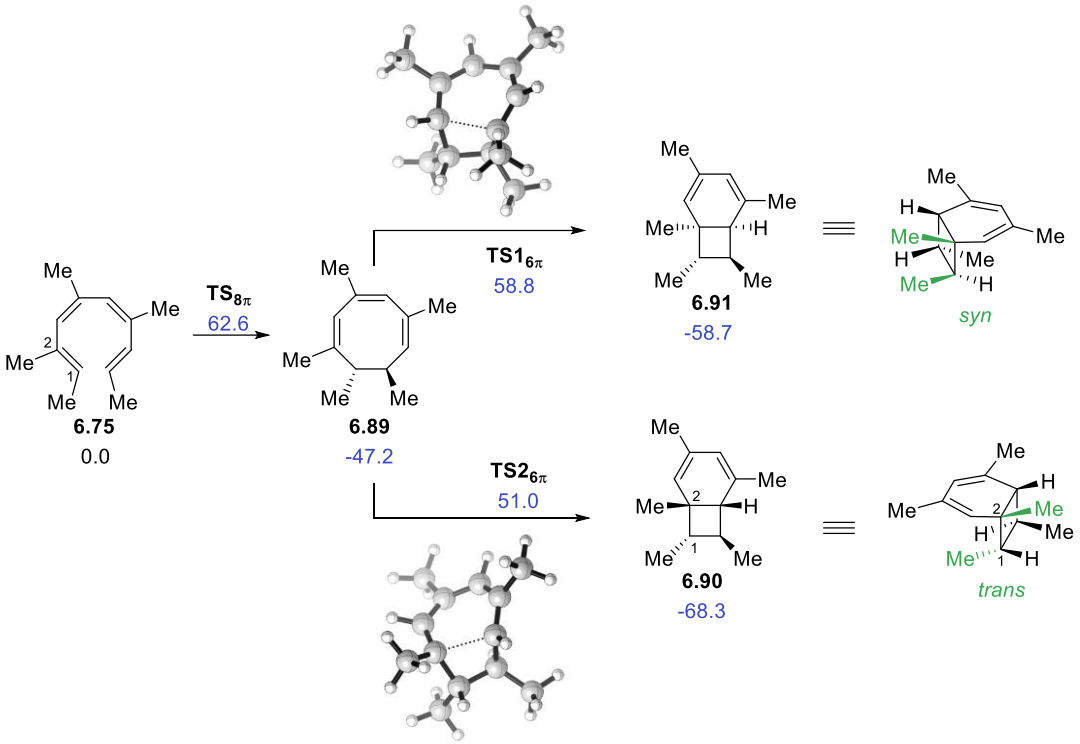

Scheme 6.14: Gibbs free energy profile (kJ/mol) and transition structures for the 8π/6π ring closure cascade of tetraene 6.75

It can be envisioned that bulkier groups would amplify the aforementioned effects on the 6π/8π cascade. Replacing the three internal methyl groups with *t*-butyl groups gives tetraene **6.76** which was modelled and presented in scheme 6.15. Starting with tetraene **6.76**, a comparatively large 89.0 kJ/mol is required to overcome the 8π transition state barrier to reach cyclooctatriene $\Delta G_{8\pi}$ **6.91**, which could be owed to potential steric clashes of three *t*-butyl groups (Scheme 6.15). $\mathbf{TS2}_{6\pi}$ is considerably lower than $\mathbf{TS1}_{6\pi}$, differing by a significant 23 kJ/mol. These large differences continue with **6.92** being 25.2 kJ/mol lower than **6.93**.

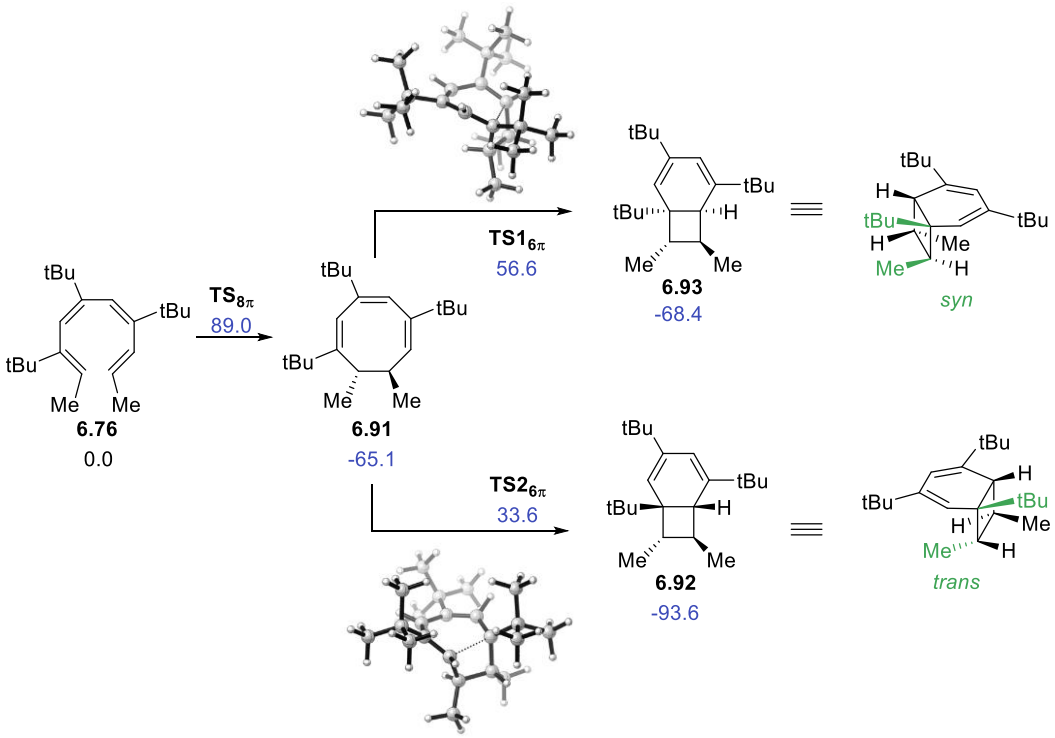

Scheme 6.15: Gibbs free energy profile (kJ/mol) and transition structures for the 8π/6π ring closure cascade of tetraene 6.76

Venturing a little beyond our scope, we wished to compare the effects different sizes of substituents at the C2 and C7 positions would have on the cascade. Installing a *t*-butyl group at C2 and a methyl group at C7 gives use tetraene **6.77** which has been modelled and presented in scheme 6.16. The 8π cyclisation to **6.94** is facile with an activation energy of 63.3 kJ/mol. **6.95** is shown to be the preferred product in terms of kinetics and thermodynamics when compared to the alternative **6.96**. This likely arises from the favoured least sterically hindered product and associated 6π transition state. In general, the facile nature of converting the methylated tetraenes to their respective BOD structures, either in the natural products or their simple derivatives, arises from the destabilising effects of the methyl groups on the backbone. However, the global minimum of this cascade is the cyclooctatriene intermediate **6.94**, which is likely owed to the cyclobutane moieties in the **6.95** and **6.96** BODs being sterically encumbered and therefore would assume a mixture of both **6.94** (major) and **6.95** (minor).

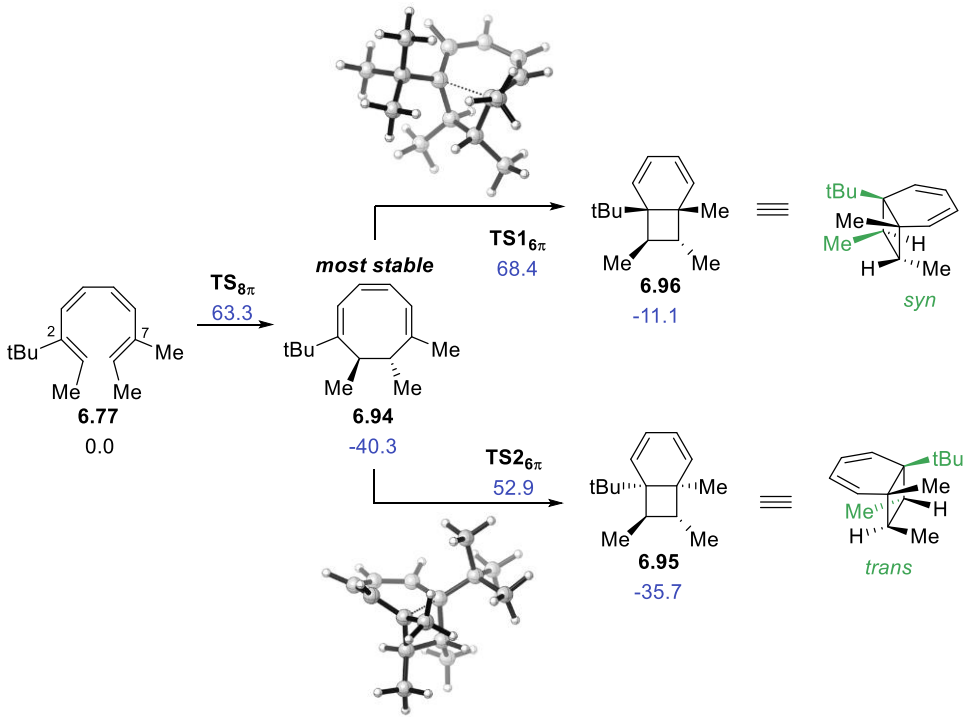

Scheme 6.16: Gibbs free energy profile (kJ/mol) and transition structures for the 8π/6π ring closure cascade of tetraene 6.77

Terminal substituents may also have an effect on the torquoselectivity of the 6π electrocyclisation, instead of solely the methyl groups on the tetraene backbone. Our calculations advised the *trans* products to be both the kinetic and thermodynamic products, however is at odds with some natural product syntheses. This was observed during the synthesis of ocellapyrones, where the kinetic product was the *syn* ocellapyrone B **6.34** and the thermodynamic product was the *trans* ocellapyrone A **6.33** (Scheme 6.17A). Similarly for the synthesis of elysiapyrones, the major product was the kinetically favoured *syn* elysiapyrone A **6.35** (Scheme 6.17B). Therefore, care needs to be taken when applying what was learnt in this section to other related natural products. The C2 substituent does have a major role in torquoselectivity, but terminal substituents may also be important. Future work might involve modelling a variety of terminal substituents to understand the inconsistency with some 2,4,6-trimethylbicyclo[4.2.0]octadiene natural product synthesis outcomes.

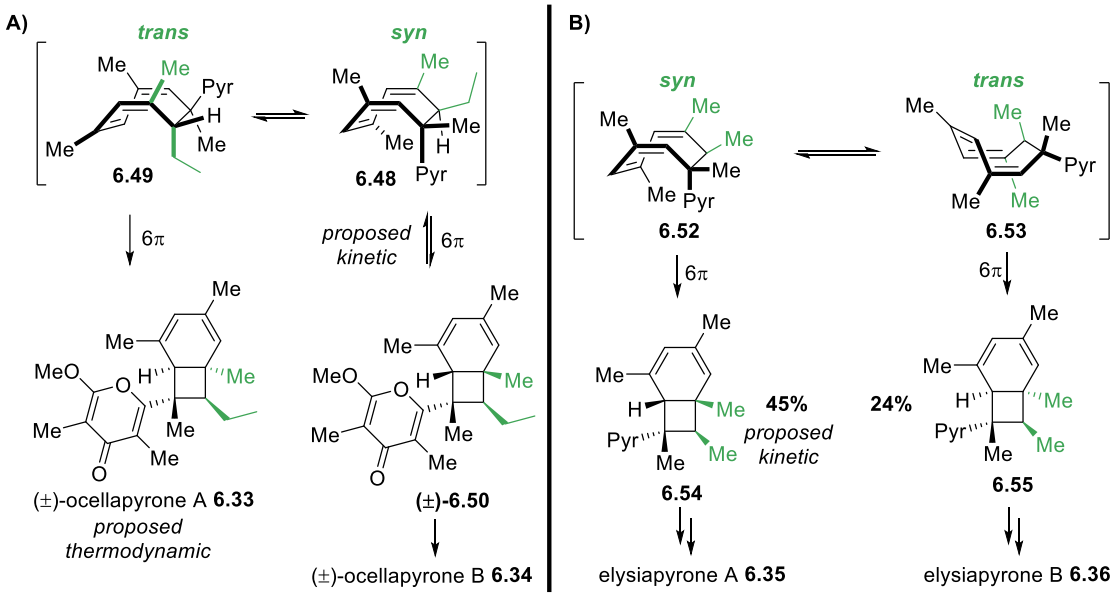

Scheme 6.17: A) Snapshot of ocellapyrone synthesis from scheme 6.6. B) Snapshot of elysiapyrone synthesis from scheme 6.7

6.4.2 Reversibility in the biosynthetic cascade of endiandric acid related natural products

There is no suggested torquoselectivity in the 8π electrocyclisation step of the biosynthetic cascade of endiandric acid derivatives, as they are isolated as racemic mixtures. This was also the original clue in favour of a non-enzymatic biosynthetic cascade. Torquoselectivity in the 6π electrocyclisation is not relevant since the subsequent IMDA only proceeds through an *endo*-selective pathway, in regards to fused **6.27** and bridged **6.28** tetracycles. Despite this, there have been efforts on the enantioselective synthesis of endiandric natural products.

6.4.2.1 Towards enantioselective synthesis of bis-methylenehydroxy BOD

In Nicolaou's hallmark work involving the syntheses of endiandric acids A-G, bis-methylenehydroxy tetraene **6.97** was synthesised and collapsed into BOD **6.98**, which served as an intermediate from which the divergent total synthesis occurred (Scheme 6.18A).[30–34] In a 2022 paper, Brown reported the enantioselective isomerization/stereoselective [2+2] cycloadditions that access bicyclo[4.2.0]octanes.[35] To test the applicability of his methodology, Brown devised an enantioselective synthesis of Nicolaou's intermediate **6.98**. Compound **6.99** was transformed into BOD **6.100** over several steps to maintain a high 96:4 enantiomeric ratio (Scheme 6.18B). In the process of removing the triflate group and silyl group deprotection, the final BOD **6.69** lost enantiopurity. It was postulated that the high temperatures during the Pd-catalysed step provided enough energy for the BOD **6.98** to racemise by cycling through the cyclooctatriene **6.101** on its way to tetraene **6.97**, losing its asymmetry (Scheme 6.18C). We conducted a computational study on this pathway to provide insight into the reversibility of this event.

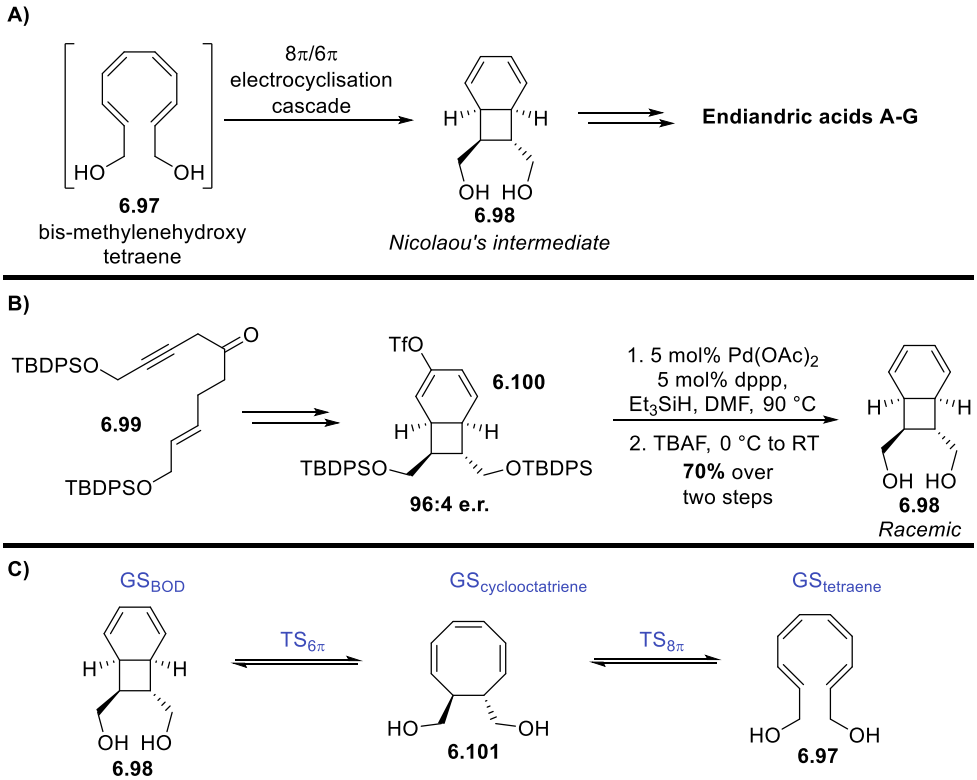

Scheme 6.18: A) Nicolaou's intermediate in the total synthesis of endiandric acids A-G. B) Brown's attempt towards asymmetric synthesis of Nicolaou's intermediate. C) Pathway for racemisation

An energy of 119.7 kJ/mol is required for reversal to **GS$_{cyclooctatriene}$ 6.101** from **GS$_{BOD}$ 6.98** (Figure 6.7). To find the rate constant, we inputted the **TS$_{6\pi}$** (119.7 kJ/mol) with the temperature of the reported reaction conditions in Scheme 6.16B (T = 90 °C = ~388.15 K) into the Eyring equation (Equation 6.1).

Equation 6.1:

$$k = \frac{k_b T}{h} e^{-\frac{\Delta G^{\ddagger}}{RT}}$$

The rate constant (k) is calculated to be ~6.302e-4 which is a half-life ($t_{1/2}$) of ~18.3 minutes. An energy of 108 kJ/mol is required for reversal to **GS$_{tetraene}$ 6.97** from **GS$_{cyclooctatriene}$ 6.101** (Figure 6.8). Repeating the Eyring equation, we calculate a rate constant (k) of ~2.367e-2 which is a half-life ($t_{1/2}$) of ~29 seconds. The reaction (in Scheme 6.18B) was reported to run for an hour at 90 °C, which according to our calculations, is enough time to allow for reversibility and therefore racemisation. If the authors were able to run their reactions at least 30 °C lower, enantiopurity of **GS$_{BOD}$ 6.98** may have been preserved.

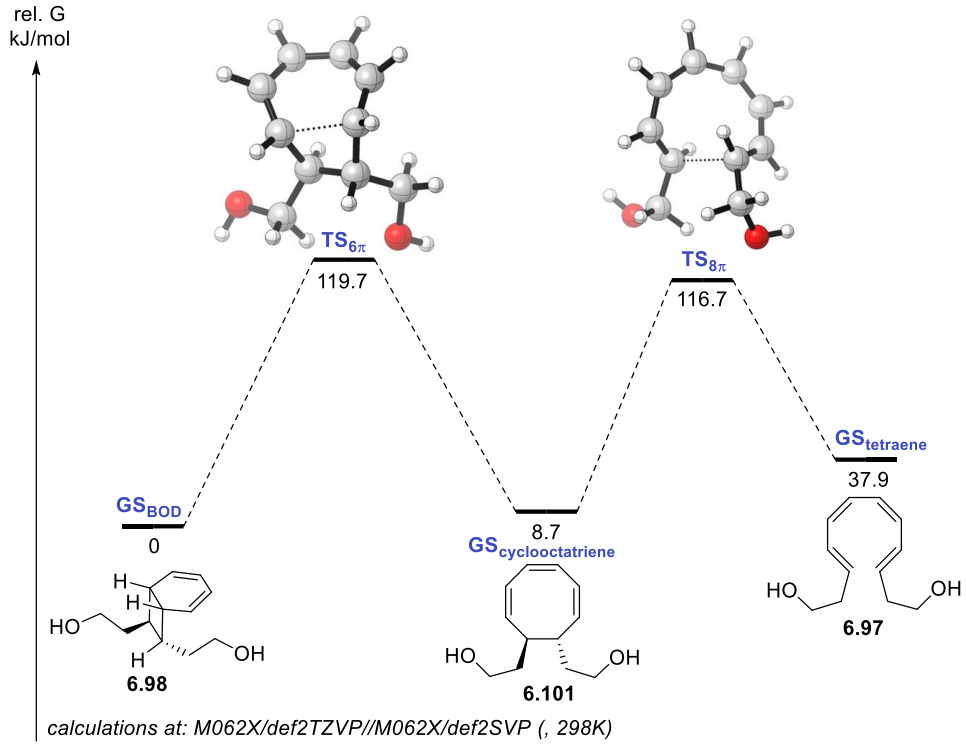

Figure 6.8: Gibbs free energy profile (kJ/mol) and transition structures for the 8π/6π ring opening cascade of BOD 6.98

6.4.2.2 Enantioselective synthesis of (−)-kingianin F

Lu, in 2021, developed an enantioselective Diels−Alder methodology that was successfully utilised in his total synthesis of (−)-kingianin F **6.102** (Scheme 6.19A).[36] Bicyclo[4.2.0]octene **6.103** was synthesised by the enantioselective DA between cyclobutanone **6.104** and butadiene **6.105** in 93% yield with a 93% enantiomeric excess. Fast forward, a diastereoselective reduction of the enoate **6.106** to **6.107** proceeded in 99% yield and 12:1 diastereomeric ratio. Careful manipulations to afford BOD **6.108** progressed in 48% yield over three steps. A final three steps deliver (−)-kingianin F **6.102** in 18% yield. Lu maintained enantiopurity of his intermediates on his path to (−)-kingianin F **6.102**, namely BOD **6.108**. Therefore, it would be insightful to calculate the pathway for the racemisation of BOD **6.108** (calculating ground and transition state energies to compounds **6.109**-**6.111**) as a comparison to bis-methylenehydroxy BOD **6.98** (Scheme 6.19B).

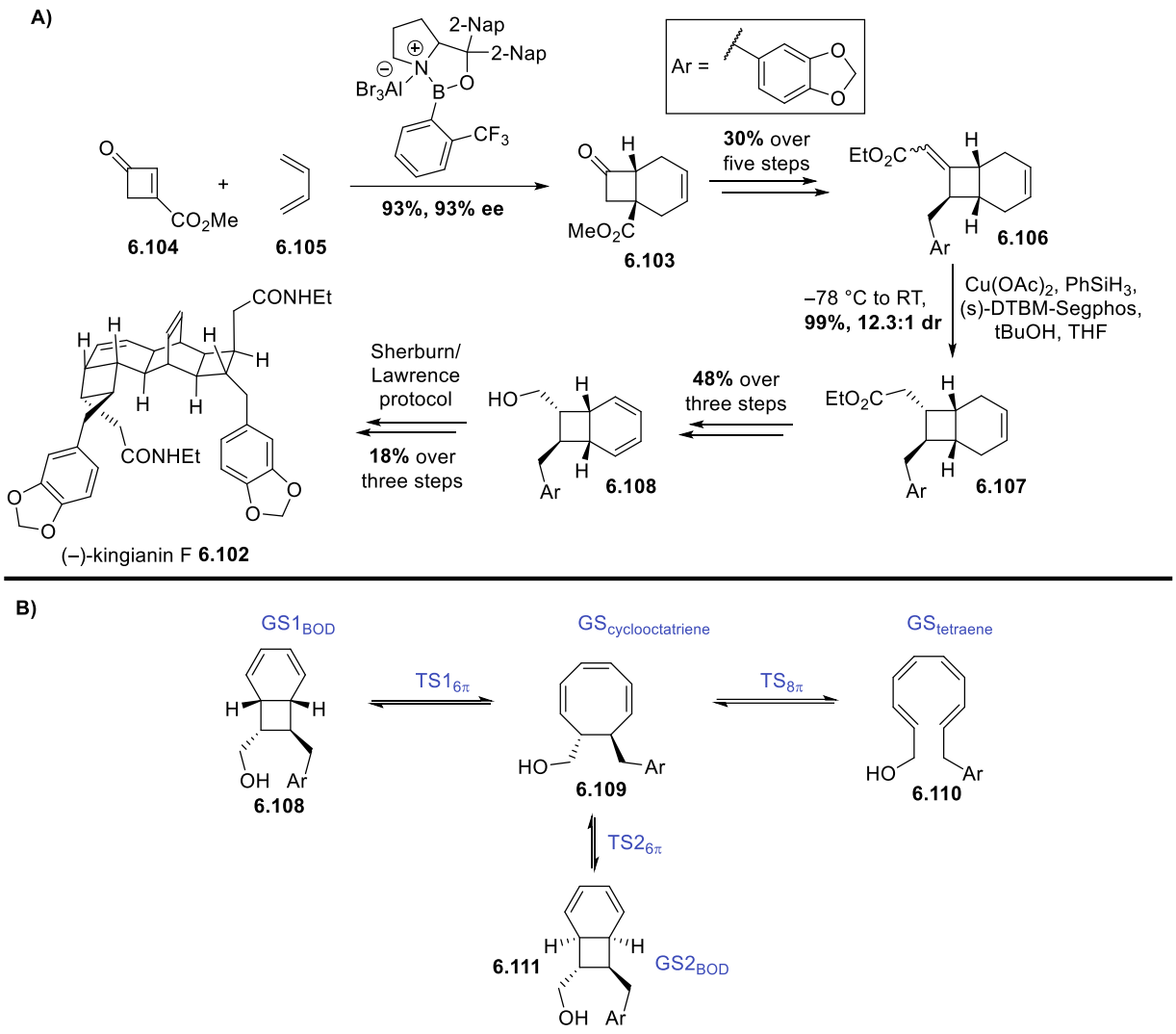

Scheme 6.19: A) Total synthesis of (−)-kingianin F. B) Proposed pathway for calculation

An energy of 115.2 kJ/mol is required for reversal to **GS$_{cyclooctatriene}$ 6.109** from Lu's intermediate **GS$_{BOD}$ 6.108** (Figure 6.9). In Lu's synthesis of intermediate **6.108**, the temperature has been reported to never exceed room temperature (25 °C) during reactions or subsequent handling. In applying equation 6.1 with a temperature of 298.15 K and **TS1$_{6\pi}$** of 115.2 kJ/mol, the rate constant (k) is calculated to be ~4.0840e-8 which is a half-life ($t_{1/2}$) of ~196 days. **TS1$_{6\pi}$** and **TS2$_{6\pi}$** are isoenergetic to each other and so the possibility of reversal to **GS$_{cyclooctatriene}$ 6.109** would lead to a 1:1 diastereomer mixture of **GS1$_{BOD}$ 6.108** and **GS2$_{BOD}$ 6.111** (both BODs are also isoenergetic). An energy of 82 kJ/mol is required for reversal to **GS$_{tetraene}$ 6.110** from **GS$_{cyclooctatriene}$ 6.109** (Figure 6.9), which we calculate a rate constant (k) of ~2.6760e-2 which is a half-life ($t_{1/2}$) of ~26 seconds. Therefore, if reversal to **GS$_{cyclooctatriene}$ 6.109** was to occur, facile racemisation would follow. Lu et al. maintained a consistent low temperature, suppressing reversibility, and maintaining enantiopurity of intermediate **6.108** to ultimately accomplish the first enantioselective synthesis of an endiandric acid derivative: (−)-kingianin F **6.102**.

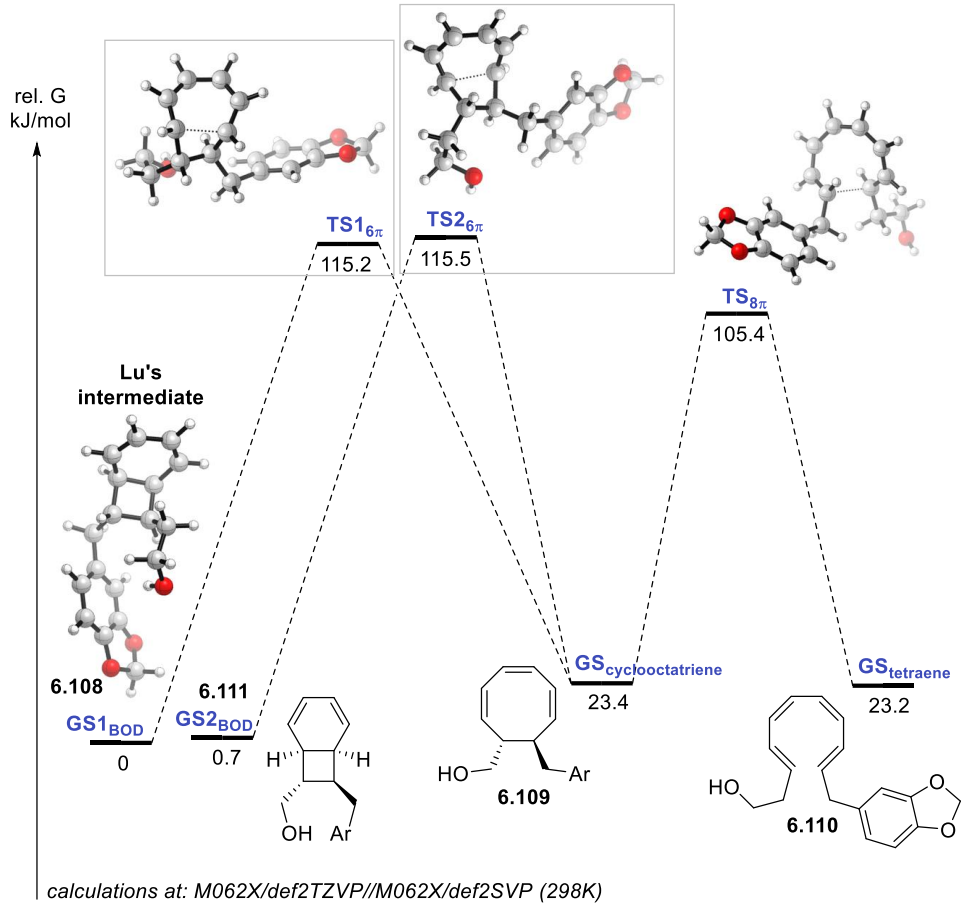

Figure 6.9: Gibbs free energy profile (kJ/mol) and transition structures for the 8π/6π ring opening cascade of BOD 6.108

6.4.3 Modelling the synthesis of SNF4435 C and D

We looked at calculating the energies of all the intermediates in the synthetic pathway to SNF4435 C **6.31** and D **6.32** starting from the tetraene **6.41** (Scheme 6.20). The kinetic and thermodynamic insight gained here would further support already established hypotheses on the predominance of **6.31** over **6.32**. This work can be considered complementary to the computational studies conducted on shimalactones A **6.37**, B **6.38**, and emeriones A **6.39**, B **6.40**.

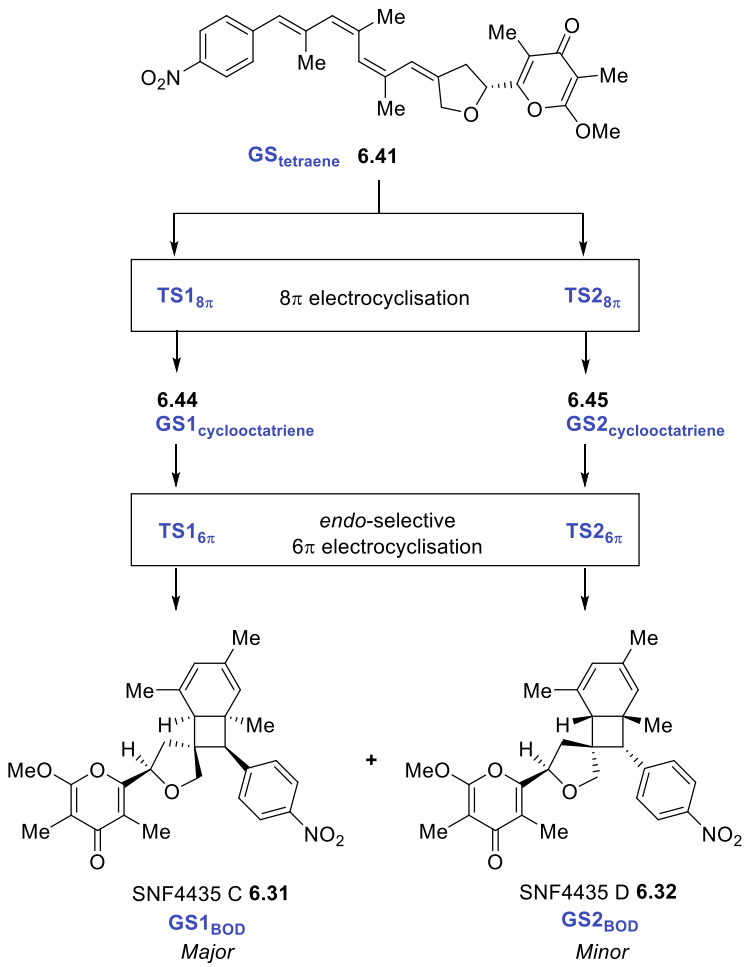

Scheme 6.20: Intermediates to be calculated in the synthetic pathway of SNF4435 C and D

Starting at tetraene **6.41**, the relative 8π electrocyclisation transition state energies were calculated to be 64.0 and 69.4 kJ/mol for **TS1$_{8\pi}$** and **TS2$_{8\pi}$**, respectively (Figure 10). The ground state cyclooctatriene energy of **6.44** is 6.4 kJ/mol lower than **6.45**. The relative 6π electrocyclisation transition state energies of **TS1$_{6\pi}$** and **TS2$_{6\pi}$** were 57.1 and 66.4 kJ/mol, respectively. The final SNF4435 C **6.31** product was found to be 3.9 kJ/mol higher than its diastereomer SNF4435 D **6.32**. The overall cascade is kinetically controlled in the initial 8π electrocyclisation, which is also the RDS, however the 6π is close in energy. Only the *endo*-6π structures were calculated, due to the *exo*-6π transition states already being established as unfavourable (refer to section 6.2.5). The computational outcomes here are consistent with experimental observations, where pathway 1 is the favoured, leading to the major product **6.31**. This work also confirms that the cascade is facile at room temperature and therefore supports a non-enzymatic biosynthesis of the SNF molecules.

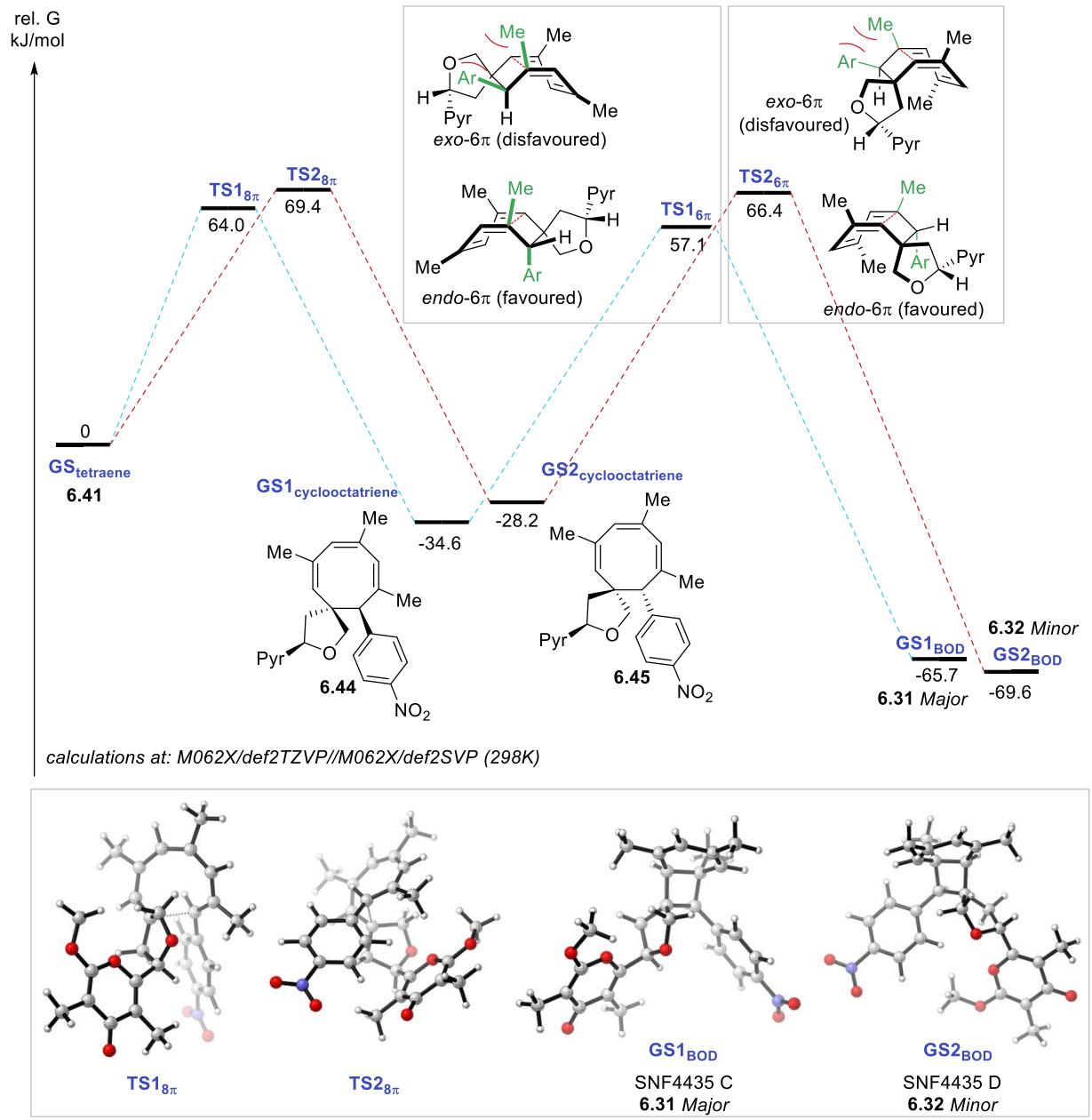

Figure 6.10: Gibbs free energy profile (kJ/mol) and transition structures for the 8π/6π cascade of SNF4435 C and D

6.4.4 Parker's cleavable chiral auxiliary

Parker in 2006, reported torquoselective 8π electrocyclisations employing cleavable chiral auxiliaries on SNF analogues (Scheme 6.21A).[37] Tetraene **6.112** is formed by cross-coupling conditions where it then undergoes a spontaneous 8π/6π electrocyclisation cascade to form BODs **6.113** and **6.114**. Tetraene **6.112a** gave the best diastereomeric ratio of 4:1 (**6.113a** + **6.114a**). This chiral auxiliary was developed by E.J. Corey for asymmetric Diels−Alder and alkylation reactions in the presence of Lewis acids.[38] It was reasoned that the low selectivities arose from the lack of Lewis acid coordination to the auxiliary to force a *s-trans*, *syn* conformation **6.115** (Scheme 6.21B). The helical *s-cis*, *syn* conformer **6.116** has the conformation for the 8π electrocyclisation transition state which eventually leads to major compound **6.113a**. We conducted computational studies on the synthetic pathway of **6.112a** to **6.113a/6.114a** to confirm the kinetic or thermodynamic influence on the product distribution.

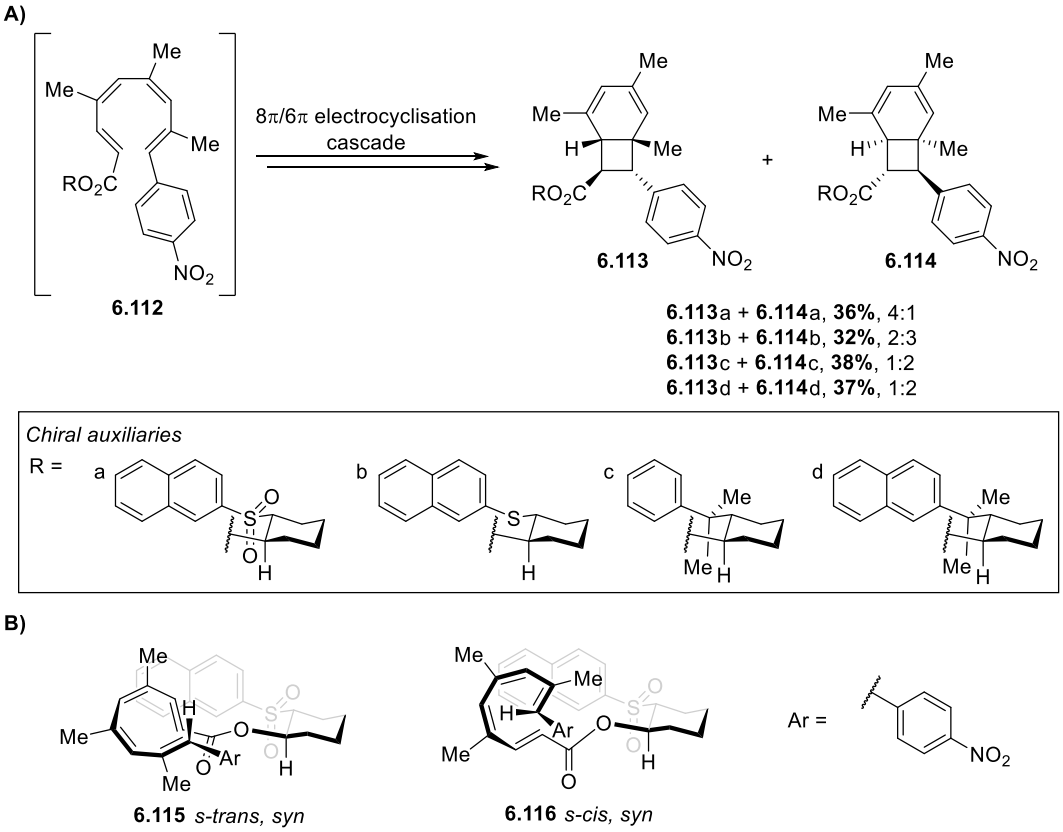

Scheme 6.21: A) Preparation of diastereomeric SNF analogues bearing cleavable chiral auxiliaries B) Helical conformation structures for the 8π electrocyclisation of tetraene 6.112a

Starting at tetraene **6.112a**, the relative 8π electrocyclisation transition state energies were calculated to be 50.0 and 62.6 kJ/mol for $\mathbf{TS1}_{8\pi}$ and $\mathbf{TS2}_{8\pi}$, respectively. **GS1** is 8.3 kJ/mol lower than **GS2**, but the following $\mathbf{TS1}_{6\pi}$ and final **BOD1** is 10.8 and 10.1 kJ/mol higher than their diastereomers, respectively. $\mathbf{TS1}_{8\pi}$ is 12.6 kJ/mol lower than $\mathbf{TS2}_{8\pi}$, which is a large difference at their energy levels, and would expect a better preference for **BOD1** than the 4:1 product ratio. The potential reversibility of both cyclooctatrienes coupled with the comparatively high 6π transition state barrier of 124.7 kJ/mol in pathway 1 may explain the mild diastereoselectivity. High reverse barrier energies of the resulting BODs are too high (over 120 kJ/mol) for the reported reaction conditions to allow for reversibility to the thermodynamic **BOD2** product.

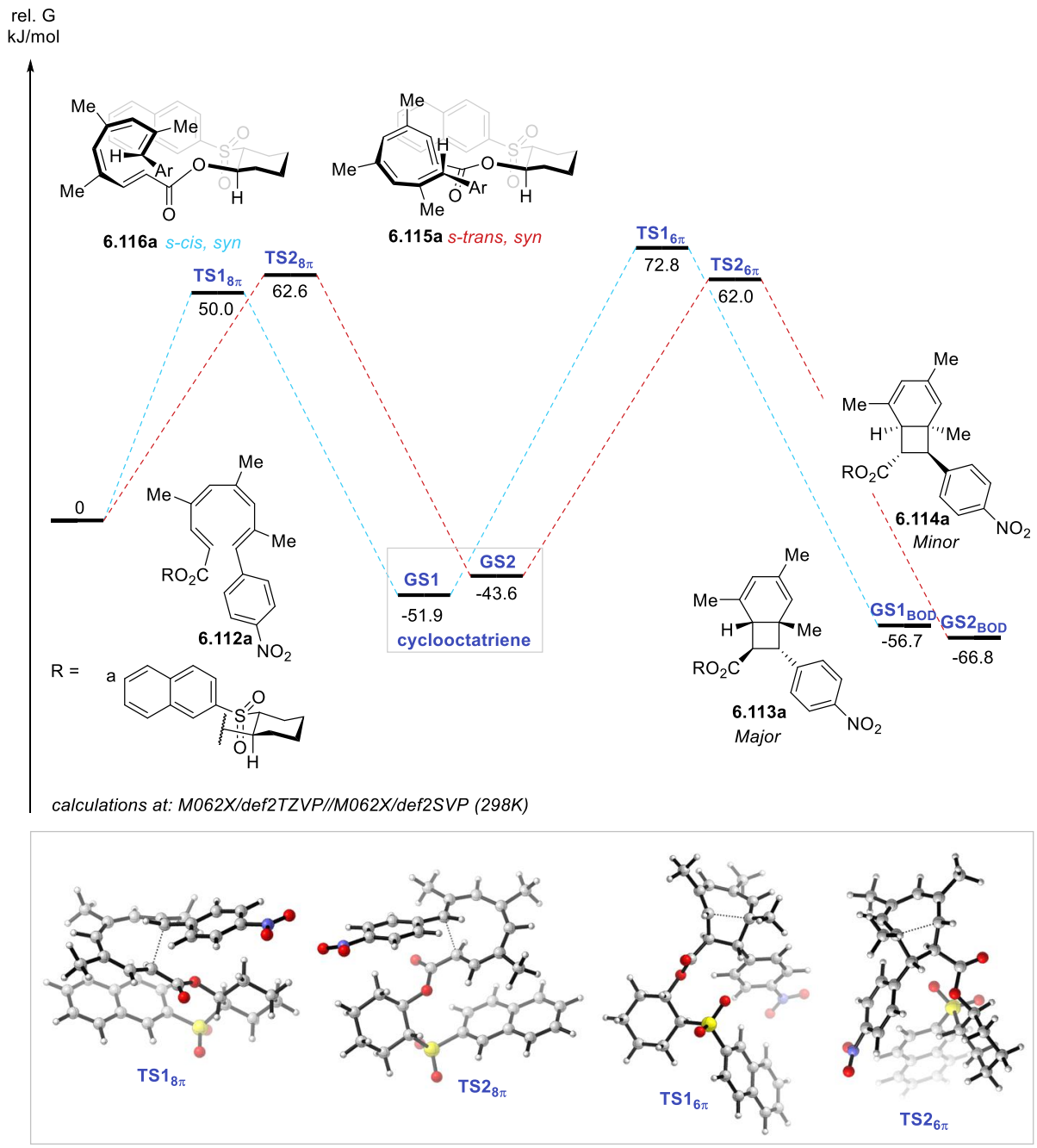

Figure 6.11: Gibbs free energy profile (kJ/mol) and transition structures for the 8π/6π cascade of tetraene 6.112a

In 2012, Parker reported an oxazoline chiral auxiliary giving slightly improved torquoselectivity.[39] Diphenyl oxazoline substrate **6.117** was synthesised and readily underwent the cascade to afford a 6:1 ratio of diastereomers **6.118** and **6.119**, in 42% yield (Scheme 6.22A). There are four postulated helical transition states, where both **6.120** and **6.121** lead to **6.118**, and both **6.122** and **6.123** lead to **6.119** (Scheme 6.22B). Product **6.118** is the major diastereomer because both conformational pairs **6.120** and **6.121** have less steric hindrance (phenyl group pointing away) compared to pairs **6.122** and **6.123**. Computational studies were conducted on this synthetic pathway to confirm the influence of the four helical transition states on the product distribution.

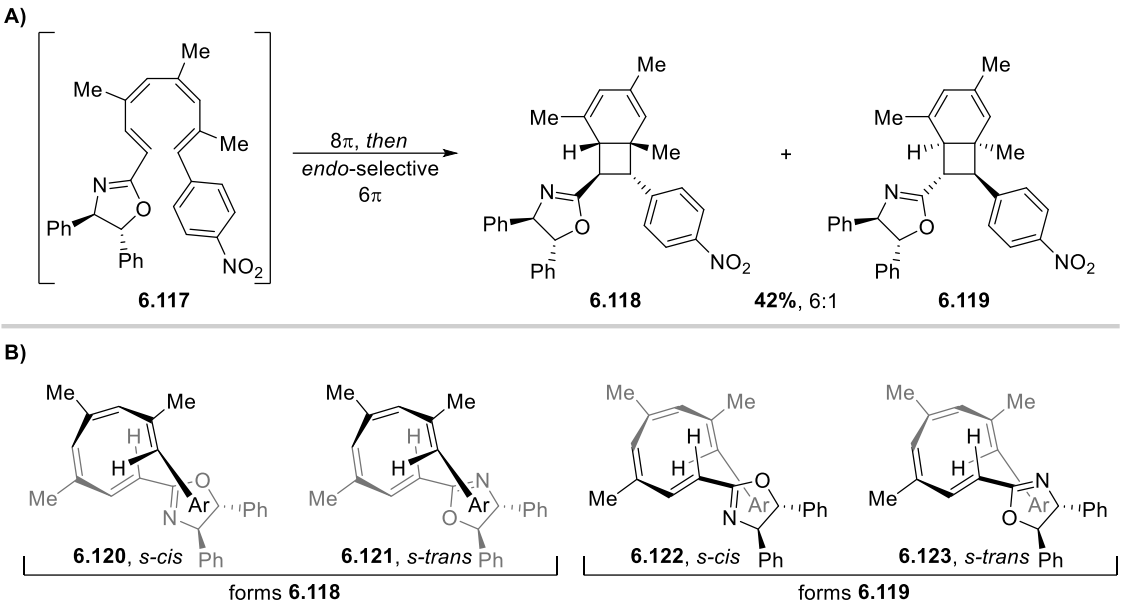

Scheme 6.22: A) Asymmetric synthesis of SNF4435 analogs with oxazoline chiral auxiliaries. B) The four possible helical 8π transition states.

Starting at tetraene **6.117**, the relative 8π electrocyclisation transition state energies were calculated to be 61.1, 59.2, 79.5 and 58.0 kJ/mol for **TS1$_{8\pi}$**, **TS2$_{8\pi}$**, **TS3$_{8\pi}$**, **TS4$_{8\pi}$**, respectively (Figure 6.12). The energies of the diastereomer pair's cyclooctatriene ground state (**GS1$_{cyclooctatriene}$** and **GS2$_{cyclooctatriene}$**), 6π transition state (**TS1$_{6\pi}$** and **TS2$_{6\pi}$**) and BOD ground state (**GS1$_{BOD}$** and **GS2$_{BOD}$**) differ by ~1.0 kJ/mol and can be considered isoenergetic to each other. This situation is so finely balanced that selectivity could arise from either the 8π or 6π step, or both. However, the reaction is likely overall to be kinetically controlled by the 8π transition state energies as well as not reversible from the BODs. **TS3$_{8\pi}$** is an outlier with a comparatively higher energy than **TS4$_{8\pi}$** (roughly 20 kJ/mol), which may be explained by a potentially unfavourable *s-cis* helical conformation.

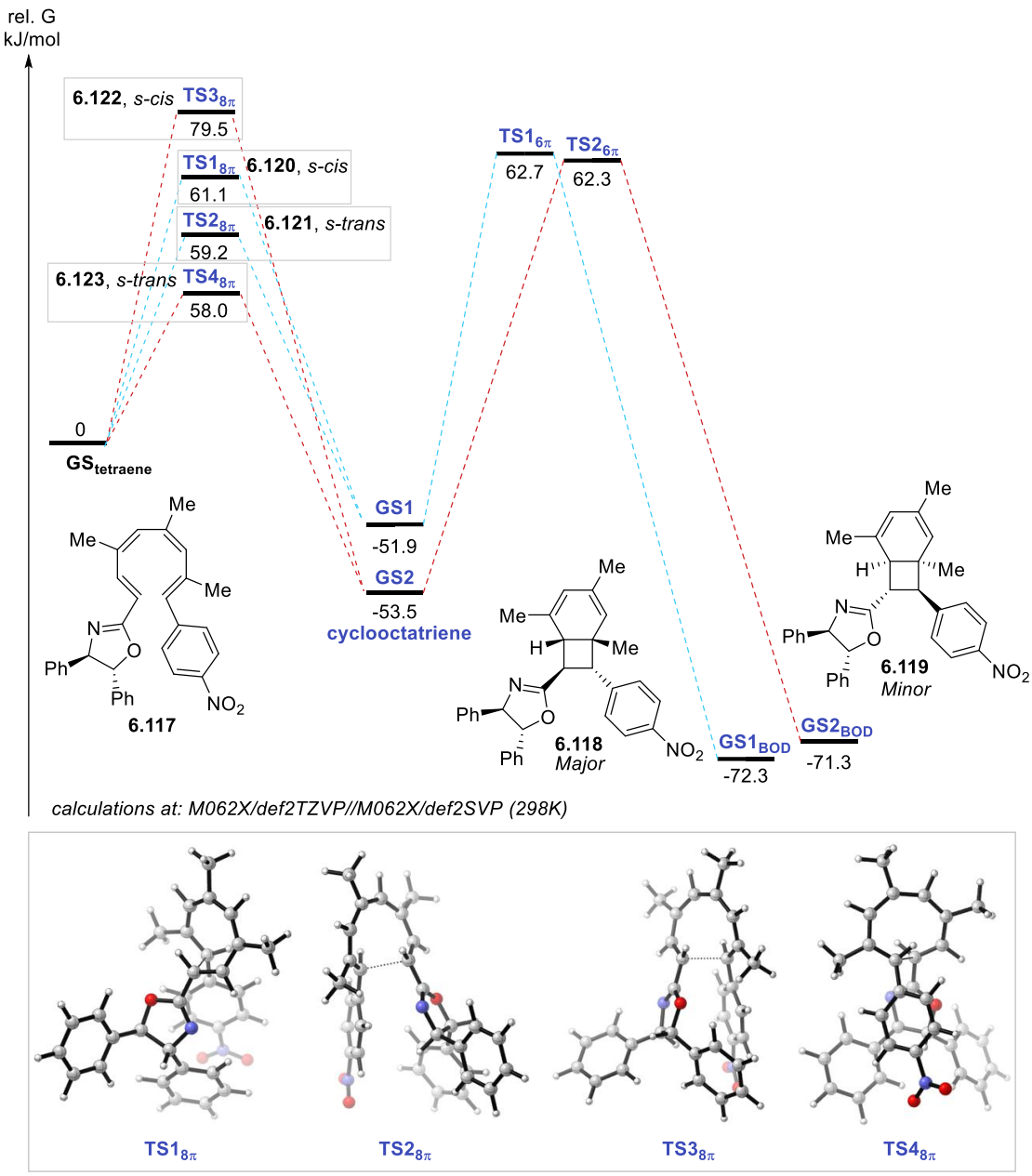

Figure 6.12: Gibbs free energy profile (kJ/mol) and transition structures for the 8π/6π cascade of tetraene 6.117

6.4.5 Hypothetical molecules with torquoselective 8π electrocyclisations

Inspired by the previous sections, we wished to conduct computational calculations on unreported, hypothetical molecules that may undergo a completely torquoselective 8π electrocyclisation. The idea behind tetraene **6.124** is based on doubling the chiral THF moiety in the SNF molecules to increase the steric hindrance during the 8π transition state (Scheme 6.23A). The strategy behind the (S)-BINOL/BINAP tetraenes (**6.125-6.127**) is for the conformation of the biaryl to restrict the 8π electrocyclisation to prefer one transition state (Scheme 6.23B). All ground and transition states from the tetraene to the BOD were calculated for these molecules.

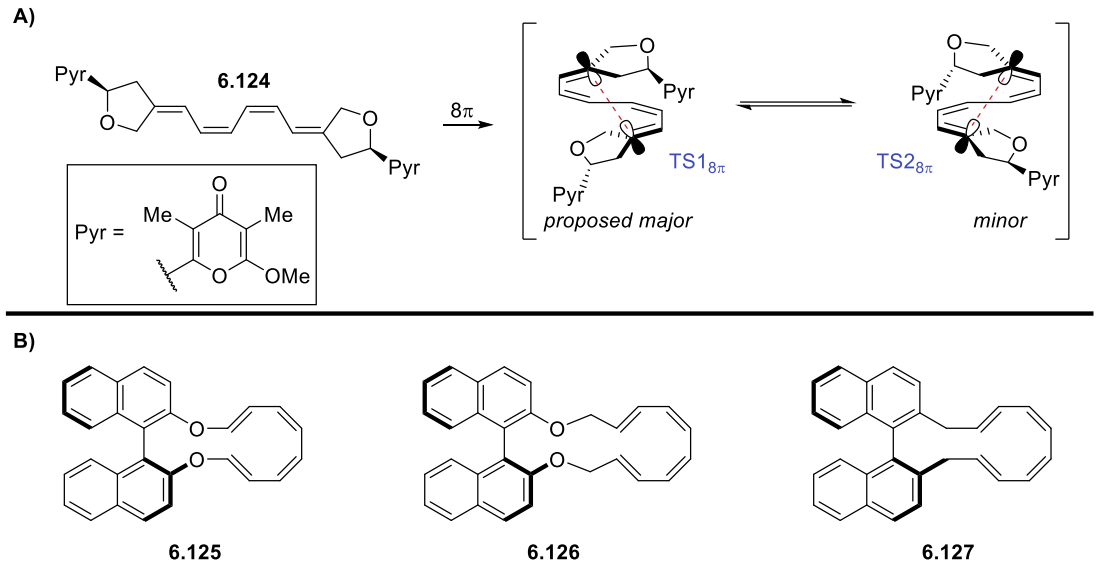

Scheme 6.23: A) Proposed hypothetical tetraene for steric-induced torquoselective 8π electrocyclisation. B) Proposed hypothetical tetraenes for ring-strain-induced torquoselective 8π electrocyclisation

6.4.5.1 Steric-based influence on torquoselectivity

Starting at tetraene **6.124**, the relative 8π electrocyclisation transition state energies were calculated to be 114.1 and 119.6 kJ/mol for **TS1$_{8π}$** and **TS2$_{8π}$**, respectively (Figure 6.13). **GS2$_{cyclooctatriene}$** is 6.7 kJ/mol lower than **GS1$_{cyclooctatriene}$**. The relative 6π electrocyclisation transition state energies of **TS1$_{8π}$** and **TS2$_{8π}$** were 114.1 and 124.5 kJ/mol, respectively. The final **GS1$_{BOD}$** product was found to be 14.9 kJ/mol lower than its diastereomer **GS2$_{BOD}$**. It is clear **GS1$_{BOD}$** is both the kinetic and thermodynamic product, where both the 8π and 6π steps in pathway 1 are important for selectivity. The thermodynamics are also finely balanced with **GS2$_{BOD}$** being destabilised relative to tetraene **6.124** and **GS1$_{BOD}$** being slightly stabilised. Therefore, we might expect **GS1$_{BOD}$** to predominate in a mixture with the starting tetraene **6.124**.

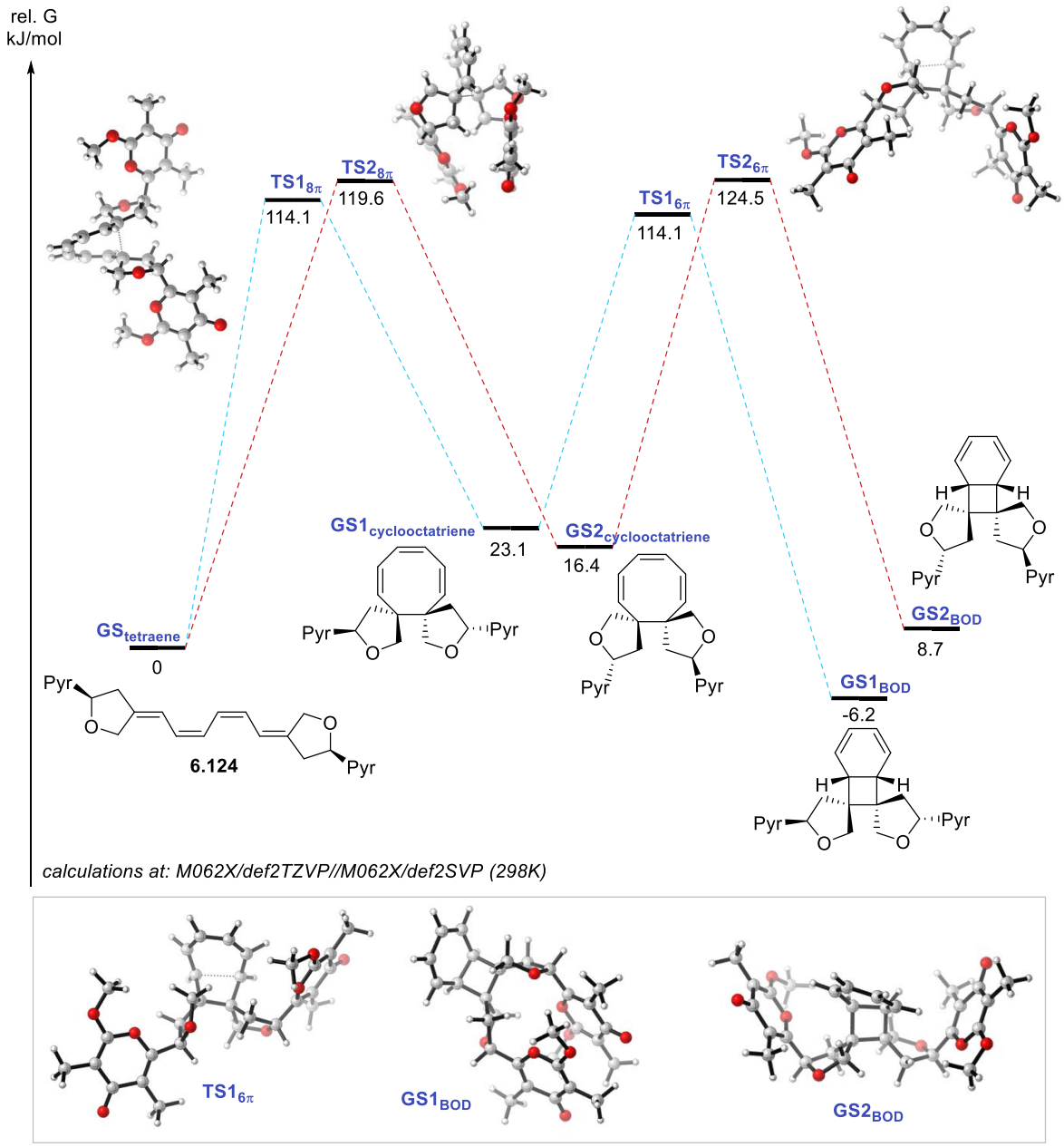

Figure 6.13: Gibbs free energy profile (kJ/mol) and transition structures for the 8π/6π cascade of tetraene 6.124

6.4.5.2 Constraint dependent torquoselectivity in the 8π electrocyclisation

The difference between **TS1$_{8\pi}$** and **TS2$_{8\pi}$** in the tetraene **6.125** cascade is quite substantial (15.7 kJ/mol difference). The activation energy of **TS1$_{8\pi}$** (38.6 kJ/mol) is considerably low, and would rapidly convert to **GS1$_{cyclooctatriene}$** at room temperature. Interestingly, **GS1$_{cyclooctatriene}$** (-45.3 kJ/mol) is the minimum within pathway 1, with **GS1$_{BOD}$** being only -24.8 kJ/mol. Sole rapid conversion of tetraene **6.125** to **GS1$_{cyclooctatriene}$** would initially occur, however the reverse 8π barrier energy (83.9 kJ/mol) is much lower than the forward 6π barrier (110.5 kJ/mol). Therefore, we would likely see an equilibrium with **GS$_{tetraene}$**, which allows an option to pathway 2. The activation energy of **TS2$_{8\pi}$** (54.3 kJ/mol) is also low, providing an opportunity to convert to **GS2$_{cyclooctatriene}$**. From here, the low forward 6π activation barrier (80.9 kJ/mol) is conducive for formation of **GS2$_{BOD}$**. Over time, the initial predominance of the kinetically favourable **GS1$_{cyclooctatriene}$** would be overridden by the thermodynamically favourable **GS2$_{BOD}$**.

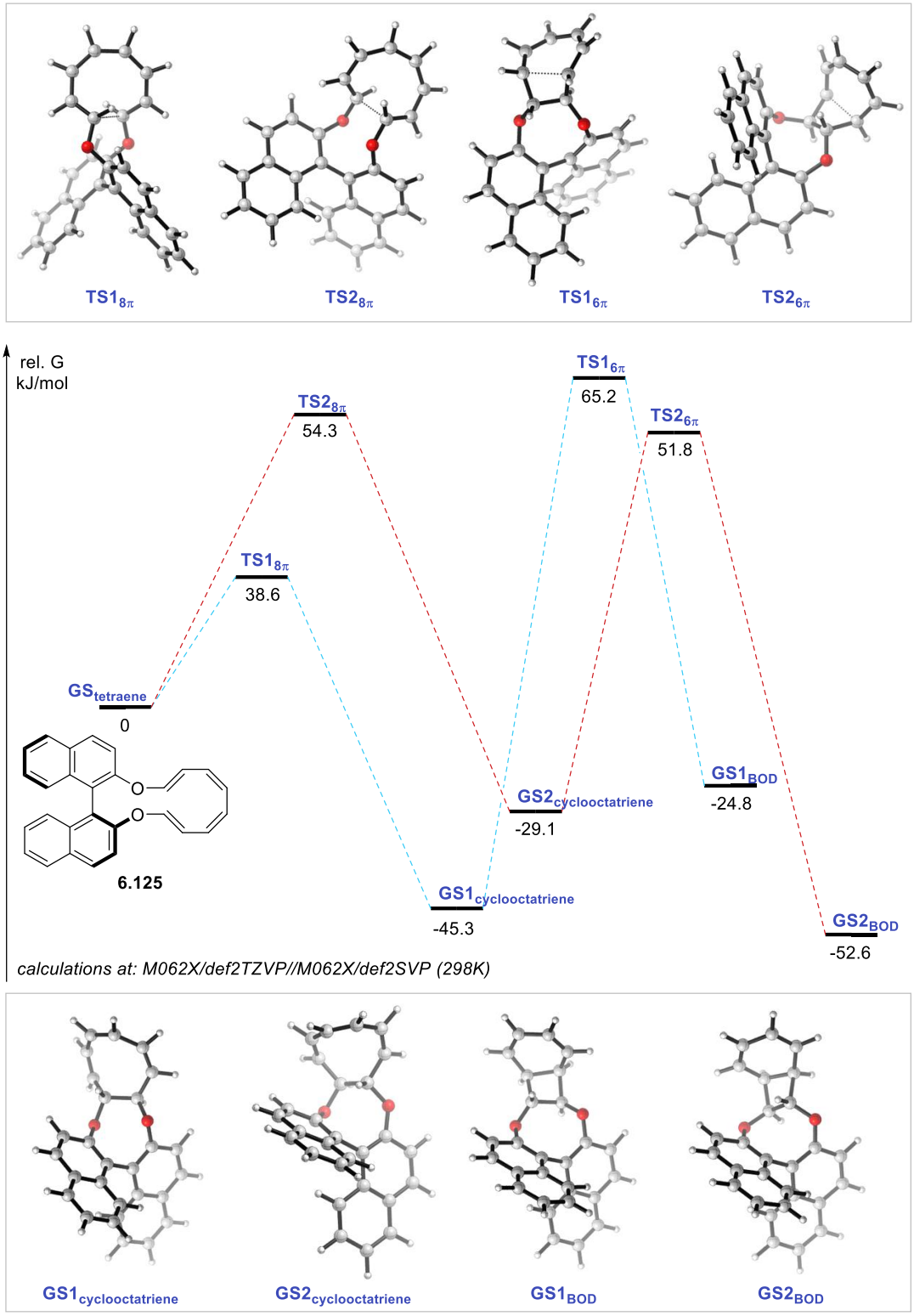

Figure 6.14: Gibbs free energy profile (kJ/mol) and transition structures for the 8π/6π cascade of tetraene 6.125

Moving onto tetraene **6.126**, **TS1$_{8\pi}$** was calculated to be 16.3 kJ/mol lower than **TS2$_{8\pi}$** (Figure 6.15). Facile formation of **GS1$_{cyclooctatriene}$** would be followed by 6π electrocyclisation (activation energy of 89.2 kJ/mol) to **GS1$_{BOD}$**. Reversal to tetraene **6.126** is possible with an activation energy of 76.4kJ/mol, but not productive. **GS1$_{BOD}$** is the overall thermodynamic product and has a reverse barrier energy of 116.9 kJ/mol, preventing reversibility. Torquoselectivity in this instance is primarily driven by kinetics in the 8π step of the cascade, with added thermodynamic favourability of the BOD.

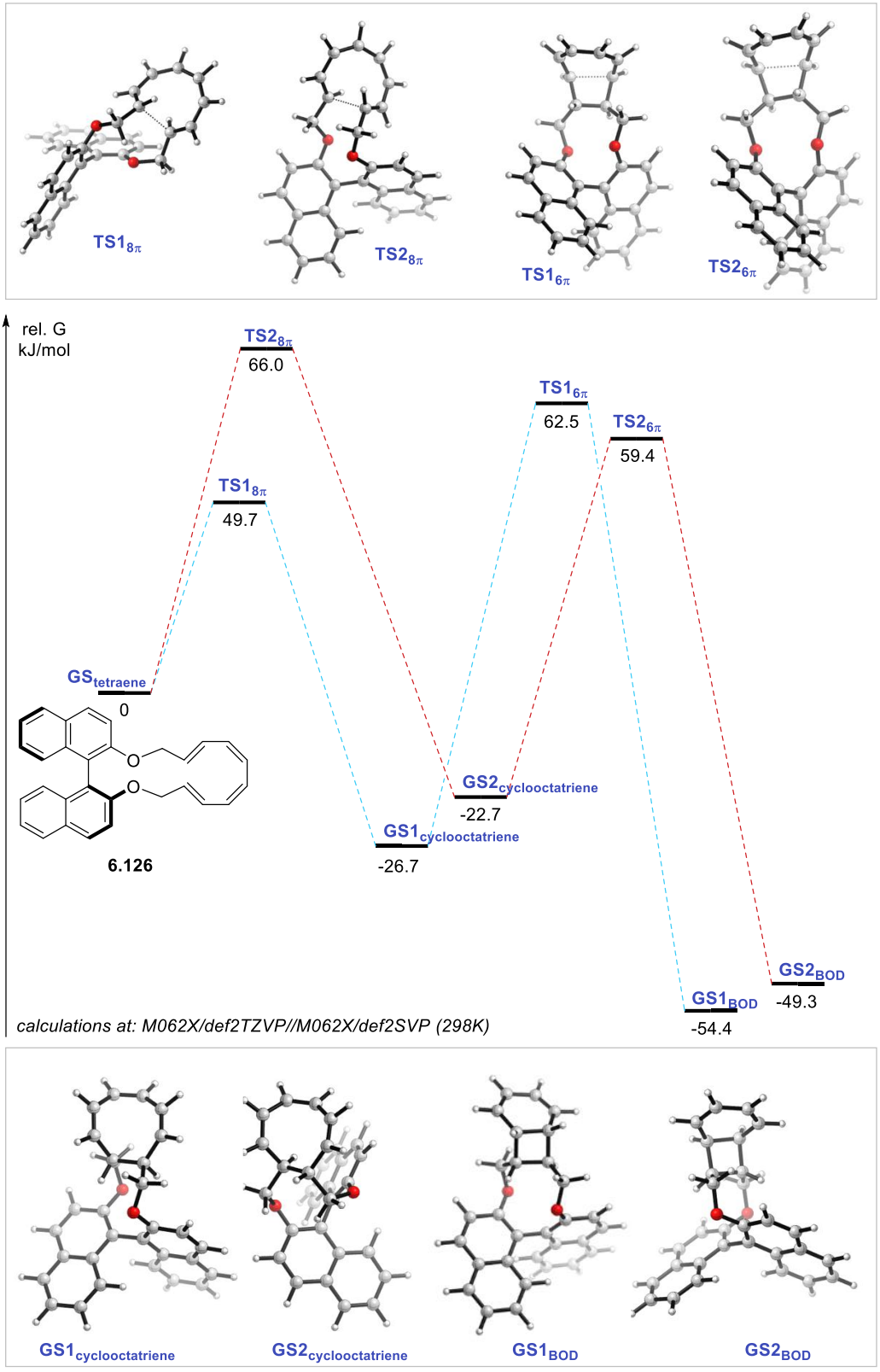

Figure 6.15: Gibbs free energy profile (kJ/mol) and transition structures for the 8π/6π cascade of tetraene 6.126

Tetraene **6.127** does not display the same strong preference for **TS1$_{8\pi}$** over **TS2$_{8\pi}$** (only 4.0 kJ/mol difference) as the previous tetraenes **6.125**-**6.126** (Figure 6.16). However, a difference of 4.0 kJ/mol at these low energy levels is still significant. Similar to tetraene **6.125**, **GS1$_{cyclooctatriene}$** of tetraene **6.127** (-48.4 kJ/mol here) is the minimum of pathway 1, but differs by being the global minimum of both pathways. Rapid sole conversion of tetraene **6.127** to **GS1$_{cyclooctatriene}$** would initially occur, however the reverse 8π barrier energy (91.9 kJ/mol) is

much lower than the forward 6π barrier (107.1 kJ/mol). Therefore, we may see reversibility to **GS$_{tetraene}$**, allowing for pathway 2 to occur. Pathway 2 may ultimately be unproductive, since its reverse 8π barrier energy from **GS2$_{cyclooctatriene}$** is low (70.1 kJ/mol) and would readily go back to **GS$_{tetraene}$**. Therefore, conversion of **GS2$_{cyclooctatriene}$** to **GS2$_{BOD}$** is not kinetically favourable and would not be formed. The energies are finely balanced in this case, where we would see both a kinetic and thermodynamic preference for **GS1$_{cyclooctatriene}$** as the major product with possibly minor amounts of **GS1$_{BOD}$** (reverse barrier energy of 97.4 kJ/mol).

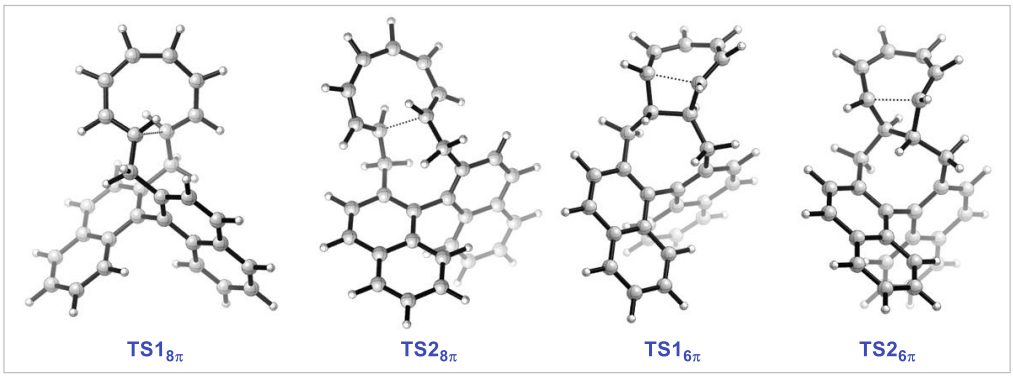

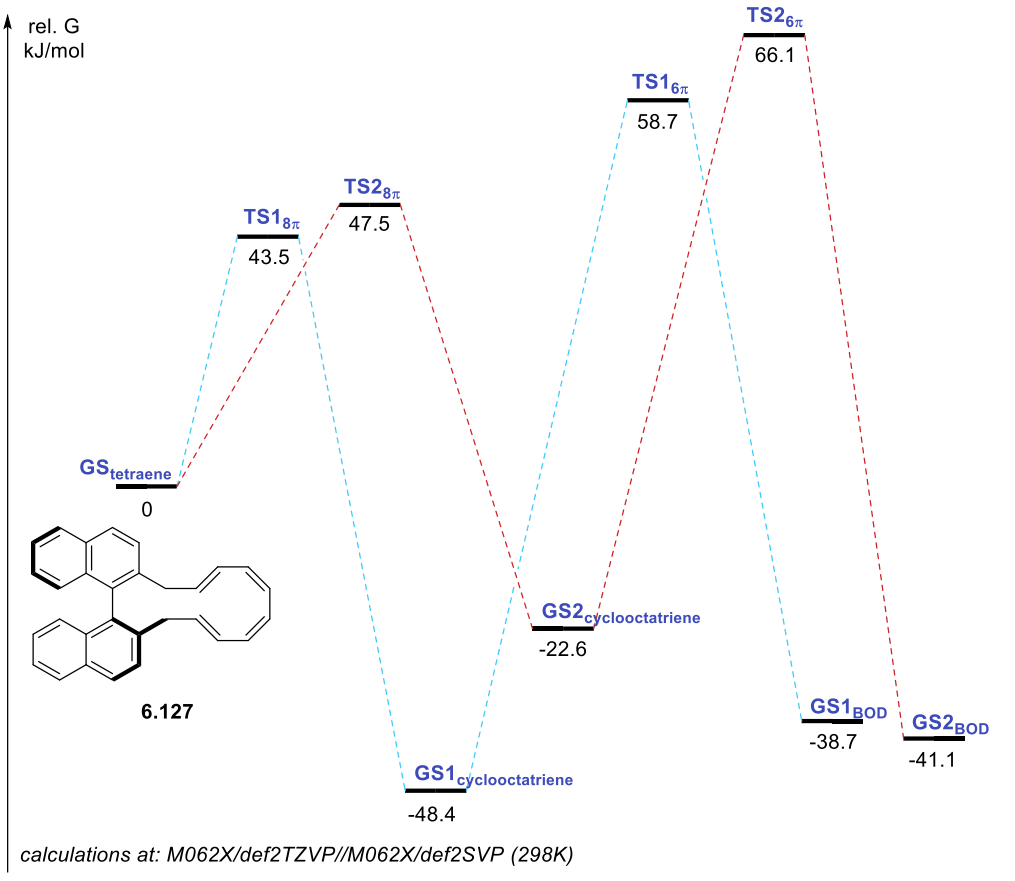

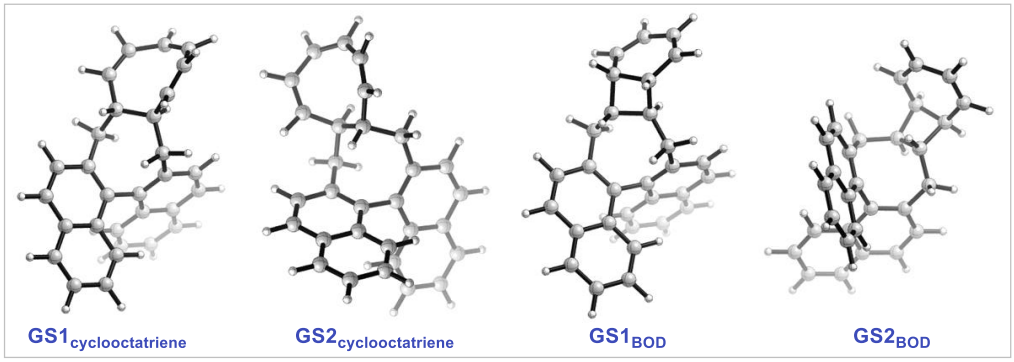

Figure 6.16: Gibbs free energy profile (kJ/mol) and transition structures for the 8π/6π cascade of tetraene 6.127

6.5 Conclusion

This chapter focused on the computational modelling of torquoselective electrocyclisations in natural product settings. The complete elucidation of the torquoselective 6π requirements in the biosynthetic cascade of 2,4,6-trimethylbicyclo[4.2.0]octadiene related natural products began with the modelling of a variety of truncated substituted tetraenes **6.69**-**6.77**. It was highlighted that the C2 substituent provides the most influence on the diastereoselectivity, with the C4 and C6 substituent offering additive effects (Scheme 6.24A). Moving on to 8π electrocyclisations, we modelled Brown and Lu's work on the enantioselective syntheses of their respective bicyclo[4.2.0]octadiene compounds (Scheme 6.24B). This revealed that their respective BOD compounds were reversible and susceptible to racemisation, however with careful temperature control, can be prevented. Our computational models of 2,4,6-trimethylbicyclo[4.2.0]octadiene related natural products such as SNF4435 C **6.31** and D **6.32** are not as susceptible to racemisation, as well as agreeing well with their synthetic outcomes. Parker made attempts at improving the 8π torquoselectivity of these natural product systems through cleavable chiral auxiliary derivatives **6.113a**-**6.114a** and **6.118**-**6.119** (Scheme 6.24C). Our models keep in line with the mild selectivities experimentally observed for **6.113a**-**6.114a**, however show that the energies for the pathways for oxazolines **6.118**-**6.119** to be isoenergetic, despite their experimental mild selectivities. Overall, it has been shown that it is difficult to impose torquoselectivity in both natural and synthesised compounds. Torquoselective 8π electrocyclisations still remain a challenge, however several proposed hypothetical compounds (Scheme 6.24D) have been computationally predicted to exhibit high levels of torquoselectivity.

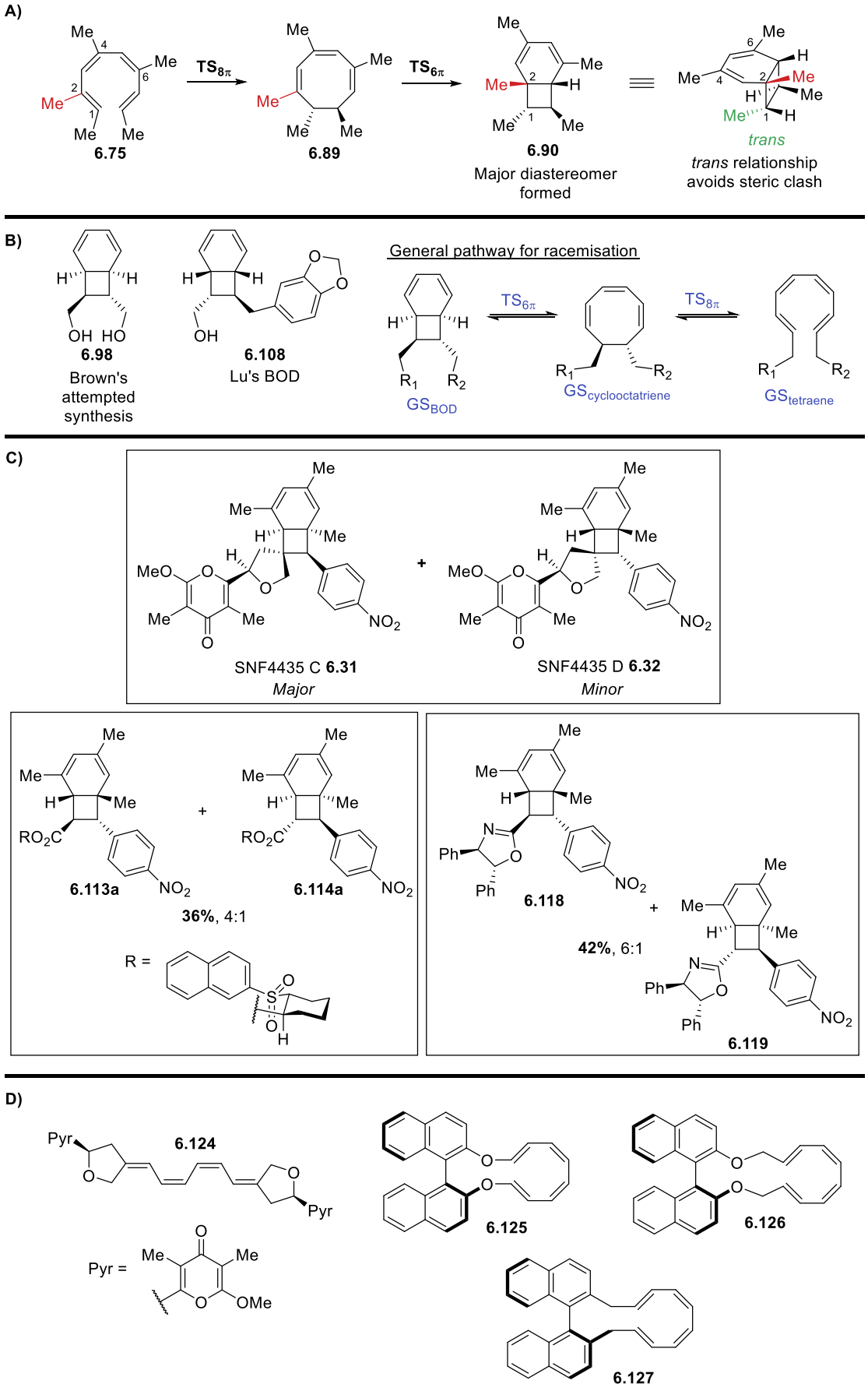

Scheme 6.24: A) 8π/6π cascade of tetraene 6.75 highlighting the influence of C2 substituent on the torquoselective 6π. B) Pathway for BOD racemisation. C) SNF4435 C and D and Parkers chiral auxiliaries 6.113a, 6.114a, 6.118 and 6.118. D) Proposed 8π torquoselective hypothetical compounds

6.6 Future directions

There are two future projects that naturally stem from this chapter. The first is to validate the proposed torquoselective hypothetical compounds. Compound **6.124** is the most synthetically accessible and provides a suitable starting point. The second is a continuation on the computational work already conducted. Houk's set of tetraenes focused on the terminal substituent effects on the 8π/6π cascade, where our set focused on the internal substituent effects (Figure 6.17). We envisioned by combining these two focuses we could model the 8π/6π cascade of every combination of methyl substitution on the tetraene backbone (see **6.128**). The purpose of this challenging task is to arrive at a conclusion as to why the 2,4,6- substitution pattern is prevalent in the aforementioned natural products and why this pattern is suitable to undergo the 8π/6π biosynthetic cascade as opposed to any other substituent combination. This potential project would provide additional, valuable insight into this class of natural products.

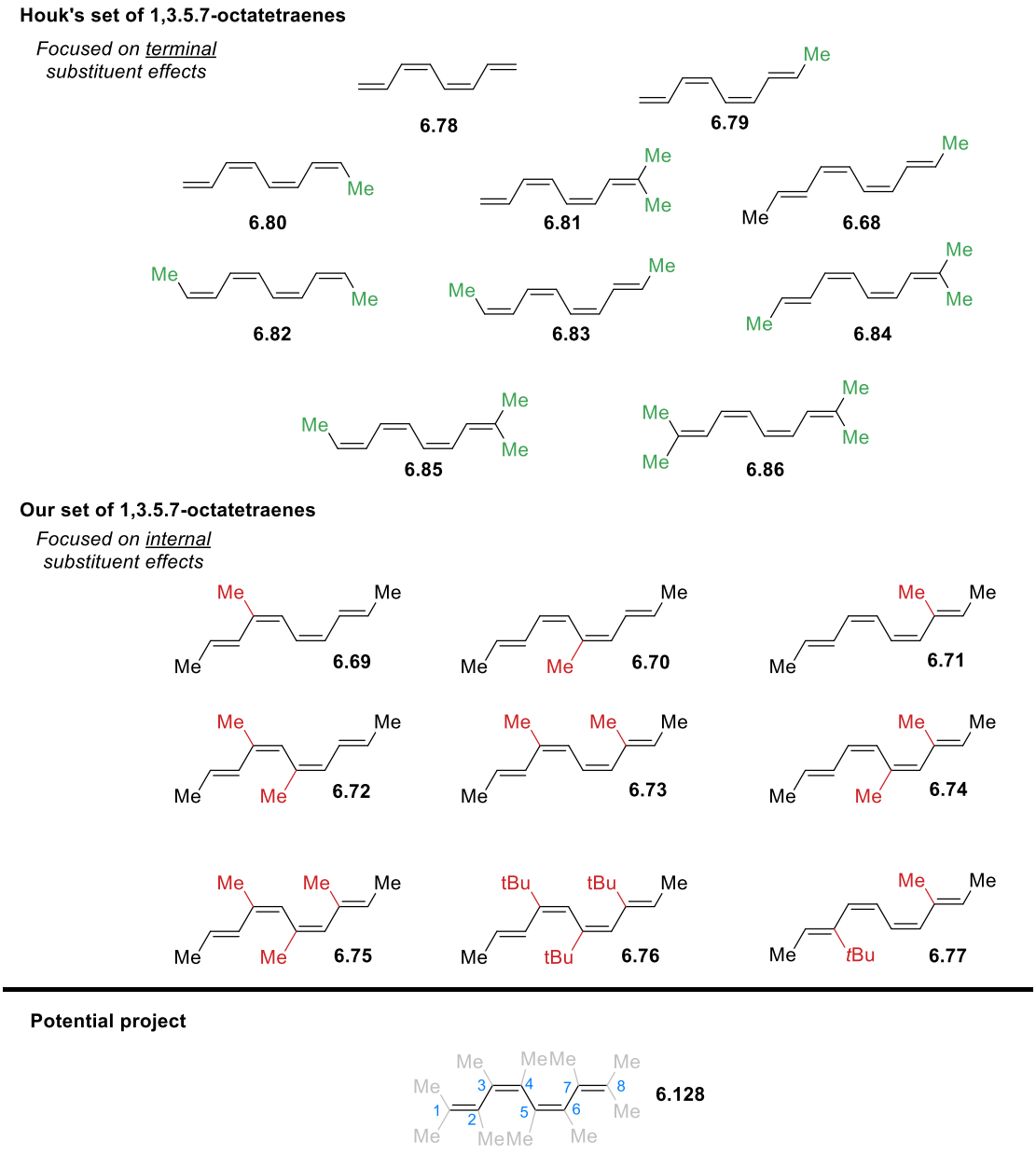

Figure 6.17: Future project inspired by the combination of Houk's and our work with the aim to computationally validate the presence of 2,4,6-trimethylbicyclo[4.2.0]octadiene related natural products in nature

6.7 References

[1] P. Muller, *Pure and Applied Chemistry* **1994**, *66*, 1077–1184.

[2] V. Gold, Ed. , *The IUPAC Compendium of Chemical Terminology*, International Union Of Pure And Applied Chemistry (IUPAC), Research Triangle Park, NC, **2019**.

[3] C. W. Jefford, G. Bernardinelli, Y. Wang, D. C. Spellmeyer, A. Buda, K. N. Houk, *J. Am. Chem. Soc.* **1992**, *114*, 1157–1165.

[4] W. Kirmse, N. G. Rondan, K. N. Houk, *J. Am. Chem. Soc.* **1984**, *106*, 7989–7991.

[5] S. Thompson, A. G. Coyne, P. C. Knipe, M. D. Smith, *Chem. Soc. Rev.* **2011**, *40*, 4217.

[6] S. E. Denmark, T. K. Jones, *J. Am. Chem. Soc.* **1982**, *104*, 2642–2645.

[7] S. E. Denmark, R. C. Klix, *Tetrahedron* **1988**, *44*, 4043–4060.

[8] S. E. Denmark, M. A. Wallace, C. B. Walker, *J. Org. Chem.* **1990**, *55*, 5543–5545.

[9] M. Rueping, W. Ieawsuwan, A. P. Antonchick, B. J. Nachtsheim, *Angew. Chem. Int. Ed.* **2007**, *46*, 2097–2100.

[10] N. A. Magomedov, P. L. Ruggiero, Y. Tang, *Org. Lett.* **2004**, *6*, 3373–3375.

[11] J. Negri, T. Morwick, J. Doyon, P. D. Wilson, E. R. Hickey, L. A. Paquette, *J. Am. Chem. Soc.* **1993**, *115*, 12189–12190.

[12] C. Hulot, G. Blond, J. Suffert, *J. Am. Chem. Soc.* **2008**, *130*, 5046–5047.

[13] C. Hulot, S. Amiri, G. Blond, P. R. Schreiner, J. Suffert, *J. Am. Chem. Soc.* **2009**, *131*, 16587–16587.

[14] W. M. Bandaranayake, J. E. Banfield, D. St. C. Black, *J. Chem. Soc. Chem. Commun.* **1980**, 902.

[15] B. Lenta, J. Chouna, P. Nkeng-Efouet, N. Sewald, *Biomolecules* **2015**, *5*, 910–942.

[16] K. A. Parker, Y.-H. Lim, *J. Am. Chem. Soc.* **2004**, *126*, 15968–15969.

[17] M. F. Jacobsen, J. E. Moses, R. M. Adlington, J. E. Baldwin, *Org. Lett.* **2005**, *7*, 2473–2476.

[18] C. M. Beaudry, D. Trauner, *Org. Lett.* **2005**, *7*, 4475–4477.

[19] A. K. Miller, D. Trauner, *Angew. Chem. Int. Ed.* **2005**, *44*, 4602–4606.

[20] R. Rodriguez, R. M. Adlington, S. J. Eade, M. W. Walter, J. E. Baldwin, J. E. Moses, *Tetrahedron* **2007**, *63*, 4500–4509.

[21] J. E. Barbarow, A. K. Miller, D. Trauner, *Org. Lett.* **2005**, *7*, 2901–2903.

[22] V. Sofiyev, G. Navarro, D. Trauner, *Org. Lett.* **2008**, *10*, 149–152.

[23] I. Fujii, M. Hashimoto, K. Konishi, A. Unezawa, H. Sakuraba, K. Suzuki, H. Tsushima, M. Iwasaki, S. Yoshida, A. Kudo, R. Fujita, A. Hichiwa, K. Saito, T. Asano, J. Ishikawa, D. Wakana, Y. Goda, A. Watanabe, M. Watanabe, Y. Masumoto, J. Kanazawa, H. Sato, M. Uchiyama, *Angew. Chem. Int. Ed.* **2020**, *59*, 8464–8470.

[24] S. Jänner, D. Isak, Y. Li, K. N. Houk, A. K. Miller, *Angew. Chem.* **2022**, *134*, DOI 10.1002/ange.202205878.

[25] A. Patel, K. N. Houk, *J. Org. Chem.* **2014**, *79*, 11370–11377.

[26] Y. Zhao, D. G. Truhlar, *Theor. Chem. Acc.* **2008**, *120*, 215–241.

[27] Y. Zhao, N. E. Schultz, D. G. Truhlar, *J. Chem. Theory Comput.* **2006**, *2*, 364–382.

[28] Y. Zhao, D. G. Truhlar, *J. Chem. Phys.* **2006**, *125*, 194101.

[29] F. Weigend, R. Ahlrichs, *Phys. Chem. Chem. Phys.* **2005**, *7*, 3297.

[30] K. C. Nicolaou, N. A. Petasis, R. E. Zipkin, J. Uenishi, *J. Am. Chem. Soc.* **1982**, *104*, 5555–5557.

[31] K. C. Nicolaou, N. A. Petasis, J. Uenishi, R. E. Zipkin, *J. Am. Chem. Soc.* **1982**, *104*, 5557–5558.

[32] K. C. Nicolaou, R. E. Zipkin, N. A. Petasis, *J. Am. Chem. Soc.* **1982**, *104*, 5558–5560.
[33] K. C. Nicolaou, N. A. Petasis, R. E. Zipkin, *J. Am. Chem. Soc.* **1982**, *104*, 5560–5562.
[34] K. C. Nicolaou, N. A. Petasis, **1984**, pp. 155–173.
[35] R. Guo, B. P. Witherspoon, M. K. Brown, *Tetrahedron* **2022**, *122*, 132932.
[36] P. Yan, C. Zhong, J. Zhang, Y. Liu, H. Fang, P. Lu, *Angew. Chem. Int. Ed.* **2021**, *60*, 4609–4613.
[37] K. A. Parker, Z. Wang, *Org. Lett.* **2006**, *8*, 3553–3556.
[38] G. Sarakinos, E. J. Corey, *Org. Lett.* **1999**, *1*, 1741–1744.
[39] K. Kim, J. W. Lauher, K. A. Parker, *Org. Lett.* **2012**, *14*, 138–141.

Chapter 7

Supporting Information

7.1 Chapter 3 Experimental[1]

Bisketene Equivalents as Diels–Alder Dienes

Isuru Dissanayake,‡ Jacob D. Hart,‡ Emma C. Becroft, Christopher J. Sumby, Christopher G. Newton†*

Department of Chemistry, The University of Adelaide, Adelaide, SA 5005, Australia

‡Equal contribution

†Present address: Department of Chemistry, University of Georgia, Athens, Georgia 30602, United States

*chris.newton@uga.edu

Supporting Information

Contents of Supplementary Information

General Experimental

NMR Spectroscopy

^{1}H NMR spectra were recorded using either an Agilent 500 MHz DD2 console, or Agilent 600 MHz DD2 console with an Oxford 600 MHz magnet and Agilent cryoprobe. ^{13}C NMR spectra were recorded using either an Agilent 500 MHz DD2 console at 125 MHz, or Agilent 600 MHz DD2 console with an Oxford 600 MHz magnet and Agilent cryoprobe at 150 MHz. ^{19}F NMR spectra were recorded using an Agilent 500 MHz DD2 console at 470 MHz. Residual solvent peaks were used as an internal reference for ^{1}H NMR spectra [$CDCl_3$ δ 7.26 ppm, $(CD_3)_2SO$ δ 2.50 ppm, C_6D_6 δ 7.16 ppm, or $(CD_3)_2CO$ δ 2.05 ppm] and ^{13}C NMR spectra [$CDCl_3$ δ 77.16 ppm, $(CD_3)_2SO$ δ 39.52 ppm, C_6D_6 δ 128.06 ppm, or $(CD_3)_2CO$ δ 29.84, ppm]. ^{19}F NMR spectra were reported relative to the ^{19}F resonance of C_6F_6 [$CDCl_3$ δ −161.64 ppm, or $(CD_3)_2CO$ δ −164.67 ppm]. Coupling constants (*J*) were quoted to the nearest 0.1 Hz. For ^{13}C NMR, coupling constants were included only in the case of coupling with ^{19}F nuclei. The following abbreviations (or combinations thereof) were used to describe ^{1}H NMR multiplicities: s = singlet, d = doublet, t = triplet, q = quartet, p = pentet, m = multiplet, br = broad.

Infrared Spectroscopy

IR spectra were recorded neat on a Perkin Elmer spectrum 100 FT-IR Spectrometer.

Mass Spectrometry

HRMS measurements (electrospray ionization - ESI) were recorded on an Agilent 6230 time-of-flight LC/MS system.

Chromatography

Flash chromatography was performed with Carl Roth silica gel 60 (0.040–0.063 mm grade). Analytical thin-layer chromatography was performed with commercial aluminium sheets coated with 0.25 mm silica gel (E. Merck, silica gel 60 F254). Compounds were either visualized under

UV-light at 254 nm, or by dipping the plates in an aqueous potassium permanganate solution followed by heating. All R_f values were measured to the nearest 0.05 cm.

Melting Points

Melting points were measured on a DigiMelt melting point apparatus, model MPA161, and are uncorrected.

Optical Rotations

Optical rotations were recorded on an Anton Paar Modular Circular Polarimeter at the specified temperature.

Preparation of Phosphate Buffered Silica (pH 7)

To a 1 L conical flask equipped with a stir bar was added 1 L of 0.2 M aqueous disodium hydrogen phosphate. Once the phosphate fully dissolved, 100 g of silica was added. The pH was adjusted to pH 7 with phosphoric acid (if necessary). The silica was filtered, dried in an oven overnight, and then stored at room temperature.

Experimental Procedures and Reagents

Commercially available chemicals were used as purchased, or where specified, purified by standard techniques. Solvent compositions are given in v/v. All reactions were carried out under an atmosphere of nitrogen in oven-dried glassware with magnetic stirring, unless otherwise indicated. Et_2O, CH_2Cl_2 and THF were purified by a Pure Solv™ Micro solvent purification system. All other solvents were used as purchased, or where specified, purified by standard techniques.

Microwave

Reaction conditions invoking microwave irradiation were carried out in a CEM Discover SP microwave synthesis system.

General Comments on Compound Characterization

All new compounds were fully characterized when possible. For compounds that have been previously characterized in the literature, if we have made any modification to the reported synthesis, we include our modified method, in addition to compound appearance, R_f, and ^{1}H NMR data.

Experimental Procedures and Characterization Data

Synthesis of Silyloxyfurans

Precursors

5-Methoxyfuran-2(5*H*)-one (S1)

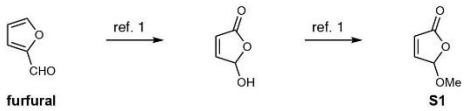

furfural S1

Prepared in two steps from furfural according to the procedure of Feringa.[1]

5-Bromo-2(5*H*)-furanone (S2)

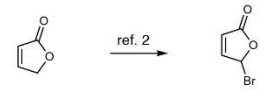

2-furanone S2

Prepared in one step from 2-furanone according to the procedure of Kulnevich.[2]

Tetracyclic anhydride (±)-S3

6-methoxy-1-tetralone (±)-S3

Prepared in three steps from 6-methoxy-1-tetralone according to the procedures of Liao[3] and Göbel.[4]

Silyl enol ether anhydride (±)-S6

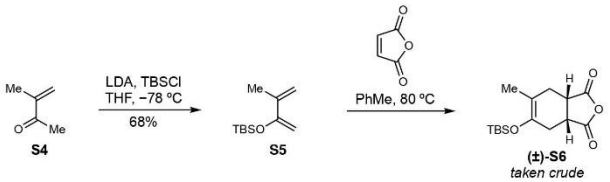

Prepared in two steps from 3-methyl-3-buten-2-one (**S4**) according to a modification of the procedures reported by Liu[5] and Ireland.[6]

***tert*-Butyldimethyl((3-methylbuta-1,3-dien-2-yl)oxy)silane (S5)**

To an oven-dried two-neck 250 ml round-bottom flask equipped with a stir bar and under nitrogen was added diisopropylamine (5.03 ml, 35.7 mmol, 1.50 mol. equiv.) and anhydrous THF (99.0 ml, 0.240 M). The solution was cooled to −78 ºC and ^{n}BuLi (2.50 M in hexanes, 14.3 ml, 35.7 mmol, 1.50 mol. equiv.) was added dropwise over 20 minutes. After stirring for 30 minutes a solution of 3-methyl-3-buten-2-one (**S4**) (2.00 g, 23.8 mmol, 1.00 mol. equiv.) in anhydrous THF (99.0 ml, 0.240 M) was added dropwise over 30 minutes. The reaction was allowed to stir for a further 30 minutes before TBSCl (5.38 g, 35.7 mmol, 1.50 mol. equiv.) was added in one portion. The reaction mixture was warmed to room temperature and stirred for 36 hours, by which time ^{1}H NMR analysis indicated the reaction has reached completion. The reaction was quenched with water and the aqueous layer extracted with hexanes (3×). The combined organics were washed with H_2O (2×), brine, dried over $MgSO_4$, filtered, and concentrated under reduced pressure. Purification by flash column chromatography [phosphate buffered silica (pH 7), eluting with petroleum ether] yielded diene **S5**. **Yield**: 3.21 g, 16.2 mmol, 68%; Spectroscopic data matched those previously reported in the literature.[5] **Appearance**: Cloudy white oil; **R$_f$**: 0.44 (petroleum ether); **^{1}H NMR** (500 MHz, $CDCl_3$): δ 5.43 (d, *J* = 2.2 Hz, 1H), 4.96 (s, 1H), 4.48 (s, 1H), 4.32 (s, 1H), 1.88 (s, 3H), 0.97 (s, 9H), 0.17 (s, 6H) ppm.

Silyl enol ether anhydride (±)-S6

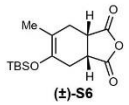

(±)-S6

To an oven-dried round-bottom flask equipped with a stir bar and under nitrogen was added diene **S5** (1.06 g, 5.35 mmol, 1.05 mol. equiv.) and anhydrous PhMe (10.2 mL, 0.500 M). Following addition of maleic anhydride (0.500 g, 5.10 mmol, 1.00 mol. equiv.) the resulting mixture was heated overnight at 80 ºC, whereby ^{1}H NMR analysis indicated the reaction had gone to completion. The reaction was concentrated under reduced pressure, and the crude mixture was submitted to the subsequent reaction without further purification. For characterization purposes a small amount was purified by flash column chromatography [phosphate buffered silica (pH 7), eluting with petroleum ether → 1:4 EtOAc:petroleum ether]. Spectroscopic data matched those previously reported in the literature.[6]
Appearance: White solid; **R$_f$**: 0.45 (1:4 EtOAc:petroleum ether); **^{1}H NMR** (500 MHz, $CDCl_3$): δ 3.39 (ddd, *J* = 10.6, 7.8, 3.0 Hz, 1H), 3.30 (ddd, *J* = 10.0, 7.0, 3.2 Hz, 1H), 2.57–2.42 (m, 3H), 2.37 (dd, *J* = 15.6, 6.9 Hz, 1H), 1.64 (s, 3H), 0.94 (s, 9H), 0.13 (s, 3H), 0.09 (s, 3H) ppm.

Indole anhydride S9

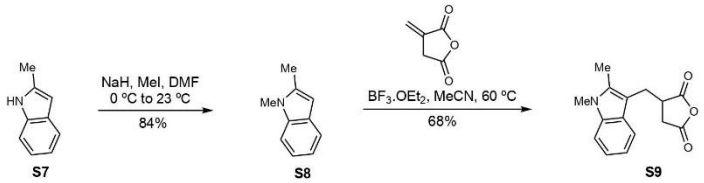

S7 S8 S9

Prepared in two steps from 2-methylindole (**S7**) according to a modification of the procedures reported by Bull[7] and Bergman.[8]

1,2-Dimethylindole (S8)

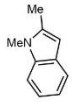

S8

To an oven-dried round-bottom flask under nitrogen and equipped with a stir bar was added 2-methylindole (**S7**) (3.231 g, 24.65 mmol, 1.00 mol. equiv.). Following addition of anhydrous DMF (30.0 mL, 0.820 M) the resulting suspension was cooled to 0 ºC, and NaH (60% dispersion in mineral oil, 1.48 g, 36.9 mmol, 1.50 mol. equiv.) was added portion-wise. The reaction mixture was allowed to warm to room temperature and stirred for 30 minutes. The

reaction mixture was cooled to 0 ºC and MeI (1.84 mL, 29.5 mmol, 1.20 mol. equiv.) was added dropwise as a solution in anhydrous THF (5.00 mL, 5.91 M). The reaction was allowed to slowly warm to room temperature overnight. The reaction mixture was quenched by the slow addition of water (20 mL) and the solution was extracted with EtOAc (3×). The combined organics were washed with H_2O, dried over $MgSO_4$, filtered, concentrated under reduced pressure and then purified via flash column chromatography (SiO_2, eluting with petroleum ether → 5:95 EtOAc:petroleum ether). **Yield**: 3.0 g, 20.72 mmol, 84%; Spectroscopic data matched those previously reported in the literature.[7] **Appearance**: Yellow solid; **R*f***: 0.61 (5:95 EtOAc:petroleum ether); **^{1}H NMR** (500 MHz, $CDCl_3$): δ 7.52 (d, *J* = 7.8 Hz, 1H), 7.26 (d, *J* = 8.1 Hz, 1H), 7.15 (t, *J* = 7.6 Hz, 1H), 7.07 (t, *J* = 7.4 Hz, 1H), 6.25 (s, 1H), 3.67 (s, 3H), 2.43 (s, 3H) ppm.

Indole anhydride S9

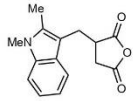

S9

To an oven-dried round-bottom flask under nitrogen and equipped with a stir bar and was added itaconic anhydride (2.22 g, 19.8 mmol, 1.20 mol. equiv.). Following addition of anhydrous acetonitrile (60 mL, 0.300 M) the resulting suspension was cooled to 0 ºC, and $BF_3.Et_2O$ (2.44 mL, 19.8 mmol, 1.20 mol. equiv.) was added. The reaction mixture was allowed to warm to room temperature and stirred for 10 minutes. 1,2-dimethylindole **S8** (2.36 g, 16.2 mmol, 1.00 mol. equiv.) was added, and the resulting mixture was heated at 60 ºC overnight. The reaction mixture was diluted with EtOAc, washed with saturated aqueous $NaHCO_3$ (3×), brine (2×), dried over $MgSO_4$, filtered and concentrated under reduced pressure. The crude anhydride **S9** was then washed with a minimum volume of cold Et_2O (3×). **Yield**: 2.83 g, 11.0 mmol, 68%; **Appearance**: Purple solid; **R*f***: 0.35 (1:4 EtOAc:petroleum ether); **^{1}H NMR** (500 MHz, $CDCl_3$): δ 7.42 (d, *J* = 7.8 Hz, 1H), 7.24 (d, *J* = 3.6 Hz, 1H), 7.17 (t, *J* = 7.6 Hz, 1H), 7.09 (t, *J* = 7.4 Hz, 1H), 3.65 (s, 3H), 3.50–3.43 (m, 1H), 3.32 (dd, *J* = 14.9, 5.4 Hz, 1H), 3.16 (dd, *J* = 14.9, 7.7 Hz, 1H), 2.85 (dd, *J* = 18.9, 9.6 Hz, 1H), 2.74 (dd, *J* = 18.9, 6.4 Hz, 1H), 2.36 (s, 3H) ppm; **^{13}C NMR** (125 MHz, $CDCl_3$): δ 173.8, 170.2, 136.9, 134.7, 127.4, 121.4, 119.7, 117.5, 109.1, 105.2, 42.2, 33.5, 29.8, 25.3, 10.7 ppm; **IR**: 2942, 1863, 1775, 1472, 1224, 1056, 924, 746 cm^{-1}; **HRMS** (ESI): calculated for $[C_{15}H_{15}NO_3+H]^+$: 258.1125, found: 258.1126.

1,2,3,4-Butanetetracarboxylic dianhydride (S10)

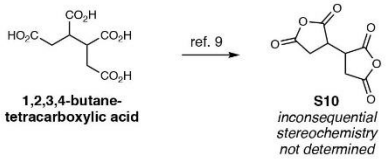

Prepared in one step from 1,2,3,4-butanetetracarboxylic acid according to the procedure of Mukherjee.[9] Although 1,2,3,4-butanetetracarboxylic dianhydride (**S10**) has been reported several times, to the best of our knowledge complete characterization data for this compound has not been published, and so we include it here. **Appearance**: White solid; $\mathbf{R_f}$: 0.31 (2:3 EtOAc:petroleum ether); **M.p.**: Degrades at 240 ºC; **^{1}H NMR** [500 MHz, $(CD_3)_2CO$]: δ 4.10–4.03 (m, 1H), 3.43–3.34 (m, 1H), 3.32–3.24 (m, 1H) ppm; **^{13}C NMR** [150 MHz, $(CD_3)_2CO$]: δ 173.7, 170.8, 41.9, 33.5 ppm; **IR**: 1852, 1768, 1223, 1064, 1030, 908, 709, 662 cm^{-1}; **HRMS** (ESI): calculated for $[C_8H_6O_6+H]^+$: 199.0237, found: 199.0228.

(*E*)-3-Ethylidenedihydrofuran-2,5-dione (S12)

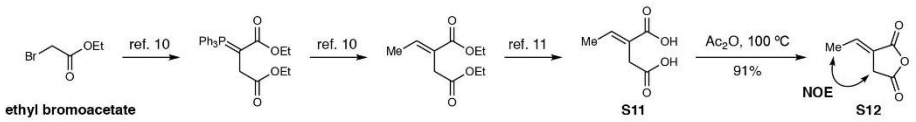

(*E*)-2-ethylidenesuccinic acid (**S11**) was prepared in 3 steps from ethyl bromoacetate according to the procedures of Lugtenburg,[10] and Zhang.[11]

(*E*)-3-Ethylidenedihydrofuran-2,5-dione (S12)

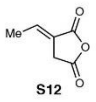
S12

To an oven-dried round-bottom flask equipped with a stir bar and under nitrogen was added (*E*)-2-ethylidenesuccinic acid (**S11**) (2.33 g, 16.2 mmol, 1.00 mol. equiv.). Following addition of acetic anhydride (16.2 mL, 1.00 M) the resulting mixture was heated at 100 ºC for 4 hours, whereby ^{1}H NMR analysis indicated the reaction had gone to completion. The flask was cooled to room temperature, concentrated under reduced pressure, and then co-evaporated with PhMe until no acetic anhydride remained. The crude mixture was filtered

through a silica plug (eluting with Et_2O). **Yield**: 1.86 g, 14.7 mmol, 91%; **Appearance**: Yellow oil; **R_f**: 0.27 (1:4 EtOAc:petroleum ether); **^{1}H NMR** [500 MHz, $(CD_3)_2CO$]: δ 7.01–6.94 (m, 1H), 3.68 (s, 2H), 1.93 (d, J = 7.2 Hz, 3H) ppm; **^{13}C NMR** (150 MHz, $(CD_3)_2CO$): δ 170.3, 166.3, 139.7, 126.2, 32.5, 16.1 ppm; **IR**: 2957, 2923, 1836, 1769, 1684, 1267, 1226, 1178, 1093, 925, 891, 714, 663 cm^{-1}; **HRMS** (ESI): calculated for $[C_6H_6O_3+H]^+$: 127.0390, found: 127.0383.

All other silyloxyfuran precursors were obtained from commercial suppliers.

2,5-Bis(silyloxy)furans

Summary

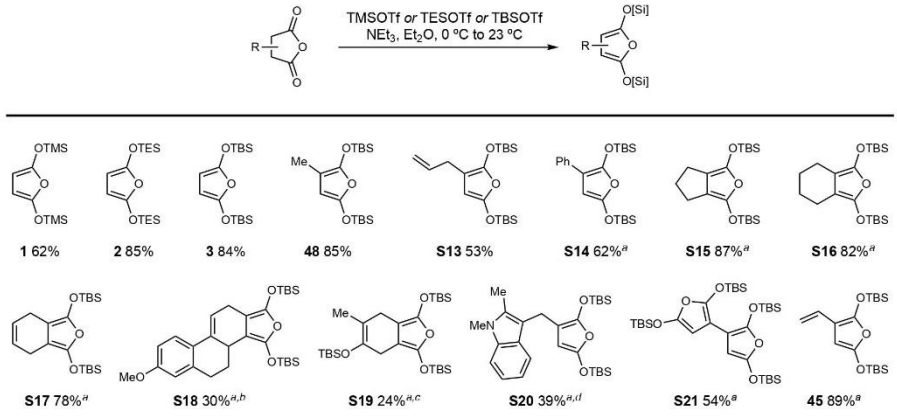

[a] ^{1}H NMR yield
[b] Reaction run in $ClCH_2CH_2Cl$ at 50 °C
[c] Yield over 2 steps from **S5**
[d] Reaction run in CH_2Cl_2

General Procedure

Prepared according to a modification of the procedure reported by Simchen.[12] To an oven-dried three-neck round-bottom flask equipped with a stir bar and under nitrogen was added the appropriate cyclic anhydride (1.00 mol. equiv.). Following addition of anhydrous Et_2O (0.250 M) the resulting suspension was cooled to 0 ºC, and anhydrous triethylamine (3.00 mol. equiv.) was added. After stirring for 10 minutes the appropriate trialkylsilyl trifluoromethanesulfonate (2.20 mol. equiv.) was added dropwise and the reaction mixture was allowed to warm to room temperature. The reaction was stirred vigorously overnight, yielding a biphasic mixture. ***Note***: All furans underwent rapid hydrolysis in the presence of untreated (i.e. acidic) silica. The relative stability of each furan towards hydrolysis was inferred from its stability on phosphate buffered silica (pH 7). The least stable furans were purified using procedure A, moderately stable furans with procedure B, and the most stable furans with procedures C or D. All furans were stored in the freezer (–20 °C) under a nitrogen atmosphere.

Purification Procedure A (furan **1**)

The reaction mixture was diluted with anhydrous Et_2O and filtered through Celite, eluting with additional anhydrous Et_2O. The filtrate was concentrated under reduced pressure and anhydrous hexanes were added. All precipitates were removed via filtration, and the solution was concentrated under reduced pressure to yield furan **1**. This was found to decompose rapidly if brought in contact with either untreated (i.e. acidic) silica, or phosphate buffered silica (pH 7).

Purification Procedure B (furan **2**)

The reaction mixture was filtered through phosphate buffered silica (pH 7), eluting with Et_2O. The filtrate was concentrated under reduced pressure to yield the corresponding furan. Attempts to purify via flash chromatography with either untreated (i.e. acidic) silica, or phosphate buffered silica (pH 7) resulted in decomposition.

Purification Procedure C (furans **S14**, **S15**, **S16**, **S18**, **S19**, **S20**, **S21**, and **45**)

The reaction mixture was filtered through phosphate buffered silica (pH 7), eluting with Et_2O, and the filtrate was concentrated under reduced pressure. A ^1H NMR yield with the specified internal standard was obtained. Each furan was used in subsequent Diels–Alder reactions without further purification. For characterization purposes a small amount was purified by flash column chromatography [phosphate buffered silica (pH 7), eluting with petroleum ether].

Purification Procedure D (furans **3**, **48**, **S13**, and **S17**)

The reaction mixture was filtered through phosphate buffered silica (pH 7), eluting with Et_2O, and the filtrate was concentrated under reduced pressure. Purification by flash column chromatography [phosphate buffered silica (pH 7), eluting with petroleum ether] yielded the corresponding furan.

Characterization Data

2,5-Bis((trimethylsilyl)oxy)furan (1)

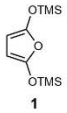

1

Synthesized from dihydrofuran-2,5-dione and trimethylsilyl trifluoromethanesulfonate using purification procedure A. **Yield**: 757 mg, 3.10 mmol, 62%; Spectroscopic data matched those previously reported in the literature.[12] **Appearance**: Yellow oil; $\mathbf{R}_f$: N/A (unstable on silica); **^{1}H NMR** (500 MHz, $CDCl_3$): δ 4.90 (s, 2H), 0.27 (s, 18H) ppm.

2,5-Bis((triethylsilyl)oxy)furan (2)

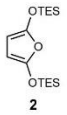

2

Synthesized from dihydrofuran-2,5-dione and triethylsilyl trifluoromethanesulfonate using purification procedure B. **Yield**: 13.9 g, 42.3 mmol, 85%; **Appearance**: Yellow oil; $\mathbf{R}_f$: N/A (unstable on silica); **^{1}H NMR** (500 MHz, $CDCl_3$): δ 4.89 (s, 2H), 0.99 (t, J = 8.0 Hz, 18H), 0.74 (q, J = 8.0 Hz, 12H) ppm; **^{13}C NMR** (150 MHz, $CDCl_3$): δ 147.4, 83.8, 6.5, 4.7 ppm; **IR**: 2957, 2880, 1626, 1461, 1255, 1183, 1004, 990, 834, 731 cm^{-1}; **HRMS** (ESI): calculated for $[C_{16}H_{32}O_3Si_2]^{\cdot+}$: 328.1884, found: 328.1888.

2,5-Bis((*tert*-butyldimethylsilyl)oxy)furan (3)

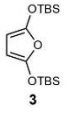

3

Synthesized from dihydrofuran-2,5-dione and *tert*-butyldimethylsilyl trifluoromethanesulfonate using purification procedure D. **Yield**: 6.90 g, 21.0 mmol, 84%; **Appearance**: Colorless oil; $\mathbf{R}_f$: 0.2 (petroleum ether); **^{1}H NMR** (500 MHz, $CDCl_3$): δ 4.88 (s, 2H), 0.95 (s, 18H), 0.21 (s, 12H) ppm; **^{13}C NMR** (150 MHz, $CDCl_3$): δ 147.5, 84.0, 25.7, 18.2, –4.7 ppm; **IR**: 2930, 2862, 1626, 1250, 1179, 990, 838, 784 cm^{-1}; **HRMS** (ESI): calculated for $[C_{16}H_{32}O_3Si_2+H]^+$: 329.1963, found: 328.1947.

((3-Methylfuran-2,5-diyl)bis(oxy))bis(*tert*-butyldimethylsilane) (48)

48

Synthesized from methylsuccinic anhydride and *tert*-butyldimethylsilyl trifluoromethanesulfonate using purification procedure D. **Yield**: 5.13 g, 15.0 mmol, 85%; **Appearance**: Colorless oil; $\mathbf{R}_f$: 0.42 (petroleum ether); **^{1}H NMR** (500 MHz, $CDCl_3$): δ 4.81 (s, 1H), 1.75 (s, 3H), 0.97 (s, 9H), 0.95 (s, 9H), 0.20 (s, 6H), 0.19 (s, 6H) ppm; **^{13}C**

NMR (150 MHz, $CDCl_3$): δ 146.9, 143.2, 92.8, 86.8, 25.7, 25.7, 18.3, 18.1, 8.9, –4.5, –4.7 ppm; **IR**: 2930, 2862, 1662, 1626, 1250, 1102, 887, 838, 784 cm^{-1}; **HRMS** (ESI): calculated for $[C_{17}H_{34}O_3Si_2+H]^+$: 343.2119, found: 343.2116.

((3-Allylfuran-2,5-diyl)bis(oxy))bis(*tert*-butyldimethylsilane) (S13)

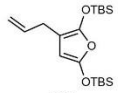

S13

Synthesized from allylsuccinic anhydride and *tert*-butyldimethylsilyl trifluoromethanesulfonate using purification procedure D. **Yield**: 1.56 g, 4.22 mmol, 53%; **Appearance**: Colorless oil; $\mathbf{R_f}$: 0.44 (petroleum ether); **^{1}H NMR** (500 MHz, $CDCl_3$): δ 5.91–5.79 (m, 1H), 5.04 (dd, J = 17.1, 1.3 Hz, 1H), 4.97 (dd, J = 10.0, 1.2 Hz, 1H), 4.83 (s, 1H), 2.92 (d, J = 6.1 Hz, 2H), 0.96 (s, 9H), 0.95 (s, 9H), 0.20 (s, 6H), 0.19 (s, 6H) ppm; **^{13}C NMR** (125 MHz, $CDCl_3$): δ 147.0, 143.2, 137.4, 114.7, 95.6, 85.8, 28.4, 25.7, 18.3, 18.1, –4.48, –4.68 ppm; **IR**: 2955, 2858, 2934, 1664, 1626, 1254, 886, 862, 837, 785 cm^{-1}; **HRMS** (ESI): calculated for $[C_{19}H_{36}O_3Si_2+H]^+$: 369.2276, found: 369.2273.

((3-Phenylfuran-2,5-diyl)bis(oxy))bis(*tert*-butyldimethylsilane) (S14)

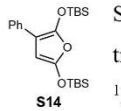

S14

Synthesized from phenylsuccinic anhydride and *tert*-butyldimethylsilyl trifluoromethanesulfonate using purification procedure C. **Yield**: 4.13 mmol, 62% (by ^{1}H NMR using 1,2-dichloroethane as an internal standard); **Appearance**: Colorless oil; $\mathbf{R_f}$: 0.2 (petroleum ether); **^{1}H NMR** (500 MHz, $CDCl_3$): δ 7.51 (dd, J = 8.4, 1.1 Hz, 2H), 7.30 (t, J = 7.8 Hz, 2H), 7.11 (t, J = 7.4 Hz, 1H), 5.31 (s, 1H), 1.01 (s, 9H), 0.98 (s, 9H), 0.25 (s, 12H) ppm; **^{13}C NMR** (150 MHz, $CDCl_3$): δ 147.4, 143.9, 133.8, 128.4, 125.5, 124.8, 98.7, 83.6, 25.8, 25.7, 18.3, 18.2, –4.2, –4.7 ppm; **IR**: 2954, 2932, 2861, 1718, 1631, 1257, 1210, 859, 839.9, 787, 727.8, 694 cm^{-1}; **HRMS** (ESI): calculated for $[C_{22}H_{36}O_3Si_2+H]^+$: 405.2276, found: 405.2283.

1,3-Bis((*tert*-butyldimethylsilyl)oxy)-5,6-dihydro-4*H*-cyclopenta[*c*]furan (S15)

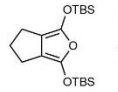

S15

Synthesized from *cis*-1,2-cyclopentanedicarboxylic anhydride and *tert*-butyldimethylsilyl trifluoromethanesulfonate using purification procedure C. **Yield**: 12.5 mmol, 87% (by ^{1}H NMR using durene as an internal standard); **Appearance**:

Colorless oil; R_f: 0.31 (1:9 EtOAc:petroleum ether); **^{1}H NMR** (500 MHz, $CDCl_3$): δ 2.37 (t, J = 6.9 Hz, 4H), 2.18 (p, J = 7.2 Hz, 2H), 0.95 (s, 18H), 0.18 (s, 10H) ppm; **^{13}C NMR** (125 MHz, $CDCl_3$): δ 137.9, 104.9, 32.3, 25.7, 23.4, 18.2, –4.5 ppm; **IR**: 2953, 2928, 2859, 1687, 1672, 1474, 1327, 1252, 1114, 1057, 876, 838, 822, 807, 785 cm^{-1}; **HRMS** (ESI): calculated for $[C_{19}H_{36}O_3Si_2+NH_4]^+$: 386.2541, found: 386.2561.

1,3-Bis((*tert*-butyldimethylsilyl)oxy)-4,5,6,7-tetrahydroisobenzofuran (S16)

S16

Synthesized from 1,2-cyclohexanedicarboxylic anhydride (predominantly *cis*) and *tert*-butyldimethylsilyl trifluoromethanesulfonate using purification procedure C. **Yield**: 2.86 mmol, 82% (by ^{1}H NMR using 1,2-dichloroethane as an internal standard); **Appearance**: Colorless oil; R_f: 0.5 (1:9 EtOAc:petroleum ether); **^{1}H NMR** (500 MHz, $CDCl_3$): δ 2.29–2.25 (m, 4H), 1.59–1.55 (m, 4H), 0.96 (s, 18H), 0.18 (s, 12H) ppm; **^{13}C NMR** (125 MHz, $CDCl_3$): δ 141.1, 94.8, 25.7, 23.6, 20.0, 18.1, –4.4 ppm; **IR**: 2930, 2858, 1671, 1649, 1349, 1282, 1250, 1099, 838, 780 cm^{-1}; **HRMS** (ESI): calculated for $[C_{20}H_{38}O_3Si_2+H]^+$: 383.2432, found: 383.2449.

1,3-Bis((*tert*-butyldimethylsilyl)oxy)-4,7-dihydroisobenzofuran (S17)

S17

Synthesized from *cis*-1,2,3,6-tetrahydrophthalic anhydride and *tert*-butyldimethylsilyl trifluoromethanesulfonate using purification procedure D. Modifications from general procedure: 4.50 mol. equiv. of triethylamine, 3.30 mol. equiv. of *tert*-butyldimethylsilyl trifluoromethanesulfonate, reaction stirred for 36 hours. **Yield**: 2.45 g , 15.0 mmol, 72%; **Appearance**: Yellow oil; R_f: 0.3 (1:9 Et_2O:petroleum ether); **^{1}H NMR** (600 MHz, $CDCl_3$): δ 5.78 (m, 2H), 2.92 (m, 4H), 0.96 (s, 18H), 0.19 (s, 12H) ppm; **^{13}C NMR** (150 MHz, $CDCl_3$): δ 141.1, 124.0, 92.1, 26.0, 20.4, 18.1, –4.4 ppm; **IR**: 2957, 2931, 2891, 2856, 1709, 1672, 1650, 1355, 1274, 1252, 1098, 854, 838, 785 cm^{-1}; **HRMS** (ESI): calculated for $[C_{20}H_{36}O_3Si_2+H]^+$: 381.2276, found: 381.2271.

Tetracyclic furan S18

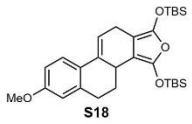

S18

Synthesized from tetracyclic anhydride **(±)-S3** and *tert*-butyldimethylsilyl trifluoromethanesulfonate. Modifications from general procedure: reaction was conducted in 1,2-dichloroethane, with warming to 50 ºC after the addition of *tert*-butyldimethylsilyl trifluoromethanesulfonate. Purified using purification procedure C. **Yield**: 1.06 mmol, 30% (by ^{1}H NMR using 1,2-dichloroethane as an internal standard); **Appearance**: Yellow oil; **R$_f$**: N/A (unstable on silica); **^{1}H NMR** (500 MHz, $CDCl_3$): δ 7.50 (d, *J* = 8.8 Hz, 1H), 6.74 (dd, *J* = 8.7, 2.6 Hz, 1H), 6.63 (d, *J* = 2.5 Hz, 1H), 6.15–6.10 (m, 1H), 3.80 (s, 3H), 3.26–3.15 (m, 2H), 3.11–2.96 (m, 2H), 2.88 (dd, *J* = 17.1, 4.6 Hz, 1H), 2.59–2.51 (m, 1H), 1.63 (qd, *J* = 12.9, 5.5 Hz, 1H), 1.00 (s, 9H), 0.99 (s, 9H), 0.24 (s, 3H) 0.22 (s, 9H) ppm; **^{13}C NMR** (125 MHz, $CDCl_3$): δ 161.2, 144.2, 143.1, 140.0, 137.3, 131.9, 128.2, 118.5, 115.9, 115.1, 99.5, 94.2, 79.7, 57.7, 34.4, 32.7, 32.2, 28.2, 28.2, 23.7, 20.6, 20.6, –1.8, –1.8, –1.8 ppm; **IR**: 2957, 2931, 2856, 1703, 1609, 1064, 1252, 910, 835, 788, 731 cm^{-1}; **HRMS** (ESI): calculated for $[C_{29}H_{44}O_4Si_2+H]^+$: 513.2851, found: 513.2827.

((6-Methyl-4,7-dihydroisobenzofuran-1,3,5-triyl)tris(oxy))tris(*tert*-butyldimethylsilane) (S19)

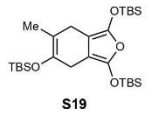

S19

Synthesized from silyl enol ether anhydride **(±)-S6** and *tert*-butyldimethylsilyl trifluoromethanesulfonate using purification procedure C. **Yield**: 1.50 mmol, 24% over 2 steps from **S5** (by ^{1}H NMR using 1,2-dichloroethane as an internal standard); **Appearance**: Pale yellow oil; **R$_f$**: 0.39 (3:97 EtOAc:petroleum ether); **^{1}H NMR** (500 MHz, $CDCl_3$): δ 2.92 (s, 2H), 2.90–2.86 (m, 2H), 1.69 (s, 3H), 0.96 (s, 27H), 0.19 (d, *J* = 3.0 Hz, 12H), 0.15 (s, 6H) ppm, **^{13}C NMR** (125 MHz, $CDCl_3$): δ 141.1, 140.4, 140.4, 109.1, 93.6, 92.6, 26.0, 25.9, 25.9, 25.7, 25.6, 18.4, 18.2, 18.1, 16.9, –3.6, –4.4, –4.4 ppm; **IR**: 2953, 2928, 2884, 2859, 1706, 1675, 1659, 1471, 1361, 1252, 876, 835, 782 cm^{-1}; **HRMS** (ESI): calculated for $[C_{27}H_{52}O_4Si_3+H]^+$: 525.3246, found: 525.3223.

3-((2,5-Bis((*tert*-butyldimethylsilyl)oxy)furan-3-yl)methyl)-1,2-dimethyl-1*H*-indole (S20)

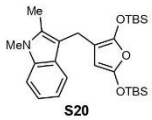

S20

Synthesized from indole anhydride **S9** and *tert*-butyldimethylsilyl trifluoromethanesulfonate using purification procedure C. Modifications from general procedure: reaction was conducted in CH_2Cl_2. **Yield**: 0.97 mmol, 39% (by ^{1}H NMR using 1,2-dichloroethane as an internal standard); **Appearance**: Colorless oil; **^{1}H NMR** (600 MHz, $CDCl_3$): δ 7.53 (d, *J* = 7.8 Hz, 1H), 7.22 (d, *J* = 8.1 Hz, 1H), 7.12 (ddd, *J* = 8.2, 7.0, 1.2 Hz, 1H), 7.03 (ddd, *J* = 7.9, 7.0, 1.0 Hz, 1H), 4.71 (s, 1H), 3.64 (s, 3H), 3.60 (s, 2H), 2.36 (s, 3H), 1.02 (s, 9H), 0.91 (s, 9H), 0.25 (s, 6H), 0.15 (s, 6H) ppm; **^{13}C NMR** (150 MHz, $CDCl_3$): δ 146.8, 142.6, 136.6, 132.9, 128.0, 120.4, 118.7, 118.6, 110.3, 108.4, 97.6, 86.0, 29.6, 25.8, 25.62, 19.0, 18.2, 18.2, 10.4, –4.3, –4.7 ppm; **IR**: 2956, 2931, 2859, 1705, 1472, 1366, 1253, 1176, 839, 789, 735 cm^{-1}; **HRMS** (ESI): calculated for $[C_{27}H_{43}NO_3Si_2+H]^+$: 486.2854, found: 486.2850.

([3,3'-Bifuran]-2,2',5,5'-tetrayltetrakis(oxy))tetrakis(*tert*-butyldimethylsilane) (S21)

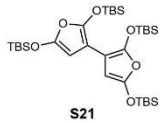

S21

Synthesized from 1,2,3,4-butanetetracarboxylic dianhydride (**S10**) and *tert*-butyldimethylsilyl trifluoromethanesulfonate using purification procedure C. **Yield**: 0.545 mmol, 54% (by ^{1}H NMR using 1,2-dichloroethane as an internal standard); **Appearance**: Orange oil; **R*f***: 0.38 (1:9 EtOAc:petroleum ether); **^{1}H NMR** (500 MHz, $CDCl_3$): δ 5.26 (s, 2H), 0.98 (s, 18H), 0.96 (s, 18H), 0.22 (s, 12H), 0.20 (s, 12H) ppm; **^{13}C NMR** (150 MHz, $CDCl_3$): δ 146.9, 142.2, 91.8, 84.6, 84.5, 25.8, 25.7, 18.3, 18.2, –4.3, –4.7 ppm; **IR**: 2957, 2932, 2861, 1724, 1696, 1628, 1606, 1581, 1366, 1251, 1195, 1170, 840, 787, 731 cm^{-1}; **HRMS** (ESI): calculated for $[C_{32}H_{62}O_6Si_4+H]^+$: 655.3696, found: 655.3699.

((3-Vinylfuran-2,5-diyl)bis(oxy))bis(*tert*-butyldimethylsilane) (45)

45

Synthesized from (*Z*)-3-ethylidenedihydrofuran-2,5-dione (**S12**) and *tert*-butyldimethylsilyl trifluoromethanesulfonate using purification procedure C. **Yield**: 4.34 mmol, 89% (by ^{1}H NMR using 1,2-dichloroethane as an internal standard); **Appearance**: Pale yellow oil; **R*f***: 0.34 (petroleum ether); **^{1}H NMR** (500 MHz, $CDCl_3$): δ 6.39 (dd, *J* = 17.5, 10.9 Hz, 1H), 5.10 (s, 1H), 5.06 (d, *J* = 17.5 Hz, 1H), 4.85 (d, *J* = 10.9 Hz, 1H), 0.98 (s, 9H), 0.96 (s, 9H), 0.22 (s, 6H), 0.22 (s, 6H) ppm; **^{13}C NMR** (125 MHz, $CDCl_3$): δ 148.0, 144.9,

126.7, 108.4, 99.7, 81.6, 25.6 (2 coincident peaks), 18.3, 18.2, –4.4, –4.7 ppm; **IR**: 2957, 2931, 2894, 2859, 1650, 1637, 1603, 1471, 1255, 1070, 1051, 835, 778 cm^{-1}; **HRMS** (ESI): calculated for $[C_{18}H_{34}O_3Si_2+H]^+$: 355.2119, found: 355.2114.

Mono(silyloxy)furans

Summary

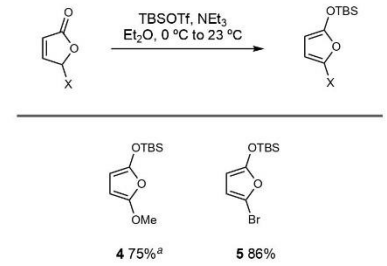

General Procedure

Prepared according to a modification of the procedure reported by Simchen.[12] To an oven-dried two-neck round-bottom flask equipped with a stir bar was added the appropriate substituted furanone (1.00 mol. equiv.). Following addition of anhydrous Et_2O (0.250 M) the resulting suspension was cooled to 0 ºC, and anhydrous triethylamine (2.25 mol. equiv.) was added. After stirring for 10 minutes, *tert*-butyldimethylsilyl trifluoromethanesulfonate (1.65 mol. equiv.) was added dropwise, and the reaction mixture was allowed to warm to room temperature. The reaction was stirred vigorously overnight, yielding a biphasic mixture. The reaction mixture was filtered through phosphate buffered silica (pH 7), eluting with Et_2O. The filtrate was concentrated under reduced pressure to yield the corresponding furan. Both furans were stored in the freezer (–20 °C) under a nitrogen atmosphere. Attempts to purify either furan via flash chromatography using untreated (i.e. acidic) silica resulted in decomposition.

Characterization Data

***tert*-Butyl((5-methoxyfuran-2-yl)oxy)dimethylsilane (4)**

4

Synthesized from 5-methoxyfuran-2(5*H*)-one (**S1**). **Yield**: 0.723 mmol, 75% (by ^{1}H NMR using durene as an internal standard); **Appearance**: Colorless oil; $\mathbf{R_f}$: 0.35 (1:39 EtOAc:petroleum ether); **^{1}H NMR** (600 MHz, $CDCl_3$): δ 4.93 (s, 2H), 3.76 (s, 3H), 0.96

(s, 9H), 0.22 (s, 6H) ppm; **^{13}C NMR** (150 MHz, $CDCl_3$): δ 152.6, 148.2, 83.8, 80.5, 58.1, 25.6, 18.2, –4.8 ppm; **IR**: 2957, 2931, 2859, 1734, 1712, 1390, 1255, 1217, 1164, 838, 791 cm^{-1}; **HRMS** (ESI): calculated for $[C_{11}H_{20}O_3Si+H]^+$: 229.1255, found: 229.1254.

((5-Bromofuran-2-yl)oxy)(*tert*-butyl)dimethylsilane (5)

5

Synthesized from 5-bromo-2(5*H*)-furanone (**S2**). **Yield**: 1.10 g, 3.97 mmol, 86%; **Appearance**: Brown oil; **R*f***: 0.31 (petroleum ether); **^{1}H NMR** (600 MHz, $CDCl_3$): δ 6.11 (d, *J* = 3.2 Hz , 1H), 5.09 (d, *J* = 3.2 Hz, 1H), 0.97 (s, 9H), 0.24 (s, 6H) ppm; **^{13}C NMR** (150 MHz, $CDCl_3$): δ 157.4, 112.7, 109.0, 86.7, 25.5, 18.2, –4.8 ppm; **IR**: 2957, 2932, 2861, 1618, 1531, 1472, 1254, 1120, 1189, 1008, 971, 840, 787, 756, 684 cm^{-1}; **HRMS** (ESI): calculated for $[C_{10}H_{17}BrO_2Si+H]^+$: 277.0254, found: 277.0247.

Stability Studies

Summary

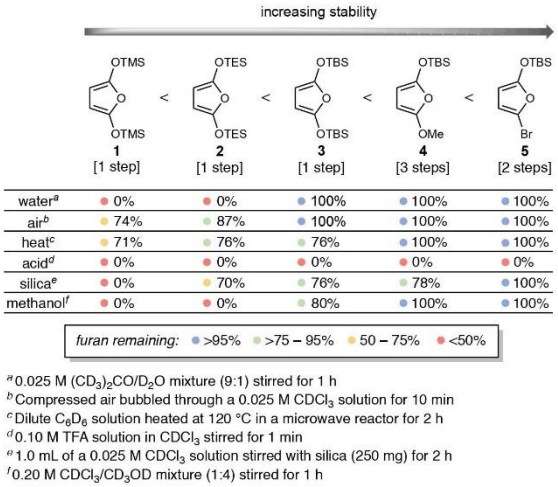

[a] 0.025 M $(CD_3)_2CO/D_2O$ mixture (9:1) stirred for 1 h
[b] Compressed air bubbled through a 0.025 M $CDCl_3$ solution for 10 min
[c] Dilute C_6D_6 solution heated at 120 °C in a microwave reactor for 2 h
[d] 0.10 M TFA solution in $CDCl_3$ stirred for 1 min
[e] 1.0 mL of a 0.025 M $CDCl_3$ solution stirred with silica (250 mg) for 2 h
[f] 0.20 M $CDCl_3/CD_3OD$ mixture (1:4) stirred for 1 h

Note: Stability studies are adapted from those disclosed by Sherburn.[13]

Water Stability

0.025 M $(CD_3)_2CO/D_2O$ (9:1) solutions of each substrate were prepared. BHT (ca. 2 mg/mL) was added to inhibit the autoxidative effects of any oxygen present in solution. An internal standard (durene) was added to each sample, and an initial ^1H NMR spectrum was obtained. The flasks were sealed, and each sample was stirred for 1 hour. A second ^1H NMR spectrum was obtained to determine whether any decomposition had occurred.

Air Stability

0.025 M $CDCl_3$ solutions of each substrate were prepared ($CDCl_3$ stored over K_2CO_3 to remove any acid). An internal standard (durene) was added to each sample, and an initial ^1H NMR spectrum was obtained. Compressed air (from an Ozito cordless air pump, flow rate of 14 L/min) was then bubbled through each sample for 10 minutes. A second ^1H NMR spectrum was obtained to determine whether any decomposition had occurred.

Heat Stability

Dilute solutions of each substrate in C_6D_6 were prepared. BHT (ca. 2 mg/mL) was added to inhibit the autoxidative effects of any oxygen present in solution. An internal standard (durene) was added to each sample, and an initial ^{1}H NMR spectrum was obtained. Each sample was heated to 120 °C for 2 hours in a microwave reactor. A second ^{1}H NMR spectrum was obtained to determine whether any decomposition had occurred.

Acid Stability

0.025 M $CDCl_3$ solutions of each substrate were prepared. BHT (ca. 2 mg/mL) was added to inhibit the autoxidative effects of any oxygen present in solution. An internal standard (durene) was added to each sample, and an initial ^{1}H NMR spectrum was obtained. To 500 µL of each substrate solution was added 500 µL of a 0.2 M TFA solution in $CDCl_3$, and the samples were stirred for ca. 1 minute. A second ^{1}H NMR spectrum was obtained to determine whether any decomposition had occurred.

Silica Stability

0.025 M $CDCl_3$ solutions of each substrate were prepared ($CDCl_3$ stored over K_2CO_3 to remove any acid). BHT (ca. 2 mg/mL) was added to inhibit the autoxidative effects of any oxygen present in solution. An internal standard (durene) was added to each sample, and an initial ^{1}H NMR spectrum was obtained. 250 mg of silica was added to 1 mL of each furan solution, and the samples were stirred for 2 hours. A second ^{1}H NMR spectrum was obtained to determine whether any decomposition had occurred.

Note: This test is not necessarily representative of subjecting a compound to flash chromatographic purification with untreated (i.e. acidic) silica. For example, bromide **5** decomposes if attempts are made to purify it by this method.

Methanol Stability

0.020 M $CDCl_3/CD_3OD$ (1:4) solutions of each substrate were prepared ($CDCl_3$ stored over K_2CO_3 to remove any acid). BHT (ca. 2 mg/mL) was added to inhibit the autoxidative effects of any oxygen present in solution. An internal standard (durene) was added to each sample, and an initial ^1H NMR spectrum was obtained. The flasks were sealed, and each sample was stirred for 1 hour. A second ^1H NMR spectrum was obtained to determine whether any decomposition had occurred.

Diels–Alder Rate Studies

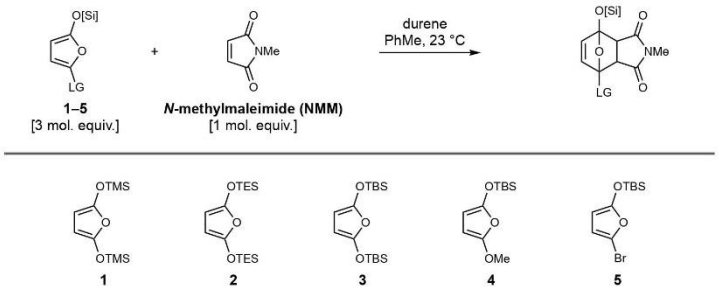

General Procedure

To an oven dried 10 mL round-bottom flask equipped with a stir bar and under nitrogen was added *N*-methylmaleimide (0.0500 g, 0.450 mmol, 1.00 mol. equiv.), durene (used as a ^{1}H NMR internal standard, 0.0250 g, 0.186 mmol, 0.410 mol. equiv.) and anhydrous PhMe (0.450 mL, 0.250 M). To this mixture was added the appropriate silylated diene (3.00 mol. equiv.) as a solution in anhydrous PhMe (0.450 mL). The percentage of *N*-methylmaleimide remaining was determined by ^{1}H NMR via comparison to durene, at the time intervals specified in the table below.

Time (minutes)	***N*-methylmaleimide Remaining (%)**				
	1	**2**	**3**	**4**	**5**
0	100.00	100.00	100.00	100.00	100.00
5	-	-	-	48.39	-
15	52.69	64.89	57.33	16.13	-
30	25.32	40.13	38.67	6.45	-
60	11.76	17.87	19.20	0.00	90.98
120	1.79	4.08	5.33	0.00	80.90
180	0.52	1.57	1.87	0.00	68.44
240	0.00	0.31	0.80	0.00	56.50
300	0.00	0.00	0.00	0.00	46.15

Reaction Kinetics

For **A** + **B** → **C**:

$$\frac{d[\mathbf{B}]}{dt} = -k[\mathbf{A}][\mathbf{B}]$$

Given initial concentrations of **A** and **B**, $[\mathbf{A}]_0$ and $[\mathbf{B}]_0$, respectively, the concentration of **B** at time *t* is:

$$[\mathbf{B}] = \frac{([\mathbf{A}]_0 - [\mathbf{B}]_0)[\mathbf{B}]_0}{([\mathbf{A}]_0 e^{k([\mathbf{A}]_0 - [\mathbf{B}]_0)t} - [\mathbf{B}]_0}$$

The rate data was fit to this equation to obtain the rate constant, *k*:

***k* ($M^{-1}min^{-1}$)**				
1	**2**	**3**	**4**	**5**
0.0164702	0.0112124	0.012082	0.0511795	0.00081359

With relative rate constants, k_{rel}:

k_{rel}				
1	**2**	**3**	**4**	**5**
0.32	0.22	0.24	1.00	0.02

Note: For $[\mathbf{A}]_0 >> [\mathbf{B}]_0$ (which is not the case here), this reduces to the expected equation for pseudo-first order kinetics:

$$[\mathbf{B}] = [\mathbf{B}]_0 e^{-k[\mathbf{A}]_0 t}$$

With pseudo-first order rate constant, k_{pseudo}:

$$k_{pseudo} = k[\mathbf{A}]_0$$

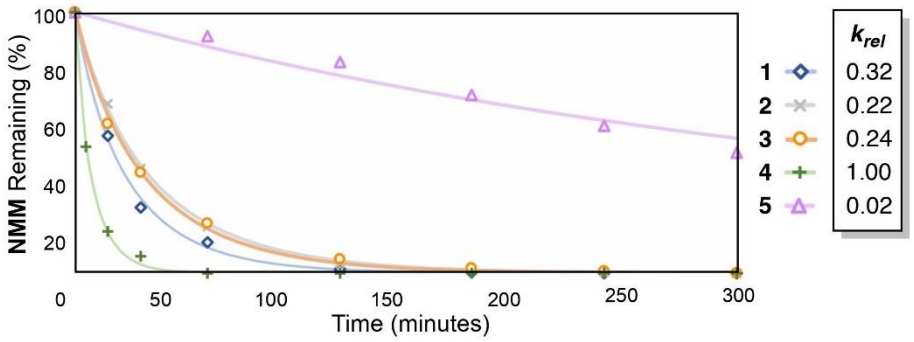
NMM Remaining (%)
100
80
60
40
20
0
50
100
150
200
250
300
Time (minutes)
k_{rel}
1 0.32
2 0.22
3 0.24
4 1.00
5 0.02

Synthesis of para-Hydroquinones

Step-wise Diels–Alder/Aromatization

Isolation of Silylated Intermediates

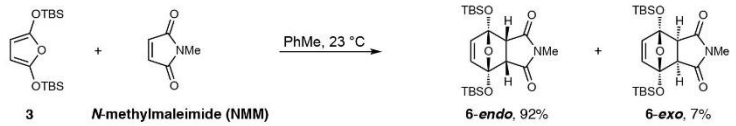

3 ***N*-methylmaleimide (NMM)** **6-*endo*, 92%** **6-*exo*, 7%**

To an oven-dried 10 mL round-bottom flask equipped with a stir bar and under nitrogen was added 2,5-bis((*tert*-butyldimethylsilyl)oxy)furan (**3**) (444 mg, 1.35 mmol, 3.00 mol. equiv.), anhydrous PhMe (0.900 mL, 0.500 M), and *N*-methylmaleimide (50 mg, 0.450 mmol, 1.00 mol. equiv.). The reaction was stirred at room temperature overnight, whereby TLC analysis indicated the reaction had gone to completion. The reaction mixture was concentrated under reduced pressure and purified via flash column chromatography [phosphate buffered SiO_2 (pH 7), eluting with petroleum ether → 1:4 EtOAc:petroleum ether], yielding **6-*endo*** (182 mg, 0.414 mmol, 92%) and **6-*exo*** (13.7 mg, 0.031 mmol, 7%).

Intermediate 6-*endo*

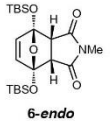

6-*endo*

Appearance: White solid; **R*f***: 0.32 (1:19 EtOAc:petroleum ether); **M.p.**: 141.1–145.9 ºC; **^{1}H NMR** (600 MHz, C_6D_6): δ 5.90 (s, 2H), 3.03 (s, 2H), 2.52 (s, 3H), 1.02 (s, 18H), 0.22 (s, 6H), 0.16 (s, 6H) ppm; **^{13}C NMR** (150 MHz, C_6D_6): δ 173.3, 137.5, 105.0, 55.3, 25.8, 24.2, 18.1, –3.1, –3.3 ppm; **IR**: 3471, 2934, 2862, 1711, 1358, 1336, 1237, 838, 784 cm^{-1}; **HRMS** (ESI): calculated for $[C_{21}H_{37}NO_5Si_2+H]^+$: 440.2283, found: 440.2286.

Assignment of Stereochemistry:

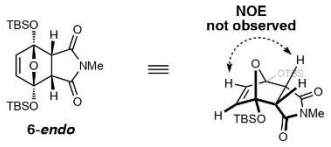

6-*endo*

Intermediate 6-*exo*

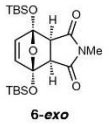

6-*exo*

Appearance: White solid; **R*f***: 0.28 (3:17 EtOAc:petroleum ether); **M.p.**: 93.6–98.6 °C; **^{1}H NMR** (600 MHz, C_6D_6): δ 5.82 (s, 2H), 2.70 (s, 3H), 2.41 (s, 2H), 1.07 (s, 18H), 0.23 (s, 6H), 0.17 (s, 6H) ppm; **^{13}C NMR** (150 MHz, C_6D_6): δ 172.0, 140.2, 104.9, 53.2, 25.9, 24.4, 18.2, –3.2, –3.4 ppm; **IR**: 3465, 2930, 2858, 1703, 1326, 1228, 887, 829, 780 cm^{-1}; **HRMS** (ESI): calculated for $[C_{21}H_{37}NO_5Si_2+H]^+$: 440.2283, found: 440.2288.

Assignment of Stereochemistry:

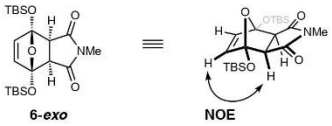

Aromatization of Silylated Intermediates

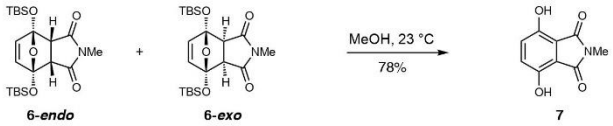

To a 50 ml round-bottom flask open to air and equipped with a stir bar was added a 92:7 mixture of **6-*endo*** and **6-*exo*** (0.953 g, 2.17 mmol, 1.00 mol. equiv.) and MeOH (4.34 mL, 0.500 M, not anhydrous). The reaction was sealed and stirred at room temperature overnight, by which time a yellow solid had crashed out of solution. The crude mixture was concentrated under reduced pressure and purified by washing with petroleum ether to yield 4,7-dihydroxy-2-methylisoindoline-1,3-dione (**7**) (0.327 g, 1.69 mmol, 78%). Characterization data is included in the diene scope section below.

Diels–Alder Reaction Scope

Diene Scope

Summary

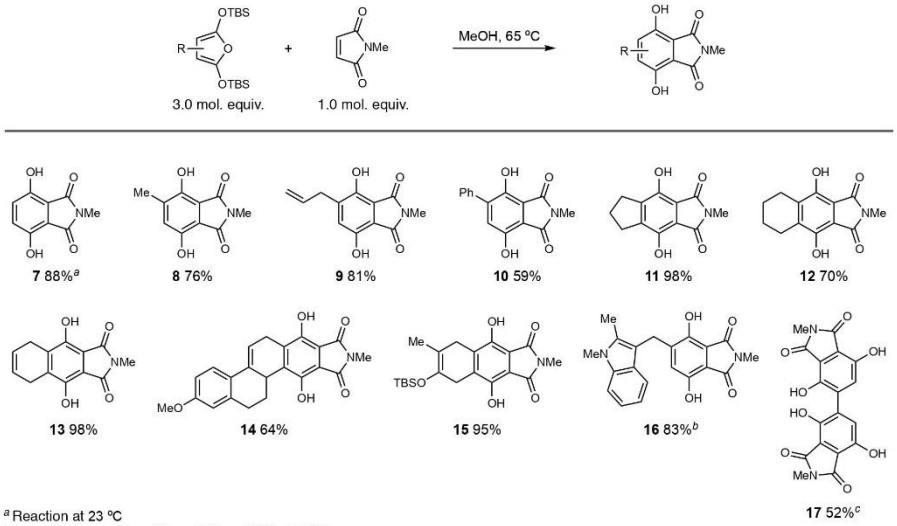

[a] Reaction at 23 °C
[b] Aromatization achieved by addition of TFA at 23 °C
[c] 1.0 mol. equiv. furan, 3.0 mol. equiv. *N*-methylmaleimide. Diels–Alder in PhMe at 23 °C, aromatization achieved by addition of H_2SO_4 at 23 °C

General Procedure

To a round-bottom flask equipped with a stir bar and under nitrogen was added the appropriate furan (3.00 mol. equiv.), MeOH (not anhydrous, 0.500 M), and *N*-methylmaleimide (1.00 mol. equiv.). The reaction was heated at reflux overnight, by which time a yellow/orange solid had crashed out of solution. The crude mixture was concentrated under reduced pressure and purified as specified to yield the corresponding *para*-hydroquinone.

Characterization Data

4,7-Dihydroxy-2-methylisoindoline-1,3-dione (7)

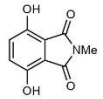
7

Synthesized from 2,5-bis((*tert*-butyldimethylsilyl)oxy)furan (**3**). Modifications from general procedure: reaction conducted at 23 ºC. Purified by washing with Et_2O. **Yield**: 0.114 g, 0.589 mmol, 72%; Spectroscopic data matched those previously reported in the literature.[14] **Appearance**: Yellow solid; **R**$_f$: 0.30 (6:4 EtOAc:petroleum ether); **^{1}H NMR** [500 MHz, $(CD_3)_2SO$]: δ 10.08 (s, 2H), 7.04 (s, 2H), 2.91 (s, 3H) ppm.

4,7-Dihydroxy-2,5-dimethylisoindoline-1,3-dione (8)

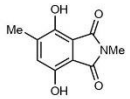
8

Synthesized from ((3-methylfuran-2,5-diyl)bis(oxy))bis(*tert*-butyldimethylsilane) (**48**). Purified by washing with petroleum ether and then Et_2O. **Yield**: 0.105 g, 0.507 mmol, 76%; **Appearance**: Yellow solid; **R**$_f$: 0.27 (3:7 EtOAc:petroleum ether); **M.p.**: 214.8–215.9 ºC; **^{1}H NMR** [500 MHz, $(CD_3)_2SO$]: δ 10.12 (br s, 1H), 9.11 (br s, 1H), 6.92 (s, 1H), 2.91 (s, 3H), 2.16 (s, 3H) ppm; **^{13}C NMR** [125 MHz, $(CD_3)_2SO$]: δ 167.9, 166.2, 148.0, 145.8, 136.7, 125.9, 114.4, 11.3, 23.1, 16.2 ppm; **IR**: 3422, 2983, 2948, 1747, 1676, 1456, 1165, 1031, 981, 757 cm^{-1}; **HRMS** (ESI): calculated for $[C_{10}H_9NO_4+H]^+$: 208.0604, found: 208.0603.

5-Allyl-4,7-dihydroxy-2-methylisoindoline-1,3-dione (9)

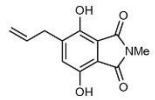
9

Synthesized from ((3-allylfuran-2,5-diyl)bis(oxy))bis(*tert*-butyldimethylsilane) (**S13**). Purified by washing with petroleum ether and then Et_2O. **Yield**: 0.200 g, 0.856 mmol, 81%; **Appearance**: Yellow solid; **R**$_f$: 0.36 (3:7 EtOAc:petroleum ether); **M.p.**: 165–168 ºC; **^{1}H NMR** [600 MHz, $(CD_3)_2SO$]: δ 10.23 (s, 1H), 9.25 (s, 1H), 6.92 (s, 1H), 5.95–5.88 (m, 1H), 5.10 (t, J = 5.1 Hz, 1H), 5.09–5.06 (m, 1H), 2.92 (s, 3H) ppm; **^{13}C NMR** [150 MHz, $(CD_3)_2SO$]: δ 167.8, 166.2, 148.2, 145.2, 138.7, 135.6, 125.2, 116.8, 114.9, 111.8, 33.4, 23.2 ppm; **IR**: 3402, 1663, 1023, 1000, 823, 762 cm^{-11}; **HRMS** (ESI): calculated for $[C_{12}H_{11}NO_4+H]^+$: 234.0766, found: 234.0759.

4,7-Dihydroxy-2-methyl-5-phenylisoindoline-1,3-dione (10)

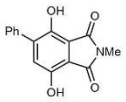

10

Synthesized from ((3-phenylfuran-2,5-diyl)bis(oxy))bis(*tert*-butyldimethylsilane) (**S14**). Purified by washing with Et_2O. **Yield**: 0.119 g, 0.441 mmol, 59%; **Appearance**: Yellow solid; $\mathbf{R}_f$: 0.30 (7:13 EtOAc:petroleum ether); **M.p.**: 235–238 ºC; **^{1}H NMR** [600 MHz, $(CD_3)_2SO$]: δ 10.44 (br s, 1H), 9.20 (br s, 1H), 7.51 (d, J = 7.7 Hz, 2H), 7.46 (t, J = 7.6 Hz, 2H), 7.40 (t, J = 7.3 Hz, 1H), 7.09 (s, 1H), 2.97 (s, 3H) ppm; **^{13}C NMR** [125 MHz, $(CD_3)_2SO$]: δ 168.0, 166.0, 148.3, 144.5, 139.1, 136.2, 129.1, 128.3, 128.1, 125.9, 116.0, 112.9, 23.3 ppm; **IR**: 3411, 2950, 2530, 1747, 1672, 1443, 1274, 1302, 1245, 1142, 923, 885, 703, 760 cm^{-1}; **HRMS** (ESI): calculated for $[C_{15}H_{11}NO_4+H]^+$: 270.0761, found: 270.0753.

4,8-Dihydroxy-2-methyl-6,7-dihydrocyclopenta[*f*]isoindole-1,3(2*H*,5*H*)-dione (11)

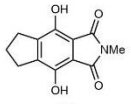

11

Synthesized from 1,3-bis((*tert*-butyldimethylsilyl)oxy)-5,6-dihydro-4*H*-cyclopenta[*c*]furan (**S15**). Purified by washing with EtOAc. **Yield**: 0.115 g, 0.492 mmol, 98%; **Appearance**: Pale-yellow solid; $\mathbf{R}_f$: 0.30 (1:3 EtOAc:petroleum ether); **M.p.**: 250–253 ºC; **^{1}H NMR** [600 MHz, $(CD_3)_2SO$]: δ 9.39 (br s, 2H), 2.91 (s, 3H), 2.82 (t, J = 7.4 Hz, 4H), 2.05 (p, J = 7.4 Hz, 2H) ppm; **^{13}C NMR** [125 MHz, $(CD_3)_2SO$]: δ 167.1, 144.5, 141.7, 113.3, 30.0, 24.1, 23.1 ppm; **IR**: 3405, 2953, 2894, 2841, 2515, 1741, 1669, 1634, 1446, 1380, 1274, 1236, 1161, 1057, 979, 938, 760 cm^{-1}; **HRMS** (ESI): calculated for $[C_{12}H_{11}NO_4+H]^+$: 234.0761, found: 234.0764.

4,9-Dihydroxy-2-methyl-5,6,7,8-tetrahydro-1*H*-benzo[*f*]isoindole-1,3(2*H*)-dione (12)

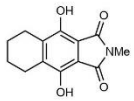

12

Synthesized from 1,3-bis((*tert*-butyldimethylsilyl)oxy)-4,5,6,7-tetrahydroisobenzofuran (**S16**). Purified by washing with Et_2O. **Yield**: 0.173 g, 0.700 mmol, 70%; **Appearance**: Pale yellow solid; $\mathbf{R}_f$: 0.34 (1:4 EtOAc:petroleum ether); **M.p.**: 237.6–239.7 ºC; **^{1}H NMR** [500 MHz, $(CD_3)_2SO$]: δ 9.21 (s, 2H), 2.93 (s, 3H), 2.63–2.54 (m, 4H) 1.73–1.60 (m, 4H) ppm; **^{13}C NMR** [125 MHz, $(CD_3)_2SO$]: δ 167.6, 145.7, 135.5, 110.3, 23.6, 23.1, 21.2 ppm; **IR**: 3400, 2952, 2930, 1747, 1671, 1452, 1187, 990, 762, 659 cm^{-1}; **HRMS** (ESI): calculated for $[C_{13}H_{13}NO_4+H]^+$: 248.0917, found: 248.0910.

4,9-Dihydroxy-2-methyl-5,8-dihydro-1*H*-benzo[*f*]isoindole-1,3(2*H*)-dione (13)

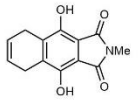

13

Synthesized from 1,3-bis((*tert*-butyldimethylsilyl)oxy)-4,7-dihydroisobenzofuran (**S17**). Purified by washing with Et_2O. **Yield**: 0.240 g, 0.980 mmol, 98%; **Appearance**: Yellow solid; **R*f***: 0.44 (3:7 EtOAc:petroleum ether); **M.p.**: >260 ºC; **^{1}H NMR** [600 MHz, $(CD_3)_2SO$]: δ 9.43 (br s, 2H), 5.86 (s, 2H), 3.24 (s, 4H), 2.94 (s, 3H) ppm; **^{13}C NMR** [150 MHz, $(CD_3)_2SO$]: δ 167.5, 145.2, 132.4, 122.8, 110.9, 24.7, 23.2 ppm; **IR**: 3417, 3361, 3038, 2862, 2533, 1744, 1559, 1455, 1214, 1001, 954, 938, 757, 578 cm^{-1}; **HRMS** (ESI): calculated for $[C_{13}H_{11}NO_4+H]^+$: 246.0761, found: 246.0756.

Pentacyclic *para*-hydroquinone 14

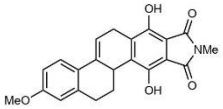

14

Synthesized from tetracyclic furan **S18**. Purified by washing with petroleum ether and then Et_2O. **Yield**: 0.121 g, 0.321 mmol, 64%; **Appearance**: Yellow solid; **R*f***: 0.37 (3:7 EtOAc:petroleum ether); **M.p.**: >260 ºC; **^{1}H NMR** [500 MHz, $(CD_3)_2SO$]: δ 9.49 (br s, 2H), 7.40 (d, *J* = 8.6 Hz, 1H), 6.76 (dd, *J* = 8.6, 2.7 Hz, 1H), 6.70 (d, *J* = 2.7 Hz, 1H), 5.99 (t, *J* = 3.8 Hz, 1H), 3.74 (s, 3H), 3.59–3.49 (m, 3H), 3.43 (dt, *J* = 25.8, 4.5 Hz, 2H), 3.14–3.04 (m, 1H), 2.95 (s, 3H), 2.88 (dd, *J* = 17.2, 5.3 Hz, 1H), 2.65 (dd, *J* = 12.3, 5.9 Hz, 1H), 1.48 (qd, *J* = 12.2, 5.4 Hz, 1H) ppm; **^{13}C NMR** [150 MHz, $(CD_3)_2SO$]: δ 167.7, 167.3, 158.5, 145.9, 145.2, 137.0, 135.2, 134.2, 132.0, 129.0, 125.3, 114.0, 113.1, 112.5, 111.8, 111.2, 55.0, 35.7, 31.4, 29.9, 26.0, 23.2 ppm; **IR**: 3414, 2944, 2869, 2831, 2527, 1747, 1675, 1603, 1496, 1443, 1377, 1274, 1224, 998, 957, 945, 760 cm^{-1}; **HRMS** (ESI): calculated for $[C_{22}H_{19}NO_5+H]^+$: 378.1336, found: 378.1338.

Silyl enol ether *para*-hydroquinone 15

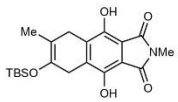

15

Synthesized from ((6-methyl-4,7-dihydroisobenzofuran-1,3,5-triyl)tris(oxy))tris(*tert*-butyldimethylsilane) (**S19**). Purified by washing with Et_2O. **Yield**: 0.166 g, 0.426 mmol, 95%; **Appearance**: White solid; **R*f***: 0.34 (1:4 EtOAc:petroleum ether); **M.p.**: 200–202 ºC; **^{1}H NMR** [600 MHz, $CDCl_3$]: δ 7.18 (br s, 2H), 3.38–3.31 (m, 4H), 3.10 (s, 3H), 1.74 (s, 3H), 0.99 (s, 9H), 0.19 (s, 5H) ppm; **^{13}C NMR** [150 MHz, $CDCl_3$]: δ 170.0, 169.9, 146.2, 146.1, 139.4, 132.8, 132.8, 109.2, 109.2, 107.3, 30.9, 29.6, 26.0,

23.6, 18.4, 15.8, –3.6 ppm; **IR**: 3417, 2931, 2856, 1750, 1687, 1468, 1258, 1079, 988, 888, 782, 757 cm^{-1}; **HRMS** (ESI): calculated for $[C_{20}H_{27}NO_5Si+H]^+$: 390.1731, found: 390.1727.

Indole-substituted *para*-hydroquinone 16

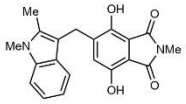

16

Synthesized from 3-((2,5-bis((*tert*-butyldimethylsilyl)oxy)furan-3-yl)methyl)-1,2-dimethyl-1*H*-indole (**S20**). Modifications from general procedure: aromatization achieved followed by addition of TFA (0.08 mL, 1.07 mmol, 6 eq.) at 23 ºC. The reaction was stirred for 1.5 hours, before being purified by washing with Et_2O, then CH_2Cl_2. **Yield**: 0.0520 g, 0.148 mmol, 83%; **Appearance**: Yellow solid; $\mathbf{R_f}$: 0.31 (1:4 EtOAc:PhMe); **M.p.**: Degraded at 240 ºC; **^{1}H NMR** [500 MHz, $(CD_3)_2SO$]: δ 9.97 (s, 1H), 9.34 (s, 1H), 7.37 (d, J = 8.2 Hz, 1H), 7.31 (d, J = 7.8 Hz, 1H), 7.06 (t, J = 7.6 Hz, 1H), 6.94 (t, J = 7.5 Hz, 1H), 6.66 (s, 1H), 3.98 (s, 2H), 3.68 (s, 3H), 2.92 (s, 3H), 2.36 (s, 3H) ppm; **^{13}C NMR** [125 MHz, $(CD_3)_2SO$]: δ 168.0, 166.1, 148.2, 145.2, 140.6, 136.4, 134.4, 127.2, 124.6, 120.3, 118.6, 117.6, 114.7, 111.3, 109.0, 107.1, 29.4, 23.5, 23.2, 10.0 ppm; **IR**: 3412, 2909, 1753, 1683, 1621, 1483, 1458, 1441, 1382, 1276, 1250, 1158, 1013, 933, 736 cm^{-1}; **HRMS** (ESI): calculated for $[C_{20}H_{18}N_2O_4+H]^+$: 351.1339, found: 351.1339.

4,4',7,7'-Tetrahydroxy-2,2'-dimethyl-[5,5'-biisoindoline]-1,1',3,3'-tetraone (17)

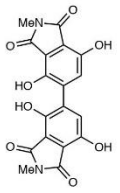

17

Synthesized from ([3,3'-bifuran]-2,2',5,5'-tetrayltetrakis(oxy))tetrakis(*tert*-butyldimethylsilane) (**S21**). Modifications from general procedure: reaction conducted in PhMe at room temperature with 1.00 mol. equiv. of **S21** and 3.00 mol. equiv. of *N*-methylmaleimide. Aromatization achieved by addition of concentrated sulfuric acid (5 drops), followed by stirring overnight. Purification via washing with CH_2Cl_2 and then EtOAc. **Yield**: 0.200 g, 0.519 mmol, 52%; **Appearance**: Yellow solid; $\mathbf{R_f}$: 0.50 (EtOAc); **M.p.**: >260 ºC; **^{1}H NMR** [500 MHz, $(CD_3)_2SO$]: δ 10.40 (br s, 2H), 9.32 (s, 2H), 6.98 (s, 2H), 2.96 (s, 6H) ppm; **^{13}C NMR** [150 MHz, $(CD_3)_2SO$]: 167.6, 166.1, 147.7, 145.0, 134.6, 126.7, 115.5, 113.8, 23.3 ppm; **IR**: 3402, 1746, 1677, 1631, 1441, 1375, 1245, 1186, 1126, 996, 978, 933, 765 cm^{-1}; **HRMS** (ESI): calculated for $[C_{18}H_{12}N_2O_8+Na]^+$: 407.0486, found: 407.0486.

Dienophile Scope

Summary

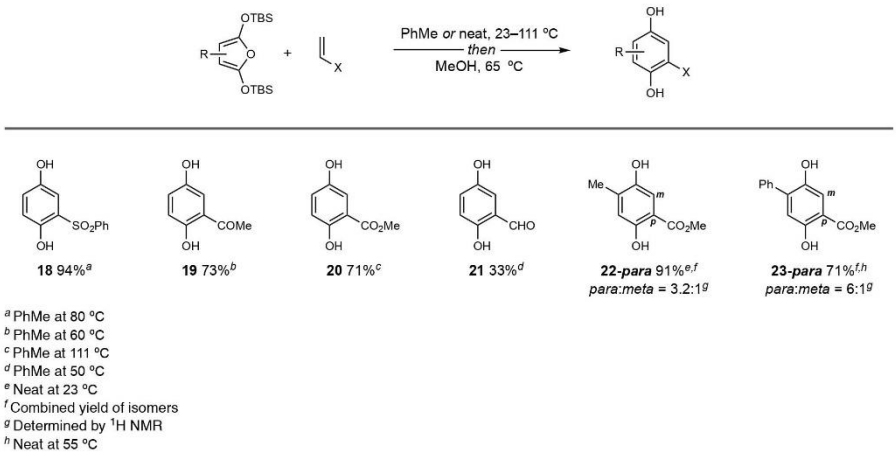

[a] PhMe at 80 °C
[b] PhMe at 60 °C
[c] PhMe at 111 °C
[d] PhMe at 50 °C
[e] Neat at 23 °C
[f] Combined yield of isomers
[g] Determined by ^{1}H NMR
[h] Neat at 55 °C

General Procedures

To an oven-dried Schlenk tube equipped with a stir bar and under nitrogen was added the appropriate furan and dienophile. The reaction was either run neat, or in anhydrous PhMe (0.500M with respect to the limiting reagent). The flask was sealed, and the reaction mixture was heated until ^{1}H NMR analysis indicated the reaction had gone to completion. The reaction mixture was allowed to cool to room temperature (if necessary), and MeOH (not anhydrous) was added. The reaction was heated at 65 °C overnight, whereby ^{1}H NMR analysis indicated the reaction had gone to completion. The reaction mixture was concentrated under reduced pressure and purified according to the specified procedure. ***Note***: Individual reaction details (e.g. molar quantities, stoichiometries) are provided below.

Characterization Data

2-(Phenylsulfonyl)benzene-1,4-diol (18)

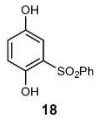

18

Synthesized from 2,5-bis((*tert*-butyldimethylsilyl)oxy)furan (**3**) (0.493 g, 1.50 mmol, 3.00 mol. equiv.), and phenyl vinyl sulfone (84.1 mg, 0.500 mmol, 1.00 mol. equiv.). Diels–Alder reaction conducted in PhMe at 80 °C overnight. Aromatization achieved with 2 mL of MeOH. Purified via flash column chromatography (SiO_2, eluting with 1:99 MeOH/CH_2Cl_2 → 1:19 MeOH/CH_2Cl_2). **Yield**: 0.117 g, 0.467 mmol, 94%; Spectroscopic data matched those previously reported in the literature.[15] **Appearance**: Off-white solid; **R*f***: 0.30 (1:19 MeOH:CH_2Cl_2); **^{1}H NMR** [500 MHz, $(CD_3)_2SO$]: δ 9.92 (br s, 1H), 9.37 (br s, 1H), 7.89 (d, *J* = 7.5 Hz, 2H), 7.65 (t, *J* = 7.3 Hz, 1H), 7.57 (t, *J* = 7.7 Hz, 2H), 7.33 (d, *J* = 3.0 Hz, 1H), 6.91 (dd, *J* = 8.7, 3.0 Hz, 1H), 6.73 (d, *J* = 8.8 Hz, 1H) ppm.

1-(2,5-Dihydroxyphenyl)ethanone (19)

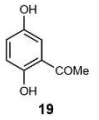

19

Synthesized from 2,5-bis((*tert*-butyldimethylsilyl)oxy)furan (**3**) (0.334 g, 1.02 mmol, 1.00 mol. equiv.) and methyl vinyl ketone (0.642 g, 9.15 mmol, 9.00 mol. equiv.). Diels–Alder reaction conducted in PhMe at 60 °C for 3 h. Aromatization achieved with 4 mL of MeOH. The mixture was concentrated under reduced pressure and washed with petroleum ether (3×). **Yield**: 0.114 g, 0.748 mmol, 74%; Spectroscopic data matched those previously reported in the literature.[16] **Appearance**: Yellow solid; **R*f***: 0.36 (3:7 EtOAc:petroleum ether); **^{1}H NMR** [500 MHz, $(CD_3)_2SO$]: δ 11.33 (s, 1H), 9.19 (s, 1H), 7.18 (d, *J* = 3.0 Hz, 1H), 6.99 (dd, *J* = 8.8, 3.0 Hz, 1H), 6.80 (d, *J* = 8.8 Hz, 1H), 2.58 (s, 3H) ppm.

Methyl 2,5-dihydroxybenzoate (20)

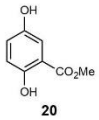

20

Synthesized from 2,5-bis((*tert*-butyldimethylsilyl)oxy)furan (**3**) (0.329 g, 1.00 mmol, 1.00 mol. equiv.) and methyl acrylate (0.630 mL, 7.00 mmol, 7.00 mol. equiv.). Diels–Alder reaction conducted in PhMe at 111 °C overnight. Aromatization achieved with 4 mL of MeOH. The crude reaction was concentrated under reduced pressure and then purified via flash column chromatography (SiO_2, eluting with petroleum ether → 1:4 EtOAc:petroleum ether). **Yield**: 0.119 g, 0.707 mmol, 71%; Spectroscopic data matched those previously reported in the

literature.[17] **Appearance**: Off-white solid; **R*f***: 0.29 (1:3 EtOAc:petroleum ether); **^{1}H NMR** (500 MHz, $CDCl_3$): δ 10.36 (s, 1H), 7.27 (d, *J* = 3.0 Hz, 1H), 7.01 (dd, *J* = 8.9, 3.0 Hz, 1H), 6.87 (d, *J* = 8.9 Hz, 1H), 5.25 (s, 1H), 3.92 (s, 3H) ppm.

2,5-Dihydroxybenzaldehyde (21)

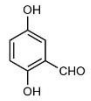

21

Synthesized from 2,5-bis((*tert*-butyldimethylsilyl)oxy)furan (**3**) (0.329 g, 1.00 mmol, 1.00 mol. equiv.), and acrolein (0.392 g, 7.00 mmol, 7.00 mol. equiv.). Reaction conducted in PhMe at 50 °C overnight. Aromatization achieved with 2 mL of MeOH. The crude reaction was concentrated under reduced pressure and then purified via flash column chromatography (SiO_2, eluting with petroleum ether → 1:4 EtOAc/petroleum ether). **Yield**: 0.050 g, 0.330 mmol, 33%; Spectroscopic data matched those previously reported in the literature.[18] **Appearance**: Yellow solid; **R*f***: 0.38 (3:7 EtOAc:petroleum ether); **^{1}H NMR** [500 MHz, $(CD_3)_2SO$]: δ 10.18 (s, 1H), 10.02 (s, 1H), 9.18 (s, 1H), 7.00–6.95 (m, 2H), 6.84 (d, *J* = 8.6 Hz, 1H) ppm.

Methyl 2,5-dihydroxy-4-methylbenzoate (22-*para*) and methyl 2,5-dihydroxy-3-methylbenzoate (22-*meta*)

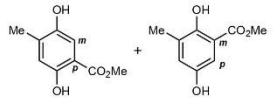

22-*para* **22-*meta***

Synthesized from ((3-methylfuran-2,5-diyl)bis(oxy))bis(*tert*-butyldimethylsilane) (**48**) (1.18 g, 3.44 mmol, 1.40 mol. equiv.) and methyl acrylate (0.211 g, 2.45 mmol, 1.00 mol. equiv.). Diels–Alder reaction conducted neat at 23 °C overnight. Aromatization achieved with 2 mL of MeOH. The crude reaction was concentrated under reduced pressure and purified via flash column chromatography (SiO_2, eluting with petroleum ether → 1:4 EtOAc:petroleum ether), yielding a mixture of **22-*para*** and **22-*meta*** as an off-white solid. **Yield**: 0.406 g, 2.23 mmol, 91%, *para*:*meta* = 3.2:1 (determined by ^{1}H NMR); **R*f***: 0.41 (3:7 EtOAc:petroleum ether).

Methyl 2,5-dihydroxy-4-methylbenzoate (22-*para*)

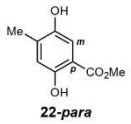

22-*para*

Spectroscopic data matched those previously reported in the literature.[19] **^{1}H NMR** (500 MHz, $CDCl_3$): δ 10.25 (s, 1H), 7.19 (s, 1H), 6.77 (s, 1H), 4.46 (br s, 1H), 3.92 (s, 3H), 2.26 (s, 3H) ppm.

Methyl 2,5-dihydroxy-3-methylbenzoate (22-*meta*)

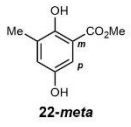

22-*meta*

Spectroscopic data matched those previously reported in the literature.[20] **^{1}H NMR** (500 MHz, $CDCl_3$): δ 10.58 (s, 1H), 7.12 (d, J = 3.6 Hz, 1H), 6.90 (d, J = 3.7 Hz, 1H), 4.50 (br s, 1H),3.93 (s, 3H), 2.24 (s, 3H) ppm.

Methyl 2,5-dihydroxy-[1,1'-biphenyl]-4-carboxylate (23-*para*) and methyl 2,5-dihydroxy-[1,1'-biphenyl]-3-carboxylate (23-*meta*)

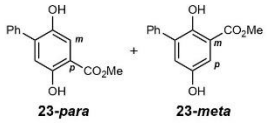

23-*para* **23-*meta***

Synthesized from ((3-phenylfuran-2,5-diyl)bis(oxy))bis(*tert*-butyldimethylsilane) (**S14**) (2.19 g, 5.40 mmol, 1.80 mol. equiv.) and methyl acrylate (0.258 g, 3.00 mmol, 1.00 mol. equiv.). Diels–Alder reaction conducted neat at 55 °C overnight. Aromatization achieved with 2 mL of MeOH. The crude reaction was concentrated under reduced pressure and purified via flash column chromatography (SiO_2, eluting with 1:9 EtOAc:petroleum ether → 3:7 EtOAc:petroleum ether), yielding a mixture of **23-*para*** and **23-*meta*** as a pale orange (minor isomer assigned by analogy to **22-*meta***). **Yield**: 0.520 g, 2.13 mmol, 71%, *para*:*meta* = 6:1 (determined by ^{1}H NMR); **R_f**: 0.40 (3:7 EtOAc:petroleum ether).

Methyl 2,5-dihydroxy-[1,1'-biphenyl]-4-carboxylate (23-*para*)

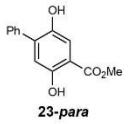

23-*para*

Spectroscopic data matched those previously reported in the literature.[21] **^{1}H NMR** (500 MHz, $CDCl_3$, mixture of two orientational isomers – minor isomer omitted for clarity): δ 10.30 (s, 1H), 7.51–7.46 (m, 5H), 7.43 (s, 1H), 6.91 (s, 1H), 4.82 (br s, 1H), 3.96 (s, 3H) ppm.

Synthesis of Benzyne Precursors

2-Iodoestrone

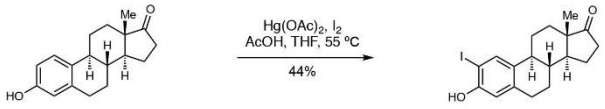

estrone 2-iodoestrone

Prepared according to a modification of the procedure reported by Potter.[22] To a 250 mL round-bottom flask open to air and equipped with a stir bar was added estrone (2.00 g, 7.40 mmol, 1.00 mol. equiv.), acetic acid (113 mL) and tetrahydrofuran (56.9 mL). The mixture was heated to 55 °C, and mercuric acetate (1.18 g, 3.70 mmol, 0.500 mol. equiv.) was added. The reaction was stirred at this temperature for 15 minutes and iodine (1.88 g, 7.40 mmol, 1.00 mol. equiv.) was added. The flask was cooled to room temperature and stirred for a further two hours before being concentrated under reduced pressure. The crude mixture was diluted with EtOAc and a solution of 5% aqueous potassium iodide (100 mL) was added. The organic later was separated and washed with saturated aqueous sodium thiosulfate, brine, dried over $MgSO_4$, filtered, and concentrated under reduced pressure. Purification via flash column chromatography (SiO_2, eluting with CH_2Cl_2) yielded pure 2-iodoestrone. **Yield**: 1.32 g, 4.74 mmol, 44%; Spectroscopic data matched those previously reported in the literature.[22] **Appearance**: White crystalline solid; **R*f***: 0.33 (CH_2Cl_2); **^{1}H NMR** (500 MHz, $CDCl_3$): δ 7.52 (s, 1H), 6.73 (s, 1H), 5.21 (s, 1H), 2.88–2.79 (m, 2H), 2.51 (dd, *J* = 19.1, 8.8 Hz, 1H), 2.37–2.29 (m, 1H), 2.25–2.10 (m, 2H), 2.09–1.92 (m, 3H), 1.67–1.35 (m, 6H), 0.91 (s, 3H) ppm.

Triflation Summary

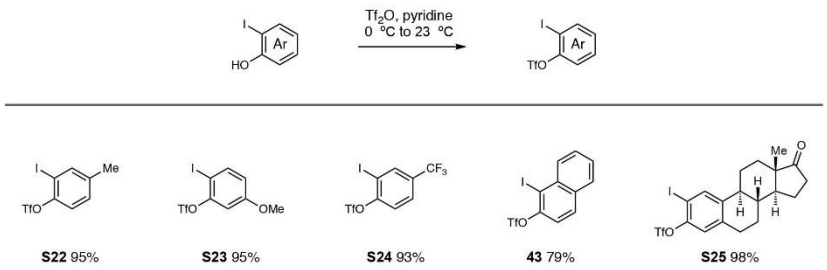

Note: 2-Iodo-4-methylphenyl trifluoromethanesulfonate was obtained from a commercial supplier.

General Procedure

To an oven-dried two-neck round-bottom flask equipped with a stir bar was added the appropriate *ortho*-iodophenol (1.00 mol. equiv.), and anhydrous pyridine (0.500 M). The reaction flask was cooled to 0 ºC and trifluoromethanesulfonic anhydride (1.25 mol. equiv.) was added dropwise. After stirring for 10 minutes the reaction was allowed to warm to room temperature and left to stir overnight. The reaction mixture was diluted with EtOAc, washed with water, 10% aqueous HCl (2×), saturated aqueous $NaHCO_3$, brine, dried over $MgSO_4$, filtered, and concentrated under reduced pressure. Purification via flash column chromatography, according to the specified conditions, yielded the corresponding triflate.

Characterization Data

2-Iodo-4-methylphenyl trifluoromethanesulfonate (S22)

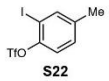

S22

Synthesized from 2-iodo-4-methylphenol. Purified via flash column chromatography (SiO_2, eluting with petroleum ether → 5:95 EtOAc:petroleum ether). **Yield**: 1.49 g, 4.07 mmol, 95%; Spectroscopic data matched those previously reported in the literature.[23]

Appearance: Colorless oil; **R_f**: 0.29 (petroleum ether); **^{1}H NMR** (500 MHz, $CDCl_3$): δ 7.72 (s, 1H), 7.22–7.17 (m, 2H), 2.35 (s, 3H) ppm.

2-Iodo-5-methoxyphenyl trifluoromethanesulfonate (S23)

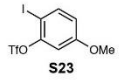

S23

Synthesized from 2-iodo-5-methoxyphenol. Purified via flash column chromatography (SiO_2, eluting with petroleum ether → 1:9 EtOAc:petroleum ether). **Yield**: 0.856 g, 2.25 mmol, 95%; **Appearance**: Yellow oil; **R_f**: 0.30 (5:95 EtOAc:petroleum ether); **^{1}H NMR** [600 MHz, $(CD_3)_2CO$]: δ 7.89 (d, J = 8.8 Hz, 1H), 7.03 (d, J = 2.7 Hz, 1H), 6.92 (dd, J = 8.8, 2.7 Hz, 1H), 3.88 (s, 3H) ppm; **^{13}C NMR** [150 MHz, $(CD_3)_2CO$]: δ 162.2, 151.7, 141.6, 119.62 (q, J = 319.7 Hz), 117.1, 109.6, 77.6, 56.5 ppm; **^{19}F NMR** [470 MHz, $(CD_3)_2CO$]: δ –74.5 ppm; **IR**: 1596, 1482, 1426, 1212, 1139, 1047, 951, 827 cm^{-1}; **HRMS** (ESI): calculated for $[C_8H_6F_3IO_4S]^{\bullet+}$: 381.8978, found: 381.8978.

2-Iodo-4-(trifluoromethyl)phenyl trifluoromethanesulfonate (S24)

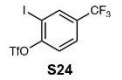

S24

Synthesized from 2-iodo-4-(trifluoromethyl)phenol. Purified via flash column chromatography (SiO_2, eluting with petroleum ether → 5:95 EtOAc:petroleum ether). **Yield**: 1.36 g, 3.01 mmol, 93%; Spectroscopic data matched those previously reported in the literature.[24] **Appearance**: Colorless oil; **R_f**: 0.29 (petroleum ether); **^{1}H NMR** (500 MHz, $CDCl_3$): δ 8.17 (s, 1H), 7.71 (d, J = 8.7 Hz, 1H), 7.45 (d, J = 8.6 Hz, 1H) ppm.

1-Iodonaphthalen-2-yl trifluoromethanesulfonate (43)

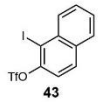

43

Synthesized from 1-iodonaphthalen-2-ol. Purified via flash column chromatography (SiO_2, eluting with petroleum ether → 1:9 EtOAc:petroleum ether). **Yield**: 0.644 g, 1.60 mmol, 79%; Spectroscopic data matched those previously reported in the literature.[25] **Appearance**: Yellow oil; **R_f**: 0.43 (2:98 EtOAc:petroleum ether); **^{1}H NMR** (500 MHz, $CDCl_3$): δ 8.24 (d, J = 8.5 Hz, 1H), 7.91 (d, J = 9.0 Hz, 1H), 7.85 (d, J = 8.1 Hz, 1H), 7.67 (t, J = 7.7 Hz, 1H), 7.63–7.58 (m, 1H), 7.42 (d, J = 9.0 Hz, 1H) ppm.

Estrone-derived keto-triflate S25

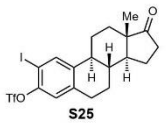

S25

Synthesized from 2-iodoestrone (see synthesis above). Purified via flash column chromatography (SiO_2, eluting with 1:9 EtOAc:petroleum ether → 2:8 EtOAc:petroleum ether). **Yield**: 0.725 g, 1.37 mmol, 98%; **Appearance**: Sticky white solid; **R*f***: 0.32 (1:4 EtOAc:petroleum ether); **^{1}H NMR** (500 MHz, $CDCl_3$): δ 7.74 (s, 1H), 7.01 (s, 1H), 2.91–2.85 (m, 2H), 2.49 (dd, *J* = 19.0, 8.8 Hz, 1H), 2.38–2.31 (m, 1H), 2.25 (td, *J* = 10.9, 4.3 Hz, 1H), 2.18–2.00 (m, 3H), 1.97 (d, *J* = 12.5 Hz, 1H), 1.67–1.38 (m, 6H), 0.90 (s, 3H) ppm; **^{13}C NMR** (125 MHz, $CDCl_3$): δ 220.1, 148.1, 142.3, 139.6, 137.7, 122.0, 118.8 (q, *J* = 320.7 Hz), 85.0, 50.4, 47.8, 43.8, 37.6, 35.8, 31.5, 29.2, 25.9, 25.7, 21.6, 13.8 ppm; **^{19}F NMR** (470 MHz, $CDCl_3$): δ –73.1 ppm; **IR**: 2932, 2864, 1737, 1475, 1422, 1245, 1207, 1136, 936, 921, 899, 834, 728 cm^{-1}; **HRMS** (ESI): calculated for $[C_{19}H_{20}F_3IO_4S+H]^+$: 529.0152, found: 529.0153; **[α]$_D^{22}$**: +94.6 (c = 0.14, $CHCl_3$).

Estrone-derived ketal S26

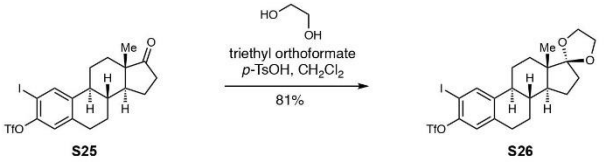

S25 **S26**

Prepared according to a modification of the procedure reported by Chen.[26] To a 100 mL round-bottom flask open to air and equipped with a stir bar was added ketone **S25** (1.75 g, 3.31 mmol, 1.00 mol. equiv.), ethylene glycol (22.3 mL, 397 mmol, 120 mol. equiv.), triethyl orthoformate (4.41 mL, 26.5 mmol, 8.00 mol. equiv.) and *para*-toluenesulfonic acid (158 mg, 0.828 mmol, 0.25 mol. equiv.). The reaction was sealed and stirred at room temperature for 24 hours by which time ^{1}H NMR analysis indicated the complete consumption of ketone **S25**. The reaction was quenched with saturated aqueous sodium bicarbonate and diluted with CH_2Cl_2. The layers were separated, and the aqueous layer washed with CH_2Cl_2. The combined organics were washed with brine, dried over $MgSO_4$, filtered, concentrated under reduced pressure, and then co-evaporated with PhMe (3×). Purification via flash column chromatography (SiO_2, eluting with 1:9 EtOAc:petroleum) yielded estrone-derived ketal **S26**. **Yield**: 1.54 g, 2.69 mmol, 81%; **Appearance**: Sticky white

solid; $\mathbf{R}_f$: 0.36 (1:9 EtOAc:petroleum ether); **^{1}H NMR** (500 MHz, $CDCl_3$): δ 7.72 (s, 1H), 6.98 (s, 1H), 3.96–3.84 (m, 4H), 2.85–2.78 (m, 2H), 2.27–2.16 (m, 2H), 2.04–1.97 (m, 1H), 1.93–1.88 (m, 1H), 1.86–1.79 (m, 1H), 1.78–1.71 (m, 2H), 1.64–1.57 (m, 1H), 1.56–1.28 (m, 5H), 0.85 (s, 3H) ppm; **^{13}C NMR** (125 MHz, $CDCl_3$): δ 148.0, 143.1, 134.0, 137.7, 122.0, 119.3, 118.9 (q, J = 320.7 Hz), 84. 9, 65.4, 64.7, 49.4, 46.1, 43.6, 38.3, 34.3, 30.6, 29.4, 26.5, 26.0, 22.4, 14.4 ppm; **^{19}F NMR** (470 MHz, $CDCl_3$): δ –73.1 ppm; **IR**: 2941, 2867, 1475, 1419, 1207, 1161, 1136, 1108, 918, 890, 852, 827, 784 cm^{-1}; **HRMS** (ESI): calculated for $[C_{21}H_{24}F_3IO_5S+H]^+$: 573.0414, found: 573.0411. **$[\alpha]_D^{25}$**: +32.8 (c = 1.0, $CHCl_3$).

2-Iodo-3-methoxyphenyl trifluoromethanesulfonate (S27)

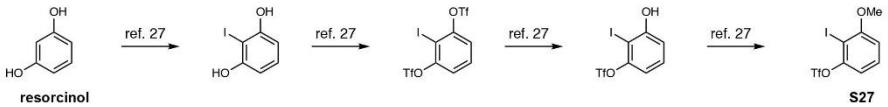

resorcinol **S27**

Prepared in four steps from resorcinol according to the procedure of Suzuki.[27]

Diels–Alder Reaction Scope

Dimethyl Acetylenedicarboxylate (DMAD) as Dienophile

Summary

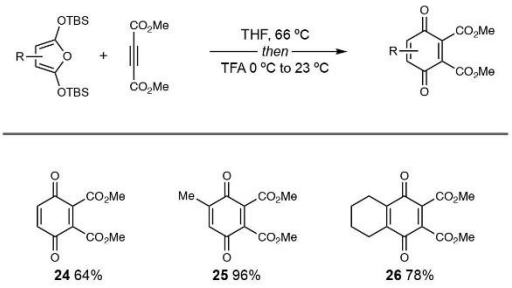

General Procedure

To a round-bottom flask equipped with a stir bar and under nitrogen was added the appropriate furan (2.00 mol. equiv.), dimethyl acetylenedicarboxylate (1.00 mol. equiv.), and anhydrous THF (0.500 M). The reaction mixture was heated at 66 °C until ^{1}H NMR analysis indicated the reaction had reached completion. The mixture was cooled to 0 °C and TFA (20.0 mol. equiv.) was added. The reaction was allowed to warm to room temperature and stirred for 1 h. The resulting solution was concentrated under reduced pressure and purified via flash column chromatography (eluting with PhMe → 1:9 EtOAc:PhMe) to yield the corresponding *para*-benzoquinone.

Dimethyl 3,6-dioxocyclohexa-1,4-diene-1,2-dicarboxylate (24)

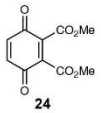

24

Synthesized from 2,5-bis((*tert*-butyldimethylsilyl)oxy)furan (**3**) (2.24 g, 6.81 mmol, 2.00 mol. equiv.), and dimethyl acetylenedicarboxylate (484 mg, 3.40 mmol, 1.00 mol. equiv.). **Yield**: 0.486 g, 2.17 mmol, 64%; Spectroscopic data matched those previously reported in the literature.[28] **Appearance**: Yellow solid; **R$_f$**: 0.36 (1:9 EtOAc:PhMe); **^{1}H NMR** (500 MHz, $CDCl_3$): δ 6.86 (s, 2H), 3.91 (s, 6H) ppm.

Dimethyl 4-methyl-3,6-dioxocyclohexa-1,4-diene-1,2-dicarboxylate (25)

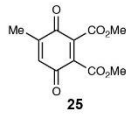

25

Synthesized from ((3-methylfuran-2,5-diyl)bis(oxy))bis(*tert*-butyldimethylsilane) (**48**) (1.37 g, 4.00 mmol, 2.00 mol. equiv.), and dimethyl acetylenedicarboxylate (284 mg, 2.00 mmol, 1.00 mol. equiv.). **Yield**: 0.458 g, 1.92 mmol, 96%; **Appearance**: Orange solid; **R*f***: 0.36 (1:19 EtOAc:PhMe); **M.p.**: 85–88 ºC; **^{1}H NMR** (500 MHz, $CDCl_3$): δ 6.69 (s, 1H), 3.90 (s, 3H), 3.89 (s, 3H), 2.11 (s, 3H) ppm; **^{13}C NMR** (125 MHz, $CDCl_3$): δ 183.9, 182.9, 162.7, 162.5, 146.2, 136.6, 135.9, 133.2, 53.4, 53.4, 16.0 ppm; **IR**: 1774, 1752, 1737, 1659, 1438, 1326, 1273, 1220, 1139, 1039, 974, 924, 902, 734 cm^{-1}; **HRMS** (ESI): calculated for $[C_{11}H_{10}O_6+H]^+$: 239.0550, found: 239.0558.

Dimethyl 1,4-dioxo-1,4,5,6,7,8-hexahydronaphthalene-2,3-dicarboxylate (26)

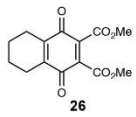

26

Synthesized from 1,3-bis((*tert*-butyldimethylsilyl)oxy)-4,5,6,7-tetrahydroisobenzofuran (**S16**) (1.06 g, 2.77 mmol, 2.00 mol. equiv.), and dimethyl acetylenedicarboxylate (197 mg, 1.38 mmol, 1.00 mol. equiv.). **Yield**: 0.302 g, 1.08 mmol, 78%; **Appearance**: Orange solid; **R*f***: 0.36 (1:19 EtOAc:PhMe); **M.p.**: 73–76 ºC; **^{1}H NMR** (500 MHz, $CDCl_3$): δ 3.89 (s, 6H), 2.49–2.42 (m, 4H), 1.74–1.68 (m, 4H) ppm; **^{13}C NMR** (125 MHz, $CDCl_3$): δ 183.2, 162.9, 143.0, 135.9, 53.3, 22.8, 20.9 ppm; **IR**: 2953, 1746, 1656, 1435, 1286, 1151, 1045, 958 cm^{-1}; **HRMS** (ESI): calculated for $[C_{14}H_{14}O_6+H]^+$: 279.0863, found: 279.0868.

Summary

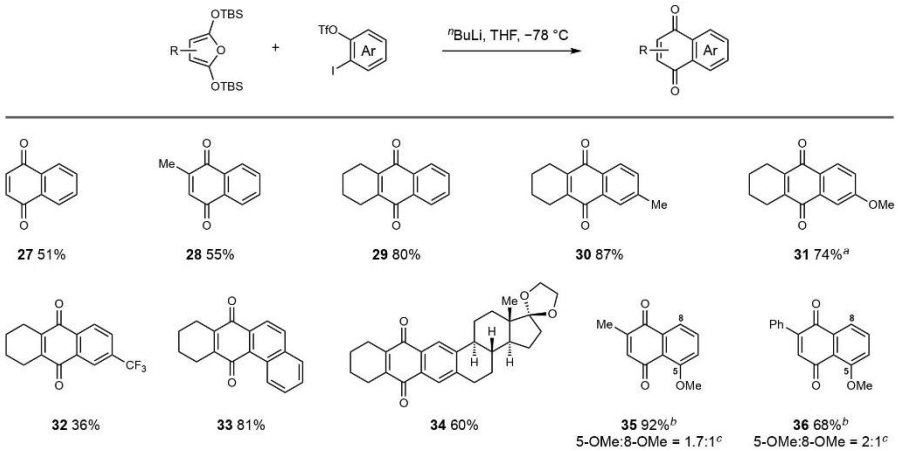

27 51% **28** 55% **29** 80% **30** 87% **31** 74%[a]

32 36% **33** 81% **34** 60% **35** 92%[b] 5-OMe:8-OMe = 1.7:1[c] **36** 68%[b] 5-OMe:8-OMe = 2:1[c]

[a] ^{1}H NMR yield
[b] Combined yield of isomers
[c] Determined by ^{1}H NMR

General Procedure

To a round-bottom flask equipped with a stir bar and under nitrogen was added the appropriate furan (2.00 mol. equiv.), the appropriate *ortho*-iodoaryl triflate (1.00 mol. equiv.), and anhydrous THF (0.500 M). The reaction mixture was cooled to –78 °C and ^{n}BuLi (2.5 M solution in THF, 2.00 mol. equiv.) was added dropwise over 5 minutes. The reaction was allowed to stir for an additional 10 minutes before being quenched with saturated aqueous NH_4Cl. The flask was warmed to room temperature and extracted with EtOAc (2×). The organics were combined and washed with 10% aqueous HCl (3×), saturated aqueous $NaHCO_3$, brine, dried over $MgSO_4$, filtered, and concentrated under reduced pressure. Purification via flash column chromatography according to the specified conditions yielded the corresponding *para*-benzoquinone.

Naphthalene-1,4-dione (27)


27

Synthesized from 2,5-bis((*tert*-butyldimethylsilyl)oxy)furan (**3**) (0.406 g, 1.24 mmol, 2.00 mol. equiv.), and 2-iodophenyl trifluoromethanesulfonate (0.218 g, 0.618 mmol, 1.00 mol. equiv.). Purified by flash chromatography (SiO_2, eluting with 1:1 CH_2Cl_2/petroleum ether → CH_2Cl_2). **Yield**: 0.049 g, 0.315 mmol, 51%; Spectroscopic data matched those previously reported in the literature.[29] **Appearance**: Yellow solid; **R*f***: 0.39 (1:9 EtOAc:petroleum ether); **^{1}H NMR** (500 MHz, $CDCl_3$): δ 8.09 (dd, *J* = 5.7, 3.3 Hz, 2H), 7.77 (dd, *J* = 5.8, 3.3 Hz, 2H), 6.99 (s, 2H) ppm.

2-Methylnaphthalene-1,4-dione (28)

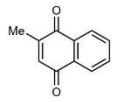
28

Synthesized from ((3-methylfuran-2,5-diyl)bis(oxy))bis(*tert*-butyldimethylsilane) (**48**) (0.400 g, 1.17 mmol, 2.00 mol. equiv.), and 2-iodophenyl trifluoromethanesulfonate (0.206 g, 0.585 mmol, 1.00 mol. equiv.). Purified by flash chromatography (eluting with petroleum ether → 3:2 EtOAc/petroleum ether). **Yield**: 0.0551 g, 0.320 mmol, 55%; Spectroscopic data matched those previously reported in the literature.[30] **Appearance**: Yellow solid; **R*f***: 0.33 (5:95 EtOAc:petroleum ether); **^{1}H NMR** (500 MHz, $CDCl_3$): δ 8.10 (dd, *J* = 5.8, 3.3 Hz, 1H), 8.06 (dd, *J* = 5.8, 3.3 Hz, 1H), 7.72 (dd, *J* = 5.7, 3.3 Hz, 2H), 6.84 (q, *J* = 1.3 Hz, 1H), 2.20 (d, *J* = 1.4 Hz, 4H) ppm.

1,2,3,4-Tetrahydroanthracene-9,10-dione (29)

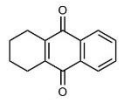
29

Synthesized from 1,3-bis((*tert*-butyldimethylsilyl)oxy)-4,5,6,7-tetrahydroisobenzofuran (**S16**) (0.236 g, 0.617 mmol, 2.00 mol. equiv.), and 2-iodophenyl trifluoromethanesulfonate (0.109 g, 0.309 mmol, 1.00 mol. equiv.). Purified by flash chromatography (SiO_2, eluting with 4:6 CH_2Cl_2/petroleum ether → 7:3 CH_2Cl_2/petroleum ether).**Yield**: 0.0521 g, 0.245 mmol, 80%; Spectroscopic data matched those previously reported in the literature. [31] **Appearance**: Yellow solid; **R*f***: 0.37 (1:19 EtOAc:petroleum ether); **^{1}H NMR** (500 MHz, $CDCl_3$): δ 8.08–8.03 (m, 2H), 7.70–7.65 (m, 2H), 2.61–2.57 (m, 4H), 1.77–1.73 (m, 4H) ppm.

6-Methyl-1,2,3,4-tetrahydroanthracene-9,10-dione (30)

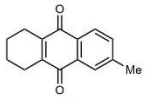

30

Synthesized from 1,3-bis((*tert*-butyldimethylsilyl)oxy)-4,5,6,7-tetrahydroisobenzofuran (**S16**) (0.442 g, 1.16 mmol, 2.00 mol. equiv.), and 2-iodo-4-methylphenyl trifluoromethanesulfonate (**S22**) (0.212 g, 0.578 mmol, 1.00 mol. equiv.). Purified by flash chromatography (SiO_2, eluting with petroleum ether → 1:1 CH_2Cl_2/petroleum ether). **Yield**: 0.113 g, 0.501 mmol, 87%; **Appearance**: Yellow solid; **M.p.**: 169–171 ºC; **R***f*: 0.36 (5:95 EtOAc:petroleum ether); **^{1}H NMR** (500 MHz, $CDCl_3$): δ 7.94 (d, *J* = 7.9 Hz, 1H), 7.84 (s, 1H), 7.46 (d, *J* = 7.9 Hz, 1H), 2.58 (p, *J* = 3.7 Hz, 4H), 2.47 (s, 3H), 1.74 (p, J = 3.6 Hz, 4H) ppm. **^{13}C NMR** (125 MHz, $CDCl_3$): δ 185.5, 185.1, 144.9, 144.7, 144.4, 134.2, 132.2, 130.1, 126.6, 126.5, 23.3 (2 coincident peaks), 21.6, 21.3 (2 coincident peaks) ppm; **IR**: 2938, 2869, 1655, 1601, 1300, 716 cm^{-1}; **HRMS** (ESI): calculated for $[C_{15}H_{14}O_2+H]^+$: 227.1067, found: 227.1069.

6-Methoxy-1,2,3,4-tetrahydroanthracene-9,10-dione (31)

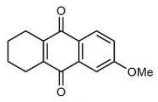

31

Synthesized from 1,3-bis((*tert*-butyldimethylsilyl)oxy)-4,5,6,7-tetrahydroisobenzofuran (**S16**) (0.406 g, 1.06 mmol, 2.00 mol. equiv.), and 2-iodo-5-methoxyphenyl trifluoromethanesulfonate (**S23**) (0.204 g, 0.533 mmol, 1.00 mol. equiv.). Purification by flash chromatography (SiO_2, eluting with petroleum ether → 7:3 CH_2Cl_2/petroleum ether) yielded **31** contaminated with an unknown silyl-containing impurity. For characterization purposes a pure sample was isolated via washing with petroleum ether and then Et_2O. **Yield** 74%, 0.395 mmol (following flash chromatography using 1,2-dichloroethane as an internal standard). **Appearance**: Yellow solid; **M.p.**: 163–165 ºC; **R***f*: 0.26 (5:95 EtOAc:petroleum ether); **^{1}H NMR** (500 MHz, $CDCl_3$): δ 8.01 (d, *J* = 8.6 Hz, 1H), 7.51 (d, *J* = 2.6 Hz, 1H), 7.14 (dd, *J* = 8.6, 2.6 Hz, 1H), 3.93 (s, 3H), 2.58 (s, 4H), 1.77–1.70 (m, 4H) ppm. **^{13}C NMR** (125 MHz, $CDCl_3$]): δ 185.2, 184.2, 163.9, 145.1, 144.4, 134.3, 128.7, 125.9, 119.9, 109.6, 56.0, 23.3, 23.3, 21.3, 21.3 ppm; **IR**: 2939, 1655, 1595, 1296 cm^{-1}; **HRMS** (ESI): calculated for $[C_{15}H_{14}O_3+H]^+$: 243.1016, found: 243.1019.

6-(Trifluoromethyl)-1,2,3,4-tetrahydroanthracene-9,10-dione (32)

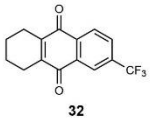
32

Synthesized from 1,3-bis((*tert*-butyldimethylsilyl)oxy)-4,5,6,7-tetrahydroisobenzofuran (**S16**) (0.400 g, 1.05 mmol, 2.00 mol. equiv.), and 2-iodo-4-(trifluoromethyl)phenyl trifluoromethanesulfonate (**S24**) (0.220 g, 0.524 mmol, 1.00 mol. equiv.). Purified by flash chromatography (SiO_2, eluting with 2:3 CH_2Cl_2/petroleum ether → 7:3 CH_2Cl_2/petroleum ether). **Yield**: 0.0533 g, 0.189 mmol, 36%; **Appearance**: Yellow solid; **M.p.**: 136–137 ºC; R_f: 0.44 (1:4 CH_2Cl_2:petroleum ether); **^{1}H NMR** (600 MHz, $CDCl_3$): δ 8.34 (s, 1H), 8.20 (d, *J* = 8.1 Hz, 1H), 7.93 (d, *J* = 8.0 Hz, 1H), 2.66–2.58 (m, 4H), 1.77 (p, *J* = 3.5 Hz, 4H) ppm. **^{13}C NMR** (150 MHz, $CDCl_3$): δ 184.0, 183.7, 145.7, 145.5, 135.2 (q, *J* = 33.6 Hz), 134.4, 132.7, 129.9 (q, *J* = 3.3 Hz), 127.1, 123.6 (q, *J* = 3.7 Hz), 123.4 (d, *J* = 273.2 Hz), 23.4, 23.4, 21.1 (2 coincident peaks) ppm; **^{19}F NMR** (470 MHz, $CDCl_3$): δ −63.2 ppm; **IR**: 2942, 2876, 1661, 1276, 1258, 1163, 1130 cm^{-1}; **HRMS** (ESI): calculated for $[C_{15}H_{11}F_3O_2+H]^+$: 281.0784, found: 281.0789.

8,9,10,11-Tetrahydrotetraphene-7,12-dione (33)

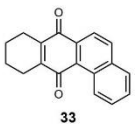
33

Synthesized from 1,3-bis((*tert*-butyldimethylsilyl)oxy)-4,5,6,7-tetrahydroisobenzofuran (**S16**) (0.475 g, 1.24 mmol, 2.00 mol. equiv.), and 1-iodonaphthalen-2-yl trifluoromethanesulfonate (**43**) (0.250 g, 0.622 mmol, 1.00 mol. equiv.). Purified by flash chromatography (SiO_2, eluting with petroleum ether → 3:2 CH_2Cl_2/petroleum ether). **Yield**: 0.132 g, 0.504 mmol, 81%; **Appearance**: Orange solid; **M.p.**: 139–140 ºC; R_f: 0.34 (5:95 EtOAc:petroleum ether); **^{1}H NMR** (500 MHz, $CDCl_3$): δ 9.55 (d, *J* = 8.8 Hz, 1H), 8.18 (d, *J* = 8.5 Hz, 1H), 8.12 (d, *J* = 8.5 Hz, 1H), 7.88 (d, *J* = 8.1 Hz, 1H), 7.70 (t, *J* = 7.8 Hz, 1H), 7.61 (t, *J* = 7.5 Hz, 1H), 2.68–2.59 (m, 4H), 1.83–1.73 (m, *J* = 6.2 Hz, 4H) ppm. **^{13}C NMR** (125 MHz, $CDCl_3$): δ 188.4, 186.0, 146.3, 142.2, 136.5, 134.6, 132.5, 130.1, 129.8, 128.8, 128.4, 128.2, 127.7, 122.0, 23.5, 22.8, 21.5, 21.2 ppm; **IR**: 2937, 1649, 1301, 761 cm^{-1}; **HRMS** (ESI): calculated for $[C_{18}H_{14}O_2+H]^+$: 263.1067, found: 263.1069.

Estrone-derived *para*-benzoquinone 34

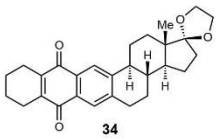
34

Synthesized from 1,3-bis((*tert*-butyldimethylsilyl)oxy)-4,5,6,7-tetrahydroisobenzofuran (**S16**) (0.284 g, 0.741 mmol, 2.00 mol. equiv.), and estrone-derived triflate **S25** (0.212 g, 0.371 mmol, 1.00 mol. equiv.). Purified by flash chromatography (eluting with CH_2Cl_2). **Yield**: 0.0962 g, 0.222 mmol, 60%; **Appearance**: Yellow solid; **M.p.**: 126 ºC; **R*f***: 0.24 (CH_2Cl_2); **^{1}H NMR** (500 MHz, $CDCl_3$): δ 7.91 (s, 1H), 7.67 (s, 1H), 3.97–3.85 (m, 4H), 3.00–2.86 (m, 2H), 2.53 (s, 4H), 2.49–2.41 (m, 1H), 2.31–2.24 (m, 1H), 2.06–1.97 (m, 1H), 1.97–1.90 (m, 1H), 1.87–1.74 (m, 3H), 1.71 (s, 4H), 1.67–1.48 (m, 3H), 1.46–1.28 (m, 3H), 0.87 (s, 3H) ppm; **^{13}C NMR** (125 MHz, $CDCl_3$): δ 185.3 (2 coincident peaks), 146.8, 144.8, 144.6, 143.4, 129.8, 129.7, 126.7, 123.4, 119.3, 65.4, 64.7, 49.6, 46.1, 44.5, 38.4, 34.3, 30.7, 29.9, 26.5, 25.9, 23.3, 23.2, 22.4, 21.3, 21.3, 14.4 ppm; **IR**: 2938, 2870, 1656, 1621, 1600, 1329, 1298, 1179, 1101, 1042, 912, 728 cm^{-1}; **HRMS** (ESI): calculated for $[C_{28}H_{32}O_4+H]^+$: 433.2373, found: 433.2371. **[α]$_D^{19}$**: +62.2 (c = 0.18, $CHCl_3$).

5-Methoxy-2-methylnaphthalene-1,4-dione (35-*5-OMe*) and 8-methoxy-2-methylnaphthalene-1,4-dione (35-*8-OMe*)

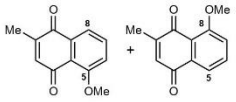
35-*5-OMe* **35**-*8-OMe*

Synthesized from ((3-methylfuran-2,5-diyl)bis(oxy))bis(*tert*-butyldimethylsilane) (**48**) (0.468 g, 1.37 mmol, 2.00 mol. equiv.), and 2-iodo-3-methoxyphenyl trifluoromethanesulfonate (**S27**) (0.261 g, 0.683 mmol, 1.00 mol. equiv.), yielding a mixture of **35**-*5-OMe* and **35**-*8-OMe*. **Yield**: 0.127 g, 0.630 mmol, 92%, **35**-*5-OMe*:**35**-*8-OMe* = 1.7:1 (determined by ^{1}H NMR). For characterization purposes a small amount of each isomer was isolated via flash chromatography using the conditions described above.

5-Methoxy-2-methylnaphthalene-1,4-dione (35-*5-OMe*)

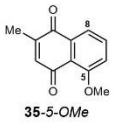
35-*5-OMe*

Spectroscopic data matched those previously reported in the literature.[32] **Appearance**: Yellow/orange solid; **R*f***: 0.27 (2:3 EtOAc:petroleum ether); **^{1}H NMR** (500 MHz, $CDCl_3$): δ 7.72 (d, *J* = 7.7 Hz, 1H), 7.63 (t, *J* = 8.0 Hz, 1H), 7.26 (d, *J* = 8.4 Hz, 1H), 6.71 (s, 1H), 3.98 (s, 3H), 2.11 (s, 3H) ppm.

8-Methoxy-2-methylnaphthalene-1,4-dione (35-*8-OMe*)

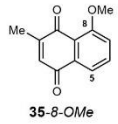

35-*8-OMe*

Spectroscopic data matched those previously reported in the literature. [33] **Appearance**: Yellow solid; **R*f***: 0.31 (2:3 EtOAc:petroleum ether); **^{1}H NMR** (500 MHz, $CDCl_3$): δ 7.71 (d, *J* = 7.6 Hz, 1H), 7.65 (t, *J* = 8.0 Hz, 1H), 7.28 (d, *J* = 8.3 Hz, 1H), 6.76 (d, *J* = 1.4 Hz, 1H), 4.00 (s, 3H), 2.16 (d, *J* = 1.4 Hz, 3H) ppm.

5-Methoxy-2-phenylnaphthalene-1,4-dione (36-*5-OMe*) and 8-methoxy-2-phenylnaphthalene-1,4-dione (36-*8-OMe*)

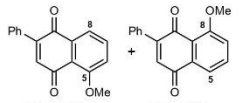

36-*5-OMe* **36**-*8-OMe*

Synthesized from ((3-phenylfuran-2,5-diyl)bis(oxy))bis(*tert*-butyldimethylsilane) (**S14**) (0.627 g, 1.55 mmol, 2.00 mol. equiv.), and 2-iodo-3-methoxyphenyl trifluoromethanesulfonate (**S27**) (0.296 g, 0.775 mmol, 1.00 mol. equiv.), yielding a mixture of **36**-*5-OMe* and **36**-*8-OMe*. **Yield**: 0.139 g, 0.525 mmol, 68%, **36**-*5-OMe*:**36**-*8-OMe* = 2:1 (determined by ^{1}H NMR). For characterization purposes a small amount of each isomer was isolated via flash chromatography using the conditions described above.

5-Methoxy-2-phenylnaphthalene-1,4-dione (36-*5-OMe*)

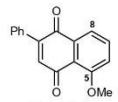

36-*5-OMe*

Spectroscopic data matched those previously reported in the literature.[32] **Appearance**: Yellow/orange solid; **R*f***: 0.31 (CH_2Cl_2); **^{1}H NMR** (500 MHz, $CDCl_3$): δ 7.84 (d, *J* = 7.7 Hz, 1H), 7.71 (t, *J* = 8.1 Hz, 1H), 7.60–7.54 (m, 2H), 7.49–7.43 (m, 3H), 7.33 (d, *J* = 8.5 Hz, 1H), 7.00 (s, 1H), 4.04 (s, 3H) ppm.

8-Methoxy-2-phenylnaphthalene-1,4-dione (36-*8-OMe*)

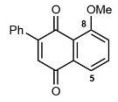

36-*8-OMe*

Spectroscopic data matched those previously reported in the literature. [34] **Appearance**: Yellow solid; **R*f***: 0.40 (CH_2Cl_2); **^{1}H NMR** (500 MHz, $CDCl_3$): δ 7.77 (d, *J* = 7.6 Hz, 1H), 7.70 (t, *J* = 8.0 Hz, 1H), 7.57–7.53 (m, 2H), 7.46–7.42 (m, 3H), 7.33 (d, *J* = 8.4 Hz, 1H), 6.99 (s, 1H), 4.02 (s, 3H) ppm.

Synthesis

N-(para-Methoxyphenyl)pyrrole 37

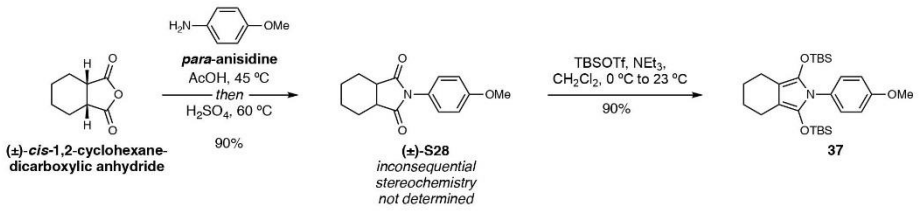

Prepared in two steps from 1,2-cyclohexanedicarboxylic anhydride. The synthesis of cyclic imide **(±)-S28** was conducted according to a modification of the procedure reported by Patil.[35]

Cyclic imide (±)-S28

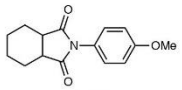

(±)-S28
inconsequential stereochemistry not determined

To a round-bottom flask equipped with a stir bar was added *para*-anisidine (0.477 g, 3.87 mmol, 1.00 mol. equiv.), 1,2-cyclohexanedicarboxylic anhydride (predominantly *cis*) (0.656 g, 4.26 mmol, 1.10 mol. equiv.), and acetic acid (30 mL). The reaction mixture was heated to 45 °C for 10 minutes before addition of concentrated H_2SO_4 (1.04 mL, 19.3 mmol, 5.00 mol. equiv.). The solution was heated to 60 °C for 1 hour, cooled to room temperature and poured over crushed ice. The solid was collected by vacuum filtration, washed with saturated aqueous $NaHCO_3$ and brine. The solid was dissolved in CH_2Cl_2, dried over $MgSO_4$, filtered and concentrated under reduced pressure. **Yield**: 0.907 g, 3.50 mmol, 90%; **M.p.**: 162.8–164.8 ºC; **Appearance**: Off-white solid; **R_f**: 0.35 (CH_2Cl_2); **^{1}H NMR** (500 MHz, $CDCl_3$): δ 7.20–7.16 (m, 2H), 6.99–6.95 (m, 2H), 3.81 (s, 4H), 3.04–2.97 (m, 2H), 1.98–1.82 (m, 5H), 1.55–1.46 (m, 5H) ppm; **^{13}C NMR** (125 MHz, $CDCl_3$): δ 179.0, 159.5, 127.6, 124.9, 114.6, 55.6, 40.2, 24.1, 21.9 ppm; **IR**: 3467, 2949, 2929, 2859, 1704, 1607, 1509, 1448, 1383, 1307, 1298, 1249, 1184, 1164, 1131. 1112, 1084, 1025, 887, 843, 828, 820, 806 cm^{-1}; **HRMS** (ESI): calculated for $[C_{15}H_{17}NO_3+H]^+$: 260.1281, found: 260.1286.

***N-(para*-Methoxyphenyl)pyrrole 37**

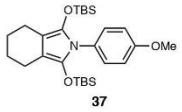

37

To an oven-dried round-bottom flask equipped with a stir bar and under nitrogen was added cyclic imide **(±)-S28** (1.18 g, 4.57 mmol, 1.00 mol. equiv.). Following addition of anhydrous CH_2Cl_2 (18 mL, 0.25 M) the resulting suspension was cooled to 0 ºC, and anhydrous triethylamine (1.91 mL, 13.7 mmol, 3.00 mol. equiv.) was added. After stirring for 10 minutes *tert*-butyldimethylsilyl trifluoromethanesulfonate (2.31 mL, 10.0 mmol, 2.20 mol. equiv.) was added dropwise, and the reaction mixture was allowed to warm to room temperature. The reaction was stirred vigorously overnight, yielding a biphasic mixture. The solution was filtered through a phosphate buffered silica (pH 7) plug, eluting with Et_2O, and used without further purification. **Yield**: 2.00 g, 4.10 mmol, 90%; **Appearance**: Yellow oil; **R*f***: N/A (unstable on silica); **^{1}H NMR** (500 MHz, $CDCl_3$): δ 7.21–7.16 (m, 2H), 6.89–6.84 (m, 2H), 3.81 (s, 3H), 2.46–2.41 (m, 4H), 1.70–1.65 (m, 4H), 0.77 (s, 18H), –0.20 (s, 12H) ppm; **^{13}C NMR** (150 MHz, $CDCl_3$): δ 158.2, 129.7, 129.6, 129.1, 113.7, 96.2, 55.7, 25.7, 24.3, 21.8, 18.1, –4.4 ppm; **IR**: 3299, 2930, 2856, 1699, 1619, 1585, 1514, 1464, 1366, 1247, 1060, 919, 835, 809, 782 cm^{-1}; **HRMS** (ESI): calculated for $[C_{27}H_{45}NO_3Si_2+H]^+$: 488.3011, found: 488.2989.

Note: Attempts to purify *N-(para*-methoxyphenyl)pyrrole **37** by flash chromatography, using either untreated (i.e. acidic) silica, or phosphate buffered silica (pH 7), resulted in reversion to cyclic imide **(±)-S28**.

***N*-Methylpyrrole 38**

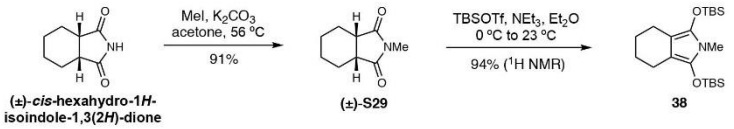

Prepared in two steps from (±)-*cis*-hexahydro-1*H*-isoindole-1,3(2*H*)-dione. The synthesis of cyclic imide **(±)-S29** was conducted according to a modification of the procedure reported by Marson.[36]

Cyclic imide (±)-S29


(±)-S29

To an oven-dried round-bottom flask equipped with a stir bar and under nitrogen was added (±)-*cis*-hexahydro-1*H*-isoindole-1,3(2*H*)-dione (4.01 g, 26.17 mmol, 1.00 mol. equiv.), anhydrous acetone (52.4 mL, 0.50 M), potassium carbonate (4.34 g, 31.4 mmol, 1.2 mol. equiv.) and methyl iodide (1.79 mL, 28.8 mmol, 1.1 mol. equiv.). The resulting solution was heated at reflux overnight. After cooling to room temperature, the reaction was filtered, concentrated under reduced pressure, and purified by flash chromatography (SiO_2, eluting with 3:7 EtOAc:petroleum ether). Spectroscopic data matched those previously reported in the literature.[37] **Yield**: 3.96 g, 23.7 mmol, 91%; **Appearance**: Pale-yellow crystalline solid; $\mathbf{R_f}$: 0.31 (3:7 EtOAc:petroleum ether); **^{1}H NMR** (500 MHz, $CDCl_3$): δ 2.94 (s, 3H), 2.82 (q, J = 8.0, 6.2 Hz, 2H), 1.88–1.79 (m, 2H), 1.75–1.67 (m, 2H), 1.47–1.35 (m, 4H) ppm.

***N*-Methylpyrrole 38**


38

To an oven-dried round-bottom flask equipped with a stir bar and under nitrogen was added cyclic imide **(±)-S29** (1.00 g, 5.98 mmol, 1.00 mol. equiv.). Following addition of anhydrous Et_2O (17.1 mL, 0.25 M) the resulting suspension was cooled to 0 °C, and anhydrous triethylamine (2.50 mL, 17.9 mmol, 3.00 mol. equiv.) was added. After stirring for 10 minutes *tert*-butyldimethylsilyl trifluoromethanesulfonate (3.02 mL, 13.2 mmol, 2.20 mol. equiv.) was added dropwise, and the reaction mixture was allowed to warm to room temperature. The reaction was stirred vigorously overnight, yielding a biphasic mixture. The solution was filtered through Celite, eluting with Et_2O, and used without further purification. **Yield**: 5.62 mmol,

94% (by ^{1}H NMR using 1,2-dichloroethane as an internal standard); **Appearance**: Yellow oil; **R_f**: N/A (unstable on silica); **^{1}H NMR** (500 MHz, $CDCl_3$): δ 3.14 (s, 3H), 2.41–2.36 (m, 4H), 1.64–1.60 (m, 4H), 1.00 (s, 18H), 0.17 (s, 12H) ppm; **^{13}C NMR** (125 MHz, $CDCl_3$): δ 129.1, 95.2, 27.2, 25.9, 24.3, 21.8, 18.3, –3.91 ppm; **IR**: 2954, 2930, 2858, 1701, 1611, 1581, 1472, 1463, 1391, 1252, 1210, 1101, 1067, 1045, 909, 835, 780, 732 cm^{-1}; **HRMS** (ESI): calculated for $[C_{21}H_{41}NO_2Si_2+H]^+$: 396.2749, found: 396.2738.

Note: Attempts to purify *N*-methylpyrrole **38** by flash chromatography, using either untreated (i.e. acidic) silica, or phosphate buffered silica (pH 7), resulted in decomposition.

10-((4-Methoxyphenyl)amino)-1,2,3,4-tetrahydroanthracen-9-ol (41)

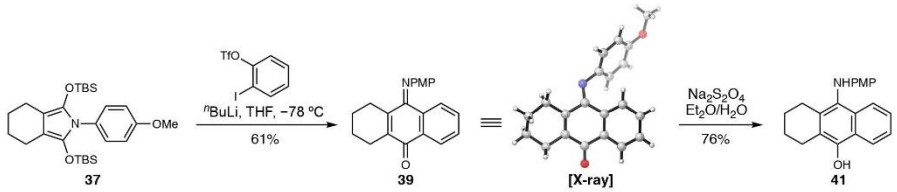

Prepared in two steps from *N-(para*-methoxyphenyl)pyrrole **37**.

10-((4-Methoxyphenyl)imino)-1,2,3,4-tetrahydroanthracen-9(10*H*)-one (39)

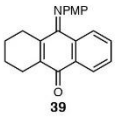

To a round-bottom flask equipped with a stir bar and under nitrogen was added *N-(para*-methoxyphenyl)pyrrole **37** (0.910 g, 1.86 mmol, 3.00 mol. equiv.), 2-iodophenyl trifluoromethanesulfonate (0.219 g, 0.621 mmol, 1.00 mol. equiv.), and anhydrous THF (1.24 mL, 0.500 M). The reaction mixture was cooled to −78 ºC and ^{n}BuLi (1.07 mL, 1.86 mmol, 3 mol. equiv., 1.75 M solution in THF) was added dropwise over 5 minutes. The reaction was allowed to stir for an additional 10 minutes before being quenched with saturated aqueous NH_4Cl. The flask was warmed to room temperature and extracted with EtOAc (2×). The organics were combined and washed with brine (2×), dried over $MgSO_4$, filtered, and concentrated under reduced pressure. The crude mixture was co-evaporated with methanol (3×) and purified by flash chromatography (SiO_2, eluting with petroleum ether → 1:19 EtOAc/petroleum ether). **Yield**: 0.120 g, 0.377 mmol, 61%; Recrystallization of pure **39** via the slow evaporation of hexane yielded red needle-like crystals suitable for X-Ray analysis. **Appearance**: Red oil (after chromatography); $\mathbf{R}_f$: 0.37 (1:9 EtOAc:petroleum ether); **^{1}H NMR** (500 MHz, $CDCl_3$): δ 8.10 (d, J = 7.7 Hz, 1H), 7.44–7.38 (m, 1H), 7.17 (d, J = 3.2 Hz, 2H), 6.88 (d, J = 8.7 Hz, 2H), 6.72 (d, J = 8.5 Hz, 2H), 3.82 (s, 3H), 2.83 (s, 2H), 2.61 (s, 2H), 1.77 (s, 4H) ppm. **^{13}C NMR** (150 MHz, $CDCl_3$): δ 185.3, 156.8, 156.2, 149.9, 145.3, 138.4, 133.0, 130.9, 130.3, 129.7, 128.4, 126.9, 119.8, 115.0, 55.6, 26.1, 23.2, 22.1, 21.6 ppm; **IR**: 3069, 2935, 2860, 2834, 1647, 1596, 1498, 1459, 1385, 1293, 1239, 1175, 1034, 911, 842, 832, 776, 698, 672 cm^{-1}; **HRMS** (ESI): calculated for $[C_{21}H_{19}NO_2+H]^{+}$: 318.1489, found: 318.1491.

10-((4-Methoxyphenyl)amino)-1,2,3,4-tetrahydroanthracen-9-ol (41)

41

To a round-bottom flask open to air and equipped with a stir bar was added *para*-iminoquinone **39** (0.0754 g, 0.238 mmol, 1.00 mol. equiv.), Et_2O (2.38 mL, 0.1 M) and saturated aqueous sodium dithionite (7.13 mL). The solution was stirred vigorously for 2 hours, then was extracted with Et_2O (3×), dried over $MgSO_4$, filtered and concentrated. The crude mixture was purified by flash chromatography (SiO_2, eluting with hexane → 1:9 EtOAc/hexane). **Yield**: 0.0574 g, 0.180 mmol, 76%; **Appearance**: Red oil; **R*f***: 0.37 (1:3 EtOAc:hexane); **^{1}H NMR** (600 MHz, $CDCl_3$): δ 8.15 (d, *J* = 8.3 Hz, 1H), 7.92 (d, *J* = 8.3 Hz, 1H), 7.42 (t, *J* = 7.5 Hz, 1H), 7.38 (t, *J* = 7.5 Hz, 1H), 6.72 (d, *J* = 8.9 Hz, 2H), 6.44 (d, *J* = 8.8 Hz, 2H), 5.19 (br s, 2H), 3.73 (s, 3H), 2.82 (*q*, J = 6.8 Hz, 4H), 1.92–1.85 (m, 2H), 1.81–1.74 (m, 2H) ppm. **^{13}C NMR** (125 MHz, $CDCl_3$): δ 152.4, 146.8, 141.9, 134.1, 130.9, 127.9, 126.0, 124.7, 123.4, 123.2, 121.3, 117.7, 115.0, 114.4, 55.9, 26.2, 23.6, 22.8, 22.6 ppm; **IR** 3388, 2933, 2861, 1590, 1507, 1450, 1378, 1287, 1231, 1179, 1100, 1055, 1032, 907, 820, 729 cm^{-1}; **HRMS** (ESI): calculated for $[C_{21}H_{21}NO_2+H]^+$: 320.1645, found: 320.1651.

Note: 10-((4-Methoxyphenyl)amino)-1,2,3,4-tetrahydroanthracen-9-ol (**41**) undergoes facile autoxidation in air, and should be stored under inert atmosphere.

10-(Methylamino)-1,2,3,4-tetrahydroanthracen-9-ol (42)

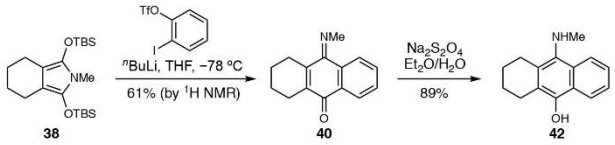

38 40 42

Prepared in two steps from *N*-methylpyrrole **38**.

10-(Methylimino)-1,2,3,4-tetrahydroanthracen-9(10*H*)-one (40)

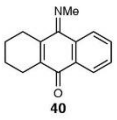

40

To a round-bottom flask equipped with a stir bar and under nitrogen was added *N*-methylpyrrole **38** (0.838 g, 2.12 mmol, 3.00 mol. equiv.), 2-iodophenyl trifluoromethanesulfonate (0.249 g, 1.04 mmol, 1.00 mol. equiv.), and anhydrous

THF (2.08 mL, 0.500 M). The reaction mixture was cooled to −78 °C and ^{n}BuLi (1.79 mL, 3.13 mmol, 3 mol. equiv., 1.75 M solution in THF) was added dropwise over 5 minutes. The reaction was stirred for an additional 10 minutes before being quenched with saturated aqueous NH_4Cl. The flask was warmed to room temperature and extracted with EtOAc (2×). The organics were combined and washed with brine (2×), dried over $MgSO_4$, filtered, and concentrated under reduced pressure. The crude mixture was co-evaporated with methanol (3×) to afford crude 10-(methylimino)-1,2,3,4-tetrahydroanthracen-9(10*H*)-one (**40**), which was used without further purification. **Yield**: 0.636 mmol, 61% (by ^{1}H NMR using 1,2-dichloroethane as an internal standard); **Appearance**: Yellow oil; $\mathbf{R}_f$: N/A (unstable on silica);

Note: Attempts to purify 10-(methylimino)-1,2,3,4-tetrahydroanthracen-9(10*H*)-one (**40**) by flash chromatography, using either untreated (i.e. acidic) silica, or phosphate buffered silica (pH 7), resulted in hydrolysis to 1,2,3,4-tetrahydroanthracene-9,10-dione (**29**). For characterization purposes a sample of 10-(methylamino)-1,2,3,4-tetrahydroanthracen-9-ol (**42**) was stirred in $CDCl_3$ for 4 hours (open to air), resulting in complete autoxidation to yield 10-(methylimino)-1,2,3,4-tetrahydroanthracen-9(10*H*)-one (**40**). **^{1}H NMR** (500 MHz, $CDCl_3$): 8.18 (d, J = 7.5 Hz, 1H), 7.80 (d, J = 7.6 Hz, 1H), 7.57 (p, J = 7.4 Hz, 2H), 3.91 (s, 3H), 2.71 (s, 2H), 2.53 (s, 2H), 1.73 (s, 4H) ppm. **^{13}C NMR** (125 MHz, $CDCl_3$): δ 185.4, 159.4, 151.1, 136.4, 133.0, 131.1, 130.2, 130.2, 128.1, 127.4, 43.5, 25.9, 22.9, 22.1, 21.7 ppm; **IR**: 3450, 2934, 2859, 1648, 1593, 1383, 1288, 1177, 842, 774, 701 cm^{-1}; **HRMS** (ESI): calculated for $[C_{25}H_{21}NO_2+H]^+$: 226.1226, found: 226.1223.

10-(methylamino)-1,2,3,4-tetrahydroanthracen-9-ol (42)

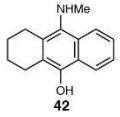

42

To a round-bottom flask open to air and equipped with a stir bar was added crude 10-(methylimino)-1,2,3,4-tetrahydroanthracen-9(10*H*)-one (**40**) (0.636 mmol), Et_2O (10.4 mL, 0.1 M) and saturated aqueous sodium dithionite (31.3 mL). The solution was stirred vigorously for 2 hours, then was extracted with Et_2O (3×), dried over $MgSO_4$, filtered and concentrated. The crude mixture was purified by flash chromatography (SiO_2, eluting with pentane → 1:1 Et_2O/pentane). **Yield**: 0.132 g, 0.581 mmol, 56%; **Appearance**: Brown oil;

R$_f$: 0.35 (2:5 Et_2O:pentane); **^{1}H NMR** (600 MHz, $CDCl_3$): 8.11 (d, J = 8.0 Hz, 1H), 8.06 (d, J = 8.2 Hz, 1H), 7.46–7.39 (m, 2H), 4.01, (br s, 2H), 2.88 (t, J = 6.0 Hz, 2H), 2.84 (s, 3H), 2.80 (t, J = 6.1 Hz, 2H), 1.90–1.84 (m, 4H) ppm. **^{13}C NMR** (150 MHz, $CDCl_3$): δ 144.7, 136.7, 127.9, 127.7, 125.3, 124.5, 123.4, 122.8, 121.4, 117.9, 37.2, 25.6, 23.8, 23.0, 22.6 ppm; **IR** 3369, 3067, 2932, 2858, 1647, 1591, 1448, 1380, 1289, 1211, 1061, 765 cm^{-1}; **HRMS** (ESI): calculated for $[C_{15}H_{17}NO+H]^+$: 228.1390, found: 228.1390.

Note: 10-(Methylamino)-1,2,3,4-tetrahydroanthracen-9-ol (**42**) undergoes facile autoxidation to **40** in air, and should be stored under inert atmosphere.

7-((4-methoxyphenyl)amino)-8,9,10,11-tetrahydrotetraphen-12-ol (44)

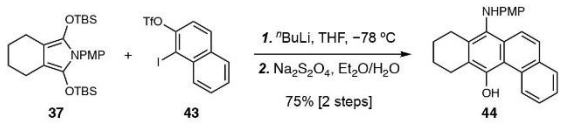

Prepared in two steps from *N-(para*-methoxyphenyl)pyrrole **37**.

7-((4-methoxyphenyl)amino)-8,9,10,11-tetrahydrotetraphen-12-ol (44)

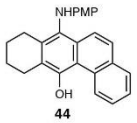

To a round-bottom flask equipped with a stir bar and under nitrogen was added *N-(para*-methoxyphenyl)pyrrole **37** (0.527 g, 1.08 mmol, 3.00 mol. equiv.), 1-iodonaphthalen-2-yl trifluoromethanesulfonate (**43**) (0.145 g, 0.361 mmol, 1.00 mol. equiv.), and anhydrous THF (0.72 mL, 0.500 M). The reaction mixture was cooled to −78 °C and ^{n}BuLi (0.618 mL, 1.08 mmol, 3.00 mol. equiv., 1.75 M solution in THF) was added dropwise over 5 minutes. The reaction was stirred for an additional 10 minutes before being quenched with saturated aqueous NH_4Cl. The flask was warmed to room temperature and extracted with EtOAc (2×). The organics were combined and washed with brine (2×), dried over $MgSO_4$, filtered, and concentrated under reduced pressure. The crude mixture was co-evaporated with methanol (3×) and purified by flash chromatography (SiO_2, eluting with hexane → 1:19 EtOAc/hexane), yielding 0.114 g of an inseparable mixture of 2 compounds (ratio of 3.6:1 by ^{1}H NMR, tentatively assigned as a mixture of the two possible *para*-iminoquinone regioisomers). **Appearance**: Red oil; **R**$_f$: 0.38

(1:9 EtOAc:petroleum ether). To a round-bottom flask open to air and equipped with a stir bar was added the mixture of *para*-iminoquinones (0.114 g), Et_2O (3.1 mL, 0.1 M) and saturated aqueous sodium dithionite (9.3 mL). The solution was stirred vigorously for 2 hours, then was extracted with Et_2O (3×), dried over $MgSO_4$, filtered and concentrated, yielding pure 7-((4-methoxyphenyl)amino)-8,9,10,11-tetrahydrotetraphen-12-ol (**44**). **Yield**: 0.0998 g, 0.270 mmol, 75%; **Appearance**: Red oil; **R_f**: 0.31 (3:7 Et_2O:pentane); **^{1}H NMR** (600 MHz, $CDCl_3$): δ 9.71 (d, *J* = 8.6 Hz, 1H), 7.92 (d, *J* = 9.1 Hz, 1H), 7.85 (d, *J* = 7.8 Hz, 1H), 7.65 (ddd, *J* = 8.5, 7.0, 1.5 Hz, 1H), 7.61 (d, *J* = 9.1 Hz, 1H), 7.57 (t, *J* = 7.4 Hz, 1H), 6.72 (d, *J* = 9.1 Hz, 2H), 6.42 (d, *J* = 8.9 Hz, 2H), 5.63 (br s, 1H), 5.13 (br s, 1H), 3.72 (s, 3H), 2.80 (q, *J* = 6.0 Hz, 4H), 1.96–1.90 (m, 2H), 1.81–1.74 (m, 2H) ppm; **^{13}C NMR** (150 MHz, $CDCl_3$): δ 152.3, 150.4, 141.9, 134.7, 132.6, 130.7, 130.6, 128.6, 128.5, 128.3, 127.7, 126.5, 125.8, 122.6, 120.4, 117.9, 115.0, 114.3, 55.8, 26.0, 23.6, 22.6, 22.4 ppm; **IR** 3562, 3393, 2933, 2861, 1507, 1448, 1342, 1310, 1231, 1200, 1180, 1108, 1038, 905, 819, 726 cm^{-1}; **HRMS** (ESI): calculated for $[C_{25}H_{23}NO_2+H]^+$: 370.1802, found: 370.1785.

Assignment of Regioselectivity:

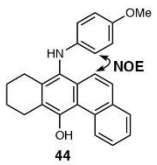

44

Summary

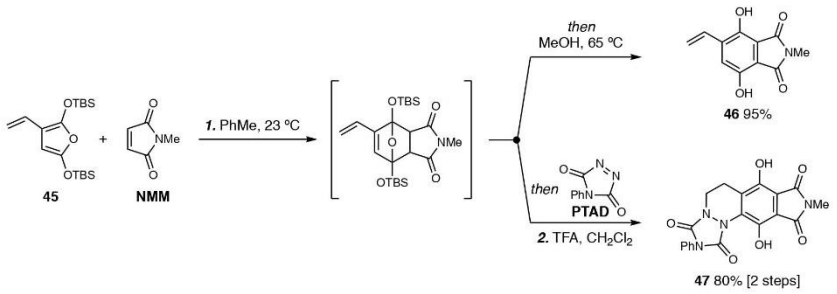

4,7-Dihydroxy-2-methyl-5-vinylisoindoline-1,3-dione (46)

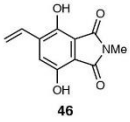

46

To a 10 mL Schlenk tube equipped with a stir bar and under a nitrogen atmosphere was added ((3-vinylfuran-2,5-diyl)bis(oxy))bis(*tert*-butyldimethylsilane) (**45**) (1.06 g, 3.00 mmol, 3.00 mol. equiv.), *N*-methylmaleimide (111.1 mg, 1.00 mmol, 1.00 mol. equiv.) and anhydrous PhMe (2 mL, 0.500 M). The flask was sealed and the reaction was stirred at room temperature overnight, by which time ^{1}H NMR analysis indicated complete consumption of *N*-methylmaleimide. Methanol (4 mL, 0.250 M) was added and the mixture was heated at 65 °C overnight. The reaction mixture cooled to room temperature, concentrated under reduced pressure, and purified via flash column chromatography (SiO_2, eluting with CH_2Cl_2), yielding pure 4,7-dihydroxy-2-methyl-5-vinylisoindoline-1,3-dione (**46**). **Yield**: 0.209 g, 0.952 mmol, 95%; **Appearance**: Yellow solid; **R$_f$**: 0.32 (1:39 EtOAc:CH_2Cl_2); **M.p.**: Degraded at 155 °C; **^{1}H NMR** (500 MHz, $CDCl_3$): δ 7.47 (br s, 1H), 7.19 (s, 1H), 6.94 (br s, 1H), 6.93 (dd, *J* = 17.7, 11.2 Hz, 1H), 5.97 (d, *J* = 17.7 Hz, 1H), 5.51 (d, *J* = 11.3 Hz, 1H), 3.12 (s, 3H) ppm; **^{13}C NMR** (125 MHz, $CDCl_3$): δ 167.0, 169.2, 148.2, 146.8, 135.7, 129.5, 121.9, 119.7, 113.1, 111.6, 23.7 ppm; **IR**: 3427, 1749, 1674, 1612, 1295, 1248, 1161, 1005, 933 cm^{-1}; **HRMS** (ESI): calculated for $[C_{11}H_9NO_4+H]^+$: 220.0604, found: 220.0602.

Tetrahydrocinnoline 47

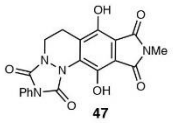

47

To a 10 mL round-bottom flask equipped with a stir bar and under nitrogen was added ((3-vinylfuran-2,5-diyl)bis(oxy))bis(*tert*-butyldimethylsilane) (**45**) (1.42 g, 4.00 mmol, 4.00 mol. equiv.), *N*-methylmaleimide (0.111 mg, 1.00 mmol, 1.00 mol. equiv.) and anhydrous PhMe (2.00 mL, 0.500 M). The reaction was stirred overnight at room temperature by which time ^{1}H NMR analysis indicated complete consumption of *N*-methylmaleimide. Anhydrous PhMe (0.500 mL), and 4-phenyl-1,2,4-triazoline-3,5-dione (batchwise addition, 1.23 g, 7.00 mmol, 7.00 mol. equiv.) was added, and the reaction mixture was stirred at room temperature for 30 minutes by which time ^{1}H NMR analysis indicated complete consumption of all mono-Diels–Alder adducts. The reaction was concentrated under reduced pressure and purified by flash column chromatography [phosphate buffered SiO_2 (pH 7), eluting with 1:9 EtOAc:CH_2Cl_2, R_f*'s* of isolated diastereomeric intermediates: 0.61 and 0.29 (1:4 EtOAc:CH_2Cl_2)]. To a 10 mL round-bottom flask equipped with a stir bar and open to air was added all intermediates, CH_2Cl_2 (2.00 mL, 0.500 M), and trifluoroacetic acid (1.53 mL, 20.0 mmol, 20.0 mol. equiv.). The reaction mixture was stirred at room temperature for 30 minutes and then concentrated under reduced pressure. Purification via washing with Et_2O, and then EtOAc, yielded tetrahydrocinnoline **47**. **Yield**: 0.314 g, 0.796 mmol, 80%; **Appearance**: Orange solid; **R*f***: 0.30 (3:7 EtOAc:CH_2Cl_2); **M.p.**: Degraded at 200 ºC; **^{1}H NMR** [600 MHz, $(CD_3)_2SO$]: 10.16 (br s, 1H), 9.96 (br s, 1H), 7.57–7.54 (m, 4H), 7.50–7.45 (m, 1H), 3.97 (t, J = 5.7 Hz, 2H), 3.06 (t, J = 5.7 Hz, 2H), 2.96 (s, 3H) ppm; **^{13}C NMR** [150 MHz, $(CD_3)_2SO$]: δ 166.9, 165.6, 149.0, 148.5, 144.2, 139.5, 131.1, 129.1, 128.6, 128.3, 126.7, 126.2, 115.2, 112.9, 40.2, 23.4, 21.3 ppm; **IR**: 3592, 3409, 3069, 2941, 2618, 1752, 1674, 1432, 1382, 1326, 1242, 1042, 1033, 927, 753, 743, 684 cm^{-1}; **HRMS** (ESI): calculated for $[C_{19}H_{14}N_4O_6+H]^+$: 395.0986, found: 395.0992.

Previous Synthetic Work

Kraus' synthesis from methylmalonic acid (9 steps, 6.8% overall yield, prepared on 69.1 mg scale):[20,38]

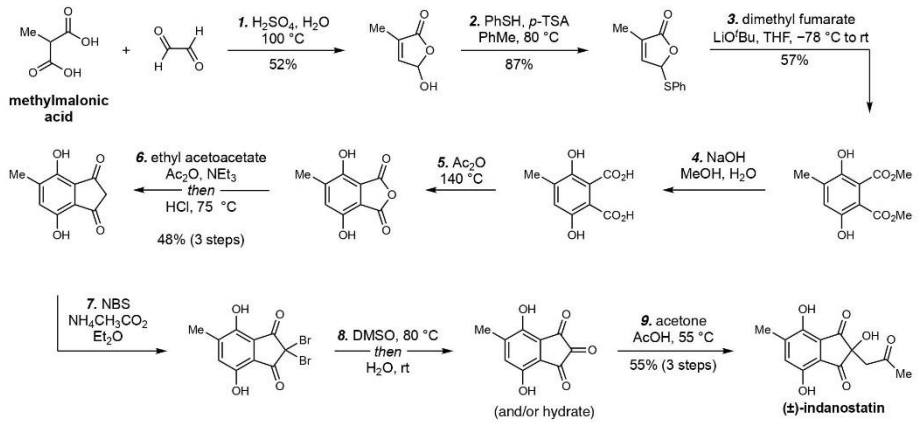

Our Synthesis

From methylsuccinic anhydride (3 steps, 43% overall yield, prepared on 1.14 g scale)

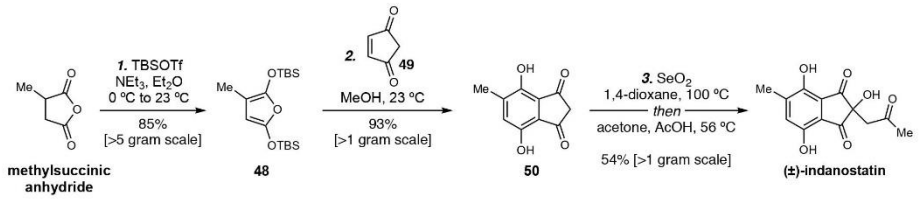

The synthesis of ((3-methylfuran-2,5-diyl)bis(oxy))bis(*tert*-butyldimethylsilane) (**48**) is described earlier in the 2,5-bis(silyloxy)furan synthesis section.

4,7-Dihydroxy-5-methyl-1*H*-indene-1,3(2*H*)-dione (50)

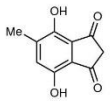
50

To a 50 mL round-bottom flask open to air and equipped with a stir bar was added ((3-methylfuran-2,5-diyl)bis(oxy))bis(*tert*-butyldimethylsilane) (**48**) (4.81 g, 14.1 mmol, 1.50 mol. equiv.), 4-cyclopentene-1,3-dione (**49**) (0.900 g, 9.37 mmol, 1.00 mol. equiv.), and MeOH (18.7 mL, 0.500M) at 23 ºC. The reaction was placed under a nitrogen atmosphere and stirred overnight by which time ^{1}H NMR analysis indicated the complete consumption of starting material. The reaction mixture was concentrated under reduced pressure, and purified by washing with Et_2O, yielding pure 4,7-dihydroxy-5-methyl-1*H*-indene-1,3(2*H*)-dione (**50**). **Yield**: 1.67 g, 8.71 mmol, 93%; Spectroscopic data matched those previously reported in the literature.[20] **Appearance**: Yellow solid; **R$_f$**: 0.25 (3:7 EtOAc:petroleum ether); **^{1}H NMR** [600 MHz, $(CD_3)_2SO$]: δ 10.04 (s, 1H), 9.18 (s, 1H), 7.07 (s, 1H), 3.25 (s, 2H), 2.21 (s, 3H) ppm.

(±)-Indanostatin

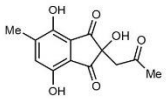
(±)-indanostatin

To a one-neck 250 mL round-bottom flask open to air and equipped with a stir bar and water condenser was added 4,7-dihydroxy-5-methyl-1*H*-indene-1,3(2*H*)-dione (**50**) (1.53 g, 7.96 mmol, 1.00 mol. equiv.), 1,4-dioxane (35.0 mL, 0.220 M), and selenium dioxide (1.06 g, 9.55 mmol, 1.20 mol. equiv.). The reaction was placed under a nitrogen atmosphere and heated to 101 ºC for 1.5 hours, by which time ^{1}H NMR analysis indicated the complete consumption of starting material. The reaction was cooled to room temperature and acetic acid (35 mL), and acetone (14 mL) were added. The flask was heated to 56 ºC and allowed to stir overnight, before being cooled to room temperature and filtered over silica (eluting with EtOAc). The crude reaction mixture was concentrated under reduced pressure, and purified via flash column chromatography (SiO_2, eluting with CH_2Cl_2 → 2:3 EtOAc:CH_2Cl_2), yielding pure (±)-indanostatin. **Yield:** 1.14 g, 4.30 mmol, 54%; Spectroscopic data matched those of the natural sample.[39] **Appearance**: Pale orange solid; **R$_f$**: 0.38 (3:7 EtOAc:CH_2Cl_2); **^{1}H NMR** [500 MHz, $(CD_3)_2SO$]: δ 10.22 (s, 1H), 9.19 (s, 1H), 7.12 (s, 1H), 6.49 (s, 1H), 3.19 (d, J = 3.0 Hz, 2H), 2.23 (s, 3H), 2.05 (s, 3H) ppm; **^{13}C NMR** [125 MHz, $(CD_3)_2SO$]: δ 206.6, 200.6, 196.8, 148.9, 146.9, 137.3, 127.3, 124.2, 122.3, 73.0, 47.8, 29.6, 16.1 ppm; **IR**: 3438, 2925, 1706, 1682, 1323, 1275, 1166, 1049, 790 cm^{-1}; **HRMS** (ESI): calculated for $[C_{13}H_{12}O_6+Na]^+$: 287.0526, found: 287.0522.

NMR Comparison Tables

^{1}H NMR

(±)-indanostatin

#	**^{1}H NMR of Natural (−)-indanostatin**[39] 400 MHZ, DMSO-d_6	**^{1}H NMR of Synthetic (±)-indanostatin** 500 MHZ, DMSO-d_6	**Δ**
1	-	-	-
2	-	-	-
3	-	-	-
3a	-	-	-
4	-	-	-
5	-	-	-
6	7.11 (s, 1H)	7.12 (s, 1H)	0.01
7	-	-	-
7a	-	-	-
8	3.17 (s, 2H)	3.19 (d, J = 3.0 Hz, 2H)	0.02
9	-	-	-
10	2.04 (s, 3H)	2.05 (s, 3H)	0.01
11	2.22 (s, 3H)	2.23 (s, 3H)	0.01
2-OH	6.45 (s, 1H)	6.49 (s, 1H)	0.04
4-OH	9.18 (s, 1H)	9.19 (s, 1H)	0.01
7-OH	10.19 (s, 1H)	10.22 (s, 1H)	0.03

^{13}C NMR

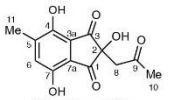

(±)-indanostatin

#	**^{13}C NMR of Natural (−)-indanostatin[39]** 100 MHZ, DMSO-d_6	**^{13}C NMR of Synthetic (±)-indanostatin** 125 MHZ, DMSO-d_6	**Δ**
1	196.5	196.8	0.3
2	72.8	73.0	0.2
3	200.4	200.6	0.2
3a	124.0	124.2	0.2
4	146.6	146.9	0.3
5	137.0	137.3	0.3
6	127.1	127.3	0.2
7	148.7	148.9	0.2
7a	122.1	122.3	0.2
8	47.6	47.8	0.2
9	206.3	206.6	0.3
10	29.4	29.6	0.2
11	15.9	16.1	0.2
2-OH	-	-	-
4-OH	-	-	-
7-OH	-	-	-

X-Ray Crystallographic Data

*para-Iminoquinone **39***

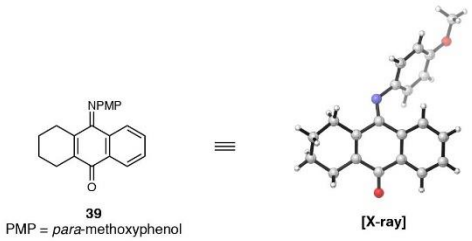

39
PMP = *para*-methoxyphenol

[X-ray]

Procedure

The tip of a suitable crystal was selected and mounted in a thin coating of Paratone-N using a MiTeGen crystal mount on an Oxford Xcalibur diffractometer fitted with an Eos detector. The data collection was conducted at 150(2) K and absorption corrections were applied using empirical methods. Using the Olex2 interface,[40] the structure was solved by Direct Methods with the ShelXS [41] structure solution program and refined with the ShelXL [42] using Least Squares minimization. Full data for the structure determination have been deposited with the Cambridge Crystallographic Data Centre as CCDC 2008987. The table below provides the crystal data and structure refinement details.

Crystal data and structure refinement

Empirical formula	$C_{21}H_{19}NO_2$
Formula weight	317.37
Temperature/K	150.(2)
Crystal system	orthorhombic
Space group	*Pbca*
a/Å	12.2553(9)
b/Å	7.6970(5)
c/Å	33.463(2)
α/°	90
β/°	90
γ/°	90
Volume/Å^3	3156.5(4)
Z	8
ρ_{calc}g/cm^3	1.336
μ/mm^{-1}	0.086
F(000)	1344.0
Crystal size/mm^3	0.80 × 0.37 × 0.05
Radiation	Mo*K*α (λ = 0.71073)
2Θ range for data collection/°	6.65 to 58.906
Index ranges	$-15 \leq h \leq 16$, $-10 \leq k \leq 9$, $-42 \leq l \leq 46$
Reflections collected	18438
Independent reflections	3938 [R_{int} = 0.0605, R_{sigma} = 0.0635]
Data/restraints/parameters	3938/0/218
Goodness-of-fit on F^2	1.056
Final R indexes [I>=2σ (I)]	R_1 = 0.0575, wR_2 = 0.0984
Final R indexes [all data]	R_1 = 0.0970, wR_2 = 0.1123
Largest diff. peak/hole / e Å^{-3}	0.24/-0.23

References

1 de Jong, J. C.; van Bolhuis, F.; Feringa, B. L. Asymmetric Diels-Alder reactions with 5-menthyloxy-2-(5H)-furanone. *Tetrahedron: Asymmetry*, **1991**, *2*, 1247.

2 Kaklyugina, T. Ya.; Badovskaya, L. A.; Sorotskaya, L. N.; Kozhina, N. D.; Jurášek, A.; Kada, R.; Kováč, J.; Kulnevich, V. G. Reaction of 2-butenolide and 4-bromo-2-butenolide with 5-aryl-2-furaldehydes and thiolates. *Collect. Czech. Chem. Commun*. **1986**, *51*, 2181.

3 Niu, G.-H.; Hou, C.-S.; Chuang, G. J.; Wu, C.-P.; Liao, C.-C. Diels–Alder Reactions of Masked *o*-Benzoquinones with 1-Vinylcyclohexenes: A Short and Efficient Entry to Highly Functionalized Decahydrophenanthrene Skeleton. *Eur. J. Org. Chem*. **2014**, 3794.

4 Schuster, T.; Kurz, M.; Göbel, M. W. Catalysis of a Diels-Alder Reaction by Amidinium Ions. *J. Org. Chem*. **2000**, *65*, 1697.

5 Liu, H.-J.; Wang, D.-X.; Kim, J. B.; Browne, E. N. C.; Wang, Y.; Activated cyclooctenones are effective dienophiles. *Can. J. Chem*. **1997**, *75*, 899.

6 Ireland, R. E.; Thompson, W. J. An Approach to the Total Synthesis of Chlorothricolide: The Synthesis of the Top Half. *J. Org. Chem.* **1979**, *44*, 3041.

7 Taylor, J. E.; Jones, M. D.; Williams, J. M. J.; Bull, S. D. Friedel-Crafts Acylation of Pyrroles and Indoles using 1,5-Diazabicyclo[4.3.0]non-5-ene (DBN) as a Nucleophilic Catalyst. *Org. Lett.* **2010**, *12*, 5740.

8 Bergman, J.; Johnson, A.-L. A Short Synthesis of the Carbazole Alkaloid Clausine E. *Org. Prep. Proced. Int.* **2006**, *593*.

9 Mukherjee, J.; Wasserman, E. P. Preparation of a particulate reversibly crosslinked polymeric material and its preparation using tetracarboxylic acid dianhydride crosslinker, Patent Number WO2011154759, Dec. 15, 2011.

10 Siebum, A. H. G.; Woo, W. S.; Lugtenburg, J. Preparation and Characterization of [5-^{13}C]-(2*S*,4*R*)-Leucine and [4-^{13}C]-(2*S*,3*S*)-Valine−Establishing Synthetic Schemes to Prepare Any Site-Directed Isotopomer of L-Leucine, L-Isoleucine and L-Valine. *Eur. J. Org. Chem*. **2003**, 4664.

11 a) Synthetic procedure: Lin, X.; Qiu, Z.; Tang, G.; Wong, J. C.; Zhang Z. Preparation of pyrrolidinylaminohydroxybenzamide derivatives and analogs for use as HDAC inhibitors, Patent Number WO2012098132, Jan 18, 2012. b) Characterization data: Shao, L.; Miyata, S.; Muramatsu, H.; Kawano, H.; Ishii, Y.; Saburi, M.; Uchida, Y. Asymmetric synthesis of (*R*)- and (*S*)-4-(substituted benzyl)dihydrofuran-2(3*H*)-ones: an application of the ruthenium-binap complex-catalysed asymmetric hydrogenation of alkylidenesuccinic acids. *J. Chem. Soc., Perkin Trans. 1*, **1990**, 1441.

12 Frick, U.; Simchen, G. Reaktionen der Trialkylsilyl- trifluormethansulfonate, VIII. Synthese von O-(Trimethylsilyl)keten- O,N-acetalen, 2,5-Bis(trimethylsiloxy)pyrrolen, -furanen und -thiophenen. *Liebigs Ann*. **1987**, 839

13 Horvath, K. L.; Magann, N. L.; Sowden, M.J.; Gardiner, M. G.; Sherburn, M. S., Unlocking Acyclic π-Bond Rich Structure Space with Tetraethynylethylene–Tetravinylethylene Hybrids. *J. Am. Chem. Soc*. **2019**, *141*, 19746.

14 Vézouët, R. L.; White, A. J. P.; Burrows, J. N.; Barrett, A. G. M. Synthetic studies on the CDEF ring system of lactonamycin. *Tetrahedron,* **2006**, *62,* 12252.

[15] Nematollahi, D.; Momeni, S.; Khazalpour, S. Different strategies in electrochemical synthesis of new mono and di-substituted hydroquinone and benzoquinone. *Electrochimica Acta*, **2014**, *147*, 310.
[16] Baranac-Stojanović, M.; Marković, R.; Stojanović, M. Catalytic oxidations of enolizable ketones using 2-alkylidene-4-oxothiazolidine vinyl bromide. *Tetrahedron*, **2011**, *67*, 8000.
[17] Mazzini, F.; Alpi, E.; Salvadori, P.; Netscher, T. First Synthesis of (8-$^{2}H_3$)-(all-*rac*)-δ-Tocopherol. *Eur. J. Org. Chem.* **2003**, 2840.
[18] Yang, D.; Fu, H. A Simple and Practical Copper-Catalyzed Approach to Substituted Phenols from Aryl Halides by Using Water as the Solvent. *Chem. Eur. J.* **2010**, *16*, 2366.
[19] Evans, D.; Wu, J. Enantioselective Rare-Earth Catalyzed Quinone Diels−Alder Reactions. *J. Am. Chem. Soc*. **2003**, *125*, 10162.
[20] Wang, S.; Kraus, G. A. Annulations of 5-Phenylthiobutenolides and First Synthesis of (±)-Indanostatin. *Synlett,* **2009**, *30,* 353.
[21] Zheng, H.; Xu, C.; Wang, Y.; Kang, T.; Liu, X.; Lina, L.; Feng, X. Catalytic asymmetric [2+2] cycloaddition between quinones and fulvenes and a subsequent stereoselective isomerization to 2,3-dihydrobenzofurans. *Chem. Commun.* **2017**, *53*, 6585.
[22] Potter, B. V. L.; Reed, M. J.; Woo, L. W. L. *Preparation of sulfamoyl steroidal imide derivatives for inhibition of steroid sulfatase*, Patent Number WO2003033518, Apr. 24, 2003.
[23] Harada, T.; Chiba, M.; Oku, A. Novel Homologation Reaction of Arylzincates Bearing a Leaving Group at the Ortho and Meta Positions. *J. Org. Chem.* **1999**, *64*, 8210.
[24] Ganta, A.; Snowden, T. S. Facile Preparation of 2-Iodophenyl Trifluoromethanesulfonates: Superior Aryne Precursors. *Synlett*, **2007**, *14*, 2227.
[25] Yoshida, S.; Hazama, Y.; Kanemoto, K.; Nakamura, Y.; Hosoya, T. Facile Synthesis of Diverse *o*-Iodoaryl Triflates from *o*-Silylaryl Triflates by Aluminum-mediated Desilyliodination. *Chem. Lett.* **2019**, *48*, 742.
[26] Li, H.; Wang, K.; Wan, Q.; Chen, Y. Design, synthesis and anti-tumor evaluation of novel steroidal glycoconjugate with furoxan derivatives. *Steroids*, **2019**, *141*, 81.
[27] Hamura, T.; Hosoya, T.; Yamaguchi, H.; Kuriyama, Y.; Tanabe, M.; Miyamoto, M.; Yasui, Y.; Matsumoto, T.; Suzuki, T. Facile Access to Versatile Polyaromatic Building Blocks: Selectively Protected Benzocyclobutenedione Derivatives via Regioselective [2+2] Cycloaddition of α-Alkoxybenzyne and Ketene Silyl Acetal. *Helv. Chim. Acta*. **2002**, *85*, 3589.
[28] Kelly, T. R.; Bell, S. H.; Ohashi, N.; Armstrong-Chong R. J. Synthesis of (±)-Fredericamycin A. *J. Am. Chem. Soc*. **1988**, *110*, 6471.
[29] Huang, L.; Zhao, J.; Guo, S.; Zhang, C.; Ma, J. Bodipy Derivatives as Organic Triplet Photosensitizers for Aerobic Photoorganocatalytic Oxidative Coupling of Amines and Photooxidation of Dihydroxylnaphthalenes. *J. Org. Chem*. **2013**, *78*, 5627.
[30] Murahashi, S.-I.; Miyaguchi, N.; Noda, S.; Naota, T.; Fujii, A.; Inubushi, Y.; Komiya, N. Ruthenium-Catalyzed Oxidative Dearomatization of Phenols to 4-(*tert*-Butylperoxy)cyclohexadienones: Synthesis of 2-Substituted Quinones from *p*-Substituted Phenols. *Eur. J. Org. Chem*. **2011**, 5355.
[31] Franck, R. W.; Gupta, R. B. Baeyer-Villiger Oxidation of Naphthaldehydes: Easy Access to Naphthoquinones. *J. Org. Chem*. **1985**, *50*, 4632.

[32] Watanabe, M.; Hisamatsu, S.; Hotokezaka, H.; Furukawa, S. Reaction of Lithiated Senecioamide and Related Compounds with Benzynes : Efficient Syntheses of Naphthols and Naphthoquinones. *Chem. Pharm. Bull.* **1986**, *34*, 2810.
[33] Wurm, G.; Goeßler, B. Untersuchungen an 1,4-Naphthochinonen, 19. Mitt.: 2-,3-und 6-Methyljuglon aus Formylnaphtholen. *Arch. Pharm. Pharm. Med. Chem*. **1989**, *322*, 569.
[34] Molina, M. T.; Navarro, C.; Moreno, A.; Csákÿ, A. G. Arylation of Benzo-Fused 1,4-Quinones by the Addition of Boronic Acids under Dicationic Pd(II)-Catalysis. *Org. Lett*. **2009**, *11*, 4938.
[35] Patil, S. V.; Mahale, K. A.; Gosavi, K. S.; Deshmukh, G. B.; Patil, N. S. Solvent-mediated One-pot Synthesis of Cyclic *N*-Substituted Imides. *Org. Prep. Proced. Int.* **2013**, *45*, 314.
[36] Khan, A.; Marson, C. M.; Porter, R. A. Synthesis of Exocyclic Enamides via Stereocontrolled Allylic Isomerization and 1,3-Transposition. *Synth. Commun*. **2017**, *31*, 1753.
[37] Barker, M. D.; Dixon, R. A.; Jones, S.; Marsh, B. J. The crucial role of the nitrogen substituent in the desymmetrisation of cyclic *meso*-imides using *B*-Me and *B*-OMe oxazaborolidine catalysts. *Tetrahedron*. **2006**, *62*, 11663.
[38] Morris, J. C.; McErlean, C. S. P. Synthesis of highly *enantio*-enriched stereoisomers of hydroxy-GR24. *Org. Biomol. Chem.* **2016**, *14*, 1236.
[39] Hayakawa, Y.; Kobayashi, T.; Izawa, M. Indanostatin, a new neuroprotective compound from *Streptomyces* sp. *J. Antibiot.* **2013**, *66*, 731.
[40] Dolomanov, O. V.; Bourhis, L. J.; Gildea, R. J.; Howard, J. A. K.; Puschmann, H. *OLEX2*: a complete structure solution, refinement and analysis program. *J. Appl. Cryst*. **2009**, *42*, 339.
[41] Sheldrick, G. M. A short history of *SHELX*. *Acta Cryst*. **2008**, *A64*, 112.
[42] Sheldrick, G. M. Crystal structure refinement with *SHELXL*. *Acta Cryst*. **2015**, *C71*, 3.

NMR Spectra

Silyloxyfurans

Precursors

S5
^{1}H NMR
$CDCl_3$, 500 MHz

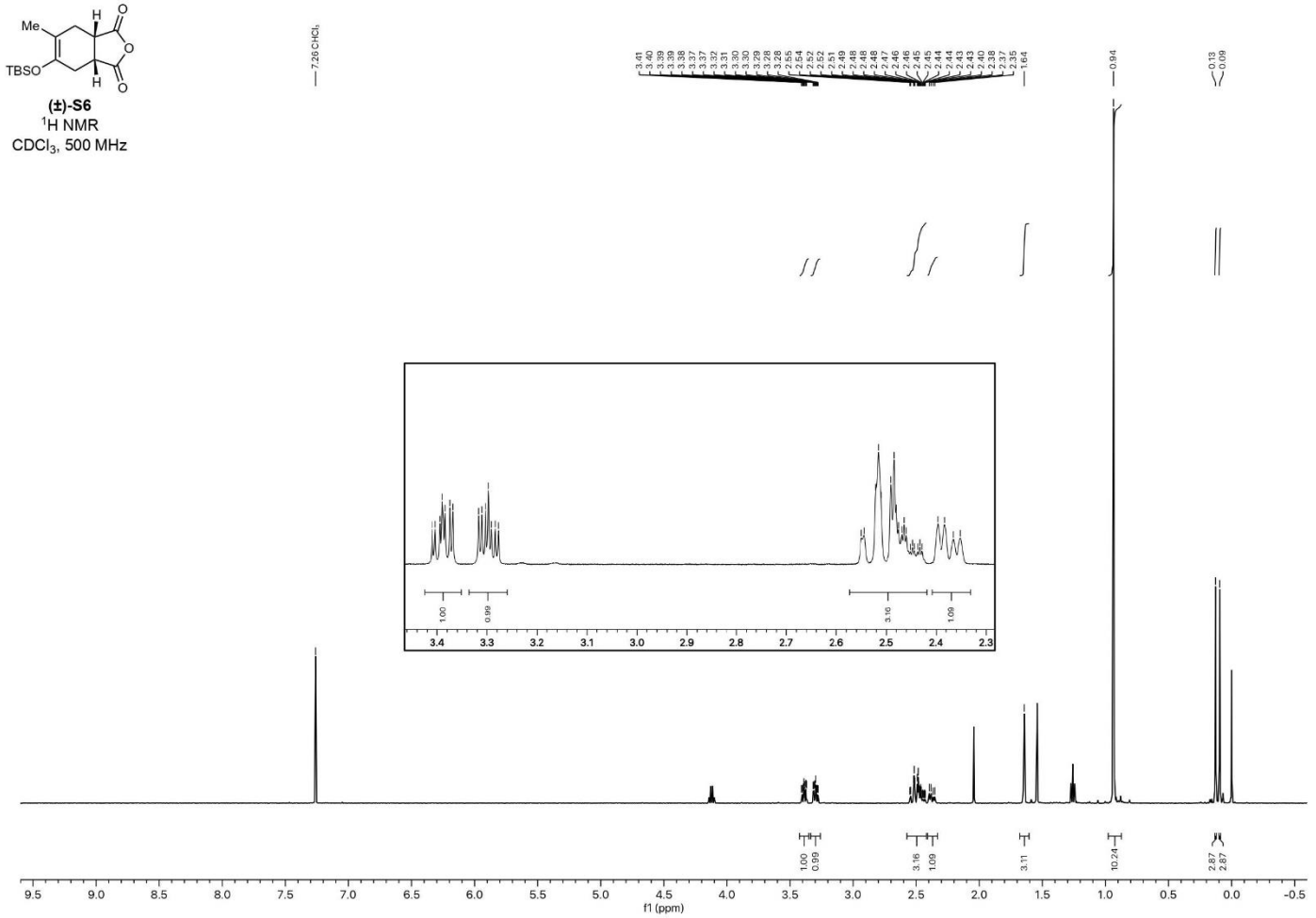
Me
TBSO
H
H
O
O
O
O
(±)-S6
1H NMR
CDCl3, 500 MHz
7.26 CHCl3
3.41
3.40
3.39
3.38
3.38
3.37
3.37
3.32
3.31
3.31
3.30
3.30
3.29
3.28
3.28
2.55
2.54
2.52
2.52
2.51
2.49
2.48
2.48
2.48
2.47
2.46
2.46
2.45
2.45
2.44
2.44
2.44
2.43
2.40
2.38
2.37
2.35
1.64
0.94
0.13
0.09
1.00
0.99
3.16
1.09
3.11
10.24
2.87
2.87
f1 (ppm)

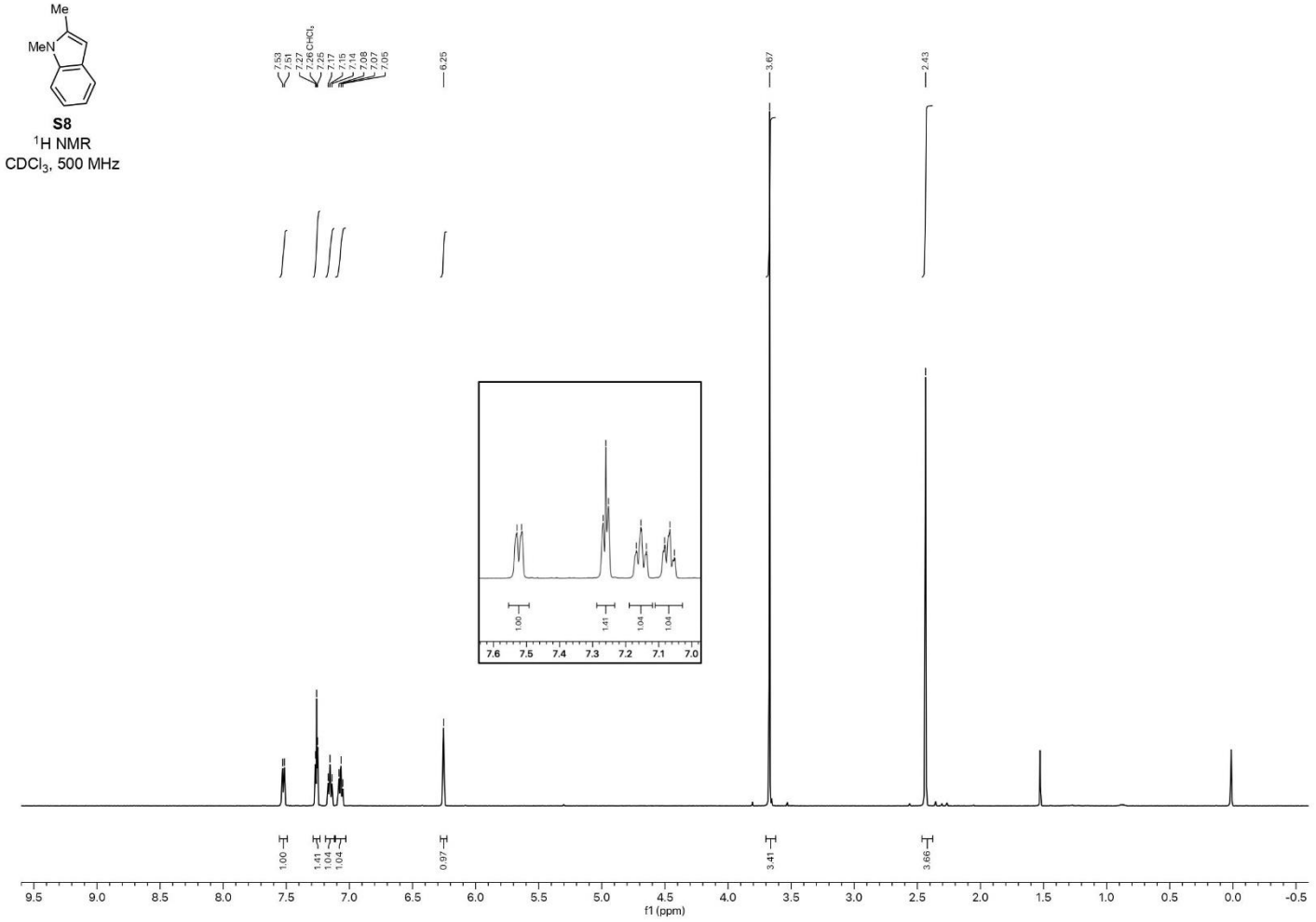
Me
MeN
S8
1H NMR
CDCl3, 500 MHz
7.53
7.51
7.27
7.26 CHCl3
7.25
7.17
7.15
7.14
7.08
7.07
7.05
6.25
3.67
2.43
1.00
1.41
1.04
1.04
0.97
3.41
3.66
f1 (ppm)

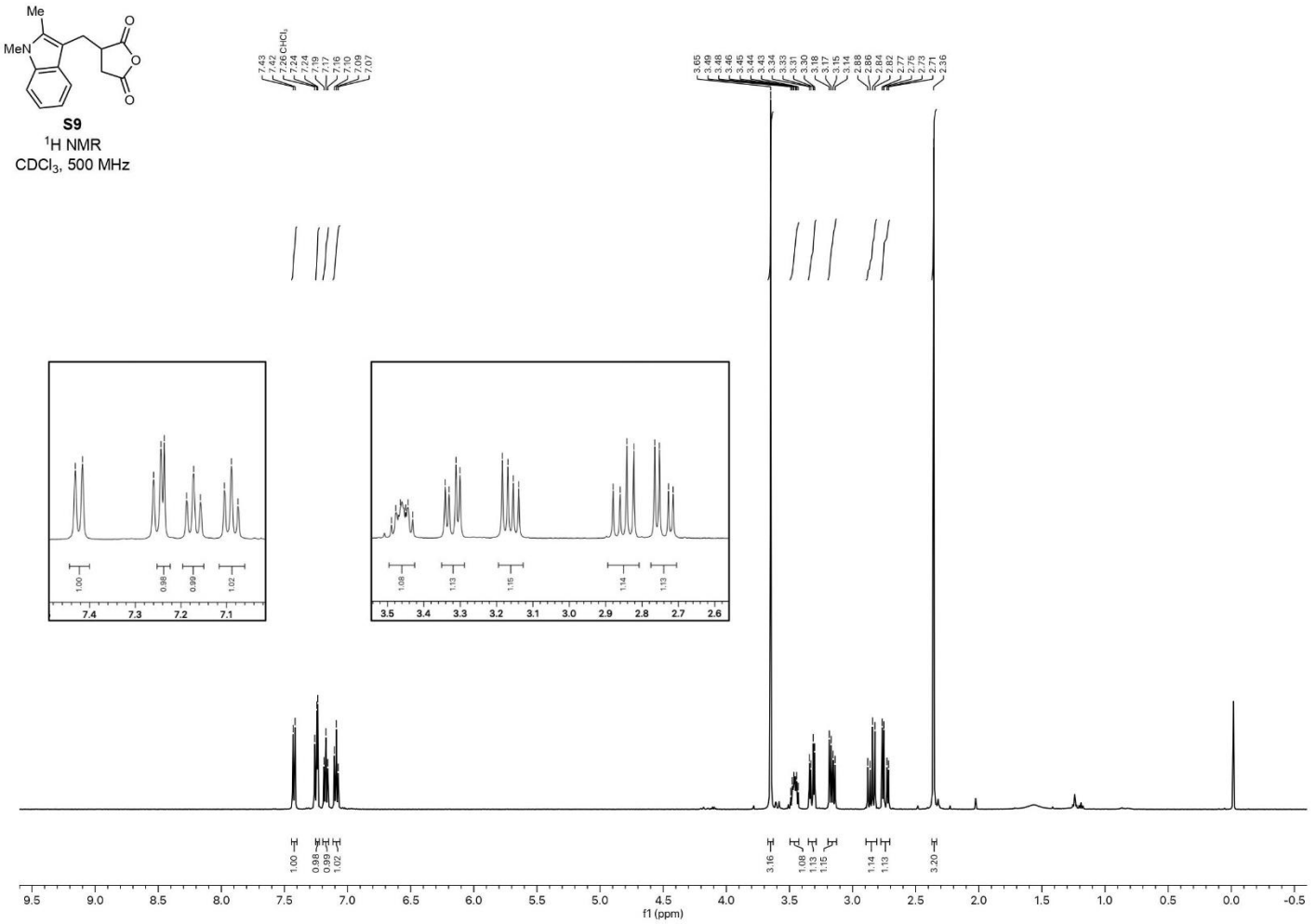
Me
MeN
O
O
O
O
S9
1H NMR
CDCl3, 500 MHz
7.43
7.42
7.26 CHCl3
7.24
7.24
7.19
7.17
7.16
7.10
7.09
7.07
3.65
3.48
3.46
3.46
3.45
3.44
3.43
3.34
3.33
3.31
3.30
3.18
3.17
3.15
3.14
2.88
2.86
2.84
2.82
2.77
2.75
2.73
2.71
2.36
1.00
0.98
0.99
1.02
3.16
1.08
1.13
1.15
1.14
1.13
3.20
f1 (ppm)

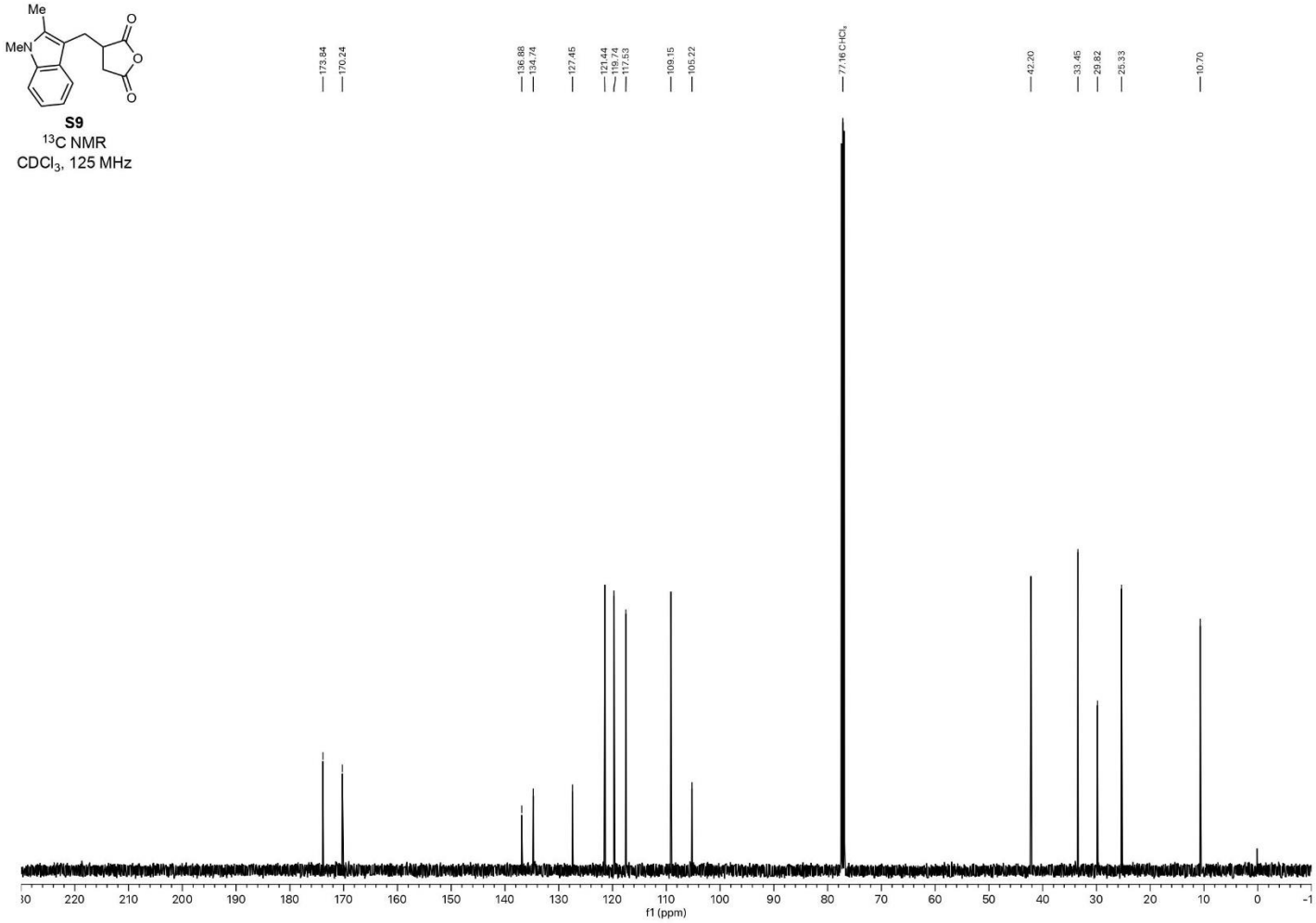
Me
MeN
O
O
O
O
S9
13C NMR
CDCl3, 125 MHz
173.84
170.24
136.88
134.74
127.45
121.44
119.74
117.53
109.15
105.22
77.16 CHCl3
42.20
33.45
29.82
25.33
10.70
f1 (ppm)

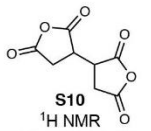

S10
^{1}H NMR
$(CD_3)_2CO$, 500 MHz

(inconsequential stereochemistry not determined)

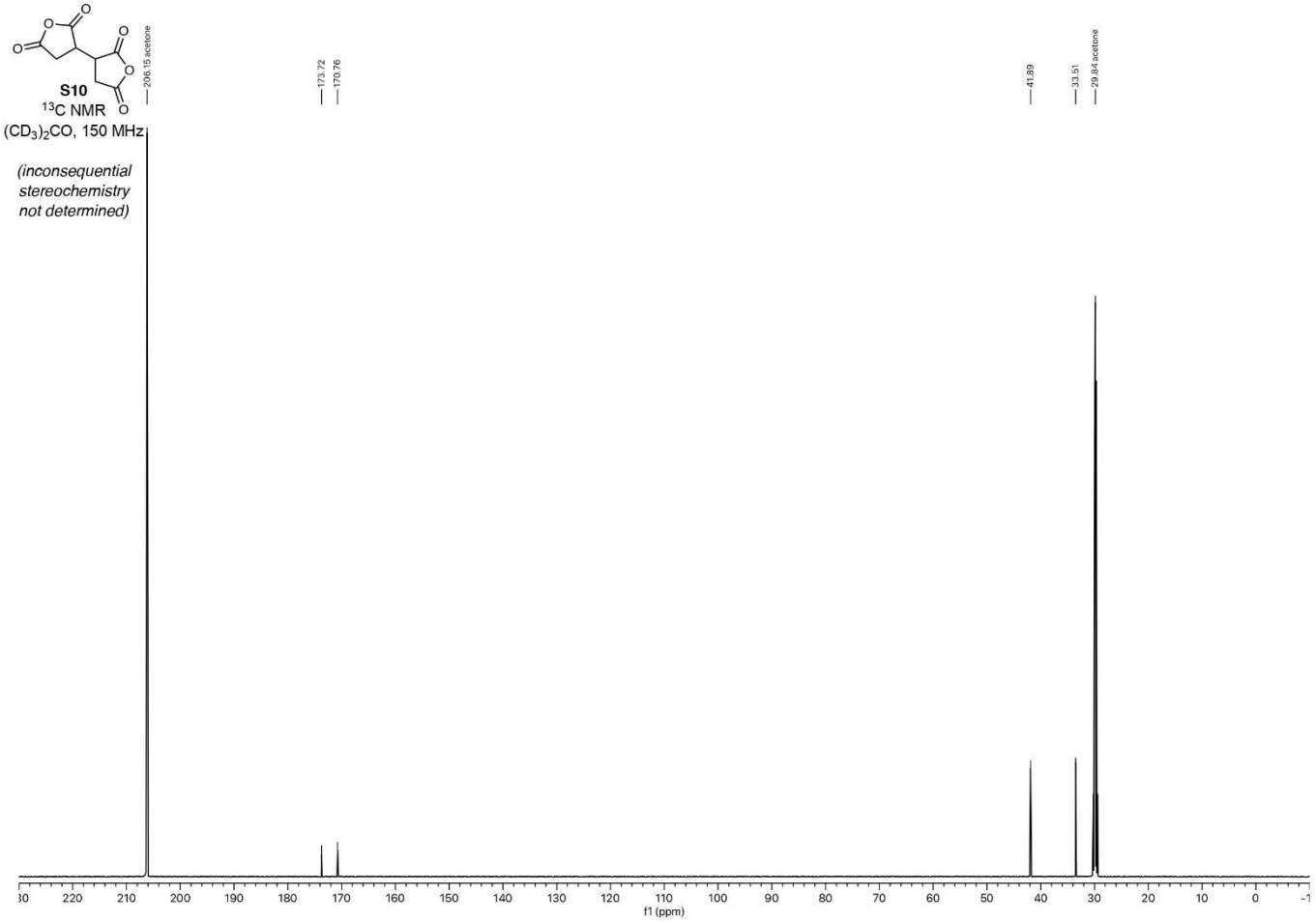
S10
13C NMR
(CD3)2CO, 150 MHz
(inconsequential stereochemistry not determined)
206.15 acetone
173.72
170.76
41.89
33.51
29.84 acetone
f1 (ppm)

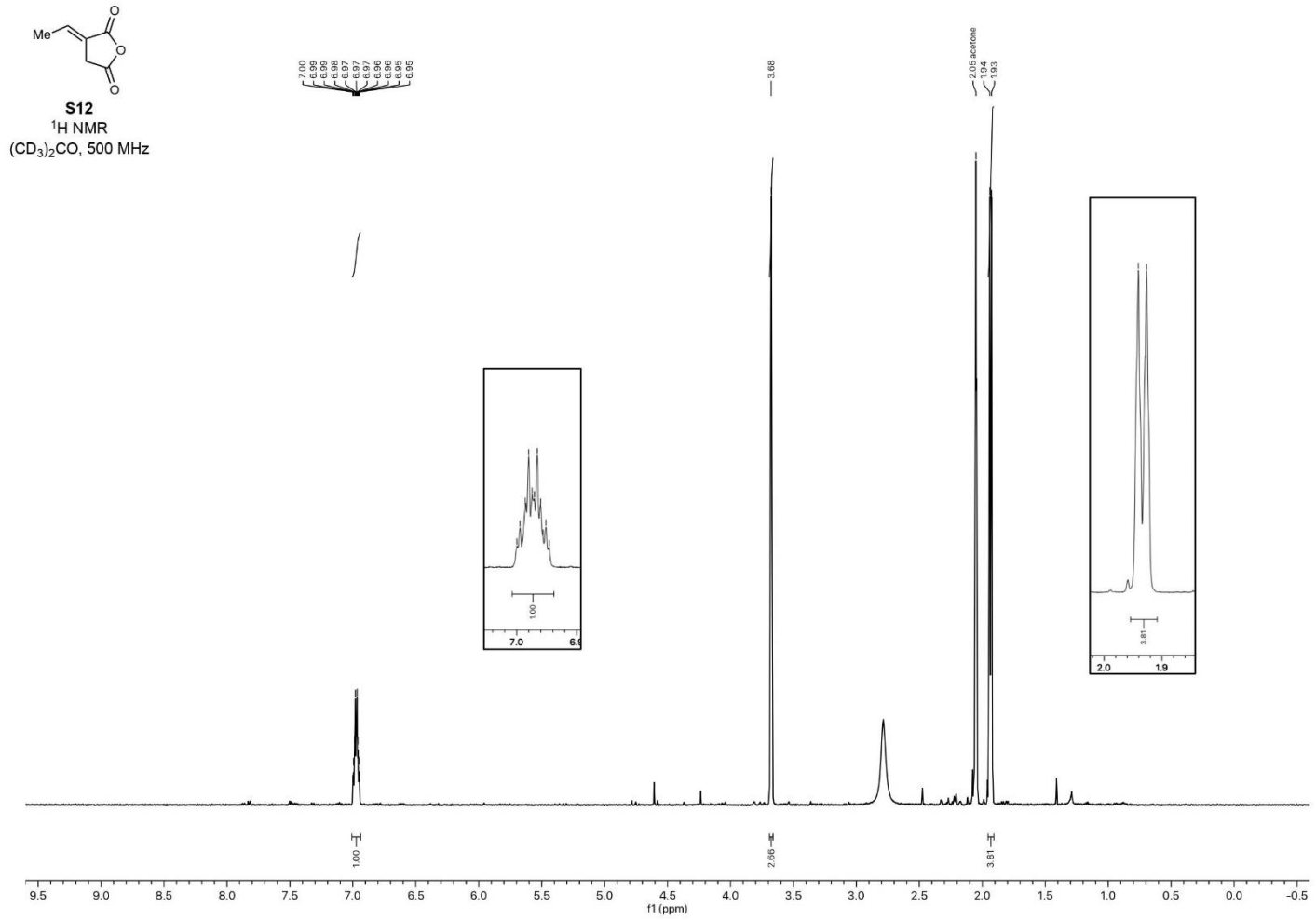
Me
O
O
O
S12
1H NMR
(CD3)2CO, 500 MHz
7.00
6.99
6.99
6.98
6.97
6.97
6.97
6.97
6.96
6.96
6.96
6.95
6.95
3.68
2.05 acetone
1.94
1.93
1.00
7.0
6.9
3.81
2.0
1.9
1.00
2.66
3.81
9.5
9.0
8.5
8.0
7.5
7.0
6.5
6.0
5.5
5.0
4.5
4.0
3.5
3.0
2.5
2.0
1.5
1.0
0.5
0.0
-0.5
f1 (ppm)

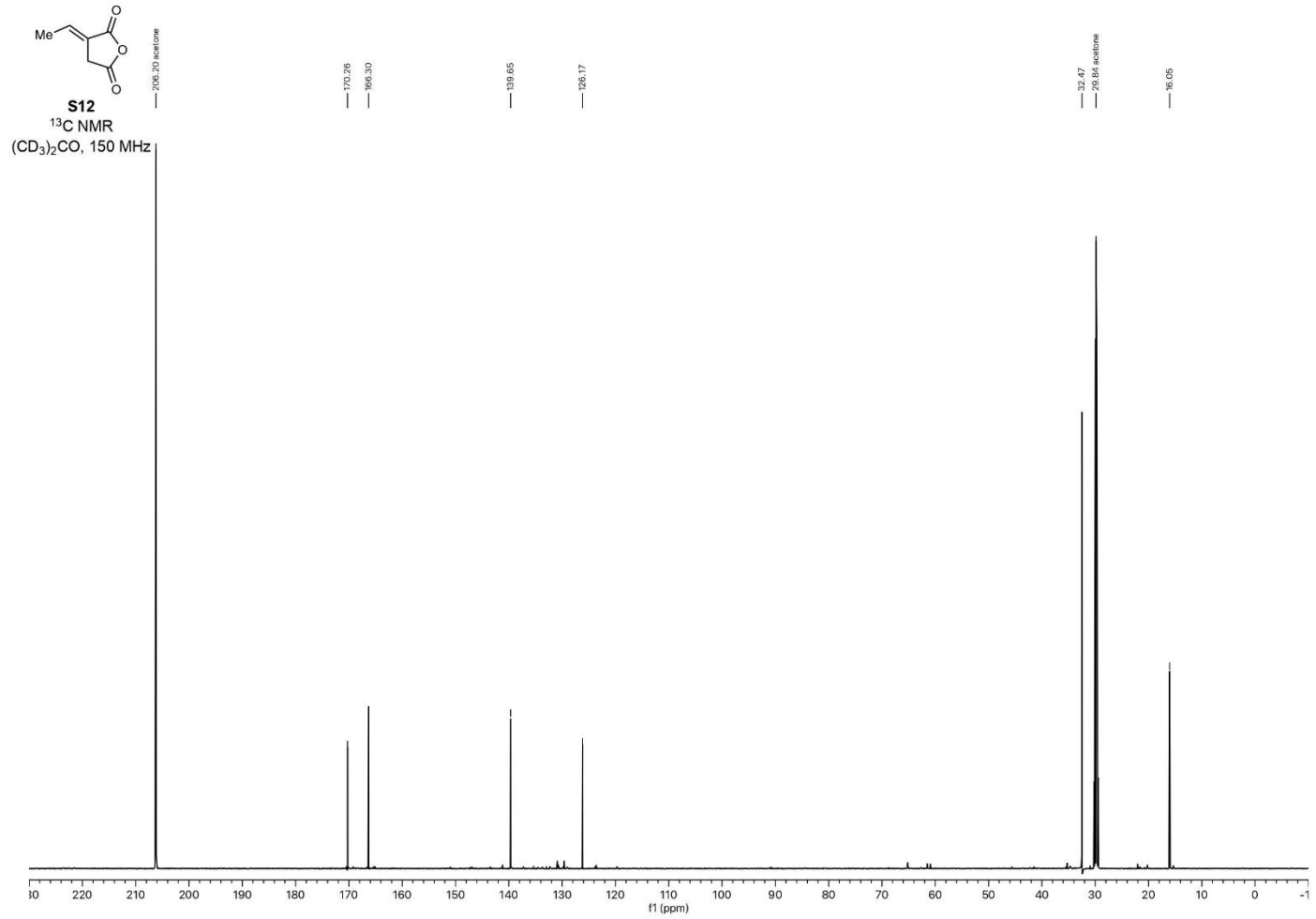
Me
O
O
O
S12
13C NMR
(CD3)2CO, 150 MHz
206.20 acetone
170.26
166.30
139.65
126.17
32.47
29.84 acetone
16.05
f1 (ppm)

2,5-Bis(silyloxy)furans

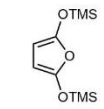

1
^{1}H NMR
$CDCl_3$, 500 MHz

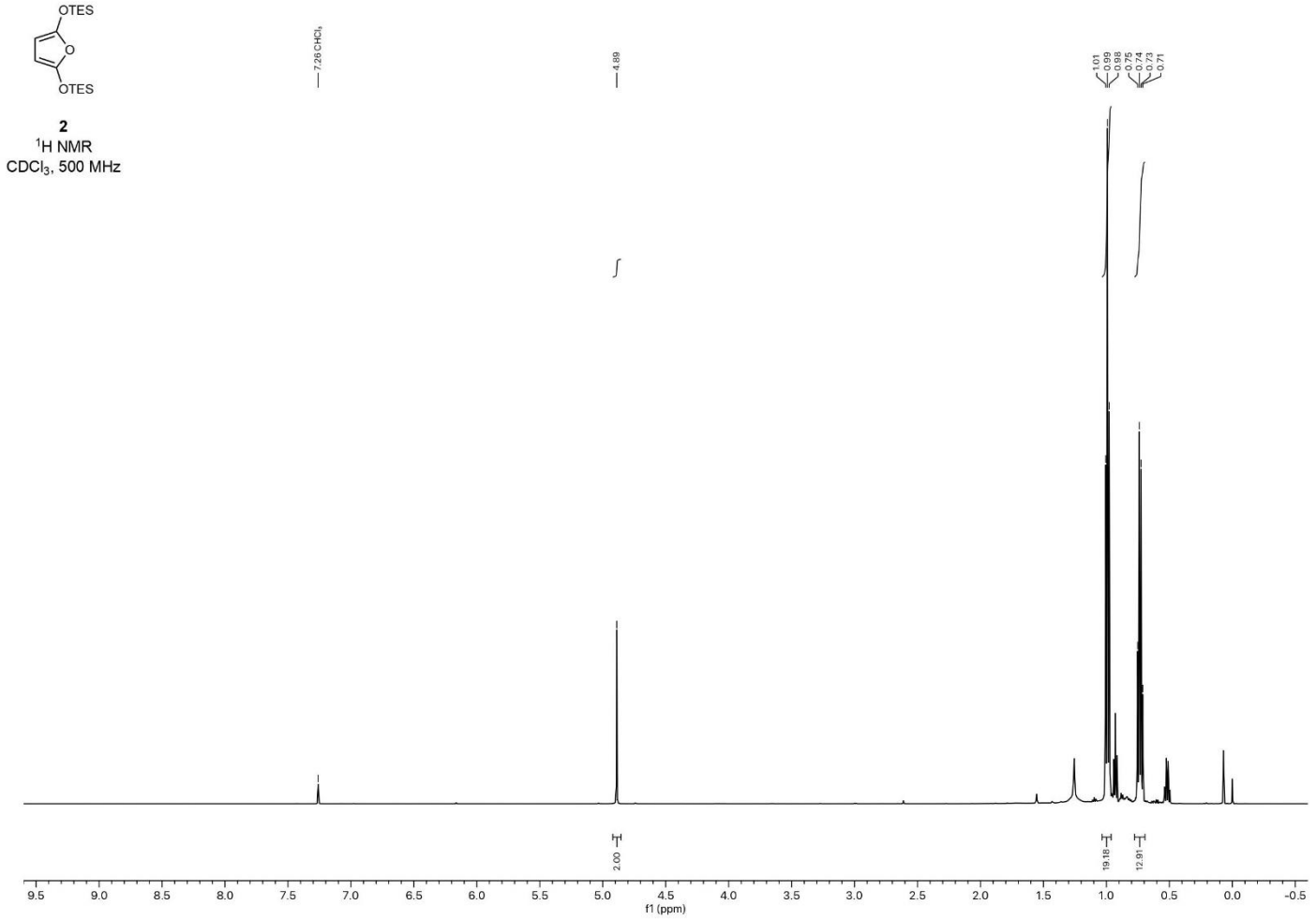
OTES
OTES
2
1H NMR
CDCl3, 500 MHz
7.26 CHCl3
4.89
1.01
0.99
0.98
0.75
0.74
0.73
0.71
2.00
19.18
12.91
9.5
9.0
8.5
8.0
7.5
7.0
6.5
6.0
5.5
5.0
4.5
4.0
3.5
3.0
2.5
2.0
1.5
1.0
0.5
0.0
-0.5
f1 (ppm)

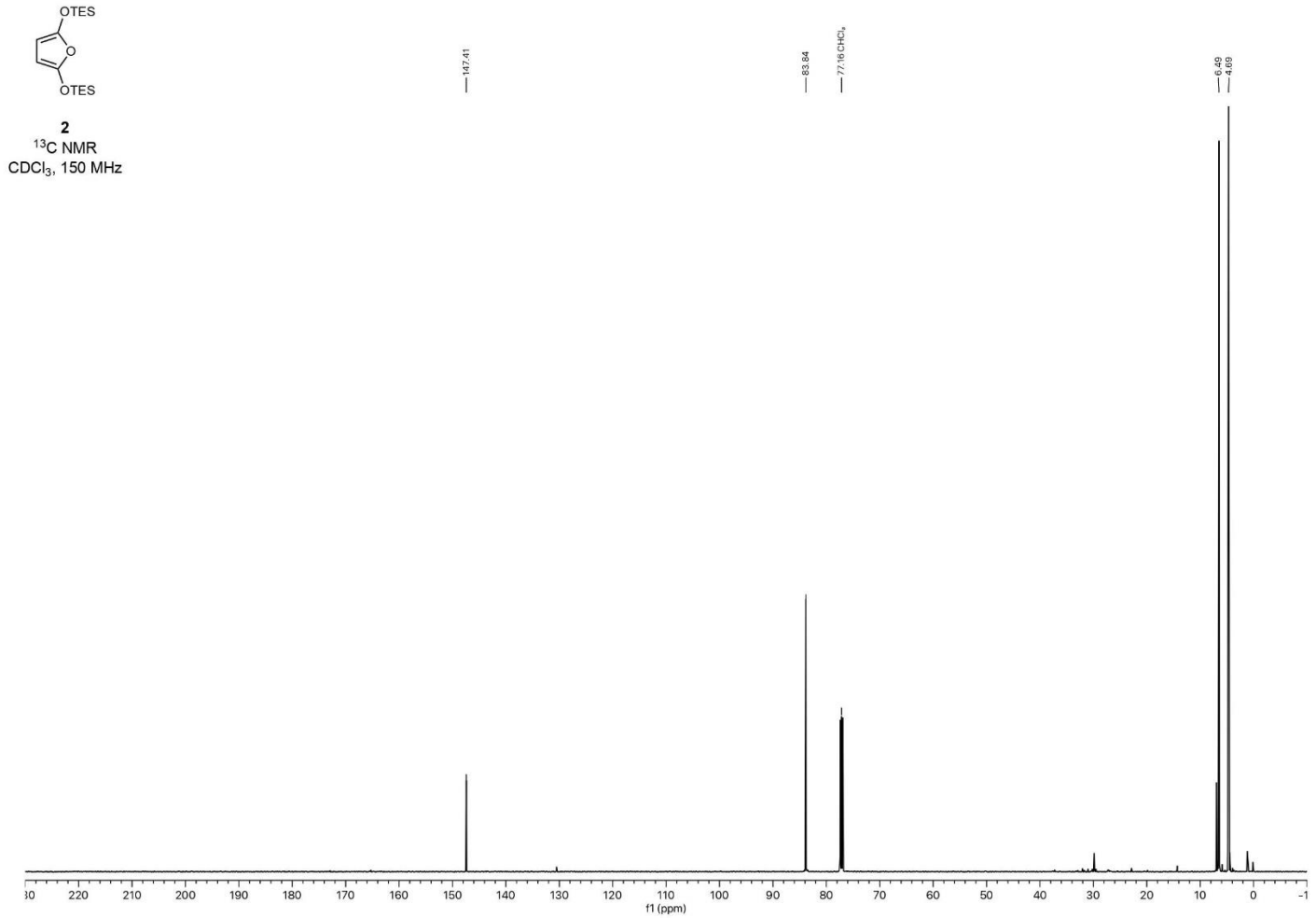
OTES
OTES
2
13C NMR
CDCl3, 150 MHz
147.41
83.84
77.16 CHCl3
6.49
4.69
f1 (ppm)

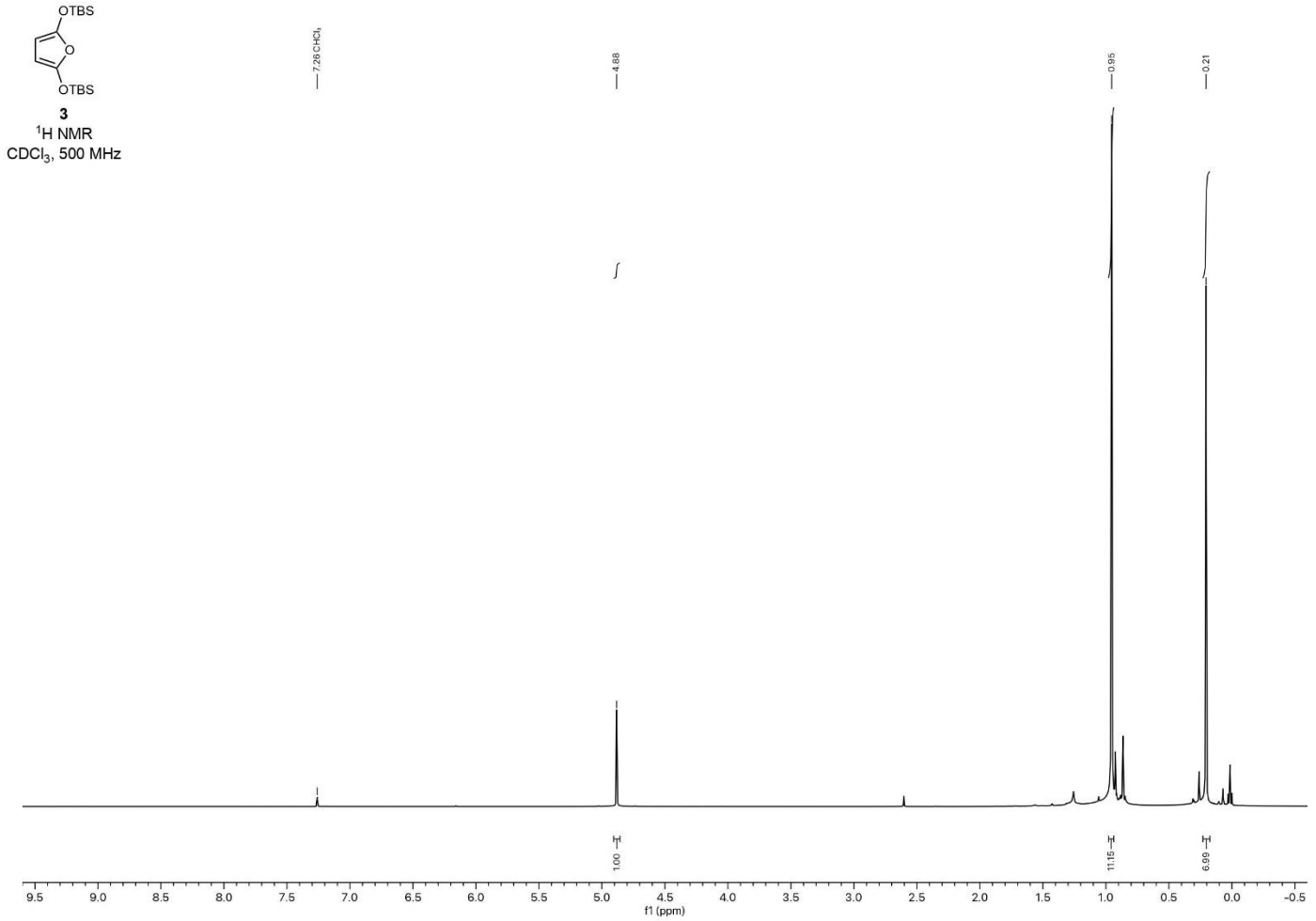
OTBS
O
OTBS
3
1H NMR
CDCl3, 500 MHz
7.26 CHCl3
4.88
0.95
0.21
1.00
11.15
6.99
9.5 9.0 8.5 8.0 7.5 7.0 6.5 6.0 5.5 5.0 4.5 4.0 3.5 3.0 2.5 2.0 1.5 1.0 0.5 0.0 -0.5
f1 (ppm)

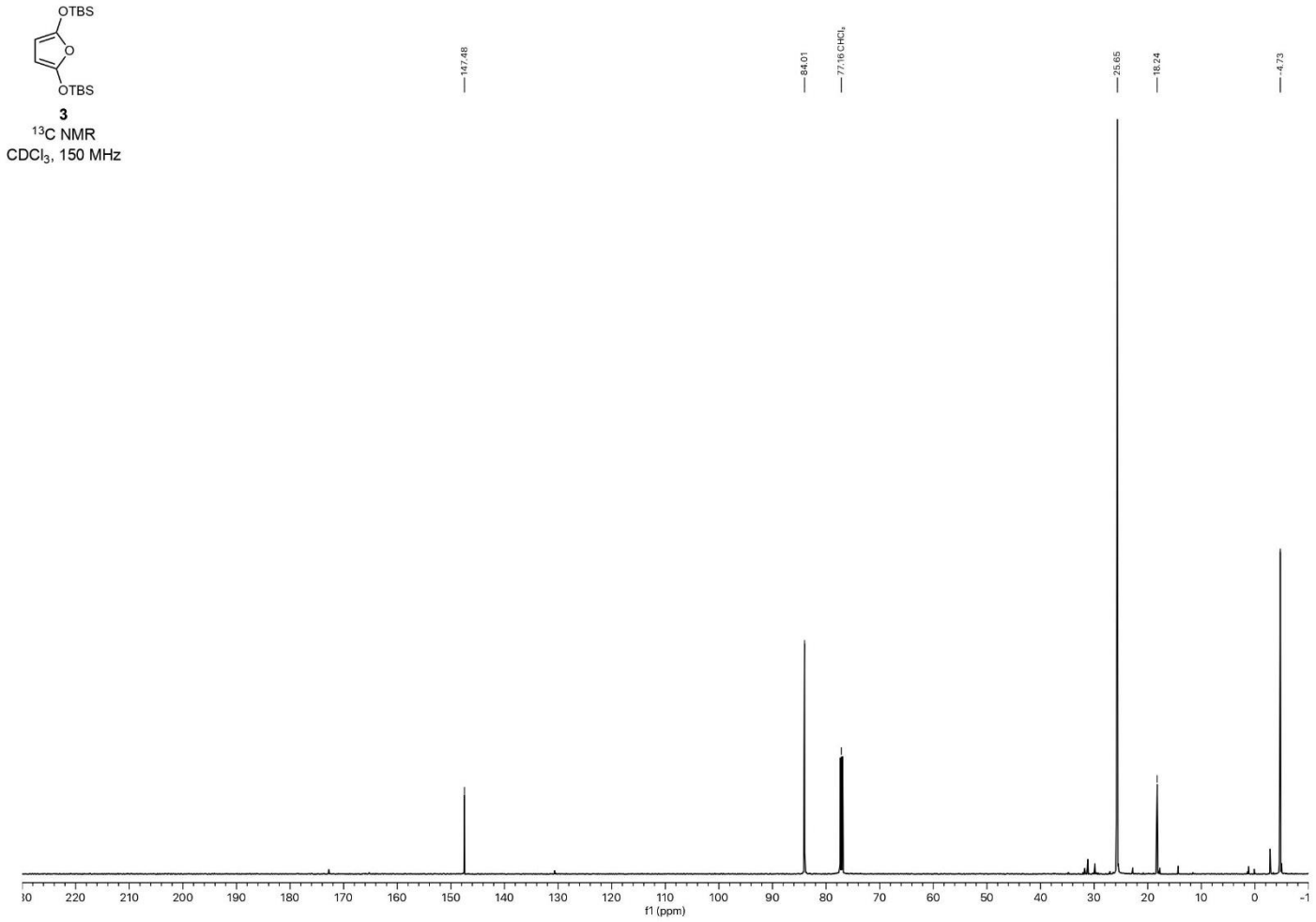
OTBS
OTBS
3
13C NMR
CDCl3, 150 MHz
147.48
84.01
77.16 CHCl3
25.65
18.24
-4.73
f1 (ppm)

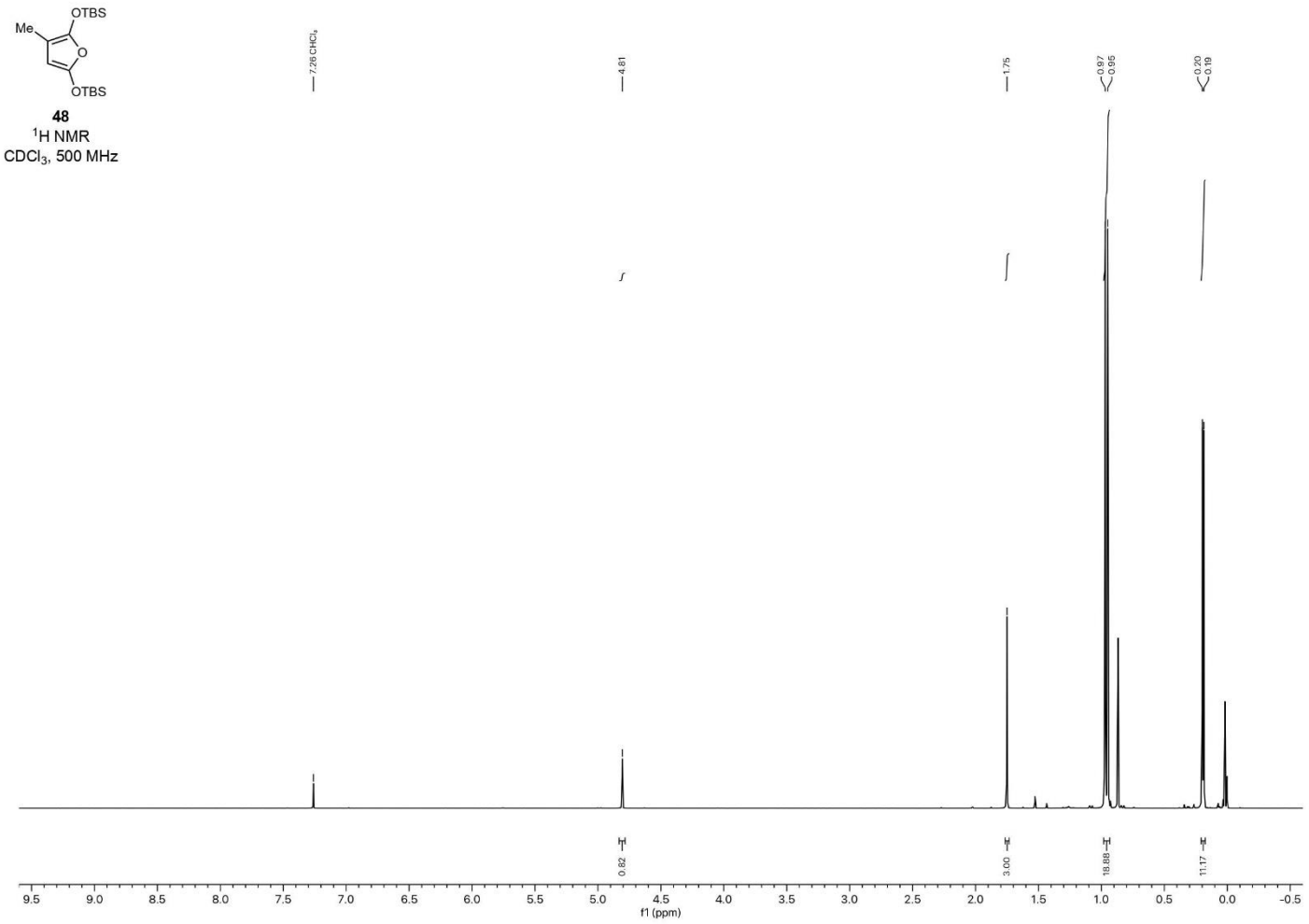
OTBS
Me
O
OTBS
48
1H NMR
CDCl3, 500 MHz
7.26 CHCl3
4.81
1.75
0.97
0.95
0.20
0.19
0.82
3.00
18.88
11.17
9.5 9.0 8.5 8.0 7.5 7.0 6.5 6.0 5.5 5.0 4.5 4.0 3.5 3.0 2.5 2.0 1.5 1.0 0.5 0.0 -0.5
f1 (ppm)

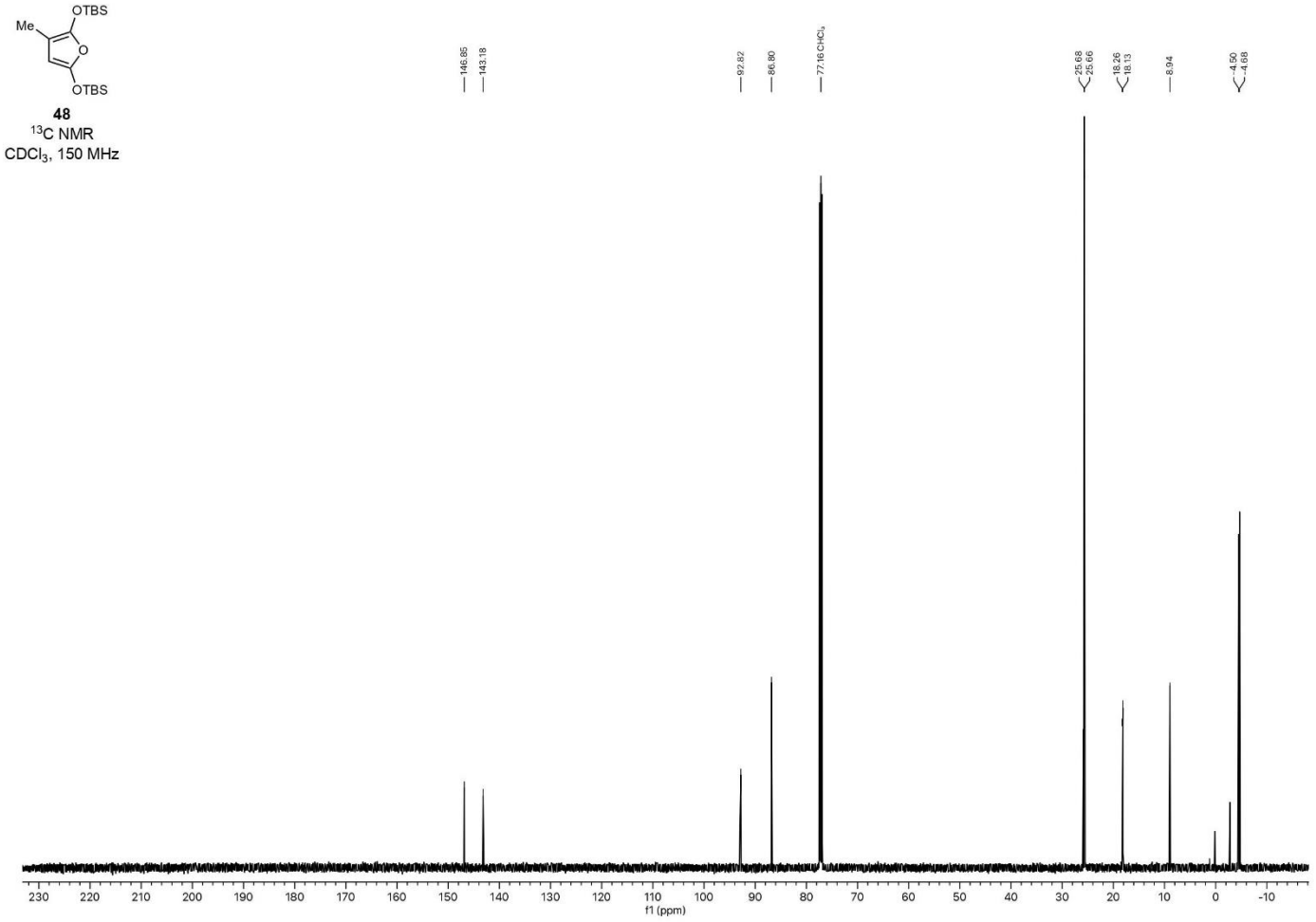
OTBS
Me
O
OTBS
48
13C NMR
CDCl3, 150 MHz
146.85
143.18
92.82
86.80
77.16 CHCl3
25.68
25.66
18.26
18.13
8.94
-4.50
-4.68
230 220 210 200 190 180 170 160 150 140 130 120 110 100 90 80 70 60 50 40 30 20 10 0 -10
f1 (ppm)

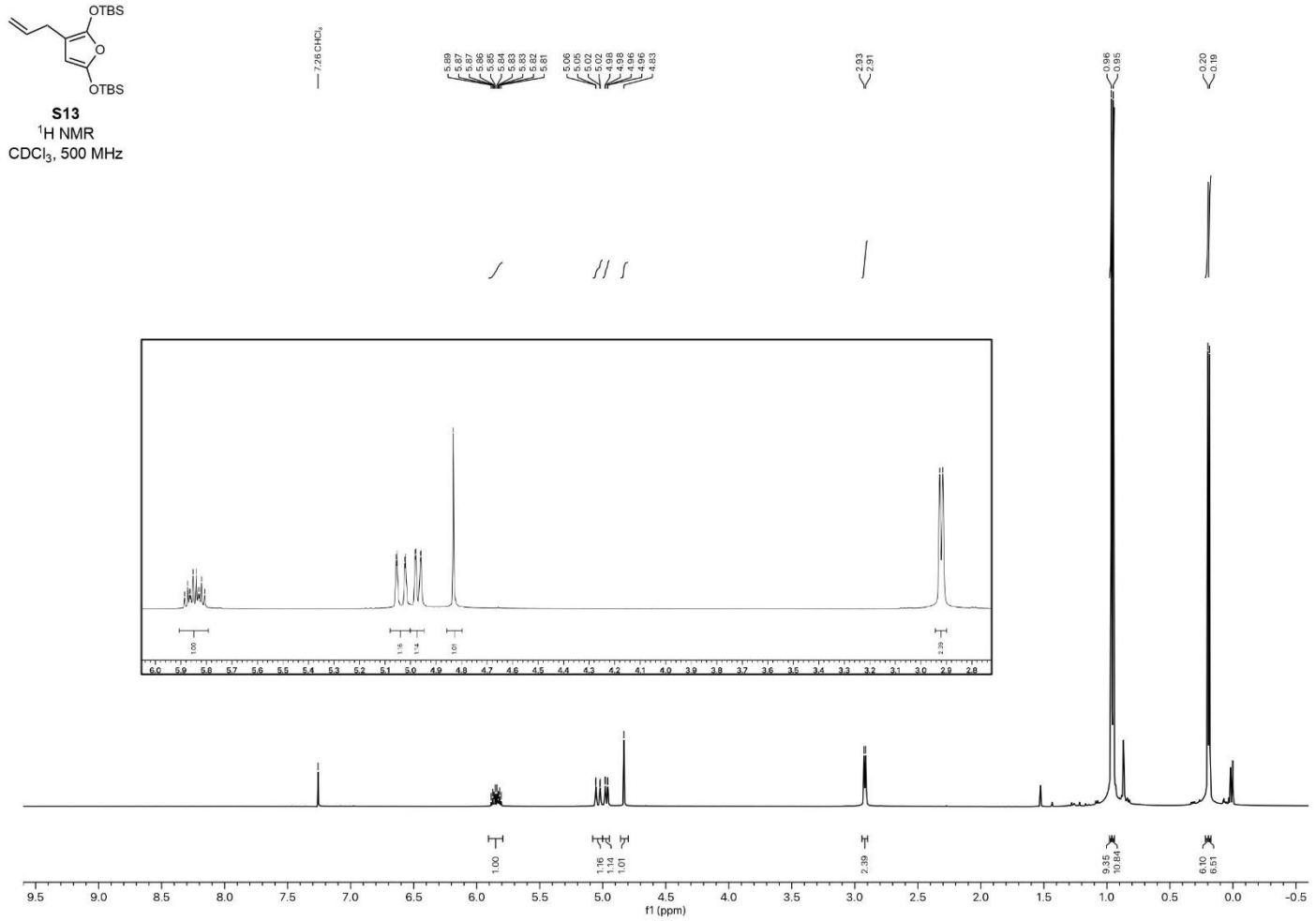
OTBS
OTBS
S13
1H NMR
CDCl3, 500 MHz
7.26 CHCl3
5.89
5.87
5.87
5.86
5.85
5.84
5.83
5.83
5.82
5.81
5.06
5.05
5.02
5.02
4.98
4.98
4.96
4.96
4.93
2.93
2.91
0.96
0.95
0.20
0.19
1.00
1.16
1.14
1.01
2.39
9.35
10.84
6.10
6.51
f1 (ppm)

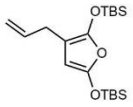

S13
^{13}C NMR
$CDCl_3$, 125 MHz

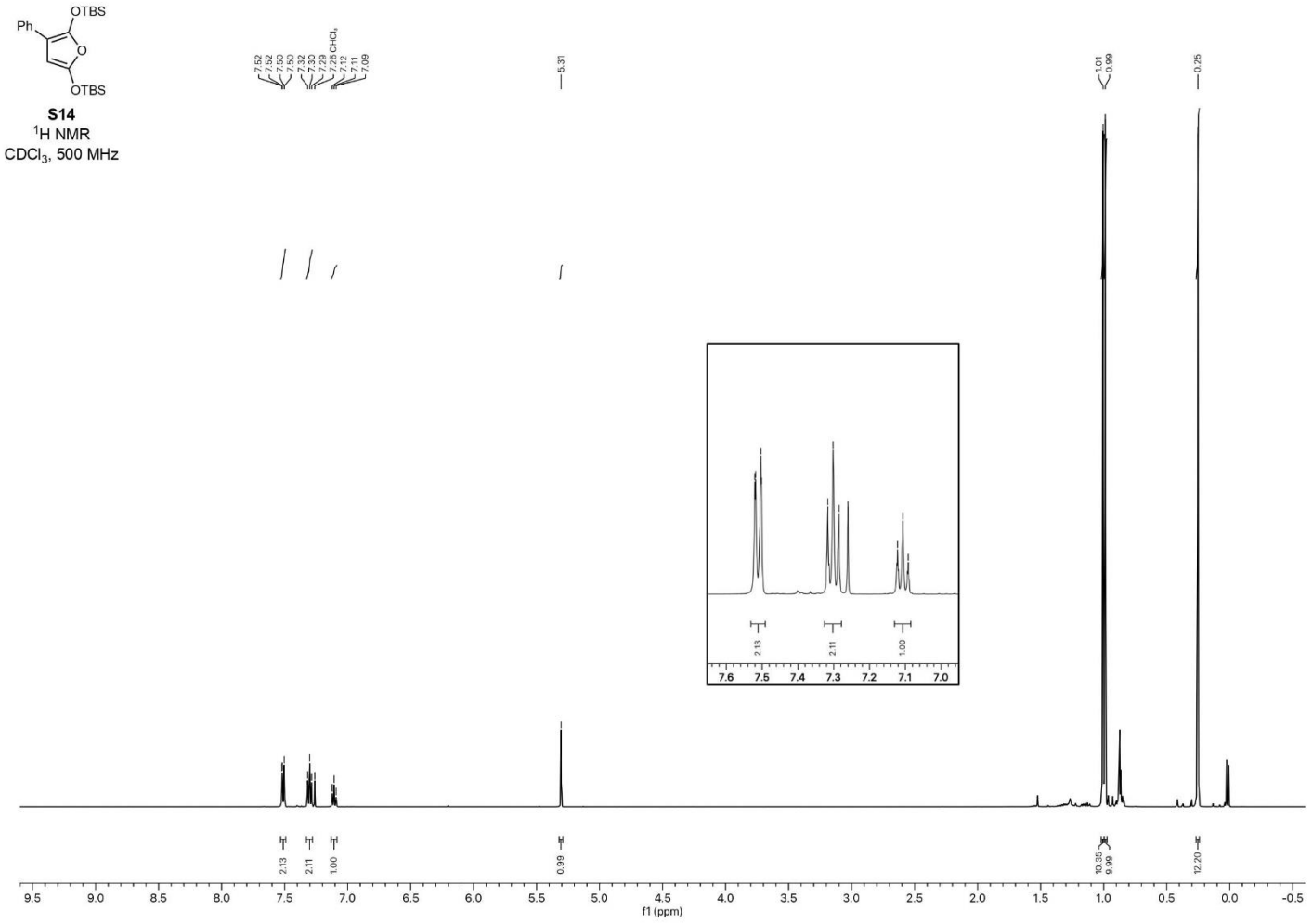
OTBS
Ph
O
OTBS
S14
1H NMR
CDCl3, 500 MHz
7.52
7.52
7.50
7.50
7.32
7.30
7.28
7.26 CHCl3
7.12
7.11
7.09
5.31
1.01
0.99
0.25
2.13
2.11
1.00
0.99
10.35
9.99
12.20
f1 (ppm)

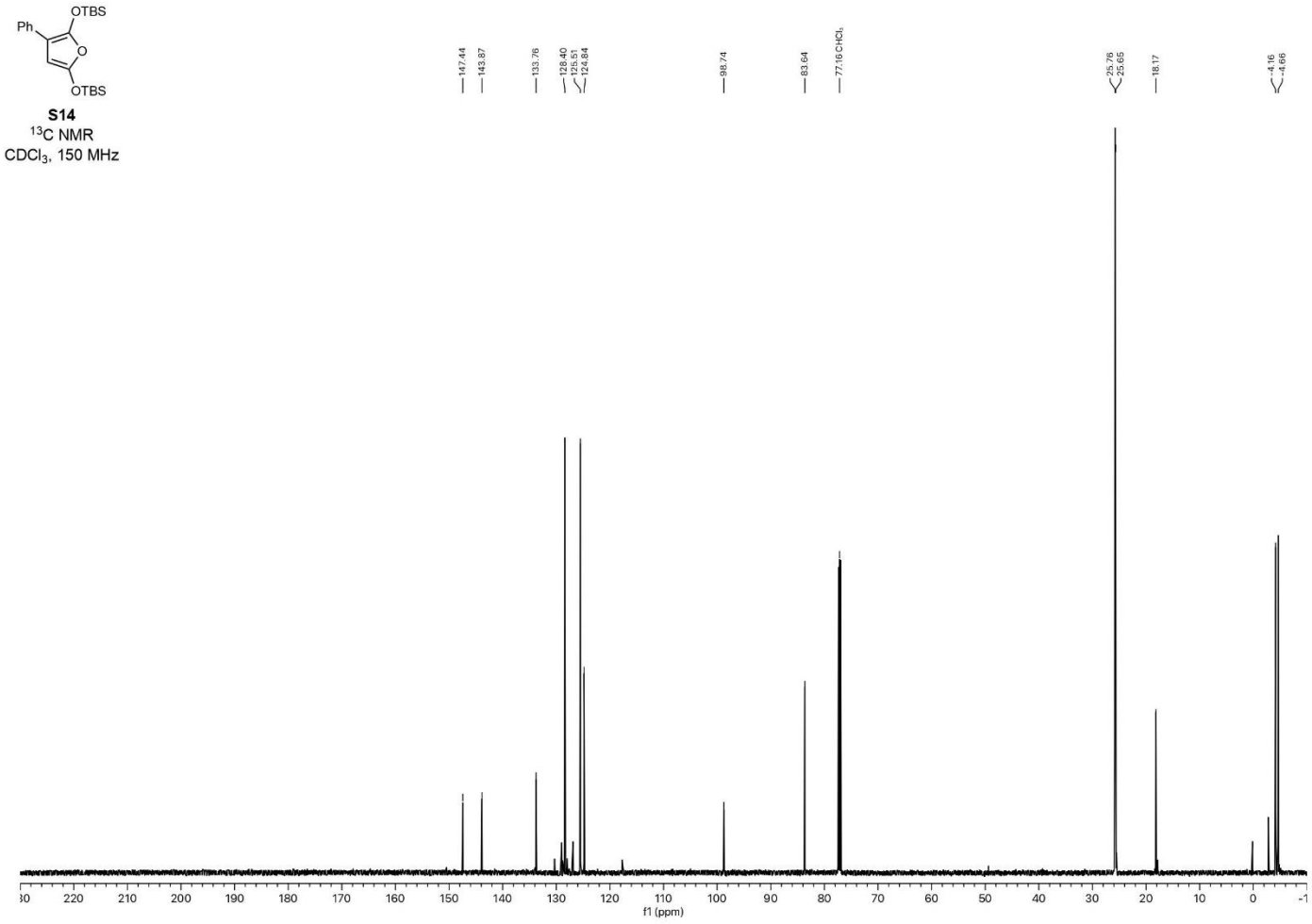
OTBS
Ph
O
OTBS
S14
13C NMR
CDCl3, 150 MHz
147.44
143.87
133.76
128.40
125.51
124.84
98.74
83.64
77.16 CHCl3
25.76
25.65
18.17
-4.16
-4.66
f1 (ppm)

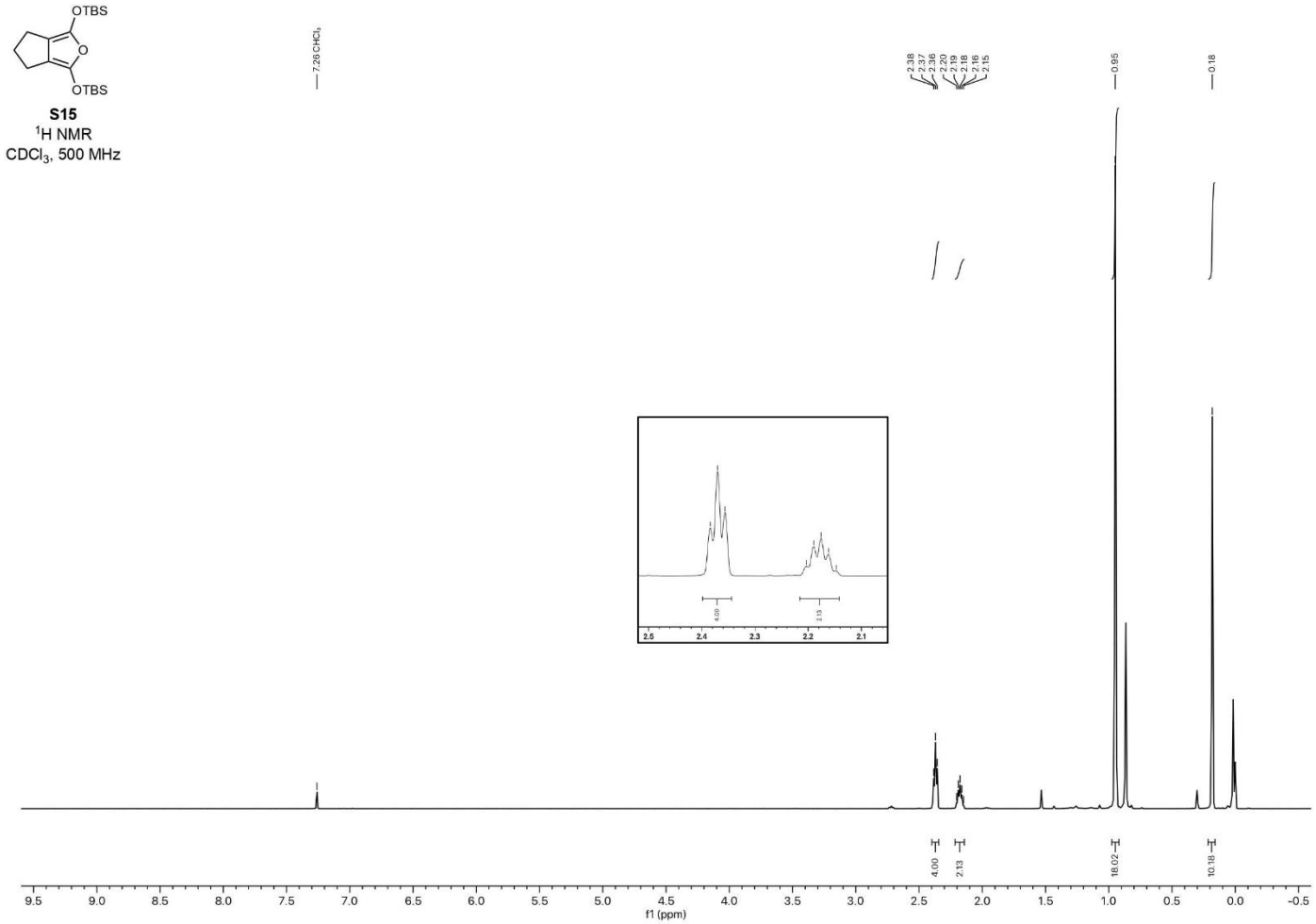
OTBS
OTBS
S15
1H NMR
CDCl3, 500 MHz
7.26 CHCl3
2.38
2.37
2.36
2.20
2.19
2.18
2.16
2.15
0.95
0.18
4.00
2.13
18.02
10.18
f1 (ppm)

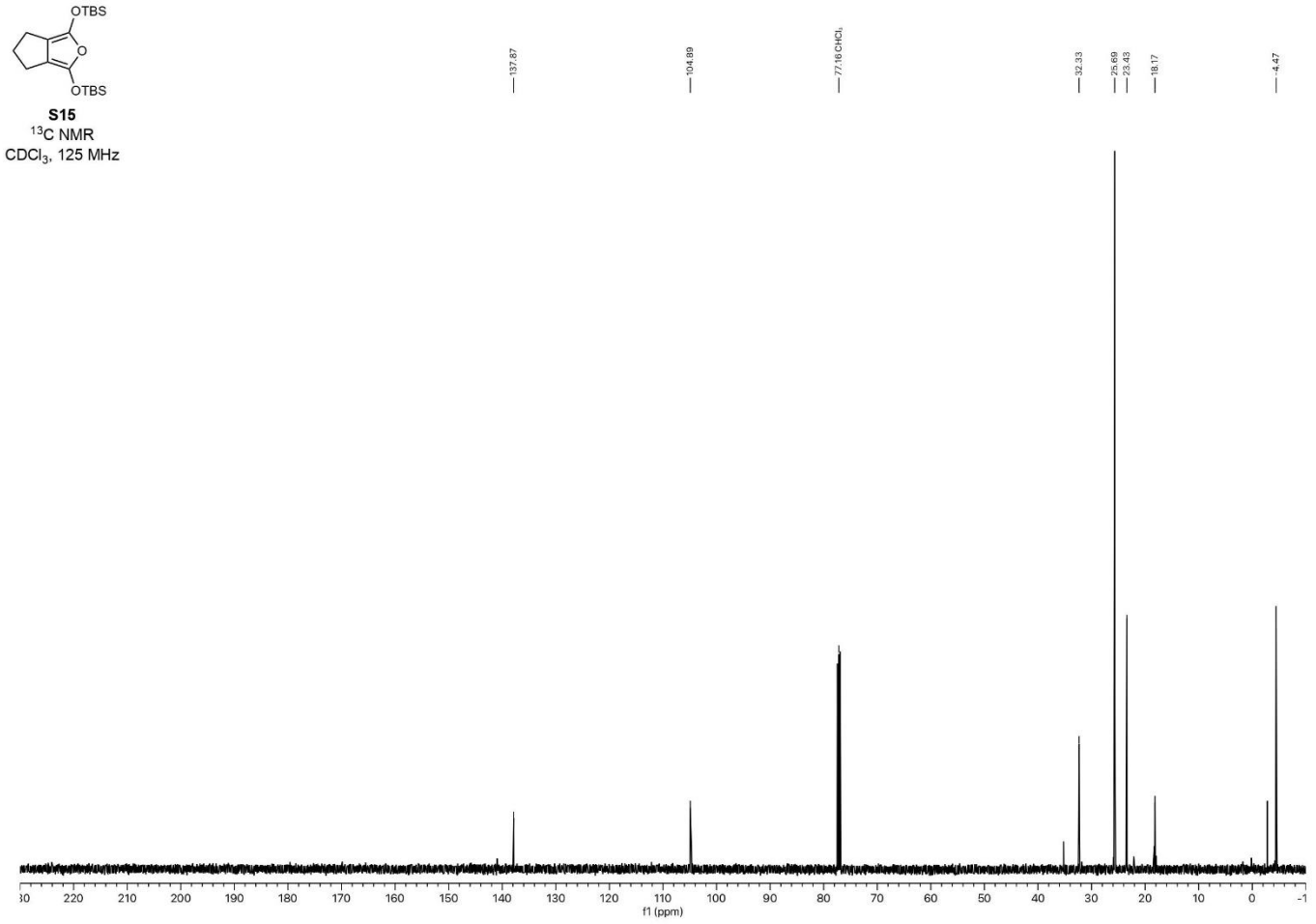
OTBS
O
OTBS
S15
13C NMR
CDCl3, 125 MHz
137.67
104.99
77.16 CHCl3
32.33
25.69
23.43
18.17
-4.47
f1 (ppm)

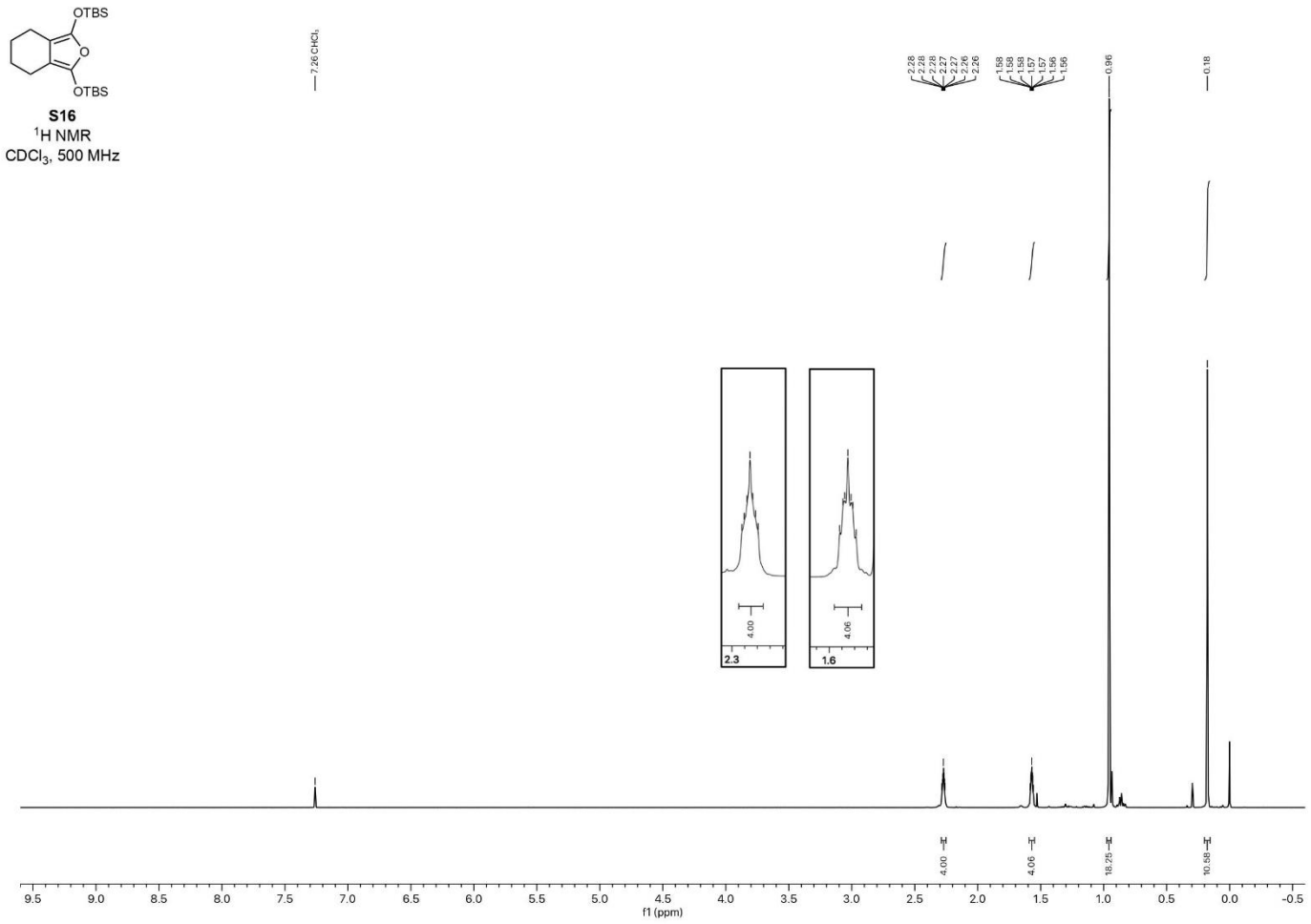
OTBS
OTBS
S16
1H NMR
CDCl3, 500 MHz
7.26 CHCl3
2.28
2.28
2.28
2.27
2.27
2.27
2.26
2.26
1.58
1.58
1.58
1.57
1.57
1.56
1.56
0.96
0.18
4.00
4.06
2.3
1.6
4.00
4.06
18.25
10.58
9.5
9.0
8.5
8.0
7.5
7.0
6.5
6.0
5.5
5.0
4.5
4.0
3.5
3.0
2.5
2.0
1.5
1.0
0.5
0.0
-0.5
f1 (ppm)

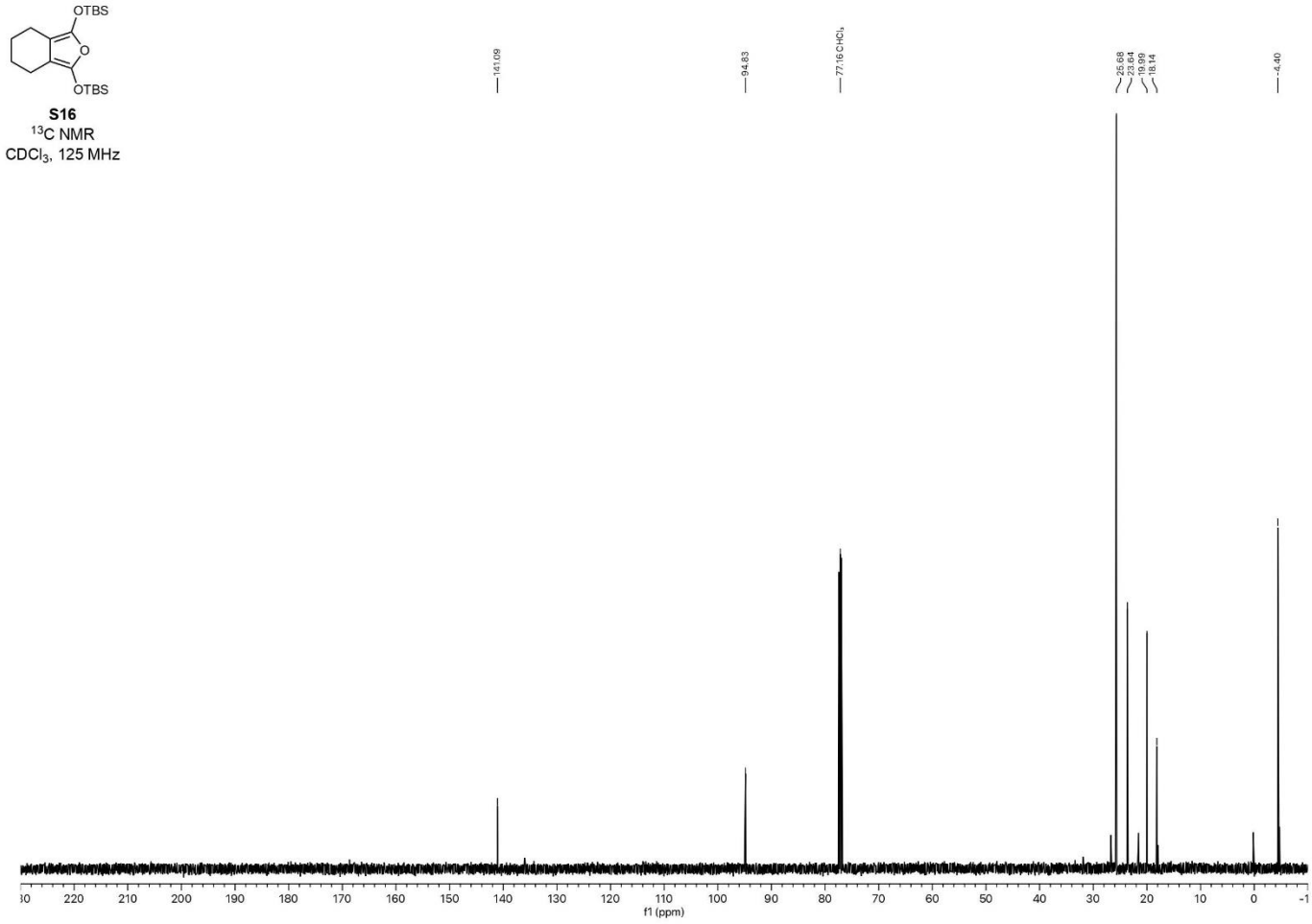
OTBS
O
OTBS
S16
13C NMR
CDCl3, 125 MHz
141.09
94.83
77.16 CHCl3
25.68
23.64
19.99
18.14
-4.40
f1 (ppm)

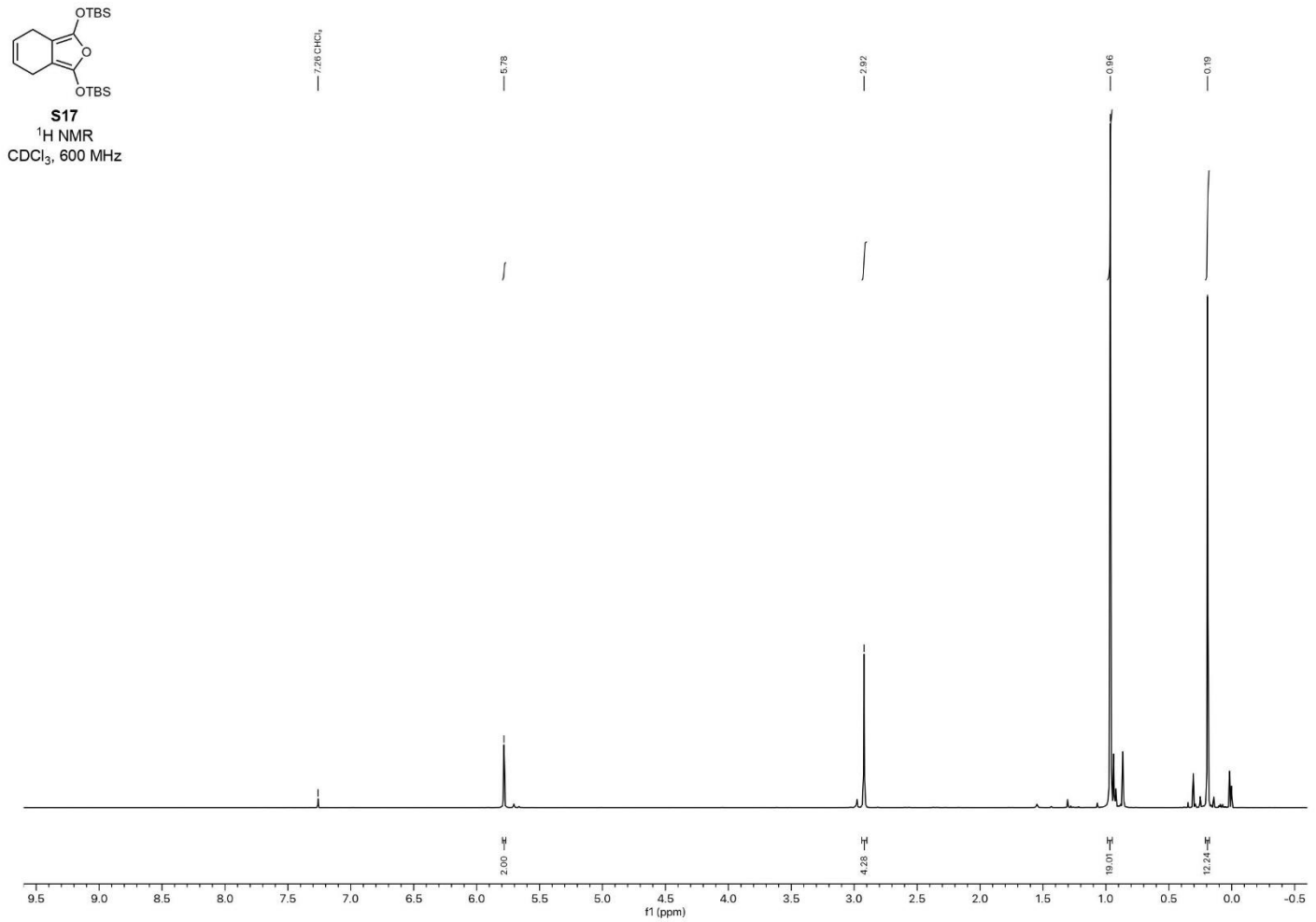
OTBS
OTBS
O
S17
1H NMR
CDCl3, 600 MHz
7.26 CHCl3
5.78
2.92
0.96
0.19
2.00
4.28
19.01
12.24
9.5
9.0
8.5
8.0
7.5
7.0
6.5
6.0
5.5
5.0
4.5
4.0
3.5
3.0
2.5
2.0
1.5
1.0
0.5
0.0
-0.5
f1 (ppm)

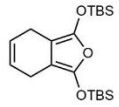

S17
^{13}C NMR
$CDCl_3$, 150 MHz

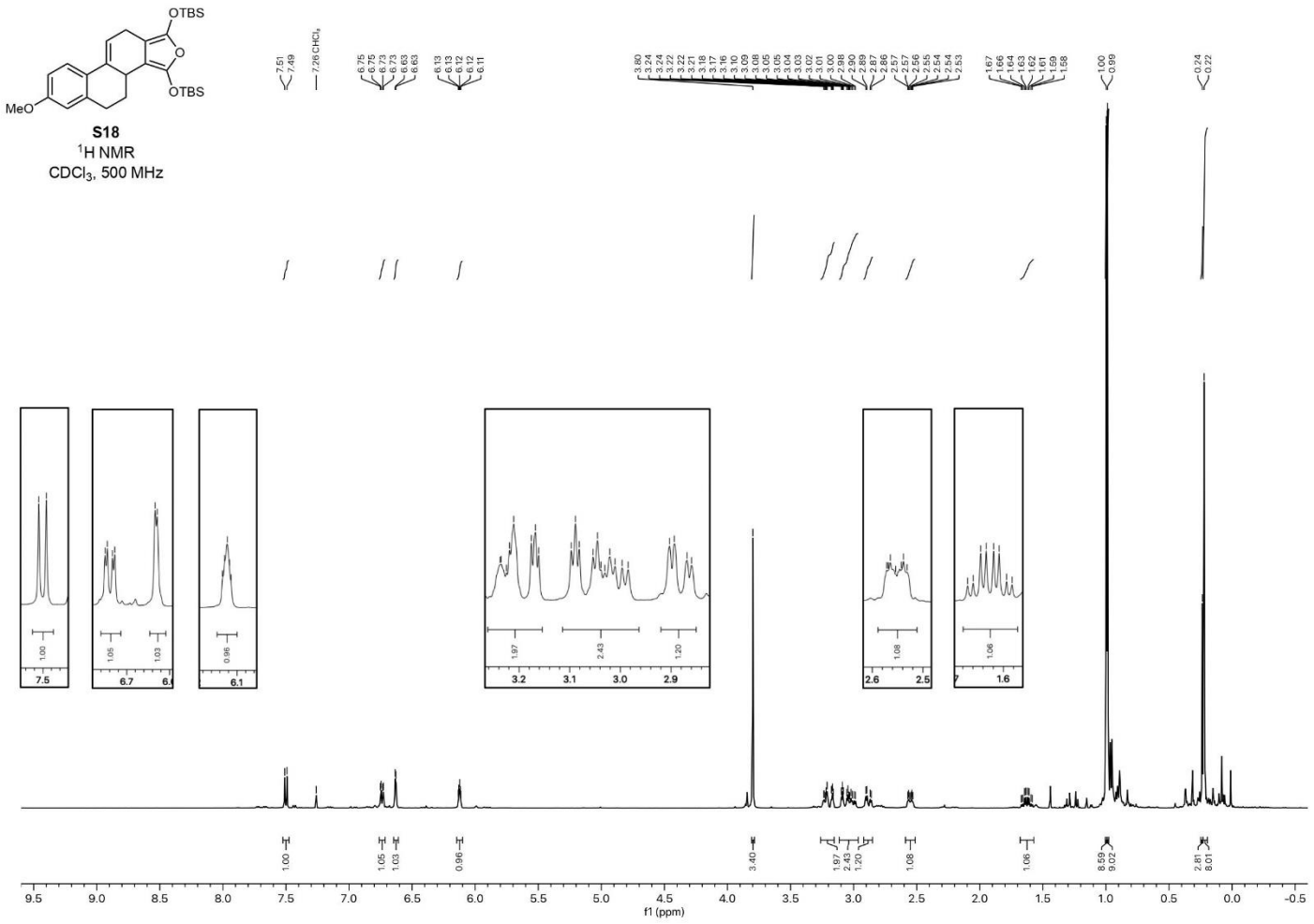
OTBS
OTBS
MeO
S18
1H NMR
CDCl3, 500 MHz
f1 (ppm)

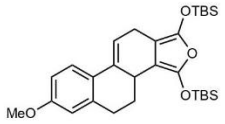

S18
^{13}C NMR
$CDCl_3$, 125 MHz

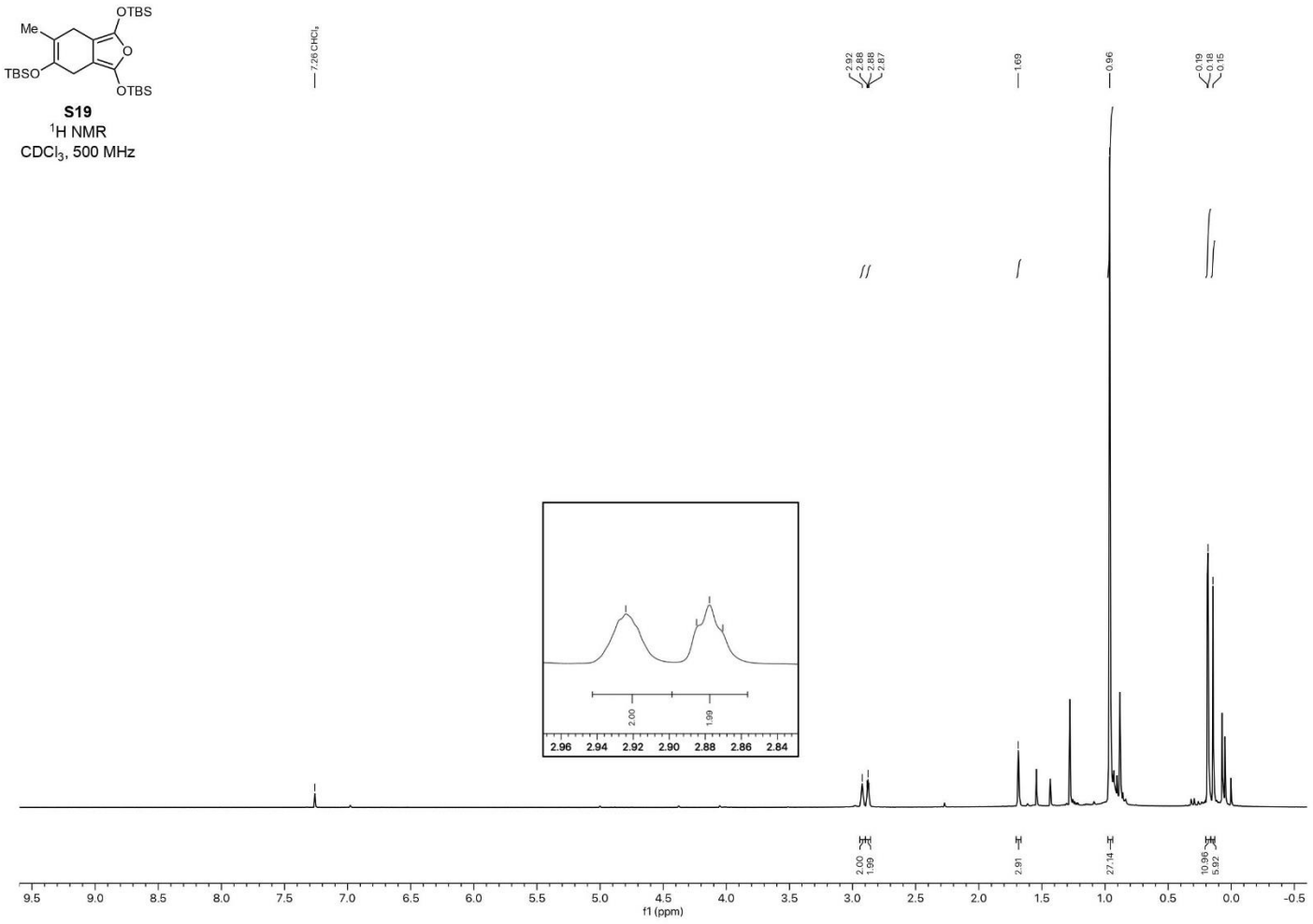
OTBS
Me
TBSO
O
OTBS
S19
1H NMR
CDCl3, 500 MHz
7.26 CHCl3
2.92
2.88
2.88
2.87
1.69
0.96
0.19
0.18
0.15
2.96 2.94 2.92 2.90 2.88 2.86 2.84
2.00
1.99
2.00
1.99
2.91
27.14
10.96
5.92
9.5 9.0 8.5 8.0 7.5 7.0 6.5 6.0 5.5 5.0 4.5 4.0 3.5 3.0 2.5 2.0 1.5 1.0 0.5 0.0 -0.5
f1 (ppm)

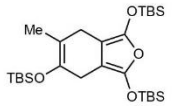

S19
^{13}C NMR
$CDCl_3$, 125 MHz

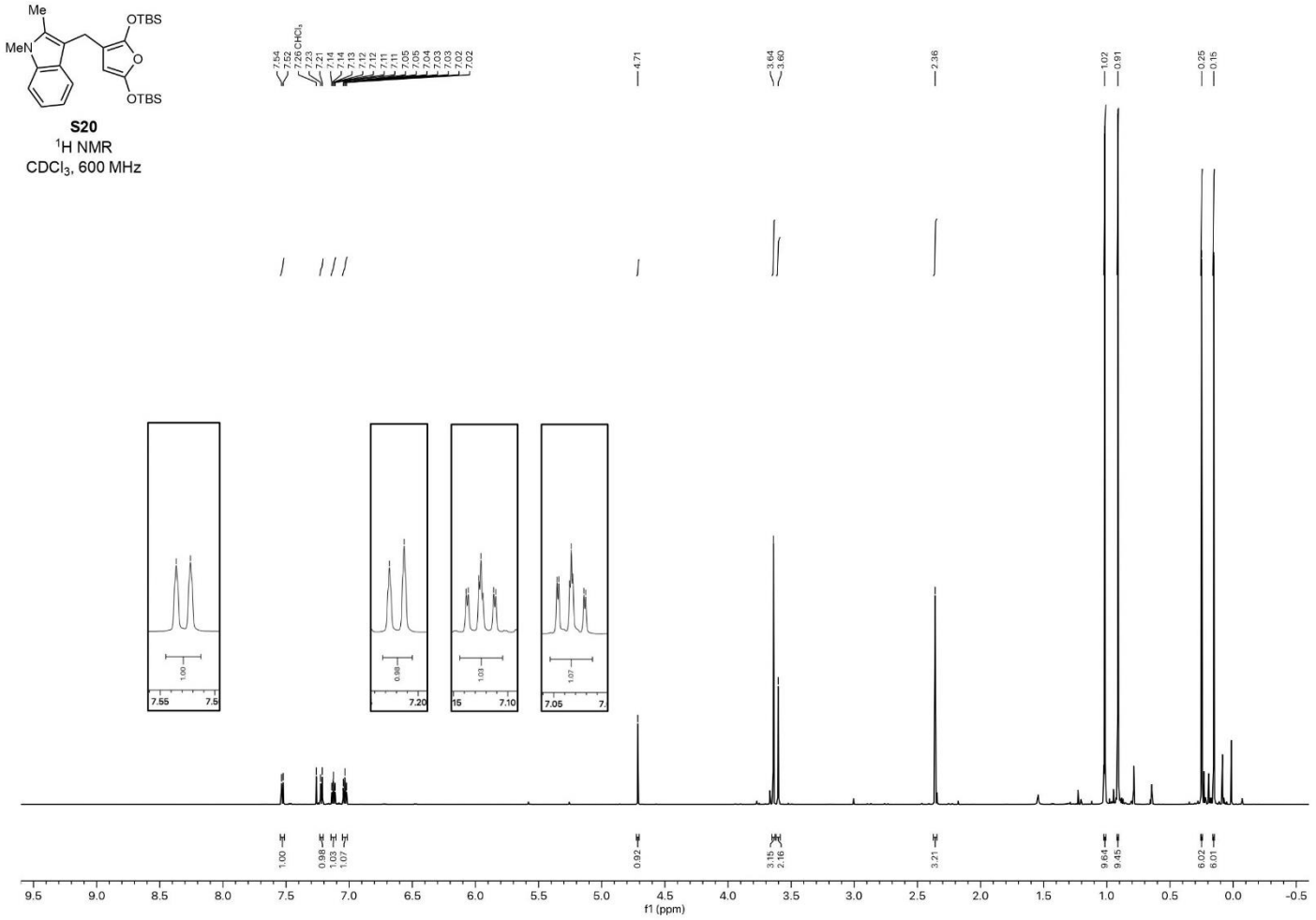
Me
MeN
OTBS
O
OTBS
S20
1H NMR
CDCl3, 600 MHz
7.54
7.52
7.26 CHCl3
7.23
7.21
7.14
7.14
7.13
7.13
7.12
7.11
7.11
7.05
7.05
7.04
7.03
7.03
7.02
7.02
7.02
4.71
3.64
3.60
2.36
1.02
0.91
0.25
0.15
1.00
0.98
1.03
1.07
0.92
3.15
2.16
3.21
9.64
9.45
6.02
6.01
f1 (ppm)

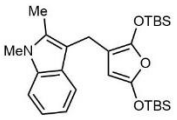

S20
^{13}C NMR
$CDCl_3$, 150 MHz

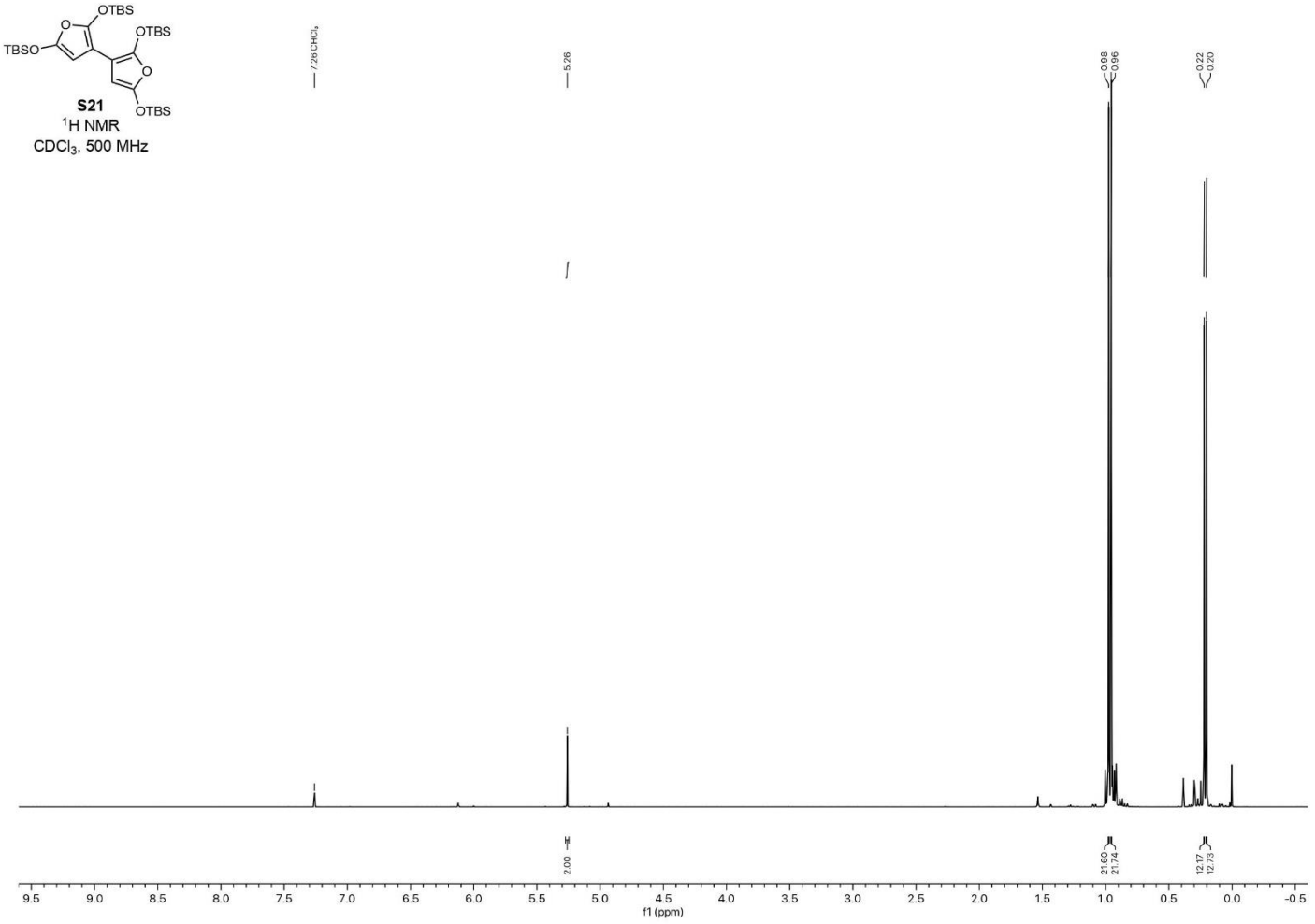
OTBS
OTBS
TBSO
OTBS
S21
1H NMR
CDCl3, 500 MHz
7.26 CHCl3
5.26
0.98
0.96
0.22
0.20
2.00
21.60
21.74
12.17
12.73
9.5 9.0 8.5 8.0 7.5 7.0 6.5 6.0 5.5 5.0 4.5 4.0 3.5 3.0 2.5 2.0 1.5 1.0 0.5 0.0 -0.5
f1 (ppm)

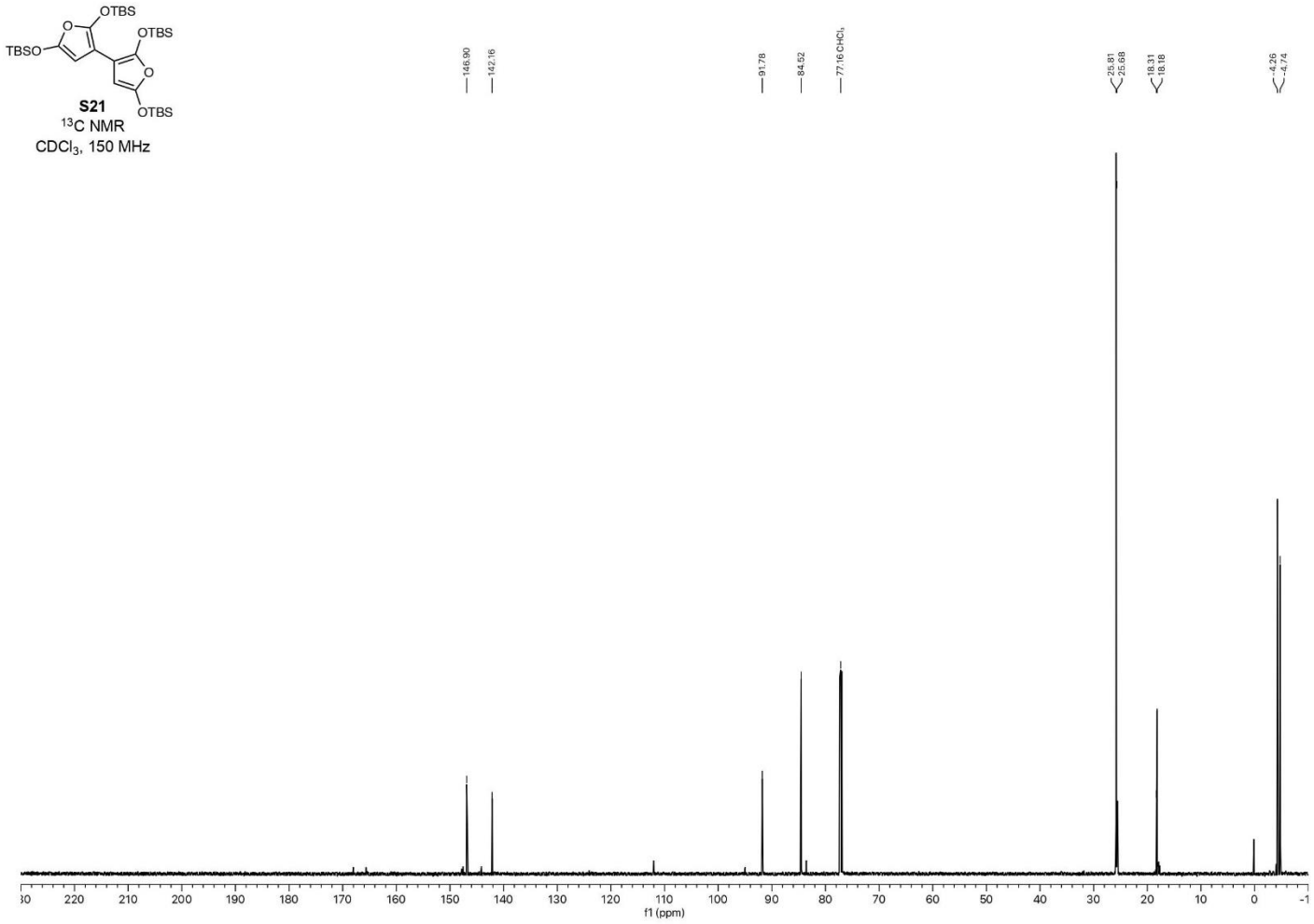
OTBS
TBSO
OTBS
OTBS
S21
13C NMR
CDCl3, 150 MHz
146.90
142.16
91.78
84.52
77.16 CHCl3
25.81
25.68
18.31
18.18
-4.26
-4.74
f1 (ppm)

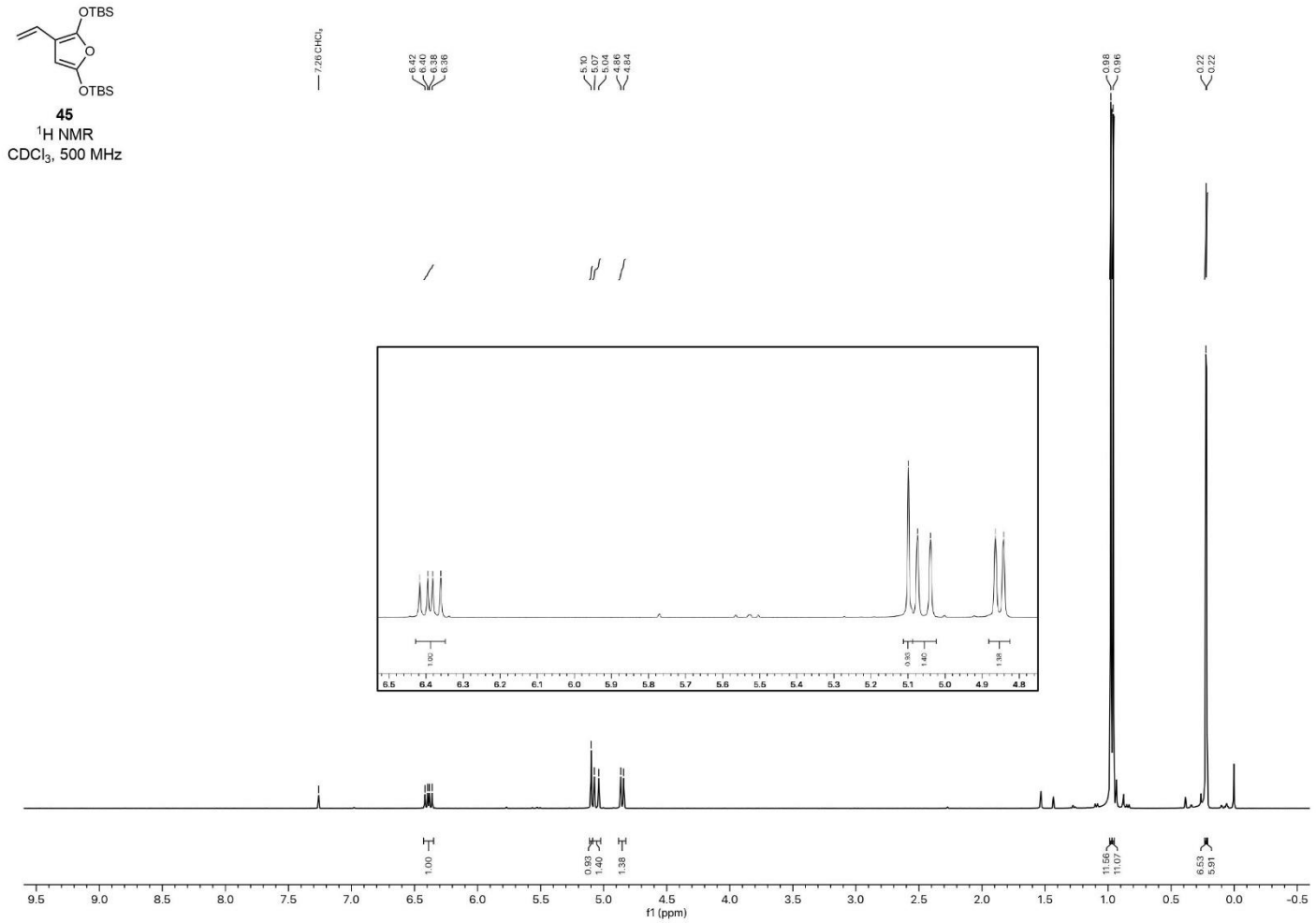
OTBS
OTBS
45
1H NMR
CDCl3, 500 MHz
7.26 CHCl3
6.42
6.40
6.38
6.36
5.10
5.07
5.04
4.86
4.84
0.98
0.96
0.22
0.22
1.00
0.93
1.40
1.38
11.56
11.07
6.53
5.91
f1 (ppm)

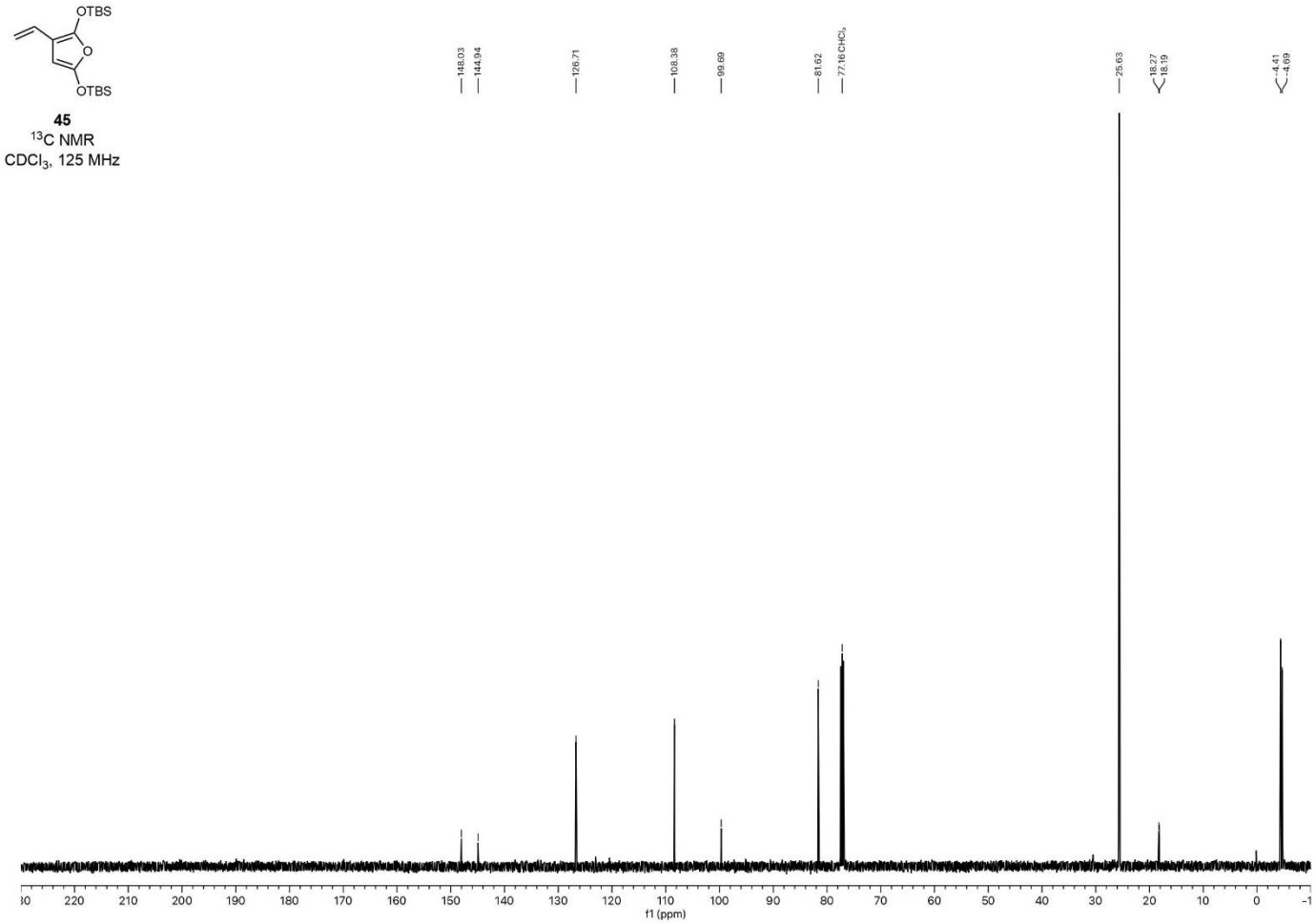
OTBS
O
OTBS
45
^{13}C NMR
$CDCl_3$, 125 MHz
148.03
144.94
126.71
108.38
99.69
81.62
77.16 $CHCl_3$
25.63
18.27
18.19
-4.41
-4.69
f1 (ppm)

Mono(silyloxy)furans

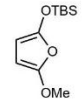

4
^{1}H NMR
$CDCl_3$, 500 MHz

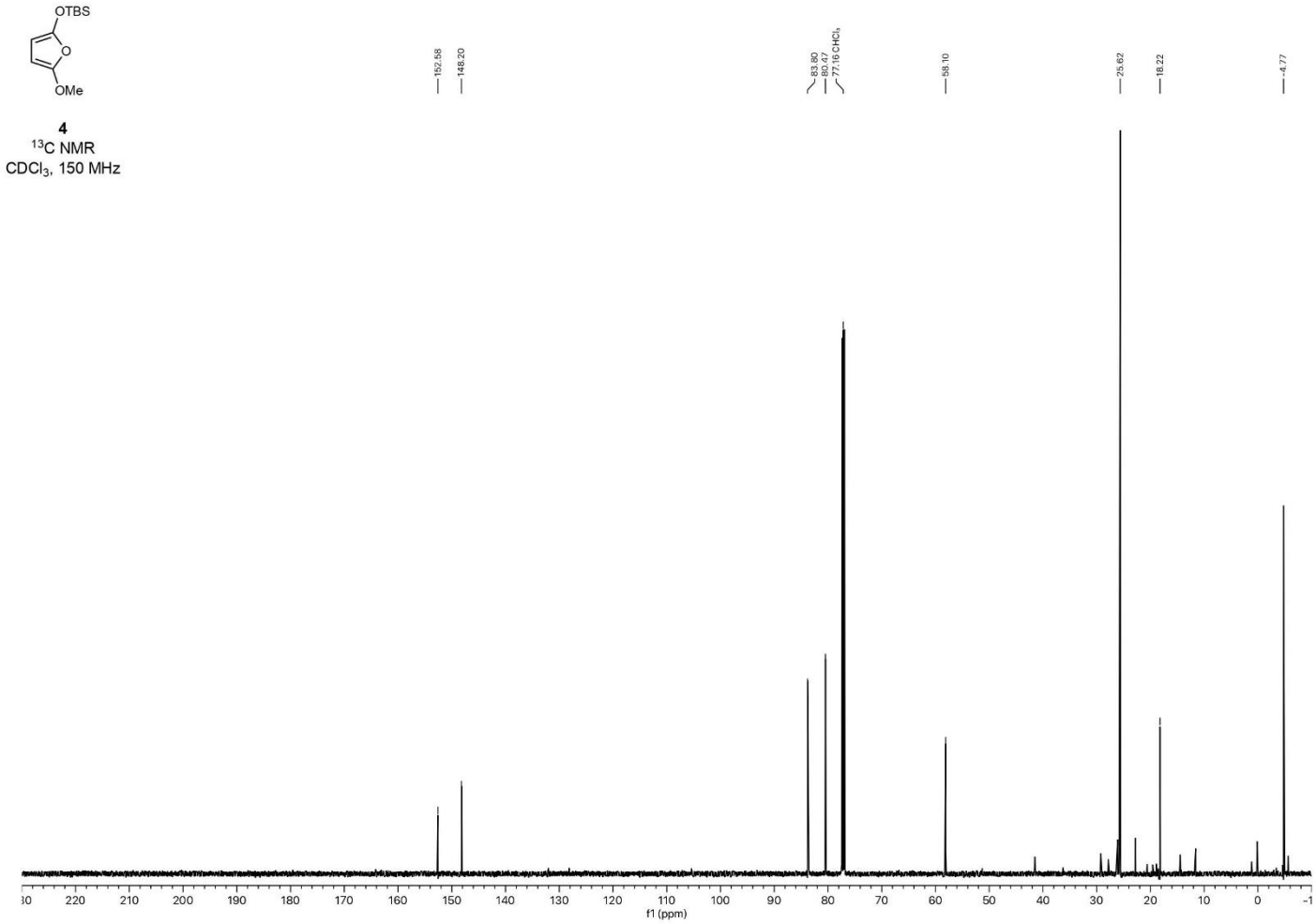
OTBS
O
OMe
4
^{13}C NMR
$CDCl_3$, 150 MHz
152.58
148.20
83.80
80.47
77.16 $CHCl_3$
59.10
25.62
18.22
-4.77
f1 (ppm)

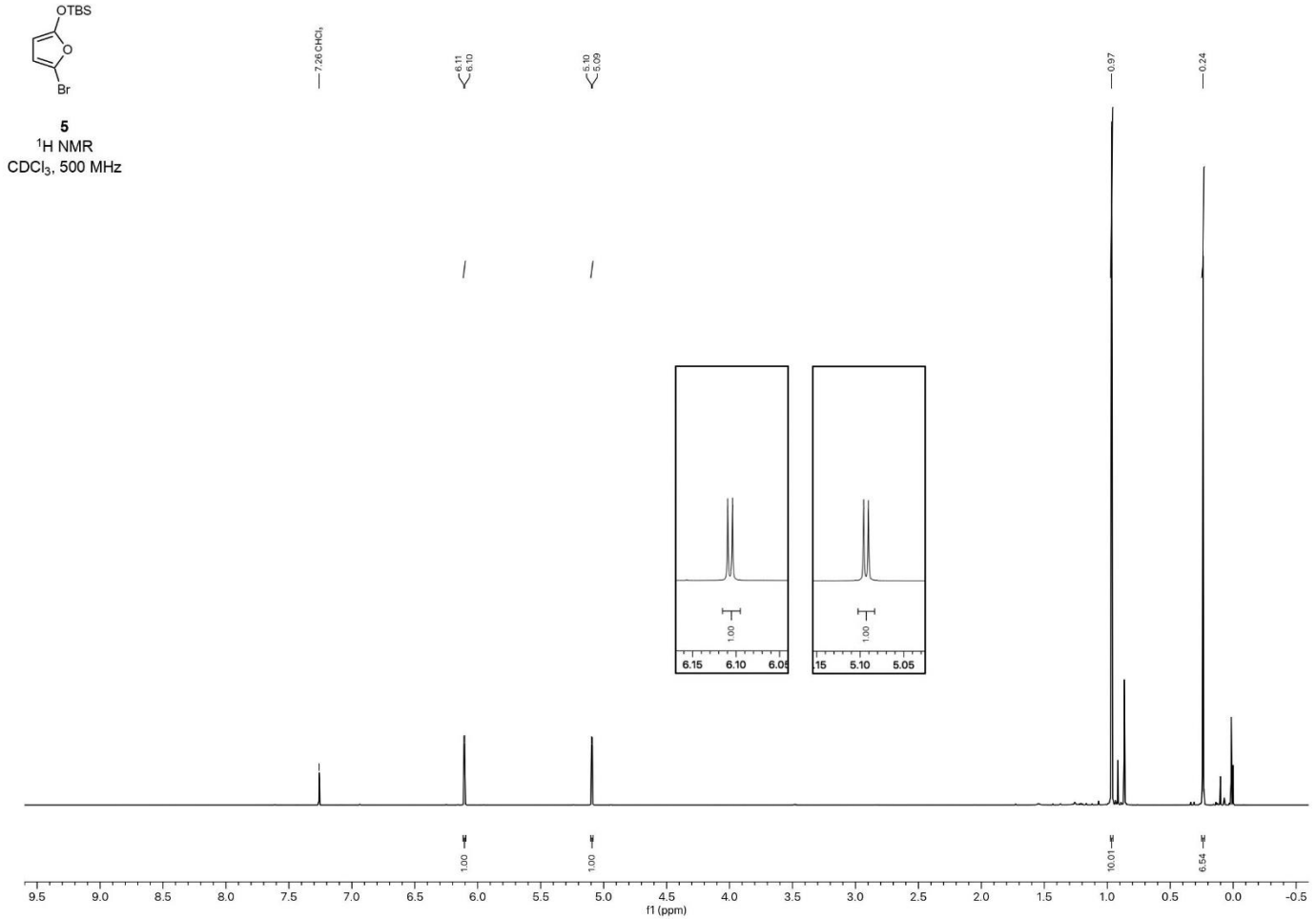
OTBS
O
Br
5
1H NMR
CDCl3, 500 MHz
7.26 CHCl3
6.11
6.10
5.10
5.09
0.97
0.24
1.00
1.00
10.01
6.54
f1 (ppm)

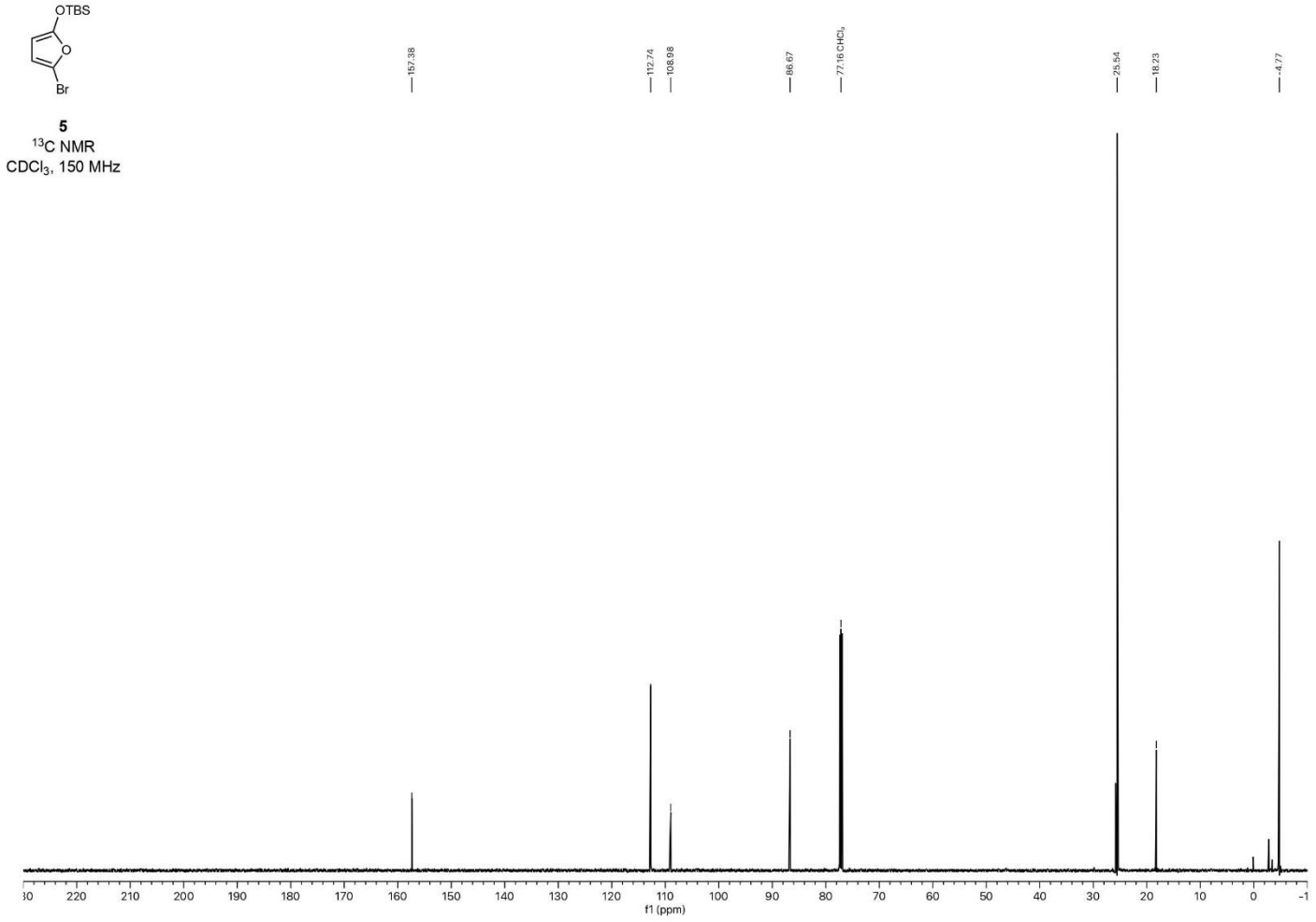
OTBS
O
Br
5
13C NMR
CDCl3, 150 MHz
157.38
112.74
108.98
86.67
77.16 CHCl3
25.54
18.23
-4.77
f1 (ppm)

Step-wise Diels–Alder/Aromatization Studies

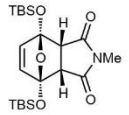

6-*endo*
^{1}H NMR
C_6D_6, 600 MHz

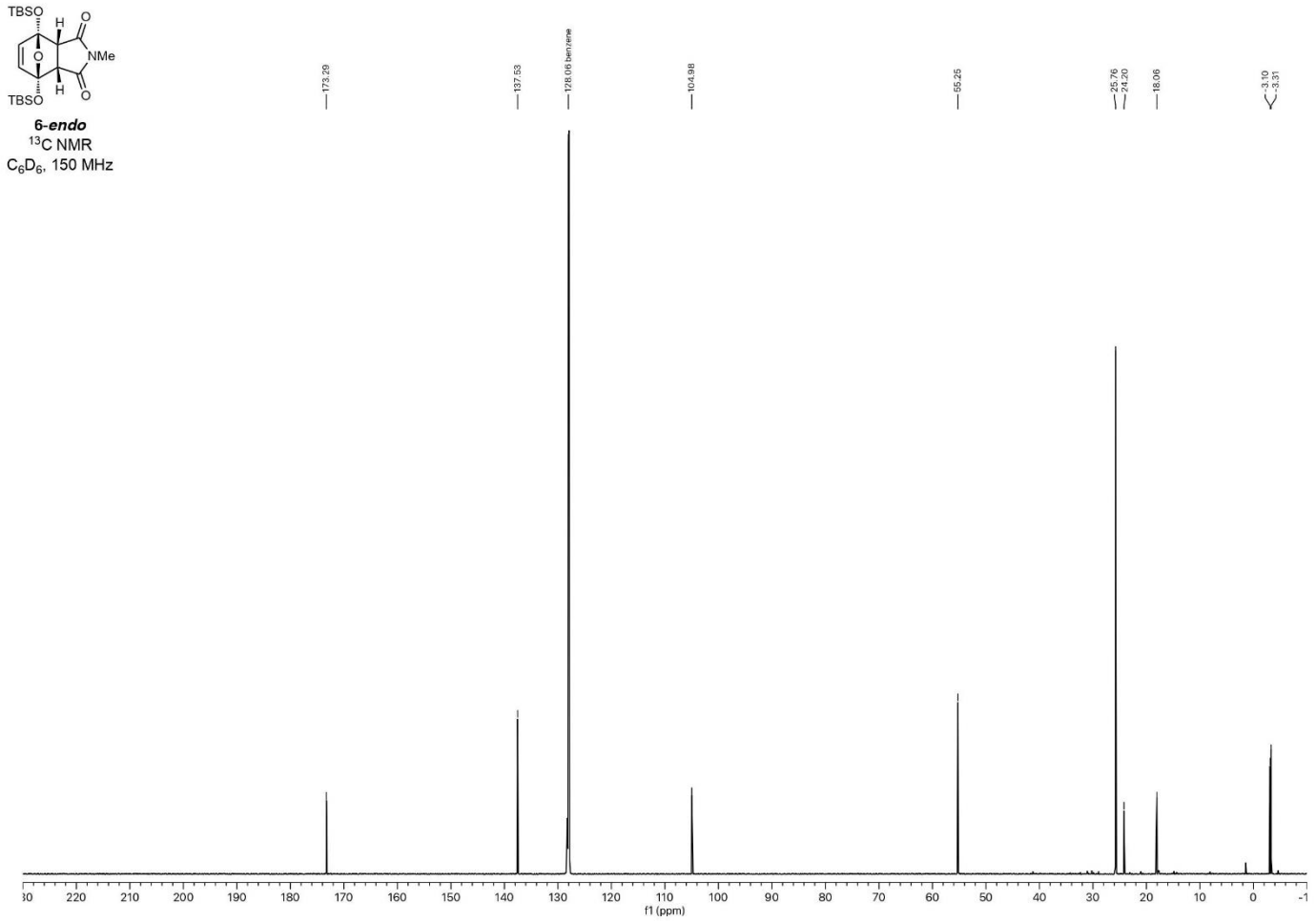
TBSO
H
O
NMe
O
TBSO
H
O
6-endo
13C NMR
C6D6, 150 MHz
173.29
137.53
128.06 benzene
104.98
55.25
25.76
24.20
18.06
-3.10
-3.31
f1 (ppm)

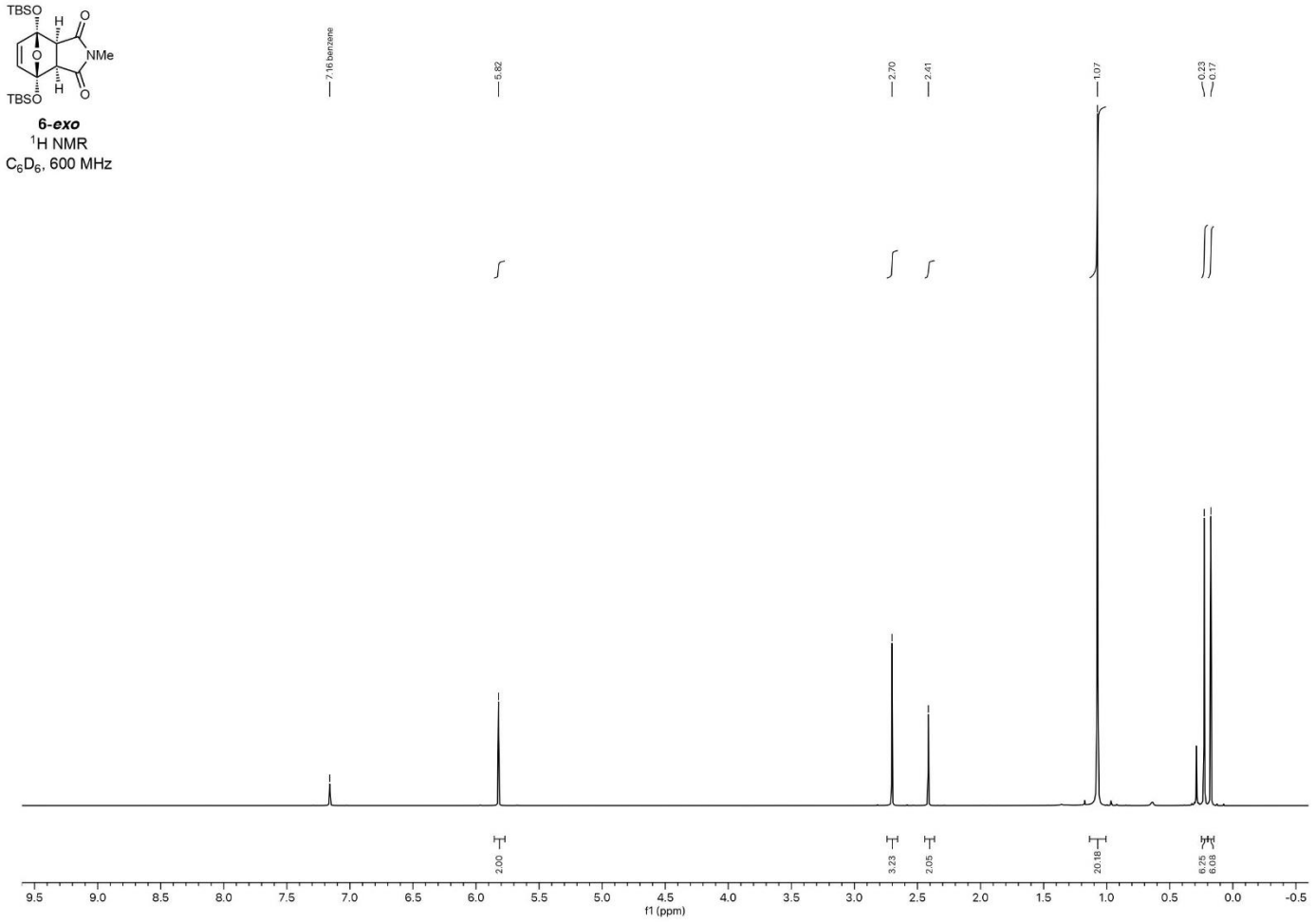
TBSO
H
O
NMe
O
O
H
TBSO
6-exo
1H NMR
C6D6, 600 MHz
7.16 benzene
5.82
2.70
2.41
1.07
0.23
0.17
2.00
3.23
2.05
20.18
6.25
6.08
9.5
9.0
8.5
8.0
7.5
7.0
6.5
6.0
5.5
5.0
4.5
4.0
3.5
3.0
2.5
2.0
1.5
1.0
0.5
0.0
-0.5
f1 (ppm)

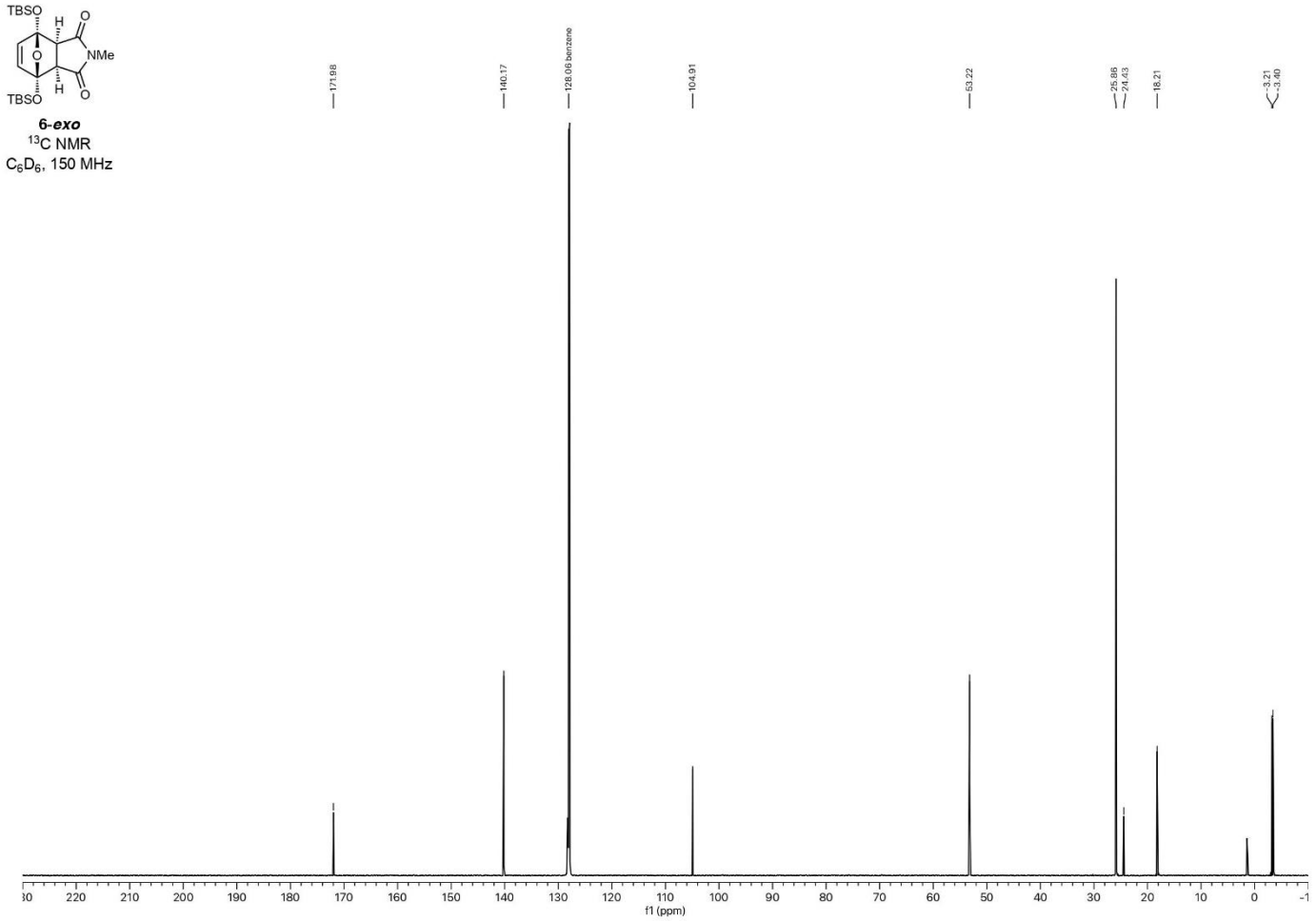
TBSO
TBSO
O
H
O
NMe
O
H
O
6-exo
13C NMR
C6D6, 150 MHz
171.98
140.17
128.05 benzene
104.91
53.22
25.86
24.43
18.21
-3.21
-3.40
f1 (ppm)

para-Hydroquinones

Diene Scope

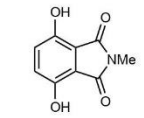

7

^{1}H NMR

$(CD_3)_2SO$, 500 MHz

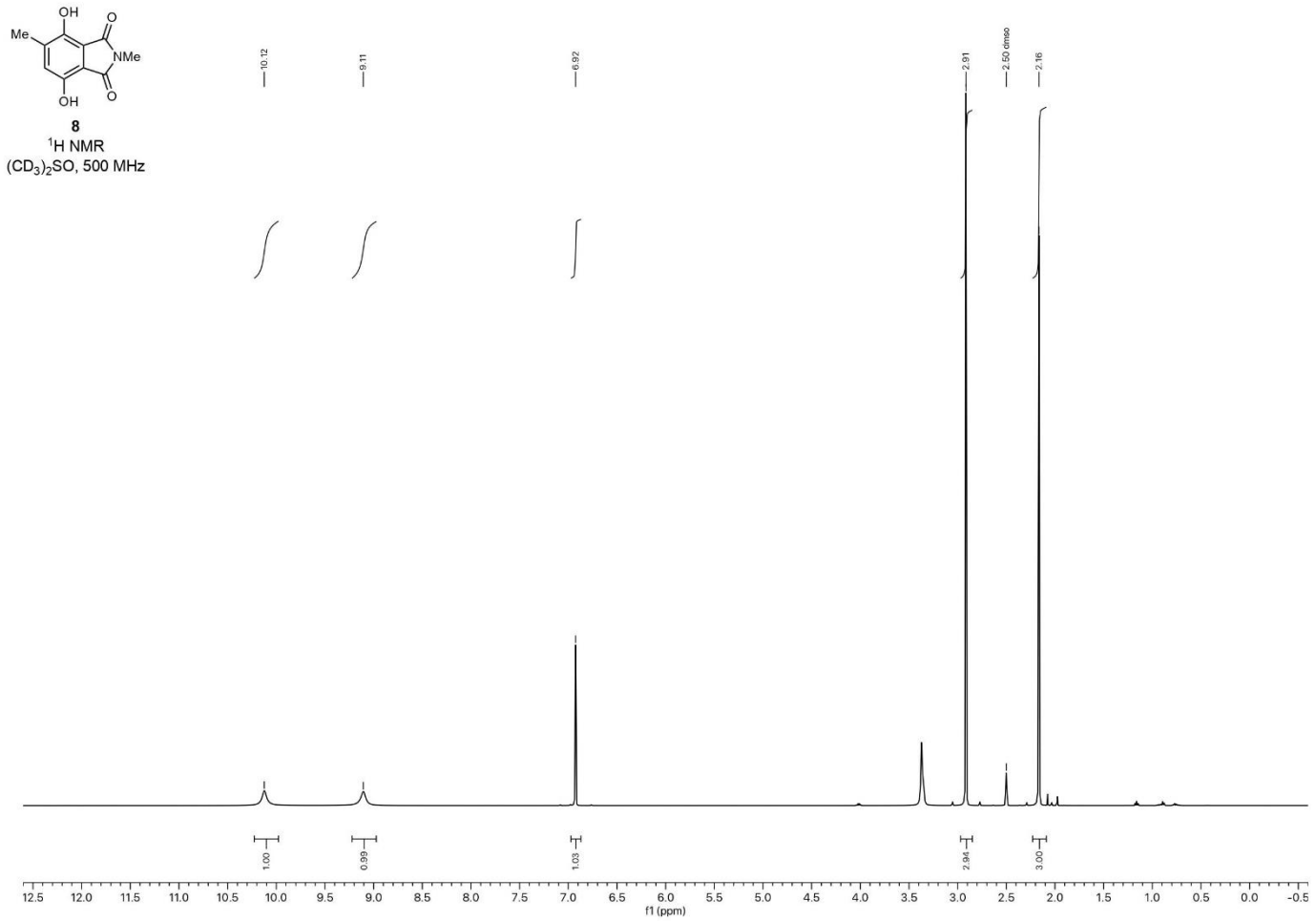
OH
O
Me
NMe
O
OH
8
1H NMR
(CD3)2SO, 500 MHz
10.12
9.11
6.92
2.91
2.50 dmso
2.16
1.00
0.99
1.03
2.94
3.00
12.5 12.0 11.5 11.0 10.5 10.0 9.5 9.0 8.5 8.0 7.5 7.0 6.5 6.0 5.5 5.0 4.5 4.0 3.5 3.0 2.5 2.0 1.5 1.0 0.5 0.0 -0.5
f1 (ppm)

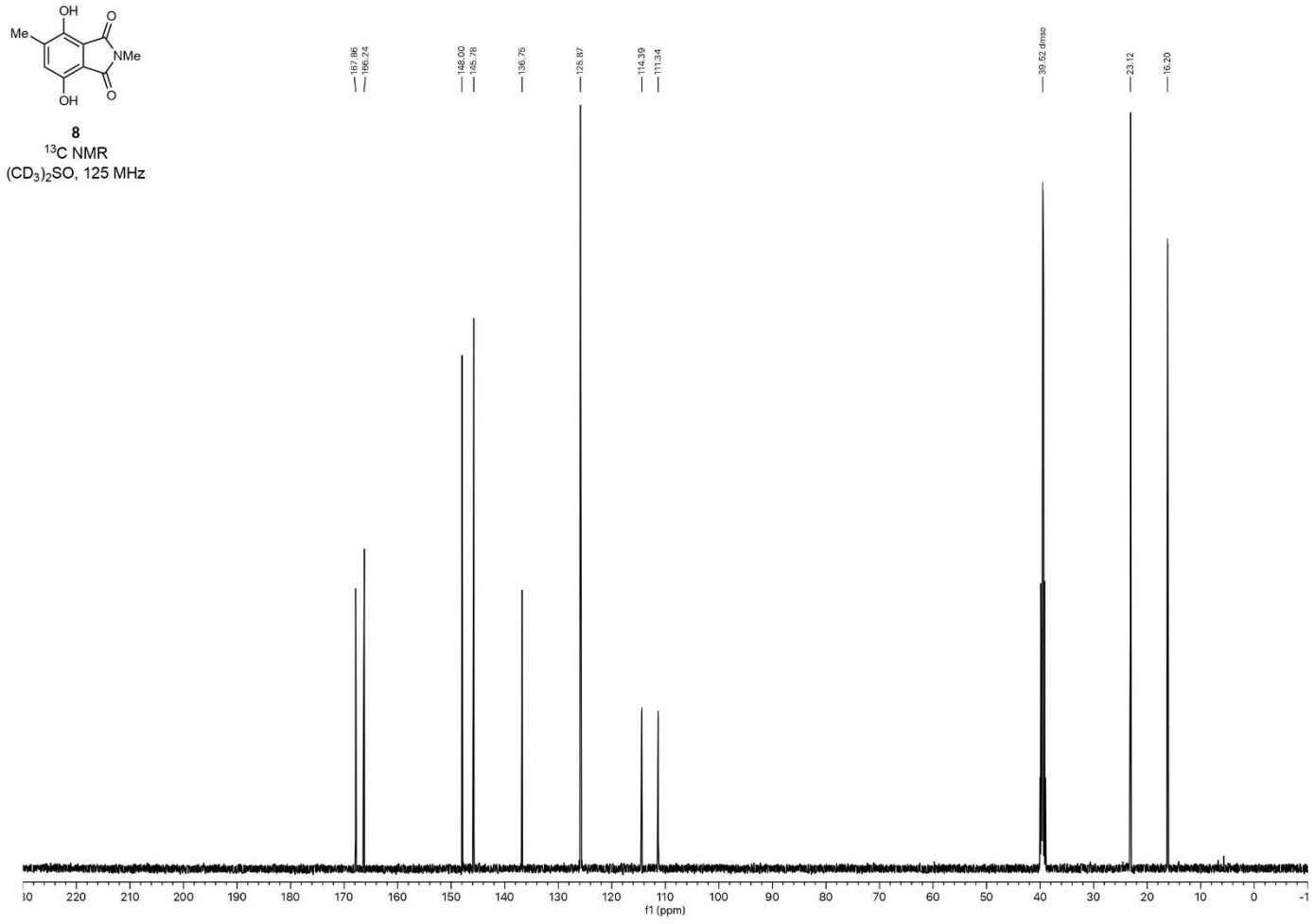
OH
O
Me
NMe
O
OH
8
13C NMR
(CD3)2SO, 125 MHz
167.86
166.24
148.00
145.78
136.75
125.87
114.39
111.34
39.52 dmso
23.12
16.20
f1 (ppm)

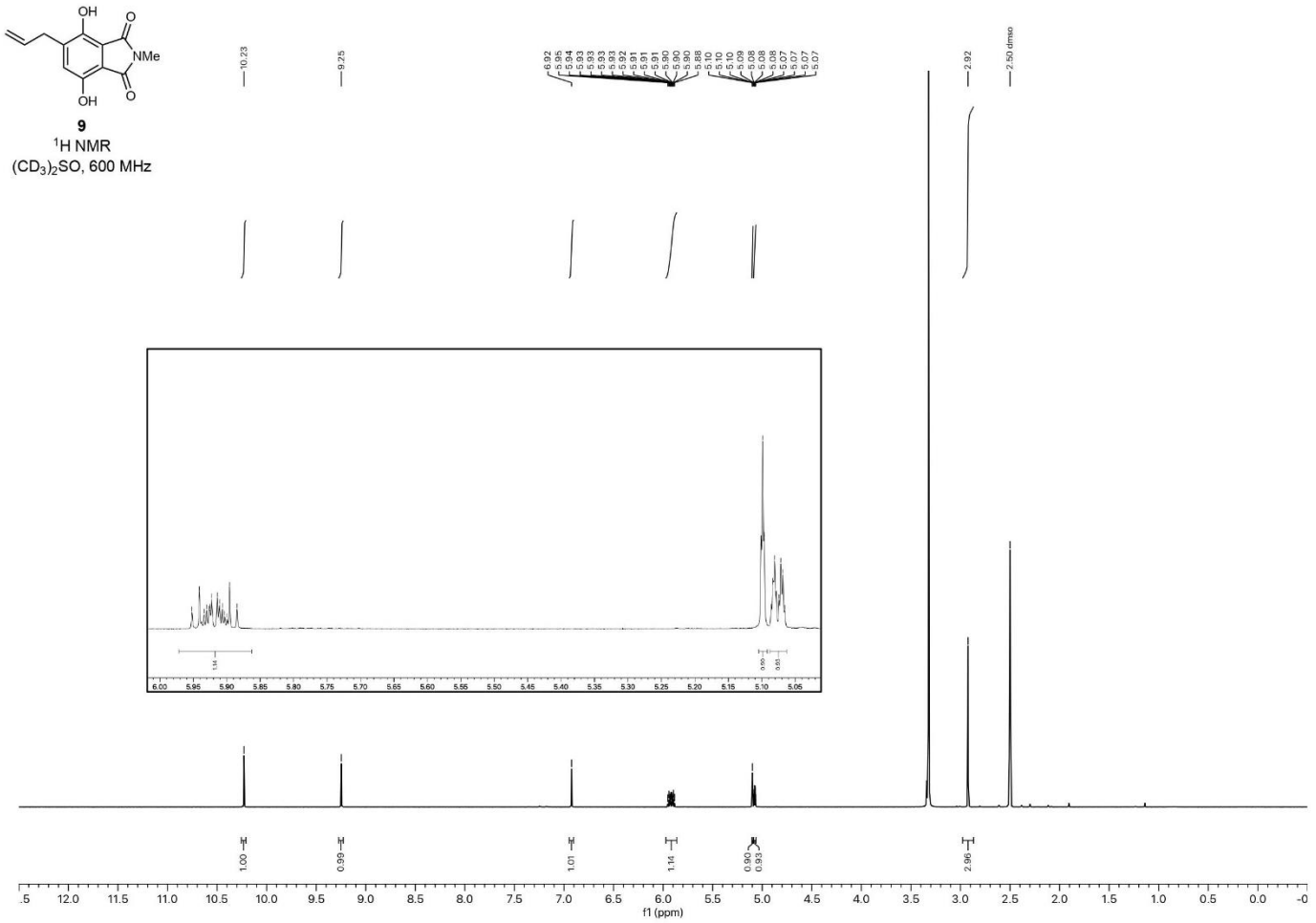
OH
O
NMe
O
OH
9
1H NMR
(CD3)2SO, 600 MHz
10.23
9.25
6.92
5.95
5.94
5.94
5.93
5.93
5.93
5.92
5.91
5.91
5.91
5.90
5.90
5.90
5.88
5.10
5.10
5.09
5.09
5.08
5.08
5.08
5.07
5.07
5.07
5.07
2.92
2.50 dmso
1.00
0.99
1.01
1.14
0.90
0.93
2.96
f1 (ppm)

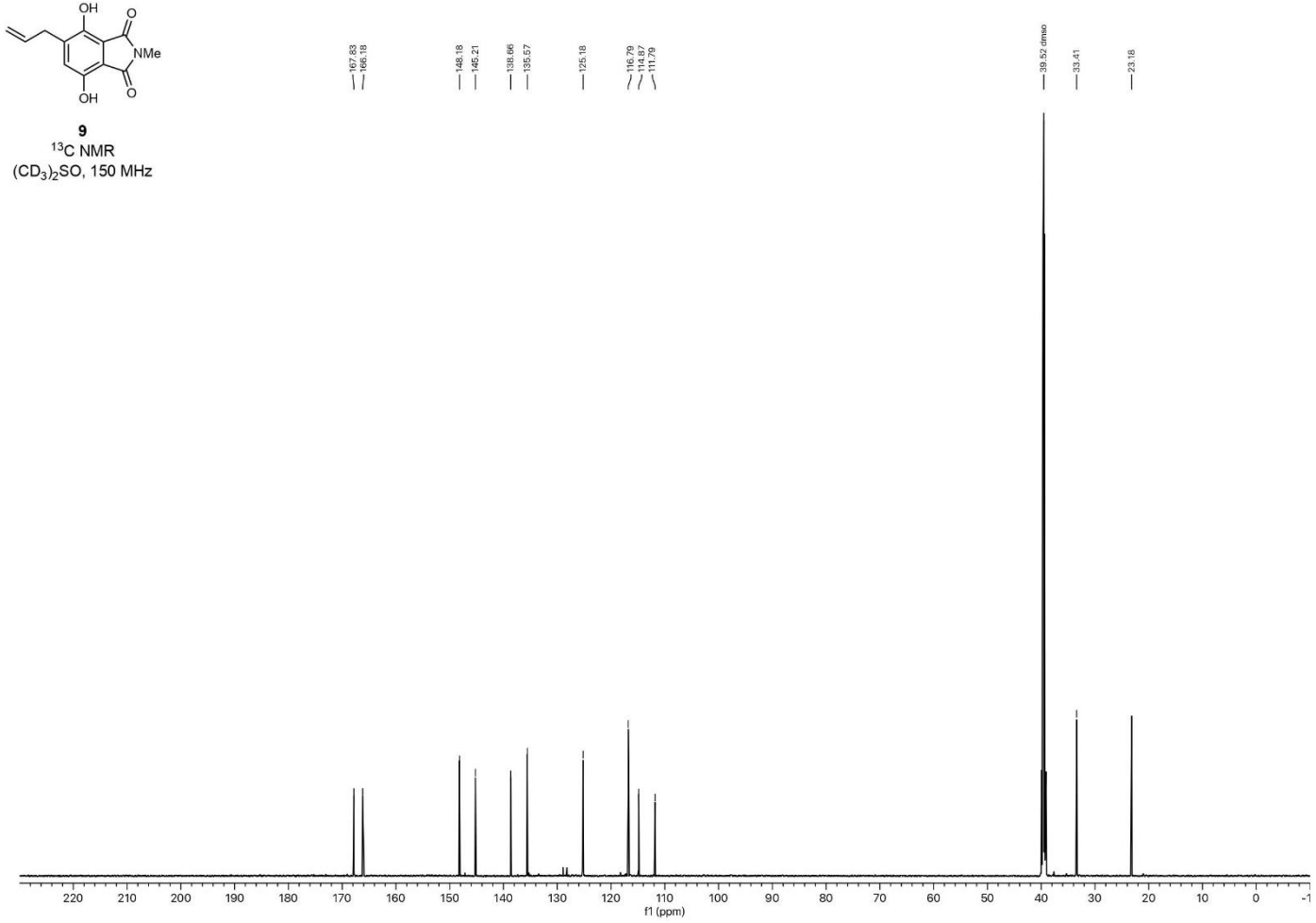
OH
O
NMe
O
OH
9
13C NMR
(CD3)2SO, 150 MHz
167.83
166.18
148.18
145.21
138.66
135.57
125.18
116.79
114.87
111.79
39.52 dmso
33.41
23.18
f1 (ppm)

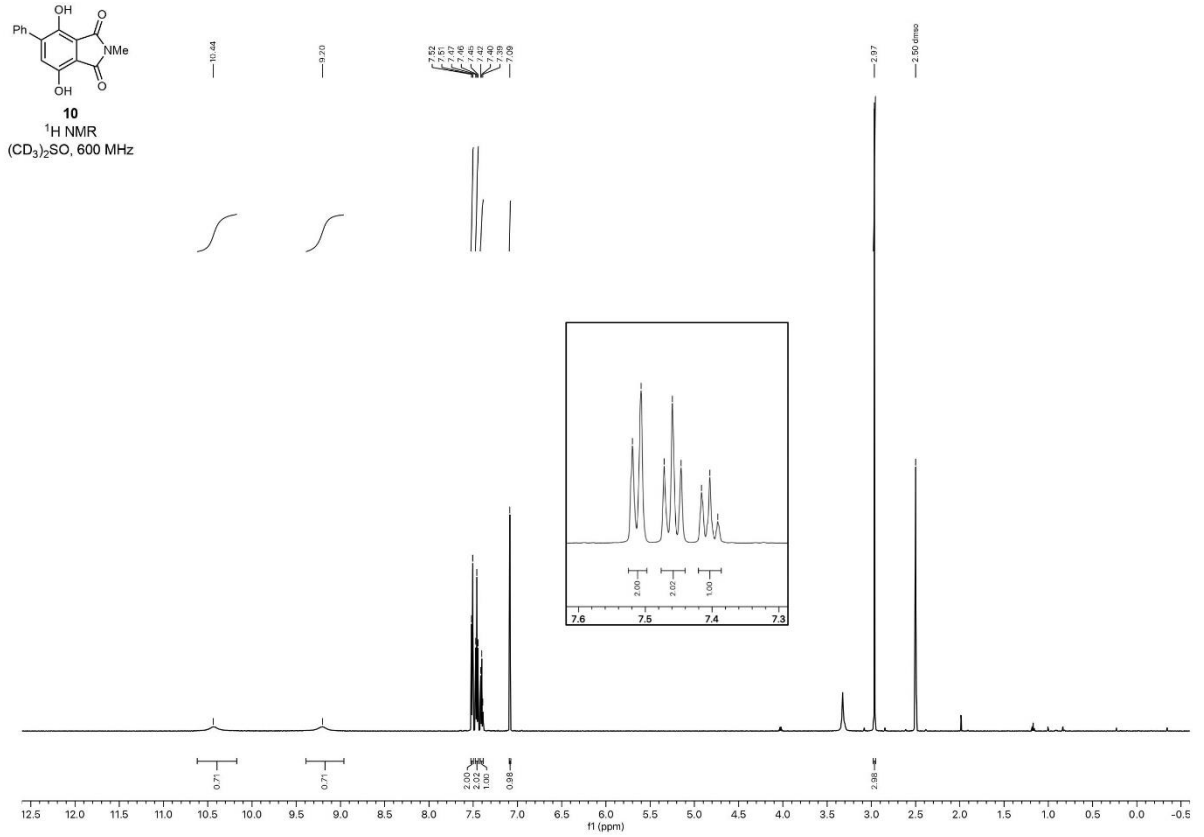
OH
Ph
O
NMe
O
OH
10
1H NMR
(CD3)2SO, 600 MHz
10.44
9.20
7.52
7.51
7.47
7.46
7.42
7.40
7.39
7.09
2.97
2.50 dmso
2.00
2.02
1.00
7.6
7.5
7.4
7.3
0.71
0.71
2.00
2.02
1.00
0.98
2.98
f1 (ppm)

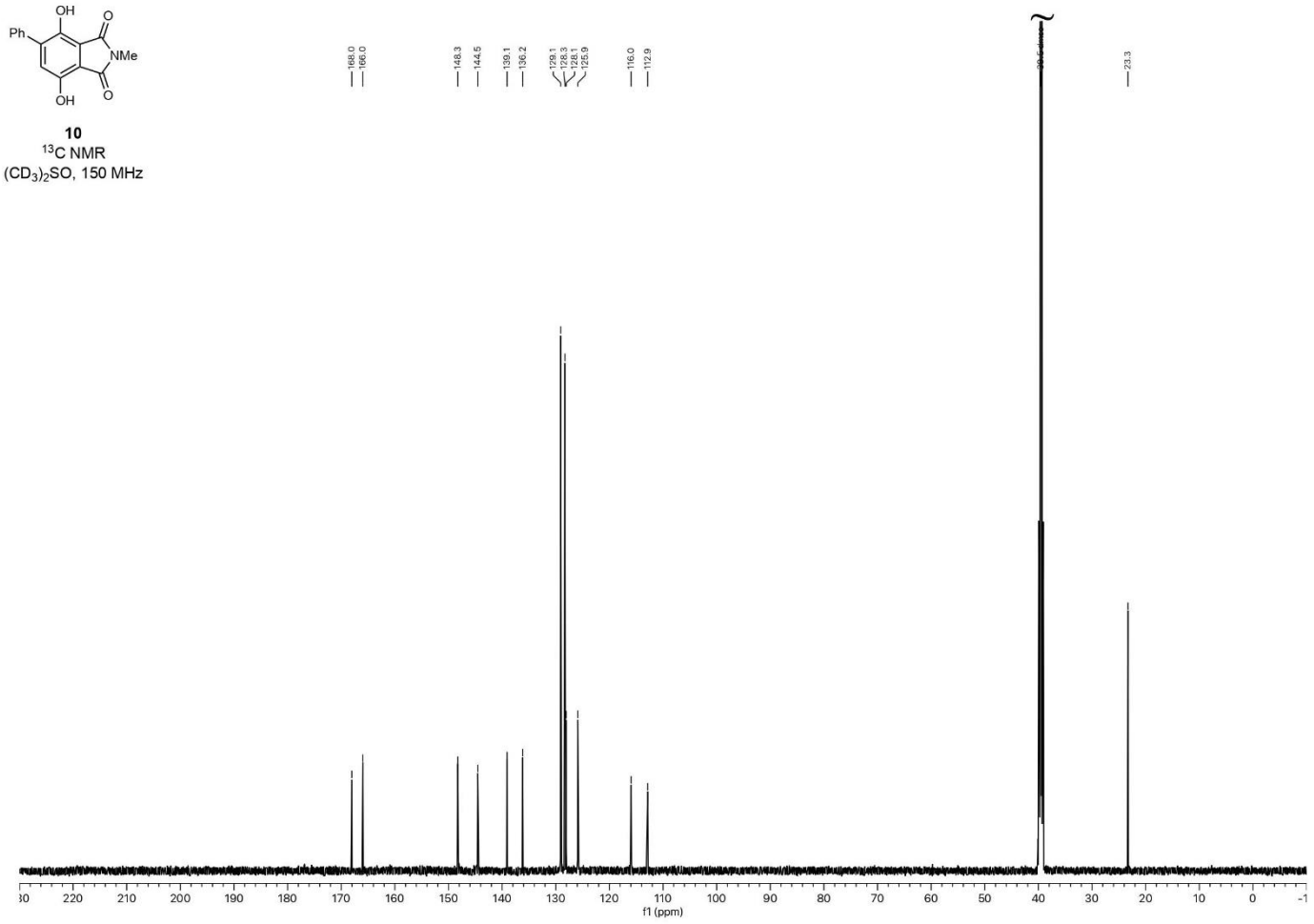
OH
Ph
O
NMe
O
OH
10
13C NMR
(CD3)2SO, 150 MHz
168.0
166.0
148.3
144.5
139.1
136.2
129.1
128.3
128.1
125.9
116.0
112.9
23.3
f1 (ppm)

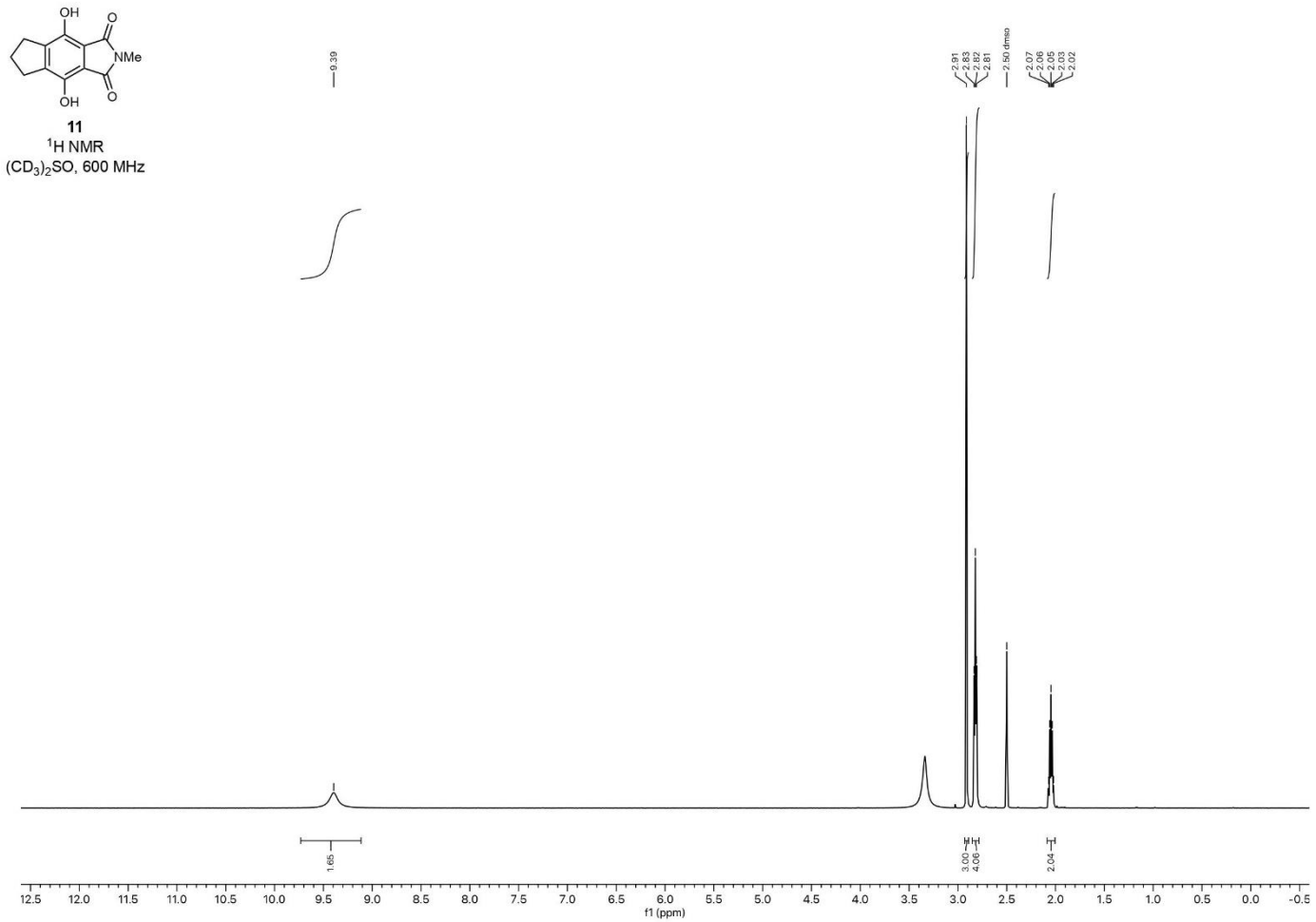
OH
O
NMe
O
OH
11
1H NMR
(CD3)2SO, 600 MHz
9.39
2.91
2.83
2.82
2.81
2.50 dmso
2.07
2.06
2.05
2.03
2.02
1.65
3.00
4.00
2.04
12.5 12.0 11.5 11.0 10.5 10.0 9.5 9.0 8.5 8.0 7.5 7.0 6.5 6.0 5.5 5.0 4.5 4.0 3.5 3.0 2.5 2.0 1.5 1.0 0.5 0.0 -0.5
f1 (ppm)

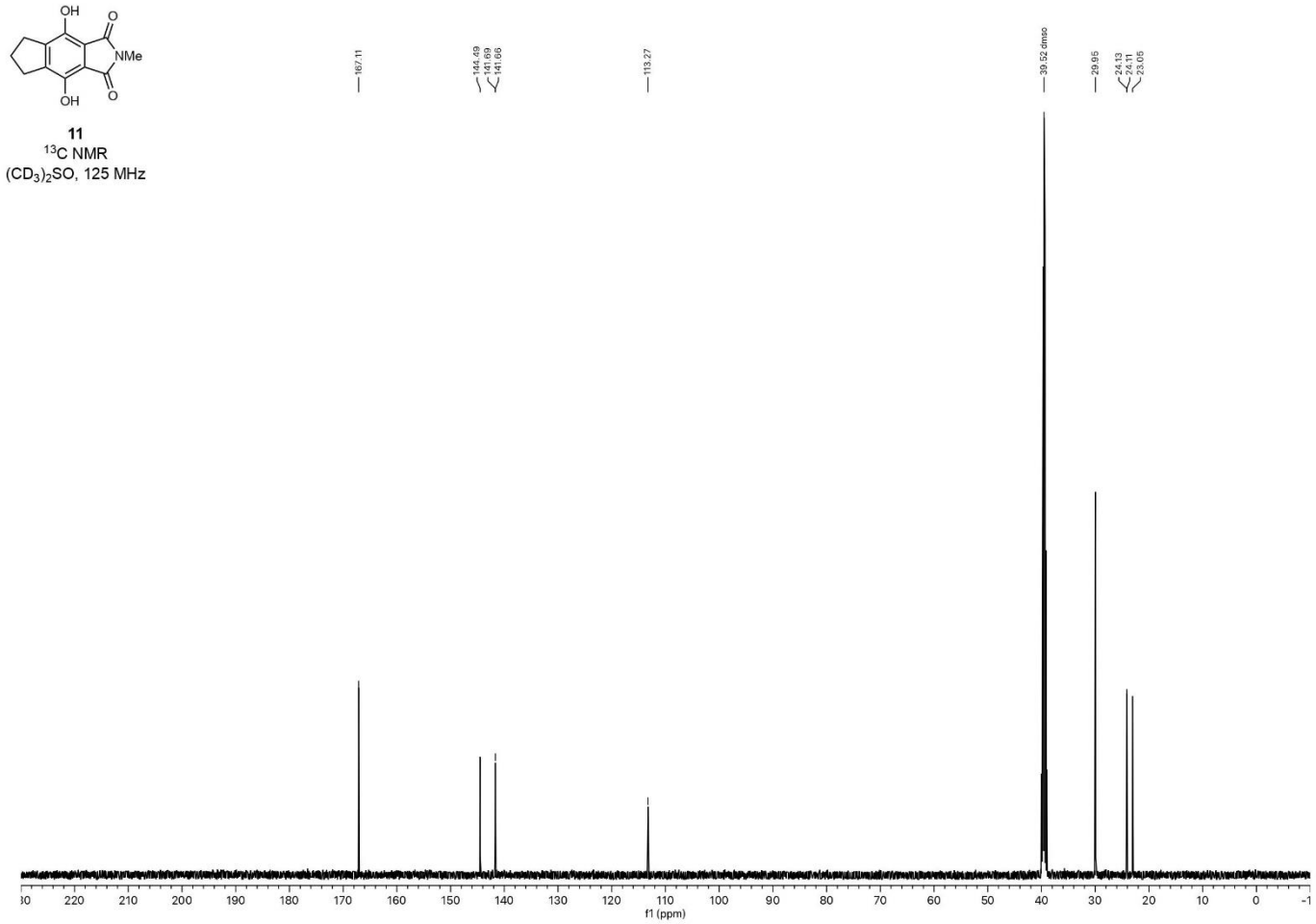

11
^{13}C NMR
$(CD_3)_2SO$, 125 MHz

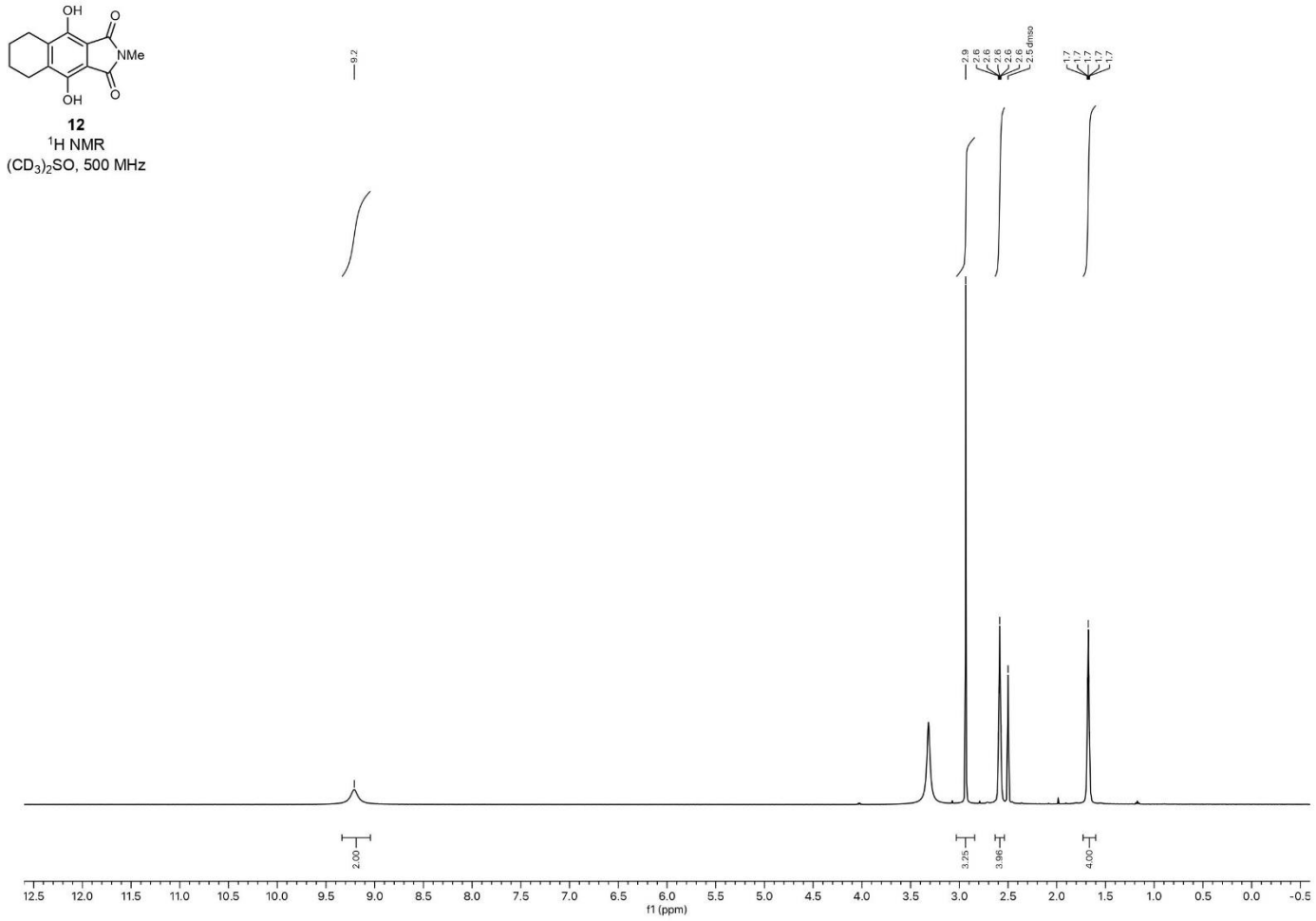
OH
O
NMe
O
OH
12
1H NMR
(CD3)2SO, 500 MHz
9.2
2.9
2.6
2.6
2.6
2.6
2.6
2.5 dmso
1.7
1.7
1.7
1.7
1.7
2.00
3.25
3.96
4.00
12.5 12.0 11.5 11.0 10.5 10.0 9.5 9.0 8.5 8.0 7.5 7.0 6.5 6.0 5.5 5.0 4.5 4.0 3.5 3.0 2.5 2.0 1.5 1.0 0.5 0.0 -0.5
f1 (ppm)

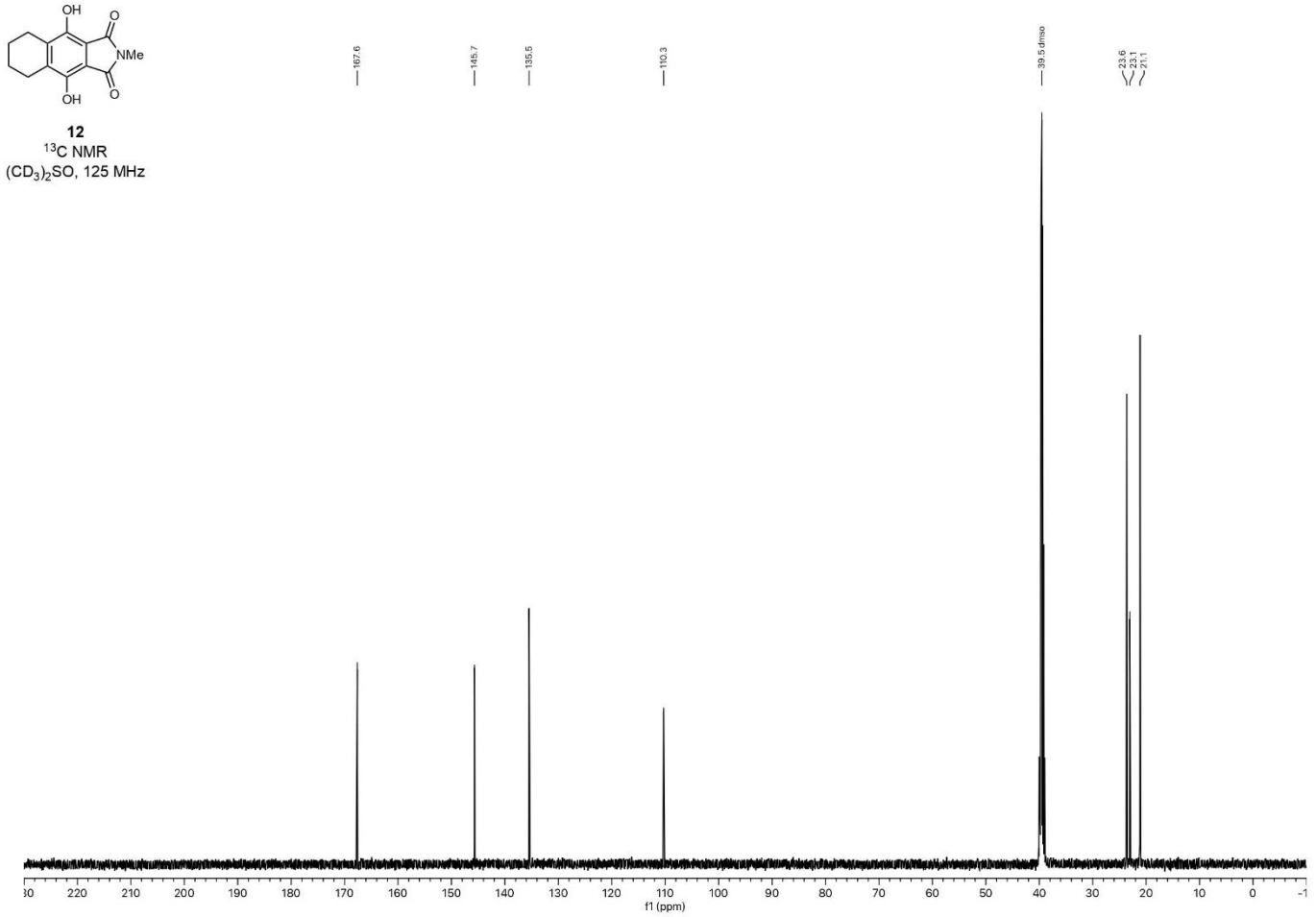

12
^{13}C NMR
$(CD_3)_2SO$, 125 MHz

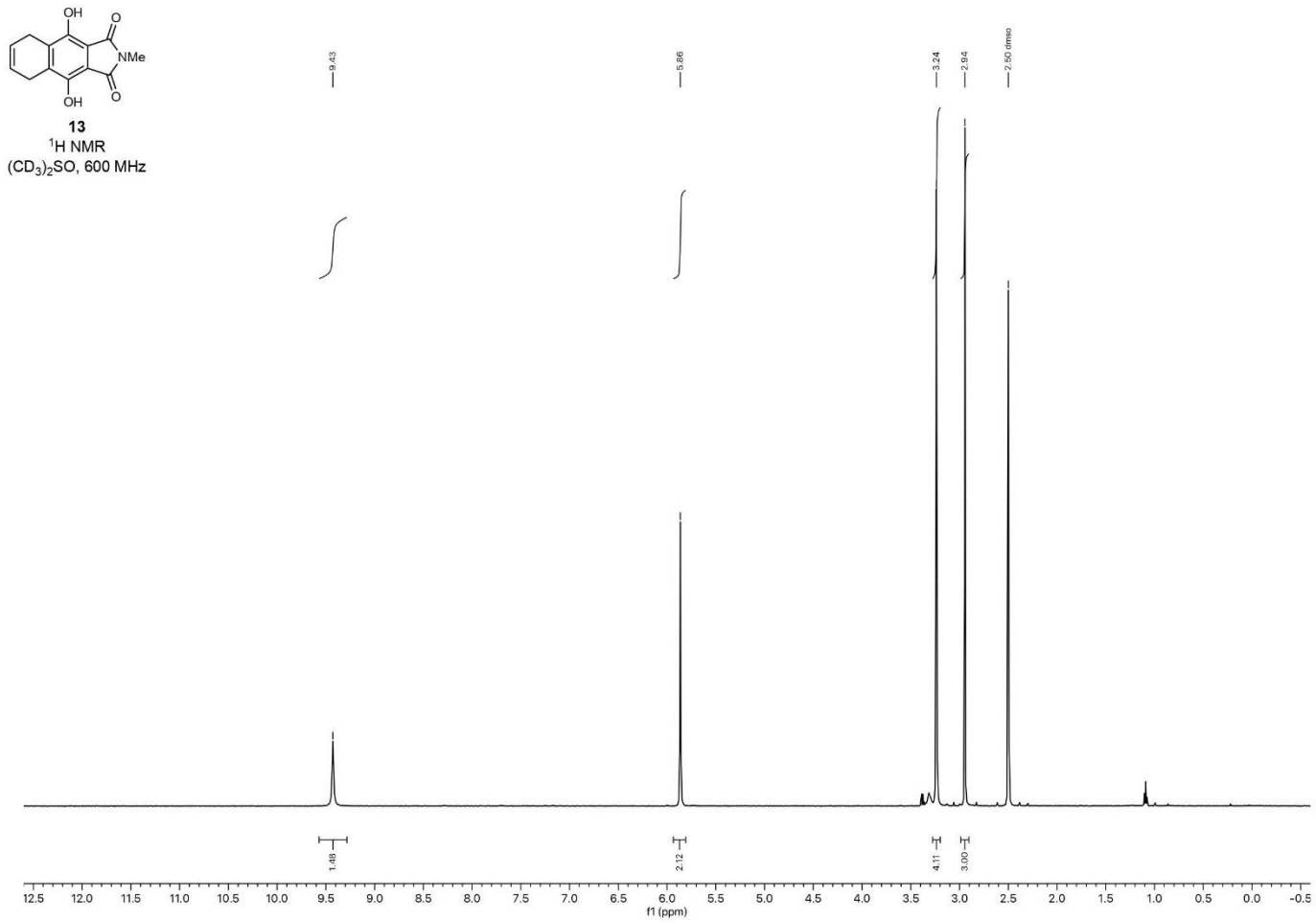
OH
O
NMe
O
OH
13
1H NMR
(CD3)2SO, 600 MHz
9.43
5.86
3.24
2.94
2.50 dmso
1.48
2.12
4.11
3.00
12.5 12.0 11.5 11.0 10.5 10.0 9.5 9.0 8.5 8.0 7.5 7.0 6.5 6.0 5.5 5.0 4.5 4.0 3.5 3.0 2.5 2.0 1.5 1.0 0.5 0.0 -0.5
f1 (ppm)

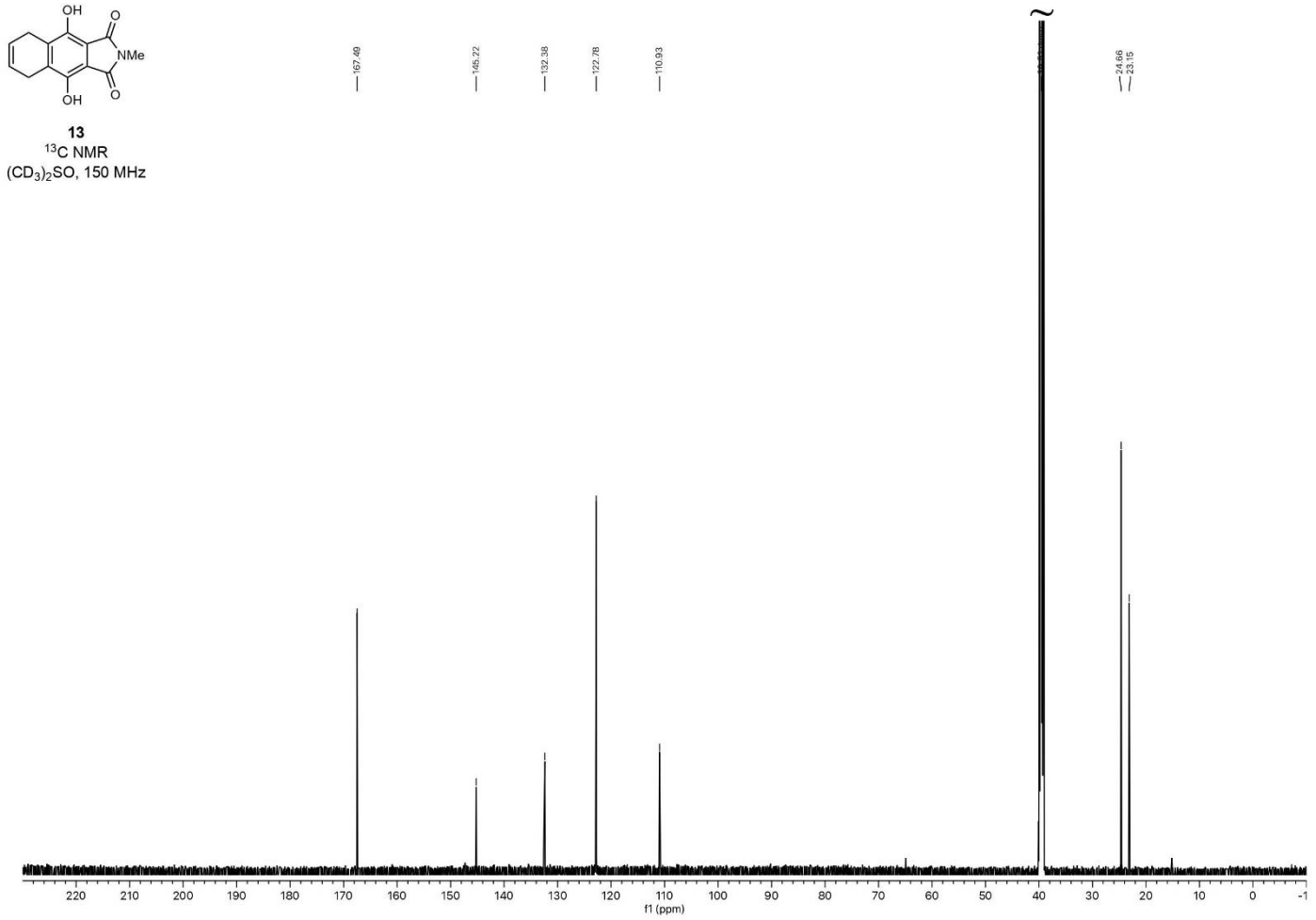
OH
O
NMe
O
OH
13
13C NMR
(CD3)2SO, 150 MHz
167.49
145.22
132.38
122.78
110.93
24.66
23.15
220
210
200
190
180
170
160
150
140
130
120
110
100
90
80
70
60
50
40
30
20
10
0
-1
f1 (ppm)

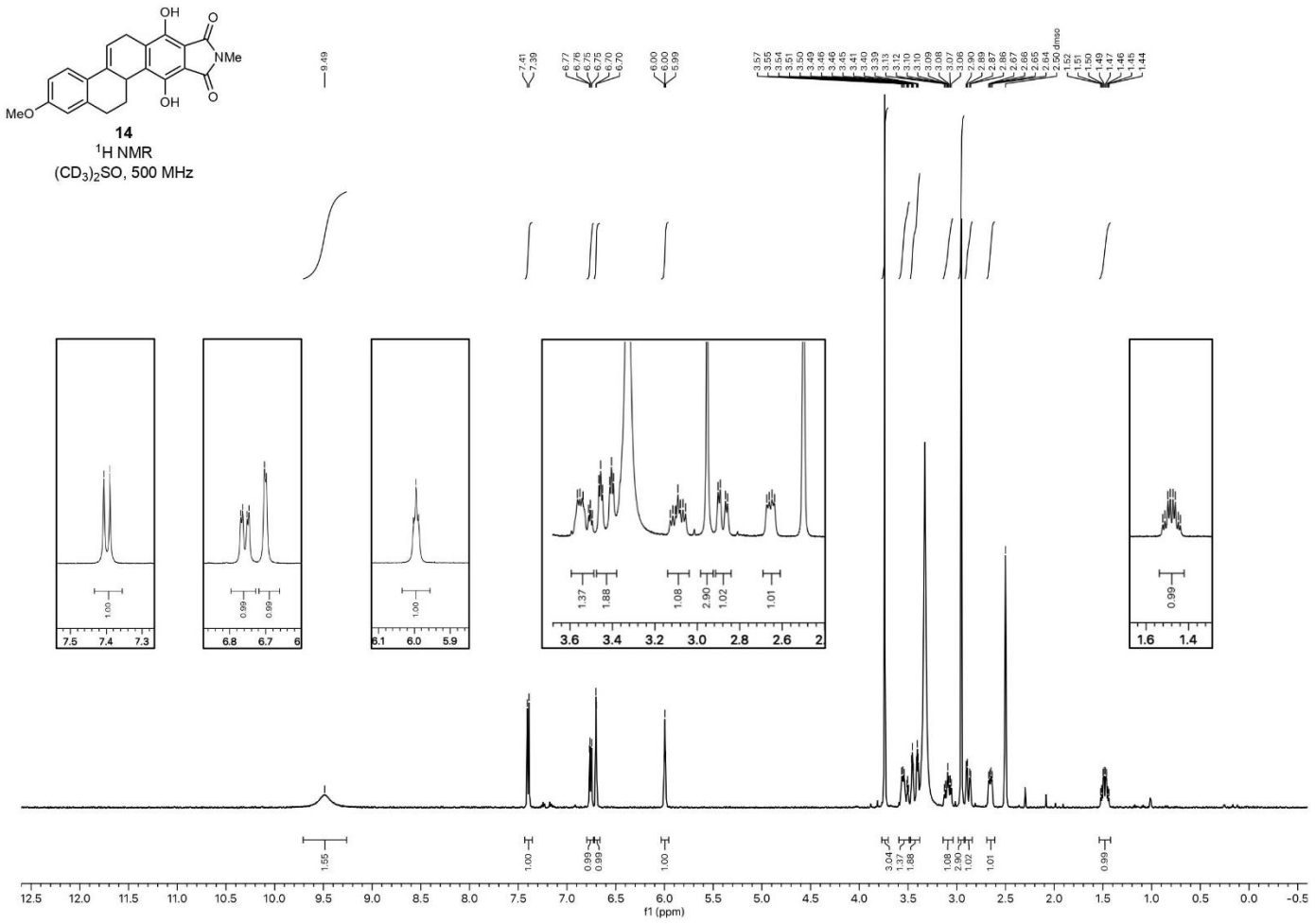
OH
O
NMe
O
OH
MeO
14
1H NMR
(CD3)2SO, 500 MHz
f1 (ppm)

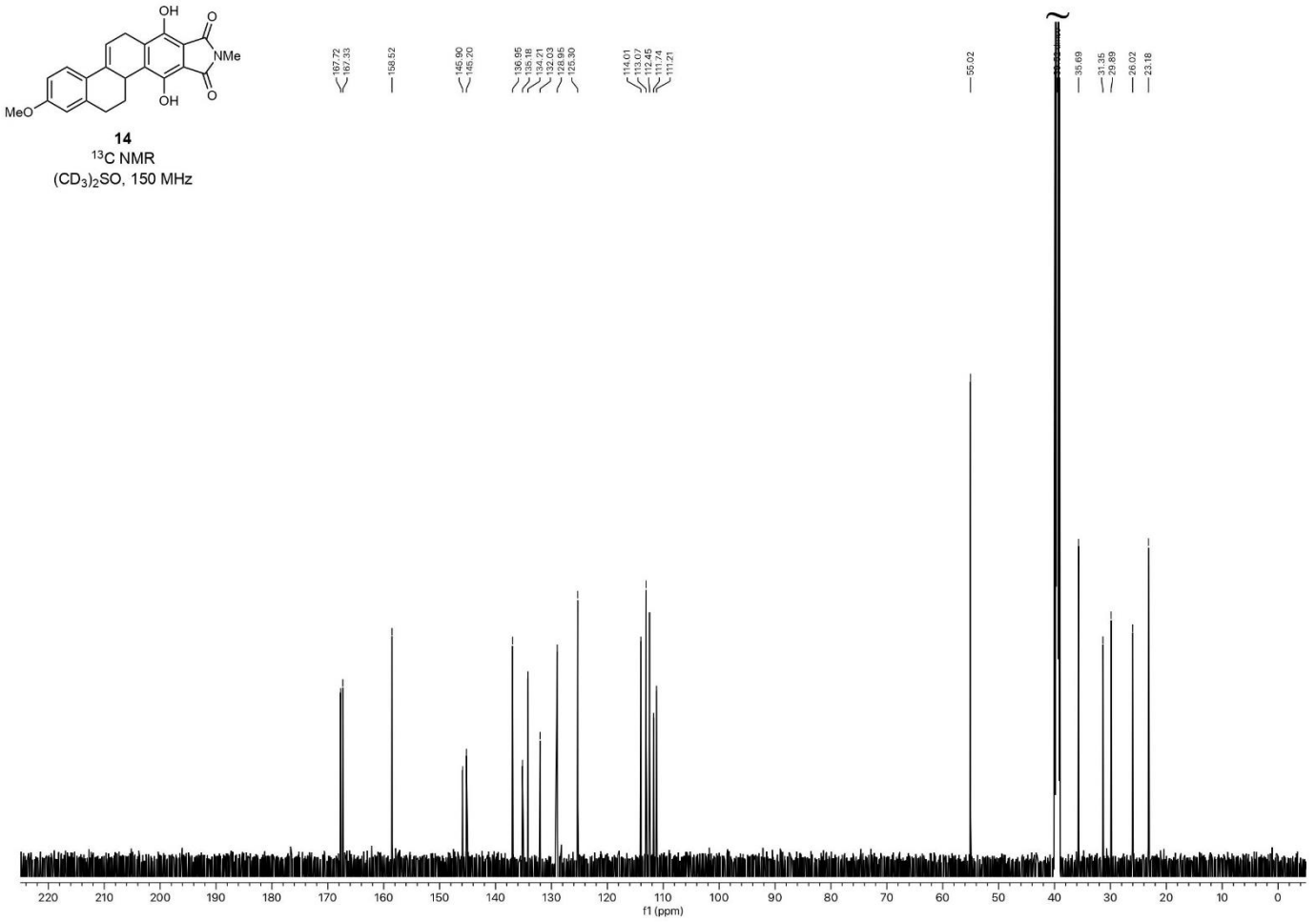
OH
O
NMe
O
MeO
OH
14
13C NMR
(CD3)2SO, 150 MHz
167.72
167.33
158.52
145.90
145.20
136.95
135.18
134.21
132.03
128.95
125.30
114.01
113.07
112.45
111.74
111.21
55.02
39.51
35.69
31.35
29.89
26.02
23.18
220
210
200
190
180
170
160
150
140
130
120
110
100
90
80
70
60
50
40
30
20
10
0
f1 (ppm)

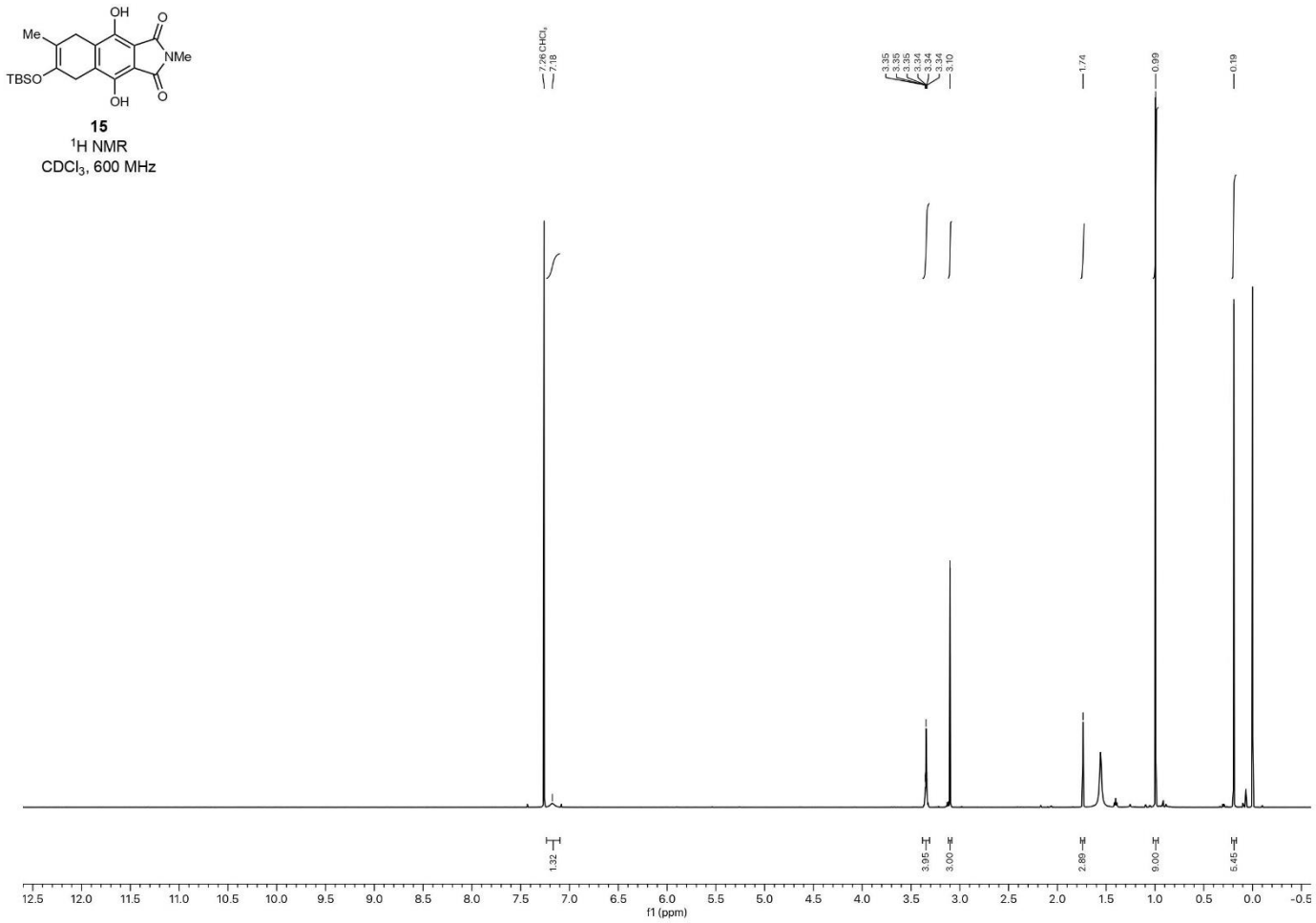
OH
Me
O
NMe
TBSO
O
OH
15
1H NMR
CDCl3, 600 MHz
7.26 CHCl3
7.18
3.35
3.35
3.35
3.34
3.34
3.10
1.74
0.99
0.19
1.32
3.95
3.00
2.89
9.00
5.45
f1 (ppm)

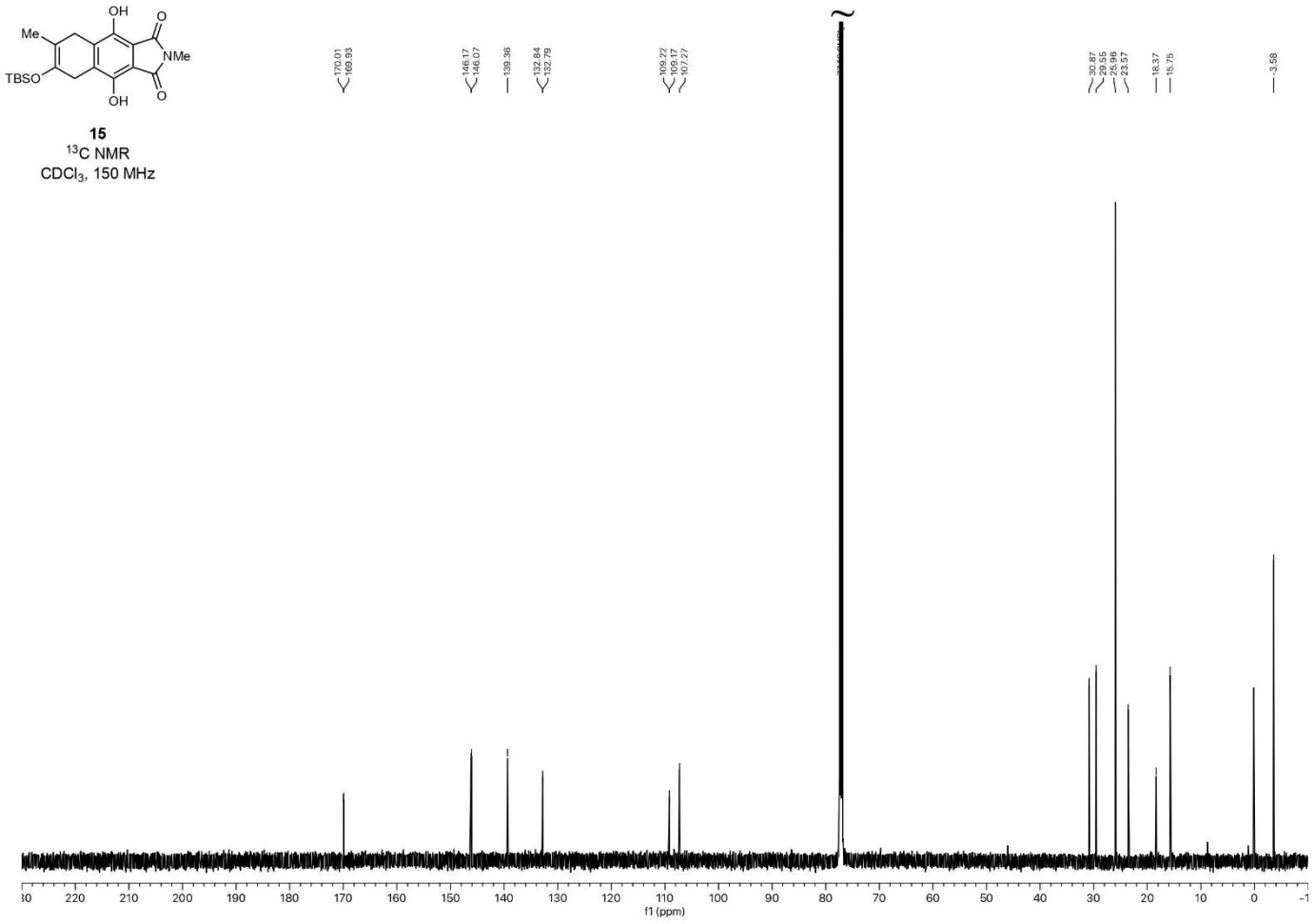
OH
O
Me
NMe
TBSO
O
OH
15
13C NMR
CDCl3, 150 MHz
170.01
169.93
146.17
146.07
139.36
132.84
132.79
109.22
109.17
107.27
30.87
29.55
25.96
23.57
18.37
15.75
-3.58
f1 (ppm)

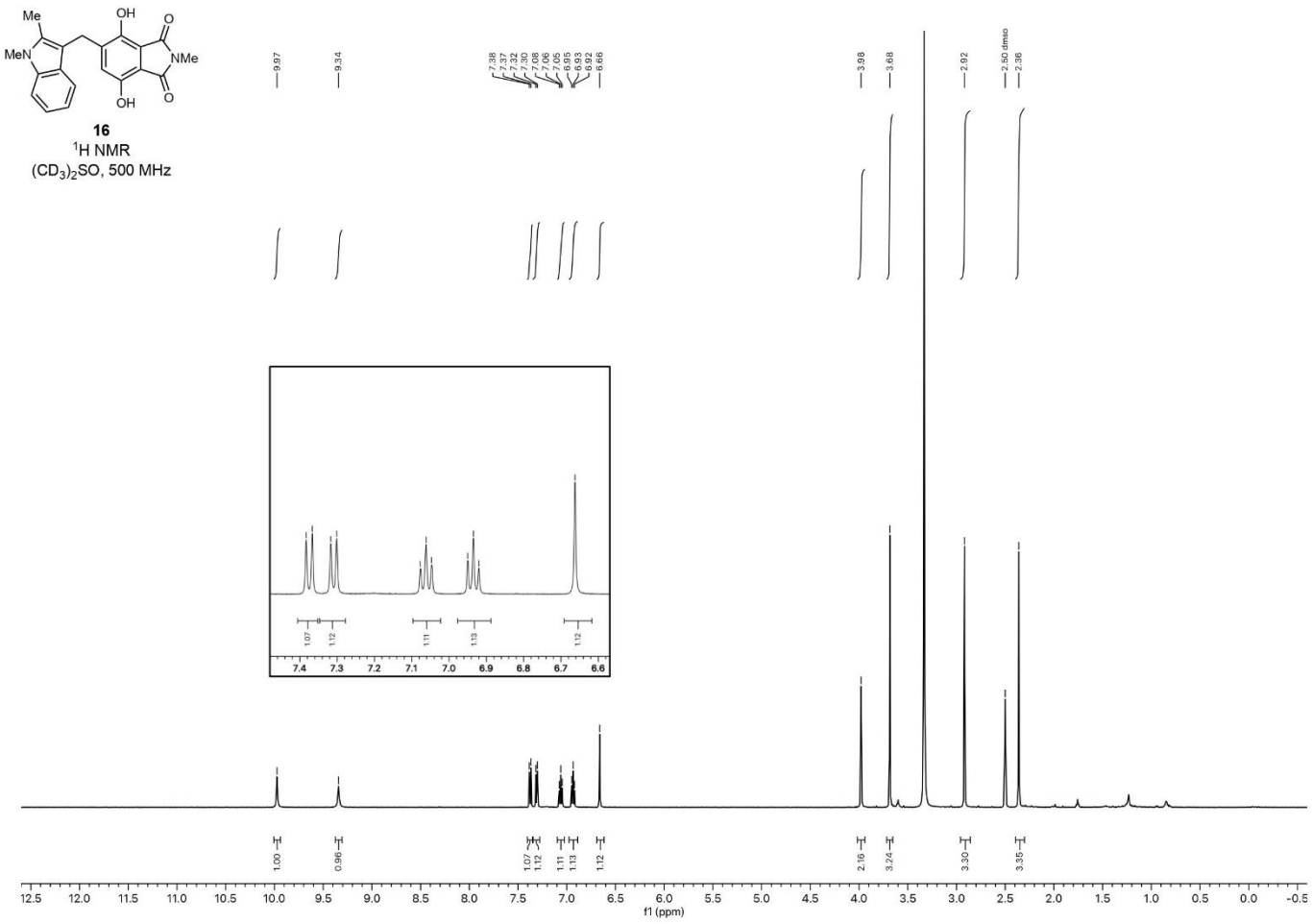
Me
MeN
OH
O
NMe
OH
O
16
1H NMR
(CD3)2SO, 500 MHz
9.97
9.34
7.38
7.37
7.32
7.30
7.08
7.06
7.05
6.95
6.93
6.92
6.66
3.98
3.68
2.92
2.50 dmso
2.36
1.00
0.96
1.07
1.12
1.11
1.13
1.12
2.16
3.24
3.30
3.35
f1 (ppm)

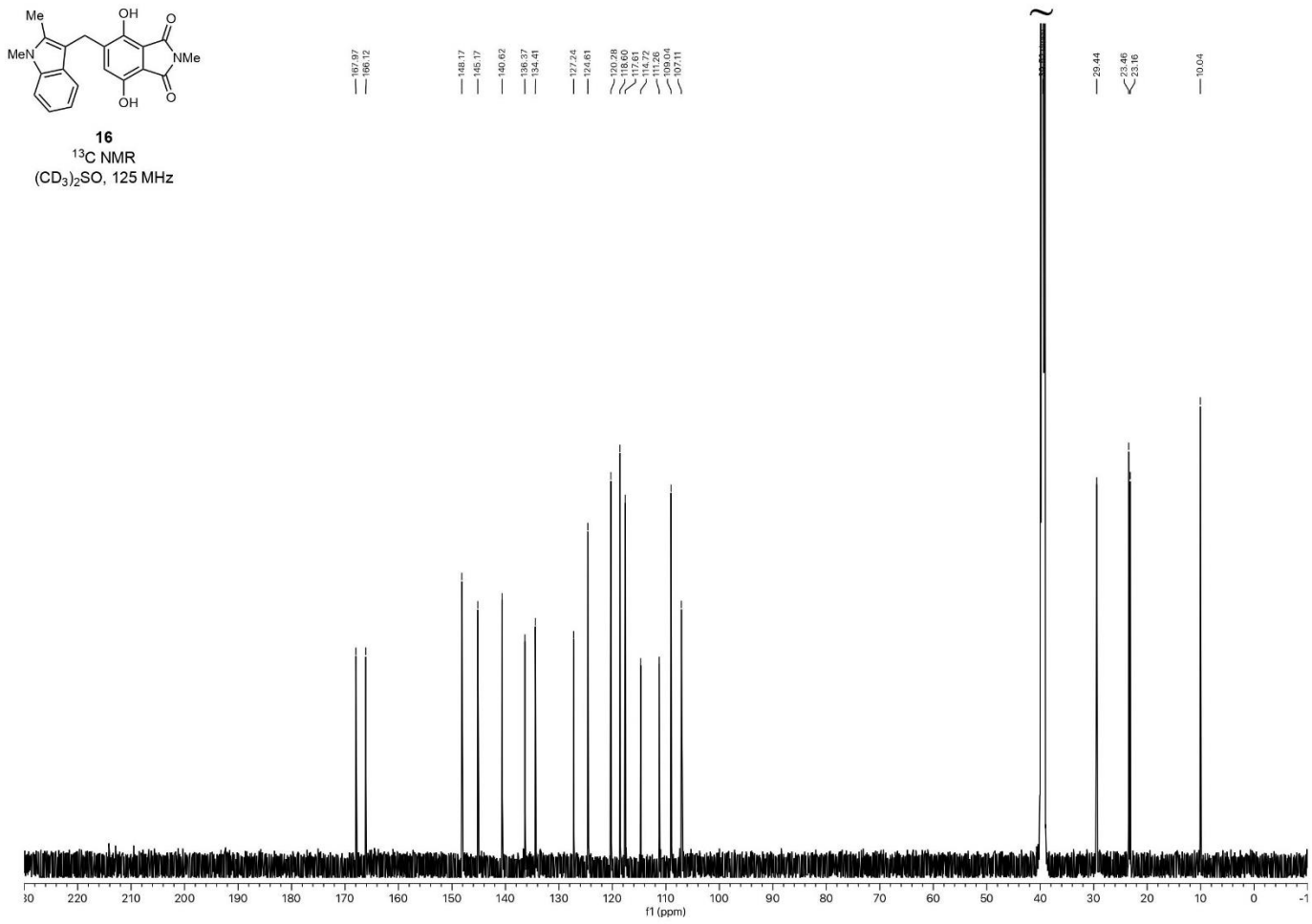
Me
OH
O
MeN
NMe
O
OH
16
^{13}C NMR
$(CD_3)_2SO$, 125 MHz
167.97
166.12
148.17
145.17
140.62
136.37
134.41
127.24
124.61
120.28
118.60
117.61
114.72
111.26
109.04
107.11
39.51
29.44
23.46
23.16
10.04
f1 (ppm)

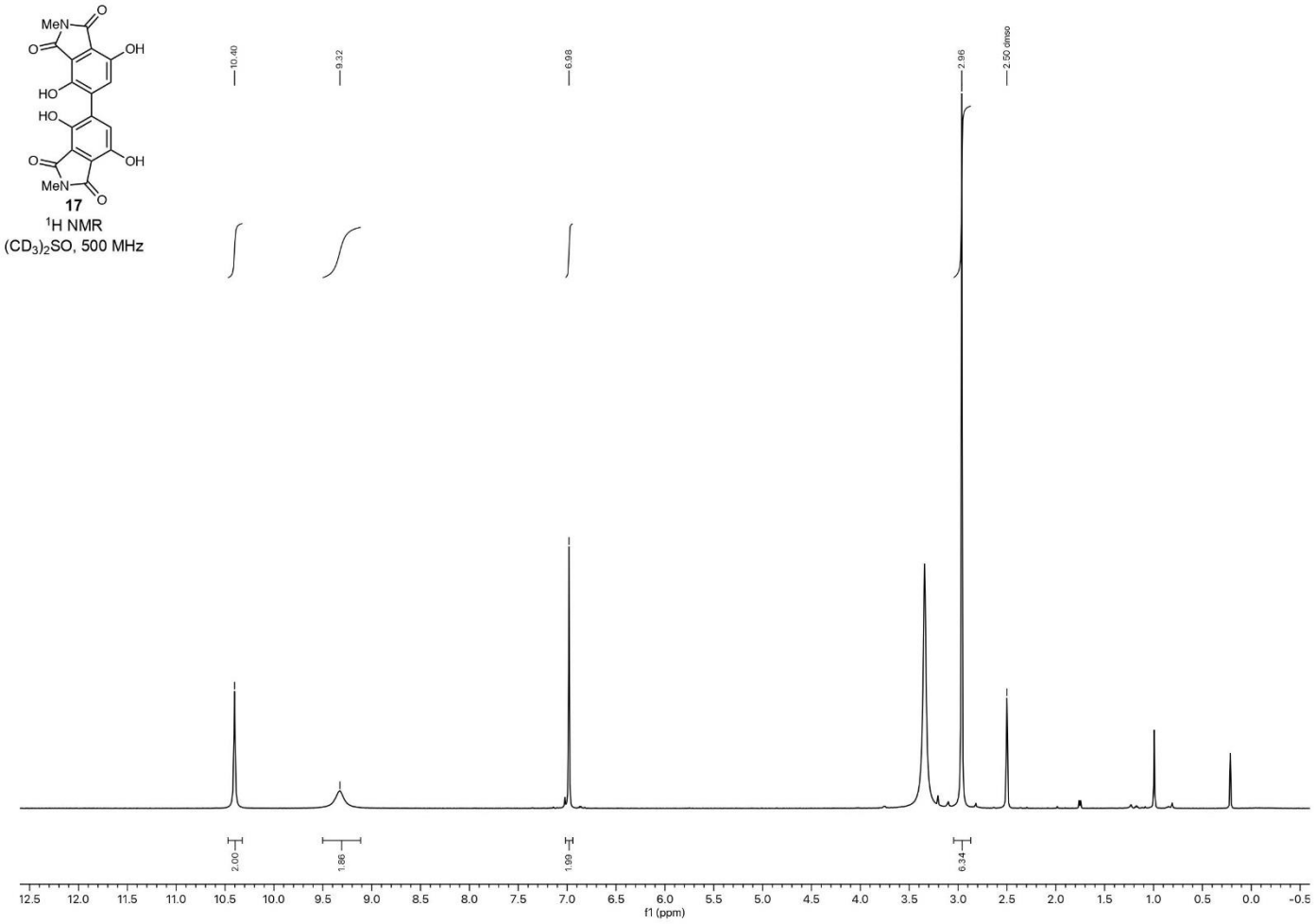
MeN
O
O
OH
HO
HO
O
OH
MeN
O
17
1H NMR
(CD3)2SO, 500 MHz
10.40
9.32
6.98
2.96
2.50 dmso
2.00
1.86
1.99
6.34
12.5 12.0 11.5 11.0 10.5 10.0 9.5 9.0 8.5 8.0 7.5 7.0 6.5 6.0 5.5 5.0 4.5 4.0 3.5 3.0 2.5 2.0 1.5 1.0 0.5 0.0 -0.5
f1 (ppm)

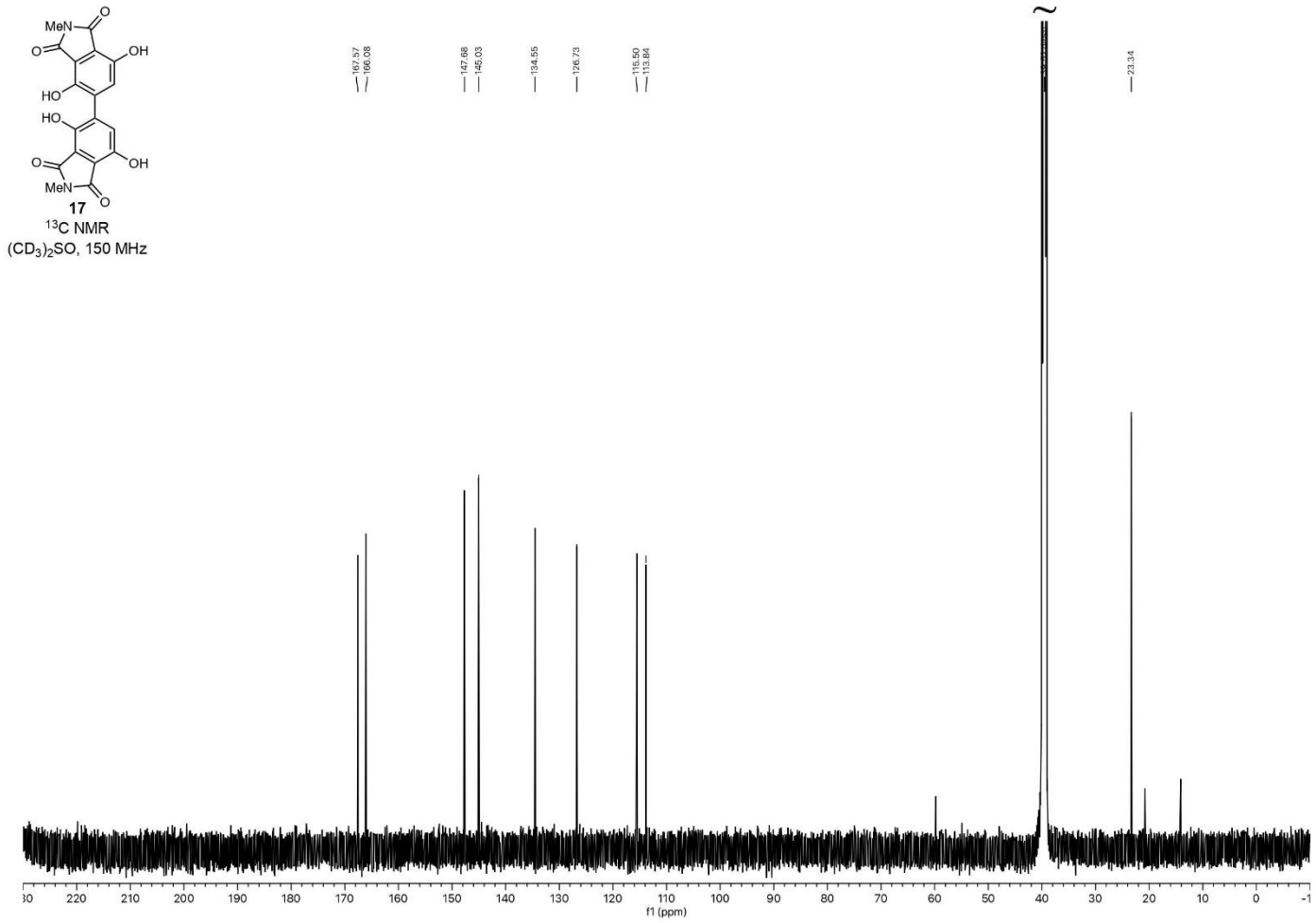
MeN
O
O
OH
HO
HO
OH
O
MeN
O
17
13C NMR
(CD3)2SO, 150 MHz
167.57
166.08
147.66
145.03
134.55
126.73
115.50
113.84
23.34
f1 (ppm)

Dienophile Scope

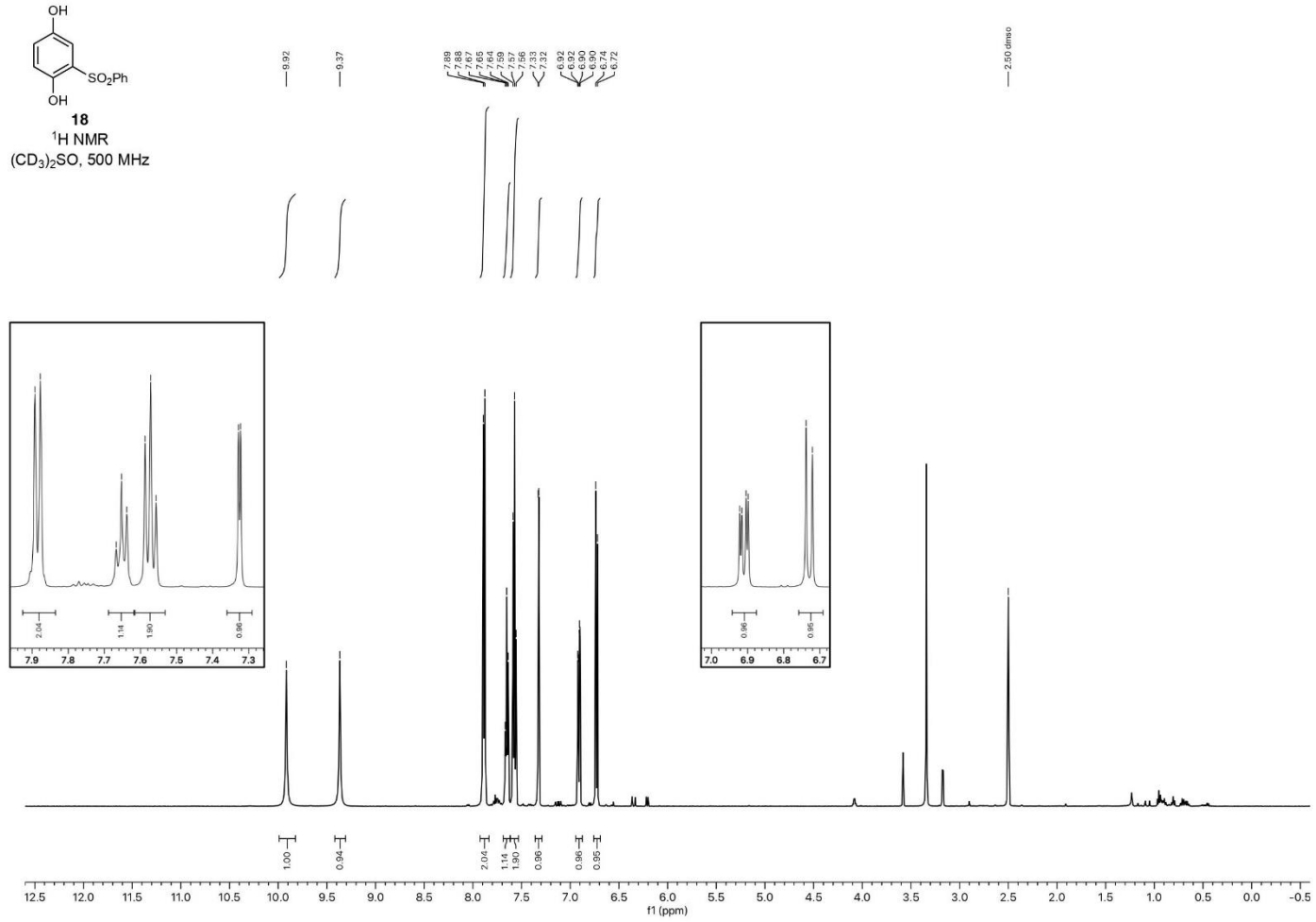

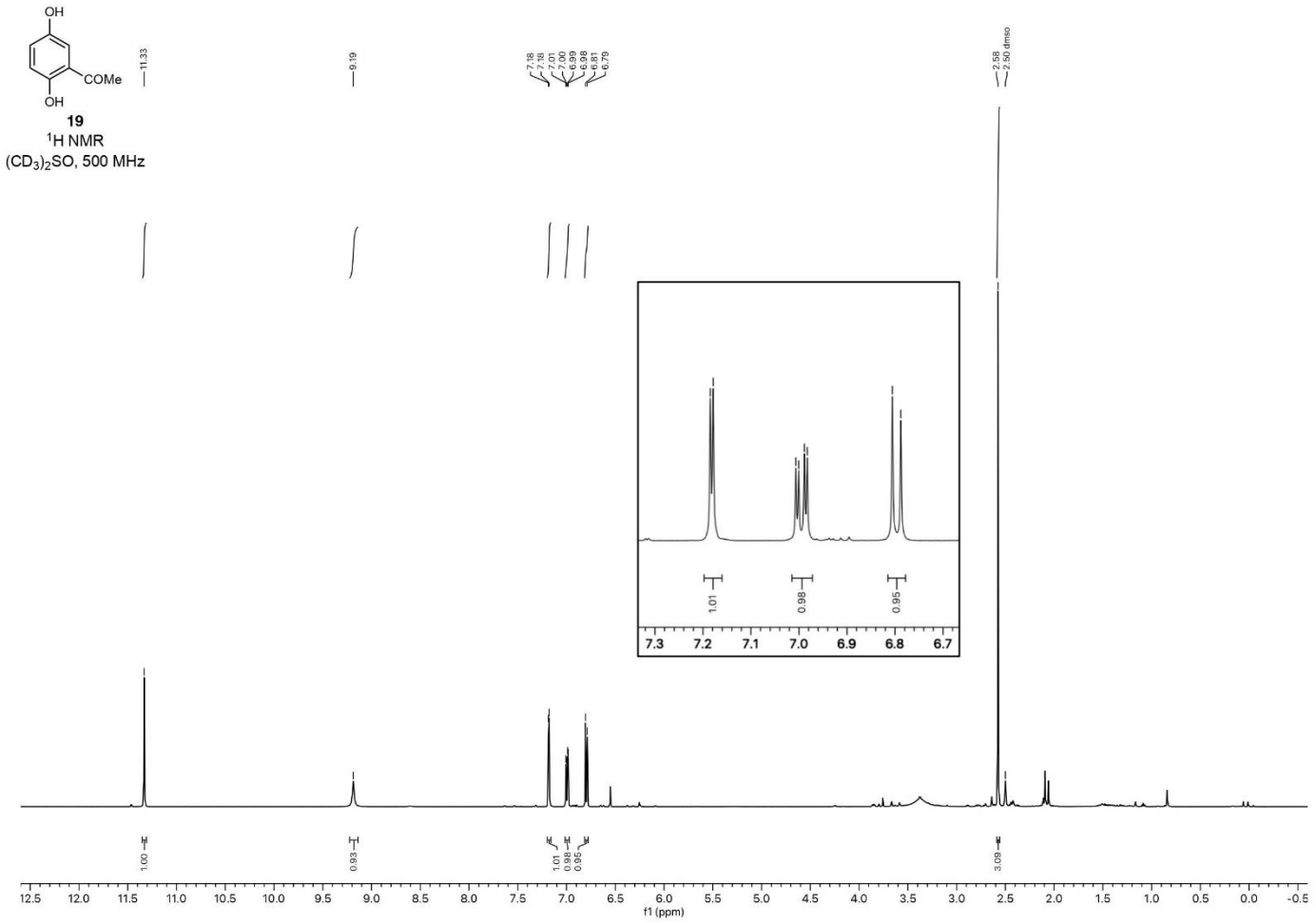
OH
COMe
OH
19
1H NMR
(CD3)2SO, 500 MHz
11.33
9.19
7.18
7.18
7.01
7.00
6.99
6.98
6.81
6.79
2.58
2.50 dmso
1.01
0.98
0.95
7.3
7.2
7.1
7.0
6.9
6.8
6.7
1.00
0.93
1.01
0.98
0.95
3.09
12.5
12.0
11.5
11.0
10.5
10.0
9.5
9.0
8.5
8.0
7.5
7.0
6.5
6.0
5.5
5.0
4.5
4.0
3.5
3.0
2.5
2.0
1.5
1.0
0.5
0.0
-0.5
f1 (ppm)

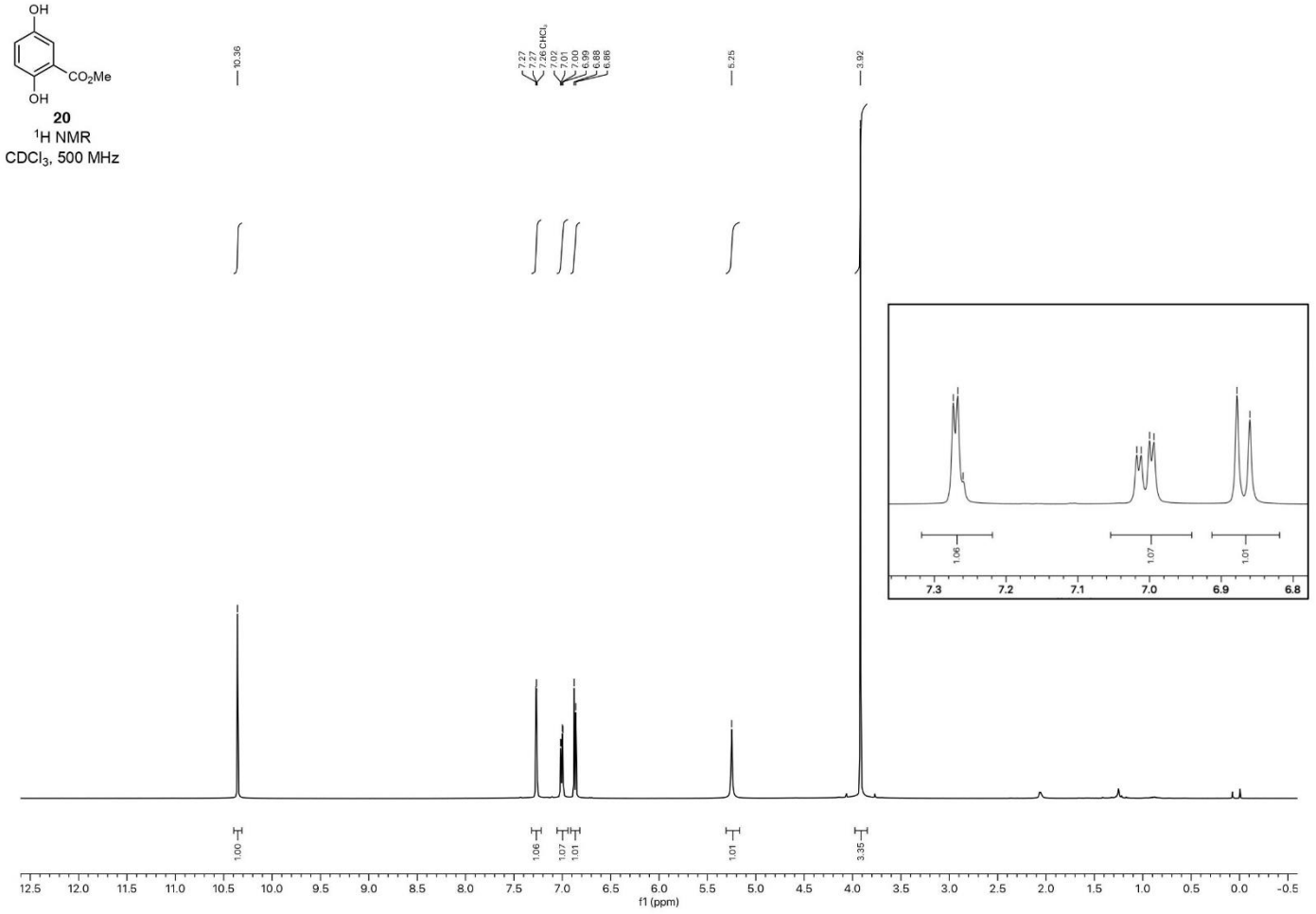
OH
CO2Me
OH
20
1H NMR
CDCl3, 500 MHz
10.36
7.27
7.26 CHCl3
7.01
7.00
6.99
6.88
6.86
5.25
3.92
1.00
1.06
1.07
1.01
1.01
3.35
f1 (ppm)

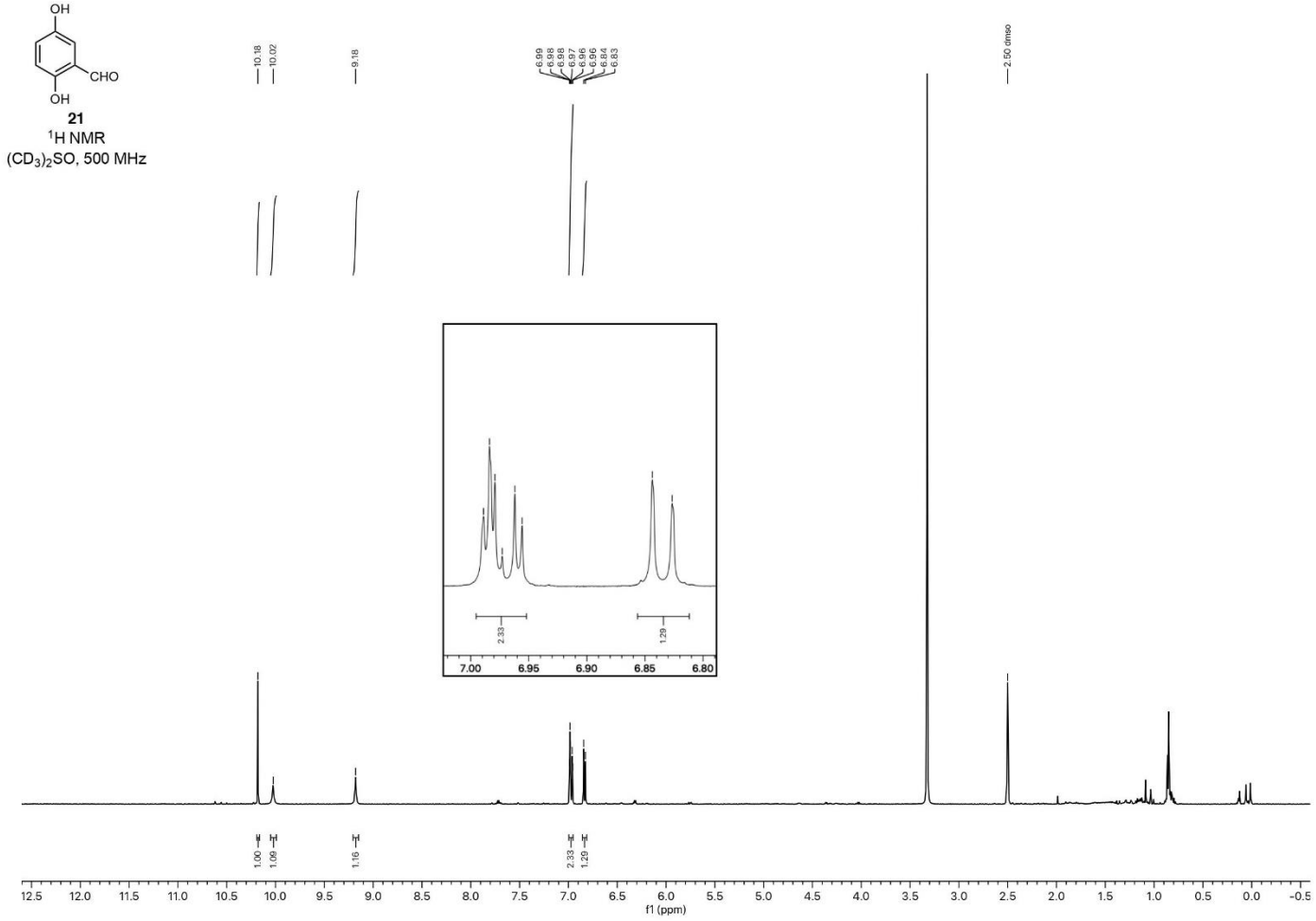
OH
CHO
OH
21
1H NMR
(CD3)2SO, 500 MHz
10.18
10.02
9.18
6.99
6.98
6.98
6.98
6.97
6.96
6.96
6.96
6.84
6.83
2.50 dmso
2.33
1.29
7.00
6.95
6.90
6.85
6.80
1.00
1.09
1.16
2.33
1.29
12.5
12.0
11.5
11.0
10.5
10.0
9.5
9.0
8.5
8.0
7.5
7.0
6.5
6.0
5.5
5.0
4.5
4.0
3.5
3.0
2.5
2.0
1.5
1.0
0.5
0.0
-0.5
f1 (ppm)

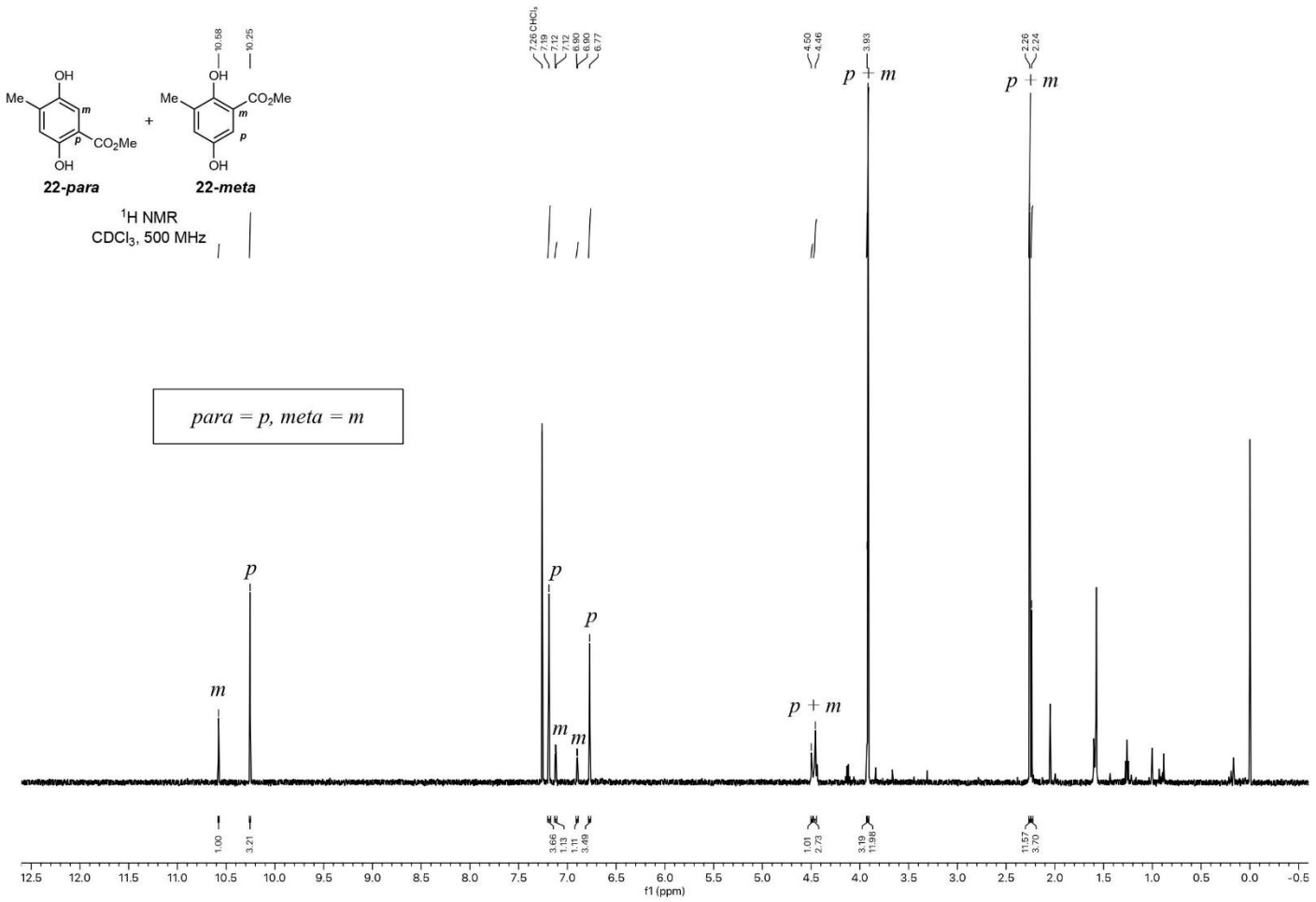
22-para
22-meta
1H NMR
CDCl3, 500 MHz
para = p, meta = m
p + m
f1 (ppm)

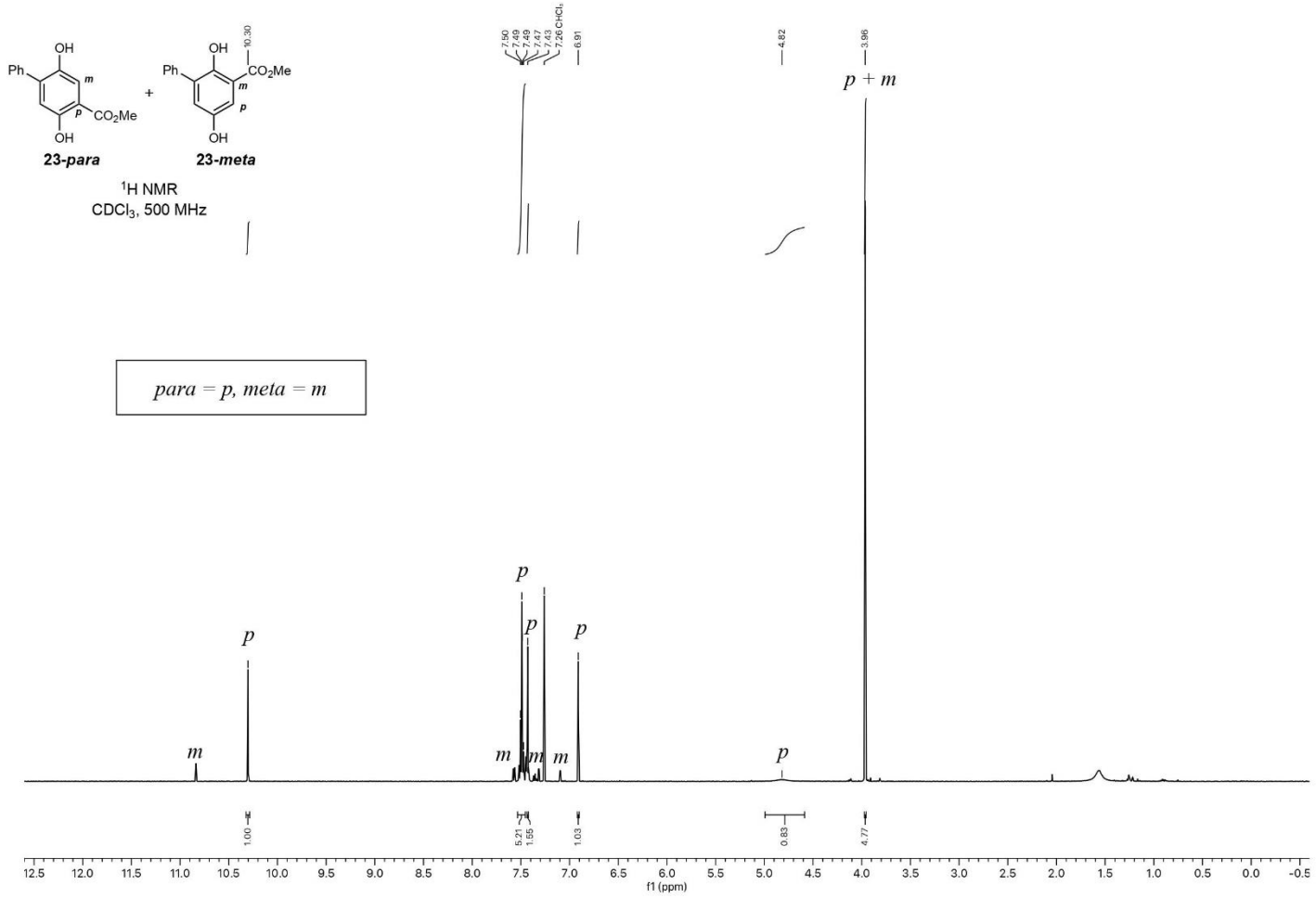
23-para
23-meta
1H NMR
CDCl3, 500 MHz
para = p, meta = m
p + m
f1 (ppm)

Benzyne Precursors

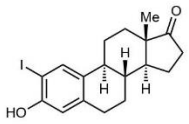

2-iodoestrone
^{1}H NMR
$CDCl_3$, 500 MHz

SI-143

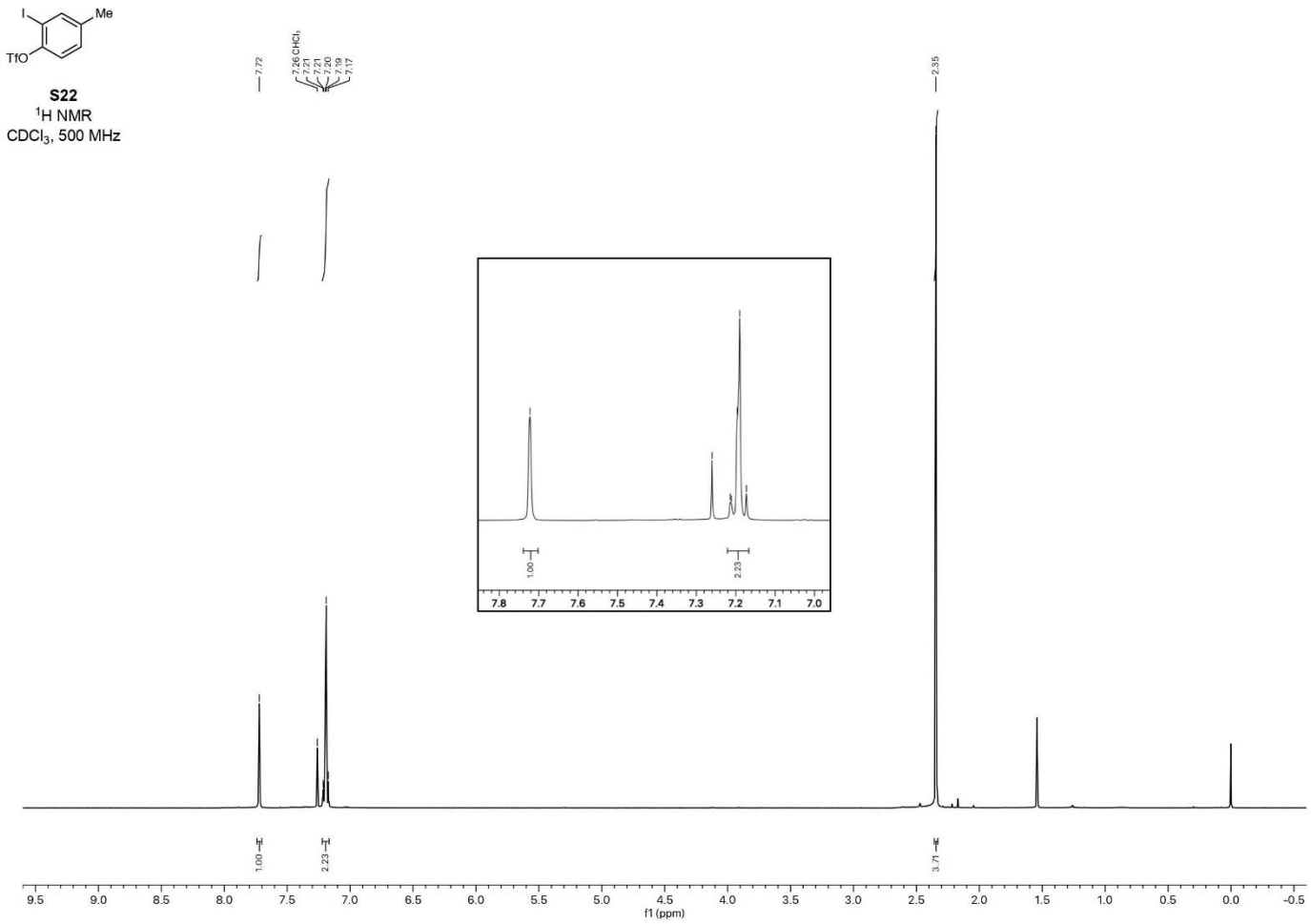
I
Me
TfO
S22
1H NMR
CDCl3, 500 MHz
7.72
7.26 CHCl3
7.21
7.21
7.20
7.19
7.17
2.35
1.00
2.23
3.71
f1 (ppm)

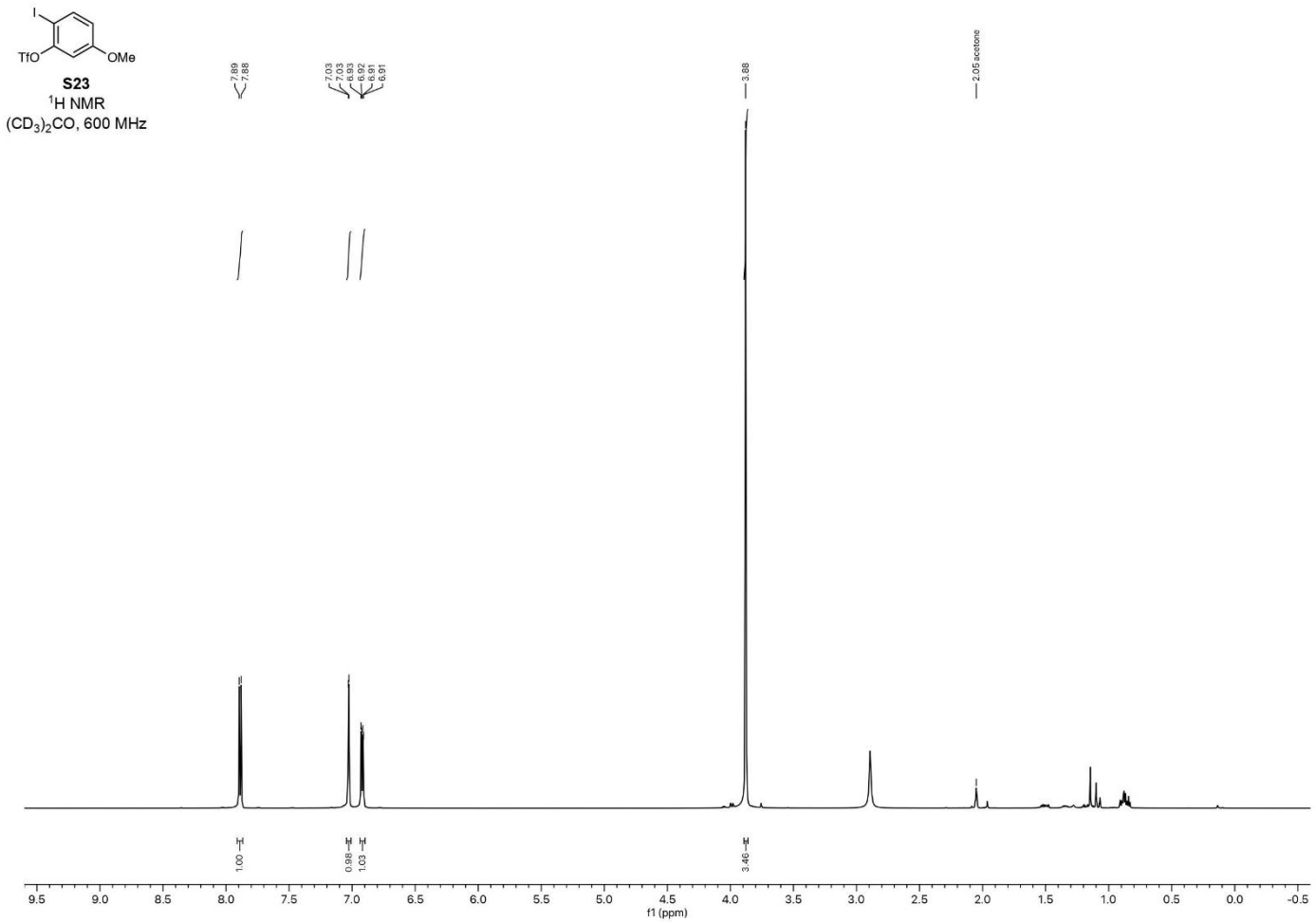
I
TfO
OMe
S23
1H NMR
(CD3)2CO, 600 MHz
7.89
7.88
7.03
7.03
6.93
6.92
6.91
6.91
3.88
2.05 acetone
1.00
0.98
1.03
3.46
9.5
9.0
8.5
8.0
7.5
7.0
6.5
6.0
5.5
5.0
4.5
4.0
3.5
3.0
2.5
2.0
1.5
1.0
0.5
0.0
-0.5
f1 (ppm)

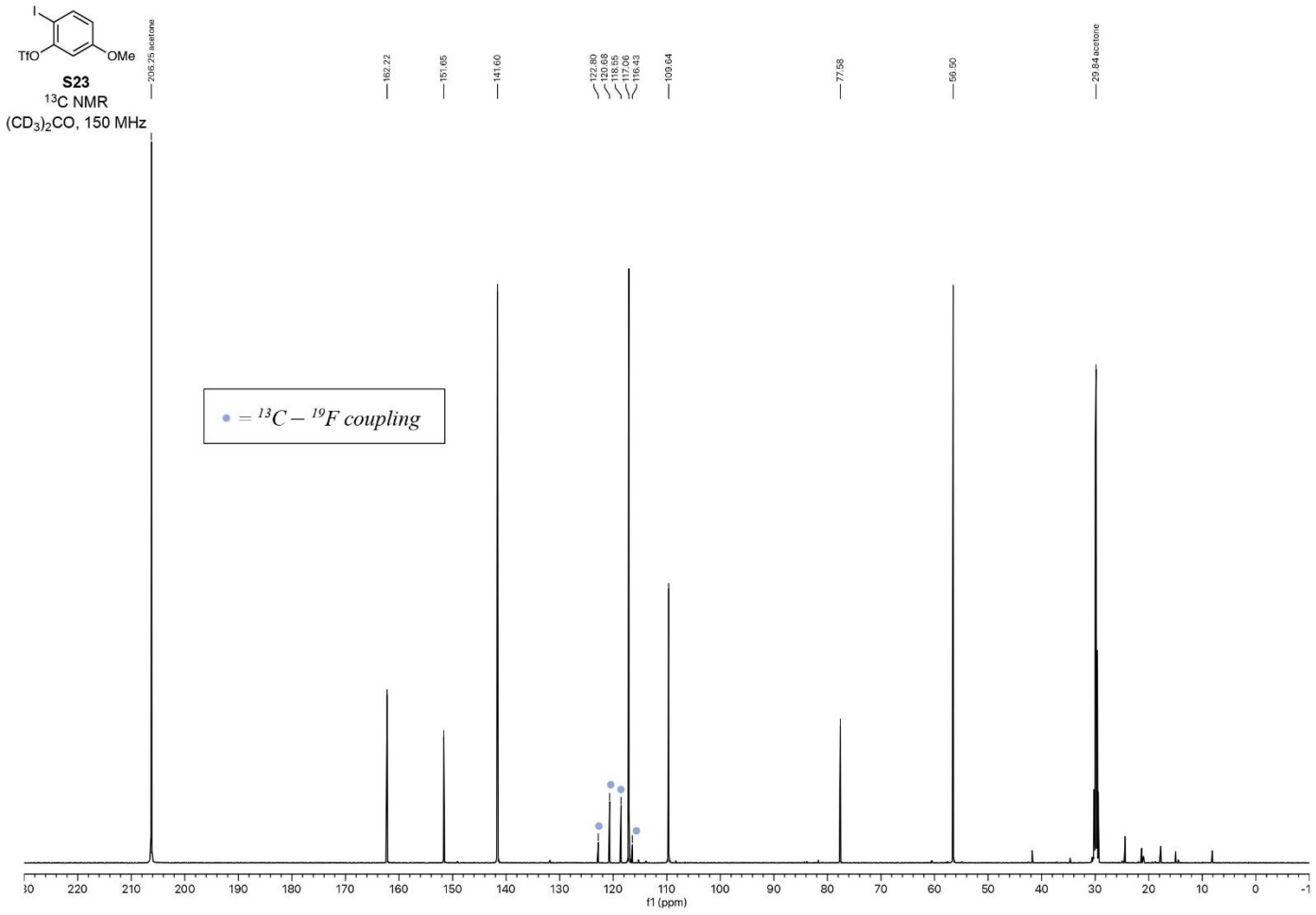
I
TfO
OMe
S23
13C NMR
(CD3)2CO, 150 MHz
206.25 acetone
162.22
151.65
141.60
122.80
120.68
118.65
117.66
116.43
109.64
77.58
56.50
29.84 acetone
● = 13C – 19F coupling
f1 (ppm)

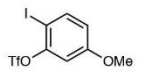

S23
^{19}F NMR
$(CD_3)_2CO$, 470 MHz

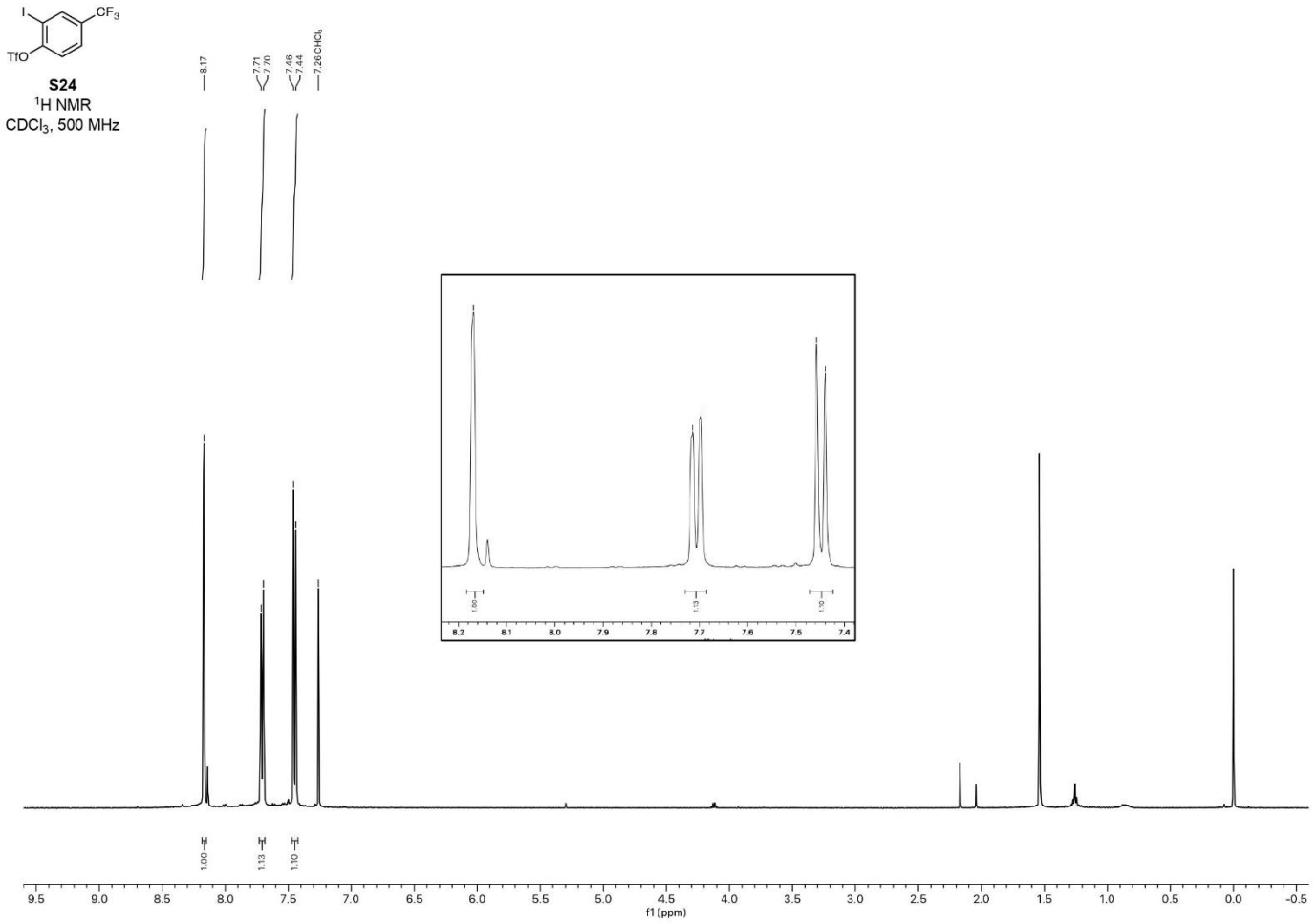
I
CF3
TfO
S24
1H NMR
CDCl3, 500 MHz
8.17
7.71
7.70
7.46
7.44
7.26 CHCl3
1.00
1.13
1.10
f1 (ppm)

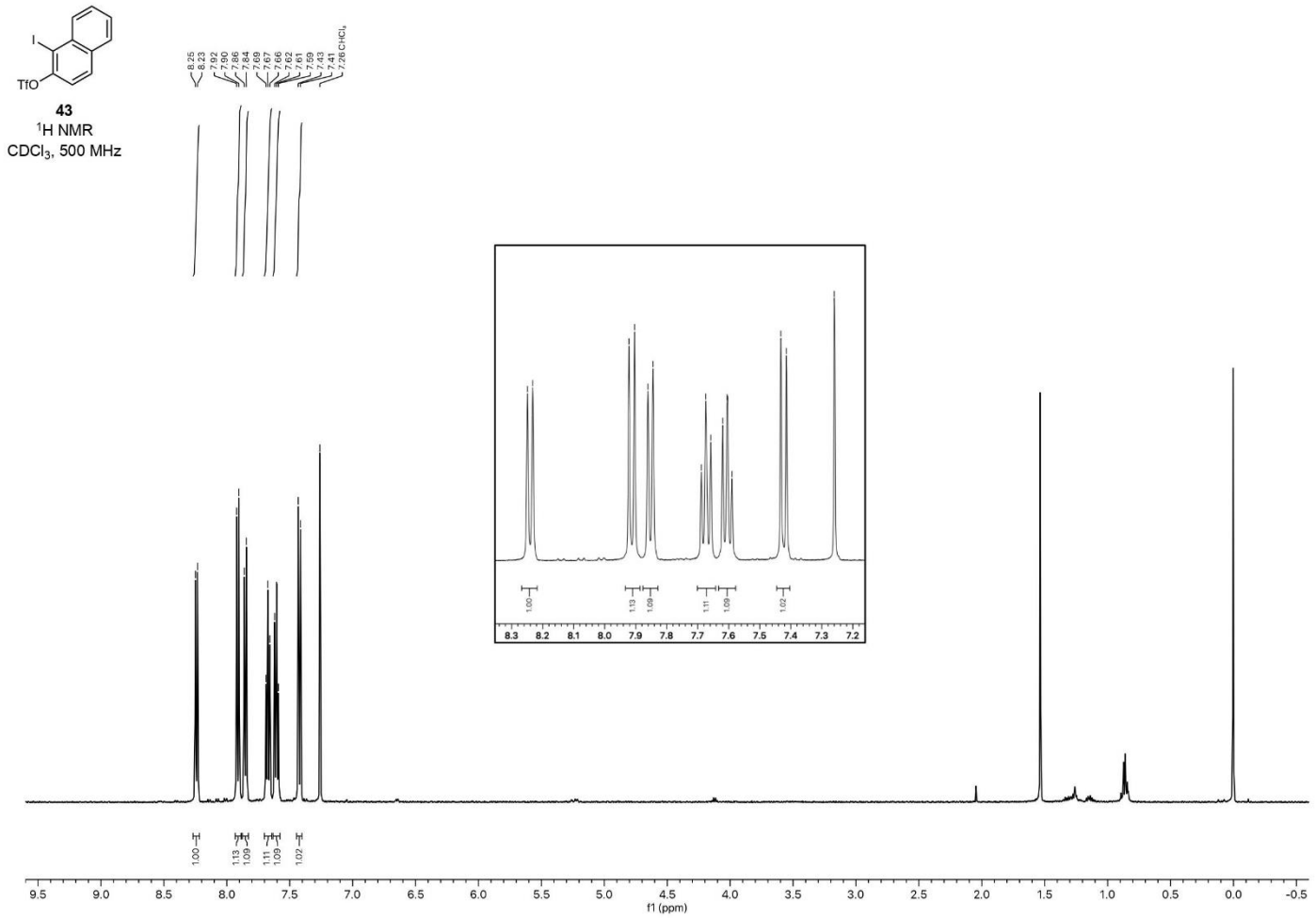
I
TfO
43
1H NMR
CDCl3, 500 MHz
8.25
8.23
7.92
7.90
7.86
7.84
7.69
7.67
7.66
7.62
7.61
7.59
7.43
7.41
7.26 CHCl3
1.00
1.13
1.09
1.11
1.09
1.02
f1 (ppm)

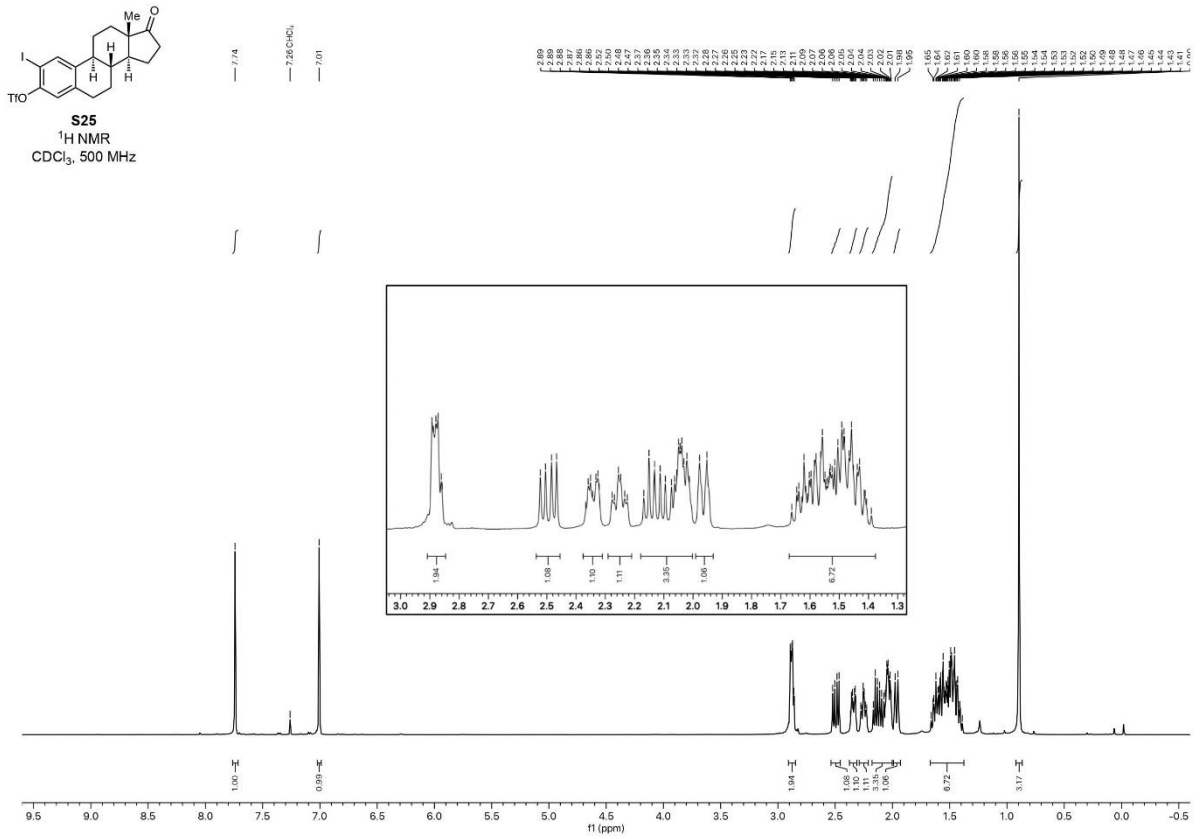
Me
O
I
H
H
H
TfO
S25
1H NMR
CDCl3, 500 MHz
7.74
7.26 CHCl3
7.01
1.00
0.99
1.94
1.08
1.10
1.11
3.35
1.06
6.72
3.17
f1 (ppm)

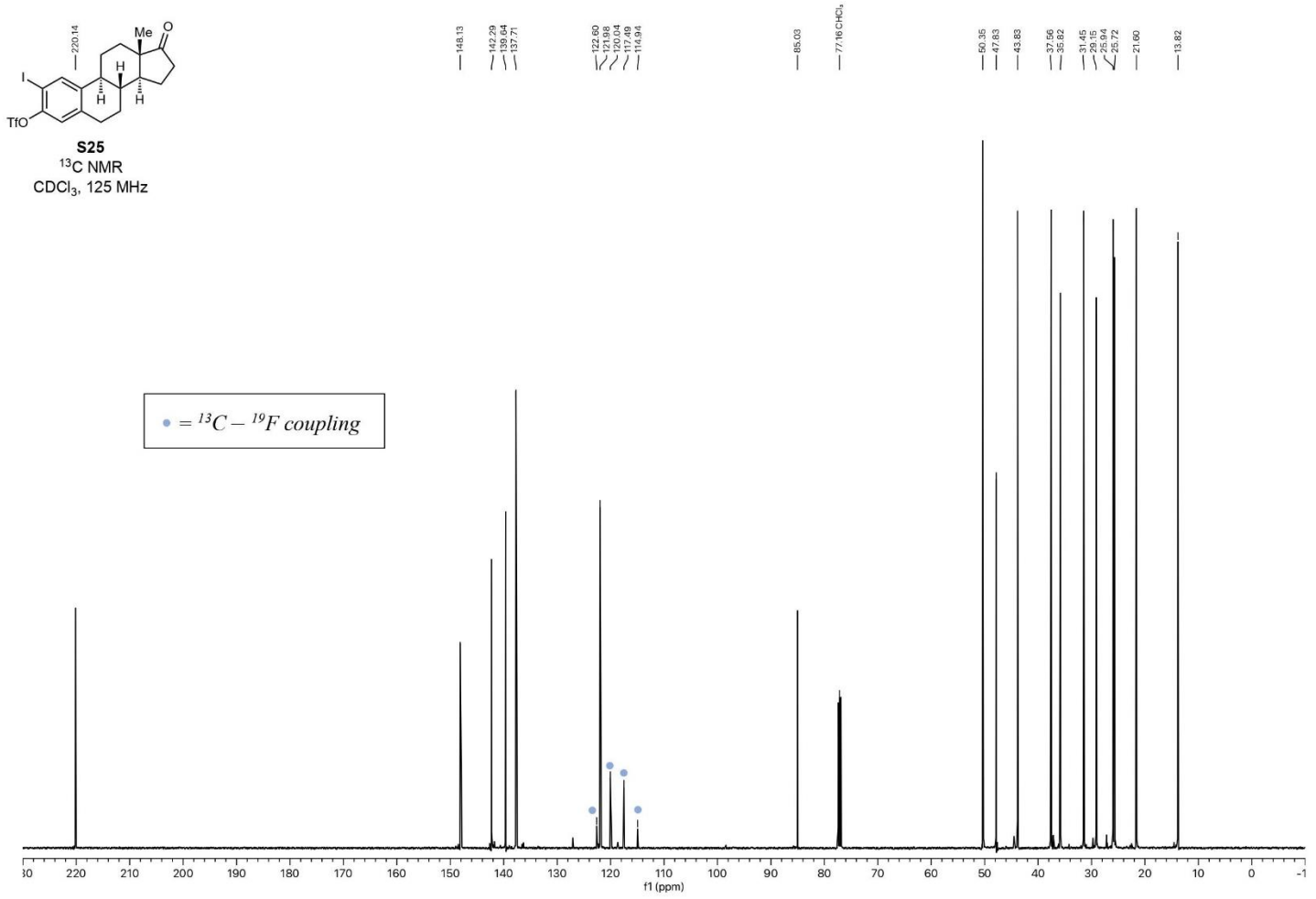
220.14
148.13
142.29
139.64
137.71
122.60
121.98
120.04
117.49
114.94
85.03
77.16 CHCl3
50.35
47.83
43.83
37.56
35.82
31.45
29.15
25.94
25.72
21.60
13.82
Me
O
H
H
H
I
TfO
S25
13C NMR
CDCl3, 125 MHz
= 13C – 19F coupling
f1 (ppm)

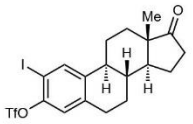

S25
^{19}F NMR
$CDCl_3$, 470 MHz

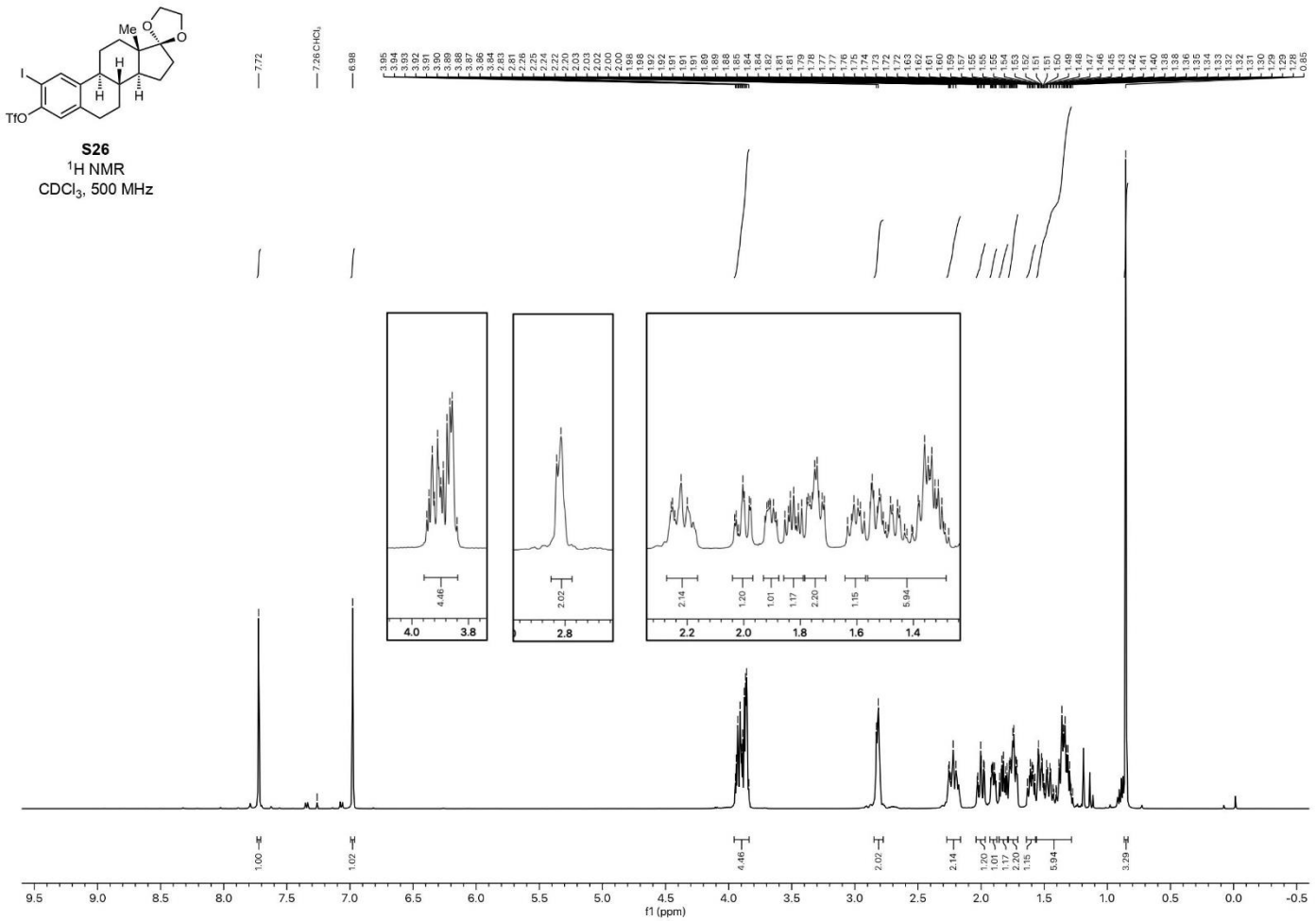
Me
O
O
H
H
H
I
TfO
S26
1H NMR
CDCl3, 500 MHz
7.72
7.26 CHCl3
6.98
f1 (ppm)

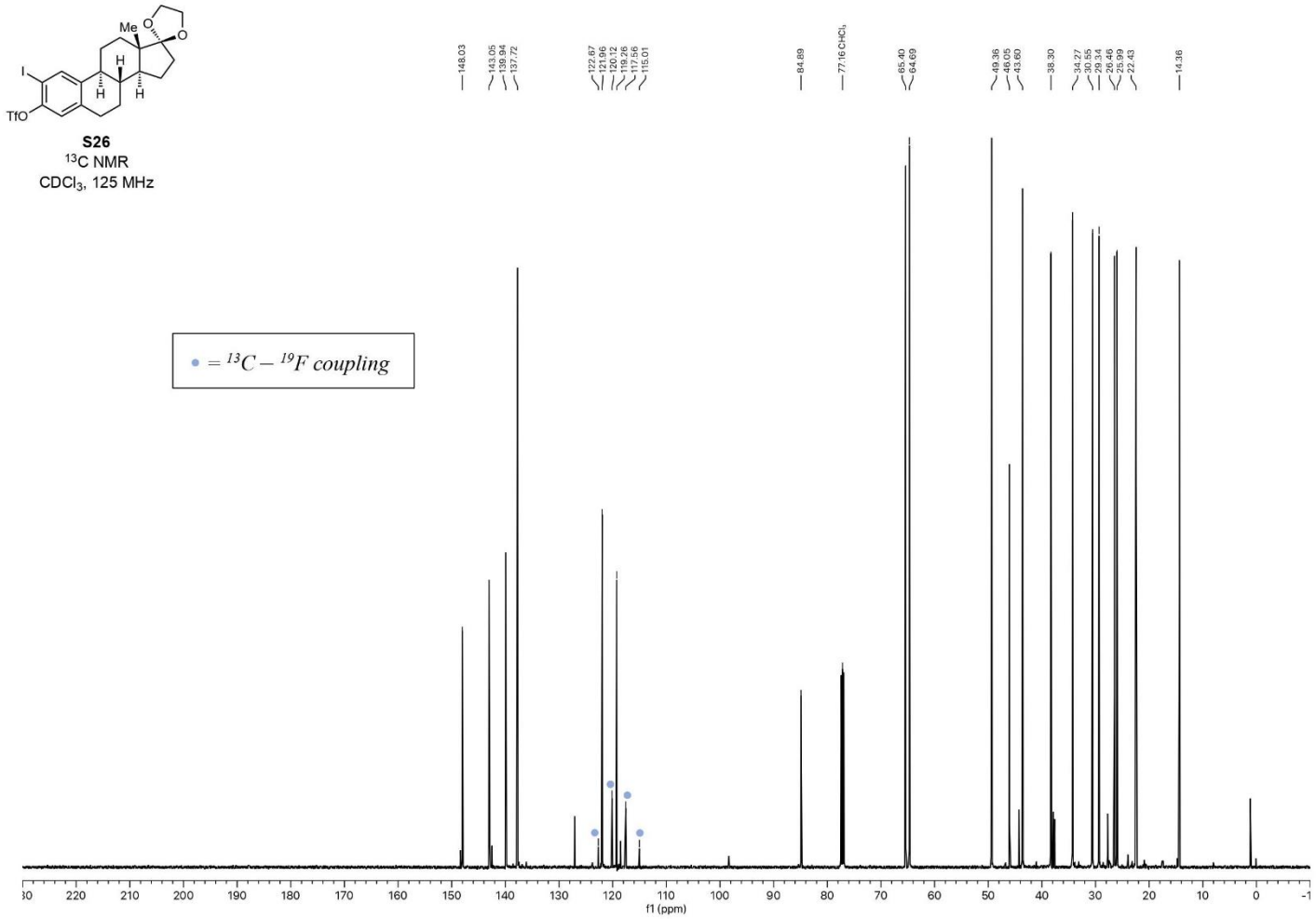
Me
O
O
H
H
H
I
TfO
S26
13C NMR
CDCl3, 125 MHz
148.03
143.05
139.94
137.72
122.67
121.96
120.32
119.26
117.56
115.01
84.89
77.16 CHCl3
65.40
64.69
49.36
48.05
43.60
38.30
34.27
30.55
29.34
29.45
25.99
22.43
14.36
• = 13C – 19F coupling
f1 (ppm)

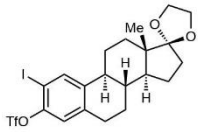

S26
^{19}F NMR
$CDCl_3$, 470 MHz

para-Benzoquinones

Dimethyl Acetylenedicarboxylate(DMAD) as Dienophile

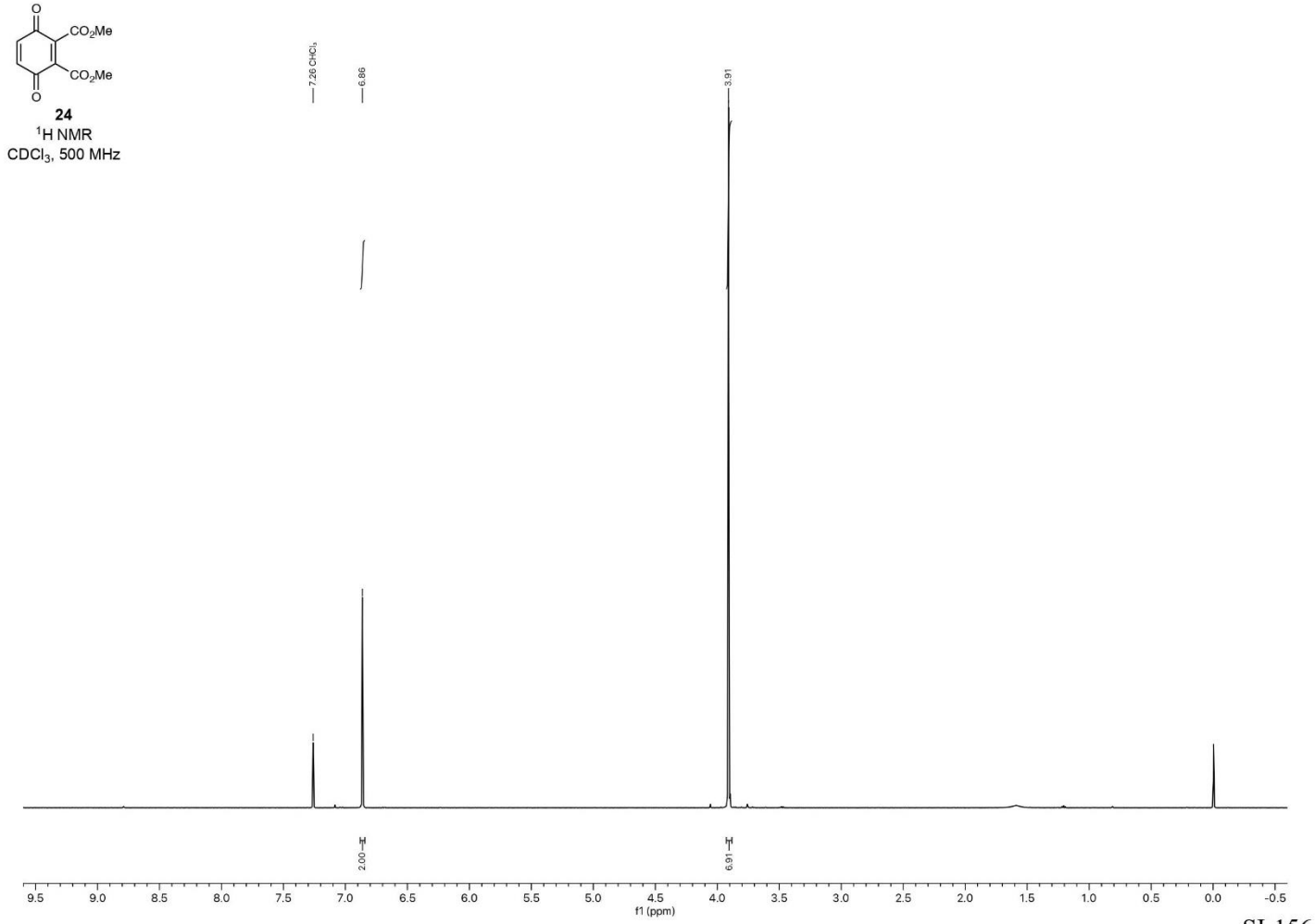

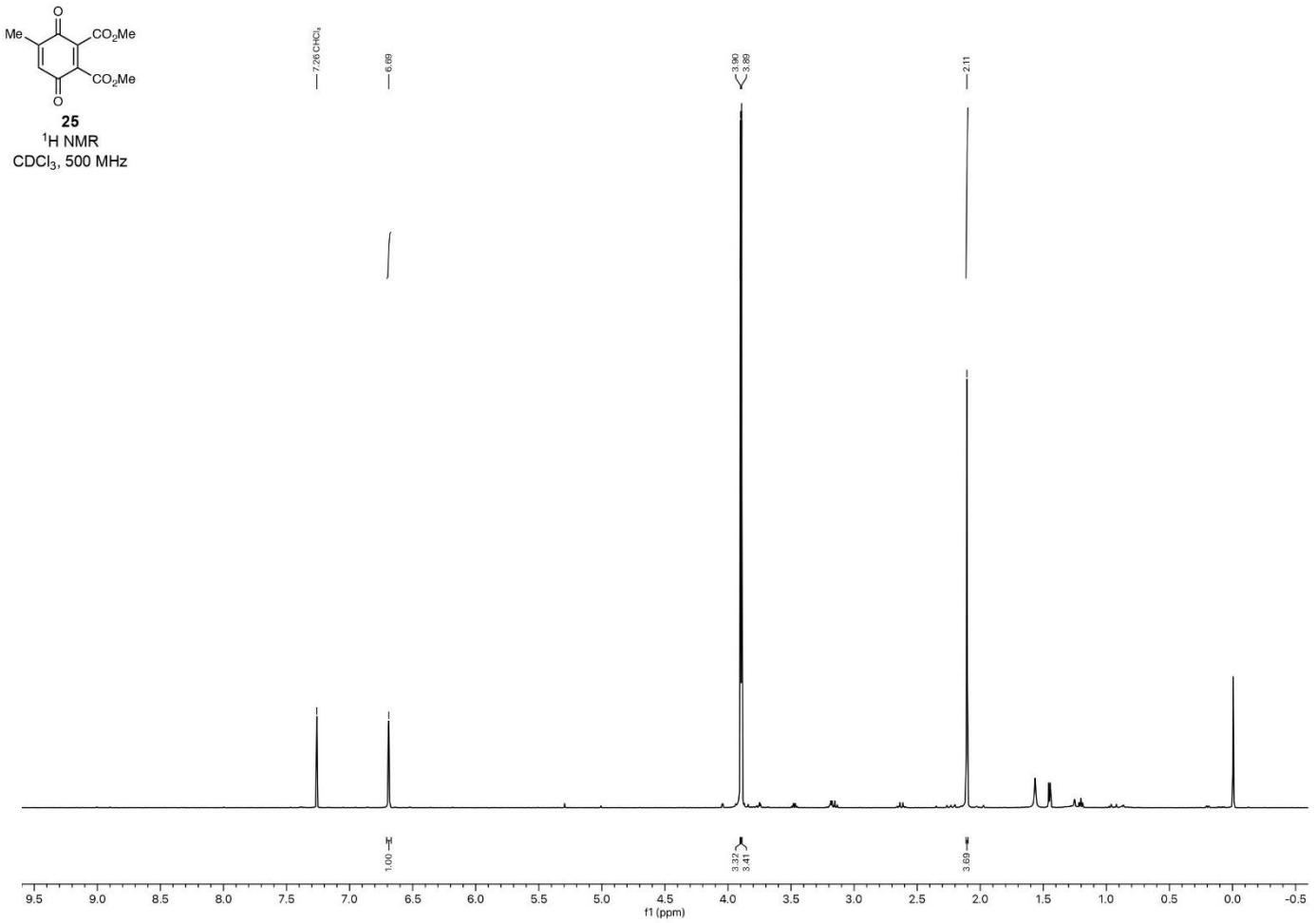
Me
CO2Me
CO2Me
O
O
25
1H NMR
CDCl3, 500 MHz
7.26 CHCl3
6.69
3.90
3.89
2.11
1.00
3.32
3.41
3.69
f1 (ppm)

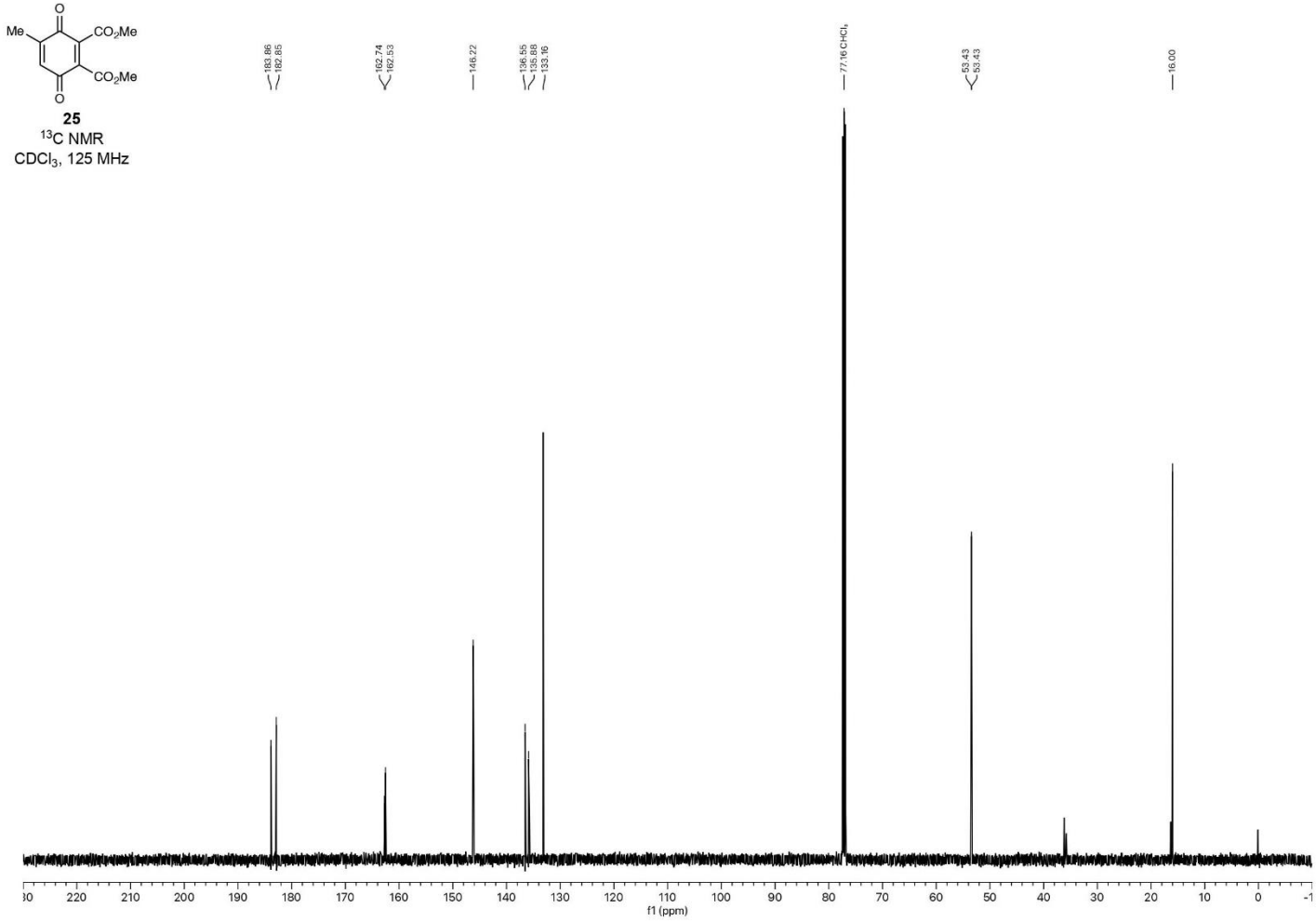
Me
CO2Me
CO2Me
O
O
O
25
13C NMR
CDCl3, 125 MHz
183.86
182.85
162.74
162.53
146.22
136.55
135.88
133.16
77.16 CHCl3
53.43
53.43
16.00
f1 (ppm)

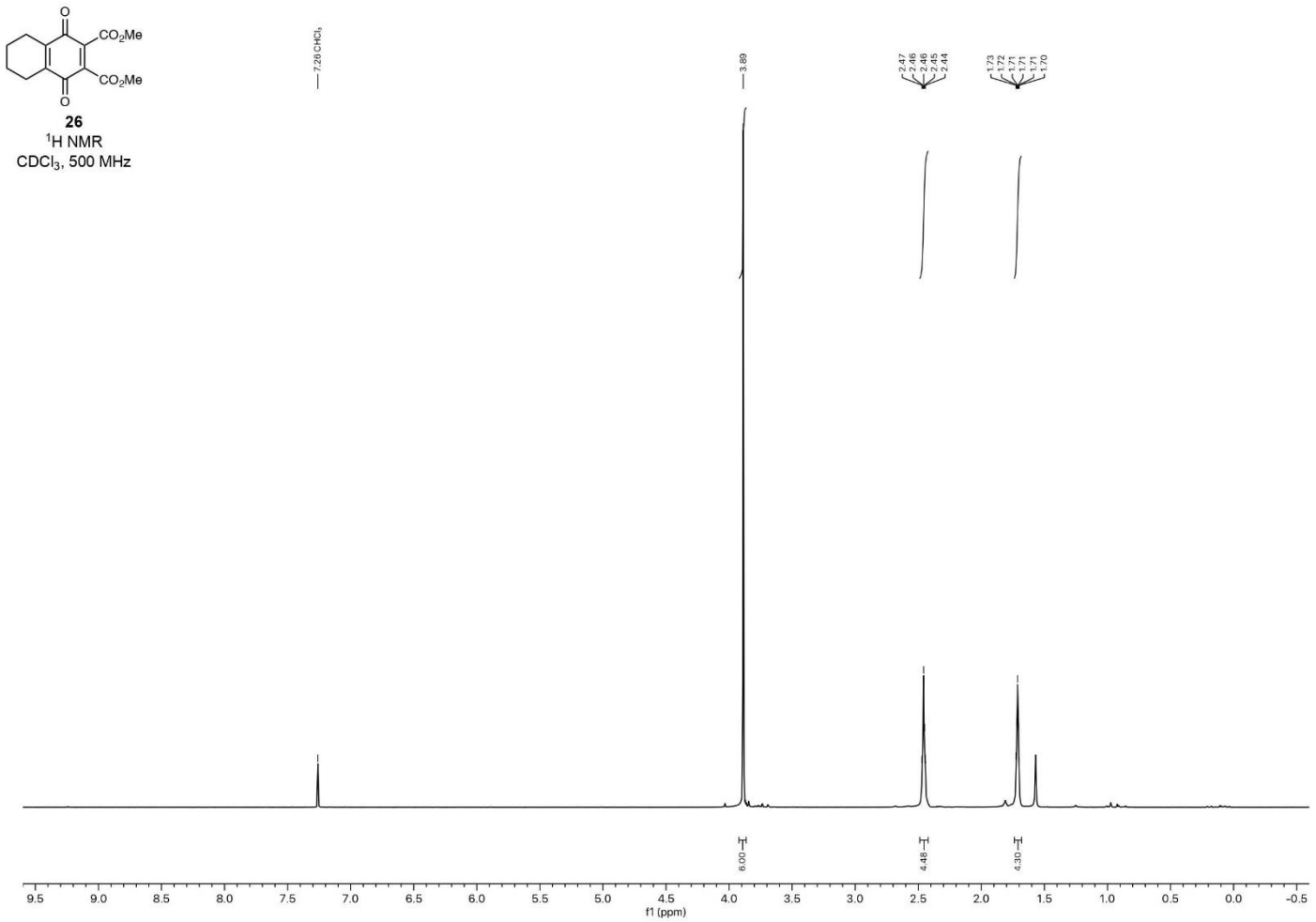
O
CO2Me
CO2Me
O
26
1H NMR
CDCl3, 500 MHz
7.26 CHCl3
3.89
2.47
2.46
2.46
2.45
2.44
1.73
1.72
1.71
1.71
1.71
1.70
6.00
4.48
4.30
9.5
9.0
8.5
8.0
7.5
7.0
6.5
6.0
5.5
5.0
4.5
4.0
3.5
3.0
2.5
2.0
1.5
1.0
0.5
0.0
-0.5
f1 (ppm)

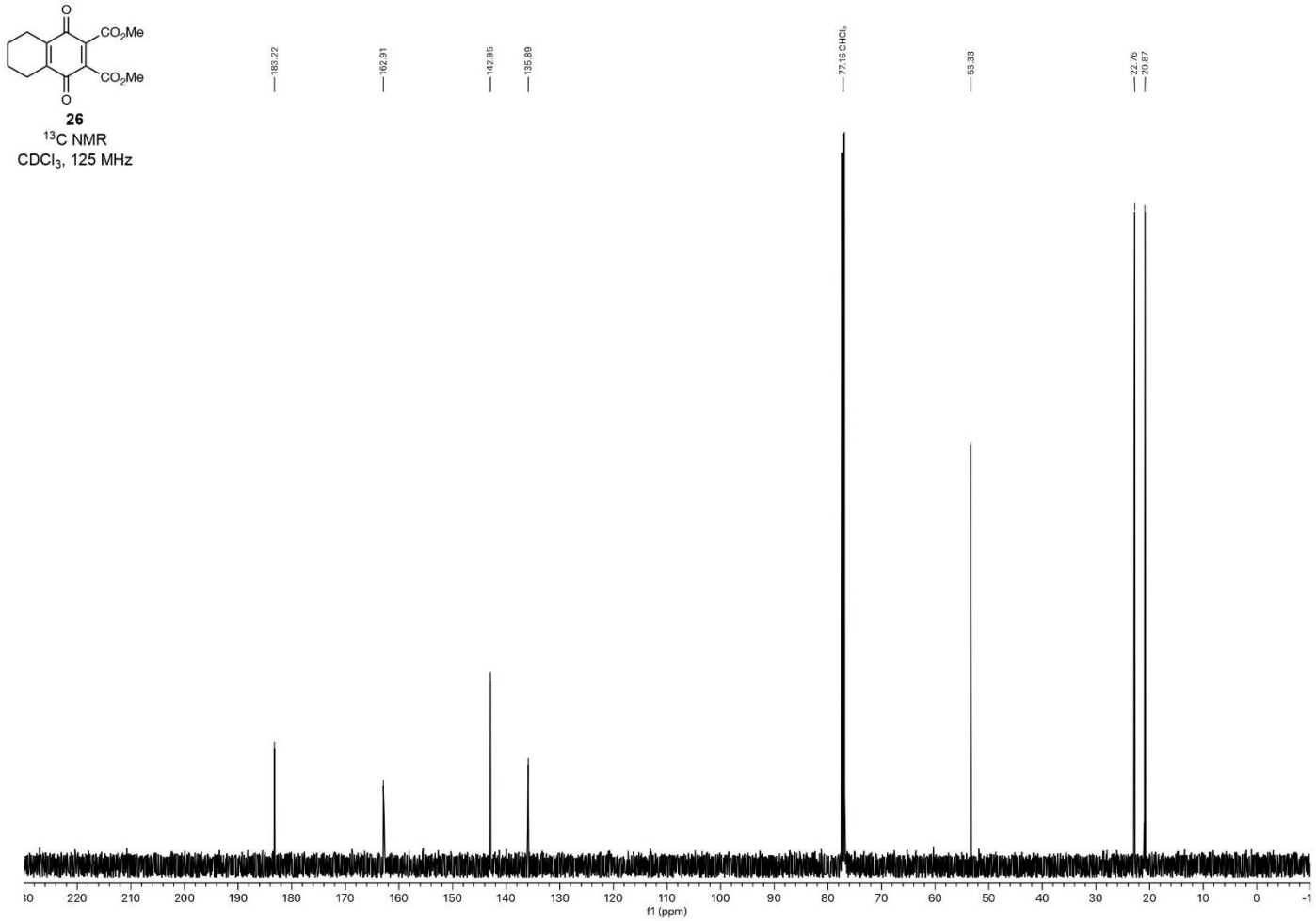
CO2Me
CO2Me
26
13C NMR
CDCl3, 125 MHz
183.22
162.91
147.95
135.89
77.16 CHCl3
53.33
22.76
20.67
f1 (ppm)

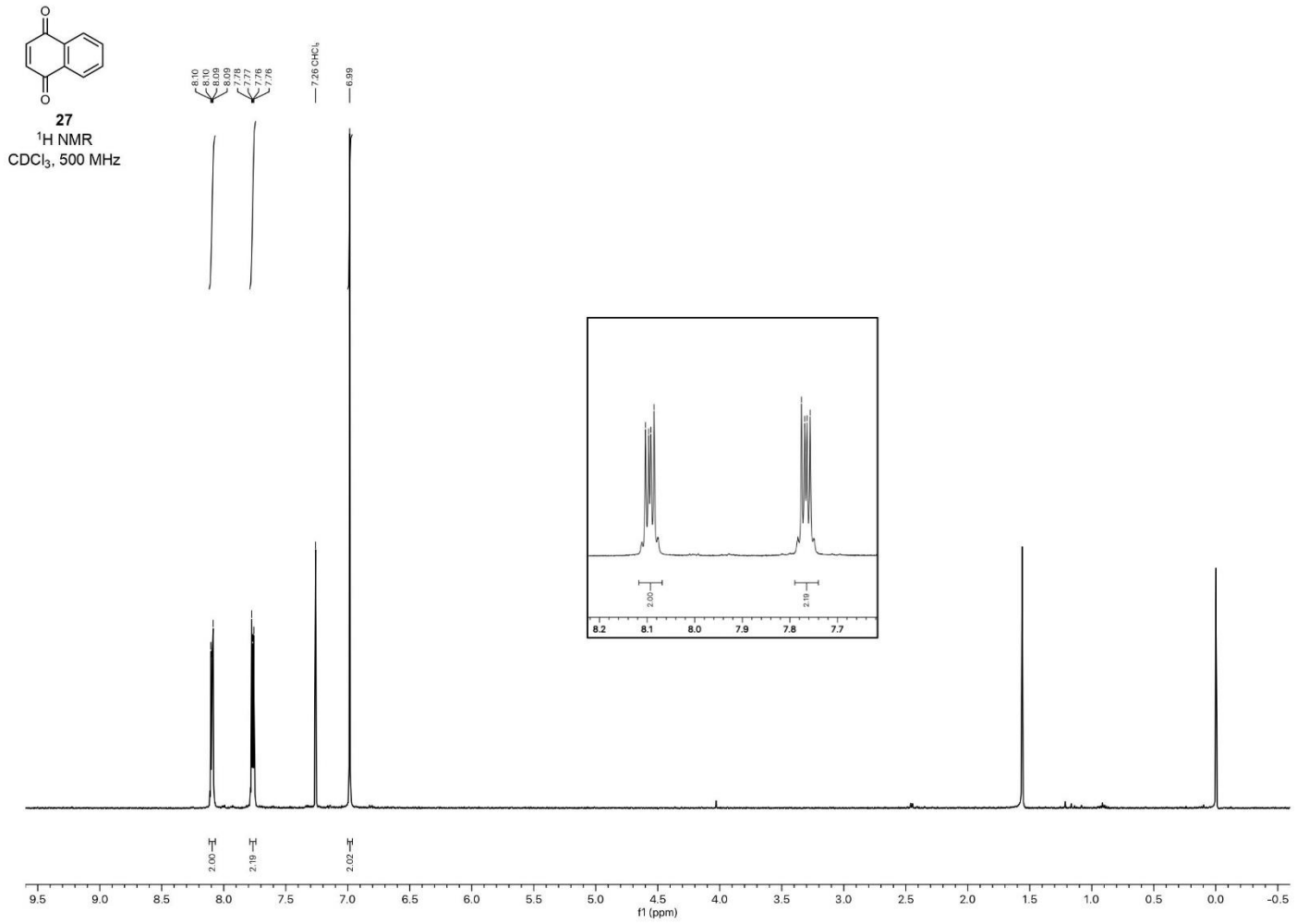
27
^{1}H NMR
$CDCl_3$, 500 MHz
8.10
8.10
8.09
8.09
7.78
7.77
7.76
7.76
7.26 $CHCl_3$
6.99
2.00
2.19
2.02
f1 (ppm)

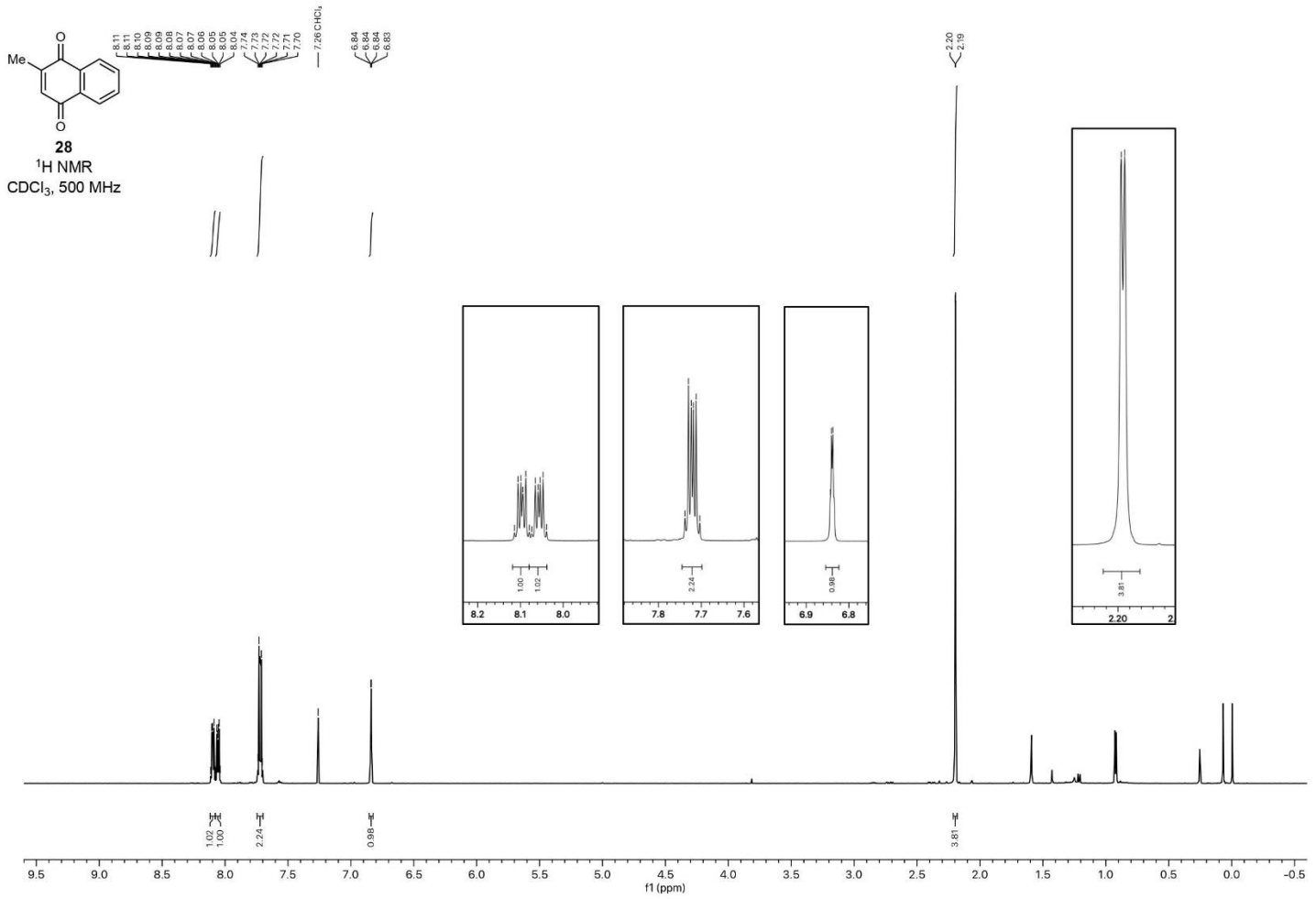
Me
O
O
28
1H NMR
CDCl3, 500 MHz
8.11
8.11
8.10
8.09
8.09
8.08
8.07
8.07
8.06
8.05
8.05
8.04
7.74
7.73
7.72
7.72
7.71
7.70
7.26 CHCl3
6.84
6.84
6.84
6.83
2.20
2.19
1.02
1.00
2.24
0.98
3.81
f1 (ppm)

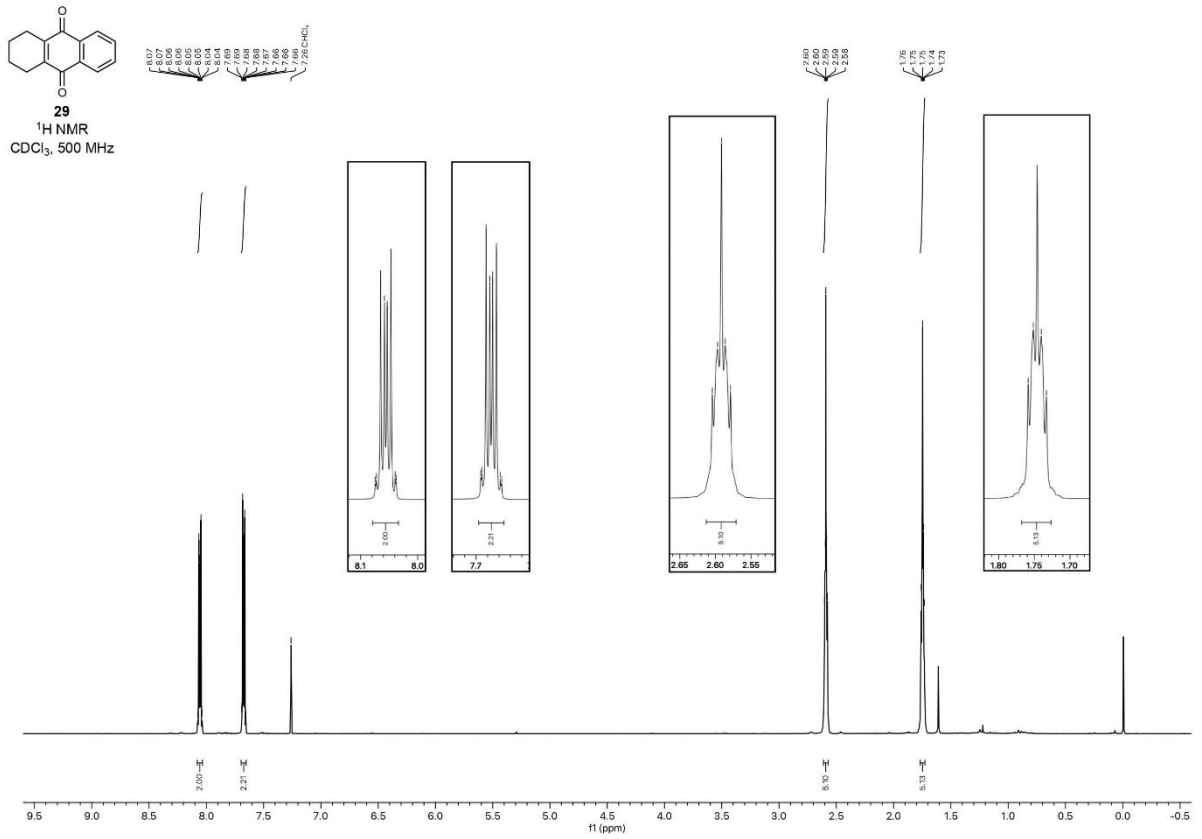
29
^{1}H NMR
$CDCl_3$, 500 MHz
f1 (ppm)

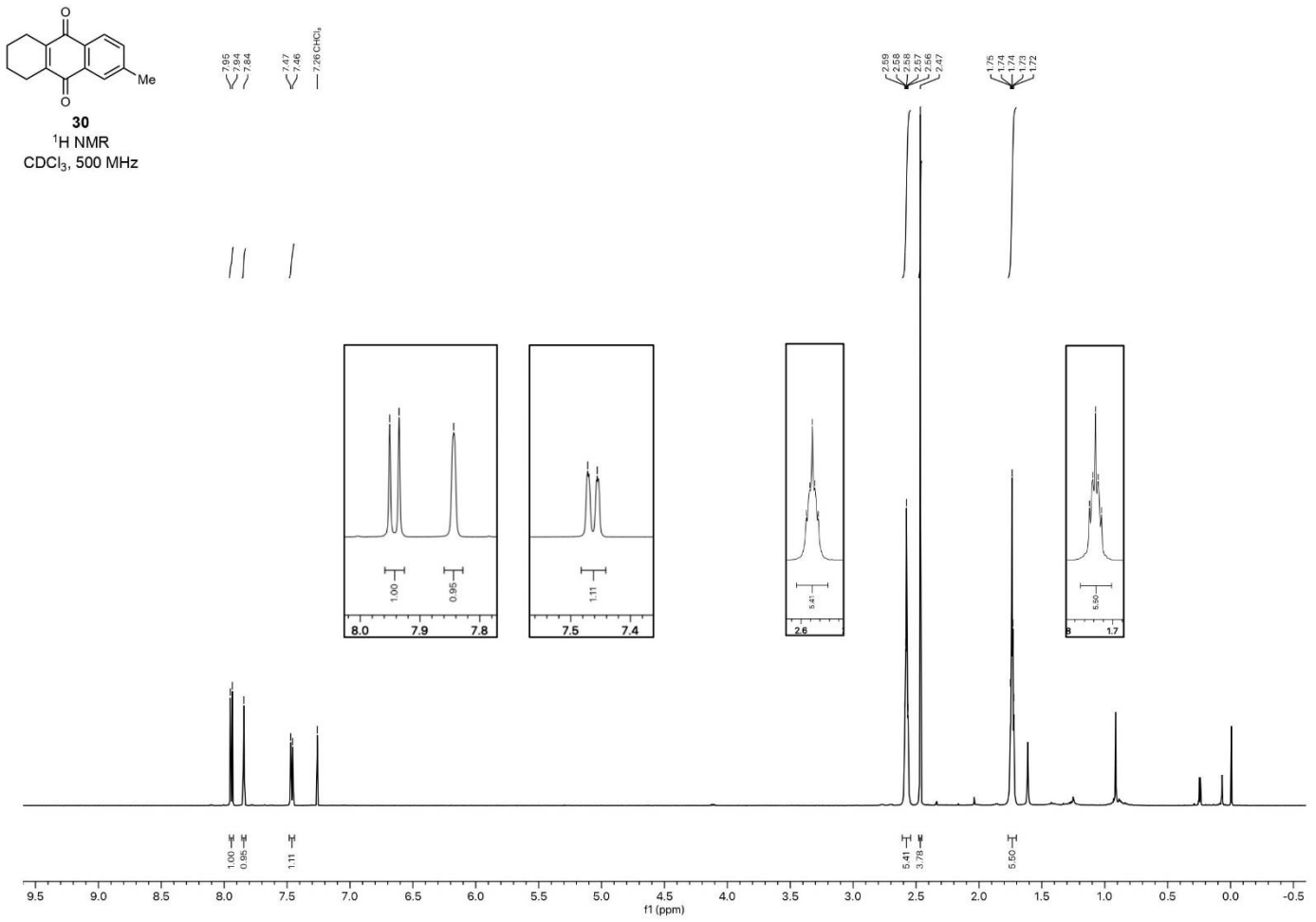
Me
30
1H NMR
CDCl3, 500 MHz
7.95
7.94
7.84
7.47
7.46
7.26 CHCl3
2.59
2.58
2.58
2.57
2.56
2.47
1.75
1.74
1.74
1.74
1.73
1.72
1.00
0.95
1.11
5.41
3.78
5.50
f1 (ppm)

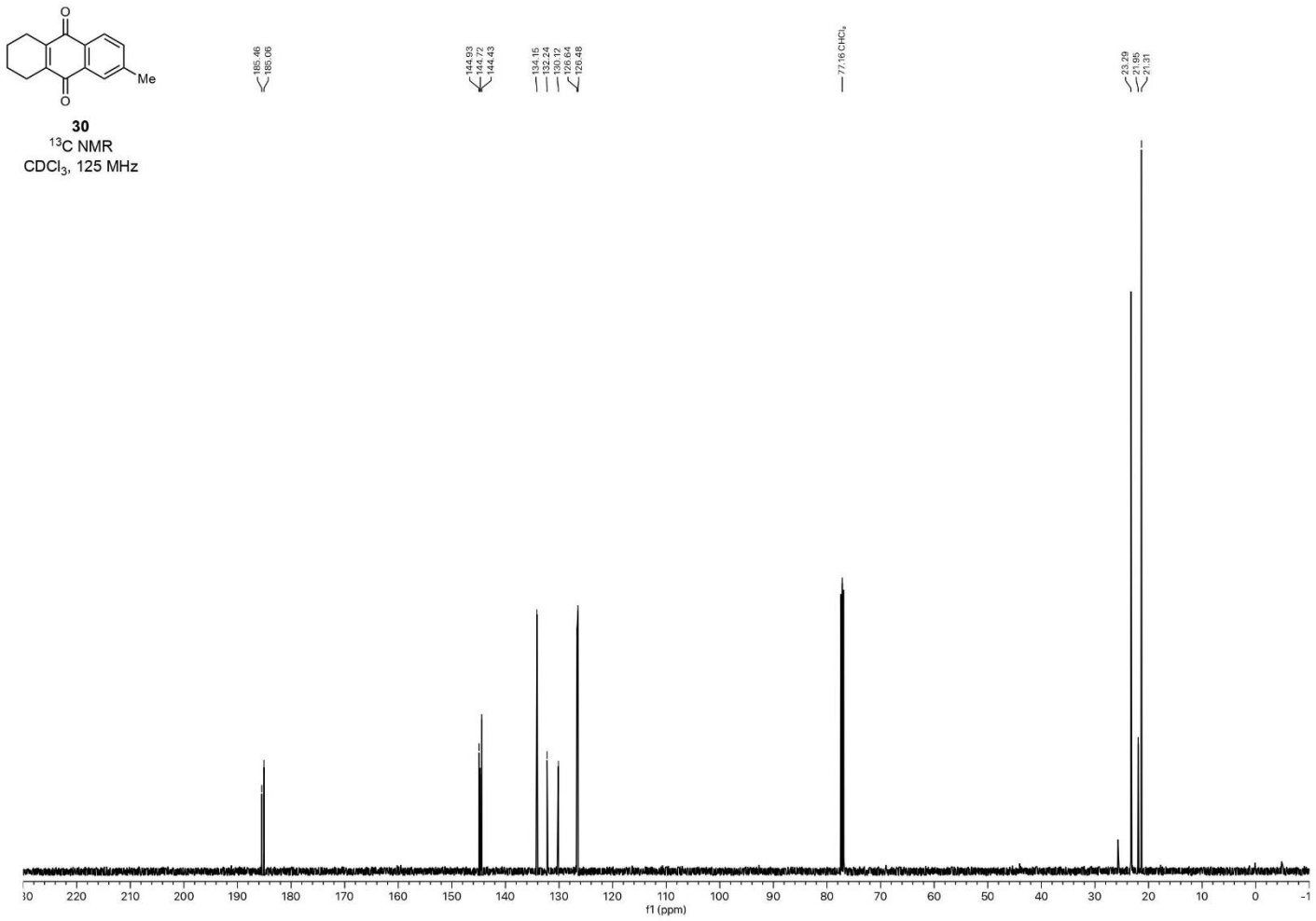
Me
30
13C NMR
CDCl3, 125 MHz
185.46
185.06
144.93
144.72
144.43
134.15
132.24
130.12
126.64
126.48
77.16 CHCl3
23.29
21.95
21.31
f1 (ppm)

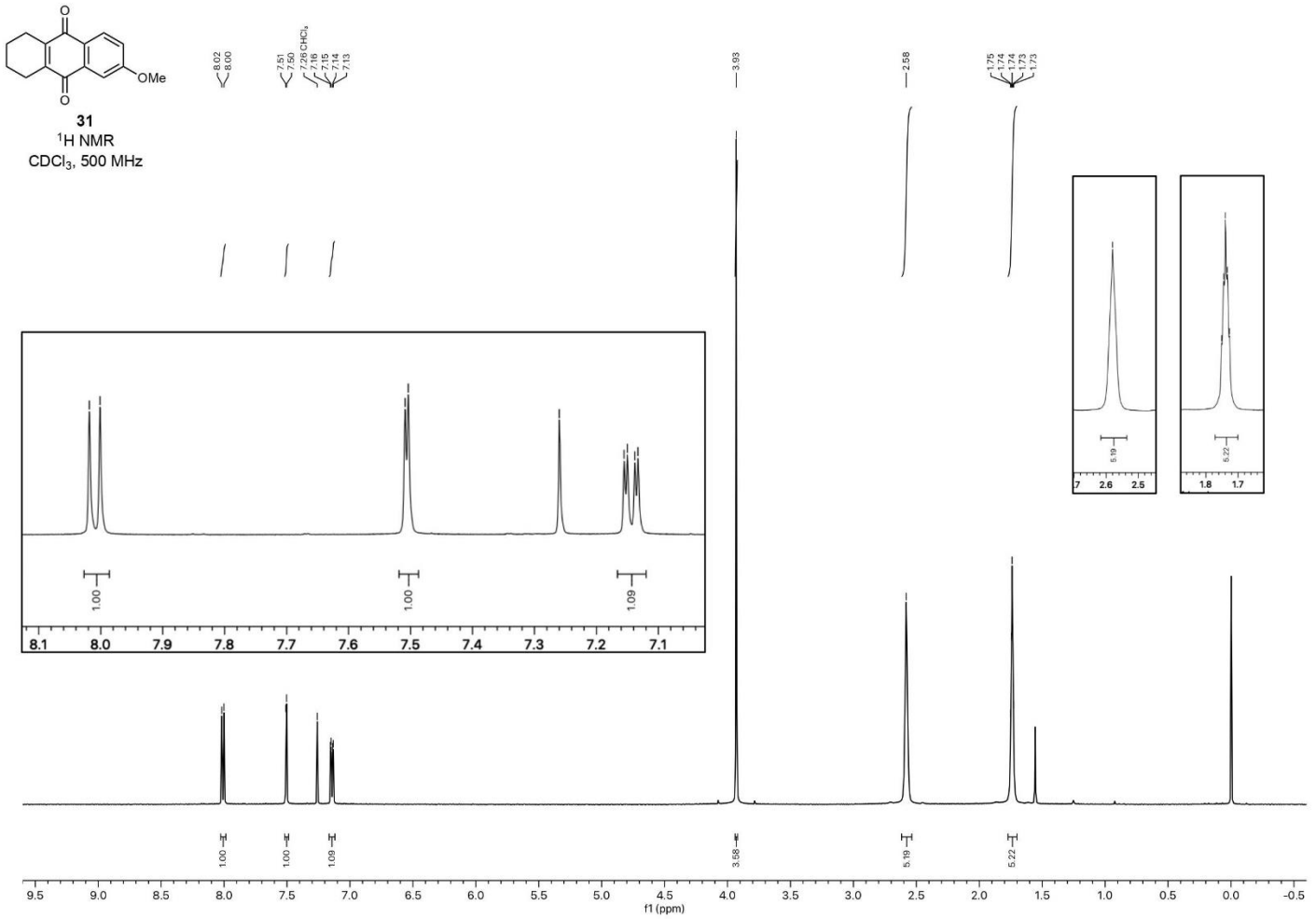
OMe
31
1H NMR
CDCl3, 500 MHz
8.02
8.00
7.51
7.50
7.26 CHCl3
7.16
7.15
7.14
7.13
3.93
2.58
1.75
1.74
1.74
1.73
1.73
1.00
1.00
1.09
5.19
5.22
f1 (ppm)

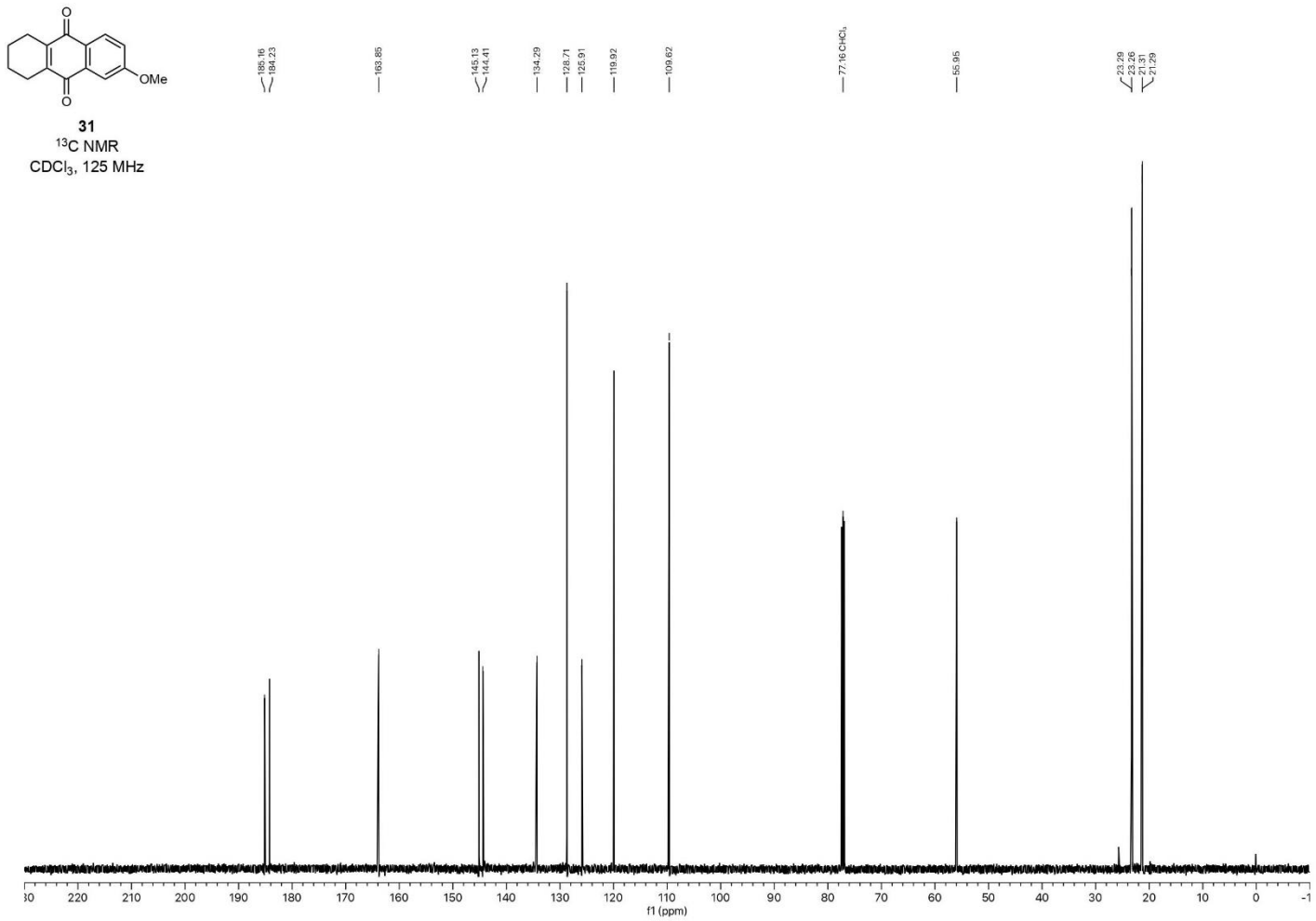
O
O
OMe
31
13C NMR
CDCl3, 125 MHz
185.16
184.23
163.85
145.13
144.41
134.29
128.71
125.91
119.92
109.62
77.16 CHCl3
55.95
23.29
23.26
21.31
21.29
f1 (ppm)

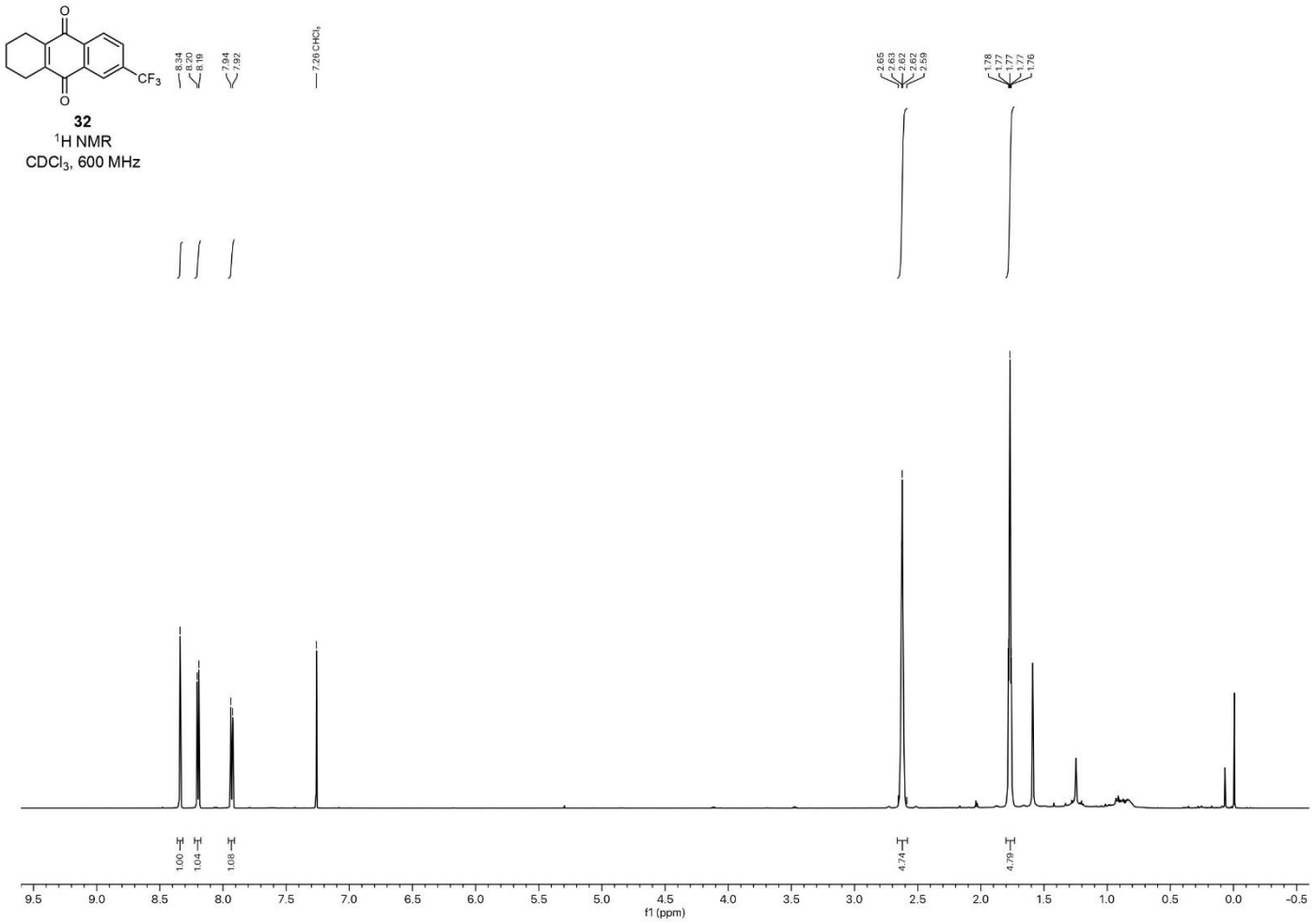
O
O
CF3
32
1H NMR
CDCl3, 600 MHz
8.34
8.20
8.19
7.94
7.92
7.26 CHCl3
2.65
2.63
2.62
2.62
2.59
1.78
1.77
1.77
1.77
1.76
1.00
1.04
1.08
4.74
4.79
9.5
9.0
8.5
8.0
7.5
7.0
6.5
6.0
5.5
5.0
4.5
4.0
3.5
3.0
2.5
2.0
1.5
1.0
0.5
0.0
-0.5
f1 (ppm)

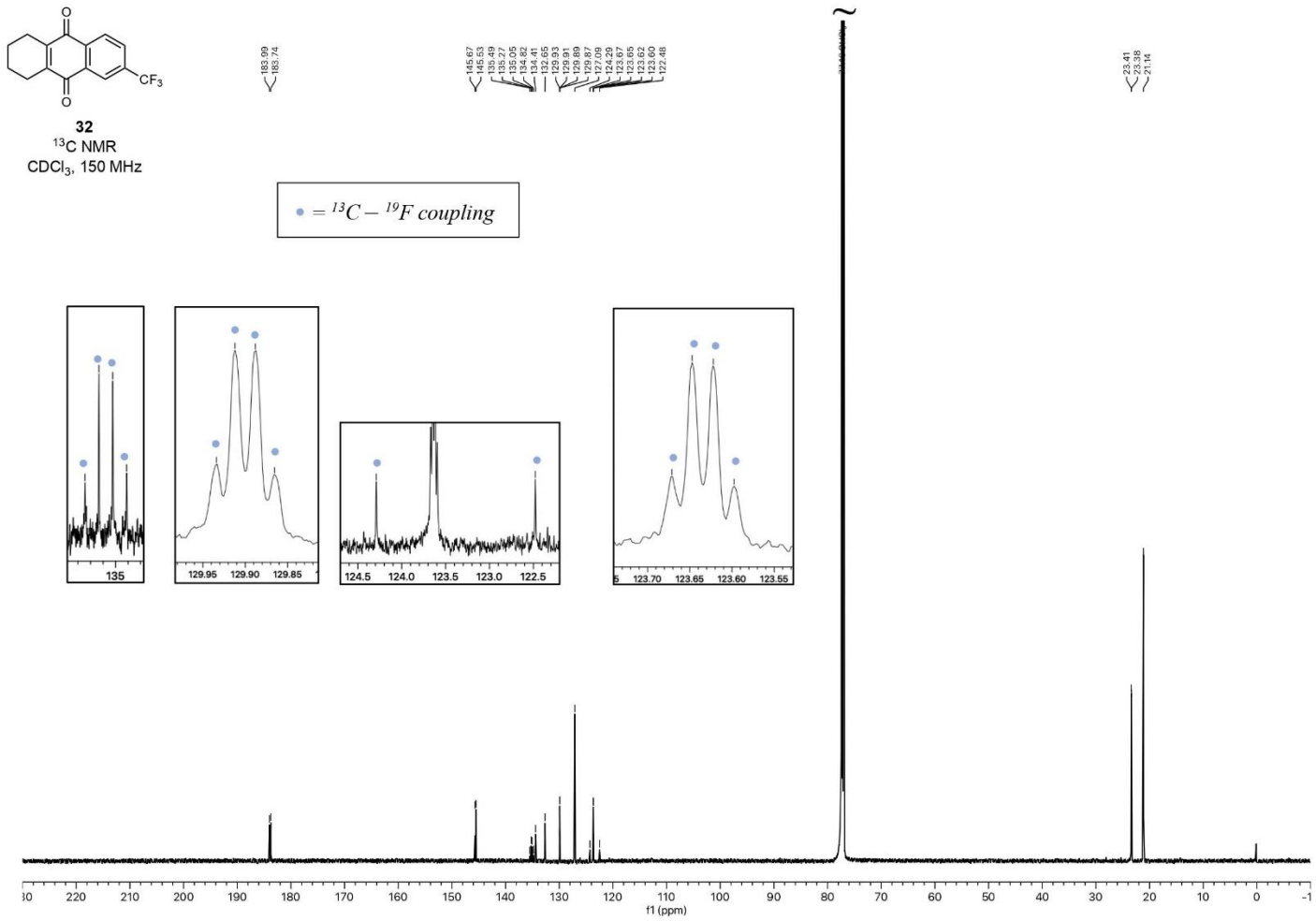
O
O
CF3
32
13C NMR
CDCl3, 150 MHz
• = 13C – 19F coupling
183.99
183.74
145.67
145.53
135.49
135.27
135.07
134.82
134.41
132.65
129.93
129.91
129.89
129.87
127.09
124.29
123.67
123.65
123.62
123.60
122.48
77.48
77.16
76.84
23.41
23.38
21.14
135
129.95
129.90
129.85
124.5
124.0
123.5
123.0
122.5
123.70
123.65
123.60
123.55
f1 (ppm)

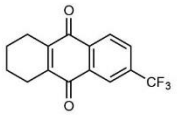

32
^{19}F NMR
$CDCl_3$, 470 MHz

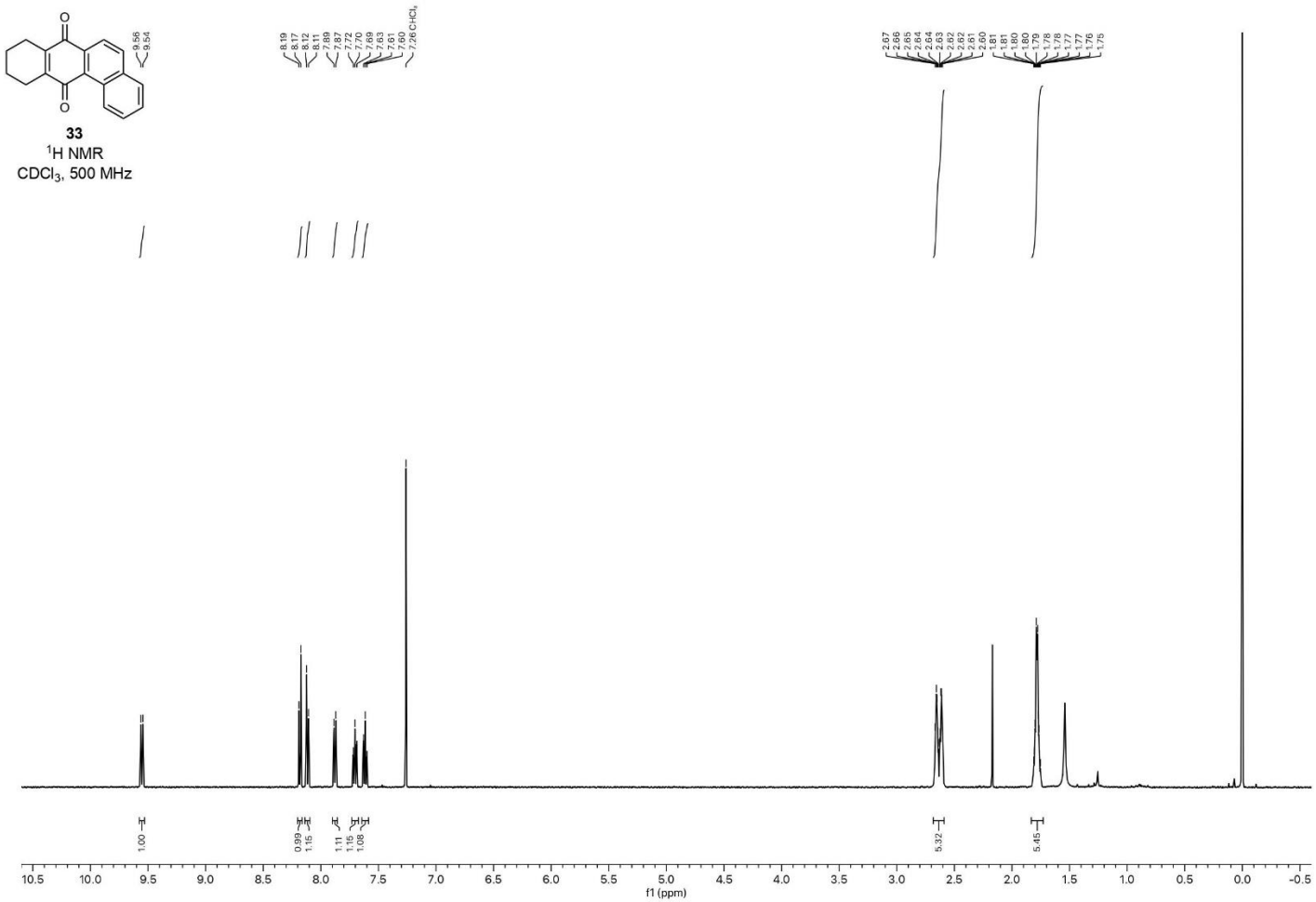
33
1H NMR
CDCl3, 500 MHz
f1 (ppm)

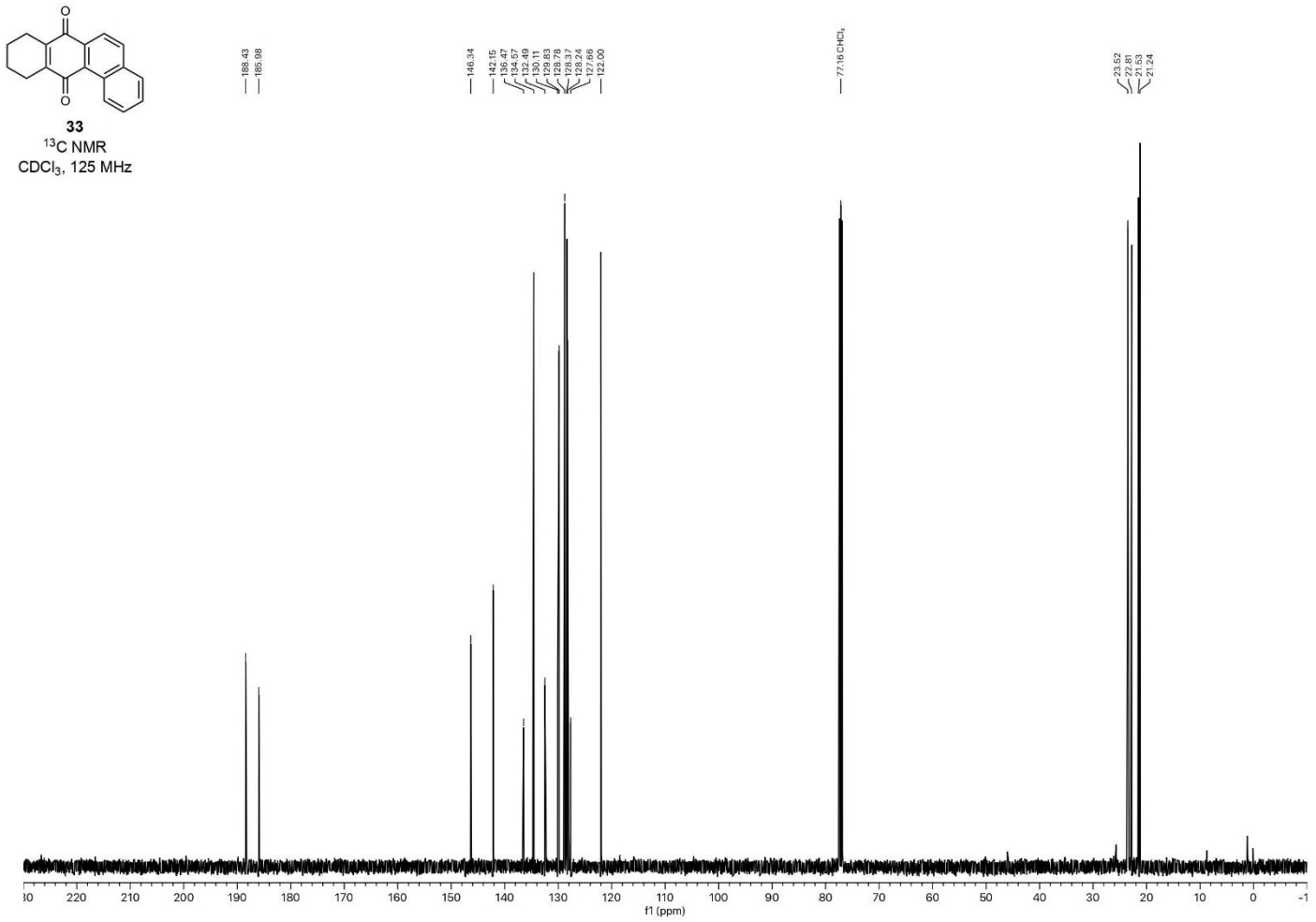

33

^{13}C NMR

$CDCl_3$, 125 MHz

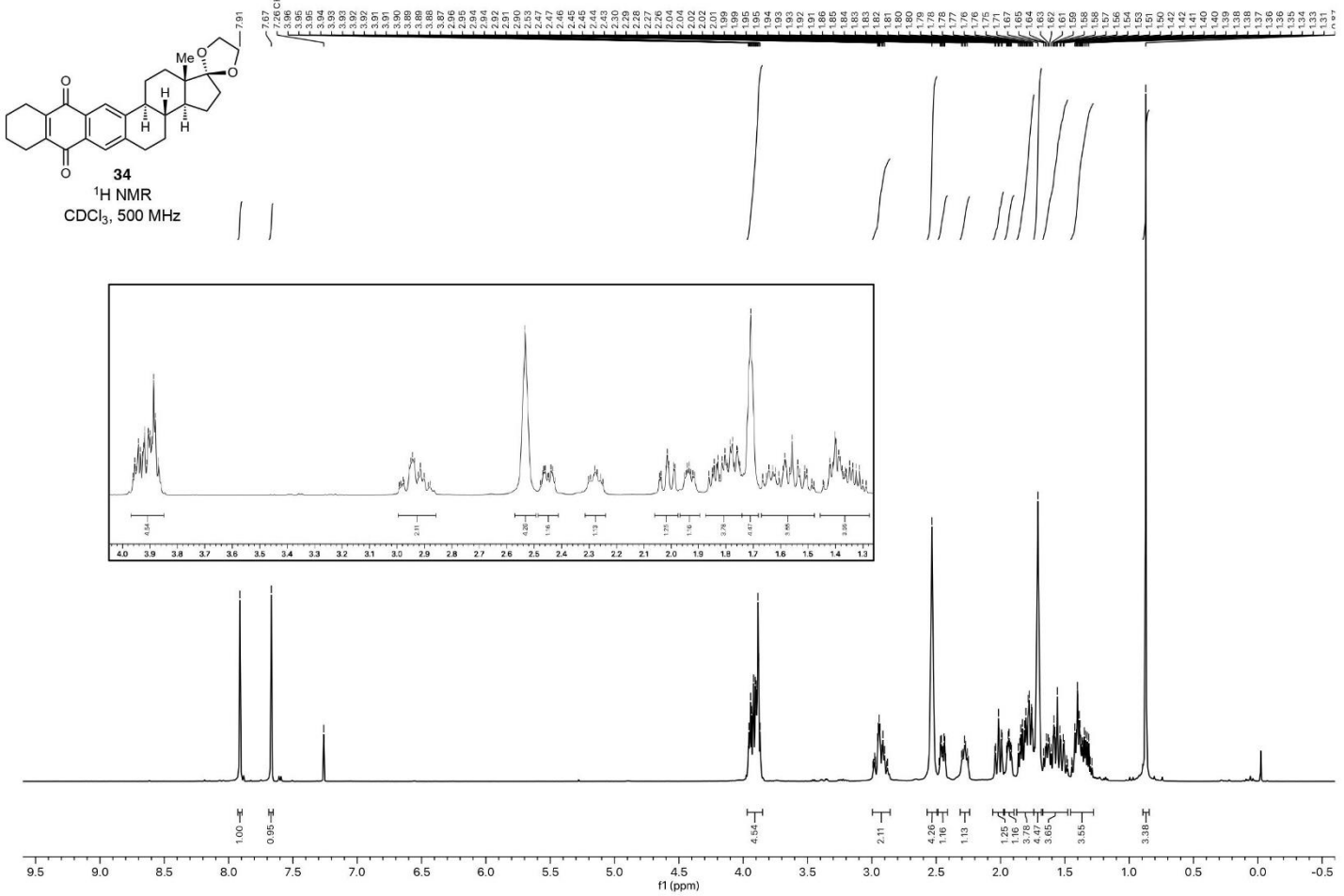
34
^{1}H NMR
$CDCl_3$, 500 MHz
f1 (ppm)

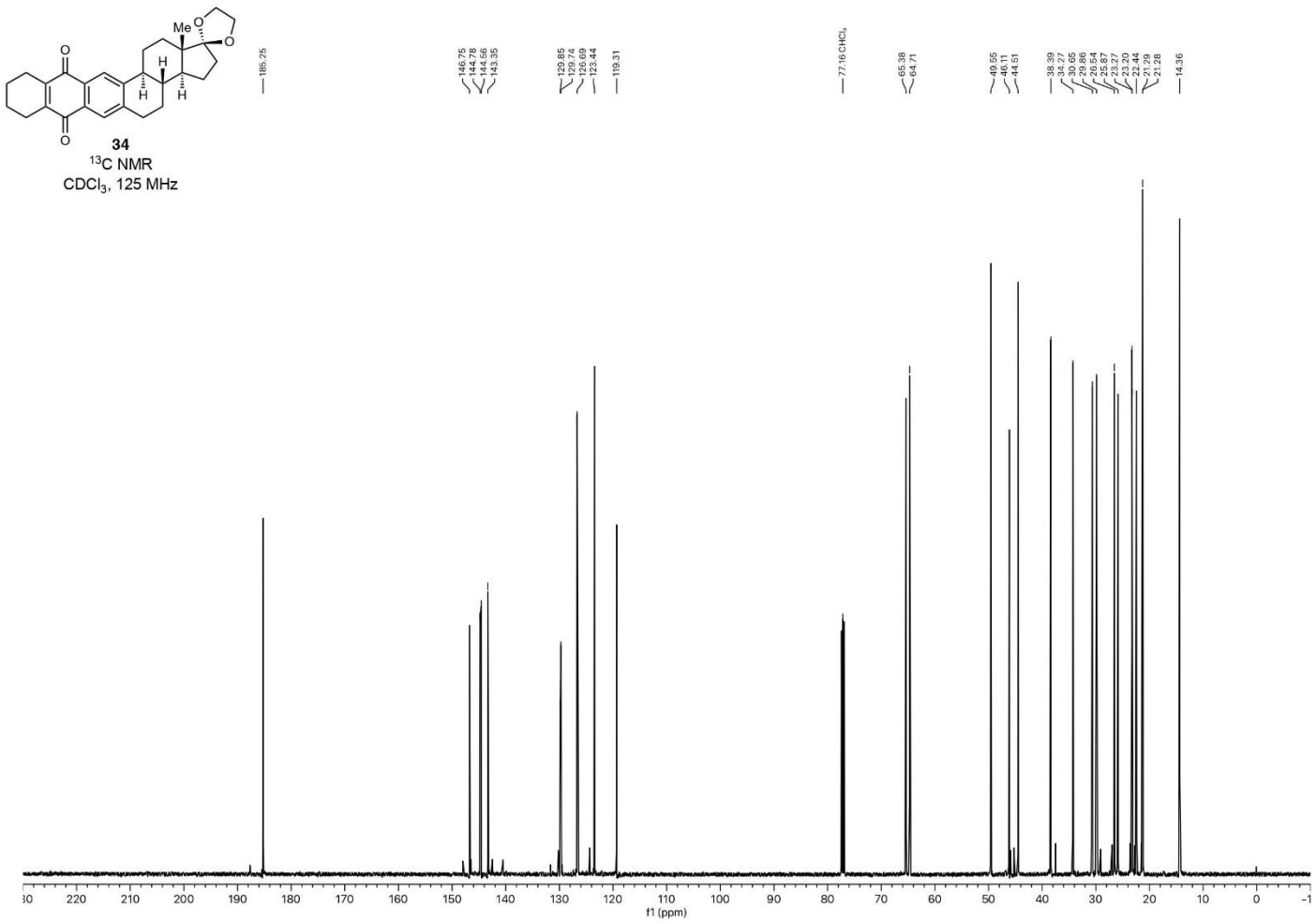
Me
O
O
H
H
H
O
O
34
^{13}C NMR
$CDCl_3$, 125 MHz
185.25
146.75
144.78
144.56
143.35
129.85
129.74
126.69
123.44
119.31
77.16 $CHCl_3$
65.38
64.71
49.55
48.11
44.51
38.39
34.27
30.65
29.86
29.54
25.87
23.27
23.20
21.44
21.29
21.28
14.36
f1 (ppm)

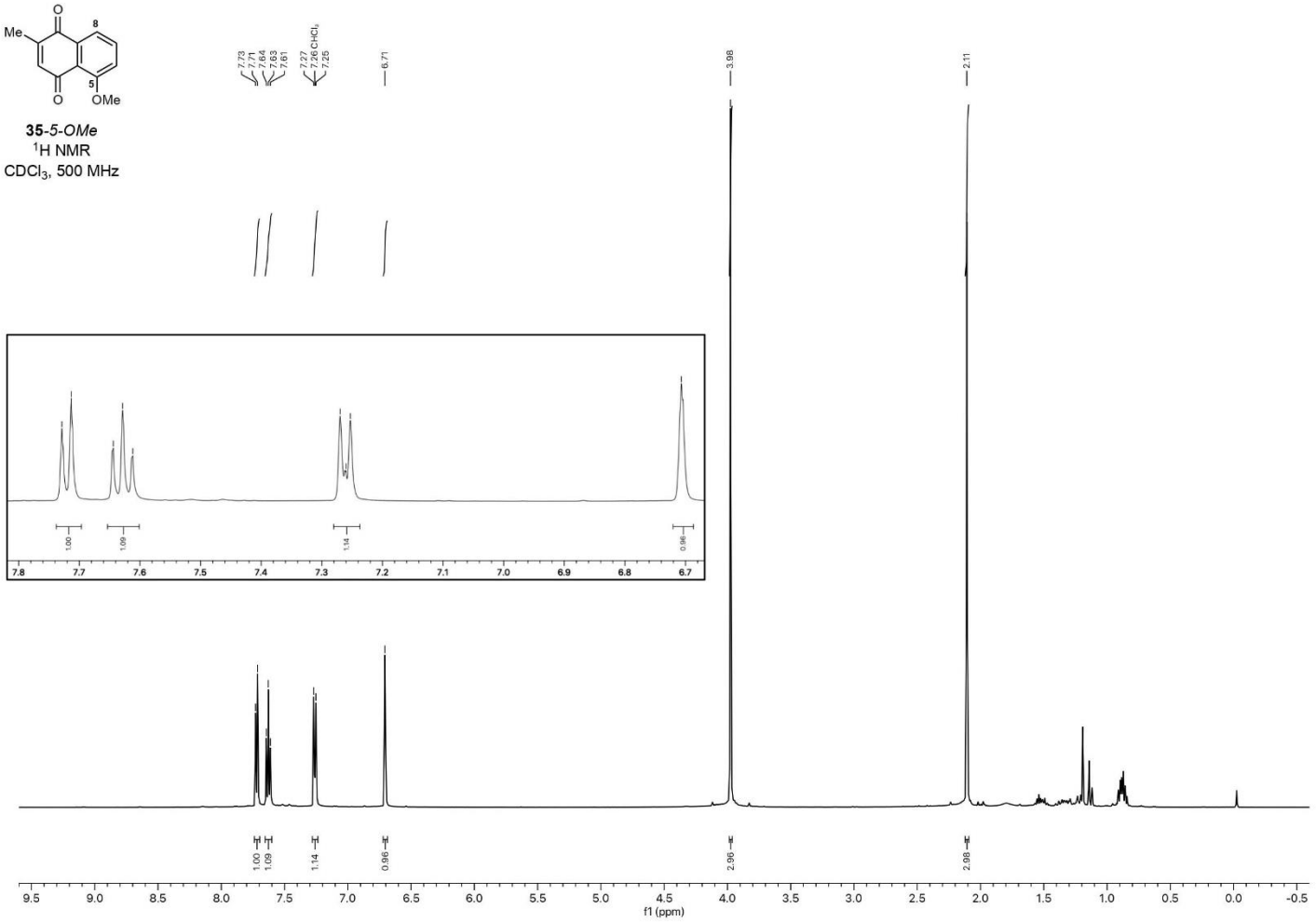
Me
O
O
8
5
OMe
35-5-OMe
1H NMR
CDCl3, 500 MHz
7.73
7.71
7.64
7.63
7.61
7.27
7.26 CHCl3
7.25
6.71
3.98
2.11
1.00
1.09
1.14
0.96
2.96
2.98
f1 (ppm)

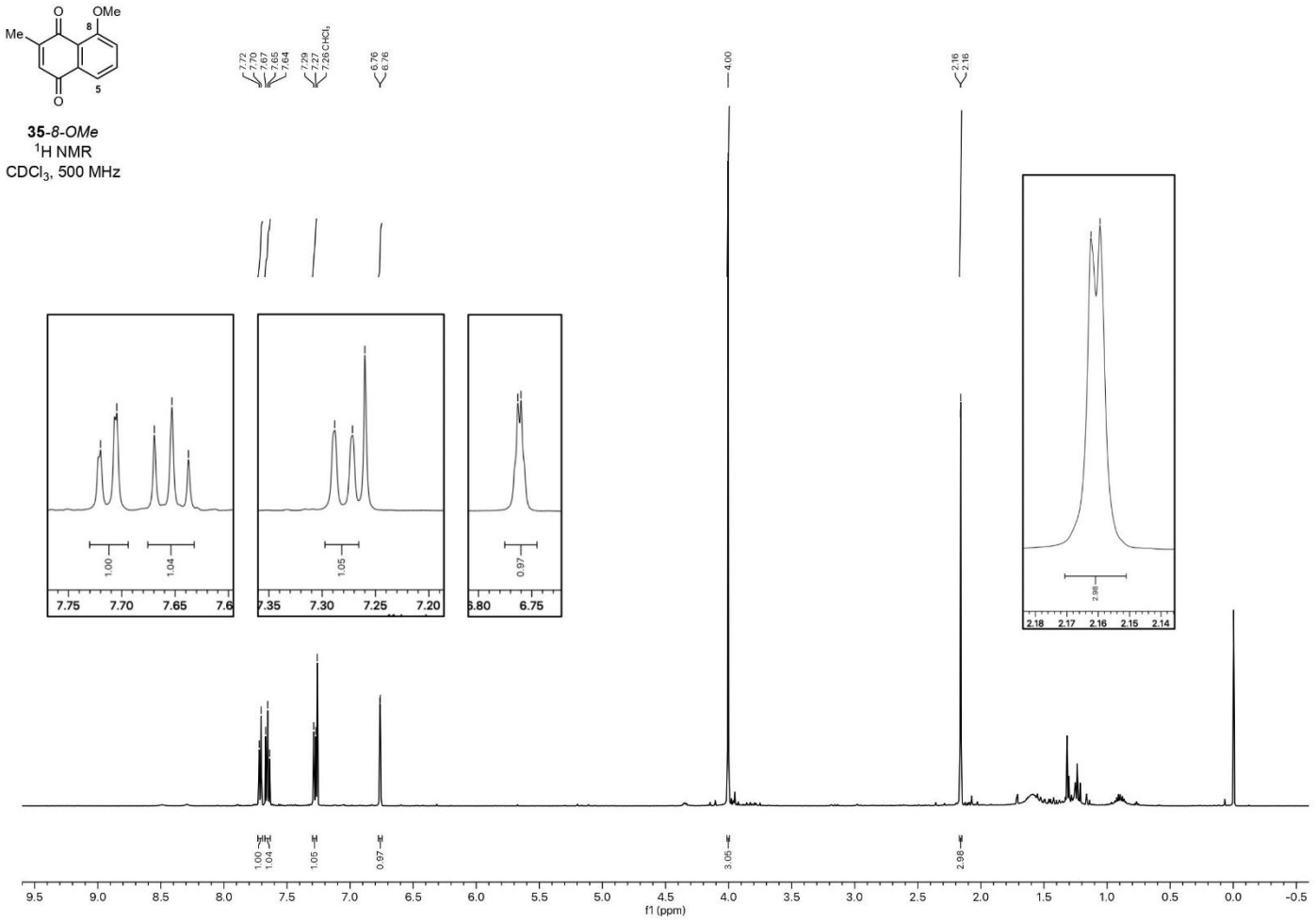
Me
O
OMe
8
5
O
35-8-OMe
1H NMR
CDCl3, 500 MHz
7.72
7.70
7.67
7.65
7.64
7.29
7.27
7.26 CHCl3
6.76
6.76
4.00
2.16
2.16
1.00
1.04
1.05
0.97
2.98
f1 (ppm)

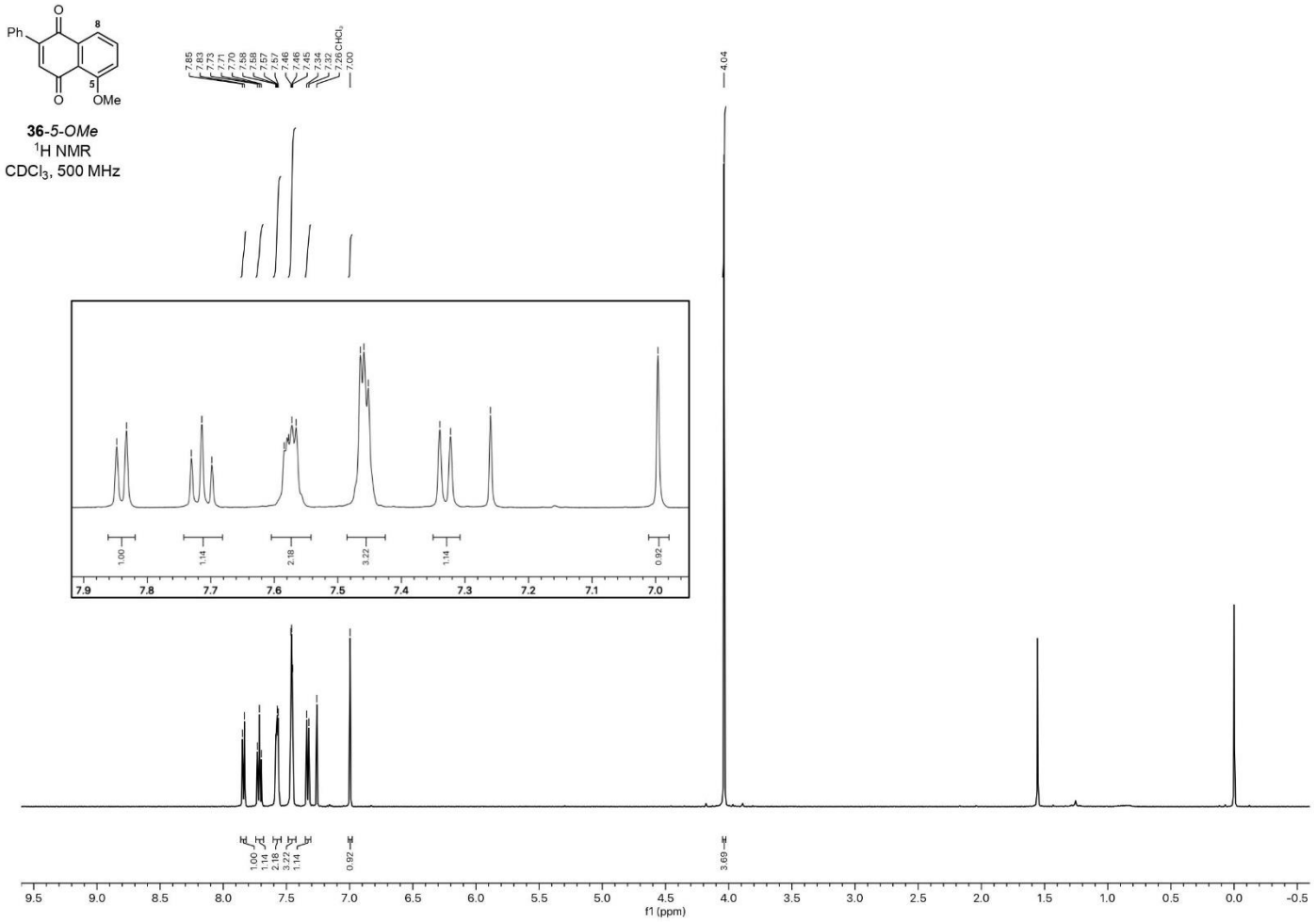
Ph
O
O
8
5
OMe
36-5-OMe
1H NMR
CDCl3, 500 MHz
7.85
7.83
7.73
7.71
7.70
7.59
7.58
7.57
7.57
7.46
7.46
7.45
7.34
7.32
7.26 CHCl3
7.00
4.04
1.00
1.14
2.18
3.22
1.14
0.92
3.69
f1 (ppm)

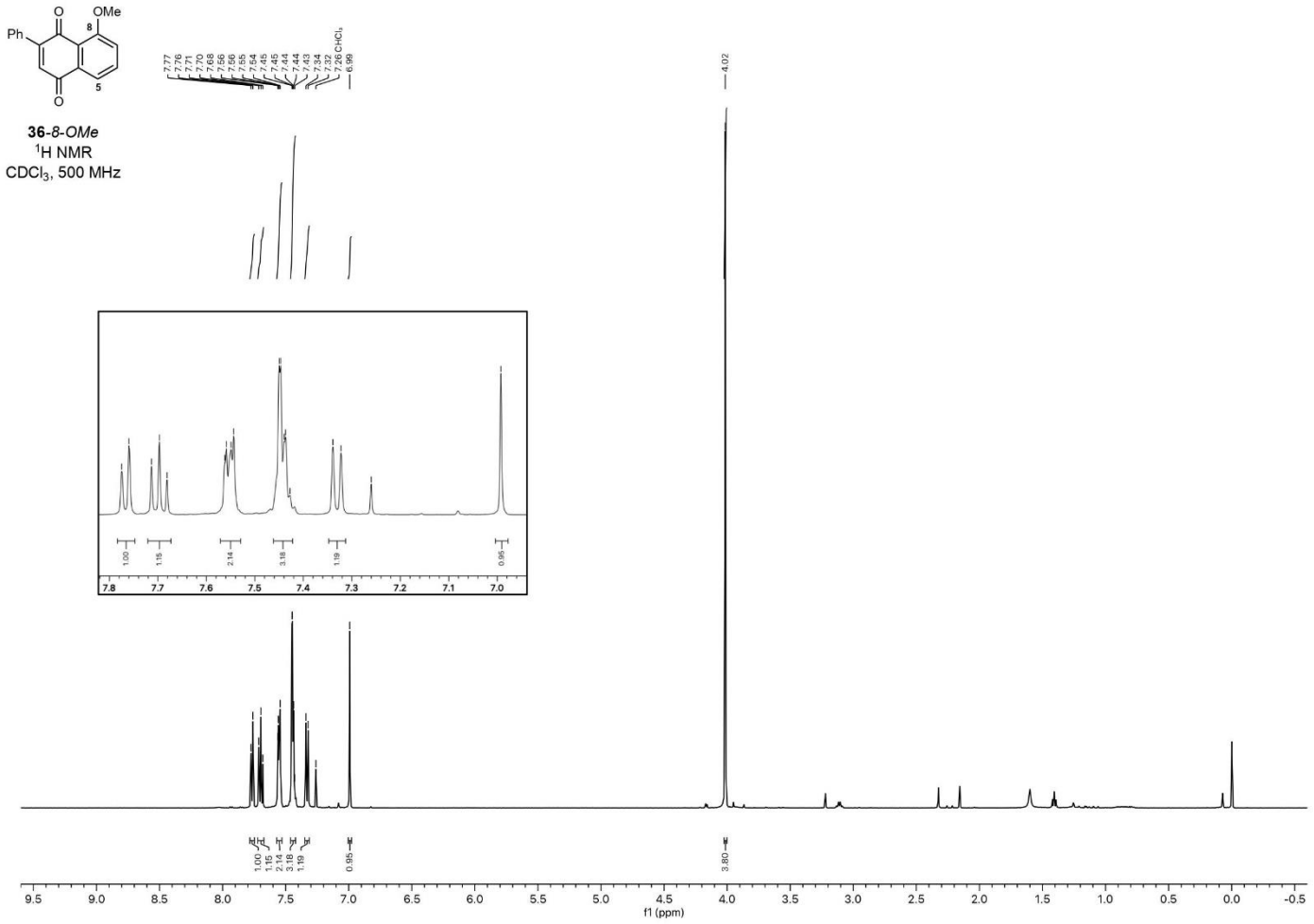
Ph
O
OMe
8
5
O
36-8-OMe
1H NMR
CDCl3, 500 MHz
7.77
7.76
7.71
7.70
7.68
7.56
7.56
7.55
7.54
7.45
7.45
7.44
7.44
7.43
7.34
7.32
7.26 CHCl3
6.99
4.02
1.00
1.15
2.14
3.18
1.19
0.95
3.80
f1 (ppm)

Pyrroles and their Precursors

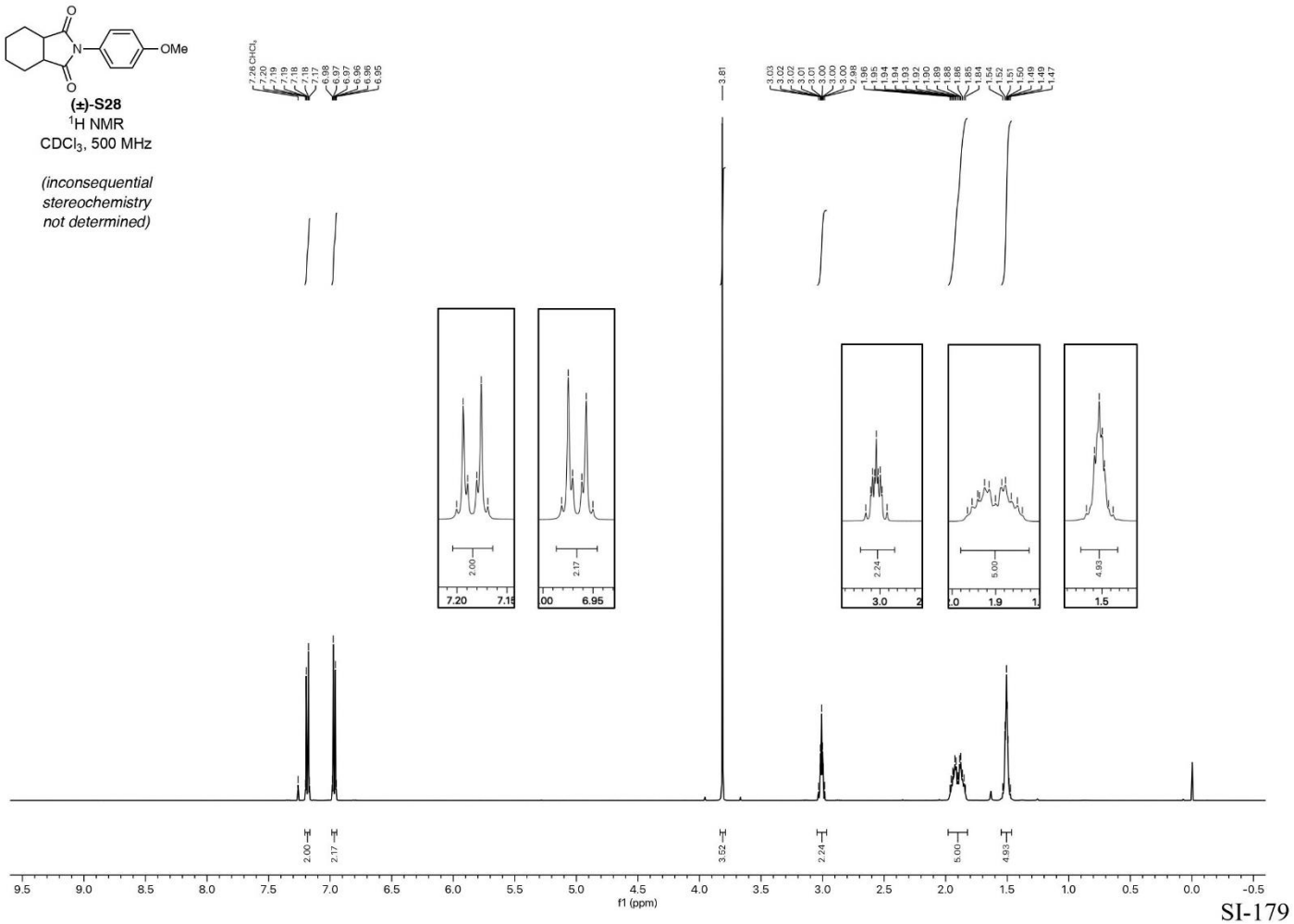

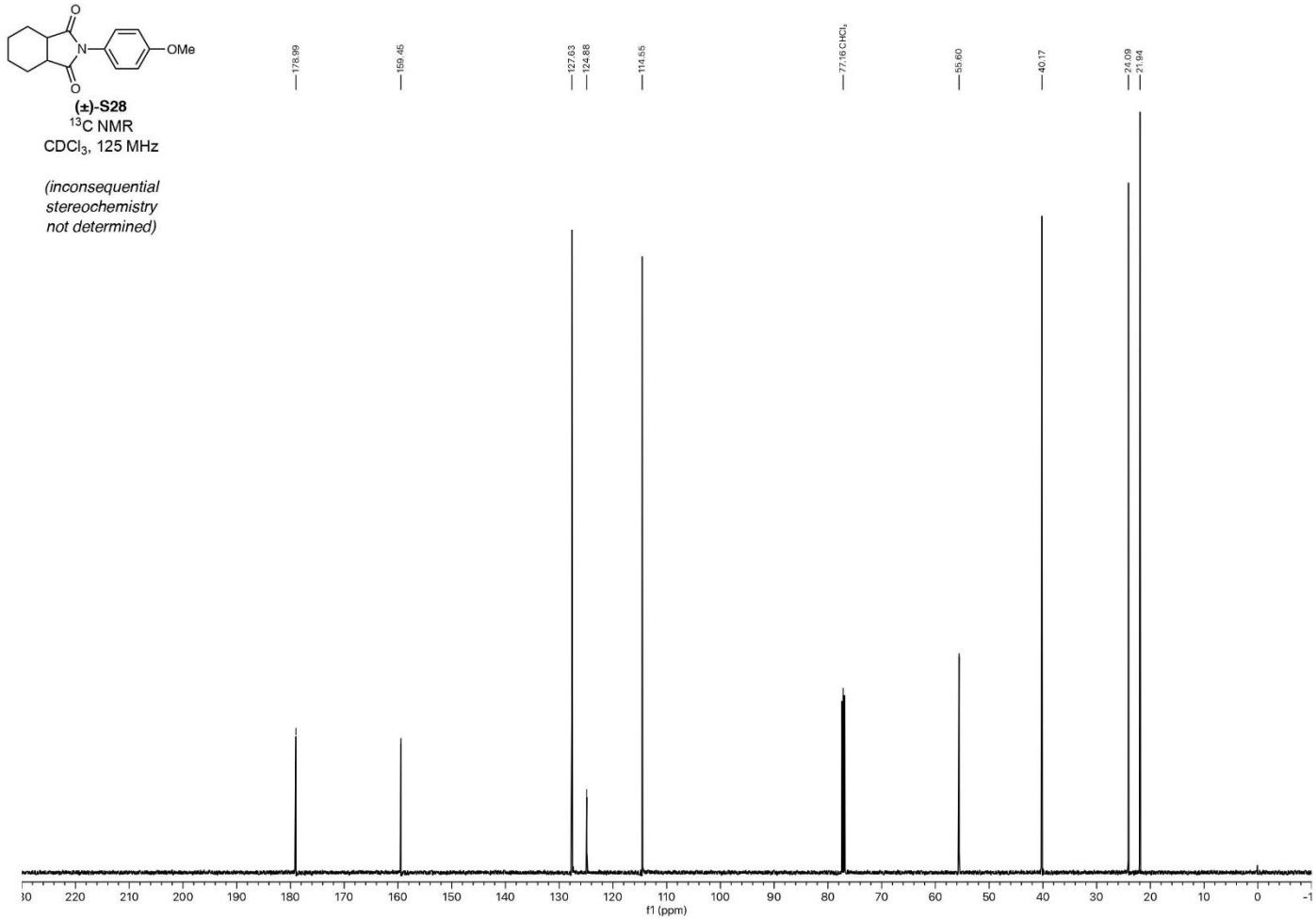
O
N
OMe
O
(±)-S28
13C NMR
CDCl3, 125 MHz
(inconsequential
stereochemistry
not determined)
178.99
159.45
127.63
124.88
114.55
77.16 CHCl3
55.60
40.17
24.09
21.94
f1 (ppm)

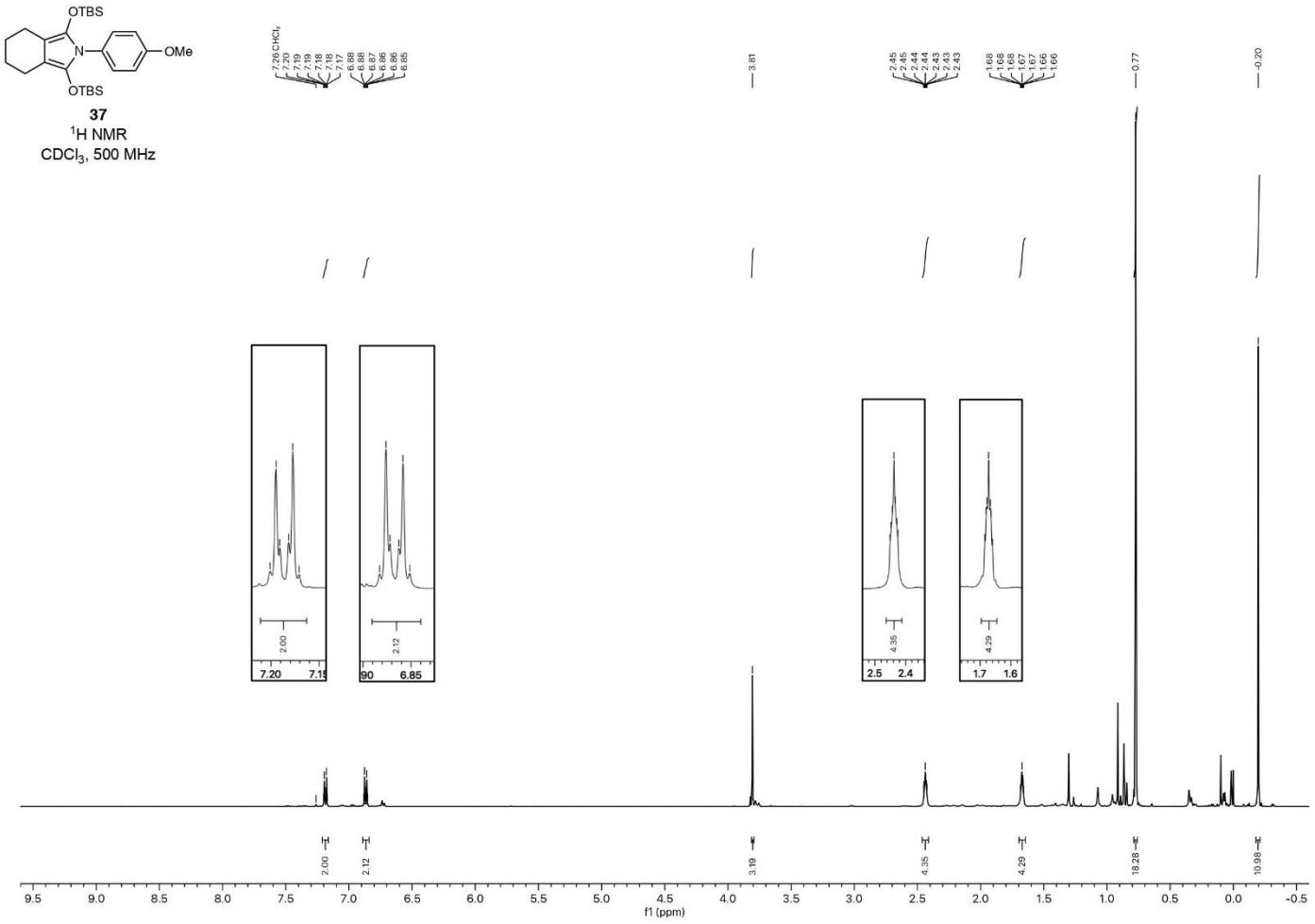
OTBS
N
OMe
OTBS
37
1H NMR
CDCl3, 500 MHz
7.26 CHCl3
7.20
7.19
7.19
7.18
7.17
6.88
6.88
6.87
6.87
6.86
6.86
6.85
3.81
2.45
2.45
2.44
2.44
2.43
2.43
2.43
1.68
1.68
1.68
1.67
1.67
1.66
1.66
0.77
-0.20
2.00
2.12
4.35
4.29
7.20
7.19
6.90
6.85
2.5
2.4
1.7
1.6
2.00
2.12
3.19
4.35
4.29
18.29
10.98
9.5
9.0
8.5
8.0
7.5
7.0
6.5
6.0
5.5
5.0
4.5
4.0
3.5
3.0
2.5
2.0
1.5
1.0
0.5
0.0
-0.5
f1 (ppm)

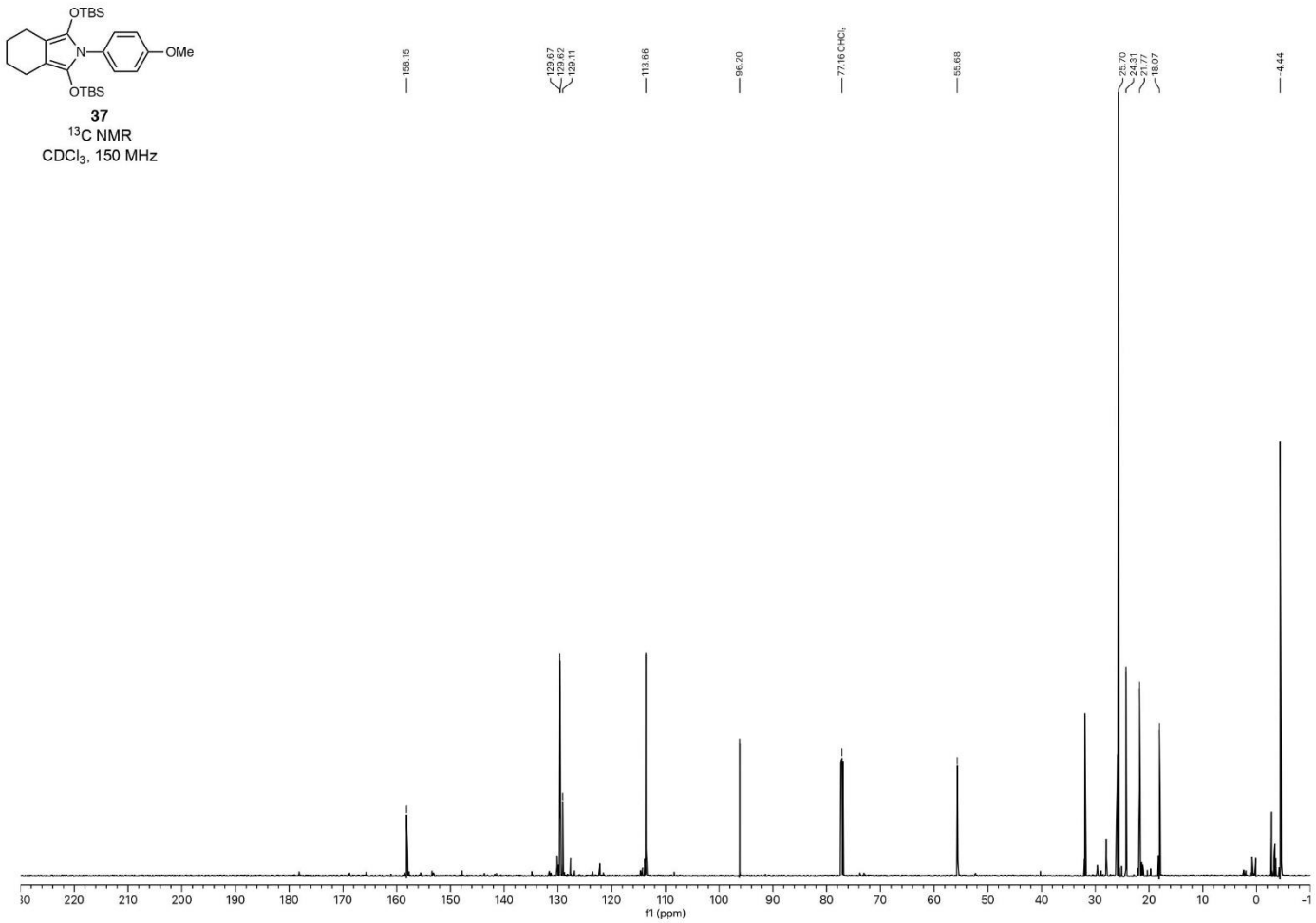
OTBS
N
OMe
OTBS
37
13C NMR
CDCl3, 150 MHz
158.15
129.67
129.62
129.11
113.66
96.20
77.16 CHCl3
55.68
25.70
24.31
21.77
18.07
-4.44
f1 (ppm)

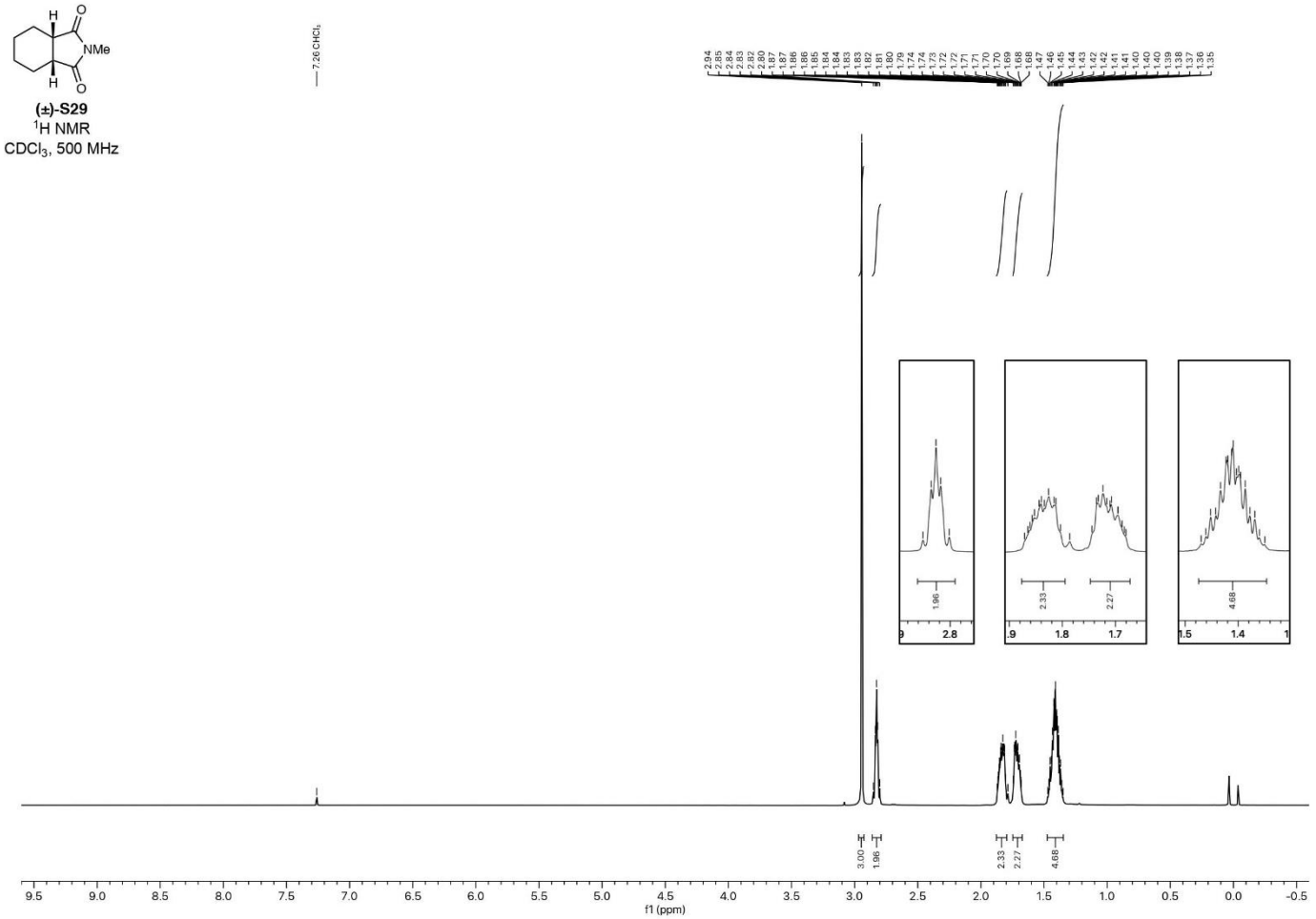
(±)-S29
1H NMR
CDCl3, 500 MHz
7.26 CHCl3
3.00
1.96
2.33
2.27
4.68
f1 (ppm)

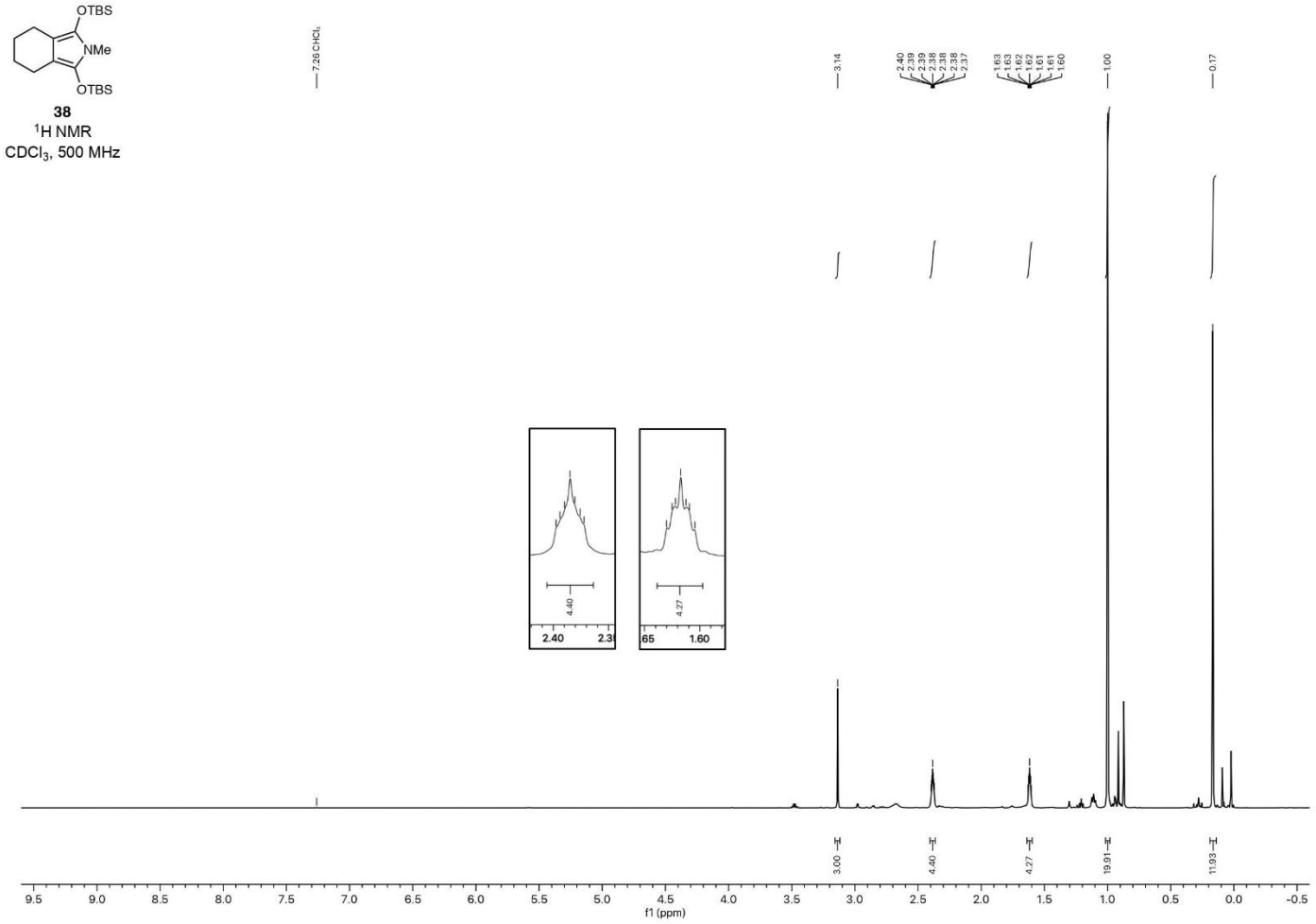
OTBS
NMe
OTBS
38
1H NMR
CDCl3, 500 MHz
7.26 CHCl3
3.14
2.40
2.39
2.38
2.38
2.38
2.37
1.63
1.63
1.62
1.62
1.61
1.61
1.60
1.00
0.17
4.40
2.40
4.27
1.60
3.00
4.40
4.27
19.91
11.93
f1 (ppm)

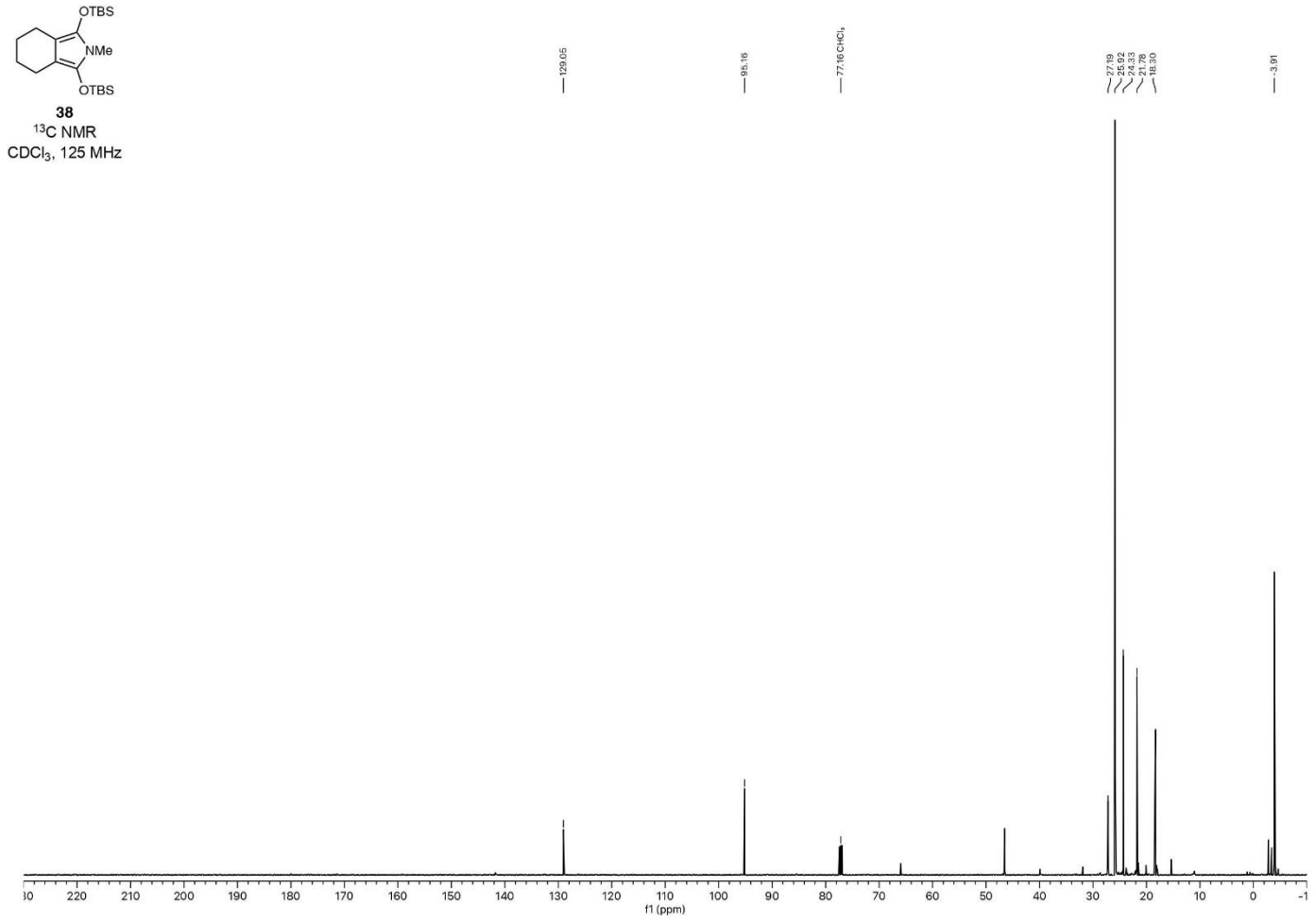
OTBS
NMe
OTBS
38
13C NMR
CDCl3, 125 MHz
129.05
95.16
77.16 CHCl3
27.19
25.92
24.33
21.78
18.30
-3.91
f1 (ppm)

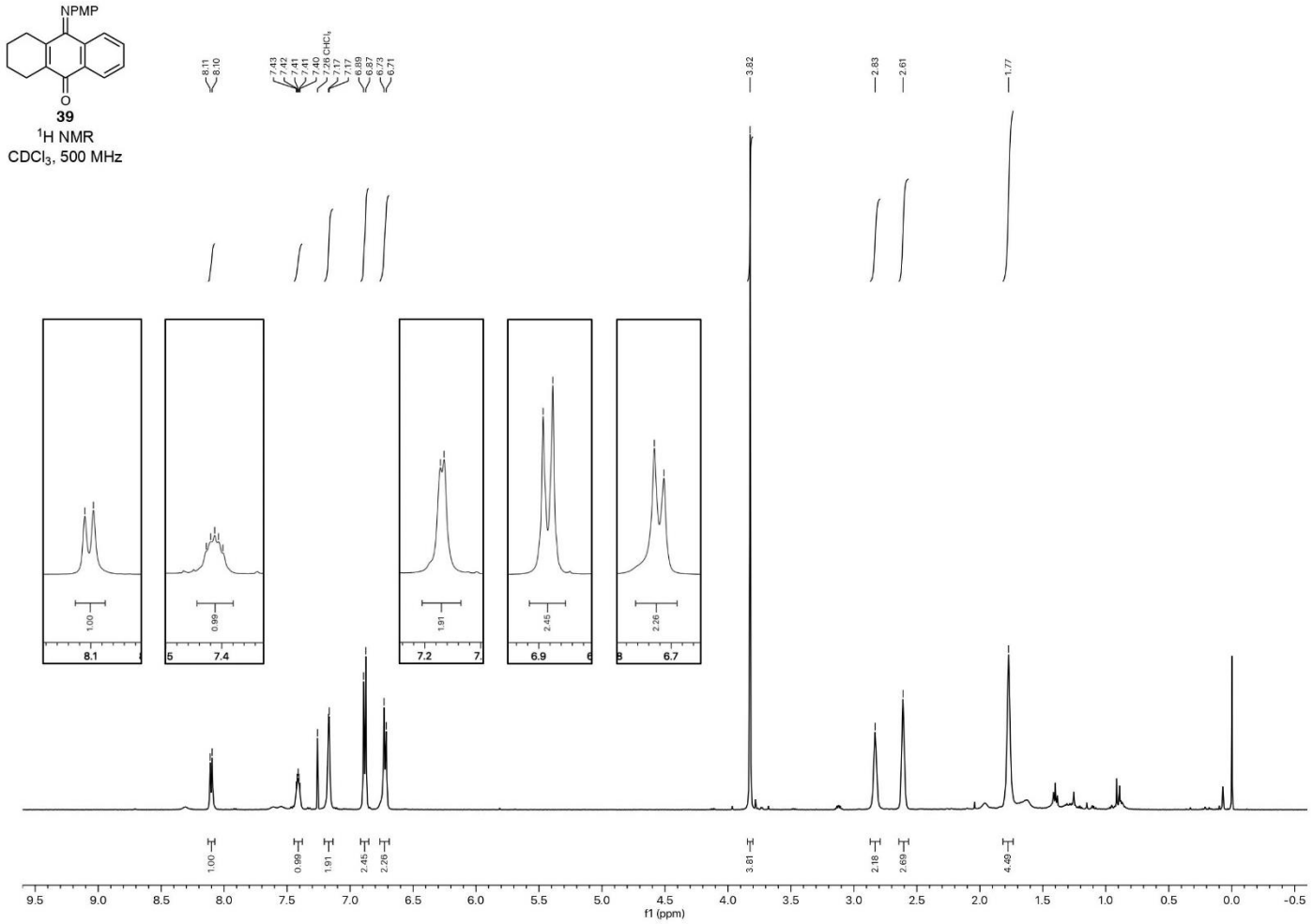
NPMP
O
39
^{1}H NMR
$CDCl_3$, 500 MHz
8.11
8.10
7.43
7.42
7.41
7.40
7.26 $CHCl_3$
7.17
7.17
6.89
6.87
6.73
6.71
3.82
2.83
2.61
1.77
1.00
0.99
1.91
2.45
2.26
3.81
2.18
2.69
4.49
f1 (ppm)

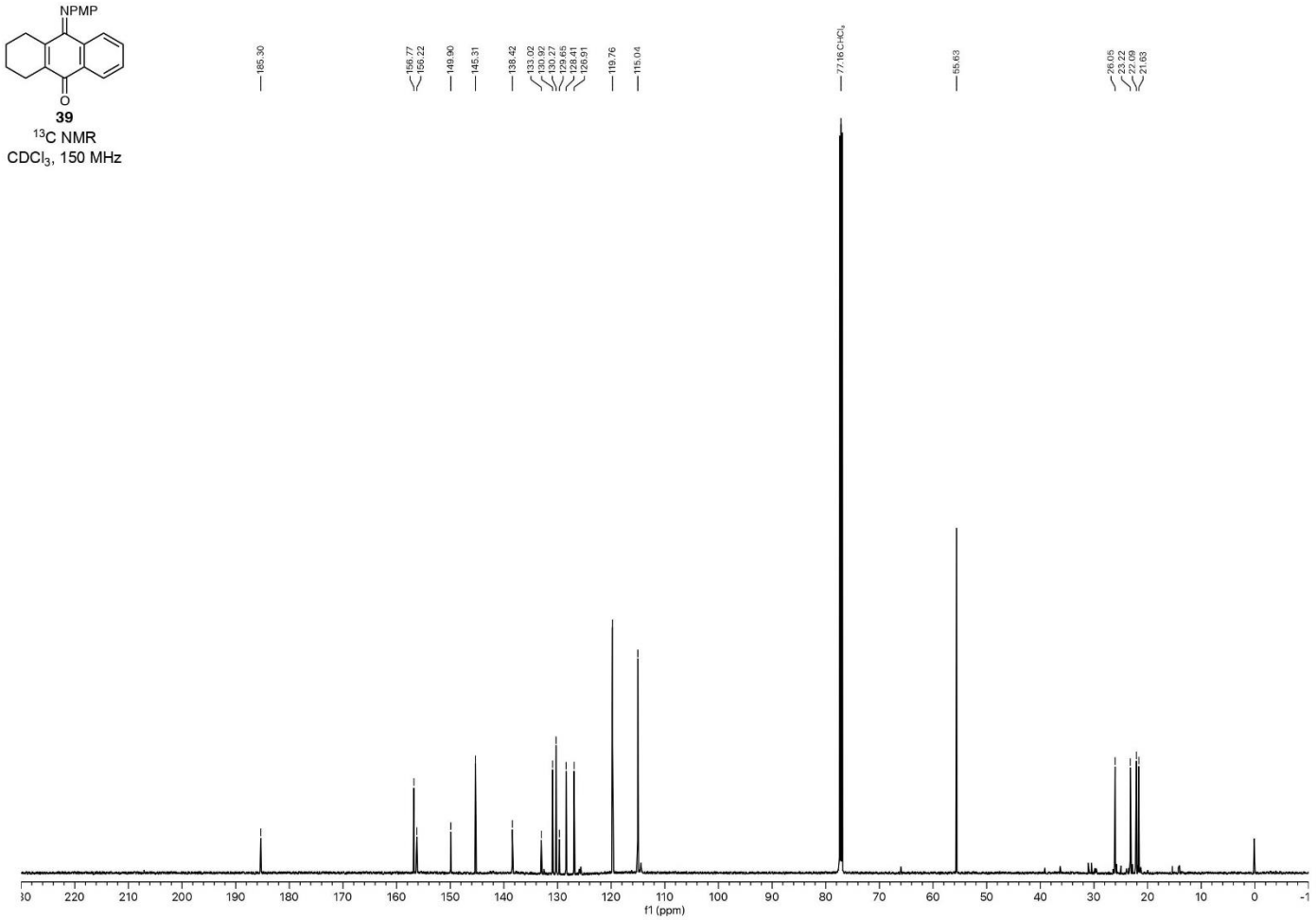
NPMP
O
39
^{13}C NMR
$CDCl_3$, 150 MHz
185.30
158.77
155.22
149.90
145.31
138.42
133.02
130.99
130.27
129.65
128.41
126.91
119.76
115.04
77.16 $CHCl_3$
55.63
26.05
23.22
22.09
21.63
f1 (ppm)

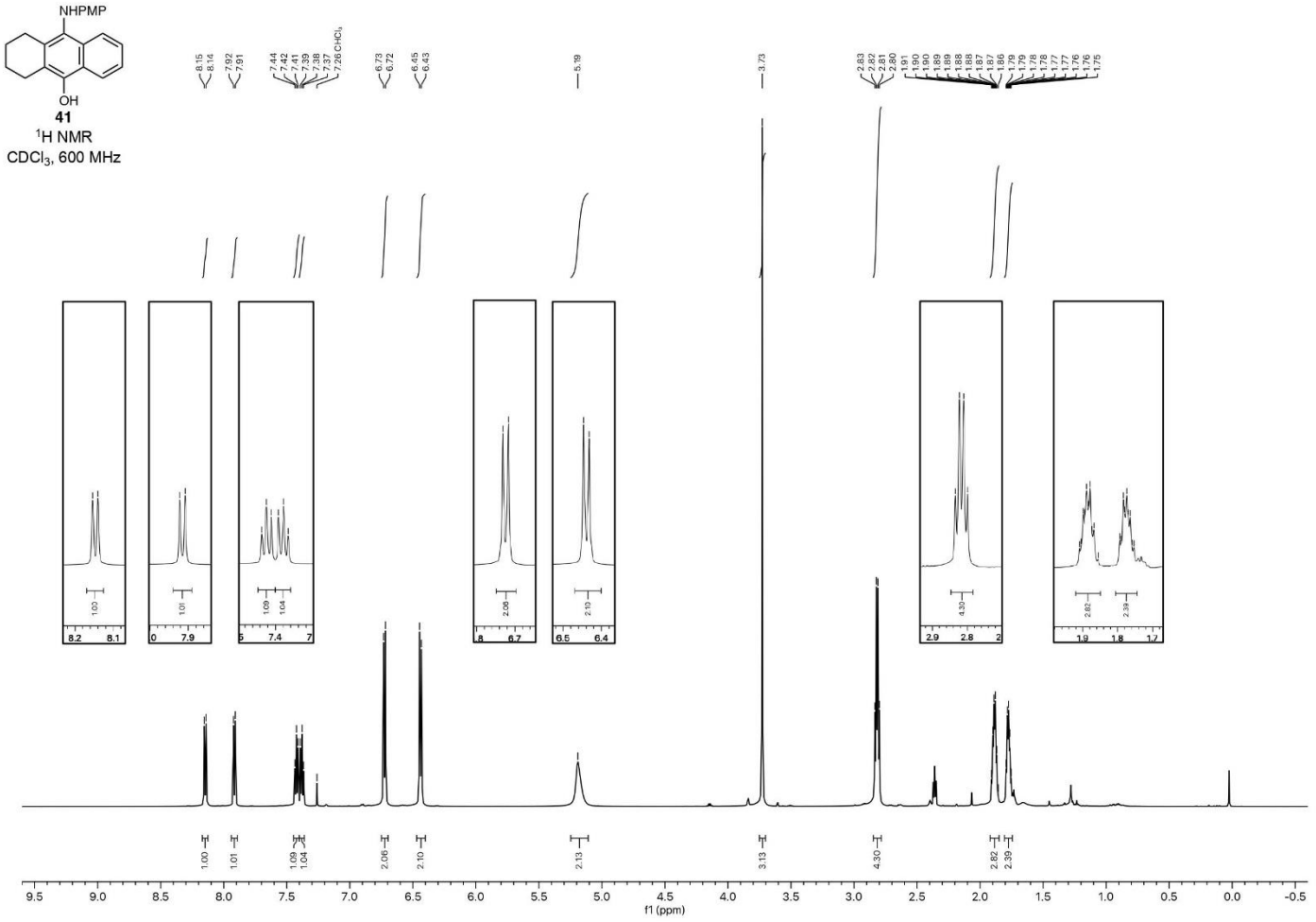
NHPMP
OH
41
^{1}H NMR
$CDCl_3$, 600 MHz
f1 (ppm)

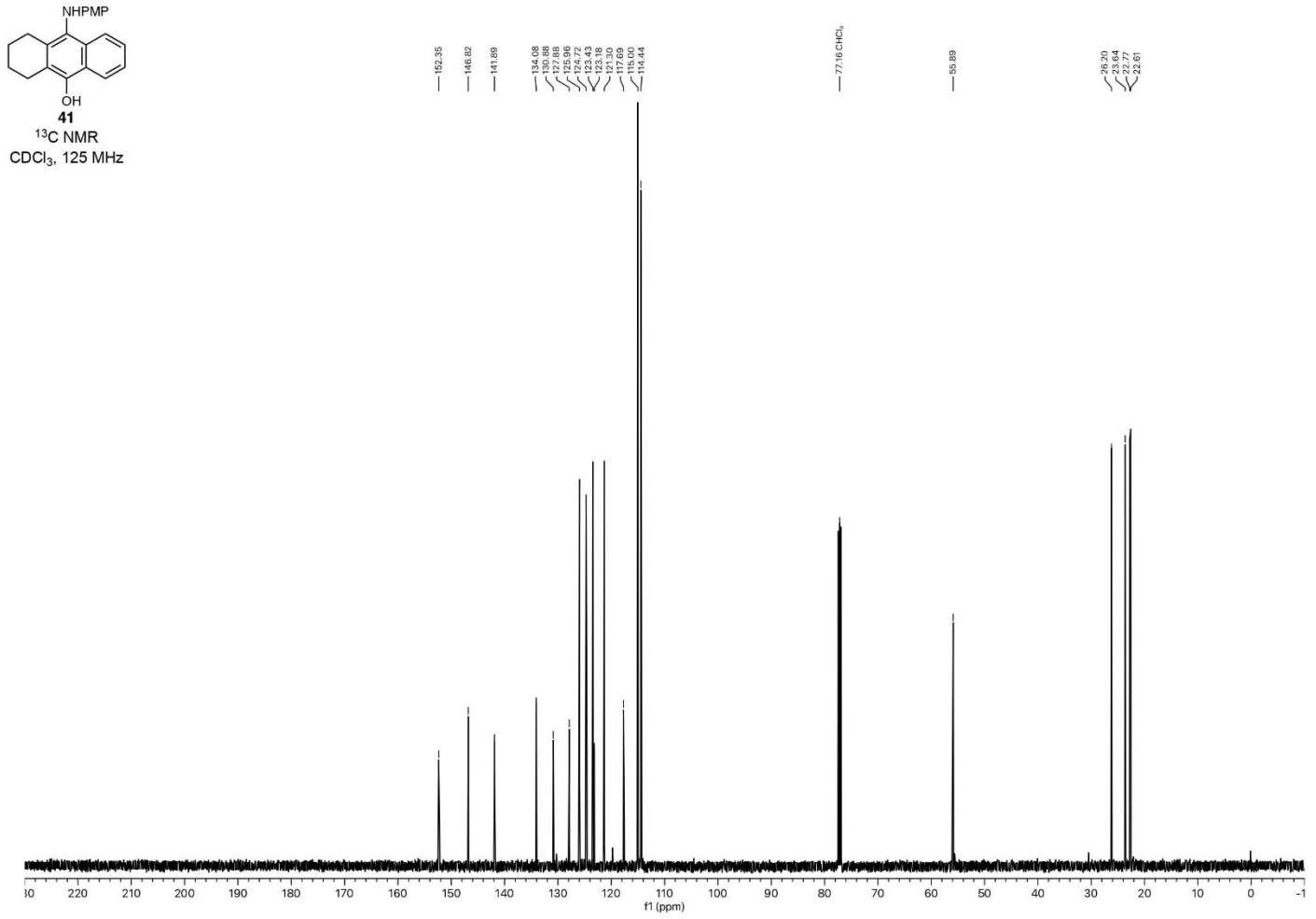
NHPMP
OH
41
^{13}C NMR
$CDCl_3$, 125 MHz
152.35
146.82
141.89
134.08
130.88
127.88
125.66
124.72
123.43
123.18
121.30
117.69
115.00
114.44
77.16 $CHCl_3$
55.89
26.20
25.64
22.77
22.61
f1 (ppm)

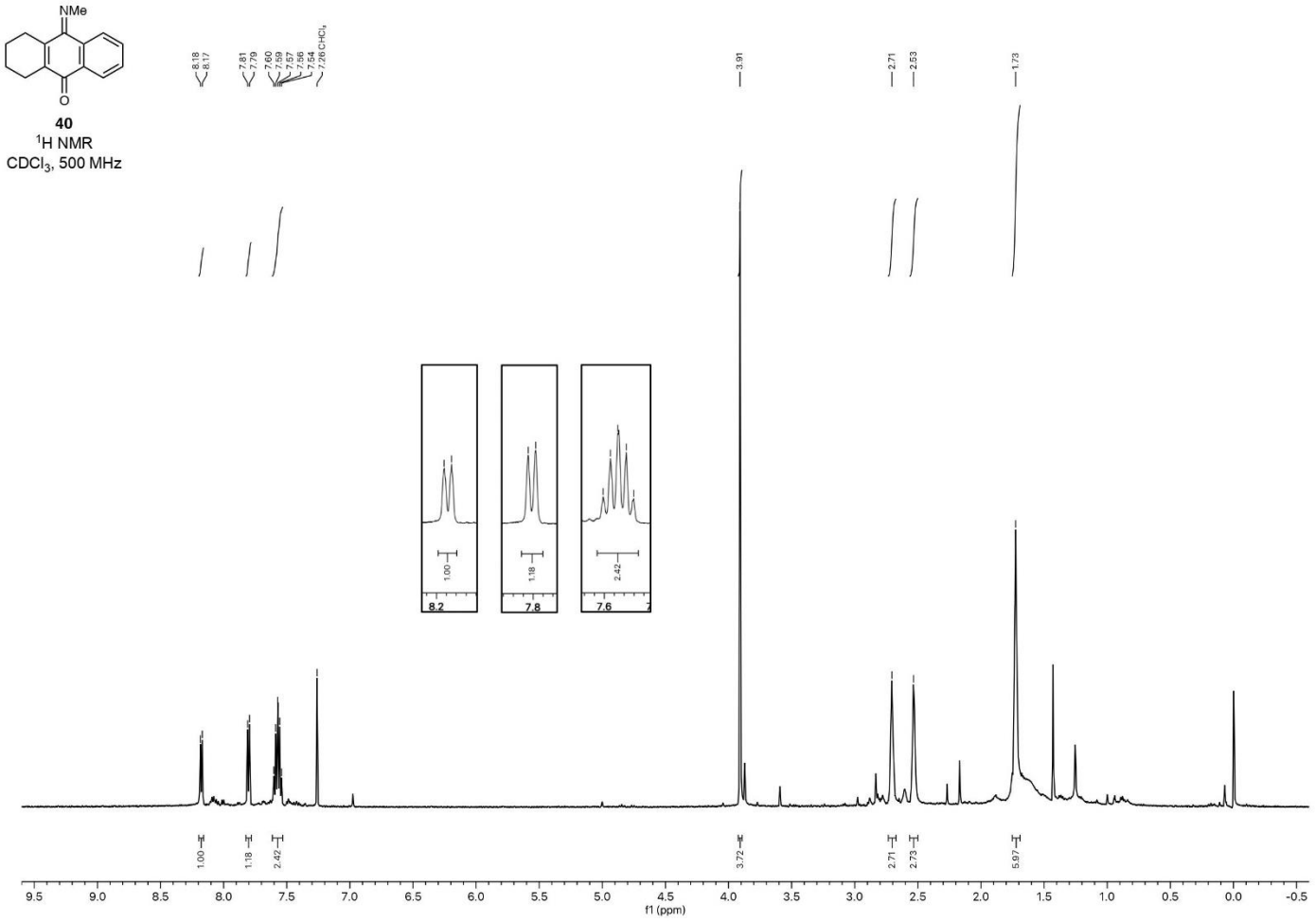
NMe
O
40
1H NMR
CDCl3, 500 MHz
8.18
8.17
7.81
7.79
7.60
7.59
7.57
7.56
7.54
7.26 CHCl3
3.91
2.71
2.53
1.73
1.00
1.18
2.42
8.2
7.8
7.6
3.72
2.73
5.97
f1 (ppm)

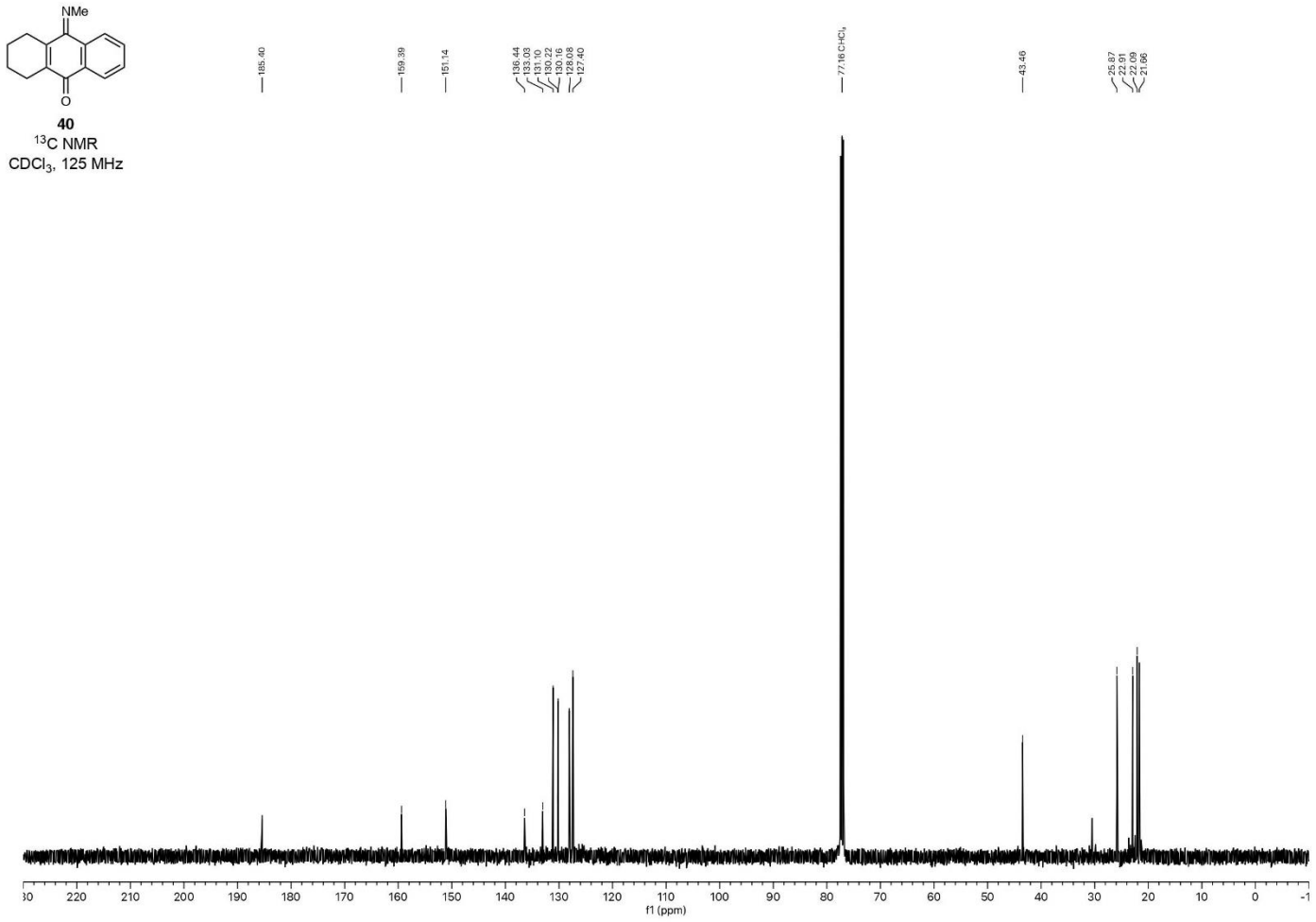

40

^{13}C NMR

$CDCl_3$, 125 MHz

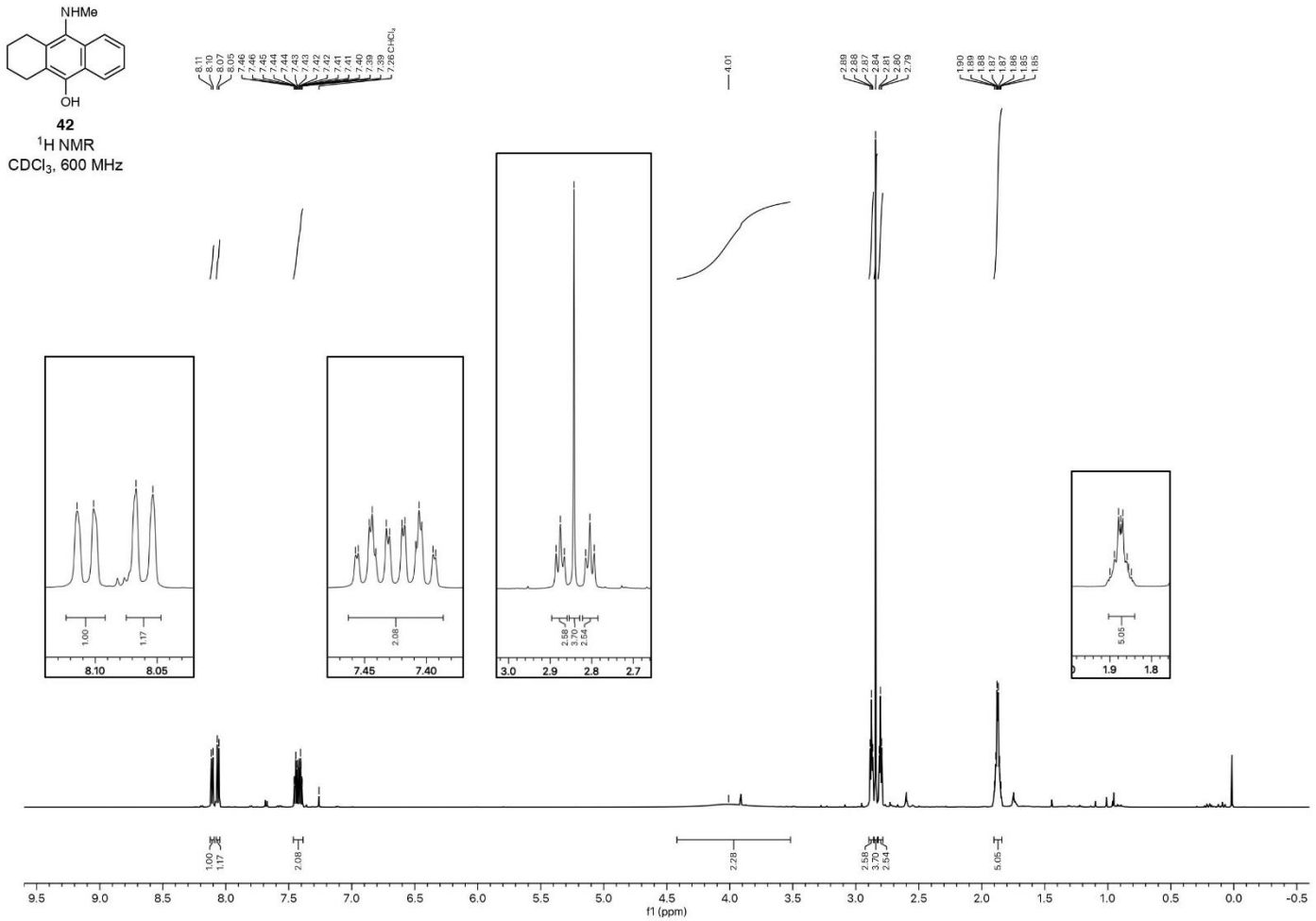
NHMe
OH
42
^{1}H NMR
$CDCl_3$, 600 MHz
f1 (ppm)

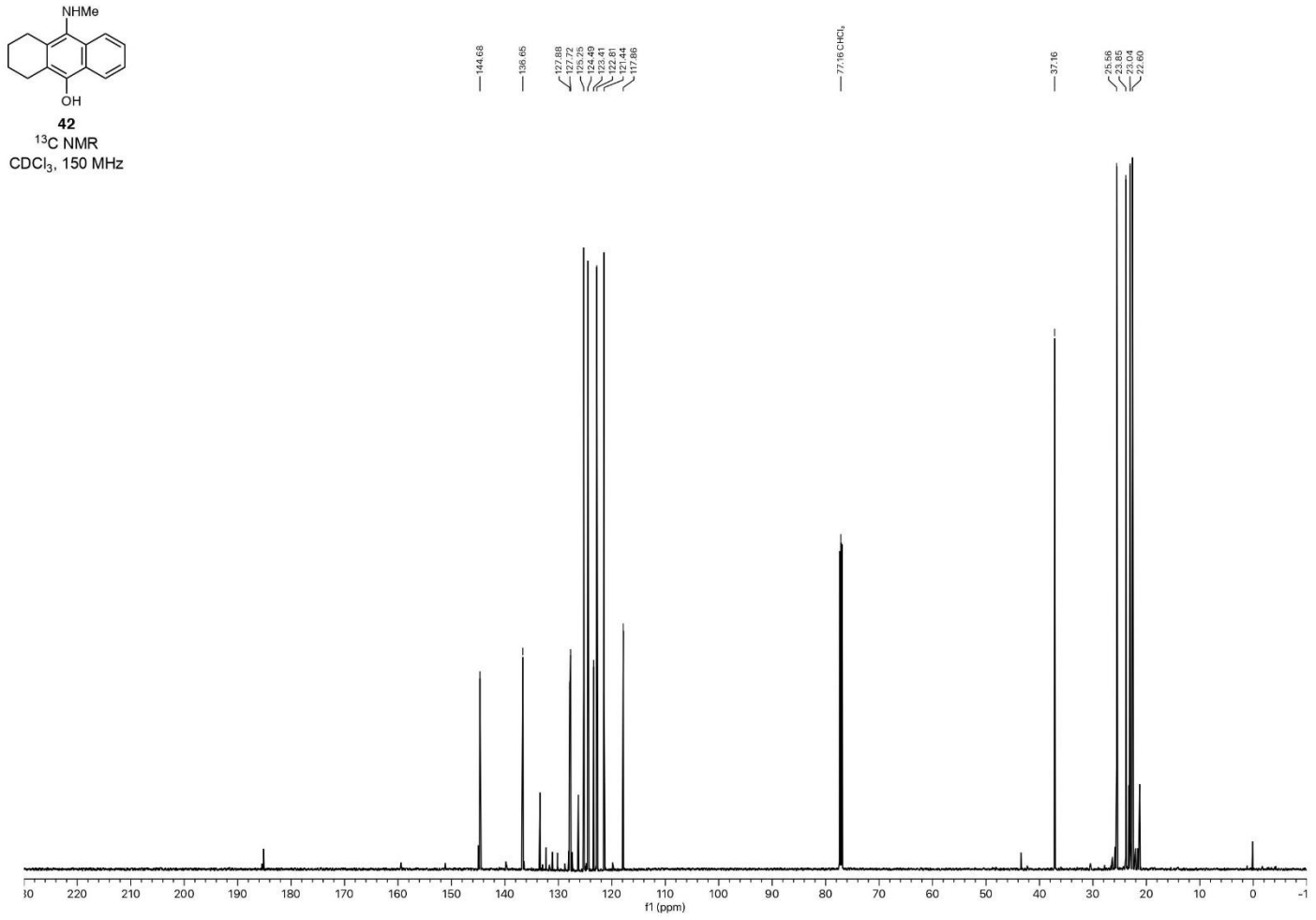
NHMe
OH
42
^{13}C NMR
$CDCl_3$, 150 MHz
144.68
136.65
127.88
127.72
125.25
124.49
123.41
122.81
121.44
117.86
77.16 $CHCl_3$
37.16
25.56
23.85
23.04
22.60
f1 (ppm)

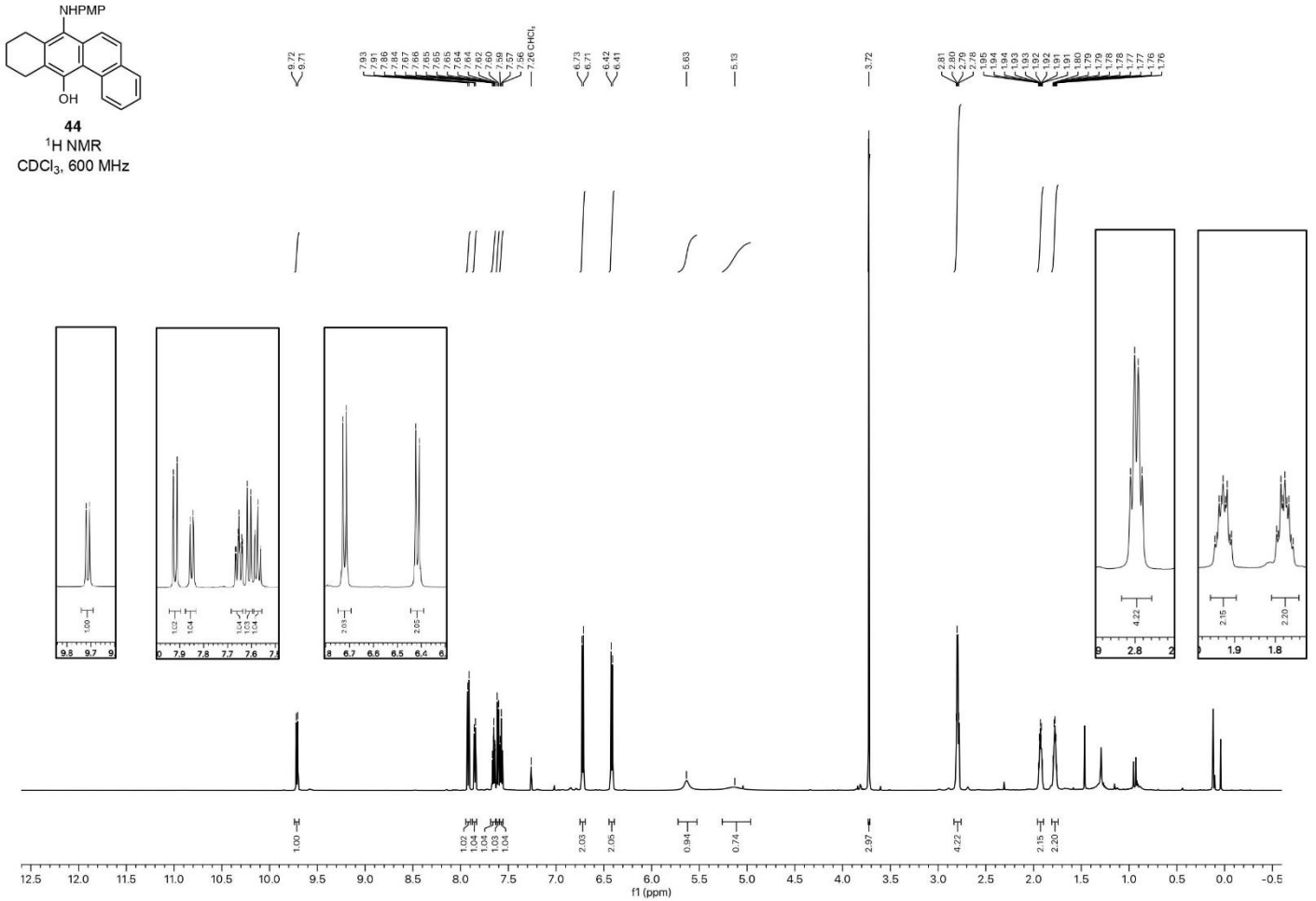
NHPMP
OH
44
^{1}H NMR
$CDCl_3$, 600 MHz
f1 (ppm)

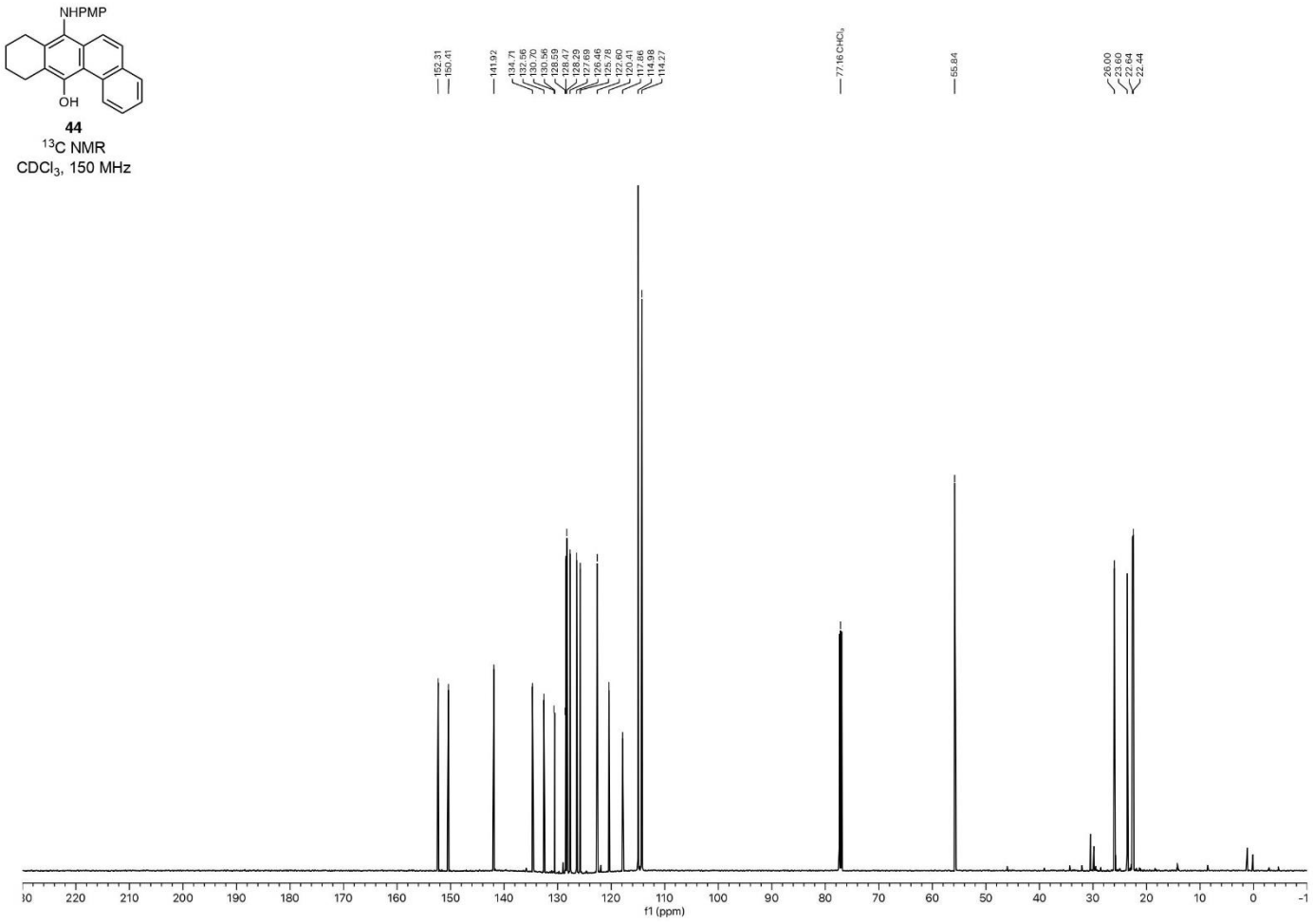
NHPMP
OH
44
^{13}C NMR
$CDCl_3$, 150 MHz
153.31
150.41
141.92
134.71
132.56
130.70
129.96
128.55
128.47
128.29
127.69
126.46
125.76
122.60
120.41
117.86
114.69
114.27
77.16 $CHCl_3$
55.84
26.00
23.60
23.44
22.44
f1 (ppm)

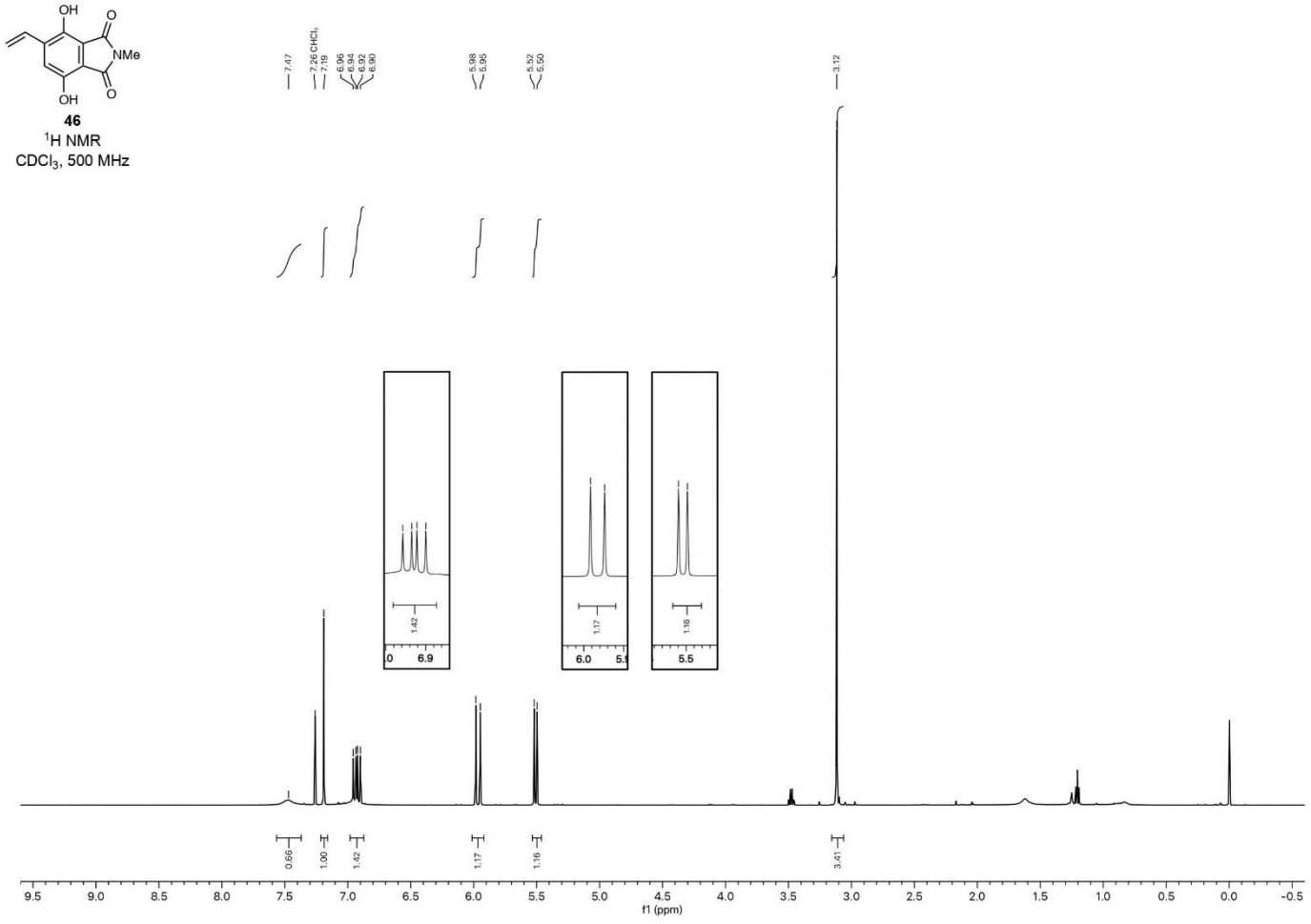
OH
O
NMe
O
OH
46
^{1}H NMR
$CDCl_3$, 500 MHz
7.47
7.26 $CHCl_3$
7.19
6.96
6.94
6.93
6.90
5.98
5.95
5.52
5.50
3.12
1.42
1.17
1.16
0.66
1.00
1.42
1.17
1.16
3.41
f1 (ppm)

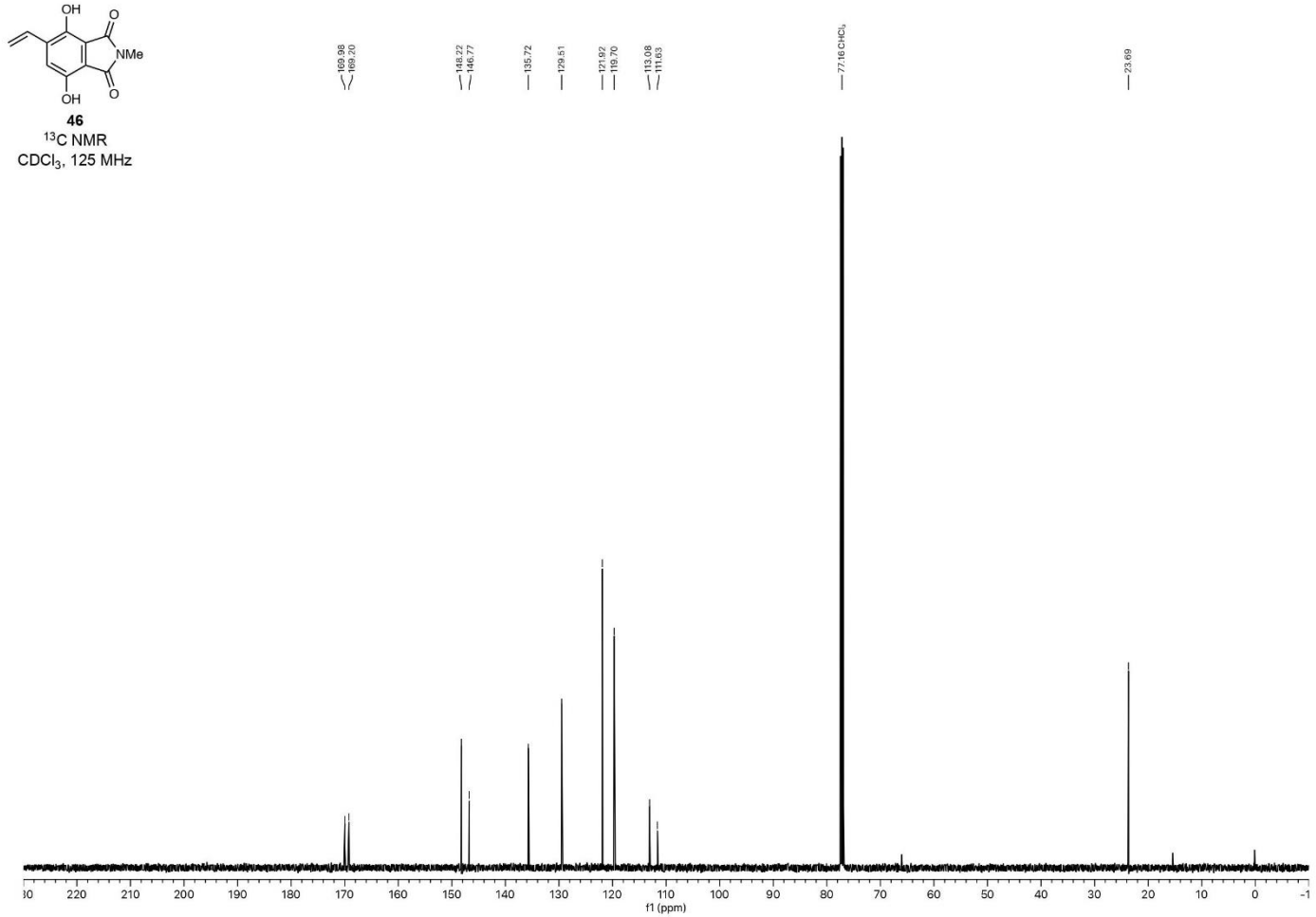
OH
O
NMe
O
OH
46
13C NMR
CDCl3, 125 MHz
169.98
169.20
148.22
146.77
135.72
129.51
121.92
119.70
113.08
111.63
77.16 CHCl3
23.69
f1 (ppm)

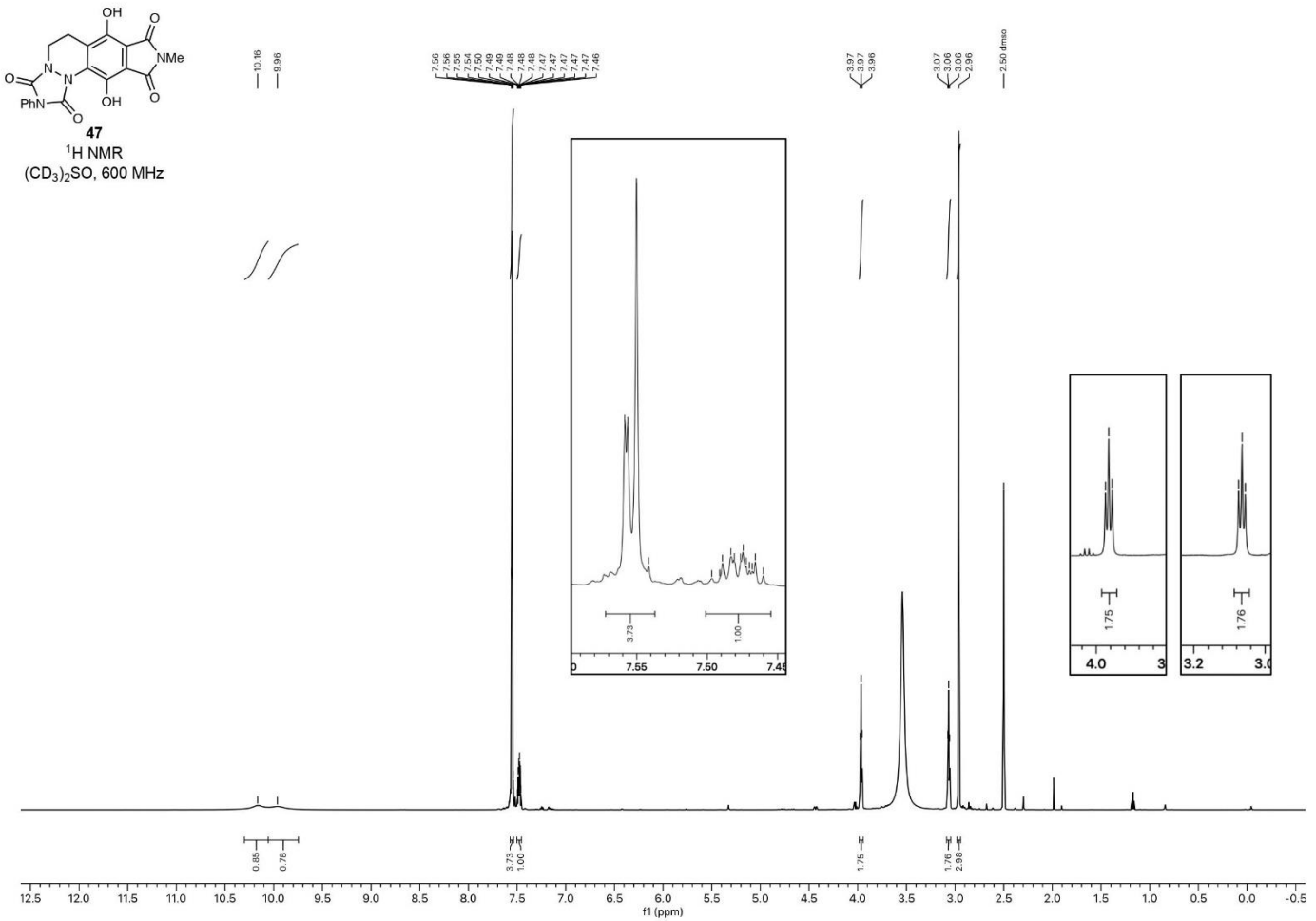
OH
O
NMe
O
N
N
O
PhN
O
OH
O
47
1H NMR
(CD3)2SO, 600 MHz
10.16
9.96
7.56
7.56
7.55
7.54
7.50
7.50
7.49
7.48
7.48
7.48
7.47
7.47
7.47
7.47
7.47
7.46
3.97
3.97
3.96
3.07
3.06
3.06
2.96
2.50 dmso
3.73
1.00
7.55
7.50
1.75
4.0
1.76
3.2
0.85
0.78
3.73
1.00
1.75
1.76
2.98
f1 (ppm)

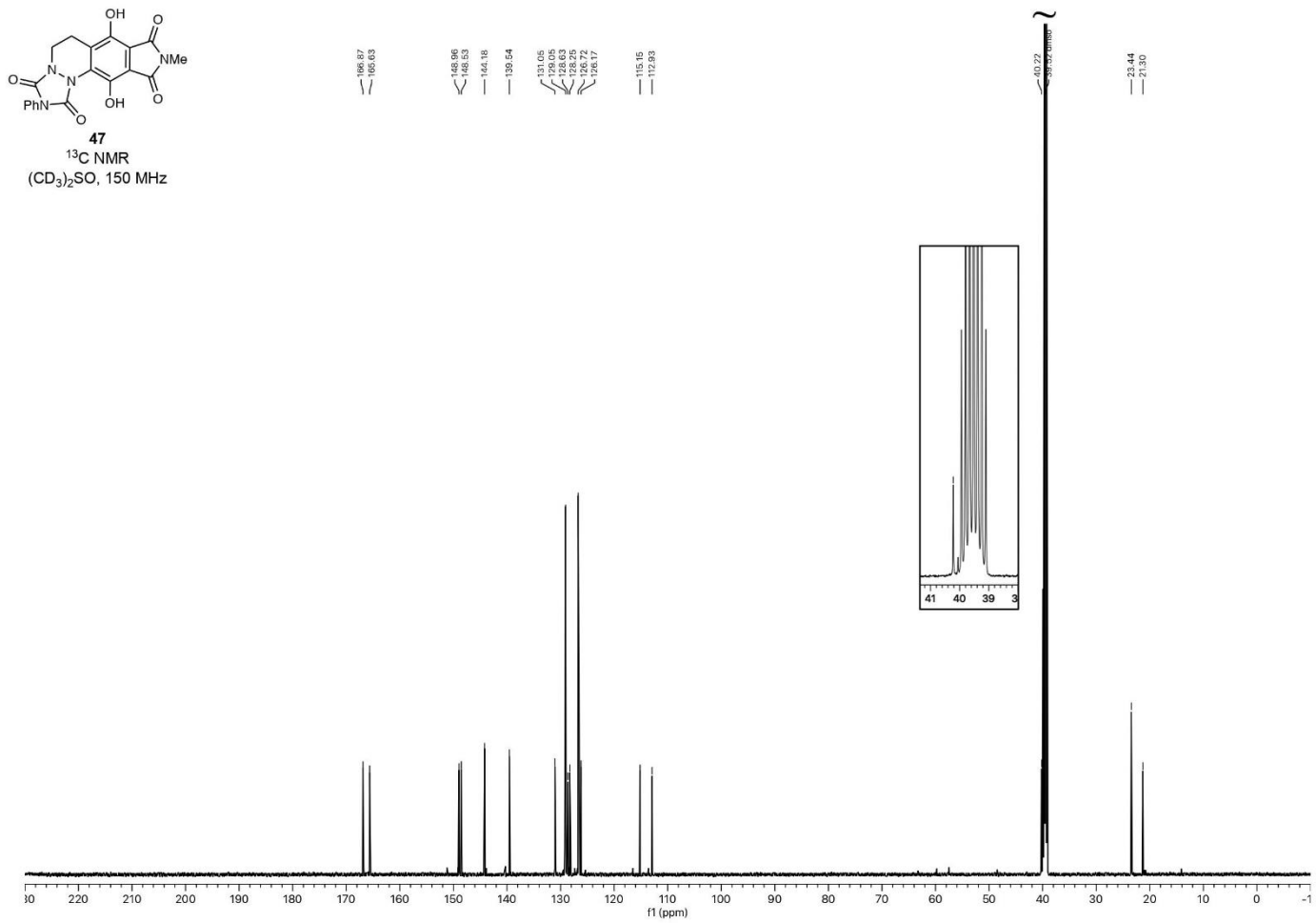
OH
O
NMe
O
N
N
O
PhN
O
OH
O
47
^{13}C NMR
$(CD_3)_2SO$, 150 MHz
166.87
165.63
148.96
148.53
144.18
139.64
131.05
129.05
128.63
128.25
126.72
126.17
115.15
112.93
49.22
39.62 dmso
23.44
21.30
41
40
39
f1 (ppm)

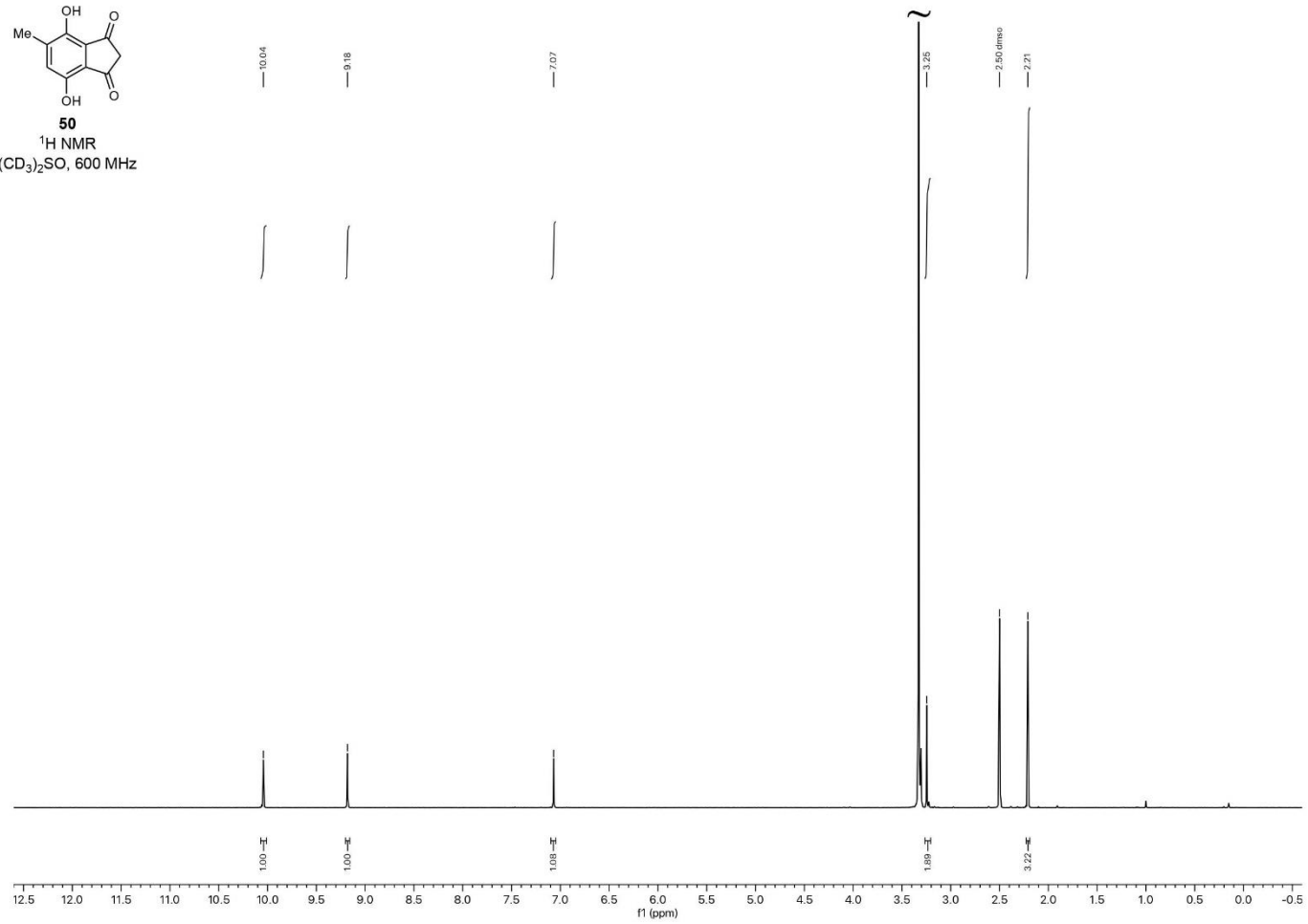
OH
Me
O
O
OH
50
1H NMR
(CD3)2SO, 600 MHz
10.04
9.18
7.07
3.25
2.50 dmso
2.21
1.00
1.00
1.08
1.89
3.22
12.5 12.0 11.5 11.0 10.5 10.0 9.5 9.0 8.5 8.0 7.5 7.0 6.5 6.0 5.5 5.0 4.5 4.0 3.5 3.0 2.5 2.0 1.5 1.0 0.5 0.0 -0.5
f1 (ppm)

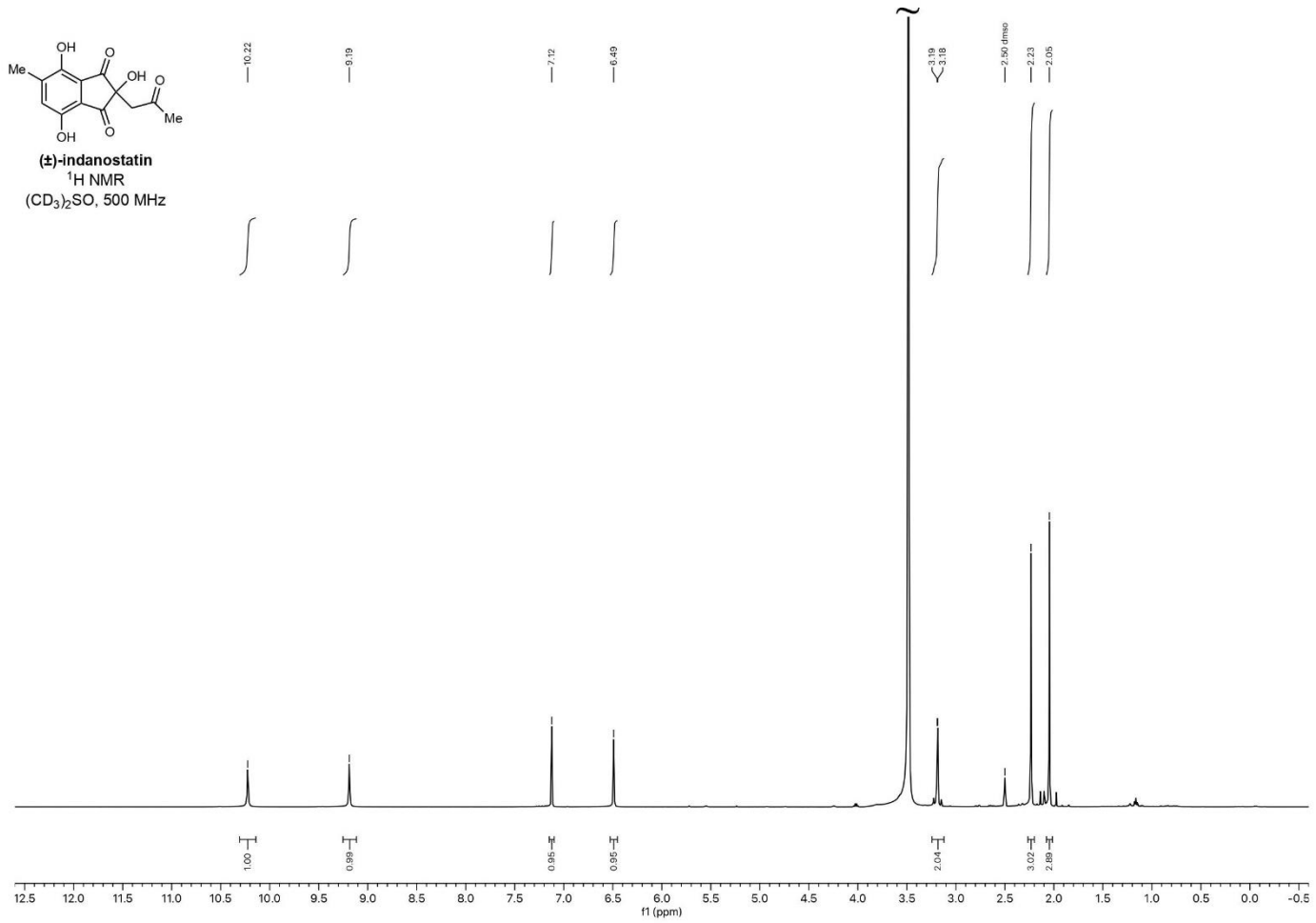
(±)-indanostatin
1H NMR
(CD3)2SO, 500 MHz
10.22
9.19
7.12
6.49
3.19
3.18
2.50 dmso
2.23
2.05
1.00
0.99
0.95
0.95
2.04
3.02
2.89
f1 (ppm)

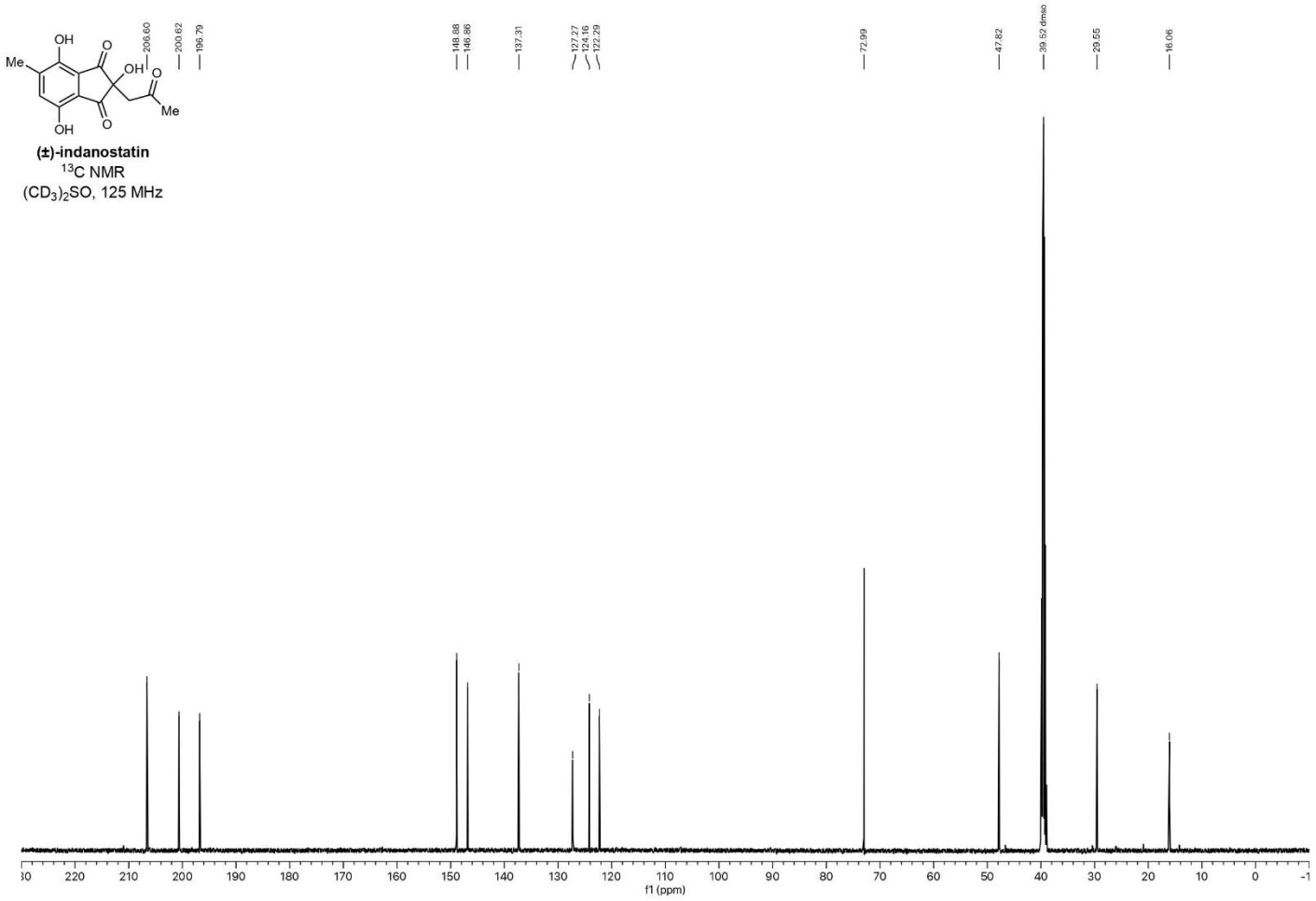
OH
Me
O
OH
O
Me
OH
O
206.60
200.62
196.79
148.88
146.86
137.31
127.27
124.16
122.29
72.99
47.82
39.52 dmso
29.55
16.06
(±)-indanostatin
13C NMR
(CD3)2SO, 125 MHz
f1 (ppm)

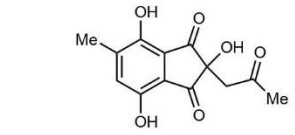

natural (−)-indanostatin (Hayakawa et. al)
^{1}H NMR
$(CD_3)_2SO$, 400 MHz

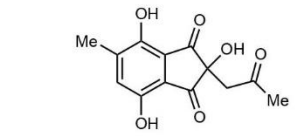

synthetic (±)-indanostatin (this work)
^{1}H NMR
$(CD_3)_2SO$, 500 MHz

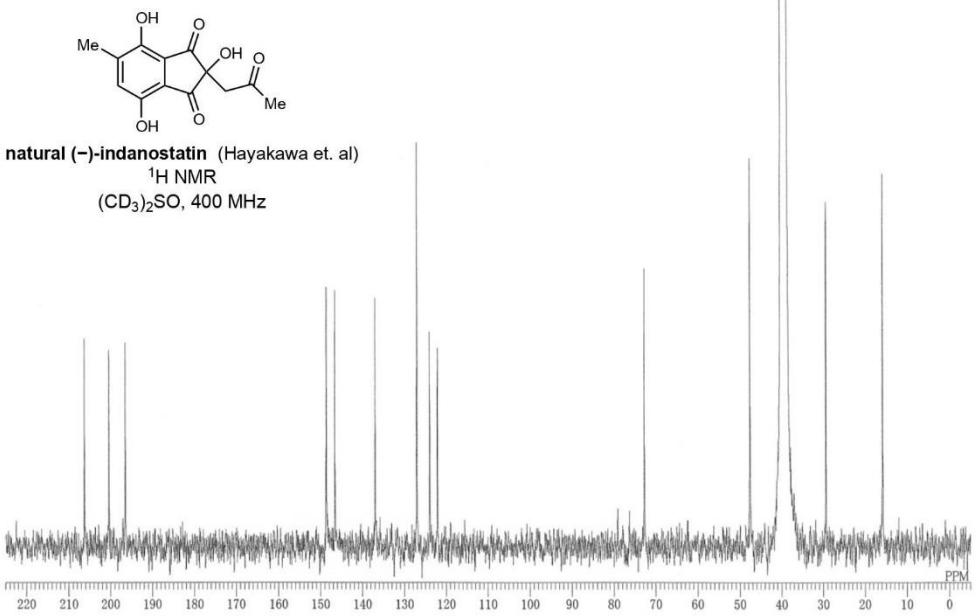

natural (−)-indanostatin (Hayakawa et. al)
^{1}H NMR
$(CD_3)_2SO$, 400 MHz

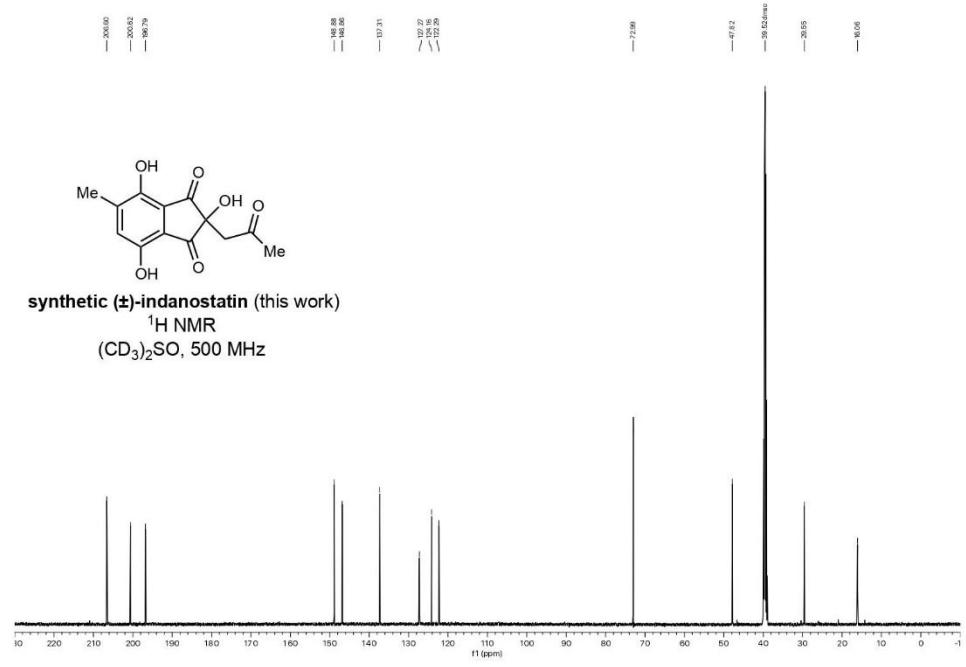

synthetic (±)-indanostatin (this work)
^{1}H NMR
$(CD_3)_2SO$, 500 MHz

7.2 Chapter 5 Experimental

General Experimental

NMR Spectroscopy

^{1}H NMR spectra were recorded using either an Agilent 500 MHz DD2 console, or Agilent 600 MHz DD2 console with an Oxford 600 MHz magnet and Agilent cryoprobe. ^{13}C NMR spectra were recorded using either an Agilent 500 MHz DD2 console at 125 MHz, or Agilent 600 MHz DD2 console with an Oxford 600 MHz magnet and Agilent cryoprobe at 150 MHz. Residual solvent peaks were used as an internal reference for ^{1}H NMR spectra [$CDCl_3$ δ 7.26 ppm] and ^{13}C NMR spectra [$CDCl_3$ δ 77.16 ppm]. Coupling constants (*J*) are quoted to the nearest 0.1 Hz. The following abbreviations (or combinations thereof) were used to describe ^{1}H NMR multiplicities: s = singlet, d = doublet, t = triplet, q = quartet, p = pentet, m = multiplet, br = broad.

Infrared Spectroscopy

IR spectra were recorded neat on a SHIMADZU IRSpirit FTIR Spectrophotometer with an ATR.

Mass Spectrometry

HRMS measurements (electrospray ionization - ESI) were recorded on an Agilent 6230 time-of-flight LC/MS system.

Chromatography

Flash column chromatography was performed using a Biotage IsoleraTM One Flash Chromatography System and iLOKTM Empty Solid Load Cartridges. Flash chromatography was performed with Carl Roth silica gel 60 (0.040–0.063 mm grade). Analytical thin-layer chromatography was performed with commercial aluminium sheets coated with 0.25 mm silica gel (E. Merck, silica gel 60 F254). Compounds were either visualized under UV-light at 254 nm, or by dipping the plates in a cerium ammonium molybdate stain, followed by heating. All R_f values were measured to the nearest 0.05 cm.

Experimental Procedures and Reagents

Commercially available chemicals were used as purchased, or where specified, purified by standard techniques. Solvent compositions are given in v/v. All reactions were carried out under an atmosphere of nitrogen in oven-dried glassware with magnetic stirring, unless otherwise indicated. Et_2O, toluene, CH_2Cl_2 and THF were purified by a Pure Solv^{TM} Micro solvent purification system. Et_2O and THF were also purified by a benzophenone/sodium still. All other solvents were used as purchased, or where specified, purified by standard techniques.

General Comments on Compound Characterization

All new compounds were fully characterized when possible. For compounds that have been previously characterized in the literature, if we have made any modification to the reported synthesis we include our modified method, in addition to compound appearance, R_f, and ^{1}H NMR data.

Experimental Procedures and Characterisation Data

Precursors

Ethyl (E)-5-iodopent-2-enoate (7.1)

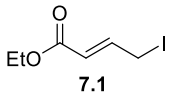
7.1

To a 120 mL sealable reaction flask under nitrogen was added ethyl (E)-5-bromopent-2-enoate (3.50 g, 18.1 mmol, 1.00 mol. equiv.), distilled acetone (69.7 mL, 0.260 M) and sodium iodide (6.79 g, 45.3 mmol, 2.50 mol. equiv.). The flask was sealed and stirred at 60 °C overnight by which time ^{1}H NMR analysis indicated completion of the reaction. The reaction mixture was allowed to cool to room temperature and then was diluted with water and extracted with hexanes. The combined organic layers were then washed with a 10% aqueous solution of $Na_2S_2O_3$, brine, dried over $MgSO_4$, filtered, and concentrated under reduced pressure. The crude product was used without further purification. Spectroscopic data matched those previously reported in the literature.[2] **Yield**: 3.78 g, 15.8 mmol, 87%; **Appearance**: Yellow oil; **R_f**: N/A; **^{1}H NMR** (500 MHz, $CDCl_3$): δ 7.04 (dt, *J* = 8.3, 15.3 Hz, 1H), 5.93 (d, *J* = 15.3 Hz, 1H), 4.20 (q, *J* = 7.2 Hz, 2H), 3.92 (d, *J* = 8.2 Hz, 2H), 1.29 (t, *J* = 7.2 Hz, 3H) ppm.

(E)-Cinnamyl alcohol (7.2)

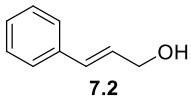
7.2

To a 250 mL round bottom flask under nitrogen was added (E)-cinnamaldehyde (2.90 mL, 22.7 mmol, 1.00 mol. equiv.) and MeOH (45.4 mL, 0.500 M). The solution was cooled to 0 °C and sodium borohydride (0.945 g, 25.0 mmol, 1.10 mol. equiv.) was added. The reaction was allowed to warm to room temperature overnight by which time ^{1}H NMR analysis indicated completion of the reaction. The reaction mixture was cooled to 0 °C and quenched with saturated aqueous $NaHCO_3$ solution. The organics was washed with water, brine, dried over $MgSO_4$ and concentrated under reduced pressure. Purification via flash column chromatography (SiO_2, eluting with 1:4 EtOAc:hexane → 2:3 EtOAc:hexane) yielded pure (E)-cinnamyl alcohol. Spectroscopic data matched those previously reported in the literature.[3] **Yield**: 2.56 g, 19.1 mmol, 84%; **Appearance**: White solid; **R_f**: 0.20 (1:4 EtOAc:hexane); **^{1}H NMR** (500 MHz, $CDCl_3$): δ 7.39 (d, *J* = 8.1 Hz, 2H), 7.32 (t, *J* = 7.5 Hz, 2H), 7.24 (t, *J* = 7.5 Hz, 1H), 6.62 (d, *J* = 15.9 Hz, 1H), 6.37 (dt, *J* = 5.7, 15.9 Hz, 1H), 4.33 (t, *J* = 4.4 Hz, 1H), 1.48 (s, 1H) ppm.

(E)-Cinnamyl iodide (7.3)

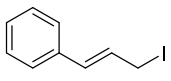
7.3

To a 25 mL round bottom flask under nitrogen was added (E)-cinnamyl alcohol (1.00 g, 7.45 mmol, 1.00 mol. equiv.) and dry Et_2O (13.5 mL, 0.550 M). The solution was cooled to –15 °C and phosphorus triiodide (1.53 g, 3.73 mmol, 0.50 mol. equiv.) was added. The reaction was allowed to stir at –15 °C for 1 hour by which time ^{1}H NMR analysis indicated completion of the reaction. The reaction mixture was quenched with water, extracted with diethyl ether, washed with water, saturated aqueous $NaHCO_3$ solution, 10% aqueous $Na_2S_2O_3$ solution, brine, dried over $MgSO_4$, filtered, and concentrated under reduced pressure. The crude product was used without further purification. Product degrades at room temperature. Spectroscopic data matched those previously reported in the literature.[4] **Yield**: 1.44 g, 5.89 mmol, 79%; **Appearance**: Off-white solid; **R_f**: N/A; **^{1}H NMR** (500 MHz, $CDCl_3$): δ 7.37 (d, *J* = 7.8 Hz, 2H), 7.32 (t, *J* = 7.8 Hz, 2H), 7.25 (t, *J* = 7.3 Hz, 1H), 6.60 (d, *J* = 15.5 Hz, 1H), 6.48–6.40 (m, 1H), 4.12 (d, *J* = 8.1 Hz, 1H) ppm.

Ethyl (E)-3,4-(methylenedioxy)cinnamate (7.4)

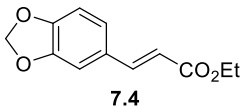
7.4

To a 250 mL round bottom flask under N2 was added ethyl(triphenylphosphoranylidene)acetate (6.03 g, 17.3 mmol, 1.30 mol. equiv.) and dry dichloromethane (66.6 mL, 0.200 M). The solution was cooled to 0 °C and piperonal (2.00 g, 13.3 mmol, 1.00 mol. equiv.) was added dropwise. ethyl(triphenylphosphoranylidene)acetate (a total of 1.00 g) was added until 1H NMR analysis indicated the piperonal was completely consumed. The reaction mixture was diluted with water and extracted with ethyl acetate. The combined organic layers were then washed with brine, dried over $MgSO_4$, filtered, and concentrated under reduced pressure. Purification via flash column chromatography (SiO_2, eluting with 1:9 EtOAc:hexane) yielded pure ethyl (E)-3,4-(methylenedioxy)cinnamate. Spectroscopic data matched those previously reported in the literature.[5] **Yield**: 2.73 g, 12.4 mmol, 93%; **Appearance**: White solid; $\mathbf{R_f}$: 0.37 (1:9 EtOAc:hexane); **^{1}H NMR** (500 MHz, $CDCl_3$): δ 7.59 (d, *J* = 15.9 Hz, 1H), 7.03 (s, 1H), 7.01 (d, *J* = 8.0 Hz, 1H), 6.81 (d, *J* = 8.0 Hz, 1H), 6.26 (d, *J* = 15.9 Hz, 1H), 6.00 (s, 2H) 4.25 (q, *J* = 7.1 Hz, 2H), 1.33 (t, *J* = 7.1 Hz, 3H) ppm.

(E)-3,4-Methylenedioxycinnamyl alcohol (7.5)

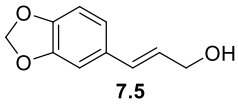
7.5

To a two-neck 250 mL two-neck round bottom flask under nitrogen was added ethyl (E)-3,4-(methylenedioxy)cinnamate (2.73 g, 12.4 mmol, 1.00 mol. equiv.) and dry CH_2Cl_2 (41.3 mL, 0.300 M) and. The solution was cooled to −78 °C and diisobutylaluminium hydride (22.7 mL, 27.3 mmol, 2.20 mol. equiv., 1.00 M solution in cyclohexane) was added dropwise. The reaction was allowed to warm to room temperature overnight by which time ^{1}H NMR analysis indicated completion of the reaction. The reaction mixture was diluted with diethyl ether, cooled to 0 °C and water (1.12 mL) was added dropwise followed by a 15% aqueous solution of sodium hydroxide (1.12 mL) and then water (2.80 mL) again. The mixture was allowed to warm to room temperature over fifteen minutes and then $MgSO_4$ was added, stirred for a further fifteen minutes, filtered, and concentrated under reduced pressure. The crude product was used without further purification. Spectroscopic data matched those previously reported in the literature.[6] **Yield**: 1.96 g, 10.9 mmol, 88%; **Appearance**: White solid; $\mathbf{R_f}$: 0.14 (1:4 EtOAc:hexane); **^{1}H NMR** (500 MHz, $CDCl_3$): δ 6.93 (s, 1H), 6.82 (d, *J* = 8.0 Hz, 1H), 6.76 (d, *J* = 8.0 Hz, 1H), 6.52 (d, *J* = 15.8 Hz, 1H), 6.20 (dt, *J* = 5.9, 15.8 Hz, 1H), 5.96 (s, 2H), 4.29 (t, *J* = 5.9 Hz, 2H), 1.42 (t, *J* = 5.9 Hz, 1H) ppm.

1,3-Benzodioxole, 5-[(1E)-3-bromo-1-propen-1-yl]- (ACI) (7.6)

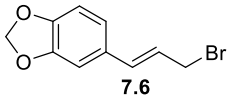
7.6

To a 50 mL round bottom flask under nitrogen was added (E)-3,4-methylenedioxycinnamyl alcohol (0.953 g, 5.35 mmol, 1.00 mol. equiv.) and dry diethyl ether (17.8 mL, 0.300 M). The reaction was cooled to 0 °C and phosphorus tribromide (0.200 mL, 2.14 mmol, 0.400 mol. equiv.) was added dropwise. The reaction was stirred at 0 °C for one hour by which time ^{1}H NMR analysis indicated completion of the reaction. The reaction mixture was quenched with a saturated solution of sodium bicarbonate at 0 °C and extracted with diethyl ether. The combined organic layers were then washed with a saturated aqueous solution of $Na_2S_2O_3$, brine, dried over $MgSO_4$, filtered, and concentrated under reduced pressure. The crude product was used without further purification. Spectroscopic data matched those previously reported in the literature.[7] **Yield**: 1.20 g, 4.96 mmol, 93%; **Appearance**: Pale yellow solid; $\mathbf{R_f}$: Degrades on silica; **^{1}H NMR** (500 MHz, $CDCl_3$): δ 6.93 (s, 1H), 6.82 (d, *J* = 8.0 Hz, 1H), 6.76 (d, *J* = 8.0 Hz, 1H), 6.56 (d, *J* = 15.5 Hz, 1H), 6.23 (dt, *J* = 7.9, 15.5 Hz, 1H), 5.97 (s, 2H), 4.15 (d, *J* = 7.9 Hz, 2H) ppm.

Ethyl (E,E)-5-phenyl-2,4-pentadienoate (7.7)

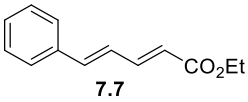

7.7

To a 100 mL round bottom flask under N_2 was added ethyl(triphenylphosphoranylidene)acetate (6.33 g, 18.2 mmol, 1.20 mol. equiv.) and dry toluene (16.8 mL, 0.900 M). The solution was cooled to 0 °C and trans-cinnamaldehyde (2.00 g, 15.1 mmol, 1.00 mol. equiv.) was added dropwise. The reaction was allowed to warm to room temperature over four hours by which time ^{1}H NMR analysis indicated completion of the reaction. The reaction mixture was diluted with water and extracted with ethyl acetate. The combined organic layers were then washed with brine, dried over $MgSO_4$, filtered, and concentrated under reduced pressure. Purification via flash column chromatography (SiO_2, eluting with 1:19 EtOAc:hexane → 1:3 EtOAc:hexane) yielded pure ethyl (E,E)-5-phenyl-2,4-pentadienoate. Spectroscopic data matched those previously reported in the literature.[8] **Yield**: 2.09 g, 10.4 mmol, 68%; **Appearance**: Yellow oil; **^{1}H NMR** (500 MHz, $CDCl_3$): δ 7.46 (d, *J* = 8.1 Hz, 2H), 7.43 (d, *J* = 8.9 Hz, 1H), 7.36 (t, *J* = 7.5 Hz, 2H), 7.31 (t, *J* = 7.2 Hz, 1H), 6.93–6.83 (m, 2H), 5.99 (d, *J* = 15.8 Hz, 1H), 4.24 (q, *J* = 7.1 Hz, 2H), 1.32 (t, *J* = 7.1 Hz, 3H) ppm.

(E,E)-5-Phenyl-2,4-pentadien-1-ol (7.8)

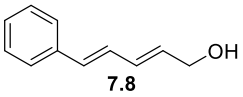

7.8

To a 250 mL round bottom flask under N_2 was added ethyl (E,E)-5-phenyl-2,4-pentadienoate (2.09 g, 10.3 mmol, 1.00 mol. equiv.) and dry CH_2Cl_2 (51.7 mL, 0.200 M) and. The solution was cooled to −78 °C and diisobutylaluminium hydride (22.7 mL, 22.7 mmol, 2.20 mol. equiv., 1.00 M solution in toluene) was added dropwise. The reaction was allowed to warm to room temperature over two hours by which time ^{1}H NMR analysis indicated completion of the reaction. The reaction mixture was diluted with diethyl ether, cooled to 0 °C and water (0.91 mL) was added dropwise followed by a 15% aqueous solution of sodium hydroxide (0.91 mL) and then water (2.27 mL) again. The mixture was allowed to warm to room temperature over fifteen minutes and then $MgSO_4$ was added, stirred for a further fifteen minutes, filtered, and concentrated under reduced pressure to yield pure (E,E)-5-phenyl-2,4-pentadien-1-ol. Spectroscopic data matched those previously reported in the literature.[9] **Yield**: 1.59 g, 9.92 mmol, 96%; **Appearance**: Off-white solid; **^{1}H NMR** (500 MHz, $CDCl_3$): δ 7.40 (d, *J* = 7.7 Hz, 2H), 7.32 (t, *J* = 7.6 Hz, 2H), 7.23 (t, *J* = 7.2 Hz, 1H), 6.79 (dd, *J* = 10.5, 15.6 Hz, 1H), 6.56 (d, *J* = 15.6 Hz, 1H), 6.43 (dd, *J* = 10.4, 15.3 Hz, 1H), 5.97 (dt, *J* = 5.9, 15.3 Hz, 1H), 4.26 (t, *J* = 5.8 Hz, 2H), 1.34 (t, *J* = 5.9 Hz, 1H) ppm.

(E,E)-5-Bromo-1-phenyl-1,3-pentadiene (7.9)

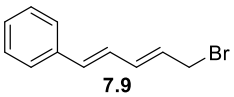

7.9

To a 250 mL round bottom flask under N_2 was added (E,E)-5-phenyl-2,4-pentadien-1-ol (5.31 g, 33.1 mmol, 1.00 mol. equiv.) and dry diethyl ether (110 mL, 0.300 M) and. The reaction was cooled to 0 °C and phosphorus tribromide (1.25 mL, 13.3 mmol, 0.400 mol. equiv.) was added dropwise. The reaction was stirred at 0 °C for one hour by which time ^{1}H NMR analysis indicated completion of the reaction. The reaction mixture was quenched with a saturated solution of sodium bicarbonate at 0 °C and extracted with diethyl ether. The combined organic layers were then washed with a saturated aqueous solution of $Na_2S_2O_3$, brine, dried over $MgSO_4$, filtered, and concentrated under reduced pressure. The crude product was used without further purification. Spectroscopic data matched those previously reported in the literature.[9] **Yield**: 5.92 g, 26.5 mmol, 80%; **Appearance**: Pale yellow solid; **R_f**: Degrades on silica; **^{1}H NMR** (500 MHz, $CDCl_3$): δ 7.40 (d, *J* = 7.4 Hz, 2H), 7.32 (t, *J* = 7.5 Hz, 2H), 7.24 (t, *J* = 7.3 Hz, 1H), 6.76 (dd, *J* = 10.5, 15.6 Hz, 1H), 6.60 (d, *J* = 15.6 Hz, 1H), 6.46 (dd, *J* = 10.5, 14.9 Hz, 1H), 6.00 (dt, *J* = 8.0, 14.9 Hz, 1H), 4.11 (d, *J* = 8.0 Hz, 2H) ppm.

Cyclooctatetraene oxide (5.122)

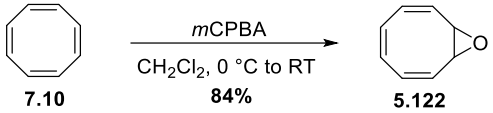

7.10 5.122

To a one-neck 250 mL round-bottom flask under nitrogen and equipped with a stir bar was added 1,3,5,7-cyclooctatetraene (2.98 g, 28.6 mmol, 1.00 mol. equiv.) and dry CH_2Cl_2 (118 mL, 0.220 M). The solution was cooled to 0 °C and mCPBA (4.49 g, 26.0 mmol, 0.900 mol. equiv.) was added and the reaction allowed to warm to room temperature. mCPBA (a total of 3.00 g) was added until ^{1}H NMR analysis indicated the 1,3,5,7-cyclooctatetraene was completely consumed. The reaction was washed with 10% aqueous $Na_2S_2O_3$ solution, saturated aqueous $NaHCO_3$, brine, dried over $MgSO_4$, filtered, and concentrated under reduced pressure. Purification via flash column chromatography (SiO_2, eluting with hexane) yielded pure cyclooctatetraene oxide. Spectroscopic data matched those previously reported in the literature.[10] **Yield**: 2.61 g, 21.8 mmol, 84%; **Appearance**: Pale yellow oil; **R_f**: 0.40 (1:19 EtOAc:hexanes); **^{1}H NMR** (500 MHz, $CDCl_3$): δ 6.11 (d, *J* = 11.8 Hz, 2H), 6.02 (d, *J* = 11.8 Hz, 2H), 5.93 (s, 2H), 3.49 (s, 2H) ppm.

ethyl (E)-4-((2Z,4Z,6Z)-8-oxocycloocta-2,4,6-trien-1-yl)but-2-enoate (5.147)

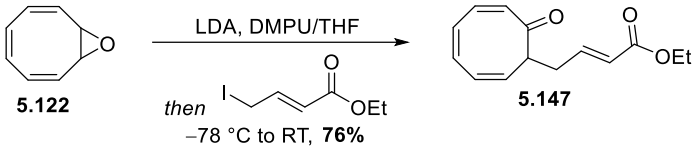

To a two-neck 50 mL round-bottom flask under nitrogen and equipped with a stir bar was added dry tetrahydrofuran (16.7 mL, 0.150 M), dry diisopropylamine (0.460 mL, 3.25 mmol, 1.30 mol. equiv.) and N, N′-dimethylpropyleneurea (2.36 mL, 1.06 M). The solution was cooled to –78 °C and then *n*-butyllithium (1.48 mL, 3.12 mmol, 1.25 mol. equiv., 2.11 M solution in THF) was added dropwise. A solution of cyclooctatetraene oxide (0.300 g, 2.50 mmol, 1.00 mol. equiv.) in tetrahydrofuran (1.50 mL, 1.67 M) was added dropwise, followed by dropwise addition of ethyl (E)-5-iodopent-2-enoate (1.02 mL, 4.24 mmol, 1.70 mol. equiv.) and then allowed to warm to room temperature overnight. The reaction mixture was diluted with hexane, washed with water, brine, dried over $MgSO_4$, filtered and concentrated under reduced pressure. Purification via flash column chromatography (SiO_2, eluting with hexane → 1:4 EtOAc:hexane) yielded pure ethyl (E)-4-((2Z,4Z,6Z)-8-oxocycloocta-2,4,6-trien-1-yl)but-2-enoate. **Yield**: 0.442 g, 1.90 mmol, 76%; **Appearance**: Yellow oil; $\mathbf{R_f}$: 0.29 (1:4 EtOAc:hexanes); **^{1}H NMR** (600 MHz, $CDCl_3$): δ 7.74 (m, 1H), 6.91–6.85 (s, 1H), 6.75 (dd, *J* = 7.3, 13.1 Hz, 1H), 6.66 (dd, *J* = 4.8, 12.3 Hz, 1H), 6.61 (d, *J* = 13.3 Hz, 1H), 6.41 (dd, *J* = 7.3, 12.3 Hz, 1H), 6.34 (dd, *J* = 4.9, 10.2 Hz, 1H), 5.82 (d, *J* = 15.6 Hz, 1H), 5.38 (t, *J* = 9.5 Hz, 1H), 4.16 (q, *J* = 7.5, 7.2 Hz, 2H), 2.95–2.88 (m, 1H), 2.88–2.82 (m, 1H), 2.66–2.60 (m, 1H), 1.27 (t, *J* = 7.2 Hz, 3H) ppm; **^{13}C NMR** (150 MHz, ($CDCl_3$): δ 192.0, 166.6, 146.2, 138.2, 136.4, 134.7, 134.2, 129.5, 127.2, 123.1, 60.4, 50.1, 31.6, 14.4 ppm; **IR**: 2982, 1717, 1660, 1269, 1197, 1177, 1149, 1042, 656 cm^{-1}; **HRMS** (ESI): calculated for $[C_{14}H_{16}O_3+H]^+$: 233.1172, found: 233.1175.

(2Z,4Z,6Z)-8-((E)-3-(benzo[d][1,3]dioxol-5-yl)allyl)cycloocta-2,4,6-trien-1-one (5.148)

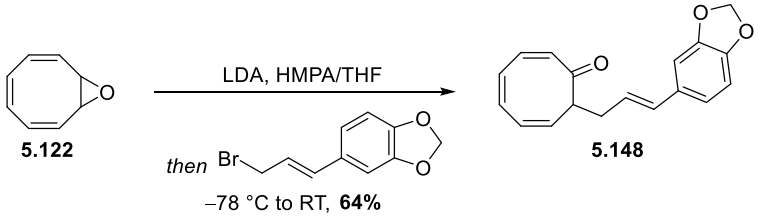

To a two-neck 50 mL round-bottom flask under nitrogen and equipped with a stir bar was added dry tetrahydrofuran (16.7 mL, 0.150 M), dry diisopropylamine (0.305 mL, 2.87 mmol, 1.15 mol. equiv.) and hexamethylphosphoramide (2.36 mL, 1.06 M). The solution was cooled to –78 °C and *n*-butyllithium (1.83 mL, 2.75 mmol, 1.10 mol. equiv., 1.50 M solution in cyclohexane) was added dropwise. A solution of cyclooctatetraene oxide (0.300 g, 2.50 mmol, 1.00 mol. equiv.) in tetrahydrofuran (1.00 mL, 2.5 M) was added dropwise, followed by dropwise addition of a solution of 5-[(1E)-3-bromo-1-propen-1-yl]-1,3-benzodioxole (2.05 g, 8.49 mmol, 3.40 mol. equiv.) in tetrahydrofuran (5.00 mL, 1.70 M) and then allowed to warm to room temperature overnight. The reaction mixture was diluted with hexane, washed with water, brine, dried over $MgSO_4$, filtered and concentrated under reduced pressure. Purification via flash column chromatography (SiO_2, dichloromethane) yielded pure (2Z,4Z,6Z)-8-((E)-3-(benzo[d][1,3]dioxol-5-yl)allyl)cycloocta-2,4,6-trien-1-one. **Yield**: 446 mg, 1.59 mmol, 64%; **Appearance**: Yellow oil; $\mathbf{R_f}$: 0.50 (dichloromethane); **^{1}H NMR** (500 MHz, $CDCl_3$): δ 6.86 (s, 1H), 6.76–6.70 (m, 3H), 6.65 (dd, *J* = 4.9, 12.2 Hz, 1H), 6.61 (d, *J* = 13.2 Hz, 1H), 6.39 (dd, *J*

= 7.1, 12.2 Hz, 1H), 6.36–6.30 (m, 2H), 5.99 (dt, *J* = 7.2, 15.1 Hz, 1H), 5.92 (s, 2H), 5.45 (t, *J* = 9.5 Hz, 1H), 2.93–2.86 (m, 1H), 2.86–2.79 (m, 1H), 2.64–2.56 (m, 1H) ppm; **^{13}C NMR** (125 MHz, ($CDCl_3$): δ 192.8, 148.1, 146.9, 138.5, 136.1, 135.7, 134.2, 132.2, 131.3, 129.0, 127.0, 126.1, 120.6, 108.3, 105.6, 101.1, 51.5, 32.4 ppm; **IR**: 2894, 1660, 1502, 1489, 1445, 1248, 1192, 1038, 964, 930, 794, 783, 656 cm^{-1}; **HRMS** (ESI): calculated for $[C_{18}H_{16}O_3+H]^+$: 281.1172, found: 281.1173.

(2Z,4Z,6Z)-8-cinnamylcycloocta-2,4,6-trien-1-one (5.149)

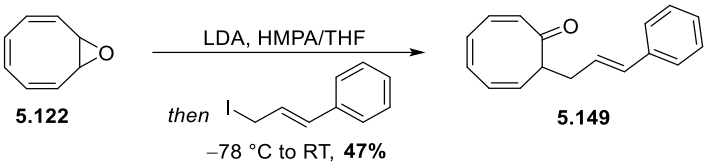

To a two-neck 50 mL round-bottom flask under nitrogen and equipped with a stir bar was added dry tetrahydrofuran (13.9 mL, 0.150 M) and dry diisopropylamine (0.338 mL, 2.39 mmol, 1.15 mol. equiv.) and hexamethylphosphoramide (1.96 mL, 1.06 M). The solution was cooled to –78 °C, and then *n*-butyllithium (1.14 mL, 2.29mmol, 1.10 mol. equiv., 2.00 M solution in cyclohexane) was added dropwise. A solution of cyclooctatetraene oxide (0.250 g, 2.08 mmol, 1.00 mol. equiv.) in tetrahydrofuran (1.00 mL, 2.08 M) was added dropwise, followed by dropwise addition of a solution of (E)-cinnamyl iodide (0.762 g, 3.12 mmol, 1.50 mol. equiv.) in THF (4 mL, 0.780 M) and then allowed to warm to room temperature overnight. The reaction mixture was diluted with diethyl ether, washed with water, brine, dried over $MgSO_4$, filtered and concentrated under reduced pressure. Purification via flash column chromatography (SiO_2, eluting with hexane → 1:4 EtOAc:hexane) yielded (2Z,4Z,6Z)-8-cinnamylcycloocta-2,4,6-trien-1-one that contained cinnamaldehyde as an impurity. To remove cinnamaldehyde, the compound was dissolved in MeOH, washed with a saturated solution of sodium sulfite, water, extracted with a 1:9 EtOAc:hexane solvent mixture, dried over $MgSO_4$, filtered and concentrated under reduced pressure to yield pure (2Z,4Z,6Z)-8-cinnamylcycloocta-2,4,6-trien-1-one. **Yield**: 0.233 g, 0.986 mmol, 47%; **Appearance**: Yellow oil; **R_f**: 0.40 (1:9 EtOAc:hexanes); **^{1}H NMR** (500 MHz, $CDCl_3$): δ 7.32 (d, *J* = 7.9 Hz, 2H), 7.28 (t, *J* = 7.3 Hz, 2H), 7.19 (t, *J* = 7.3 Hz, 1H), 6.73 (dd, *J* = 7.3, 13.2 Hz, 1H), 6.67–6.60 (m, 2H), 6.45–6.37 (m, 2H), 6.33 (dd, *J* = 4.9, 10.2 Hz, 1H), 6.17 (dt, *J* = 7.1, 15.8 Hz, 1H), 5.46 (t, *J* = 9.5 Hz, 1H), 2.96–2.89 (m, 1H), 2.88–2.82 (m, 1H), 2.68–2.60 (m, 1H) ppm; **^{13}C NMR** (125 MHz, ($CDCl_3$): δ 192.8, 138.5, 137.6, 136.2, 135.7, 134.2, 131.8, 129.0, 128.6, 127.9, 127.2, 127.0, 126.2, 51.5, 32.5 ppm; **IR**: 3023, 1660, 1621, 1149, 965, 734, 693, 656 cm^{-1}; **HRMS** (ESI): calculated for $[C_{17}H_{16}O+H]^+$: 237.1274, found: 237.1277.

(2Z,4Z,6Z)-8-((2E,4E)-5-phenylpenta-2,4-dien-1-yl)cycloocta-2,4,6-trien-1-one (5.193)

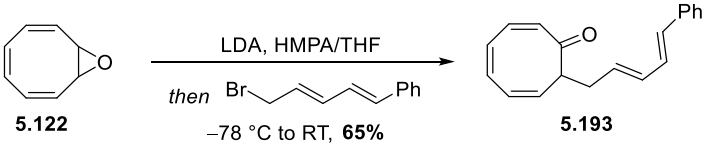

To a two-neck 50 mL round-bottom flask under nitrogen and equipped with a stir bar was added dry tetrahydrofuran (27.7 mL, 0.150 M) and dry diisopropylamine (0.734 mL, 5.20 mmol, 1.25 mol. equiv.) and hexamethylphosphoramide (3.90 mL, 1.06 M). The solution was cooled to –78 °C, and then *n*-butyllithium (2.00 mL, 4.99 mmol, 1.20 mol. equiv., 2.50 M solution in THF) was added dropwise. A solution of cyclooctatetraene oxide (0.500 g, 4.16 mmol, 1.00 mol. equiv.) in tetrahydrofuran (2.50 mL, 1.67 M) was added dropwise, followed by dropwise addition of a solution of ((1E,3E)-5-bromopenta-1,3-dien-1-yl)benzene (1.39 g, 6.24 mmol, 1.50 mol. equiv.) in THF (4 mL, 1.56 M) and then allowed to warm to room temperature

overnight. The reaction mixture was diluted with hexane, washed with water, brine, dried over $MgSO_4$, filtered and concentrated under reduced pressure. Purification via flash column chromatography (SiO_2, eluting with hexane → 1:4 EtOAc:hexane) yielded pure (2Z,4Z,6Z)-8-((2E,4E)-5-phenylpenta-2,4-dien-1-yl)cycloocta-2,4,6-trien-1-one. **Yield**: 0.707 g, 2.70 mmol, 65%; **Appearance**: Yellow oil; $\mathbf{R_f}$: 0.37 (1:4 EtOAc:hexanes); **^{1}H NMR** (500 MHz, $CDCl_3$): δ 7.36 (d, *J* = 7.7 Hz, 2H), 7.29 (t, *J* = 7.5 Hz, 2H), 7.19 (t, *J* = 7.3 Hz, 1H), 6.77–6.64 (m, 3H), 6.62 (d, *J* = 13.2 Hz, 1H), 6.44 (d, *J* = 15.9 Hz, 1H), 6.40 (dd, *J* = 7.3, 12.2 Hz, 1H), 6.34 (dd, *J* = 4.9, 10.3 Hz, 1H), 6.24 (dd, *J* = 10.4, 15.8 Hz, 1H), 5.57 (dt, *J* = 7.0, 14.6 Hz, 1H), 5.43 (t, *J* = 9.4 Hz, 1H), 2.90–2.78 (m, 2H), 2.63–2.55 (m, 1H) ppm; **^{13}C NMR** (125 MHz, ($CDCl_3$): δ 192.8, 138.5, 137.6, 136.2, 135.7, 134.2, 132.4, 132.4, 130.9, 129.2, 129.0, 128.7, 127.4, 127.0, 126.3, 51.4, 32.3 ppm; **IR**: 2931, 1656, 1623, 1449, 990, 970, 750, 736, 693, 656 cm^{-1}; **HRMS** (ESI): calculated for $[C_{19}H_{18}O+H]^+$: 263.1430, found: 263.1423.

4-(((2Z,4Z,6Z)-8-oxocycloocta-2,4,6-trien-1-yl)methyl)furan-2(5H)-one (5.150)

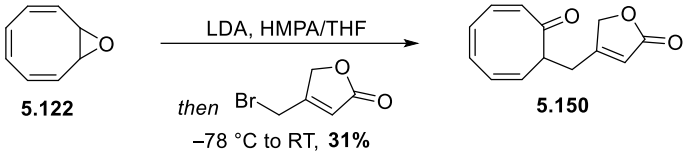

To a two-neck 25 mL round-bottom flask under nitrogen and equipped with a stir bar was added dry tetrahydrofuran (11.1 mL, 0.150 M) and dry diisopropylamine (0.258 mL, 1.83 mmol, 1.10 mol. equiv.) and hexamethylphosphoramide (1.57 mL, 1.06 M). The solution was cooled to –78 °C, and then *n*-butyllithium (0.873 mL, 1.75 mmol, 1.05 mol. equiv., 2.00 M solution in THF) was added dropwise. A solution of cyclooctatetraene oxide (0.200 g, 1.66 mmol, 1.00 mol. equiv.) in tetrahydrofuran (1.00 mL, 1.66 M) was added dropwise, followed by dropwise addition of a solution of 4-(bromomethyl)-2(5H)-furanone (0.441 g, 2.50 mmol, 1.50 mol. equiv.) in THF (2 mL, 1.25 M) and then allowed to warm to room temperature overnight. The reaction mixture was diluted with diethyl ether, washed with water, brine, dried over $MgSO_4$, filtered and concentrated under reduced pressure. Purification via flash column chromatography (SiO_2, eluting with 3:7 EtOAc:hexane → 1:1 EtOAc:hexane) yielded pure 4-(((2Z,4Z,6Z)-8-oxocycloocta-2,4,6-trien-1-yl)methyl)furan-2(5H)-one. **Yield**: 110.7 mg, 0.511 mmol, 31%; **Appearance**: Pale yellow oil; $\mathbf{R_f}$: 0.27 (1:1 EtOAc:hexanes); **^{1}H NMR** (500 MHz, $CDCl_3$): δ 6.81 (dd, *J* = 7.4, 13.3 Hz, 1H), 6.71 (dd, *J* = 4.8, 12.2 Hz, 1H), 6.64 (d, *J* = 13.3 Hz, 1H), 6.48 (dd, *J* = 4.8, 12.2 Hz, 1H), 6.40 (dd, *J* = 4.5, 10.0 Hz, 1H), 5.72 (s, 1H), 5.40 (t, *J* = 9.3 Hz, 1H), 4.73 (s, 2H), 3.12 (dd, *J* = 6.7, 16.5 Hz, 1H), 3.02 (q, *J* = 7.3, 7.3 Hz, 1H), 2.82 (dd, *J* = 7.1, 16.5 Hz, 1H) ppm; **^{13}C NMR** (125 MHz, ($CDCl_3$): δ 191.4, 173.9, 167.9, 138.0, 136.9, 134.0, 133.7, 130.1, 127.8, 116.8, 73.5, 49.7, 28.0 ppm; **IR**: 2926, 1778, 1751, 1559, 1445, 1172, 1152, 1132, 1024, 888, 742 cm^{-1}; **HRMS** (ESI): calculated for $[C_{13}H_{12}O_3+H]^+$: 217.0859, found: 217.0865.

Ethyl (1aR,1a1S,5S,6aR,7R)-1-oxo-1,1a,1a1,2,4a,5,6,6a-octahydro-2,5-methanocyclobuta[cd]indene-7-carboxylate (Ethyl ester tetracycle) (5.161)

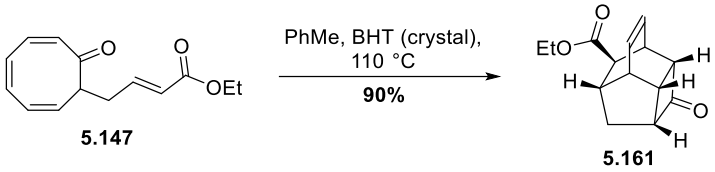

5.147 5.161

To a one-neck 500 mL round-bottom flask under nitrogen and equipped with a stir bar was added ethyl (E)-4-((2Z,4Z,6Z)-8-oxocycloocta-2,4,6-trien-1-yl)but-2-enoate (0.723 g, 3.11 mmol), dry degassed toluene (311 mL, 0.01 M) and butylated hydroxytoluene (crystal). The reaction was heated to 110 °C for 24 hours by which time ^{1}H NMR analysis indicated the complete consumption of the starting material. The reaction mixture was concentrated under reduced pressure and purified via flash column chromatography (SiO_2, eluting with 1:4 EtOAc:petroleum ether) yielding pure ethyl ester tetracycle. **Yield**: 0.653 g, 2.80 mmol, 90%; **Appearance**: Pale yellow oil; $\mathbf{R_f}$: 0.45 (1:4 EtOAc:hexanes); **^{1}H NMR** (600 MHz, $CDCl_3$): δ 6.44–6.40 (m, 1H), 6.28–6.24 (m, 1H), 4.12–4.02 (m, 2H), 3.40 (dt, *J* = 5.4, 5.4, 8.9 Hz, 1H), 3.25–3.21 (m, 1H), 3.06 (dt, *J* = 5.3, 5.3, 8.3 Hz, 1H), 2.97-2.93 (m, 1H), 2.74 (t, *J* = 4.9 Hz, 1H), 2.49–2.45 (m, 1H), 2.18-2.15 (m, 1H), 1.95 (ddd, *J* = 5.0, 8.9, 12.9 Hz, 1H), 1.64 (d, *J* = 12.9 Hz, 1H), 1.21 (t, *J* = 7.1 Hz, 3H) ppm; **^{13}C NMR** (150 MHz, ($CDCl_3$): δ 211.0, 172.8, 134.0, 131.9, 62.4, 60.8, 60.0, 50.4, 40.3, 37.4, 34.6, 34.3, 30.9, 14.3 ppm; **IR**: 2975, 1760, 1728, 1185, 1027, 692 cm^{-1}; **HRMS** (ESI): calculated for $[C_{14}H_{16}O_3+H]^+$: 233.1172, found: 233.1173.

(1aS,1a1S,5S,6aR,7R)-7-(benzo[d][1,3]dioxol-5-yl)-1a1,2,4a,5,6,6a-hexahydro-2,5-methanocyclobuta[cd]inden-1(1aH)-one (1,3-Benzodioxole tetracycle) (5.162)

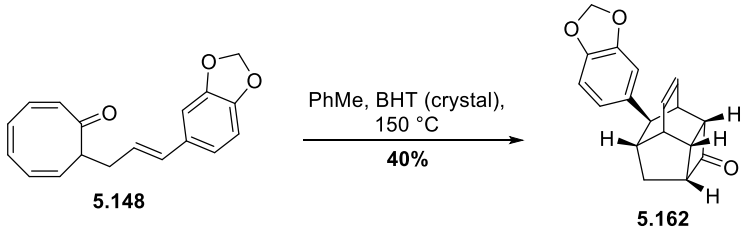

5.148 5.162

To a 120 mL sealed flask under nitrogen and equipped with a stir bar was added (2Z,4Z,6Z)-8-((E)-3-(benzo[d][1,3]dioxol-5-yl)allyl)cycloocta-2,4,6-trien-1-one (81.5 mg, 0.291 mmol), dry degassed toluene (29.1 mL, 0.01 M) and butylated hydroxytoluene (crystal). The reaction was heated to 150 °C overnight by which time ^{1}H NMR analysis indicated the complete consumption of the starting material. The reaction mixture was concentrated under reduced pressure and purified via flash column chromatography (SiO_2, eluting with 1:4 EtOAc:hexanes) yielding pure 1,3-benzodioxole tetracycle. **Yield**: 32.8 mg, 0.117 mmol, 40%; **Appearance**: Yellow oil; $\mathbf{R_f}$: 0.51 (1:4 EtOAc:hexanes); **^{1}H NMR** (500 MHz, $CDCl_3$): δ 6.66 (d, *J* = 8.1 Hz, 1H), 6.55 (s, 1H), 6.54 (t, *J* = 7.3 Hz, 1H), 6.56–6.51 (m, 2H), 6.49 (d, *J* = 8.1 Hz, 1H), 6.06 (t, *J* = 7.3 Hz, 1H), 5.89 (s, 2H), 3.42 (dt, *J* = 8.6, 5.3 Hz, 1H), 3.10 (dt, *J* = 8.0, 5.3 Hz, 1H), 3.04 (q, *J* = 5.2, 5.3 Hz, 1H), 2.88 (t, *J* = 7.4 Hz, 1H), 2.53–2.47 (m, 2H), 2.45 (t, *J* = 4.6 Hz,1H), 1.96 (ddd, *J* = 4.8, 8.7, 13.2 Hz, 1H), 1.75 (d, *J* = 13.2 Hz, 1H) ppm; **^{13}C NMR** (125 MHz, ($CDCl_3$): δ 211.6, 147.2, 145.8, 138.9, 133.4, 132.4, 121.8, 109.4, 107.7, 100.9, 63.8, 59.6, 50.5, 42.6, 40.9, 36.7, 35.5, 34.8 ppm; **IR**: 2941, 1760, 1502, 1489, 1442, 1255, 1232, 1214, 1107, 1037, 928, 796, 699 cm^{-1}; **HRMS** (ESI): calculated for $[C_{18}H_{16}O_3+H]^+$: 281.1172, found: 281.1171.

(1aS,1a1S,5S,6aR,7R)-7-phenyl-1a1,2,4a,5,6,6a-hexahydro-2,5-methanocyclobuta[cd]inden-1(1aH)-one (Phenyl tetracycle) (5.163)

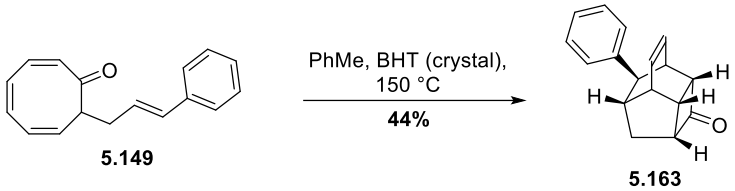

5.149 5.163

To a 120 mL sealed flask under nitrogen and equipped with a stir bar was added (2Z,4Z,6Z)-8-cinnamylcycloocta-2,4,6-trien-1-one (231 mg, 0.976 mmol), dry degassed toluene (97.6 mL, 0.01 M) and butylated hydroxytoluene (crystal). The reaction was heated to 150 °C overnight by which time ^{1}H NMR analysis indicated the complete consumption of the starting material. The reaction mixture was concentrated under reduced pressure and purified via flash column chromatography (SiO_2, eluting with 1:19 EtOAc:hexanes → 1:9 EtOAc:hexane) yielding pure phenyl tetracycle. **Yield**: 102 mg, 0.433 mmol, 44%; **Appearance**: Pale yellow oil; $\mathbf{R_f}$: 0.44 (1:9 EtOAc:hexanes); **^{1}H NMR** (500 MHz, $CDCl_3$): δ 7.23 (t, *J* = 7.2 Hz, 2H), 7.16 (t, *J* = 7.3 Hz, 1H), 7.05 (d, *J* = 7.2 Hz, 2H), 6.58–6.53 (m, 1H), 6.06–6.01 (m, 1H), 3.45 (dt, *J* = 5.3, 8.7 Hz, 1H), 3.13 (dt, *J* = 5.2, 8.0 Hz, 1H), 3.10–3.05 (m, 1H), 2.96–2.93 (m, 1H), 2.58 (d, *J* = 3.0 Hz, 1H), 2.56 (t, *J* = 4.8 Hz, 1H), 2.54–2.50 (m, 1H), 1.99 (ddd, *J* = 4.8, 8.7, 12.6 Hz, 1H), 1.78 (d, *J* = 12.6 Hz, 1H) ppm; **^{13}C NMR** (125 MHz, ($CDCl_3$): δ 211.6, 144.7, 133.4, 132.2, 128.8, 127. 9, 126.1, 63.8, 59.6, 50.8, 42.0, 40.9, 36.4, 35.5, 34.8 ppm; **IR**: 2941, 1758, 1492, 1448, 1108, 1031, 744, 713, 697, 667 cm^{-1}; **HRMS** (ESI): calculated for $[C_{17}H_{16}O+H]^+$: 237.1274, found: 237.1276.

Diels−Alder reaction of (2Z,4Z,6Z)-8-((2E,4E)-5-phenylpenta-2,4-dien-1-yl)cycloocta-2,4,6-trien-1-one (5.193)

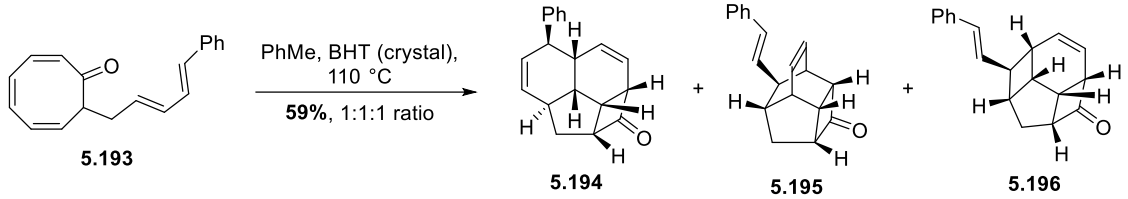

To a 500 mL round-bottom flask under nitrogen and equipped with a stir bar was added (2Z,4Z,6Z)-8-((2E,4E)-5-phenylpenta-2,4-dien-1-yl)cycloocta-2,4,6-trien-1-one (707.4 mg, 2.70 mmol), dry degassed toluene (270 mL, 0.01 M) and butylated hydroxytoluene (crystal). The reaction was heated to 110 °C overnight by which time ^{1}H NMR analysis indicated the complete consumption of the starting material. The reaction mixture was concentrated under reduced pressure and purified via flash column chromatography (SiO_2, eluting with hexane → 1:4 EtOAc:hexanes) to a 1:1:1 mixture of three compounds (see below). **Combined Yield**: 415 mg, 1.59 mmol, 59%. For characterisation, the three compounds were separated via preparative TLC.

Phenyl fused tetracycle (5.194)

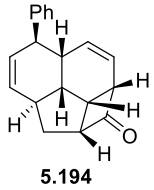

Stereochemistry determined by analogy to fused tetracyclic natural products in literature.[11–13] **Appearance**: Pale yellow oil; **R_f**: 0.47 (1:9 EtOAc:hexanes); **^{1}H NMR** (500 MHz, $CDCl_3$): δ 7.32 (t, *J* = 7.5 Hz, 2H), 7.27–7.20 (m, 3H), 6.11 (d, *J* = 9.8 Hz, 1H), 5.81 (d, *J* = 11.1 Hz, 1H), 5.72–5.64 (m, 2H), 3.63 (q, *J* = 7.2, 7.7 Hz, 2H), 3.35 (s, 1H), 2.87 (q, *J* = 7.6, 8.2 Hz, 1H), 2.75 (s, 1H), 2.45 (br t, *J* = 11.8 Hz, 1H), 2.25 (dd, *J* = 5.3, 12.2 Hz, 1H), 2.14–2.11 (m, 1H), 1.56–1.46 (m, 1H) ppm; **^{13}C NMR** (125 MHz, ($CDCl_3$): δ 215.4, 147.1, 133.9, 130.9, 130.7, 128.7, 127.6, 126.5, 120.4, 63.5, 57.1, 49.8, 41.7, 40.1, 36.8, 33.0, 29.6 ppm; **IR**: 2926, 1764, 1677, 1490, 1449, 1028, 913, 759, 699 cm^{-1}; **HRMS** (ESI): calculated for $[C_{19}H_{18}O+H]^+$: 263.1430, found: 263.1428.

2D NMR analysis of Phenyl fused tetracycle

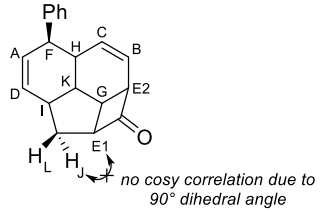

Position	^{1}H (500 MHz) NMR, $CDCl_3$	^{13}C (125 MHz) NMR, $CDCl_3$ (see HSQC in NMR data section)	COSY (500 MHz) correlations, $CDCl_3$
A	6.11 (d, *J* = 9.8 Hz, 1H)	130.7	D, F
B	5.81 (d, *J* = 11.1 Hz, 1H)	133.9	C, E2, H
C	5.72–5.64 (m, 2H)	120.4	B, E2, H
D	5.72–5.64 (m, 2H)	130.9	A, F, I
E1	3.63 (q, *J* = 7.2, 7.7 Hz, 2H)	63.5	G, L

E2	3.63 (q, *J* = 7.2, 7.7 Hz, 2H)	57.1	B, G
F	3.35 (s, 1H)	49.8	A, D, H, I
G	2.87 (q, *J* = 7.6, 8.2 Hz, 1H)	29.6	E1, E2, K
H	2.75 (s, 1H)	40.1	B, C, F, K
I	2.45 (br t, *J* = 11.8 Hz, 1H)	36.8	D, J, K, L
J	2.25 (dd, *J* = 5.3, 12.2 Hz, 1H)	33.0	I, L
K	2.14–2.11 (m, 1H)	41.7	G, H, I
L	1.56–1.46 (m, 1H)	33.0	E1, I, J, K
Ph	7.32 (t, *J* = 7.5 Hz, 2H), 7.27–7.20 (m, 3H)	147.1, 128.7, 127.6, 126.5	-
C=O	-	215.4	-

Styrenyl bridged tetracycle (5.195)

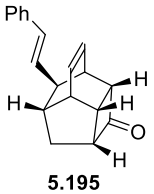

5.195

Stereochemistry determined by analogy to bridged tetracyclic products in literature.[11,12] **Appearance**: Pale yellow oil; **R_f**: 0.40 (1:9 EtOAc:hexanes); **^{1}H NMR** (500 MHz, $CDCl_3$): δ 7.30–7.24 (m, 4H), 7.21–7.16 (m, 1H), 6.50 (t, *J* = 7.5 Hz, 1H), 6.33 (t, *J* = 7.4 Hz, 1H), 6.27 (d, *J* = 15.9 Hz, 1H), 5.96 (dd, *J* = 8.5, 15.9 Hz, 1H), 3.41 (dt, *J* = 5.5, 9.9 Hz, 1H), 3.08 (dt, *J* = 5.4, 8.0 Hz, 1H), 2.96 (q, *J* = 5.4, 5.3 Hz, 1H), 2.84–2.78 (m, 1H), 2.48 (dt, *J* = 5.3, 9.4 Hz, 1H), 2.13–2.09 (m, 1H), 2.09–2.03 (m, 1H), 1.91 (ddd, *J* = 4.8, 8.6, 12.6 Hz, 1H), 1.73 (d, *J* = 12.6 Hz, 1H) ppm; **^{13}C NMR** (125 MHz, ($CDCl_3$): δ 211.7, 137.5, 134.0, 133.1, 132.9, 129.4, 128.6, 127.2, 126.2, 63.6, 59.6, 50.1, 41.8, 40.7, 34.8, 34.6, 34.6 ppm; **IR**: 2939, 1760, 1697, 1490, 1448, 1206, 1110, 1027, 965, 746, 693 cm^{-1}; **HRMS** (ESI): calculated for $[C_{19}H_{18}O+H]^+$: 263.1430, found: 263.1426.

2D NMR analysis of Styrenyl bridged tetracycle

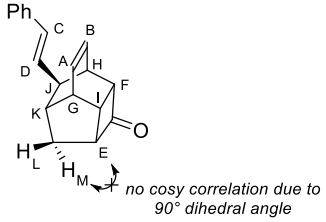

Position	^{1}H (500 MHz) NMR, $CDCl_3$	Key COSY (500 MHz) correlations, $CDCl_3$
A	6.50 (t, *J* = 7.5 Hz, 1H)	B, G
B	6.33 (t, *J* = 7.4 Hz, 1H)	A, H
C	6.27 (d, *J* = 15.9 Hz, 1H)	D
D	5.96 (dd, *J* = 8.5, 15.9 Hz, 1H)	C, J
E	3.41 (dt, *J* = 5.5, 9.9 Hz, 1H)	F, I, L

F	3.08 (dt, *J* = 5.4, 8.0 Hz, 1H)	E, H, I
G	2.96 (q, *J* = 5.4, 5.3 Hz, 1H)	A, I, K
H	2.84–2.78 (m, 1H)	B, F, J
I	2.48 (dt, *J* = 5.3, 9.4 Hz, 1H)	E, F, G
J	2.13–2.09 (m, 1H)	D, H, K
K	2.09–2.03 (m, 1H)	G, J, L, M
L	1.91 (ddd, *J* = 4.8, 8.6, 12.6 Hz, 1H)	E, K, L
M	1.73 (d, *J* = 12.6 Hz, 1H)	K, L
Ph	7.30–7.24 (m, 4H), 7.21–7.16 (m, 1H)	-
C=O	-	-

4/6/5/4 tetracycle (5.196)

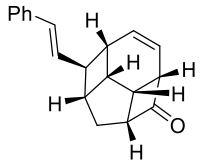

5.196

(Degrades rapidly >0 °C)

Characterised in a mixture with minor amounts of other products. Stereochemistry determined by analogy to other products in mixture. **Appearance**: Pale yellow oil; **R_f**: 0.35 (1:9 EtOAc:hexanes); **^{1}H NMR** (500 MHz, $CDCl_3$): δ 7.36 (t, *J* = 7.7 Hz, 2H), 7.28 (d, *J* = 7.5 Hz, 2H), 7.24 (t, *J* = 7.3 Hz, 1H), 6.00–5.90 (m, 2H), 5.77 (d, *J* = 10.2 Hz, 1H), 5.55 (d, *J* = 10.2 Hz, 1H), 3.68 (br s, 1H), 3.60–3.50 (m, 2H), 3.32 (q, *J* = 8.5, 8.3 Hz, 1H), 3.19–3.11 (m, 1H), 2.97–2.88 (m, 1H), 2.70 (br s, 1H), 2.26–2.18 (m, 1H), 1.95–1.85 (m, 1H) ppm; **^{13}C NMR** (150 MHz, ($CDCl_3$): δ 209.4, 142.8, 132.6, 129.7, 128.6, 128.5, 127.5, 126.5, 126.2, 63.8, 58.7, 44.9, 44.6, 41.7, 36.9, 36.4, 34.9 ppm.

2D NMR analysis of 4/6/5/4 tetracycle

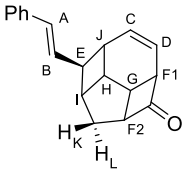

Position	^{1}H (500 MHz) NMR, $CDCl_3$	^{13}C (150 MHz) NMR, $CDCl_3$ (see HSQC in NMR data section)	COSY (600 MHz) correlations, $CDCl_3$	Key HMBC (600 MHz) correlations, $CDCl_3$
A	6.00–5.90 (m, 2H)	127.5	B	
B	6.00–5.90 (m, 2H)	132.6	A, E	L, I, H
C	5.77 (d, *J* = 10.2 Hz, 1H)	126.2	D, J, F1	G
D	5.55 (d, *J* = 10.2 Hz, 1H)	129.7	C, J, F1	H
E	3.68 (br s, 1H)	44.6	B, I, J	
F1	3.60–3.50 (m, 2H)	58.7	C, D, G	G, H, F2
F2	3.60–3.50 (m, 2H)	63.8	C, D, G, K/L	G, H, K, L

G	3.32 (q, *J* = 8.5, 8.3 Hz, 1H)	34.9	F1, F2, H	H, K
H	3.19–3.11 (m, 1H)	41.7	G, I, J	I, K
I	2.97–2.88 (m, 1H)	44.9	E, H, K/L	G, H, K, L
J	2.70 (br s, 1H)	36.4	C, D, E, H	G, H
K	2.26–2.18 (m, 1H)	36.9	F2, I, L	F, G, H, I
L	1.95–1.85 (m, 1H)	36.9	F2, I, K	F, G, H, I
Ph	7.36 (t, *J* = 7.7 Hz, 2H), 7.28 (d, *J* = 7.5 Hz, 2H), 7.24 (t, *J* = 7.3 Hz, 1H)	142.8, 128.6, 128.5, 126.5	-	
C=O		209.4	-	F1, F2, G, K, L, H

Ethyl (1aR,1a1S,5S,6aR,7R)-1-(methoxymethylene)-1,1a,1a1,2,4a,5,6,6a-octahydro-2,5-methanocyclobuta[cd]indene-7-carboxylate (Methyl vinyl ether tetracycle) (5.169)

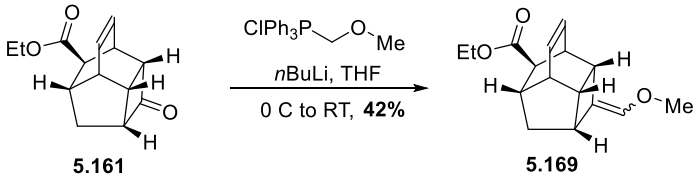

To a two-neck 10 mL round-bottom flask under nitrogen and equipped with a stir bar was added (methoxymethyl)triphenylphosphonium chloride (295 mg, 0.861 mmol, 2.00 mol. equiv.) and dry tetrahydrofuran (2.90 mL, 0.150 M). Upon cooling the solution to 0 °C, *n*-butyllithium (0.344 mL, 0.861 mmol, 2.00 mol. equiv., 2.50 M solution in THF) was added dropwise. To the reaction mixture, a solution of ethyl ester tetracycle (100 mg, 0.431 mmol, 1.00 mol. equiv.) in tetrahydrofuran (0.430 mL, 1.00 M) was added dropwise, and then allowed to warm to room temperature overnight. The reaction mixture was diluted with diethyl ether, quenched with saturated aqueous ammonium chloride, washed with water, brine, dried over $MgSO_4$, filtered and concentrated under reduced pressure. Purification via flash column chromatography (SiO_2, eluting with 1:9 EtOAc:hexane) yielded pure inseparable E/Z mixture of methyl vinyl ether tetracycle (1.00:0.78, major:minor, unassigned E/Z isomers). **Yield**: 47.6 mg, 0.181 mmol, 42%; **Appearance**: Yellow oil; $\mathbf{R_f}$: 0.41 (1:4 EtOAc:hexanes); **^{1}H NMR** (600 MHz, $CDCl_3$): δ 6.25 (t, *J* = 7.4 Hz, 1.94H, minor), 6.22–6.15 (m, 1.98H, major), 5.87 (s, 0.78H, minor), 5.85 (s, 1.00H, major), 4.14-4.00 (m, 4.19H), 3.58 (s, 3.33H, major), 3.56 (s, 2.55H, minor), 3.28 (t, *J* = 6.6 Hz, 1.15H), 3.18–3.14 (m, 0.95H), 3.08 (t, *J* = 6.2 Hz, 0.92H), 2.97–2.92 (m, 1.21H), 2.85 (d, *J* = 3.6 Hz, 1.10H, major), 2.79 (d, *J* = 3.6 Hz, 0.90H, minor), 2.79–2.75 (m, 0.93H), 2.70–2.65 (m, 2.20H), 2.62–2.57 (m, 3.26H), 2.41–2.35 (m, 2.07H), 1.83 (ddd, *J* = 5.1, 7.3, 12.4 Hz, 2.35H), 1.67–1.63 (m, 1.71H), 1.48 (d, *J* = 12.3 Hz, 1.02H), 1.22 (t, *J* = 7.1 Hz, 6.13H) ppm; **^{13}C NMR** (150 MHz, ($CDCl_3$): δ 175.0, 175.0, 140.6 (major), 140.5 (minor), 132.1, 132.1, 132.0, 131.7, 118.9 (minor), 118.7 (major), 60.4 (major), 60.3 (minor), 59.4 (major), 59.2 (minor), 49.4, 49.0, 41.0, 40.9, 40.9, 40.8, 40.8, 40.5, 40.4, 40.2, 39.6, 38.6, 38.4, 37.6, 36.4, 35.2, 14.4, 14.4 ppm; **IR**: 2962, 2934, 1728, 1700, 1191, 1118, 693 cm^{-1}; **HRMS** (ESI): calculated for $[C_{16}H_{20}O_3+H]^+$: 261.1485, found: 261.1484.

Ethyl (1S,1aR,1a1R,5S,6aR,7R)-1-formyl-1,1a,1a1,2,4a,5,6,6a-octahydro-2,5-methanocyclobuta[cd]indene-7-carboxylate (Aldehyde ester tetracycle) (5.171)

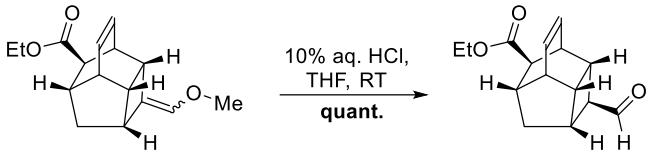

5.169 **5.171**

To a one-neck 10 mL round-bottom flask open to air and equipped with a stir bar was added methyl vinyl ether tetracycle (316 mg, 1.21 mmol), tetrahydrofuran (2.38 mL, 0.510 M), 10% aqueous HCl solution (2.38 mL, 0.510 M). The reaction was stirred at room temperature overnight by which time ^{1}H NMR analysis indicated the complete consumption of the starting material. The reaction mixture was diluted with ethyl acetate, quenched with sodium bicarbonate. The aqueous layer was extracted with ethyl acetate and the combined organic layers were washed with brine, dried over $MgSO_4$ and concentrated under reduced pressure to yield pure aldehyde ester tetracycle. **Yield**: 299 mg, 1.21 mmol, quantitative yield; **Appearance**: Pale yellow oil; **R_f**: 0.42 (2:8 EtOAc:hexanes); **^{1}H NMR** (500 MHz, $CDCl_3$): δ 9.85 (s, 1H), 6.26–6.17 (m, 2H), 4.17–4.04 (m, 2H), 3.14 (q, *J* = 4.9, 4.8 Hz, 1H), 2.93 (t, *J* = 6.3 Hz, 1H), 2.80–2.73 (m, 2H), 2.72–2.66 (m, 2H), 2.39 (dt, *J* = 5.5, 10.8 Hz, 1H), 2.32–2.25 (m, 1H), 2.05 (ddd, *J* = 5.2, 7.2, 13.1 Hz, 1H), 1.67 (d, *J* = 13.1 Hz, 1H), 1.24 (t, *J* = 7.1 Hz, 3H) ppm; **^{13}C NMR** (125 MHz, $CDCl_3$): δ 201.6, 174.0, 131.6, 131.3, 60.6, 51.3, 49.1, 41.9, 40.6, 38.4, 38.3, 35.4, 34.6, 34.0, 14.4 ppm; **IR**: 2961, 1731, 1700, 1205, 1185, 1038, 692 cm^{-1}; **HRMS** (ESI): calculated for $[C_{15}H_{18}O_3+H]^+$: 247.1329, found: 247.1306 (mass error: –9.1894).

Ethyl (1S,1aR,1a1R,5S,6aR,7R)-1-(hydroxy(phenyl)methyl)-1,1a,1a1,2,4a,5,6,6a-octahydro-2,5-methanocyclobuta[cd]indene-7-carboxylate (Phenyl alcohol tetracycle) (5.172)

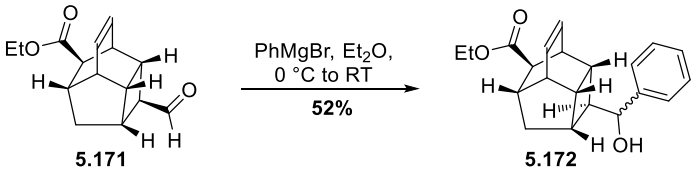

To a two-neck 10 mL round-bottom flask under nitrogen and equipped with a stir bar was added aldehyde ester tetracycle (92.2 mg, 0.374 mmol, 1.00 mol. equiv.) and diethyl ether (1.87 mL, 0.200 M). The solution was cooled to 0 °C and a solution of phenyl magnesium bromide (0.570 mL, 0.374 mmol, 0.657 M solution in diethyl ether) was added and the reaction allowed to warm to room temperature. The reaction was stirred at room temperature overnight by which time ^{1}H NMR analysis indicated the complete consumption of the starting material. The reaction mixture was diluted with diethyl ether and quenched with ammonium chloride. The mixture was then extracted with diethyl ether, washed with brine, dried over $MgSO_4$, filtered and concentrated under reduced pressure. Purification via flash column chromatography (SiO_2, eluting with 1:9 EtOAc:hexane) yielded separate phenyl alcohol tetracycle diastereomer A and B (inconsequential 1:1 diastereomeric ratio). **Yield**: 63.6 mg, 0.195 mmol, 52%; **Appearance**: Pale yellow oil

Diastereomer A

R_f: 0.24 (1:4 EtOAc: hexanes); **^{1}H NMR** (500 MHz, $CDCl_3$): δ 7.39–7.33 (m, 4H), 7.32–7.27 (m, 1H), 6.24–6.18 (m, 2H), 4.68 (d, *J* = 8.6 Hz, 1H), 4.14–4.02 (m, 2H), 3.11 (q, *J* = 4.7, 4.9 Hz, 1H), 2.82 (d, *J* = 3.8 Hz, 1H), 2.69 (q, *J* = 5.5, 5.6 Hz, 1H), 2.59 (t, *J* = 5.3 Hz, 1H), 2.36 (dt, *J* = 5.6, 10.0 Hz, 1H), 2.29 (t, *J* = 6.3 Hz, 1H), 2.16–2.09 (m, 2H), 1.91 (br s, 1H), 1.83 (ddd, *J* = 5.7, 7.6, 13.0 Hz, 1H), 1.44 (d, *J* = 12.9 Hz, 1H), 1.23 (t, *J* = 7.0 Hz, 3H) ppm; **^{13}C NMR** (150 MHz, $CDCl_3$): δ 174.7, 143.1, 131.9, 131.4, 128.6, 127.9, 126.9, 77.7, 60.4, 49.1, 46.5, 42.0, 40.2, 38.4, 38.4, 37.3, 36.6, 35.2, 14.4 ppm; **IR**: 3451, 3045, 2958, 2929, 1728, 1208, 1181, 1042, 700 cm^{-1}; **HRMS** (ESI): calculated for $[C_{21}H_{24}O_3+H]^+$: 325.1798, found: 325.1800.

Diastereomer B

R_f: 0.21 (1:4 EtOAc:hexanes); **^{1}H NMR** (600 MHz, $CDCl_3$): δ 7.37–7.33 (m, 4H), 7.32–7.28 (m, 1H), 6.21–6.16 (m, 1H), 6.10–6.05 (m, 1H), 4.67 (d, *J* = 9.2 Hz, 1H), 4.13–3.99 (m, 2H), 2.80–2.70 (m, 4H), 2.64 (t, *J* = 5.2 Hz, 1H), 2.37 (dt, *J* = 5.5, 10.3 Hz, 1H), 2.11 (dt, *J* = 2.1, 9.3 Hz, 1H), 2.02 (ddd, *J* = 5.5, 7.6, 13.0 Hz, 1H), 1.88 (br s, 1H), 1.69–1.62 (m, 2H), 1.20 (t, *J* = 7.1 Hz, 3H) ppm; **^{13}C NMR** (150 MHz, $CDCl_3$): δ 174.6, 142.8, 131.8, 131.4, 128.6, 128.0, 127.0, 78.2, 60.4, 49.2, 46.5, 42.0, 40.1, 38.7, 38.5, 37.9, 36.2, 34.6, 14.4 ppm; **IR**: 3454, 3045, 2959, 2928, 1731, 1208, 1179, 1040, 700 cm^{-1}; **HRMS** (ESI): calculated for $[C_{21}H_{24}O_3+H]^+$: 325.1798, found: 325.1803.

Kingianic acid B ethyl ester (7.11)

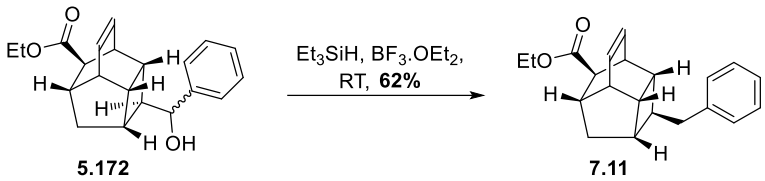

5.172 7.11

To a 5 mL vial under nitrogen and equipped with a stir bar was added phenyl alcohol tetracycle (28.5 mg, 0.088 mmol, 1.00 mol. equiv.) and dry dichloromethane (0.420 mL, 0.210 M). To the solution was added triethylsilane (28.1 µL, 0.176 mmol, 2.00 mol. equiv.) and then boron trifluoride diethyl etherate (16.7 µL, 0.176 mmol, 2.00 mol. equiv.). The reaction was stirred at room temperature for 1 hour by which time ^{1}H NMR analysis indicated the complete consumption of the starting material. The reaction mixture was diluted with dichloromethane and quenched with a saturate aqueous ammonium chloride solution. The organic layer was dried over $MgSO_4$, filtered and concentrated under reduced pressure. The crude product was purified via flash column chromatography (SiO_2, eluting with 1:19 EtOAc:hexane) yielding pure kingianic acid B ethyl ester. **Yield**: 16.7 mg, 0.054 mmol, 62%; **Appearance**: Pale yellow oil; $\mathbf{R_f}$: 0.36 (1:19 EtOAc:hexanes); **^{1}H NMR** (500 MHz, $CDCl_3$): δ 7.29 (t, *J* = 7.5 Hz, 2H), 7.20 (t, *J* = 7.3 Hz, 1H), 7.17 (d, *J* = 7.7 Hz, 2H), 6.21 (t, *J* = 7.4 Hz, 1H), 6.15 (t, *J* = 7.2 Hz, 1H), 4.15–4.01 (m, 2H), 2.97 (q, *J* = 4.8, 4.9 Hz, 1H), 2.91–2.77 (m, 2H), 2.81 (s, 1H), 2.71 (q, *J* = 5.6, 5.6 Hz, 1H), 2.61 (t, *J* = 4.7 Hz, 1H), 2.43 (dt, *J* = 10.1, 5.6 Hz, 1H), 2.37 (t, *J* = 7.1 Hz, 1H), 2.08 (t, *J* = 8.1 Hz, 1H), 1.90 (ddd, *J* = 13.0, 7.5, 5.5 Hz, 1H), 1.79–1.73 (m, 1H), 1.56 (d, *J* = 12.7 Hz, 1H), 1.22 (t, *J* = 7.1 Hz, 3H) ppm; **^{13}C NMR** (125 MHz, $CDCl_3$): δ 174.7, 141.1, 132.0, 131.4, 128.9, 128.4, 126.0, 60.4, 49.3, 42.2, 42.1, 40.4, 40.1, 39.9, 39.1, 38.6, 38.5, 35.1, 14.4 ppm; **IR**: 2956, 2925, 1731, 1460, 1453, 1366, 1298, 1202, 1175, 1040, 743, 696 cm^{-1}; **HRMS** (ESI): calculated for $[C_{21}H_{24}O_2+H]^+$: 309.1849, found: 309.1852.

Kingianic acid B (5.173)

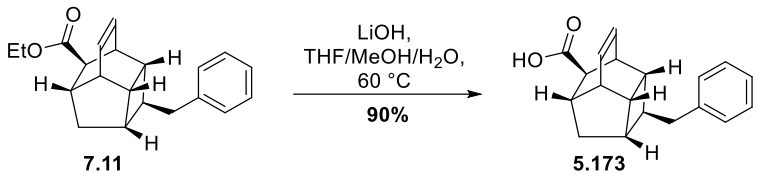

To a 5 mL vial open to air and equipped with a stir bar was added kingianic ester B (10.6 mg, 34.4 µmol, 1.00 mol. equiv.), tetrahydrofuran (0.115 mL, 0.300 M), methanol (0.115 mL, 0.300 M), water (0.115 mL, 0.300 M) and lithium hydroxide (8.23 mg, 0.344 mmol, 10.0 mol. equiv.). The reaction was heated to 60 °C for 3 hours by which time ^{1}H NMR analysis indicated the complete consumption of the starting material. The reaction was acidified with 1M aqueous HCl solution, extracted with diethyl ether, dried over $MgSO_4$, filtered, and concentrated under reduced pressure. The crude product was purified via flash column chromatography (SiO_2, eluting with 1:9 EtOAc:hexane → 1:4 EtOAc:hexane) yielding pure kingianic acid B. **Yield**: 8.70 mg, 31.8 µmol, 90%; **Appearance**: Pale yellow oil; $\mathbf{R_f}$: 0.30 (1:4 EtOAc:hexanes); **^{1}H NMR** (600 MHz, $CDCl_3$): δ 7.29 (t, *J* = 7.5 Hz, 2H), 7.19 (t, *J* = 7.4 Hz, 1H), 7.16 (d, *J* = 7.5 Hz, 2H), 6.25–6.19 (m, 2H), 3.00–2.96 (m, 1H), 2.90–2.78 (m, 2H), 2.87 (d, *J* = 3.7 Hz, 1H), 2.74–2.69 (m, 1H), 2.56 (t, *J* = 5.3 Hz, 1H), 2.44 (dt, *J* = 9.7, 5.6 Hz, 1H), 2.37 (t, *J* = 6.8 Hz, 1H), 2.07 (t, *J* = 8.2 Hz, 1H), 1.90 (ddd, *J* = 12.9, 7.6, 5.5 Hz, 1H), 1.79–1.74 (m, 1H), 1.55 (d, *J* = 12.9 Hz, 1H) ppm; **^{13}C NMR** (150 MHz, $CDCl_3$): δ 180.4, 141.0, 132.1, 131.4, 128.8, 128.4, 126.0, 49.1, 42.1, 42.0, 40.4, 40.0, 39.8, 39.0, 38.6, 38.4, 34.9 ppm; **IR**: 3026, 2956, 2924, 2855, 1697, 1496, 1453, 1412, 1298, 1239, 743, 693 cm^{-1}; **HRMS** (ESI): calculated for $[C_{19}H_{20}O_2+H]^+$: 281.1536, found: 281.1542.

NMR comparison table for kingianic acid B (5.173)

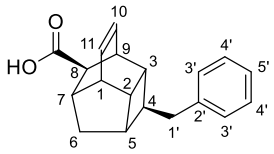

	Kingianic acid B (4.173)			
	Synthetic natural product		Isolated natural product[12]	
Position	^{1}H (600 MHz) NMR, $CDCl_3$	^{13}C (150 MHz) NMR, $CDCl_3$	^{1}H (600 MHz) NMR, $CDCl_3$	^{13}C (150 MHz) NMR, $CDCl_3$
1	2.74–2.69 (m, 1H)	42.0	2.72 (dd, *J* = 1.62, 5.1 Hz, 1H)	41.8
2	2.44 (dt, *J* = 9.7, 5.6 Hz, 1H)	39.8	2.44 (dt, *J* = 9.3, 3.7 Hz, 1H)	39.7
3	1.76 (m, 1H)	39.0	1.76 (m, 1H)	38.9
4	2.07 (t, *J* = 8.2 Hz, 1H)	40.4	2.07 (t, *J* = 8.0 Hz, 1H)	40.2
5	2.37 (t, *J* = 6.8 Hz, 1H)	40.0	2.37 (t, *J* = 6.0 Hz, 1H)	39.9
6	1.90 (ddd, *J* = 12.9, 7.6, 5.5 Hz, 1H), 1.55 (d, *J* = 12.9 Hz, 1H)	38.6	1.90 (ddd, *J* = 13.0, 7.4, 5.4 Hz, 1H), 1.54 (d, *J* = 12.8 Hz, 1H)	38.4
7	2.56 (t, *J* = 5.3 Hz, 1H)	38.4	2.56 (t, *J* = 4.9 Hz, 1H)	38.3
8	2.87 (d, *J* = 3.7 Hz, 1H)	49.1	2.87 (d, *J* = 2.6 Hz, 1H)	48.8
9	3.00–2.96 (m, 1H)	34.9	2.98 (m, 1H)	34.8
10	6.25–6.19 (m, 1H)	131.4	6.22 (m, 1H)	131.3
11	6.25–6.19 (m, 1H)	132.1	6.22 (m, 1H)	132.0
1’	2.90–2.78 (m, 2H)	42.1	2.83 (m, 1H), 2.86 (m, 1H)	41.9
2’	-	141.0	-	140.9
3’	7.16 (d, *J* = 7.5 Hz, 2H)	128.9	7.15 (d, *J* = 7.1 Hz, 2H)	128.7, 128.6
4’	7.29 (t, *J* = 7.5 Hz, 2H)	128.4	7.28 (t, *J* = 7.6 Hz, 2H)	128.3, 128.4
5’	7.19 (t, *J* = 7.4 Hz, 1H)	126.0	7.19 (t, *J* = 7.3 Hz, 1H)	125.8
C=O	-	180.4	-	179.4

Ethyl (1aR,1a1R,5S,6aR,7R)-1-(benzo[d][1,3]dioxol-5-yl(hydroxy)methyl)-1,1a,1a1,2,4a,5,6,6a-octahydro-2,5-methanocyclobuta[cd]indene-7-carboxylate (1,3-Benzodioxole alcohol tetracycle) (7.12)

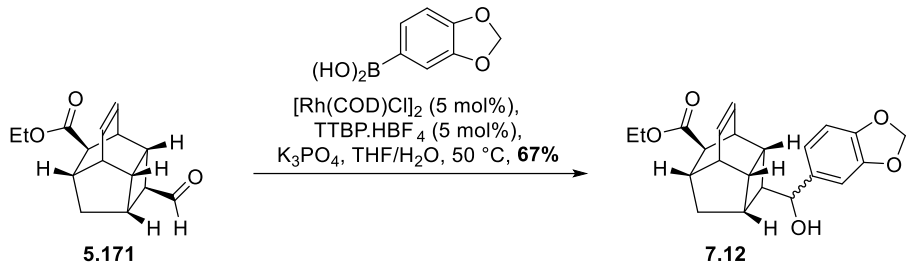

To an oven-dried 10 mL sealed reaction tube under nitrogen and equipped with a stir bar was added chloro(1,5-cyclooctadiene)rhodium(I) dimer (5.39 mg, 10.9 µmol, 5.00 mol%), Tri-tert-butylphosphonium tetrafluoroborate (3.17 mg, 10.9 µmol, 5.00 mol%), 3,4-methylenedioxyphenylboronic acid (72.5 mg, 0.437 mmol, 2.00 mol. equiv.), a solution of aldehyde ester tetracycle (53.8 mg, 0.218 mmol, 1.00 mol. equiv.) in degassed THF (0.440 mL, 0.500 M) and a degassed aqueous solution of K_3PO_4 (0.131 mL, 0.655 mmol, 5.00 M). The reaction mixture was heated to 50 °C overnight by which time ^{1}H NMR analysis indicated the complete consumption of the starting material. The reaction mixture was diluted with dichloromethane and quenched with ammonium chloride. The mixture was then washed with brine, dried over $MgSO_4$, filtered and concentrated under reduced pressure. Purification via flash column chromatography (SiO_2, eluting with 1:9 EtOAc:hexane → 1:4 EtOAc:hexane) yielded separate 1,3-benzodioxole alcohol tetracycle diastereomer A and B (inconsequential 1:1 diastereomeric ratio). **Yield**: 54.0 mg, 0.146 mmol, 67%; **Appearance**: Yellow oil

Diastereomer A

R_f: 0.25 (1:4 EtOAc:hexanes); **^{1}H NMR** (600 MHz, $CDCl_3$): δ 6.85 (s, 1H), 6.82–6.75 (m, 2H), 6.24–6.17 (m, 2H), 5.96 (s, 2H), 4.59 (d, *J* = 8.9 Hz, 1H), 4.14–4.02 (m, 2H), 3.15–3.09 (m, 1H), 2.82 (d, *J* = 3.8 Hz, 1H), 2.68 (q, *J* = 5.3, 5.3 Hz, 1H), 2.59 (t, *J* = 5.2 Hz, 1H), 2.35 (dt, *J* = 5.6, 9.7 Hz, 1H), 2.24 (t, *J* = 6.3 Hz, 1H), 2.12–2.07 (m, 1H), 2.04 (d, *J* = 9.0 Hz, 1H), 1.85 (br s, 1H), 1.83 (ddd, *J* = 5.4, 7.6, 13.0 Hz, 1H), 1.45 (d, *J* = 12.8 Hz, 1H), 1.23 (t, *J* = 7.1 Hz, 3H) ppm; **^{13}C NMR** (150 MHz, $CDCl_3$): δ 174.6, 148.0, 147.3, 137.2, 131.9, 131.5, 120.5, 108.2, 107.1, 101.2, 77.6, 60.4, 49.1, 46.6, 42.0, 40.2, 38.4 (two coincident peaks), 37.3, 36.7, 35.2, 14.4 ppm; **IR**: 3413, 2931, 1724, 1713, 1503, 1487, 1442, 1242, 1208, 1181, 1038, 936, 809, 696 cm^{-1}; **HRMS** (ESI): calculated for $[C_{22}H_{24}O_5+H]^+$: 369.1696, found: 369.1703.

Diastereomer B

R_f: 0.19 (1:4 EtOAc:hexanes); **^{1}H NMR** (600 MHz, $CDCl_3$): δ 6.85 (s, 1H), 6.80–6.74 (m, 2H), 6.20–6.15 (m, 1H), 6.10–6.05 (m, 1H), 5.96 9s, 2H), 4.57 (d, *J* = 9.3 Hz, 1H), 4.14–3.99 (m, 2H), 2.82–2.75 (m, 2H), 2.75–2.67 (m, 2H), 2.63 (t, *J* = 4.9 Hz, 1H), 2.36 (dt, *J* = 5.5, 10.4 Hz, 1H), 2.06–1.98 (m, 2H), 1.91 (br s, 1H), 1.66 (d, *J* = 12.9 Hz, 1H), 1.63–1.58 (m, 1H), 1.21 (t, *J* = 7.2 Hz, 3H) ppm; **^{13}C NMR** (150 MHz, $CDCl_3$): δ 174.6, 147.9, 147.3, 136.9, 131.8, 131.4, 120.6, 108.1, 107.1, 101.2, 78.1, 60.5, 49.2, 46.6, 41.9, 40.1, 38.7, 38.5, 38.1, 36.3, 34.5, 14.4 ppm; **IR**: 3461, 2925, 1727, 1717, 1553, 1486, 1442, 1244, 1208, 1179, 1040, 937, 810, 732, 692 cm^{-1}; **HRMS** (ESI): calculated for $[C_{22}H_{24}O_5+H]^+$: 369.1696, found: 369.1696.

Kingianic acid A ethyl ester (5.174)

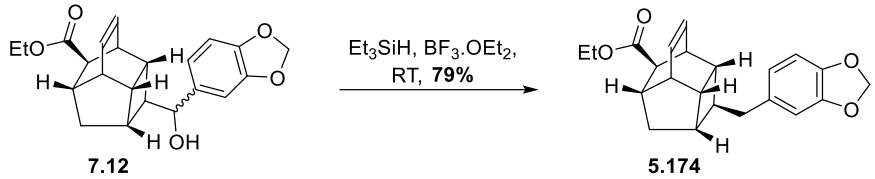

7.12 5.174

To a 5 mL vial under nitrogen and equipped with a stir bar was added 1,3-benzodioxole alcohol tetracycle (37.6 mg, 0.102 mmol, 1.00 mol. equiv.) and dry dichloromethane (0.490 mL, 0.210 M). To the solution was added triethylsilane (32.6 µL, 0.204 mmol, 2.00 mol. equiv.) and then boron trifluoride diethyl etherate (14.6 µL, 0.153 mmol, 1.50 mol. equiv.). The reaction was stirred at room temperature for 5 minutes by which time ^{1}H NMR analysis indicated the complete consumption of the starting material. The reaction mixture was diluted with dichloromethane and quenched with a saturate aqueous ammonium chloride solution. The organic layer was dried over $MgSO_4$, filtered and concentrated under reduced pressure to yield pure kingianic acid A ethyl ester. Spectroscopic data matched those previously reported in the literature.[14] **Yield**: 28.3 mg, 0.080 mmol, 79%; **Appearance**: Pale yellow oil; **R_f**: 0.38 (1:9 EtOAc:hexanes); **^{1}H NMR** (600 MHz, $CDCl_3$): δ 6.73 (d, J = 7.8 Hz, 1H), 6.66 (s, 1H), 6.61 (d, J = 7.4 Hz, 1H), 6.23–6.18 (m, 1H), 6.17–6.12 (m, 1H), 5.93 (s, 2H), 4.15 – 4.02 (m, 2H), 2.96 (q, J = 5.0, 4.8 Hz, 1H), 2.82–2.75 (m, 2H), 2.74–2.67 (m, 2H), 2.60 (t, J = 4.8 Hz, 1H), 2.41 (dt, J = 5.9, 10.2 Hz, 1H), 2.33 (t, J = 6.3 Hz, 1H), 1.99 (t, J = 8.1 Hz, 1H), 1.90 (dt, J = 6.4, 12.9 Hz, 1H), 1.75 – 1.70 (m, 1H), 1.54 (d, J = 12.1 Hz, 1H), 1.22 (t, J = 7.2 Hz, 3H).

Kingianic acid A (5.21)

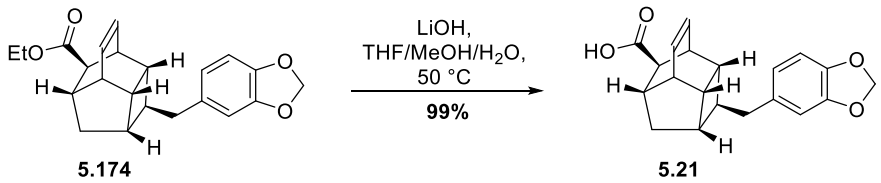

To a 5 mL vial open to air and equipped with a stir bar was added kingianic ester A (28.3 mg, 80.3 µmol, 1.00 mol. equiv.), tetrahydrofuran (0.270 mL, 0.300 M), methanol (0.270 mL, 0.300 M), water (0.270 mL, 0.300 M) and lithium hydroxide (19.23 mg, 0.803 mmol, 10.0 mol. equiv.). The reaction was heated to 50 °C overnight by which time ^{1}H NMR analysis indicated the complete consumption of the starting material. The reaction was acidified with 1M aqueous HCl solution, extracted with dichloromethane, dried over $MgSO_4$, filtered, and concentrated under reduced pressure to yield pure kingianic acid A. **Yield**: 25.9 mg, 79.8 µmol, 99%; **Appearance**: Pale yellow oil; $\mathbf{R_f}$: 0.24 (1:3 EtOAc:hexanes); **^{1}H NMR** (600 MHz, $CDCl_3$): δ 6.73 (d, *J* = 7.9 Hz, 1H), 6.65 (s, 1H), 6.60 (d, *J* = 7.9 Hz, 1H), 6.25–6.19 (m, 2H), 5.93 (s, 2H), 3.00–2.95 (m, 1H), 2.86 (d, *J* = 3.7 Hz, 1H), 2.80–2.69 (m, 2H), 2.73–2.70 (m, 1H), 2.56 (t, *J* = 5.3 Hz, 1H), 2.42 (dt, *J* = 9.8, 5.7 Hz, 1H), 2.34 (t, *J* = 6.4 Hz, 1H), 1.99 (t, *J* = 8.2 Hz, 1H), 1.90 (dt, *J* = 13.0, 6.6 Hz, 1H), 1.73 (m, 1H), 1.55 (d, *J* = 12.9 Hz, 1H) ppm; **^{13}C NMR** (150 MHz, $CDCl_3$): δ 179.3, 147.7, 145.8, 134.9, 132.1, 131.5, 121.6, 109.2, 108.2, 100.9, 48.9, 42.0, 41.8, 40.7, 39.9, 39.8, 38.9, 38.6, 38.4, 34.9 ppm; **IR**: 2951, 2921, 1701, 1503, 1489, 1443, 1244, 1040, 938, 926, 692 cm^{-1}; **HRMS** (ESI): calculated for $[C_{20}H_{20}O_2+H]^+$: 325.1434, found: 325.1435.

NMR comparison table for kingianic acid A (5.21)

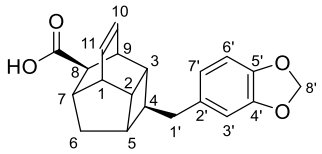

	Kingianic acid A (4.21)			
	Synthetic natural product		Isolated natural product[12]	
Position	**^{1}H (600 MHz) NMR, $CDCl_3$**	**^{13}C (150 MHz) NMR, $CDCl_3$**	**^{1}H (600 MHz) NMR, $CDCl_3$**	**^{13}C (150 MHz) NMR, $CDCl_3$**
1	2.73–2.70 (m, 1H)	42.0	2.71 (m, 1H)	41.8
2	2.42 (dt, *J* = 9.8, 5.7 Hz, 1H)	39.8	2.42 (dt, *J* = 8.5, 5.5 Hz, 1H)	39.7
3	1.76–1.71 (m, 1H)	38.9	1.73 (m, 1H)	38.8
4	1.99 (t, *J* = 8.2 Hz, 1H)	40.7	2.00 (t, *J* = 8.5 Hz, 1H)	40.6
5	2.34 (t, *J* = 6.4 Hz, 1H)	39.9	2.34 (t, *J* = 6.5 Hz, 1H)	39.8
6	1.90 (dt, *J* = 13.0, 6.6 Hz, 1H), 1.55 (d, *J* = 12.9 Hz, 1H)	38.6	1.90 (ddd, *J* = 13.0, 7.5, 5.5 Hz, 1H), 1.55 (d, *J* = 13.0 Hz, 1H)	38.5
7	2.56 (t, *J* = 5.3 Hz, 1H)	38.4	2.57 (t, *J* = 5.0 Hz, 1H)	38.3
8	2.86 (d, *J* = 3.7 Hz, 1H)	48.9	2.86 (d, *J* = 3.5 Hz, 1H)	48.8
9	3.00–2.95 (m, 1H)	34.9	2.98 (dt, *J* = 7.0, 4.0 Hz, 1H)	34.8
10	6.25–6.19 (m, 1H)	131.5	6.22 (t, *J* = 4.0 Hz, 1H)	131.3
11	6.25–6.19 (m, 1H)	132.1	6.22 (t, *J* = 4.0 Hz, 1H)	132.0
1’	2.80–2.69 (m, 2H)	41.8	2.72 (m, 1H), 2.78 (m, 1H)	41.7
2’	-	134.9	-	134.7
3’	6.65 (s, 1H)	109.2	6.66 (s, 1H)	109.1
4’		147.7	-	147.5
5’		145.8	-	145.7
6’	6.73 (d, *J* = 7.9 Hz, 1H)	108.2	6.72 (d, *J* = 8.0 Hz, 1H)	108.1
7’	6.60 (d, *J* = 7.9 Hz, 1H)	121.6	6.60 (d, *J* = 8.0 Hz, 1H)	121.5
8’	5.93 (s, 2H)	100.9	5.92 (s, 2H)	100.8
C=O	-	179.3	-	179.3

Ethyl (1aR,1a1R,5S,6aR,7R)-1-(1-hydroxy-3-phenylallyl)-1,1a,1a1,2,4a,5,6,6a-octahydro-2,5-methanocyclobuta[cd]indene-7-carboxylate (Styrenyl alcohol tetracycle) (5.175)

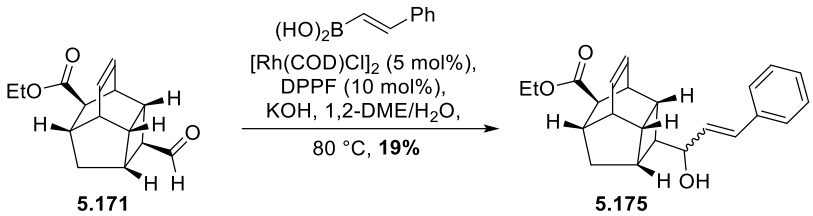

5.171 5.175

To an oven-dried 10 mL sealed reaction tube under nitrogen and equipped with a stir bar was added chloro(1,5-cyclooctadiene)rhodium(I) dimer (5.07 mg, 10.3 μmol, 5.00 mol%), 1,1′-bis(diphenylphosphino)ferrocene (11.4 mg, 20.6 μmol, 10.0 mol%), *trans*-2-phenylvinylboronic acid (60.9 mg, 0.412 mmol, 2.00 mol. equiv.), potassium hydroxide (11.6 mg, 0.206 mmol, 1.00 mol. equiv.), a solution of aldehyde ester tetracycle (50.7 mg, 0.206 mmol, 1.00 mol. equiv.) in degassed dimethoxyethane (0.883 mL, 0.233 M) and degassed distilled water (0.146 mL, 1.41 M). The reaction mixture was heated to 80 °C overnight by which time ^{1}H NMR analysis indicated the complete consumption of the starting material. The reaction mixture was diluted with dichloromethane and quenched with ammonium chloride. The mixture was then extracted with dichloromethane, dried over $MgSO_4$, filtered and concentrated under reduced pressure. Purification via flash column chromatography (SiO_2, eluting with 1:9 EtOAc:hexane → 1:4 EtOAc:hexane) yielded separate styrenyl alcohol tetracycle diastereomer A and B (inconsequential 1:1 diastereomeric ratio). **Yield**: 13.5 mg, 0.038 mmol, 19%; **Appearance**: Orange oil

Diastereomer A

R_f: 0.28 (1:4 EtOAc:hexanes); **^{1}H NMR** (500 MHz, $CDCl_3$): δ 7.40 (d, *J* = 7.5 Hz, 2H), 7.32 (t, *J* = 7.5 Hz, 2H), 7.27–7.22 (m, 1H), 6.63 (d, *J* = 15.8 Hz, 1H), 6.27–6.17 (m, 3H), 4.33 (t, *J* = 7.7 Hz, 1H), 4.16 – 4.02 (m, 2H), 3.14–3.07 (m, 1H), 2.83 (s, 1H), 2.71 (q, *J* = 5.9, 5.1 Hz, 1H), 2.64 (t, *J* = 5.3 Hz, 1H), 2.48–2.42 (m, 1H), 2.35 (q, *J* = 5.8, 6.3 Hz, 1H), 2.05–2.00 (m, 1H), 1.98–1.89 (m, 2H), 1.65 (br s, 1H) 1.58 (d, *J* = 12.1 Hz, 1H), 1.23 (t, *J* = 6.9 Hz, 3H) ppm; **^{13}C NMR** (125 MHz, $CDCl_3$): δ 174.6, 136.8, 131.8, 131.5, 131.4, 130.4, 128.7, 127.9, 126.6, 75.9, 60.4, 49.1, 45.3, 42.0, 40.7, 38.5, 37.1, 36.1, 35.1, 14.4 ppm; **IR**: 3440, 2956, 2928, 1731, 1495, 1449, 1366, 1298, 1208, 1181, 1040, 967, 750, 693 cm^{-1}; **HRMS** (ESI): calculated for $[C_{23}H_{26}O_3+H]^+$: 351.1955, found: 351.1959.

Diastereomer B

R_f: 0.24 (1:4 EtOAc:hexanes); **^{1}H NMR** (500 MHz, $CDCl_3$): δ 7.40 (d, *J* = 7.5 Hz, 2H), 7.33 (t, *J* = 7.5 Hz, 2H), 7.27–7.23 (m, 1H), 6.62 (d, *J* = 16.0 Hz, 1H), 6.25–6.12 (m, 3H), 4.32 (t, *J* = 8.0 Hz, 1H), 4.16 – 4.02 (m, 2H), 3.04–2.99 (m, 1H), 2.81 (s, 1H), 2.77–2.70 (m, 1H), 2.67–2.61 (m, 2H), 2.40–2.34 (m, 1H), 2.06–1.98 (m, 1H), 1.91 (d, *J* = 7.9 Hz, 1H), 1.82 (m, 1H), 1.68 (br s, 1H) 1.63 (d, *J* = 13.5 Hz, 1H), 1.23 (t, *J* = 7.2 Hz, 3H) ppm; **^{13}C NMR** (125 MHz, $CDCl_3$): δ 174.6, 136.8, 131.8, 131.7, 131.5, 130.1, 128.7, 127.9, 126.6, 76.3, 60.4, 49.2, 45.4, 42.0, 40.5, 38.6, 38.4, 37.3, 36.1, 34.8, 14.4 ppm; **IR**: 3451, 2956, 2928, 1728, 1449, 1366, 1305, 1298, 1208, 1181, 1041, 967, 750, 693 cm^{-1}; **HRMS** (ESI): calculated for $[C_{23}H_{26}O_3+H]^+$: 351.1955, found: 351.1956.

Kingianic acid D ethyl ester (7.13)

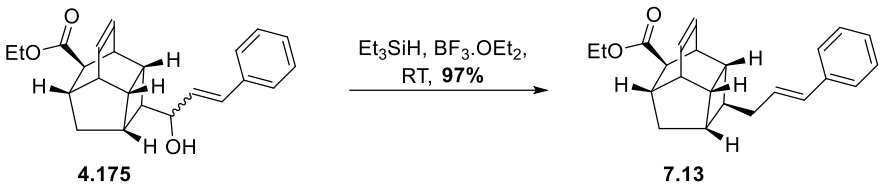

4.175 7.13

To a 5 mL vial under nitrogen and equipped with a stir bar was added styrenyl alcohol tetracycle (13.5 mg, 38.5 µmol, 1.00 mol. equiv.) and dry dichloromethane (0.183 mL, 0.210 M). To the solution was added triethylsilane (12.3 µL, 77.0 µmol, 2.00 mol. equiv.) and then boron trifluoride diethyl etherate (5.50 µL, 57.8 µmol, 1.50 mol. equiv.). Immediate ^{1}H NMR analysis indicated the complete consumption of the starting material. The reaction mixture was diluted with dichloromethane and quenched with a saturate aqueous ammonium chloride solution. The organic layer was dried over $MgSO_4$, filtered and concentrated under reduced pressure to yield pure kingianic acid D ethyl ester. **Yield**: 12.5 mg, 37.4 µmol, 97%; **Appearance**: Yellow oil; **R_f**: 0.46 (1:9 EtOAc:hexanes); **^{1}H NMR** (500 MHz, $CDCl_3$): δ 7.35 (d, J = 7.7 Hz, 2H), 7.30 (t, J = 7.5 Hz, 2H), 7.20 (t, J = 7.4 Hz, 1H), 6.40 (d, J = 15.9 Hz, 1H), 6.24–6.15 (m, 3H), 4.16 – 4.02 (m, 2H), 3.04 (q, J = 4.9, 4.9 Hz, 1H), 2.83 (d, *J* = 3.8 Hz, 1H), 2.71 (q, *J* = 5.5, 5.6 Hz, 1H), 2.62 (t, J = 5.3 Hz, 1H), 2.49–2.32 (m, 4H), 1.96–1.85 (m, 2H), 1.78 – 1.72 (m, 1H), 1.59 (d, J = 12.8 Hz, 1H), 1.23 (t, J = 7.1 Hz, 3H) ppm. **^{13}C NMR** (125 MHz, $CDCl_3$): δ 174.8, 137.9, 131.9, 131.4, 131.1, 128.9, 128.6, 127.1, 126.1, 60.4, 49.3, 42.1, 40.2, 40.1, 39.6, 39.1, 38.6, 38.5, 35.1, 14.4 ppm; **IR**: 2956, 2926, 1731, 1495, 1449, 1265, 1298, 1205, 1178, 1042, 964, 743, 692 cm^{-1}; **HRMS** (ESI): calculated for $[C_{23}H_{26}O_2+H]^+$: 335.2006, found: 335.2016.

Kingianic acid D (5.176)

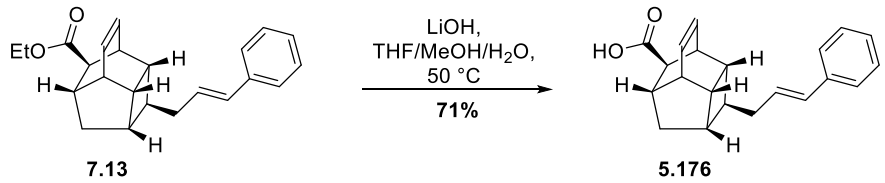

To a 5 mL vial open to air and equipped with a stir bar was added kingianic ester D (10.9 mg, 32.6 µmol, 1.00 mol. equiv.), tetrahydrofuran (0.110 mL, 0.300 M), methanol (0.110 mL, 0.300 M), water (0.110 mL, 0.300 M) and lithium hydroxide (7.80 mg, 0.326 mmol, 10.0 mol. equiv.). The reaction was at 50 °C overnight by which time ^{1}H NMR analysis indicated the complete consumption of the starting material. The reaction was acidified with 1M aqueous HCl solution, extracted with ethyl acetate, dried over $MgSO_4$, filtered, and concentrated under reduced pressure. Purification via flash column chromatography (SiO_2, eluting with 1:4 EtOAc:hexane) yielded pure kingianic acid D. **Yield**: 7.1 mg, 23.1 µmol, 71%; **Appearance**: Yellow oil; **R_f**: 0.37 (3:7 EtOAc:hexanes); **^{1}H NMR** (500 MHz, $CDCl_3$): δ 7.35 (d, *J* = 6.9 Hz, 2H), 7.30 (t, *J* = 7.5 Hz, 2H), 7.20 (t, *J* = 7.5 Hz, 1H), 6.40 (d, *J* = 15.8 Hz, 1H), 6.27–6.16 (m, 3H), 3.06 (t, *J* = 4.0 Hz, 1H), 2.89 (d, *J* = 3.7 Hz, 1H), 2.75–2.69 (m, 1H), 2.58 (t, *J* = 5.2 Hz, 1H), 2.50–2.38 (m, 3H), 2.36 (t, *J* = 7.1 Hz, 1H), 1.98–1.90 (m, 1H), 1.87 (t, *J* = 7.5 Hz, 1H), 1.79–1.73 (m, 1H), 1.59 (d, *J* = 12.8 Hz, 1H) ppm; **^{13}C NMR** (125 MHz, $CDCl_3$): δ 180.6, 137.9, 132.1, 131.5, 131.1, 128.8, 128.7, 127.1, 126.1, 49.1, 42.0, 40.1, 40.0, 39.6, 39.1, 39.0, 38.6, 38.4, 34.9 ppm; **IR**: 2955, 2924, 1697, 1412, 1306, 1249, 1238, 964, 908, 739, 690 cm^{-1}; **HRMS** (ESI): calculated for $[C_{21}H_{22}O_2+H]^+$: 307.1693, found: 307.1692.

NMR comparison table for kingianic acid D (5.176)

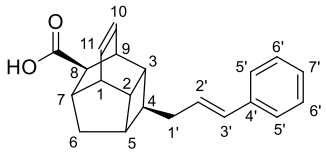

	Kingianic acid D (4.176)			
	Synthetic natural product		Isolated natural product[12]	
Position	**^{1}H (500 MHz) NMR, $CDCl_3$**	**^{13}C (125 MHz) NMR, $CDCl_3$**	**^{1}H (600 MHz) NMR, $CDCl_3$**	**^{13}C (150 MHz) NMR, $CDCl_3$**
1	2.75–2.69 (m, 1H)	42.0	2.73 (m, 1H)	41.9
2	2.50–2.38 (m, 1H)	40.0	2.40 (m, 1H)	39.8
3	1.79–1.73 (m, 1H)	39.1	1.76 (m, 1H)	39.0
4	1.87 (t, *J* = 7.5 Hz, 1H)	39.0	1.88 (t, *J* = 7.4 Hz, 1H)	38.9
5	2.36 (t, *J* = 7.1 Hz, 1H)	40.1	2.36 (t, *J* = 7.4 Hz, 1H)	39.9
6	1.98–1.90 (m, 1H), 1.59 (d, *J* = 12.8 Hz, 1H)	38.6	1.93 (m, 1H), 1.61 (d, *J* = 12.7 Hz, 1H)	38.4
7	2.58 (t, *J* = 5.2 Hz, 1H)	38.4	2.58 (t, *J* = 5.1 Hz, 1H)	38.3
8	2.89 (d, *J* = 3.7 Hz, 1H)	49.1	2.90 (d, *J* = 3.8 Hz, 1H)	48.6
9	3.06 (t, *J* = 4.0 Hz, 1H)	34.9	3.06 (t, *J* = 3.8 Hz, 1H)	34.8
10	6.27–6.16 (m, 1H)	131.5	6.22 (d, *J* = 3.1 Hz, 1H)	131.4
11	6.27–6.16 (m, 1H)	132.1	6.22 (d, *J* = 3.0 Hz, 1H)	131.9
1'	2.50–2.38 (m, 2H)	39.6	2.43 (m, 2H)	39.4
2'	6.27–6.16 (m, 1H)	128.6	6.19 (m, 1H)	128.7
3'	6.40 (d, *J* = 15.8 Hz, 1H)	131.1	6.38 (d, *J* = 15.8 Hz, 1H)	131.0
4'	-	137.9	-	137.7
5'	7.35 (d, *J* = 6.9 Hz, 2H)	126.1	7.35 (d, *J* = 7.2 Hz, 2H)	126.0
6'	7.30 (t, *J* = 7.5 Hz, 2H)	128.8	7.30 (t, *J* = 7.6 Hz, 2H)	128.5
7'	7.20 (t, *J* = 7.5 Hz, 1H)	127.1	7.20 (t, *J* = 7.3 Hz, 1H)	127.0
C=O	-	180.6	-	177.5

Kingianic acid A aldehyde (5.177)

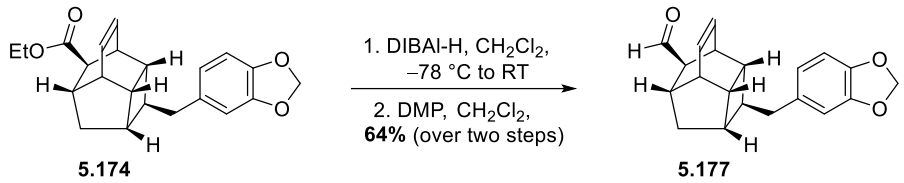

5.174 5.177

To a 10 mL round-bottom flask under nitrogen and equipped with a stir bar was added kingianic ethyl ester A (149.6 mg, 0.424 mmol, 1.00 mol. equiv.) and dry dichloromethane (2.12 mL, 0.200 M). The solution was cooled to −78 °C and diisobutylaluminium hydride (0.934 mL, 0.934 mmol, 2.20 mol. equiv., 1.00 M solution in cyclohexane) was added dropwise. The reaction was allowed to warm to room temperature over two hours by which time ^{1}H NMR analysis indicated completion of the reaction. The reaction mixture was diluted with diethyl ether, cooled to 0 °C and water (0.04 mL) was added dropwise followed by a 15% aqueous solution of sodium hydroxide (0.04 mL) and then water (0.09 mL) again. The mixture was allowed to warm to room temperature over fifteen minutes and then $MgSO_4$ was added, stirred for a further fifteen minutes, filtered, and concentrated under reduced pressure to yield the crude kingianic alcohol A (120 mg). A solution of the crude alcohol (120 mg, 0.387 mmol, 1.00 mol. equiv.) in dry dichloromethane (3.87 mL, 0.100 M) was cooled to 0 °C and Dess-Martin periodinane (0.246 g, 0.580 mmol, 1.50 mol. equiv.) was added. The reaction was allowed to stir at room temperature for one hour by which time ^{1}H NMR analysis indicated completion of the reaction. The reaction was quenched with a saturated aqueous solution of sodium bicarbonate, extracted with ethyl acetate, washed with water, brine, dried over $MgSO_4$, filtered, and concentrated under reduced pressure. The crude product was purified via flash column chromatography (SiO_2, eluting with 1:9 EtOAc:hexane) yielding pure kingianic acid A aldehyde. **Yield**: 83.9 mg, 0.272 mmol, 64% (over two steps); **Appearance**: Clear oil; $\mathbf{R_f}$: 0.39 (1:9 EtOAc:hexane); **^{1}H NMR** (500 MHz, $CDCl_3$): δ 9.48 (s, 1H), 6.73 (d, J = 7.8 Hz, 1H), 6.66 (s, 1H), 6.61 (d, J = 7.8 Hz, 1H), 6.26–6.21 (m, 1H), 6.20–6.16 (m, 1H), 5.93 (s, 2H), 2.98 (q, J = 5.0, 4.8 Hz, 1H), 2.84–2.67 (m, 5H), 2.45 (dt, J = 5.5, 9.9 Hz, 1H), 2.38 (t, J = 6.8 Hz, 1H), 2.02 (t, J = 8.2 Hz, 1H), 1.96–1.89 (m, 1H), 1.82–1.77 (m, 1H), 1.55 (d, J = 12.7 Hz, 1H) ppm; **^{13}C NMR** (125 MHz, ($CDCl_3$): δ 203.9, 147.7, 145.8, 134.8, 133.0, 131.9, 121.6, 109.1, 108.2, 100.9, 57.7, 42.7, 41.8, 40.8, 40.3, 39.8, 39.1, 38.5, 38.0, 33.7 ppm; **IR**: 2924, 1721, 1502, 1489, 1443, 1244, 1187, 1040, 938, 926, 807 cm^{-1}; **HRMS** (ESI): calculated for $[C_{20}H_{20}O_3+H]^+$: 309.1458, found: 309.1477.

Endiandric acid M ethyl ester (7.14)

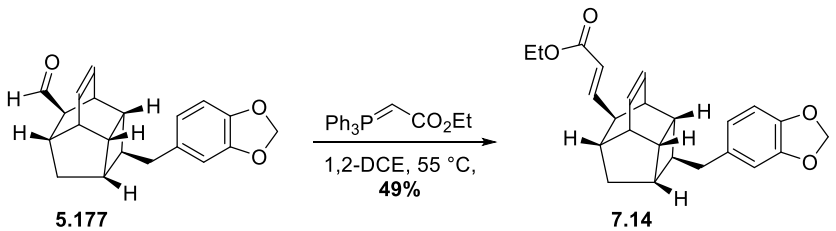

5.177 7.14

To a 10 mL round bottom flask under nitrogen was added kingianic aldehyde A (66.0 mg, 0.214 mmol, 1.00 mol. equiv.), dry 1,2-dichloroethane (1.10 mL, 0.200 M) and ethyl(triphenylphosphoranylidene)acetate (149 mg, 0.428 mmol, 2.00 mol. equiv.), The mixture was heated at 55 °C overnight by which time ^{1}H NMR analysis indicated completion of the reaction. The reaction mixture was concentrated under reduced pressure and purified via flash column chromatography (SiO_2, eluting with 1:9 EtOAc:hexane) yielding pure endiandric acid M ethyl ester. **Yield**: 39.8 mg, 0.105 mmol, 49%; **Appearance**: Clear oil; $\mathbf{R_f}$: 0.46 (1:9 EtOAc:hexane); **^{1}H NMR** (500 MHz, $CDCl_3$): δ 6.75 (dd, J = 8.1, 15.7 Hz, 1H), 6.72 (d, J =

8.0 Hz, 1H), 6.66 (s, 1H), 6.61 (d, *J* = 8.0 Hz 1H), 6.26–6.21 (m, 1H), 6.20–6.14 (m, 1H), 5.92 (s, 2H), 5.68 (d, *J* = 15.7 Hz, 1H), 4.16 (q, *J* = 7.1, 7.1 Hz, 2H), 2.81–2.65 (m, 4H), 2.52 (dt, *J* = 4.2, 5.6 Hz, 1H), 2.43 (dt, *J* = 5.4, 8.7 Hz, 1H), 2.34 (t, *J* = 5.9 Hz, 1H), 2.10 (t, *J* = 8.1 Hz, 1H), 1.91 (t, *J* = 5.2 Hz, 1H), 1.89–1.82 (m, 1H), 1.75–1.69 (m, 1H), 1.57 (d, *J* = 12.6 Hz, 1H), 1.27 (t, *J* = 7.1 Hz, 3H) ppm; **^{13}C NMR** (125 MHz, ($CDCl_3$): δ 167.1, 154.0, 147.6, 145.7, 135.0, 132.7, 130.6, 121.6, 119.8, 109.1, 108.1, 100.8, 60.2, 47.3, 42.3, 41.9, 41.9, 40.1, 40.0, 39.8, 39.7, 39.0, 37.3, 14.4 ppm; **IR**: 2924, 1713, 1647, 1502, 1489, 1442, 1244, 1171, 1037, 937,923, 809 cm^{-1}; **HRMS** (ESI): calculated for $[C_{24}H_{26}O_4+H]^+$: 379.1904, found: 379.1888.

Endiandric acid M (4.178)

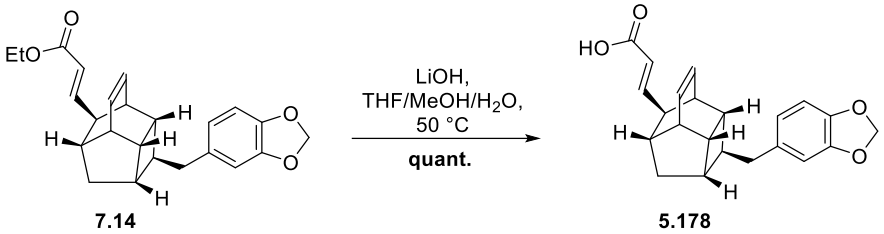

7.14 **5.178**

To a 5 mL vial open to air and equipped with a stir bar was added endiandric ethyl ester M (39.8 mg, 105 µmol, 1.00 mol. equiv.), tetrahydrofuran (0.350 mL, 0.300 M), methanol (0.350 mL, 0.300 M), water (0.350 mL, 0.300 M) and lithium hydroxide (25.2 mg, 1.05 mmol, 10.0 mol. equiv.). The reaction was heated to 60 °C for 2 hours by which time ^{1}H NMR analysis indicated the complete consumption of the starting material. The reaction was acidified with 1M aqueous HCl solution, extracted with ethyl acetate, dried over $MgSO_4$, filtered, and concentrated under reduced pressure to yield pure endiandric acid M. **Yield**: 36.9 mg, 105 µmol, quant.; **Appearance**: Pale yellow oil; **R_f**: 0.21 (3:7 EtOAc:hexanes); **^{1}H NMR** (500 MHz, $CDCl_3$): δ 6.86 (dd, *J* = 8.1, 15.7 Hz, 1H), 6.73 (d, *J* = 8.0 Hz, 1H), 6.66 (s, 1H), 6.61 (d, *J* = 8.0 Hz 1H), 6.27–6.22 (m, 1H), 6.19–6.14 (m, 1H), 5.93 (s, 2H), 5.68 (d, *J* = 15.7 Hz, 1H), 2.82–2.67 (m, 4H), 2.55–2.51 (m, 1H), 2.44 (dt, *J* = 5.5, 9.8 Hz, 1H), 2.35 (t, *J* = 6.0 Hz, 1H), 2.13–2.08 (m, 1H), 1.91 (t, *J* = 4.7 Hz, 1H), 1.90–1.83 (m, 1H), 1.76–1.70 (m, 1H), 1.59 (d, *J* = 12.6 Hz, 1H) ppm; **^{13}C NMR** (125 MHz, $CDCl_3$): δ 172.4, 157.0, 147.6, 145.7, 134.9, 132.6, 130.8, 121.6, 119.1, 109.2, 108.2, 100.9, 47.4, 42.3, 41.9, 41.8, 40.1, 40.0, 39.8, 39.7, 38.9, 37.3 ppm; **IR**: 2963, 2924, 1689, 1644, 1502, 1489, 1442, 1278, 1244, 1208, 1189, 1038, 937, 923, 809, 732 cm^{-1}; **HRMS** (ESI): calculated for $[C_{22}H_{22}O_4+H]^+$: 351.1591, found: 351.1593.

NMR comparison table for endiandric acid M (5.178)

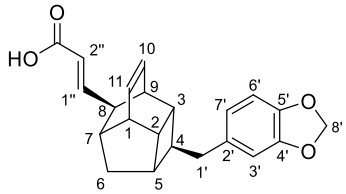

	Endiandric acid M (4.178)			
	Synthetic natural product		Isolated natural product[11,12]	
Position	**^{1}H (500 MHz) NMR, $CDCl_3$**	**^{13}C (125 MHz) NMR, $CDCl_3$**	**^{1}H (500 MHz) NMR, $CDCl_3$**	**^{13}C (150 MHz) NMR, $CDCl_3$**
1	2.82–2.67 (m, 4H)	42.3	2.69	42.3
2	2.44 (dt, *J* = 5.5, 9.8 Hz, 1H)	40.0	2.44	40.1
3	1.76–1.70 (m, 1H)	39.8	1.73	39.8
4	1.91 (t, *J* = 4.5 Hz, 1H)	41.8	1.92	41.8
5	2.35 (t, *J* = 6.0 Hz, 1H)	39.7	2.35	39.7
6	1.90–1.83 (m, 1H), 1.59 (d, *J* = 12.6 Hz, 1H)	38.9	1.86, 1.58	39.0
7	2.13–2.08 (m, 1H)	40.1	2.10	40.2
8	2.82–2.67 (m, 4H)	47.4	2.78	47.4
9	2.55–2.51 (m, 1H)	37.3	2.53	37.3
10	6.19–6.14 (m, 1H)	132.6	6.16	132.6
11	6.27–6.22 (m, 1H)	130.8	6.24	130.8
1’	2.82–2.67 (m, 4H)	41.9	2.76, 2.71	41.9
2’	-	134.9	-	135.0
3’	6.66 (s, 1H)	109.2	6.66	109.2
4’	-	147.6	-	147.7
5’	-	145.7	-	145.8
6’	6.73 (d, *J* = 8.0 Hz, 1H)	108.2	6.73	108.2
7’	6.61 (d, *J* = 8.0 Hz 1H)	121.6	6.61	121.6
8’	5.93 (s, 2H)	100.9	5.93	100.9
1’’	6.86 (dd, *J* = 8.1, 15.7 Hz, 1H)	157.0	6.85	156.9
2’’	5.68 (d, *J* = 15.7 Hz, 1H)	119.1	5.69	118.9
C=O	-	172.4	-	171.3

Additional Experiments

(1aR,1a1S,5S,6aR,7R)-1-oxo-1,1a,1a1,2,4a,5,6,6a-octahydro-2,5-methanocyclobuta[cd]indene-7-carboxylic acid (Carboxylic acid tetracycle) (5.183)

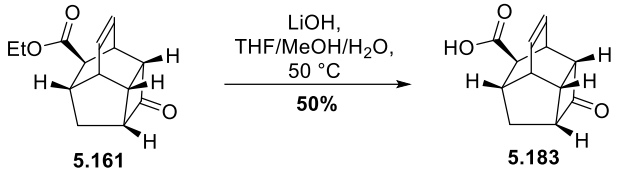

To a 15 mL sealable reaction tube open to air and equipped with a stir bar was added ethyl ester tetracycle (167.4 mg, 0.721 mmol, 1.00 mol. equiv.), tetrahydrofuran (2.40 mL, 0.300 M), methanol (2.40 mL, 0.300 M), water (2.40 mL, 0.300 M) and lithium hydroxide (86.3 mg, 3.60 mmol, 5.00 mol. equiv.). The reaction was heated to 50 °C overnight by which time ^{1}H NMR analysis indicated the complete consumption of the starting material. The reaction was acidified with 1M aqueous HCl solution, extracted with dichloromethane, washed with brine, dried over $MgSO_4$, filtered, and concentrated under reduced pressure. The crude product was purified via flash column chromatography (SiO_2, eluting with 49.5:49.5:1 EtOAc:hexane:acetic acid) yielding carboxylic acid tetracycle. **Yield**: 73.8 mg, 0.361 mmol, 50%; **Appearance**: white solid; $\mathbf{R_f}$: 0.40 (49.5:49.5:1 EtOAc:hexane:acetic acid); **^{1}H NMR** (500 MHz, $CDCl_3$): δ 10.40 (br s, 1H), 6.45 (t, *J* = 7.5 Hz, 1H), 6.33 (t, *J* = 7.4 Hz, 1H), 3.42 (dt, *J* = 5.3, 5.3, 8.7 Hz, 1H), 3.28–3.22 (m, 1H), 3.08 (dt, *J* = 5.4, 5.4, 7.7 Hz, 1H), 3.01–2.94 (m, 1H), 2.72 (t, *J* = 5.1 Hz, 1H), 2.50 (dt, *J* = 5.7, 5.7, 7.1 Hz, 1H), 2.26–2.22 (m, 1H), 1.97 (ddd, *J* = 5.1, 8.8, 12.9 Hz, 1H), 1.66 (d, *J* = 12.9 Hz, 1H) ppm; **^{13}C NMR** (125 MHz, ($CDCl_3$): δ 210.7, 178.5, 134.1, 132.1, 62.2, 60.0, 50.3, 40.3, 37.4, 34.5, 34.2, 30.6 ppm; **IR**: 3139, 2971, 2939, 1763, 1744, 1701, 1268, 1221, 1185, 1158, 689 cm^{-1}; **HRMS** (ESI): calculated for $[C_{12}H_{12}O_3+H]^+$: 205.0859, found: 205.0862.

(1aR,1a1S,5S,6aR,7R)-N-isobutyl-1-oxo-1,1a,1a1,2,4a,5,6,6a-octahydro-2,5-methanocyclobuta[cd]indene-7-carboxamide (Amide tetracycle) (5.184)

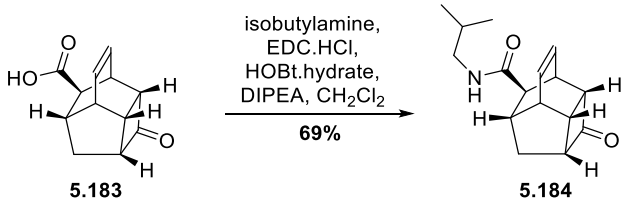

To a 10 mL round-bottom flask open to air and equipped with a stir bar was added carboxylic acid tetracycle (73.8 mg, 0.361 mmol, 1.00 mol. equiv.), dichloromethane (1.45 mL, 0.250 M), isobutylamine (35.9 µL, 0.361 mmol, 1.00 mol. equiv.), N-(3-dimethylaminopropyl)-N'-ethylcarbodiimide hydrochloride (83.1 mg, 0.434 mmol, 1.20 mol. equiv.), hydroxybenzotriazole hydrate (66.4 mg, 0.434 mmol, 1.20 mol. equiv.), and N,N-diisopropylethylamine (0.151 mL, 0.344 mmol, 2.40 mol. equiv.). The reaction was allowed to stir at room temperature overnight by which time ^{1}H NMR analysis indicated the complete consumption of the starting material. The reaction was diluted with ethyl acetate, washed with water, brine, dried over $MgSO_4$, filtered, and concentrated under reduced pressure. The crude product was purified via flash column chromatography (SiO_2, eluting with 1:1 EtOAc:hexane) yielding amide tetracycle. **Yield**: 64.2 mg, 0.248 mmol, 69%; **Appearance**: white solid; $\mathbf{R_f}$: 0.35 (1:1 EtOAc:hexanes); **^{1}H NMR** (500 MHz, $CDCl_3$): δ 6.49 (t, *J* = 7.5 Hz, 1H), 6.26 (t, *J* = 7.2 Hz, 1H), 5.46 (br s, 1H), 3.40 (dt, *J* = 5.4, 9.8 Hz, 1H), 3.11–2.92 (m, 5H), 2.73 (t, *J* = 4.9 Hz, 1H), 2.48 (dt, *J* = 5.3, 9.2 Hz, 1H), 2.06 (d, *J* = 2.3 Hz, 1H), 1.95 (ddd, *J* = 4.9, 8.8, 13.4 Hz, 1H), 1.77–1.66 (m, 1H), 1.63 (d, *J* = 12.8 Hz, 1H), 0.88 (s, 3H), 0.87 (s, 3H) ppm; **^{13}C**

NMR (125 MHz, ($CDCl_3$): δ 211.0, 172.2, 134.2, 130.8, 62.8, 60.0, 51.3, 47.1, 40.5, 37.5, 34.6, 34.6, 32.5, 28.7, 20.2, 20.2 ppm; **IR**: 3324, 2956, 2934, 1760, 1653, 1533, 1467, 1368, 1261, 1234, 1158, 1110, 685 cm^{-1}; **HRMS** (ESI): calculated for $[C_{16}H_{21}NO_2+H]^+$: 260.1645, found: 260.1643.

(1aS,1a1S,5S,6aR,7R)-1-oxo-1,1a,1a1,2,4a,5,6,6a-octahydro-2,5-methanocyclobuta[cd]indene-7-carbaldehyde (Aldehyde tetracycle) (5.179)

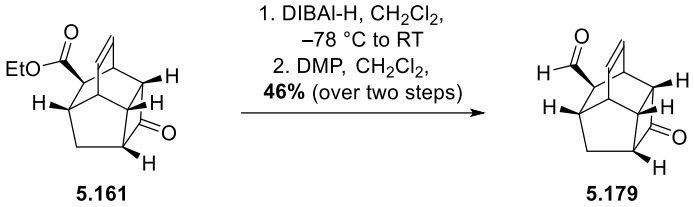

5.161 5.179

To a two-necked 50 mL round-bottom flask under nitrogen and equipped with a stir bar was added ethyl ester tetracycle (647.5 mg, 2.79 mmol, 1.00 mol. equiv.) and dry dichloromethane (14.0 mL, 0.200 M). The solution was cooled to −78 °C and diisobutylaluminium hydride (22.7 mL, 22.7 mmol, 2.20 mol. equiv., 1.00 M solution in toluene) was added dropwise. The reaction was allowed to warm to room temperature overnight by which time ^{1}H NMR analysis indicated completion of the reaction. The reaction mixture was diluted with diethyl ether, cooled to 0 °C and water (0.44 mL) was added dropwise followed by a 15% aqueous solution of sodium hydroxide (0.44 mL) and then water (1.10 mL) again. The mixture was allowed to warm to room temperature over fifteen minutes and then $MgSO_4$ was added, stirred for a further fifteen minutes, filtered, and concentrated under reduced pressure to yield the crude diol (337.4 mg).
A solution of the crude diol (337 mg, 1.75 mmol, 1.00 mol. equiv.) in dry dichloromethane (18 mL, 0.100 M) was cooled to 0 °C and Dess-Martin periodinane (1.86 g, 4.39 mmol, 2.50 mol. equiv.) was added. The reaction was allowed to stir at room temperature for 30 minutes by which time ^{1}H NMR analysis indicated completion of the reaction. The reaction was quenched with a saturated aqueous solution of sodium bicarbonate, extracted with ethyl acetate, washed with water, brine, dried over $MgSO_4$, filtered, and concentrated under reduced pressure. The crude product was purified via flash column chromatography (SiO_2, eluting with 1:4 EtOAc:hexane) yielding aldehyde tetracycle. **Yield**: 234 mg, 1.24 mmol, 46% (over two steps); **Appearance**: Clear oil; $\mathbf{R_f}$: 0.27 (1:4 EtOAc:hexane); **^{1}H NMR** (500 MHz, $CDCl_3$): δ 9.41 (s, 1H), 6.48–6.43 (m, 1H), 6.30–6.26 (m, 1H), 3.44 (dt, *J* = 5.4, 5.4, 9.1 Hz, 1H), 3.24 (q, *J* = 5.3, 5.2 Hz, 1H), 3.13 (dt, *J* = 5.2, 5.2, 8.3 Hz, 1H), 2.98 (q, *J* = 5.3, 5.3 Hz, 1H), 2.83 (t, *J* = 4.9 Hz, 1H), 2.53 (dt, *J* = 5.3, 5.3, 8.0 Hz, 1H), 2.13 (d, *J* = 2.8 Hz, 1H), 1.97 (ddd, *J* = 4.9, 8.9, 12.8 Hz, 1H), 1.63 (d, *J* = 12.8 Hz, 1H) ppm; **^{13}C NMR** (125 MHz, ($CDCl_3$): δ 210.5, 201.0, 135.6, 131.6, 62.4, 59.9, 58.5, 41.0, 36.5, 35.0, 34.0, 29.4 ppm; **IR**: 2936, 1760, 1724, 1110, 1052, 1035, 703, 665 cm^{-1}; **HRMS** (ESI): calculated for $[C_{12}H_{12}O_2+H]^+$: 189.0910, found: 189.0909.

Ethyl (E)-3-((1aS,1a1S,5R,6aR,7R)-1-oxo-1,1a,1a1,2,4a,5,6,6a-octahydro-2,5-methanocyclobuta[cd]inden-7-yl)acrylate (Unsaturated ester tetracycle) (5.180)

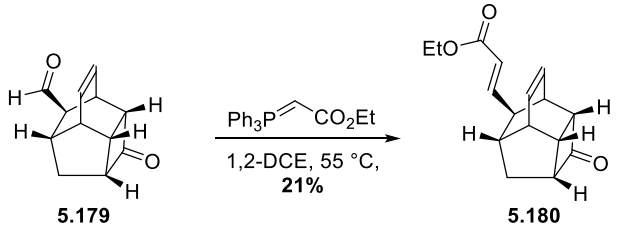

5.179 5.180

To a 10 mL round-bottom flask under nitrogen and equipped with a stir bar was added aldehyde tetracycle (50.0 mg, 0.266 mmol, 1.00 mol. equiv.), toluene (0.295 mL, 0.900 M) and ethyl(triphenylphosphoranylidene)acetate (92.5 mg, 0.266 mmol, 1.00 mol. equiv.). The reaction was stirred at room temperature overnight by which time ^{1}H NMR analysis indicated the complete consumption of the starting material. The reaction was concentrated under reduced pressure and was purified via flash column chromatography (SiO_2, eluting with 1:4 EtOAc:hexane) yielding unsaturated ester tetracycle. **Yield**: 14.1 mg, 0.055 mmol, 21%; **Appearance**: Clear oil; **R$_f$**: 0.43 (1:4 EtOAc:hexane); **^{1}H NMR** (500 MHz, $CDCl_3$): δ 6.64 (dd, *J* = 8.2, 15.8 Hz, 1H), 6.49–6.44 (m, 1H), 6.30–6.24 (m, 1H), 5.66 (d, *J* = 15.8 Hz, 1H), 4.14 (q, *J* = 7.1, 7.2 Hz, 2H), 3.42–3.36 (m, 1H), 3.42–3.36 (m, 1H), 3.09–3.03 (m, 1H), 2.94 (q, *J* = 5.1, 5.2 Hz, 1H), 2.81–2.75 (m, 1H), 2.51–2.45 (m, 1H), 2.12-2.07 (m, 1H), 2.04 (t, *J* = 4.9 Hz, 1H) 1.89 (ddd, *J* = 4.8, 8.8, 12.7 Hz, 1H), 1.65 (d, *J* = 12.7 Hz, 1H), 1.25 (t, *J* = 7.1 Hz, 3H) ppm; **^{13}C NMR** (125 MHz, ($CDCl_3$): δ 211.1, 166.7, 151.3, 133.4, 132.3, 120.9, 63.4, 60.4, 59.5, 48.9, 40.8, 40.6, 34.6, 34.4, 33.6, 14.4 ppm; **IR**: 2939, 1763, 1713, 1650, 1301, 1274, 1261, 1249, 1182, 1158, 1037 cm^{-1}; **HRMS** (ESI): calculated for $[C_{16}H_{18}O_3+H]^+$: 259.1329, found: 259.1338.

Ethyl (1S,1aR,1a1R,5S,6aR,7R)-1-(hydroxy(4-methoxyphenyl)methyl)-1,1a,1a1,2,4a,5,6,6a-octahydro-2,5-methanocyclobuta[cd]indene-7-carboxylate (Anisole alcohol tetracycle) (7.15)

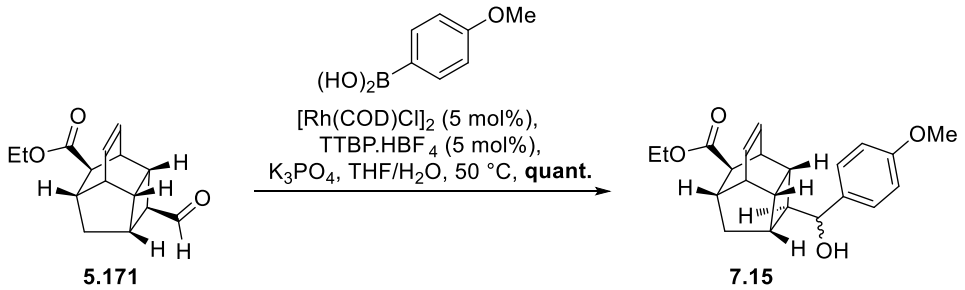

5.171 7.15

To an oven-dried 10 mL sealed reaction tube under nitrogen and equipped with a stir bar was added chloro(1,5-cyclooctadiene)rhodium(I) dimer (5.00 mg, 10.2 µmol, 5.00 mol%), Tri-tert-butylphosphonium tetrafluoroborate (2.94 mg, 10.2 µmol, 5.00 mol%), (4-methoxyphenyl)boronic acid (61.7 mg, 0.406 mmol, 2.00 mol. equiv.), a solution of aldehyde ester tetracycle (50.0 mg, 0.203 mmol, 1.00 mol. equiv.) in degassed THF (0.410 mL, 0.500 M) and a degassed aqueous solution of K_3PO_4 (0.110 mL, 0.655 mmol, 5.50 M). The reaction mixture was heated to 50 °C overnight by which time ^{1}H NMR analysis indicated the complete consumption of the starting material. The reaction mixture was diluted with dichloromethane and quenched with ammonium chloride. The mixture was then extracted with dichloromethane, dried over $MgSO_4$, filtered and concentrated under reduced pressure. Purification via flash column chromatography (SiO_2, eluting with 1:4 EtOAc:hexane → 3:7 EtOAc:hexane) yielded a rough 1:1 diastereomeric mixture of anisole alcohol tetracycle. **Yield**: 72.0 mg, 0.203 mmol, quant.; **Appearance**: Yellow oil **R$_f$**: 0.45 and 0.36 (3:7 EtOAc:hexanes); **^{1}H NMR** (500 MHz, $CDCl_3$): δ 7.30–7.24 (m, 4H), 6.88 (d, *J* = 8.6 Hz, 4H), 6.25–6.15 (m, 3H), 6.09–6.04 (m, 1H), 4.62 (t, *J* = 8.6 Hz, 2H), 4.15–3.99 (m, 4H), 3.81 (s, 6H), 3.15–3.11 (m, 1H), 2.81 (d, *J* = 3.8 Hz, 1H), 2.80–2.76 (m, 2H), 2.75–2.66 (m, 2H), 2.63 (t, *J* = 5.2 Hz, 1H), 2.59 (t, *J* = 5.2 Hz, 1H), 2.35 (dq, *J* = 5.0, 4.9, 9.5 Hz, 2H), 2.24 (t, *J* = 7.2 Hz, 1H), 2.14–2.07 (m, 3H), 2.02 (ddd, *J* = 5.5, 7.7, 12.9 Hz, 1H), 1.86–1.76 (m, 3H), 1.67 (d, *J* = 12.9 Hz, 1H), 1.62–1.55 (m, 1H), 1.44 (d, *J* = 12.9 Hz, 1H), 1.23 (t, *J* = 7.2 Hz, 3H), 1.20 (t, *J* = 7.2 Hz, 3H) ppm; **^{13}C NMR** (125 MHz, $CDCl_3$): δ 174.7, 174.6, 159.3, 159.3, 135.3, 135.0, 131.9, 131.8, 131.4, 131.4, 128.2, 128.1, 113.9, 77.7, 77.3, 60.4, 55.4, 49.2, 49.2, 46.5, 42.0, 41.9, 40.1, 40.1, 38.7, 38.5, 38.4, 38.4, 38.0, 37.3, 36.7, 36.3, 35.2, 34.5, 14.4 ppm; **IR**: 3445, 2956, 2929, 1727, 1612, 1512,

1303, 1245, 1206, 1175, 1035, 827, 732, 693 cm^{-1}; **HRMS** (ESI): calculated for $[C_{22}H_{26}O_4+H]^+$: 355.1904, found: 355.1899.

Ethyl (1S,1aR,1a1R,5S,6aR,7R)-1-((4-fluorophenyl)(hydroxy)methyl)-1,1a,1a1,2,4a,5,6,6a-octahydro-2,5-methanocyclobuta[cd]indene-7-carboxylate (Fluorophenyl alcohol tetracycle) (7.16)

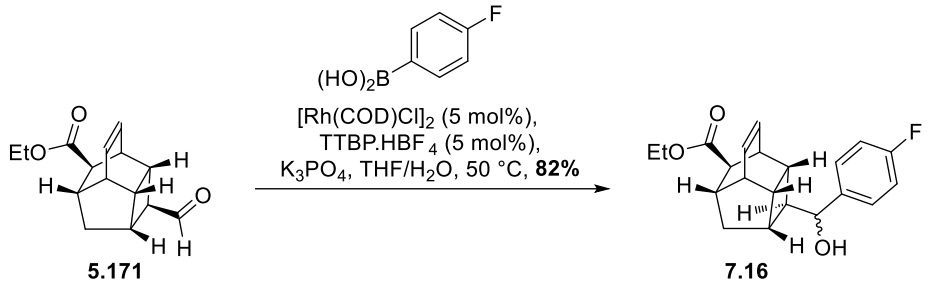

5.171 7.16

To an oven-dried 10 mL sealed reaction tube under nitrogen and equipped with a stir bar was added chloro(1,5-cyclooctadiene)rhodium(I) dimer (5.00 mg, 10.2 µmol, 5.00 mol%), Tri-tert-butylphosphonium tetrafluoroborate (2.9 mg, 10.2 µmol, 5.00 mol%), (4-fluorophenyl)boronic acid (56.8 mg, 0.406 mmol, 2.00 mol. equiv.), a solution of aldehyde ester tetracycle (50.0 mg, 0.203 mmol, 1.00 mol. equiv.) in degassed THF (0.410 mL, 0.500 M) and a degassed aqueous solution of K_3PO_4 (0.110 mL, 0.655 mmol, 5.50 M). The reaction mixture was heated to 50 °C overnight by which time 1H NMR analysis indicated the complete consumption of the starting material. The reaction mixture was diluted with dichloromethane and quenched with ammonium chloride. The mixture was then extracted with dichloromethane, dried over $MgSO_4$, filtered and concentrated under reduced pressure. Purification via flash column chromatography (SiO2, eluting with 1:4 EtOAc:hexane → 3:7 EtOAc:hexane) yielded a 1:1 diastereomeric mixture of fluorophenyl alcohol tetracycle. **Yield**: 57.3 mg, 0.167 mmol, 82%; **Appearance**: Clear oil $\mathbf{R_f}$: 0.53 and 0.47 (3:7 EtOAc:hexanes); **^{1}H NMR** (500 MHz, $CDCl_3$): δ 7.34–7.28 (m, 4H), 7.03 (t, *J* = 8.5 Hz, 4H), 6.24–6.15 (m, 3H), 6.10–6.04 (m, 1H), 4.65 (t, *J* = 9.2 Hz, 2H), 4.14–3.98 (m, 4H), 3.09 (q, *J* = 4.9, 4.8 Hz, 1H), 2.80 (d, *J* = 3.8 Hz, 1H), 2.76 (s, 2H), 2.74–2.66 (m, 3H), 2.62 (t, *J* = 5.2 Hz, 2H), 2.59 (t, *J* = 5.2 Hz, 1H), 2.38–2.31 (m, 2H), 2.25 (t, *J* = 7.4 Hz, 1H), 2.14–1.98 (m, 6H), 1.82 (ddd, *J* = 5.4, 7.7, 13.0 Hz, 1H), 1.64 (s, *J* = 13.1 Hz, 1H), 1.62–1.57 (m, 1H), 1.42 (d, *J* = 12.8 Hz, 1H), 1.22 (t, *J* = 7.0 Hz, 3H), 1.20 (t, *J* = 7.0 Hz, 3H) ppm; **^{13}C NMR** (125 MHz, $CDCl_3$): δ 174.6, 174.5, 162.8 (d, *J* = 245.8 Hz), 161.4 (d, *J* = 245.8 Hz), 138.9 (d, *J* = 3.3 Hz), 138.6 (d, *J* = 3.0 Hz), 131.9, 131.7, 131.4, 128.6, 128.5, 128.5, 128.4, 115.5 (d, *J* = 21.5 Hz), 77.4, 77.0, 60.5, 60.4, 49.2, 49.1, 46.7, 42.0, 41.9, 40.2, 40.1, 38.6, 38.4, 38.4, 38.3, 37.9, 37.3, 36.5, 36.2, 35.1, 34.5, 14.4 ppm; **^{19}F NMR** (470 MHz, $CDCl_3$): δ –114.6, –114.7 ppm; **IR**: 3453, 2958, 292, 1724, 1604, 1510, 1299, 1219, 1179, 1158, 1040, 830, 695 cm^{-1}; **HRMS** (ESI): calculated for $[C_{21}H_{23}FO_3+H]^+$: 343.1704, found: 343.1703.

Ethyl (1S,1aR,1a1R,5S,6aR,7R)-1-(hydroxy(1H-indol-5-yl)methyl)-1,1a,1a1,2,4a,5,6,6a-octahydro-2,5-methanocyclobuta[cd]indene-7-carboxylate (Indole alcohol tetracycle) (7.17)

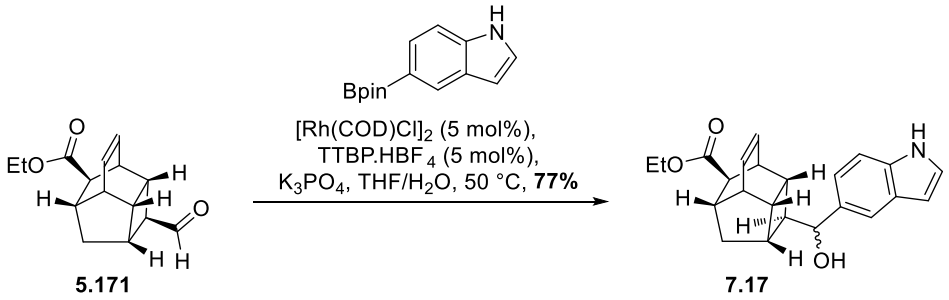

5.171 7.17

To an oven-dried 10 mL sealed reaction tube under nitrogen and equipped with a stir bar was added chloro(1,5-cyclooctadiene)rhodium(I) dimer (5.00 mg, 10.2 µmol, 5.00 mol%), Tri-tert-butylphosphonium tetrafluoroborate (2.94 mg, 10.2 µmol, 5.00 mol%), 5-(4,4,5,5-tetramethyl-1,3,2-dioxaborolan-2-yl)-1H-indole (98.7 mg, 0.406 mmol, 2.00 mol. equiv.), a solution of aldehyde ester tetracycle (50.0 mg, 0.203 mmol, 1.00 mol. equiv.) in degassed THF (0.410 mL, 0.500 M) and a degassed aqueous solution of K_3PO_4 (0.110 mL, 0.655 mmol, 5.00 M). The reaction mixture was heated to 50 °C overnight by which time ^{1}H NMR analysis indicated the complete consumption of the starting material. The reaction was diluted with dichloromethane and quenched with ammonium chloride. The mixture was then extracted with dichloromethane, dried over $MgSO_4$, filtered and concentrated under reduced pressure. Purification via flash column chromatography (SiO_2, eluting with 1:4 EtOAc:hexane → 2:3 EtOAc:hexane) yielded a rough 1:1 diastereomeric mixture of indole alcohol tetracycle. **Yield**: 56.9 mg, 0.157 mmol, 77%; **Appearance**: Light orange oil **R*f***: 0.38 and 0.32 (2:3 EtOAc:hexanes); **^{1}H NMR** (500 MHz, $CDCl_3$): δ 8.25 (br s, 2H), 7.61 (d, *J* = 8.2 Hz, 2H), 7.38 (d, *J* = 8.3 Hz, 2H), 7.24–7.18 (m, 4H), 6.55 (s, 2H), 6.26–6.20 (m, 2H), 6.20–6.14 (m, 1H), 6.06–6.00 (m, 1H), 4.80–4.73 (m, 2H), 4.15–3.97 (m, 4H), 3.17 (br s, 1H), 2.87 (d, *J* = 3.8 Hz, 1H), 2.83–2.77 (m, 2H), 2.77–2.71 (m, 2H), 2.71–2.66 (m, 1H), 2.64 (br t, *J* = 5.0 Hz, 1H), 2.58 (br t, *J* = 5.0 Hz, 1H), 2.40 (dq, *J* = 5.2, 5.1, 9.9 Hz, 1H), 2.28 (t, *J* = 7.1 Hz, 1H), 2.23–2.16 (m, 3H), 2.07–2.00 (m, 1H), 1.98–1.84 (m, 2H), 1.82–1.75 (m, 1H), 1.70 (d, *J* = 12.9 Hz, 1H), 1.67–1.57 (m, 2H), 1.42 (d, *J* = 13.4 Hz, 1H), 1.29–1.21 (m, 6H), 1.18 (t, *J* = 7.1 Hz, 3H) ppm; **^{13}C NMR** (125 MHz, $CDCl_3$): δ 174.9, 174.8, 135.7, 135.6, 134.5, 134.2, 131.9, 131.8, 131.4, 131.4, 127.8, 127.8, 124.9 (two coincident peaks), 121.0, 121.0, 119.3, 119.1, 111.3 (two coincident peaks), 102.6 (two coincident peaks), 79.0, 78.5, 60.4, 49.2, 49.1, 46.6, 42.0, 41.9, 40.1, 40.0, 38.7, 38.5, 38.4, 38.3, 38.2, 37.4, 37.0, 36.4, 35.2, 34.5, 24.9 (two coincident peaks), 14.4, 14.3 ppm; **IR**: 3404, 3370, 2958, 2931, 1713, 1209, 1181, 1040, 729, 695 cm^{-1}; **HRMS** (ESI): calculated for $[C_{23}H_{25}NO_3+H]^+$: 364.1907, found: 364.1905.

Ethyl (1S,1aR,1a1R,5S,6aR,7R)-1-((4-cyanophenyl)(hydroxy)methyl)-1,1a,1a1,2,4a,5,6,6a-octahydro-2,5-methanocyclobuta[cd]indene-7-carboxylate (Benzonitrile alcohol tetracycle) (7.18)

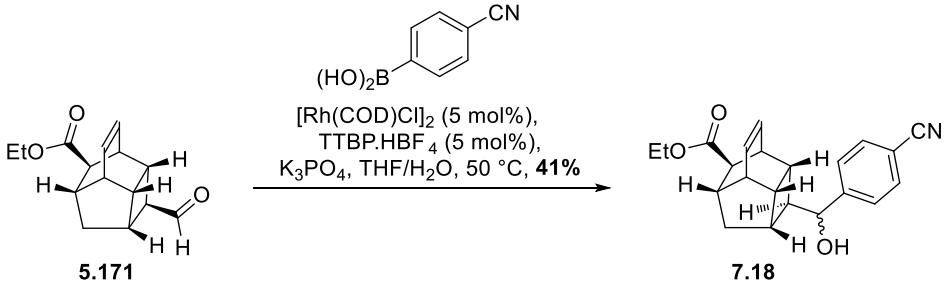

5.171 7.18

To an oven-dried 10 mL sealed reaction tube under nitrogen and equipped with a stir bar was added chloro(1,5-cyclooctadiene)rhodium(I) dimer (5.00 mg, 10.2 µmol, 5.00 mol%), Tri-tert-butylphosphonium tetrafluoroborate (2.94 mg, 10.2 µmol, 5.00 mol%), 4-cyanophenylboronic acid (59.7 mg, 0.406 mmol, 2.00 mol. equiv.), a solution of aldehyde ester tetracycle (50.0 mg,

0.203 mmol, 1.00 mol. equiv.) in degassed THF (0.410 mL, 0.500 M) and a degassed aqueous solution of K_3PO_4 (0.110 mL, 0.655 mmol, 5.00 M). The reaction mixture was heated to 50 °C overnight by which time ^{1}H NMR analysis indicated the complete consumption of the starting material. The reaction mixture was diluted with dichloromethane and quenched with ammonium chloride. The mixture was then extracted with dichloromethane, dried over $MgSO_4$, filtered and concentrated under reduced pressure. Purification via flash column chromatography (SiO_2, eluting with 1:4 EtOAc:hexane → 2:3 EtOAc:hexane) yielded a rough 1:1 diastereomeric mixture of benzonitrile alcohol tetracycle. **Yield**: 29.4 mg, 0.084 mmol, 41%; **Appearance**: Yellow oil **R$_f$**: 0.53 and 0.43 (2:3 EtOAc:hexanes); **^{1}H NMR** (500 MHz, $CDCl_3$): δ 7.65 (d, *J* = 7.7 Hz, 4H), 7.50–7.45 (m, 4H), 6.24–6.16 (m, 3H), 6.09 (t, *J* = 7.3 Hz, 1H), 4.77 (d, *J* = 8.1 Hz, 1H), 4.74 (d, *J* = 8.5 Hz, 1H), 4.13–4.01 (m, 4H), 3.07–3.02 (m, 1H), 2.80–2.68 (m, 5H), 2.67–2.59 (m, 2H), 2.40–2.33 (m, 2H), 2.33–2.28 (m, 1H), 2.08–1.93 (m, 6H), 1.90–1.82 (m, 1H), 1.68–1.64 (m, 1H), 1.61 (d, *J* = 12.9 Hz, 1H), 1.43 (d, *J* = 12.9 Hz, 1H), 1.37 (d, *J* = 12.3 Hz, 1H), 1.27–1.18 (m, 6H) ppm; **^{13}C NMR** (125 MHz, $CDCl_3$): δ 174.4, 174.3, 148.6, 148.4, 132.3 (two coincident peaks), 131.8, 131.6, 131.5, 131.4, 127.6, 127.5, 118.9 (two coincident peaks), 111.5, 111.5, 76.9, 76.6, 60.5, 60.5, 49.1, 49.1, 46.6, 46.6, 41.9, 41.9, 40.2, 40.1, 38.5, 38.3, 38.3, 38.3, 37.5, 37.1, 36.1, 36.0, 34.9, 34.4, 14.4 (two coincident peaks) ppm; **IR**: 3465, 2958, 2929, 2228, 1721, 1366, 1299, 1206, 1179, 1082, 1040, 914, 827, 732, 693, 572 cm^{-1}; **HRMS** (ESI): calculated for $[C_{22}H_{23}NO_3+H]^+$: 350.1751, found: 350.1748.

Ethyl (1S,1aR,1a1R,5S,6aR,7R)-1-((4-(dimethylamino)phenyl)(hydroxy)methyl)-1,1a,1a1,2,4a,5,6,6a-octahydro-2,5-methanocyclobuta[cd]indene-7-carboxylate (Aniline alcohol tetracycle) (7.19)

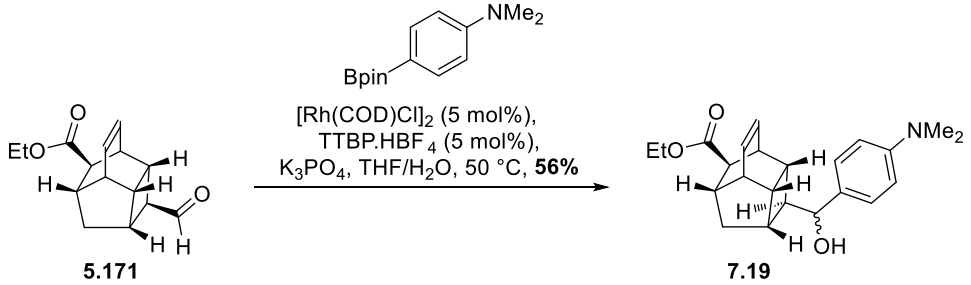

5.171 7.19

To an oven-dried 10 mL sealed reaction tube under nitrogen and equipped with a stir bar was added chloro(1,5-cyclooctadiene)rhodium(I) dimer (5.00 mg, 10.2 µmol, 5.00 mol%), Tri-tert-butylphosphonium tetrafluoroborate (2.94 mg, 10.2 µmol, 5.00 mol%), N,N-dimethyl-4-(4,4,5,5-tetramethyl-1,3,2-dioxaborolan-2-yl)aniline (100.3 mg, 0.406 mmol, 2.00 mol. equiv.), a solution of aldehyde ester tetracycle (50.0 mg, 0.203 mmol, 1.00 mol. equiv.) in degassed THF (0.410 mL, 0.500 M) and a degassed aqueous solution of K_3PO_4 (0.110 mL, 0.655 mmol, 5.50 M). The reaction mixture was heated to 50 °C overnight by which time ^{1}H NMR analysis indicated the complete consumption of the starting material. The reaction mixture was diluted with dichloromethane and quenched with ammonium chloride. The mixture was then extracted with dichloromethane, dried over $MgSO_4$, filtered and concentrated under reduced pressure. Purification via flash column chromatography (SiO_2, eluting with 1:9 EtOAc:hexane → 1:4 EtOAc:hexane) yielded a rough 1:1 diastereomeric mixture of aniline alcohol tetracycle. **Yield**: 41.7 mg, 0.113 mmol, 56%; **Appearance**: Brown oil **R$_f$**: 0.34 and 0.29 (3:7 EtOAc:hexanes); **^{1}H NMR** (500 MHz, $CDCl_3$): δ 7.20 (dd, *J* = 5.1, 8.5 Hz, 4H), 6.70 (d, *J* = 8.5 Hz, 4H), 6.23–6.19 (m, 2H), 6.19–6.15 (m, 1H), 6.08–6.03 (m, 1H), 4.57 (d, *J* = 5.0 Hz, 1H), 4.55 (d, *J* = 5.0 Hz, 1H), 4.14–3.98 (m, 4H), 3.15 (p, *J* = 4.1, 4.1, 4.3, 4.3 Hz, 1H), 2.94 (s, 12H), 2.85 (d, *J* = 3.8 Hz, 1H), 2.80 (s, 2H), 2.74–2.69 (m, 2H), 2.69–2.65 (m, 1H), 2.62 (t, *J* = 5.2 Hz, 1H), 2.59 (t, *J* = 5.2 Hz, 1H), 2.34 (dp, *J* = 4.7, 4.7, 4.2, 4.2, 13.0 Hz, 2H), 2.22 (t, *J* = 6.7 Hz, 1H), 2.14–2.08 (m, 3H), 2.01 (ddd, *J* = 5.4, 7.7, 13.0 Hz, 1H), 1.98 (br s, 1H), 1.81 (ddd, *J* = 5.3, 7.6, 12.9

Hz, 1H), 1.67 (d, *J* = 12.9 Hz, 1H), 1.61–1.55 (m, 1H), 1.45 (d, *J* = 12.9 Hz, 1H), 1.23 (t, *J* = 6.5 Hz, 3H), 1.19 (t, *J* = 7.1 Hz, 3H) ppm; **^{13}C NMR** (125 MHz, $CDCl_3$): δ 174.7, 174.6, 150.3, 150.3, 131.9, 131.8, 131.4, 131.3, 131.0, 130.7, 127.9, 127.8, 112.5 (two coincident peaks), 77.8, 77.5, 60.3 (two coincident peaks), 49.2, 49.1, 46.2, 46.2, 42.0, 41.9, 40.7 (two coincident peaks), 40.1, 40.0, 38.7, 38.5, 38.4, 38.1, 37.4, 36.9, 36.4, 35.2, 34.6, 14.4 (two coincident peaks) ppm; **IR**: 3445, 2956, 2929, 1731, 1614, 1523,1340, 1206, 1178, 1164, 1041, 816, 696 cm^{-1}; **HRMS** (ESI): calculated for $[C_{23}H_{29}NO_3+H]^+$: 368.2220, found: 368.2233.

Ethyl (1S,1aR,1a1R,5S,6aS,7R)-1-(4-methoxybenzyl)-1,1a,1a1,2,4a,5,6,6a-octahydro-2,5-methanocyclobuta[cd]indene-7-carboxylate (Anisole tetracycle) (7.20)

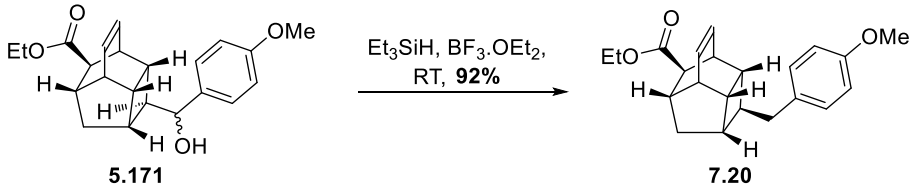

5.171 **7.20**

To a 5 mL vial under nitrogen and equipped with a stir bar was added anisole alcohol tetracycle (77.6 mg, 0.219 mmol, 1.00 mol. equiv.) and dry dichloromethane (1.04 mL, 0.210 M). To the solution was added triethylsilane (70.0 µL, 0.438 µmol, 2.00 mol. equiv.) and then boron trifluoride diethyl etherate (31.0 µL, 0.328 mmol, 1.50 mol. equiv.). Immediate ^{1}H NMR analysis indicated the complete consumption of the starting material. The reaction mixture was diluted with dichloromethane and quenched with a saturate aqueous ammonium chloride solution. The organic layer was dried over $MgSO_4$, filtered and concentrated under reduced pressure to yield pure anisole tetracycle. **Yield**: 68.3 mg, 0.202 mmol, 92%; **Appearance**: Dark yellow oil; **R_f**: 0.30 (1:19 EtOAc:hexanes); **^{1}H NMR** (500 MHz, $CDCl_3$): δ 7.08 (d, *J* = 8.3 Hz, 2H), 6.83 (d, *J* = 8.3 Hz, 2H), 6.21 (t, *J* = 7.3 Hz, 1H), 6.15 (t, *J* = 7.3 Hz, 1H), 4.15–4.01 (m, 2H), 3.79 (s, 3H), 2.95 (q, *J* = 4.9, 5.1 Hz, 1H), 2.85–2.68 (m, 4H), 2.60 (t, *J* = 5.3 Hz, 1H), 2.41 (dt, *J* = 5.6, 9.8 Hz, 1H), 2.34 (t, *J* = 7.2 Hz, 1H), 2.02 (t, *J* = 8.2 Hz, 1H), 1.93–1.86 (m, 1H), 1.76–1.70 (m, 1H) 1.54 (d, *J* = 13.0 Hz, 1H), 1.23 (t, *J* = 7.1 Hz, 3H). **^{13}C NMR** (125 MHz, $CDCl_3$): δ 174.8, 157.9, 133.2, 132.0, 131.4, 129.7, 113.8, 60.4, 55.4, 49.3, 42.1, 41.3, 40.6, 39.9, 39.0, 38.6, 38.5, 35.1, 14.4 ppm; **IR**: 2955, 2926, 1731, 1512, 1299, 1245, 1204, 1177, 1038, 692 cm^{-1}; **HRMS** (ESI): calculated for $[C_{22}H_{26}O_3+H]^+$: 339.1955, found: 339.1965.

Ethyl (1S,1aR,1a1R,5S,6aS,7R)-1-(4-fluorobenzyl)-1,1a,1a1,2,4a,5,6,6a-octahydro-2,5-methanocyclobuta[cd]indene-7-carboxylate (Fluorophenyl tetracycle) (7.21)

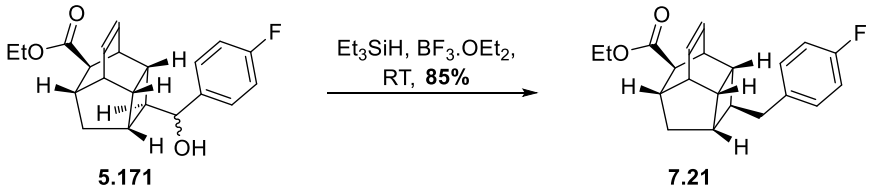

5.171 **7.21**

To a 5 mL vial under nitrogen and equipped with a stir bar was added fluorophenyl alcohol tetracycle (37.2 mg, 109 mmol, 1.00 mol. equiv.) and dry dichloromethane (0.517 mL, 0.210 M). To the solution was added triethylsilane (35.0 µL, 0.217 mmol, 2.00 mol. equiv.) and then boron trifluoride diethyl etherate (16.0 µL, 0.163 mmol, 1.50 mol. equiv.). Immediate ^{1}H NMR analysis indicated the complete consumption of the starting material. The reaction mixture was diluted with dichloromethane and quenched with a saturate aqueous ammonium chloride solution. The organic layer was dried over $MgSO_4$, filtered and concentrated under reduced pressure. The crude product was purified via flash column chromatography (SiO_2, eluting with 1:19 EtOAc:hexane) yielding pure fluorophenyl tetracycle. **Yield**: 30.3 mg, 0.093 mmol, 85%; **Appearance**: Yellow oil; **R_f**: 0.38 (1:19 EtOAc:hexanes); **^{1}H NMR** (500 MHz, $CDCl_3$): δ 7.11

(dd, *J* = 5.4, 8.3 Hz, 2H), 6.97 (t, *J* = 8.7 Hz, 2H), 6.23–6.12 (m, 2H), 4.15 – 4.01 (m, 2H), 2.95 (q, *J* = 4.9, 4.8 Hz, 1H), 2.87–2.73 (m, 3H), 2.71 (q, *J* = 5.5, 5.6 Hz, 1H), 2.61 (t, *J* = 5.3 Hz, 1H), 2.42 (dt, *J* = 5.5, 9.6 Hz, 1H), 2.34 (t, *J* = 7.2 Hz, 1H), 2.02 (t, *J* = 8.1 Hz, 1H), 1.94–1.86 (m, 1H), 1.75–1.69 (m, 1H), 1.54 (d, *J* = 13.0 Hz, 1H), 1.22 (t, *J* = 7.1 Hz, 3H). **^{13}C NMR** (125 MHz, $CDCl_3$): δ 174.7, 161.4 (d, *J* = 243.3 Hz), 136.7 (d, *J* = 3.3 Hz), 131.9, 131.4, 130.1, 130.1, 115.1 (d, *J* = 3.3 Hz), 60.4, 49.3, 42.0, 41.3, 40.5, 40.0, 39.9, 39.0, 38.6, 38.5, 35.0, 14.4 ppm; **^{19}F NMR** (470 MHz, $CDCl_3$): δ –117.7 ppm; **IR**: 2955, 2924, 1733, 1509, 1221, 1208, 1175, 1158, 1041, 831, 692 cm^{-1}; **HRMS** (ESI): calculated for $[C_{21}H_{23}FO_2+H]^+$: 327.1755, found: 327.1753.

Procedure for dipotassium cyclooctatetraenide (K_2COT) (5.212) synthesis

To a dry 20 mL sealed reaction tube under nitrogen and equipped with a stir bar was added potassium metal (600 mg, 15.4 mmol, 3.20 mol. equiv.), dry tetrahydrofuran (9.6 mL, 0.500 M) and 1,3,5,7-cyclooctatetraene (0.540 mL, 4.80 mmol, 1.00 mol. equiv.). The reaction was stirred at room temperature where over the course of 12 hours the colour changed from yellow to dark brown to dark blue signifying the presence of the dipotassium cyclooctatetraenide. The solution was stored at room temperature and used without further purification.

(1E,3Z,5Z,7E)-1,8-bis(4,4,5,5-tetramethyl-1,3,2-dioxaborolan-2-yl)octa-1,3,5,7-tetraene (Bis-Bpin tetraene) (5.224)

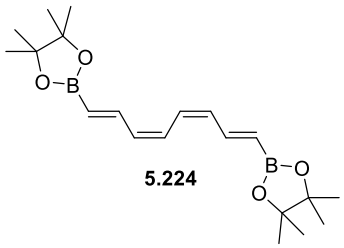

5.224

To a 10 mL round-bottom flask under nitrogen and equipped with a stir bar was added pinacolborane (1.00 mL, 6.88 mmol, 13.2 mol. equiv.). A solution of K_2COT (1.00 mL, 0.521 mmol, 1.00 mol. equiv., 0.500 M in THF) was carefully added dropwise where the blue colour was allowed to dissipate before adding another drop of K_2COT. Upon completion of the addition of K2COT, the reaction mixture was diluted with hexane, the solids filtered off and the solution concentrated under reduced pressure at room temperature to yield crude product. The product was used without further purification. **Crude yield**: 0.173 g, 0.483 mmol, 93%; **Appearance**: Off-white solid; $\mathbf{R_f}$: N/A (unstable on silica); **^{1}H NMR** (500 MHz, $CDCl_3$): δ 7.51 (dd, *J* = 11.5, 17.4 Hz, 2H), 6.74–6.67 (m, 2H), 6.19–6.13 (m, 2H), 5.65 (d, *J* = 17.4 Hz, 2H), 1.27 (s, 24H) ppm; **^{13}C NMR** (125 MHz, ($CDCl_3$): δ 143.7, 132.9, 127.4, 123.5 (carbon adjacent to boron), 83.5, 24.9 ppm; **IR**: 2979, 2931, 1613, 1546, 1475, 1459, 1379, 1339, 1142, 970, 850, 669 cm^{-1}; **HRMS** (ESI): calculated for $[C_{20}H_{32}B_2O_4+H]^+$: 359.2560, found: 359.2546.

(1E,3Z,5Z,7E)-1,8-diphenylocta-1,3,5,7-tetraene (5.233)

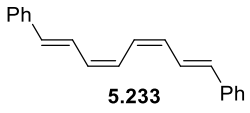

5.233

To an oven-dried 10 mL sealed reaction tube under nitrogen and equipped with a stir bar was added tetrakis(triphenylphosphine)palladium(0) (8.8 mg, 7.6 µmol, 5.00 mol%), a solution of bis-Bpin tetraene (54.3 mg, 0.151 mmol, 1.00 mol. equiv.) in degassed THF (0.760 mL, 0.200 M), degassed aqueous solution of K_2CO_3 (0.303 mL, 0.607 mmol, 2.00 M) and bromobenzene (0.04 mL, 0.379 mmol, 2.50 mol. equiv.). The reaction mixture was heated to 70 °C overnight by which time ^{1}H NMR analysis indicated the complete consumption of the starting material. The reaction mixture was diluted with dichloromethane and quenched with ammonium chloride. The mixture was extracted with dichloromethane, dried over $MgSO_4$, filtered and concentrated under reduced pressure. Purification via flash column chromatography (SiO_2, eluting with hexane → 1:9 EtOAc:hexane) yielded product. **Yield**: 8.0 mg, 0.031 mmol, 20%; **Appearance**: Orange solid; $\mathbf{R_f}$: 0.18 (hexanes); **^{1}H NMR** (500 MHz, $CDCl_3$): δ 7.46 (d, *J* = 7.4 Hz, 4H), 7.36–7.30 (m, 8H), 7.26–7.23 (m, 2H), 6.68–6.63 (m, 4H), 6.29 (ddd, *J* = 2.4, 6.9, 11.4 Hz, 1H) ppm; **^{13}C NMR** (150 MHz, $CDCl_3$): δ 137.5, 134.3, 130.6, 128.8, 127.9, 126.7, 124.8, 124.1 ppm; **IR**: 2924, 2852, 1727, 1489, 1446, 1259, 1071, 1007, 987, 953, 799, 736, 690 cm^{-1}; **HRMS** (ESI): calculated for $[C_{20}H_{18}+H]^+$: 259.1481, found: 259.1480.

(1R,6S,7S,8S)-7,8-dibenzylbicyclo[4.2.0]octa-2,4-diene (5.234)

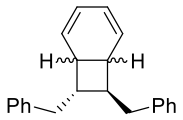

5.234

To an oven-dried 10 mL sealed reaction tube under nitrogen and equipped with a stir bar was added tetrakis(triphenylphosphine)palladium(0) (9.3 mg, 8.1 µmol, 5.00 mol%), a solution of bis-Bpin tetraene (57.7 mg, 0.161 mmol, 1.00 mol. equiv.) in degassed THF (0.806 mL, 0.200 M), degassed aqueous solution of K_2CO_3 (0.322 mL, 0.645 mmol, 2.00 M) and benzyl bromide (0.05 mL, 0.403 mmol, 2.50

mol. equiv.). The reaction mixture was heated to 70 °C overnight by which time ^{1}H NMR analysis indicated the complete consumption of the starting material. The reaction mixture was diluted with dichloromethane and quenched with ammonium chloride. The mixture was extracted with dichloromethane, dried over $MgSO_4$, filtered and concentrated under reduced pressure. Purification via flash column chromatography (SiO_2, eluting with hexane) yielded product. **Yield**: 5.0 mg, 0.017 mmol, 11%; **Appearance**: Pale yellow oil; **R_f**: 0.26 (hexanes); **^{1}H NMR** (500 MHz, $CDCl_3$): δ 7.29–7.21 (m, 4H), 7.19–7.13 (m, 4H), 7.06 (d, *J* = 7.1 Hz, 2H), 5.88–5.83 (m, 1H), 5.60–5.54 (m, 2H), 5.31–5.25 (m, 1H), 3.18 (t, *J* = 9.0 Hz, 1H), 2.93–2.79 (m, 2H), 2.73 (p, *J* = 8.1, 1H), 2.68–2.59 (m, 2H), 2.55–2.44 (m, 2H) ppm; **^{13}C NMR** (150 MHz, $CDCl_3$): δ 141.5, 141.0, 128.9, 128.7, 128.5, 128.4, 127.2, 126.6, 125.9, 125.9, 124.3, 121.4, 53.7, 51.7, 41.8, 36.7, 36.4, 35.0 ppm; **IR**: 3026, 2924, 2852, 1603, 1583, 1495, 1455, 1375, 941, 907, 730, 699 cm^{-1}; **HRMS** (ESI): calculated for $[C_{22}H_{22}+H]^+$: 287.17943, found: 287.1793.

2,2'-((1R,2R,7S,8R)-bicyclo[5.1.0]octa-3,5-diene-2,8-diyl)bis(4,4,5,5-tetramethyl-1,3,2-dioxaborolane) (5.204)

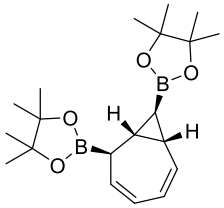

5.204

To an oven-dried 25 mL sealed reaction tube under nitrogen and equipped with a stir bar was added tetrakis(triphenylphosphine)platinum(0) (118 mg, 94.5 µmol, 3.00 mol%), bis(pinacolato)diboron (800 mg, 3.15 mmol, 1.00 mol. equiv.), dry degassed toluene (15.8 mL, 0.200 M) and 1,3,5,7-cyclooctatetraene (0.530 mL, 4.73 mmol, 1.50 mol. equiv.). The reaction mixture was heated to 50 °C overnight by which time ^{1}H NMR analysis indicated the complete consumption of the starting material. The reaction mixture was under reduced pressure and then purified via flash column chromatography (SiO_2, eluting with 1:9 EtOAc:hexane) to yield product. **Yield**: 0.382 g, 1.07 mmol, 34%; **Appearance**: Yellow oil; **R_f**: 0.32 (1:9 EtOAc:hexanes); **^{1}H NMR** (500 MHz, $(CD_3)_2SO$): δ 6.01 (dd, *J* = 6.1, 11.6 Hz, 1H), 5.68 (dd, *J* = 5.6, 10.8 Hz, 1H), 5.60 (dd, *J* = 8.3, 10.8 Hz, 1H), 5.46 (dd, *J* = 5.6, 11.6 Hz, 1H), 2.13 (dd, *J* = 5.8, 8.4 Hz, 1H), 1.76 (dt, *J* = 6.1, 8.3 Hz, 1H), 1.24–1.18 (m, 1H), 1.20–1.17 (m, 12H), 1.14 (s, 12H), 0.92 (t, *J* = 6.0 Hz, 1H) ppm; **^{13}C NMR** (125 MHz, $(CD_3)_2SO$): δ 134.2, 132.0, 127.1, 124.4, 83.0, 82.6, 41.3, 26.0, 24.5 (two coincident peaks), 24.4 (two coincident peaks) ppm; **IR**: 2978, 1475, 1448, 1372, 1325, 1167, 1142, 981, 850, 673 cm^{-1}; **HRMS** (ESI): calculated for $[C_{20}H_{32}B_2O_4+H]^+$: 359.2560, found: 359.2563.

2D NMR analysis of 2,2'-((1R,2R,7S,8R)-bicyclo[5.1.0]octa-3,5-diene-2,8-diyl)bis(4,4,5,5-tetramethyl-1,3,2-dioxaborolane) (5.204)

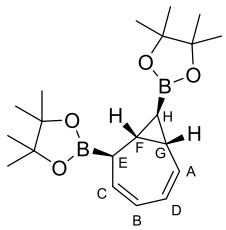

See associated 1D NOESY spectra for relative stereochemistry assignment

Position	^{1}H (500 MHz) NMR, $(CD_3)_2SO$	COSY (600 MHz) correlations, $(CD_3)_2SO$
A	6.01 (dd, *J* = 6.1, 11.6 Hz	D, G
B	5.68 (dd, *J* = 5.6, 10.8 Hz, 1H)	C, D

C	5.60 (dd, *J* = 8.3, 10.8 Hz, 1H)	B, E
D	5.46 (dd, *J* = 5.6, 11.6 Hz	A, B
E	2.13 (dd, *J* = 5.8, 8.4 Hz, 1H),	C, F
F	1.76 (dt, *J* = 6.1, 8.3 Hz, 1H)	E, G, H
G	1.24–1.18 (m, 1H)	A, F, H
H	0.92 (t, *J* = 6.0 Hz, 1H)	F, G
Bpin groups	1.20–1.17 (m, 12H), 1.14 (s, 12H)	-

NMR Data

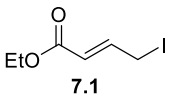

7.1

^{1}H NMR

$CDCl_3$, 500 MHz

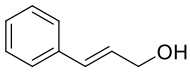

7.2

^{1}H NMR

$CDCl_3$, 500 MHz

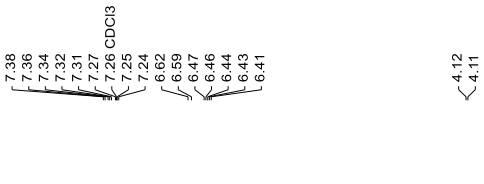

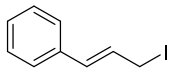

7.3

^{1}H NMR

$CDCl_3$, 500 MHz

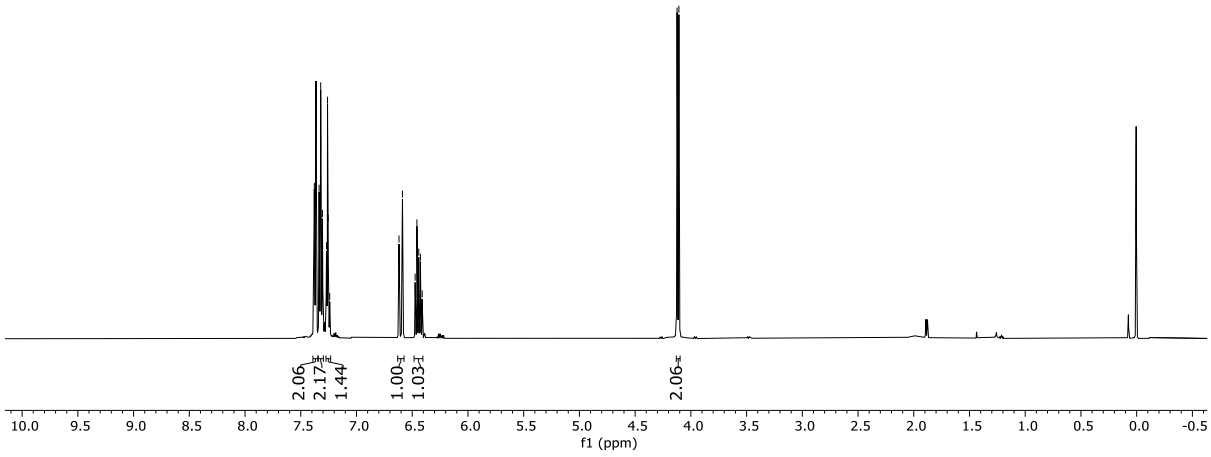

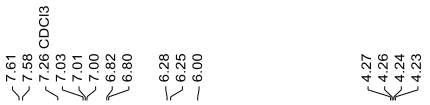

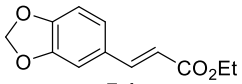

7.4

^{1}H NMR

$CDCl_3$, 500 MHz

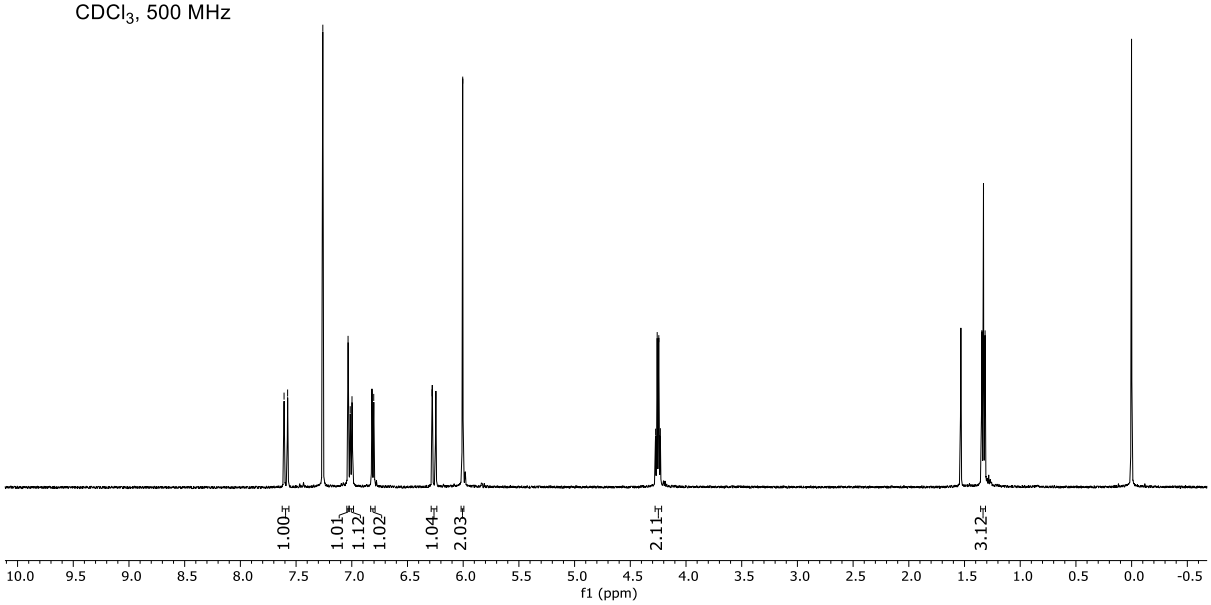

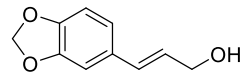

7.5

^{1}H NMR

$CDCl_3$, 500 MHz

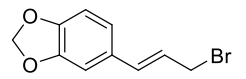

7.6

^{1}H NMR

$CDCl_3$, 500 MHz

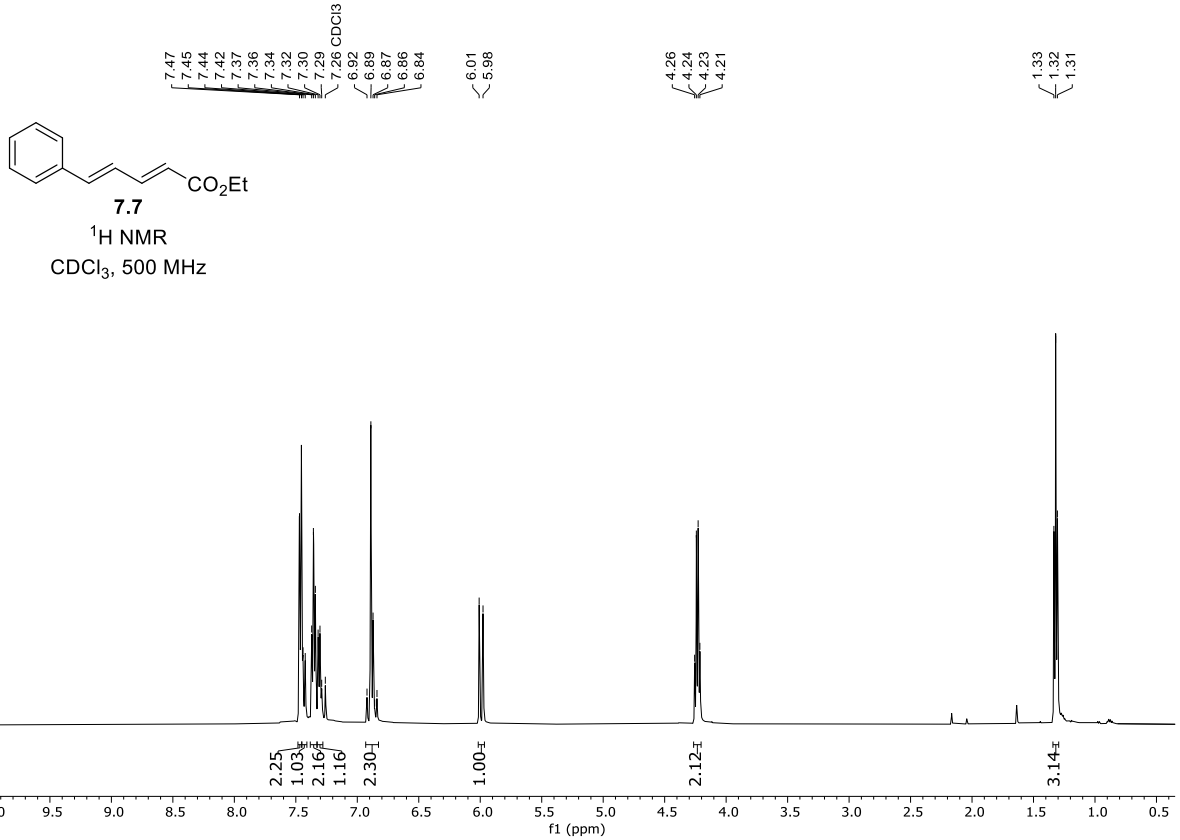

7.7

^{1}H NMR

$CDCl_3$, 500 MHz

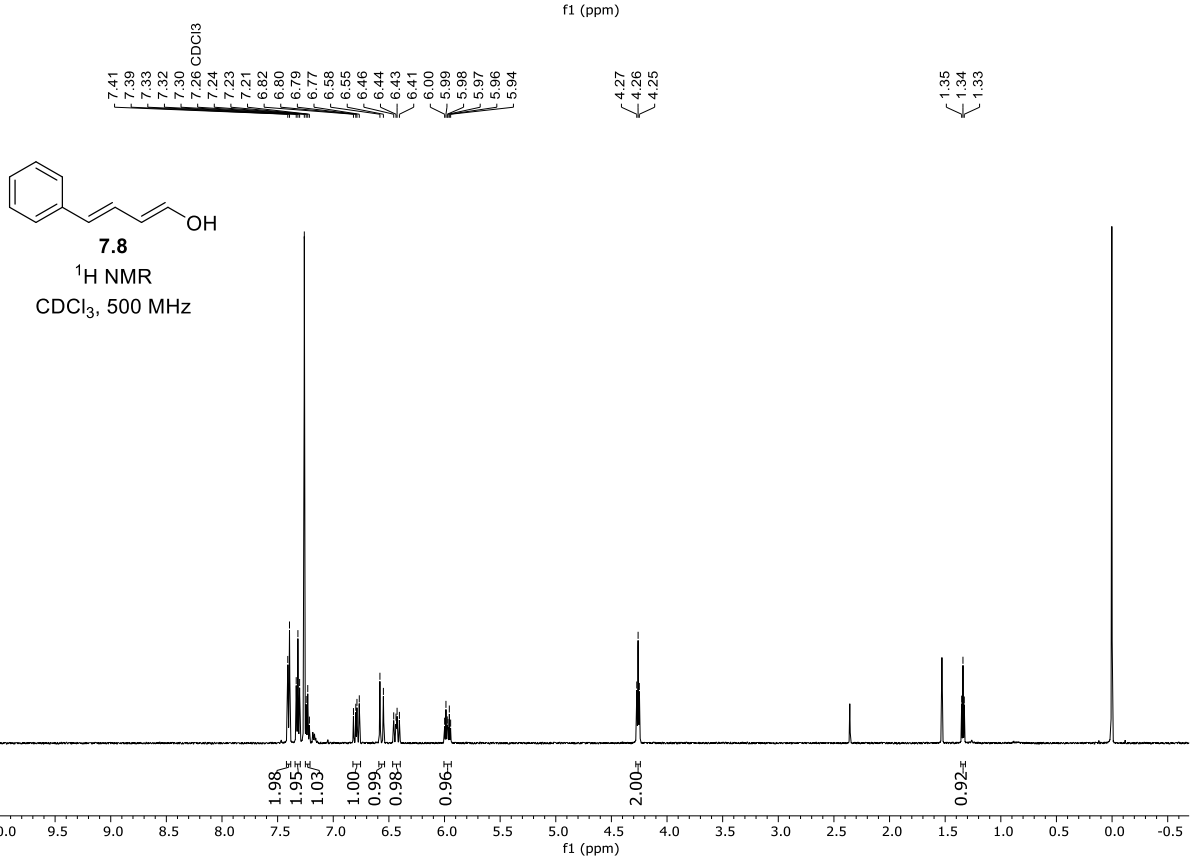

7.8

^{1}H NMR

$CDCl_3$, 500 MHz

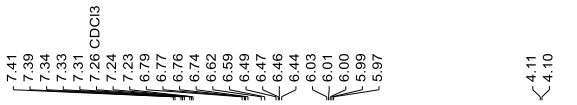

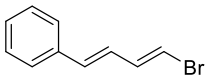

7.9

^{1}H NMR

$CDCl_3$, 500 MHz

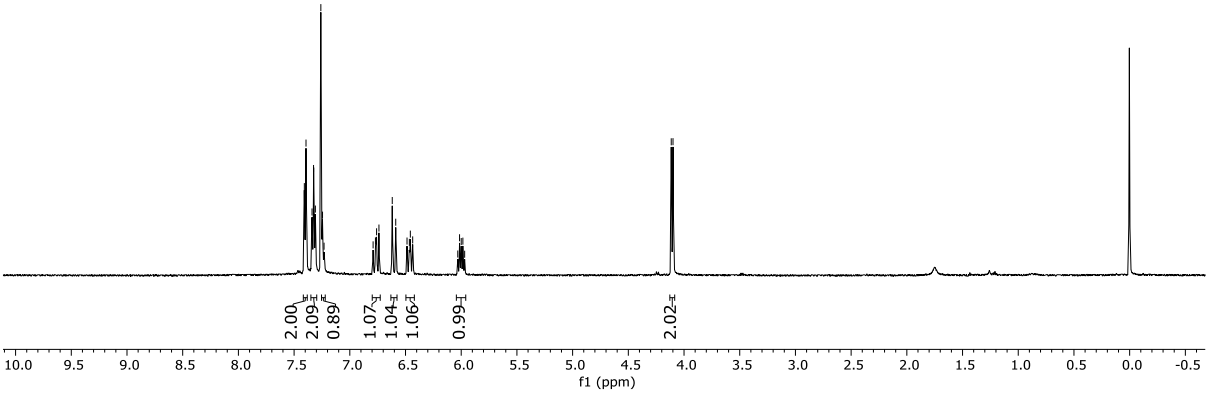

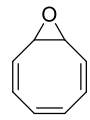

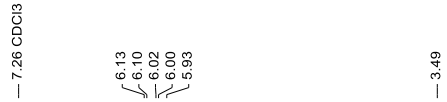

5.122

^{1}H NMR

$CDCl_3$, 500 MHz

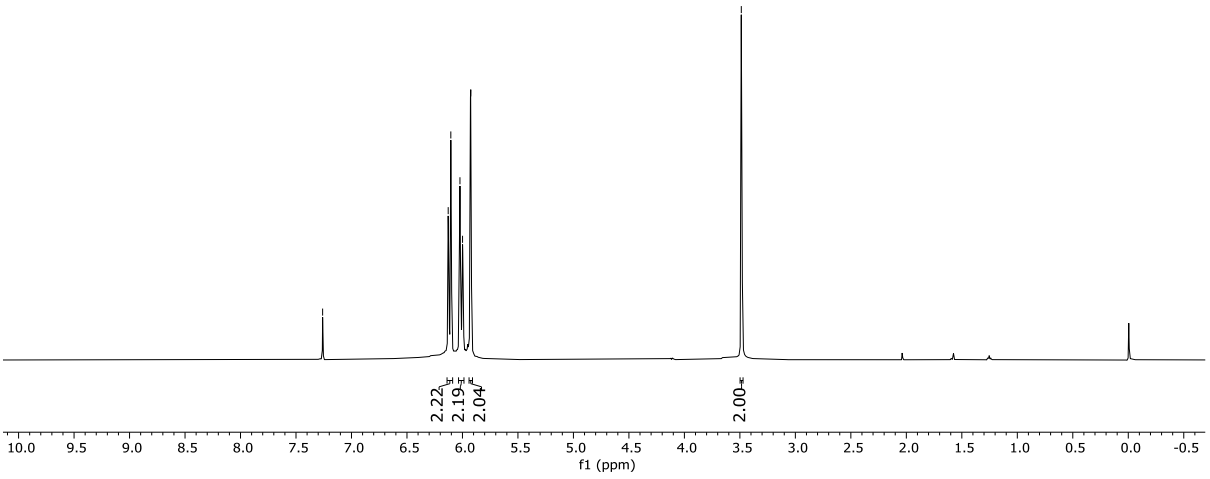

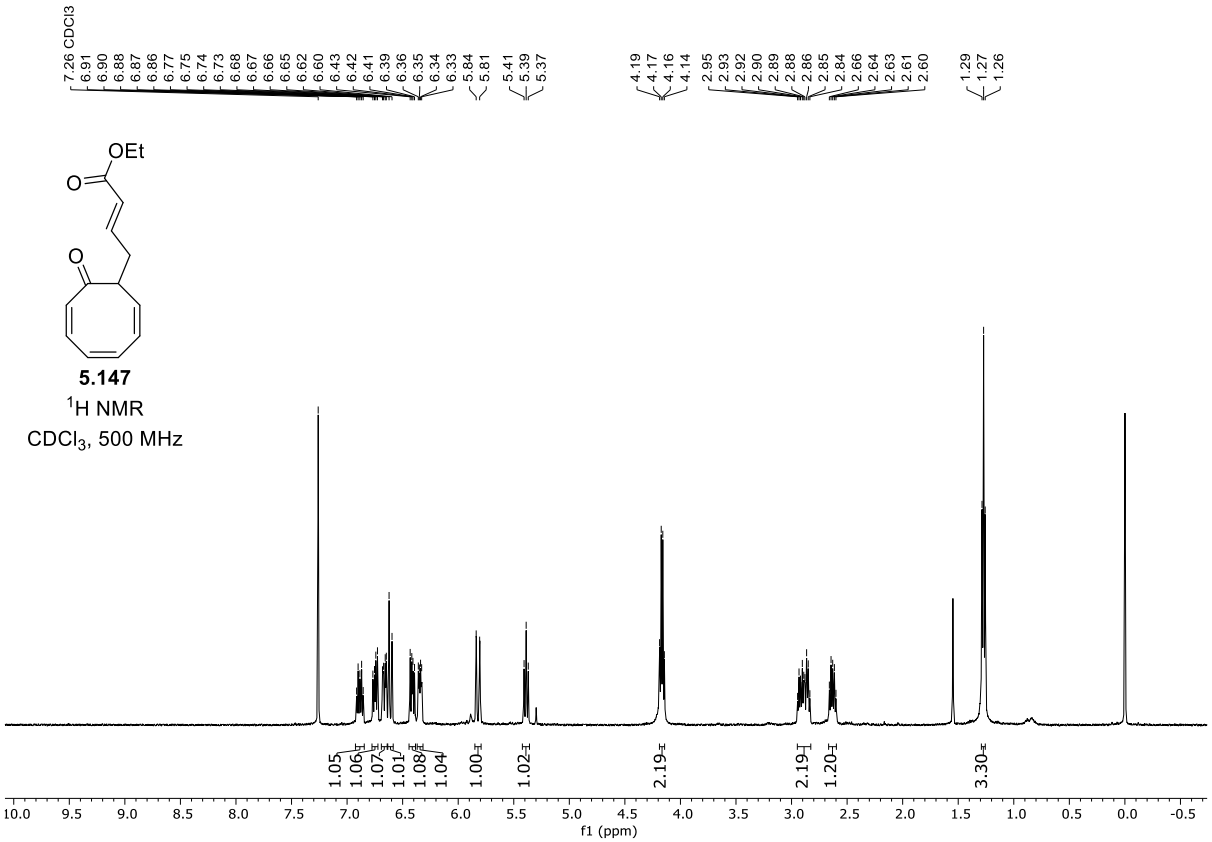
7.26 CDCl3
6.91
6.90
6.88
6.87
6.86
6.77
6.75
6.74
6.73
6.68
6.67
6.66
6.65
6.62
6.60
6.43
6.42
6.41
6.39
6.36
6.35
6.34
6.33
5.84
5.81
5.41
5.39
5.37
4.19
4.17
4.16
4.14
2.95
2.93
2.92
2.90
2.89
2.88
2.86
2.85
2.84
2.66
2.64
2.63
2.61
2.60
1.29
1.27
1.26
OEt
O
O
5.147
1H NMR
CDCl3, 500 MHz
1.05
1.06
1.07
1.01
1.08
1.04
1.00
1.02
2.19
2.19
1.20
3.30
f1 (ppm)

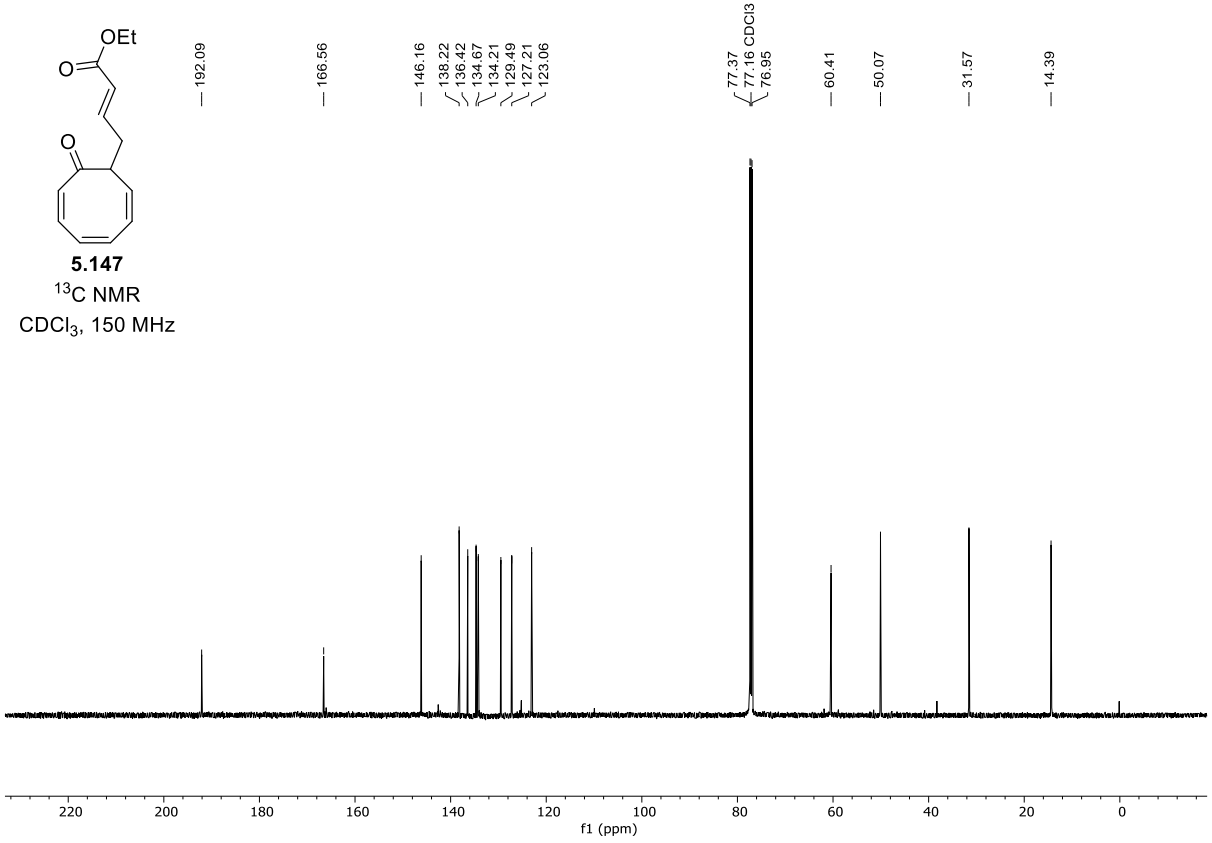
OEt
O
O
5.147
13C NMR
CDCl3, 150 MHz
192.09
166.56
146.16
138.22
136.42
134.67
134.21
129.49
127.21
123.06
77.37
77.16 CDCl3
76.95
60.41
50.07
31.57
14.39
f1 (ppm)

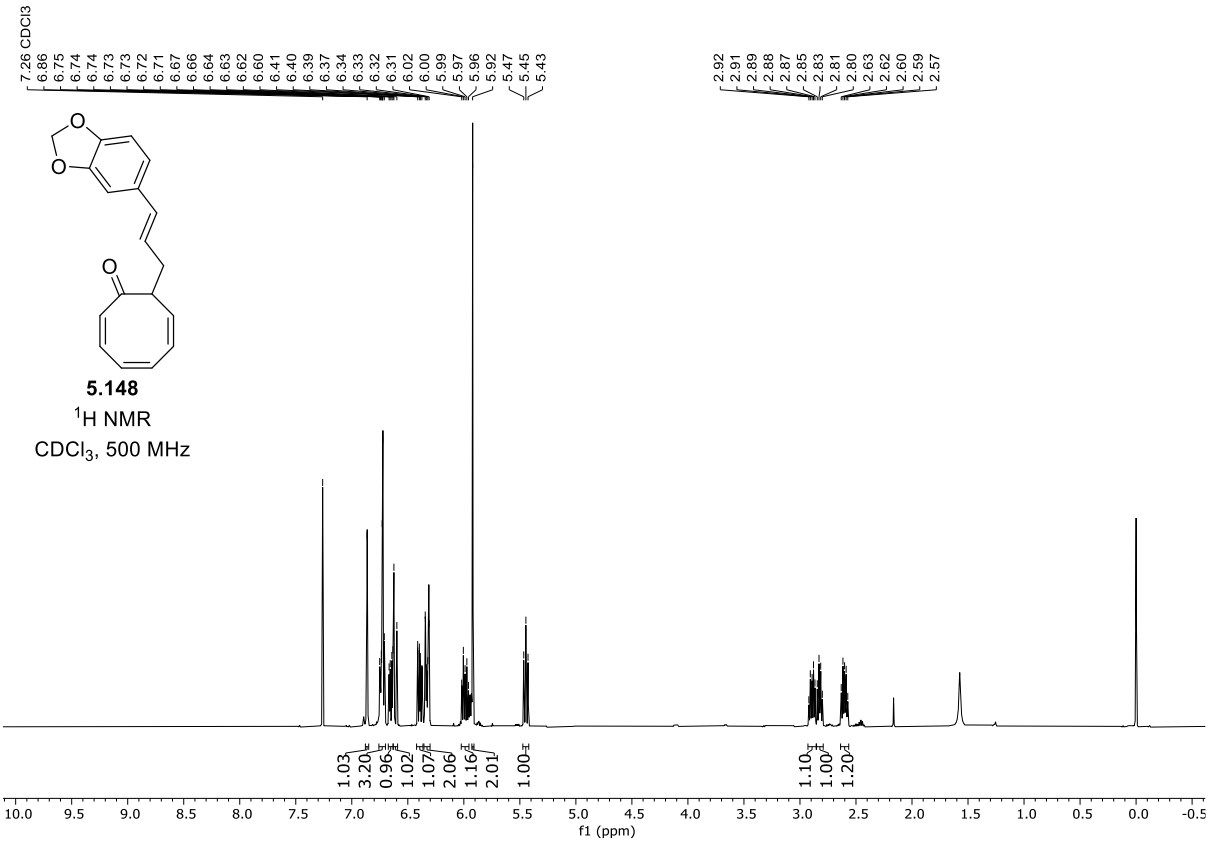
7.26 CDCl3
6.86
6.75
6.74
6.74
6.73
6.73
6.72
6.71
6.67
6.66
6.64
6.63
6.62
6.60
6.41
6.40
6.39
6.37
6.34
6.33
6.32
6.31
6.02
6.00
5.99
5.97
5.96
5.92
5.47
5.45
5.43
2.92
2.91
2.89
2.88
2.87
2.85
2.83
2.81
2.80
2.63
2.62
2.60
2.59
2.57
O
O
O
5.148
1H NMR
CDCl3, 500 MHz
1.03
3.20
0.96
1.02
1.07
2.06
1.16
2.01
1.00
1.10
1.00
1.20
10.0
9.5
9.0
8.5
8.0
7.5
7.0
6.5
6.0
5.5
5.0
4.5
4.0
3.5
3.0
2.5
2.0
1.5
1.0
0.5
0.0
-0.5
f1 (ppm)

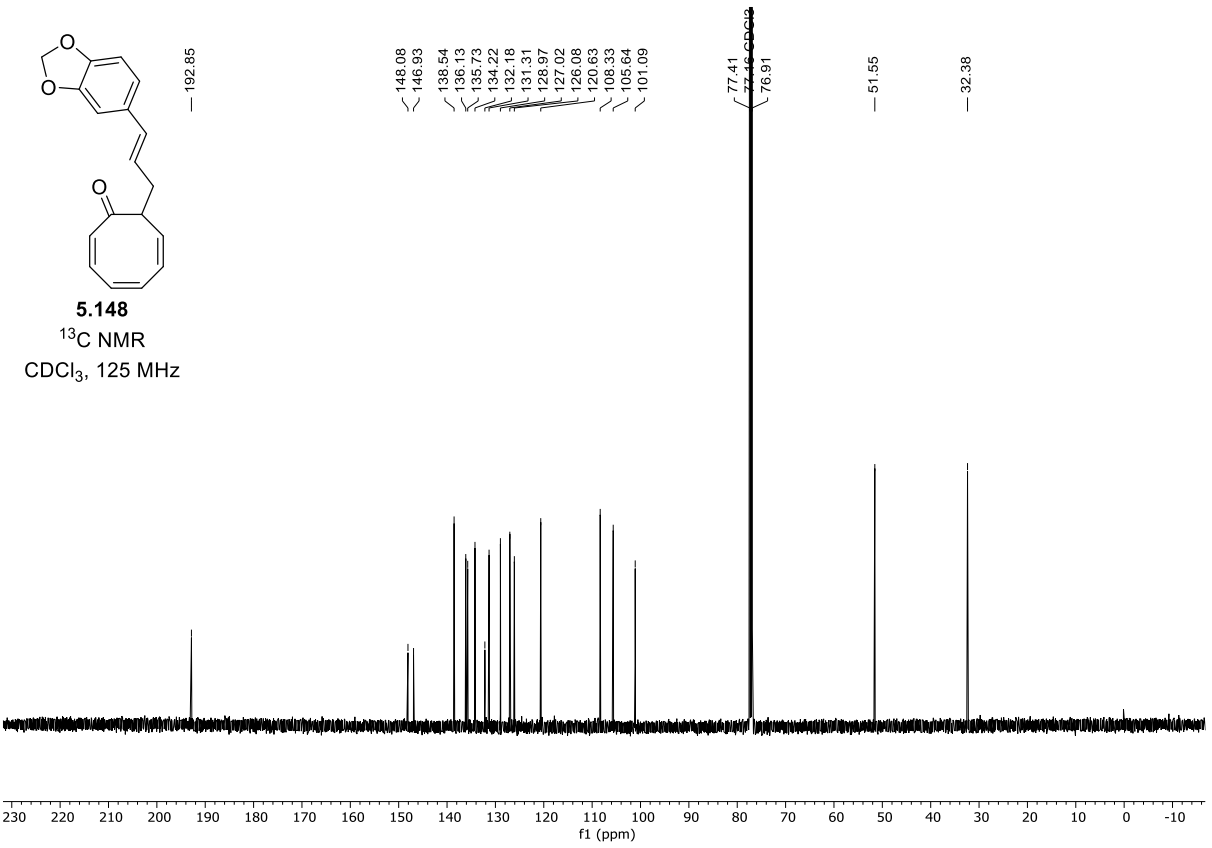
O
O
O
5.148
13C NMR
CDCl3, 125 MHz
192.85
148.08
146.93
138.54
136.13
135.73
134.22
132.18
131.31
128.97
127.02
126.08
120.63
108.33
105.64
101.09
77.41
77.16 CDCl3
76.91
51.55
32.38
230
220
210
200
190
180
170
160
150
140
130
120
110
100
90
80
70
60
50
40
30
20
10
0
-10
f1 (ppm)

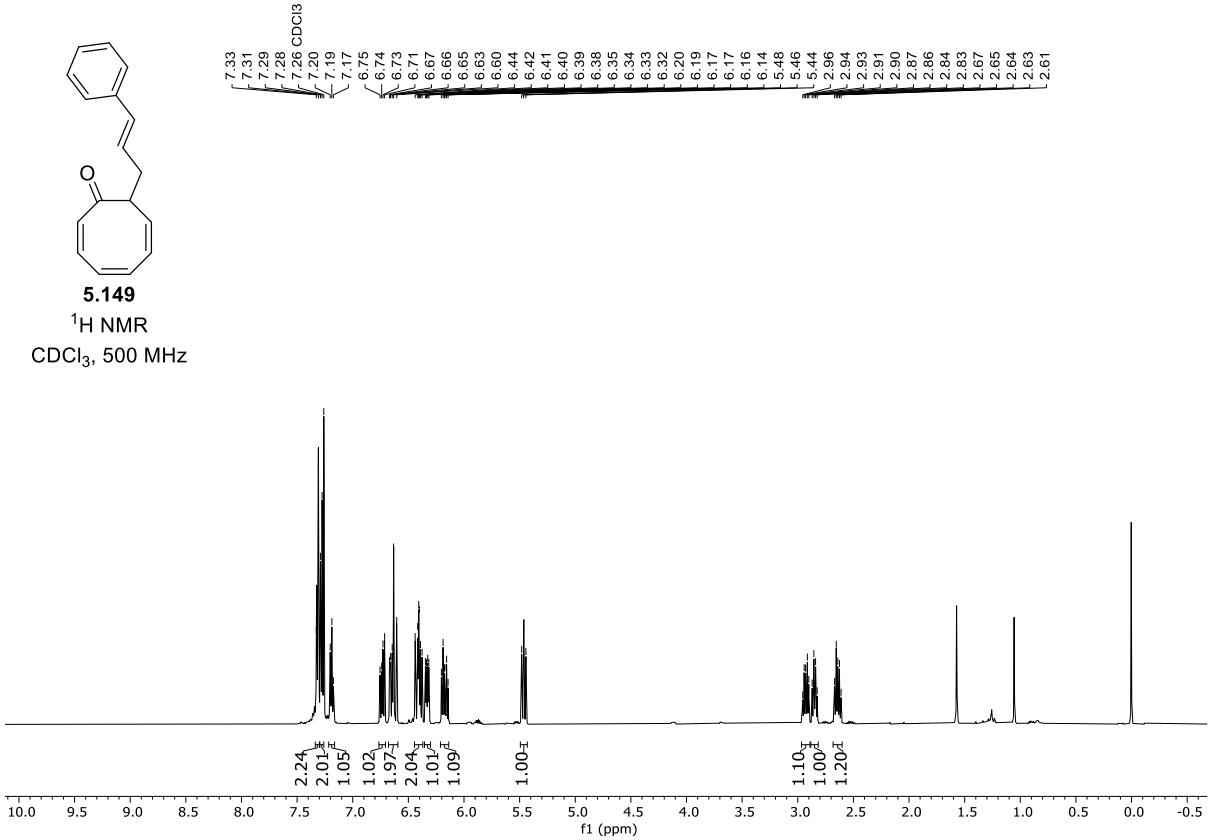
7.33
7.31
7.29
7.28
7.26 CDCl3
7.20
7.19
7.17
6.75
6.74
6.73
6.71
6.67
6.66
6.65
6.63
6.60
6.44
6.42
6.41
6.40
6.39
6.38
6.35
6.34
6.33
6.32
6.20
6.19
6.17
6.17
6.16
6.14
5.48
5.46
5.44
2.96
2.94
2.93
2.91
2.90
2.87
2.86
2.84
2.83
2.67
2.65
2.64
2.63
2.61
O
5.149
1H NMR
CDCl3, 500 MHz
2.24
2.01
1.05
1.02
1.97
2.04
1.01
1.09
1.00
1.10
1.00
1.20
10.0
9.5
9.0
8.5
8.0
7.5
7.0
6.5
6.0
5.5
5.0
4.5
4.0
3.5
3.0
2.5
2.0
1.5
1.0
0.5
0.0
-0.5
f1 (ppm)

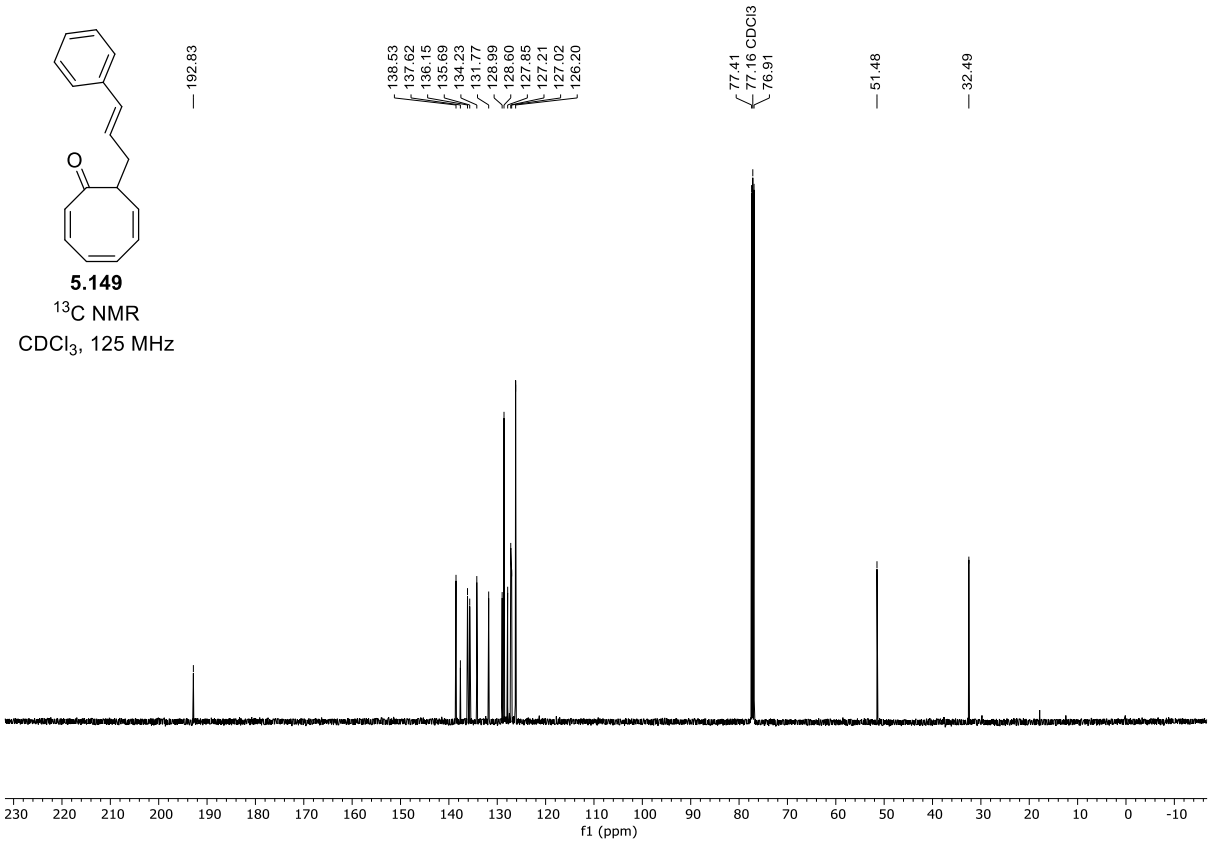
192.83
138.53
137.62
136.15
135.69
134.23
131.77
128.99
128.60
127.85
127.21
127.02
126.20
77.41
77.16 CDCl3
76.91
51.48
32.49
O
5.149
13C NMR
CDCl3, 125 MHz
230
220
210
200
190
180
170
160
150
140
130
120
110
100
90
80
70
60
50
40
30
20
10
0
-10
f1 (ppm)

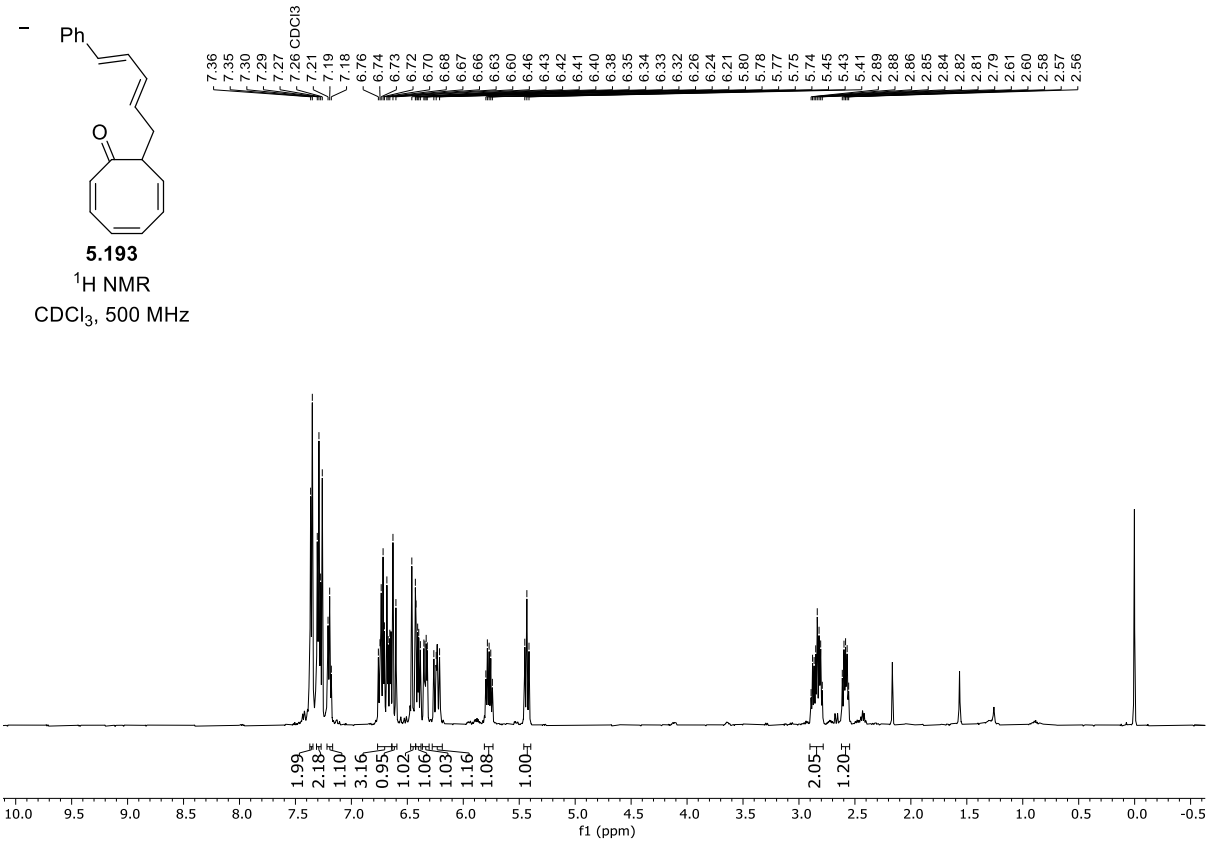

5.193

^{1}H NMR

$CDCl_3$, 500 MHz

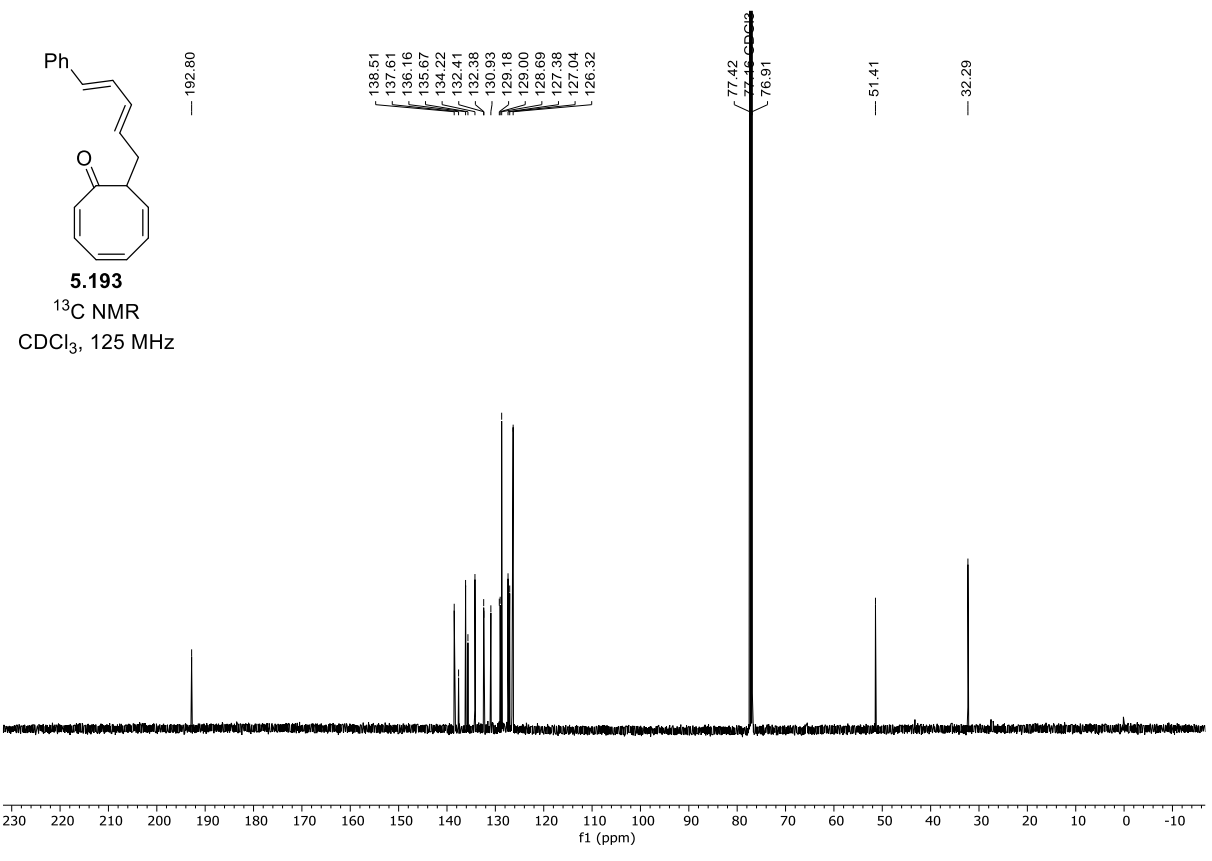

5.193

^{13}C NMR

$CDCl_3$, 125 MHz

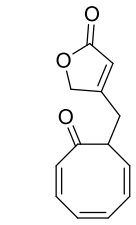

5.150

^{1}H NMR

$CDCl_3$, 500 MHz

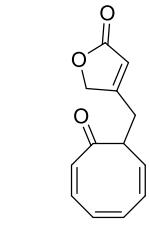

5.150

^{13}C NMR

$CDCl_3$, 125 MHz

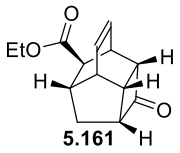

5.161

^{1}H NMR

$CDCl_3$, 500 MHz

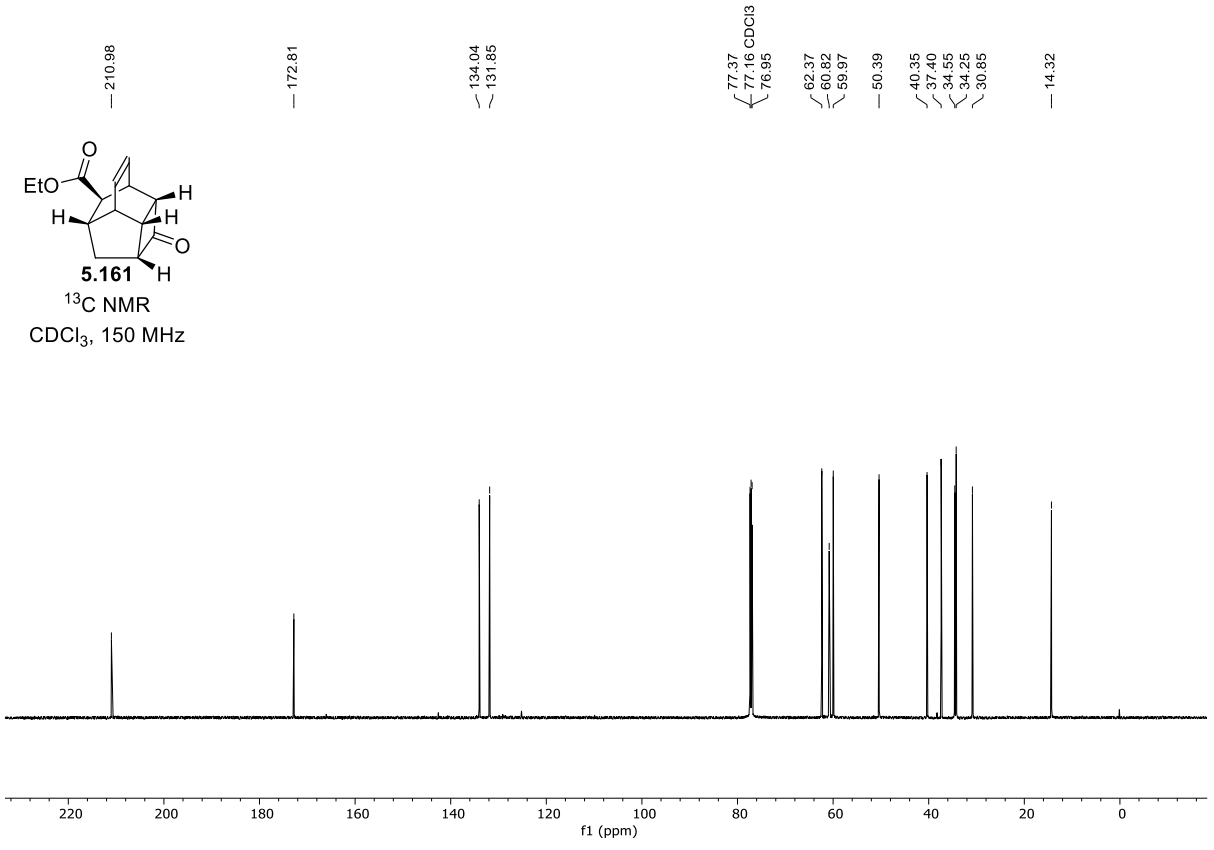

5.161

^{13}C NMR

$CDCl_3$, 150 MHz

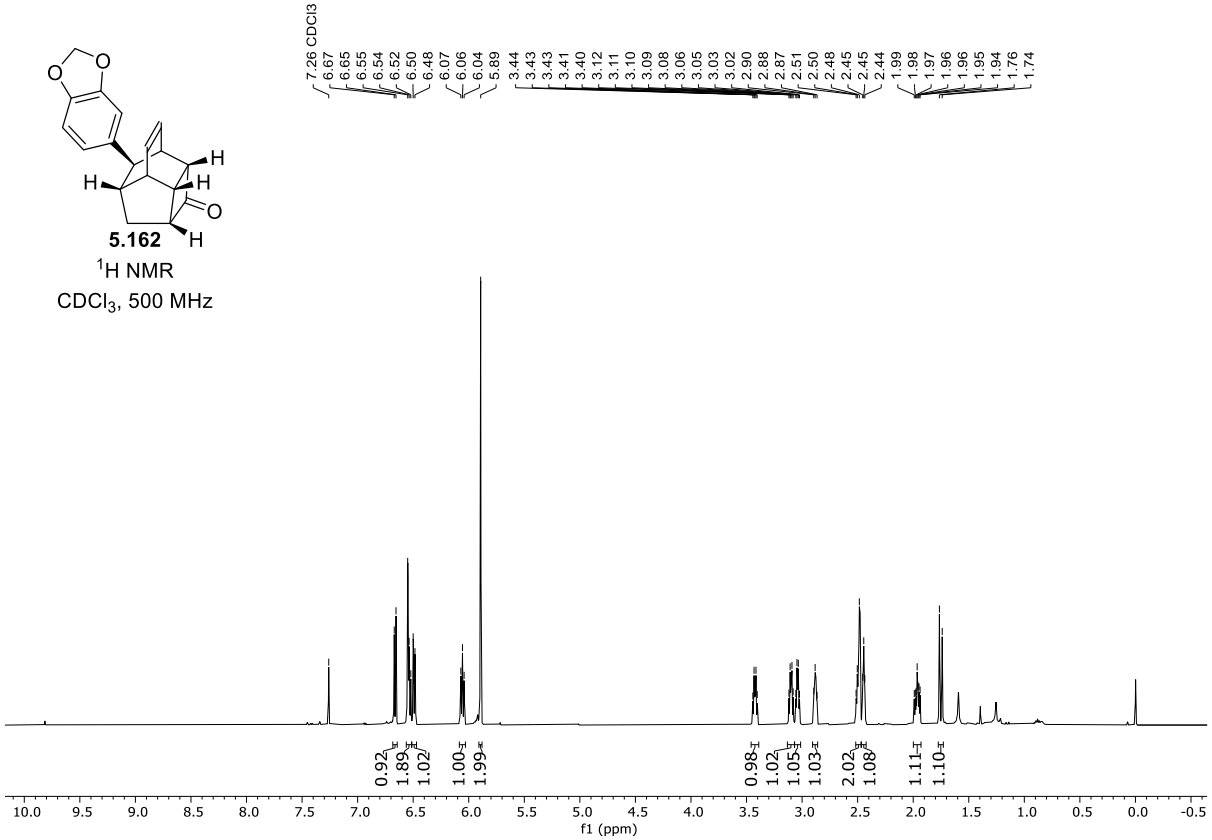

^{1}H NMR

$CDCl_3$, 500 MHz

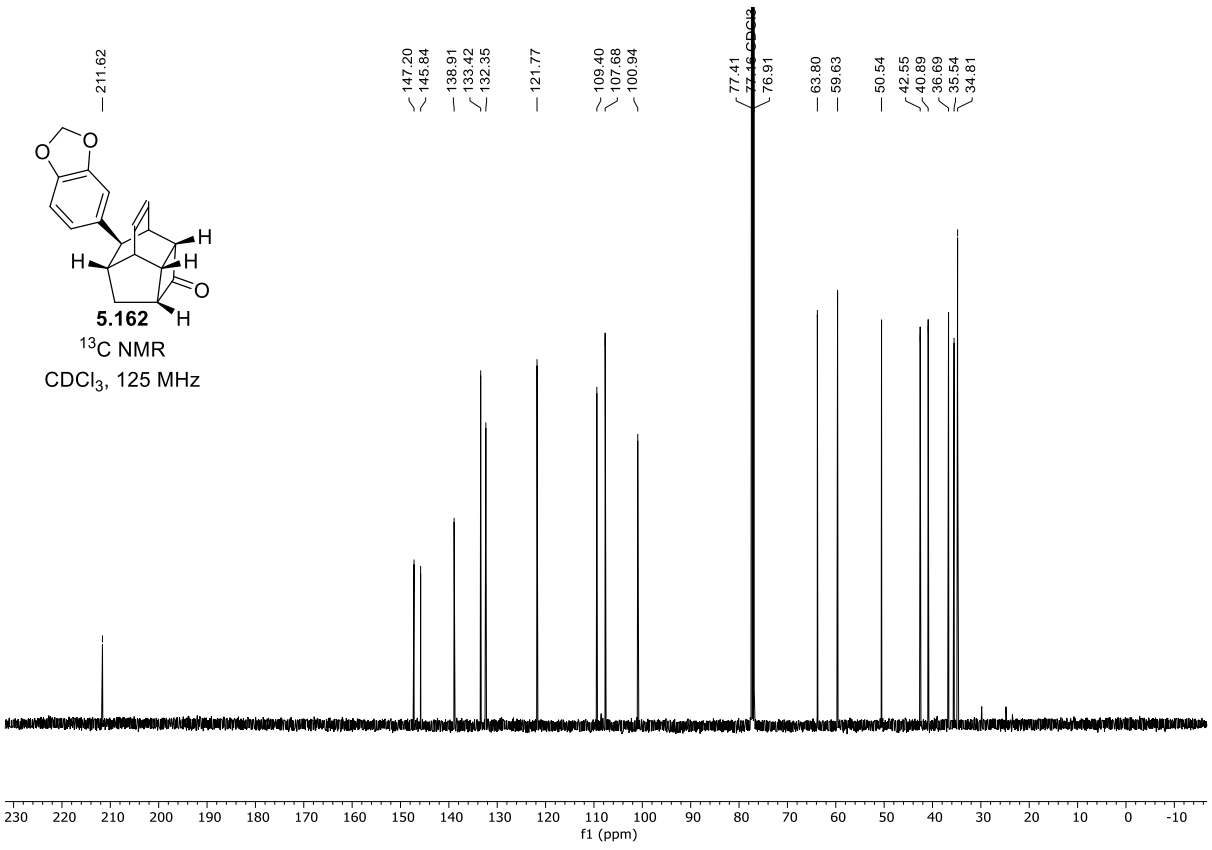

^{13}C NMR

$CDCl_3$, 125 MHz

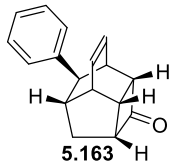

5.163

^{1}H NMR

$CDCl_3$, 500 MHz

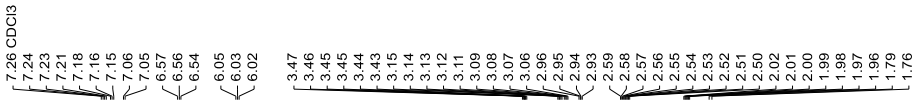

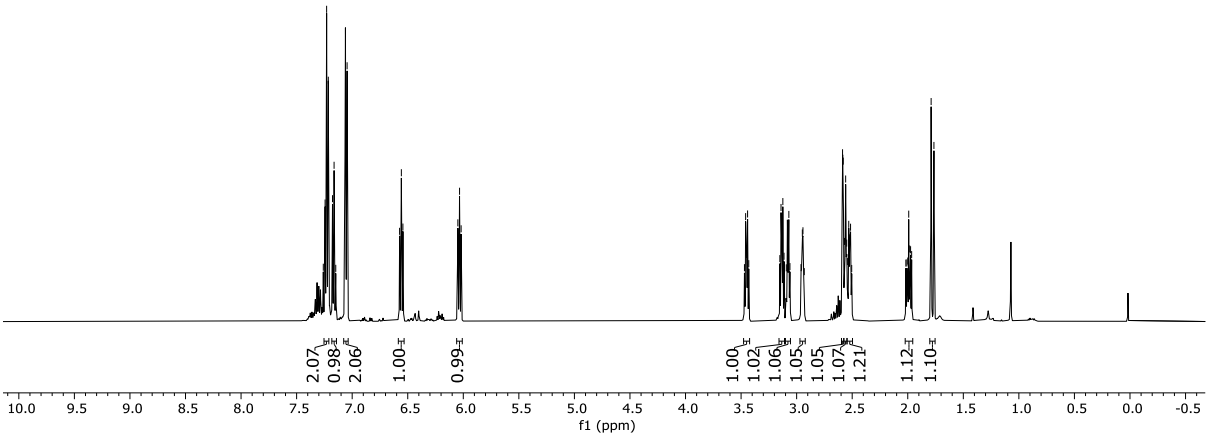

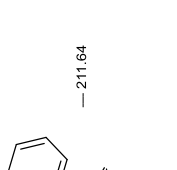

5.163

^{13}C NMR

$CDCl_3$, 125 MHz

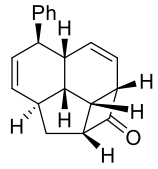

5.194

^{1}H NMR

$CDCl_3$, 500 MHz

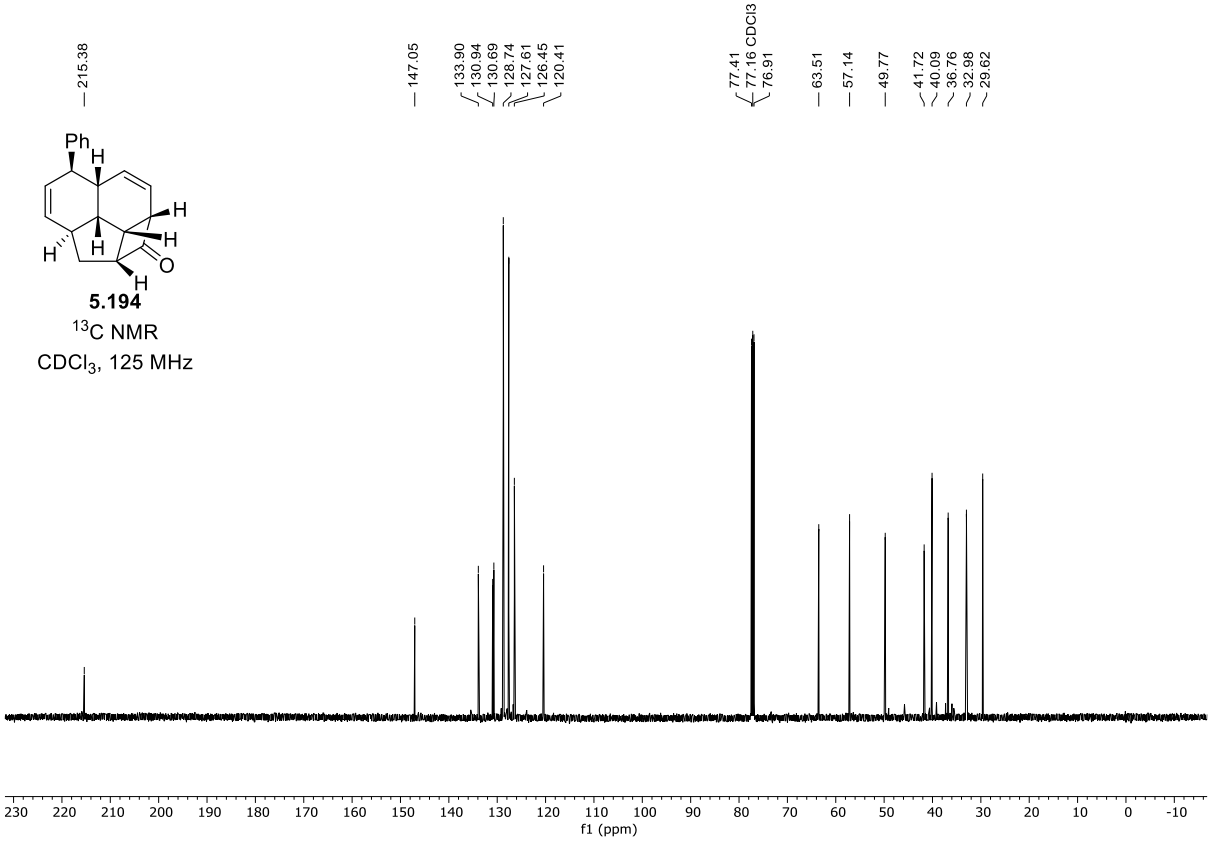

5.194

^{13}C NMR

$CDCl_3$, 125 MHz

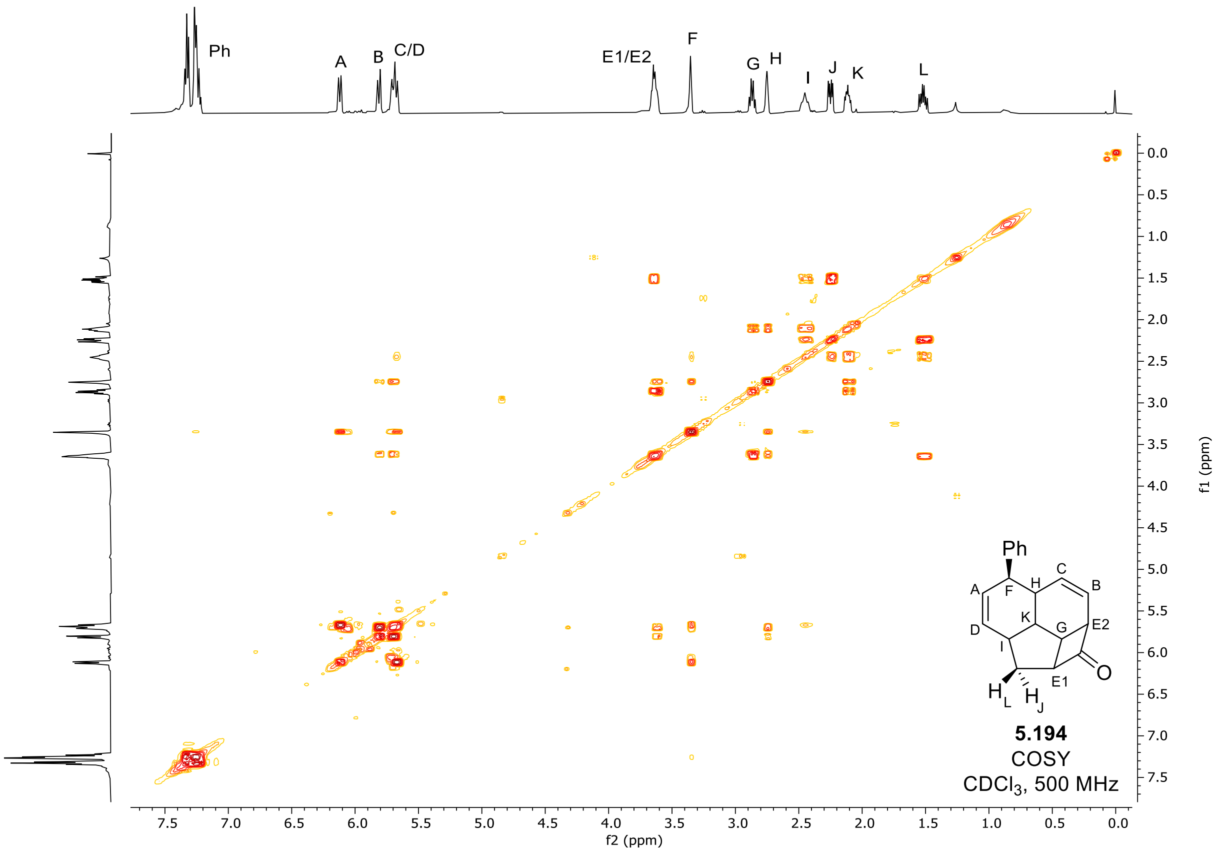

Ph
A
B
C/D
E1/E2
F
G
H
I
J
K
L
5.194
COSY
$CDCl_3$, 500 MHz
f2 (ppm)
f1 (ppm)

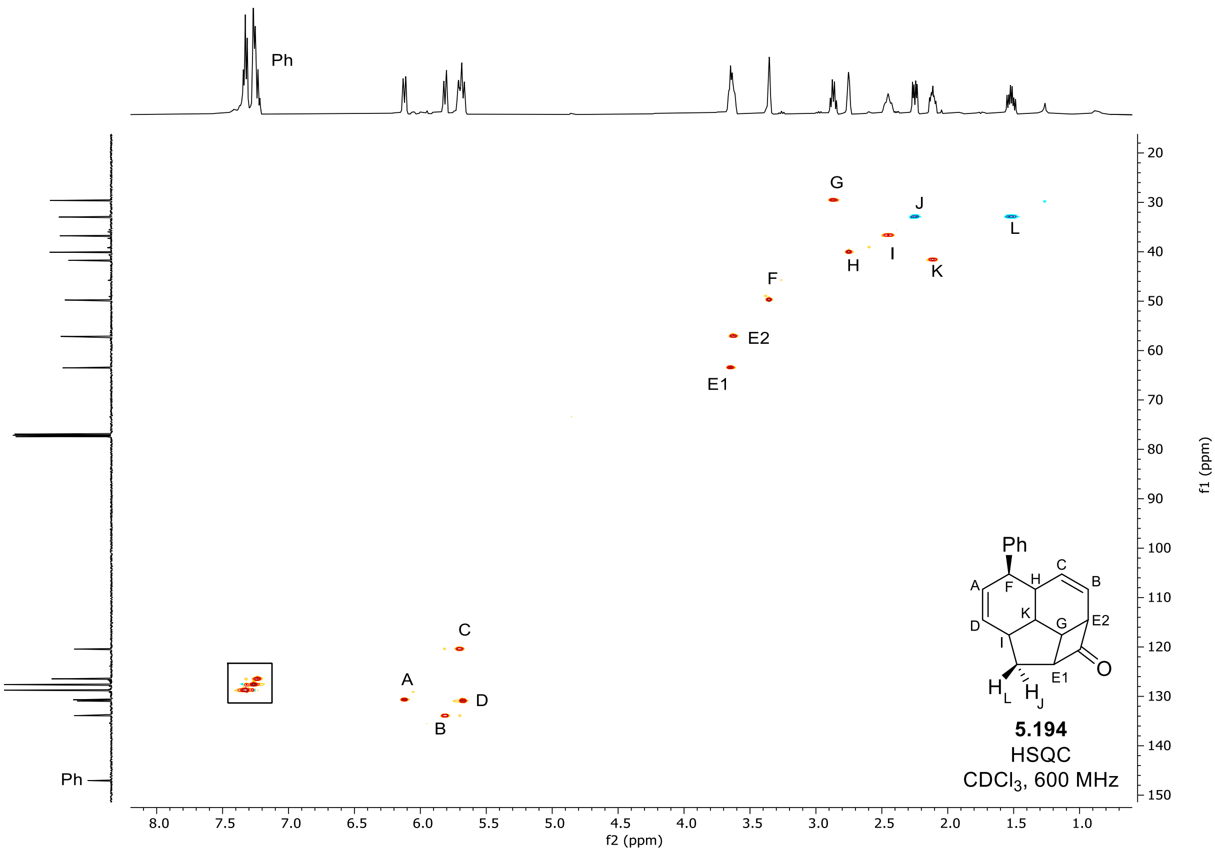

Ph
G
J
L
H
I
K
F
E2
E1
C
A
D
B
5.194
HSQC
$CDCl_3$, 600 MHz
f2 (ppm)
f1 (ppm)

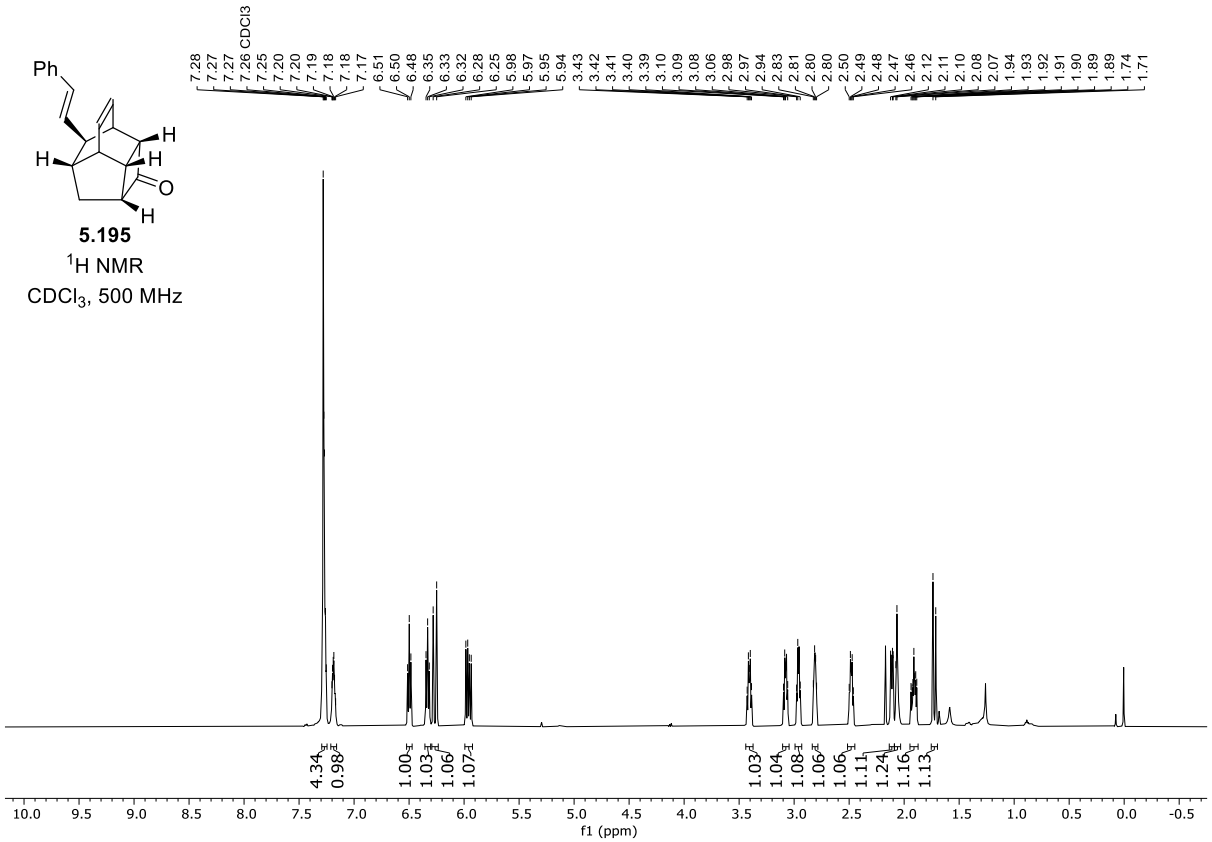
Ph
H
H
H
O
H
5.195
1H NMR
CDCl3, 500 MHz
7.28
7.27
7.27
7.26 CDCl3
7.25
7.20
7.20
7.19
7.18
7.18
7.17
6.51
6.50
6.48
6.35
6.33
6.32
6.28
6.25
5.98
5.97
5.95
5.94
3.43
3.42
3.41
3.40
3.39
3.10
3.09
3.08
3.06
2.98
2.97
2.94
2.83
2.81
2.80
2.80
2.50
2.49
2.48
2.47
2.46
2.12
2.11
2.10
2.08
2.07
1.94
1.93
1.92
1.91
1.90
1.89
1.89
1.74
1.71
4.34
0.98
1.00
1.03
1.06
1.07
1.03
1.04
1.08
1.06
1.06
1.11
1.24
1.16
1.13
f1 (ppm)

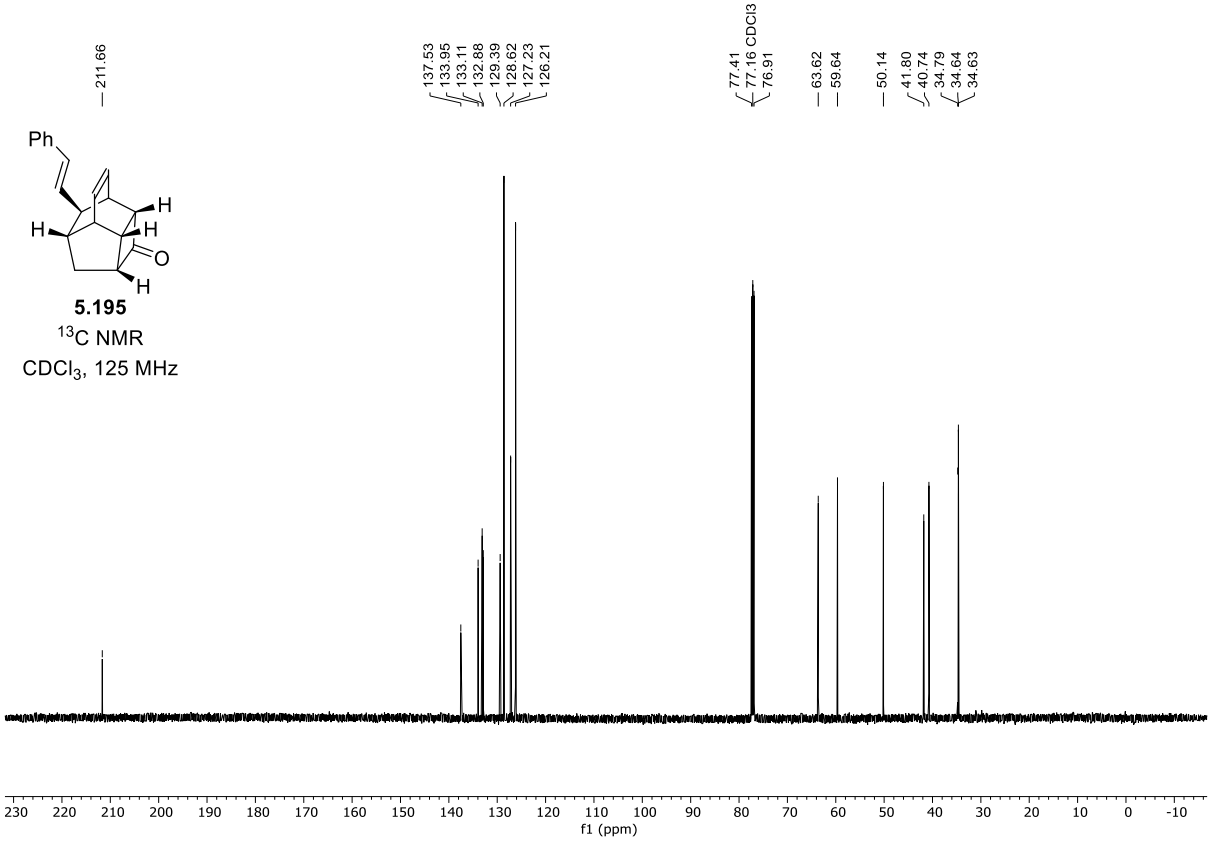
211.66
137.53
133.95
133.11
132.88
129.39
128.62
127.23
126.21
77.41
77.16 CDCl3
76.91
63.62
59.64
50.14
41.80
40.74
34.79
34.64
34.63
Ph
H
H
H
O
H
5.195
13C NMR
CDCl3, 125 MHz
f1 (ppm)

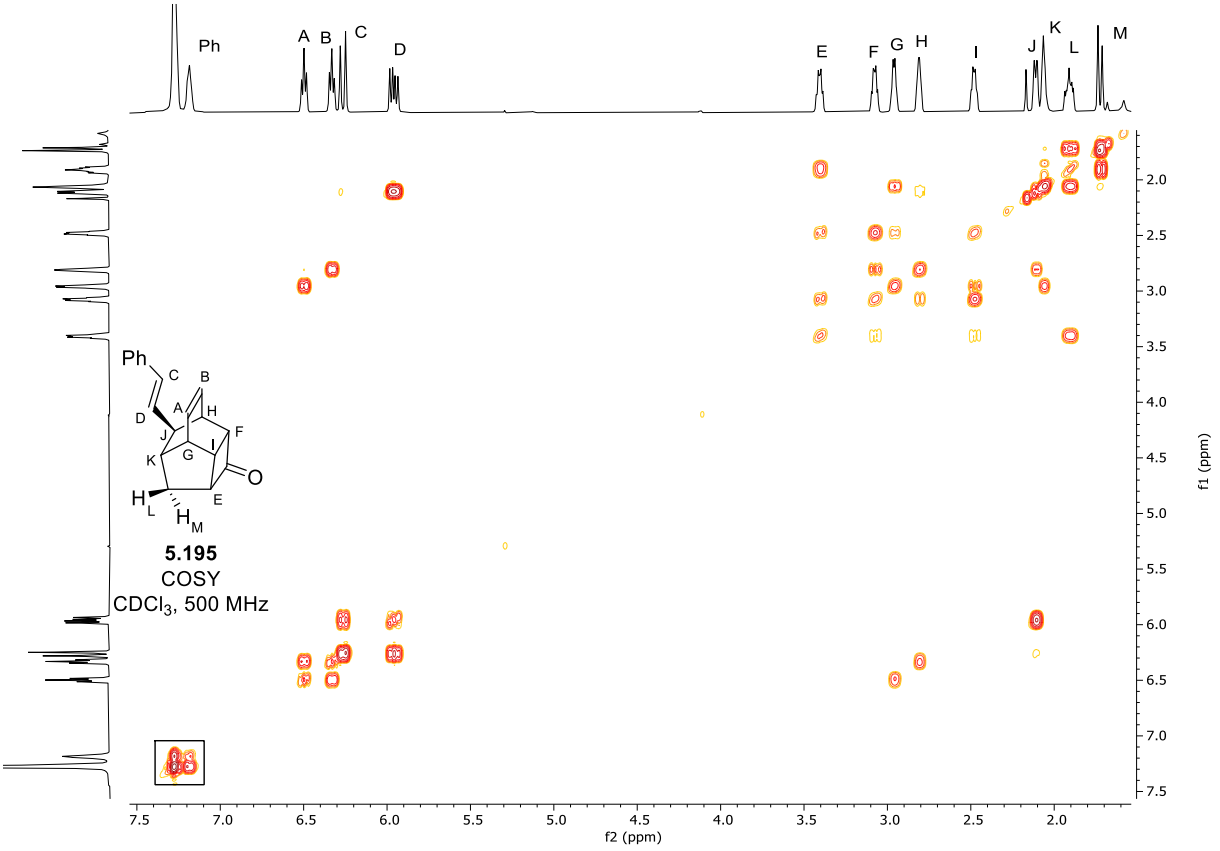

5.195
COSY
$CDCl_3$, 500 MHz

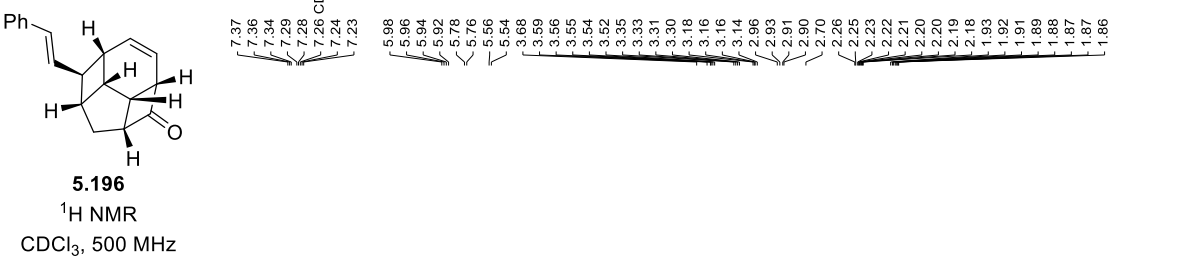

5.196
^{1}H NMR
$CDCl_3$, 500 MHz

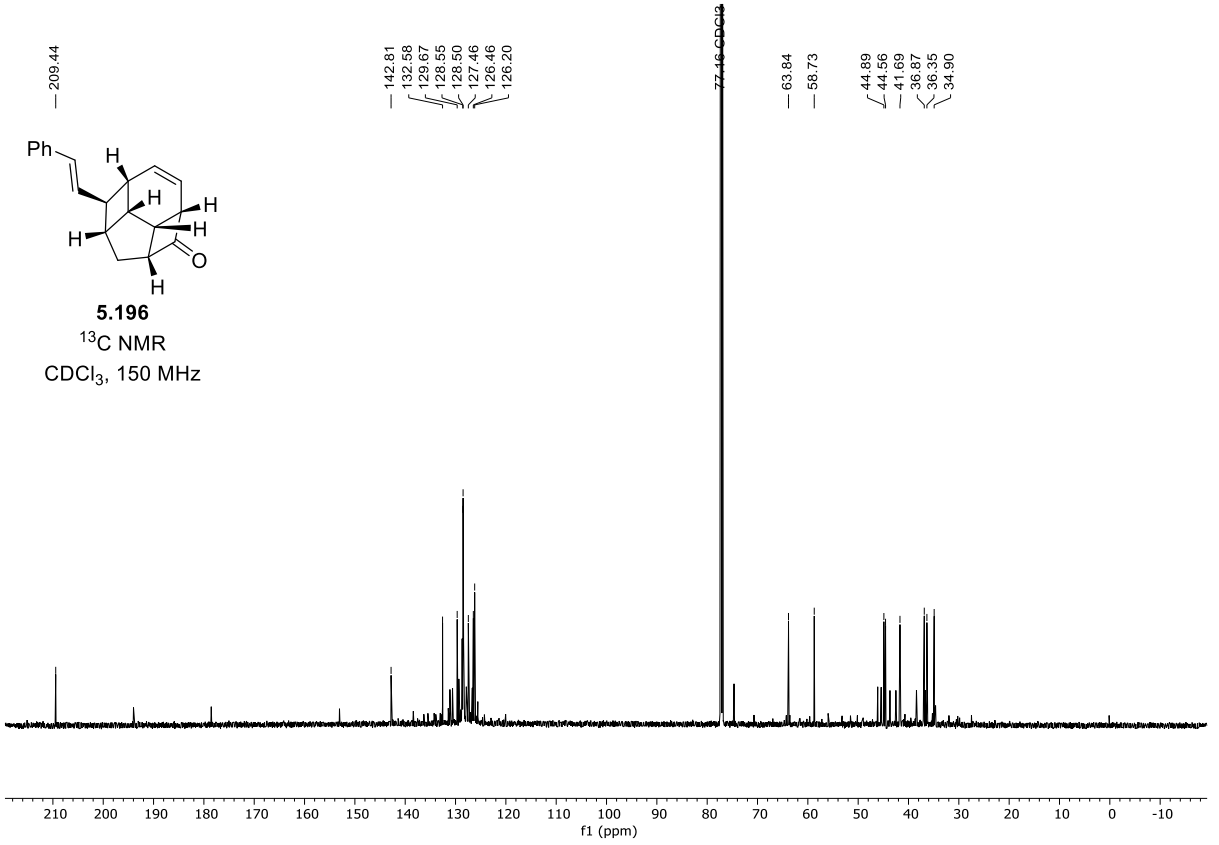

5.196

^{13}C NMR

$CDCl_3$, 150 MHz

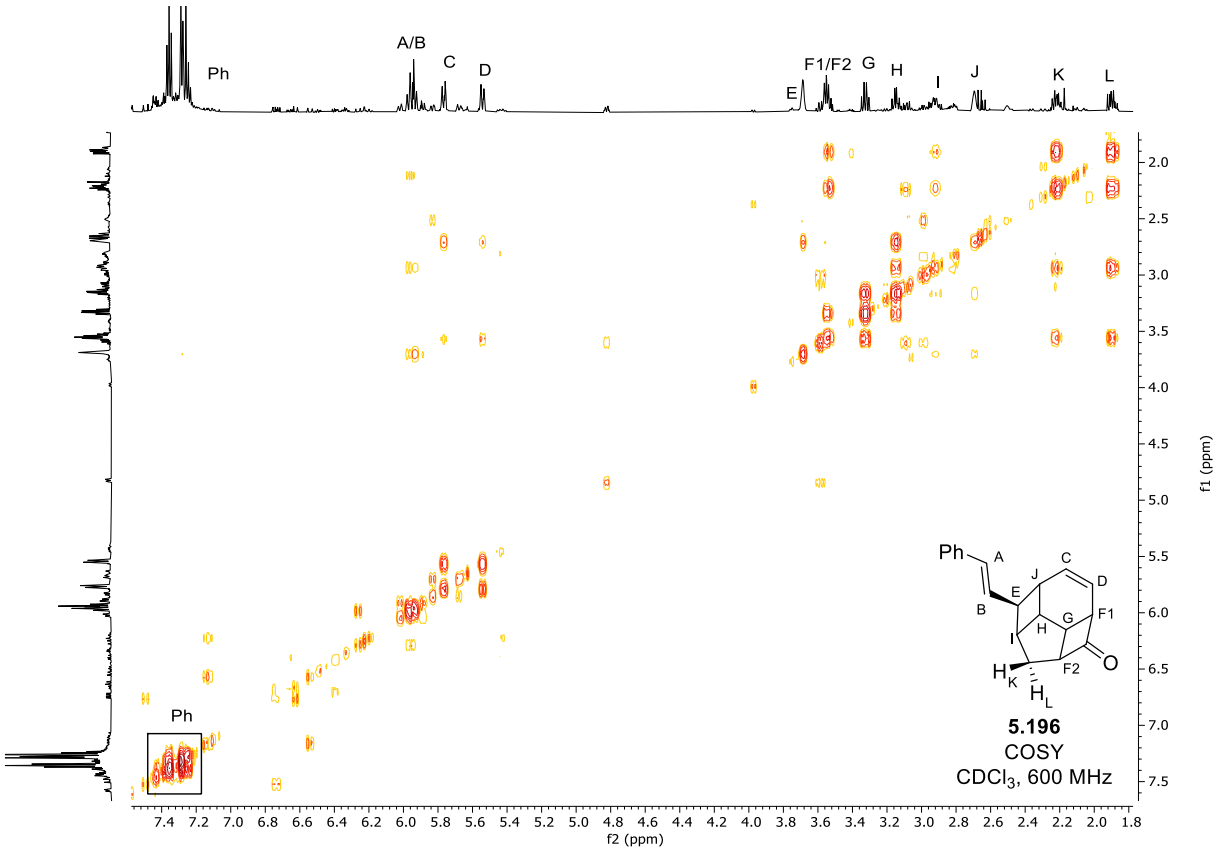

5.196

COSY

$CDCl_3$, 600 MHz

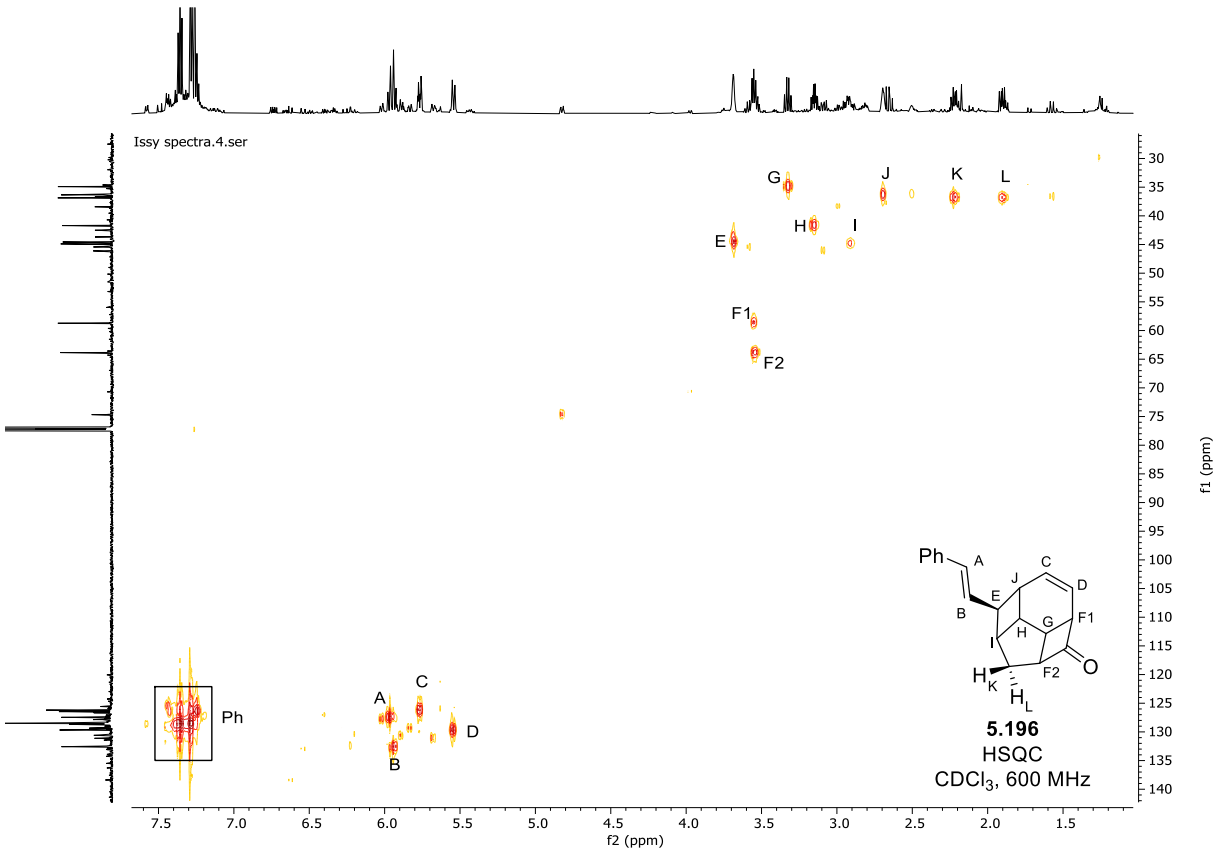
Issy spectra.4.ser
G
J
K
L
H
I
E
F1
F2
Ph
A
B
C
D
f1 (ppm)
f2 (ppm)
5.196
HSQC
CDCl3, 600 MHz

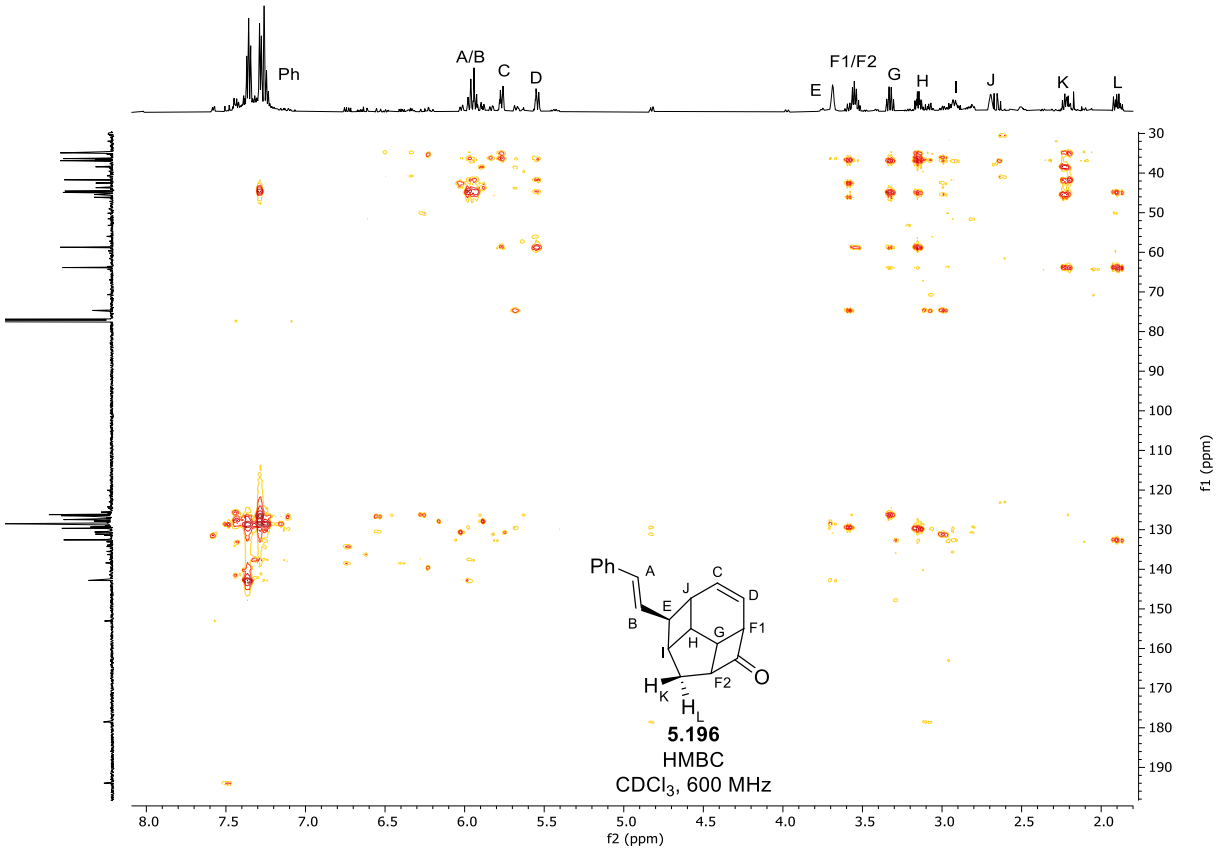
Ph
A/B
C
D
F1/F2
E
G
H
I
J
K
L
f1 (ppm)
f2 (ppm)
5.196
HMBC
CDCl3, 600 MHz

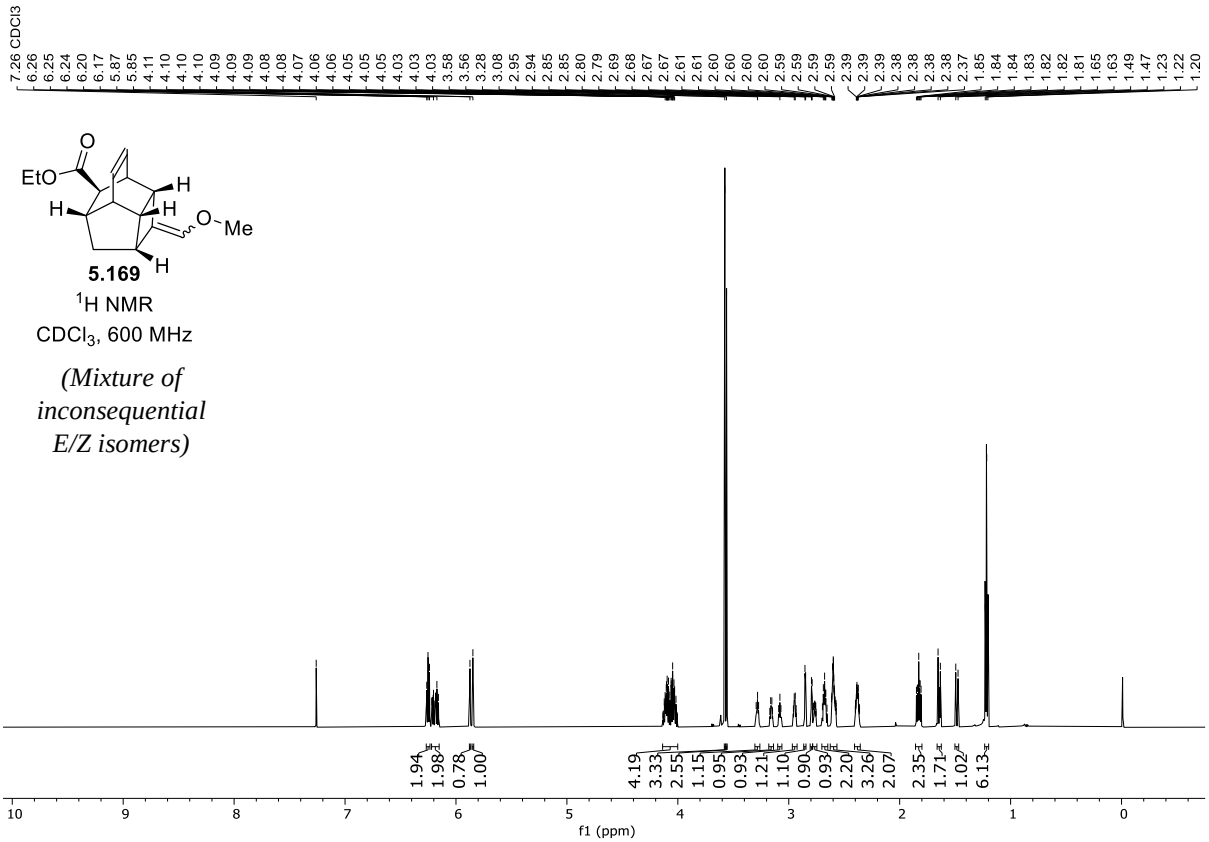

5.169

^{1}H NMR

$CDCl_3$, 600 MHz

(Mixture of inconsequential E/Z isomers)

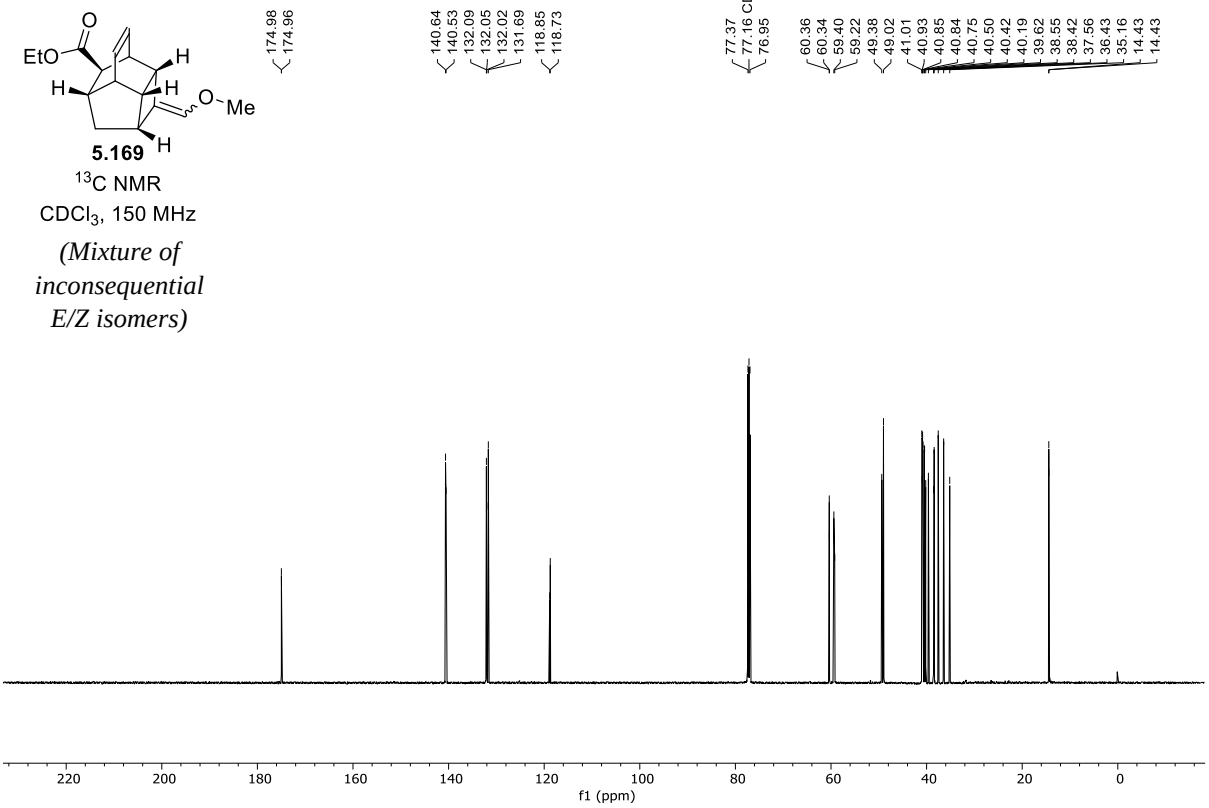

5.169

^{13}C NMR

$CDCl_3$, 150 MHz

(Mixture of inconsequential E/Z isomers)

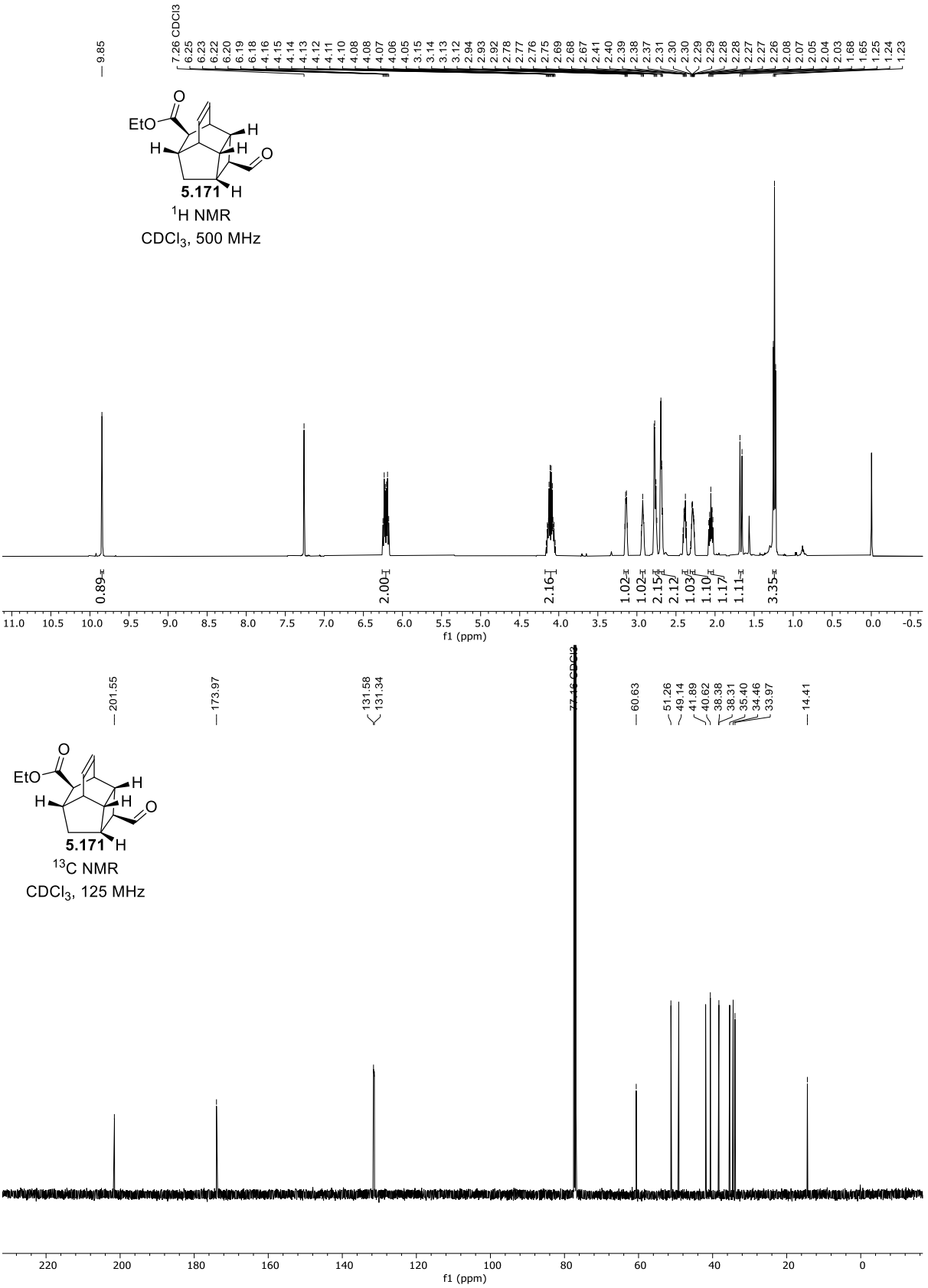
9.85
7.26 CDCl3
6.25
6.23
6.22
6.20
6.19
6.18
4.16
4.15
4.14
4.13
4.12
4.11
4.10
4.08
4.08
4.07
4.06
4.05
3.15
3.14
3.13
3.12
2.94
2.93
2.92
2.78
2.77
2.76
2.75
2.69
2.68
2.67
2.41
2.40
2.39
2.38
2.37
2.31
2.30
2.30
2.29
2.29
2.28
2.28
2.27
2.27
2.26
2.08
2.07
2.05
2.04
2.03
1.68
1.65
1.25
1.24
1.23
EtO
O
H
H
H
O
5.171
H
1H NMR
CDCl3, 500 MHz
0.89
2.00
2.16
1.02
1.02
2.15
2.12
1.03
1.10
1.17
1.11
3.35
f1 (ppm)
201.55
173.97
131.58
131.34
77.16 CDCl3
60.63
51.26
49.14
41.89
40.62
38.38
38.31
35.40
34.46
33.97
14.41
EtO
O
H
H
H
O
5.171
H
13C NMR
CDCl3, 125 MHz
f1 (ppm)

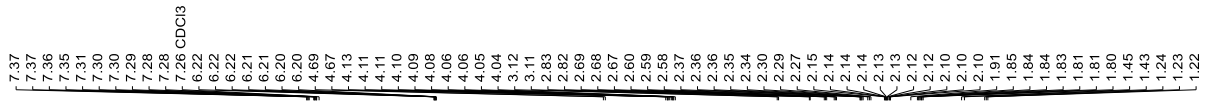

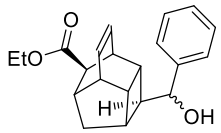

diastereomer A 5.172

^{1}H NMR

$CDCl_3$, 500 MHz

(Inconsequential Stereochemistry Not determined)

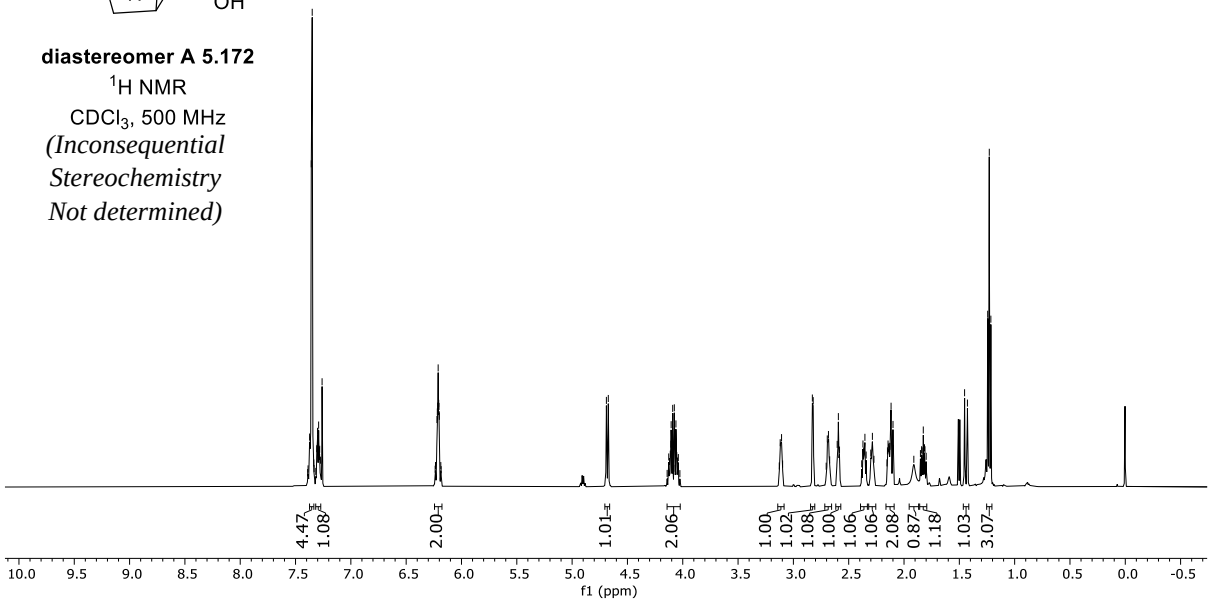

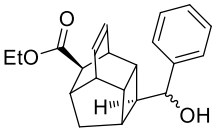

diastereomer A 5.172

^{13}C NMR

$CDCl_3$, 150 MHz

(Inconsequential Stereochemistry Not determined)

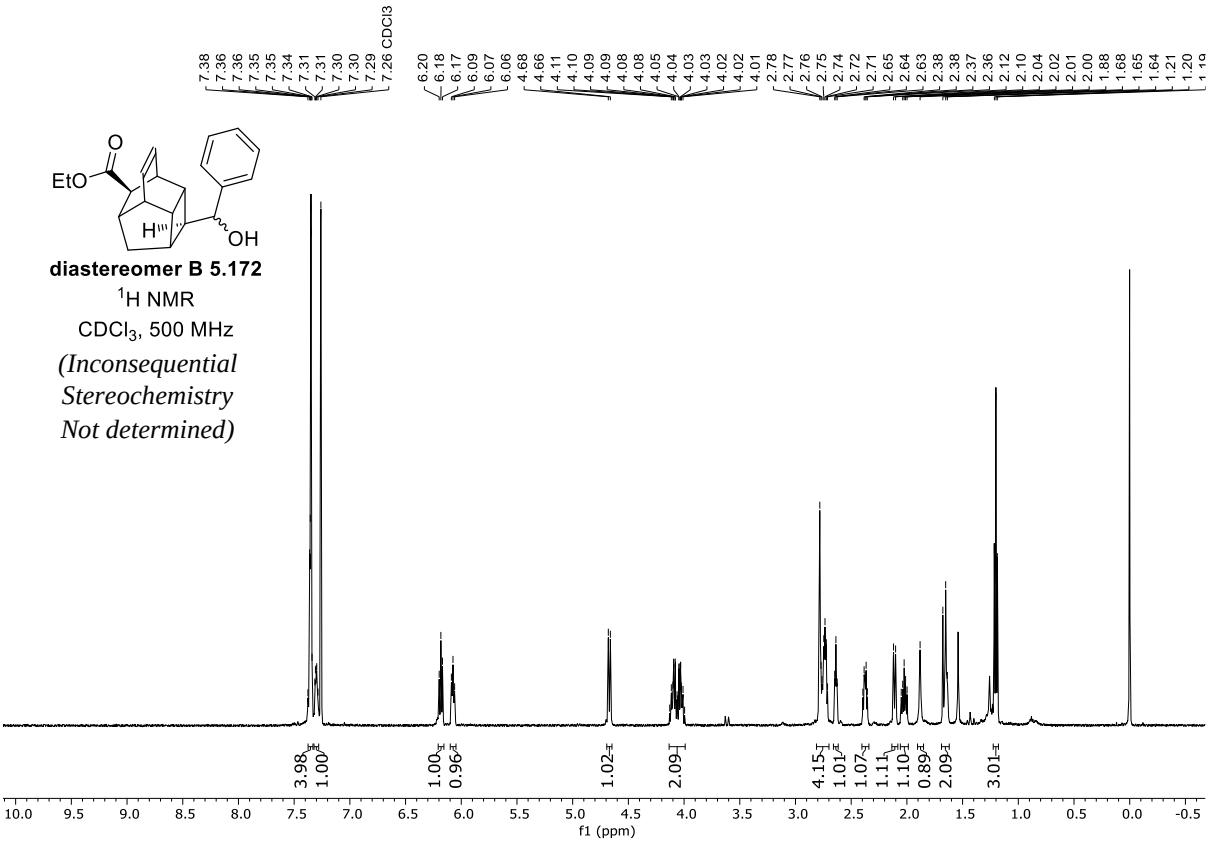
EtO
O
H
OH
diastereomer B 5.172
1H NMR
CDCl3, 500 MHz
(Inconsequential
Stereochemistry
Not determined)
f1 (ppm)

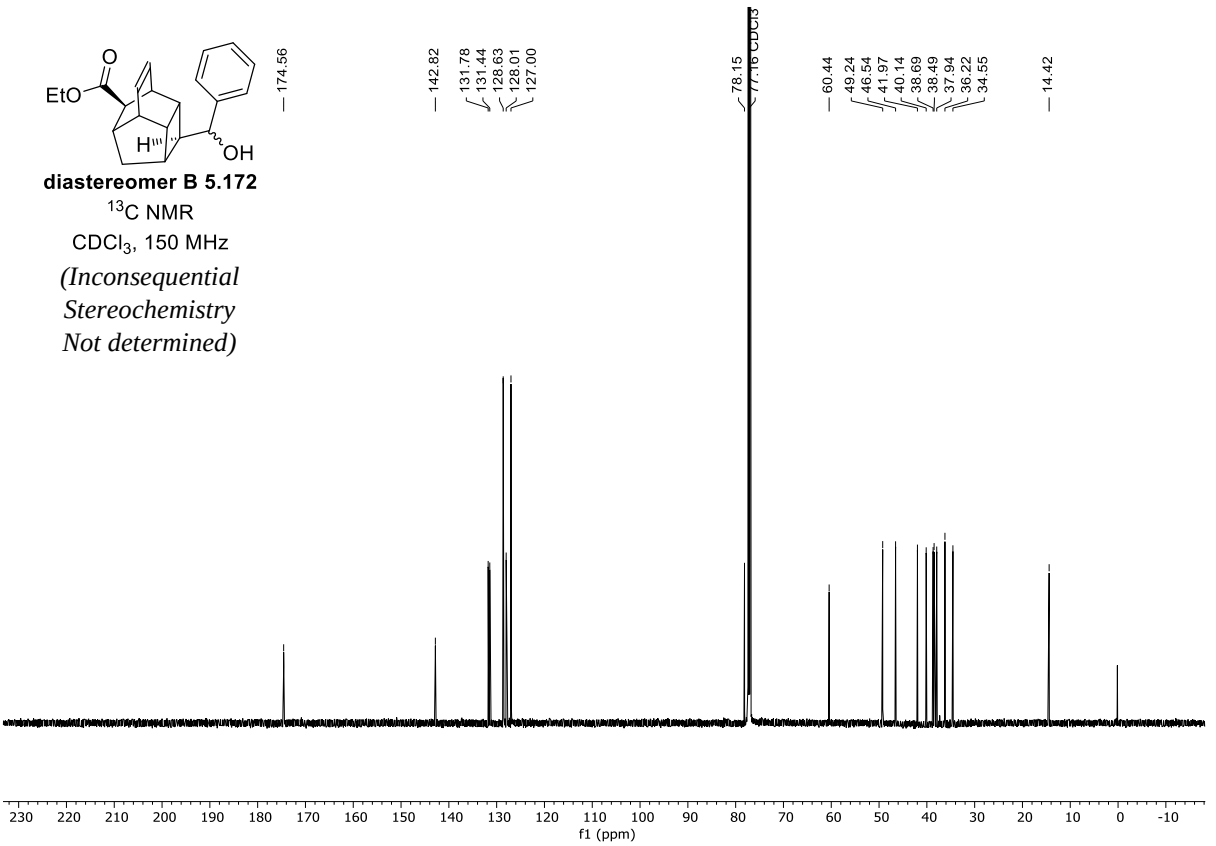
EtO
O
H
OH
diastereomer B 5.172
13C NMR
CDCl3, 150 MHz
(Inconsequential
Stereochemistry
Not determined)
f1 (ppm)

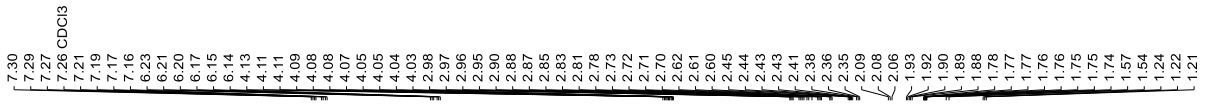

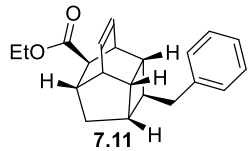

7.11

^{1}H NMR

$CDCl_3$, 500 MHz

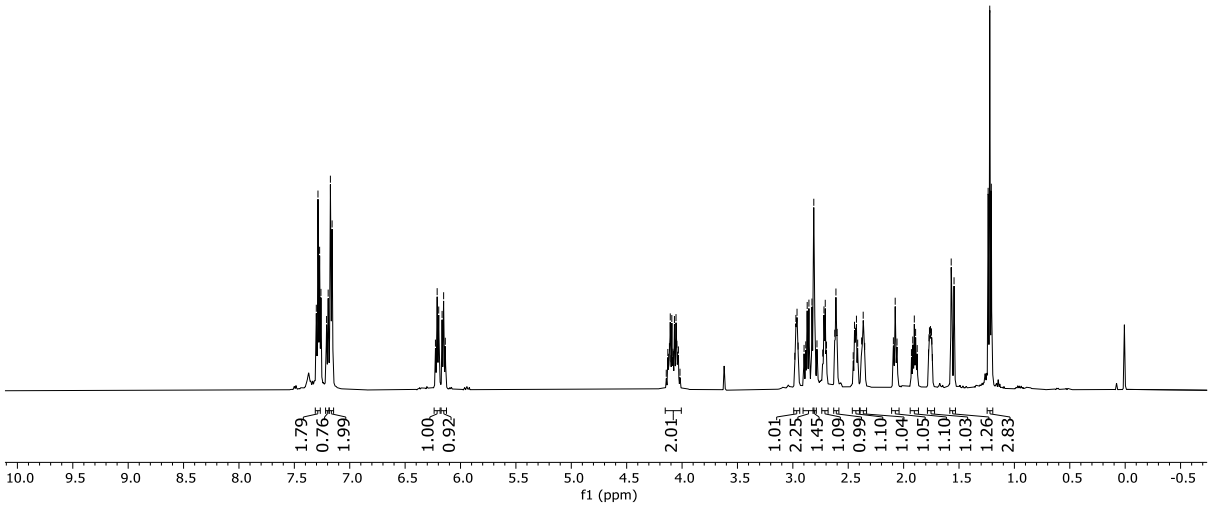

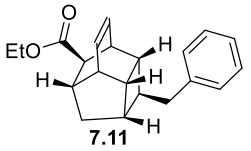

7.11

^{13}C NMR

$CDCl_3$, 125 MHz

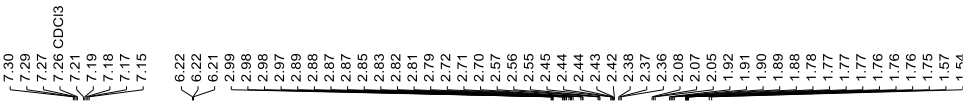

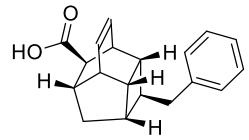

kingianic acid B (5.173)

^{1}H NMR

$CDCl_3$, 600 MHz

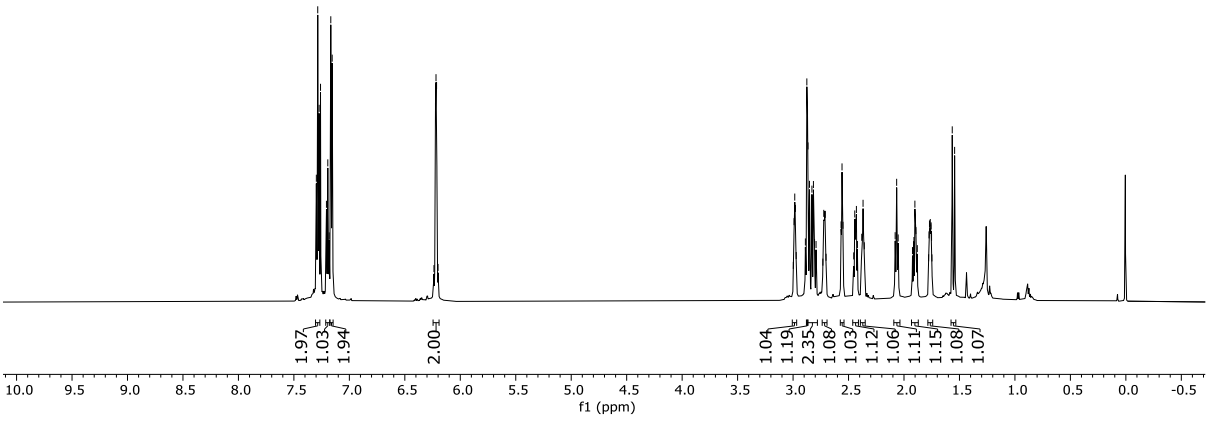

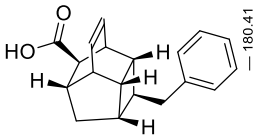

kingianic acid B (5.173)

^{13}C NMR

$CDCl_3$, 150 MHz

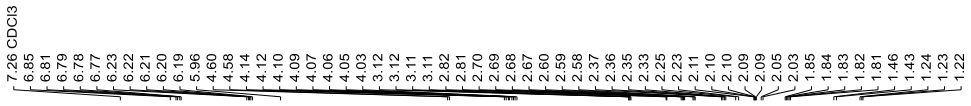

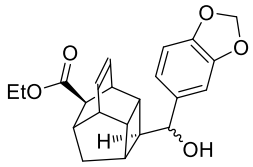

diastereomer A 7.12

^{1}H NMR

$CDCl_3$, 600 MHz

(Inconsequential Stereochemistry Not determined)

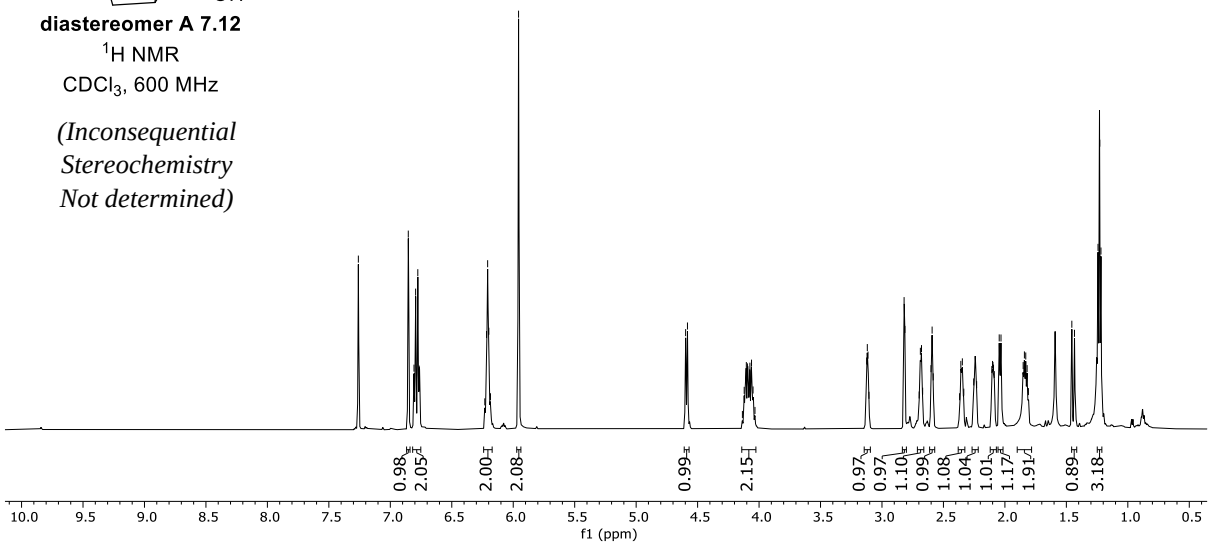

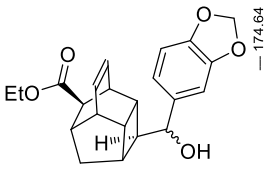

diastereomer A 7.12

^{13}C NMR

$CDCl_3$, 150 MHz

(Inconsequential Stereochemistry Not determined)

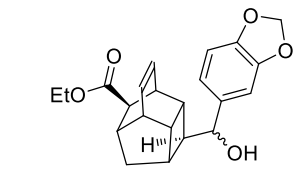

diastereomer B 7.12

^{1}H NMR

$CDCl_3$, 600 MHz

(Inconsequential Stereochemistry Not determined)

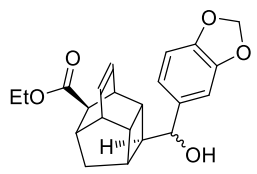

diastereomer B 7.12

^{13}C NMR

$CDCl_3$, 150 MHz

(Inconsequential Stereochemistry Not determined)

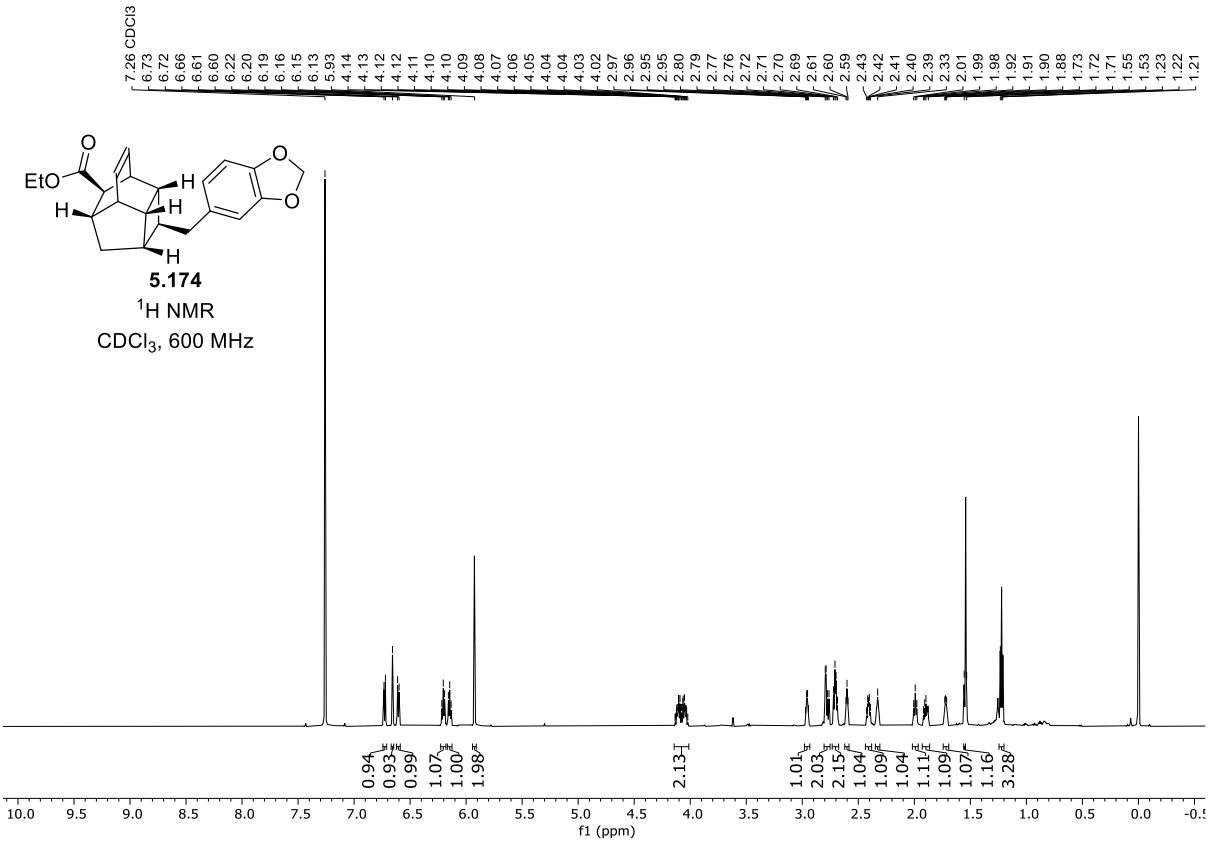
7.26 CDCl3
EtO
O
O
O
H
H
H
H
5.174
1H NMR
CDCl3, 600 MHz
0.94
0.93
0.99
1.07
1.00
1.98
2.13
1.01
2.03
2.15
1.04
1.09
1.04
1.11
1.09
1.07
1.16
3.28
f1 (ppm)

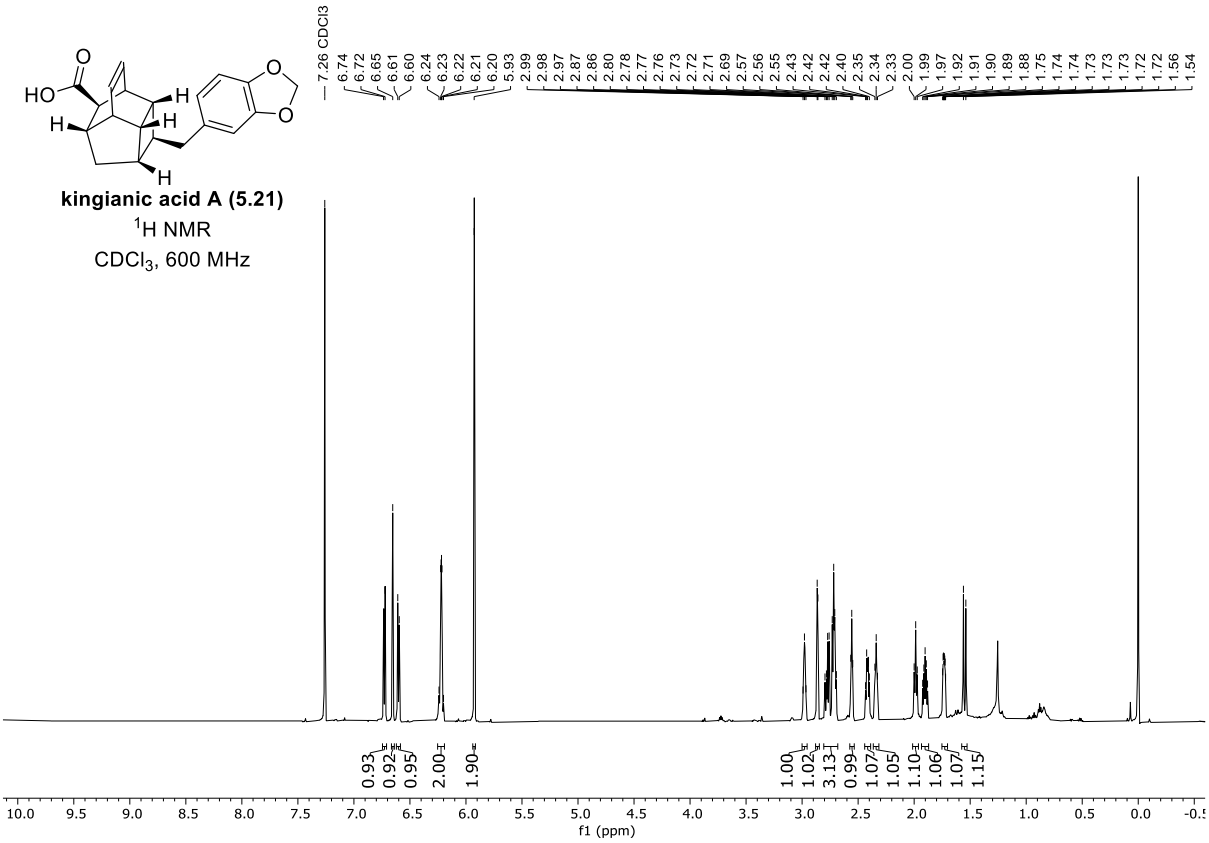
7.26 CDCl3
HO
O
O
O
H
H
H
H
kingianic acid A (5.21)
1H NMR
CDCl3, 600 MHz
0.93
0.92
0.95
2.00
1.90
1.00
1.02
3.13
0.99
1.07
1.05
1.10
1.06
1.07
1.15
f1 (ppm)

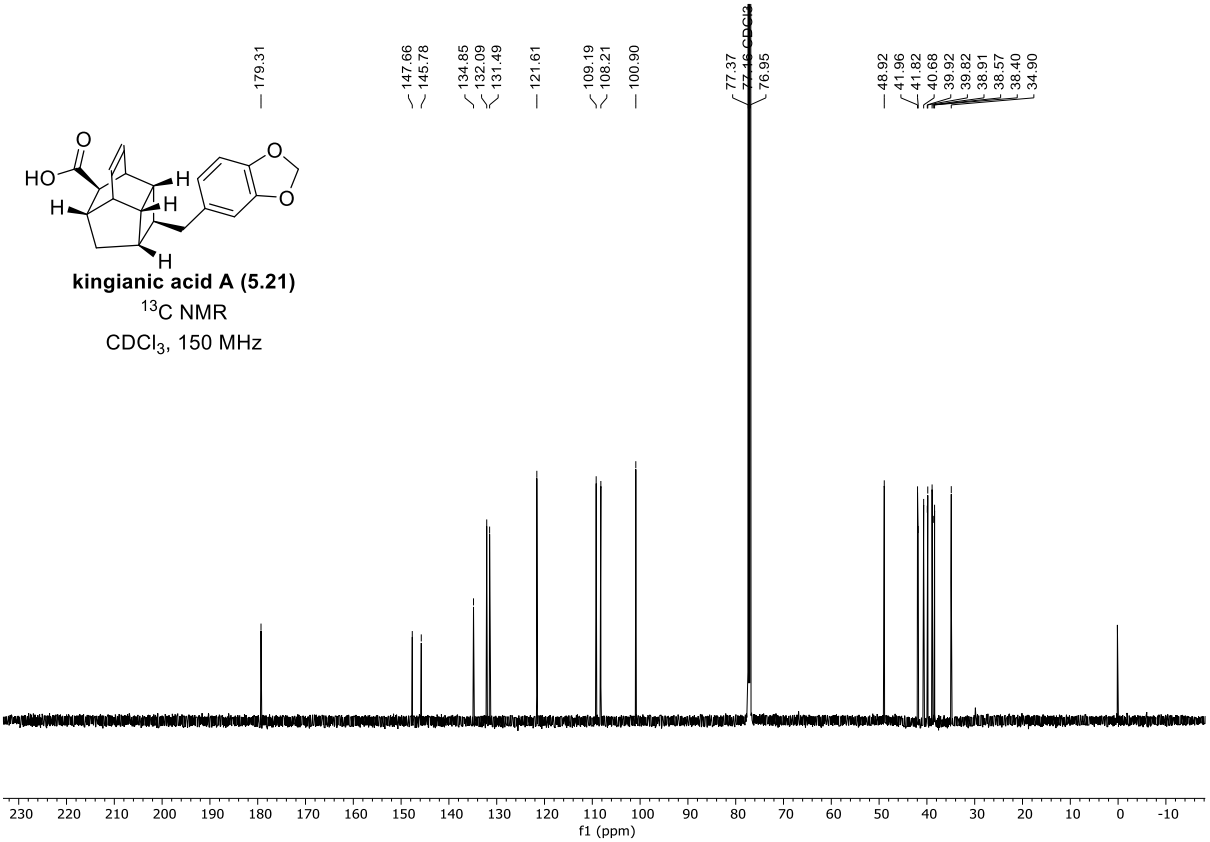

kingianic acid A (5.21)

^{13}C NMR

$CDCl_3$, 150 MHz

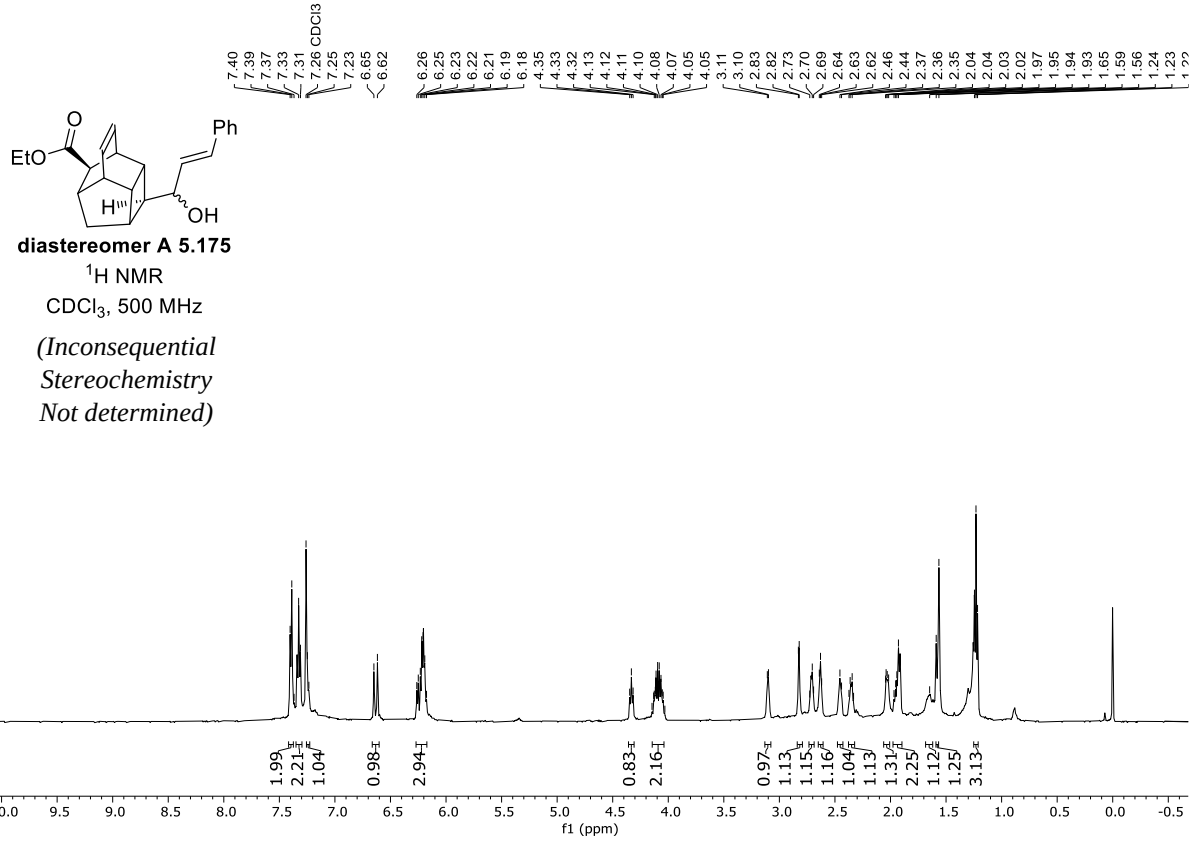

diastereomer A 5.175

^{1}H NMR

$CDCl_3$, 500 MHz

(Inconsequential Stereochemistry Not determined)

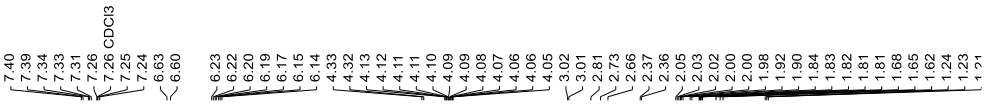

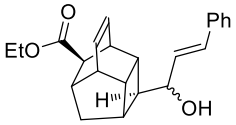

diastereomer B 5.175

^{1}H NMR

$CDCl_3$, 500 MHz

(Inconsequential Stereochemistry Not determined)

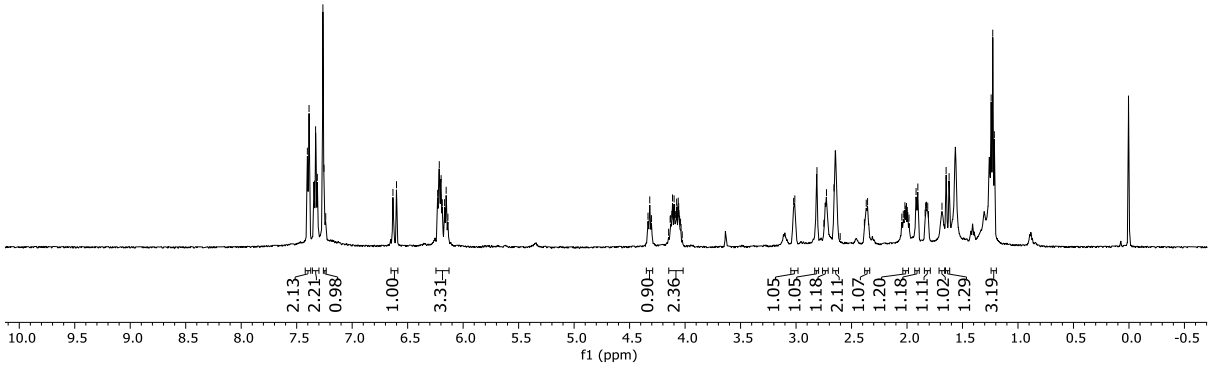

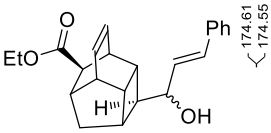

diastereomers A and B 5.175

^{13}C NMR

$CDCl_3$, 125 MHz

(Inconsequential Diastereomeric mixture)

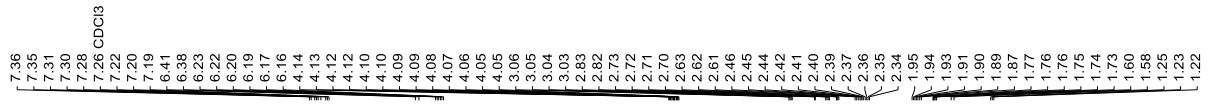

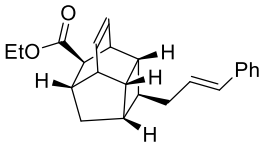

7.13

^{1}H NMR

$CDCl_3$, 500 MHz

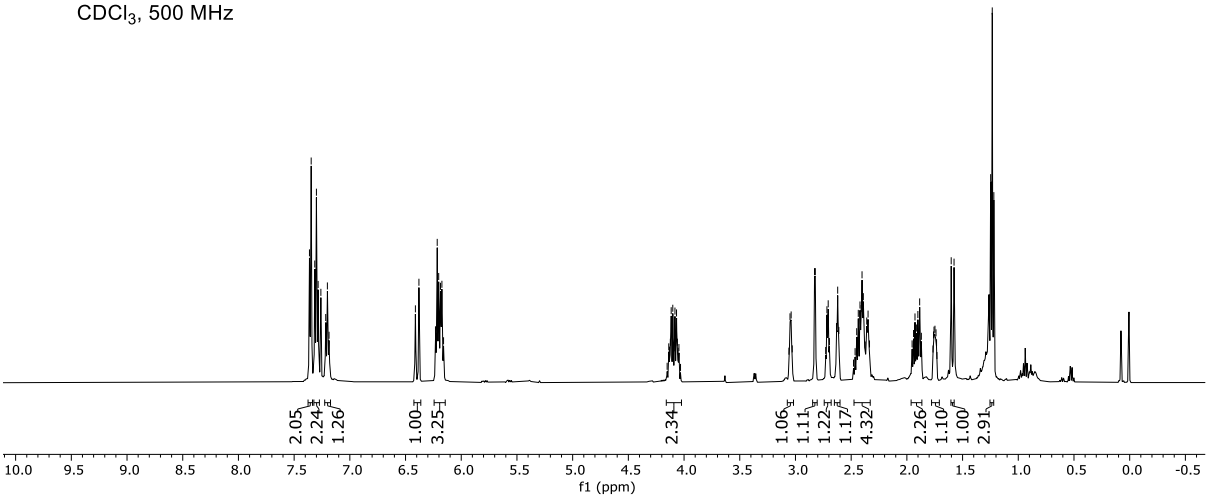

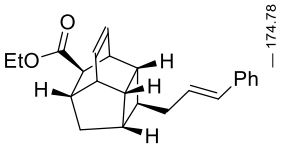

7.13

^{13}C NMR

$CDCl_3$, 125 MHz

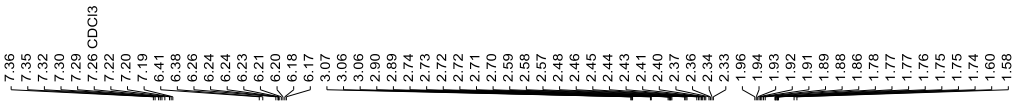

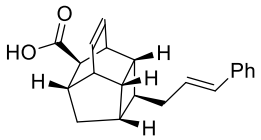

kingianic acid D (5.176)

^{1}H NMR

$CDCl_3$, 500 MHz

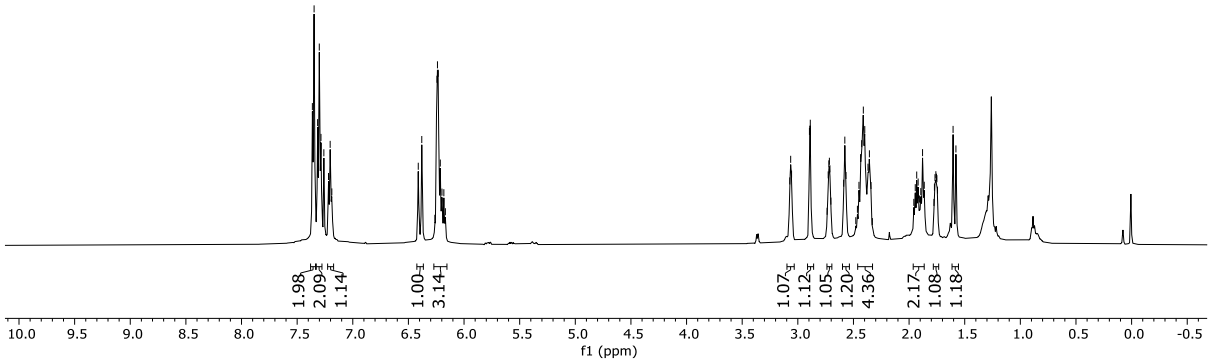

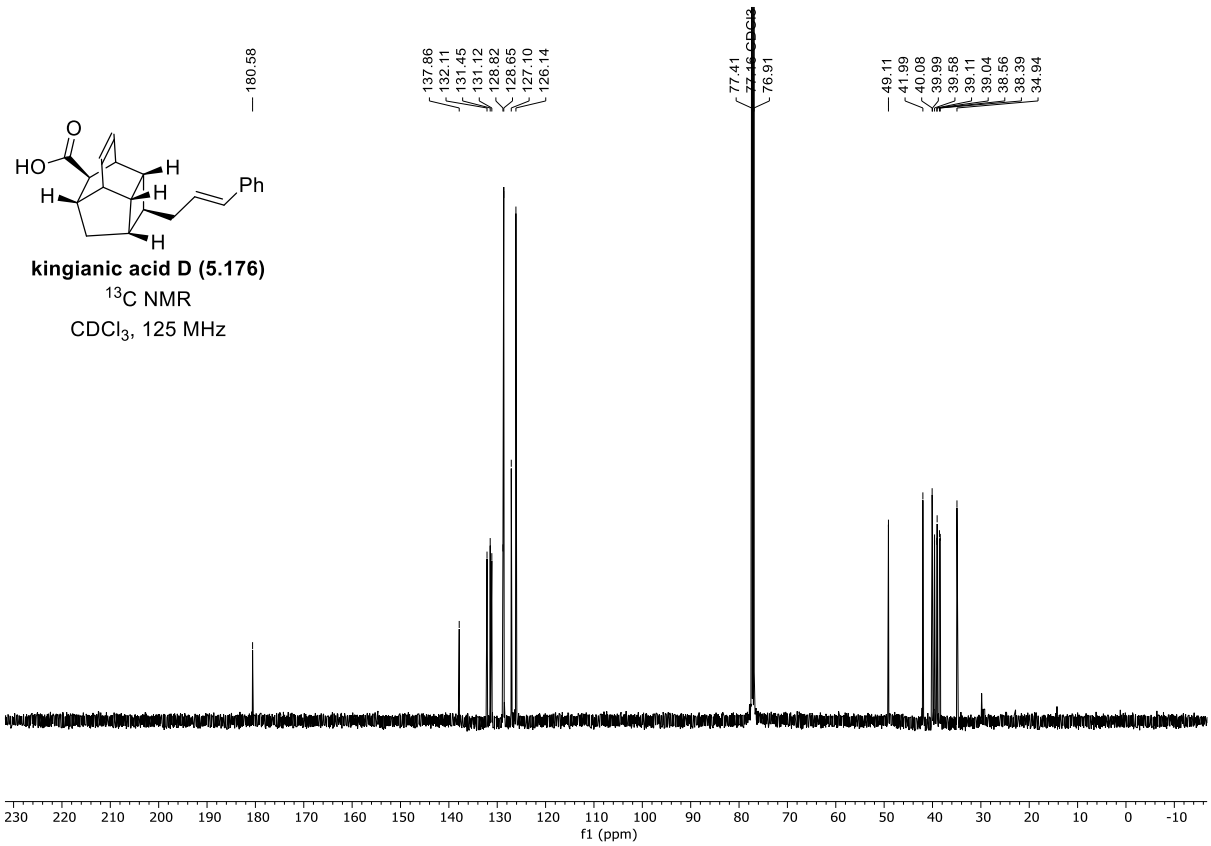

kingianic acid D (5.176)

^{13}C NMR

$CDCl_3$, 125 MHz

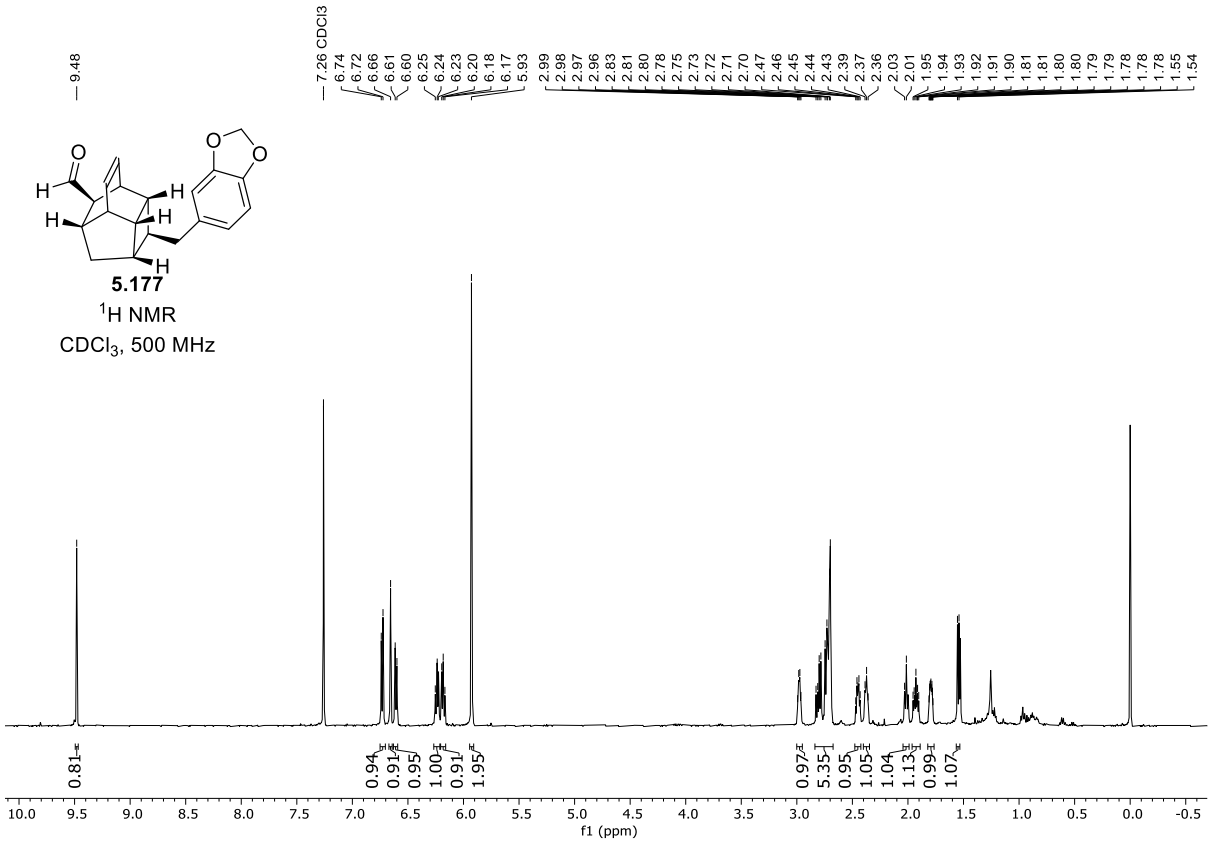
9.48
7.26 CDCl3
6.74
6.72
6.66
6.61
6.60
6.25
6.24
6.23
6.20
6.18
6.17
5.93
2.99
2.98
2.97
2.96
2.83
2.81
2.80
2.78
2.75
2.73
2.72
2.71
2.70
2.47
2.46
2.45
2.44
2.43
2.39
2.37
2.36
2.03
2.01
1.95
1.94
1.93
1.92
1.91
1.90
1.81
1.81
1.80
1.80
1.79
1.79
1.78
1.78
1.78
1.55
1.54
O
O
O
H
H
H
H
H
5.177
1H NMR
CDCl3, 500 MHz
0.81
0.94
0.91
0.95
1.00
0.91
1.95
0.97
5.35
0.95
1.05
1.04
1.13
0.99
1.07
10.0
9.5
9.0
8.5
8.0
7.5
7.0
6.5
6.0
5.5
5.0
4.5
4.0
3.5
3.0
2.5
2.0
1.5
1.0
0.5
0.0
-0.5
f1 (ppm)

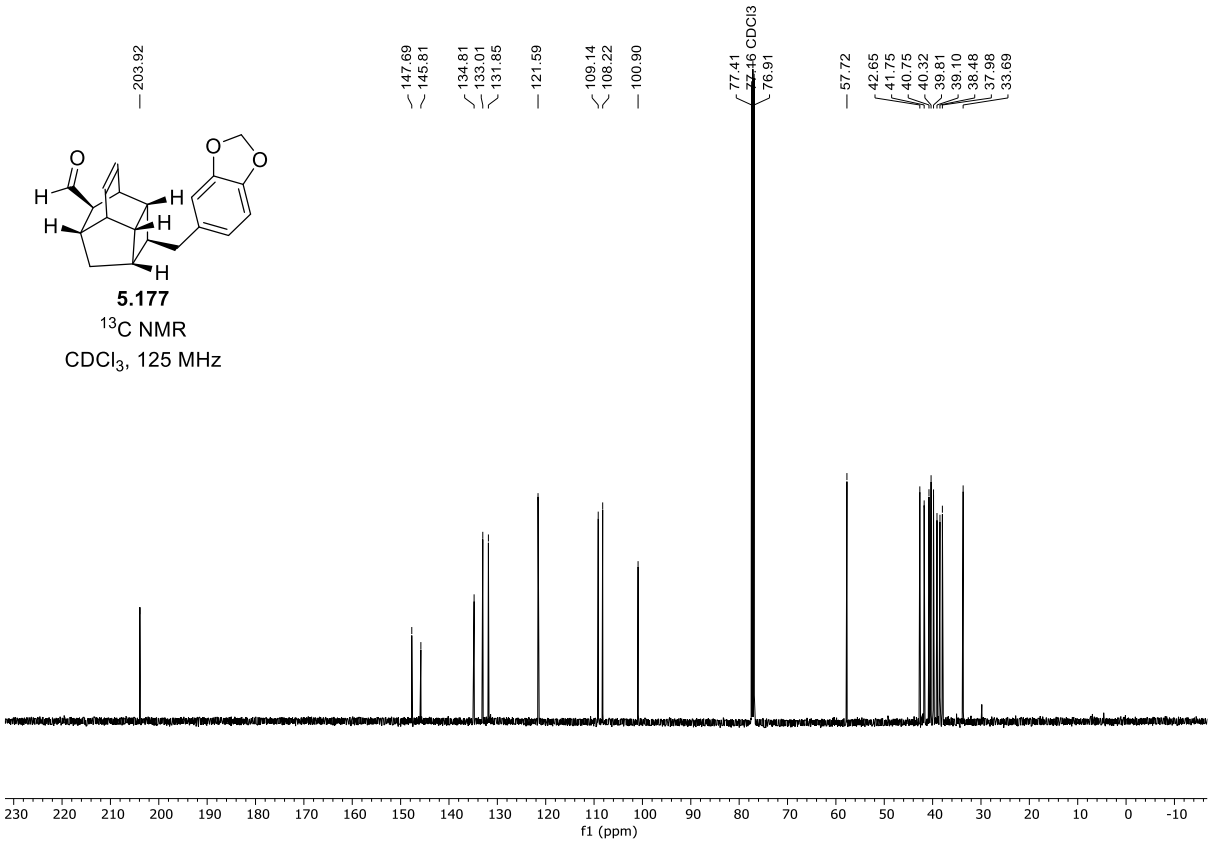
203.92
147.69
145.81
134.81
133.01
131.85
121.59
109.14
108.22
100.90
77.41
77.16 CDCl3
76.91
57.72
42.65
41.75
40.32
39.81
39.10
38.48
37.98
33.69
O
O
O
H
H
H
H
H
5.177
13C NMR
CDCl3, 125 MHz
230
220
210
200
190
180
170
160
150
140
130
120
110
100
90
80
70
60
50
40
30
20
10
0
-10
f1 (ppm)

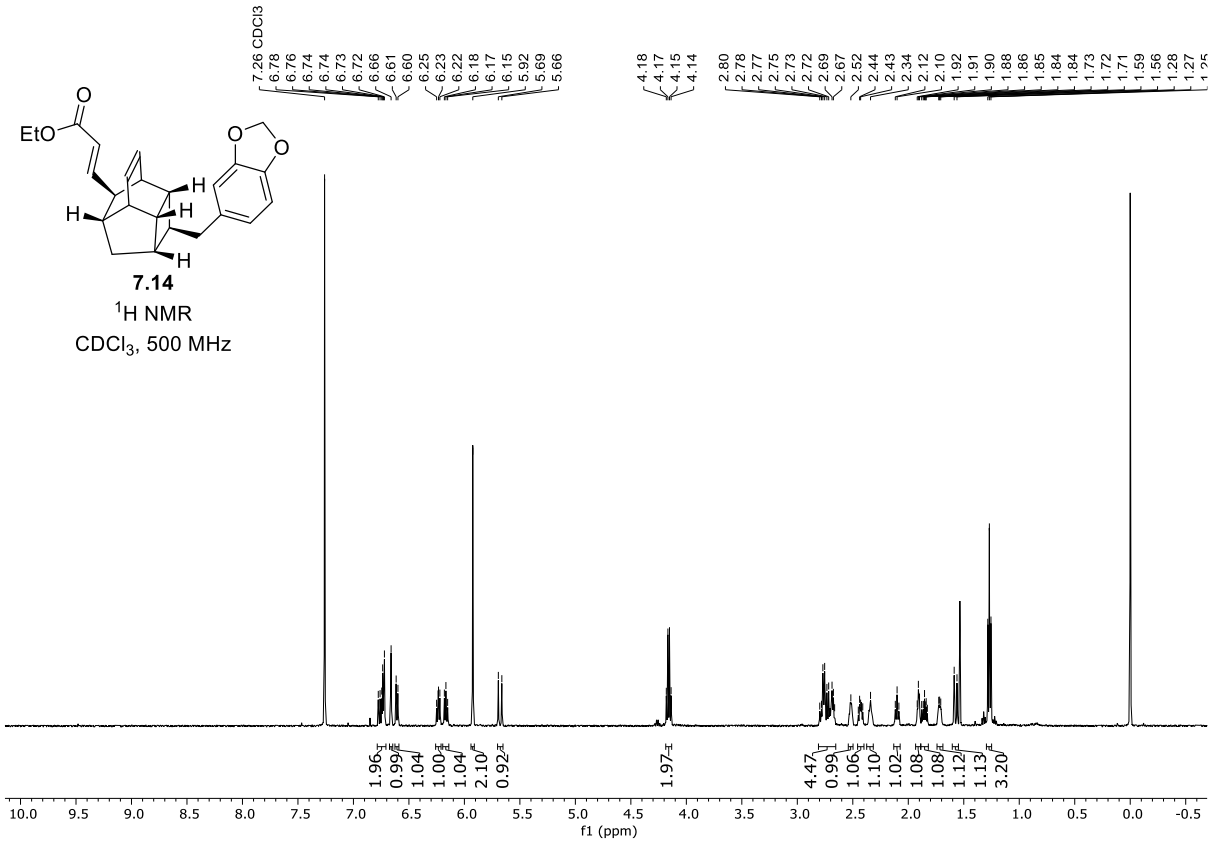

7.14

^{1}H NMR

$CDCl_3$, 500 MHz

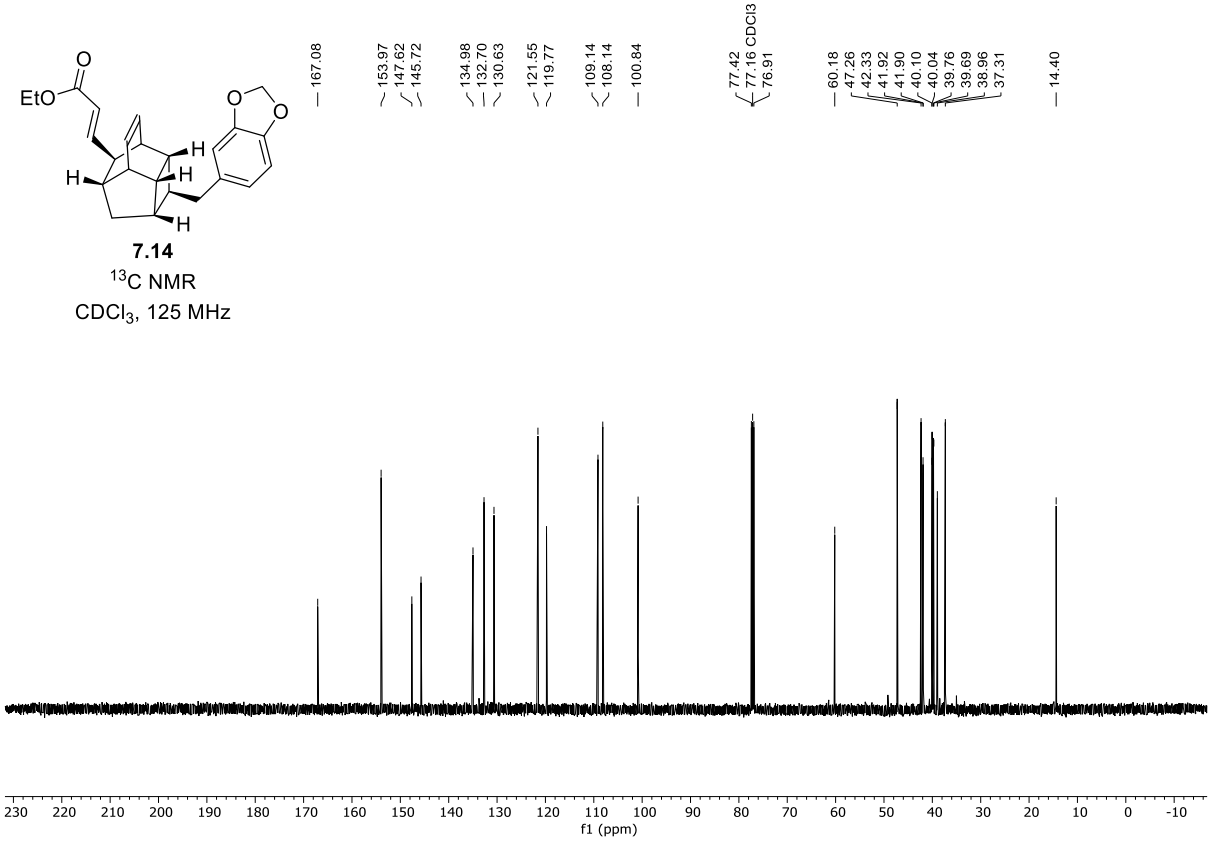

7.14

^{13}C NMR

$CDCl_3$, 125 MHz

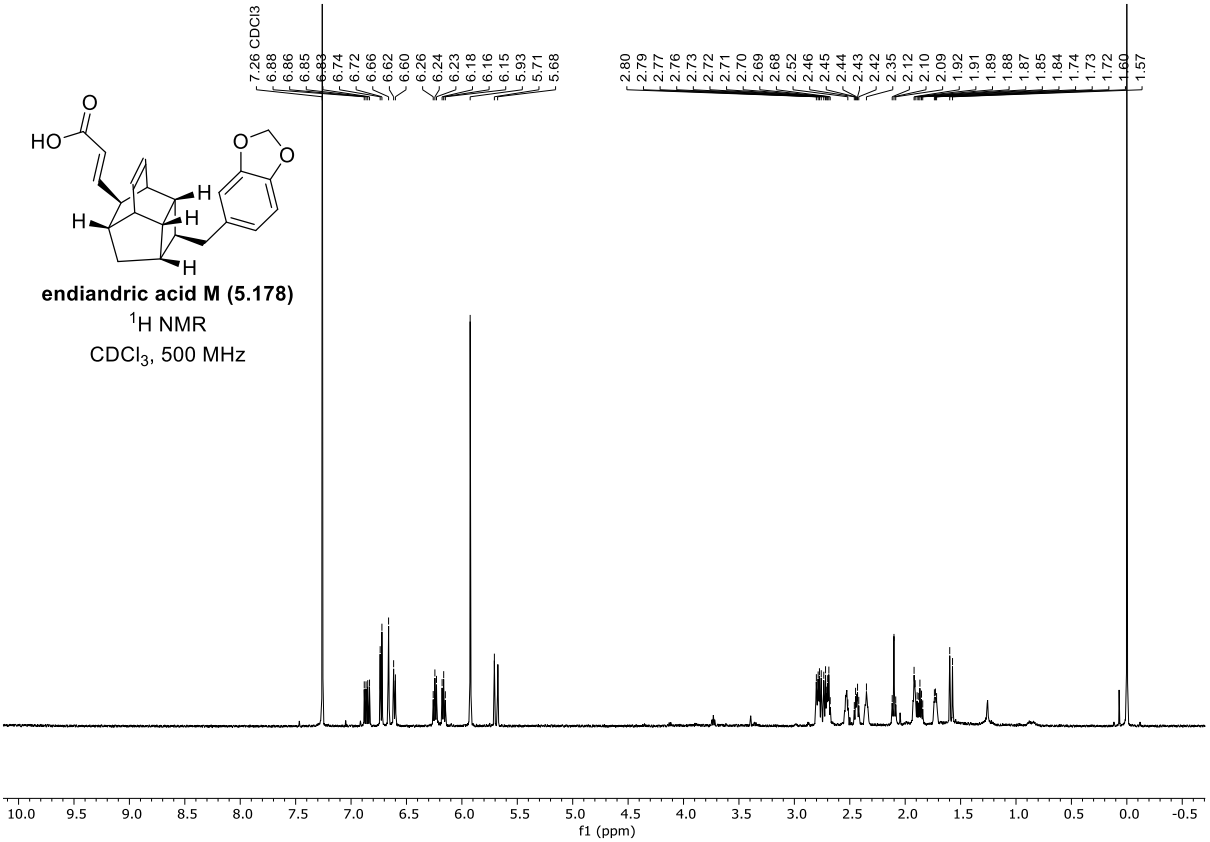

endiandric acid M (5.178)

^{1}H NMR

$CDCl_3$, 500 MHz

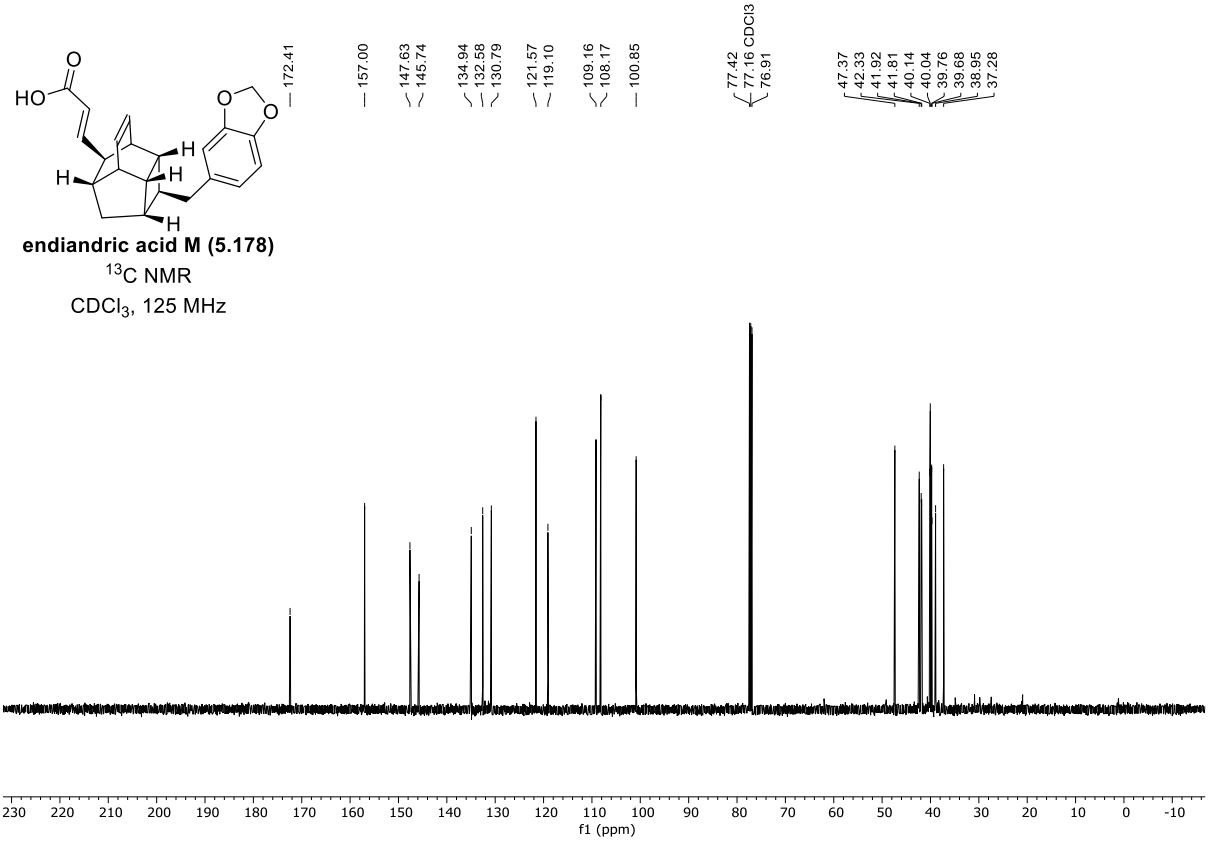

endiandric acid M (5.178)

^{13}C NMR

$CDCl_3$, 125 MHz

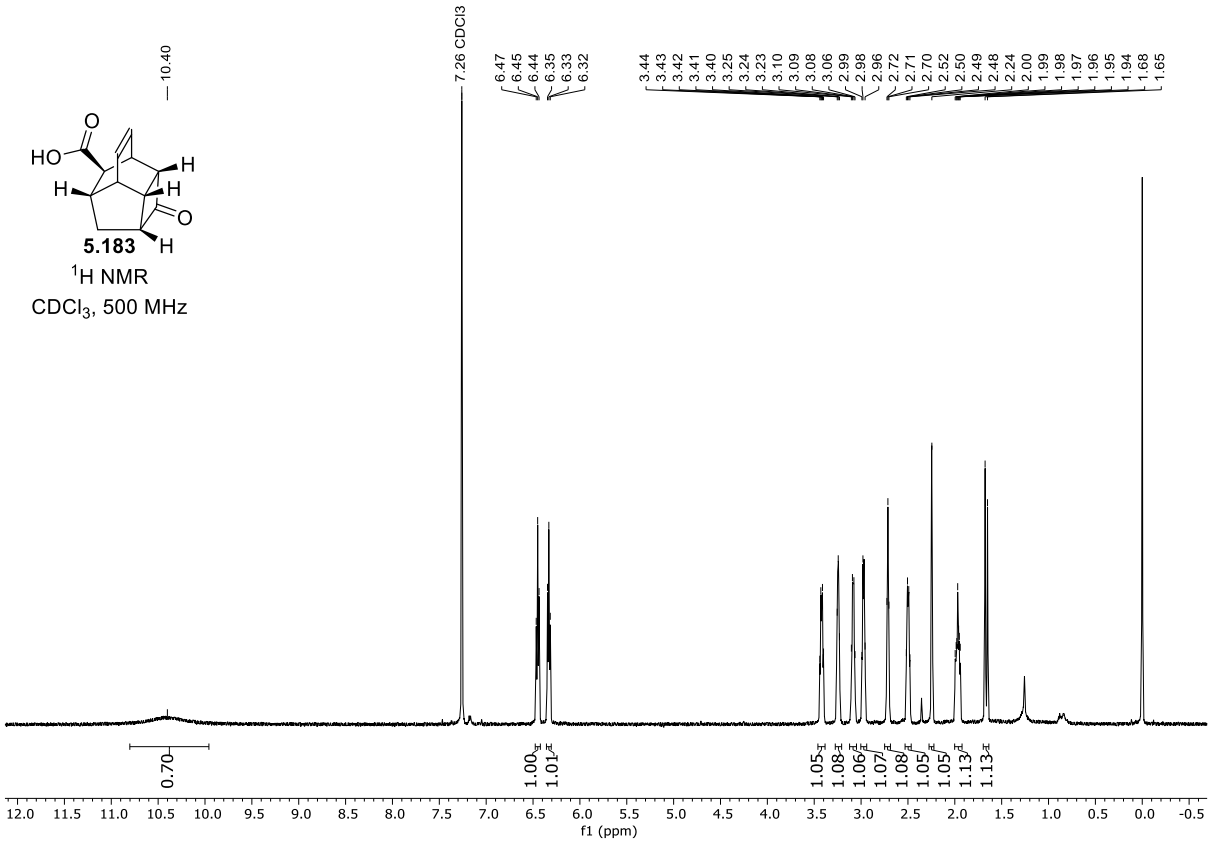

^{1}H NMR

$CDCl_3$, 500 MHz

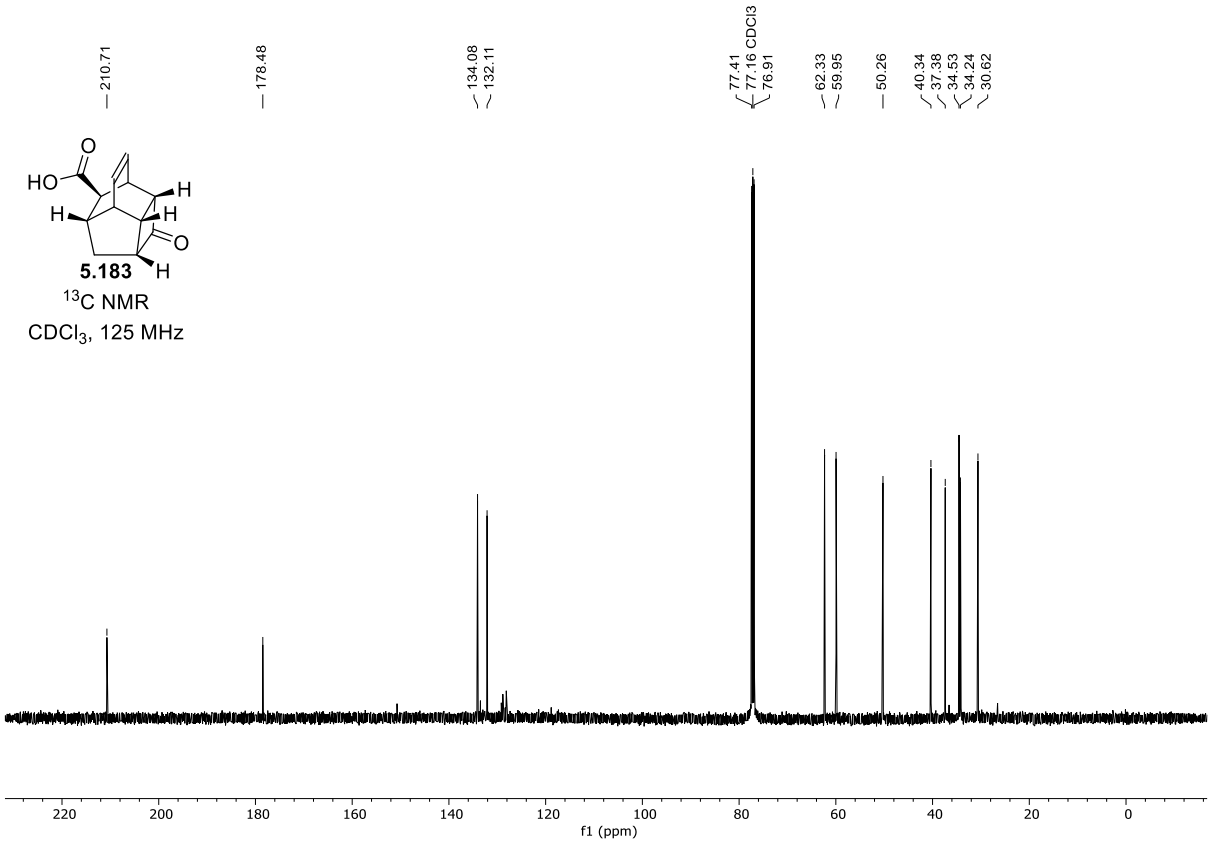

^{13}C NMR

$CDCl_3$, 125 MHz

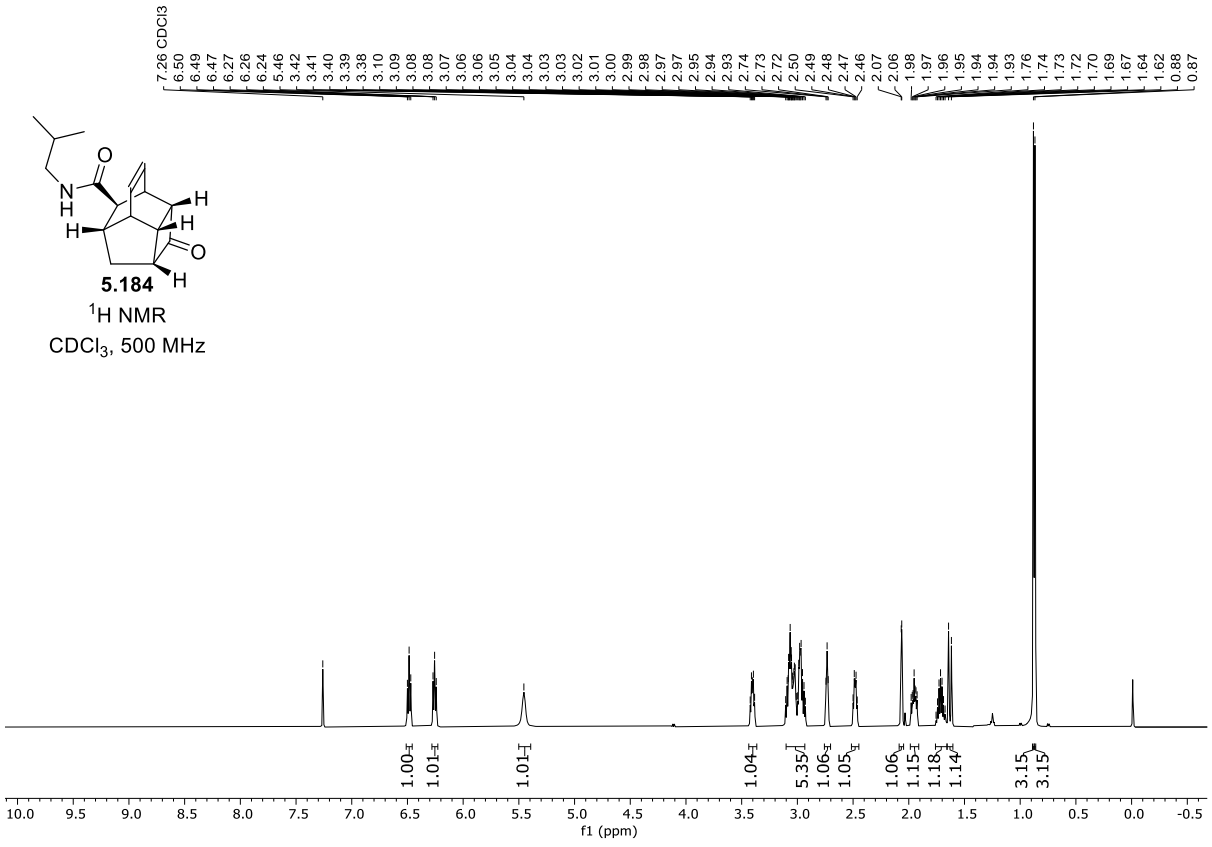
7.26 CDCl3
6.50 6.49 6.47 6.27 6.26 6.24 5.46 3.42 3.41 3.40 3.39 3.38 3.10 3.09 3.08 3.08 3.07 3.06 3.06 3.05 3.04 3.04 3.03 3.03 3.02 3.01 3.00 2.99 2.98 2.97 2.97 2.95 2.94 2.93 2.74 2.73 2.72 2.50 2.49 2.48 2.47 2.46 2.07 2.06 1.98 1.97 1.96 1.95 1.94 1.94 1.93 1.76 1.74 1.73 1.72 1.70 1.69 1.67 1.64 1.62 0.88 0.87
5.184
1H NMR
CDCl3, 500 MHz
1.00 1.01 1.01 1.04 5.35 1.06 1.05 1.06 1.15 1.18 1.14 3.15 3.15
f1 (ppm)

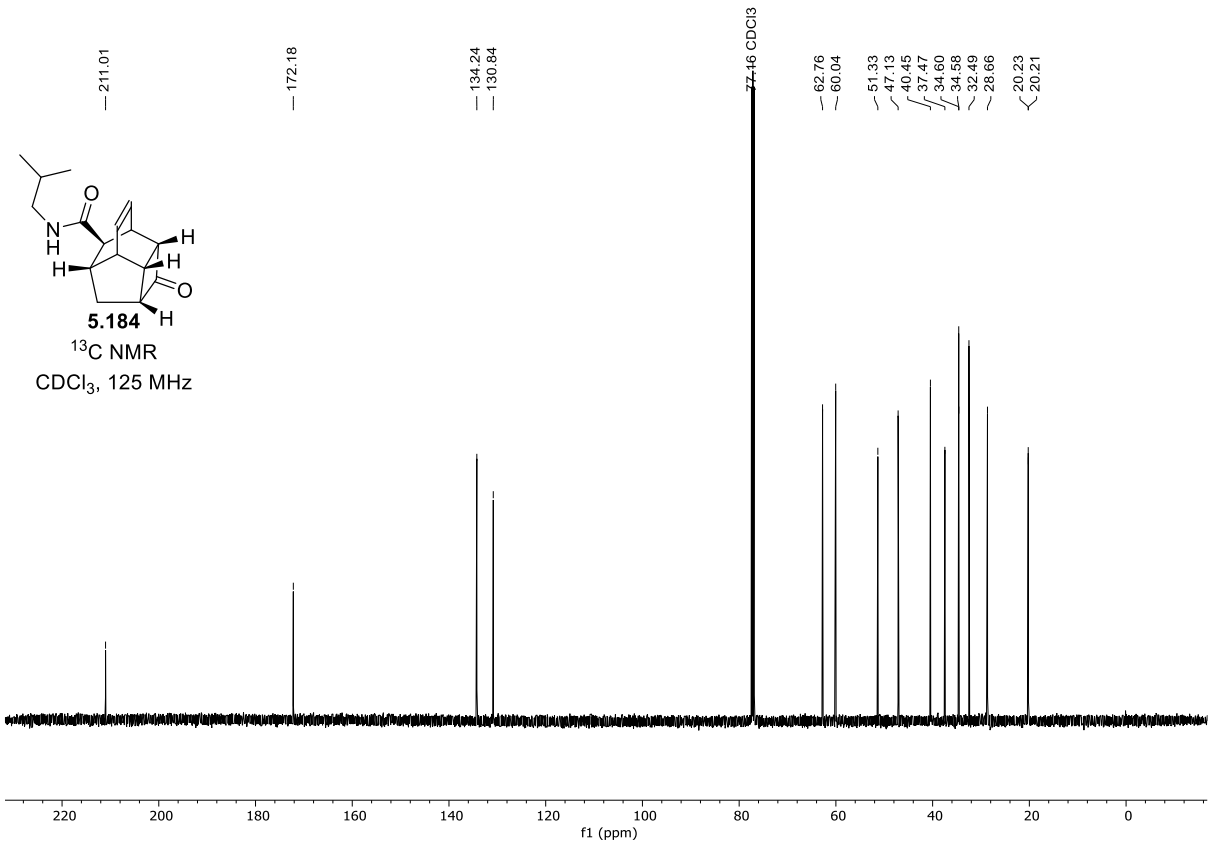
211.01
172.18
134.24
130.84
77.16 CDCl3
62.76
60.04
51.33
47.13
40.45
37.47
34.60
34.58
32.49
28.66
20.23
20.21
5.184
13C NMR
CDCl3, 125 MHz
f1 (ppm)

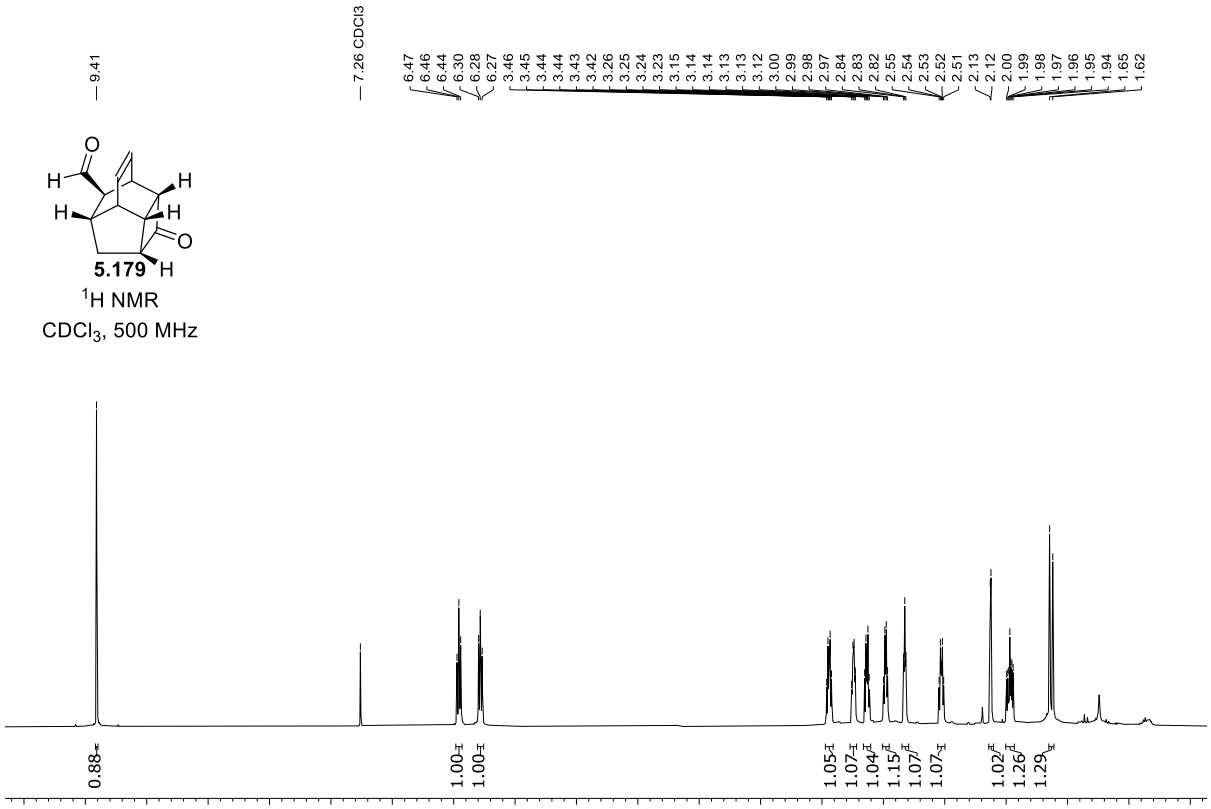
9.41
7.26 CDCl3
6.47
6.46
6.44
6.30
6.28
6.27
3.46
3.45
3.44
3.44
3.43
3.42
3.26
3.25
3.24
3.23
3.15
3.14
3.14
3.13
3.13
3.12
3.00
2.99
2.98
2.97
2.84
2.83
2.82
2.55
2.54
2.53
2.52
2.51
2.13
2.12
2.00
1.99
1.98
1.97
1.96
1.95
1.94
1.65
1.62
5.179
1H NMR
CDCl3, 500 MHz
0.88
1.00
1.00
1.05
1.07
1.04
1.15
1.07
1.07
1.02
1.26
1.29
f1 (ppm)
210.52
201.04
135.63
131.59
77.41
77.16 CDCl3
76.91
62.38
59.86
58.45
40.96
36.51
35.03
33.98
29.35
5.179
13C NMR
CDCl3, 125 MHz
f1 (ppm)

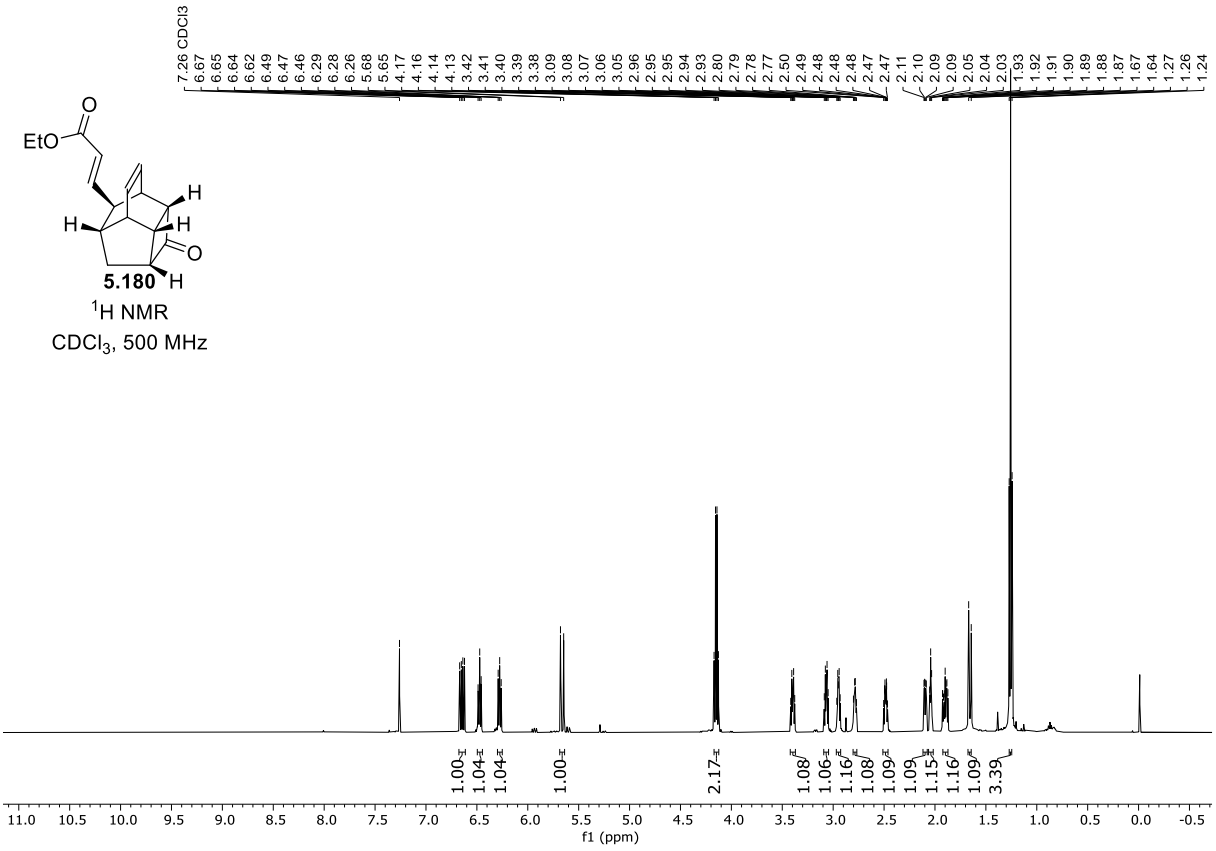
7.26 CDCl3
6.67 6.65 6.64 6.62 6.49 6.47 6.46 6.29 6.28 6.26 5.68 5.65 4.17 4.16 4.14 4.13 3.42 3.41 3.40 3.39 3.38 3.09 3.08 3.07 3.06 3.05 2.96 2.95 2.94 2.93 2.80 2.79 2.78 2.77 2.50 2.49 2.48 2.48 2.48 2.47 2.47 2.11 2.10 2.09 2.09 2.05 2.04 2.03 1.93 1.92 1.91 1.90 1.89 1.88 1.87 1.67 1.64 1.27 1.26 1.24
EtO
O
H
H
H
O
5.180
H
1H NMR
CDCl3, 500 MHz
1.00 1.04 1.04 1.00 2.17 1.08 1.06 1.16 1.08 1.09 1.09 1.15 1.16 1.09 3.39
11.0 10.5 10.0 9.5 9.0 8.5 8.0 7.5 7.0 6.5 6.0 5.5 5.0 4.5 4.0 3.5 3.0 2.5 2.0 1.5 1.0 0.5 0.0 -0.5
f1 (ppm)

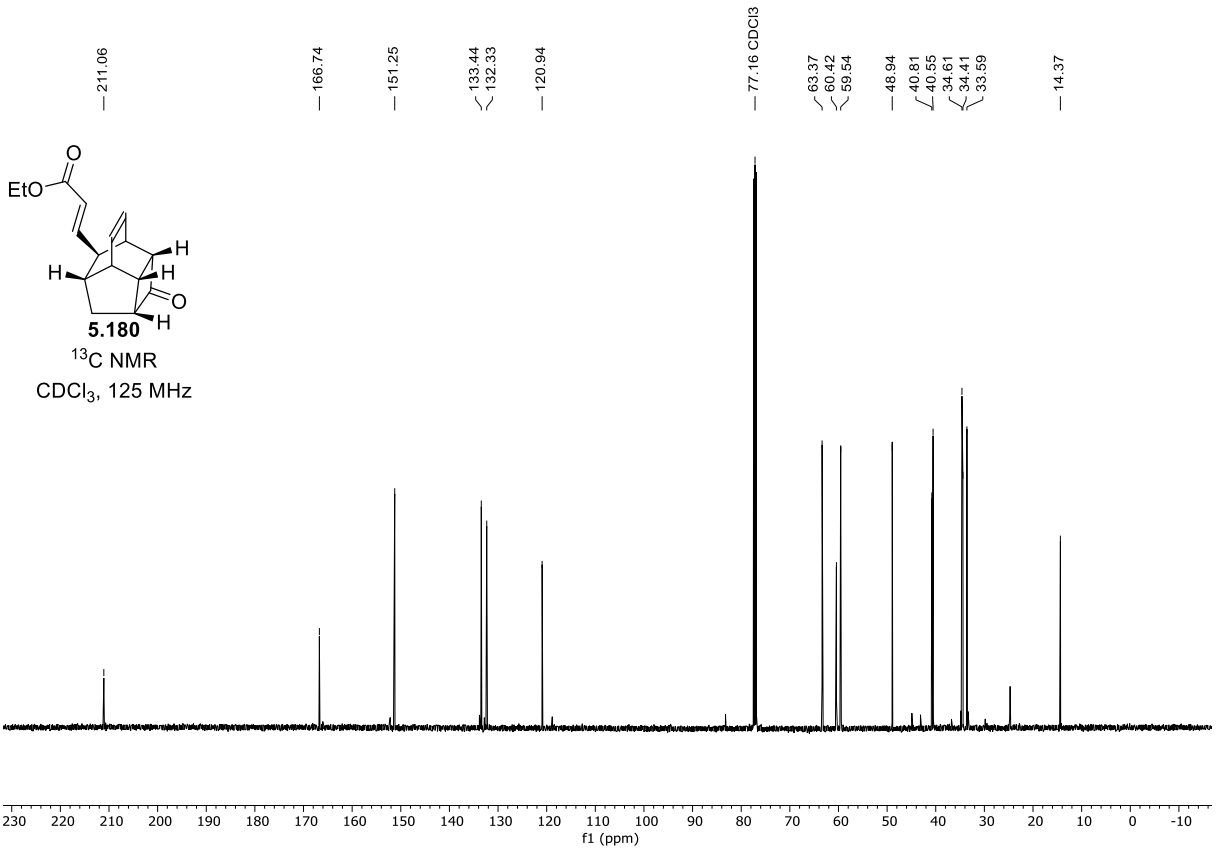
211.06
166.74
151.25
133.44
132.33
120.94
77.16 CDCl3
63.37
60.42
59.54
48.94
40.81
40.55
34.61
34.41
33.59
14.37
EtO
O
H
H
H
O
5.180
H
13C NMR
CDCl3, 125 MHz
230 220 210 200 190 180 170 160 150 140 130 120 110 100 90 80 70 60 50 40 30 20 10 0 -10
f1 (ppm)

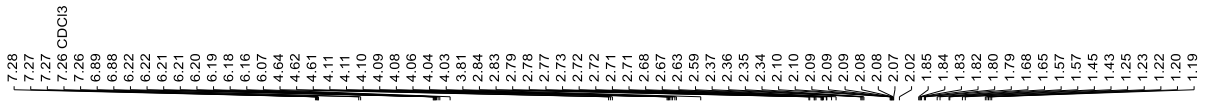

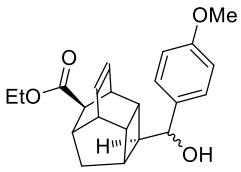

7.15

^{1}H NMR

$CDCl_3$, 500 MHz

(Mixture of Inconsequential Diastereomers)

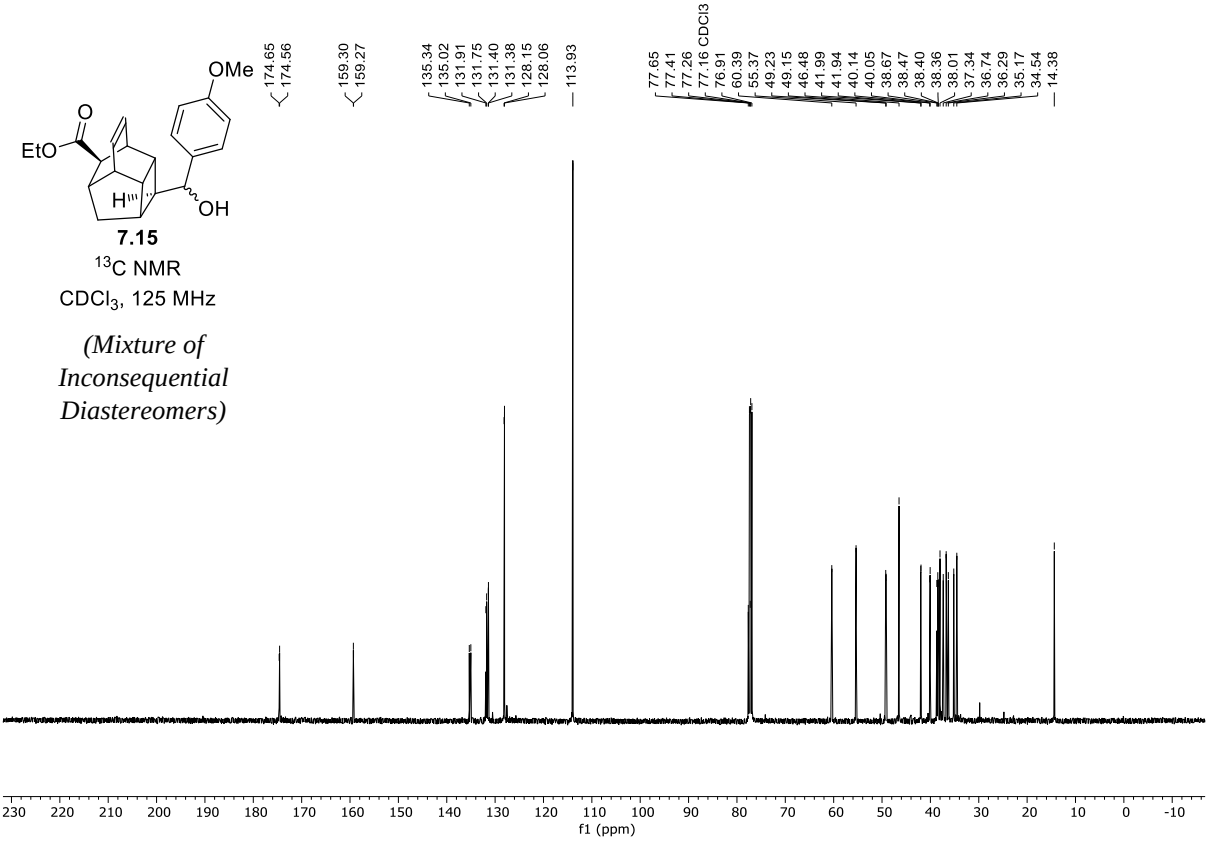

7.15

^{13}C NMR

$CDCl_3$, 125 MHz

(Mixture of Inconsequential Diastereomers)

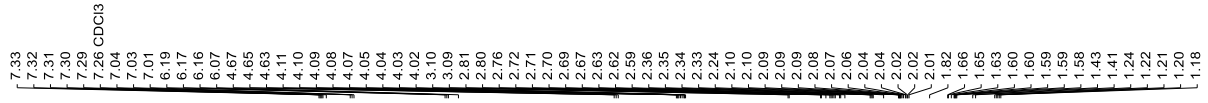

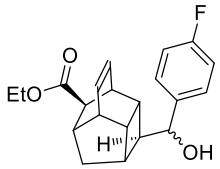

7.16

^{1}H NMR

$CDCl_3$, 500 MHz

(Mixture of Inconsequential Diastereomers)

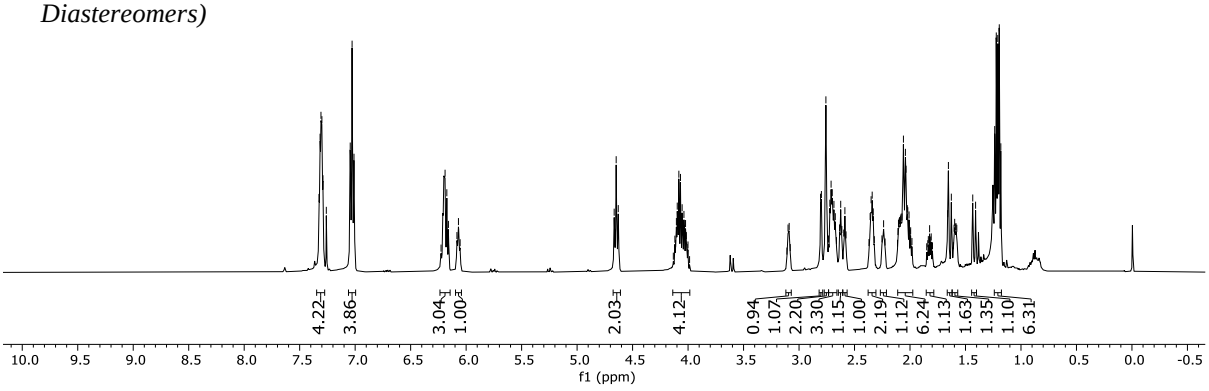

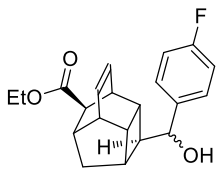

7.16

^{13}C NMR

$CDCl_3$, 125 MHz

(Mixture of Inconsequential Diastereomers)

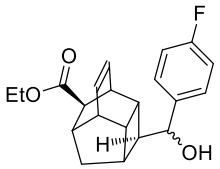

7.16

^{19}F NMR

$CDCl_3$, 470 MHz

(Mixture of Inconsequential Diastereomers)

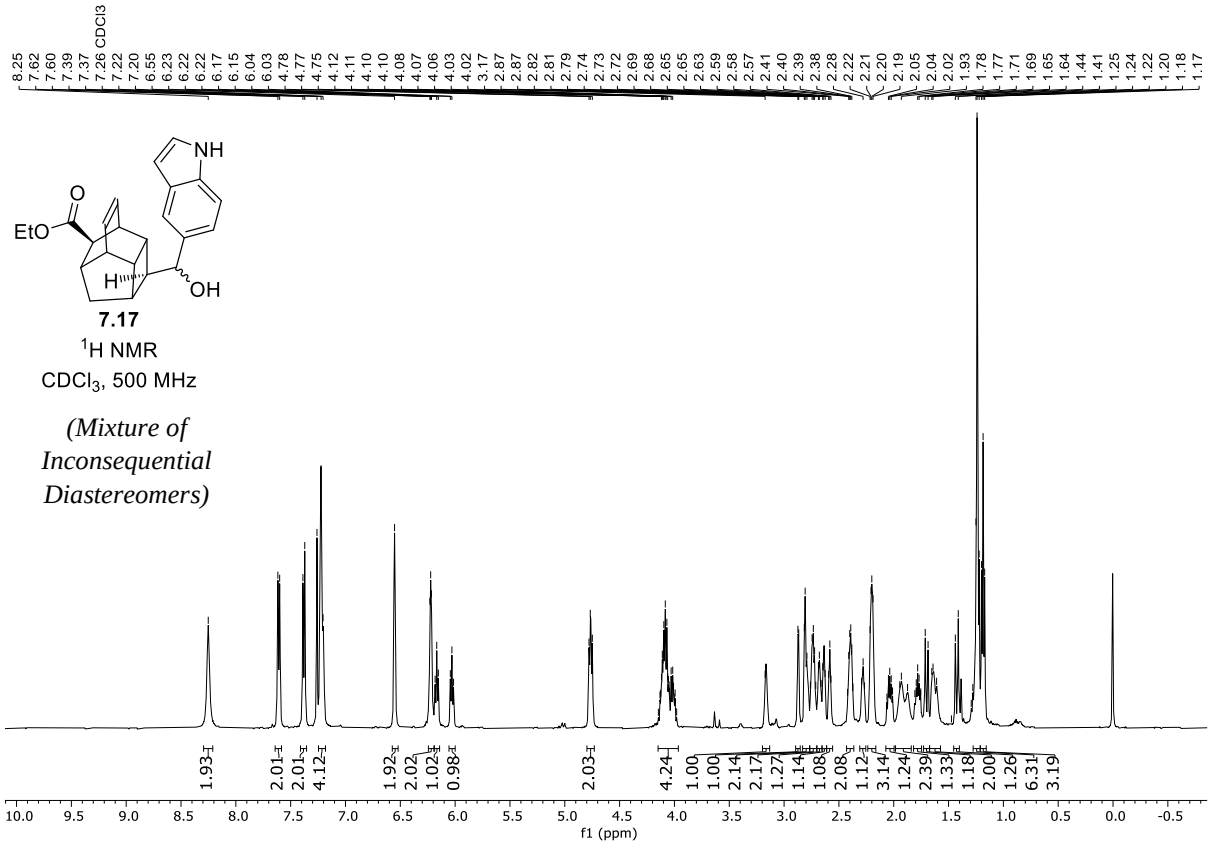

7.17

^{1}H NMR

$CDCl_3$, 500 MHz

(Mixture of Inconsequential Diastereomers)

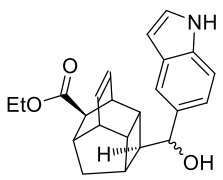

7.17

^{13}C NMR

$CDCl_3$, 125 MHz

(Mixture of Inconsequential Diastereomers)

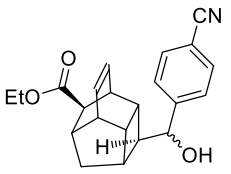

7.18

^{1}H NMR

$CDCl_3$, 500 MHz

(Mixture of Inconsequential Diastereomers)

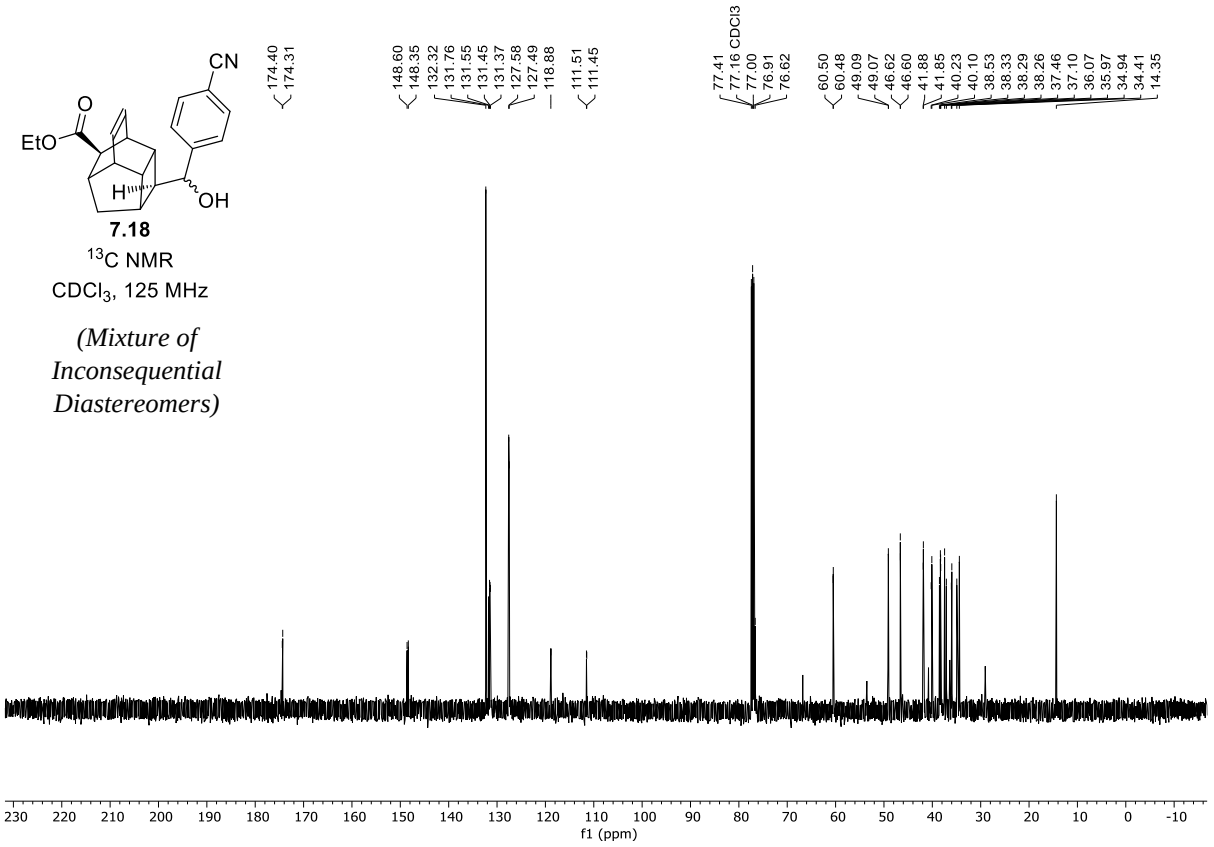

7.18

^{13}C NMR

$CDCl_3$, 125 MHz

(Mixture of Inconsequential Diastereomers)

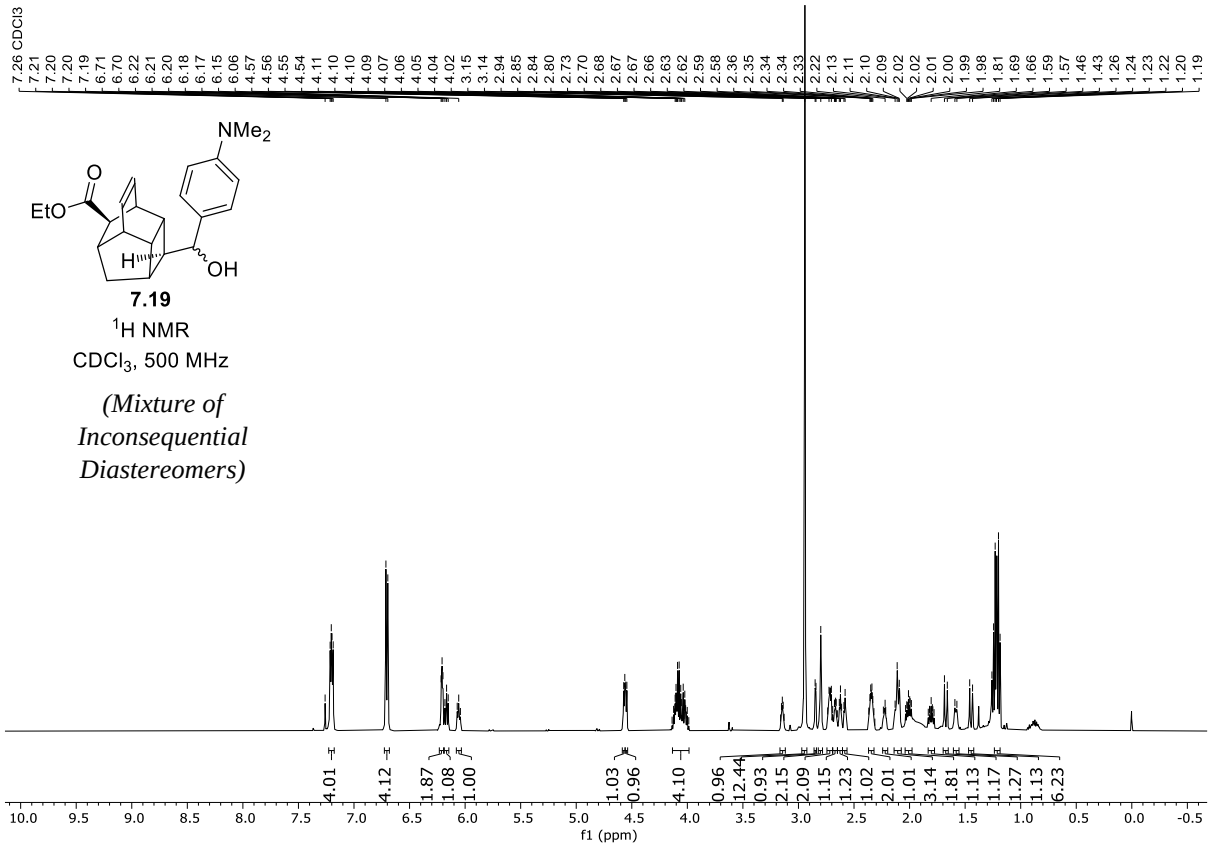

7.19

^{1}H NMR

$CDCl_3$, 500 MHz

(Mixture of Inconsequential Diastereomers)

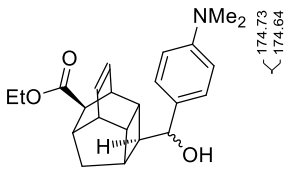

7.19

^{13}C NMR

$CDCl_3$, 125 MHz

(Mixture of Inconsequential Diastereomers)

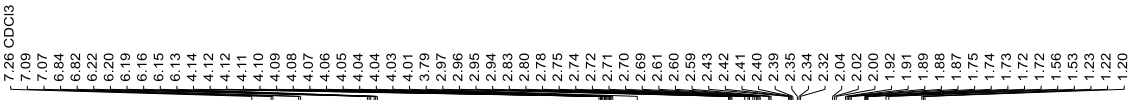

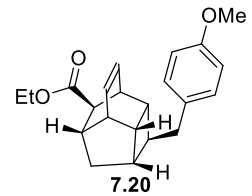

7.20

^{1}H NMR

$CDCl_3$, 500 MHz

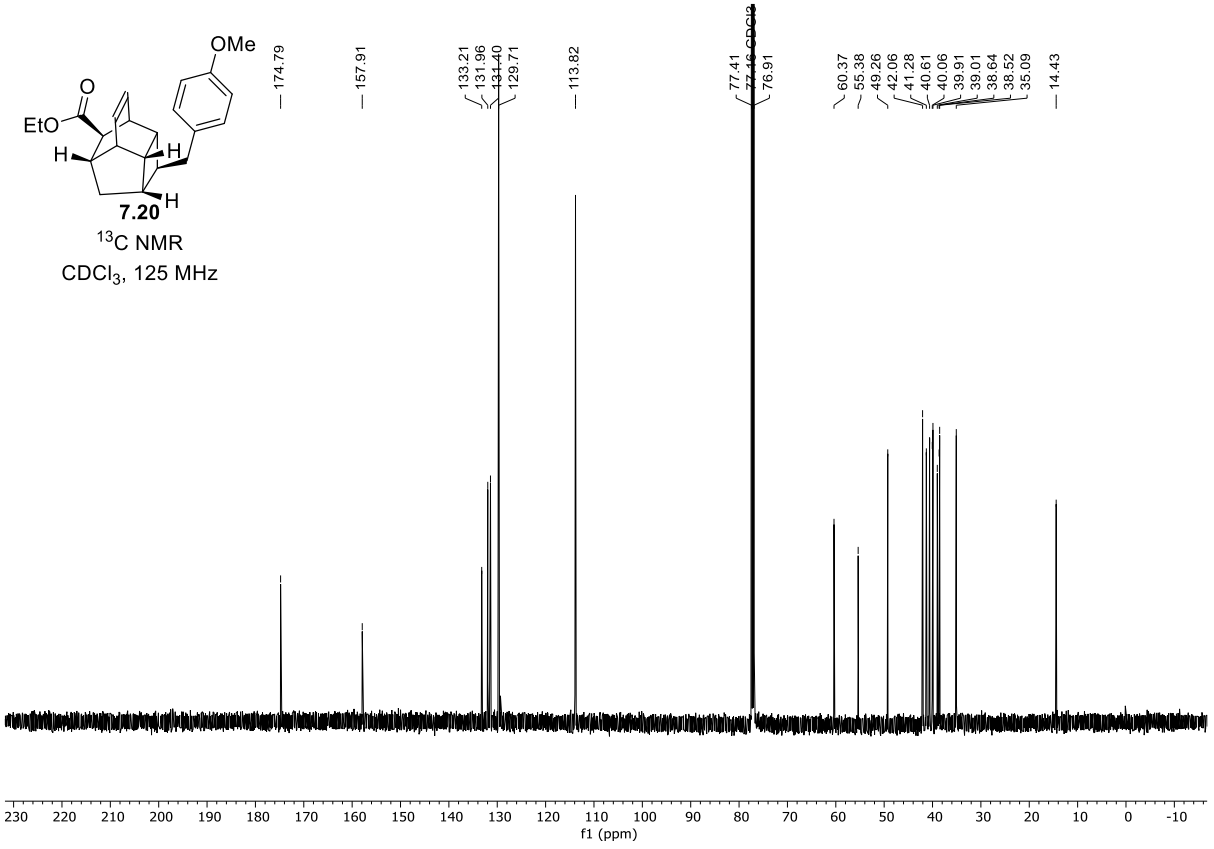

^{13}C NMR

$CDCl_3$, 125 MHz

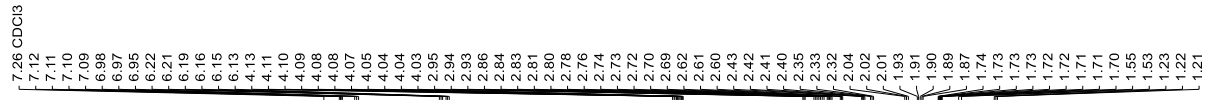

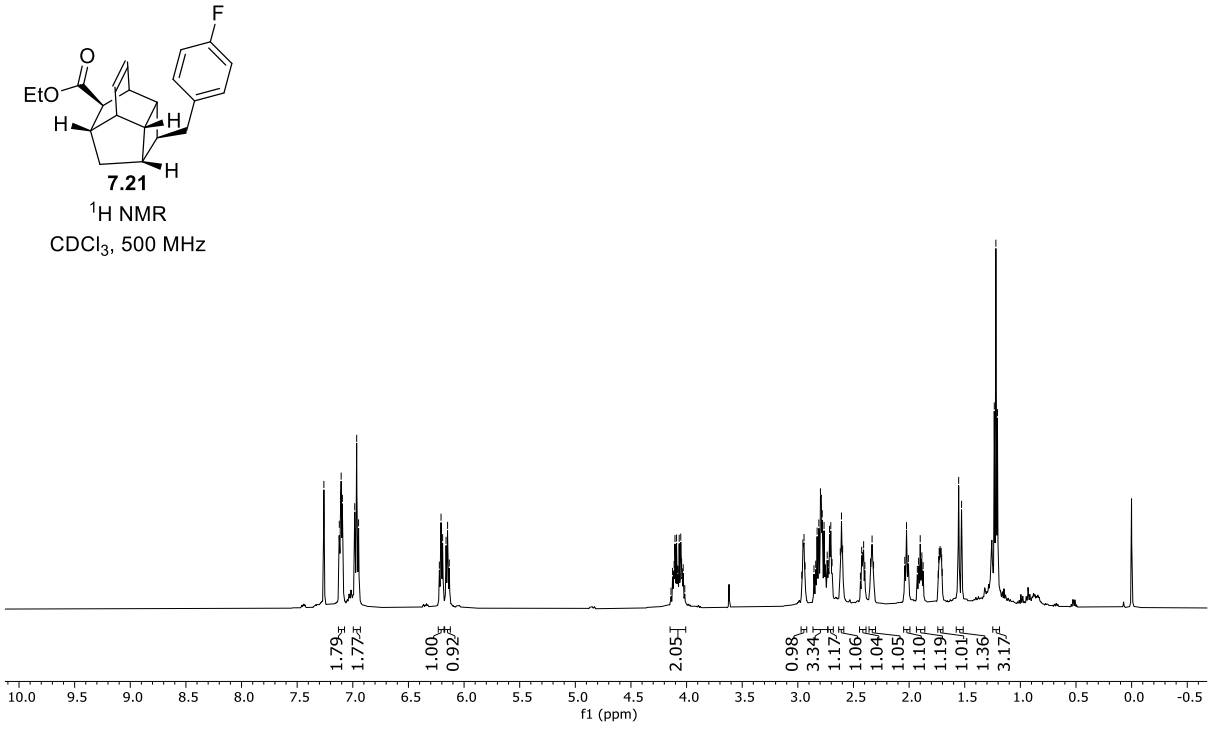

^{1}H NMR

$CDCl_3$, 500 MHz

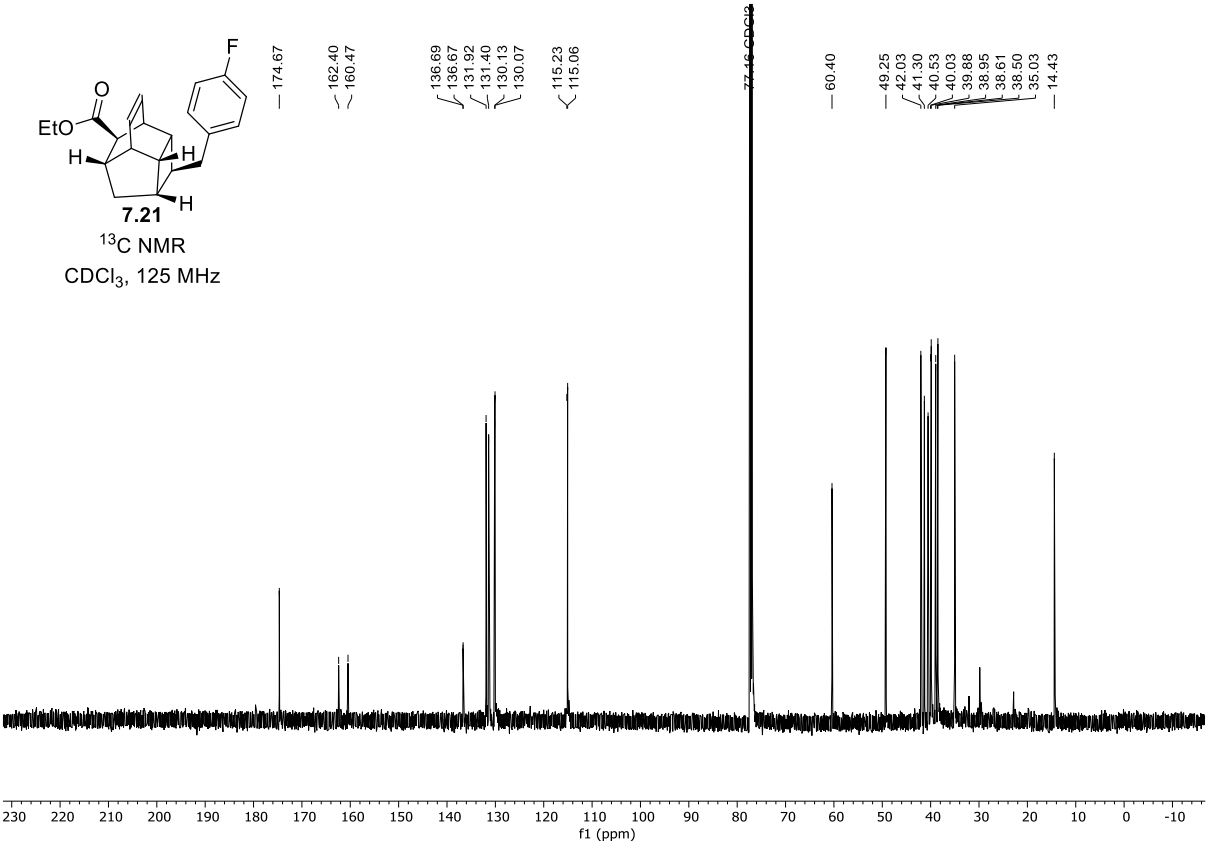

^{13}C NMR

$CDCl_3$, 125 MHz

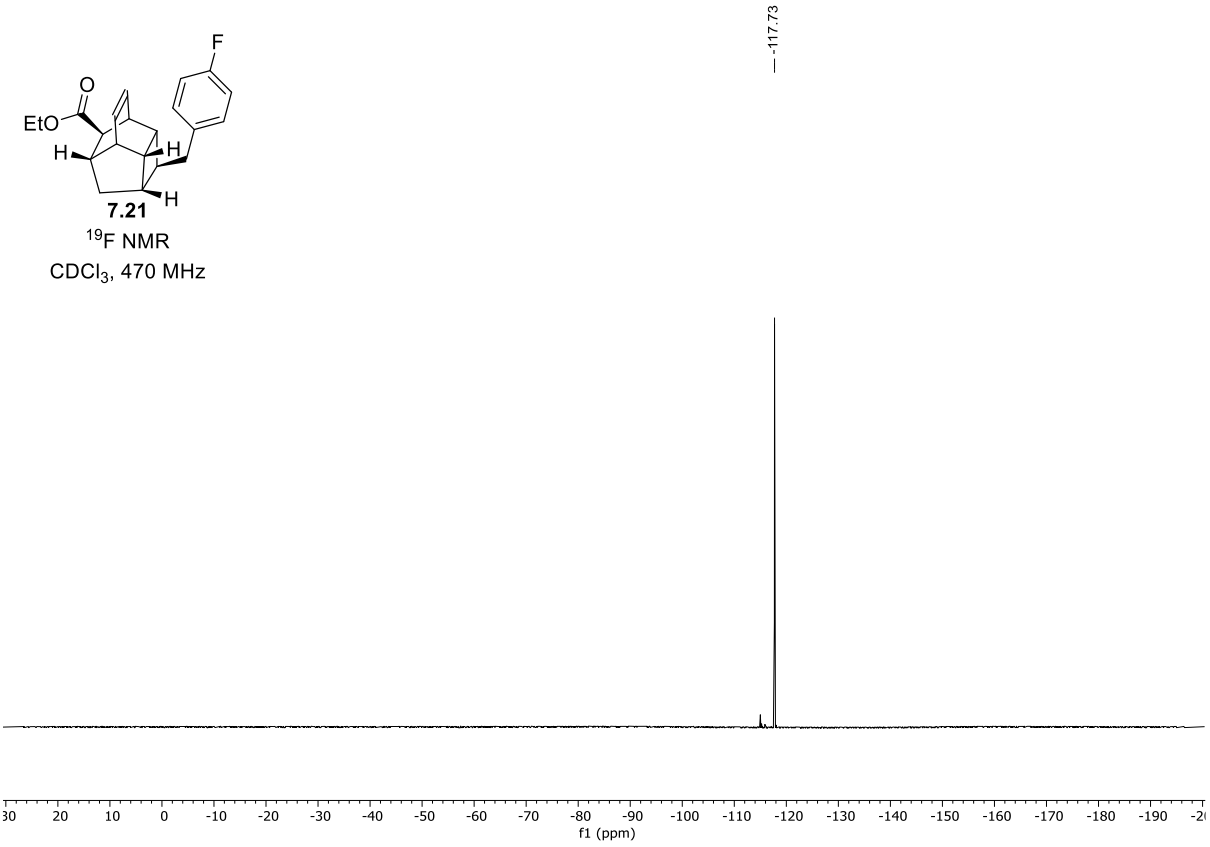

^{19}F NMR

$CDCl_3$, 470 MHz

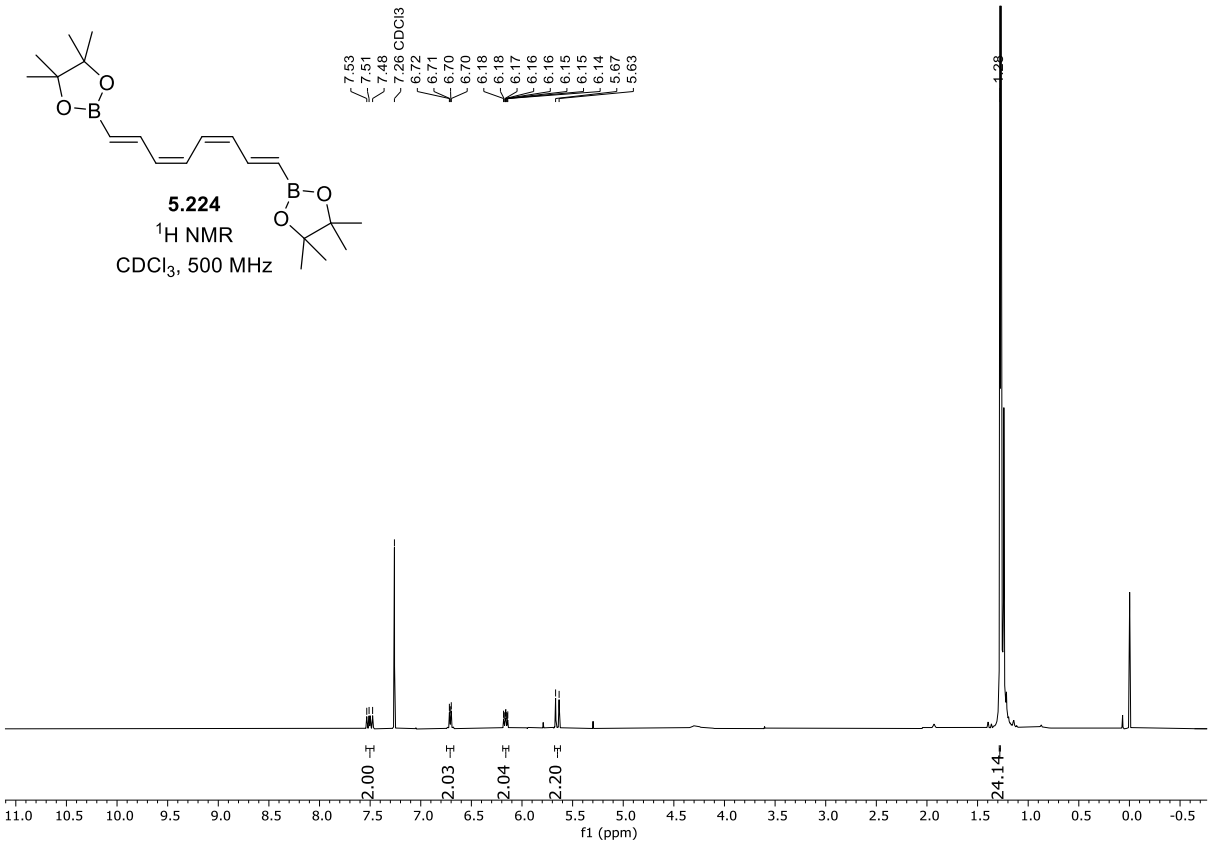

5.224
^{1}H NMR
$CDCl_3$, 500 MHz

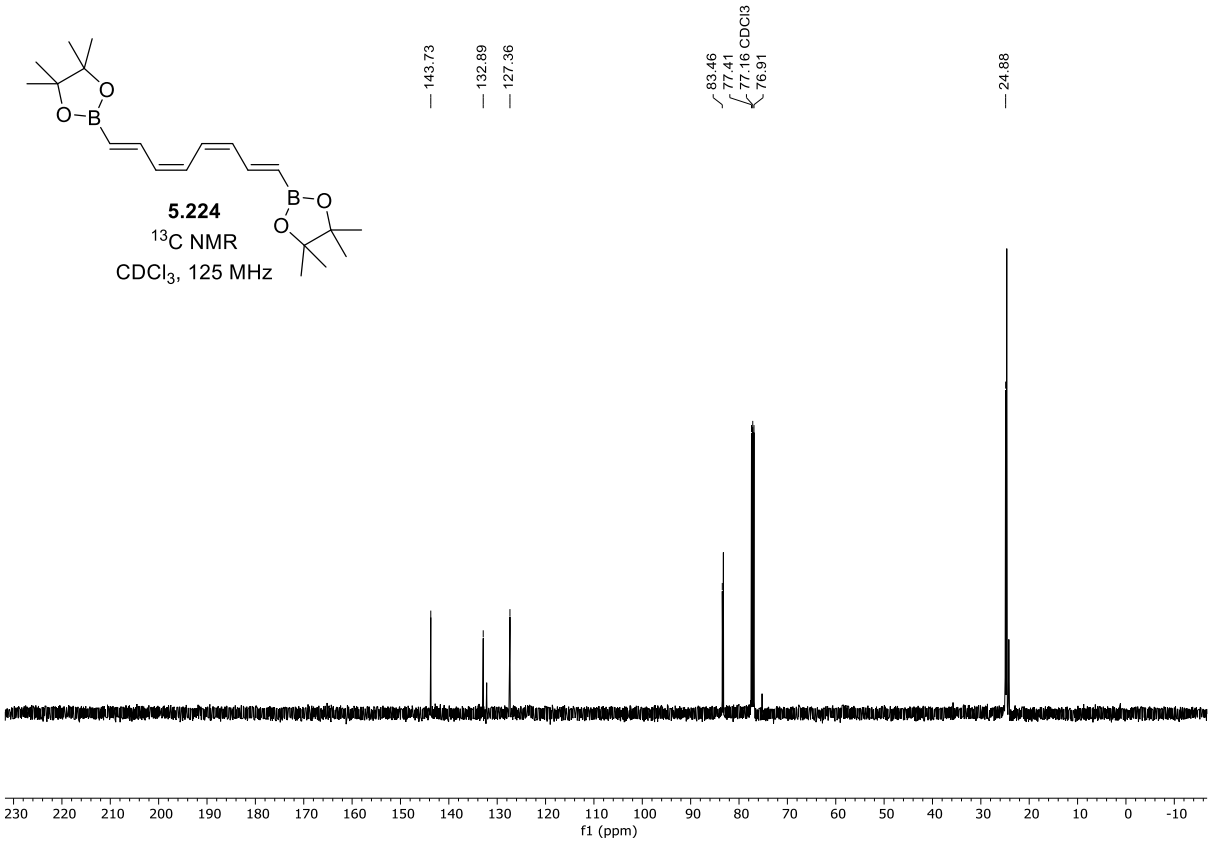

5.224
^{13}C NMR
$CDCl_3$, 125 MHz

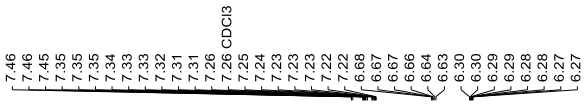

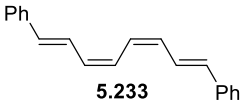

5.233

^{1}H NMR

$CDCl_3$, 500 MHz

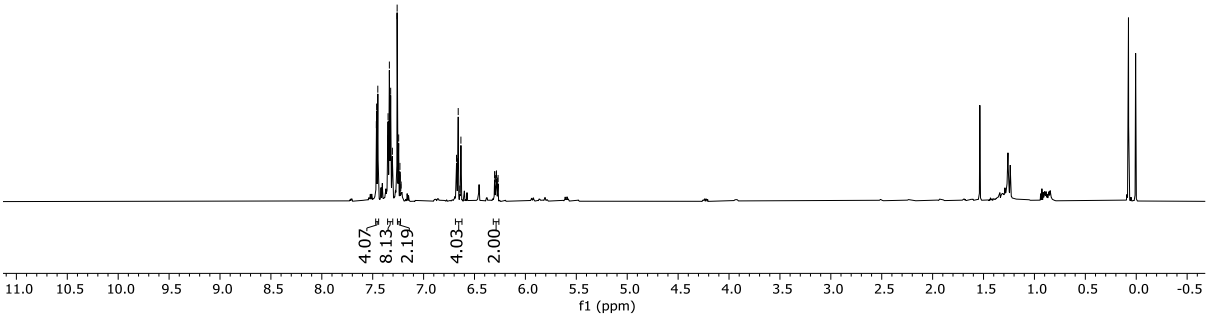

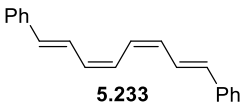

5.233

^{13}C NMR

$CDCl_3$, 125 MHz

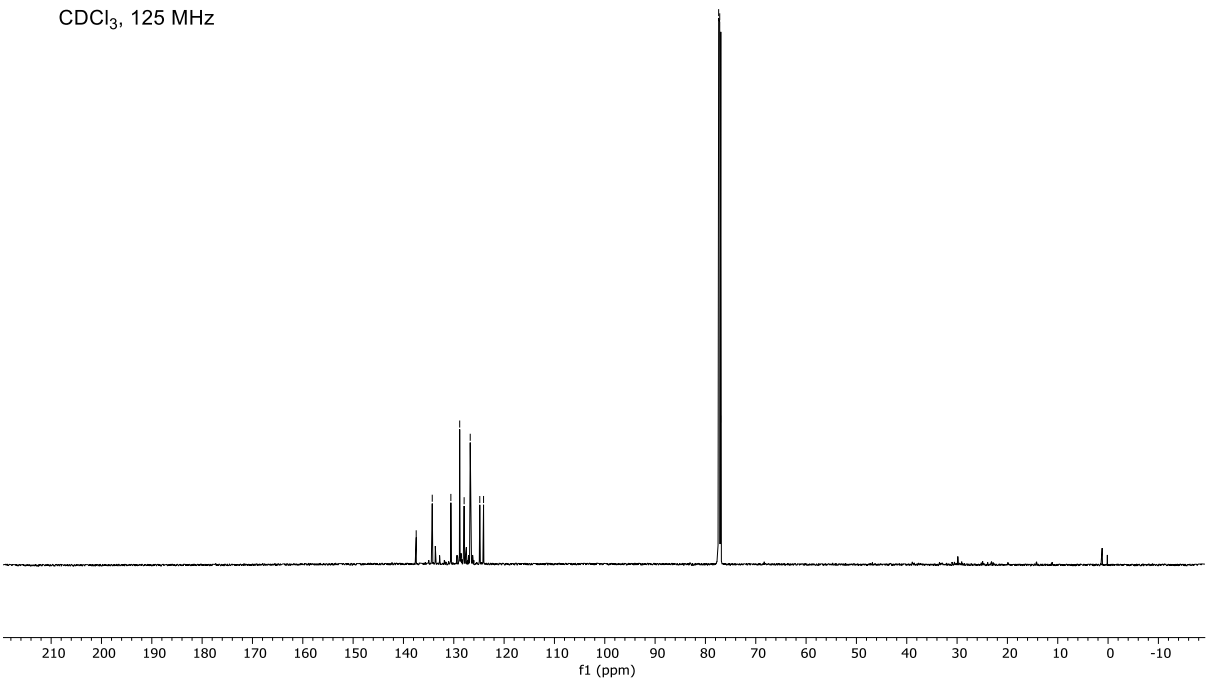

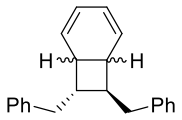

5.234

^{1}H NMR

$CDCl_3$, 500 MHz

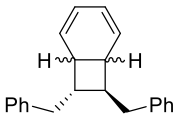

5.234

^{13}C NMR

$CDCl_3$, 125 MHz

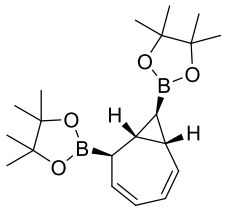

5.204

^{1}H NMR

$(CD_3)_2SO$, 500 MHz

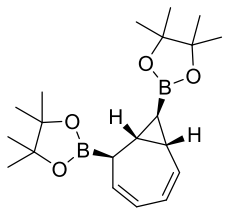

5.204

^{13}C NMR

$(CD_3)_2SO$, 125 MHz

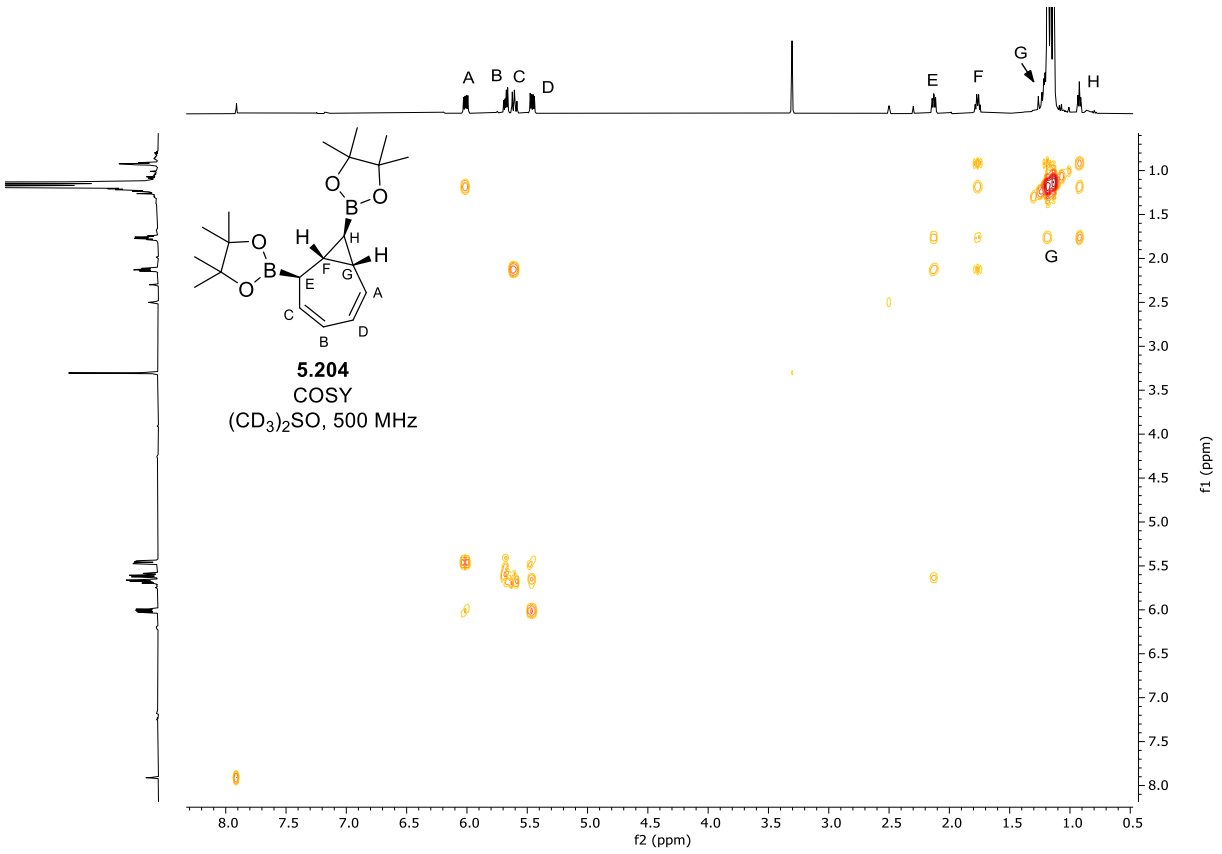

5.204
COSY
$(CD_3)_2SO$, 500 MHz

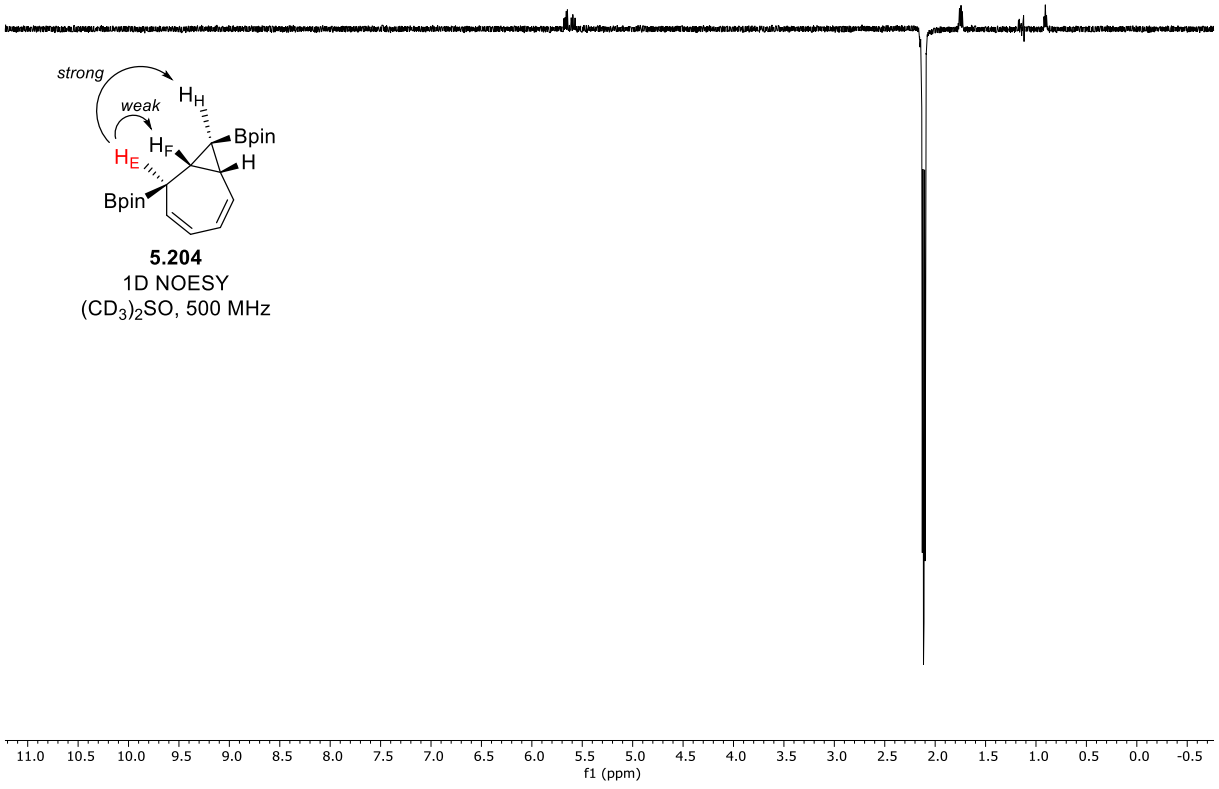

5.204
1D NOESY
$(CD_3)_2SO$, 500 MHz

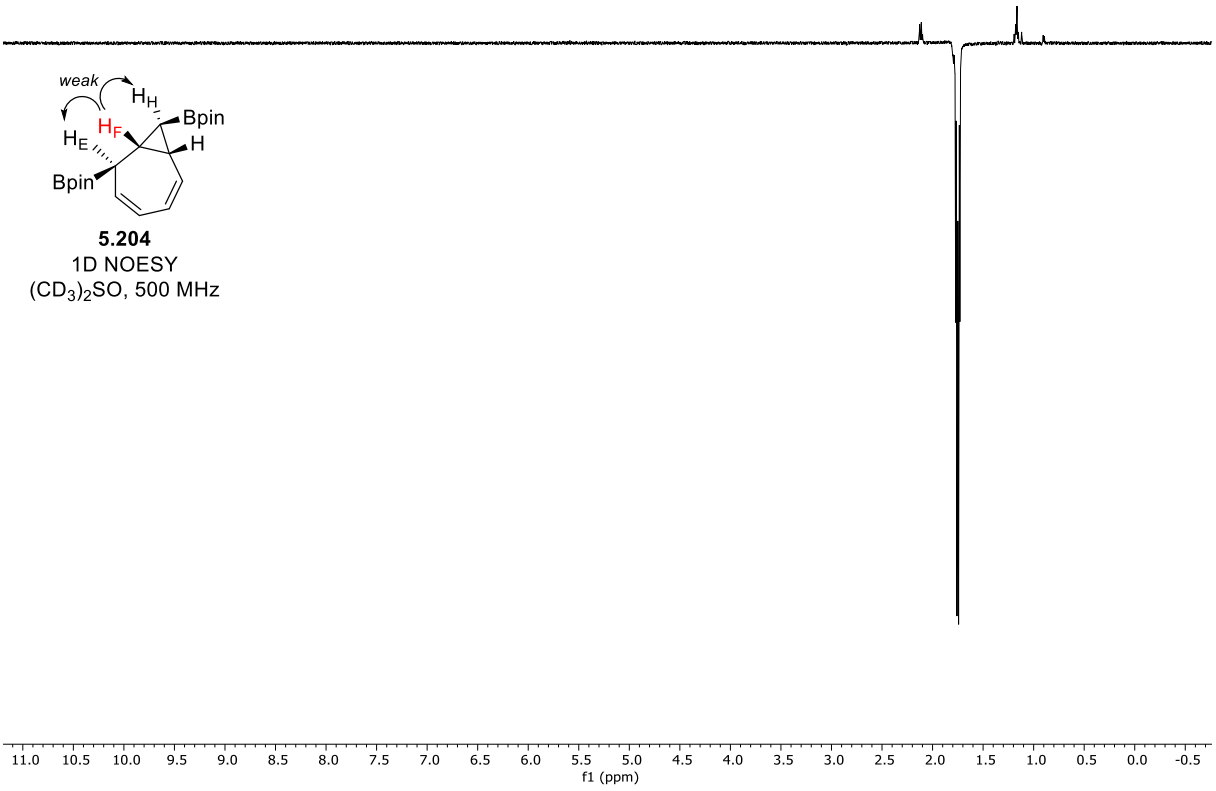

5.204
1D NOESY
$(CD_3)_2SO$, 500 MHz

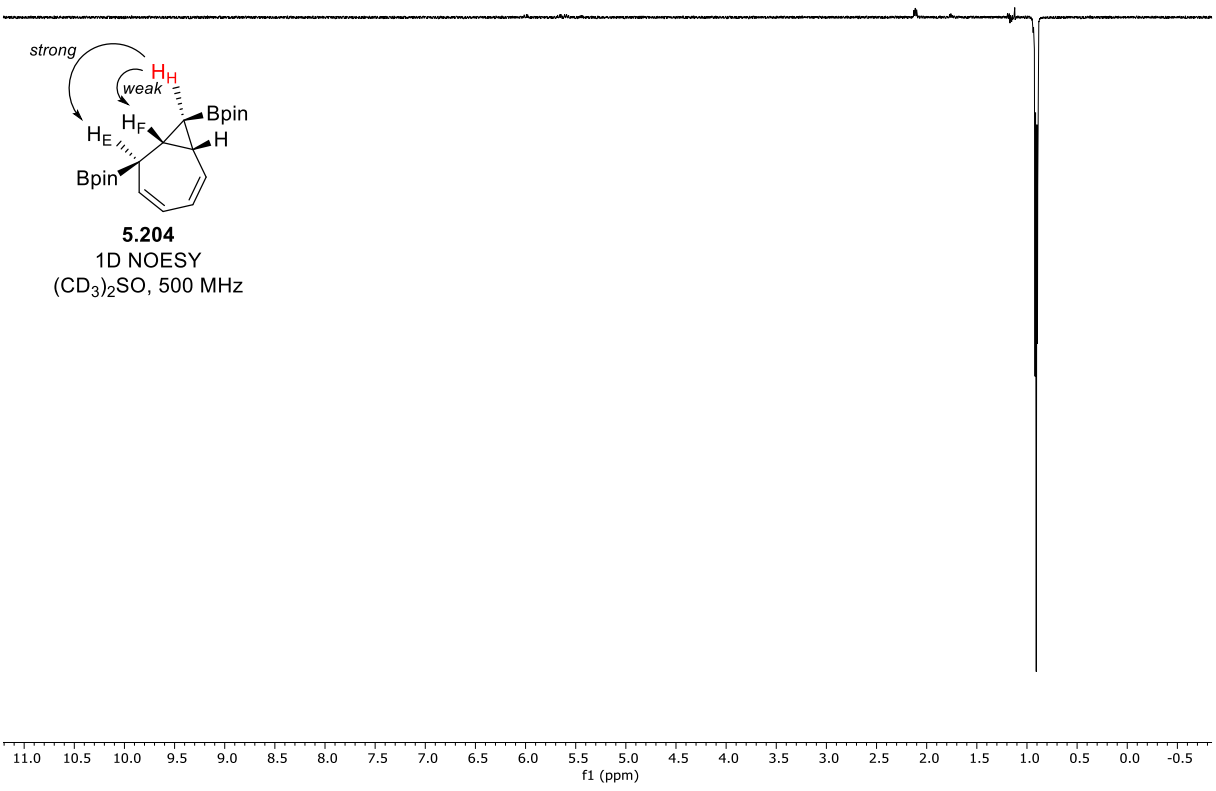

5.204
1D NOESY
$(CD_3)_2SO$, 500 MHz

7.3 Chapter 6 Experimental

Computational Methods

Geometry optimisations, frequency calculations, and single point energy calculations were performed using Gaussian 16.[15] Ground state conformers were assessed using Spartan14 through a sequence of MMFF, Semi-empirical/PM6, HF/3-21G calculations, and the lowest energy conformer selected. Geometry optimisations and frequency calculations were conducted using the M062X functional,[16–18] and def2SVP basis set[19] . Ground states and transition structures were verified by inspecting the number of imaginary vibrational frequencies (ground state – zero, transition structure – one). Transition structures were verified using intrinsic reaction coordinate calculations. Finally, the single point energies were calculated with the same functional and the def2TZVP basis set.[20] The Gibbs free energies were calculated by applying the free energy correction (M062X/def2SVP) to the electronic energy (M062X/def2TZVP), and the results are summarised in Tables S1 to S8.

Structure	Number of imaginary frequencies	Free energy correction (Hartree)	Electronic energy (Hartree)	Relative Gibbs free energy (kJ/mol)
Trimethyl				
Trimethyl_tetraene_GS	0	0.248757	-507.298437	0.000
Trimethyl_tetraene_8π_TS	1	0.253028	-507.278848	62.644
Trimethyl_cyclooctatriene_GS	0	0.257082	-507.324735	-47.188
Trimethyl_cyclooctatriene_endo_6π_TS	1	0.255663	-507.282947	58.801
Trimethyl_cyclooctatriene_exo_6π_TS	1	0.25445	-507.284694	51.029
Trimethyl_BOD_endo_GS	0	0.25888	-507.330909	-58.677
Trimethyl_BOD_exo_GS	0	0.257928	-507.333634	-68.331
Dimethyl A				
Dimethyl_A_tetraene_GS	0	0.222551	-467.993693	0.000
Dimethyl_A_tetraene_8π_TS	1	0.226827	-467.968957	76.171
Dimethyl_A_cyclooctatriene_GS	0	0.231384	-468.015406	-33.816
Dimethyl_A_cyclooctatriene_endo_6π_TS	1	0.22933	-467.972351	73.832
Dimethyl_A_cyclooctatriene_exo_6π_TS	1	0.228624	-467.973105	69.998

Dimethyl_A _BOD_endo_GS	0	0.232755	-468.020413	-43.363
Dimethyl_A _BOD_exo_GS	0	0.231824	-468.021719	-49.236
Dimethyl B				
Dimethyl_B_tetraene _GS	0	0.223089	-467.993487	0.000
Dimethyl_B _tetraene_8π_TS	1	0.227364	-467.973404	63.952
Dimethyl_B _cyclooctatriene_GS	0	0.2314	-468.013332	-30.283
Dimethyl_B _cyclooctatriene_end o_6π_TS	1	0.230507	-467.973066	73.091
Dimethyl_B _cyclooctatriene_exo _6π_TS	1	0.22914	-467.975049	64.296
Dimethyl_B _BOD_endo_GS	0	0.233259	-468.019014	-40.320
Dimethyl_B _BOD_exo_GS	0	0.232293	-468.021795	-50.158
Dimethyl C				
Dimethyl_C_tetraene _GS	0	0.223838	-467.992446	0.000
Dimethyl_C _tetraene_8π_TS	1	0.227843	-467.971489	65.538
Dimethyl_C _cyclooctatriene_GS	0	0.232494	-468.015881	-38.802
Dimethyl_C _cyclooctatriene_end o_6π_TS	1	0.230348	-467.973827	65.976
Dimethyl_C _cyclooctatriene_exo _6π_TS	1	0.229717	-467.974836	61.670
Dimethyl_C _BOD_endo_GS	0	0.233138	-468.017318	-40.884
Dimethyl_C _BOD_exo_GS	0	0.232109	-468.020373	-51.607
Monomethyl A				
Monomethyl_A_tetr aene_GS	0	0.197534	-428.688379	0.000
Monomethyl _A _tetraene_8π_TS	1	0.201839	-428.663357	76.998
Monomethyl _A _cyclooctatriene_GS	0	0.205792	-428.704355	-20.264
Monomethyl _A _cyclooctatriene_end o_6π_TS	1	0.204002	-428.662345	85.334
Monomethyl _A _cyclooctatriene_exo _6π_TS	1	0.20343	-428.663336	81.230

Monomethyl _A _BOD_endo_GS	0	0.206974	-428.708469	-27.962
Monomethyl _A _BOD_exo_GS	0	0.206244	-428.709861	-33.533
Monomethyl B				
Monomethyl_B_tetra ene_GS	0	0.197805	-428.689803	0.000
Monomethyl _B _tetraene_8π_TS	1	0.202326	-428.661832	85.308
Monomethyl _B _cyclooctatriene_GS	0	0.205633	-428.704363	-17.675
Monomethyl _B _cyclooctatriene_end o_6π_TS	1	0.203908	-428.663522	85.024
Monomethyl _B _cyclooctatriene_exo _6π_TS	1	0.204024	-428.663322	85.854
Monomethyl _B _BOD_endo_GS	0	0.206618	-428.706713	-21.259
Monomethyl _B _BOD_exo_GS	0	0.206191	-428.70844	-26.914
Monomethyl C				
Monomethyl_B_tetra ene_GS	0	0.197127	-428.685855	0.000
Monomethyl _B _tetraene_8π_TS	1	0.202557	-428.665701	67.171
Monomethyl _B _cyclooctatriene_GS	0	0.206764	-428.70441	-23.414
Monomethyl _B _cyclooctatriene_end o_6π_TS	1	0.205116	-428.663977	78.416
Monomethyl _B _cyclooctatriene_exo _6π_TS	1	0.204483	-428.665185	73.582
Monomethyl _B _BOD_endo_GS	0	0.20751	-428.705443	-24.168
Monomethyl _B _BOD_exo_GS	0	0.206491	-428.708557	-35.019
Tributyl				
Tributyl_tetraene_G S	0	0.491654	-861.057174	0.000
Tributyl_tetraene_8π _TS	1	0.498259	-861.029896	88.960
Tributyl_cyclooctatri ene_GS	0	0.499592	-861.089925	-65.147
Tributyl_cyclooctatri ene_6π1_TS	1	0.499684	-861.043646	56.601
Tributyl_cyclooctatri ene_6π2_TS	1	0.49731	-861.050039	33.583

Tributyl_BOD1_GS	0	0.501856	-861.093424	-68.389
Tributyl_BOD2_GS	0	0.500605	-861.101785	-93.625
Butylmethyl				
Butylmethyl_tetraene_GS	0	0.304082	-585.906747	0.000
Butylmethyl_tetraene_8π_TS	1	0.31038	-585.888927	63.322
Butylmethyl_cyclooctatriene_GS	0	0.313325	-585.931344	-40.312
Butylmethyl_cyclooctatriene_6π1_TS	1	0.311469	-585.89397	52.941
Butylmethyl_cyclooctatriene_6π2_TS	1	0.312875	-585.889505	68.355
Butylmethyl_BOD1_GS	0	0.315346	-585.93159	-35.652
Butylmethyl_BOD2_GS	0	0.315716	-585.922621	-11.132
Unsubstituted Tetraene				
Unsubstituted_tetraene_GS	0	0.17113	-389.381461	0.000
Unsubstituted_tetraene_8π_TS	1	0.177641	-389.35589	84.231
Unsubstituted_cyclooctatriene_GS	0	0.179996	-389.39288	-6.703
Unsubstituted_cyclooctatriene_6π_TS	1	0.178721	-389.353564	93.174
Unsubstituted_BOD_GS	0	0.180521	-389.396602	-15.097

Table S1: Calculated relative free energies of methyl tetraene compounds (6.68-6.77)

Trimethyl Cartesian Coordinates

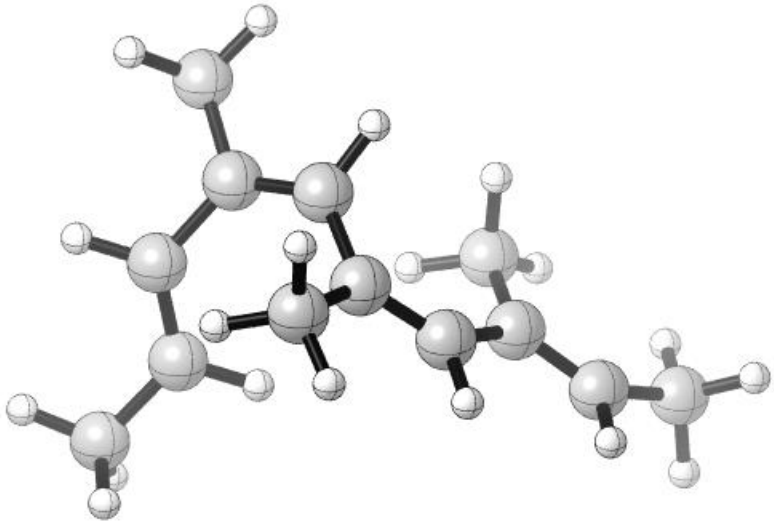

Trimethyl_tetraene_GS
E(M062X/def2TZVP) = -507.298437 Hartree
Free energy correction (M062X/def2SVP) = 0.248757 Hartree
G = -1331258.935

C	-1.84651600	1.14179200	-0.05127200
C	-0.70371400	1.15522700	0.66083300
H	-0.25214400	2.13589000	0.84995900
C	-0.02512000	-0.00317500	1.30456000
C	1.23061300	-0.41751900	1.03924300
H	1.61046300	-1.22965800	1.66875600
C	2.18772300	0.02860000	0.01180300
C	-2.56182100	-0.08220200	-0.46600400
H	-3.65282400	0.01086300	-0.54835900
C	3.42456800	-0.50936300	0.04630800
H	3.62148700	-1.23333100	0.84512600
C	-1.99805900	-1.24975300	-0.80360900
H	-0.90671700	-1.33581500	-0.76365400
C	4.58445800	-0.24505300	-0.86197800
H	4.92116100	-1.17623100	-1.34472100
H	5.44394100	0.13564500	-0.28764300
H	4.36172000	0.48348100	-1.64992700
C	-2.75891400	-2.46340100	-1.23625300
H	-2.44705300	-2.78833200	-2.24082600
H	-3.84119400	-2.27550200	-1.25179200
H	-2.56396700	-3.30911400	-0.55813100
C	-0.81806700	-0.65500300	2.41271900
H	-1.02795700	0.07401900	3.21108800
H	-0.27764200	-1.50616800	2.84806000
H	-1.79051100	-1.00636700	2.03676300
C	1.74877000	1.02151400	-1.03371400
H	2.48812800	1.12274800	-1.83596200
H	1.58624200	2.01740900	-0.59723400
H	0.79330500	0.71369300	-1.48133300

C	-2.48005800	2.42767800	-0.51770600
H	-2.54349700	2.45641000	-1.61677500
H	-1.91545000	3.30468800	-0.17597300
H	-3.51067900	2.50962300	-0.13700600

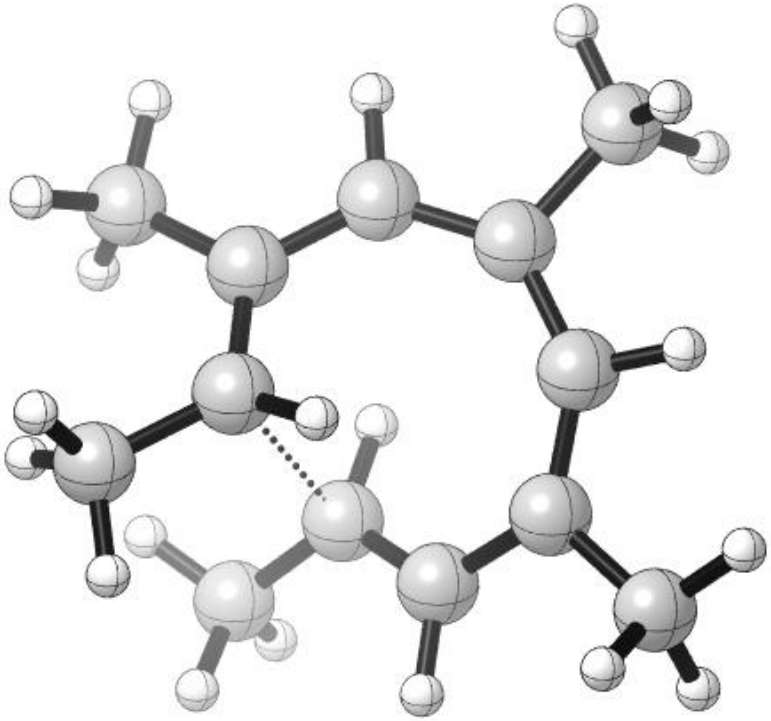

Trimethyl_tetraene_8π_TS
E(M062X/def2TZVP) = -507.278848 Hartree
Free energy correction (M062X/def2SVP) = 0.253028 Hartree
G = -1331196.290

C	1.72905000	-1.10247900	0.10673000
C	1.94831700	0.27855400	0.11553100
H	3.00499600	0.49942600	0.30925300
C	1.23760600	1.50095100	-0.10935300
C	-0.11271600	1.86400800	-0.11041500
H	-0.29038300	2.88978300	-0.44733000
C	-1.28955400	1.17194800	0.25407900
C	0.56691700	-1.79390200	-0.29592700
H	0.50789000	-2.85870300	-0.03908200
C	-1.23405800	-0.06349300	0.88254600
H	-0.29607800	-0.29309300	1.38545600
C	-0.52660200	-1.20535200	-0.90217800
H	-0.34290300	-0.26092400	-1.41493000
C	-2.44604100	-0.78733200	1.39041400
H	-2.22128900	-1.84661100	1.57812200
H	-3.28930400	-0.73440500	0.68782000
H	-2.78579800	-0.35009000	2.34476300
C	-1.69433200	-2.00867600	-1.39456100
H	-2.61431800	-1.40840000	-1.43000100
H	-1.87613900	-2.88730700	-0.75952400

H	-1.50386300	-2.36569200	-2.41959300
C	2.86995500	-1.98308000	0.58164800
H	3.16388000	-2.70792000	-0.19200900
H	2.56593200	-2.56216100	1.46763600
H	3.75491900	-1.39506800	0.85471900
C	2.20065100	2.66069900	-0.34551500
H	2.82888100	2.82203400	0.54460100
H	1.67147600	3.59843000	-0.55409400
H	2.87861600	2.45332000	-1.18646100
C	-2.62131100	1.75223800	-0.15731600
H	-3.34169100	1.76113200	0.67404700
H	-3.07474600	1.16173200	-0.97198800
H	-2.50736400	2.78000800	-0.52550700

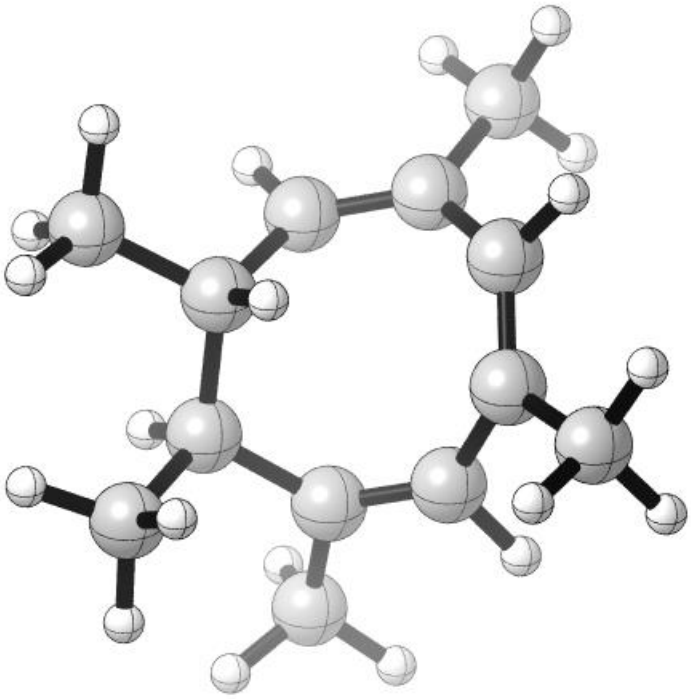

Trimethyl_cyclooctatriene_GS
E(M062X/def2TZVP) = -507.324735 Hartree
Free energy correction (M062X/def2SVP) = 0.257082 Hartree
G = -1331306.123

C	-0.06095200	-1.60584600	0.38305700
C	-1.95358400	-0.22967000	-0.51240600
C	-1.17099300	-1.32632900	-0.55753800
H	-2.85744300	-0.22216300	-1.13448300
C	-1.73593600	0.94089200	0.35339500
C	1.04863200	-0.93972000	0.75035200
C	-0.55398800	1.57699100	0.37495800
H	-0.43387200	2.43234700	1.05211900
C	0.61092300	1.26664300	-0.52718200
H	0.21991300	0.74609400	-1.41578400
C	1.63034000	0.32256500	0.13496100
H	2.10402600	0.88435200	0.96192000

C	2.73781500	-0.07710000	-0.85394800
H	3.42228700	-0.81788900	-0.41888800
H	3.34053000	0.78826200	-1.16046200
H	2.28737800	-0.52470100	-1.75343100
C	1.26663900	2.57461200	-0.98080000
H	2.01739700	2.41203000	-1.76549400
H	1.76143500	3.07472300	-0.13226500
H	0.50884700	3.26286900	-1.38106900
H	-0.20051900	-2.57746900	0.87782800
C	-2.91063800	1.38444100	1.18461700
H	-3.20859300	0.59578400	1.89252700
H	-3.78408700	1.58526000	0.54377700
H	-2.68044400	2.29635200	1.75135800
C	-1.50941400	-2.47743500	-1.47104300
H	-0.67897600	-2.67472900	-2.16663800
H	-2.41546500	-2.27615100	-2.05742700
H	-1.66330200	-3.40207100	-0.89207700
C	1.90916900	-1.51522500	1.84909800
H	2.96232800	-1.60078900	1.54076800
H	1.55984400	-2.50540600	2.16837000
H	1.89064100	-0.84562200	2.72422300

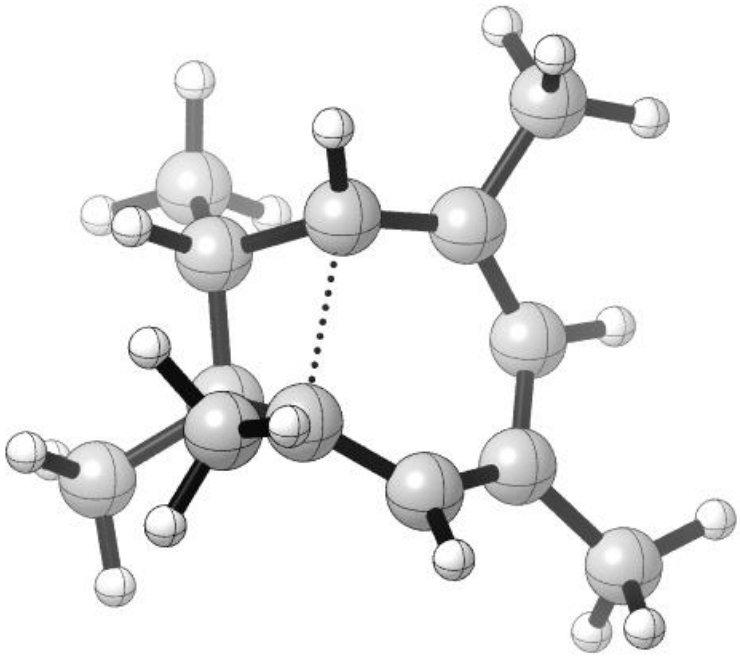

Trimethyl_cyclooctatriene_endo_6π_TS
E(M062X/def2TZVP) = -507.282947 Hartree
Free energy correction (M062X/def2SVP) = 0.255663 Hartree
G = -1331200.134

C	1.03873100	1.32721300	0.27550000
C	1.68706800	-0.99861400	-0.37888800
C	1.75768700	0.40558600	-0.50085800
H	2.67657000	0.78213400	-0.96198100
C	0.70723300	-1.59697100	0.41493000

H	0.99014400	-2.49112800	0.98397400
C	-0.25910700	1.14053300	0.80322800
H	-0.43783400	1.74100500	1.70928000
C	-0.55013400	-1.01912000	0.63150300
C	-1.30226500	-0.43620000	-0.56962000
H	-0.59812600	-0.40093100	-1.41477100
C	-1.50880300	0.97294400	-0.05926200
H	-2.37500000	0.96542500	0.62507000
C	1.78364400	2.56562700	0.73614300
H	1.31453400	3.48517100	0.35310500
H	2.83699000	2.55693700	0.42757600
H	1.75265500	2.62550200	1.83576900
C	-1.71220900	2.06790800	-1.09778600
H	-1.76983300	3.05973000	-0.62390700
H	-2.64174700	1.91101000	-1.66639000
H	-0.86787900	2.07791700	-1.80437300
C	-2.54831300	-1.20190300	-0.99539000
H	-3.01199000	-0.72012800	-1.86920400
H	-3.29951200	-1.22911700	-0.19156300
H	-2.30478300	-2.23817100	-1.27348800
C	2.84128500	-1.82621100	-0.88838500
H	3.76949600	-1.24334800	-0.95963900
H	2.61759400	-2.22341900	-1.89103500
H	3.01964300	-2.69127100	-0.23356200
C	-1.40029000	-1.54941300	1.76137300
H	-2.17789500	-0.82936300	2.05491900
H	-0.78634400	-1.76854100	2.64445300
H	-1.91383400	-2.47768800	1.46084000

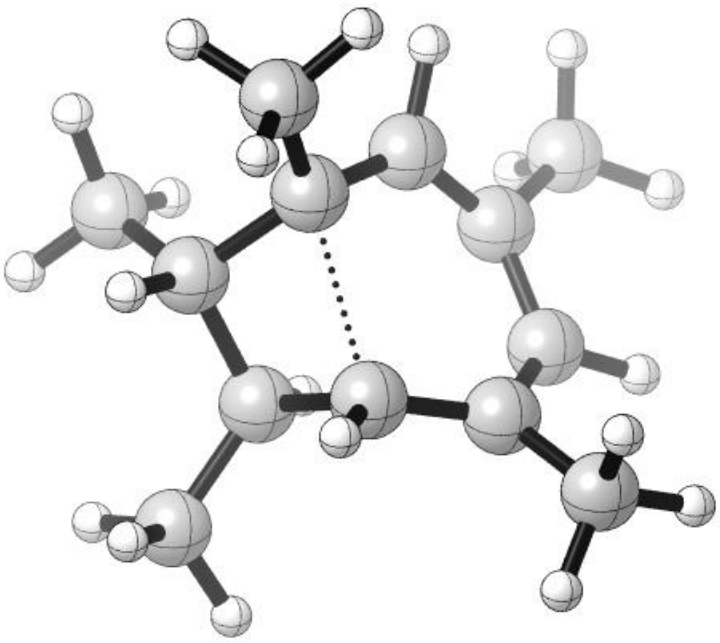

Trimethyl_cyclooctatriene_exo_6π_TS
E(M062X/def2TZVP) = -507.284694 Hartree
Free energy correction (M062X/def2SVP) = 0.254450 Hartree

G = -1331207.906

C	-0.27714100	-1.51862500	0.34836600
C	-1.94109500	0.08562500	-0.51224200
C	-1.34577900	-1.19449100	-0.50152700
H	-2.97703500	0.12505200	-0.86471100
C	-1.43867800	1.17283600	0.20379000
C	0.74670100	-0.70894500	0.88836000
C	-0.05656000	1.25421800	0.41778600
H	0.29218400	1.97902900	1.16824400
C	0.93992300	0.99571400	-0.70044700
H	0.40382800	0.51704000	-1.53472800
C	1.79671600	-0.04117800	-0.00831800
H	2.49325900	0.49371600	0.66304400
C	2.58714800	-1.00170200	-0.88688200
H	3.10099300	-1.76890200	-0.28827700
H	3.35120300	-0.46373900	-1.46850300
H	1.91061100	-1.51401700	-1.58740200
C	1.65382100	2.24271900	-1.20304200
H	2.40110400	1.98806000	-1.97000200
H	2.17561000	2.75171000	-0.37732400
H	0.94242700	2.95454400	-1.64640000
H	-0.36556800	-2.52075200	0.79212400
C	-2.38619100	2.13203900	0.88372500
H	-3.40825900	2.01712000	0.49835100
H	-2.07953100	3.17935600	0.75394400
H	-2.42044400	1.92850700	1.96636100
C	-2.09808700	-2.32889800	-1.15569300
H	-1.70973800	-2.51174300	-2.16981600
H	-3.17066900	-2.10925400	-1.24796400
H	-1.97608100	-3.26450000	-0.59108300
C	1.27748700	-1.11549600	2.24479800
H	2.22255700	-1.67664300	2.14304900
H	0.56030000	-1.72788700	2.80692400
H	1.50367000	-0.21959500	2.84212100

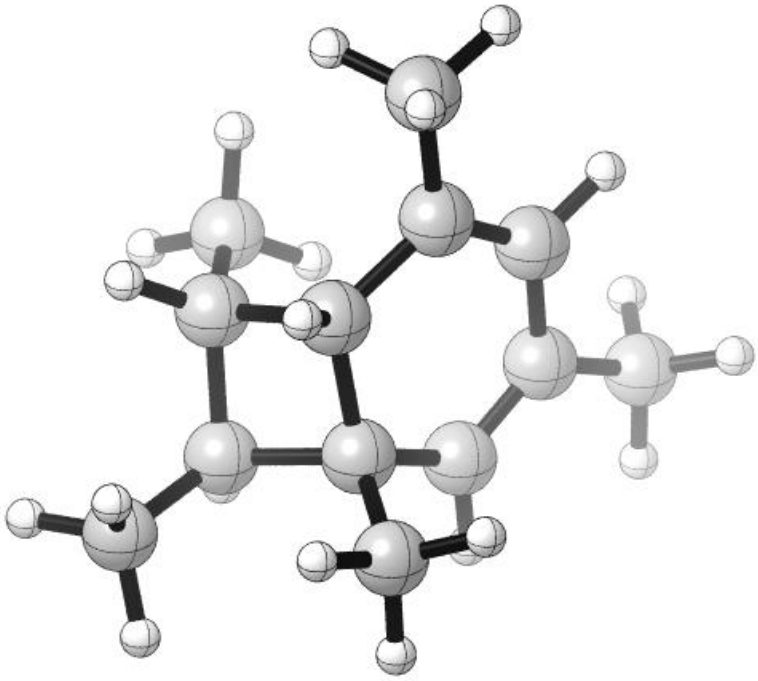

Trimethyl_BOD_endo_GS
E(M062X/def2TZVP) = -507.330909 Hartree
Free energy correction (M062X/def2SVP) = 0.258880 Hartree
G = -1331317.612

C	-1.68630000	-1.05995700	0.20014800
C	-1.06120200	1.18279000	-0.63435400
C	0.71700600	-0.73274700	-0.45599100
C	0.38328000	0.77706900	-0.58303400
C	-0.42684500	-1.51973600	0.12924900
C	-2.00596900	0.30636500	-0.25710600
H	-0.19998000	-2.53983100	0.46070100
H	0.91729100	1.21279700	-1.44353200
H	-3.05899800	0.60448600	-0.26703400
C	1.18732700	1.05837100	0.72884400
H	1.94160000	1.85313200	0.61271900
C	1.79196500	-0.36936500	0.62279200
H	1.68057400	-0.95502200	1.55067300
C	-1.36094300	2.58627600	-1.06659700
H	-2.43506400	2.80889000	-1.01858600
H	-1.01197600	2.75986100	-2.09727600
H	-0.82581200	3.30868300	-0.42794200
C	0.36404400	1.31404400	1.98026900
H	-0.15775400	2.28144100	1.93013700
H	1.01741400	1.32585800	2.86585600
H	-0.39289600	0.52984200	2.12232500
C	3.24090300	-0.39460800	0.16651700
H	3.39168500	0.24012000	-0.72020700
H	3.57350100	-1.41202200	-0.08708300
H	3.89686100	-0.01119100	0.96242700
C	-2.82309500	-1.87990100	0.74280400

H	-2.48843500	-2.87803700	1.05345700
H	-3.61316700	-1.99812900	-0.01535400
H	-3.28464900	-1.38149200	1.60994200
C	1.19838600	-1.42455000	-1.72762800
H	0.37687500	-1.46871600	-2.45829800
H	1.52147500	-2.45658900	-1.51883200
H	2.04011400	-0.88839100	-2.18957000

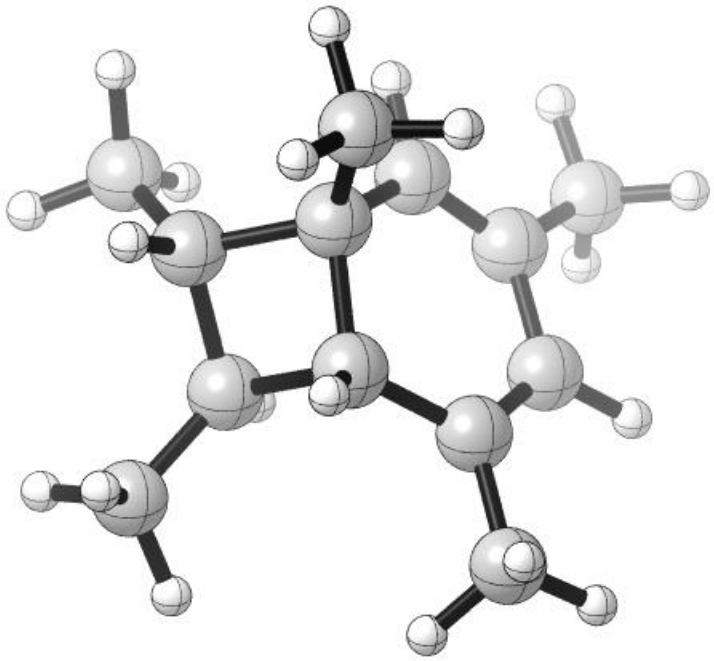

Trimethyl_BOD_exo_GS
E(M062X/def2TZVP) = -507.333634 Hartree
Free energy correction (M062X/def2SVP) = 0.257928 Hartree
G = -1331327.266

C	2.19697100	-1.02444800	-0.63576500
C	2.71007400	-1.02406300	0.72294400
H	2.00370700	-1.25861800	1.52221500
C	3.98509300	-0.75972400	1.08800900
C	0.92072800	-1.28325400	-1.00035900
H	0.67776500	-1.24840800	-2.06664800
C	-0.18969100	-1.60874000	-0.11747900
C	5.09217200	-0.42311200	0.20547000
H	4.90296900	-0.37287200	-0.87139800
C	6.33560800	-0.17668800	0.64806200
C	-1.43104300	-1.86015600	-0.56341200
C	7.49796700	0.19381100	-0.21755900
H	7.21210300	0.11550100	-1.27999700
H	-0.00416000	-1.65378200	0.96033600
H	2.90459500	-0.79600800	-1.43564800
H	4.22866300	-0.79759400	2.15410400
H	-1.62847300	-1.80876400	-1.64081900
H	6.52351400	-0.22577000	1.72809400
H	8.33856200	-0.50073200	-0.05410000

C	-2.60480700	-2.18649700	0.31179700
H	-2.27384900	-2.22506700	1.36226200
H	-2.98815300	-3.18842400	0.06075400
C	-3.73712100	-1.18767400	0.16502100
C	-5.80989400	0.63092100	-0.09537100
C	-3.47033000	0.18390300	0.36842400
C	-5.02530700	-1.60597400	-0.16470300
C	-6.09458400	-0.70070700	-0.29930900
C	-4.52228500	1.06146000	0.23302500
H	-2.46867500	0.53650600	0.61758600
H	-5.21221100	-2.66965800	-0.32313300
H	-7.10142600	-1.03018600	-0.55224300
O	-6.64285800	1.70942300	-0.13175600
O	-4.53910600	2.41298300	0.40526900
C	-5.80229000	2.84709200	-0.06516100
H	-5.69048800	3.28440800	-1.07449600
H	-6.22559400	3.58054400	0.63282200
C	8.01353000	1.60669200	0.06657300
H	8.27448900	1.69428600	1.13206000
H	7.20440900	2.33620100	-0.12527200
O	9.17809100	1.90807400	-0.65522400
H	8.96448700	1.88753500	-1.59404100

Dimethyl A Cartesian Coordinates

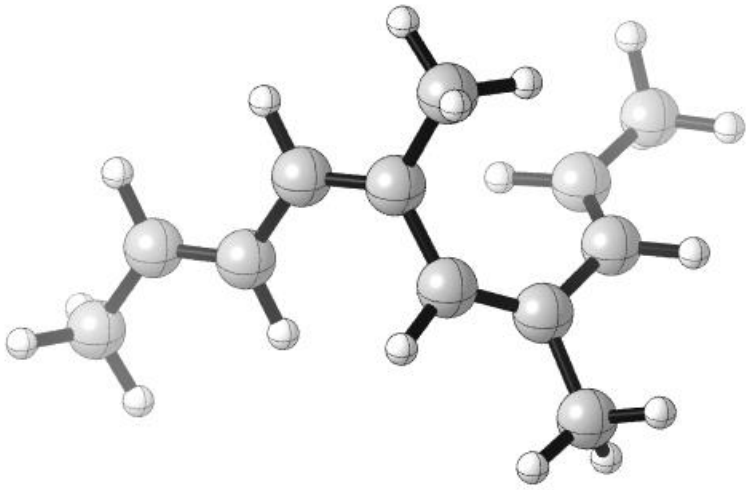

Dimethyl_A_tetraene_GS
E(M062X/def2TZVP) = -467.993693 Hartree
Free energy correction (M062X/def2SVP) = 0.222551 Hartree
G = -1228133.133

C	1.50100000	-1.27934700	0.05341000
C	0.33838200	-1.04129000	0.69261700
H	-0.29318900	-1.91308700	0.90210100
C	-0.18463500	0.25601700	1.19289200
C	-1.42866200	0.67680700	0.88180300
H	-1.79346700	1.60405500	1.33700400

C	-2.34396800	0.00227100	-0.03036600
H	-1.97748200	-0.89919300	-0.53431500
C	2.43019000	-0.23180400	-0.41619800
H	3.49776100	-0.48696300	-0.38648000
C	-3.58808700	0.43145000	-0.29165100
H	-3.93865200	1.34067100	0.21159100
C	2.06898000	0.94920500	-0.93396300
H	0.99969800	1.17960500	-1.00510800
C	-4.54762100	-0.23586900	-1.22537200
H	-5.46952900	-0.53447000	-0.70185600
H	-4.10356200	-1.13268000	-1.67837800
H	-4.85257300	0.44471300	-2.03589700
C	3.02409100	1.99013800	-1.42630200
H	2.83501400	2.23226300	-2.48341600
H	4.06678000	1.65921400	-1.32583200
H	2.90304800	2.92879400	-0.86262700
C	1.93041300	-2.68786500	-0.26938300
H	2.90592500	-2.90654300	0.19389300
H	2.05706700	-2.81958000	-1.35516200
H	1.20378000	-3.42628900	0.09297900
C	0.67539600	1.02094000	2.16584900
H	0.84210800	0.42007500	3.07367000
H	0.19928100	1.96686400	2.45688000
H	1.66512600	1.23863400	1.74093800

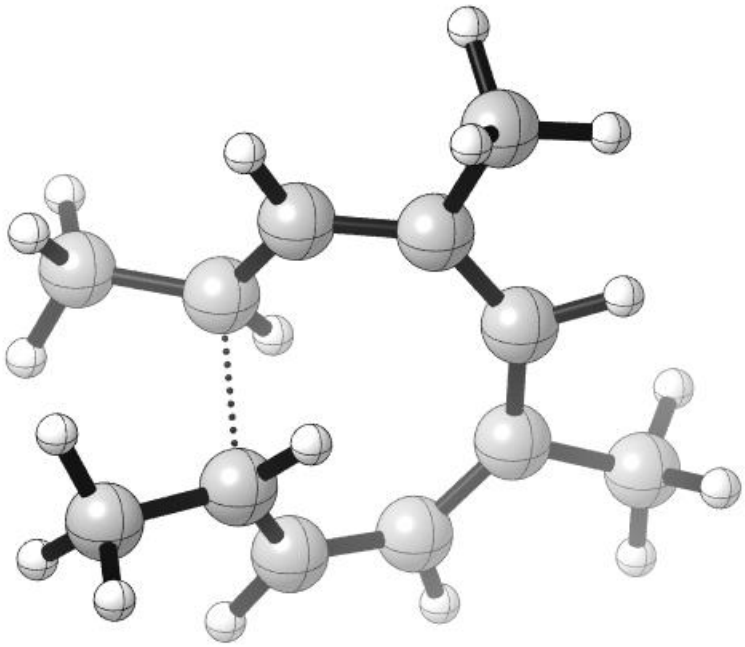

Dimethyl_A_tetraene_8π_TS
E(M062X/def2TZVP) = -467.968957 Hartree
Free energy correction (M062X/def2SVP) = 0.226827 Hartree
G = -1228056.962

C	-0.80721200	1.55385000	-0.15029900
C	-1.70494300	0.47730600	-0.11922900

H	-2.72662500	0.82347400	-0.31804800
C	-1.71687500	-0.92435100	0.14486000
C	-0.72509700	-1.91465600	0.17674100
H	-1.07561800	-2.88306500	0.54420200
C	0.62812400	-1.89554500	-0.19022200
H	1.23027500	-2.75824200	0.11753000
C	0.53884600	1.57598600	0.25976500
H	1.12687600	2.45825600	-0.02212800
C	1.27405300	-0.84011900	-0.81590300
H	0.63893000	-0.16103600	-1.38357900
C	1.19318900	0.53635800	0.90161600
H	0.55844300	-0.16704000	1.43976100
C	2.70187700	-0.93720200	-1.26790200
H	3.19122300	0.04724300	-1.27722900
H	2.75154800	-1.33187100	-2.29554600
H	3.28449500	-1.60926900	-0.62166800
C	2.59557300	0.68127800	1.41632900
H	3.11243700	-0.28764500	1.46023400
H	2.58228000	1.08868000	2.44003200
H	3.18691900	1.36496400	0.79070300
C	-1.33665300	2.86762800	-0.69664800
H	-1.11965700	3.70265100	-0.01506700
H	-2.42067400	2.83293900	-0.86252400
H	-0.86039200	3.10345200	-1.66157000
C	-3.13183400	-1.43649600	0.39344300
H	-3.75775200	-1.27773000	-0.49862000
H	-3.61209600	-0.90098700	1.22553400
H	-3.14490500	-2.50899500	0.62266600

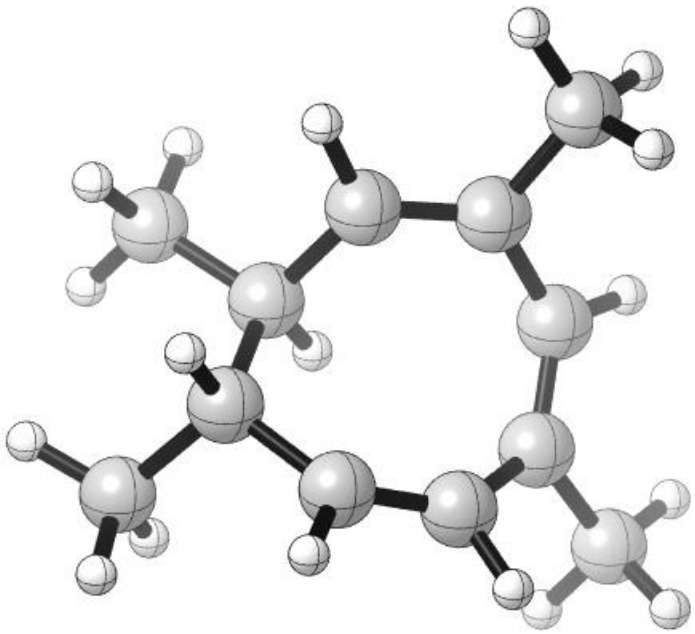

Dimethyl_A_cyclooctatriene_GS
E(M062X/def2TZVP) = -468.015406 Hartree
Free energy correction (M062X/def2SVP) = 0.231384 Hartree

G = -1228166.950

C	1.20871200	1.36014300	0.13460900
C	1.47698800	-1.11511700	-0.25190300
C	1.80347500	0.17029300	-0.49267200
H	2.63436500	0.35513700	-1.18511100
C	0.54469100	-1.59051900	0.79646200
H	0.98106400	-2.41917900	1.36970800
C	-0.11907800	1.55155000	0.17200900
H	-0.49685700	2.45564100	0.66708500
C	-0.70124500	-1.25583400	1.16811300
H	-1.09766300	-1.83762100	2.00895700
C	-1.72818700	-0.32146000	0.58024400
H	-2.13256900	0.27791500	1.41744300
C	-1.16064000	0.66451900	-0.45431500
H	-0.68052200	0.06613200	-1.24598800
C	2.18155800	2.36297100	0.69816100
H	2.89284700	2.68987400	-0.07711200
H	2.77636200	1.91668800	1.50982100
H	1.66436900	3.24919700	1.08888500
C	-2.25540300	1.52763300	-1.08729100
H	-1.81031400	2.29356000	-1.73787500
H	-2.84071200	2.04456600	-0.30900800
H	-2.94915500	0.93212900	-1.69573000
C	-2.88347400	-1.16677200	0.02469300
H	-3.75834000	-0.54973800	-0.22037300
H	-3.20218700	-1.92234700	0.75723700
H	-2.56247100	-1.69645500	-0.88584900
C	2.20351600	-2.23112600	-0.96151100
H	2.95093700	-1.84291900	-1.66537700
H	1.49406100	-2.86217000	-1.51890500
H	2.71130100	-2.88810800	-0.23740600

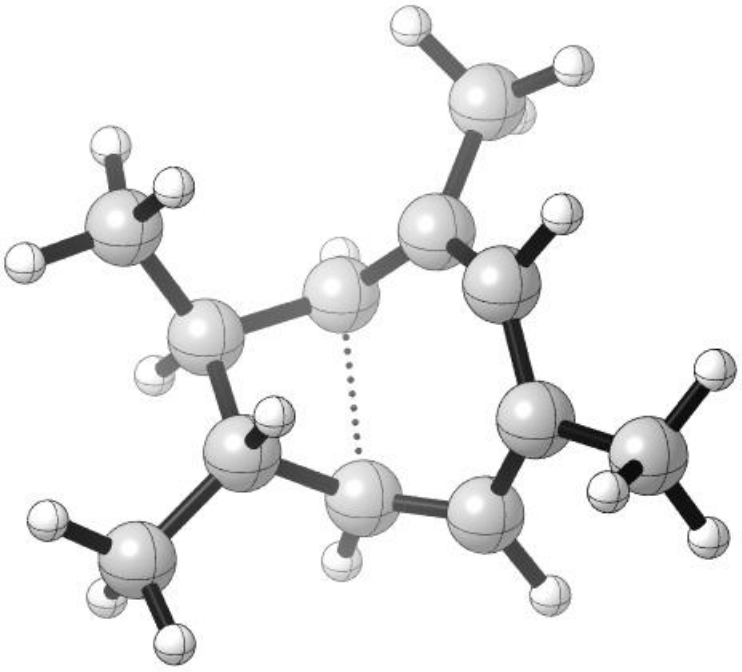

Dimethyl_A_cyclooctatriene_endo_6π_TS
E(M062X/def2TZVP) = -467.972351 Hartree
Free energy correction (M062X/def2SVP) = 0.229330 Hartree
G = -1228059.302

C	-1.06718800	-1.39670100	0.79830400
C	-1.47308200	0.58721300	-0.55253400
C	-1.80148200	-0.73573500	-0.19174600
H	-2.22285300	1.09300600	-1.16973700
C	-0.57640800	1.42959600	0.12729400
C	0.28029000	-1.11073100	1.01046700
H	0.73725100	-1.47290800	1.94054100
C	0.58980500	1.03528600	0.82144700
H	0.85887900	1.73836200	1.62509600
C	1.80709600	0.39005100	0.16176000
H	2.57127100	0.26967300	0.94945100
C	1.25231200	-0.98215900	-0.15320000
H	0.66576500	-0.92463700	-1.08374700
C	2.25730200	-2.12061000	-0.25268600
H	1.75294500	-3.08135200	-0.43101200
H	2.83914600	-2.20830600	0.67835700
H	2.96408700	-1.94982900	-1.07886600
C	2.39767100	1.19051800	-0.99084600
H	3.28641900	0.69181900	-1.40725600
H	2.69799900	2.19787100	-0.66428900
H	1.65160400	1.30160700	-1.79287200
H	-1.60785400	-2.05140400	1.48992300
C	-0.99353500	2.87995900	0.28627600
H	-1.01696900	3.14080400	1.35632500
H	-1.99002900	3.07488600	-0.13050300
H	-0.27470800	3.56220300	-0.19331700
C	-3.10457800	-1.32040700	-0.67640200

H	-2.93411500	-1.97726700	-1.54381900
H	-3.81991900	-0.54419500	-0.97958500
H	-3.56813700	-1.93801900	0.10651200

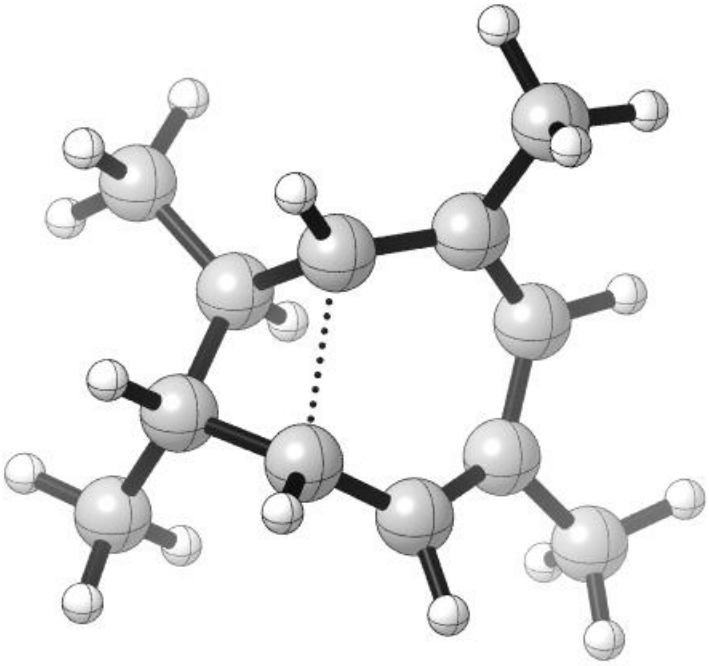

Dimethyl_A_cyclooctatriene_exo_6π_TS
E(M062X/def2TZVP) = -467.973105 Hartree
Free energy correction (M062X/def2SVP) = 0.228624 Hartree
G = -1228063.135

C	1.12960900	1.32453500	0.07092200
C	1.42310200	-1.11374200	-0.24373300
C	1.75384200	0.22878900	-0.52710200
H	2.72376200	0.38413400	-1.01139700
C	0.52604900	-1.45595100	0.78134800
H	0.84772500	-2.32545700	1.37003900
C	-0.21552700	1.21393300	0.44900800
H	-0.61060800	1.99244200	1.11740700
C	-0.57567600	-0.74306900	1.28987500
H	-0.78643200	-0.97671900	2.34373300
C	-1.83197500	-0.41567100	0.48157000
H	-2.52385200	0.11120700	1.16183000
C	-1.26018600	0.60837600	-0.47535000
H	-0.73600600	0.08289900	-1.28917400
C	1.94555000	2.53206500	0.46680900
H	2.92861900	2.52250000	-0.02282100
H	2.12191300	2.53013300	1.55468900
H	1.43948300	3.47462000	0.21554900
C	-2.23577500	1.61683500	-1.06440400
H	-1.71568600	2.34715600	-1.70122300
H	-2.75416900	2.16918100	-0.26483200
H	-2.99864900	1.11465700	-1.67857700
C	-2.53897600	-1.62479600	-0.11438700

H	-3.44270500	-1.32152900	-0.66487200
H	-2.84252500	-2.33669200	0.66774500
H	-1.86580800	-2.15084200	-0.80843700
C	2.31386600	-2.19729000	-0.80194400
H	3.30509300	-1.81149600	-1.07712500
H	1.86528600	-2.63335600	-1.70815200
H	2.44113400	-3.01691300	-0.08005300

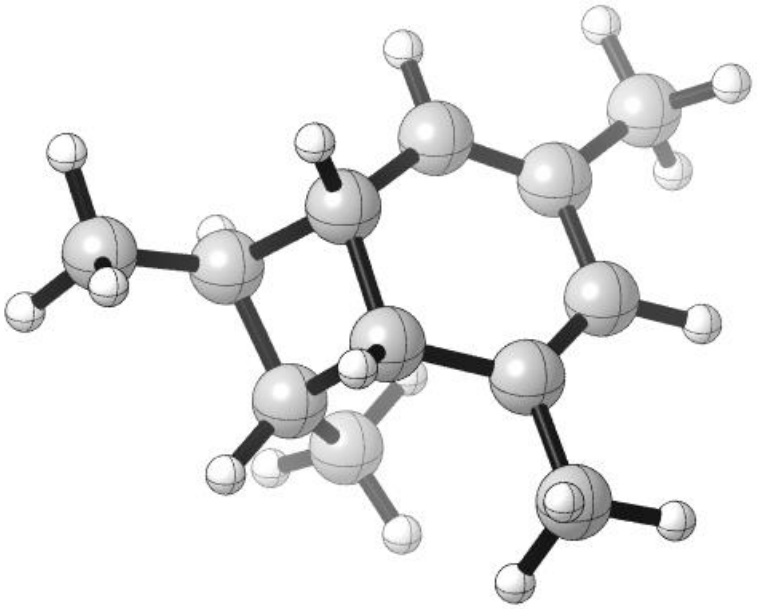

Dimethyl_A_BOD_endo_GS
E(M062X/def2TZVP) = -468.020413 Hartree
Free energy correction (M062X/def2SVP) = 0.232755 Hartree
G = -1228176.496

H	2.87415400	0.88386300	0.00175800
C	1.87643500	0.46720100	-0.16831400
C	0.55033800	-1.58239100	-0.35512800
C	-0.52221800	0.72008800	-0.65617900
C	-0.65425100	-0.81607700	-0.81509900
C	0.85438000	1.28829300	-0.45635200
C	1.72226600	-0.99787400	-0.05786100
H	0.45543400	-2.67123900	-0.28578800
H	-1.01967000	1.25132700	-1.48199700
H	-0.94374100	-1.15689700	-1.82449800
C	-1.85018200	-0.79453700	0.17996000
H	-1.75024700	-1.51521500	1.00846600
C	-1.47312500	0.65832700	0.58547400
H	-2.31993200	1.36114900	0.52743000
C	-0.79965400	0.76988000	1.94310800
H	0.04199700	0.06655600	2.02165000
H	-1.51918300	0.53524400	2.74211200
H	-0.40986000	1.78293200	2.12251800
C	0.99203200	2.77786300	-0.54892500

H	2.01686600	3.10808900	-0.33393000
H	0.30919000	3.27399600	0.16074200
H	0.71220300	3.13295400	-1.55391000
C	-3.21023100	-0.92804700	-0.48174300
H	-3.35775100	-1.93781200	-0.89286700
H	-3.30865100	-0.21019700	-1.31172500
H	-4.02141300	-0.72766300	0.23407700
C	2.92859600	-1.77477800	0.38882200
H	3.77232300	-1.61226600	-0.30029300
H	2.72098000	-2.85160400	0.43516400
H	3.26098200	-1.44090500	1.38450000

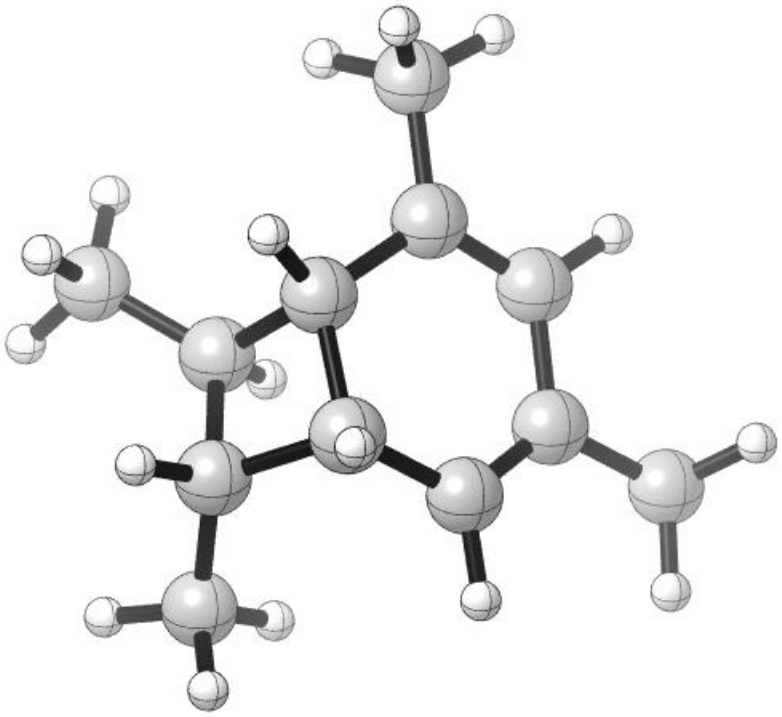

Dimethyl_A_BOD_exo_GS
E(M062X/def2TZVP) = -468.021719 Hartree
Free energy correction (M062X/def2SVP) = 0.231824 Hartree
G = -1228182.369

C	1.89494100	-0.64147400	-0.07490200
C	0.70886800	1.51523600	0.18009500
C	-0.30826100	-0.71197600	1.11142400
C	-0.49950400	0.75752900	0.65152000
C	0.91937900	-1.34502300	0.52460000
C	1.80449100	0.82839000	-0.18146500
H	-0.32868100	-0.89080800	2.19963600
H	1.02927100	-2.42918500	0.63226100
H	-1.05205300	1.33783000	1.40882100
H	2.67829000	1.36209400	-0.56791100
C	-1.48954100	0.24693300	-0.43218600
H	-0.91505900	0.02803400	-1.34831300
C	-1.64007700	-1.05832100	0.38251800
H	-2.47136100	-0.93503300	1.09713900

C	0.59611500	3.00665100	0.08439800
H	1.50944600	3.45968900	-0.32322300
H	0.39909700	3.44569400	1.07574700
H	-0.25196500	3.29170500	-0.55957500
C	-2.72855500	1.05628000	-0.75856600
H	-2.47522300	1.99848200	-1.26749100
H	-3.28339100	1.30455100	0.15963300
H	-3.40487600	0.49317500	-1.41998500
C	-1.78344700	-2.36935300	-0.36467600
H	-0.95880300	-2.49943800	-1.08161000
H	-2.73055600	-2.39692700	-0.92453100
H	-1.77531100	-3.22985600	0.32142300
C	3.13310000	-1.28613700	-0.63236100
H	3.11779700	-2.37522800	-0.49608500
H	4.03393100	-0.88624700	-0.14062000
H	3.23438600	-1.07093800	-1.70772400

Dimethyl B Cartesian Coordinates

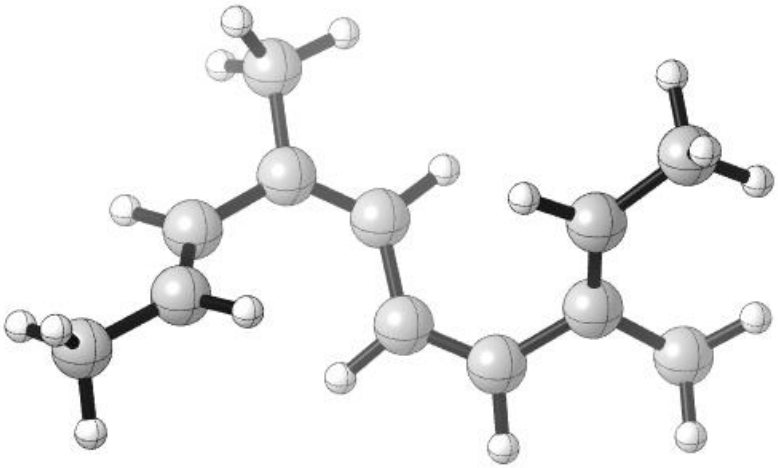

Dimethyl_B_tetraene_GS
E(M062X/def2TZVP) = -467.993487 Hartree
Free energy correction (M062X/def2SVP) = 0.223089 Hartree
G = -1228131.18

C	-1.60744000	1.09584300	-0.44910800
C	-0.35905400	0.58637800	-0.56120600
H	0.46865400	1.29460900	-0.67253300
C	-0.00297000	-0.82496400	-0.62854900
H	-0.81550500	-1.51480700	-0.87539700
C	1.23502600	-1.34355800	-0.48907500
H	1.35739300	-2.41123600	-0.70393000
C	2.47153500	-0.63015100	-0.11430200
C	-2.81531400	0.28342100	-0.21964300
H	-3.72501400	0.62669400	-0.73052700
C	2.46572500	0.30975300	0.84995000
H	1.51056900	0.48924000	1.35474100
C	-2.91059100	-0.77467000	0.59766100

H	-2.02173000	-1.07969900	1.16133700
C	3.61673700	1.13157500	1.34249900
H	3.39085300	2.20528800	1.24645000
H	4.54949700	0.93637000	0.80053400
H	3.79771500	0.94632800	2.41296900
C	-4.16064700	-1.56621900	0.82301000
H	-4.01148700	-2.62353000	0.55374300
H	-4.99592400	-1.17401100	0.22708700
H	-4.45237000	-1.55010300	1.88451900
C	-1.85097700	2.57808300	-0.56260600
H	-2.31689800	2.97213300	0.35421500
H	-2.54724200	2.79204300	-1.38970700
H	-0.91885900	3.12752300	-0.74674900
C	3.70024400	-1.07868300	-0.86517800
H	3.59870400	-0.85713600	-1.93878800
H	3.81612100	-2.17033400	-0.77640200
H	4.62187700	-0.61023300	-0.50228300

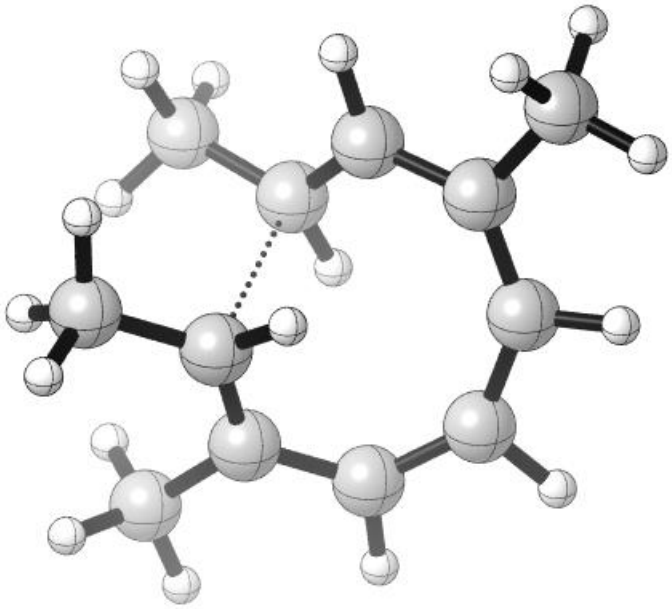

Dimethyl_B_tetraene_8π_TS
E(M062X/def2TZVP) = -467.973404 Hartree
Free energy correction (M062X/def2SVP) = 0.227364 Hartree
G = -1228067.228

C	2.13912700	-0.01079100	0.06249800
C	1.77465800	-1.35326300	-0.06487900
H	2.63937100	-2.01855400	0.03443200
C	0.59986600	-2.11592900	-0.32721400
C	-0.78227900	-1.95214800	-0.30631800
H	-1.33260300	-2.81039100	-0.70489200
C	-1.59104800	-0.88512300	0.14996400
C	1.34197100	1.12240200	-0.21870400
H	1.71534400	2.09135100	0.13559700
C	-1.03702800	0.15357800	0.88041400

H	-0.08034800	-0.05884200	1.35531600
C	0.11211700	1.08712300	-0.84206700
H	-0.11017600	0.19632400	-1.43002700
C	-1.84414900	1.26303400	1.48544300
H	-1.20571200	2.11901600	1.74478700
H	-2.33067800	0.92317900	2.41570300
H	-2.63748500	1.61644300	0.81212000
C	-0.63415900	2.33342400	-1.21581500
H	-1.71912300	2.16137300	-1.25313900
H	-0.32875100	2.67288100	-2.21887700
H	-0.43524500	3.15072800	-0.50815800
C	3.54899300	0.28601500	0.53436500
H	3.52750700	0.88749600	1.45647000
H	4.10847600	0.86560100	-0.21529800
H	4.11016700	-0.63240600	0.74671500
C	-3.04548400	-0.84815200	-0.25178700
H	-3.70530200	-0.64670600	0.60511000
H	-3.35252500	-1.79872700	-0.70690500
H	-3.22988800	-0.05497700	-0.99634700
H	0.87146400	-3.14480500	-0.58801000

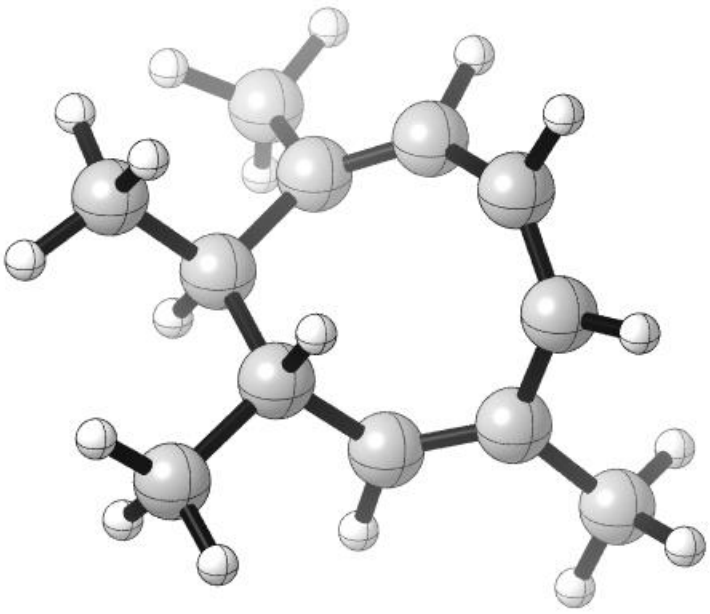

Dimethyl_B_cyclooctatriene_GS
E(M062X/def2TZVP) = -468.013332 Hartree
Free energy correction (M062X/def2SVP) = 0.231400 Hartree
G = -1228161.462

C	-2.01995500	0.12107700	-0.17667600
C	-0.81157000	-1.48403400	1.30851200
C	-1.87370600	-0.70540000	1.03235100
H	-2.72370900	-0.73134500	1.72379600
C	0.32458800	-1.80383200	0.42742200
H	0.46516700	-2.88921000	0.33835100

C	-1.04810800	0.96309200	-0.56234200
H	-1.19439300	1.53726200	-1.48629000
C	1.18790300	-1.06339400	-0.29451900
C	1.40772400	0.44020600	-0.24268400
H	1.64586100	0.76001100	-1.27469900
C	0.19896000	1.27015800	0.22347400
H	0.01207900	1.00228200	1.27539200
C	-3.31153300	-0.03126300	-0.93584900
H	-4.17226100	0.17648400	-0.28025900
H	-3.43083500	-1.06198500	-1.30343500
H	-3.35619700	0.65390000	-1.79263400
C	0.48354600	2.77388800	0.15008100
H	-0.42121700	3.34587700	0.39985400
H	0.79360500	3.06103700	-0.86805000
H	1.27477900	3.08042400	0.84686200
C	2.63946300	0.72766700	0.63271600
H	2.98506700	1.76356700	0.51741100
H	3.48193300	0.07029100	0.38017600
H	2.38901600	0.55939200	1.69150300
H	-0.86633900	-2.09267500	2.21810100
C	2.14554200	-1.77315500	-1.22113400
H	3.18910100	-1.47033500	-1.04790300
H	1.91117100	-1.51104000	-2.26568200
H	2.08004700	-2.86398900	-1.12060500

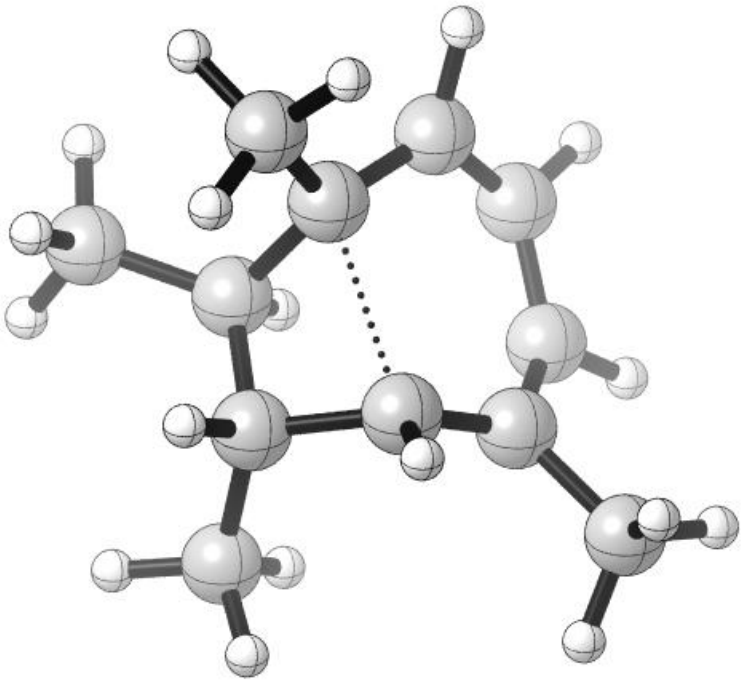

Dimethyl_B_cyclooctatriene_endo_6π_TS
E(M062X/def2TZVP) = -467.973066 Hartree
Free energy correction (M062X/def2SVP) = 0.230507 Hartree
G = -1228058.089

C	0.36336900	-2.00791900	-0.22501900

C	-1.69390600	-0.87470800	-0.94764400
C	-0.74278900	-1.90430000	-1.06029400
H	-2.61692300	-1.02066900	-1.51594000
C	-1.75512800	0.03408800	0.12037900
C	0.96013400	-0.88129900	0.35865000
C	-0.65626600	0.51729900	0.86728500
H	-0.93998300	0.81993500	1.88779200
C	0.45698000	1.38094800	0.27668600
H	1.09813500	1.70008300	1.11679900
C	1.21482700	0.34546600	-0.52390000
H	0.68523900	0.18414100	-1.47503400
C	2.67919000	0.64388200	-0.81875600
H	3.16285400	-0.19948600	-1.33371400
H	3.24241200	0.85310300	0.10329200
H	2.76405900	1.52716400	-1.46924400
C	-0.03080100	2.61723900	-0.46660700
H	0.81337100	3.21764500	-0.83906200
H	-0.63953700	3.26021900	0.18734900
H	-0.65322600	2.31945500	-1.32460500
H	0.69153900	-3.00852100	0.07876100
C	-3.13475600	0.39211600	0.63925200
H	-3.20124000	0.14405200	1.71054600
H	-3.93021500	-0.15388000	0.11587800
H	-3.33312600	1.47124700	0.54800600
C	1.90818900	-1.08443000	1.51581600
H	2.03283000	-0.16263400	2.10242900
H	2.90803600	-1.37705300	1.15460800
H	1.54354400	-1.87114100	2.18877600
H	-1.04202300	-2.77396700	-1.65172100

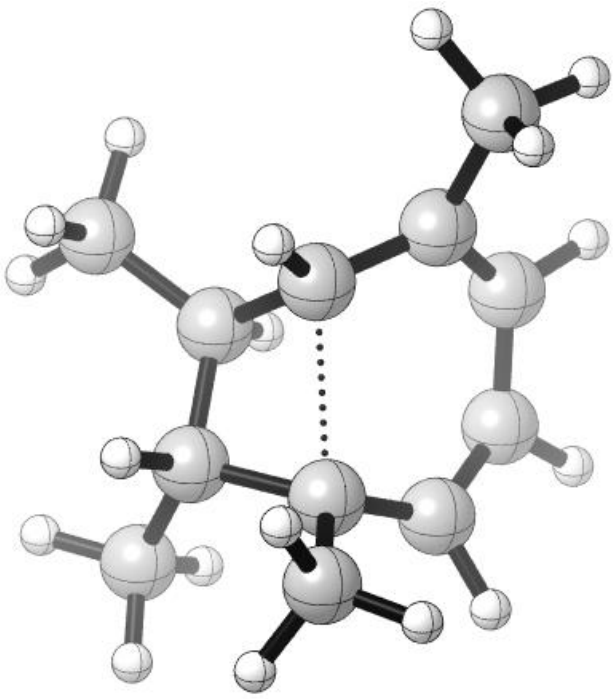

Dimethyl_B_cyclooctatriene_exo_6π_TS

E(M062X/def2TZVP) = -467.975049 Hartree
Free energy correction (M062X/def2SVP) = 0.229140 Hartree
G = -1228066.884

C	1.89459000	0.15411900	0.06678700
C	0.76378600	-1.45648100	-1.39833600
C	1.85305700	-0.61936800	-1.09491600
H	2.78267900	-0.81311800	-1.63771600
C	-0.30985900	-1.71434400	-0.54314300
H	-0.64180700	-2.76164000	-0.55329900
C	0.68580900	0.62021000	0.60325700
H	0.71525700	1.02142000	1.62721600
C	-0.86702800	-0.90851000	0.47708900
C	-1.56505700	0.41888000	0.15881500
H	-1.92655700	0.82508900	1.12129400
C	-0.38093400	1.25353100	-0.27549300
H	-0.14582800	1.02055300	-1.32555600
C	3.19263600	0.32497100	0.81889100
H	4.04779200	-0.00052800	0.21155500
H	3.18535600	-0.29172900	1.73214000
H	3.35874800	1.36709200	1.12617500
C	-0.51349200	2.76067300	-0.10691100
H	0.41226500	3.27496700	-0.40327500
H	-0.72545500	3.01772800	0.94292200
H	-1.33379900	3.15643600	-0.72491200
C	-2.73638700	0.30429500	-0.80786200
H	-3.21979200	1.28199000	-0.95557700
H	-3.50152600	-0.39435100	-0.43725200
H	-2.38419800	-0.06264000	-1.78356000
C	-1.46373100	-1.64017000	1.65790900
H	-2.56200200	-1.70153400	1.56623100
H	-1.25349600	-1.08619700	2.58503100
H	-1.05969500	-2.65500300	1.76828800
H	0.93171300	-2.18537300	-2.19622700

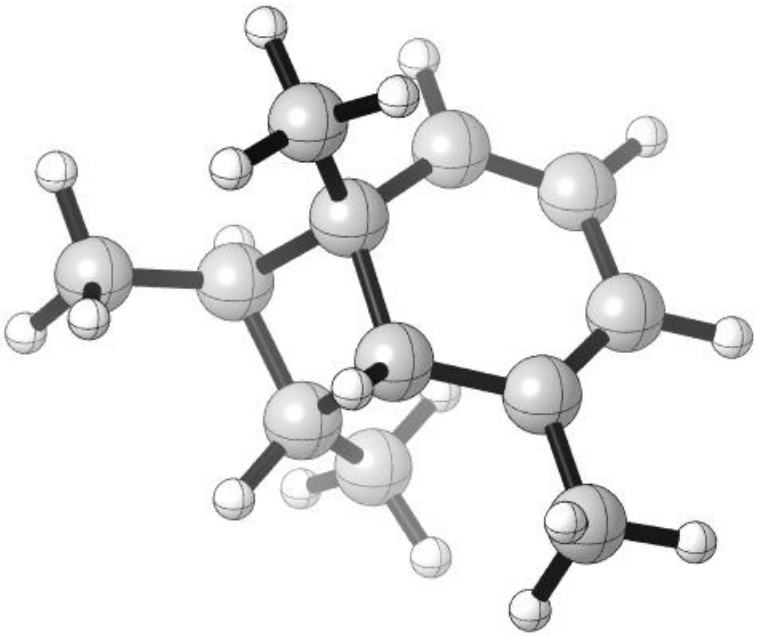

Dimethyl_B_BOD_endo_GS
E(M062X/def2TZVP) = -468.019014 Hartree
Free energy correction (M062X/def2SVP) = 0.233259 Hartree
G = -1228171.5

H	3.16777100	1.00066700	-0.52028200
C	2.09812000	0.84110000	-0.36324100
C	-0.17276500	1.58426500	-0.93576300
C	0.20745400	-0.32113500	0.69749400
C	-0.78756900	0.73727200	0.14846700
C	1.68040900	-0.08308600	0.51844000
C	1.14970100	1.64528500	-1.14531500
H	-0.85699500	2.20445000	-1.52448800
H	-0.00391700	-0.52261000	1.76064700
C	-1.65413500	-0.42817900	-0.43534900
H	-1.88495300	-0.29407800	-1.50549600
C	-0.47798000	-1.41373100	-0.18757600
H	-0.78083100	-2.30612300	0.38333600
C	0.27575400	-1.83766100	-1.43712700
H	0.58466300	-0.96419200	-2.02824900
H	-0.36613500	-2.47083200	-2.06830200
H	1.18004800	-2.41267200	-1.18786900
C	2.61082100	-0.94694600	1.31459600
H	3.66294200	-0.74241900	1.07618800
H	2.40957600	-2.01345400	1.11882400
H	2.45926100	-0.79197000	2.39504700
C	-2.92228600	-0.77264000	0.32704800
H	-3.66032700	0.04198000	0.28565000
H	-2.70762500	-0.97983300	1.38667200
H	-3.38765800	-1.67452700	-0.09806000
C	-1.43679300	1.65224300	1.18224200
H	-1.90099000	1.07805700	1.99708100

H	-2.21270500	2.28379200	0.72162900
H	-0.67606000	2.31558400	1.62033500
H	1.54955000	2.30745900	-1.91616200

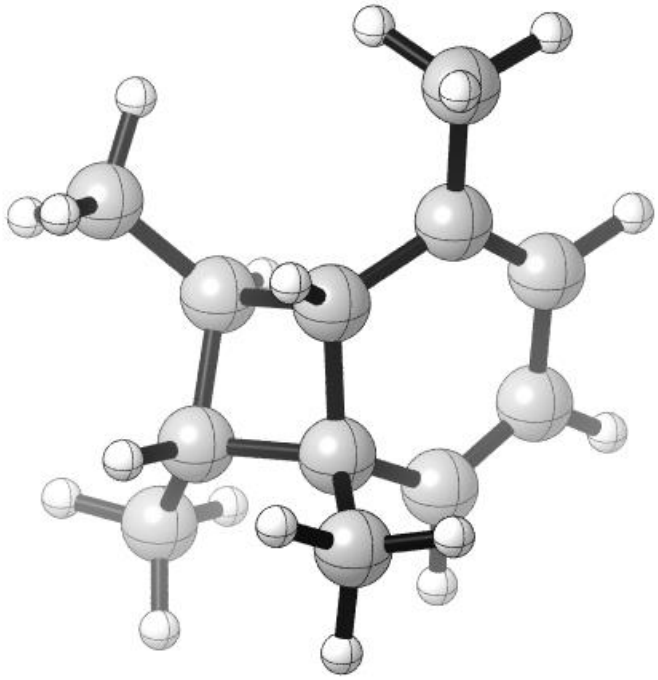

Dimethyl_B_BOD_exo_GS
E(M062X/def2TZVP) = -468.021795 Hartree
Free energy correction (M062X/def2SVP) = 0.232293 Hartree
G = -1228181.338

C	0.78530200	-1.89690700	-1.07607800
C	1.81602800	0.04254800	0.02024000
C	-0.65353400	-0.68285500	0.56869200
C	0.45364200	0.40997400	0.53517100
C	-0.40538200	-1.73635900	-0.47952600
C	1.93691700	-1.03927700	-0.76846100
H	-1.22679400	-2.42596300	-0.69925500
H	0.52890400	0.89765300	1.52293900
H	2.90901400	-1.30256600	-1.19242300
C	-0.46547100	1.25880000	-0.38521900
H	-0.24676500	0.99256700	-1.43311400
C	-1.66089300	0.41205400	0.10422700
H	-2.08511800	0.88496300	1.00767900
C	2.95951200	0.94388600	0.37484300
H	3.89552900	0.62140300	-0.10002800
H	3.11080300	0.96834100	1.46617100
H	2.74919100	1.98027900	0.06364300
C	-0.51049400	2.76405100	-0.21409900
H	0.43475100	3.23508000	-0.52312500
H	-0.69480300	3.03046500	0.83829100
H	-1.31562400	3.20673700	-0.82049000
C	-2.76878600	0.07140400	-0.87301700

H	-2.35576800	-0.37273300	-1.79113600
H	-3.33218500	0.97384100	-1.15442600
H	-3.48325300	-0.64554800	-0.43988900
C	-0.94546400	-1.34562400	1.90950400
H	-0.09660100	-1.97019400	2.22601900
H	-1.83569800	-1.99102100	1.84141900
H	-1.12996100	-0.58754600	2.68623000
H	0.92611100	-2.70592900	-1.79617800

Dimethyl C Cartesian Coordinates

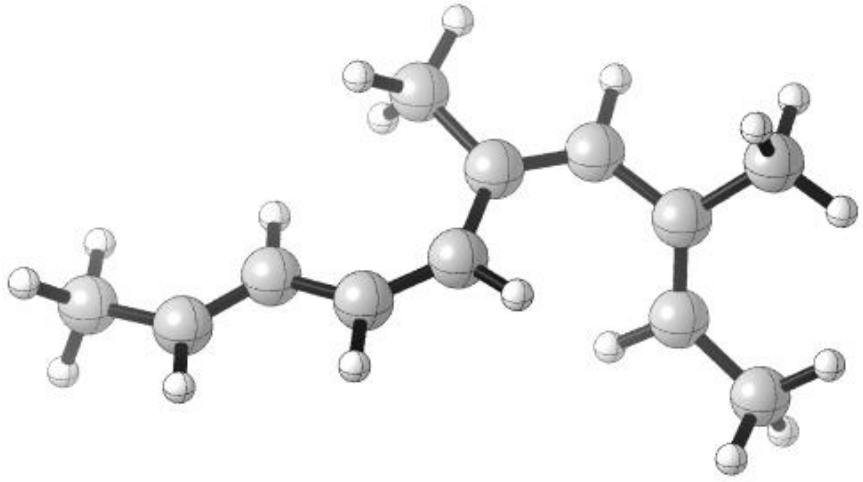

Dimethyl_C_tetraene_GS
E(M062X/def2TZVP) = -467.992446 Hartree
Free energy correction (M062X/def2SVP) = 0.223838 Hartree
G = -1228126.48

C	-1.53109200	-0.69128000	0.65820600
H	-1.65664900	-1.61335800	1.23605800
C	-0.27339400	-0.20001000	0.59630400
H	0.49400700	-0.79441900	1.09877400
C	0.23766900	1.03828700	-0.00522400
C	1.56242400	1.21600300	-0.22827000
H	1.87916500	2.21785900	-0.54422800
C	2.66052000	0.24384300	-0.07439800
C	-2.76304600	-0.20619400	0.04647700
H	-2.72827100	0.67445900	-0.59741200
C	2.53472400	-1.02478100	-0.50873600
H	1.58896500	-1.28560600	-0.99514800
C	-3.94561600	-0.81657500	0.22617500
H	-3.97741100	-1.70601600	0.86702700
C	3.54192200	-2.12986400	-0.42970800
H	3.12211500	-2.99249500	0.11137100
H	4.46824900	-1.83519100	0.07706600
H	3.80200900	-2.49125600	-1.43696600
C	-5.23870000	-0.37789100	-0.38317400
H	-5.67104200	-1.17294700	-1.01087200
H	-5.10393200	0.51717500	-1.00540900

H	-5.98562600	-0.14930800	0.39326800
C	-0.70766200	2.17621600	-0.30390400
H	-1.25930200	2.00289900	-1.24056500
H	-0.15207700	3.11595400	-0.42114100
H	-1.44906900	2.30095900	0.49835200
C	3.91128300	0.81497300	0.54619800
H	3.72078500	1.11968400	1.58682900
H	4.22053200	1.72128700	0.00225100
H	4.75335900	0.11394900	0.54107200

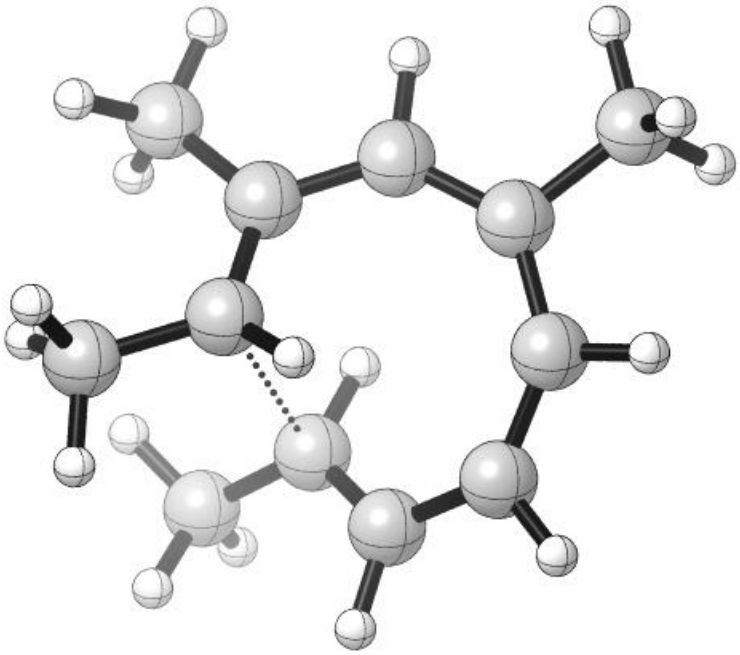

Dimethyl_C_tetraene_8π_TS
E(M062X/def2TZVP) = -467.971489 Hartree
Free energy correction (M062X/def2SVP) = 0.227843 Hartree
G = -1228060.943

C	0.88147600	-2.12468100	0.44307900
C	1.87376500	-1.15208500	0.36827200
H	2.84868700	-1.56496000	0.65423700
C	2.01090900	0.21536100	-0.03291900
C	1.10596700	1.26517700	-0.20224500
H	1.55202100	2.15821900	-0.65113600
C	-0.26602700	1.41443300	0.11259900
C	-0.46118600	-2.12115600	0.02223800
H	-1.10126000	-2.93257300	0.38557800
C	-0.94493100	0.47628000	0.87249600
H	-0.32517500	-0.18842900	1.47208400
C	-1.03199400	-1.11933000	-0.73843800
H	-0.34753800	-0.50816800	-1.32710300
C	-2.36062400	0.65311800	1.33550600
H	-2.79615500	-0.30723000	1.64478800
H	-3.00400500	1.08842500	0.55836000
H	-2.39919500	1.32683000	2.20856000

C	-2.44874700	-1.18621300	-1.22478200
H	-2.87560200	-0.18378800	-1.37026000
H	-3.08979800	-1.73931900	-0.52383000
H	-2.49288200	-1.69755200	-2.20013400
C	-1.01321200	2.58194000	-0.48752500
H	-1.61041400	3.11961600	0.26370200
H	-1.71029700	2.24235800	-1.27281500
H	-0.32217400	3.29639300	-0.95311900
C	3.47047600	0.58458200	-0.27247900
H	3.93512100	-0.07917100	-1.01638300
H	4.04791700	0.48063500	0.65967200
H	3.58055200	1.61949900	-0.61870600
H	1.21494900	-3.05534400	0.91169400

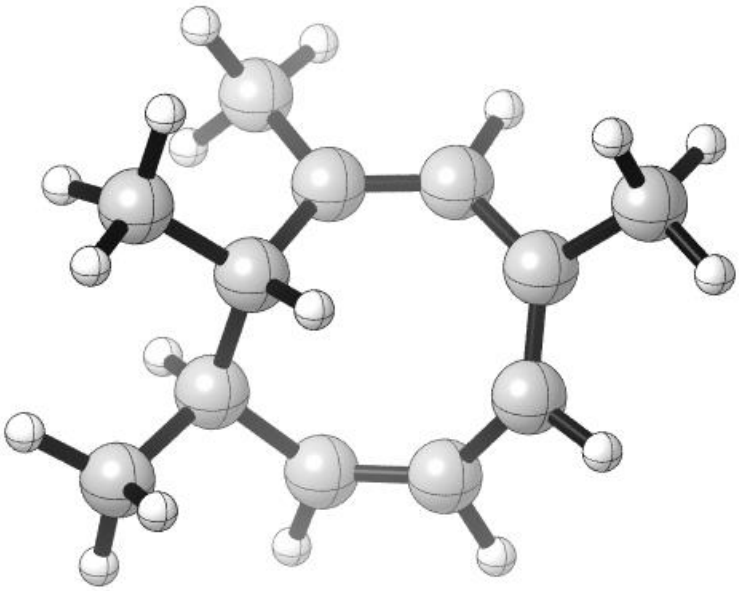

Dimethyl_C_cyclooctatriene_GS
E(M062X/def2TZVP) = -468.015881 Hartree
Free energy correction (M062X/def2SVP) = 0.232494 Hartree
G = -1228165.283

C	0.54323100	-2.02919300	-0.63072800
C	2.07469100	-0.14929000	0.16302600
C	1.64660400	-1.42931300	0.13411200
H	2.29085300	-2.16667900	0.62713100
C	1.37295600	0.95002400	-0.51267600
H	1.99898500	1.60826800	-1.12819600
C	-0.73576400	-1.68484300	-0.86195900
H	-1.28473000	-2.37609400	-1.51233800
C	0.06436300	1.23527400	-0.40653900
C	-0.86335200	0.46346200	0.51166300
H	-0.24604500	-0.06460100	1.25468600
C	-1.62383800	-0.61261200	-0.28346000
H	-2.12883300	-0.10956400	-1.13012200
C	-2.71758800	-1.30158100	0.54613800

H	-3.17366600	-2.12518000	-0.02177000
H	-3.51896200	-0.60466800	0.82633800
H	-2.28558500	-1.72718500	1.46528700
C	-1.80882200	1.40365600	1.26661900
H	-2.32100400	0.87607300	2.08204600
H	-2.58000200	1.82436000	0.60204200
H	-1.24951600	2.23948200	1.71147900
C	-0.54001300	2.36754400	-1.19195000
H	-1.42037400	2.02206200	-1.75882400
H	0.18199300	2.78646200	-1.90430000
H	-0.88739900	3.17843800	-0.53379800
C	3.36596700	0.22222800	0.84440800
H	3.87420200	-0.65729100	1.26083200
H	3.18517800	0.94231400	1.65756100
H	4.04801600	0.71377000	0.13214900
H	0.84627600	-2.97209900	-1.10213800

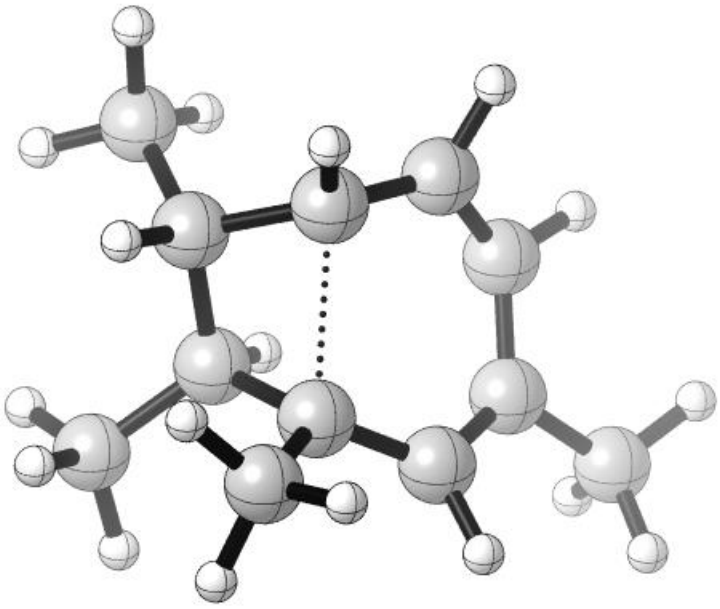

Dimethyl_C_cyclooctatriene_endo_6π_TS
E(M062X/def2TZVP) = -467.973827 Hartree
Free energy correction (M062X/def2SVP) = 0.230348 Hartree
G = -1228060.504

C	-0.54185000	-1.72765700	0.79722100
C	-2.02186600	-0.03427400	-0.26461300
C	-1.58709500	-1.36323700	-0.05033500
H	-2.32284000	-2.14103600	-0.27720700
C	-1.29489900	1.03416500	0.25568100
H	-1.86001600	1.89975300	0.62331300
C	0.61418600	-0.99594900	1.14020900
H	1.00619100	-1.25684500	2.13433900
C	0.09375100	0.98887900	0.46715500
C	0.98024800	0.43598400	-0.65464200
H	0.32061500	-0.06193400	-1.38187500

C	1.70868600	-0.62713800	0.13774700
H	2.51703000	-0.13655600	0.70727100
C	2.29381400	-1.80105800	-0.63501500
H	2.72791800	-2.54948600	0.04466600
H	3.08728500	-1.46619100	-1.32063200
H	1.50672300	-2.29487300	-1.22502600
C	1.83678700	1.46241800	-1.38381100
H	2.42659000	0.97468900	-2.17431100
H	2.54154400	1.95861600	-0.69946600
H	1.21530100	2.23659500	-1.85799400
C	0.71278900	2.05041100	1.34633600
H	1.71065300	1.75307100	1.69988400
H	0.08445100	2.24693800	2.22468400
H	0.83271600	2.99584100	0.79170400
C	-3.41538200	0.19276000	-0.79615800
H	-4.08629900	-0.64721400	-0.57004000
H	-3.39447600	0.31709700	-1.89035000
H	-3.84969700	1.11107200	-0.37611300
H	-0.73870100	-2.63136200	1.38850100

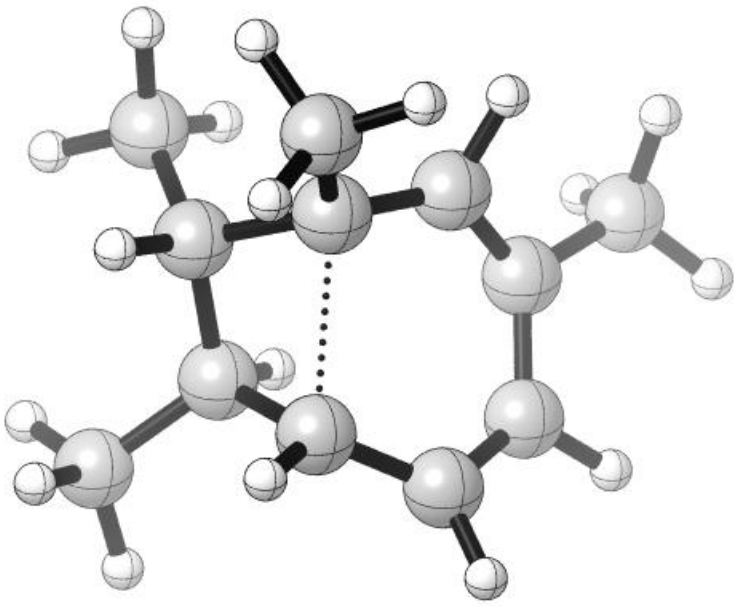

Dimethyl_C_cyclooctatriene_exo_6π_TS
E(M062X/def2TZVP) = -467.974836 Hartree
Free energy correction (M062X/def2SVP) = 0.229717 Hartree
G = -1228064.81

C	1.07180100	1.00143900	0.10778500
C	1.75623000	-1.36146300	0.20999700
C	1.88216000	-0.05865300	-0.32393900
H	2.65086400	-1.98882100	0.15604400
C	0.72390900	-1.72823300	1.06437400
C	-0.24667700	1.01053600	0.61887400
C	-0.52398400	-1.10339300	0.98193400

H	-1.22264400	-1.24671700	1.81712900
C	-1.20017400	-0.88195700	-0.36311400
H	-0.45539300	-1.06367400	-1.15409000
C	-1.44361100	0.60647800	-0.25142900
H	-2.34778800	0.75262800	0.36727900
C	-1.58904300	1.39609300	-1.54522200
H	-1.66848100	2.47669700	-1.35309100
H	-2.49090100	1.08658800	-2.09503400
H	-0.71244000	1.22875200	-2.18900000
C	-2.42152300	-1.75809300	-0.60131000
H	-2.89898400	-1.51580200	-1.56292000
H	-3.16807200	-1.60951400	0.19471600
H	-2.14786700	-2.82293800	-0.61710300
H	1.62462000	1.94461500	0.22758500
C	-0.56497200	2.09626600	1.62257900
H	-1.07719600	2.94292500	1.13337600
H	0.33329300	2.47129500	2.13029200
H	-1.25308000	1.70859500	2.38849500
C	3.13985200	0.27527800	-1.08995200
H	3.46054500	1.30918500	-0.89737700
H	2.96276600	0.18901600	-2.17339400
H	3.96569700	-0.40364000	-0.83627500
H	0.94125400	-2.42497900	1.87991000

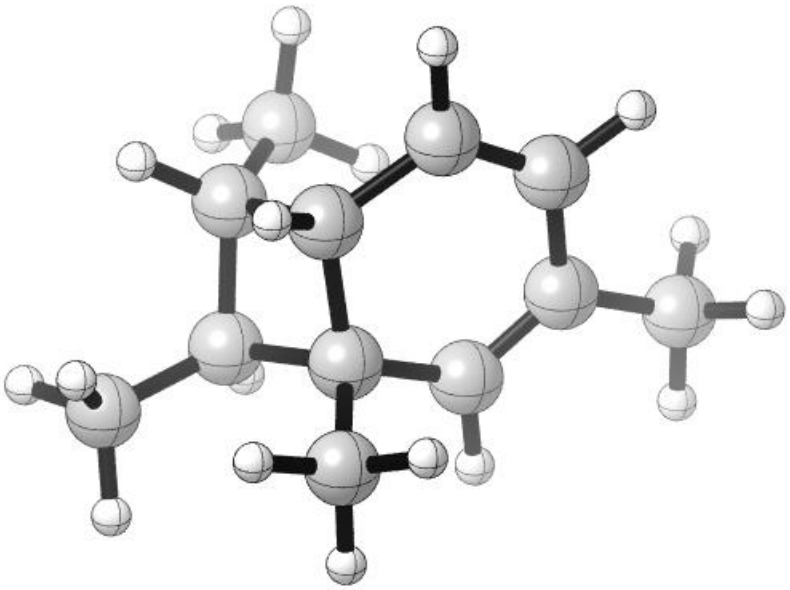

Dimethyl_C_BOD_endo_GS
E(M062X/def2TZVP) = -468.017318 Hartree
Free energy correction (M062X/def2SVP) = 0.233138 Hartree
G = -1228167.365

C	1.93638000	-0.37459800	-0.26278300
C	0.86411200	0.96151100	1.50900600
C	-0.51388000	-0.77850600	0.15189200
C	-0.48090100	0.47331900	1.07153200

C	0.78038100	-0.96997000	-0.59753000
C	1.97681700	0.56574400	0.87640100
H	0.75815900	-1.68108800	-1.43202100
H	-1.12734400	0.31465700	1.94853200
H	2.95481400	0.93944700	1.19179900
C	-1.26637600	1.27967000	-0.01522500
H	-2.16210500	1.78074300	0.38528700
C	-1.59253400	-0.06228900	-0.72725800
H	-1.33445300	-0.05581400	-1.79968800
C	-0.45865100	2.26544800	-0.84244000
H	-0.14502000	3.13236200	-0.24301300
H	-1.06278500	2.63358300	-1.68558900
H	0.44605400	1.79246900	-1.25024800
C	-3.02719600	-0.52759500	-0.54413200
H	-3.33133000	-0.47783700	0.51270900
H	-3.16986600	-1.56290600	-0.88741300
H	-3.71168500	0.11722200	-1.11541600
C	-0.90201800	-2.09527900	0.81687300
H	-0.11699600	-2.39788700	1.52601400
H	-1.01271500	-2.89827200	0.07111900
H	-1.84833100	-2.00795700	1.37007700
C	3.22346000	-0.61609900	-0.99989000
H	3.08967100	-1.33370000	-1.81961800
H	3.99497700	-1.00708400	-0.31807300
H	3.61496200	0.32364700	-1.42048400
H	0.92642700	1.66026700	2.34734100

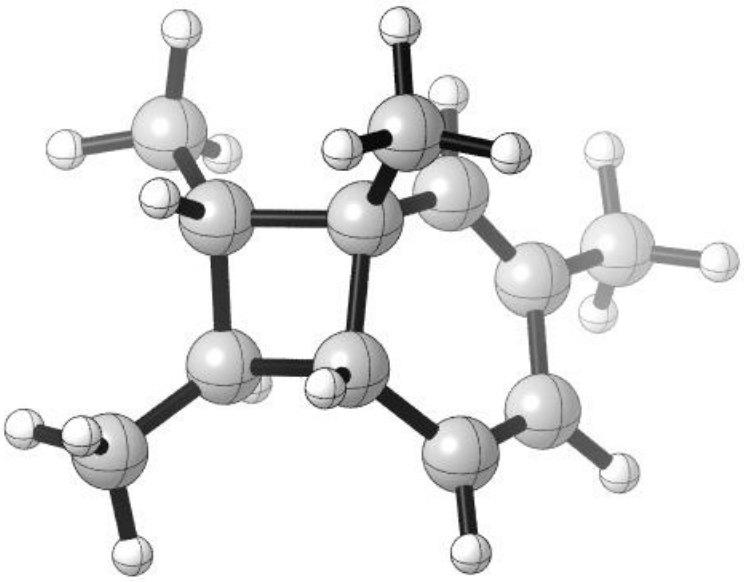

Dimethyl_C_BOD_exo_GS
E(M062X/def2TZVP) = -468.020373 Hartree
Free energy correction (M062X/def2SVP) = 0.232109 Hartree
G = -1228178.087

H	-2.63349900	2.09566900	-0.05725800
C	-1.78992100	1.41301000	0.07577200

C	-1.04838500	-0.91659400	-0.00347200
C	0.53338300	0.92320800	0.70773100
C	0.22743900	-0.60233800	0.73524700
C	-0.62774200	1.85584000	0.57463900
C	-1.98608600	-0.00156100	-0.30272700
H	-1.23091000	-1.96999100	-0.24566100
H	1.17003300	1.19469200	1.56605000
C	1.50046600	-0.80930300	-0.14040300
H	2.35770700	-0.95507500	0.54046800
C	1.42899500	0.68120500	-0.53789000
H	0.80153400	0.77887600	-1.43977400
C	2.71317400	1.47037900	-0.69254900
H	3.33092200	1.38951400	0.21535700
H	2.50940500	2.53681700	-0.87065400
H	3.30833600	1.09793300	-1.54028000
C	1.51943700	-1.86096000	-1.23218600
H	1.42881900	-2.87658300	-0.81695000
H	2.46063600	-1.81645300	-1.80063700
H	0.68818000	-1.70650500	-1.93646700
C	0.22209700	-1.29230700	2.09400600
H	1.15231900	-1.07948900	2.64300900
H	0.13414800	-2.38431200	1.97766600
H	-0.62815200	-0.94608000	2.70068000
C	-3.27460400	-0.35354100	-0.99207700
H	-4.13790000	-0.08344000	-0.36372600
H	-3.33152800	-1.42646900	-1.21670800
H	-3.37832900	0.20539400	-1.93529200
H	-0.51124200	2.90327300	0.86362500

Monomethyl A Cartesian Coordinates

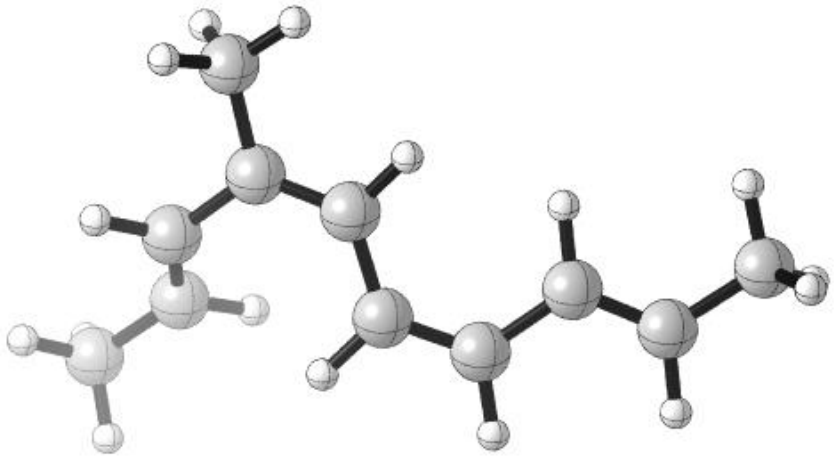

Monomethyl_A_tetraene_GS
E(M062X/def2TZVP) = -428.688379 Hartree
Free energy correction (M062X/def2SVP) = 0.197534 Hartree
G = -1125002.714

C	1.57720600	1.16949200	-0.10444600

C	0.28087100	0.79845900	-0.22371800
H	-0.46754600	1.58760100	-0.10536800
C	-0.21228800	-0.52770000	-0.56269900
H	0.52928900	-1.24325600	-0.92596000
C	-1.50105300	-0.93119500	-0.50357900
H	-1.73508000	-1.94558600	-0.84120200
C	-2.63368600	-0.15227700	-0.02331400
H	-2.44330200	0.85789600	0.35349900
C	2.71843600	0.23916400	-0.17954200
H	3.60367400	0.61115200	-0.71290600
C	-3.89415600	-0.61378700	-0.00971900
H	-4.07679100	-1.62935700	-0.38112700
C	2.79058000	-0.96428200	0.40533400
H	1.93330800	-1.30903900	0.99448400
C	-5.08352100	0.15119000	0.47643300
H	-5.83449800	0.26600800	-0.32099700
H	-4.79799600	1.15223000	0.82706700
H	-5.58261200	-0.37540000	1.30507300
C	3.97640600	-1.87472000	0.33633500
H	4.36633900	-2.09189400	1.34274000
H	4.78520900	-1.43439200	-0.26241000
H	3.70362200	-2.84308100	-0.11136200
C	1.95217900	2.61191700	0.11231900
H	2.61124700	2.96440200	-0.69763800
H	2.51203600	2.73462400	1.05269700
H	1.06725300	3.26052300	0.14298700

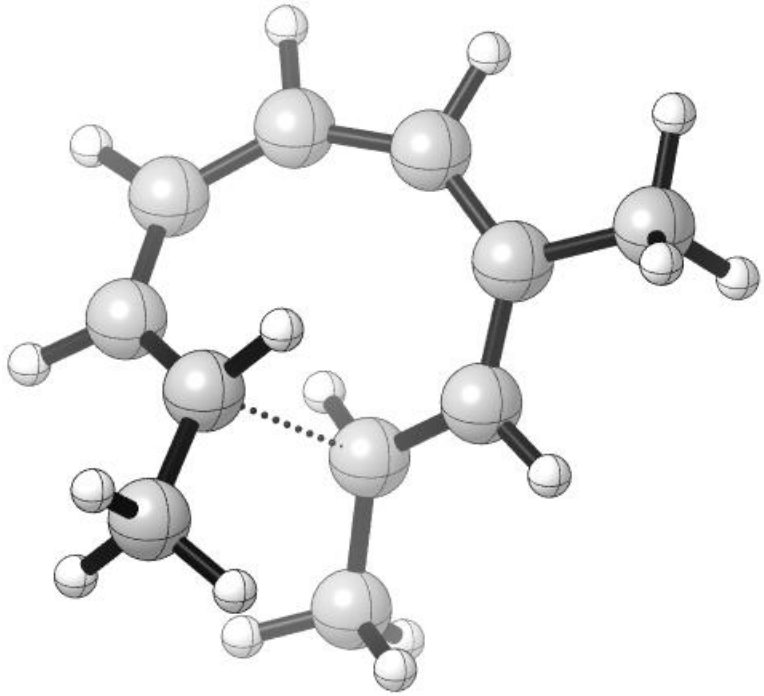

Monomethyl_A_tetraene_8π_TS
E(M062X/def2TZVP) = -428.663357 Hartree
Free energy correction (M062X/def2SVP) = 0.201839 Hartree
G = -1124925.716

C	1.77290300	-0.43230200	0.11541900
C	1.82875900	0.95396600	-0.07813300
H	2.85027800	1.33516300	0.02895700
C	0.94379000	2.01380000	-0.40953500
H	1.51014000	2.90800200	-0.69188500
C	-0.43164100	2.24993700	-0.43745200
H	-0.71002300	3.20672100	-0.88819300
C	-1.50242200	1.47044800	0.02723800
H	-2.51011400	1.76363600	-0.28812000
C	0.69253600	-1.29308200	-0.16534700
H	0.75887300	-2.31397400	0.23152200
C	-1.35571800	0.31894900	0.78318400
H	-0.42093600	0.22527900	1.33523400
C	-0.46278200	-0.93249700	-0.83619000
H	-0.39680700	-0.04642100	-1.46699300
C	-2.53055800	-0.42870300	1.34082100
H	-2.31146500	-1.49990500	1.45480300
H	-3.41792700	-0.32057400	0.70092000
H	-2.78769500	-0.04389500	2.34091900
C	-1.50613300	-1.94002100	-1.22085400
H	-2.50465500	-1.48510600	-1.28407700
H	-1.54621100	-2.77353400	-0.50518200
H	-1.27858300	-2.36027300	-2.21377200
C	3.01281900	-1.10335000	0.67475700
H	3.37559800	-1.89828600	0.00647900
H	2.79137700	-1.57298400	1.64593400
H	3.82883300	-0.38671800	0.83000600

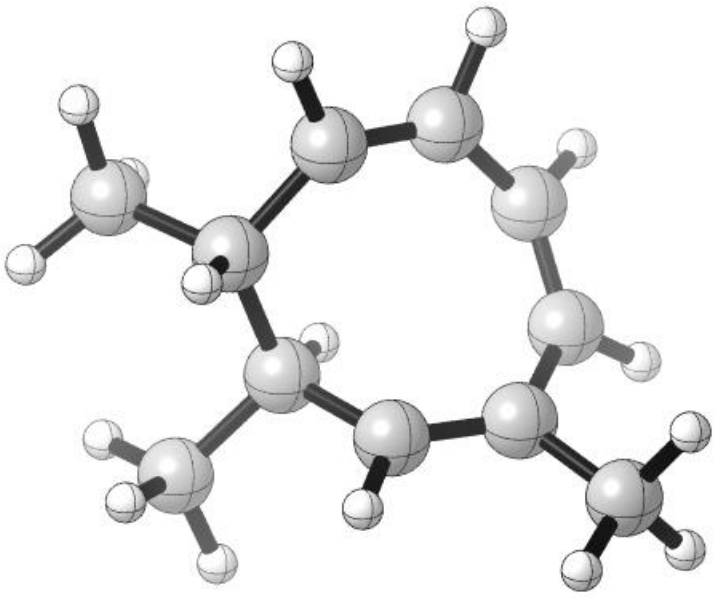

Monomethyl_A_cyclooctatriene_GS
E(M062X/def2TZVP) = -428.704355 Hartree
Free energy correction (M062X/def2SVP) = 0.205792 Hartree
G = -1125022.977

C	-0.01518300	2.11192900	-0.15205700
C	-1.84513400	0.64493600	0.83873100
C	-1.05192000	1.73166200	0.82163500
H	-1.28956800	2.52071900	1.54337900
H	-2.67243300	0.63592900	1.55774900
C	-1.76551100	-0.50044300	-0.07964700
C	0.98991700	1.45177700	-0.75262900
H	1.57377300	2.05590600	-1.45729000
C	-0.60581600	-1.12819700	-0.32962100
H	-0.61709500	-1.96270100	-1.04295400
C	0.72033300	-0.85047600	0.32475200
H	0.54021300	-0.32619300	1.27752400
C	1.57937700	0.07878400	-0.54986200
H	1.66246400	-0.39068000	-1.54795600
C	3.00581700	0.25195700	-0.00753200
H	3.56117700	0.99295400	-0.60038800
H	3.57003100	-0.68973600	-0.03750900
H	2.97587600	0.60926500	1.03364900
C	1.42505500	-2.17734700	0.62152900
H	2.31616900	-2.03882600	1.24807200
H	1.73807400	-2.66870200	-0.31449400
H	0.74573100	-2.86112400	1.14972000
H	-0.09120100	3.17021200	-0.42942900
C	-3.06658700	-0.93503300	-0.70275200
H	-3.49454300	-0.12899200	-1.31820900
H	-3.80858500	-1.17185900	0.07640500
H	-2.93216300	-1.82346900	-1.33356300

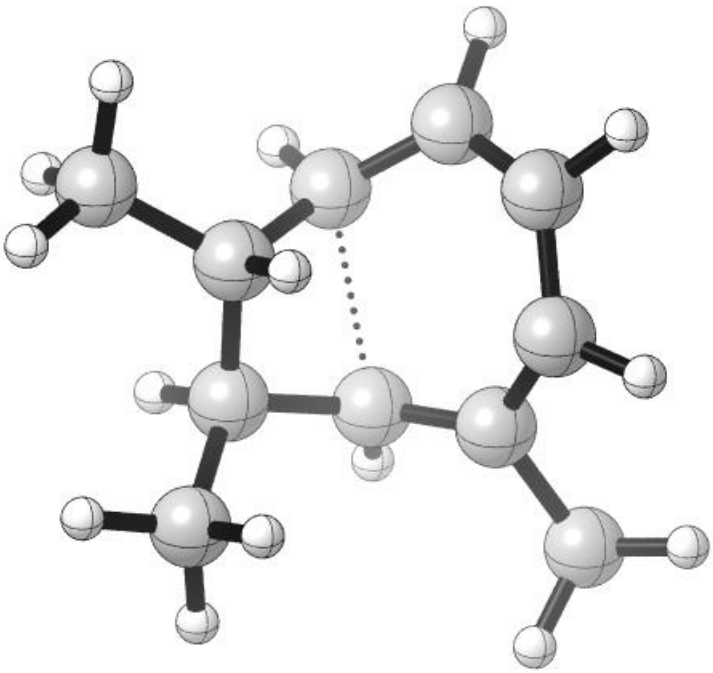

Monomethyl_A_cyclooctatriene_endo_6π_TS
E(M062X/def2TZVP) = -428.662345 Hartree
Free energy correction (M062X/def2SVP) = 0.204002 Hartree

G = -1124917.38

C	-1.54886300	-0.30016400	0.03387200
C	-0.89212700	2.00731600	-0.64107400
C	-1.57708000	0.79763100	-0.84427500
H	-2.43667500	0.85279600	-1.51845700
H	-1.31781400	2.89149100	-1.12322200
C	0.05575300	2.16816800	0.36665100
H	0.10447300	3.12555100	0.89404600
C	-0.46931900	-0.69227600	0.85769500
H	-0.80211800	-1.23769700	1.75462300
C	0.81250300	1.08081200	0.80419900
H	1.35991900	1.18605900	1.74990700
C	1.45693000	0.12254000	-0.18710600
H	1.03366300	0.32516000	-1.18359500
C	0.88209500	-1.17583100	0.33481200
H	1.47681100	-1.47506400	1.21552100
C	-2.86366100	-1.02252000	0.26265400
H	-2.79975100	-2.08139800	-0.03177800
H	-3.69383500	-0.55835300	-0.28501500
H	-3.11295200	-1.00275700	1.33552100
C	0.79796800	-2.34719900	-0.63404000
H	0.29341200	-3.21029500	-0.17343300
H	1.80030600	-2.67274500	-0.95208700
H	0.22524000	-2.05588800	-1.52807200
C	2.97424000	0.22336600	-0.24790600
H	3.38992400	-0.52196600	-0.94281300
H	3.41634400	0.04491700	0.74495700
H	3.29241800	1.21912300	-0.58899500

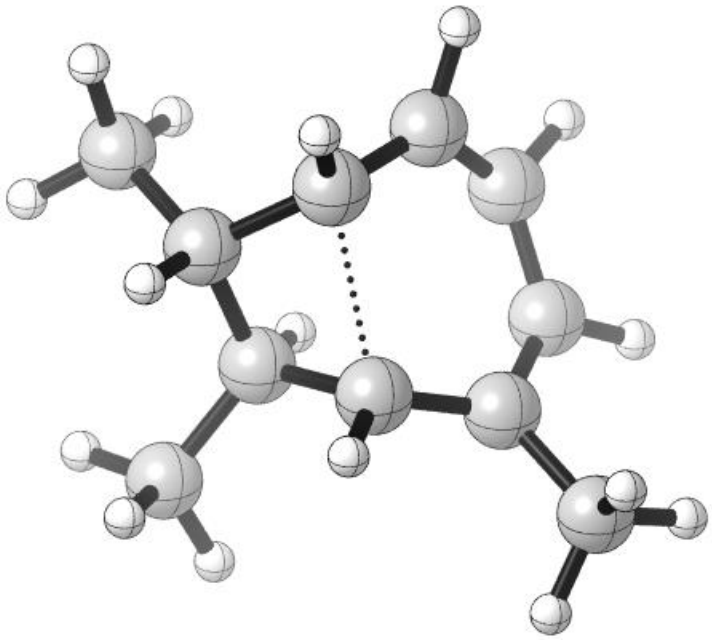

Monomethyl_A_cyclooctatriene_exo_6π_TS
E(M062X/def2TZVP) = -428.663336 Hartree

Free energy correction (M062X/def2SVP) = 0.203430 Hartree
G = -1124921.483

C	0.12978900	-1.96575800	0.24216400
C	-1.73583800	-0.77254900	-0.87738400
C	-0.80333400	-1.82172200	-0.78840200
H	-1.04435300	-2.72296900	-1.35892000
H	-2.64019000	-0.97581000	-1.45841900
C	-1.72905800	0.31360200	0.00020700
C	0.74027400	-0.97026000	1.03089600
H	1.01709300	-1.32941800	2.03298500
C	-0.50526300	0.73748400	0.53925900
H	-0.55128400	1.42766000	1.39404400
C	0.72971900	0.91860500	-0.32976400
H	0.55149400	0.41457600	-1.29256300
C	1.69780400	0.08965700	0.48619700
H	2.02130800	0.70242100	1.34581000
C	2.92465700	-0.46758600	-0.22193400
H	3.51244900	-1.11511700	0.44580400
H	3.58152700	0.34448700	-0.56938000
H	2.61780300	-1.06701300	-1.09249300
C	1.11052500	2.37092300	-0.57823700
H	2.03829600	2.43970200	-1.16630800
H	1.27289900	2.89910200	0.37452700
H	0.32005200	2.89946700	-1.13070200
H	0.25919300	-3.00027900	0.58449900
C	-3.03189400	0.89530600	0.49471600
H	-3.88035100	0.52671200	-0.09707400
H	-3.03362700	1.99387400	0.46103200
H	-3.20658700	0.59639800	1.54084600

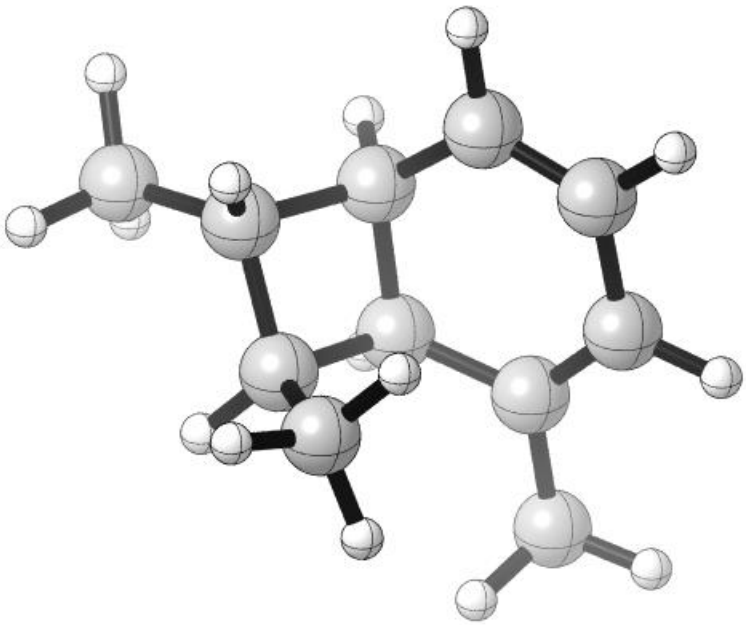

Monomethyl_A_BOD_endo_GS
E(M062X/def2TZVP) = -428.708469 Hartree

Free energy correction (M062X/def2SVP) = 0.206974 Hartree
G = -1125030.675

H	1.66098000	2.80586800	0.90588500
C	1.20632100	1.94976700	0.40311900
C	1.56324400	-0.34126800	-0.42235200
C	-0.75985500	0.84987500	-0.65335000
C	0.09036100	-0.44682800	-0.70865100
C	-0.08859600	1.98747300	0.05803500
C	2.05824100	0.78723400	0.11255900
H	-1.14025400	1.20186300	-1.62801000
H	-0.69050300	2.87591700	0.27077000
H	-0.05751300	-0.97893700	-1.66087600
H	3.12383100	0.85602500	0.34520400
C	-0.82257700	-1.07383500	0.39737000
H	-1.22794900	-2.06187400	0.12566600
C	-1.83341700	0.08666000	0.17433800
H	-2.11737200	0.59735200	1.10944400
C	2.39687500	-1.55103200	-0.71770900
H	3.44529200	-1.40550000	-0.42579200
H	2.36235600	-1.79518800	-1.79183900
H	2.00482900	-2.43208000	-0.18273700
C	-0.23211600	-1.12324800	1.79670400
H	0.58587100	-1.85541000	1.86782200
H	-1.00767800	-1.40739800	2.52399500
H	0.16894000	-0.14178900	2.08804000
C	-3.06967700	-0.29980500	-0.61784400
H	-2.78631900	-0.80712700	-1.55386700
H	-3.66775400	0.58455900	-0.88348300
H	-3.70957700	-0.98624500	-0.04353100

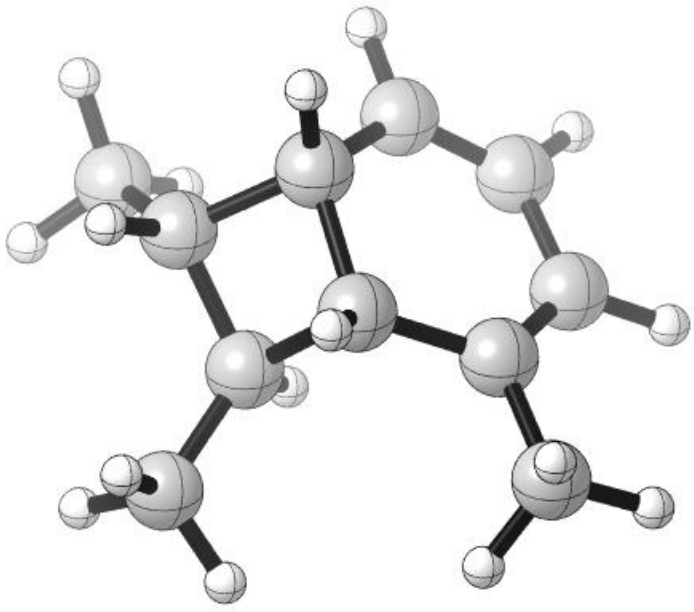

Monomethyl_A_BOD_exo_GS
E(M062X/def2TZVP) = -428.709861 Hartree

Free energy correction (M062X/def2SVP) = 0.206244 Hartree
G = -1125036.246

H	-2.89791700	-1.28027300	-0.94833300
C	-1.93347400	-1.05474600	-0.48670100
C	0.25669000	-1.96293900	0.17874400
C	-0.36573700	0.45480100	0.64573300
C	0.58710200	-0.72913200	0.96735000
C	-1.72214500	0.14824900	0.07370600
C	-0.89961800	-2.09884000	-0.48769000
H	0.97887000	-2.78443200	0.19214000
H	-0.45268700	1.13310600	1.51054900
H	0.69890700	-0.99621300	2.03161100
H	-1.10883100	-3.02558200	-1.02631600
C	1.75680800	0.12405000	0.39513000
H	2.19778700	0.70895300	1.21985900
C	0.71151400	1.00111900	-0.33216100
H	0.52145800	0.57109000	-1.33029600
C	-2.74855200	1.23945200	0.10903100
H	-3.68171000	0.93723200	-0.38438600
H	-2.36929600	2.14715300	-0.38854600
H	-2.97814100	1.52383100	1.14870400
C	0.94776500	2.49483500	-0.43010100
H	1.10356200	2.92972300	0.56948600
H	0.09451200	3.01055300	-0.89571900
H	1.83967100	2.71449300	-1.03689700
C	2.85101900	-0.53181100	-0.42372900
H	3.46327500	-1.21172200	0.18787100
H	3.52223100	0.22674900	-0.85399200
H	2.42008300	-1.11489200	-1.25160800

Monomethyl B Cartesian Coordinates

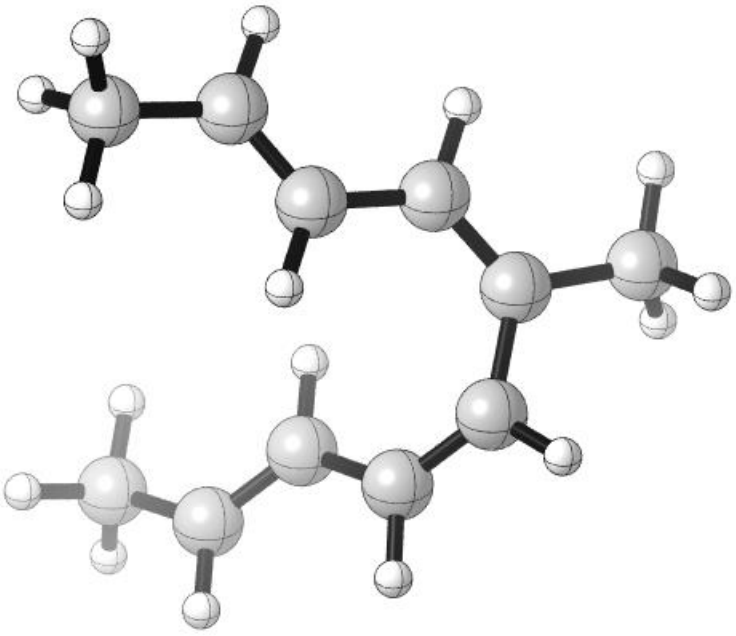

Monomethyl_B_tetraene_GS
E(M062X/def2TZVP) = -428.689803 Hartree
Free energy correction (M062X/def2SVP) = 0.197805 Hartree
G = -1125005.741

C	0.01060000	1.71519600	0.91913800
H	0.34367900	2.39102100	1.71371600
C	-1.29381900	1.37915200	0.88576500
H	-1.95562500	1.85320700	1.62012900
C	-1.96540900	0.50020500	-0.09215800
C	-1.55804600	-0.75380900	-0.38764700
H	-2.13150200	-1.30866600	-1.13879400
C	-0.44924200	-1.47697500	0.22361700
H	0.06145900	-0.99899700	1.06567900
C	1.03623100	1.29505300	-0.02973700
H	0.71105200	0.71158000	-0.89709800
C	-0.04214000	-2.68725200	-0.18799900
H	-0.56078500	-3.15041300	-1.03620600
C	2.33540200	1.59643700	0.11366100
H	2.64052200	2.17639900	0.99324000
C	1.07954200	-3.46489900	0.42436100
H	0.72854900	-4.43694700	0.80532900
H	1.53686400	-2.91259400	1.25637900
H	1.86376500	-3.68229800	-0.31779400
C	3.41609400	1.19679000	-0.83969300
H	3.93257800	2.08026400	-1.24673100
H	3.01055900	0.61527300	-1.67842800
H	4.18300400	0.58805000	-0.33560400
C	-3.20123900	1.08710500	-0.72353800
H	-3.92839700	1.37876000	0.05156900
H	-3.68681300	0.37322800	-1.40165400
H	-2.95675900	2.00011600	-1.28835100

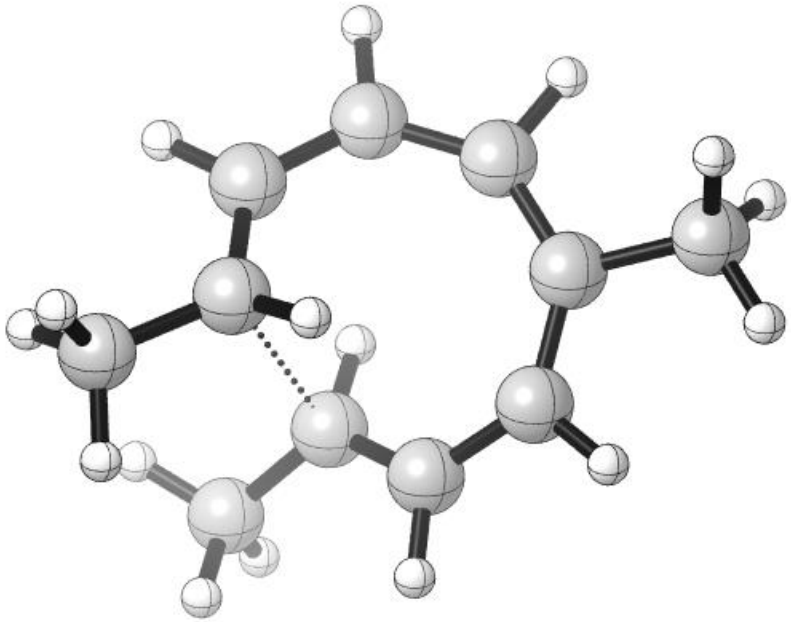

Monomethyl_B_tetraene_8π_TS
E(M062X/def2TZVP) = -428.661832 Hartree
Free energy correction (M062X/def2SVP) = 0.202326 Hartree
G = -1124920.433

C	0.52025200	1.85561100	-0.69786800
C	1.64430000	1.05364000	-0.49819800
H	2.54973200	1.55292300	-0.86415700
C	1.97168400	-0.20118400	0.09491200
C	1.20504300	-1.31990100	0.44261000
H	1.75446300	-2.07444000	1.01290000
C	-0.12954000	-1.66635200	0.17626500
H	-0.52800600	-2.52295100	0.73217800
C	-0.80295300	1.74215800	-0.24428400
H	-1.54604400	2.39876400	-0.71027500
C	-0.99655000	-0.97565300	-0.65391600
H	-0.53741400	-0.33599500	-1.40675900
C	-1.24055400	0.80154800	0.67448700
H	-0.48114800	0.38946600	1.33826700
C	-2.37050500	-1.48774100	-0.97175900
H	-3.06951900	-0.66660200	-1.18542400
H	-2.77833100	-2.08728200	-0.14533000
H	-2.34074900	-2.12734100	-1.86866000
C	-2.64799200	0.78709100	1.19287900
H	-2.96255100	-0.22579600	1.48149700
H	-3.35650800	1.17385800	0.44658500
H	-2.72752200	1.41872000	2.09236500
H	0.71796400	2.73498900	-1.31802900
C	3.46762900	-0.34116300	0.34853500
H	4.02186400	-0.29602600	-0.60206900
H	3.71314200	-1.29460800	0.83203900
H	3.84574600	0.47398900	0.98289100

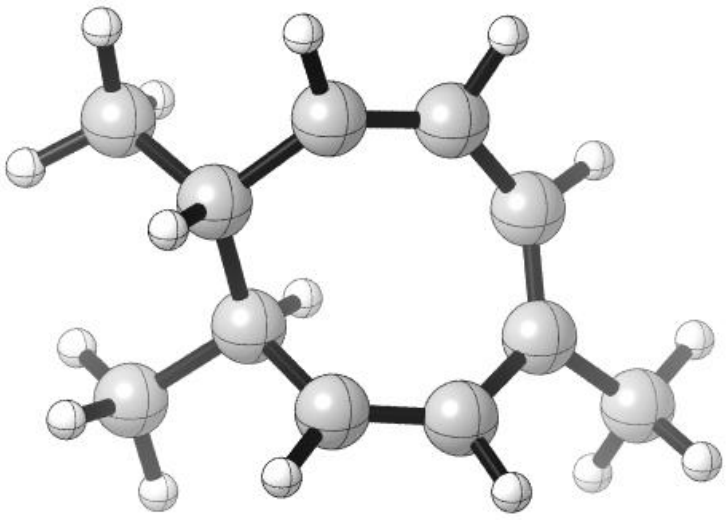

Monomethyl_B_cyclooctatriene_GS
E(M062X/def2TZVP) = -428.704363 Hartree

Free energy correction (M062X/def2SVP) = 0.205633 Hartree
G = -1125023.416

C	0.37691700	1.94806400	0.20446400
C	2.03219200	0.02212400	-0.07843000
C	1.51074300	1.22585500	-0.39484300
H	2.09483100	1.83519900	-1.09461300
C	1.40831600	-0.89087500	0.89078200
H	2.07269900	-1.33296800	1.64198400
C	-0.87650700	1.61243900	0.55577300
H	-1.45835700	2.42828000	1.00083200
C	0.11842600	-1.24763300	0.87912700
H	-0.24020100	-1.92922700	1.66005800
C	-0.89799500	-0.84156700	-0.15311200
H	-0.36381400	-0.53106300	-1.06638700
C	-1.70588100	0.37223300	0.33578100
H	-2.15225900	0.10007200	1.31073200
C	-2.86135200	0.73227800	-0.60928500
H	-3.35929900	1.65580500	-0.28058800
H	-3.62024900	-0.06083300	-0.64667800
H	-2.48010400	0.90095500	-1.62848100
C	-1.79250700	-2.03856700	-0.48578600
H	-2.43771000	-1.84020000	-1.35183200
H	-2.43835300	-2.29072600	0.37136900
H	-1.18095200	-2.92184400	-0.71822300
H	0.62578300	3.00075300	0.38653600
C	3.33775000	-0.44254900	-0.66844700
H	3.77403300	0.31304600	-1.33464200
H	3.19983100	-1.37531600	-1.23707100
H	4.06350700	-0.66274200	0.13085300

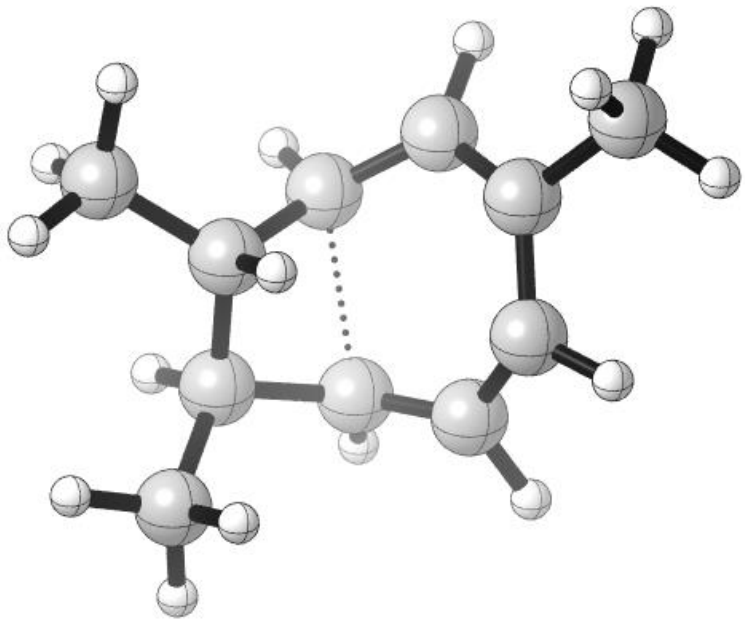

Monomethyl_B_cyclooctatriene_endo_6π_TS
E(M062X/def2TZVP) = -428.663522 Hartree

Free energy correction (M062X/def2SVP) = 0.203908 Hartree
G = -1124920.717

C	-0.35549000	-1.76967700	0.30869500
C	-1.96640900	0.07434200	-0.16304000
C	-1.41403100	-1.20407500	-0.40488900
H	-2.07062900	-1.90616700	-0.92832300
C	-1.34212800	0.93720800	0.73916500
H	-1.97810900	1.56383800	1.37361100
C	0.72718800	-1.13613500	0.95350800
H	1.10639200	-1.71111800	1.81078600
C	0.03949400	0.89972700	0.95274700
H	0.42752400	1.42496300	1.83516100
C	1.01382000	0.85209700	-0.21604200
H	0.44744900	0.58909200	-1.12372800
C	1.81870700	-0.35093000	0.22535500
H	2.53490500	-0.01118800	0.99378400
C	2.56514600	-1.13500600	-0.84452500
H	3.04890100	-2.02807800	-0.42142500
H	3.34658400	-0.51689000	-1.31257600
H	1.86531800	-1.46625100	-1.62677400
C	1.77902000	2.14646700	-0.44786700
H	2.50283400	2.03384600	-1.26925600
H	2.33564900	2.43641400	0.45719000
H	1.09741900	2.96953400	-0.70700100
H	-0.49227200	-2.83566800	0.53206900
C	-3.36378400	0.36745600	-0.64830200
H	-3.95127400	-0.54884100	-0.79603000
H	-3.33361900	0.90347700	-1.60996100
H	-3.89627600	1.01418800	0.06365300

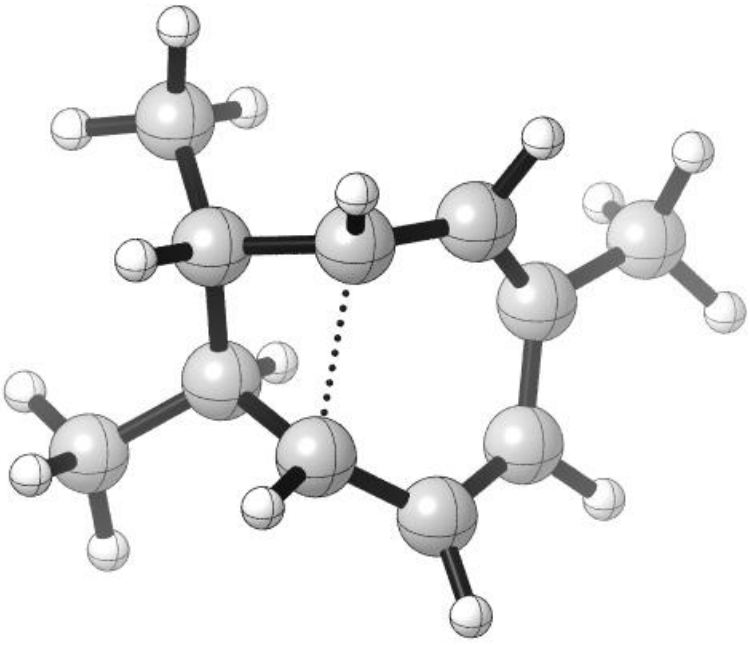

Monomethyl_B_cyclooctatriene_exo_6π_TS

E(M062X/def2TZVP) = -428.663322 Hartree
Free energy correction (M062X/def2SVP) = 0.204024 Hartree
G = -1124919.887

C	1.12278500	0.93646200	0.70012200
C	1.62386000	-1.27788500	-0.23871300
C	1.83897500	0.11791100	-0.18690600
H	2.46571400	-1.87560500	-0.60114900
C	0.59406400	-1.91420200	0.44341400
C	-0.17941100	0.79193400	1.21828200
H	-0.29608100	1.25433100	2.20913100
C	-0.60912500	-1.25218900	0.70841700
H	-1.28291800	-1.70112900	1.44966900
C	-1.32179000	-0.45515100	-0.37545900
H	-0.62243400	-0.32030100	-1.21613100
C	-1.45078000	0.85544300	0.36979700
H	-2.30402100	0.76329700	1.06424200
C	-1.60865900	2.12606100	-0.45295300
H	-1.61371700	3.01993900	0.18857100
H	-2.55094900	2.11254300	-1.02182000
H	-0.77263600	2.22265400	-1.16238600
C	-2.60880800	-1.09202400	-0.87798800
H	-3.10383400	-0.44622400	-1.61902300
H	-3.31243000	-1.25509600	-0.04652100
H	-2.41148600	-2.06377800	-1.35322400
H	1.74552100	1.70188300	1.18267100
H	0.78849500	-2.89923000	0.87881400
C	3.09921300	0.66811100	-0.80938300
H	3.50852000	1.49570700	-0.21228900
H	2.88765400	1.06868700	-1.81306300
H	3.87265900	-0.10450100	-0.91926900

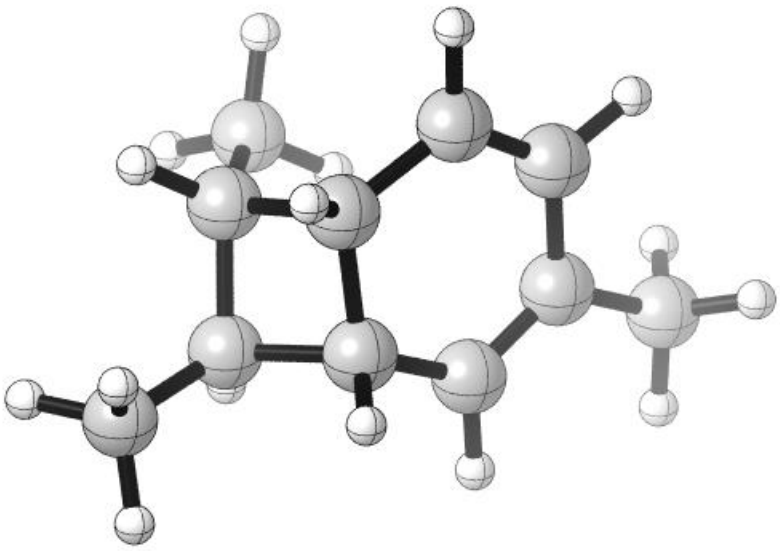

Monomethyl_B_BOD_endo_GS
E(M062X/def2TZVP) = -428.706713 Hartree

Free energy correction (M062X/def2SVP) = 0.206618 Hartree
G = -1125026.999

C	-1.90244500	-0.47029400	0.01800300
C	-0.72490000	1.43063600	-1.02864300
C	0.48865900	-0.83094200	-0.63924600
C	0.57172300	0.68406400	-0.96687700
C	-0.81435500	-1.25608300	-0.02768900
C	-1.85711100	0.89075100	-0.55955400
H	0.73826200	-1.50570700	-1.47668200
H	-0.86451900	-2.27112900	0.38125600
H	1.14934100	0.86104500	-1.88528000
H	-2.79305800	1.45487500	-0.59743600
C	1.49123100	0.88618500	0.28382600
H	2.43003600	1.41537400	0.05409300
C	1.66153800	-0.65667700	0.36759000
H	1.44692200	-1.06135200	1.37076100
C	0.83295500	1.50945400	1.50293000
H	0.60275100	2.57231400	1.34038200
H	1.50171000	1.43265700	2.37367500
H	-0.10786400	0.99480500	1.74743500
C	2.99715800	-1.17104800	-0.13927400
H	3.21031300	-0.77035700	-1.14316400
H	3.00308600	-2.26905500	-0.20843800
H	3.81821000	-0.86519700	0.52620800
H	-0.73038300	2.43868900	-1.45174400
C	-3.20364200	-0.91179600	0.62586000
H	-3.13909300	-1.93537100	1.01695700
H	-4.01371000	-0.87475200	-0.11952100
H	-3.49687100	-0.24233000	1.44994000

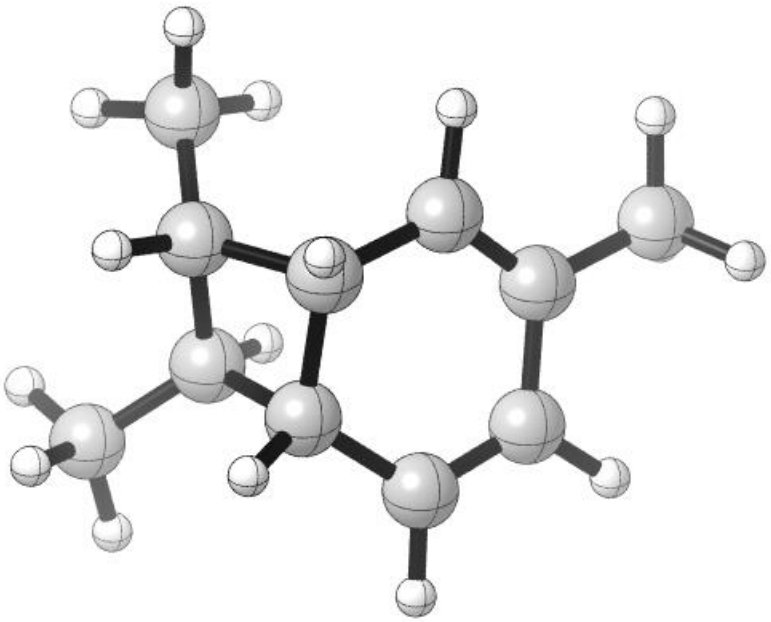

Monomethyl_B_BOD_exo_GS
E(M062X/def2TZVP) = -428.708440 Hartree

Free energy correction (M062X/def2SVP) = 0.206191 Hartree
G = -1125032.655

H	2.55588600	-1.96318000	-0.49887100
C	1.73768300	-1.33308600	-0.13977200
C	1.07349100	0.93158500	0.51143900
C	-0.55982500	-1.01000900	0.67915300
C	-0.21324800	0.44142600	1.11083300
C	0.57432800	-1.88052600	0.23633800
C	1.97571500	0.12454000	-0.07271800
H	1.29162800	2.00154300	0.59670200
H	-1.17445100	-1.51017500	1.44347000
H	-0.21200900	0.64612300	2.19473600
C	-1.50042400	0.91206200	0.37172400
H	-2.34019000	0.88926800	1.08656500
C	-1.48454400	-0.41597700	-0.41924400
H	-0.88575900	-0.27482300	-1.33500400
C	-2.79577900	-1.10368500	-0.73999300
H	-3.38540500	-1.26267800	0.17629000
H	-2.62974900	-2.08384200	-1.21142300
H	-3.40222300	-0.49894300	-1.43144400
C	-1.50540100	2.21749500	-0.39870400
H	-1.40548200	3.08479200	0.27142200
H	-2.44512500	2.33442800	-0.95933300
H	-0.67312600	2.24692000	-1.11811800
H	0.43130100	-2.96314600	0.19391100
C	3.27050500	0.63160100	-0.64295500
H	3.36155800	1.71978100	-0.53120700
H	3.34944600	0.38399300	-1.71317700
H	4.12869500	0.15738500	-0.14112900

Monomethyl C Cartesian Coordinates

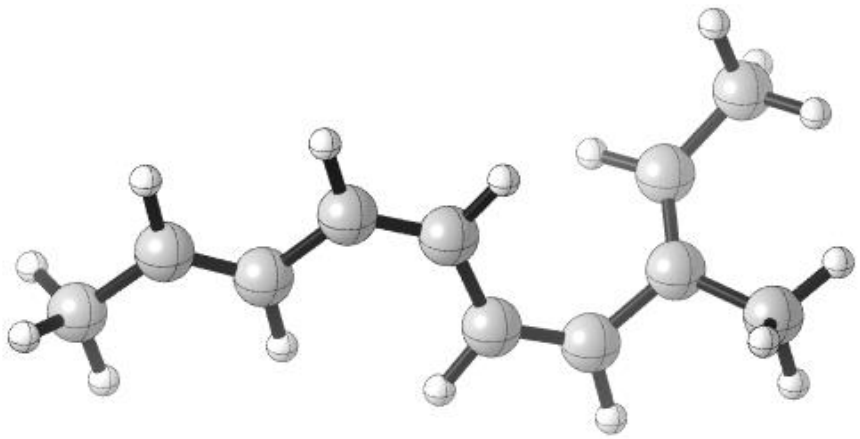

Monomethyl_C_tetraene_GS
E(M062X/def2TZVP) = -428.685855 Hartree
Free energy correction (M062X/def2SVP) = 0.197127 Hartree
G = -1124997.155

C	-1.67360600	0.66227900	0.61361900
H	-1.88445000	1.58155700	1.16895100
C	-0.38718800	0.25701200	0.52981600
H	0.37749500	0.87751900	1.00346100
C	0.07884700	-0.96571400	-0.10973200
H	-0.68140300	-1.70391400	-0.37825600
C	1.36407300	-1.30075800	-0.34916100
H	1.55403300	-2.30863400	-0.73609600
C	2.56842500	-0.47922600	-0.11619300
C	-2.83316000	0.00359000	0.02867500
H	-2.67061000	-0.90527900	-0.55951500
C	2.59817800	0.81802100	-0.47467600
H	1.70031400	1.21337900	-0.96139800
C	-4.08720100	0.46165100	0.16771600
H	-4.24122900	1.37709400	0.75159200
C	3.72414100	1.79201800	-0.31406300
H	4.04787100	2.17679900	-1.29378200
H	4.59792300	1.36245300	0.18965900
H	3.39466600	2.66554200	0.27018900
C	-5.30544100	-0.17972800	-0.41547900
H	-6.02346800	-0.45609300	0.37253900
H	-5.04805400	-1.08581200	-0.98043100
H	-5.83162900	0.51164500	-1.09229200
C	3.72718100	-1.23036700	0.48971700
H	3.94775100	-2.12744300	-0.10996400
H	3.47285800	-1.58023700	1.50205700
H	4.64243300	-0.63124700	0.55184200

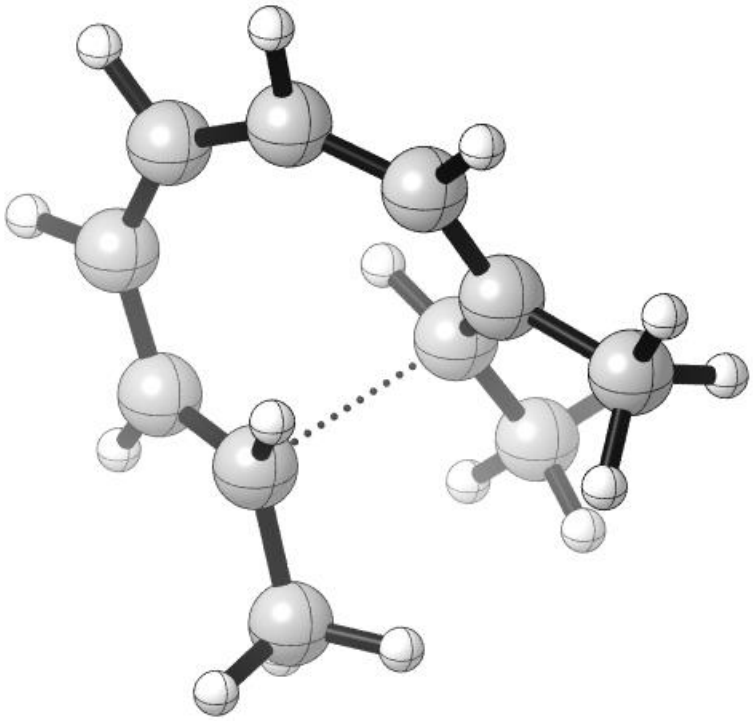

Monomethyl_C_tetraene_8π_TS
E(M062X/def2TZVP) = -428.665701 Hartree
Free energy correction (M062X/def2SVP) = 0.202557 Hartree

G = -1124929.985

C	-2.35923700	0.61672400	0.38400300
C	-2.39354400	-0.76160000	0.20775500
H	-3.38726100	-1.17631700	0.40806100
C	-1.49241400	-1.78566500	-0.20649000
C	-0.11992600	-1.95776900	-0.34333600
H	0.15812900	-2.90139600	-0.82394000
C	0.97513500	-1.14531900	0.04278600
C	-1.36291400	1.55986500	0.05808300
H	-1.46584000	2.56333500	0.48586400
C	0.78945900	-0.05167800	0.86891400
H	-0.14016500	-0.03206600	1.43583500
C	-0.24839900	1.28128800	-0.70379000
H	-0.29874500	0.39599200	-1.33817600
C	1.91230900	0.78336100	1.40670100
H	1.54538100	1.75777000	1.75770400
H	2.69738700	0.95935100	0.65826200
H	2.38654100	0.28208800	2.26784700
C	0.74467000	2.33181900	-1.10010900
H	1.75061600	1.90910200	-1.23371400
H	0.80123200	3.13568000	-0.35252600
H	0.45801600	2.78447300	-2.06333400
H	-3.26288100	1.03244700	0.83919300
H	-2.03901300	-2.70197200	-0.45480300
C	2.33847500	-1.44576000	-0.53259100
H	3.11930700	-1.46200100	0.24198400
H	2.63161700	-0.68233600	-1.27337600
H	2.34399300	-2.41575000	-1.04643600

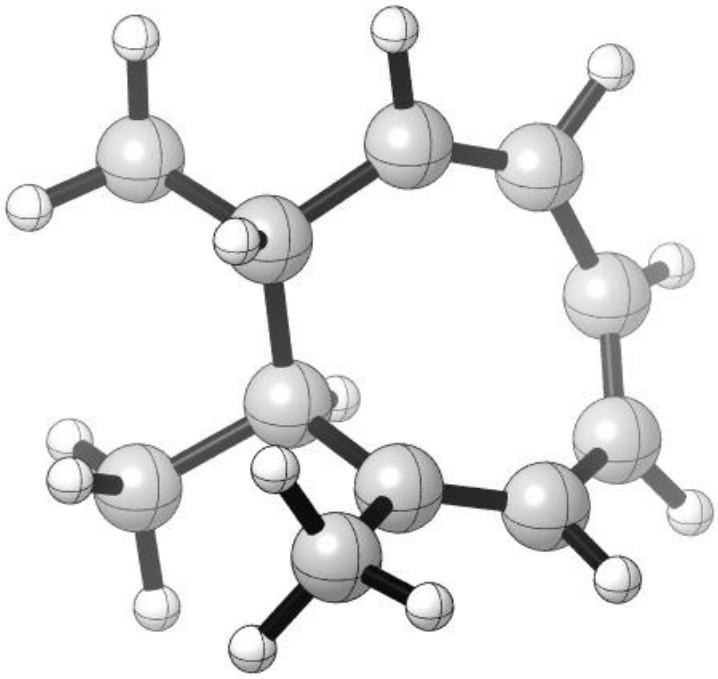

Monomethyl_C_cyclooctatriene_GS
E(M062X/def2TZVP) = -428.704410 Hartree

Free energy correction (M062X/def2SVP) = 0.206764 Hartree
G = -1125020.57

C	1.58215400	1.57722600	0.39711000
C	2.24099300	-0.64323800	-0.65539500
C	2.29044900	0.69908400	-0.54595400
H	3.06871100	1.20805800	-1.12424400
C	1.33629900	-1.53048200	0.07110200
H	1.78963000	-2.41842100	0.52645800
C	0.31926300	1.64038000	0.85548000
H	0.14396800	2.42930500	1.59655600
C	0.00882300	-1.35701000	0.20211700
C	-0.73835000	-0.24313500	-0.50526800
H	-0.10756200	0.11789700	-1.33222800
C	-0.95552800	0.94907900	0.44390500
H	-1.43504300	0.56354300	1.36378600
C	-1.89697700	2.01233800	-0.14146000
H	-1.95291700	2.88772000	0.52144300
H	-2.91694400	1.62721100	-0.27343700
H	-1.52273200	2.35512800	-1.11872100
C	-2.05243300	-0.75370100	-1.10655100
H	-2.48060800	-0.01775400	-1.79978900
H	-2.80405100	-0.95879400	-0.32790000
H	-1.88377000	-1.68233000	-1.67076500
H	2.24849800	2.34452500	0.80917200
H	2.99013600	-1.11999200	-1.29618500
C	-0.80850600	-2.30146000	1.04056400
H	-1.41888400	-1.74387400	1.77039000
H	-0.16637900	-2.99823000	1.59404300
H	-1.50918100	-2.88847600	0.42751700

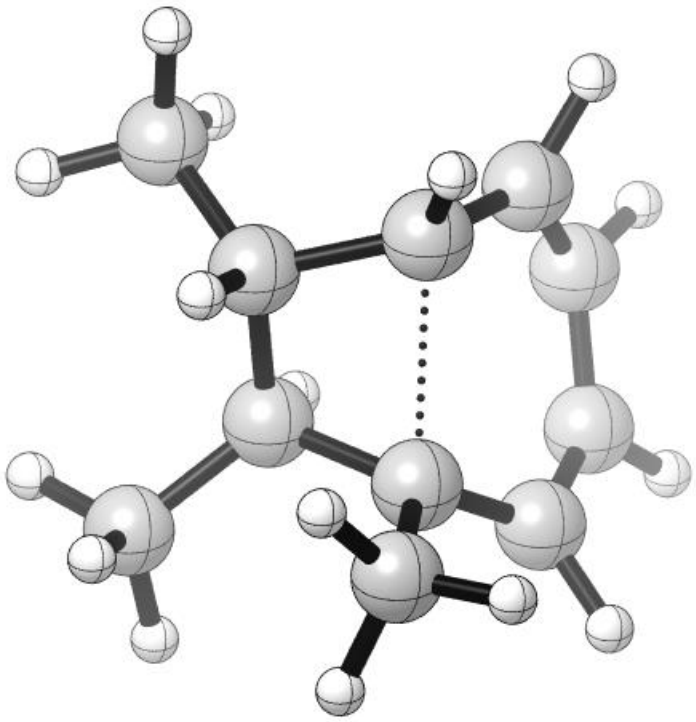

Monomethyl_C_cyclooctatriene_endo_6π_TS
E(M062X/def2TZVP) = -428.663977 Hartree
Free energy correction (M062X/def2SVP) = 0.205116 Hartree
G = -1124918.74

C	1.43750000	1.37021300	0.54426300
C	2.15261700	-0.53476000	-0.85580000
C	2.15468000	0.83553000	-0.52572200
H	3.00344600	1.41844300	-0.89302400
C	1.31009300	-1.44817300	-0.23829500
H	1.69387900	-2.45678200	-0.04602900
C	0.23155100	0.91097100	1.11505200
H	0.13821300	1.16778500	2.18061100
C	0.05540000	-1.08100900	0.28132700
C	-0.86481900	-0.22211300	-0.59446100
H	-0.26238000	0.15847000	-1.43354100
C	-1.10717700	0.91336200	0.37488000
H	-1.87629300	0.58938700	1.09723800
C	-1.51493500	2.25926200	-0.20782300
H	-1.58359600	3.02885300	0.57549400
H	-2.49518600	2.19361600	-0.70427800
H	-0.76993500	2.59234500	-0.94637000
C	-2.09321000	-0.93160600	-1.14807700
H	-2.68361600	-0.24238200	-1.77008100
H	-2.74641300	-1.29602000	-0.34080600
H	-1.80956800	-1.78993600	-1.77511700
H	1.97809000	2.14218300	1.10681800
H	3.02458000	-0.90415800	-1.40184700
C	-0.62624600	-2.03090100	1.23777500
H	-1.41101100	-1.52581600	1.81937900

H	0.09570300	-2.46314000	1.94267000
H	-1.10863700	-2.85749500	0.69016500

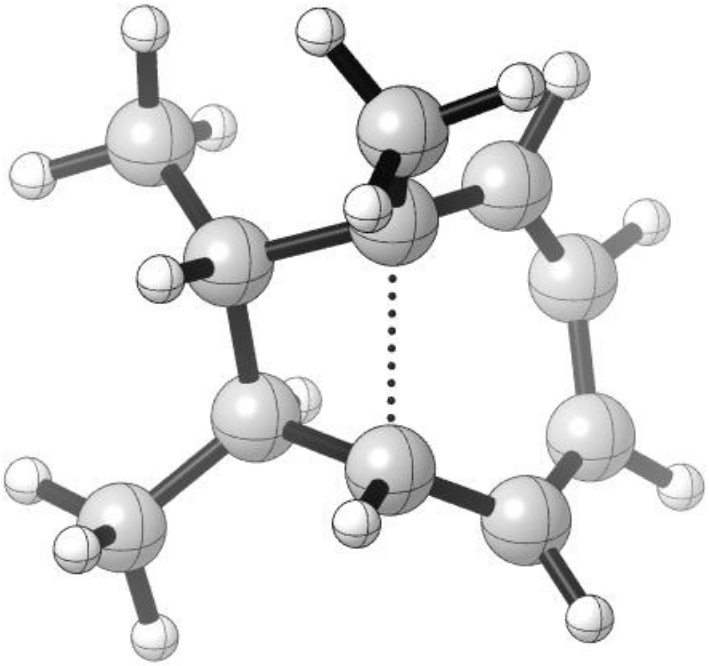

Monomethyl_C_cyclooctatriene_exo_6π_TS
E(M062X/def2TZVP) = -428.665185 Hartree
Free energy correction (M062X/def2SVP) = 0.204483 Hartree
G = -1124923.573

C	-0.87255800	-1.41425100	-0.51083900
C	-2.36567500	0.56805400	-0.48153900
C	-1.85552800	-0.60168500	-1.07811600
H	-2.48987900	-1.06795900	-1.83696900
H	-3.37010900	0.87470700	-0.78370300
C	-1.80204200	1.09998200	0.67260800
C	0.17364500	-1.08626800	0.38520400
C	-0.44205000	0.91711300	0.94644400
H	-0.09371900	1.13522100	1.96496700
C	0.60710100	1.15155000	-0.13104400
H	0.09303600	1.20938300	-1.10331200
C	1.33088300	-0.17272400	-0.03702900
H	2.01980200	-0.11796900	0.82559700
C	2.10024000	-0.64343400	-1.26392100
H	2.50993200	-1.65476800	-1.12167800
H	2.94234700	0.03110000	-1.48120900
H	1.43489400	-0.66537200	-2.13998600
C	1.44568800	2.40440200	0.07704200
H	2.22018500	2.49358500	-0.69982300
H	1.94912100	2.37763100	1.05627000
H	0.82169600	3.30895100	0.03936700
H	-1.05958100	-2.48905700	-0.64279100
H	-2.46089300	1.55398000	1.41914700
C	0.57845600	-2.16803800	1.36105400

H	1.47566500	-2.70222300	1.00307200
H	-0.22374400	-2.89770400	1.53229400
H	0.84228900	-1.71770400	2.32957700

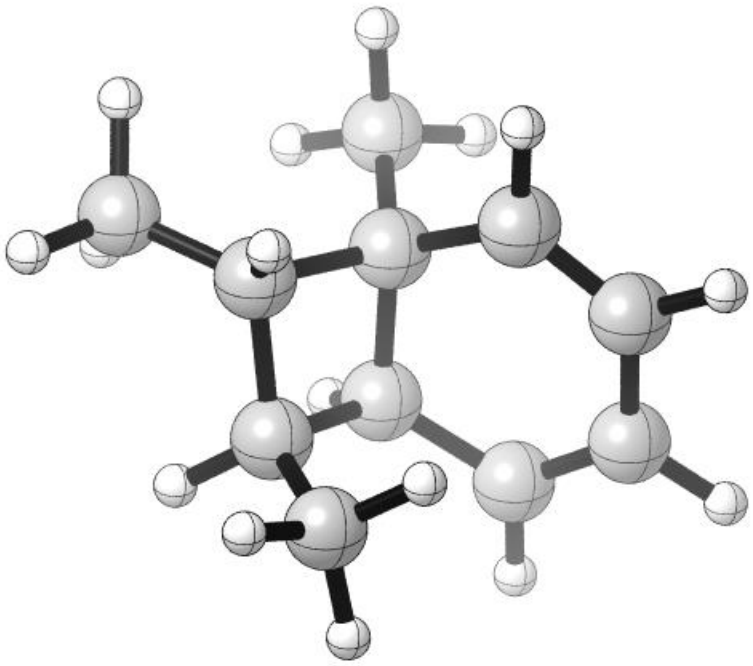

Monomethyl_C_BOD_endo_GS
E(M062X/def2TZVP) = -428.705443 Hartree
Free energy correction (M062X/def2SVP) = 0.207510 Hartree
G = -1125021.323

C	1.97147000	-0.80314900	-0.93665000
C	1.63822900	0.38773700	1.17654000
C	-0.36046000	-0.78585200	-0.02075300
C	0.15536600	0.25284700	1.01540100
C	0.67175700	-1.10105200	-1.07382200
C	2.47765000	-0.09962100	0.25153400
H	0.31946700	-1.64408700	-1.95755700
H	-0.31345700	0.07132600	1.99497900
H	3.55713500	0.01763000	0.36568100
C	-0.63081900	1.37736800	0.26333700
H	-1.28670800	1.96099200	0.92890600
C	-1.39582100	0.27544000	-0.52105100
H	-1.36221400	0.42329600	-1.61371600
C	0.19272500	2.32186900	-0.59585800
H	0.81151900	2.99025600	0.02014200
H	-0.47164800	2.94465100	-1.21404400
H	0.86297900	1.76578800	-1.26652000
C	-2.83339100	0.07750300	-0.07146000
H	-2.90144300	-0.00404500	1.02417900
H	-3.27847400	-0.82995800	-0.50556800
H	-3.44822300	0.93716000	-0.37737900
H	2.02769000	0.90642600	2.05630700
H	2.68361900	-1.09027900	-1.71292600

C	-0.90293200	-2.09457900	0.54446200
H	-0.08349100	-2.67109800	0.99921100
H	-1.35382000	-2.71259300	-0.24796400
H	-1.66558700	-1.91653200	1.31618200

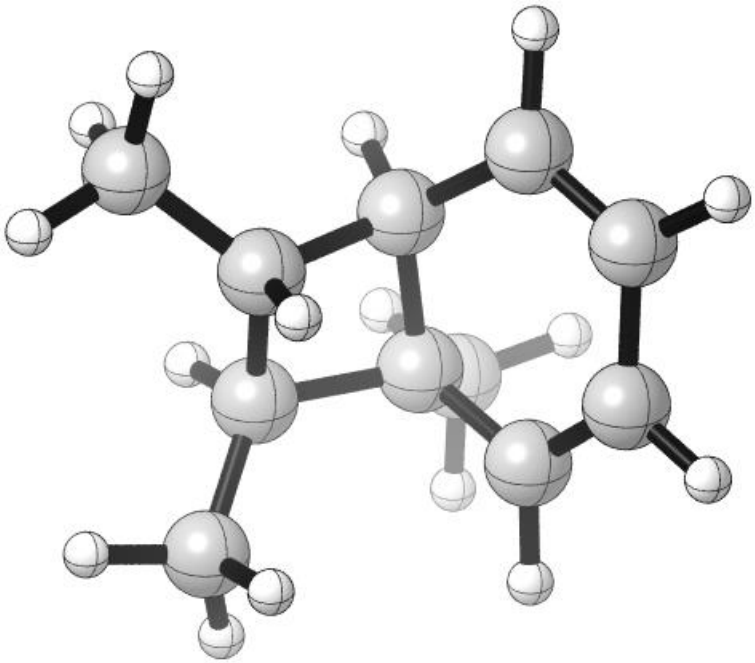

Monomethyl_C_BOD_exo_GS
E(M062X/def2TZVP) = -428.708557 Hartree
Free energy correction (M062X/def2SVP) = 0.206491 Hartree
G = -1125032.174

H	-3.16524900	1.57399300	-0.78049200
C	-2.27223200	1.02029200	-0.48423200
C	-1.10467700	-1.14107800	-0.57126300
C	-0.13554300	0.80838300	0.71396400
C	-0.13890400	-0.73651800	0.51362600
C	-1.37986000	1.56029100	0.35880900
C	-2.08117100	-0.33658500	-1.01731400
H	-1.02404200	-2.16488800	-0.95133700
H	0.20332100	1.05260600	1.73438700
C	1.32754900	-0.61030000	0.00165800
H	1.99765400	-0.71157400	0.87364300
C	1.07243300	0.89038200	-0.25881900
H	0.68384200	1.01204700	-1.28395600
C	2.17819800	1.88952000	0.01457700
H	2.55450300	1.78129400	1.04372000
H	1.82337200	2.92342600	-0.11023600
H	3.02545400	1.74201900	-0.67239800
C	1.82127200	-1.48093800	-1.13714600
H	1.82509800	-2.54629000	-0.85949100
H	2.84885800	-1.20724600	-1.41999200
H	1.18125700	-1.36305400	-2.02453700
H	-1.53743400	2.56020200	0.77022500

H	-2.78116300	-0.69849300	-1.77334700
C	-0.35468600	-1.60714500	1.74543800
H	0.34577600	-1.32609400	2.54674300
H	-0.19407300	-2.67055200	1.50643700
H	-1.38146400	-1.49521000	2.12485300

Tributyl Cartesian Coordinates

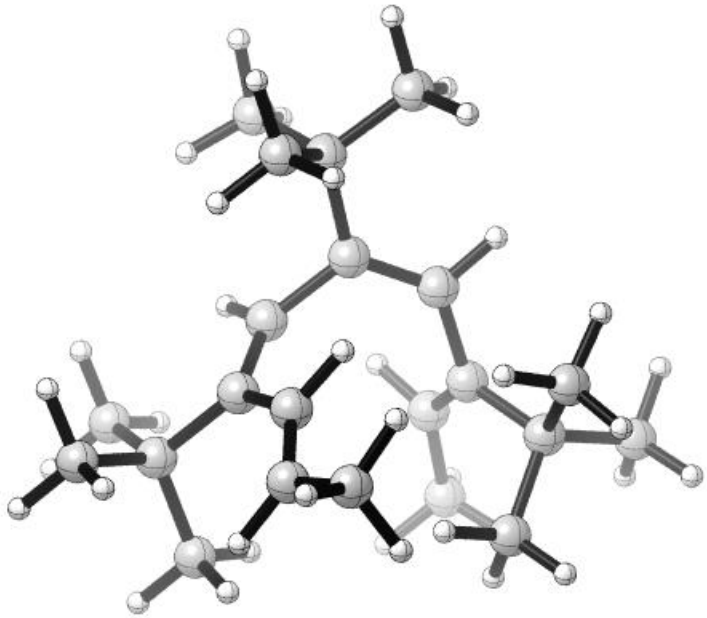

Tributyl_tetraene_GS
E(M062X/def2TZVP) = -861.057174 Hartree
Free energy correction (M062X/def2SVP) = 0.491654 Hartree
G = -2259414.773

C	-1.49431900	-0.51859700	-0.04128000
C	-1.11841500	0.56772400	-0.75110700
H	-1.55007900	0.72285000	-1.74199400
C	-0.14160200	1.60988700	-0.32675100
C	1.18204400	1.36760500	-0.31603300
H	1.84698400	2.16663400	0.02230500
C	1.86944500	0.11739200	-0.73802300
C	-0.95009200	-0.66358400	1.32473600
H	-0.40561200	0.22252600	1.66526000
C	1.61239000	-0.35062600	-1.97336700
H	0.87912300	0.22387200	-2.54990300
C	-1.01040600	-1.68109600	2.19852500
H	-1.52215800	-2.61222300	1.94545800
C	2.16619200	-1.53433000	-2.71275400
H	2.41758000	-1.24563500	-3.74428100
H	1.40813600	-2.33209500	-2.78768100
H	3.06153500	-1.96912600	-2.25861300
C	-0.37722100	-1.63665000	3.55613000
H	-1.11488100	-1.83994200	4.34795000
H	0.07787400	-0.65590300	3.75288900
H	0.40794300	-2.40444900	3.65036400

C	-0.74453400	2.97011700	0.05169600
C	2.87893900	-0.50248700	0.25106000
C	-2.43135000	-1.57336700	-0.64419900
C	2.52532500	-1.97693300	0.51257800
H	2.56048700	-2.58971700	-0.39609700
H	1.50953300	-2.05133000	0.92880100
H	3.23269700	-2.40848700	1.23859100
C	2.83523300	0.20877100	1.61334000
H	3.16269400	1.25591600	1.54737900
H	3.50837200	-0.30593100	2.31546000
H	1.82084500	0.19064000	2.03743000
C	4.31033500	-0.36910300	-0.29439900
H	4.56249400	0.69010500	-0.45381800
H	4.44237200	-0.88948900	-1.25168700
H	5.03238300	-0.78734200	0.42464600
C	-1.59355100	2.80891400	1.32361200
H	-2.35178500	2.02151800	1.20085400
H	-2.11044800	3.75280600	1.55669400
H	-0.96085700	2.54566400	2.18502700
C	0.32395400	4.03419300	0.30688800
H	0.95513900	4.19136400	-0.58021000
H	0.97374200	3.75991900	1.15095500
H	-0.15972600	4.99021900	0.55656800
C	-1.65201300	3.45153000	-1.09371800
H	-2.50784300	2.77692700	-1.24010900
H	-1.09193100	3.51297500	-2.03941200
H	-2.04993500	4.45149800	-0.86362100
C	-2.95260300	-1.15668100	-2.02482600
H	-2.13511000	-1.04583200	-2.75225600
H	-3.50993000	-0.20925200	-1.97872700
H	-3.63456700	-1.93191800	-2.40363000
C	-1.65015200	-2.88704400	-0.84048200
H	-0.77994300	-2.70879100	-1.49031700
H	-2.29382800	-3.64019900	-1.32088500
H	-1.27724100	-3.30957000	0.09981900
C	-3.66219300	-1.78907000	0.25333000
H	-4.23272700	-0.85216100	0.34317500
H	-3.40134600	-2.11649200	1.26604800
H	-4.32242400	-2.54894400	-0.19217200

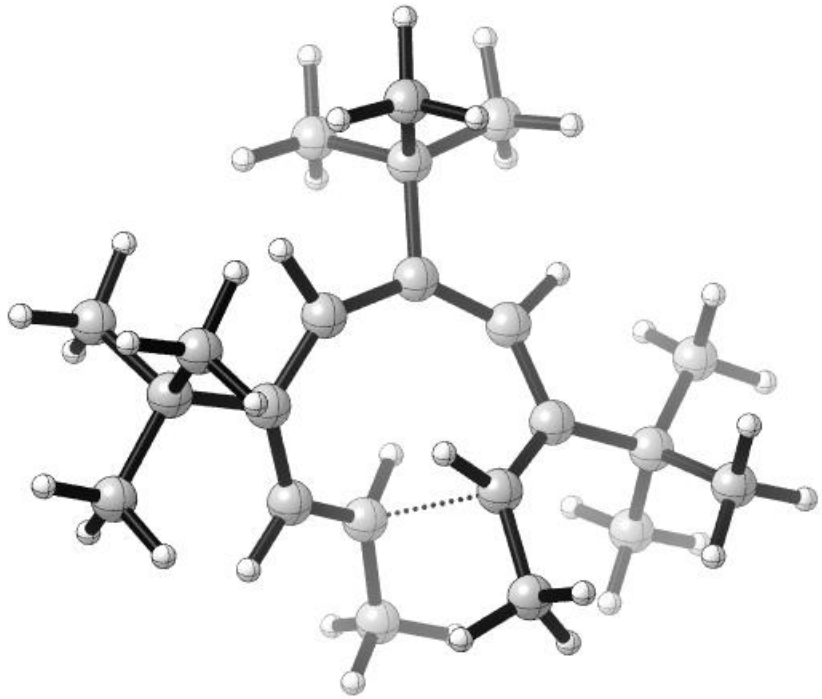

Tributyl_tetraene_8π_TS
E(M062X/def2TZVP) = -861.029896 Hartree
Free energy correction (M062X/def2SVP) = 0.498259 Hartree
G = -2259325.813

C	-1.87025800	-0.77497700	-0.12295900
C	-1.41269000	0.53410900	0.05628800
H	-2.25627400	1.18285100	0.29405700
C	-0.22407500	1.33175800	-0.03212000
C	1.13943300	1.03371400	0.05581700
H	1.76670200	1.89337000	-0.13261400
C	1.88032500	-0.13804600	0.36998200
C	-1.12674000	-1.85555400	-0.64843100
H	-1.54185300	-2.86139200	-0.56148300
C	1.17665300	-1.26063400	0.78999500
H	0.18080500	-1.02265600	1.15848000
C	0.14085600	-1.75477700	-1.18377100
H	0.46363400	-0.77420900	-1.53445500
C	1.68099100	-2.58877800	1.27907900
H	0.87466900	-3.33299700	1.20559300
H	1.96692300	-2.52957800	2.34209400
H	2.54548200	-2.97177000	0.72367700
C	0.81637900	-2.95104300	-1.78709100
H	1.90821900	-2.90113700	-1.69025000
H	0.59363600	-3.00959700	-2.86520300
H	0.46638600	-3.88339900	-1.32138900
C	-3.35221400	-1.01425800	0.27271200
C	-0.57970100	2.85338100	-0.16859500
C	3.41430700	-0.11785200	0.17280700
C	3.82142700	-1.06429100	-0.96933600
H	3.29279700	-0.80330200	-1.89905400

H	3.60806200	-2.11515200	-0.73578900
H	4.90343700	-0.98314400	-1.15744800
C	4.12664200	-0.53093900	1.47245400
H	3.83484300	0.13514000	2.29819100
H	5.21775400	-0.45843200	1.34341800
H	3.89671400	-1.56082100	1.76886300
C	3.94848000	1.27465700	-0.19781000
H	3.54490100	1.63143900	-1.15635100
H	5.04245100	1.22151600	-0.29598400
H	3.71864800	2.02175600	0.57593700
C	0.63380200	3.76207100	-0.41214300
H	0.28156100	4.79469100	-0.54813800
H	1.18547600	3.47584300	-1.31978300
H	1.33259200	3.76227200	0.43663900
C	-1.53003200	3.06909600	-1.36061300
H	-1.77334300	4.13777400	-1.46431200
H	-2.47438600	2.51941900	-1.25153900
H	-1.05441800	2.73219000	-2.29405700
C	-1.24540100	3.34861600	1.12938700
H	-1.46588700	4.42459100	1.05229500
H	-0.57322800	3.19531200	1.98667000
H	-2.19246700	2.83476400	1.34537900
C	-3.58043400	-0.60982900	1.73896400
H	-4.62815600	-0.78950900	2.02614300
H	-3.36063800	0.45288600	1.91264000
H	-2.93390300	-1.19906100	2.40676700
C	-4.27241500	-0.18521900	-0.64087200
H	-5.32762700	-0.38283400	-0.39632400
H	-4.10683300	-0.44739500	-1.69638800
H	-4.10348900	0.89520200	-0.52875600
C	-3.77524900	-2.48160000	0.13130600
H	-4.82961600	-2.58359300	0.42688700
H	-3.18214500	-3.14231700	0.78047800
H	-3.68193800	-2.83635700	-0.90519300

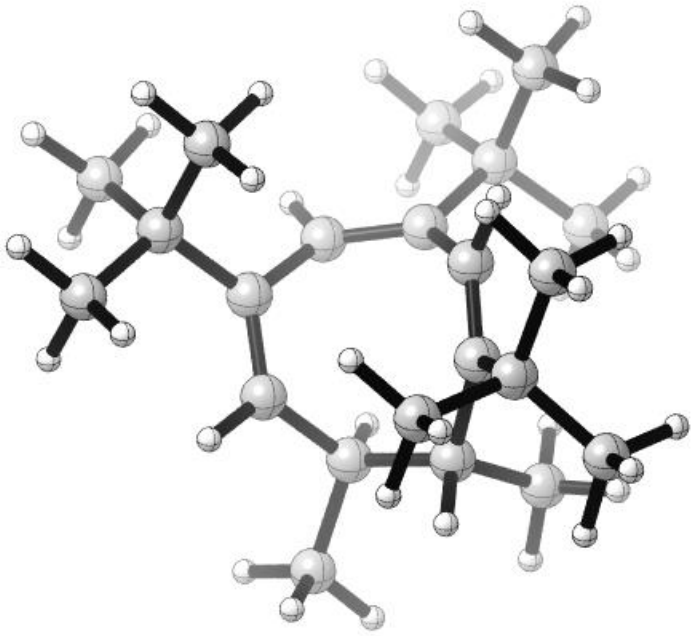

Tributyl_cyclooctatriene_GS
E(M062X/def2TZVP) = -861.089925 Hartree
Free energy correction (M062X/def2SVP) = 0.499592 Hartree
G = -2259479.919

C	1.58159500	-0.89655000	0.38124500
C	0.56528700	1.36834100	0.03311300
C	1.57913000	0.58507200	0.45223600
H	2.49152600	1.05704500	0.82514600
C	-0.60970700	0.77389500	-0.65854100
H	-0.67221100	1.08943800	-1.70290600
C	0.65790700	-1.59759200	1.05581400
H	0.64318700	-2.68939300	0.98320300
C	-1.52403600	-0.11606300	-0.23442100
C	-1.67847400	-0.56518000	1.21652900
H	-2.31607700	-1.46305900	1.21073500
C	-0.37580500	-0.97452700	1.95743500
H	0.05818400	-0.05129800	2.37160900
C	2.65001200	-1.52917200	-0.51464000
C	-0.69765600	-1.92175400	3.11547900
H	0.20849300	-2.15534700	3.69255200
H	-1.10634500	-2.87077400	2.73269300
H	-1.43623000	-1.49097400	3.80587200
C	-2.41517300	0.51609200	2.01816500
H	-2.62371000	0.18070800	3.04448400
H	-3.37036700	0.78962700	1.54987600
H	-1.79583100	1.42205700	2.07093400
C	0.65737400	2.90116100	0.02465600
C	-2.51667100	-0.74908400	-1.22541400
C	-2.17123100	-2.24644600	-1.34555600
H	-1.13961000	-2.37236500	-1.70715200
H	-2.85365600	-2.73660700	-2.05727100
H	-2.25850000	-2.77191100	-0.38362800

C	-3.96858700	-0.59776100	-0.74018000
H	-4.25116500	0.46426300	-0.67914000
H	-4.13317800	-1.05546400	0.24523100
H	-4.65049200	-1.08990900	-1.45027400
C	-2.43431400	-0.14118200	-2.62888700
H	-1.44406200	-0.29352900	-3.08160900
H	-2.64830300	0.93790000	-2.61451700
H	-3.17692900	-0.62448100	-3.28055000
C	-0.52417800	3.49284000	0.80756800
H	-0.51975400	4.59109800	0.72996500
H	-0.45862500	3.22628400	1.87343500
H	-1.48349500	3.12219300	0.41721100
C	0.59101500	3.40790000	-1.42811000
H	1.36551300	2.92847300	-2.04640500
H	0.75620300	4.49576400	-1.45147800
H	-0.38901000	3.21289200	-1.88545000
C	1.95876900	3.40854900	0.64907100
H	2.83814500	3.07931100	0.07590100
H	2.07022200	3.05964600	1.68612700
H	1.95756500	4.50850500	0.66044400
C	2.41071200	-1.06039900	-1.95986900
H	3.16823700	-1.48978100	-2.63396400
H	2.46270600	0.03592400	-2.03453700
H	1.41496700	-1.37589500	-2.30752700
C	4.04684500	-1.07355400	-0.06116200
H	4.81945100	-1.55341900	-0.68113400
H	4.22714800	-1.34922000	0.98885100
H	4.17213800	0.01412100	-0.16062600
C	2.59956400	-3.05726100	-0.47795200
H	3.38499400	-3.47036000	-1.12814100
H	1.63150600	-3.43581400	-0.83791400
H	2.76309500	-3.43959300	0.54046700

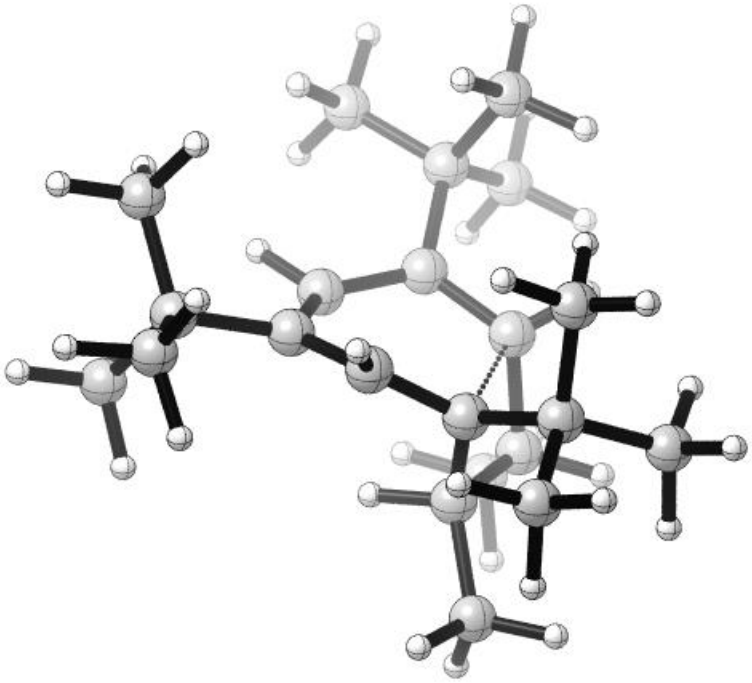

Tributyl_cyclooctatriene_6π1_TS
E(M062X/def2TZVP) = -861.043646 Hartree
Free energy correction (M062X/def2SVP) = 0.499684 Hartree
G = -2259358.172

C	0.53224600	1.30331500	-0.39816200
C	-1.46209000	0.18569000	0.45069400
C	-0.75583700	1.36862400	0.14289200
H	-2.52112000	0.33630800	0.66042600
C	-1.06900500	-1.12043700	0.10458800
C	1.44143000	0.27483300	-0.10707000
C	0.26386600	-1.57163100	0.12549500
H	0.44794100	-2.45029100	-0.50803800
C	1.15047100	-1.54030300	1.37497100
H	2.03072400	-2.16671600	1.16463800
C	1.56356400	-0.08375600	1.38817500
H	0.75019300	0.46825600	1.88205700
C	2.84416600	0.28580200	2.13130600
H	3.02894700	1.36920000	2.08820500
H	3.73485100	-0.22939700	1.74757700
H	2.73730100	0.01146600	3.19199900
C	0.47954200	-2.05423300	2.64276000
H	1.16866500	-2.00869100	3.50030900
H	0.15371400	-3.09874700	2.52614200
H	-0.40786400	-1.44534400	2.87512400
H	0.78316600	2.02698300	-1.17828100
C	-2.12284600	-2.06531200	-0.52430900
C	-1.54277700	2.69114300	0.16997600
C	2.60083500	0.06872100	-1.10223600
C	-1.93649300	2.97310200	1.62946600
H	-1.04025000	3.06469600	2.26148100

H	-2.55904800	2.16468500	2.03958500
H	-2.50648000	3.91290500	1.69791600
C	-0.69561000	3.86573300	-0.33177500
H	0.25337900	3.93860200	0.21916100
H	-1.24870000	4.80633000	-0.19193100
H	-0.46578300	3.77342800	-1.40339700
C	-2.80929700	2.61313800	-0.69825800
H	-3.52974200	1.87696600	-0.31518400
H	-2.55362700	2.33467200	-1.73188200
H	-3.31515300	3.59080700	-0.71922100
C	-3.55412100	-1.53001000	-0.40593800
H	-3.84755900	-1.38486400	0.64475600
H	-4.25054300	-2.25668300	-0.84969300
H	-3.67921000	-0.57639700	-0.93851800
C	-2.08208800	-3.44597300	0.14891100
H	-1.09472800	-3.91801400	0.04769700
H	-2.82728100	-4.11827000	-0.30424900
H	-2.30628600	-3.35858700	1.22313500
C	3.35576600	-1.25248200	-0.89750600
H	3.82032800	-1.33225700	0.09281500
H	4.15951900	-1.32678200	-1.64559200
H	2.68829000	-2.11483000	-1.03827500
C	3.60410000	1.23320000	-0.99207900
H	4.09245300	1.25629900	-0.00896900
H	3.10536000	2.20068000	-1.14907200
H	4.38877500	1.12650500	-1.75748100
C	2.03796500	0.03638200	-2.53265000
H	2.84379100	-0.18370700	-3.24955300
H	1.58602300	0.99422300	-2.82355600
H	1.26508600	-0.74212900	-2.62080300
C	-1.79751100	-2.20525300	-2.02213700
H	-0.80596200	-2.65049200	-2.18685600
H	-1.81594800	-1.21986800	-2.51195000
H	-2.54086600	-2.85270900	-2.51320700

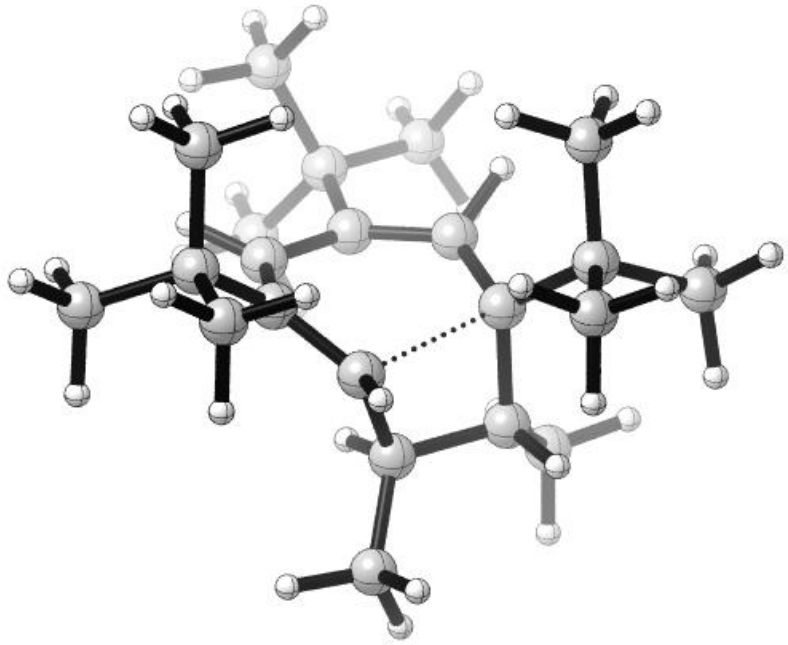

Tributyl_cyclooctatriene_6π2_TS
E(M062X/def2TZVP) = -861.050039 Hartree
Free energy correction (M062X/def2SVP) = 0.497310 Hartree
G = -2259381.19

C	1.25385000	-1.02422800	0.23269200
C	0.64831300	1.37925700	0.08466800
C	1.57237000	0.33600000	0.30892800
H	2.62651100	0.62223800	0.25239200
C	-0.65250200	1.11436000	-0.37011100
H	-0.99643200	1.81248500	-1.13913000
C	-0.02931200	-1.41421200	0.63291300
H	-0.36114500	-2.43095200	0.39864300
C	-1.48373600	-0.00329300	-0.13935300
C	-1.94539300	-0.28181700	1.30403000
H	-2.69383300	-1.09100100	1.26979100
C	-0.66813100	-0.84915400	1.89209700
H	-0.04198900	-0.01880800	2.25373100
C	2.26931200	-1.98534100	-0.40589400
C	-0.83872400	-1.87721200	3.00179400
H	0.13608700	-2.26125300	3.33748400
H	-1.43837600	-2.73217000	2.65067500
H	-1.35014200	-1.43995400	3.87295700
C	-2.53718900	0.91067700	2.04655000
H	-2.83496100	0.61921500	3.06581000
H	-3.42264900	1.31951000	1.53947700
H	-1.78784100	1.71354000	2.12172400
C	1.21414500	2.81057000	-0.00837800
C	-2.45982300	-0.40883200	-1.26300600
C	1.71359400	-3.40691900	-0.52579100
H	2.47296300	-4.06467800	-0.97409900
H	0.82174000	-3.43820700	-1.16977100

H	1.44338100	-3.81925800	0.45760300
C	3.52858800	-2.03287800	0.47457200
H	4.27386800	-2.71428900	0.03533600
H	3.28270900	-2.39237500	1.48477800
H	3.99536400	-1.04206600	0.56985000
C	2.64441300	-1.49111600	-1.81248700
H	3.36133300	-2.17888300	-2.28796200
H	3.09970200	-0.49099500	-1.77658700
H	1.74931500	-1.42916900	-2.45023300
C	1.86174000	3.15166400	1.34360800
H	2.28432700	4.16818500	1.31987100
H	2.67052000	2.44984300	1.59189300
H	1.11590800	3.10622600	2.15198700
C	0.12055600	3.85087600	-0.28064500
H	0.54303200	4.86226500	-0.18576500
H	-0.70958600	3.75473400	0.43476000
H	-0.28976700	3.76259900	-1.29686800
C	2.26370400	2.91744100	-1.12694500
H	2.62278800	3.95469800	-1.21407700
H	1.82838100	2.62076300	-2.09322900
H	3.13706000	2.27794400	-0.93660300
C	-1.95476900	0.03080100	-2.64349900
H	-0.90656800	-0.27173900	-2.78936100
H	-2.01943900	1.11846000	-2.78631800
H	-2.56519000	-0.43857800	-3.42962200
C	-3.84639800	0.21065500	-1.01771400
H	-3.78133400	1.30787900	-0.95720400
H	-4.29844500	-0.16034200	-0.08628100
H	-4.52578900	-0.04637400	-1.84530700
C	-2.59740400	-1.94025400	-1.29982000
H	-1.64742800	-2.40518900	-1.60091300
H	-3.36753800	-2.22701300	-2.03222100
H	-2.88977100	-2.35955800	-0.32648200

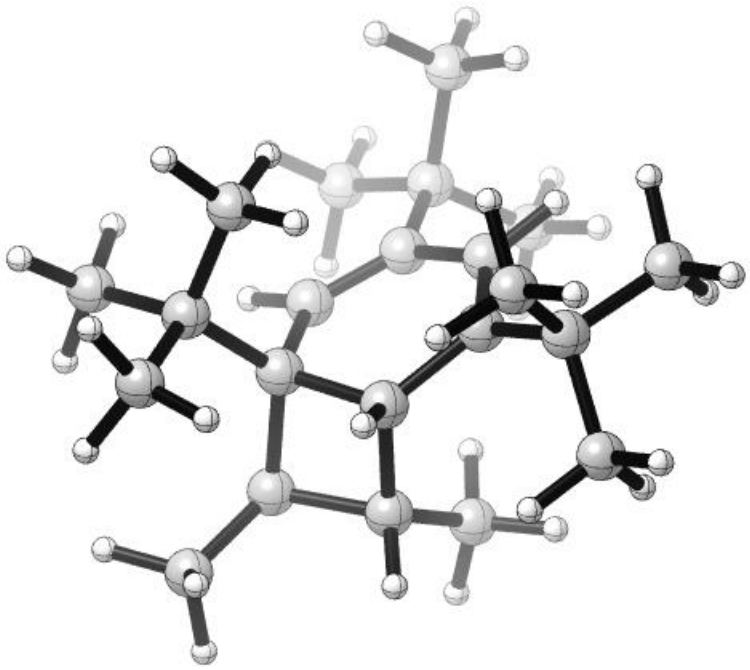

Tributyl_BOD1_GS
E(M062X/def2TZVP) = -861.093424 Hartree
Free energy correction (M062X/def2SVP) = 0.501856 Hartree
G = -2259483.162

H	2.12958900	1.46026800	-0.58049400
C	1.27525300	0.85810600	-0.27013400
C	0.46355800	-1.39921000	0.15802600
C	-1.08143300	0.57678000	0.32934300
C	-0.98410300	-0.95662000	0.11922800
C	0.06696600	1.43193200	-0.13594500
C	1.51255400	-0.57854400	-0.01531000
H	0.62432900	-2.46084800	0.35513100
H	-2.02124700	0.95426400	-0.09698000
C	-1.55761900	-1.15934000	1.57364000
H	-0.89784800	-1.81387800	2.16757900
C	-1.29807500	0.34633500	1.86134500
H	-2.20115800	0.85867200	2.23203500
C	-0.14126700	0.64331700	2.80086600
H	0.78716700	0.16749100	2.45847000
H	-0.37305100	0.26072200	3.80683800
H	0.04340700	1.72364800	2.88580300
C	-0.21662800	2.89981300	-0.44461500
C	-2.99793300	-1.57803900	1.82650700
H	-3.21487300	-2.59443000	1.46703700
H	-3.71508000	-0.88718000	1.36280000
H	-3.18147900	-1.56204000	2.91212900
C	2.96782600	-1.04609000	0.02678200
C	-1.67682000	-1.54738400	-1.15314400
C	-3.18374100	-1.25466700	-1.24258800
H	-3.42332400	-0.20148600	-1.03292600
H	-3.77567800	-1.88538200	-0.56970400

H	-3.52485500	-1.46512400	-2.26778500
C	-1.48899900	-3.07059400	-1.20572400
H	-0.44102700	-3.34689200	-1.38856400
H	-2.09138100	-3.49707400	-2.02237000
H	-1.81113700	-3.54475800	-0.26480800
C	-1.02096800	-0.91450400	-2.39055000
H	0.07026400	-1.04697000	-2.38290500
H	-1.23295900	0.16475400	-2.43743000
H	-1.42054500	-1.37677300	-3.30653700
C	-0.99265800	3.53823200	0.71890900
H	-0.38582500	3.54844600	1.63620700
H	-1.92763100	2.99936000	0.93181600
H	-1.25339200	4.57881900	0.47242900
C	-1.06978100	2.98492300	-1.72375800
H	-0.52835300	2.55368100	-2.57871300
H	-1.30115100	4.03633600	-1.95467700
H	-2.02521200	2.44977000	-1.61741700
C	1.06793100	3.70070300	-0.67018600
H	1.62016700	3.33907400	-1.54962600
H	1.73235900	3.64093100	0.20463100
H	0.82229800	4.75908300	-0.84259100
C	3.71794700	-0.26814300	1.12059400
H	4.77780200	-0.56548500	1.14226700
H	3.28318600	-0.47483500	2.11026700
H	3.67513700	0.81770500	0.95228700
C	3.08419200	-2.54129800	0.32844800
H	4.14442800	-2.83309700	0.35695000
H	2.58764500	-3.14674200	-0.44433900
H	2.63755600	-2.78989900	1.30235700
C	3.62440600	-0.77795400	-1.33841600
H	4.67282300	-1.11370500	-1.32745900
H	3.61987200	0.29033400	-1.59700800
H	3.09552000	-1.32327900	-2.13462100

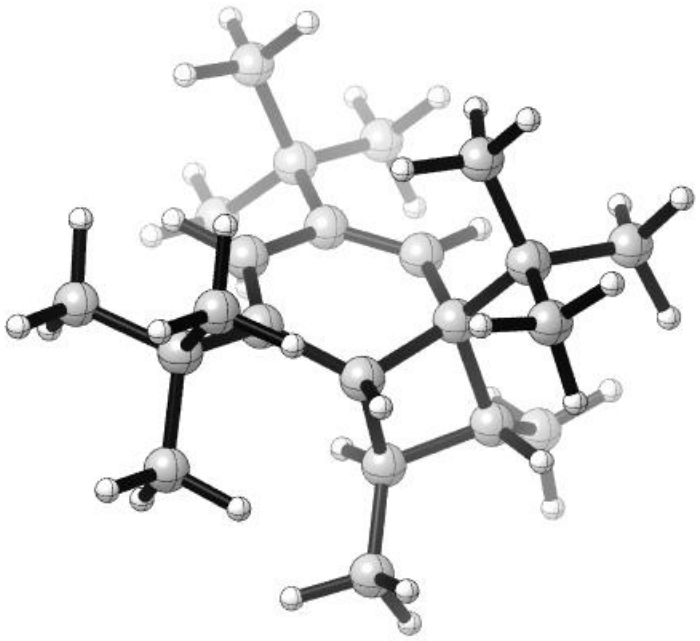

Tributyl_BOD2_GS
E(M062X/def2TZVP) = -861.101785 Hartree
Free energy correction (M062X/def2SVP) = 0.500605 Hartree
G = -2259508.398

C	1.54148800	-0.53076100	0.03214100
C	-0.84295000	-1.20816800	-0.04930000
C	-0.16246800	1.32601400	-0.05648000
C	-1.19358000	0.21295400	0.30445600
C	1.24061300	0.77939200	0.02796500
C	0.46149400	-1.52729200	-0.12103100
H	2.04199600	1.51892300	0.07895800
H	-2.18897000	0.48414400	-0.07467700
H	0.75805600	-2.55450200	-0.33412200
C	-1.10391100	0.67274100	1.78840900
H	-0.29818900	0.10654300	2.28447100
C	-0.53622200	2.01918900	1.29290300
H	-1.37564900	2.71290100	1.11593100
C	-1.97216700	-2.19328400	-0.33259400
C	-2.34306100	0.71416700	2.66197100
H	-2.65871700	-0.28562900	2.99058100
H	-3.18500700	1.17937000	2.12408100
H	-2.15166200	1.31526700	3.56475300
C	0.51847400	2.70018600	2.14713100
H	1.33664000	2.00494200	2.38799400
H	0.07785100	3.04421500	3.09537600
H	0.95456100	3.57663000	1.64484500
C	2.97049300	-1.06527900	0.13528200
C	-0.37157500	2.14365500	-1.36929200
C	0.11649800	1.32549400	-2.57268700
H	1.20599900	1.18226100	-2.54950800
H	-0.14346600	1.83539700	-3.51340200

H	-0.35276000	0.32869500	-2.57912300
C	-1.85010900	2.48310800	-1.60225800
H	-1.93718200	3.18265200	-2.44740400
H	-2.31551700	2.96238300	-0.72817200
H	-2.43648300	1.58882800	-1.85810900
C	0.41292300	3.45953500	-1.28554200
H	1.48173800	3.28915200	-1.08896300
H	0.01469600	4.10750100	-0.48961000
H	0.33461200	4.00987100	-2.23581800
C	-3.00039200	-2.15150000	0.80737000
H	-2.53263200	-2.42701000	1.76506100
H	-3.81810700	-2.86047600	0.60640800
H	-3.44348000	-1.15134100	0.91713900
C	-1.46297100	-3.62925100	-0.47819000
H	-0.77630200	-3.72970800	-1.33109700
H	-2.31055900	-4.30915800	-0.64952700
H	-0.93762200	-3.95955400	0.43018600
C	-2.66153600	-1.78696900	-1.64796600
H	-1.95279700	-1.83598700	-2.48799900
H	-3.06524900	-0.76485500	-1.59839300
H	-3.50070000	-2.46674800	-1.86291500
C	3.06140300	-2.01055600	1.34459100
H	4.07853100	-2.42263700	1.43272400
H	2.36135100	-2.85376900	1.25572600
H	2.82467100	-1.47085700	2.27399000
C	3.32532600	-1.83420700	-1.14894900
H	4.35563400	-2.21749100	-1.08866600
H	3.25273700	-1.17426600	-2.02647000
H	2.66015800	-2.69347800	-1.31419700
C	3.99421900	0.05669000	0.31994700
H	5.00207600	-0.37273700	0.41887900
H	3.78485900	0.64514200	1.22566800
H	4.00296200	0.74023800	-0.54186000

Butylmethyl Cartesian Coordinates

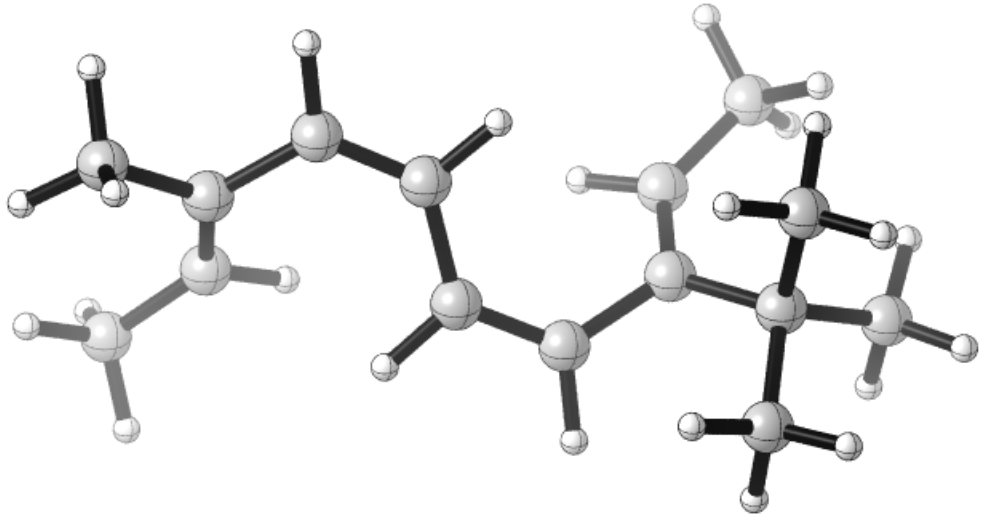

Butylmethyl_tetraene_GS
E(M062X/def2TZVP) = -585.906747 Hartree
Free energy correction (M062X/def2SVP) = 0.304082 Hartree
G = -1537499.797

C	-2.35594100	0.84085300	0.97999600
C	-1.08144700	0.47107900	0.73876400
H	-0.28383100	1.05647700	1.20614300
C	-0.65292200	-0.68812600	-0.03755100
C	0.60008900	-0.93034300	-0.47552700
H	0.78407400	-1.90481700	-0.93560600
C	1.75028600	-0.00282700	-0.38640700
C	-3.58524200	0.24558900	0.41981600
C	1.55313100	1.27357600	-0.77550700
H	0.56086000	1.49103400	-1.18495900
C	-3.65658600	-0.10045800	-0.87938300
C	2.47913700	2.45574000	-0.75736100
H	1.91191100	3.36295500	-0.50315900
H	2.91664000	2.62864200	-1.75465900
H	3.30300600	2.36425900	-0.04192800
C	-4.81018700	-0.71995300	-1.60597400
H	-5.15369300	-0.06457100	-2.42166800
H	-5.66659600	-0.93157800	-0.95514300
H	-4.50325300	-1.66736800	-2.07631000
H	-1.41654000	-1.44808600	-0.22813700
C	3.07392000	-0.56220400	0.17390000
H	-2.51412200	1.65922500	1.69175200
C	4.26322100	-0.22599100	-0.73906200
H	4.44019800	0.85153100	-0.83223300
H	4.09521700	-0.62851400	-1.74917400
H	5.18199200	-0.68233300	-0.33902400
C	3.28639600	0.01061100	1.58574300
H	3.36259300	1.10607200	1.57997900
H	4.20952100	-0.39519600	2.02880100
H	2.44333600	-0.26404300	2.23775500
C	3.02736200	-2.09268000	0.30414000
H	2.20349200	-2.42123600	0.95356600
H	3.97097800	-2.44762300	0.74439700
H	2.91194000	-2.58125300	-0.67475400
H	-2.77403800	0.11022600	-1.49276300
C	-4.71897700	0.11440700	1.40554300
H	-4.91518700	1.08723100	1.88314600
H	-4.45032800	-0.58574400	2.21154700
H	-5.65161300	-0.23092700	0.94565800

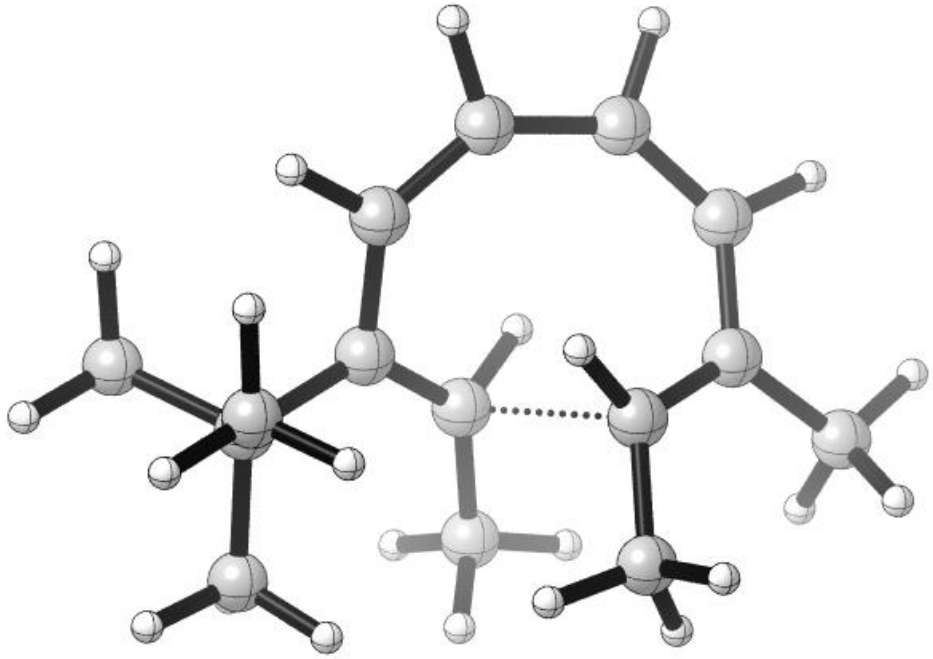

Butylmethyl_tetraene_8π_TS
E(M062X/def2TZVP) = -585.888927 Hartree
Free energy correction (M062X/def2SVP) = 0.310380 Hartree
G = -1537436.475

C	-0.73062100	1.76119000	0.03227900
C	0.44810100	2.49722900	0.05720300
H	0.24723500	3.56035600	0.22830600
C	1.84954000	2.28503900	-0.11697800
C	2.74058900	1.21904500	-0.11198000
H	3.76036800	1.49236100	-0.40143500
C	2.55554200	-0.14563000	0.21807100
C	-1.01464400	0.41371800	-0.33125500
C	1.38497500	-0.56502500	0.82615800
H	0.79920000	0.20798900	1.32211100
C	0.00200500	-0.27745100	-0.97604800
H	0.76389400	0.39132200	-1.37573400
C	1.16313400	-1.97389500	1.28726600
H	0.09657900	-2.16663400	1.47225400
H	1.69868200	-2.16095800	2.23377700
H	1.52501500	-2.71002600	0.55529000
C	0.02564500	-1.62898100	-1.63936600
H	1.05851500	-1.86212100	-1.93424800
H	-0.57919200	-1.62575400	-2.56061500
H	-0.33533300	-2.44775200	-1.00873000
C	3.62698400	-1.14121600	-0.15761200
H	3.90577800	-1.78317400	0.69151400
H	4.53127400	-0.62997400	-0.51245600
H	3.28938200	-1.80836900	-0.96807900
C	-2.39878400	-0.11373900	0.09295000
C	-2.57294400	0.06434600	1.61193400
H	-2.50199600	1.11840200	1.91315800

H	-1.79787300	-0.49448600	2.15955700
H	-3.55643800	-0.31524600	1.93008900
C	-2.63189000	-1.59485400	-0.22133700
H	-2.55647900	-1.80728800	-1.29564600
H	-3.64635800	-1.87103700	0.10302400
H	-1.92700200	-2.24309200	0.31796800
C	-3.48710500	0.68606100	-0.64619200
H	-3.38677200	0.55980700	-1.73435600
H	-3.43668800	1.76058700	-0.42425800
H	-4.48462500	0.32798200	-0.34749200
H	-1.59592000	2.35160500	0.34538500
H	2.36560500	3.24048500	-0.25994500

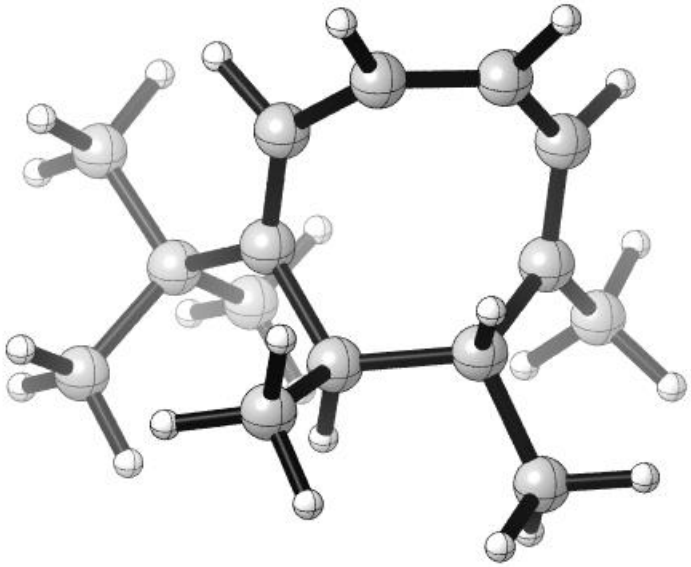

Butylmethyl_cyclooctatriene_GS
E(M062X/def2TZVP) = -585.931344 Hartree
Free energy correction (M062X/def2SVP) = 0.313325 Hartree
G = -1537540.109

C	-2.13285100	1.34172700	0.75987900
C	-0.69329000	2.22413500	-1.05551000
C	-1.87763600	2.18341000	-0.41608200
H	-0.58509300	2.93425900	-1.88310800
C	0.55177500	1.59134200	-0.57808300
C	-1.91290700	0.01586800	0.79350700
C	0.84326800	0.30622100	-0.30881000
C	-0.03299600	-0.86501800	-0.74481200
H	0.30625400	-1.75823200	-0.19542000
C	-1.55512900	-0.73606000	-0.47819400
H	-1.96434000	-0.14482300	-1.31021300
C	-2.22270700	-2.11441700	-0.51938700
H	-3.30898200	-2.02978700	-0.36972200
H	-1.82235500	-2.77889700	0.26158800
H	-2.05952500	-2.60404900	-1.48875500
C	0.20319500	-1.11375500	-2.24349400

H	-0.33049400	-2.00737800	-2.59702000
H	1.26902600	-1.24527600	-2.46981200
H	-0.15562600	-0.24479800	-2.81602600
H	-2.50898800	1.84086900	1.66059600
C	-2.07686900	-0.76856400	2.06646800
H	-1.16830700	-1.35552300	2.27872300
H	-2.90950300	-1.48541600	2.00216100
H	-2.25881200	-0.10221400	2.91966600
C	2.15198300	-0.07220500	0.40598100
H	1.32743900	2.33701500	-0.37936500
H	-2.67201100	2.85874500	-0.75160300
C	3.06675200	1.13092400	0.65394800
H	3.36772800	1.61038600	-0.28908700
H	3.97948100	0.79526800	1.16776200
H	2.58202900	1.88557800	1.28947900
C	2.95781300	-1.11259100	-0.39031100
H	3.27530800	-0.70357500	-1.36134800
H	2.38829900	-2.03469800	-0.57285900
H	3.86206800	-1.38950900	0.17285600
C	1.78082400	-0.66622400	1.77860300
H	1.19588700	-1.59259800	1.68251500
H	1.18965400	0.05530300	2.36242800
H	2.69351900	-0.90942600	2.34435200

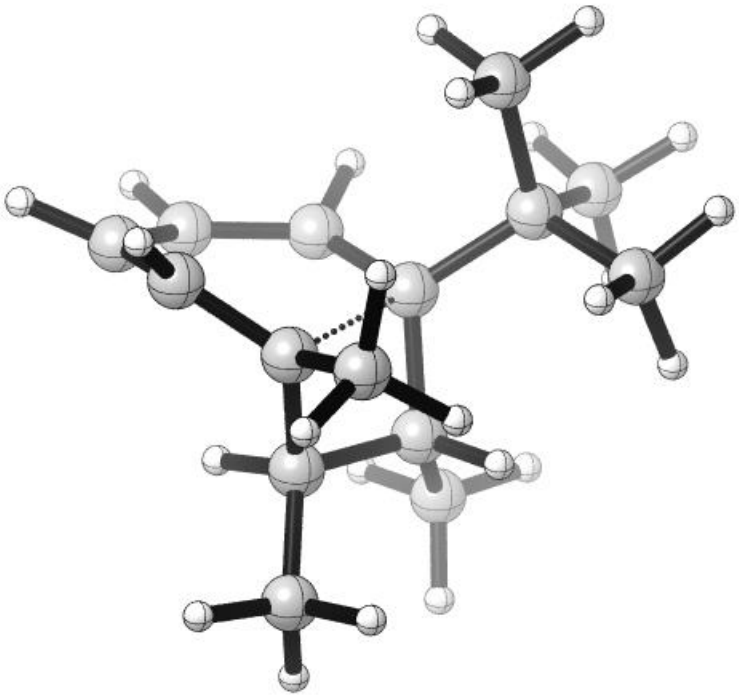

Butylmethyl_cyclooctatriene_6π1_TS
E(M062X/def2TZVP) = -585.893970 Hartree
Free energy correction (M062X/def2SVP) = 0.311469 Hartree
G = -1537446.856

C	-1.83467400	1.53435100	0.68194100
C	-0.70270500	1.99450000	-1.43442000

C	-1.73204700	2.24250600	-0.50313300
H	-0.59532000	2.72359300	-2.24202100
C	0.39833200	1.18138800	-1.18568400
C	-1.33913300	0.22358800	0.81259600
C	0.56323700	0.08072100	-0.29845500
C	-0.19420300	-1.22537100	-0.58707000
H	0.06573100	-1.95036400	0.19944000
C	-1.61294700	-0.77240500	-0.31811800
H	-1.97481500	-0.20502800	-1.18803800
C	-2.62657700	-1.86369000	0.00533900
H	-3.60539500	-1.43186800	0.26169700
H	-2.29657500	-2.49073000	0.84721100
H	-2.76993500	-2.52217900	-0.86434600
C	0.07210200	-1.86096400	-1.94701300
H	-0.54298500	-2.76486800	-2.07686000
H	1.12416200	-2.15803000	-2.06531200
H	-0.17573900	-1.15236300	-2.75168500
H	-2.23283600	2.04560400	1.56600400
C	-1.28194200	-0.35828100	2.20728900
H	-0.76442200	-1.32661900	2.23248800
H	-2.30279000	-0.53263400	2.58700500
H	-0.77597900	0.32319300	2.90498600
C	1.97032400	0.00081700	0.34604600
H	1.32156100	1.58025600	-1.62426900
H	-2.28689500	3.17663700	-0.62010200
C	2.21504000	1.29772400	1.13265400
H	1.45367300	1.41878500	1.91803500
H	2.16013800	2.17929500	0.47816300
H	3.20883200	1.28135000	1.60640000
C	3.07159300	-0.15856400	-0.72090200
H	2.91902500	-1.06799700	-1.31934600
H	4.05255500	-0.24096300	-0.22733100
H	3.11941700	0.69913000	-1.40532800
C	2.10561000	-1.17698000	1.31908100
H	2.06524200	-2.14740300	0.80331500
H	1.32294900	-1.15643800	2.08938700
H	3.07834200	-1.11639100	1.82958900

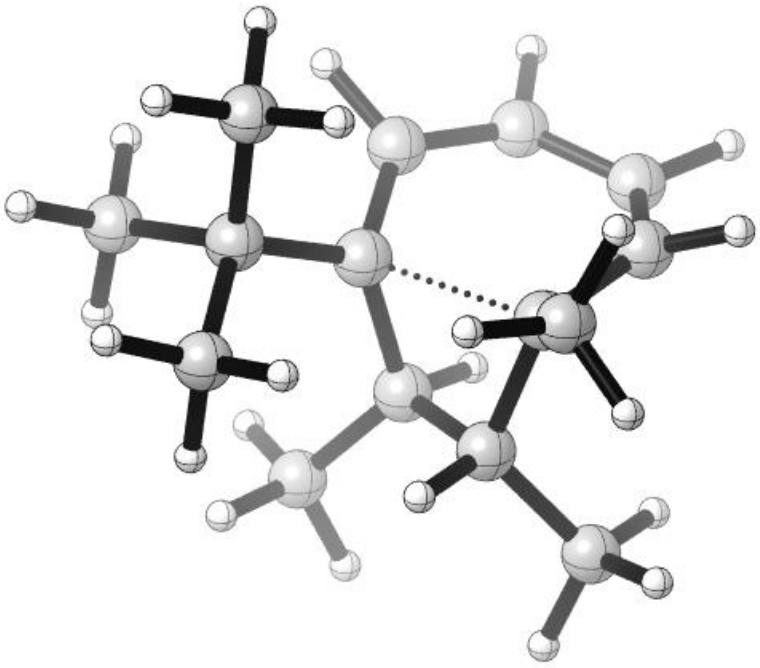

Butylmethyl_cyclooctatriene_6π2_TS
E(M062X/def2TZVP) = -585.889505 Hartree
Free energy correction (M062X/def2SVP) = 0.312875 Hartree
G = -1537431.442

C	-0.42049900	1.67064400	-0.85053700
C	2.00287800	1.90476100	-0.57895200
C	0.78155700	2.26271300	-1.19019100
H	0.76732300	3.20719400	-1.73977200
C	2.10621000	1.03772000	0.49890500
H	2.88921100	1.31099700	1.21992100
C	-0.52581100	0.35633400	-0.33067300
C	1.24894300	-0.02227400	0.90649600
C	1.11466600	-1.27921300	0.03225000
H	0.51444600	-2.00871900	0.59826400
C	0.28409700	-0.70941100	-1.09589700
H	0.97886400	-0.14285000	-1.73307900
C	-0.44175700	-1.67698100	-2.02687100
H	-0.98990300	-1.13144800	-2.80884500
H	-1.14897300	-2.33981700	-1.51196200
H	0.29923800	-2.31576600	-2.53139700
C	2.43758200	-1.92937300	-0.35583800
H	2.26871000	-2.85142100	-0.93268200
H	3.03117600	-2.19691200	0.53132100
H	3.03495700	-1.23778800	-0.96911400
C	1.28808200	-0.29998900	2.39663700
H	2.06884300	-1.04838900	2.62124800
H	0.34007400	-0.71653700	2.76002600
H	1.50009000	0.60721400	2.97798700
C	-1.87414500	0.02439300	0.35084700
H	-1.31355000	2.30136700	-0.90654400
H	2.84626400	2.57894300	-0.74997900

C	-3.01102200	0.08076800	-0.69010300
H	-3.06203500	1.06118900	-1.18345100
H	-3.97840300	-0.09868100	-0.19536400
H	-2.88238400	-0.68551000	-1.46657800
C	-2.14927300	1.07091400	1.44304100
H	-2.22770200	2.08597200	1.03046600
H	-1.33732900	1.07381700	2.18549400
H	-3.09498200	0.84229500	1.95811200
C	-1.93786400	-1.35412600	1.02632300
H	-1.22077800	-1.44233700	1.85083300
H	-1.76165200	-2.18267000	0.33045400
H	-2.94338000	-1.49142400	1.45202900

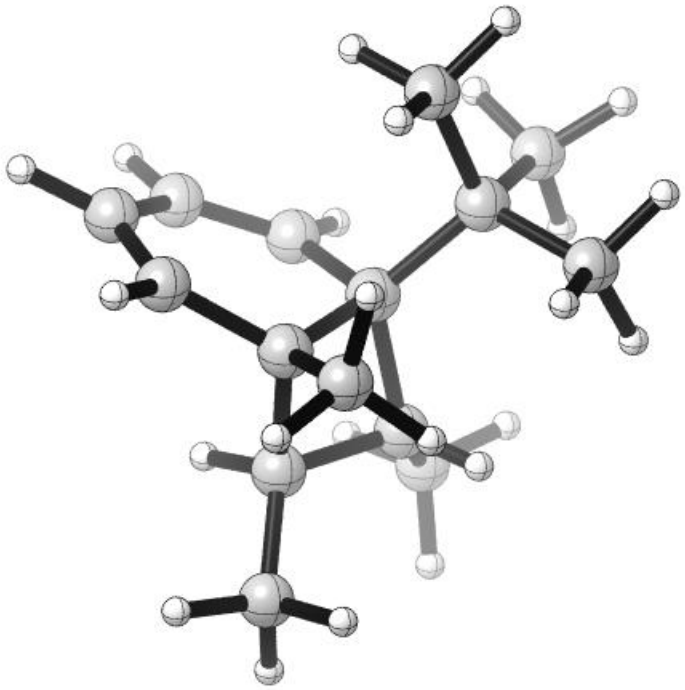

Butylmethyl_BOD1_GS
E(M062X/def2TZVP) = -585.931590 Hartree
Free energy correction (M062X/def2SVP) = 0.315346 Hartree
G = -1537535.449

H	-0.07248100	2.52185200	-2.54641600
C	-0.18472500	1.96958700	-1.61089900
C	-1.25479300	1.85970800	0.56648800
C	0.32265200	-0.08669500	-0.22041700
C	-0.89950300	0.40002600	0.67105400
C	0.37928100	0.76037600	-1.47853600
C	-0.93809900	2.58402600	-0.51500100
H	-1.79927600	2.31781600	1.39760100
C	-1.78311300	-0.57474600	-0.17908900
H	-2.10493900	-0.03627400	-1.08423800
C	-0.51053700	-1.37593700	-0.51488800
H	-0.33106400	-2.09944300	0.29631000
C	-0.44302600	-2.08906600	-1.85367100

H	-0.65840600	-1.39949500	-2.68327300
H	-1.18847200	-2.89809000	-1.88898600
H	0.54299400	-2.54357200	-2.03309900
C	-2.97507700	-1.28080500	0.43852500
H	-3.75207800	-0.56254100	0.74159200
H	-2.69386600	-1.87162200	1.32210400
H	-3.42990300	-1.96919400	-0.28988500
C	-0.91287400	-0.01582600	2.14240300
H	-0.76430400	-1.09366800	2.28194100
H	-1.89782800	0.23447200	2.56645200
H	-0.15520900	0.51822700	2.73209700
C	1.77157800	-0.21289700	0.36440500
H	0.94165400	0.34926900	-2.31954900
H	-1.22882300	3.63330900	-0.59281200
C	2.78027900	-0.53120100	-0.75638000
H	2.92574400	0.31726200	-1.43817200
H	2.46230100	-1.40274600	-1.34940900
H	3.75858200	-0.76762000	-0.31200200
C	2.17126900	1.12779600	0.99606100
H	2.05137900	1.94939600	0.27422300
H	3.22540200	1.10021000	1.31375800
H	1.55897900	1.36245900	1.87777600
C	1.92019900	-1.33306100	1.40401200
H	1.27470800	-1.19912000	2.27828500
H	2.95940700	-1.34778600	1.76646500
H	1.71443900	-2.32081100	0.96483000

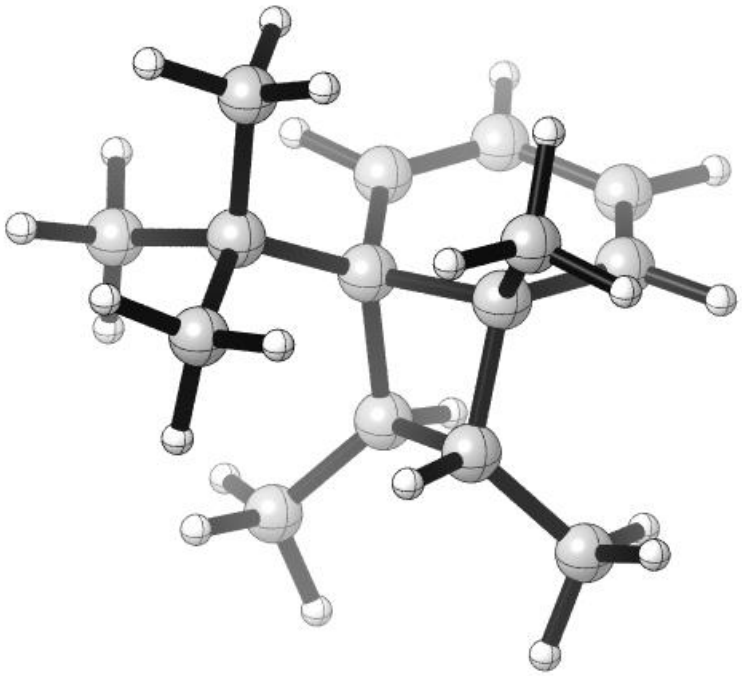

Butylmethyl_BOD2_GS
E(M062X/def2TZVP) = -585.922621 Hartree
Free energy correction (M062X/def2SVP) = 0.315716 Hartree
G = -1537510.929

C	-2.13323000	-1.83685900	-0.62246200
C	0.22331600	-1.48877300	-1.15108700
C	-0.91066400	-0.11020200	0.76455800
C	0.29938300	-0.25854600	-0.27431700
C	-2.13106500	-0.88500600	0.31848300
C	-0.90427800	-2.18940200	-1.33292500
H	-3.05062300	-0.67111600	0.87309500
H	-0.91595200	-3.04424000	-2.01176200
C	-0.32392800	1.00827000	-0.98022000
H	-1.10511000	0.60206900	-1.64385400
C	-1.03342500	1.38029300	0.33151300
H	-0.36815800	1.98454700	0.96659700
C	0.42662200	2.06271400	-1.77764600
H	0.84248400	1.64654600	-2.70686100
H	1.24318100	2.54046500	-1.22229900
H	-0.28092400	2.85523600	-2.06808700
C	-2.39583000	2.04556200	0.25071800
H	-3.06143200	1.50178900	-0.43617400
H	-2.30077000	3.07928700	-0.11417200
H	-2.88492300	2.08908200	1.23635600
C	-0.79024000	-0.38141000	2.26693100
H	-0.68154800	-1.45698800	2.46808300
H	-1.72196800	-0.04992700	2.75345400
H	0.03633500	0.14868300	2.75123800
C	1.76111300	-0.11706100	0.28964900
H	1.11854000	-1.80019900	-1.68990500
H	-3.05159900	-2.38169600	-0.84976000
C	2.78280900	-0.06732100	-0.86743000
H	2.89453200	-1.03428800	-1.37483200
H	3.77260300	0.19094600	-0.46210400
H	2.52392100	0.68740300	-1.62041000
C	2.10821300	-1.34923300	1.14276900
H	1.92290100	-2.28166700	0.58941800
H	1.52809500	-1.38731900	2.07273300
H	3.17494000	-1.32386700	1.41458200
C	2.02330400	1.14007200	1.13969100
H	1.37945200	1.21458900	2.02171300
H	1.91076400	2.06649700	0.56331500
H	3.06266700	1.10558200	1.50028300

Unsubstituted Cartesian Coordinates

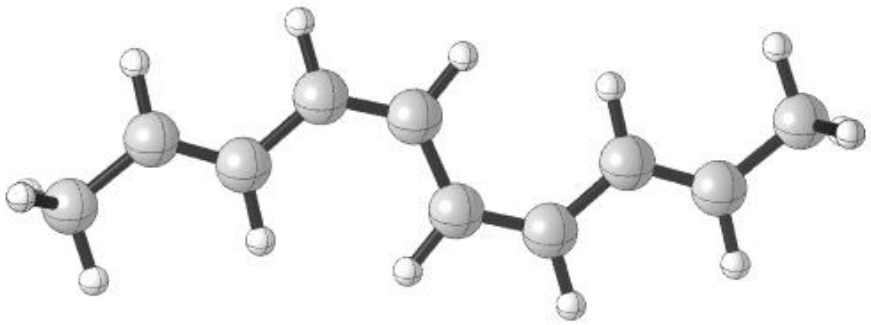

Unsubstituted_tetraene_GS
E(M062X/def2TZVP) = -389.381461 Hartree
Free energy correction (M062X/def2SVP) = 0.171130 Hartree
G = -1021871.724

C	-1.60281800	0.96845100	-0.00044200
C	-0.28419000	0.66831500	-0.00075900
H	0.41575500	1.50672000	-0.00115200
C	0.28418900	-0.66831400	-0.00075700
C	1.60281800	-0.96845000	-0.00044100
H	1.88425000	-2.02604200	-0.00063900
C	2.71301200	-0.02727500	0.00016700
C	-2.71301200	0.02727500	0.00017000
H	-2.48778100	-1.04377800	0.00075600
C	3.99938300	-0.41137500	0.00013300
H	4.21771500	-1.48608500	-0.00039000
C	-3.99938200	0.41137500	0.00013900
H	-4.21771600	1.48608500	-0.00038300
C	5.17250600	0.51527500	0.00071300
H	5.80893700	0.34857100	-0.88249300
H	5.80917200	0.34721000	0.88348400
H	4.85209300	1.56581000	0.00155100
C	-5.17250600	-0.51527500	0.00071000
H	-5.80923300	-0.34714600	0.88342500
H	-4.85209200	-1.56581100	0.00164300
H	-5.80887600	-0.34863600	-0.88255300
H	2.48778200	1.04377800	0.00074900
H	-0.41575500	-1.50671900	-0.00114600
H	-1.88425100	2.02604200	-0.00064400

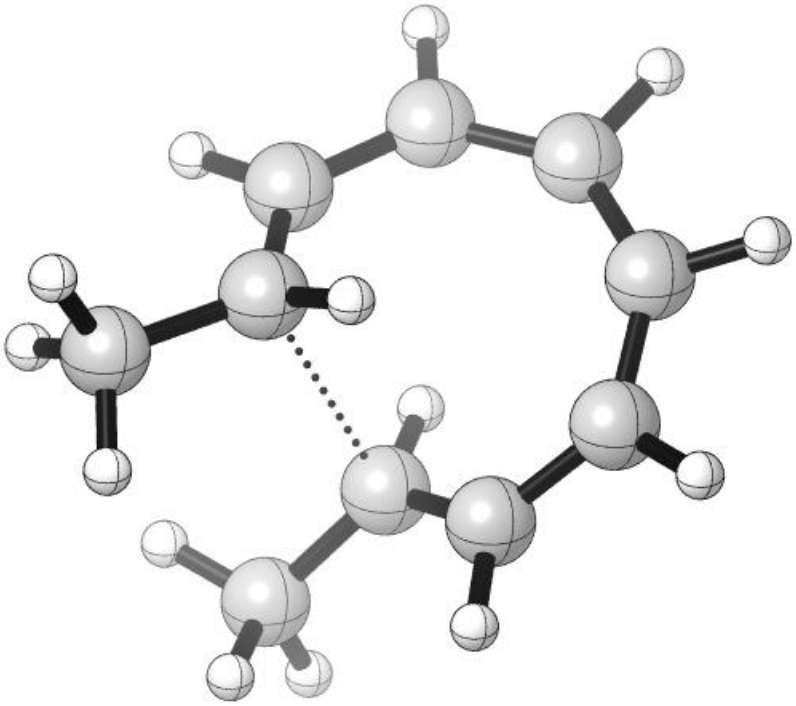

Unsubstituted_tetraene_8π_TS
E(M062X/def2TZVP) = -389.355890 Hartree
Free energy correction (M062X/def2SVP) = 0.177641 Hartree
G = -1021787.493

C	1.73471500	-0.10531300	1.28557600
C	0.70302700	-0.10091200	2.22267400
H	1.07387100	-0.26831900	3.23960900
C	-0.70302700	0.10091200	2.22267400
C	-1.73471500	0.10531300	1.28557600
H	-2.69712400	0.43858300	1.68467500
C	-1.74756700	-0.26270000	-0.07141400
C	1.74756700	0.26270000	-0.07141400
H	2.63093500	-0.02024400	-0.65488900
C	-0.70302700	-0.88923400	-0.72650100
H	0.01638500	-1.41453400	-0.09897400
C	0.70302700	0.88923400	-0.72650100
H	-0.01638500	1.41453400	-0.09897400
C	-0.81246500	-1.35826600	-2.14656200
H	-1.17617300	-2.39813200	-2.17666600
H	0.16261100	-1.34404800	-2.65386200
H	-1.51534200	-0.73956900	-2.72252400
C	0.81246500	1.35826600	-2.14656200
H	1.17617300	2.39813200	-2.17666600
H	-0.16261100	1.34404800	-2.65386200
H	1.51534200	0.73956900	-2.72252400
H	-1.07387100	0.26831900	3.23960900
H	2.69712400	-0.43858300	1.68467500
H	-2.63093500	0.02024400	-0.65488900

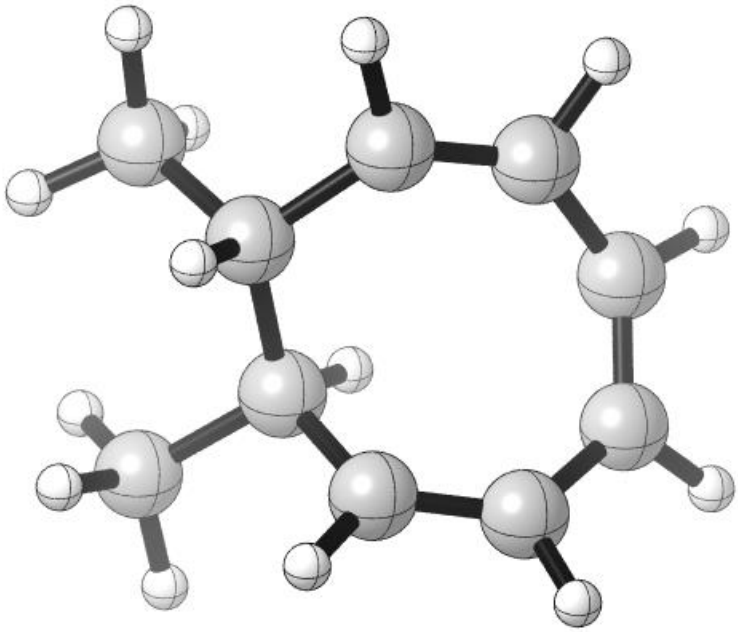

Unsubstituted_cyclooctatriene_GS
E(M062X/def2TZVP) = -389.392880 Hartree
Free energy correction (M062X/def2SVP) = 0.179996 Hartree
G = -1021878.428

C	-1.13355000	1.70603300	-0.09800100
C	-2.31054700	-0.48636700	0.44952400
C	-2.02809700	0.81419900	0.65752400
H	-2.65469800	1.33720400	1.38778000
C	-1.64093600	-1.36148400	-0.51179200
H	-2.27964000	-2.00284100	-1.12747400
C	0.10844900	1.59223400	-0.60042700
H	0.45925700	2.47722200	-1.14451500
C	-0.31139000	-1.44536000	-0.65535600
C	0.71188700	-0.75583200	0.20570700
H	0.23562100	-0.48473100	1.16267200
C	1.18930500	0.55178800	-0.44850400
H	1.54843100	0.30199000	-1.46429100
C	2.36298100	1.19548900	0.30402300
H	2.61751000	2.17137100	-0.13385800
H	3.26369700	0.56832500	0.26731500
H	2.09392600	1.36065200	1.35894100
C	1.86779700	-1.72021800	0.48568600
H	2.55401400	-1.32787200	1.24777400
H	2.44773400	-1.90843000	-0.43279100
H	1.48318500	-2.68505900	0.84510400
H	-3.14776700	-0.91452200	1.01012200
H	-1.60361100	2.67981700	-0.28083100
H	0.08695500	-2.11602100	-1.42625300

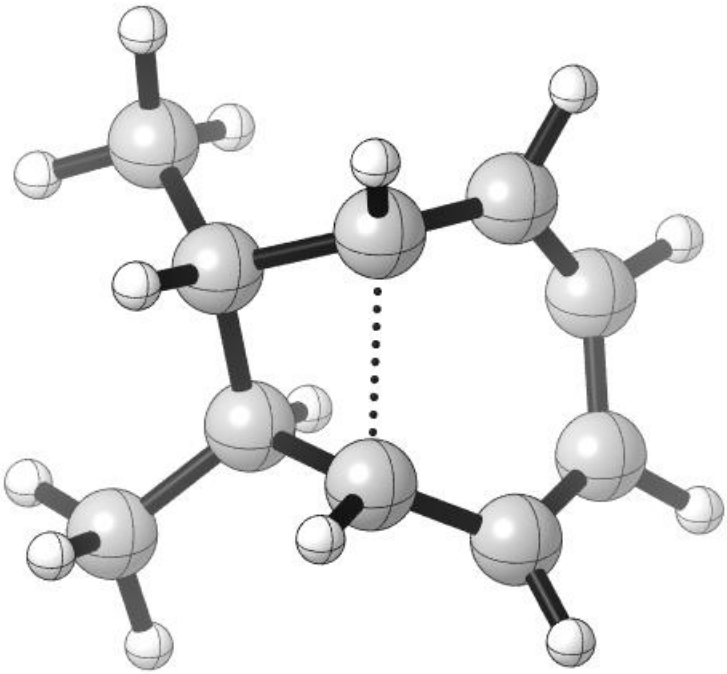

Unsubstituted_cyclooctatriene_ 6π_TS
E(M062X/def2TZVP) = -389.353564 Hartree
Free energy correction (M062X/def2SVP) = 0.178721 Hartree
G = -1021778.55

C	-1.10018000	-1.53074300	0.19546200
C	-2.20273900	0.54356700	-0.58930000
C	-1.91418400	-0.83056000	-0.69801100
H	-2.62085500	-1.42409000	-1.28434700
C	-1.56386900	1.35613000	0.34052300
H	-2.14104600	2.14802900	0.82752700
C	-0.01638000	-1.06393800	0.96843600
H	0.11271800	-1.62861000	1.90324500
C	-0.26140100	1.06983400	0.76606400
C	0.83291200	0.73349300	-0.23802500
H	0.35482500	0.51535000	-1.20628600
C	1.30406100	-0.56457100	0.38013300
H	1.95825700	-0.31144700	1.23262700
C	2.01794200	-1.56118100	-0.52175600
H	2.24339700	-2.49534700	0.01409100
H	2.96780700	-1.14636800	-0.89232300
H	1.38349100	-1.80991700	-1.38602800
C	1.87363900	1.82857100	-0.41780800
H	2.66378000	1.50923100	-1.11415500
H	2.34896500	2.07529700	0.54457700
H	1.41900600	2.74589400	-0.81893300
H	-1.47802600	-2.52908700	0.45063900
H	-3.13260000	0.88502100	-1.05139600
H	0.10147900	1.58243800	1.66646700

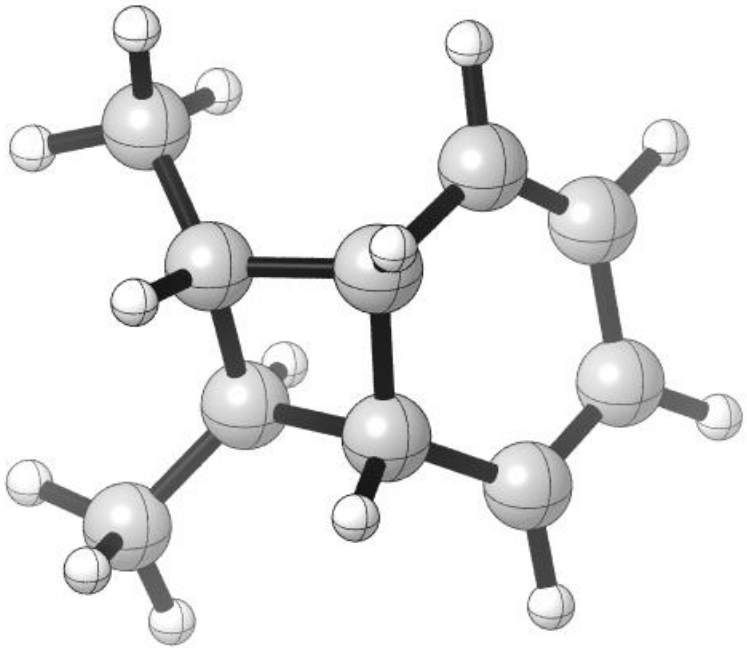

Unsubstituted_BOD_ GS
E(M062X/def2TZVP) = -389.396602 Hartree
Free energy correction (M062X/def2SVP) = 0.180521 Hartree
G = -1021886.821

C	2.34701000	-0.63981300	-0.43128100
C	1.12878800	1.41579000	0.15399800
C	0.16626400	-0.87619600	0.68760700
C	0.11812300	0.65360500	0.96264400
C	1.44514300	-1.44288900	0.15113100
C	2.14193000	0.81592400	-0.48937900
H	1.61631700	-2.52044400	0.21113000
H	0.18437300	0.97065100	2.01703900
H	2.86588600	1.41717000	-1.04324900
C	-1.32510700	0.66003100	0.37922900
H	-2.03418600	0.48020000	1.20470400
C	-1.01037600	-0.68790100	-0.30951500
H	-0.58740900	-0.48447300	-1.30796100
C	-1.79941100	1.81992000	-0.47378500
H	-1.88174500	2.74790500	0.11209400
H	-2.78997100	1.60663700	-0.90299300
H	-1.10085200	2.00325900	-1.30420600
C	-2.09067500	-1.74664500	-0.39398800
H	-2.50089100	-1.96377100	0.60456600
H	-1.69917600	-2.68596600	-0.81208400
H	-2.92114400	-1.41579300	-1.03618600
H	3.26300100	-1.05133500	-0.85960000
H	-0.18562300	-1.44121400	1.56453500
H	1.04129200	2.50621700	0.13224500

Structure	Number of imaginary frequencies	Free energy correction (Hartree)	Electronic energy (Hartree)	Relative Gibbs free energy (kJ/mol)
Bismethylenehydroxy_tetraene_GS	0	0.179757	-539.822768	0.000
Bismethylenehydroxy_tetraene_8π_TS	1	0.18568	-539.798679	78.797
Bismethylenehydroxy_cyclooctatriene_GS	0	0.189285	-539.843443	-29.266
Bismethylenehydroxy_cyclooctatriene_6π_TS	1	0.186188	-539.798051	81.779
Bismethylenehydroxy_BOD_GS	0	0.190221	-539.847676	-37.923

Table S2: Calculated relative free energies of bis-methylene alcohol compound

Bis-methylene alcohol compound Cartesian Coordinates

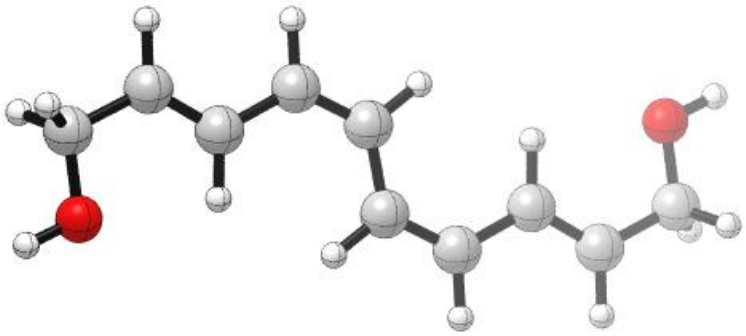

Bismethylenehydroxy_tetraene_GS
E(M062X/def2TZVP) = -539.822768 Hartree
Free energy correction (M062X/def2SVP) = 0.179757 Hartree
G = -1416832.725

C	2.19697100	-1.02444800	-0.63576500
C	2.71007400	-1.02406300	0.72294400
H	2.00370700	-1.25861800	1.52221500
C	3.98509300	-0.75972400	1.08800900
C	0.92072800	-1.28325400	-1.00035900
H	0.67776500	-1.24840800	-2.06664800
C	-0.18969100	-1.60874000	-0.11747900
C	5.09217200	-0.42311200	0.20547000
H	4.90296900	-0.37287200	-0.87139800
C	6.33560800	-0.17668800	0.64806200
C	-1.43104300	-1.86015600	-0.56341200
C	7.49796700	0.19381100	-0.21755900
H	7.21210300	0.11550100	-1.27999700
H	-0.00416000	-1.65378200	0.96033600
H	2.90459500	-0.79600800	-1.43564800
H	4.22866300	-0.79759400	2.15410400
H	-1.62847300	-1.80876400	-1.64081900
H	6.52351400	-0.22577000	1.72809400
H	8.33856200	-0.50073200	-0.05410000
C	-2.60480700	-2.18649700	0.31179700

H	-2.27384900	-2.22506700	1.36226200
H	-2.98815300	-3.18842400	0.06075400
C	-3.73712100	-1.18767400	0.16502100
C	-5.80989400	0.63092100	-0.09537100
C	-3.47033000	0.18390300	0.36842400
C	-5.02530700	-1.60597400	-0.16470300
C	-6.09458400	-0.70070700	-0.29930900
C	-4.52228500	1.06146000	0.23302500
H	-2.46867500	0.53650600	0.61758600
H	-5.21221100	-2.66965800	-0.32313300
H	-7.10142600	-1.03018600	-0.55224300
O	-6.64285800	1.70942300	-0.13175600
O	-4.53910600	2.41298300	0.40526900
C	-5.80229000	2.84709200	-0.06516100
H	-5.69048800	3.28440800	-1.07449600
H	-6.22559400	3.58054400	0.63282200
C	8.01353000	1.60669200	0.06657300
H	8.27448900	1.69428600	1.13206000
H	7.20440900	2.33620100	-0.12527200
O	9.17809100	1.90807400	-0.65522400
H	8.96448700	1.88753500	-1.59404100

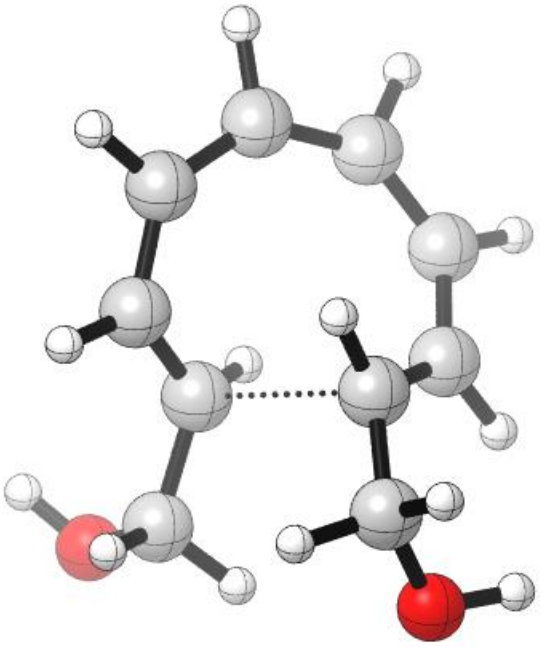

Bismethylenehydroxy_tetraene_8π_TS
E(M062X/def2TZVP) = -539.798679 Hartree
Free energy correction (M062X/def2SVP) = 0.185680 Hartree
G = -1416753.929

C	1.94610000	1.27222500	0.96940200
C	2.75992000	0.37948000	0.27902800
H	3.82228500	0.55661500	0.47797600
C	2.58986200	-0.68485300	-0.65020500
H	3.54064500	-0.93793300	-1.13116400

C	1.55276600	-1.50270300	-1.08589900
H	1.81130000	-2.13256700	-1.94195100
C	0.23744800	-1.65926400	-0.60750600
H	-0.46797600	-2.17201700	-1.26888800
C	0.56464300	1.52633100	0.86554000
H	0.10710500	2.11253400	1.67171000
C	-0.23527400	-1.12655200	0.57387500
H	0.50213400	-0.85923400	1.33145200
C	-0.26042800	1.02104000	-0.12082600
H	0.20392000	0.71120900	-1.05690300
C	-1.61686500	-1.42435500	1.09897600
H	-1.53275900	-2.21741900	1.86784500
H	-2.01360500	-0.54150500	1.62199000
C	-1.70562900	1.42803200	-0.23621900
H	-2.31523400	0.57191100	-0.55862600
H	-2.07663000	1.74752400	0.75781200
H	2.47684600	1.88067800	1.70737900
O	-2.54987900	-1.76228300	0.10953400
H	-2.32894600	-2.63107200	-0.24199500
O	-1.87924100	2.43374700	-1.20622200
H	-1.29137400	3.16327600	-0.98012100

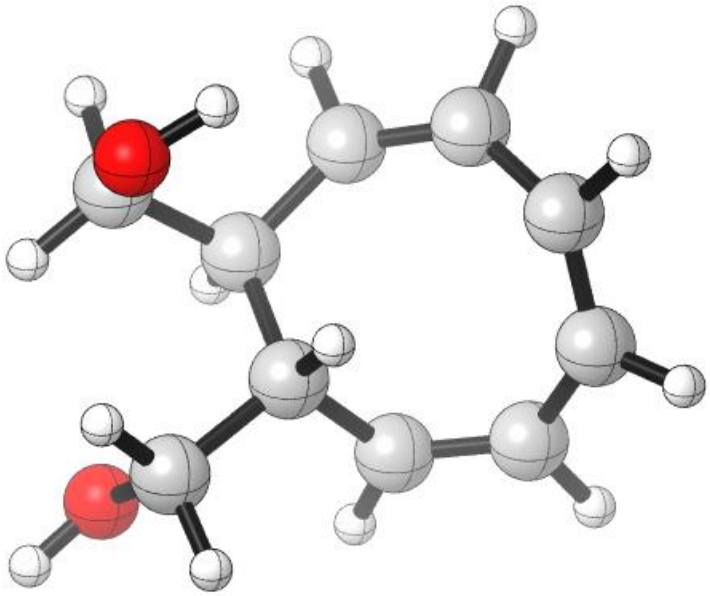

Bismethylenehydroxy_cyclooctatriene_GS
E(M062X/def2TZVP) = -539.843443 Hartree
Free energy correction (M062X/def2SVP) = 0.189285 Hartree
G = -1416861.992

C	1.83430700	-1.71798400	-0.21388900
C	2.54710200	0.58132300	0.50073500
C	2.62727700	-0.76263400	0.55911200
H	3.39310500	-1.18443600	1.21833400
C	1.80411500	1.43909600	-0.43724400
H	2.41471000	2.28910200	-0.76527000

C	0.50754100	-1.63595700	-0.38336300
H	-0.00439900	-2.38938500	-0.99142100
C	0.57572600	1.40080500	-0.98829900
C	-0.64389000	0.55957000	-0.71807800
C	-0.38348200	-0.60660300	0.25033400
H	3.24903800	1.13455700	1.13337600
H	2.36952300	-2.57219700	-0.64037800
H	0.37577500	2.20790300	-1.70377800
H	-1.00284400	0.14184800	-1.67340800
H	0.11030200	-0.19558700	1.14418500
C	-1.75311200	1.49139300	-0.20815800
H	-1.87967300	2.32907900	-0.92074300
H	-2.70544600	0.94511600	-0.17938500
C	-1.68581600	-1.25111400	0.71331800
H	-1.44437200	-2.13582300	1.33033500
H	-2.23345200	-0.53466900	1.35035900
O	-2.43063200	-1.61082000	-0.42959600
H	-3.22881400	-2.07005800	-0.15166000
O	-1.49392800	1.95307600	1.09248900
H	-0.59558200	2.30912500	1.09949100

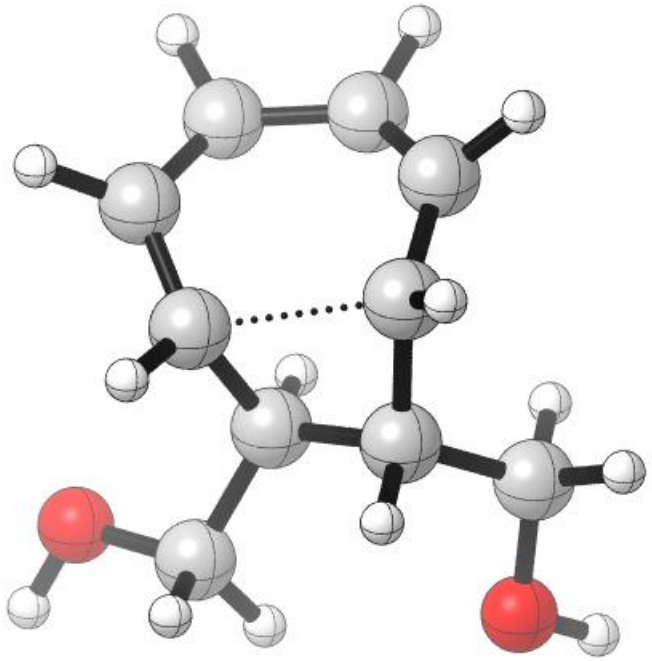

Bismethylenehydroxy_cyclooctatriene_6π_TS
E(M062X/def2TZVP) = -539.798051 Hartree
Free energy correction (M062X/def2SVP) = 0.186188 Hartree
G = -1416750.946

C	1.98869400	1.21038300	0.28182600
C	2.24066700	-0.93245300	-0.87271000
C	2.50570000	0.44611300	-0.75646200
H	3.35034700	0.82978800	-1.33428100
H	2.87325900	-1.48500800	-1.57274500
C	1.58021000	-1.68405400	0.10171500

C	0.76551400	0.88406000	0.87726300
H	0.52567900	1.36402100	1.83449200
C	0.60166000	-1.26538800	1.02872200
H	0.60567400	-1.85803400	1.95433900
C	-0.78955300	-0.79153400	0.61826300
H	-1.38299500	-0.63523100	1.53556700
C	-0.45206100	0.55657800	0.02535500
H	-0.12981400	0.44278500	-1.02228800
C	-1.54247700	1.60765700	0.08227100
H	-1.87727400	1.71290600	1.13452800
H	-2.40521400	1.24463400	-0.50283100
C	-1.54028600	-1.77337000	-0.25969900
H	-0.97003600	-1.90779000	-1.19878100
H	-1.58442700	-2.75788800	0.24557600
H	2.60682100	2.00761700	0.70478200
H	2.01755200	-2.67592200	0.27378300
O	-1.02049600	2.81516100	-0.41531800
H	-1.71327600	3.48179200	-0.39301600
O	-2.82680500	-1.25130300	-0.49699200
H	-3.28630000	-1.82249800	-1.11990400

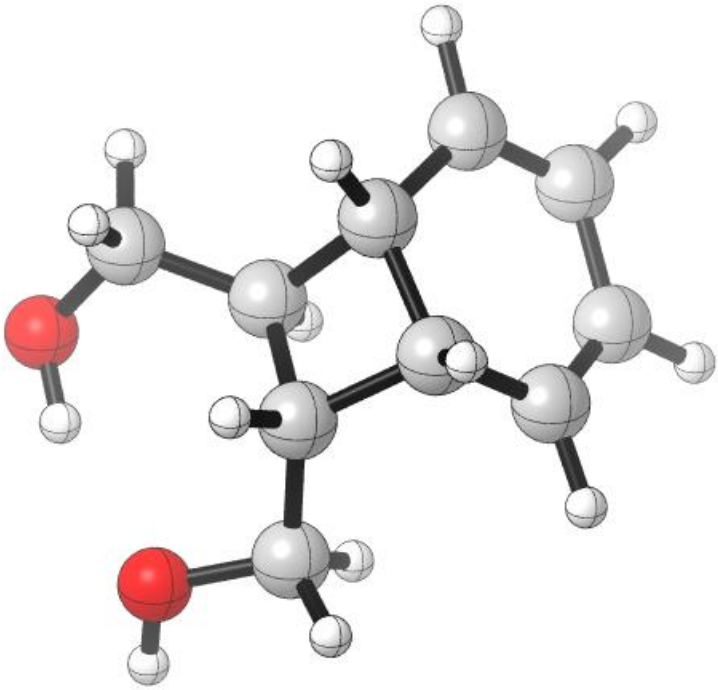

Bismethylenehydroxy_BOD_GS
E(M062X/def2TZVP) = -539.847676 Hartree
Free energy correction (M062X/def2SVP) = 0.190221 Hartree
G = -1416870.648

C	-2.59202200	0.86392700	-0.73691700
C	-2.08304400	-1.40122000	0.04139600
C	-0.84230700	0.67154600	1.03358000
C	-0.89259600	-0.86311900	0.77429600
C	-1.68056300	1.44775600	0.05561500

C	-2.85054900	-0.58341200	-0.69271100
H	-1.56216200	2.53565400	0.03672100
H	-0.71040700	-1.41959700	1.70665100
H	-3.69664100	-0.97564800	-1.25992100
C	0.43501100	-0.72959800	-0.01665900
C	0.67133500	0.62149800	0.69720900
H	-3.19622200	1.47546900	-1.41019400
H	-1.07000400	1.00994400	2.05802000
H	-2.29587000	-2.47176500	0.08859700
H	1.25271200	0.45553900	1.61992800
H	0.21435700	-0.55141100	-1.08292800
C	1.31674600	1.73872700	-0.08493200
H	0.76818700	1.88803200	-1.03264800
H	1.27247500	2.68435900	0.48639700
C	1.49687100	-1.80353200	0.10113700
H	1.10039100	-2.75963100	-0.27776500
H	1.72560400	-1.95551200	1.17755000
O	2.64172400	-1.49647600	-0.64041500
H	2.84625300	-0.55905400	-0.49567400
O	2.65951000	1.35843700	-0.32278700
H	3.06816100	1.97250300	-0.94120300

Structure	Number of imaginary frequencies	Free energy correction (Hartree)	Electronic energy (Hartree)	Relative Gibbs free energy (kJ/mol)
Lu_tetraene_GS	0	0.288672	-923.494936	0.000
Lu_tetraene_8π_TS	1	0.294358	-923.469307	82.217
Lu_cyclooctatriene_GS	0	0.299704	-923.505899	4.954
Lu_cyclooctatriene_6π1_TS	1	0.297496	-923.468721	92.055
Lu_cyclooctatriene_6π2_TS	1	0.298058	-923.469157	91.034
Lu_BOD1_GS	0	0.301723	-923.516819	-22.464
Lu_BOD2_GS	0	0.299578	-923.514398	-17.517

Table S3: Calculated relative free energies of Lu compound

Lu compound Cartesian Coordinates

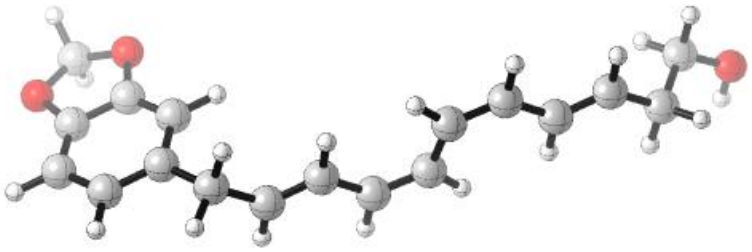

Lu_tetraene_GS
E(M062X/def2TZVP) = -923.494936 Hartree
Free energy correction (M062X/def2SVP) = 0.288672 Hartree
G = -2423878.046

C	2.19697100	-1.02444800	-0.63576500
C	2.71007400	-1.02406300	0.72294400
H	2.00370700	-1.25861800	1.52221500
C	3.98509300	-0.75972400	1.08800900
C	0.92072800	-1.28325400	-1.00035900
H	0.67776500	-1.24840800	-2.06664800
C	-0.18969100	-1.60874000	-0.11747900
C	5.09217200	-0.42311200	0.20547000
H	4.90296900	-0.37287200	-0.87139800
C	6.33560800	-0.17668800	0.64806200
C	-1.43104300	-1.86015600	-0.56341200
C	7.49796700	0.19381100	-0.21755900
H	7.21210300	0.11550100	-1.27999700
H	-0.00416000	-1.65378200	0.96033600
H	2.90459500	-0.79600800	-1.43564800
H	4.22866300	-0.79759400	2.15410400
H	-1.62847300	-1.80876400	-1.64081900
H	6.52351400	-0.22577000	1.72809400
H	8.33856200	-0.50073200	-0.05410000
C	-2.60480700	-2.18649700	0.31179700

H	-2.27384900	-2.22506700	1.36226200
H	-2.98815300	-3.18842400	0.06075400
C	-3.73712100	-1.18767400	0.16502100
C	-5.80989400	0.63092100	-0.09537100
C	-3.47033000	0.18390300	0.36842400
C	-5.02530700	-1.60597400	-0.16470300
C	-6.09458400	-0.70070700	-0.29930900
C	-4.52228500	1.06146000	0.23302500
H	-2.46867500	0.53650600	0.61758600
H	-5.21221100	-2.66965800	-0.32313300
H	-7.10142600	-1.03018600	-0.55224300
O	-6.64285800	1.70942300	-0.13175600
O	-4.53910600	2.41298300	0.40526900
C	-5.80229000	2.84709200	-0.06516100
H	-5.69048800	3.28440800	-1.07449600
H	-6.22559400	3.58054400	0.63282200
C	8.01353000	1.60669200	0.06657300
H	8.27448900	1.69428600	1.13206000
H	7.20440900	2.33620100	-0.12527200
O	9.17809100	1.90807400	-0.65522400
H	8.96448700	1.88753500	-1.59404100

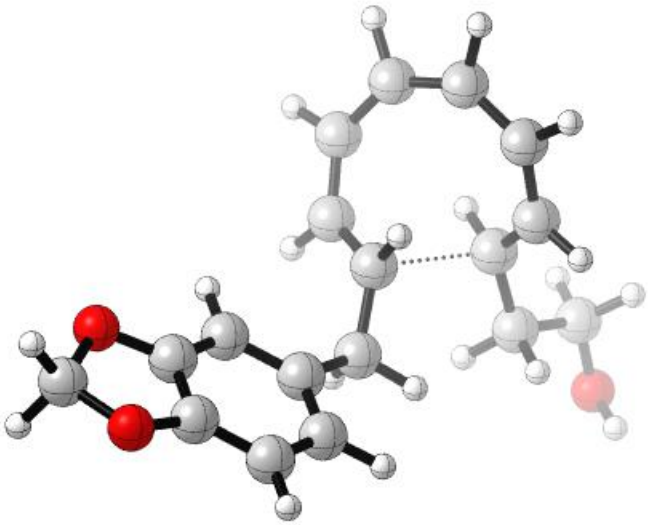

Lu_tetraene_8π_TS
E(M062X/def2TZVP) = -923.469307 Hartree
Free energy correction (M062X/def2SVP) = 0.294358 Hartree
G = -2423795.829

C	2.58080000	2.88945100	1.12292700
C	2.15373700	3.20125200	-0.19520300
H	2.29893700	4.26499900	-0.41162400
C	1.56996700	2.52803700	-1.26619600
C	2.88017300	1.74281200	1.85563800
H	3.06204000	1.92864900	2.91801800
C	3.00465300	0.40068200	1.45586000
C	1.02805400	1.23354800	-1.35656400

H	0.81354700	0.85510300	-2.36275400
C	2.99920600	-0.03720100	0.14370200
C	0.81820700	0.38508200	-0.28390800
H	1.51329300	3.11844400	-2.18521800
H	2.74618600	3.80160200	1.70607700
H	3.04604800	-0.35177400	2.25204000
C	3.26809100	-1.46875100	-0.21548800
H	2.76781100	-1.73996800	-1.15794500
H	2.87097900	-2.13448000	0.57087300
C	4.76442900	-1.74544200	-0.39104700
H	5.29186400	-1.51860500	0.55442100
H	5.17345400	-1.06676900	-1.15393200
O	5.01721100	-3.05085600	-0.83809000
H	4.72590100	-3.66539300	-0.15633000
H	3.25457600	0.70098800	-0.61699400
H	0.74401100	0.84315200	0.70268800
C	0.11933500	-0.93836300	-0.44405000
H	0.58432600	-1.69322300	0.20681400
H	0.24431800	-1.29079000	-1.48184100
C	-1.35821900	-0.86538000	-0.10070000
C	-4.05895300	-0.79181600	0.51738500
C	-2.17323900	0.10857300	-0.71772200
C	-1.91543100	-1.76163000	0.81109100
C	-3.28304700	-1.74278400	1.14155200
C	-3.51117900	0.11402900	-0.39358700
H	-1.76133800	0.83896100	-1.41478700
H	-1.27088300	-2.50631000	1.28167200
H	-3.71313100	-2.44012400	1.85919000
O	-4.49248800	0.95685400	-0.82206000
O	-5.38667400	-0.52243000	0.66781400
C	-5.70873300	0.40103900	-0.35622400
H	-6.21510700	-0.12729300	-1.18515700
H	-6.34832800	1.19546100	0.04868700

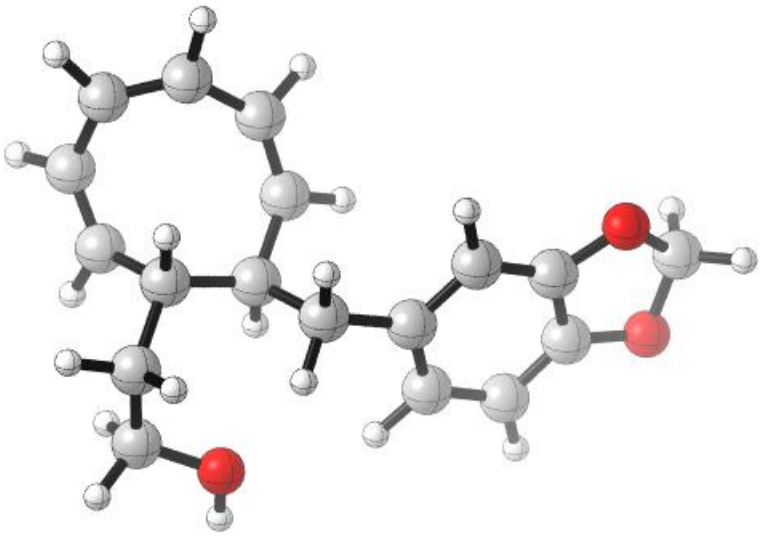

Lu_cyclooctatriene_GS

E(M062X/def2TZVP) = -923.505899 Hartree
Free energy correction (M062X/def2SVP) = 0.299704 Hartree
G = -2423877.865

C	2.75960700	-2.92114600	0.21731200
C	4.00391100	-2.46831400	-0.02906900
H	4.84401000	-3.05359700	0.35825400
C	4.32286700	-1.29597900	-0.84324100
C	0.92744600	-1.26682200	-0.57839200
C	1.48766700	-2.47153400	-0.37104800
H	0.87878300	-3.31923400	-0.70872800
C	3.72005200	-0.10527100	-0.71995200
H	4.01688900	0.68810800	-1.41444800
C	2.74090600	0.27173900	0.36234400
C	1.28311000	0.11919600	-0.10337900
C	0.28076000	0.51951300	1.00833700
H	0.42225500	-0.15922800	1.86493600
H	5.11746100	-1.40987100	-1.58787200
H	2.67958200	-3.84335000	0.80303900
H	-0.04590100	-1.29850400	-1.07938000
C	3.09490800	1.67272600	0.90351300
H	4.16663700	1.66298900	1.15796300
C	2.85589100	2.85427800	-0.02473400
H	3.26838500	2.64376700	-1.02932200
H	3.40755400	3.72516200	0.37282000
O	1.47477700	3.14263900	-0.10095600
H	1.35087100	3.91078500	-0.66755400
C	-1.15908100	0.49041900	0.55613800
C	-3.76461100	0.47768500	-0.38636100
C	-1.63365900	1.51154300	-0.27225400
C	-2.01230400	-0.56862200	0.92633100
C	-3.30288100	-0.54590900	0.43975100
C	-2.95093900	1.52682400	-0.75981600
H	-0.94534500	2.31697800	-0.53713100
H	-1.66750000	-1.37836000	1.57009500
H	-3.32370900	2.32809000	-1.39680500
O	-4.32390700	-1.42074600	0.67355200
O	-5.08112200	0.25617600	-0.67517600
C	-5.34604700	-1.06323900	-0.23834200
H	-5.32476300	-1.75147400	-1.10444100
H	-6.32077500	-1.09927800	0.26431800
H	1.11414400	0.81599300	-0.94222700
H	2.56087800	1.86987600	1.84545000
H	2.88219400	-0.43650700	1.19556800
H	0.51474600	1.54059900	1.33327700

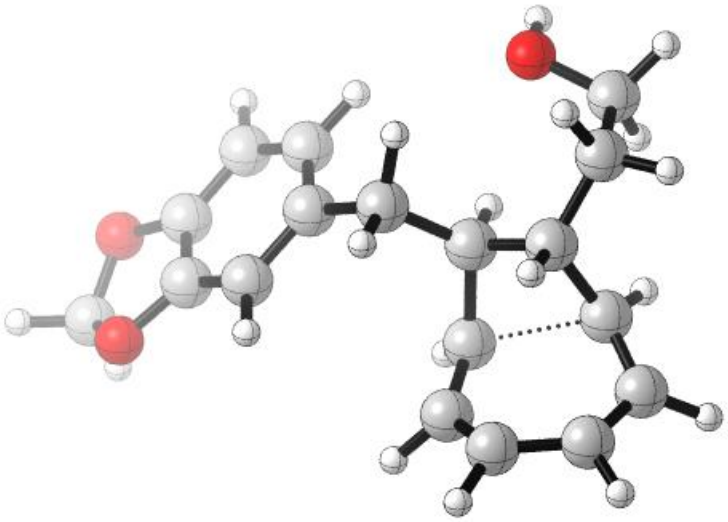

Lu_cyclooctatriene_6π1_TS
E(M062X/def2TZVP) = -923.468721 Hartree
Free energy correction (M062X/def2SVP) = 0.297496 Hartree
G = -2423786.051

C	2.36498000	-2.90278400	0.47310800
C	3.69271100	-2.64239400	0.08225500
H	4.42532700	-3.42640000	0.29030000
C	4.00860600	-1.63759200	-0.82547700
C	1.12628500	-1.04791500	-0.73906100
C	1.24635800	-2.30737200	-0.11493100
H	0.40482100	-2.99633200	-0.26525800
C	3.20590500	-0.49585600	-0.93938500
H	3.34669700	0.13249400	-1.82839800
C	2.74381000	0.25699500	0.30154700
C	1.26821100	0.29262900	-0.02067100
C	0.30175300	0.53365200	1.14032300
H	0.46067900	-0.24602500	1.90224000
H	4.82012300	-1.81392000	-1.53812900
H	2.19672000	-3.84463000	1.00222900
H	0.35684900	-1.03541600	-1.52392700
C	3.47453400	1.57668900	0.57078300
H	4.55829600	1.39537800	0.48926800
C	3.09273600	2.73406400	-0.33495600
H	3.07107600	2.40305600	-1.39184100
H	3.86019100	3.52490000	-0.25868100
O	1.83125300	3.22544900	0.07043000
H	1.58115200	3.95401700	-0.50663100
C	-1.13877000	0.54404000	0.69426800
C	-3.73778900	0.59009800	-0.26614500
C	-1.66622000	1.68773700	0.08804600
C	-1.93380600	-0.61296500	0.82316200
C	-3.22251300	-0.55771600	0.33434700
C	-2.98194300	1.73564800	-0.40195300
H	-1.02403700	2.56682500	-0.00170600

H	-1.54795100	-1.51729300	1.29497400
H	-3.39666500	2.63168200	-0.86220900
O	-4.19532900	-1.51401100	0.36877700
O	-5.04031200	0.36511100	-0.61056400
C	-5.23447100	-1.02831500	-0.46111700
H	-5.17541300	-1.51892700	-1.45107500
H	-6.20627200	-1.21934400	0.01126100
H	1.09290400	1.07756500	-0.77284300
H	3.28704200	1.90328000	1.60634400
H	2.90242700	-0.40363800	1.16760800
H	0.55886700	1.50846900	1.58247500

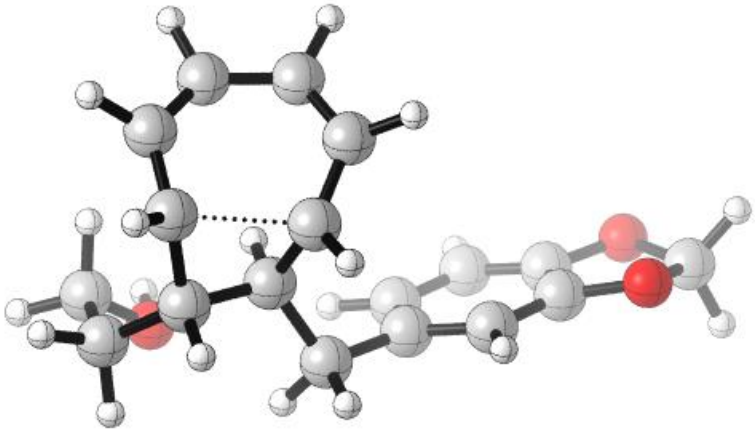

Lu_cyclooctatriene_6π2_TS
E(M062X/def2TZVP) = -923.469157 Hartree
Free energy correction (M062X/def2SVP) = 0.298058 Hartree
G = -2423785.72

C	2.55466700	1.89509900	1.57782000
C	1.21432300	2.25712100	1.33845900
H	0.70204400	2.79664700	2.13886100
C	0.67629700	2.26422000	0.05884300
C	3.30446300	1.21009300	-0.75326300
C	3.49683100	1.65381600	0.57621400
H	4.49635000	2.04510300	0.80678500
C	1.16952700	1.40193100	-0.92932600
H	0.89493000	1.61727400	-1.97076500
C	1.39013900	-0.07366300	-0.63995100
C	2.80294600	-0.17442300	-1.16604400
C	0.35595100	-1.02207100	-1.24648600
H	0.71771300	-2.04847100	-1.08171500
H	2.74677500	-0.16264500	-2.26821700
H	-0.05761100	3.03329300	-0.19956600
H	2.94857100	2.14122500	2.56781200
H	4.07218800	1.60261500	-1.43716200
H	1.39363100	-0.21857700	0.44961700
H	0.29734000	-0.85375900	-2.33448200
C	3.68758500	-1.35944300	-0.76206400

H	4.73692600	-1.10862200	-0.98865000
H	3.43511100	-2.23827600	-1.37792800
C	3.58100900	-1.78172500	0.69210300
H	3.65245000	-0.89429600	1.34676400
H	4.42653600	-2.44908900	0.93910900
O	2.35021400	-2.45524200	0.87475800
H	2.23401400	-2.63610800	1.81278400
C	-1.00505600	-0.85556800	-0.61805000
C	-3.43745200	-0.49091000	0.65700300
C	-1.25621700	-1.41895800	0.63597200
C	-1.99726700	-0.08139200	-1.25170600
C	-3.19860000	0.07797300	-0.59250400
C	-2.48062500	-1.24693400	1.30151600
H	-0.46491500	-2.01017800	1.10217300
H	-1.82828600	0.37659900	-2.22687800
H	-2.67527000	-1.68571100	2.27939200
O	-4.29829700	0.79206500	-0.97171600
O	-4.68977500	-0.13815200	1.07420800
C	-5.31819700	0.42887000	-0.05930800
H	-5.88485800	1.32052000	0.23722600
H	-5.98271500	-0.32113800	-0.52851700

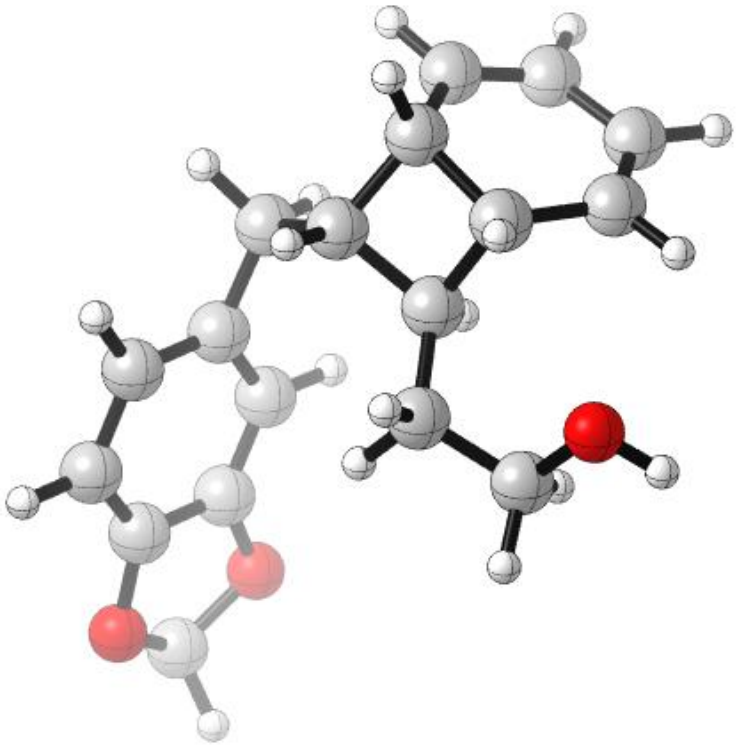

Lu_BOD1_GS
E(M062X/def2TZVP) = -923.516819 Hartree
Free energy correction (M062X/def2SVP) = 0.301723 Hartree
G = -2423901.235

H	4.88009300	0.25716500	2.28548300
C	4.24009300	-0.08454200	1.46963200

C	3.17454900	-2.03120700	0.40599300
C	2.92292100	0.30830400	-0.57818300
C	2.77334700	-1.22434000	-0.79598400
C	3.84333600	0.76443000	0.51101800
C	3.84113600	-1.50047100	1.44229200
H	3.14143600	0.83342700	-1.51875200
H	4.13639500	1.81544200	0.51946500
H	4.13388900	-2.13578500	2.28107500
H	2.93997500	-3.10007800	0.40111100
H	3.26324300	-1.64213500	-1.69128000
C	1.24192600	-0.99975500	-0.96112300
C	1.39618000	0.38499400	-0.29279200
C	0.96011200	2.88608000	-0.22602200
H	0.24708100	3.65892800	-0.56684600
O	2.27766500	3.21130000	-0.61470800
C	-1.90095100	-1.33971000	-1.50651000
C	-2.87926800	-0.21228000	0.79502300
C	-1.14335900	-1.39804400	-0.33389900
C	-3.15824200	-0.71465600	-1.55613400
C	-3.62239400	-0.15661000	-0.38342500
C	-1.64235700	-0.82059400	0.85200600
H	-3.74538200	-0.66874800	-2.47245300
H	-1.07393100	-0.84905000	1.78216800
O	-3.56429800	0.43288200	1.78159700
O	-4.78037100	0.52597800	-0.14731500
C	-4.86057500	0.66405500	1.25905400
H	-5.18702600	1.68013400	1.51440200
H	2.52841800	4.04029100	-0.19592200
H	-1.50079800	-1.79345600	-2.41582500
C	0.58977800	1.54965200	-0.84045100
H	0.73873900	1.61811200	-1.93180900
C	0.24798000	-1.98402900	-0.35107800
H	0.56129300	-2.21853400	0.67809700
H	0.25967300	-2.92925700	-0.91747300
H	-0.48400300	1.36358200	-0.67234100
H	0.87420800	2.81829000	0.87551500
H	1.23085800	0.28705000	0.79575600
H	-5.56184300	-0.08800300	1.66609200
H	1.00842900	-0.85630000	-2.02954600

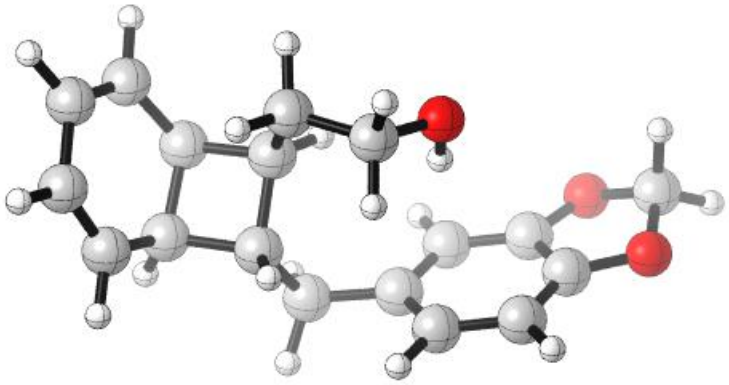

Lu_BOD2_GS
E(M062X/def2TZVP) = -923.514398 Hartree
Free energy correction (M062X/def2SVP) = 0.299578 Hartree
G = -2423900.51

H	-5.64271900	-0.15757800	1.50991300
C	-4.87926100	-0.17244600	0.72962900
C	-3.95411700	0.97437600	-1.23042000
C	-2.89042400	-1.22878500	-0.33979400
C	-2.79254100	0.02671600	-1.25145300
C	-3.96067100	-1.14835800	0.70970400
C	-4.91083900	0.88193000	-0.29691600
H	-2.96940200	-2.19077800	-0.87476900
H	-3.97731100	-1.93504000	1.47009700
H	-5.74210700	1.58953700	-0.28637200
H	-3.99809600	1.75952000	-1.98950000
H	-2.56124600	-0.25077000	-2.28978800
C	-1.48049700	0.44752200	-0.51073000
H	-0.63333100	0.60754200	-1.19762200
C	-1.45565600	-0.94261000	0.18293400
H	-1.39966400	-0.87679600	1.28252700
C	-1.57476100	1.63559600	0.43615700
H	-2.43842400	1.50597700	1.10986600
H	-1.75532900	2.55279100	-0.14679700
C	-0.30988200	1.82011600	1.27093600
H	-0.19094200	0.96723700	1.96735400
H	-0.41333200	2.72243400	1.89159500
O	0.84586100	1.99366700	0.49060800
C	-0.37584600	-1.89366800	-0.33158200
H	-0.51681400	-2.88718300	0.12442000
H	-0.49835600	-2.02192300	-1.41938000
C	1.01174500	-1.37343700	-0.03831300
C	3.47648200	-0.25197600	0.57491700
C	1.46632200	-1.29417200	1.28186000
C	1.82295500	-0.88565200	-1.08638000
C	3.04435700	-0.33625800	-0.74942500
C	2.70898500	-0.73068700	1.61584600
H	0.82800300	-1.67305900	2.08312000

H	1.50137400	-0.93580200	-2.12708800
H	3.05538700	-0.66565300	2.64626500
O	4.71282200	0.31648100	0.60096200
O	4.00615700	0.17811500	-1.56196200
C	4.90939800	0.84731600	-0.69719700
H	5.93973800	0.66077800	-1.02259100
H	4.67949000	1.92849600	-0.69228800
H	1.07985800	1.14103700	0.10553700

Structure	Number of imaginary frequencies	Free energy correction (Hartree)	Electronic energy (Hartree)	Relative Gibbs free energy (kJ/mol)
SNF_tetraene_GS	0	0.472026	-1591.501048	0.000
SNF_tetraene_8π1_TS	1	0.475884	-1591.480537	63.981
SNF_tetraene_8π2_TS	1	0.480198	-1591.482768	69.450
SNF_cyclooctatriene 1_GS	0	0.480495	-1591.522677	-34.552
SNF_cyclooctatriene 2_GS	0	0.481801	-1591.521557	-28.182
SNF_cyclooctatriene 1_6pi_TS	1	0.475752	-1591.483029	57.091
SNF_cyclooctatriene 2_6pi_TS	1	0.478651	-1591.482393	66.373
SNF_BOD1_GS	0	0.47893	-1591.532964	-65.669
SNF_BOD2_GS	0	0.480302	-1591.535833	-69.599

Table S4: Calculated relative free energies of SNF4435 compounds

SNF4435 compounds Cartesian Coordinates

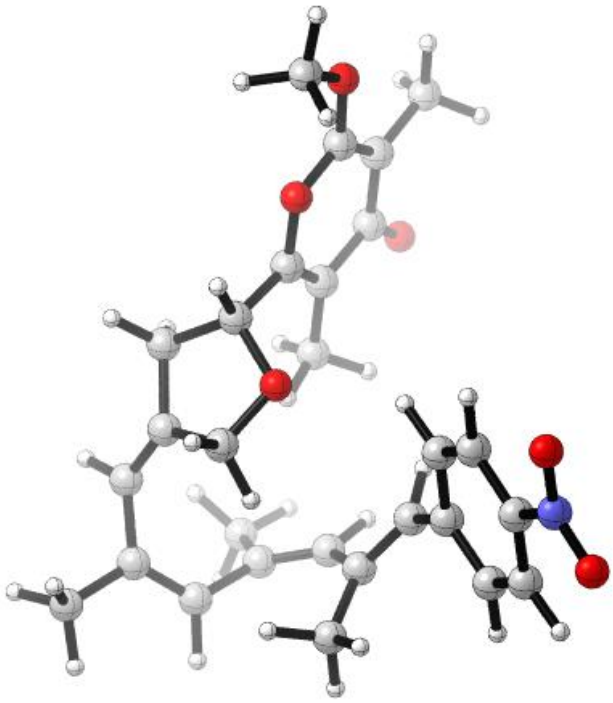

SNF_tetraene_GS
E(M062X/def2TZVP) = -1591.501048 Hartree
Free energy correction (M062X/def2SVP) = 0.472026 Hartree
G = -4177246.697

C	0.15408100	3.77677500	1.19062400
C	0.67274800	4.53242000	0.01338400
H	1.55527800	5.16480000	0.16524400

C	0.08262200	4.55290700	-1.19383500
C	0.71218100	2.67178500	1.72009500
H	0.17064000	2.20710100	2.55043800
C	1.89772900	1.91447200	1.27195100
C	-1.12275800	3.72819900	-1.48403100
H	-2.07165800	4.26696100	-1.60619300
C	-1.12400600	2.39967800	-1.61957100
C	1.84608000	0.57465200	1.42537300
H	0.92429900	0.15084300	1.83887100
C	-2.32880600	1.50556600	-1.81175800
H	-3.15300700	1.78956700	-1.14372900
H	-2.70426800	1.53959400	-2.84481300
C	0.05850200	1.46808300	-1.54301000
H	0.88193500	1.83410500	-0.92378700
H	0.44060600	1.25955600	-2.56314500
O	-0.46342500	0.28994000	-0.96343300
C	-1.76839700	0.09318200	-1.48060500
C	2.83680900	-0.41682900	0.96172700
C	4.61893700	-2.33945000	0.05604500
C	2.40141400	-1.45005800	0.11381000
C	4.18362300	-0.38197100	1.35602100
C	5.08393000	-1.34103500	0.90426700
C	3.28968600	-2.41351900	-0.34800000
H	1.35489400	-1.46379400	-0.19820200
H	4.52047200	0.39731700	2.04133000
H	6.13160400	-1.33708500	1.20051300
H	2.97885800	-3.21710600	-1.01349700
N	5.56810300	-3.35852800	-0.42948400
O	5.13643000	-4.21842400	-1.15948500
O	6.71661200	-3.26734700	-0.06764600
C	-2.58465600	-0.70112400	-0.49436400
C	-3.76200000	-2.72678200	-0.32534200
C	-3.71449100	-1.26192600	1.60011300
C	-4.14068600	-2.50043400	0.95755500
C	-2.88816100	-0.35132300	0.77053400
H	-1.70863100	-0.50672000	-2.40580100
O	-3.01208800	-1.87679200	-1.04062700
O	-4.01274600	-0.97822400	2.74876500
C	-2.46206600	0.93001600	1.41725400
H	-3.33533500	1.58580200	1.56174200
H	-1.68797300	1.46029600	0.85067500
H	-2.08599000	0.70376800	2.42568100
C	-4.97523800	-3.45867700	1.74686300
H	-4.45137300	-3.73188700	2.67409400
H	-5.20080100	-4.36429100	1.17309700
H	-5.91566200	-2.97654200	2.05137500
O	-4.10778900	-3.82188000	-0.99730200
C	-3.60951500	-4.01895400	-2.30812600
H	-4.00417400	-4.98598700	-2.63423900

H	-2.51085000	-4.04364000	-2.31539800
H	-3.95590400	-3.22780100	-2.98747000
C	3.03712800	2.64002300	0.60791400
H	3.87208200	1.96988900	0.37579600
H	2.70465900	3.10318100	-0.33338600
H	3.40170300	3.45511900	1.25101300
C	-1.12229000	4.32921600	1.77398300
H	-0.98673900	5.37807500	2.07998200
H	-1.45436800	3.74664700	2.64377600
H	-1.92304800	4.31741100	1.01730600
C	0.57699200	5.42408500	-2.31757100
H	1.43573800	6.03405300	-2.00750100
H	-0.22262800	6.09779500	-2.66392700
H	0.87061000	4.81063500	-3.18343700

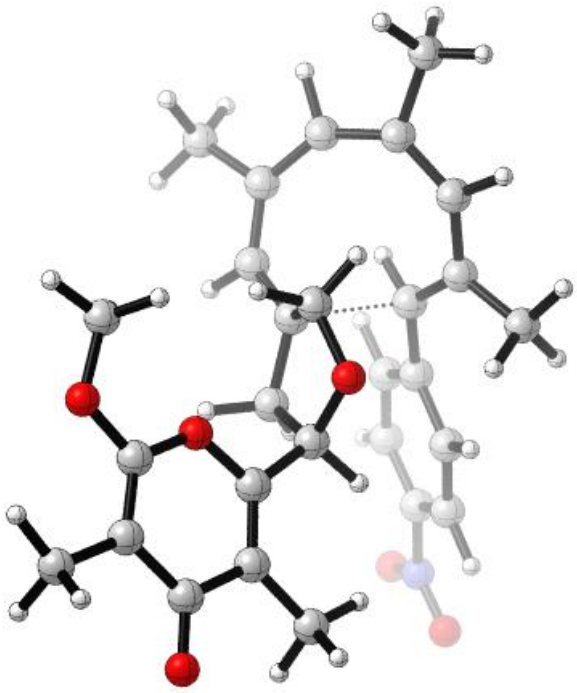

SNF_tetraene_8π1_TS
E(M062X/def2TZVP) = -1591.480537 Hartree
Free energy correction (M062X/def2SVP) = 0.475884 Hartree
G = -4177182.716

C	2.36396600	3.92643900	0.80563700
C	2.10321500	3.96123300	-0.58409300
H	2.38148100	4.94700400	-0.97863300
C	1.61837300	3.15720100	-1.63965500
C	2.37264800	2.91159600	1.78293600
H	2.44532900	3.29990700	2.80258200
C	2.33460600	1.50791400	1.72219100
C	0.99170000	1.90692200	-1.61632600
H	0.96317600	1.37519000	-2.57388900
C	2.47683600	0.86225600	0.48667200
H	2.92532100	1.49349700	-0.27717300

C	2.70475100	-0.56790000	0.24491000
C	3.13270800	-3.24054500	-0.44135400
C	3.40211200	-0.91923800	-0.92902300
C	2.21438800	-1.61199300	1.05523600
C	2.42816200	-2.94427800	0.71961000
C	3.62421400	-2.24388800	-1.27820700
H	3.77554000	-0.12337100	-1.57639500
H	1.64043000	-1.38720200	1.95062000
H	2.05410800	-3.75933600	1.33762200
H	4.16734600	-2.52245700	-2.17984200
N	3.35951800	-4.65144800	-0.79972900
O	3.97177500	-4.87440600	-1.81640400
O	2.91773800	-5.49208900	-0.05393700
C	0.46232500	1.21523000	-0.52623800
C	-0.32859200	1.82242500	0.60186700
H	0.19925300	2.54752800	1.22983500
H	-1.20525400	2.32887800	0.15480400
C	-0.17540000	-0.14492800	-0.72942300
H	0.55155500	-0.93483900	-0.96177800
H	-0.87910900	-0.08841800	-1.57441400
O	-0.73173800	0.73491000	1.40550700
C	-0.92446600	-0.41523200	0.59515800
H	-0.49674500	-1.27214000	1.12685000
C	1.83580000	3.76111400	-3.01812700
H	1.24703500	4.68468100	-3.12753200
H	1.52522100	3.07401900	-3.81486300
H	2.89031400	4.02623000	-3.18019000
C	2.73474600	5.30487100	1.34637500
H	3.69703400	5.63128400	0.92284100
H	2.83716100	5.30416300	2.43790600
H	1.98397000	6.05908600	1.07133200
C	2.11468500	0.77789200	3.02303800
H	2.23944700	1.46435500	3.86968300
H	2.81708700	-0.05749400	3.15066600
H	1.08673200	0.38401300	3.06479100
C	-4.56018100	-1.80075600	0.37623600
C	-2.39342000	-0.66799100	0.38957500
C	-4.28185100	0.44379500	-0.47420500
C	-5.11696000	-0.59462100	-0.22659500
C	-3.10610000	-1.77250100	0.68439100
O	-2.97247800	0.42786600	-0.18722500
O	-4.68506000	1.57654400	-1.04452100
O	-5.23729900	-2.78394700	0.62585800
C	-3.79557800	2.67622300	-1.10481200
H	-3.49518100	2.99524900	-0.09598500
H	-4.34949100	3.48170700	-1.59638100
H	-2.89642400	2.43364000	-1.68967000
C	-6.57779400	-0.57002000	-0.54798400
H	-6.81611700	-1.35076200	-1.28511600

H	-6.88695800	0.40475900	-0.94116900
H	-7.16045600	-0.80500100	0.35411300
C	-2.56821600	-3.02373000	1.30674300
H	-3.13505600	-3.24372900	2.22212400
H	-1.50000400	-2.97478400	1.54369500
H	-2.74692400	-3.87148100	0.63026400

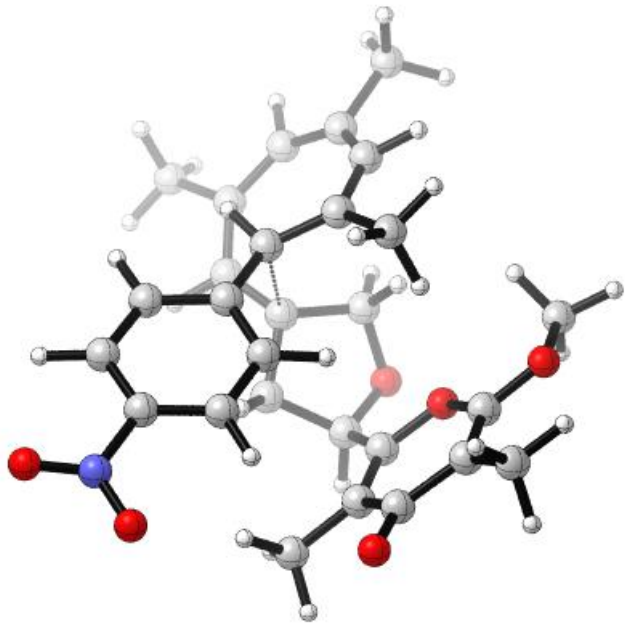

SNF_tetraene_8π2_TS
E(M062X/def2TZVP) = -1591.482768 Hartree
Free energy correction (M062X/def2SVP) = 0.480198 Hartree
G = -4177177.248

C	4.28566100	-0.15533200	-1.08187100
C	4.51742100	-1.18009700	-0.14343000
H	5.57980700	-1.44973900	-0.13931100
C	3.81786100	-1.99731700	0.77861900
C	3.13295300	0.41437500	-1.67176900
H	3.37794100	1.27282500	-2.30675100
C	1.76722900	0.11191300	-1.65803100
C	2.54091600	-1.83111300	1.30498800
H	2.12860800	-2.69146700	1.84363000
C	1.69846800	-0.71530900	1.19685300
C	1.29695600	-1.05534800	-1.02795600
H	2.04349100	-1.84219000	-0.97388200
C	0.39227300	-0.73672900	1.97394300
H	0.50158800	-1.38696300	2.85375400
C	2.22099100	0.70826400	1.29465500
H	2.07752000	1.28740000	0.36790000
H	3.28957200	0.72911600	1.55105000
O	1.49158700	1.29902200	2.35787100
C	0.21066400	0.73165900	2.41075600
H	-0.14187400	0.80379800	3.44982600
C	-0.08211100	-1.55881800	-1.02767400

C	-2.63862100	-2.64066700	-0.76648300
C	-0.27348700	-2.94867900	-0.89473400
C	-1.22343200	-0.73303900	-1.03303700
C	-2.50298400	-1.26347500	-0.89904600
C	-1.54182800	-3.49796800	-0.77377000
H	0.60062800	-3.60285100	-0.87747800
H	-1.12288700	0.34798100	-1.09582200
H	-3.38452200	-0.61968900	-0.86176600
H	-1.70223800	-4.57011600	-0.67269300
N	-3.98356300	-3.21276100	-0.58193900
O	-4.08454900	-4.41649500	-0.61372400
O	-4.89441600	-2.44159100	-0.40157000
C	0.85432400	1.09296700	-2.35571800
H	1.43733300	1.74036400	-3.02333100
H	0.32845000	1.75259200	-1.65048400
H	0.08721400	0.58128500	-2.95273100
C	5.56203600	0.47317200	-1.63696900
H	5.63090700	0.33529400	-2.72615700
H	6.46546900	0.05326700	-1.17998800
H	5.56516400	1.55692500	-1.44633200
C	4.60815700	-3.19654800	1.27082900
H	4.94309000	-3.82780700	0.43509400
H	4.01656300	-3.81584900	1.95625300
H	5.50830000	-2.86671800	1.81167000
H	-0.46112800	-1.11088100	1.39008800
C	-0.78356900	1.46881800	1.52779300
C	-2.91660300	1.95354200	0.44799200
C	-0.89459800	3.16390600	-0.08901800
C	-2.22314100	2.99491800	-0.30640700
C	-2.10671500	1.22447100	1.44753100
O	-0.18202400	2.41701200	0.76418000
O	-4.09474500	1.68545700	0.26416900
C	-2.82356200	0.19848100	2.26994500
H	-2.20623400	-0.21183900	3.07876800
H	-3.17200700	-0.62999300	1.63269400
H	-3.72986000	0.64958800	2.69744500
C	-3.00695200	3.80975600	-1.28597500
H	-3.43461000	3.15721500	-2.06111000
H	-2.38513100	4.57766500	-1.75926100
H	-3.85768000	4.28667000	-0.77857700
O	-0.15960600	4.07046800	-0.72800500
C	1.21183300	4.21314400	-0.38730400
H	1.34223200	4.34133600	0.69519500
H	1.55908600	5.10264100	-0.92141000
H	1.78934400	3.33478800	-0.71434300

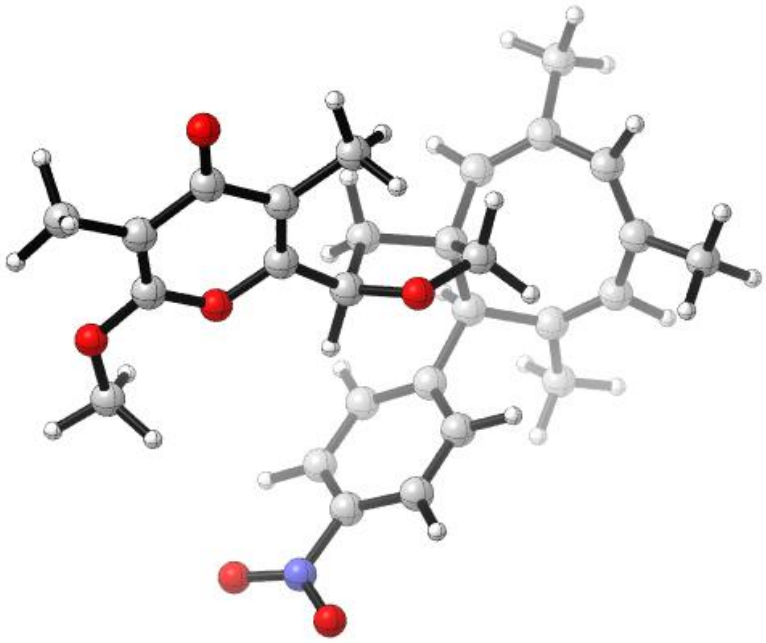

SNF_cyclooctatriene1_GS
E(M062X/def2TZVP) = -1591.522677 Hartree
Free energy correction (M062X/def2SVP) = 0.480495 Hartree
G = -4177281.249

C	-4.62525100	-0.89478600	0.98304900
C	-4.32927400	-2.08657200	0.43139400
H	-4.54828300	-2.98463400	1.02142400
C	-3.80180800	-2.30961000	-0.92211800
C	-3.74378100	1.10214200	-0.47552600
C	-4.60638100	0.41753400	0.30116400
H	-5.52852700	0.97198300	0.52110500
C	-2.72043000	-1.66640400	-1.38528400
H	-2.42471800	-1.85440700	-2.42448200
C	-1.82188200	-0.69790500	-0.64811900
C	-2.34149700	0.74472200	-0.94713100
C	-0.37386900	-0.88301500	-1.16866100
H	-0.16509700	-0.29973100	-2.07693700
H	-0.21510100	-1.94479300	-1.40738100
C	-1.34539400	1.81441200	-0.52597200
C	0.68625200	3.52564300	0.25946200
C	-1.20995700	2.18414200	0.81870700
C	-0.48576400	2.38287600	-1.47467800
C	0.54775400	3.23179000	-1.09122700
C	-0.19260500	3.04107400	1.22262100
H	-1.89825900	1.77678700	1.56102900
H	-0.61019300	2.13312300	-2.53053000
H	1.24783900	3.65703900	-1.80864000
H	-0.05328000	3.32350900	2.26491500
N	1.81229700	4.37704400	0.68672900
O	2.69135500	4.57683800	-0.11942200
O	1.78784300	4.80904300	1.81189800

H	-2.38580500	0.79646400	-2.04897100
C	-1.59594500	-0.98768500	0.85581400
H	-1.77581300	-2.05673000	1.06130200
H	-2.25006100	-0.40578500	1.51695800
O	-0.25855800	-0.65228100	1.16441400
C	0.52563800	-0.47735900	0.00766700
H	0.81702600	0.58214000	-0.07121900
C	-4.17282400	2.46124900	-0.98302400
H	-3.53947100	3.26291700	-0.57363700
H	-5.21601400	2.67736000	-0.72248200
H	-4.07413600	2.50976200	-2.07943900
C	-5.16128500	-0.82432200	2.39134200
H	-5.26433600	-1.82244000	2.83543300
H	-6.14239900	-0.32476200	2.41426500
H	-4.48776500	-0.22912800	3.02923700
C	-4.53898600	-3.32568100	-1.75476500
H	-4.57064400	-4.29617800	-1.23524200
H	-4.06144300	-3.47178900	-2.73214900
H	-5.58211400	-3.01275300	-1.91292600
C	1.82307300	-1.24017600	0.09373000
C	3.39330900	-3.05515600	0.54219200
C	4.10350900	-0.92391100	-0.36966800
C	4.44523100	-2.16582200	0.05501200
C	2.01574300	-2.49772900	0.53436700
O	2.84621200	-0.46224600	-0.36372300
O	3.62922100	-4.18754300	0.93056900
C	0.90860700	-3.36981900	1.05127700
H	1.28898600	-4.39502900	1.13178200
H	0.02859800	-3.36153300	0.39179800
H	0.57992500	-3.03293200	2.04447800
C	5.85271800	-2.67277100	0.05154300
H	6.14578600	-2.97026500	1.06876600
H	6.55182400	-1.91699800	-0.32333500
H	5.92422000	-3.57756500	-0.56947900
O	4.98611900	-0.04334000	-0.83335600
C	4.54897600	1.25805200	-1.18909100
H	5.44591300	1.79471000	-1.51221600
H	4.09439700	1.77971700	-0.33560000
H	3.82204400	1.21938700	-2.01245100

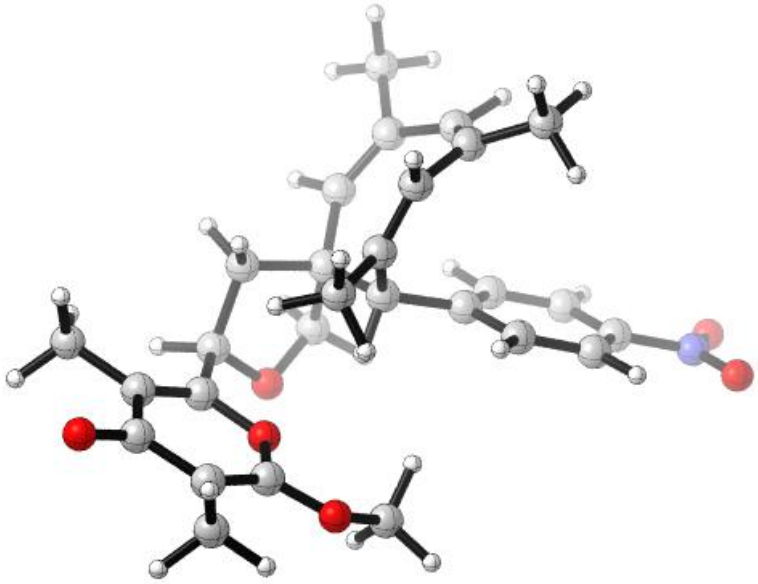

SNF_cyclooctatriene2_GS
E(M062X/def2TZVP) = -1591.521557 Hartree
Free energy correction (M062X/def2SVP) = 0.481801 Hartree
G = -4177274.879

C	-2.71556200	-2.44892300	1.13897900
C	-2.26675700	-1.66425300	2.13666600
C	-0.88326600	-1.22691000	2.37221700
C	-1.00715500	-2.87494400	-0.72372800
C	-2.03182500	-3.21468000	0.08080000
C	-0.04627700	-0.64378000	1.49922700
C	-0.37657900	-0.43778300	0.02379500
C	-0.09800800	-1.68201100	-0.85901200
H	-0.57221700	-1.24174700	3.42378500
H	-3.79372900	-2.65012500	1.16067600
H	-0.73588800	-3.64722000	-1.45486600
C	-1.72195500	0.25999400	-0.16801100
C	-4.09505100	1.69742500	-0.43017600
C	-1.95519900	1.42128500	0.58789700
C	-2.71480400	-0.15206000	-1.06572800
C	-3.90489600	0.55843500	-1.20001400
C	-3.13347100	2.14703400	0.46762200
H	-1.19908900	1.75309200	1.30322400
H	-2.58286500	-1.06151700	-1.64957200
H	-4.68872600	0.23992500	-1.88523000
H	-3.32285600	3.04654300	1.05116900
N	-5.35400400	2.45264100	-0.56673600
O	-5.48580500	3.44029100	0.11540400
O	-6.17127900	2.03479300	-1.35101900
H	0.36012200	0.29751500	-0.33998300
C	1.24126100	-0.02743600	1.98370200
H	1.23765500	1.05950100	1.78639900
H	2.12864000	-0.42644200	1.46806800

H	1.37917600	-0.17917100	3.06172500
C	-3.23590600	-1.12220200	3.15880300
H	-4.25693700	-1.48402400	2.98375700
H	-3.24444700	-0.02079700	3.12972300
H	-2.92981400	-1.41389300	4.17592000
C	-2.68597300	-4.56490500	-0.13054000
H	-3.74947600	-4.44216800	-0.38950900
H	-2.65019100	-5.15812300	0.79582500
H	-2.19797700	-5.13657700	-0.92993200
C	1.36151400	-2.17761800	-0.65752000
H	1.42500900	-3.22671600	-0.97714700
C	0.04257600	-1.22617200	-2.33492700
H	-0.70774900	-0.49416300	-2.65595000
H	-0.01053200	-2.10732500	-3.00309500
O	1.30156600	-0.60208600	-2.41992900
C	2.21812800	-1.30142300	-1.61058700
H	2.84950300	-1.95031700	-2.23919100
C	3.13487500	-0.33263500	-0.89962700
C	3.19004900	1.85908000	-0.06330100
C	5.07694900	0.41673100	0.38407500
C	4.40815900	1.70865600	0.51231800
C	4.34278100	-0.62362500	-0.37558800
O	2.56973900	0.89272200	-0.75313900
O	6.17249600	0.19058100	0.87094800
C	5.09737800	2.79615800	1.27351800
H	6.11138600	2.94041200	0.87467500
H	5.21567600	2.50635100	2.32810200
H	4.54184800	3.73899400	1.21922200
C	5.01406500	-1.95896000	-0.46515300
H	5.12581600	-2.38271800	0.54380800
H	6.03392800	-1.82765800	-0.85261000
H	4.47335000	-2.67806000	-1.09145100
O	2.47802000	2.98050000	0.01678200
C	1.33307100	3.12898700	-0.81013500
H	1.56698900	2.89843100	-1.85805500
H	1.02627400	4.17455300	-0.71047800
H	0.51507700	2.47303000	-0.47724400
H	1.68344000	-2.14326900	0.38957600

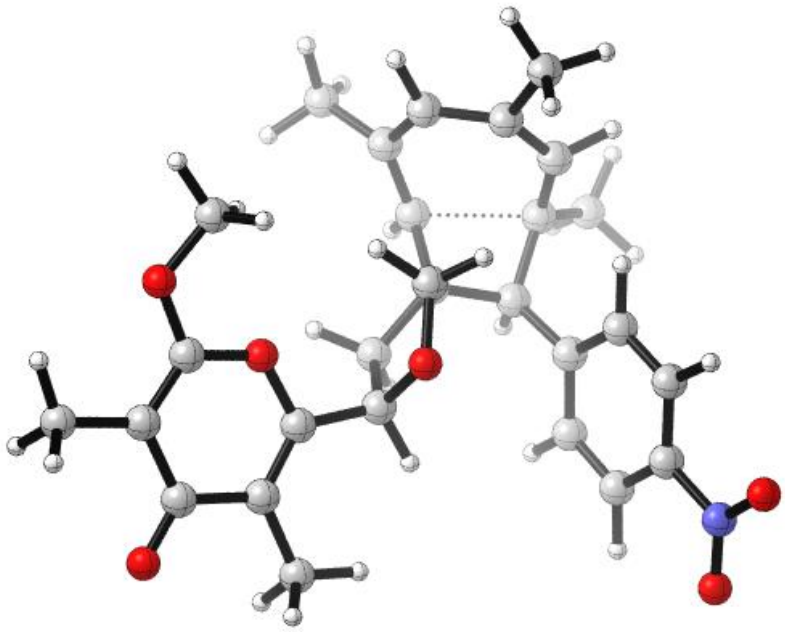

SNF_cyclooctatriene1_6π_TS
E(M062X/def2TZVP) = -1591.483029 Hartree
Free energy correction (M062X/def2SVP) = 0.475752 Hartree
G = -4177189.606

C	1.63967100	3.42126700	1.15016500
C	0.33726800	3.81824000	0.78031400
H	-0.16187200	4.51125200	1.46534500
C	-0.17034400	3.67065600	-0.50840900
C	2.44287200	2.34495000	-1.04062700
C	2.58661100	2.97357800	0.21867400
H	3.60019700	3.34419700	0.42923200
C	0.30258400	2.62033200	-1.30892600
H	0.10565500	2.70129500	-2.38722400
C	0.39181300	1.16777500	-0.85571800
C	1.85012500	0.95001400	-1.26425600
C	-0.62810000	0.25664600	-1.56231900
H	-0.29085500	-0.05451000	-2.56110100
H	-1.57423600	0.80545900	-1.68265800
C	2.58394000	-0.24214700	-0.69020400
C	3.76616600	-2.52748000	0.35092800
C	3.24565900	-0.20173900	0.54304400
C	2.54727000	-1.45446900	-1.39555900
C	3.12955500	-2.60726200	-0.88219400
C	3.84002200	-1.34329200	1.07263100
H	3.30126800	0.73743300	1.09501000
H	2.05335400	-1.49247200	-2.36965200
H	3.10961800	-3.55693300	-1.41428300
H	4.35765500	-1.33392600	2.03036600
N	4.39694700	-3.74161600	0.90550400
O	4.31467200	-4.75567800	0.25575400
O	4.95403500	-3.64061900	1.97143400
H	1.83052300	0.80971300	-2.35731600

C	0.09314300	0.81043400	0.60771300
H	-0.78706200	1.37189500	0.96140800
H	0.92507900	0.98817600	1.29846500
O	-0.15367300	-0.57733200	0.59505100
C	-0.81548700	-0.93894800	-0.60168000
H	-0.34017300	-1.85071700	-0.98518500
C	3.52020600	2.66578700	-2.05382100
H	4.25456600	1.84296800	-2.10449000
H	4.04565900	3.60103700	-1.82335300
H	3.07731400	2.76068100	-3.05657000
C	2.12662300	3.78600700	2.53115000
H	1.56347000	4.62822600	2.95537500
H	3.19552100	4.04260700	2.52336300
H	2.00423200	2.93031100	3.21500000
C	-1.06820000	4.73149900	-1.10005400
H	-0.54414100	5.25469700	-1.91578800
H	-1.34527400	5.48447600	-0.35066700
H	-1.98822700	4.30489500	-1.52537800
C	-2.26765300	-1.22263800	-0.32276500
C	-4.42793800	-2.36377500	-0.23036200
C	-4.13402200	-0.11006500	0.58918000
C	-4.96905800	-1.15917400	0.39061400
C	-2.98200700	-2.33651400	-0.57491600
O	-2.83842400	-0.12167300	0.25169100
O	-4.52829100	1.04250200	1.12600600
O	-5.11015000	-3.34975300	-0.45557300
C	-6.41628400	-1.14231100	0.76887400
H	-7.04412100	-1.25423600	-0.12732300
H	-6.68606100	-0.21426000	1.28514600
H	-6.64056900	-2.00233300	1.41581700
C	-2.45295100	-3.59180600	-1.19624000
H	-2.70727500	-4.44416800	-0.55136300
H	-1.37067100	-3.57498200	-1.36302100
H	-2.96393800	-3.77341500	-2.15277000
C	-3.55627200	2.02252600	1.44436700
H	-2.83019600	1.63545700	2.17405400
H	-4.10933500	2.85988300	1.88069500
H	-3.01535000	2.36047000	0.54780500

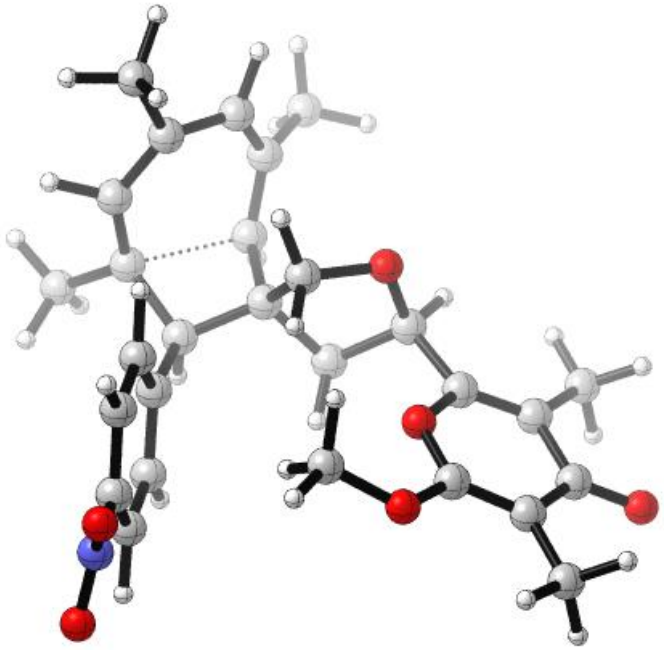

SNF_cyclooctatriene2_6π_TS
E(M062X/def2TZVP) = -1591.482393 Hartree
Free energy correction (M062X/def2SVP) = 0.478651 Hartree
G = -4177180.325

C	3.35215100	-2.59635900	1.32445700
C	3.90269900	-1.30222500	1.40803300
C	4.09969100	-0.48535600	0.28610400
C	2.28959300	-2.30915800	-0.83451800
C	2.83318400	-3.14244100	0.15272700
C	3.47356200	-0.45026800	-0.98044600
C	2.01459400	-0.06149700	-1.23113200
C	1.24332500	-1.21401800	-0.59785400
H	5.03549900	0.08924300	0.34123200
H	3.59458300	-3.27256600	2.15000100
H	2.18575900	-2.76275700	-1.83066900
C	1.60481400	1.35603400	-0.88844000
C	0.69086700	3.90096200	-0.26082400
C	0.90782000	2.12107000	-1.83322500
C	1.85117700	1.91053500	0.37766700
C	1.38524400	3.17857500	0.70505500
C	0.45341700	3.40382900	-1.53426300
H	0.71634100	1.70314900	-2.82383700
H	2.40838000	1.33101700	1.11590100
H	1.54322300	3.61674300	1.68952200
H	-0.08538200	4.01391400	-2.25776100
N	0.16103500	5.23178300	0.09131400
O	-0.22614100	5.93227100	-0.81075500
O	0.14131300	5.52455800	1.26342400
H	1.86387100	-0.17492300	-2.31703200
C	4.36390500	-0.03891800	-2.13292200
H	4.18575200	1.01775000	-2.39995300

H	4.12432900	-0.63824600	-3.02416200
H	5.42890400	-0.17563600	-1.90776100
C	4.57991500	-0.90373200	2.69704400
H	3.87808900	-0.34818200	3.34040100
H	5.43931800	-0.24421100	2.51106600
H	4.92126900	-1.77850400	3.26672400
C	2.98568200	-4.61981100	-0.12372000
H	3.66070100	-5.10450700	0.59281500
H	3.39328700	-4.77335300	-1.13456200
H	2.01283300	-5.13292100	-0.08372400
C	-0.09483800	-1.52487200	-1.29362900
H	-0.59010500	-0.57353500	-1.54743100
H	0.03094100	-2.10219000	-2.21927100
C	0.71518200	-1.05173200	0.83199600
H	0.20857100	-0.07413000	0.90834400
H	1.45772800	-1.13309600	1.62987500
O	-0.21218200	-2.10092000	0.99375800
C	-0.91176700	-2.28482400	-0.22453200
H	-0.95267300	-3.36110100	-0.43361500
C	-2.31470100	-1.75320100	-0.09000800
C	-4.75621200	-1.62394300	-0.11051700
C	-3.37949500	0.26641900	0.49770700
C	-4.62641200	-0.23672300	0.32103700
C	-3.48908900	-2.37801500	-0.30135700
O	-2.26203600	-0.44461700	0.29946400
O	-3.14738500	1.52074300	0.87465600
O	-5.83799100	-2.15464300	-0.30356200
C	-5.87324400	0.56025800	0.54068000
H	-6.45216400	0.62048900	-0.39248100
H	-5.64631600	1.57275400	0.89259600
H	-6.51625600	0.05267700	1.27400400
C	-3.65584900	-3.80297100	-0.72925600
H	-4.17216900	-3.83638700	-1.69936700
H	-4.31725800	-4.31655100	-0.01780800
H	-2.71018700	-4.35009600	-0.80599400
C	-1.81202200	1.93571000	1.10658900
H	-1.36159500	1.36915000	1.93505600
H	-1.86361300	2.99712400	1.37228300
H	-1.19268200	1.80729500	0.20581100

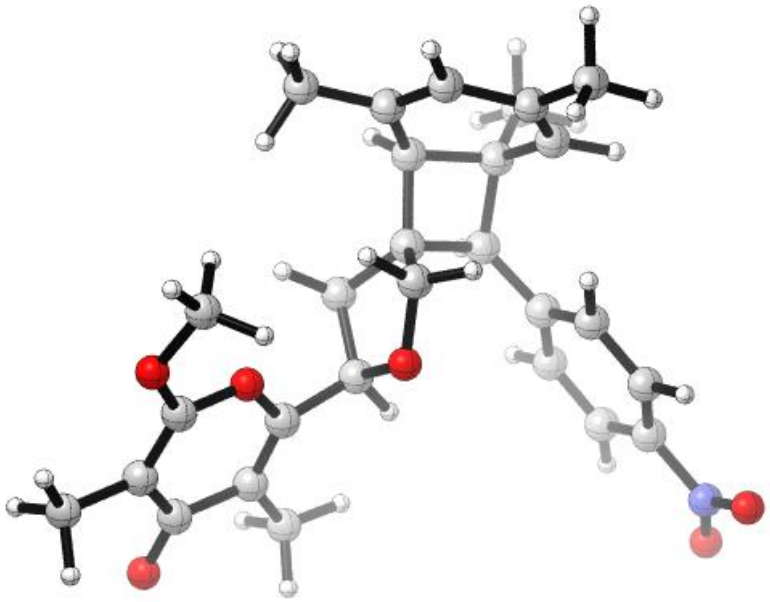

SNF_BOD1_GS
E(M062X/def2TZVP) = -1591.532964 Hartree
Free energy correction (M062X/def2SVP) = 0.478930 Hartree
G = -4177312.366

C	-2.46175800	2.05557600	1.24474000
C	-2.77903900	3.36129600	-0.87640700
C	-0.68277800	3.78052500	0.37066300
C	-1.51939400	4.09112300	-0.63219400
C	-1.00738100	2.61227100	1.25797700
C	-3.19228100	2.40896800	-0.02336500
H	-0.69213400	2.82124500	2.29412000
H	-1.27803100	4.92110800	-1.30295600
H	-4.15684900	1.91737900	-0.18840300
C	-1.84384200	0.61857500	1.30466400
C	-0.48094000	1.21436100	0.83606800
C	-3.33985400	2.41434000	2.43930800
H	-4.28178100	1.84491400	2.41204500
H	-3.58750500	3.48595400	2.42461600
H	-2.82690900	2.18699700	3.38651600
C	-3.56714800	3.75470300	-2.09389700
H	-4.48986000	3.16759500	-2.18588700
H	-2.96911700	3.61196600	-3.00765500
H	-3.83642300	4.82153000	-2.05229900
C	0.60174800	4.50485800	0.63551500
H	1.45544000	3.80715400	0.59426500
H	0.60301800	4.93857200	1.64812800
H	0.77438400	5.31012800	-0.09037100
C	0.76517000	0.59884300	1.46377600
H	0.62607400	0.29154900	2.50915500
H	1.60155500	1.31464500	1.41980100
C	-0.13553700	1.02298800	-0.63694400
H	-0.98800800	1.08490800	-1.32373800

H	0.60272600	1.78963300	-0.94109700
H	-1.72191100	0.39216500	2.37564000
C	-2.42956800	-0.61033800	0.66329700
C	-3.41236400	-2.97662400	-0.42908400
C	-2.48588700	-1.79166200	1.42076000
C	-2.88819000	-0.65401500	-0.66386500
C	-3.38072500	-1.83162300	-1.21540500
C	-2.97139000	-2.98078000	0.88748500
H	-2.14170000	-1.77604700	2.45702900
H	-2.87150200	0.24391700	-1.27887500
H	-3.73907000	-1.88008600	-2.24226600
H	-3.01887200	-3.90119900	1.46704800
N	-3.93723600	-4.22819800	-1.00944700
O	-3.94100800	-5.20780200	-0.30403400
O	-4.32924100	-4.18972200	-2.15039700
O	0.42011000	-0.27119200	-0.70829500
C	1.03974200	-0.59705000	0.52711700
H	0.57174600	-1.51290900	0.91545100
C	4.71343300	-1.88987500	0.44890800
C	2.50639300	-0.84788900	0.31245800
C	4.34393600	0.18714700	-0.72849200
C	5.21652200	-0.78037400	-0.35396600
C	3.25807500	-1.87769200	0.74830600
O	3.04654900	0.18456000	-0.39742000
O	4.69809400	1.24219600	-1.45878300
O	5.43073300	-2.79414300	0.84426300
C	3.68819000	2.10435300	-1.95141300
H	2.93058700	1.54493400	-2.51795300
H	4.19733600	2.81758500	-2.60679200
H	3.19389700	2.64414500	-1.13072600
C	6.66564500	-0.77019100	-0.72510600
H	7.28751800	-0.72815600	0.18107100
H	6.90932600	0.08060700	-1.37109800
H	6.92531500	-1.70745500	-1.23774900
C	2.76058100	-3.04806100	1.53867200
H	3.07121400	-3.97632800	1.03970000
H	1.67369400	-3.05456700	1.67422800
H	3.24645600	-3.05818700	2.52505900

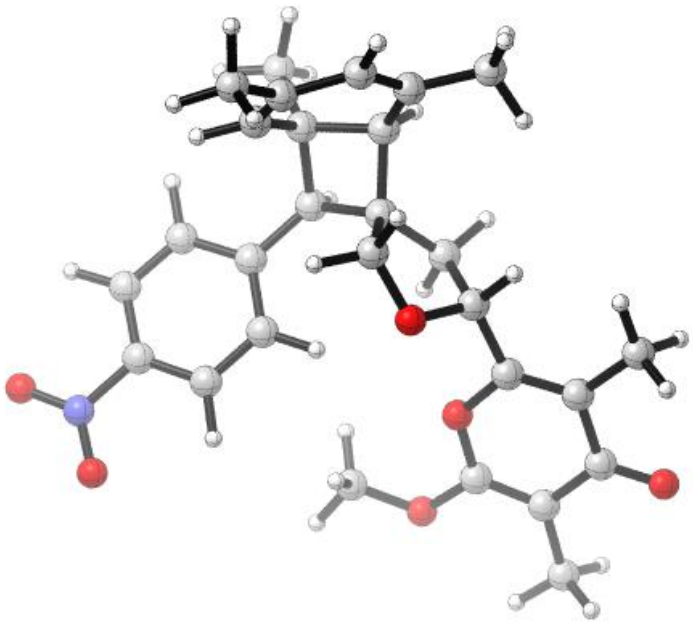

SNF_BOD2_GS
E(M062X/def2TZVP) = -1591.535833 Hartree
Free energy correction (M062X/def2SVP) = 0.480302 Hartree
G = -4177316.297

C	-1.66769400	-2.63069900	0.94583500
C	-2.83723800	-3.76891000	-0.87289700
C	-3.65067600	-1.56688000	-0.17446300
C	-3.67778100	-2.57119100	-1.06764700
C	-2.83415400	-1.62330600	1.09297400
C	-1.87770200	-3.82611600	0.06503000
C	-0.73025400	-1.45859400	0.49305600
C	-1.74567400	-0.50900100	1.18781500
H	-4.30065800	-0.69776400	-0.32023800
H	-2.99821000	-4.61826100	-1.54359900
H	-1.34012200	-2.95445000	1.94787300
C	0.72509400	-1.43036200	0.99420900
H	0.96075900	-2.26058500	1.67405600
H	0.92500900	-0.48559200	1.52300200
C	-0.56503600	-1.29526800	-1.03705800
H	-0.68276200	-2.27431100	-1.53449000
H	-1.27280700	-0.59135500	-1.49185700
C	-3.74729600	-1.82483800	2.29791000
H	-3.17302500	-1.79773000	3.23696200
H	-4.24730300	-2.80201300	2.22220800
H	-4.53335800	-1.05626500	2.34943600
C	-4.54776800	-2.54386900	-2.29236100
H	-5.23948300	-3.40055000	-2.29403100
H	-3.93646100	-2.62409200	-3.20474400
H	-5.13733100	-1.62015000	-2.34878800
C	-0.96183400	-4.99674100	0.25367400
H	0.08952100	-4.68716900	0.12402100
H	-1.17430400	-5.80198500	-0.46134400

H	-1.04612200	-5.40110600	1.27480000
C	-2.00066700	0.88924600	0.69509200
C	-2.47931900	3.50775400	-0.09783600
C	-1.03479200	1.59897300	-0.03356000
C	-3.20879200	1.52711300	1.01557000
C	-3.46052300	2.83637600	0.62248700
C	-1.27045400	2.91221400	-0.43326000
H	-0.09131800	1.11822000	-0.30394300
H	-3.96409400	0.98817300	1.58998500
H	-4.39242800	3.34574500	0.86223000
H	-0.54040800	3.48323100	-1.00560800
N	-2.72963100	4.89970100	-0.51890100
O	-1.84399000	5.46898200	-1.11008700
O	-3.80233800	5.37903800	-0.24256600
H	-1.45072500	-0.44042100	2.25060900
O	0.74723300	-0.81062600	-1.24265800
C	1.55704300	-1.47340200	-0.29804700
H	1.70932000	-2.52079000	-0.60900500
C	5.32255500	-0.52437400	-0.11717000
C	2.89364000	-0.80119500	-0.20507900
C	3.80574000	1.33015000	0.19077400
C	5.08801500	0.89296500	0.12341100
C	4.11278100	-1.36899100	-0.29914300
O	2.73901600	0.53072600	0.04933600
O	3.49115700	2.60170700	0.41605000
O	6.44119800	-1.00723600	-0.18202500
C	2.14085300	3.01087000	0.29459900
H	1.74462500	2.75733400	-0.69953700
H	2.14144500	4.09692400	0.42976600
H	1.51092300	2.54144500	1.06353600
C	6.27184800	1.79347400	0.28343400
H	6.85329200	1.50130300	1.17026400
H	5.96936600	2.84201900	0.37982000
H	6.94252500	1.68079900	-0.58021200
C	4.39498700	-2.81421600	-0.57068000
H	5.07982900	-2.88833900	-1.42669300
H	3.49906700	-3.41092100	-0.77023100
H	4.93502700	-3.24707600	0.28365900

Structure	Number of imaginary frequencies	Free energy correction (Hartree)	Electronic energy (Hartree)	Relative Gibbs free energy (kJ/mol)
Parkerester_tetraene_GS	0	0.558236	-2220.782711	0.000
Parkerester_tetraene_8π 1_TS	1	0.558857	-2220.7643	49.969
Parkerester_tetraene_8π 2_TS	1	0.561644	-2220.762264	62.631

Parkerester_cyclooctatriene1_GS	0	0.560376	-2220.804619	-51.901
Parkerester_cyclooctatriene2_GS	0	0.561801	-2220.802888	-43.615
Parkerester_cyclooctatriene1_6π_TS	1	0.560495	-2220.757223	72.850
Parkerester_cyclooctatriene2_6π_TS	1	0.558729	-2220.75958	62.025
Parkerester_BOD1_GS	0	0.565015	-2220.81107	-56.658
Parkerester_BOD2_GS	0	0.562295	-2220.812211	-66.795

Table S5: Calculated relative free energies of Parker Chiral Ester compound

Parker Chiral Ester Compound Cartesian Coordinates

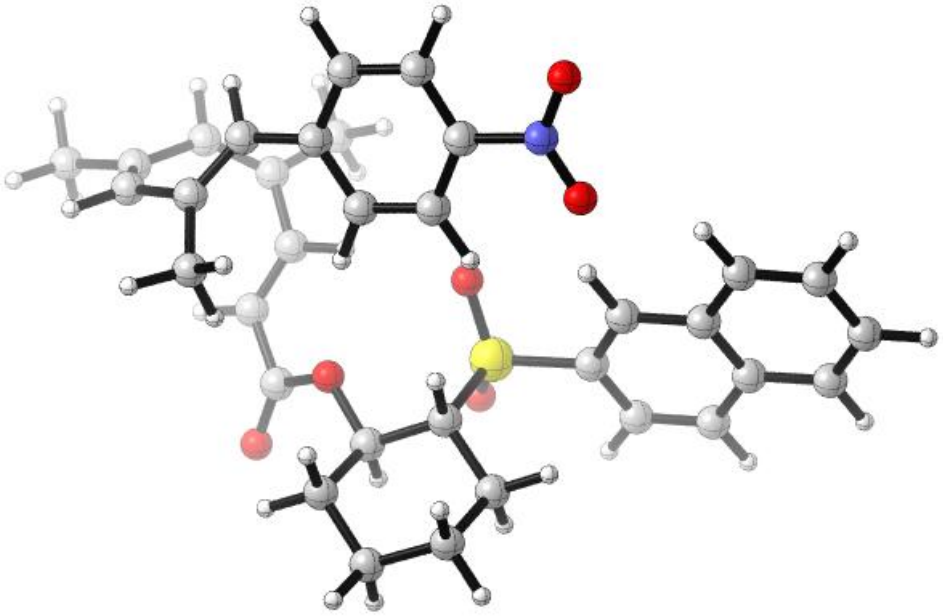

Parkerester_tetraene_GS
E(M062X/def2TZVP) = -2220.782711 Hartree
Free energy correction (M062X/def2SVP) = 0.558236 Hartree
G = -5829199.359

C	-5.93153800	0.52176400	-0.84749900
C	-5.07267700	0.80685800	-2.02357700
H	-5.55174100	1.43572100	-2.78512900
C	-3.82715500	0.37943400	-2.29800600
C	-5.57980500	0.66639000	0.44607900
H	-6.32072600	0.36666600	1.19643300
C	-4.27052300	1.09056600	0.97798700
C	-3.03826400	-0.50197900	-1.41536900
H	-1.99622300	-0.20592700	-1.22956600
C	-3.46494700	-1.67431800	-0.92658000
C	-3.63099500	2.16157900	0.46374900
H	-4.16643300	2.76023300	-0.27894100
C	-2.25364400	2.58851400	0.74359400
C	0.37832900	3.41875300	1.06952600

C	-1.91684200	3.95562600	0.69630400
C	-1.22830200	1.64963900	0.95273200
C	0.08658700	2.06166500	1.11806800
C	-0.60740700	4.38205800	0.86592100
H	-2.70344800	4.68986100	0.51430400
H	-1.44712000	0.58102500	0.90973500
H	0.89448900	1.34455700	1.24605800
H	-0.33048900	5.43431700	0.82665600
N	1.77890300	3.84311100	1.18317200
O	2.62364900	2.97177300	1.24391800
O	2.01472100	5.02445000	1.20247600
C	-3.75561800	0.25717600	2.12322700
H	-3.31841500	-0.68554600	1.75762900
H	-4.58974300	-0.00819500	2.78960100
H	-2.99254700	0.78403000	2.71007900
C	-7.31896500	0.05882400	-1.21376800
H	-7.81662000	0.80109300	-1.85796500
H	-7.94148100	-0.10302900	-0.32450800
H	-7.27226600	-0.87867700	-1.78994400
C	-3.09060300	0.82619800	-3.53313200
H	-2.16638200	1.35363400	-3.24744100
H	-3.70507300	1.49444700	-4.14988700
H	-2.78511600	-0.03915200	-4.14054800
H	-4.45459400	-2.07758700	-1.14987100
C	-2.58966900	-2.56001100	-0.13000700
O	-2.77036100	-3.73477600	0.04303900
O	-1.53517100	-1.89778000	0.40613500
C	-0.50552100	-2.69179900	0.98184200
C	1.94976600	-2.70008700	1.47340000
C	0.32973400	-3.89551800	3.01026800
C	1.64977600	-3.13227300	2.91164800
C	-0.82201500	-3.08322600	2.41985300
C	0.78623900	-1.88195000	0.91430800
H	2.09482100	-3.58813000	0.83437100
H	0.41626500	-4.84762100	2.46071100
H	1.60143300	-2.23424000	3.55046800
H	-0.98657600	-2.16339000	3.00697000
H	0.66518000	-0.93485500	1.46532000
H	-0.38655500	-3.59912100	0.36868400
H	2.87977000	-2.11612500	1.43537600
H	0.11281800	-4.15385700	4.05642600
H	2.48076300	-3.74462600	3.29012000
H	-1.75702000	-3.65964700	2.42101800
S	1.02376100	-1.36965100	-0.82516100
O	0.70176600	-2.53139900	-1.65189700
O	0.32295200	-0.09842200	-1.01467000
C	2.76883700	-1.04886300	-0.98339900
H	2.60339500	0.96470000	-0.23306400
C	3.26262100	0.17396000	-0.59971100

C	4.94480700	-1.84581400	-1.60609700
C	4.65952300	0.42057900	-0.69143100
C	3.59667700	-2.07521300	-1.50026800
C	5.51146400	-0.60369500	-1.20271400
C	5.22231400	1.66292100	-0.28577900
H	3.14138600	-3.01343300	-1.81971400
H	7.55747400	-1.13171900	-1.69402100
H	5.60341000	-2.61692200	-2.01044600
C	6.57530800	1.87364500	-0.39097000
H	4.56088100	2.42984600	0.12191900
H	7.00347400	2.82613200	-0.07610000
C	7.42362600	0.86000300	-0.90443300
H	8.49600800	1.04504800	-0.98314800
C	6.90622400	-0.34934400	-1.29963600

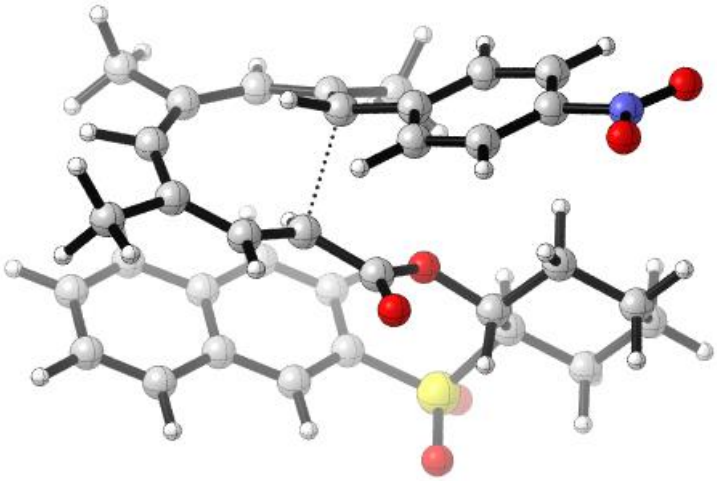

Parkerester_tetraene_8π1_TS
E(M062X/def2TZVP) = -2220.764300 Hartree
Free energy correction (M062X/def2SVP) = 0.558857 Hartree
G = -5829149.391

C	-2.80875700	-2.66309600	1.45111600
C	-2.94654900	-3.01645100	0.08393100
H	-3.83684400	-3.64586200	-0.04212500
C	-2.35724000	-2.77747600	-1.17324600
C	-1.80920400	-2.03917900	2.22227800
H	-2.16708500	-1.71938700	3.20614800
C	-0.45057400	-1.75422100	2.01090100
C	-1.31891900	-1.89293800	-1.48370100
H	-0.85076900	-1.95696400	-2.47089600
C	0.20959600	-2.27555800	0.89041800
H	-0.30754100	-3.10336200	0.40471300
C	1.65933300	-2.23770000	0.58972500
C	4.35233800	-2.22987600	-0.13193900
C	2.06686600	-2.59332200	-0.71150400
C	2.65732200	-1.91521600	1.52671300
C	4.00237400	-1.90887200	1.17270300

C	3.40316500	-2.58543400	-1.08445500
H	1.30827600	-2.85761200	-1.45010200
H	2.39436600	-1.69071500	2.55617700
H	4.78318500	-1.66068300	1.88979200
H	3.72188100	-2.84087200	-2.09345000
N	5.77535700	-2.19692900	-0.51666600
O	6.05790600	-2.56080200	-1.63210800
O	6.56480100	-1.80382200	0.30896200
C	-0.79195100	-0.97118000	-0.59174500
C	-2.96435200	-3.55362800	-2.32503000
H	-3.96395600	-3.15451800	-2.56063600
H	-3.08149100	-4.61895300	-2.08292000
H	-2.35194400	-3.46839500	-3.23146900
C	-4.03314600	-3.07548200	2.26375800
H	-4.07803300	-2.55302900	3.22789100
H	-3.99544700	-4.15550700	2.47861300
H	-4.96740600	-2.88087900	1.71935100
C	0.18158100	-0.74813700	2.94517600
H	-0.59405100	-0.14019600	3.42877500
H	0.84168400	-0.07156300	2.38386000
H	0.77168500	-1.22679600	3.74212600
H	-1.41155800	-0.58314600	0.21163100
C	0.30837100	-0.08922400	-1.04080900
O	0.87357500	-0.15075000	-2.10121800
O	0.63305100	0.78791400	-0.07630600
C	1.58961400	1.79851900	-0.38787900
C	2.24753200	4.13859500	0.29892100
C	4.02208900	2.42295000	-0.21940400
C	3.64795200	3.62916400	0.64125400
C	2.99208700	1.30956800	-0.05051100
C	1.20723400	3.02012200	0.43053000
H	2.22655400	4.50079800	-0.74188200
H	4.06496200	2.72714800	-1.27845600
H	3.68550600	3.34423100	1.70634400
H	2.98735800	0.95835700	0.99565700
H	1.05882000	2.73921900	1.48609900
H	1.51952300	2.04098300	-1.46058800
H	1.95175800	4.97845300	0.94147400
H	5.02178300	2.04947000	0.04462100
H	4.37342100	4.44389400	0.50521800
H	3.21568400	0.43945000	-0.68718500
S	-0.37164800	3.74144700	-0.12030300
O	-0.66036100	4.82520500	0.81386800
O	-0.23459700	3.99493700	-1.55358200
C	-1.66252600	2.52067200	0.07993200
H	-1.90088000	2.31225000	-2.03119100
C	-2.26191000	2.01388100	-1.04423800
C	-3.13990500	1.30436800	1.53116600
C	-3.35815000	1.11638500	-0.91107500

C	-2.09477100	2.18173500	1.38552700
C	-3.80698300	0.76204500	0.39451300
C	-4.01391700	0.56278400	-2.04345200
H	-1.61235700	2.63806500	2.25151600
H	-5.26115000	-0.37802500	1.52753100
H	-3.49420200	1.02931900	2.52693700
C	-5.07726000	-0.29276600	-1.88499700
H	-3.65816800	0.83313700	-3.03937800
H	-5.57946200	-0.70756600	-2.76030800
C	-5.53490400	-0.63263700	-0.58716600
H	-6.38659500	-1.30599000	-0.47499600
C	-4.91370700	-0.11853700	0.52520500

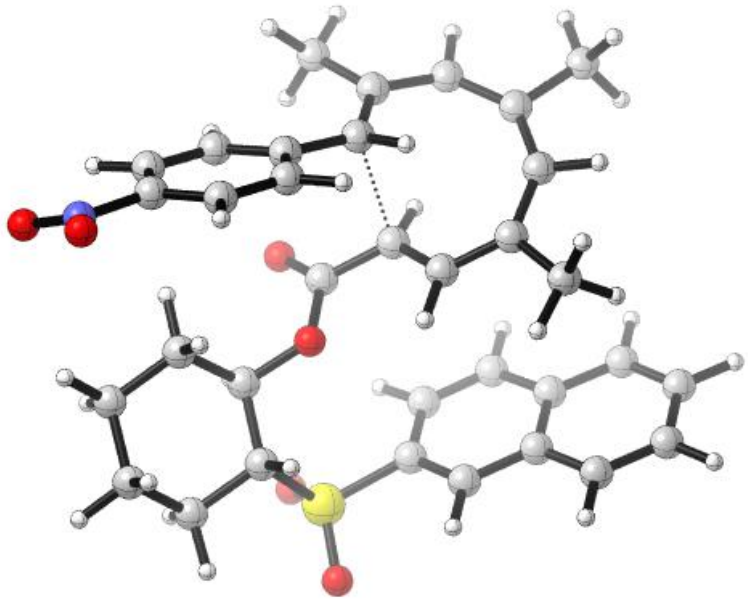

Parkerester_tetraene_8π2_TS
E(M062X/def2TZVP) = -2220.762264 Hartree
Free energy correction (M062X/def2SVP) = 0.561644 Hartree
G = -5829136.728

C	2.20942500	4.13680800	-0.48163900
C	2.56592400	3.24191800	0.56852600
H	3.45510600	3.62427500	1.09109700
C	2.18633700	2.00511700	1.12158700
C	1.06510500	4.33672900	-1.27775700
H	1.22657600	5.05695600	-2.08664900
C	-0.24609300	3.82482600	-1.23816800
C	1.25590800	1.09057600	0.60595700
H	0.96431600	0.23859700	1.22793900
C	-0.63790500	3.04101100	-0.14776000
H	-0.00880000	3.17225500	0.73335300
C	-1.96941600	2.51239900	0.18244300
C	-4.39739900	1.41697100	1.00623000
C	-2.21863000	2.22627400	1.54170700
C	-2.98179200	2.22017900	-0.75330500

C	-4.19667600	1.68138900	-0.34256000
C	-3.42542800	1.68819900	1.96488400
H	-1.43618800	2.43579000	2.27639400
H	-2.81263000	2.36767300	-1.81748200
H	-4.97948500	1.42989400	-1.05886700
H	-3.62476900	1.46501400	3.01350600
N	-5.65364900	0.77717600	1.42807700
O	-5.87687000	0.71429400	2.61312400
O	-6.37497600	0.34432800	0.55935000
C	0.63011300	1.25409300	-0.61723000
C	2.89714400	1.61727600	2.40325200
H	3.97830000	1.48470100	2.22117900
H	2.51174800	0.66563100	2.80329100
H	2.78111500	2.39411700	3.17880700
C	3.32866400	5.14190500	-0.74966700
H	3.47755700	5.78950200	0.13225800
H	3.10453600	5.79309400	-1.60699000
H	4.28622600	4.63171300	-0.94659100
C	-1.13139000	4.08033300	-2.43116900
H	-0.68656900	4.84882100	-3.08109200
H	-2.13777500	4.41766100	-2.13457000
H	-1.24261000	3.15816400	-3.02975100
H	1.10745300	1.86047800	-1.38541800
C	-0.33814500	0.26869100	-1.15626200
O	-0.90052500	0.38215400	-2.21668300
O	-0.53307600	-0.76098100	-0.32006400
C	-1.42879100	-1.80455500	-0.70959900
C	-1.95736800	-4.22038700	-0.14460500
C	-3.83405000	-2.57765500	-0.44799300
C	-3.34601300	-3.79598400	0.33319900
C	-2.84752900	-1.42245400	-0.30090400
C	-0.94805600	-3.07051100	-0.01572700
H	-2.00774400	-4.51794700	-1.20721400
H	-3.93501000	-2.84531700	-1.51550100
H	-3.31007200	-3.55473500	1.41134000
H	-2.81514200	-1.08225000	0.75139000
H	-0.72223100	-2.86158700	1.04398300
H	-1.37176400	-1.94050900	-1.80245400
H	-1.58101400	-5.08717900	0.41905700
H	-4.82933200	-2.25354900	-0.10311500
H	-4.04340200	-4.64098900	0.21641000
H	-3.15034000	-0.56209500	-0.91566000
S	0.59961600	-3.69768400	-0.74607500
O	0.95256400	-4.88144800	0.03176900
O	0.37352700	-3.77732600	-2.18793200
C	1.89701700	-2.49324200	-0.48926300
H	2.35055500	-3.26954100	1.45347700
C	2.60740500	-2.53753600	0.68275500
C	3.30780900	-0.76786200	-1.38673300

C	3.71872600	-1.66935200	0.86401100
C	2.23973100	-1.61481800	-1.54742900
C	4.07526700	-0.77232600	-0.18663000
C	4.51125500	-1.70759800	2.04479700
H	1.65932000	-1.64102100	-2.47358600
H	5.48162000	0.75686800	-0.81846600
H	3.59267600	-0.08199800	-2.18979800
C	5.61243800	-0.89678500	2.17489300
H	4.23533000	-2.40649600	2.83907600
H	6.22238300	-0.94227600	3.08020300
C	5.96469000	0.00095300	1.13368600
H	6.84311500	0.64094600	1.24921100
C	5.21063800	0.06706300	-0.01429800

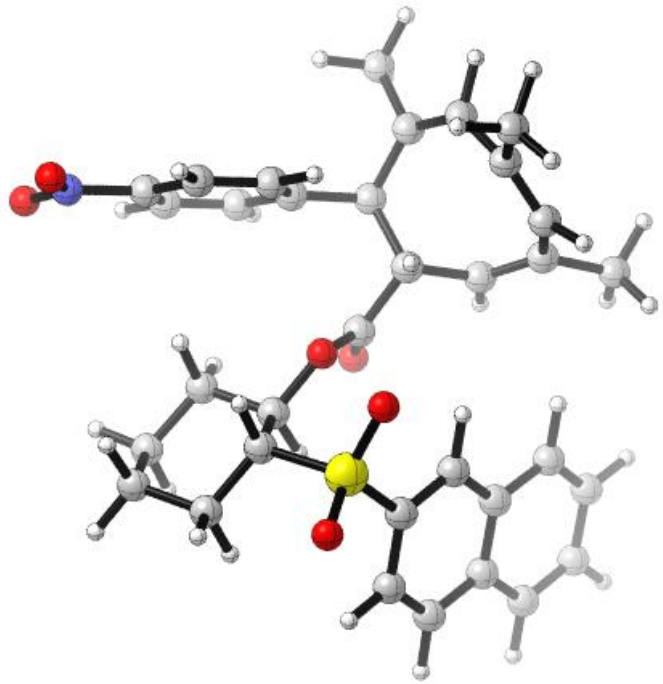

Parkerester_cyclooctatriene1_GS
E(M062X/def2TZVP) = -2220.804619 Hartree
Free energy correction (M062X/def2SVP) = 0.560376 Hartree
G = -5829251.26

C	0.71890400	3.90532400	1.49168400
C	-0.59063200	4.07340000	1.76328700
C	-1.66994100	4.26285300	0.76454000
C	0.84547800	2.73407900	-0.65771700
C	1.31090600	3.68939500	0.16327800
C	-2.09976900	3.60966100	-0.33149500
C	-1.61189500	2.28720300	-0.89535600
C	-0.26999500	1.79424600	-0.30469900
H	-2.26948900	5.14902100	1.01402300
H	1.42124800	3.96561900	2.33156900
H	1.29726400	2.58615600	-1.64468500
C	-2.69610400	1.22847800	-0.75685600

C	-4.62169300	-0.74214200	-0.48795000
C	-3.18920700	0.56223600	-1.88292900
C	-3.18578600	0.88550800	0.51076900
C	-4.15074300	-0.10361100	0.65624000
C	-4.16166400	-0.42765300	-1.75943800
H	-2.80108900	0.81846900	-2.87090700
H	-2.80303300	1.40475500	1.39235800
H	-4.54501500	-0.39045700	1.62973300
H	-4.56105500	-0.95994000	-2.62124300
N	-5.63714400	-1.80434400	-0.34292100
O	-5.99422900	-2.37230300	-1.34679500
O	-6.04022300	-2.03881200	0.77029900
H	-1.44326700	2.43048700	-1.97597200
C	-3.26637800	4.16769200	-1.10912800
H	-4.10901400	3.45864400	-1.12384300
H	-2.97767600	4.34101800	-2.15816300
H	-3.61829800	5.11689800	-0.68685100
C	-1.05139300	4.27773500	3.18522500
H	-0.21254400	4.23419400	3.89104100
H	-1.78173000	3.50387800	3.46846400
H	-1.55784600	5.24948400	3.29658400
C	2.48433500	4.55888000	-0.20264600
H	3.29251700	4.45035800	0.53899700
H	2.19446700	5.62035300	-0.20601900
H	2.88088900	4.30243400	-1.19469500
H	-0.37038400	1.69483600	0.78429800
C	0.01044800	0.41318600	-0.86626700
O	0.39148900	0.18396000	-1.98262100
O	-0.25411500	-0.52940200	0.04369300
C	-0.06183600	-1.89212500	-0.31979600
C	0.27618500	-4.17391500	0.67727900
C	-1.11273000	-3.90528700	-1.41036000
C	-0.91803000	-4.70035500	-0.12005200
C	-1.25156600	-2.41162800	-1.12109500
C	0.10183600	-2.68614600	0.97014600
H	1.20057800	-4.31824700	0.09120000
H	-0.24580500	-4.06742600	-2.07307000
H	-1.82752700	-4.62292600	0.49900200
H	-2.16537100	-2.21498700	-0.53425200
H	-0.77953500	-2.50973000	1.61103500
H	0.85332200	-1.96741600	-0.93156800
H	0.40554400	-4.71272300	1.62408400
H	-1.99816100	-4.26169700	-1.95568900
H	-0.77448900	-5.76773600	-0.34088500
H	-1.32254500	-1.83135000	-2.05195600
S	1.43654300	-2.04955100	2.04471300
O	0.96856600	-0.81409300	2.66095200
O	1.87739600	-3.17082800	2.87050400
C	2.76852600	-1.64502000	0.92896500

H	2.26482600	0.43528700	0.92165600
C	2.93069200	-0.34106900	0.53405400
C	4.64531600	-2.37655900	-0.38053400
C	3.98129500	-0.00914900	-0.36277700
C	3.63586600	-2.67985900	0.49756300
C	4.84158900	-1.04265100	-0.83748600
C	4.19899800	1.32832600	-0.79066300
H	3.50102100	-3.68802000	0.89202900
H	6.54331100	-1.49541500	-2.10421300
H	5.32685100	-3.15605900	-0.72641900
C	5.21802600	1.62445500	-1.66165000
H	3.53558500	2.10707000	-0.41295300
H	5.37907600	2.65382700	-1.98568000
C	6.06797100	0.59671300	-2.14326700
H	6.87346400	0.84476100	-2.83594000
C	5.88601600	-0.70359600	-1.73992100

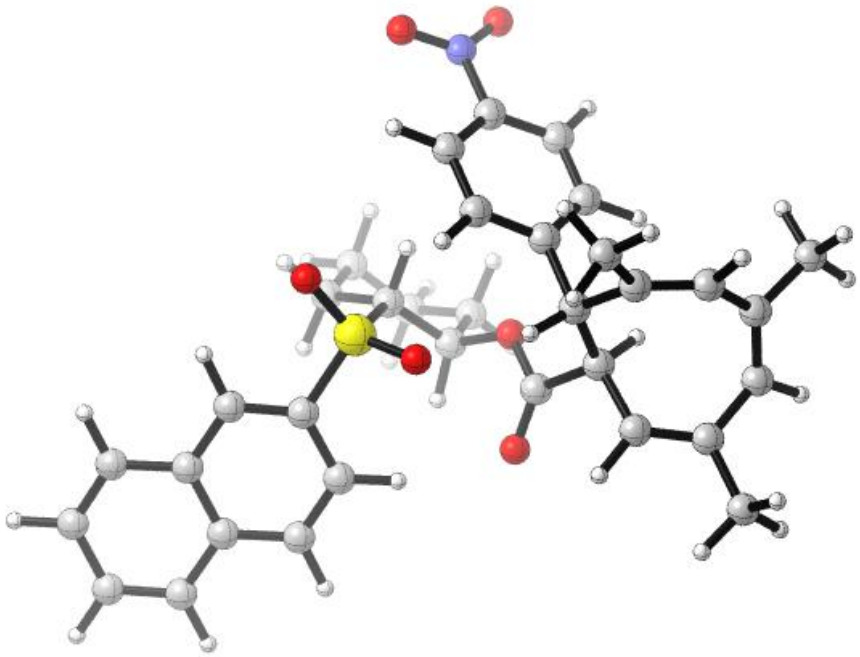

Parkerester_cyclooctatriene2_GS
E(M062X/def2TZVP) = -2220.802888 Hartree
Free energy correction (M062X/def2SVP) = 0.561801 Hartree
G = -5829242.974

C	-5.37115200	-1.99355000	0.27990400
C	-4.81363600	-3.01756500	0.95656200
H	-5.31055000	-3.35569800	1.87420500
C	-3.62769900	-3.77421900	0.52507900
C	-3.82194000	-1.18950700	-1.65569600
C	-4.97703600	-1.57579300	-1.08561200
H	-5.84139900	-1.57785800	-1.76395800
C	-2.48486000	-3.15116800	0.20143900
H	-1.61905300	-3.73781400	-0.11684500
C	-2.26173400	-1.67248700	0.34926200

C	-2.49022200	-0.89289500	-0.97441200
C	-2.40116600	0.62193200	-0.82133600
C	-2.23039600	3.37443700	-0.51733700
C	-3.19226400	1.28422900	0.12773700
C	-1.56138900	1.37786600	-1.64668100
C	-1.46395900	2.76020600	-1.49957200
C	-3.10771700	2.65986900	0.29564800
H	-3.87925600	0.70902400	0.75290700
H	-0.94331000	0.87531400	-2.39050900
H	-0.78961400	3.35378000	-2.11533000
H	-3.70091000	3.19156200	1.03768700
N	-2.11743200	4.83289100	-0.32928900
O	-1.34190600	5.42861500	-1.03731800
O	-2.80425000	5.33901300	0.52654100
H	-1.68824100	-1.19028900	-1.66589100
C	-3.79584500	-0.87642100	-3.13017700
H	-3.45752500	0.15604200	-3.31003000
H	-4.78340400	-1.00405100	-3.59055600
H	-3.08304000	-1.54054000	-3.64404800
C	-6.61323600	-1.31096500	0.79561300
H	-6.93093500	-1.72496300	1.76132800
H	-7.44148600	-1.41905300	0.07739600
H	-6.44262000	-0.22957700	0.91606100
C	-3.76552600	-5.27257200	0.48775800
H	-4.08476500	-5.65402200	1.47059900
H	-2.81709700	-5.75530400	0.21915900
H	-4.53485800	-5.57528400	-0.23892500
H	-2.96470800	-1.27523800	1.09708100
C	-0.87176800	-1.43642300	0.92719800
O	-0.03879600	-2.28010100	1.11340700
O	-0.71656100	-0.15040200	1.27627000
C	0.53774200	0.32503100	1.74881800
C	2.34091000	2.05196800	1.21486900
C	1.46618000	1.85879100	3.55405700
C	1.98003200	2.81964500	2.48494300
C	0.25233600	1.09194000	3.03960400
C	1.14138900	1.25603000	0.69611900
H	3.16762200	1.35811400	1.44166100
H	2.26800200	1.15112300	3.82547000
H	1.20399700	3.56919400	2.25709200
H	-0.56920000	1.79500700	2.82262900
H	0.34889800	1.94348600	0.35214000
H	1.20697100	-0.52789100	1.94552200
H	2.68599100	2.72821000	0.41970600
H	1.19958800	2.40213800	4.47162300
H	2.86130400	3.36990200	2.84389700
H	-0.12284400	0.37735100	3.78630400
S	1.58409900	0.43238400	-0.86792000
O	0.58739600	-0.59198500	-1.18770100

O	1.84577800	1.51386500	-1.81685000
C	3.11219600	-0.42605200	-0.55221500
H	4.26248900	1.10008900	-1.50937200
C	4.28350500	0.14248800	-0.98425200
C	4.24933600	-2.33993500	0.33553300
C	5.51262400	-0.53008200	-0.75187800
C	3.06643800	-1.68567100	0.09787700
C	5.49488400	-1.78571100	-0.07506200
C	6.75557700	0.01509500	-1.17545600
H	2.10342700	-2.11701000	0.38358300
H	6.71328200	-3.41533600	0.67625500
H	4.24557700	-3.31102800	0.83411600
C	7.92908700	-0.65468600	-0.93278500
H	6.75795100	0.97458000	-1.69604100
H	8.87913900	-0.23035300	-1.25990600
C	7.91364700	-1.90168200	-0.25777900
H	8.85324300	-2.42404400	-0.07233800
C	6.72741000	-2.45380600	0.15961300

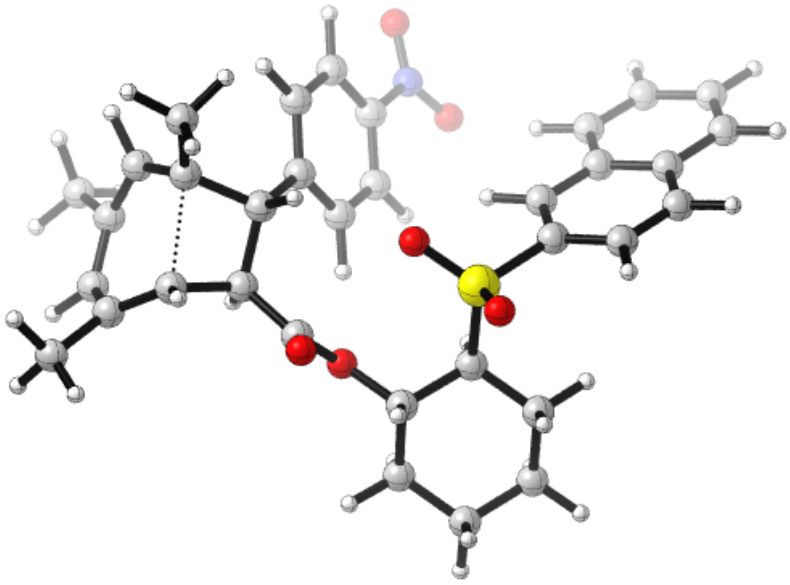

Parkerester_cyclooctatriene1_6π_TS
E(M062X/def2TZVP) = -2220.757223 Hartree
Free energy correction (M062X/def2SVP) = 0.560495 Hartree
G = -5829126.509

C	-5.54818100	0.46431900	-0.89824700
C	-5.01991800	1.73004400	-0.57374600
C	-4.44414200	1.98847300	0.68426000
C	-4.29846600	-0.80232800	0.72500800
C	-5.44773500	-0.64845800	-0.05336300
C	-3.69927300	1.12612300	1.50540100
C	-2.38358900	0.51409500	0.98593600
C	-2.92377200	-0.61213600	0.10714600
H	-4.76372000	2.93877100	1.13455300
H	-6.31719300	0.46011500	-1.67797000

H	-4.31276900	-1.53796600	1.53701600
C	-1.43392700	1.51128900	0.35089500
C	0.34262600	3.34148400	-0.76149600
C	-1.27505000	2.78990000	0.90603900
C	-0.68955600	1.18224400	-0.78980200
C	0.20263100	2.09106000	-1.35281200
C	-0.39164700	3.71213500	0.35973800
H	-1.85937800	3.07659000	1.78056300
H	-0.79769700	0.19206600	-1.23306300
H	0.78770600	1.84899000	-2.23968900
H	-0.26098000	4.70721100	0.78175000
N	1.28965400	4.30605600	-1.33975800
O	1.24418500	5.44442700	-0.94498600
O	2.06573100	3.89578900	-2.17671000
H	-1.85608700	0.05844200	1.84037500
C	-3.73427600	1.36373700	2.99688000
H	-2.83910200	1.90666900	3.34474600
H	-3.73252900	0.39950800	3.52649000
H	-4.63074300	1.91981200	3.30118200
C	-5.40784300	2.91017600	-1.43013400
H	-6.27428300	2.68860400	-2.06767100
H	-4.57104700	3.19427000	-2.08674400
H	-5.63923400	3.78839300	-0.80969100
C	-6.65747500	-1.52634900	0.15852700
H	-7.29293400	-1.52931400	-0.73821500
H	-7.27326400	-1.14130100	0.98771100
H	-6.38126300	-2.56207300	0.39525800
H	-3.01634900	-0.28796000	-0.93826900
C	-2.12305600	-1.89780800	0.17954100
O	-2.23716100	-2.71820200	1.04404800
O	-1.26593300	-2.02254200	-0.85560200
C	-0.34556200	-3.11167200	-0.84879300
C	0.56197200	-4.92555700	-2.36630100
C	2.13162400	-3.66268300	-0.87017400
C	1.96689600	-4.34566100	-2.22658800
C	1.07736100	-2.57482000	-0.65484000
C	-0.48409600	-3.83018100	-2.18736300
H	0.41273600	-5.70766900	-1.60322300
H	2.01923200	-4.40452000	-0.06337900
H	2.14666300	-3.61653100	-3.03447700
H	1.23363900	-1.71433200	-1.32676200
H	-0.37992000	-3.07680300	-2.98599400
H	-0.59245500	-3.78773700	-0.01544800
H	0.43432900	-5.40799000	-3.34574500
H	3.13713400	-3.22623300	-0.77207600
H	2.72643600	-5.13321600	-2.33344100
H	-1.50562800	-4.23138900	-2.25355900
S	1.25824500	-1.90548500	1.03131100
O	0.23917000	-0.87279900	1.22577000

O	1.34937600	-3.03974400	1.94463500
C	2.84131400	-1.08969400	0.98516700
H	2.02591000	0.62007600	-0.02344000
C	2.92174200	0.13961200	0.37935700
C	5.17983700	-1.08835500	1.51689800
C	4.17723200	0.79460300	0.29110800
C	3.96331100	-1.72204100	1.57196900
C	5.32232200	0.17374800	0.87387600
C	4.31685800	2.04761700	-0.36609400
H	3.83048400	-2.68616900	2.06473400
H	7.45150100	0.37000900	1.24208000
H	6.05979000	-1.54839900	1.97064000
C	5.54253000	2.66217500	-0.43176800
H	3.44247400	2.50380500	-0.83491000
H	5.64110400	3.62076800	-0.94257800
C	6.68052200	2.05423000	0.15772400
H	7.64753600	2.55620200	0.10094300
C	6.57503100	0.84054800	0.79245000

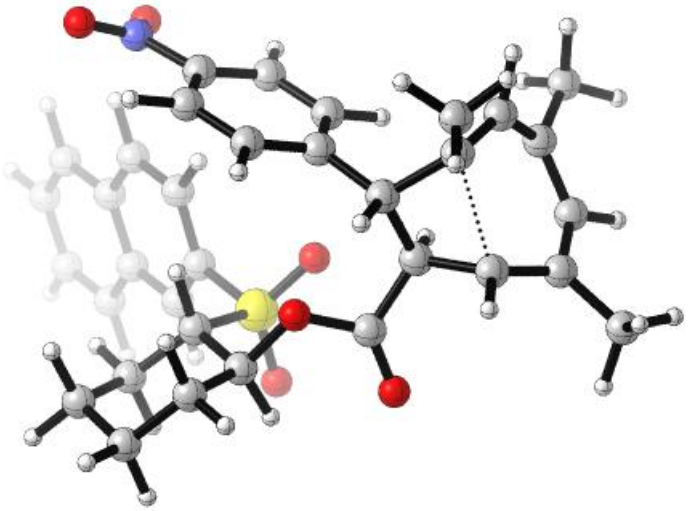

Parkerester_cyclooctatriene2_6π_TS
E(M062X/def2TZVP) = -2220.759580 Hartree
Free energy correction (M062X/def2SVP) = 0.558729 Hartree
G = -5829137.334

C	4.31200400	-1.51463700	2.21947100
C	4.62442700	-0.23305800	2.72277800
H	4.81551000	-0.17744000	3.79877800
C	5.01813000	0.83471100	1.92087800
C	4.51577700	-1.10282800	-0.30546800
C	4.51022900	-1.87621200	0.87867800
H	4.88798100	-2.90165200	0.75898700
C	4.54772100	0.89257300	0.60245100
H	5.03352200	1.61081100	-0.07123600
C	3.09329000	0.62966700	0.27800200
C	3.25865000	-0.39031300	-0.82522100

C	2.07118500	-1.26289400	-1.16289300
C	-0.20736200	-2.72536400	-1.75864700
C	1.42063000	-2.00141700	-0.16580800
C	1.56794100	-1.29893100	-2.46891100
C	0.42616900	-2.03107200	-2.78265300
C	0.27884900	-2.73617000	-0.45420700
H	1.79750400	-1.97731900	0.85708600
H	2.06628400	-0.71921400	-3.24855700
H	0.01235900	-2.06256400	-3.78946100
H	-0.25440200	-3.29301400	0.31497000
N	-1.46232800	-3.43571800	-2.05235000
O	-1.77053000	-3.58145300	-3.20883000
O	-2.11892300	-3.81646800	-1.10697100
H	3.54990600	0.14814000	-1.74142500
C	5.41040200	-1.59258300	-1.42031200
H	4.82410000	-2.17155300	-2.15574700
H	6.23319600	-2.21699300	-1.04964900
H	5.84496400	-0.73710100	-1.95862000
C	4.06714800	-2.62257300	3.21570400
H	4.52611300	-2.40569600	4.18974100
H	4.45310100	-3.58379900	2.84737900
H	2.98577800	-2.75040900	3.38418500
C	6.02275300	1.84682200	2.41045000
H	6.90358100	1.85408900	1.74953300
H	6.36631000	1.61833600	3.42738700
H	5.59567500	2.86012300	2.40019800
H	2.58271100	0.18282500	1.14619100
C	2.29303700	1.86779000	-0.04156900
O	2.40882900	2.92860900	0.49975200
O	1.40839400	1.61815900	-1.02927900
C	0.33698300	2.52619900	-1.24477600
C	-0.78578700	3.89701600	-3.04613700
C	-2.19147100	2.60623600	-1.40709900
C	-2.07518800	3.10431100	-2.84742800
C	-0.97549100	1.77044800	-1.00506700
C	0.42411100	3.04518800	-2.67530300
H	-0.80950200	4.79828000	-2.41100700
H	-2.25337100	3.46528900	-0.71892800
H	-2.08690600	2.24321900	-3.53676300
H	-0.93382200	0.80399500	-1.53609600
H	0.49149100	2.17224200	-3.34658600
H	0.41562400	3.35848900	-0.52682300
H	-0.69769300	4.24282500	-4.08595000
H	-3.10945400	2.01512900	-1.27539400
H	-2.95251100	3.71981800	-3.09263900
H	1.36255200	3.60955300	-2.77647800
S	-1.08045800	1.35146800	0.76618600
O	0.01023500	0.43428300	1.09932000
O	-1.22981200	2.61214500	1.48894000

C	-2.60991000	0.44727900	0.89509000
H	-3.58882700	2.06302800	1.89076500
C	-3.68598800	1.05045600	1.49293700
C	-3.85167700	-1.56021700	0.44482600
C	-4.91623000	0.34429700	1.58710000
C	-2.66904200	-0.86955400	0.37652400
C	-5.00121900	-0.97417100	1.04832300
C	-6.06317200	0.92064100	2.19778000
H	-1.77644000	-1.32259500	-0.05510200
H	-6.29791100	-2.68043400	0.72299000
H	-3.90875600	-2.57265900	0.03992300
C	-7.24231700	0.22027700	2.26696100
H	-5.98787700	1.92869700	2.60987000
H	-8.11823700	0.66929600	2.73705200
C	-7.32891300	-1.08887800	1.72991400
H	-8.27166700	-1.63427900	1.79200700
C	-6.23613300	-1.67189300	1.13587100

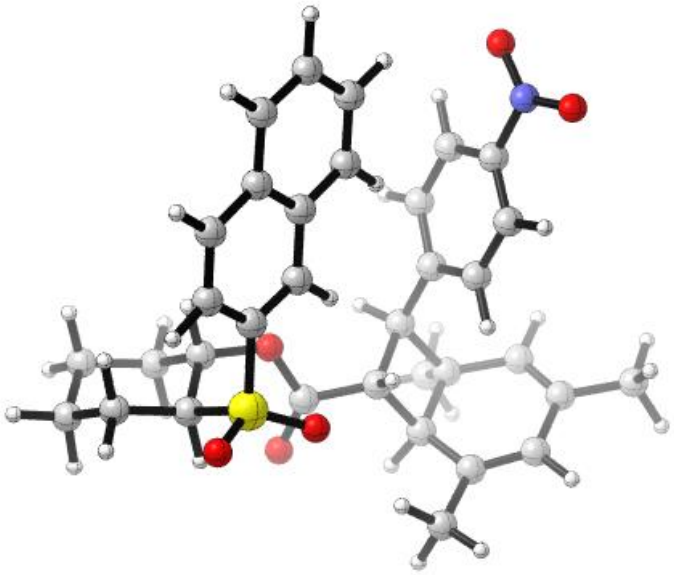

Parkerester_BOD1_GS
E(M062X/def2TZVP) = -2220.811070 Hartree
Free energy correction (M062X/def2SVP) = 0.565015 Hartree
G = -5829256.017

C	-1.39664800	-3.31348900	-0.01810200
C	-3.06481100	-3.28907800	-1.83538000
C	-3.83020800	-2.58043600	0.38358300
C	-4.11413900	-2.82289500	-0.90569000
C	-2.47015900	-2.79675300	0.98197200
C	-1.80278000	-3.53219800	-1.44814200
C	-0.57661600	-2.02987800	0.18841900
C	-1.60201200	-1.48896100	1.22264000
H	-4.61640700	-2.22025100	1.05571500
H	-3.34472600	-3.43235500	-2.88315600
H	-0.85109500	-4.19533800	0.35510700

C	-2.57294100	-3.63862800	2.24895300
H	-1.57606400	-3.81082600	2.68427800
H	-3.02346000	-4.61587400	2.02178200
H	-3.19901000	-3.13507500	3.00231000
C	-5.48417200	-2.61121900	-1.48375800
H	-5.86661200	-3.54277300	-1.92904400
H	-5.44954500	-1.86247400	-2.29125500
H	-6.19678000	-2.26853800	-0.72288000
C	-0.70068000	-3.96298800	-2.36672600
H	0.13087400	-3.23813400	-2.33460200
H	-1.04838700	-4.05690700	-3.40358400
H	-0.28660800	-4.93031000	-2.04066100
C	-2.24074400	-0.15945900	0.94275600
C	-3.49465600	2.27373400	0.46514800
C	-2.62270500	0.20574700	-0.35981300
C	-2.51477700	0.72495300	1.99530700
C	-3.13560500	1.95028400	1.76759800
C	-3.25825200	1.41765100	-0.60603600
H	-2.42906200	-0.47436500	-1.19247700
H	-2.22539500	0.45187600	3.01167500
H	-3.33176800	2.65817700	2.57148700
H	-3.56005000	1.71782600	-1.60827600
N	-4.10378500	3.58862500	0.20185500
O	-4.61445200	3.76139500	-0.87633600
O	-4.04556900	4.41472400	1.08513600
H	-1.19203500	-1.47832200	2.24260900
H	-0.51040600	-1.40811200	-0.71842600
C	0.84126000	-2.20249900	0.65328300
O	1.45750400	-3.23250100	0.65385200
O	1.34391700	-1.02247100	1.05939600
C	2.74837200	-0.86432800	1.25194600
C	4.74960200	-1.23233700	2.70870400
C	5.03682000	-0.83073000	0.22875300
C	5.59325900	-1.53270200	1.46941800
C	3.57630300	-1.22340100	0.01415500
C	3.28282800	-1.59936500	2.47909200
H	4.82505100	-0.15781400	2.94836700
H	5.10253100	0.26431700	0.35885300
H	5.60239100	-2.62060500	1.29000100
H	3.48798500	-2.30211200	-0.19497100
H	3.17565000	-2.68216900	2.32185800
H	2.85572800	0.21921000	1.42242600
H	5.13897000	-1.77772600	3.58005600
H	5.61006300	-1.08763500	-0.67114700
H	6.63721600	-1.22750500	1.62997000
H	2.66473000	-1.32150700	3.34563300
S	2.92066100	-0.51627500	-1.52774000
O	3.99941600	-0.56264400	-2.50894700
O	1.64613000	-1.18539700	-1.80351400

C	2.57174000	1.19421600	-1.17091100
H	0.60068200	0.74920500	-0.44623200
C	1.34604100	1.52100300	-0.64674300
C	3.27571100	3.49249400	-1.18875400
C	1.05363800	2.87484100	-0.34719000
C	3.55280400	2.17504900	-1.46110000
C	2.02663300	3.87829500	-0.62410300
C	-0.19424100	3.24172600	0.22221400
H	4.49416900	1.86541100	-1.91726300
H	2.44262800	6.00719400	-0.54387700
H	4.01232100	4.26587600	-1.41469900
C	-0.47881800	4.55628800	0.49562900
H	-0.91086500	2.44921400	0.43860100
H	-1.44413700	4.83024000	0.92762300
C	0.48420900	5.55994200	0.21118300
H	0.24925000	6.60304400	0.42783400
C	1.70449800	5.23184000	-0.32988600

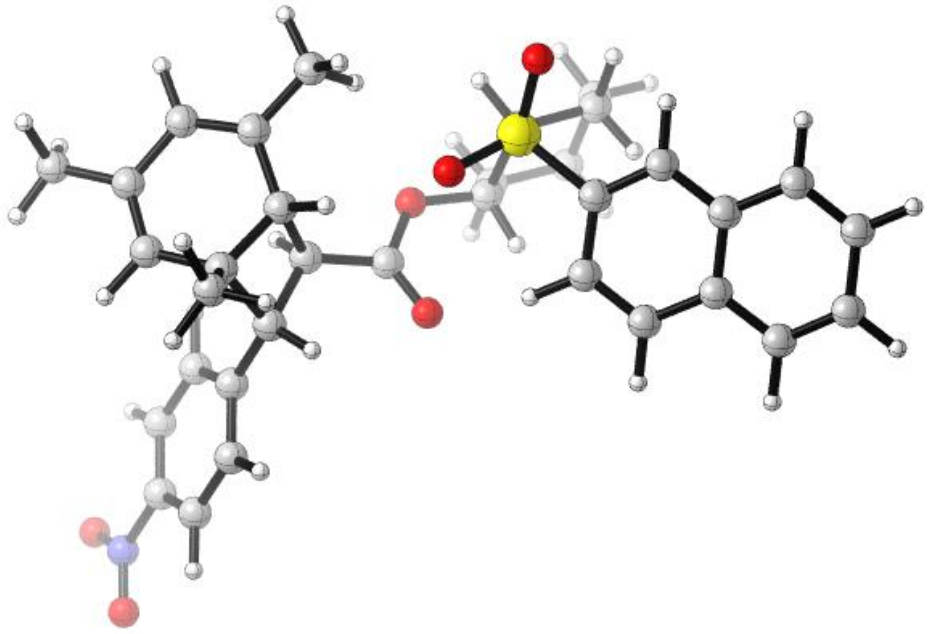

Parkerester_BOD2_GS
E(M062X/def2TZVP) = -2220.812211 Hartree
Free energy correction (M062X/def2SVP) = 0.562295 Hartree
G = -5829266.154

C	-2.77092200	-0.94274400	-1.88948400
C	-4.02187900	-2.99437800	-1.17254900
C	-1.55776500	-3.09142200	-0.98442000
C	-2.75056000	-3.70756000	-0.94175900
C	-1.52473100	-1.61468900	-1.25277600
C	-4.02641400	-1.71581500	-1.58668900
H	-0.61011800	-1.33536100	-1.79396000
H	-2.80320600	-4.77695500	-0.71673200
H	-4.97916000	-1.21143600	-1.78155200

C	-2.54103000	0.26378300	-0.91136200
C	-1.70305400	-0.66653100	-0.02461400
C	-2.70095900	-0.60077200	-3.37101500
H	-3.56714200	0.01249300	-3.66654000
H	-2.71101100	-1.51859500	-3.97723800
H	-1.78200700	-0.04017700	-3.59991400
C	-5.28772100	-3.77073800	-0.94034300
H	-6.17841000	-3.15909100	-1.13300400
H	-5.33386800	-4.14003800	0.09616800
H	-5.32314900	-4.65527100	-1.59539200
C	-0.25321200	-3.77231600	-0.70664000
H	0.21245100	-3.31066500	0.17896900
H	0.45719200	-3.62331400	-1.53360400
H	-0.38804900	-4.84677900	-0.52554000
H	-1.85348900	0.97186800	-1.39677500
C	-3.71853400	1.01814800	-0.36789900
C	-5.94043100	2.42020500	0.53409400
C	-4.05731700	2.25974900	-0.92362300
C	-4.52711400	0.49585100	0.65266500
C	-5.63975700	1.19184000	1.11215700
C	-5.16803600	2.97070200	-0.48137400
H	-3.43099100	2.67768000	-1.71402500
H	-4.29044300	-0.47568200	1.08827700
H	-6.27800900	0.80423400	1.90435400
H	-5.44310200	3.93768200	-0.89919800
N	-7.11815700	3.16541200	1.01766300
O	-7.35663400	4.22846600	0.49694900
O	-7.76885500	2.66446200	1.90309500
H	-2.28669200	-1.18361200	0.75011300
C	-0.45947400	-0.08551000	0.58193300
O	-0.04934600	1.02767000	0.38986400
O	0.15170300	-0.98119300	1.37782200
C	1.40279400	-0.65257200	1.97406000
C	2.56638000	-0.72258100	4.23211700
C	3.80942100	-1.46088700	2.18507100
C	3.59851200	-1.70164800	3.67846400
C	2.49124500	-1.56986300	1.41449000
C	1.24638300	-0.85945300	3.48010900
H	2.94815700	0.30735100	4.12952600
H	4.22628000	-0.44957300	2.04376000
H	3.25174400	-2.73556400	3.84226600
H	2.12536900	-2.61126000	1.43833800
H	0.83145200	-1.86956200	3.63230100
H	1.64510500	0.40029000	1.75921200
H	2.40210400	-0.89345300	5.30545600
H	4.52719800	-2.17509800	1.75728600
H	4.55759000	-1.59856600	4.20569000
H	0.49613000	-0.14412700	3.84658600
S	2.80838500	-1.36693100	-0.36819900

O	3.67394200	-2.48442000	-0.73527300
O	1.53433500	-1.16400000	-1.05798600
C	3.74808200	0.13917400	-0.53425000
H	5.57318000	-0.94667000	-0.77410200
C	5.10303300	0.03804500	-0.72738900
C	3.81329300	2.53351200	-0.64044000
C	5.87822300	1.21847700	-0.87668600
C	3.07264400	1.38571500	-0.50620900
C	5.22391100	2.48497300	-0.82464700
C	7.28521600	1.16959400	-1.07617900
H	1.98715700	1.41878800	-0.38791500
H	5.50204100	4.63355200	-0.93049500
H	3.31919900	3.50669000	-0.62062000
C	8.01019600	2.32731000	-1.21229000
H	7.77595600	0.19545400	-1.11922200
H	9.08928900	2.28263100	-1.36471100
C	7.36167000	3.58730700	-1.15758700
H	7.94957700	4.49958300	-1.26809800
C	6.00348300	3.66471300	-0.96958500

Structure	Number of imaginary frequencies	Free energy correction (Hartree)	Electronic energy (Hartree)	Relative Gibbs free energy (kJ/mol)
Parkeroxazoline_tetraene_GS	0	0.478297	-1572.415676	0.000
Parkeroxazoline_tetraene_8π1_TS	1	0.488548	-1572.402645	61.127
Parkeroxazoline_tetraene_8π2_TS	1	0.488392	-1572.403239	59.158
Parkeroxazoline_tetraene_8π3_TS	1	0.489561	-1572.396656	79.511
Parkeroxazoline_tetraene_8π4_TS	1	0.487332	-1572.402619	58.003
Parkeroxazoline_cyclooctatriene1_GS	0	0.488951	-1572.446116	-51.948
Parkeroxazoline_cyclooctatriene2_GS	0	0.488258	-1572.446004	-53.474
Parkeroxazoline_cyclooctatriene1_6π_TS	1	0.483587	-1572.397068	62.744
Parkeroxazoline_cyclooctatriene2_6π_TS	1	0.48282	-1572.396456	62.337
Parkeroxazoline_BOD1_GS	0	0.485119	-1572.450053	-72.346
Parkeroxazoline_BOD2_GS	0	0.484775	-1572.449308	-71.293

Table S6: Calculated relative free energies of Parker Chiral Oxazoline compound

Parker Chiral Oxazoline compound Cartesian Coordinates

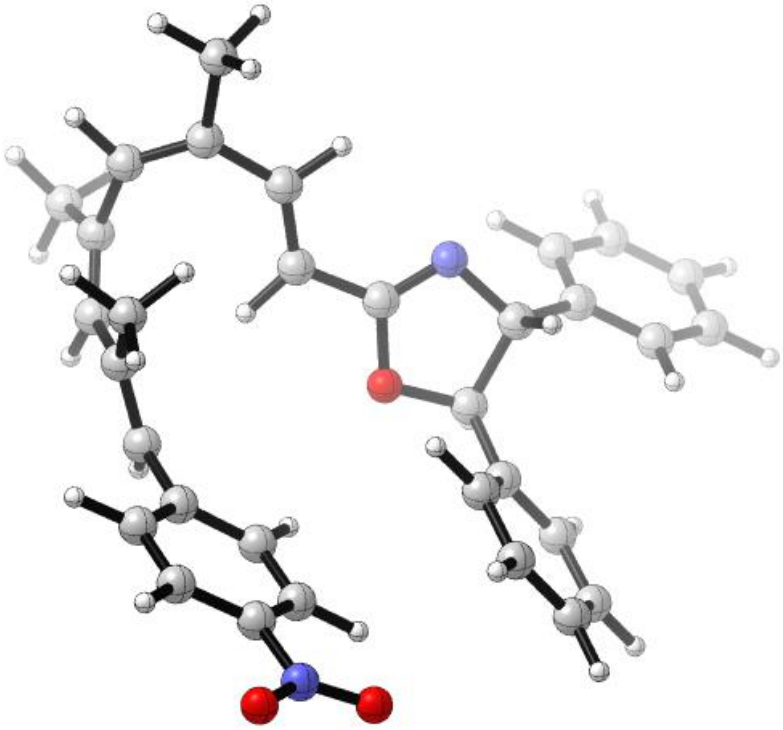

Parkeroxazoline_tetraene_GS
E(M062X/def2TZVP) = -1572.415676 Hartree

Free energy correction (M062X/def2SVP) = 0.478297 Hartree
G = -4127121.589

C	-1.35920600	4.74110600	-0.96441000
C	-1.06673500	5.07230900	0.44978600
H	-1.53328700	6.00988500	0.78126100
C	-0.20287800	4.51142700	1.32273400
C	-2.05010000	3.68519200	-1.43874500
H	-2.13330600	3.61749900	-2.52855100
C	-2.67384100	2.55962400	-0.71941400
C	0.63076700	3.31549000	1.11145300
H	1.48374500	3.21889900	1.79365000
C	0.46647600	2.30152000	0.24535700
C	-2.81827900	1.41099300	-1.41705100
H	-2.45216500	1.39925400	-2.44962600
C	1.37853900	1.15327400	0.24030900
C	-3.29279900	0.10544500	-0.91330500
C	-4.08469400	-2.38744800	0.01132500
C	-2.46067900	-1.01468700	-1.07681300
C	-4.54717700	-0.06429500	-0.30443000
C	-4.95009900	-1.30974100	0.16512100
C	-2.84941800	-2.26619300	-0.61444400
H	-1.47939300	-0.89123300	-1.54021000
H	-5.21733100	0.79138700	-0.21058100
H	-5.91637200	-1.46308800	0.64300800
H	-2.20822400	-3.13972400	-0.72085400
N	-4.48460400	-3.70421500	0.53916500
O	-3.65686400	-4.58553500	0.52267500
O	-5.60938100	-3.81800900	0.96202800
C	-3.02438500	2.69508700	0.73746200
H	-3.65909700	1.87230200	1.08161800
H	-3.53598300	3.64920700	0.92662300
H	-2.11087200	2.69273400	1.34920600
C	-0.82968600	5.78559600	-1.91770100
H	-1.11971600	5.57390400	-2.95494100
H	0.26844300	5.83469200	-1.85731700
H	-1.20795800	6.78346700	-1.64421900
C	-0.00033700	5.14449700	2.67898600
H	-0.25326500	4.43255400	3.48006200
H	-0.61837800	6.04200900	2.80496900
H	1.05517500	5.42285900	2.82168100
H	-0.35573200	2.23680000	-0.46115900
N	2.46411100	1.01785400	0.88559100
O	0.96120300	0.10730800	-0.52371900
C	2.01258300	-0.86129100	-0.50197800
H	2.55198000	-0.80019100	-1.46180000
C	2.93359500	-0.34070600	0.65234500
H	2.74479600	-0.93473800	1.56439800
C	4.40003400	-0.45132500	0.31192100

C	7.08449200	-0.72971100	-0.43556700
C	5.04984100	-1.68246200	0.45172100
C	5.10653300	0.64121000	-0.19562800
C	6.44370300	0.50184000	-0.56617300
C	6.38456100	-1.82267700	0.07561100
H	4.50394100	-2.53567100	0.86313900
H	4.59934700	1.60356400	-0.28055400
H	6.99028700	1.36239700	-0.95547900
H	6.88285700	-2.78661700	0.19039900
H	8.13104700	-0.83649300	-0.72487000
C	1.47947300	-2.25207700	-0.29919500
C	0.56746800	-4.85868900	0.15792600
C	0.38981600	-2.47959500	0.54771500
C	2.10918900	-3.33774000	-0.91401200
C	1.65837700	-4.63705500	-0.68171100
C	-0.06686400	-3.77752900	0.77199100
H	-0.11345900	-1.62866000	1.01243100
H	2.95640700	-3.16072900	-1.58109600
H	2.15387600	-5.47836100	-1.16854400
H	-0.93631400	-3.94942300	1.40937500
H	0.20309600	-5.87237900	0.32968000

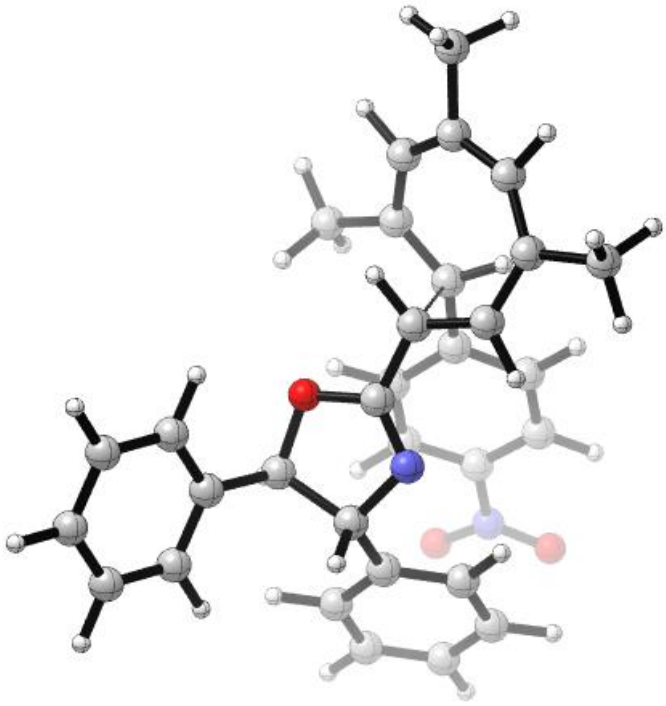

Parkeroxazoline_tetraene_8π1_TS
E(M062X/def2TZVP) = -1572.402645 Hartree
Free energy correction (M062X/def2SVP) = 0.488548 Hartree
G = -4127060.462

C	5.12278600	-0.62265700	-0.48388000
C	4.97011100	-0.77597200	0.92095800
H	5.94025800	-1.03106200	1.37301100
C	3.99115000	-0.65617500	1.92458300

C	4.23734500	-0.56440200	-1.57686700
H	4.73728500	-0.29550400	-2.51390600
C	2.86109300	-0.81217600	-1.73936400
C	2.69084000	-0.14683400	1.80864400
H	2.00088900	-0.28790500	2.64782300
C	2.17407600	0.44988700	0.66884000
C	2.11139300	-1.34685400	-0.68419800
H	2.71408600	-1.85747200	0.06843800
C	0.79858600	0.94669900	0.66004300
C	0.72378300	-1.83935800	-0.72486300
C	-1.83604000	-2.95716500	-0.74698400
C	0.40886600	-2.95553900	0.07420200
C	-0.30955400	-1.26614900	-1.48943800
C	-1.58220900	-1.82555600	-1.51275400
C	-0.85878000	-3.52061900	0.06696100
H	1.18807600	-3.39950400	0.70032400
H	-0.12942700	-0.35836200	-2.06359200
H	-2.38408300	-1.39185000	-2.11144600
H	-1.09919000	-4.39428500	0.67400500
N	-3.16836900	-3.57017300	-0.79147900
O	-3.41178200	-4.44412300	0.01402300
O	-3.94705000	-3.16749300	-1.62872000
C	2.24271300	-0.41556600	-3.05813600
H	3.02062800	-0.26858800	-3.82472900
H	1.69457400	0.53965300	-2.96187600
H	1.53496700	-1.17478000	-3.43032900
C	6.59875600	-0.55497800	-0.87764300
H	7.11870600	0.26543600	-0.35304500
H	6.73758100	-0.40675200	-1.95987700
H	7.11262300	-1.49483700	-0.60593700
C	4.42942600	-1.10033700	3.31045500
H	5.14540900	-0.37747900	3.74321000
H	4.92800000	-2.08436300	3.28723400
H	3.57410900	-1.16842000	4.00144900
H	2.84764300	0.92228700	-0.04427000
N	-0.08015400	0.77165500	1.55884200
O	0.43393600	1.62027200	-0.45868300
C	-0.91874000	2.03742800	-0.27548400
H	-1.49761900	1.61625600	-1.11402400
C	-1.31576300	1.37363400	1.08699400
H	-1.60921400	2.16516400	1.80142500
C	-2.45624200	0.36867100	1.03086600
C	-4.59817300	-1.45271500	1.02998800
C	-3.55959700	0.56174200	0.19216600
C	-2.43896800	-0.75186300	1.86759800
C	-3.50244300	-1.65331900	1.86915700
C	-4.62058300	-0.34315800	0.18706000
H	-3.60311900	1.42383800	-0.48100200
H	-1.57235800	-0.91619900	2.51161600

H	-3.46754600	-2.53362600	2.51764700
H	-5.46581500	-0.18503000	-0.48902200
H	-5.41809900	-2.17580400	1.01204500
C	-1.03071700	3.54792100	-0.29145300
C	-1.30130700	6.34220600	-0.31286900
C	0.08139400	4.36410500	-0.50946800
C	-2.28002800	4.14473800	-0.08153900
C	-2.41688200	5.53148500	-0.09501300
C	-0.05427700	5.75431400	-0.51663100
H	1.05877400	3.90506900	-0.67339700
H	-3.16043900	3.52058000	0.10630100
H	-3.40029200	5.98147700	0.06991100
H	0.82603700	6.38246700	-0.68396100
H	-1.40571400	7.43135800	-0.32012300

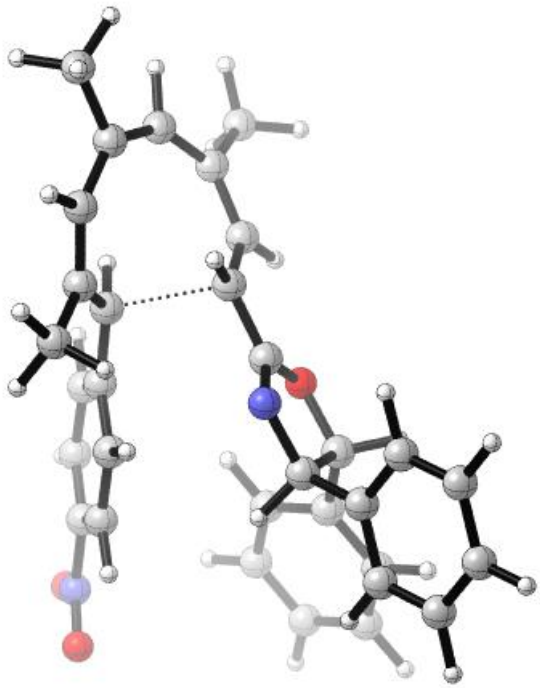

Parkeroxazoline_tetraene_8π2_TS
E(M062X/def2TZVP) = -1572.403239 Hartree
Free energy correction (M062X/def2SVP) = 0.488392 Hartree
G = -4127062.431

C	5.31050500	0.67822300	-0.26007600
C	5.09280800	0.52991900	1.13350200
H	6.05251100	0.54066100	1.66524800
C	4.02880800	0.41768900	2.05151300
C	4.51823300	0.49252300	-1.41237800
H	5.00701200	0.86429300	-2.32115000
C	3.26559100	-0.08949500	-1.66146600
C	2.65831500	0.57992100	1.81648900
H	1.97221400	0.29753300	2.62254700
C	2.09512500	0.98729600	0.61295100
C	2.59205000	-0.78264400	-0.64353100

H	3.24277900	-1.13428800	0.15846200
C	0.65018100	1.17344200	0.47819700
C	1.37892600	-1.60596100	-0.79302100
C	-0.83724600	-3.29125800	-1.01015400
C	1.30292800	-2.80655700	-0.06083400
C	0.28455800	-1.25931000	-1.60834100
C	-0.81808700	-2.09729000	-1.72259500
C	0.20921300	-3.65590700	-0.16884900
H	2.13218300	-3.08462800	0.59613100
H	0.27744100	-0.30633400	-2.13625300
H	-1.67077700	-1.83122000	-2.34837700
H	0.15379300	-4.59148700	0.38914500
N	-2.01020900	-4.16815700	-1.11547900
O	-2.04959100	-5.14225500	-0.39109600
O	-2.86962600	-3.86604100	-1.91291100
C	2.65486300	0.14958000	-3.02078100
H	3.42322200	0.47605100	-3.73943900
H	1.89542500	0.95168400	-2.96454700
H	2.16734800	-0.75201300	-3.42690400
C	6.74528000	1.07902000	-0.60789900
H	6.75602400	1.85960600	-1.38781100
H	7.31023200	0.21506700	-1.00469800
H	7.29591000	1.47337400	0.26022200
C	4.40376500	0.07231700	3.48338300
H	3.85396700	0.69809000	4.20675600
H	5.48175100	0.20123300	3.67283700
H	4.15314200	-0.98163700	3.70569800
H	2.67695900	1.60227100	-0.07018700
N	0.06989900	1.69507000	-0.53051700
O	-0.12367000	0.71258500	1.48328500
C	-1.46157100	1.12156000	1.19536200
H	-1.68800300	1.98831700	1.84108200
C	-1.36320700	1.58777400	-0.29695700
H	-1.76129900	0.79043600	-0.95232300
C	-2.13824900	2.85619100	-0.56777500
C	-3.63265400	5.20055200	-0.94142500
C	-3.49764100	2.78773000	-0.89154800
C	-1.53127000	4.10947800	-0.44412100
C	-2.27354500	5.27534000	-0.63155100
C	-4.24330900	3.95302000	-1.07215000
H	-3.97749000	1.80974200	-1.00533300
H	-0.46329900	4.16394400	-0.21445300
H	-1.78604400	6.25062400	-0.53879200
H	-5.30590300	3.88481500	-1.32452000
H	-4.21393400	6.11567400	-1.08791300
C	-2.45278300	0.01914200	1.44561400
C	-4.36264800	-2.00818000	1.73354100
C	-2.06767500	-1.32199200	1.40014500
C	-3.79744000	0.33979500	1.65978400

C	-4.74950300	-0.66928200	1.79726600
C	-3.01882500	-2.33150700	1.54454200
H	-1.01336000	-1.57100400	1.25635400
H	-4.10196600	1.39002400	1.71582200
H	-5.79947900	-0.40801100	1.95876100
H	-2.71029500	-3.38046900	1.50317400
H	-5.10776900	-2.80182400	1.83720800

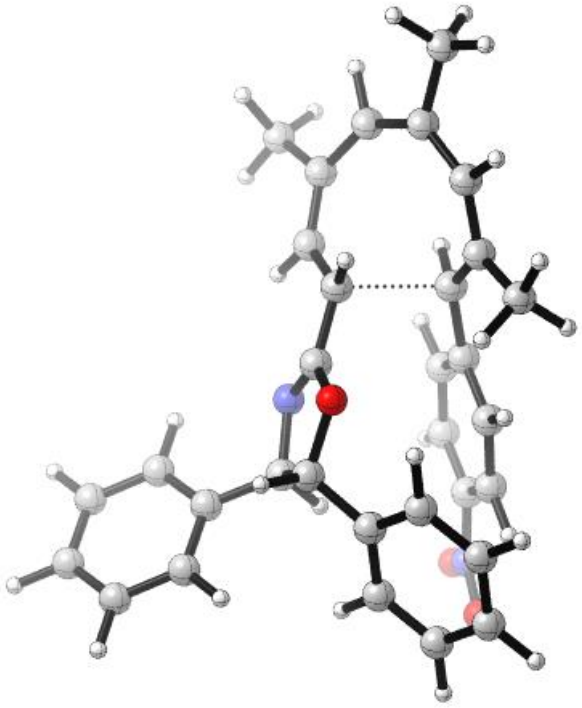

Parkeroxazoline_tetraene_8π3_TS
E(M062X/def2TZVP) = -1572.396656 Hartree
Free energy correction (M062X/def2SVP) = 0.489561 Hartree
G = -4127042.078

C	-5.35705700	-0.00054500	-0.55576600
C	-5.12642100	1.19333700	0.15306300
H	-6.08224500	1.69128300	0.37174800
C	-4.05080700	1.98319900	0.65510000
C	-4.54475200	-1.10298900	-0.95886100
H	-5.04300400	-1.73303500	-1.70379800
C	-3.27689100	-1.57113800	-0.61287400
C	-2.68928300	1.84390800	0.42202800
H	-2.00215700	2.44824500	1.02369800
C	-2.54317200	-0.95754600	0.44598600
H	-3.19468600	-0.44836700	1.15671100
C	-1.26775500	-1.34936600	1.06873200
C	1.23359800	-1.72090700	2.29049900
C	-0.94317900	-0.71668600	2.29348400
C	-0.29133200	-2.18677900	0.49119100
C	0.94702400	-2.38105600	1.09620100
C	0.29024100	-0.89293300	2.90684300
H	-1.67119800	-0.03758800	2.74754600

H	-0.45945400	-2.66863400	-0.46525500
H	1.70009800	-3.01365600	0.62821600
H	0.54363800	-0.38540600	3.83859200
N	2.56513000	-1.87172900	2.89688700
O	2.74258500	-1.39186000	4.00674900
O	3.42129200	-2.45931400	2.24819000
C	-2.08976200	0.93266000	-0.47412400
C	-4.48454600	3.14310500	1.54299400
H	-5.11387800	3.85553600	0.97614700
H	-3.62027300	3.70456400	1.93347000
H	-5.08629100	2.79817200	2.40462800
C	-6.82618200	-0.13755600	-0.97981000
H	-7.48201600	-0.19316400	-0.09064000
H	-7.01098000	-1.04447300	-1.57745100
H	-7.16018600	0.73214500	-1.57460800
C	-2.69265400	-2.66330300	-1.47784300
H	-3.43377700	-3.02944600	-2.20648100
H	-2.34514400	-3.52430900	-0.88180200
H	-1.82642100	-2.28046500	-2.04870800
H	-2.62753000	0.66083700	-1.38125700
C	-0.63160900	0.96796900	-0.61087000
N	0.18205100	1.51986400	0.20081200
O	-0.11738500	0.27260300	-1.65900400
C	1.53194800	1.22093200	-0.25653500
H	1.99197200	0.56926400	0.51120400
C	1.32254700	0.41068300	-1.58342000
H	1.61735200	1.02431700	-2.45283700
C	1.98036300	-0.94990100	-1.67701000
C	3.13416600	-3.51302500	-1.85525100
C	1.36812800	-1.95841500	-2.43763700
C	3.19008100	-1.23520900	-1.03016900
C	3.76515300	-2.50779200	-1.11926800
C	1.93345500	-3.23193300	-2.51915900
H	0.42466000	-1.74490500	-2.94585700
H	3.68408700	-0.48066900	-0.41295300
H	4.69007200	-2.71794500	-0.57577700
H	1.43148500	-4.01214500	-3.10030300
H	3.57262100	-4.51411200	-1.90897300
C	2.40059700	2.46092400	-0.40671100
C	4.04349900	4.73794800	-0.65201000
C	3.58660400	2.41250000	-1.15644300
C	2.04506600	3.66674800	0.21516000
C	2.86084200	4.79618500	0.09229800
C	4.40396300	3.54023300	-1.27785600
H	3.88107900	1.48717600	-1.66226500
H	1.11741300	3.71170200	0.78972900
H	2.56687700	5.73168600	0.57980400
H	5.32426700	3.48190800	-1.86762000
H	4.68018800	5.62359500	-0.74804800

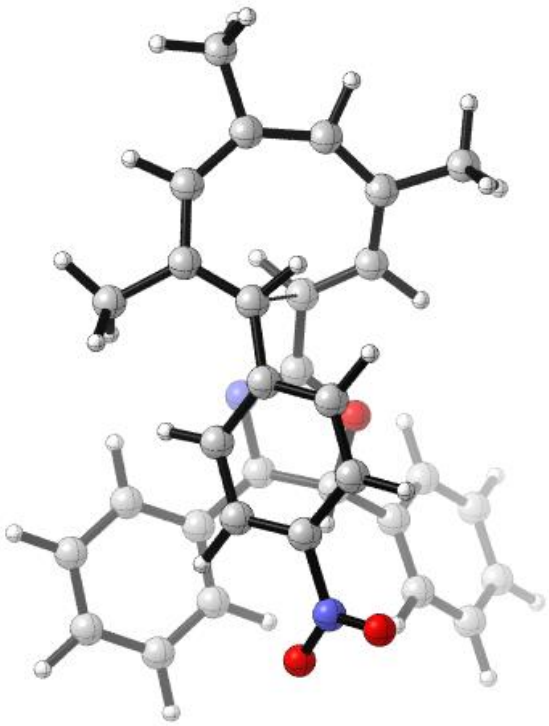

Parkeroxazoline_tetraene_8π4_TS
E(M062X/def2TZVP) = -1572.402619 Hartree
Free energy correction (M062X/def2SVP) = 0.487332 Hartree
G = -4127063.586

C	-5.34789200	-0.07030400	-0.49657600
C	-5.09464000	1.18840300	0.10609300
H	-6.04703200	1.69364600	0.31816400
C	-4.01335000	2.01581800	0.47892100
C	-4.57331700	-1.22055400	-0.76369000
H	-5.09109100	-1.94282700	-1.40471200
C	-3.29604200	-1.64414200	-0.37111700
C	-2.65862200	1.84479100	0.18296000
H	-1.93707100	2.48504700	0.70239900
C	-2.58598200	-0.90150000	0.58852300
H	-3.23249200	-0.28784400	1.21695300
C	-1.30164800	-1.20504600	1.24266500
C	1.19082200	-1.39723700	2.48471100
C	-1.06836800	-0.62042000	2.50343900
C	-0.24968500	-1.92159800	0.64530400
C	0.99687600	-2.01331100	1.25390700
C	0.16256000	-0.71855700	3.13407800
H	-1.87017300	-0.05236600	2.98380500
H	-0.36620800	-2.36706500	-0.33853000
H	1.82427900	-2.52401000	0.75683500
H	0.34791300	-0.25455200	4.10384300
N	2.52867000	-1.40489400	3.08623500
O	2.61939800	-1.12855600	4.26250800
O	3.46632800	-1.66997100	2.36074600
C	-2.15375900	0.84948900	-0.65200200

C	-4.35544400	3.22754200	1.33019700
H	-3.72588600	4.09557400	1.07218900
H	-4.19060300	3.00703500	2.40208600
H	-5.41074100	3.52680800	1.21751900
C	-6.81132600	-0.20045200	-0.92140800
H	-7.47864100	-0.09481900	-0.04761000
H	-7.02856200	-1.17543400	-1.38420000
H	-7.09068400	0.58664800	-1.64339600
C	-2.70680700	-2.83130000	-1.09011400
H	-3.48160700	-3.36438500	-1.66300100
H	-2.23756900	-3.55046700	-0.39856700
H	-1.93646800	-2.49934700	-1.81113100
H	-2.78210200	0.46665300	-1.45522900
C	-0.72020600	0.75488100	-0.93258100
N	-0.19920200	0.11308900	-1.90147700
O	0.10650500	1.35734300	-0.05336600
C	1.24442800	0.26032100	-1.78335000
H	1.59113500	0.91130700	-2.60953100
C	1.44595200	1.00328800	-0.41786600
H	1.81859400	0.30511500	0.34769800
C	2.33348200	2.21853600	-0.46438500
C	4.03769900	4.43606000	-0.63786400
C	3.57409600	2.20963700	0.17957700
C	1.94565100	3.35492500	-1.18318300
C	2.79073000	4.45920000	-1.26648500
C	4.42779500	3.30998100	0.08623900
H	3.87649700	1.33222200	0.76220100
H	0.96852300	3.37654200	-1.67714000
H	2.47582500	5.34374100	-1.82779400
H	5.39987000	3.28762200	0.58709700
H	4.70541700	5.30059900	-0.70998100
C	1.99549400	-1.05395000	-1.88472200
C	3.38729200	-3.49187800	-1.98414900
C	3.33116800	-1.13091900	-1.47582000
C	1.37494000	-2.20587900	-2.37599800
C	2.06386600	-3.41801400	-2.41987200
C	4.02216500	-2.34023600	-1.51943000
H	3.84236000	-0.23733400	-1.10651600
H	0.33785300	-2.14169100	-2.71403000
H	1.56096700	-4.31382800	-2.79661900
H	5.06097000	-2.38210100	-1.17973800
H	3.92501200	-4.44384100	-2.01148900

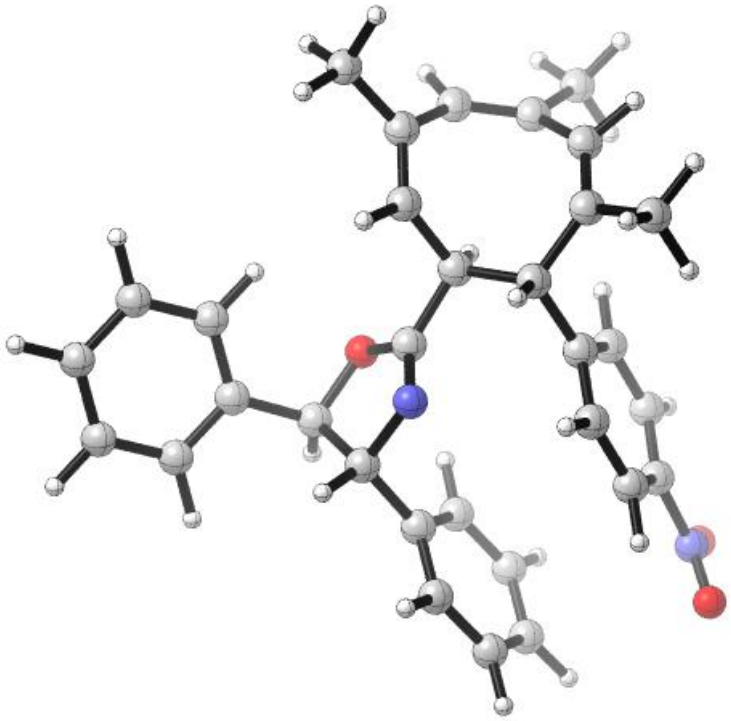

Parkeroxazoline_cyclooctatriene1_GS
E(M062X/def2TZVP) = -1572.446116 Hartree
Free energy correction (M062X/def2SVP) = 0.488951 Hartree
G = -4127173.537

C	2.74313000	-3.46458800	-1.04075900
C	1.59051200	-4.15742500	-0.94145100
C	0.75719200	-4.29398900	0.27728300
C	2.57282300	-1.61033100	0.55238400
C	3.31046400	-2.57759000	-0.01504500
C	0.17587500	-3.44416900	1.14488900
C	0.11309400	-1.92840200	1.08347200
C	1.15625000	-1.28048600	0.15513700
H	0.55197100	-5.35310000	0.48521500
H	3.34245700	-3.60582300	-1.94809600
H	3.01621800	-0.97985900	1.33127700
C	-1.29656900	-1.48926800	0.70638300
C	-3.79905000	-0.58202600	-0.05078000
C	-2.04645800	-0.67659100	1.56466000
C	-1.83945500	-1.85988400	-0.52947800
C	-3.09087000	-1.39712900	-0.92572300
C	-3.30855000	-0.22414800	1.19914200
H	-1.61086200	-0.36120000	2.51334600
H	-1.26899600	-2.51485200	-1.19283400
H	-3.52049600	-1.64510900	-1.89493600
H	-3.89943700	0.42767700	1.84076400
N	-5.08870300	-0.02492400	-0.48659800
O	-5.76975800	0.52945900	0.34260600
O	-5.37886000	-0.13763300	-1.65549700
C	-0.61245700	-4.00242100	2.30315200
H	-1.65506400	-3.64853700	2.27459800

H	-0.18414000	-3.65407200	3.25644200
H	-0.61540500	-5.09940300	2.30494500
C	1.14073100	-5.04816000	-2.07365100
H	1.83177000	-5.00061900	-2.92486900
H	0.13760100	-4.75597900	-2.42178500
H	1.06569000	-6.09493900	-1.73920700
C	4.75672900	-2.79577100	0.33948200
H	5.38511800	-2.73763800	-0.56319800
H	4.90517800	-3.79796800	0.76914900
H	5.11172200	-2.04728700	1.05998400
H	0.98918500	-1.62851800	-0.87455500
C	0.98545900	0.20892700	0.13670700
O	1.39521300	0.82565000	-1.00293300
N	0.50151400	0.92956500	1.05759000
C	0.39613700	2.28665300	0.50332200
H	0.74394100	3.02548400	1.23860400
C	1.34692200	2.22686400	-0.72588300
H	0.91824300	2.73296800	-1.60191500
C	-1.05815700	2.55273200	0.15737600
C	-3.78144800	2.93076200	-0.41146000
C	-1.62054400	2.02833500	-1.01299100
C	-1.87638500	3.26098500	1.04062600
C	-3.23094300	3.44632700	0.76129500
C	-2.97028500	2.22328200	-1.30009600
H	-1.00147700	1.44606700	-1.70089900
H	-1.44803700	3.66551800	1.96064100
H	-3.85975800	3.99740000	1.46243600
H	-3.40058500	1.80004600	-2.20997100
H	-4.84285400	3.06361500	-0.62707200
C	2.73099200	2.76687400	-0.43796600
C	5.25716400	3.82904500	0.13754100
C	2.88860400	4.13931700	-0.21401200
C	3.84767300	1.93156300	-0.38071400
C	5.10521900	2.46347200	-0.09010200
C	4.14365900	4.66855900	0.07264500
H	2.01818500	4.79924400	-0.26630200
H	3.72867400	0.86400100	-0.57211100
H	5.97270200	1.80288000	-0.04581000
H	4.25497300	5.74030600	0.24393500
H	6.24159600	4.24200800	0.36219600
H	0.30469900	-1.54251500	2.09736800

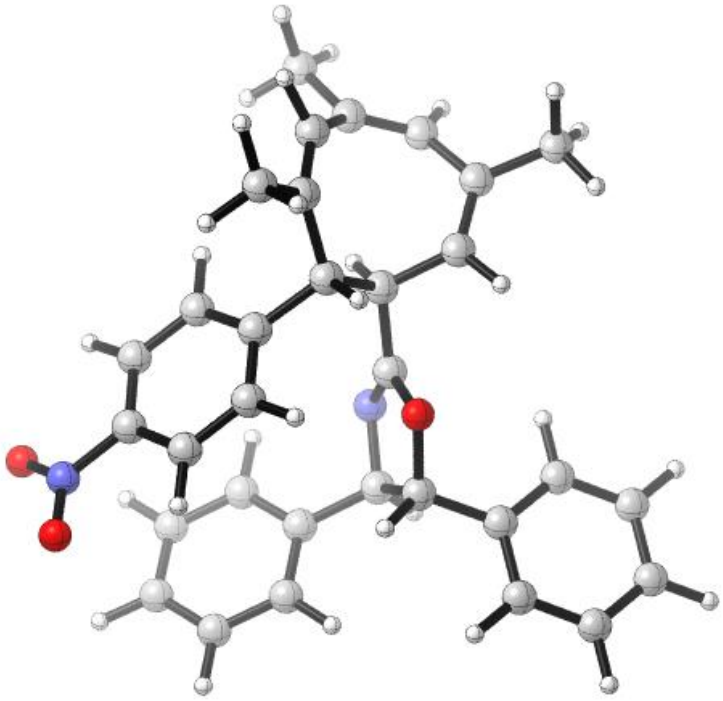

Parkeroxazoline_cyclooctatriene2_GS
E(M062X/def2TZVP) = -1572.446004 Hartree
Free energy correction (M062X/def2SVP) = 0.488258 Hartree
G = -4127175.062

C	3.99962100	2.58104100	-0.87820500
C	4.52066000	1.38137500	-1.20509500
H	5.08296200	1.31714500	-2.14450400
C	4.45686200	0.14815000	-0.40724600
C	2.46768900	2.45562700	1.24771700
C	3.41340600	2.95673300	0.43060500
H	3.85890300	3.89349000	0.79264700
C	3.29228400	-0.30562200	0.08131200
H	3.27582200	-1.22280100	0.68016200
C	1.96373300	0.35441300	-0.16333700
C	1.55945400	1.26187400	1.02600700
C	0.10690900	1.70199900	0.89633100
C	-2.55049700	2.41859300	0.58125200
C	-0.25678900	2.68107000	-0.03735300
C	-0.89003900	1.09087900	1.66542900
C	-2.22875000	1.44534500	1.51701800
C	-1.58773500	3.04547200	-0.20360500
H	0.51938400	3.16500100	-0.63495700
H	-0.60933700	0.31839300	2.38398100
H	-3.02212500	0.98008300	2.09996300
H	-1.89598700	3.79710000	-0.92854800
N	-3.96504500	2.78429600	0.39729400
O	-4.76750900	2.32510300	1.17352500
O	-4.23672400	3.51345900	-0.52775600
C	2.17471600	3.16264500	2.54852800
H	1.12606900	3.49635300	2.58983000

H	2.82440000	4.03464400	2.69313000
H	2.32291300	2.47509800	3.39650000
C	4.15358400	3.75362800	-1.81600800
H	4.67989800	3.46882800	-2.73585800
H	4.70960400	4.57151500	-1.33103500
H	3.16786600	4.16025200	-2.09135000
C	5.75237900	-0.59275600	-0.21269700
H	6.21184000	-0.82497100	-1.18635800
H	5.60031300	-1.53272100	0.33342500
H	6.47380200	0.02533700	0.34282800
H	1.61839900	0.63561300	1.93111700
H	1.99669100	0.95485000	-1.08127200
C	0.87931100	-0.65811300	-0.36192800
N	0.15514100	-0.80253400	-1.38799100
O	0.61529400	-1.42804600	0.72210700
C	-0.89893200	-1.75181200	-1.03854800
H	-0.90038100	-2.58307300	-1.76293400
C	-0.47753000	-2.28682500	0.37250000
H	-1.26914100	-2.13184600	1.11876600
C	-2.26053100	-1.07248500	-1.08030800
C	-4.76353400	0.20064100	-1.16930600
C	-3.34346300	-1.57538100	-0.35031300
C	-2.45372800	0.06127000	-1.87572400
C	-3.69845500	0.68849400	-1.92493300
C	-4.58318000	-0.93875000	-0.38544000
H	-3.22419400	-2.47562800	0.25743600
H	-1.60932500	0.45604900	-2.44073500
H	-3.83175400	1.58368000	-2.53504400
H	-5.41196500	-1.33211000	0.20515100
H	-5.72449300	0.71740200	-1.17810900
C	-0.03599800	-3.72764200	0.37634800
C	0.74527700	-6.41390500	0.29318400
C	1.17224800	-4.09273900	-0.22823000
C	-0.84434900	-4.71548900	0.93989600
C	-0.45801700	-6.05563700	0.89647600
C	1.56064300	-5.42898000	-0.26798400
H	1.81050700	-3.32234400	-0.66874800
H	-1.78289600	-4.43454400	1.42429600
H	-1.09659600	-6.81978800	1.34193900
H	2.50486200	-5.70561400	-0.73941100
H	1.05131700	-7.46052600	0.26150400

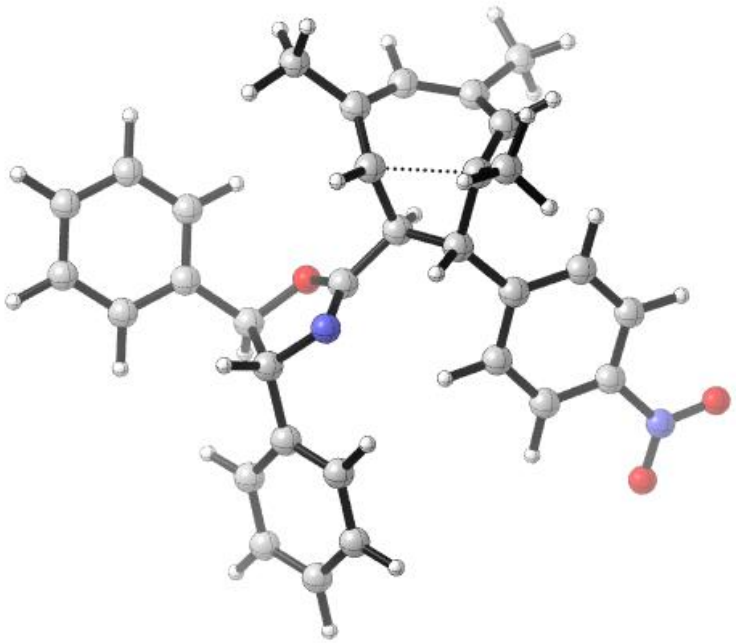

Parkeroxazoline_cyclooctatriene1_6π_TS
E(M062X/def2TZVP) = -1572.397068 Hartree
Free energy correction (M062X/def2SVP) = 0.483587 Hartree
G = -4127058.844

C	0.38918500	4.05565100	0.93230400
C	-1.01615500	4.08606800	0.79684700
C	-1.66789000	3.68093600	-0.37766000
C	0.74708100	2.42486300	-0.78712200
C	1.23340400	3.49584300	-0.02501600
C	-1.31169900	2.72994700	-1.36368800
C	-1.19658900	1.23429400	-1.05214200
C	0.00334900	1.26796000	-0.12855300
H	-2.50440100	4.34040900	-0.65183700
H	0.81322900	4.74307900	1.67111800
H	1.31821100	2.11767500	-1.67261500
C	-2.43457400	0.51070500	-0.55930700
C	-4.62419300	-0.92568600	0.37215900
C	-2.35057200	-0.87731100	-0.35562400
C	-3.64771600	1.15534600	-0.29060300
C	-4.75096300	0.44200700	0.17373100
C	-3.43671300	-1.60346800	0.11552800
H	-1.41446600	-1.39332700	-0.57331900
H	-3.73715900	2.23018700	-0.44235800
H	-5.70288200	0.92631200	0.38497100
H	-3.38169400	-2.67816500	0.28245000
N	-5.78880700	-1.68531100	0.86558300
O	-5.65263700	-2.87528800	1.01767700
O	-6.80366000	-1.06862300	1.08508600
C	-1.79931900	3.00591200	-2.76732600
H	-2.71884400	2.43044900	-2.97430500
H	-1.04728300	2.67274300	-3.49762900

H	-1.99749500	4.07160500	-2.93908200
C	-1.80703000	4.89047700	1.79988000
H	-1.18337500	5.63816300	2.30810300
H	-2.22574200	4.22679500	2.57217900
H	-2.65402600	5.40237300	1.32106800
C	2.54787300	4.15931600	-0.35678800
H	3.29704300	3.43791800	-0.71050900
H	2.94962000	4.67886600	0.52490700
H	2.41089200	4.91841100	-1.14382600
H	-0.27858900	1.53558100	0.89795600
C	0.86600500	0.04769900	-0.09263800
O	1.58645800	-0.11389000	1.03809300
N	1.04247700	-0.78272800	-1.03474200
C	2.02644500	-1.75776500	-0.56495200
H	2.84811100	-1.81148900	-1.29784500
C	2.55684600	-1.12177900	0.76065900
H	2.54366200	-1.83064600	1.59978200
C	1.42733600	-3.14903600	-0.42984500
C	0.35504200	-5.74051600	-0.25484200
C	0.30545700	-3.50881800	-1.18501200
C	2.01517800	-4.11051600	0.39853000
C	1.48344600	-5.39652600	0.48718100
C	-0.22935200	-4.79304300	-1.09434000
H	-0.13858000	-2.76881200	-1.85164800
H	2.90172100	-3.86239000	0.98705200
H	1.95282900	-6.13136500	1.14296400
H	-1.10771600	-5.05540100	-1.68650800
H	-0.06567800	-6.74421700	-0.18112900
C	3.93110200	-0.50260100	0.61842600
C	6.49392400	0.58794000	0.32318600
C	5.02288300	-1.32704300	0.32489400
C	4.13133500	0.87122600	0.76527700
C	5.40952900	1.41230700	0.61426800
C	6.29770500	-0.78664400	0.18001200
H	4.87329100	-2.40374300	0.20263100
H	3.28087800	1.51268600	1.00218600
H	5.55615600	2.48775400	0.72986900
H	7.14144400	-1.43974400	-0.04757200
H	7.49182700	1.01324500	0.20796100
H	-0.86011200	0.72727500	-1.97228600

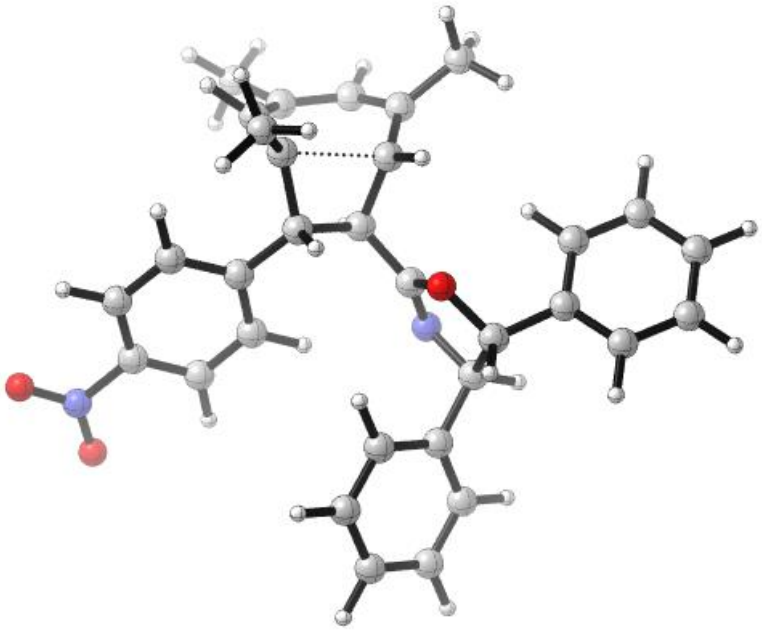

Parkeroxazoline_cyclooctatriene2_6π_TS
E(M062X/def2TZVP) = -1572.396456 Hartree
Free energy correction (M062X/def2SVP) = 0.482820 Hartree
G = -4127059.251

C	1.38885000	-3.92804500	-1.04895400
C	0.04329100	-3.99502300	-1.46821800
H	-0.15239200	-4.63807000	-2.33237400
C	-1.03169400	-3.61797300	-0.65870200
C	1.09708000	-2.75364000	1.19489200
C	1.74153200	-3.60148500	0.27221700
H	2.53946900	-4.23654200	0.68229100
C	-0.84260300	-2.57586300	0.25544000
H	-1.59910900	-2.42576100	1.03547100
C	-0.13430100	-1.29808900	-0.17162400
C	0.94538300	-1.25266300	0.90047500
C	2.22109500	-0.49878800	0.57464300
C	4.52974900	0.95083800	0.03211100
C	2.18317000	0.61151900	-0.28146300
C	3.45246600	-0.87708500	1.13079400
C	4.61194500	-0.15744900	0.86787600
C	3.33480300	1.34639900	-0.55341300
H	1.24754800	0.91174700	-0.75677300
H	3.51273100	-1.75712700	1.77140200
H	5.57473400	-0.43730300	1.29199700
H	3.31738100	2.21360500	-1.21175500
N	5.75515400	1.72309100	-0.24800800
O	6.78175900	1.34156400	0.26142300
O	5.65341000	2.68785200	-0.96644300
C	1.22974100	-3.09154000	2.66235600
H	1.94916300	-2.42808400	3.17116500
H	1.53185200	-4.13557400	2.81770800
H	0.26221200	-2.94045000	3.16442200

C	2.43961400	-4.56656900	-1.92349200
H	2.00290500	-5.28013600	-2.63497300
H	3.19700400	-5.08577700	-1.31877800
H	2.96671700	-3.79476600	-2.50513600
C	-2.28083800	-4.46514200	-0.63705700
H	-2.44800100	-4.92793500	-1.61969800
H	-3.17380000	-3.88403500	-0.36974600
H	-2.18101400	-5.28460000	0.09297900
H	0.49574000	-0.79444700	1.79964600
H	0.30327900	-1.41506000	-1.17071200
C	-1.04448600	-0.11233200	-0.20380000
N	-1.17225300	0.72760100	-1.14357300
O	-1.77375800	0.08332400	0.92599900
C	-2.07971600	1.77270400	-0.66008700
H	-2.87055500	1.95350000	-1.40163600
C	-2.68268500	1.15116600	0.64366500
H	-2.65182700	1.86051600	1.48167500
C	-1.31475200	3.05800800	-0.42289000
C	0.14586300	5.41031600	0.01089100
C	-1.61340000	4.21764900	-1.13850600
C	-0.27943600	3.08846600	0.51986500
C	0.44919000	4.25489700	0.73429300
C	-0.88761000	5.39037000	-0.92266400
H	-2.41758100	4.20094700	-1.87736900
H	-0.03819200	2.18538300	1.08890400
H	1.25855500	4.26321000	1.46598100
H	-1.12860300	6.28987600	-1.49115000
H	0.71773800	6.32448400	0.17607700
C	-4.08338200	0.62442700	0.45088200
C	-6.69384100	-0.26897800	-0.02373900
C	-4.30745600	-0.65823300	-0.05784800
C	-5.17482000	1.45355800	0.72286800
C	-6.47476800	1.01049000	0.48558900
C	-5.60780100	-1.10110500	-0.29406300
H	-3.45978800	-1.31498500	-0.26598700
H	-5.00444400	2.45437000	1.12756500
H	-7.31997300	1.66433400	0.70562000
H	-5.77371100	-2.10397700	-0.69099400
H	-7.71074100	-0.61892800	-0.20661000

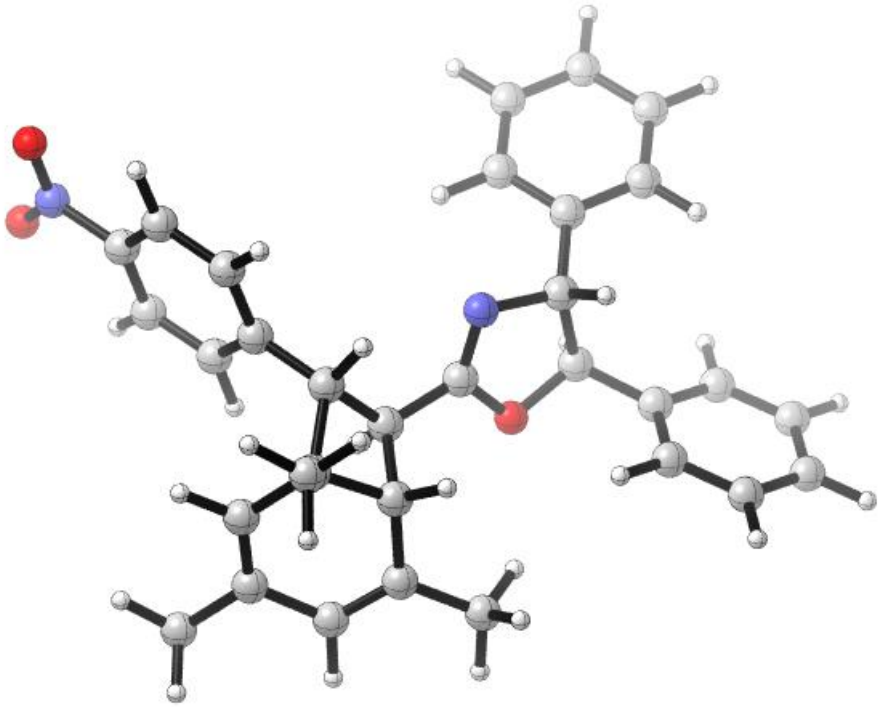

Parkeroxazoline_BOD1_GS
E(M062X/def2TZVP) = -1572.450053 Hartree
Free energy correction (M062X/def2SVP) = 0.485119 Hartree
G = -4127193.934

C	-0.34369000	-2.49122500	0.64006800
C	-1.16915400	-4.21105100	-0.88694200
C	-2.81901600	-2.82340400	0.27987500
C	-2.55041700	-3.73944100	-0.66599700
C	-1.77377700	-2.24636200	1.19662900
C	-0.11022800	-3.65864500	-0.27385200
C	-0.40821600	-1.07592600	-0.01135900
C	-1.53296400	-0.71145600	0.96825900
H	-3.85374600	-2.50812200	0.45220400
H	-1.02147700	-5.03678600	-1.58910800
H	0.39069600	-2.47856100	1.46272800
C	-2.04784400	-2.65465000	2.63710400
H	-1.28702500	-2.23771300	3.31449600
H	-2.04344700	-3.75036500	2.73442100
H	-3.03536600	-2.28797900	2.95870500
C	-3.62101200	-4.34571000	-1.52897300
H	-3.65580400	-5.43764700	-1.39091900
H	-3.41013800	-4.16563300	-2.59470000
H	-4.61072600	-3.93355500	-1.29461000
C	1.30878600	-4.08123800	-0.49995200
H	1.89636700	-3.23051200	-0.88234900
H	1.37729500	-4.91037300	-1.21596700
H	1.77684800	-4.39687800	0.44697600
C	-2.66773600	0.17801900	0.55227800
C	-4.82202200	1.78849000	-0.13945000
C	-3.18492500	0.15809100	-0.75182200

C	-3.26018700	1.02719300	1.49710700
C	-4.34064000	1.83728200	1.16293600
C	-4.26191300	0.96242600	-1.10759000
H	-2.74637400	-0.50372100	-1.49973500
H	-2.85823600	1.05807700	2.51149200
H	-4.81018700	2.50537200	1.88298700
H	-4.67622900	0.96274900	-2.11437900
N	-5.96525800	2.64512300	-0.50925000
O	-6.35979600	2.58469300	-1.64885400
O	-6.43314000	3.35049000	0.35166100
H	-0.75104700	-1.17527100	-1.05165400
H	-1.06767500	-0.29566800	1.87368300
C	0.82675100	-0.25316700	0.03746300
O	1.82212000	-0.65995700	-0.78852900
N	1.04950400	0.73117200	0.80318200
C	2.89091400	0.28282700	-0.64794400
H	2.92353200	0.89647400	-1.56202400
C	2.42443400	1.15589500	0.57005500
H	3.02428600	0.89467400	1.45873700
C	2.58229000	2.63581100	0.31249800
C	2.94930300	5.34796900	-0.27932600
C	1.49970400	3.42097800	-0.08911700
C	3.84864500	3.22015500	0.42569000
C	4.03281800	4.56871700	0.12700700
C	1.68387600	4.77218200	-0.38247400
H	0.51011300	2.96584200	-0.15321300
H	4.69506200	2.61185100	0.75617300
H	5.02390100	5.01557700	0.22028200
H	0.83121300	5.37987200	-0.68967600
H	3.09067000	6.40527700	-0.50818200
C	4.20985900	-0.40829500	-0.44314300
C	6.68854800	-1.61223800	0.04461300
C	5.37467900	0.12669300	-0.99754600
C	4.29292100	-1.55267300	0.35681900
C	5.52605300	-2.15396000	0.59578500
C	6.61110900	-0.47041400	-0.75053100
H	5.31056000	1.01649600	-1.62849600
H	3.38033100	-1.97585000	0.78280200
H	5.58193600	-3.05067800	1.21481700
H	7.51566000	-0.04625200	-1.18881600
H	7.65413400	-2.08380000	0.23254500

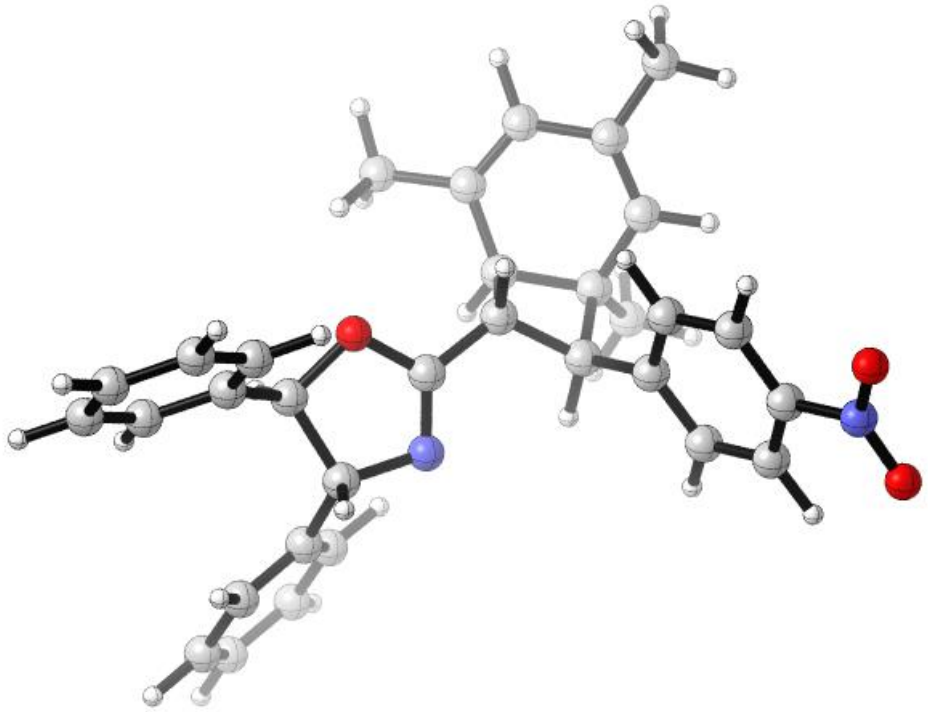

Parkeroxazoline_BOD2_GS
E(M062X/def2TZVP) = -1572.449308 Hartree
Free energy correction (M062X/def2SVP) = 0.484775 Hartree
G = -4127192.881

C	2.09460600	-1.91284900	1.27606100
C	3.08759200	-3.35819400	-0.52087700
C	0.65390900	-3.58747700	-0.15341400
C	1.78413000	-4.01687100	-0.73676400
C	0.71861800	-2.36712900	0.71682500
C	3.21953900	-2.37984300	0.39099900
H	-0.02308000	-2.42006500	1.53079000
H	1.75678600	-4.87945200	-1.40892200
H	4.20114400	-1.92415900	0.55985800
C	1.65457900	-0.43357800	0.98573300
C	0.60175200	-0.98085300	0.01047600
C	2.40119600	-2.22700900	2.73338600
H	3.32691100	-1.72033900	3.04857300
H	2.54070900	-3.30915000	2.87301800
H	1.58276600	-1.88996400	3.38775100
C	4.24119700	-3.84862900	-1.35011900
H	5.16441100	-3.30093700	-1.12201700
H	4.02377900	-3.73679200	-2.42381000
H	4.41751700	-4.92056400	-1.17017900
C	-0.69581800	-4.19848600	-0.37291700
H	-1.38455900	-3.43856500	-0.77654100
H	-1.12389300	-4.55007900	0.57950300
H	-0.65166700	-5.04435200	-1.07096600
C	2.66872900	0.58185600	0.54689900
C	4.60453600	2.43362700	-0.18519800
C	3.12748700	1.53865800	1.46249500

C	3.20720700	0.57806700	-0.74865300
C	4.17540100	1.50250700	-1.12456000
C	4.09774700	2.47047800	1.10789800
H	2.70699000	1.55696400	2.46959400
H	2.87312000	-0.16567800	-1.47320100
H	4.60420600	1.51700200	-2.12509200
H	4.46235400	3.22302900	1.80499000
N	5.63163700	3.41765300	-0.57631400
O	5.98718800	4.21283100	0.25982400
O	6.05203700	3.36317700	-1.70710900
H	0.97104100	-1.07202400	-1.02128600
H	1.12524300	-0.05100100	1.87050200
C	-0.73467200	-0.33368200	0.01387400
O	-1.61871100	-0.82580700	-0.89299600
N	-1.13080800	0.58197900	0.79469000
C	-2.89136400	-0.25812500	-0.56300500
H	-3.46708600	-1.02044900	-0.01166900
C	-2.50255300	0.90284000	0.41047000
H	-2.49194400	1.85718700	-0.14381100
C	-3.65006400	0.17582500	-1.78445900
C	-5.09357500	1.11663800	-3.98844200
C	-2.97857300	0.62885500	-2.92340800
C	-5.04753400	0.18961500	-1.75829000
C	-5.76673900	0.66376800	-2.85463300
C	-3.69894600	1.09428200	-4.02152800
H	-1.88810700	0.59963200	-2.94695900
H	-5.57342100	-0.17408300	-0.87211000
H	-6.85733500	0.67073200	-2.82616200
H	-3.16846700	1.43970400	-4.91015800
H	-5.65563700	1.48130800	-4.84935800
C	-3.46366700	1.03101100	1.56626600
C	-5.33455700	1.17206100	3.64620500
C	-3.23383800	0.35796600	2.76891000
C	-4.63360100	1.78254300	1.41646600
C	-5.56719300	1.84963000	2.44980600
C	-4.16438100	0.42963800	3.80432000
H	-2.30865700	-0.20818600	2.88996600
H	-4.81047700	2.32162900	0.48225000
H	-6.47547000	2.44084200	2.32331600
H	-3.97277200	-0.09303200	4.74284400
H	-6.06121900	1.22897100	4.45797000

Structure	Number of imaginary frequencies	Free energy correction (Hartree)	Electronic energy (Hartree)	Relative Gibbs free energy (kJ/mol)
THFpyr_tetraene_GS	0	0.515534	-1765.291509	0.000
THFpyr_tetraene_8π1_TS	1	0.523418	-1765.255936	114.096
THFpyr_tetraene_8π2_TS	1	0.531738	-1765.262155	119.613
THFpyr_cyclooctatriene1_GS	0	0.527794	-1765.294986	23.060
THFpyr_cyclooctatriene2_GS	0	0.528708	-1765.298426	16.428
THFpyr_cyclooctatriene1_6π_TS	1	0.525646	-1765.258163	114.099
THFpyr_cyclooctatriene2_6π_TS	1	0.523204	-1765.251762	124.493
THFpyr_BOD1_GS	0	0.527384	-1765.305735	-6.238
THFpyr_BOD2_GS	0	0.540113	-1765.312786	8.669

Table S7: Calculated relative free energies of Double THFpyr compound

Double THFpyr compound Cartesian Coordinates

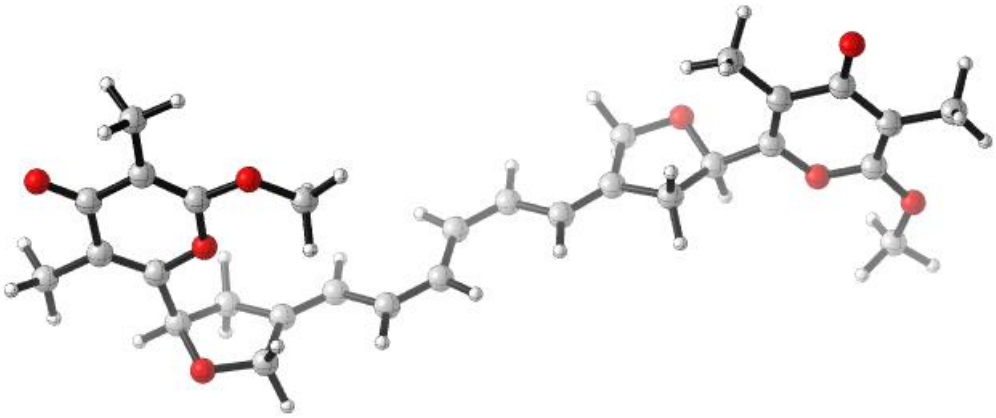

THFpyr_tetraene_GS
E(M062X/def2TZVP) = -1765.291509 Hartree
Free energy correction (M062X/def2SVP) = 0.515534 Hartree
G = -4633419.322

C	-1.09240200	-1.57327500	0.40542900
C	-0.55154800	-1.31781300	-0.91662900
H	-1.24261100	-1.38108500	-1.75989700
C	0.73439700	-1.00214700	-1.19880700
C	-2.38021100	-1.88491600	0.68586600
H	-2.63799700	-2.04156400	1.73764200
C	-3.46657800	-2.02192300	-0.27146100
C	1.82352600	-0.86485200	-0.24536300

H	1.61568900	-1.03327200	0.81396600
C	3.07741700	-0.54086500	-0.59994900
C	-4.74796900	-2.19700700	0.08823800
C	4.26514100	-0.38377700	0.31315800
H	4.27712200	0.61904600	0.77055100
H	4.29949800	-1.13022800	1.11739800
C	3.58421800	-0.30063100	-2.00949100
H	3.05640700	0.51267600	-2.52967200
H	3.48312600	-1.21986800	-2.61821400
O	4.94146500	0.06247900	-1.87496900
C	5.43349200	-0.50752500	-0.68073900
H	5.66320400	-1.57818800	-0.84023900
H	-0.40300200	-1.50486800	1.24953700
H	-3.23531900	-1.95832900	-1.33771700
H	0.98685100	-0.83271700	-2.24953800
C	8.29103600	1.92371300	0.35829500
C	6.71688300	0.15889000	-0.26067300
C	8.89282700	-0.41732400	0.42029800
C	9.26786500	0.87117000	0.61490900
C	6.95333400	1.47589600	-0.10517800
O	7.67454900	-0.78105600	-0.00209800
O	9.70769700	-1.44738000	0.63601900
O	8.54280500	3.10707000	0.51422100
C	9.26439000	-2.75765500	0.33412800
H	8.39464800	-3.03362300	0.94640700
H	10.10545700	-3.41766100	0.56733100
H	9.00016800	-2.85226400	-0.72848700
C	10.63233900	1.26769600	1.08231500
H	11.07986900	1.97249300	0.36694600
H	11.28759500	0.39736100	1.19844700
H	10.56189000	1.80112000	2.04155700
C	5.95419600	2.56323100	-0.35347700
H	5.70441400	3.06072800	0.59592400
H	5.04728100	2.19720300	-0.84294600
H	6.42257900	3.33247700	-0.98292100
C	-5.28869800	-2.25964300	1.49990600
H	-4.95744800	-3.16322700	2.03755500
H	-4.96983500	-1.37917100	2.08670000
C	-5.93580200	-2.30558500	-0.82945100
H	-6.08602700	-3.35417500	-1.13245200
H	-5.84196100	-1.69236000	-1.73542800
O	-6.69600300	-2.29951400	1.38161400
C	-7.09709900	-1.88308800	0.08906000
H	-8.02575300	-2.40976700	-0.15145000
C	-8.56091800	1.72114300	-0.16668200
C	-7.36203600	-0.39996000	0.04942200
C	-6.18979900	1.63154700	0.29473700
C	-7.28991300	2.39348200	0.07561700
C	-8.53129900	0.23483200	-0.16591000

O	-6.20496800	0.29007300	0.28384900
O	-4.99225400	2.14731500	0.55075900
O	-9.59911600	2.32936900	-0.36837400
C	-3.85267400	1.30417000	0.51798100
H	-3.90794400	0.52529700	1.29127000
H	-2.99315600	1.95417700	0.70777900
H	-3.74616000	0.81617400	-0.46158600
C	-7.26628300	3.88928400	0.07878700
H	-7.88599900	4.27671800	0.90092200
H	-7.71088700	4.26885200	-0.85207000
H	-6.24622100	4.27481800	0.18466300
C	-9.85344000	-0.42053000	-0.42016300
H	-9.82739200	-1.51228600	-0.34279600
H	-10.21934700	-0.13509200	-1.41693000
H	-10.58847000	-0.02546800	0.29455000

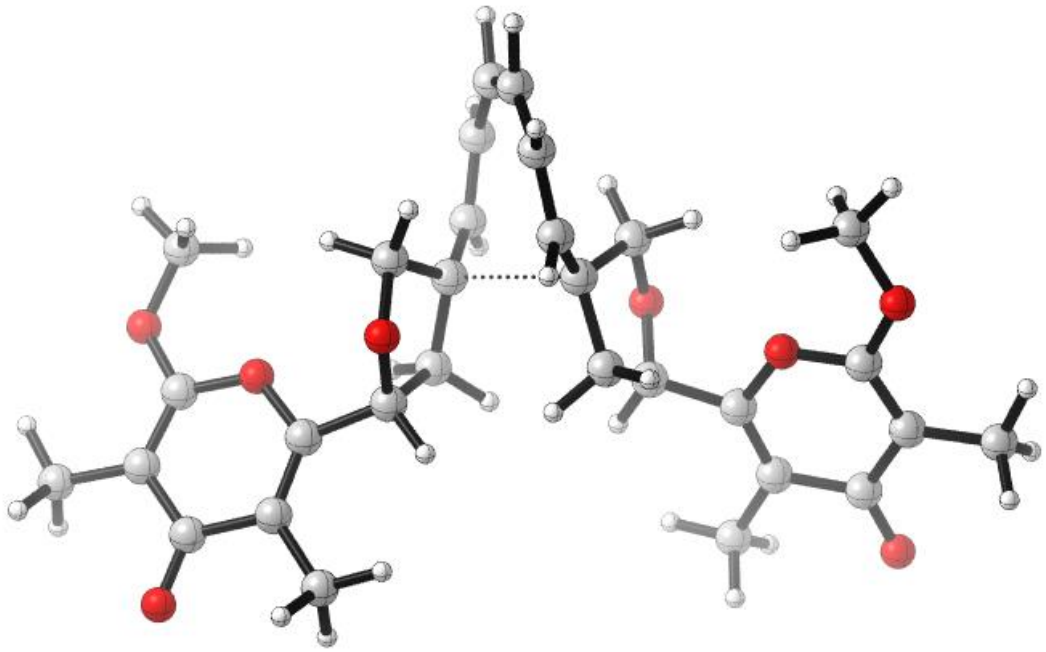

THFpyr_tetraene_8π1_TS
E(M062X/def2TZVP) = -1765.255936 Hartree
Free energy correction (M062X/def2SVP) = 0.523418 Hartree
G = -4633305.226

C	0.21508100	4.46194500	0.67001300
C	-0.21499800	4.46192100	-0.67007900
H	-0.26528600	5.47997600	-1.06895000
C	-0.54393400	3.50708500	-1.64253100
C	0.54401300	3.50714400	1.64250000
H	0.59091700	3.92555200	2.65314800
C	0.76662200	2.12678700	1.59361200
C	-0.76655100	2.12673300	-1.59358700
H	-0.66098900	1.59952900	-2.54778300
C	1.06036000	1.34374700	0.48325200
C	-1.06032000	1.34374500	-0.48319800

C	-1.92933700	1.79646700	0.66466300
H	-1.54720600	2.62977500	1.26158200
H	-2.90627500	2.09727400	0.24220000
C	-1.41207200	-0.12539600	-0.64527500
H	-0.54978100	-0.76032300	-0.88026300
H	-2.12407800	-0.23735600	-1.47669100
O	-2.06787100	0.66681000	1.49658800
C	-2.07890400	-0.50575200	0.70137300
H	-1.50930100	-1.27355900	1.23849900
C	-5.43934700	-2.48049500	0.58639700
C	-3.48665400	-1.00944800	0.52004700
C	-5.52651200	-0.28091200	-0.40927100
C	-6.18175200	-1.42445000	-0.09287400
C	-4.01299300	-2.19242800	0.89270000
O	-4.23502000	-0.06318900	-0.12304500
O	-6.10248000	0.72859800	-1.05646200
O	-5.94694100	-3.54446200	0.89936000
C	-5.42294900	1.96759700	-1.15281800
H	-5.23346600	2.39030200	-0.15513200
H	-6.08935200	2.63072600	-1.71257200
H	-4.46823400	1.86262700	-1.68817200
C	-7.62338200	-1.66177600	-0.41422300
H	-7.72234600	-2.49566100	-1.12474500
H	-8.09250200	-0.76814200	-0.84059500
H	-8.16028200	-1.96255300	0.49651100
C	-3.28685400	-3.29328900	1.60197400
H	-3.85553600	-3.57431000	2.49900300
H	-2.26337700	-3.03246400	1.89089800
H	-3.26587200	-4.18964500	0.96558100
H	0.66106500	1.59962600	2.54783200
H	0.26537600	5.48001400	1.06884400
H	-0.59082600	3.92545200	-2.65319700
C	1.41207100	-0.12539900	0.64537500
H	2.12408600	-0.23736200	1.47678400
H	0.54976100	-0.76028600	0.88039300
C	1.92936400	1.79638900	-0.66465000
H	2.90634100	2.09712800	-0.24223200
H	1.54727100	2.62971200	-1.26157000
O	2.06777100	0.66670000	-1.49655300
C	2.07885400	-0.50582200	-0.70127800
H	1.50923600	-1.27366300	-1.23834000
C	5.43932600	-2.48052400	-0.58640300
C	3.48661800	-1.00949700	-0.51998800
C	5.52650600	-0.28093000	0.40924000
C	6.18175200	-1.42445600	0.09281400
C	4.01295800	-2.19247200	-0.89265600
O	4.23499600	-0.06322700	0.12307300
O	6.10248900	0.72859300	1.05639700
O	5.94691600	-3.54449000	-0.89937300

C	5.42296700	1.96760100	1.15271900
H	5.23345300	2.39026100	0.15502000
H	6.08939200	2.63075200	1.71242100
H	4.46827000	1.86266000	1.68810800
C	7.62339900	-1.66175200	0.41410900
H	7.72239700	-2.49526000	1.12507100
H	8.09265800	-0.76793600	0.83994700
H	8.16013100	-1.96306900	-0.49654300
C	3.28680700	-3.29334000	-1.60190500
H	2.26331000	-3.03253200	-1.89077400
H	3.26587700	-4.18970300	-0.96552000
H	3.85544900	-3.57433900	-2.49896600

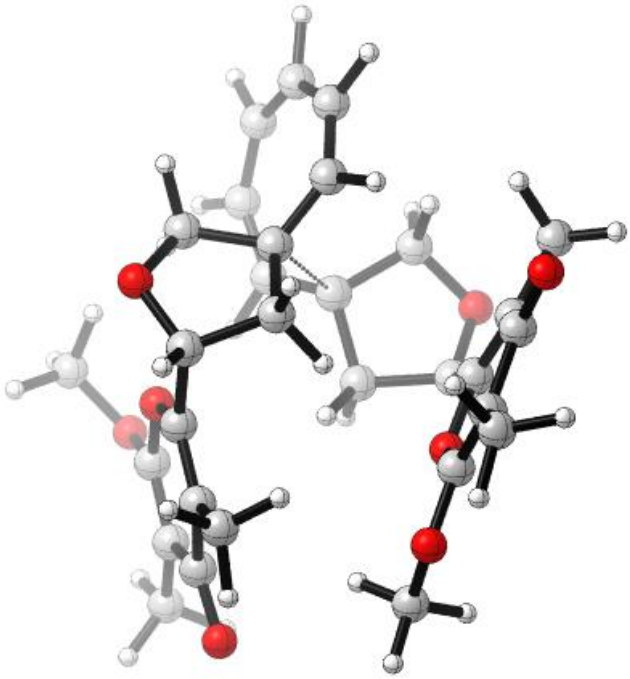

THFpyr_tetraene_8π2_TS
E(M062X/def2TZVP) = -1765.262155 Hartree
Free energy correction (M062X/def2SVP) = 0.531738 Hartree
G = -4633299.71

C	-1.71195400	4.52513900	-0.07587300
C	-0.49836900	4.81163700	0.56898300
H	-0.38608700	5.88765800	0.73670300
C	0.62203200	4.09671500	1.02667200
C	-2.33915500	3.40423300	-0.64759900
H	-3.39844000	3.56801900	-0.87075700
C	-1.87892300	2.12985000	-0.96235800
C	0.85420200	2.73778400	1.20422200
H	1.90390100	2.44589800	1.33181700
C	-0.08428200	1.69731400	1.21967000
C	-0.55113300	1.68895400	-1.03257600
C	0.41327100	0.31665400	1.63028800
H	0.80499100	-0.29278900	0.80620700

H	1.22532500	0.42707100	2.36438700
C	-1.42019100	1.88207000	1.93560300
H	-2.27895600	1.96189200	1.25640500
H	-1.40001500	2.78474400	2.56423400
O	-1.57753600	0.75258500	2.78101600
C	-0.81788400	-0.32024000	2.30192000
H	-0.52953700	-0.94673800	3.15738700
H	-2.34592100	5.41561900	-0.13587300
H	-2.65190500	1.38208000	-1.17067700
H	1.47637400	4.73555700	1.27057300
C	-1.98918600	-3.16335300	-0.04640000
C	-1.58106400	-1.19256400	1.33055000
C	-3.32144800	-1.14606400	-0.23193000
C	-3.09662600	-2.41479800	-0.64782600
C	-1.26024900	-2.47072500	1.03656000
O	-2.57953600	-0.52852900	0.70350800
O	-4.27453400	-0.36066700	-0.73526900
O	-1.69499200	-4.28989700	-0.41788100
C	-4.94518700	0.51275000	0.16711100
H	-5.35113900	-0.05187200	1.01925300
H	-5.76331000	0.96437800	-0.40248900
H	-4.26888900	1.29559000	0.53728400
C	-3.92005900	-3.09285700	-1.69636000
H	-3.29922400	-3.31892200	-2.57566300
H	-4.76816000	-2.47139400	-2.00376500
H	-4.28235900	-4.05820100	-1.31593700
C	-0.17490100	-3.21201100	1.76550800
H	-0.15694600	-4.24596200	1.39940100
H	-0.35924200	-3.22828200	2.84992600
H	0.82213500	-2.77532000	1.60195000
C	0.49866000	2.58212500	-1.68931900
H	0.03138400	3.44372200	-2.18651400
H	1.25780400	2.96397700	-0.99365500
C	-0.28796800	0.28987100	-1.57567500
H	-1.05682100	0.03800100	-2.32166800
H	-0.29538300	-0.51062200	-0.82420300
O	1.11573900	1.77767000	-2.68344900
C	1.07825700	0.44182600	-2.27722000
H	1.14438800	-0.19142100	-3.17506300
C	4.09422600	0.08207400	0.20266000
C	2.20863800	0.03630700	-1.34798100
C	2.84070400	-1.93889500	-0.20818800
C	3.85450200	-1.33372700	0.45795500
C	3.24316700	0.73317300	-0.83135800
O	2.01720400	-1.28480700	-1.03969100
O	2.55003700	-3.22798400	-0.07726800
O	4.96332100	0.71223300	0.78362200
C	1.62484200	-3.82887900	-0.97609000
H	0.61987300	-3.40106200	-0.87001400

H	1.58956400	-4.88772300	-0.70364300
H	1.96746800	-3.71792000	-2.01452100
C	4.75374900	-2.05067800	1.41456200
H	4.54166700	-3.12552100	1.43491000
H	4.63653500	-1.63986700	2.42833900
H	5.80336500	-1.88626100	1.13243400
C	3.66142800	2.12862300	-1.19223100
H	4.75300500	2.12691400	-1.31600900
H	3.46177900	2.82356700	-0.36209900
H	3.18055700	2.48651900	-2.10506500

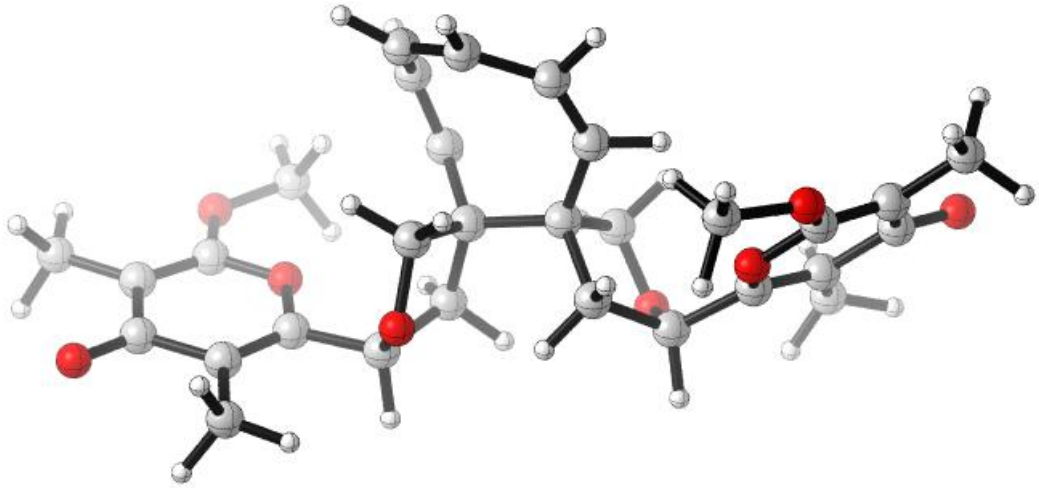

THFpyr_cyclooctatriene1_GS
E(M062X/def2TZVP) = -1765.294986 Hartree
Free energy correction (M062X/def2SVP) = 0.527794 Hartree
G = -4633396.263

C	-0.03652600	-1.71327400	3.00520400
C	-1.18735700	-1.04786600	3.21302700
H	-1.97741400	-1.55795200	3.77251700
C	-1.42172900	0.34526900	2.83908300
C	1.58079500	-0.41161000	1.44420800
C	1.23502800	-1.21243300	2.46947200
H	2.09181300	-1.60190200	3.03198900
C	-1.15263400	0.89427300	1.64729300
H	-1.31472200	1.97301500	1.55511800
C	-0.69978600	0.21074500	0.37255700
C	0.85466900	0.23704000	0.28588200
C	-1.33484000	0.95369900	-0.84931800
H	-0.56157000	1.28690700	-1.55267800
H	-1.90775100	1.83546900	-0.54315700
C	-1.24436400	-1.23383100	0.16999200
H	-2.13519600	-1.40194700	0.80002400
H	-0.50881500	-2.01817100	0.38497100
O	-1.58948800	-1.32701100	-1.19538000
C	-2.21477500	-0.10551300	-1.52595300
H	-2.19349500	-0.02210700	-2.62228500

C	-3.67173200	-0.12118600	-1.08400200
C	-5.95615500	-0.98857000	-0.94220400
C	-5.26013400	1.01155600	0.22650900
C	-6.25233500	0.13180900	-0.05571400
C	-4.56801500	-1.05575100	-1.45845300
O	-4.00892400	0.90248400	-0.24593500
O	-6.79145200	-1.82234500	-1.25075000
C	-4.26321200	-2.19670800	-2.37780600
H	-4.32989900	-3.14268900	-1.82026200
H	-3.26725400	-2.13275900	-2.82712200
H	-5.03752800	-2.24455500	-3.15577900
C	-7.64148600	0.26121400	0.48389400
H	-7.92784000	-0.66808500	0.99673900
H	-8.35606800	0.39303700	-0.34184300
H	-7.72877700	1.10563500	1.17637600
O	-5.44746800	2.08082200	0.99703000
C	-4.33608700	2.87360200	1.36752800
H	-4.73273200	3.65891700	2.01842700
H	-3.86087500	3.33024500	0.48699800
H	-3.59185900	2.27478200	1.91128600
H	-1.84969100	0.99011500	3.61472900
H	0.01981100	-2.73259000	3.40098000
H	2.66385500	-0.25623400	1.35535000
C	1.36294900	1.70467900	0.11484300
H	2.20442900	1.90879500	0.80033500
H	0.58159000	2.45397700	0.29645600
O	1.78416900	1.83579200	-1.22586500
C	1.38910400	-0.43154900	-1.02328400
H	0.57145100	-0.59022700	-1.73519300
H	1.85115900	-1.40536500	-0.83086900
C	2.36450800	0.60646900	-1.59346100
H	2.40236200	0.57947900	-2.69360300
C	6.01147400	1.15620900	-0.30320200
C	3.78282600	0.47876600	-1.04965800
C	5.25239600	-1.13523500	-0.16268900
C	6.23496300	-0.23511600	0.08122000
C	4.68616200	1.46956000	-0.90323000
O	4.07385200	-0.81160500	-0.71346300
O	5.36202900	-2.43137000	0.11784600
O	6.85576100	2.01962600	-0.13505200
C	4.20395900	-3.24591900	0.05349700
H	3.40613500	-2.85278500	0.70237700
H	4.51430500	-4.23505600	0.40364700
H	3.82713300	-3.31906600	-0.97626800
C	7.54458500	-0.59759200	0.70621300
H	7.56865800	-1.65061700	1.00797200
H	7.72867800	0.04234600	1.58077900
H	8.36591000	-0.40391100	0.00071700
C	4.45918400	2.89961900	-1.29515400

H	5.42839800	3.33420100	-1.56943700
H	4.07824400	3.47980300	-0.44017800
H	3.74111600	3.00401500	-2.11433000

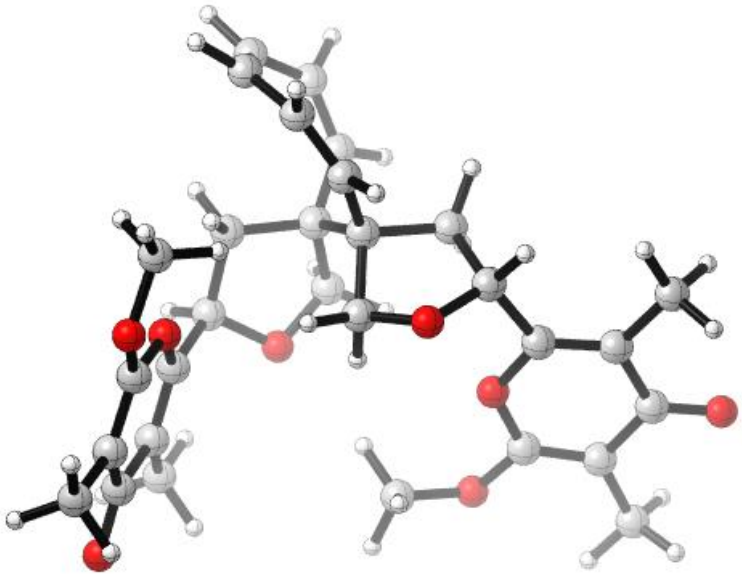

THFpyr_cyclooctatriene2_GS
E(M062X/def2TZVP) = -1765.298426 Hartree
Free energy correction (M062X/def2SVP) = 0.528708 Hartree
G = -4633402.895

C	-2.22888600	4.36695600	-0.04267600
C	-1.90732700	4.64784100	-1.31932500
C	-0.66215600	4.31113400	-2.00589900
C	-0.52553600	2.75480800	1.09043600
C	-1.44586400	3.73639300	1.02574900
C	-0.02317300	3.13458200	-1.98495900
C	-0.44448900	1.83645400	-1.33462900
C	0.11885900	1.79428200	0.11512100
H	-0.22745000	5.10847500	-2.61764400
H	-3.18999900	4.76049600	0.30413800
H	-0.16675700	2.54977500	2.10664000
C	1.65078300	2.05011000	0.15413100
H	1.88116500	3.11238600	0.29990500
C	0.06420100	0.40188100	0.79613400
H	0.27856000	-0.40301700	0.08015200
H	-0.90678700	0.20094600	1.27171700
O	1.04650700	0.45328800	1.80583600
C	2.16369500	1.17810800	1.32844900
H	2.53654100	1.79213300	2.15667300
C	3.26185500	0.24131300	0.89393700
C	3.53380300	-1.70653600	-0.40514600
C	5.49698800	-0.69760000	0.58501200
C	4.87383300	-1.75463100	-0.20560100
C	4.57948700	0.31577500	1.16539900
O	2.74743400	-0.73515300	0.09055100

O	6.69840900	-0.65132400	0.79167100
C	5.74577600	-2.83850500	-0.75598400
H	5.15099400	-3.63617500	-1.21467600
H	6.36948700	-3.25398200	0.04788500
H	6.43691600	-2.42813200	-1.50716700
C	5.23906300	1.35627700	2.01686700
H	4.53689100	2.06682200	2.46597200
H	5.97177400	1.91022400	1.41273000
H	5.81565800	0.86162100	2.81089200
O	2.87339300	-2.60115600	-1.12967900
C	1.48292600	-2.79386100	-0.89264700
H	0.87797300	-2.00092300	-1.35396200
H	1.27146600	-2.83552100	0.18537700
H	1.23212700	-3.75369300	-1.35526600
H	2.12252300	1.73835500	-0.78793200
H	-1.70295100	4.15327100	2.00627000
H	-2.61884800	5.25646600	-1.88631800
H	0.92897100	3.08246900	-2.52552400
C	0.10360700	0.67494300	-2.19713000
O	-0.73093500	-0.42879000	-1.96594900
C	-2.06245000	0.03567200	-1.80061300
H	-2.58010200	-0.03775200	-2.77359900
C	-1.96341700	1.52013600	-1.38149100
H	-2.44973100	1.70720500	-0.41950500
H	-2.45589700	2.15145000	-2.13002200
H	0.07451300	0.96905300	-3.26295600
H	1.13196900	0.37472500	-1.94547700
C	-3.64532700	-3.03227300	-0.02332900
C	-2.77081100	-0.89922000	-0.84310200
C	-3.81763300	-0.99040000	1.26091100
C	-4.07444600	-2.31898800	1.17560700
C	-2.96552800	-2.21493700	-1.05749400
O	-3.18949400	-0.29234200	0.30280800
O	-4.16731500	-0.24779900	2.30757200
O	-3.83146700	-4.22730100	-0.18171800
C	-3.86414000	1.13633300	2.30815100
H	-2.78054800	1.31189200	2.24460700
H	-4.24665500	1.52421700	3.25720800
H	-4.35608400	1.65204900	1.47017800
C	-4.77323400	-3.09012900	2.25003600
H	-5.04834300	-2.44749000	3.09356100
H	-4.12656800	-3.90481300	2.60676100
H	-5.67656700	-3.56587200	1.84170900
C	-2.53481000	-2.93980000	-2.29350100
H	-2.01612900	-2.29326200	-3.00921000
H	-3.40934200	-3.41051800	-2.76522400
H	-1.86494300	-3.76498700	-2.01112500

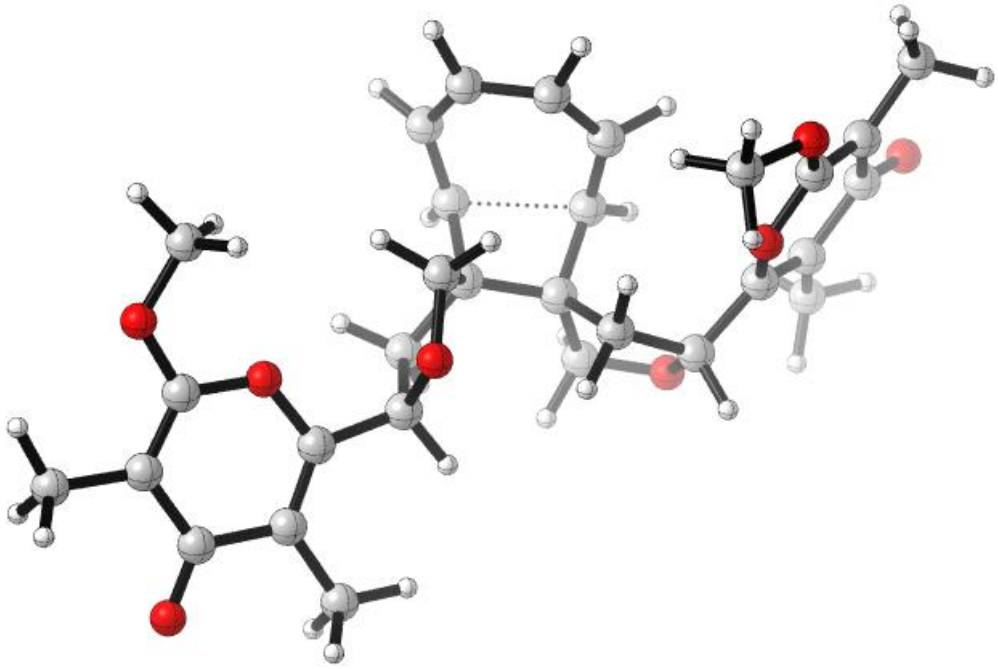

THFpyr_cyclooctatriene1_6π_TS
E(M062X/def2TZVP) = -1765.258163 Hartree
Free energy correction (M062X/def2SVP) = 0.525646 Hartree
G = -4633305.223

C	1.72072200	2.69599100	-0.59290600
C	0.57431000	3.17747600	-1.24214400
H	0.40303200	4.25572600	-1.18931800
C	-0.08970000	2.43501600	-2.22304100
C	1.78539600	0.31811600	-1.43411100
C	2.35702400	1.49411100	-0.93439500
H	3.45329300	1.55709700	-0.98271900
C	-0.13667500	1.04203600	-2.20786900
H	-0.39639000	0.54688800	-3.15104600
C	-0.55269500	0.24287500	-0.97381700
C	0.73459800	-0.54183600	-0.70657600
C	-1.83544000	-0.56558100	-1.22942800
H	-1.69613000	-1.46711600	-1.83867300
H	-2.54426100	0.09002300	-1.75891100
C	-1.03703000	1.03419400	0.25157200
H	-1.70492700	1.85217500	-0.06983300
H	-0.23541100	1.45944000	0.86569900
O	-1.73419000	0.08499200	1.03215900
C	-2.35982700	-0.86710000	0.18543100
H	-2.06299500	-1.87264600	0.51675000
C	-3.85509700	-0.74246000	0.29193600
C	-6.21035200	-1.33483900	0.56954600
C	-5.50264400	0.92709100	0.10021400
C	-6.52599300	0.07062900	0.34031100
C	-4.76924900	-1.69936700	0.54364400
O	-4.21729700	0.55321200	0.06154900
O	-5.68039900	2.22524100	-0.13009600

O	-7.06775400	-2.17597900	0.78281600
C	-7.96038600	0.49345300	0.38034200
H	-8.53101300	-0.03302800	-0.39862200
H	-8.06509400	1.57469700	0.23751300
H	-8.40728700	0.20500400	1.34252200
C	-4.47575700	-3.14464400	0.80173700
H	-3.40591500	-3.37456700	0.84820300
H	-4.94129100	-3.75871000	0.01744700
H	-4.95478800	-3.44522600	1.74373600
C	-4.54619600	3.06595500	-0.24594600
H	-3.92134000	3.01297100	0.65687700
H	-4.93839800	4.07994100	-0.36962200
H	-3.93652400	2.79520500	-1.12050000
H	2.48871800	-0.28806300	-2.02109400
H	2.32363100	3.44463000	-0.07077800
H	-0.44188600	2.97351000	-3.10893300
C	0.79740100	-1.96477000	-1.26791500
H	0.89995400	-2.00251600	-2.36316500
H	-0.09916900	-2.53937900	-0.97540300
O	1.94777000	-2.54310700	-0.68385400
C	2.27759800	-1.87906700	0.52336400
C	1.15195700	-0.85424100	0.73950200
H	0.31378300	-1.31517900	1.27992900
H	1.47896000	0.02937500	1.29664400
C	5.91535300	-0.73271200	-0.35013600
C	3.65452200	-1.23986500	0.42478100
C	4.85203700	0.53242100	1.41334000
C	5.93033900	0.36857700	0.61052000
C	4.67565900	-1.55583300	-0.39893800
O	3.76303000	-0.24336900	1.35094100
O	4.77366000	1.47516900	2.35025900
O	6.86212700	-0.95656100	-1.08584100
C	3.51613300	1.73869900	2.94730900
H	2.76698500	2.00267000	2.18473400
H	3.67563100	2.58659600	3.62047400
H	3.15741900	0.87223400	3.51962000
C	7.14594000	1.23769200	0.67589500
H	8.02034800	0.64097900	0.97458900
H	7.01313300	2.06280300	1.38460100
H	7.37091200	1.63900300	-0.32239000
C	4.66858900	-2.66984300	-1.40594300
H	5.70923800	-2.96324600	-1.58953100
H	4.25216600	-2.32671700	-2.36592500
H	4.07494400	-3.52799100	-1.07846300
H	2.30188100	-2.61639300	1.34444800

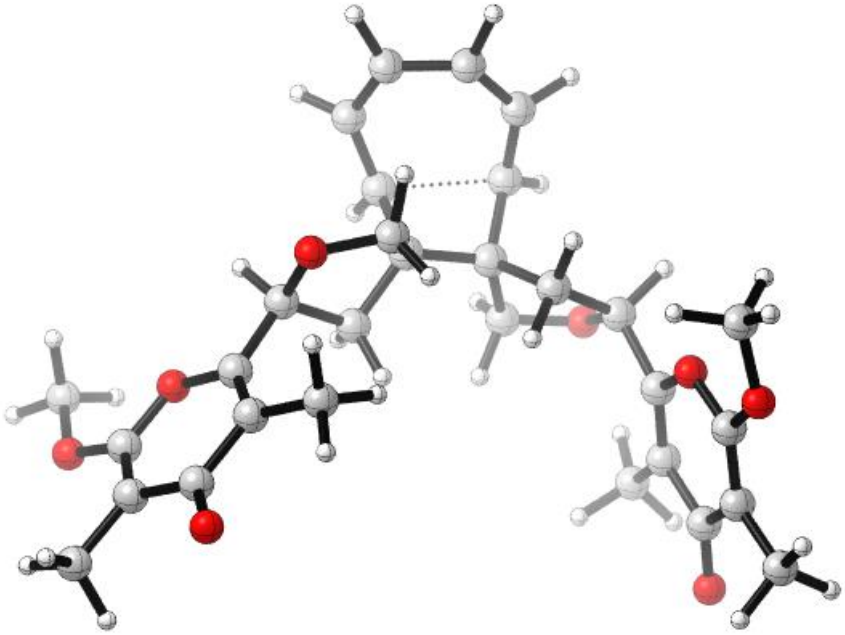

THFpyr_cyclooctatriene2_6π_TS
E(M062X/def2TZVP) = -1765.251762 Hartree
Free energy correction (M062X/def2SVP) = 0.523204 Hartree
G = -4633294.829

C	-0.39053400	4.80149000	-1.37531800
C	1.00459100	4.81918900	-1.22594800
H	1.56088900	5.48729100	-1.88786800
C	1.63325800	4.32024700	-0.08687400
C	-1.08794200	3.50583800	0.69214400
C	-1.27790300	4.40477400	-0.36964900
H	-2.16994600	5.03972300	-0.29575600
C	1.09735600	3.29366600	0.69273100
H	1.50204600	3.20849400	1.70957200
C	0.61553600	1.93941500	0.14168000
C	-0.83248300	1.99510000	0.59882300
C	1.49069900	0.79618200	0.68116400
H	0.98492800	-0.17185000	0.53287300
H	1.74846300	0.89432100	1.74453500
C	0.85994000	1.70933400	-1.35583700
H	0.67276900	2.57558100	-1.99631200
H	0.21690100	0.87894100	-1.69966300
O	2.22178600	1.35012000	-1.47514000
C	2.71663600	0.88635500	-0.23794300
C	3.47424300	-0.40808000	-0.38603700
C	4.05806000	-2.64623800	-1.17081600
C	5.34999700	-1.49133400	0.52179200
C	5.18482000	-2.59809700	-0.24227100
C	3.17741800	-1.44837100	-1.18901400
O	4.54114300	-0.42342000	0.46554600
O	6.33724900	-1.36182100	1.40564100
O	3.84805000	-3.61313100	-1.88371600
C	6.09863700	-3.78085400	-0.17964600

H	5.53162500	-4.67852900	0.10683400
H	6.91458300	-3.62266700	0.53416500
H	6.51637200	-3.98235300	-1.17653100
C	2.00366600	-1.47327900	-2.12551300
H	2.15265500	-0.77773800	-2.96203600
H	1.06865600	-1.18864300	-1.62131400
H	1.90220500	-2.49247600	-2.51630000
C	6.49582900	-0.13498300	2.09333600
H	6.66147000	0.69506100	1.39205700
H	7.37594100	-0.26240900	2.73100500
H	5.61721400	0.08942600	2.71401600
H	-1.71928400	3.74667900	1.55963100
H	-0.79791000	5.43294500	-2.16917600
H	2.50503800	4.86677300	0.28679200
C	-1.09803800	1.39621700	1.98773400
H	-0.68094000	1.99026300	2.81296000
H	-0.71158600	0.36283300	2.05262800
O	-2.50432600	1.41260600	2.09618700
C	-3.06808300	1.13104400	0.83472300
C	-1.91078600	1.24082000	-0.19011600
H	-1.54602700	0.23273400	-0.44603000
H	-2.20253400	1.75230700	-1.11606500
C	-4.55397600	-2.47269800	1.23620200
C	-3.73939400	-0.22164200	0.75420500
C	-4.84083400	-1.45468000	-0.93329000
C	-5.03266600	-2.53523800	-0.14082500
C	-3.88266600	-1.21002700	1.66013000
O	-4.22373200	-0.33834000	-0.52212600
O	-5.25227500	-1.39635700	-2.19781800
O	-4.68965500	-3.40371500	2.01198400
C	-4.90257000	-0.27555500	-2.98830400
H	-5.32793300	0.65019000	-2.57662800
H	-5.32278300	-0.46741000	-3.98028800
H	-3.81085700	-0.16731900	-3.06275600
C	-5.71391000	-3.78486600	-0.60124500
H	-5.04845400	-4.64800600	-0.45680300
H	-6.00429400	-3.71930100	-1.65571100
H	-6.60712600	-3.97414400	0.01172600
C	-3.41301400	-1.19982900	3.08581700
H	-4.16959400	-1.71017500	3.69550100
H	-3.22904000	-0.19222600	3.46253600
H	-2.49500300	-1.80094800	3.18135400
H	-3.83911500	1.89369100	0.62930100
H	3.42944400	1.62800600	0.16627300

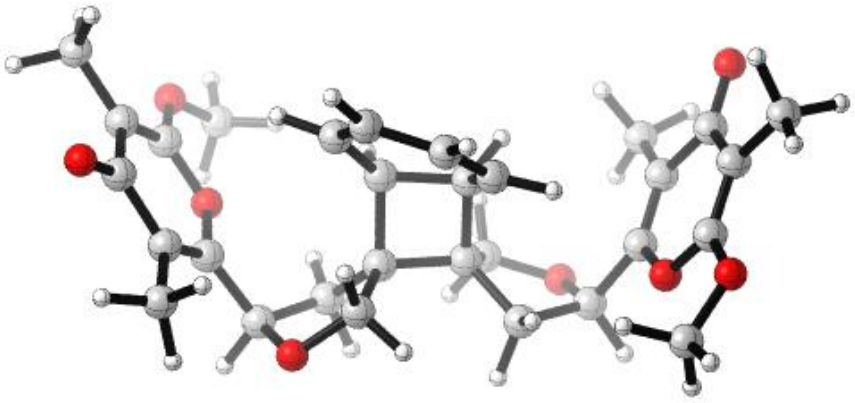

THFpyr_BOD1_GS
E(M062X/def2TZVP) = -1765.305735 Hartree
Free energy correction (M062X/def2SVP) = 0.527384 Hartree
G = -4633425.561

C	0.73199600	0.49001200	0.39599000
C	0.53417500	-1.56598100	1.78884500
C	-1.52506000	-0.29211000	1.42183700
C	-0.88151100	-1.27797500	2.06476300
C	-0.81863000	0.51195200	0.37363900
C	1.28367300	-0.75935300	1.02107000
H	-1.18721800	1.54908500	0.37734500
H	-1.39733800	-1.87316600	2.82044500
H	2.35382500	-0.95858900	0.90520300
C	0.70668000	0.52442100	-1.16286600
C	-0.76866800	0.03134800	-1.12529600
C	-1.78066800	0.63204200	-2.10441100
H	-1.34219400	0.68859000	-3.11253600
H	-2.13497400	1.62815300	-1.81363100
C	-0.97042600	-1.48664300	-1.35306600
H	-0.11942300	-1.95074000	-1.86989600
H	-1.13498700	-2.01839200	-0.40324100
O	-2.10780100	-1.63397700	-2.19538800
C	-2.86084100	-0.45102400	-2.13985400
H	-3.47557700	-0.40337600	-3.05264000
C	-5.19975200	-1.21006000	0.89831900
C	-3.77607500	-0.41621100	-0.92367900
C	-4.74680200	1.14049100	0.55823500
C	-5.37067600	0.18649000	1.29101700
C	-4.36630200	-1.46077800	-0.30795000
O	-3.96179600	0.86974000	-0.49359400
O	-4.85218300	2.44148400	0.82045700
O	-5.71953800	-2.12406400	1.51622600
C	-4.12352400	3.36821900	0.03834200
H	-3.03997800	3.20412000	0.13535400
H	-4.38003000	4.35718600	0.42994800
H	-4.40431200	3.30345400	-1.02221700
C	-6.23359000	0.49053400	2.47441500

H	-5.85114200	-0.03608200	3.36048400
H	-7.25146600	0.11116700	2.30310600
H	-6.27518200	1.56625800	2.67779300
C	-4.23571700	-2.89589300	-0.72367500
H	-3.43199000	-3.38241200	-0.14816000
H	-4.00668700	-3.01145100	-1.78643100
H	-5.16774700	-3.41303400	-0.46375400
H	-2.56793500	-0.06830700	1.65913600
H	0.98874600	-2.43484900	2.26871900
H	1.23028100	1.36476800	0.84807600
C	0.91528200	1.94291100	-1.71296100
H	0.71702700	2.72001600	-0.95543600
H	0.27615100	2.14075900	-2.58841800
O	2.27313000	2.02338500	-2.12243600
C	1.76585000	-0.24180100	-1.94684100
H	2.05341700	-1.19758400	-1.49251900
H	1.40759500	-0.43060900	-2.97158800
C	2.91050400	0.77992900	-1.99009800
H	3.56259400	0.62411100	-2.86510700
C	4.93201700	1.12390000	1.35861400
C	3.78775700	0.67389400	-0.75408800
C	5.09301000	-1.01863300	0.25966600
C	5.41936500	-0.25217600	1.32659400
C	4.07291800	1.56086000	0.22226800
O	4.31483400	-0.59043100	-0.74510500
O	5.52186500	-2.26828100	0.09888000
O	5.19635300	1.88424100	2.27442100
C	4.84609300	-3.10821400	-0.82018000
H	4.95108600	-2.73968000	-1.84931700
H	3.77676700	-3.18521700	-0.56957900
H	5.31601900	-4.09220700	-0.72891900
C	6.27259700	-0.73241900	2.45713000
H	5.76479400	-0.53684800	3.41192800
H	7.21739000	-0.16970500	2.48524600
H	6.49396500	-1.80174200	2.36705300
C	3.59615700	2.97994400	0.32350100
H	4.45105000	3.60580200	0.61306700
H	2.87509600	3.07073500	1.15170000
H	3.15445600	3.34695700	-0.60458900

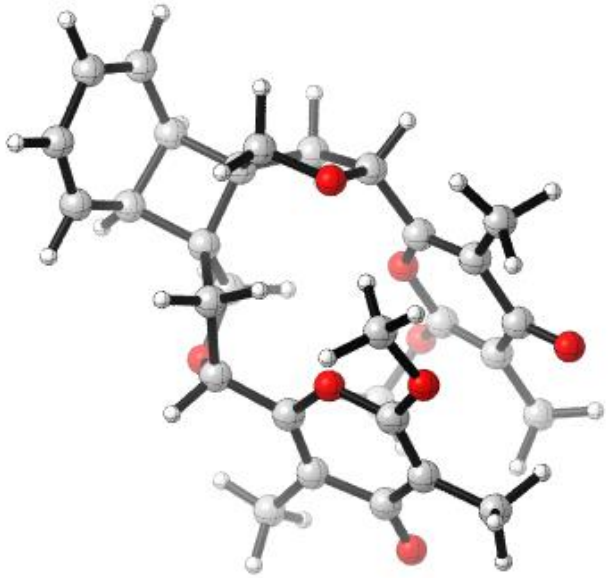

THFpyr_BOD2_GS
E(M062X/def2TZVP) = -1765.312786 Hartree
Free energy correction (M062X/def2SVP) = 0.540113 Hartree
G = -4633410.653

C	4.32887700	0.06817800	-1.07487900
C	6.20601700	-0.46671800	0.43914000
C	4.74157600	1.40872500	1.06201300
C	5.74601500	0.57555100	1.37131300
C	3.99483700	1.33320800	-0.23696600
C	5.57313200	-0.69140500	-0.72026100
C	2.96422200	-0.55032800	-0.66511400
C	2.50543900	0.85827600	-0.16361100
H	4.47366500	2.21403500	1.75181300
H	7.09659600	-1.04010500	0.70307000
H	4.30849900	0.29199100	-2.15208200
C	2.15962900	-1.29950900	-1.73311300
H	2.85671500	-1.93678100	-2.29714900
H	1.64837000	-0.64988900	-2.45086100
C	2.96233400	-1.60713600	0.43816300
H	3.67908100	-2.41481600	0.20197500
H	3.18897300	-1.22185500	1.44109200
O	1.63184800	-2.09504000	0.43340700
C	1.19372500	-2.19156600	-0.92124100
H	1.28975200	-3.24371400	-1.24240900
C	-2.67773200	-2.05071000	-0.59241000
C	-0.27869300	-1.83438000	-1.01079300
C	-1.77486300	-0.35705900	-2.07299800
C	-2.86622300	-0.90535800	-1.49260900
C	-1.28138100	-2.50349500	-0.40070000
O	-0.51751400	-0.77858500	-1.82222800
O	-1.77841500	0.61123000	-2.98966000
O	-3.61117100	-2.62525900	-0.05668300
C	-1.98592800	1.94471500	-2.52890300

H	-2.87866900	2.00686300	-1.88694700
H	-2.13028000	2.56095900	-3.42286200
H	-1.10544500	2.30044800	-1.97192200
C	-4.25528600	-0.42642400	-1.78228000
H	-4.58561700	0.31605000	-1.03685800
H	-4.94410900	-1.27948000	-1.72952500
H	-4.31108000	0.03671700	-2.77633000
C	-1.09165300	-3.73598100	0.42846500
H	-1.74259200	-3.66691600	1.31047500
H	-0.05033200	-3.88008200	0.73944200
H	-1.43405300	-4.61739800	-0.13606800
H	4.10166800	2.29611400	-0.76376600
H	6.27673600	0.69064800	2.31832500
H	5.94239900	-1.44958700	-1.41533100
C	1.58585200	1.64722200	-1.09835300
H	2.10066000	2.09456500	-1.96082100
H	0.76615400	1.00777400	-1.46444700
O	1.06940200	2.69019600	-0.29893500
C	1.75700900	0.97573700	1.17494500
H	1.24551300	0.03570000	1.40206400
H	2.43820400	1.19413000	2.00590700
C	0.74827500	2.12663300	0.96005000
H	0.87745900	2.93016700	1.70107500
C	-3.14571600	1.80398900	0.79941600
C	-0.71114900	1.67790800	1.02486700
C	-2.05723800	-0.07990600	1.82638600
C	-3.22645600	0.53018600	1.50261300
C	-1.79310900	2.40686400	0.68022400
O	-0.85157700	0.43306100	1.55573800
O	-2.00277500	-1.25821000	2.43177900
O	-4.12436400	2.37786900	0.33621000
C	-0.75249400	-1.69799400	2.94889200
H	-0.35713400	-0.97033000	3.67309000
H	-0.02237800	-1.85121800	2.14089500
H	-0.95883700	-2.64663300	3.45399000
C	-4.55419600	-0.08728100	1.82343000
H	-4.59207400	-0.41024800	2.87327600
H	-4.74025500	-0.97385800	1.19849100
H	-5.33961600	0.65578400	1.63822300
C	-1.73898700	3.82734800	0.20755600
H	-2.17514400	4.47920500	0.98033200
H	-2.37982000	3.94788200	-0.67672200
H	-0.72146900	4.15603500	-0.02588900

Structure	Number of imaginary frequencies	Free energy correction (Hartree)	Electronic energy (Hartree)	Relative Gibbs free energy (kJ/mol)
SBINOL				
SBINOL_tetraene_GS	0	0.350937	-1229.346351	0.000
SBINOL_tetraene_8π1_TS	1	0.350731	-1229.331457	38.563
SBINOL_tetraene_8π2_TS	1	0.354466	-1229.329214	54.259
SBINOL_cyclooctatriene1_GS	0	0.354776	-1229.367443	-45.298
SBINOL_cyclooctatriene2_GS	0	0.35447	-1229.360953	-29.062
SBINOL_cyclooctatriene1_6π_TS	1	0.354665	-1229.325229	65.244
SBINOL_cyclooctatriene2_6π_TS	1	0.353633	-1229.32932	51.793
SBINOL_BOD1_GS	0	0.356513	-1229.361364	-24.777
SBINOL_BOD2_GS	0	0.355446	-1229.370907	-52.633
MSBINOL				
MSBINOL_tetraene_GS	0	0.405653	-1307.957772	0.000
MSBINOL_tetraene_8π1_TS	1	0.408142	-1307.941346	49.661
MSBINOL_tetraene_8π2_TS	1	0.407905	-1307.934904	65.953
MSBINOL_cyclooctatriene1_GS	0	0.409809	-1307.972108	-26.728
MSBINOL_cyclooctatriene2_GS	0	0.409576	-1307.970358	-22.745
MSBINOL_cyclooctatriene1_6π_TS	1	0.408737	-1307.937068	62.455
MSBINOL_cyclooctatriene2_6π_TS	1	0.409282	-1307.938758	59.449
MSBINOL_BOD1_GS	0	0.410739	-1307.98356	-54.353
MSBINOL_BOD2_GS	0	0.410619	-1307.981533	-49.346
SBINAP				
SBINAP_tetraene_GS	0	0.398865	-1157.524179	0.000

SBINAP_tetraene_8π1_TS	1	0.399871	-1157.508611	43.515
SBINAP_tetraene_8π2_TS	1	0.401894	-1157.509113	47.508
SBINAP_cyclooctatriene1_GS	0	0.402889	-1157.546635	-48.393
SBINAP_cyclooctatriene2_GS	0	0.402462	-1157.53639	-22.616
SBINAP_cyclooctatriene1_6π_TS	1	0.402348	-1157.505308	58.690
SBINAP_cyclooctatriene2_6π_TS	1	0.401246	-1157.501379	66.113
SBINAP_BOD1_GS	0	0.40404	-1157.544087	-38.681
SBINAP_BOD2_GS	0	0.40304	-1157.544016	-41.121

Table S8: Calculated relative free energies of BINOL-tetraene compounds

SBINOL Cartesian Coordinates

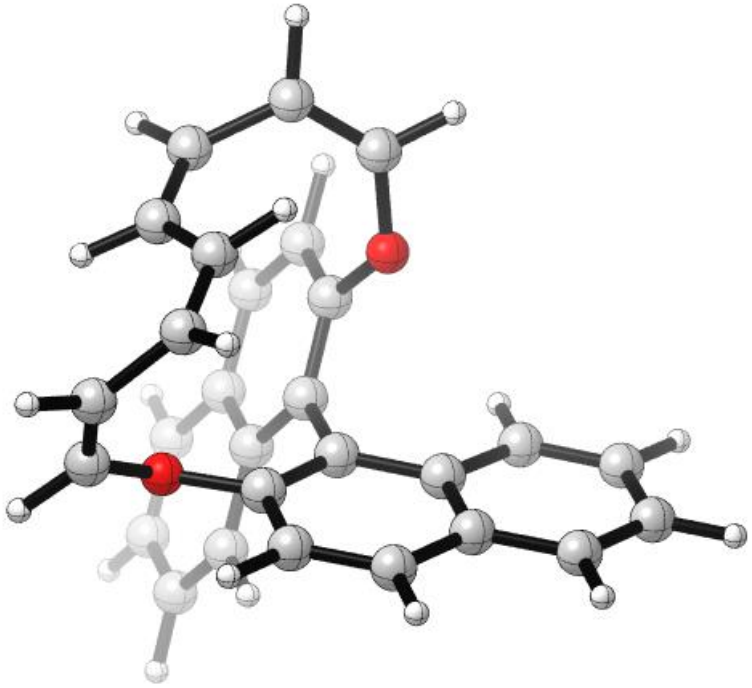

SBINOL_tetraene_GS
E(M062X/def2TZVP) = -1229.346351 Hartree
Free energy correction (M062X/def2SVP) = 0.350937 Hartree
G = -3226727.459

C	-0.11682800	-0.72023800	3.11144400
C	0.11682800	0.72023800	3.11144400
H	-0.76362100	1.36108100	3.20784700
C	1.33265100	1.29902700	3.09981900
C	-1.33265100	-1.29902700	3.09981900
C	-2.59701600	-0.56725200	2.90900500
C	2.59701600	0.56725200	2.90900500

C	-2.89535900	0.14620800	1.81638300
H	-3.81993500	0.72158100	1.72809600
C	2.89535900	-0.14620800	1.81638300
H	3.81993500	-0.72158100	1.72809600
H	1.39568300	2.38390100	3.23494400
C	1.53575400	0.83142900	0.12346000
C	0.33554300	0.66367500	-0.53765900
C	1.65745600	3.15810300	-0.50518300
C	-0.23767800	1.78186900	-1.22733000
C	2.20791600	2.08116900	0.13549700
C	0.42372800	3.04365400	-1.20039000
C	-1.45632200	1.67699100	-1.95466400
H	3.15720900	2.16936500	0.66329900
H	0.36982000	5.11159000	-1.84378800
H	2.17179800	4.12125400	-0.49781300
C	-1.98677100	2.76568200	-2.60345100
H	-1.96681300	0.71440100	-1.99326900
H	-2.92123300	2.66204100	-3.15717900
C	-1.33265100	4.02125500	-2.56435400
H	-1.76650300	4.87707000	-3.08328000
C	-0.15123600	4.15236500	-1.87791700
C	-1.53575400	-0.83142900	0.12346000
C	-0.33554300	-0.66367500	-0.53765900
C	-1.65745600	-3.15810300	-0.50518300
C	0.23767800	-1.78186900	-1.22733000
C	-2.20791600	-2.08116900	0.13549700
C	-0.42372800	-3.04365400	-1.20039000
C	1.45632200	-1.67699100	-1.95466400
H	-3.15720900	-2.16936500	0.66329900
H	-0.36982000	-5.11159000	-1.84378800
H	-2.17179800	-4.12125400	-0.49781300
C	1.98677100	-2.76568200	-2.60345100
H	1.96681300	-0.71440100	-1.99326900
H	2.92123300	-2.66204100	-3.15717900
C	1.33265100	-4.02125500	-2.56435400
H	1.76650300	-4.87707000	-3.08328000
C	0.15123600	-4.15236500	-1.87791700
H	-3.36590400	-0.62006800	3.68529000
H	-1.39568300	-2.38390100	3.23494400
H	0.76362100	-1.36108100	3.20784700
H	3.36590400	0.62006800	3.68529000
O	-2.10322500	0.26901400	0.71348600
O	2.10322500	-0.26901400	0.71348600

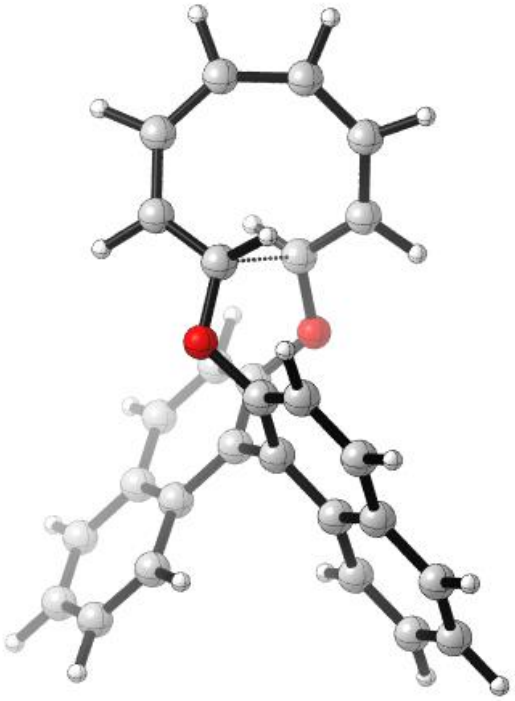

SBINOL_tetraene_8π1_TS
E(M062X/def2TZVP) = -1229.331457 Hartree
Free energy correction (M062X/def2SVP) = 0.350731 Hartree
G = -3226688.896

C	-5.40644600	0.57272400	-0.40824100
C	-5.40645100	-0.57285900	0.40823400
H	-6.41711900	-0.96634900	0.55813100
C	-4.44297900	-1.30844800	1.10879100
C	-4.44297000	1.30830600	-1.10879800
H	-4.82098800	2.24421400	-1.52903700
C	-3.10242700	1.05588200	-1.39936700
C	-3.10243500	-1.05603000	1.39935500
H	-2.51269000	-1.86599400	1.83818500
C	-2.38285000	-0.09757700	-1.10891900
H	-2.86205000	-1.07507500	-1.02683600
C	-2.38285100	0.09742600	1.10890800
H	-2.86205400	1.07492400	1.02682500
H	-6.41711100	0.96622000	-0.55813700
H	-4.82100200	-2.24435300	1.52903300
H	-2.51267900	1.86584300	-1.83819700
C	-0.21100900	1.06197800	1.11248100
C	0.81783300	0.69472600	0.26718000
C	0.58674400	3.32679900	1.26205700
C	1.78552600	1.67538500	-0.11015200
C	-0.33761000	2.37739500	1.61623400
C	1.66882300	3.00337400	0.39925000
C	2.85794500	1.37593900	-0.99734100
H	-1.16015700	2.60554700	2.29555800
H	2.53849000	4.98873000	0.42248100
H	0.50689300	4.34488100	1.64779700

C	3.77315100	2.34030200	-1.34166400
H	2.94135700	0.36622800	-1.40218400
H	4.58900400	2.09416000	-2.02279000
C	3.66556100	3.65517400	-0.82379300
H	4.40079200	4.41012600	-1.10542300
C	2.63519800	3.97676800	0.02378300
C	-0.21091700	-1.06205000	-1.11249100
C	0.81788900	-0.69472400	-0.26717700
C	0.58701400	-3.32681000	-1.26206100
C	1.78565700	-1.67530600	0.11016100
C	-0.33741200	-2.37747900	-1.61624400
C	1.66906100	-3.00330300	-0.39924500
C	2.85804500	-1.37577900	0.99735900
H	-1.15993700	-2.60569800	-2.29557300
H	2.53888500	-4.98859000	-0.42247800
H	0.50724200	-4.34489800	-1.64780000
C	3.77332500	-2.34007200	1.34168600
H	2.94137400	-0.36606400	1.40220800
H	4.58915300	-2.09386800	2.02281900
C	3.66584200	-3.65494900	0.82380800
H	4.40113100	-4.40984500	1.10544000
C	2.63551000	-3.97662300	-0.02377500
O	-1.08181200	-0.08501300	-1.51799200
O	-1.08183100	0.08486900	1.51797500

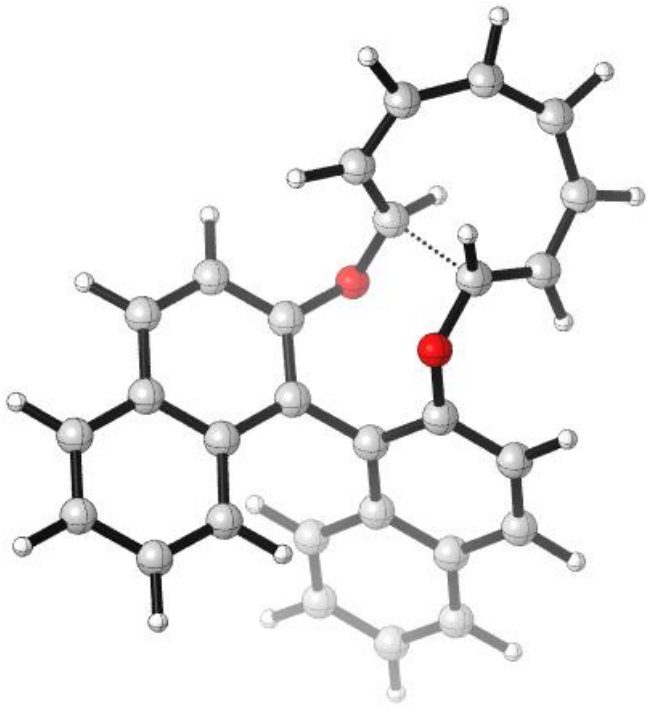

SBINOL_tetraene_8π2_TS
E(M062X/def2TZVP) = -1229.329214 Hartree
Free energy correction (M062X/def2SVP) = 0.354466 Hartree
G = -3226673.201

C	0.70048400	0.09356400	5.44321900

C	-0.70048400	-0.09356400	5.44321900
H	-1.07827800	-0.24168300	6.46013600
C	-1.73701000	-0.10585300	4.49601000
C	1.73701000	0.10585300	4.49601000
H	2.69827500	0.45153200	4.88464900
C	1.73701000	-0.26651400	3.15110000
C	-1.73701000	0.26651400	3.15110000
H	-2.59295100	-0.01391100	2.53449700
C	0.61232800	-0.86169400	2.57330700
H	-0.03532700	-1.44789000	3.22287600
C	-0.61232800	0.86169400	2.57330700
H	1.07827800	0.24168300	6.46013600
H	-2.69827500	-0.45153200	4.88464900
H	2.59295100	0.01391100	2.53449700
C	-1.31740800	0.83886200	0.29046400
C	-0.73452800	0.12170000	-0.73605600
C	-3.49434000	0.74937500	-0.74330800
C	-1.57463400	-0.37513000	-1.78799500
C	-2.69201100	1.18348100	0.27788000
C	-2.96417100	-0.05304200	-1.78976400
C	-1.07419000	-1.20776800	-2.82924000
H	-3.07920300	1.80721900	1.08417200
H	-4.85365700	-0.28011700	-2.82496100
H	-4.55296100	1.01482000	-0.76541300
C	-1.90341200	-1.67221900	-3.82115900
H	-0.01951200	-1.48376100	-2.82721600
H	-1.49979800	-2.31408900	-4.60549400
C	-3.27793400	-1.33130800	-3.83275600
H	-3.92340000	-1.70371200	-4.62928900
C	-3.79365400	-0.54205700	-2.83562100
C	1.31740800	-0.83886200	0.29046400
C	0.73452800	-0.12170000	-0.73605600
C	3.49434000	-0.74937500	-0.74330800
C	1.57463400	0.37513000	-1.78799500
C	2.69201100	-1.18348100	0.27788000
C	2.96417100	0.05304200	-1.78976400
C	1.07419000	1.20776800	-2.82924000
H	3.07920300	-1.80721900	1.08417200
H	4.85365700	0.28011700	-2.82496100
H	4.55296100	-1.01482000	-0.76541300
C	1.90341200	1.67221900	-3.82115900
H	0.01951200	1.48376100	-2.82721600
H	1.49979800	2.31408900	-4.60549400
C	3.27793400	1.33130800	-3.83275600
H	3.92340000	1.70371200	-4.62928900
C	3.79365400	0.54205700	-2.83562100
O	0.51337000	-1.31902700	1.29119500
O	-0.51337000	1.31902700	1.29119500
H	0.03532700	1.44789000	3.22287600

SBINOL_cyclooctatriene1_GS
E(M062X/def2TZVP) = -1229.367443 Hartree
Free energy correction (M062X/def2SVP) = 0.354776 Hartree
G = -3226772.757

C	-0.46208600	1.01019700	0.91259500
C	0.67225700	0.71313600	0.18077500
C	0.01941800	3.37713200	0.88340700
C	1.50244600	1.79269000	-0.27185300
C	-0.78705900	2.34228200	1.27427600
C	1.17689300	3.13216800	0.09543900
C	2.63125900	1.58204100	-1.11439600
H	-1.68113600	2.50671700	1.87799600
H	1.74471100	5.21751000	-0.05026000
H	-0.21859500	4.40420100	1.16691100
C	3.40580500	2.63569800	-1.53554700
H	2.87326500	0.56758000	-1.43176000
H	4.26331700	2.44988800	-2.18392700
C	3.09819500	3.96094500	-1.14219800
H	3.72458000	4.78768700	-1.47990100
C	2.00418200	4.19959200	-0.34874800
C	0.02017400	-1.44166500	-0.84214000
C	0.96471500	-0.70584700	-0.15077100
C	1.41872400	-3.41264600	-0.84719900
C	2.17544700	-1.35495000	0.26415600
C	0.24939500	-2.79415100	-1.20068700
C	2.40603300	-2.71484900	-0.10028900
C	3.15243300	-0.69955200	1.06721900
H	-0.52022600	-3.31321000	-1.77453100
H	3.77313600	-4.39179100	0.00937500
H	1.60565600	-4.45041100	-1.12997900
C	4.30089300	-1.34724500	1.45289800
H	2.97526400	0.32874900	1.38273900
H	5.03282600	-0.82572200	2.07136600
C	4.54133400	-2.68694000	1.06120400

H	5.46017800	-3.18724500	1.36995000
C	3.60961700	-3.35357700	0.30589400
O	-1.15573400	-0.86047500	-1.22982800
O	-1.28637300	0.00653000	1.33978400
C	-2.51435200	-0.14318200	0.63250500
H	-2.79427200	0.81056100	0.15229100
C	-3.55036300	-0.57163900	1.62059500
H	-3.16408400	-1.16239800	2.45620300
C	-4.84856000	-0.24552700	1.56679900
H	-5.49342900	-0.53883800	2.40062300
C	-5.46705700	0.53825200	0.50344500
H	-6.19462300	1.29053400	0.82422400
C	-4.58916900	-0.63765500	-1.59731900
H	-5.13542300	-0.89115500	-2.51283700
C	-5.29054100	0.39669300	-0.82657700
C	-2.31322200	-1.19099700	-0.46267000
H	-2.13793400	-2.16413200	0.03055100
C	-3.44172900	-1.31936000	-1.44286800
H	-3.20730200	-2.04342500	-2.22925500
H	-5.87956600	1.07019100	-1.45711600

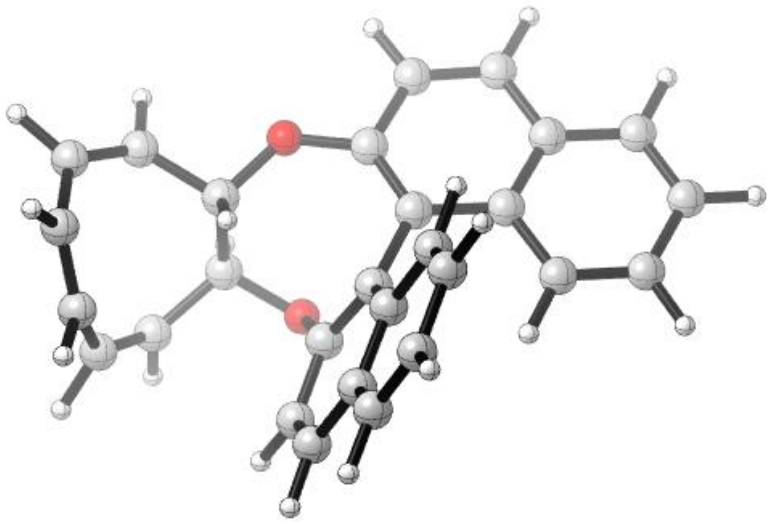

SBINOL_cyclooctatriene2_GS
E(M062X/def2TZVP) = -1229.360953 Hartree
Free energy correction (M062X/def2SVP) = 0.354470 Hartree
G = -3226756.521

C	-0.68062800	0.35873500	1.35905100
C	0.26382000	0.44601900	0.35325000
C	-1.07110700	2.74225000	1.33082600
C	0.48488700	1.71888200	-0.27200000
C	-1.32529600	1.51065900	1.87518800
C	-0.18755500	2.87408400	0.22563500
C	1.34603100	1.87019300	-1.39631000
H	-2.01507300	1.38297100	2.70857700
H	-0.47455000	5.01071800	0.00651200

H	-1.55550400	3.63569200	1.72967500
C	1.53548700	3.09910500	-1.97973200
H	1.85169900	0.99035100	-1.79529300
H	2.19346800	3.19090500	-2.84503400
C	0.88349200	4.24871200	-1.46931300
H	1.04891100	5.21988000	-1.93778200
C	0.04091100	4.13449100	-0.39233200
C	0.54292500	-1.93857800	-0.48944300
C	1.07449800	-0.74952600	-0.01607400
C	2.74883600	-2.93778100	-0.72415900
C	2.50321000	-0.68412400	0.20511200
C	1.39630900	-3.02222600	-0.85714500
C	3.34414300	-1.76948400	-0.17346800
C	3.12381000	0.43625600	0.82910700
H	0.90961000	-3.91319700	-1.25369400
H	5.36393200	-2.53428400	-0.28362900
H	3.38794900	-3.77174900	-1.02047400
C	4.48489100	0.48407700	1.02323300
H	2.51000600	1.26717600	1.17360400
H	4.92584900	1.35501700	1.51055900
C	5.31485000	-0.58146600	0.60748000
H	6.39336300	-0.52810000	0.76102800
C	4.74658200	-1.68851600	0.02669000
O	-0.75654700	-2.25839200	-0.70664200
O	-1.02156100	-0.87561500	1.84211400
C	-2.11647900	-1.48797000	1.13857000
H	-2.08387500	-2.53677200	1.46679400
C	-1.90054000	-1.48918000	-0.37655600
H	-1.80861800	-0.45881600	-0.75221800
C	-3.02772500	-2.17900400	-1.09176100
H	-2.89488300	-3.25665400	-1.21881200
C	-3.39975300	-0.85606100	1.61227600
H	-3.58303700	-1.05491200	2.67297900
C	-4.22126500	0.03046300	1.02709400
H	-4.97450700	0.46814600	1.69363400
C	-4.07531800	-1.55391300	-1.64274300
H	-4.76945100	-2.13337800	-2.25886000
C	-4.33684000	-0.12474900	-1.50150400
H	-4.62695400	0.42043900	-2.40495600
C	-4.32316300	0.55846300	-0.33907300
H	-4.58753800	1.61975300	-0.38778000

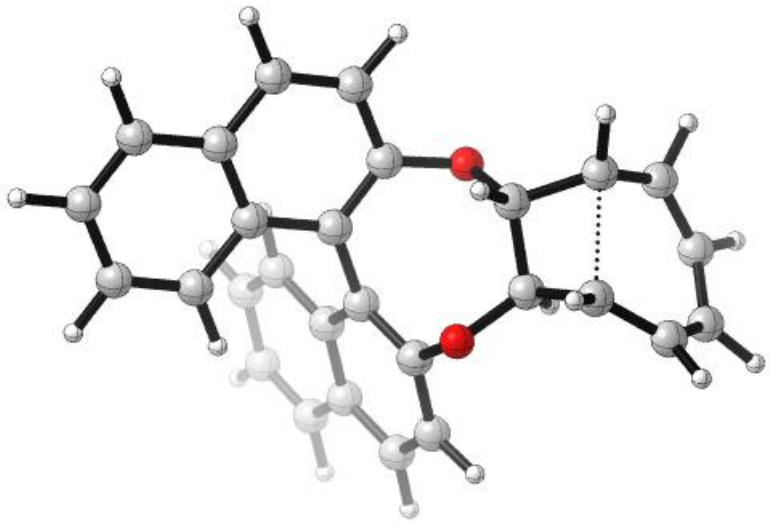

SBINOL_cyclooctatriene1_6π_TS
E(M062X/def2TZVP) = -1229.325229 Hartree
Free energy correction (M062X/def2SVP) = 0.354665 Hartree
G = -3226662.216

C	0.51321700	1.00872800	-1.08460300
C	-0.50600300	0.67336600	-0.21261600
C	-0.04364500	3.36239900	-1.00115100
C	-1.30111700	1.73717300	0.34554200
C	0.73806500	2.35132000	-1.48694800
C	-1.07252100	3.08464000	-0.06026000
C	-2.31564000	1.49360700	1.31486300
H	1.54998300	2.53381300	-2.19188700
H	-1.68006900	5.15169400	0.15806700
H	0.12105200	4.39450800	-1.31657000
C	-3.06354700	2.52382500	1.83241100
H	-2.49103800	0.47319400	1.65573200
H	-3.83039500	2.31114400	2.57865500
C	-2.84622100	3.85738900	1.41101900
H	-3.45005700	4.66517800	1.82664200
C	-1.86838300	4.12745900	0.48663800
C	-0.06886900	-1.56096900	0.89650500
C	-0.86568700	-0.73955600	0.11904100
C	-1.73905800	-3.31427800	0.94071000
C	-2.13606200	-1.24976200	-0.32908500
C	-0.51255100	-2.84203300	1.31833600
C	-2.57530100	-2.53906700	0.09209300
C	-2.98041600	-0.50846700	-1.20430000
H	0.15899500	-3.42112800	1.95324300
H	-4.15394400	-4.01827900	-0.00856800
H	-2.08455100	-4.29527000	1.27267800
C	-4.18913300	-1.01346800	-1.61927100
H	-2.65314300	0.47022200	-1.55537400
H	-4.81424100	-0.42834700	-2.29530500
C	-4.62913000	-2.28601000	-1.18261200

H	-5.59282600	-2.67299000	-1.51639100
C	-3.83456400	-3.03043100	-0.34715800
O	1.19975000	-1.20342200	1.27533600
O	1.38335300	0.07120100	-1.58054300
C	2.40905100	-0.22607600	-0.64896900
H	2.62832800	0.66479700	-0.03995900
C	3.68256200	-0.75522000	-1.26572900
H	3.51476200	-1.47517700	-2.07395400
C	4.83109100	0.05170600	-1.31145400
H	5.47409000	0.03400500	-2.19566700
C	5.23277400	0.77661900	-0.20274700
H	6.01834600	1.52812300	-0.31299900
C	4.35703100	-0.84494800	1.45690400
H	4.73359900	-1.27218800	2.39385000
C	4.92346300	0.37834600	1.11758500
C	2.13852500	-1.39405300	0.22934000
H	1.79194900	-2.22258200	-0.41159700
C	3.54875100	-1.70678200	0.67652400
H	3.68908500	-2.76785400	0.92173000
H	5.44516100	0.91216600	1.91568200

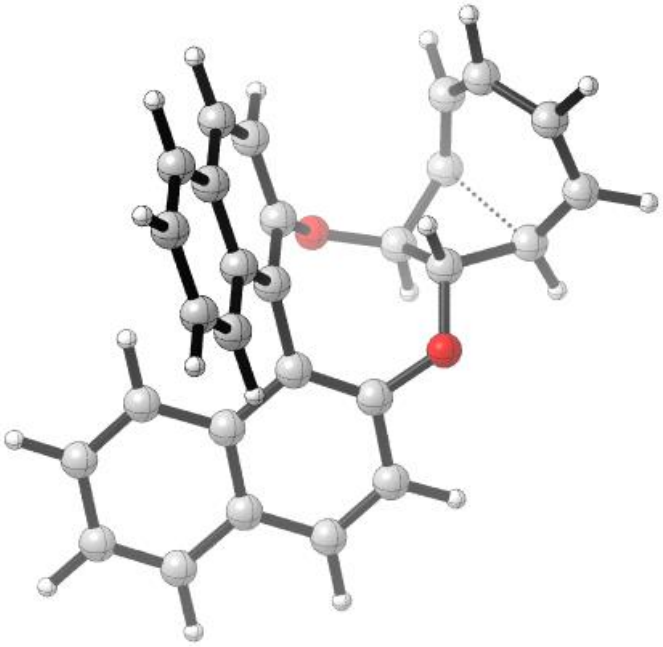

SBINOL_cyclooctatriene2_6π_TS
E(M062X/def2TZVP) = -1229.329320 Hartree
Free energy correction (M062X/def2SVP) = 0.353633 Hartree
G = -3226675.666

C	-0.63741900	0.52690400	1.29609600
C	0.30022900	0.54787800	0.28035700
C	-0.89063500	2.92613200	1.24421300
C	0.63746900	1.80429400	-0.32096900
C	-1.22953400	1.71577800	1.78960200
C	0.03659400	3.00196800	0.16909300

C	1.56158100	1.90117200	-1.39977800
H	-1.94891700	1.62646300	2.60379200
H	-0.08548800	5.15533200	-0.03864300
H	-1.33613700	3.84867500	1.62169800
C	1.87037900	3.11930800	-1.95477900
H	2.02023100	0.98940800	-1.78456800
H	2.57779700	3.17218300	-2.78360900
C	1.27739500	4.30807100	-1.46284900
H	1.53350900	5.26852900	-1.91213200
C	0.38088400	4.24673800	-0.42533800
C	0.41980300	-1.71340000	-0.86411800
C	1.00955700	-0.70232300	-0.12440300
C	2.50072400	-2.95413200	-0.99620900
C	2.39336300	-0.84546800	0.25074900
C	1.17762400	-2.83410600	-1.30848700
C	3.14490600	-1.97016300	-0.19594000
C	3.05369600	0.11618800	1.06697200
H	0.65364500	-3.58024800	-1.90603200
H	5.06793100	-2.96354300	-0.18872800
H	3.07632000	-3.81370000	-1.34510800
C	4.37822700	-0.03122400	1.40584300
H	2.49456000	0.97727000	1.43335400
H	4.85888700	0.71796700	2.03673800
C	5.12218300	-1.14441000	0.94988200
H	6.17269900	-1.24784200	1.22463600
C	4.51194200	-2.09343800	0.16689500
O	-0.87640600	-1.74119700	-1.27399600
O	-1.02475400	-0.66350800	1.83555600
C	-1.84690700	-1.47306900	1.00690600
H	-1.51731300	-2.51052700	1.16681600
C	-1.91223500	-1.21481500	-0.47351600
H	-2.06628600	-0.14838400	-0.69281800
C	-3.19718700	-1.97225200	-0.73771300
H	-3.04890200	-3.05325700	-0.82945900
C	-3.32480000	-1.37264300	1.34727700
H	-3.59620400	-1.98864700	2.21432200
C	-4.09283400	-0.19612000	1.23278900
H	-4.62589800	0.11202000	2.14067200
C	-4.23448200	-1.36933700	-1.45454300
H	-4.82321800	-1.95916800	-2.16204900
C	-4.61233400	-0.05993900	-1.18654400
H	-5.27293600	0.46127800	-1.88348400
C	-4.45874800	0.51591000	0.08886900
H	-4.96164000	1.47281400	0.24998400

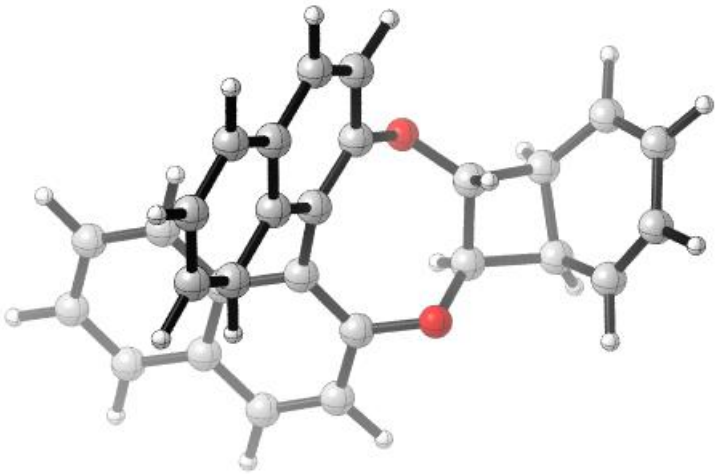

SBINOL_BOD1_GS
E(M062X/def2TZVP) = -1229.361364 Hartree
Free energy correction (M062X/def2SVP) = 0.356513 Hartree
G = -3226752.236

C	0.47380000	1.06139500	-1.15198100
C	-0.48303000	0.66731500	-0.23195400
C	-0.21585100	3.38001900	-1.04445800
C	-1.29952400	1.69192800	0.37235400
C	0.59610100	2.41298900	-1.56774400
C	-1.16913900	3.04920700	-0.04359000
C	-2.24504700	1.39700800	1.39614900
H	1.36060000	2.63817400	-2.31183200
H	-1.87173000	5.08133300	0.21142900
H	-0.12776500	4.41805600	-1.37083200
C	-3.01507000	2.38686300	1.95813400
H	-2.34820300	0.36973800	1.74556400
H	-3.72537000	2.13405900	2.74659700
C	-2.89341100	3.72970800	1.52834200
H	-3.51413900	4.50482400	1.97961600
C	-1.98634300	4.04933000	0.54945000
C	-0.04481900	-1.59353900	0.88292600
C	-0.81910200	-0.75759600	0.09566400
C	-1.76382100	-3.29820400	0.96132300
C	-2.10076500	-1.24928000	-0.34931900
C	-0.52458100	-2.85317500	1.32826700
C	-2.57487100	-2.51898400	0.09267900
C	-2.92578900	-0.50357400	-1.23962600
H	0.13502000	-3.44012300	1.96806100
H	-4.18757400	-3.96173000	0.01235600
H	-2.13572700	-4.26288300	1.31185700
C	-4.14413000	-0.98730500	-1.65192500
H	-2.57603200	0.46106200	-1.60714500
H	-4.75168200	-0.39899500	-2.34101600
C	-4.61672500	-2.24086900	-1.19573000
H	-5.58789900	-2.61065100	-1.52716000

C	-3.84366200	-2.98820100	-0.34314600
O	1.24902100	-1.29538800	1.23538000
O	1.40094300	0.19263200	-1.67273100
C	2.34863900	-0.15205700	-0.69258700
H	2.50647600	0.69553400	-0.00482800
C	3.73185700	-0.73210000	-1.06173800
C	4.87351900	0.22959900	-1.17666400
C	4.23669100	-0.81747800	1.43493700
C	2.09808300	-1.39867100	0.11982300
H	1.73798800	-2.19542800	-0.55280900
C	3.62616800	-1.54769500	0.27444100
C	5.47522200	0.68680800	-0.06867600
C	5.08398400	0.20915200	1.26609700
H	5.52980100	0.69155200	2.13791400
H	6.28385400	1.41648000	-0.14026100
H	3.64135800	-1.39030100	-1.93642200
H	3.97628100	-2.59121400	0.25807200
H	5.18659000	0.56753600	-2.16641600
H	3.99813500	-1.18054500	2.43737100

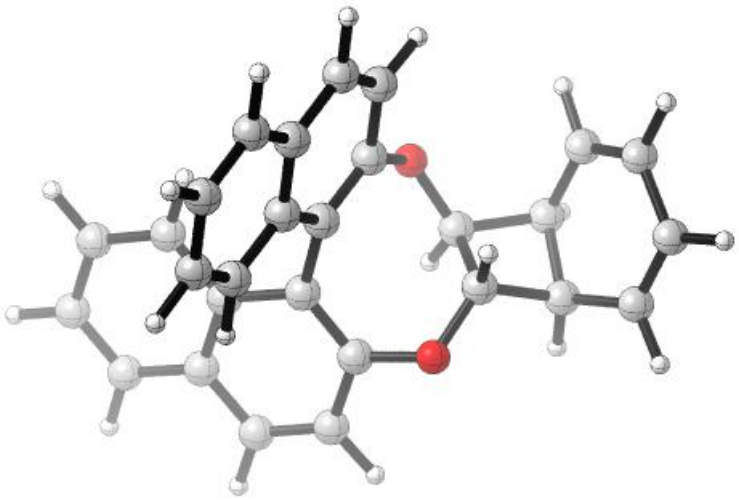

SBINOL_BOD2_GS
E(M062X/def2TZVP) = -1229.370907 Hartree
Free energy correction (M062X/def2SVP) = 0.355446 Hartree
G = -3226780.093

C	0.58233700	0.84501000	-1.18658300
C	-0.39039400	0.64376300	-0.22424700
C	0.29224400	3.24450600	-1.11933200
C	-1.02578000	1.79379700	0.35906500
C	0.91917600	2.14707700	-1.64119900
C	-0.68494400	3.10113400	-0.09592700
C	-2.00535900	1.67288200	1.38496900
H	1.68989900	2.22954800	-2.40769500
H	-1.04955300	5.22509600	0.11740300
H	0.54707500	4.24653400	-1.46997600

C	-2.60542200	2.78634400	1.92307600
H	-2.27353500	0.67992400	1.74727100
H	-3.35008200	2.66960800	2.71183500
C	-2.26608100	4.08248200	1.46684700
H	-2.75109900	4.95699700	1.90248700
C	-1.32468700	4.23191400	0.47862600
C	-0.20196300	-1.54300700	1.03916400
C	-0.88022600	-0.71572500	0.16070500
C	-2.02564700	-3.13428200	1.09867800
C	-2.16938500	-1.13671600	-0.31958700
C	-0.78363200	-2.74828300	1.51804100
C	-2.74640900	-2.35008100	0.15588700
C	-2.90840100	-0.36644700	-1.26142500
H	-0.19938500	-3.34018000	2.22280400
H	-4.44882900	-3.68473800	0.06141600
H	-2.47302800	-4.05825800	1.47030900
C	-4.14270000	-0.78239600	-1.70146200
H	-2.47984400	0.56226900	-1.63942700
H	-4.68779300	-0.17768800	-2.42776700
C	-4.71272500	-1.98659200	-1.22461700
H	-5.69362200	-2.30339200	-1.58130900
C	-4.02465600	-2.75157200	-0.31528200
O	1.04859100	-1.28368300	1.50491000
O	1.28386700	-0.17720300	-1.74885600
C	1.85639100	-1.13301700	-0.89027500
H	1.35374900	-2.10384900	-1.02169900
C	2.01420800	-0.81137100	0.59828700
C	4.96022800	0.55247200	-0.47058900
C	3.39149100	-1.31611800	-0.96575300
C	4.48800900	-0.98839100	1.37548100
C	3.36475600	-1.56580500	0.57029600
C	5.20427600	0.03264700	0.88459100
C	4.13646100	-0.06479800	-1.33044600
H	3.18218000	-2.62385800	0.80212100
H	5.50172500	1.44661600	-0.78525100
H	3.71289700	-2.15134300	-1.60665300
H	5.99812100	0.48858800	1.47889700
H	4.01045100	0.31305000	-2.34782800
H	4.68725800	-1.38826200	2.37151600
H	2.19675700	0.26385100	0.75117800

MSBINOL Cartesian Coordinates

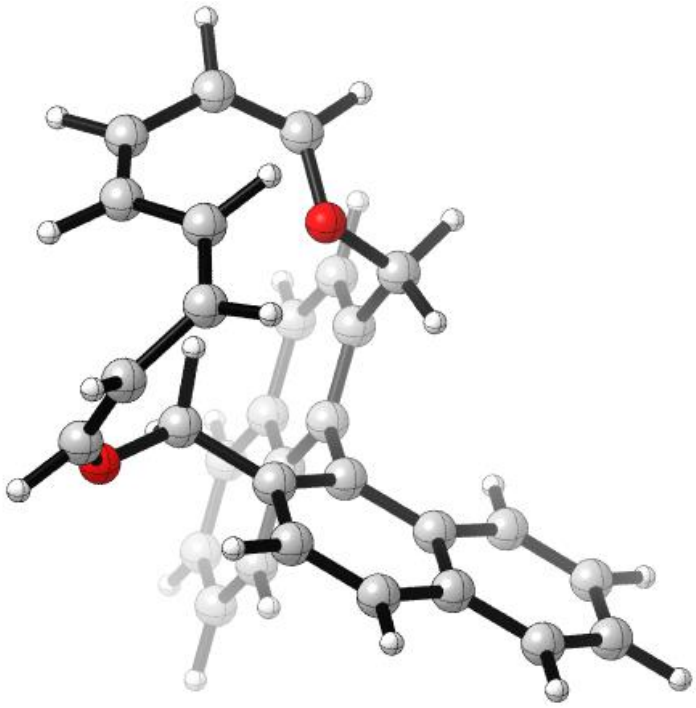

MSBINOL_tetraene_GS
E(M062X/def2TZVP) = -1307.957772 Hartree
Free energy correction (M062X/def2SVP) = 0.405653 Hartree
G = -3432978.088

C	4.22271800	0.53371500	0.23119400
C	3.93986400	-0.71610700	-0.46286600
H	3.96420000	-0.69328200	-1.55430800
C	3.67906300	-1.88566800	0.15196600
C	4.18707700	1.76539900	-0.31892600
C	3.71534500	2.12990600	-1.65435100
C	3.62026900	-2.10685900	1.60551700
C	2.65714400	1.61666200	-2.30396400
H	2.35595500	2.00886600	-3.28435000
C	2.84101300	-1.58668000	2.57135200
H	3.02422900	-1.90107900	3.60265100
H	3.58250500	-2.78009500	-0.47309200
C	0.13588100	-1.19718700	0.80825500
C	-0.86549200	-0.69723400	-0.00732100
C	-0.73971100	-3.44917800	0.54976600
C	-1.84293000	-1.57579200	-0.57720900
C	0.18116300	-2.58941300	1.09014600
C	-1.77242500	-2.97162000	-0.29945800
C	-2.89400100	-1.10144100	-1.41356500
H	0.96232300	-2.97348300	1.74492700
H	-2.67108000	-4.91222900	-0.64884700
H	-0.69271300	-4.51720300	0.77194000
C	-3.81491700	-1.97045600	-1.94742700
H	-2.96201100	-0.03323600	-1.62568200
H	-4.61376500	-1.58926500	-2.58529000
C	-3.73783400	-3.35861200	-1.67543400

H	-4.47482700	-4.03724900	-2.10707700
C	-2.73912600	-3.84469200	-0.86854600
C	-0.32927500	1.35601900	-1.35089100
C	-0.97122500	0.77210600	-0.27369900
C	-1.20083400	3.54505200	-0.75206100
C	-1.77487900	1.57817200	0.59963600
C	-0.44941800	2.75433000	-1.57988400
C	-1.88464600	2.97856600	0.35763900
C	-2.46768600	1.02245000	1.71243900
H	0.06772000	3.19549300	-2.43508600
H	-2.75348900	4.84598100	1.03208200
H	-1.28928800	4.61763700	-0.93513800
C	-3.22608500	1.81852600	2.53662500
H	-2.38768300	-0.04870800	1.90387000
H	-3.75003800	1.37658600	3.38521800
C	-3.33370700	3.20971400	2.29375000
H	-3.93883200	3.82993400	2.95650500
C	-2.67770000	3.77448400	1.22803500
H	4.21594800	2.96050200	-2.15688300
H	4.54158700	2.60104400	0.29253300
H	4.52204300	0.44609300	1.28066300
H	4.32104600	-2.85609700	1.98910300
O	1.90896700	0.59576100	-1.84134300
O	1.79156500	-0.74751900	2.56251400
C	0.55548100	0.54354500	-2.26411800
H	0.47920000	0.91733800	-3.29986700
H	0.26983900	-0.51471100	-2.25075400
C	1.16485100	-0.25219100	1.39495700
H	0.66206600	0.66985500	1.71701000
H	1.89294700	0.02828300	0.62115600

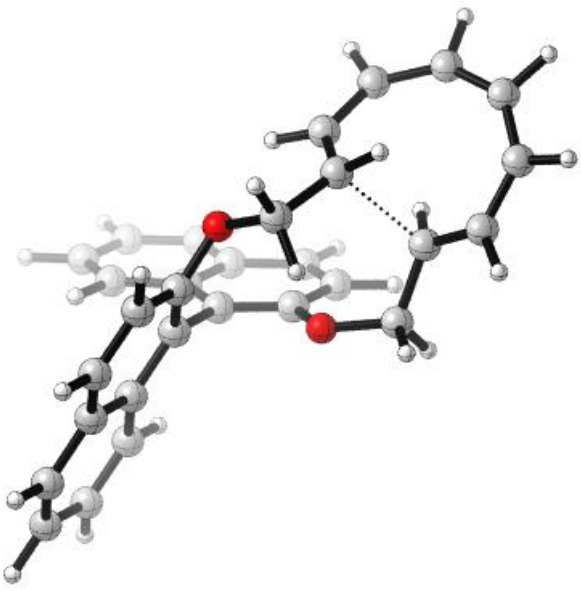

MSBINOL_tetraene_8π1_TS

E(M062X/def2TZVP) = -1307.941346 Hartree
Free energy correction (M062X/def2SVP) = 0.408142 Hartree
G = -3432928.427

C	-5.27781400	0.74555900	-0.87593300
C	-5.91105000	-0.24573800	-0.08814400
H	-7.00098800	-0.18090300	-0.17364400
C	-5.51553600	-1.24936000	0.79865000
C	-3.99617000	0.99965400	-1.37151700
H	-3.89652800	1.97548300	-1.85512200
C	-2.83321600	0.21615000	-1.39286700
C	-4.26079600	-1.52816300	1.35853800
H	-4.16010400	-2.47318200	1.90399400
C	-2.76793400	-1.10869700	-0.98720800
H	-3.69616100	-1.67962700	-0.98296400
C	-3.13615700	-0.73402900	1.20046800
H	-3.30709800	0.30947400	0.94020100
H	-6.00026000	1.49543600	-1.21571100
H	-6.32787800	-1.90581100	1.12279900
H	-1.90160800	0.69781000	-1.70011300
C	-0.28488300	0.48085500	1.03785500
C	0.84726700	0.60740400	0.24178100
C	-0.50631300	2.88238900	1.20534300
C	1.30842100	1.90809100	-0.11862700
C	-0.96035800	1.62771200	1.52930200
C	0.62780500	3.06131400	0.37531700
C	2.42787000	2.10437400	-0.98060900
H	-1.83899300	1.52195100	2.16413300
H	0.56121000	5.22759100	0.40769400
H	-1.02727100	3.76349400	1.58513100
C	2.84938600	3.36835300	-1.31026700
H	2.94537500	1.23178100	-1.38089100
H	3.70658300	3.49549300	-1.97325600
C	2.18048400	4.51219300	-0.80390500
H	2.52978600	5.50955900	-1.07405800
C	1.09271800	4.35726400	0.01676000
C	0.80074300	-1.47688400	-1.07925800
C	1.51067900	-0.63337200	-0.24425800
C	2.61431900	-3.06742700	-1.16238900
C	2.82793700	-1.01170700	0.16622500
C	1.34853500	-2.70014400	-1.53961500
C	3.38592500	-2.23759800	-0.30573800
C	3.60241200	-0.21576900	1.05857700
H	0.75489800	-3.32599400	-2.20766800
H	5.11111000	-3.54850700	-0.27187200
H	3.04747100	-4.00384000	-1.51960500
C	4.86326600	-0.60672600	1.43822000
H	3.17747400	0.71320700	1.44056000
H	5.43936100	0.01736700	2.12306900

C	5.42283600	-1.81444800	0.95206000
H	6.42676100	-2.11030900	1.25948600
C	4.69601700	-2.61037000	0.10272700
O	-0.43687000	-1.08364100	-1.48210600
O	-0.68157700	-0.78328800	1.31791800
C	-1.52948000	-1.93262300	-1.21968000
H	-1.71597600	-2.59372700	-2.08783200
H	-1.31626300	-2.57903300	-0.35201500
C	-1.89187800	-1.03683200	1.99309500
H	-1.91390200	-0.48376000	2.95070700
H	-1.85964300	-2.10705100	2.24106200

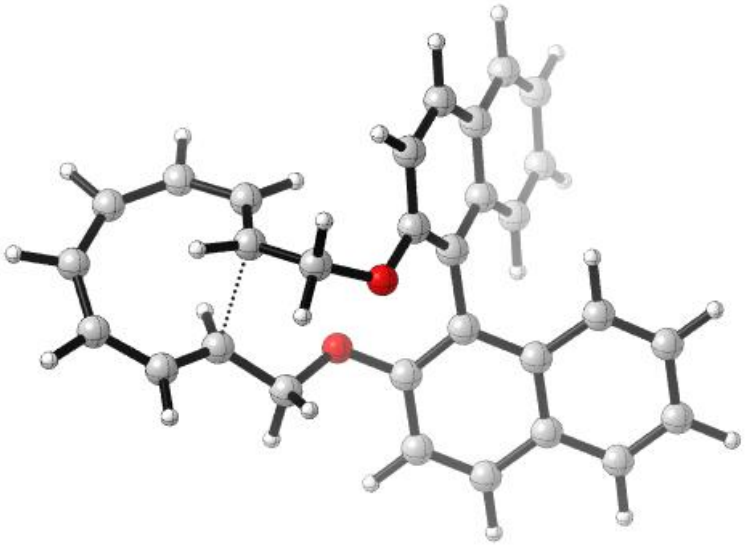

MSBINOL_tetraene _8π2_TS
E(M062X/def2TZVP) = -1307.934904 Hartree
Free energy correction (M062X/def2SVP) = 0.407905 Hartree
G = -3432912.136

C	-5.97941500	-0.15904500	-0.54888600
C	-5.31518900	1.04819300	-0.92651300
H	-5.99360400	1.70525300	-1.48130200
C	-4.06228500	1.62167200	-0.75595700
C	-5.61250400	-1.42732800	-0.11957800
H	-6.45135900	-2.06489000	0.17337200
C	-4.33494700	-2.02269800	-0.01821400
C	-2.96590200	1.23719500	0.05287500
H	-2.00440000	1.70060400	-0.17197100
C	-3.19427300	-1.45668200	-0.53652600
H	-3.30750800	-0.69681800	-1.30880100
C	-3.07415000	0.25944200	1.01552900
H	-7.06336700	-0.06285200	-0.67163400
H	-3.90545300	2.53470100	-1.33714700
H	-4.25868600	-2.95713100	0.54876600
C	-0.07270600	0.81447500	1.21984100
C	0.92673700	0.61798600	0.28075500
C	0.29107100	3.20637600	1.22262600

C	1.58085200	1.76356000	-0.28156800
C	-0.36830400	2.11255500	1.71584500
C	1.26401400	3.06868800	0.19770500
C	2.53285600	1.65077400	-1.33597900
H	-1.13553200	2.23686900	2.47968000
H	1.66431600	5.19081800	0.02605800
H	0.06213400	4.20311300	1.60470500
C	3.14039600	2.76464900	-1.86223500
H	2.77012000	0.66270100	-1.73094000
H	3.86090300	2.65265100	-2.67383600
C	2.83891000	4.05722500	-1.36677800
H	3.33369000	4.93182900	-1.79104400
C	1.91708300	4.20124600	-0.36066300
C	0.42258300	-1.64030800	-0.67602800
C	1.32892300	-0.76405900	-0.10141900
C	2.10192100	-3.37757500	-0.86373500
C	2.66552000	-1.22257000	0.15856000
C	0.81739400	-2.94930200	-1.06417700
C	3.05690500	-2.53526600	-0.23821100
C	3.62615800	-0.42154900	0.84293300
H	0.09265900	-3.60483100	-1.54572100
H	4.66015900	-3.98981500	-0.30861500
H	2.40364700	-4.37886100	-1.17743100
C	4.89634300	-0.88656600	1.08243800
H	3.34133600	0.57166200	1.18858400
H	5.60973500	-0.25371000	1.61246700
C	5.28860800	-2.17859900	0.65509100
H	6.30284400	-2.53155400	0.84623600
C	4.38205400	-2.98416500	0.01390500
O	-0.85629400	-1.22417200	-0.88484200
O	-0.73074800	-0.28173000	1.67590400
H	-4.09543500	0.01722200	1.31725700
C	-1.86804700	-2.14805100	-0.53778300
H	-1.64814800	-2.59943600	0.44672800
H	-1.91020200	-2.96781900	-1.27904200
C	-2.07873300	-0.17461100	2.06226800
H	-2.18857500	0.47815300	2.94970600
H	-2.35418200	-1.18459700	2.39871800

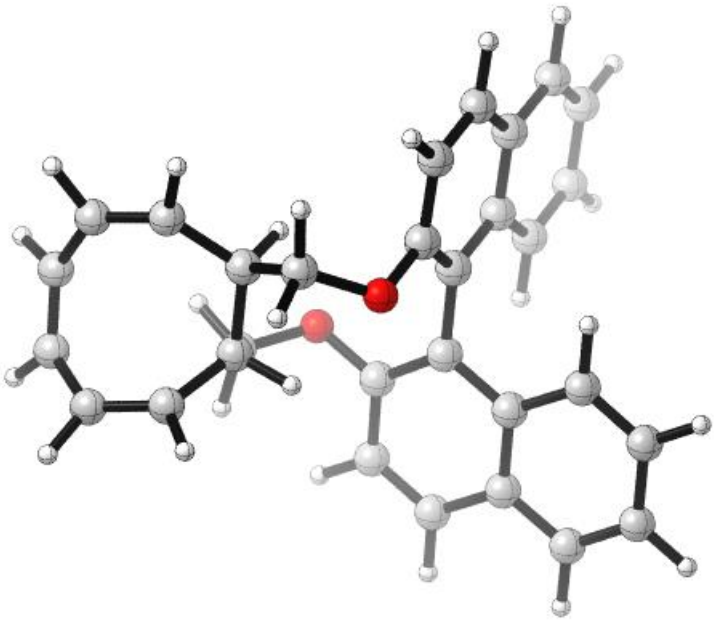

MSBINOL_cyclooctatriene1_GS
E(M062X/def2TZVP) = -1307.972108 Hartree
Free energy correction (M062X/def2SVP) = 0.409809 Hartree
G = -3433004.816

C	0.35832500	1.15748100	1.33506600
C	1.09553200	0.71139500	0.25467300
C	1.30561100	3.38114100	1.15626500
C	1.97601400	1.62364100	-0.41462800
C	0.47305700	2.49962900	1.79139900
C	2.07515200	2.97264200	0.03387500
C	2.76113200	1.22398000	-1.53286300
H	-0.09403200	2.80999600	2.66941400
H	3.00798600	4.90230200	-0.28295300
H	1.39725200	4.40849700	1.51444200
C	3.59258100	2.11722200	-2.16475400
H	2.69159300	0.19461400	-1.88668600
H	4.18451600	1.79164100	-3.02146000
C	3.68849700	3.45705200	-1.71643700
H	4.35335700	4.15463400	-2.22761500
C	2.94416400	3.87219700	-0.64004800
C	0.08025300	-1.15444700	-1.07238500
C	1.04567100	-0.71257300	-0.18757400
C	1.03822200	-3.37992900	-1.11620000
C	2.05543400	-1.62552600	0.26070700
C	0.08312500	-2.49682700	-1.54227400
C	2.04674000	-2.97378900	-0.20114000
C	3.07709700	-1.22882700	1.16928600
H	-0.67434500	-2.80493100	-2.26344900
H	3.02513400	-4.90460400	-0.11087400
H	1.04248700	-4.40749800	-1.48536400
C	4.03064400	-2.12396900	1.59119800
H	3.09228600	-0.19999000	1.53133900

H	4.80443000	-1.80065600	2.28912500
C	4.01919200	-3.46288700	1.13016100
H	4.78312100	-4.16198700	1.47314900
C	3.04643700	-3.87520000	0.25327100
O	-0.86527400	-0.28210600	-1.52691100
O	-0.46120700	0.28780900	1.99906300
C	-2.49747500	0.72583000	0.75559500
H	-1.80591700	1.31587400	0.12245700
C	-3.77397000	1.52426100	0.80574900
H	-3.72965500	2.34382600	1.53310900
C	-4.87954000	1.52200000	0.04368900
H	-5.57365600	2.34784000	0.23846800
C	-5.33153600	0.65925200	-1.05757000
H	-5.78176100	1.20026700	-1.89707500
C	-4.93197100	-1.57371300	-0.02587500
H	-5.64329700	-2.33728900	0.30741400
C	-5.39305200	-0.68327600	-1.09467300
C	-2.53704600	-0.69532600	0.16112000
H	-1.66674300	-1.20721400	0.60053100
C	-3.72930200	-1.53384100	0.56193700
H	-3.55360900	-2.24228600	1.37725200
H	-5.89500200	-1.14693400	-1.95009100
C	-2.22260200	-0.66542500	-1.34000100
H	-2.42765400	-1.64893700	-1.79393700
H	-2.81374000	0.08481700	-1.87654600
C	-1.81753900	0.68244700	2.12768800
H	-2.28851700	-0.06659600	2.78069900
H	-1.89548400	1.66130900	2.62990600

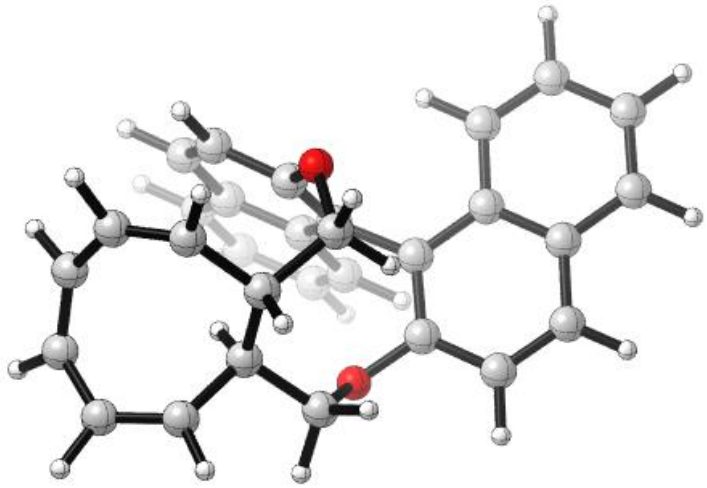

MSBINOL_cyclooctatriene2_GS
E(M062X/def2TZVP) = -1307.970358 Hartree
Free energy correction (M062X/def2SVP) = 0.409576 Hartree
G = -3433000.833

C	-0.29300700	0.29758100	1.32273600
C	0.48981700	0.71814100	0.26537200

C	-1.33662100	2.47668100	1.50851100
C	0.34624500	2.05658000	-0.22508100
C	-1.19789800	1.19181600	1.95761000
C	-0.57926000	2.94255700	0.39849300
C	1.11277400	2.53842200	-1.32227000
H	-1.76812500	0.80739300	2.80311400
H	-1.42714100	4.93595500	0.39489500
H	-2.03358800	3.16121400	1.99668300
C	0.96167300	3.82745000	-1.77444400
H	1.82386900	1.86667600	-1.80491300
H	1.55716900	4.17844900	-2.61856400
C	0.03834200	4.70493000	-1.15612500
H	-0.07237200	5.72525100	-1.52586400
C	-0.71322000	4.26862400	-0.09270500
C	1.13379200	-0.90135100	-1.48610300
C	1.48531300	-0.20144400	-0.35058900
C	3.26672400	-2.03141800	-1.54522000
C	2.77828800	-0.39851200	0.22391700
C	2.02645300	-1.82201600	-2.09211900
C	3.67590100	-1.32941500	-0.37846500
C	3.19452600	0.29446500	1.39492300
H	1.70654800	-2.34264600	-2.99621200
H	5.63880200	-2.24317100	-0.26859300
H	3.96176700	-2.73597800	-2.00644500
C	4.43981400	0.07597400	1.93165000
H	2.50572600	1.00244400	1.85818200
H	4.74567700	0.61575000	2.82903900
C	5.33353500	-0.84533000	1.33053900
H	6.31952600	-1.00742000	1.76819500
C	4.95792800	-1.53074100	0.20200200
O	-0.09702800	-0.69133800	-2.02843700
O	-0.20265000	-0.94718300	1.87452800
C	-1.85746500	-2.21297200	0.49734100
H	-1.95070900	-3.28801400	0.24822800
C	-2.12103100	-1.45531400	-0.82256100
H	-2.12500500	-0.37061100	-0.63397700
C	-3.46992800	-1.85655000	-1.36718600
H	-3.48970500	-2.76166400	-1.98665600
C	-2.85037200	-1.92824700	1.59550400
H	-2.70229400	-2.57567900	2.46749900
C	-3.77350600	-0.96681400	1.75943400
H	-4.23642600	-0.95036100	2.75381500
C	-4.60652500	-1.16454400	-1.21931200
H	-5.49773800	-1.48728200	-1.76695300
C	-4.72990800	0.02283300	-0.37464300
H	-5.25773900	0.88614700	-0.79125200
C	-4.29746600	0.10468800	0.89741500
H	-4.49219300	1.04436400	1.42554500
C	-1.07147700	-1.71484700	-1.92646100

H	-1.58508400	-1.73207400	-2.89793100
H	-0.58503400	-2.69899200	-1.78953100
C	-0.44753100	-2.11469300	1.11174100
H	-0.34113500	-2.92858300	1.84242200
H	0.32718100	-2.27220400	0.34712900

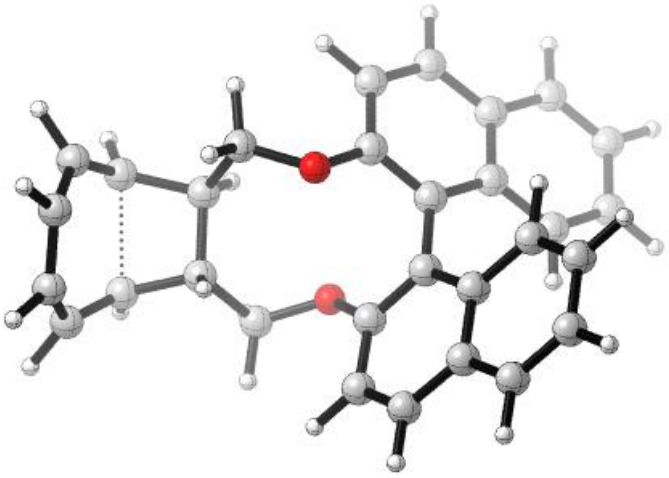

MSBINOL_cyclooctatriene1_6π_TS
E(M062X/def2TZVP) = -1307.937068 Hartree
Free energy correction (M062X/def2SVP) = 0.408737 Hartree
G = -3432915.633

C	0.10799000	1.04178000	1.10586500
C	1.14272700	0.74849200	0.23049700
C	0.58192600	3.40632500	0.97124600
C	1.93153500	1.80897800	-0.30513900
C	-0.17872500	2.38031500	1.47424500
C	1.65359600	3.15540200	0.07723900
C	2.98711400	1.57432700	-1.23417000
H	-0.99161200	2.59757100	2.16601300
H	2.22073700	5.23516800	-0.14897700
H	0.36659600	4.43715100	1.25980000
C	3.73003700	2.61587100	-1.73239500
H	3.19604100	0.55028300	-1.54640700
H	4.53377800	2.41504800	-2.44248600
C	3.46245400	3.95135900	-1.33740800
H	4.06364700	4.76752100	-1.74033400
C	2.44419400	4.21093600	-0.45544900
C	0.32172000	-1.28563500	-0.88614200
C	1.33585700	-0.67319000	-0.16476100
C	1.51105000	-3.38887000	-0.88721200
C	2.48046600	-1.43084000	0.22125900
C	0.40795200	-2.65457700	-1.24575300
C	2.57374400	-2.80510600	-0.15185200
C	3.53885800	-0.86622600	0.99167100
H	-0.39152300	-3.12153000	-1.81977600
H	3.77570900	-4.60688500	-0.06604100

H	1.58195900	-4.44102800	-1.17057500
C	4.62898600	-1.62072700	1.34853600
H	3.46883500	0.17885700	1.29629500
H	5.42846700	-1.16982800	1.93852200
C	4.72668000	-2.98173700	0.96196200
H	5.60074300	-3.56679900	1.25108500
C	3.71813500	-3.55758800	0.23165700
O	-0.71361800	-0.49402500	-1.26292900
O	-0.56582300	-0.01973900	1.61945600
C	-2.87324600	-0.00352300	0.80064500
H	-2.80856500	0.92153600	0.20342900
C	-4.30215000	-0.19078600	1.30560200
H	-4.37299100	-0.69139900	2.27973100
C	-5.29728000	0.74604000	1.00896900
H	-6.00881700	1.04880400	1.78368400
C	-5.53078300	1.17537700	-0.29500100
H	-6.16269500	2.05134800	-0.46211600
C	-4.99586800	-1.02396000	-1.28701600
H	-5.54652400	-1.69593800	-1.95654000
C	-5.33818200	0.32657700	-1.40133600
C	-2.72468100	-1.22639800	-0.09012500
H	-2.21219100	-2.03131700	0.46325100
C	-4.19202700	-1.62194000	-0.29971700
H	-4.39551600	-2.68949800	-0.14805900
H	-5.81593200	0.64193000	-2.33289900
C	-2.01445300	-1.00276700	-1.42252100
H	-2.03531800	-1.92315000	-2.03008200
H	-2.55707000	-0.23198000	-1.98690600
C	-1.91763500	0.07029600	1.98811800
H	-2.09089000	-0.80266400	2.63559300
H	-2.13129400	0.96768300	2.59249100

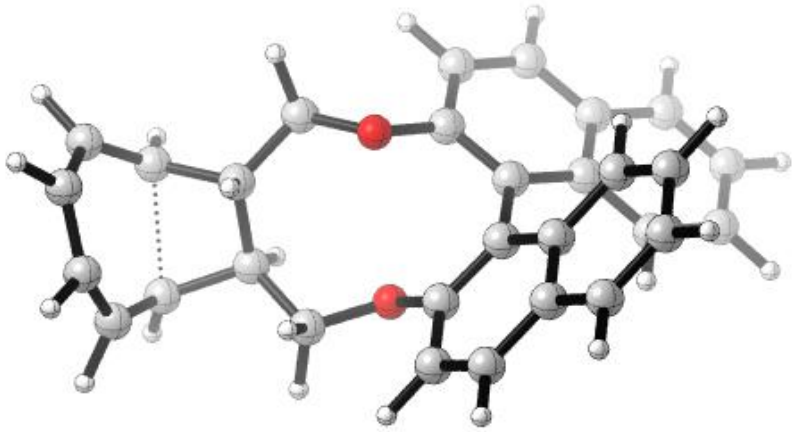

MSBINOL_cyclooctatriene2_6π_TS
E(M062X/def2TZVP) = -1307.938758 Hartree
Free energy correction (M062X/def2SVP) = 0.409282 Hartree
G = -3432918.639

C	0.07905200	1.13190100	0.99407200
C	1.13000800	0.73041000	0.18389900
C	0.77082500	3.44988300	0.87080600
C	2.00508400	1.72688000	-0.35944800
C	-0.08580400	2.49651500	1.35455600
C	1.82701000	3.09801500	-0.00817900
C	3.04837000	1.40297500	-1.27586600
H	-0.88771800	2.77453200	2.03871800
H	2.55010100	5.12483600	-0.25730800
H	0.64802500	4.49583600	1.15892500
C	3.87075500	2.37752600	-1.78583300
H	3.18437800	0.36449100	-1.57783900
H	4.65865400	2.10351400	-2.48912900
C	3.70513000	3.73468900	-1.41348100
H	4.36957300	4.49678000	-1.82280900
C	2.70066100	4.08241500	-0.54633500
C	0.35982000	-1.42717300	-0.80012900
C	1.33382300	-0.71299900	-0.11862600
C	1.73338300	-3.42252300	-0.82226900
C	2.52972200	-1.38901100	0.28871700
C	0.57422500	-2.78159900	-1.17277400
C	2.73352400	-2.75451000	-0.07068100
C	3.53151700	-0.74971700	1.07691800
H	-0.18199700	-3.29998200	-1.76250500
H	4.06264000	-4.46185600	0.03857100
H	1.89939100	-4.45952300	-1.12090800
C	4.66717800	-1.42086900	1.45852300
H	3.38252400	0.28551100	1.38403500
H	5.41614800	-0.91011400	2.06568900
C	4.87581900	-2.76971200	1.07714900
H	5.78570500	-3.28764300	1.38322800
C	3.92457400	-3.41894300	0.33204700
O	-0.78524300	-0.78621200	-1.13770700
O	-0.76471800	0.18328500	1.46777100
C	-2.98539200	-0.60565500	1.04716200
H	-2.63172600	-1.56674300	1.45667700
C	-3.07809700	-0.71612000	-0.46167300
H	-3.12983300	0.28691600	-0.91285600
C	-4.44264400	-1.38250800	-0.55556200
H	-4.42035800	-2.47486100	-0.45047100
C	-4.46502900	-0.45122300	1.39029400
H	-4.74560700	-0.92867000	2.33943000
C	-5.20648700	0.71781400	1.11868400
H	-5.74468300	1.15564700	1.96887300
C	-5.45251800	-0.83099200	-1.35149200
H	-6.11294800	-1.48200400	-1.93192100
C	-5.74181900	0.52791500	-1.29146400
H	-6.38754600	0.97331300	-2.05226600
C	-5.54724400	1.27738200	-0.11586200

H	-6.01783500	2.26375500	-0.09308000
C	-1.99585800	-1.51270100	-1.16808900
H	-1.87894300	-2.48472100	-0.65920800
H	-2.29235600	-1.70636300	-2.21384800
C	-2.13049700	0.50524300	1.63291300
H	-2.38165900	1.44643100	1.11578300
H	-2.35879300	0.63448700	2.70585100

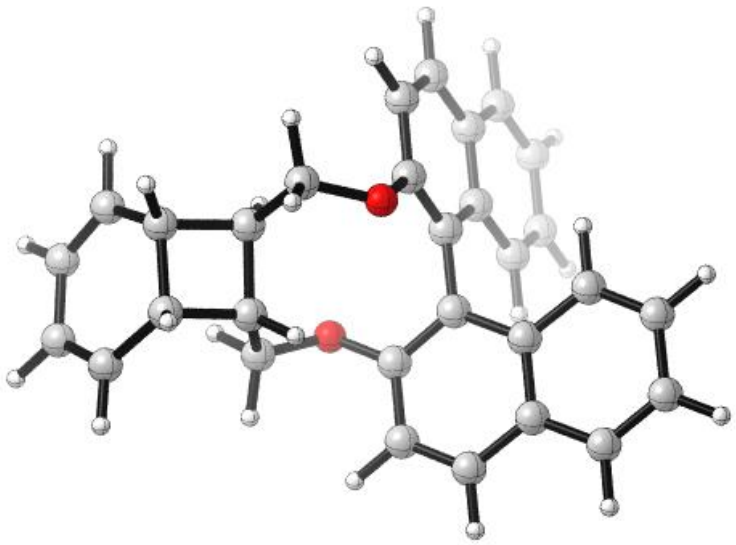

MSBINOL_BOD1_GS
E(M062X/def2TZVP) = -1307.983560 Hartree
Free energy correction (M062X/def2SVP) = 0.410739 Hartree
G = -3433032.442

C	0.34316300	1.07847800	1.36130600
C	1.11548700	0.72611700	0.27176100
C	1.04058200	3.39122800	1.19683500
C	1.89129900	1.72938000	-0.39142000
C	0.30938600	2.42043600	1.82844800
C	1.84914000	3.07686200	0.07152700
C	2.70763700	1.42446200	-1.51706600
H	-0.28738200	2.66333800	2.70806300
H	2.57467900	5.09645800	-0.22930600
H	1.01955100	4.42041200	1.56090400
C	3.43926800	2.40571300	-2.14153400
H	2.74240500	0.39629100	-1.88005800
H	4.05850800	2.15298200	-3.00353900
C	3.39674800	3.74375500	-1.67857200
H	3.98326700	4.51200300	-2.18429800
C	2.61719700	4.06861300	-0.59603800
C	0.17948300	-1.18061800	-1.02873700
C	1.16213100	-0.68984600	-0.19056200
C	1.24525300	-3.35353100	-1.11583600
C	2.23832200	-1.54507100	0.20697600
C	0.22514800	-2.52252200	-1.49626600
C	2.27792200	-2.89282900	-0.25547300

C	3.27979800	-1.09247300	1.06561700
H	-0.54875200	-2.87580100	-2.17797000
H	3.36261800	-4.76817600	-0.21535400
H	1.28261900	-4.38163700	-1.48175100
C	4.30000800	-1.93426100	1.43808100
H	3.25547600	-0.06342700	1.42702500
H	5.08905800	-1.56916600	2.09725700
C	4.33774300	-3.27267200	0.97576800
H	5.15432300	-3.92917500	1.27934500
C	3.34626900	-3.73833100	0.14791200
O	-0.80991100	-0.33859300	-1.44102200
O	-0.35175700	0.10357600	2.01691300
C	-2.49214500	0.38557000	0.93204400
H	-2.12480300	1.22999900	0.32557200
C	-4.03800100	0.32247100	1.06415400
C	-4.76665900	1.31449700	0.20498500
C	-4.96187900	-1.43480200	-0.62527400
C	-2.50102200	-0.95402300	0.15724700
H	-1.84527000	-1.71990000	0.60124800
C	-4.01359800	-1.12763800	0.49717400
C	-5.48233500	0.95082700	-0.86825500
C	-5.62674400	-0.46046700	-1.26111600
H	-6.30407500	-0.70128200	-2.08272300
H	-5.99388500	1.70832700	-1.46482800
H	-4.39039200	0.40559600	2.10688300
H	-4.13296400	-1.87327000	1.29566900
H	-4.69628100	2.36879300	0.48805900
H	-5.09516300	-2.47854200	-0.92115600
C	-2.14760700	-0.78865600	-1.30894200
H	-2.31734000	-1.72403100	-1.86841900
H	-2.77023200	-0.01061900	-1.77209500
C	-1.73020100	0.33104300	2.23976000
H	-2.07318800	-0.51897600	2.84860700
H	-1.90020300	1.24966700	2.82870200

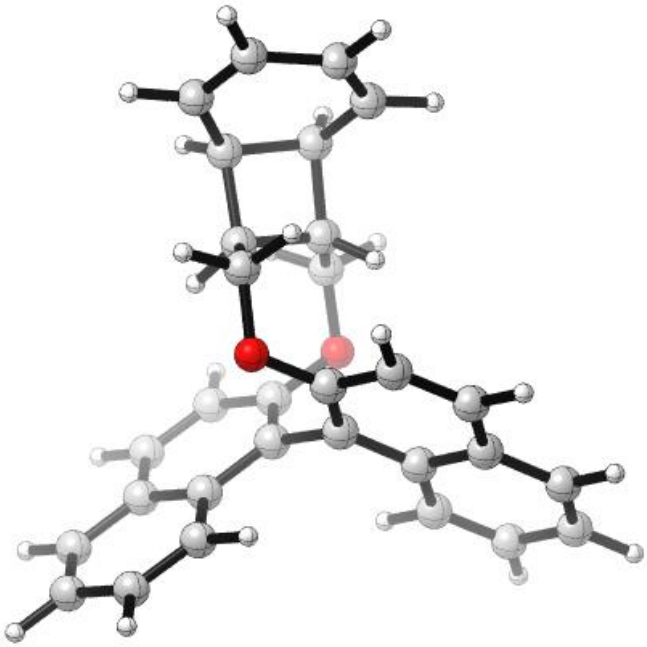

MSBINOL_BOD2_GS
E(M062X/def2TZVP) = -1307.981533 Hartree
Free energy correction (M062X/def2SVP) = 0.410619 Hartree
G = -3433027.435

C	-0.02475500	0.67343700	-1.40361700
C	-0.95957000	0.75010100	-0.39003600
C	-0.10343200	3.06124800	-1.76967000
C	-1.50841400	2.02512000	-0.04126500
C	0.40511200	1.83305200	-2.10052000
C	-1.07030600	3.19138100	-0.73493900
C	-2.47618800	2.17226900	0.99088500
H	1.13543500	1.71566400	-2.90270500
H	-1.26992500	5.34119300	-0.92204700
H	0.22041700	3.95667900	-2.30407300
C	-2.98089400	3.40919600	1.31073900
H	-2.81173300	1.28438100	1.52805800
H	-3.72322200	3.50243000	2.10483700
C	-2.54659700	4.56673100	0.61912100
H	-2.95645900	5.54254300	0.88342700
C	-1.61251800	4.45666500	-0.38080300
C	-0.86738500	-0.68779100	1.62494200
C	-1.34056100	-0.48874800	0.34309900
C	-1.94397900	-2.84593000	1.77995400
C	-2.15614200	-1.49716100	-0.26243200
C	-1.17222900	-1.86847500	2.35090400
C	-2.45441200	-2.68860100	0.46212000
C	-2.67498600	-1.35501000	-1.57929200
H	-0.78825900	-1.96620000	3.36773000
H	-3.48225700	-4.59624300	0.42102100
H	-2.18589600	-3.75506100	2.33420500
C	-3.44913400	-2.34126600	-2.14031400

H	-2.44561300	-0.44810900	-2.13992900
H	-3.83863900	-2.21453900	-3.15150500
C	-3.74692700	-3.52332500	-1.41842700
H	-4.36353500	-4.29796300	-1.87646200
C	-3.25938800	-3.68995200	-0.14611500
O	-0.11016400	0.27899700	2.22486600
O	0.48216100	-0.54197600	-1.76214600
C	1.98177900	-1.10772000	0.08526000
H	1.22793400	-1.86139900	0.35904200
C	2.03477600	0.13534900	1.02966800
C	5.25043800	-0.85682000	-1.04121500
C	3.43607400	-1.46918000	0.52761900
C	4.41477600	0.90054000	0.45876400
C	3.56220800	-0.08098500	1.21026600
C	5.18217800	0.53947700	-0.57914800
C	4.45212400	-1.80219600	-0.52661100
H	3.87865500	-0.10650500	2.26818600
H	5.97838300	-1.11086700	-1.81414600
H	3.40047000	-2.27583800	1.27336400
H	5.79267500	1.28486900	-1.09224600
H	4.52390900	-2.83561300	-0.87498700
H	4.39960900	1.94007900	0.79907700
H	1.76862100	1.08933600	0.54771100
C	1.27585700	0.02006600	2.34090700
H	1.44642000	-0.98001400	2.78679200
H	1.65617000	0.77114000	3.04785600
C	1.82781900	-0.80421800	-1.39772400
H	2.48181800	0.03884500	-1.68708300
H	2.12710100	-1.67850400	-1.99059100

SBINAP Cartesian Coordinates

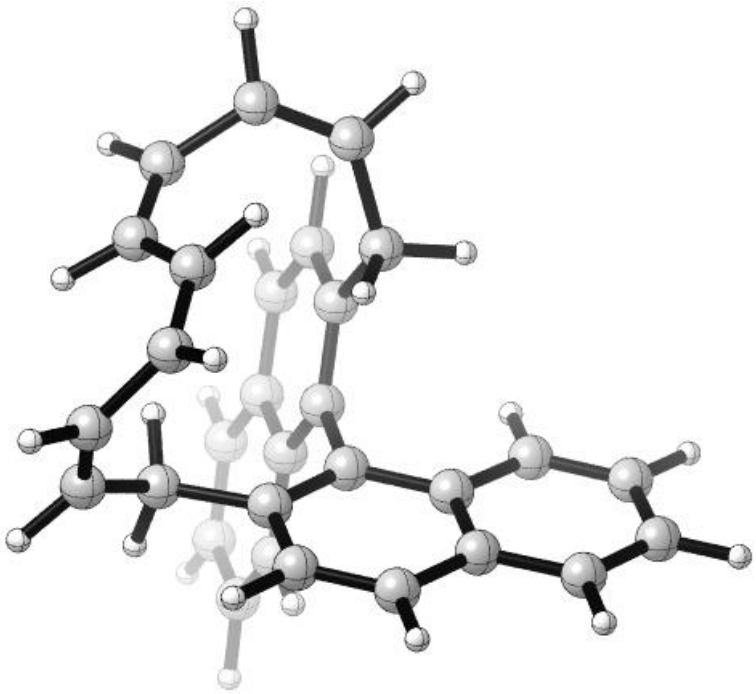

SBINAP_tetraene_GS
E(M062X/def2TZVP) = -1157.524179 Hartree
Free energy correction (M062X/def2SVP) = 0.398865 Hartree
G = -3038032.512

C	0.47792100	-0.55049900	3.39658100
C	-0.47792100	0.55049900	3.39658100
H	-1.53166300	0.28109000	3.51424700
C	-0.15116900	1.85647300	3.34116000
C	0.15116900	-1.85647300	3.34116000
C	-1.20961700	-2.39397400	3.17529800
C	1.20961700	2.39397400	3.17529800
C	-2.03898700	-2.13767800	2.15268500
H	-3.02181900	-2.61726100	2.17457400
C	2.03898700	2.13767800	2.15268500
H	3.02181900	2.61726100	2.17457400
H	-0.95262700	2.59232700	3.46804600
C	0.47792100	1.66261900	0.17025300
C	-0.21449900	0.71616800	-0.56876800
C	-1.05507200	3.40236000	-0.58137600
C	-1.35083100	1.09987900	-1.35596800
C	0.03992300	3.01653800	0.14552900
C	-1.78281600	2.45712500	-1.35168000
C	-2.06713700	0.16590100	-2.15823700
H	0.58758900	3.75448000	0.73327000
H	-3.23679700	3.87693100	-2.10362100
H	-1.37920600	4.44520500	-0.58242900
C	-3.15920700	0.55864600	-2.89466700
H	-1.73034800	-0.87180000	-2.18810400
H	-3.69224000	-0.17164000	-3.50540200
C	-3.59484600	1.90621100	-2.87429300

H	-4.46373100	2.20465500	-3.46258900
C	-2.91717200	2.83279100	-2.12116500
C	-0.47792100	-1.66261900	0.17025300
C	0.21449900	-0.71616800	-0.56876800
C	1.05507200	-3.40236000	-0.58137600
C	1.35083100	-1.09987900	-1.35596800
C	-0.03992300	-3.01653800	0.14552900
C	1.78281600	-2.45712500	-1.35168000
C	2.06713700	-0.16590100	-2.15823700
H	-0.58758900	-3.75448000	0.73327000
H	3.23679700	-3.87693100	-2.10362100
H	1.37920600	-4.44520500	-0.58242900
C	3.15920700	-0.55864600	-2.89466700
H	1.73034800	0.87180000	-2.18810400
H	3.69224000	0.17164000	-3.50540200
C	3.59484600	-1.90621100	-2.87429300
H	4.46373100	-2.20465500	-3.46258900
C	2.91717200	-2.83279100	-2.12116500
C	1.73067000	1.28370200	0.94593800
H	1.66003800	0.22287800	1.23306300
H	2.58624300	1.33544200	0.25228100
C	-1.73067000	-1.28370200	0.94593800
H	-2.58624300	-1.33544200	0.25228100
H	-1.66003800	-0.22287800	1.23306300
H	-1.54526600	-3.10499300	3.93892800
H	0.95262700	-2.59232700	3.46804600
H	1.53166300	-0.28109000	3.51424700
H	1.54526600	3.10499300	3.93892800

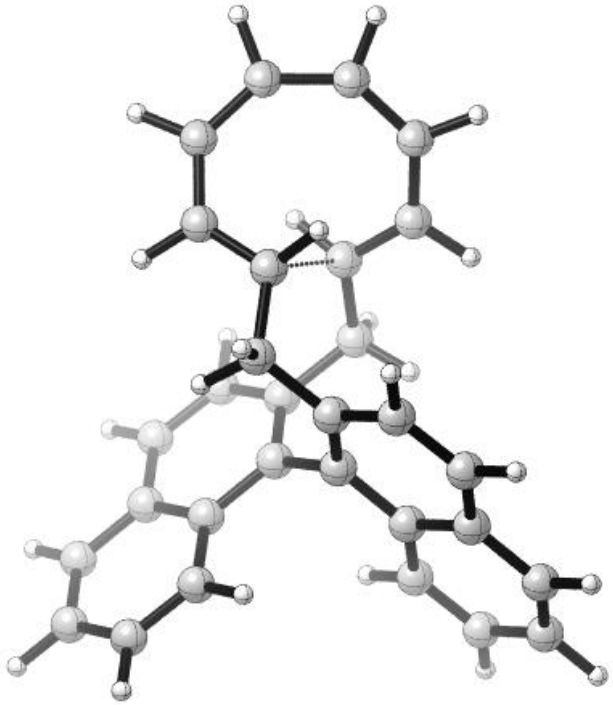

SBINAP_tetraene_8π1_TS
E(M062X/def2TZVP) = -1157.508611 Hartree

Free energy correction (M062X/def2SVP) = 0.399871 Hartree
G = -3037989.00

C	5.34493100	0.67172300	0.21220300
C	5.34496300	-0.67256700	-0.21218300
H	6.35938700	-1.08518800	-0.23043700
C	4.39336800	-1.60010000	-0.65722100
C	4.39329500	1.59921600	0.65723900
H	4.78248200	2.61512600	0.77003900
C	3.05479300	1.43522900	1.02270800
C	3.05485900	-1.43615200	-1.02266500
H	2.47705800	-2.34666300	-1.21620900
C	2.38608500	0.21582900	1.10121500
H	3.00554600	-0.67306100	1.21736500
C	2.38614500	-0.21675400	-1.10111600
H	3.00559800	0.67214100	-1.21728200
H	6.35933700	1.08438900	0.23046000
H	4.78259900	-2.61599200	-0.77002500
H	2.47698300	2.34573400	1.21627000
C	0.09914600	0.93281000	-1.30906300
C	-0.83833900	0.67174800	-0.32606000
C	-0.67584600	3.23283800	-1.47924000
C	-1.74545600	1.69253000	0.10110300
C	0.17233100	2.23301400	-1.87959500
C	-1.66186700	2.98917200	-0.48487000
C	-2.72756900	1.45737800	1.10446400
H	0.91799900	2.42556800	-2.65460500
H	-2.49135100	4.99171000	-0.51448900
H	-0.61162400	4.22761300	-1.92484700
C	-3.58463200	2.45772500	1.49567500
H	-2.79111300	0.46659300	1.55788400
H	-4.33367700	2.26143000	2.26420100
C	-3.50371600	3.74475800	0.90874400
H	-4.19033400	4.52973500	1.22885600
C	-2.56299600	4.00229600	-0.05787400
C	0.09872300	-0.93326500	1.30909800
C	-0.83866000	-0.67170900	0.32611600
C	-0.67736600	-3.23294600	1.47912400
C	-1.74625900	-1.69203500	-0.10109900
C	0.17129700	-2.23354600	1.87953300
C	-1.66328900	-2.98874800	0.48479300
C	-2.72825900	-1.45635600	-1.10444800
H	0.91687700	-2.42651200	2.65452400
H	-2.49374500	-4.99089100	0.51430500
H	-0.61360800	-4.22778000	1.92466600
C	-3.58580300	-2.45626700	-1.49571500
H	-2.79132900	-0.46551700	-1.55781800
H	-4.33475200	-2.25956400	-2.26423000
C	-3.50551000	-3.74337300	-0.90885300

H	-4.19250600	-4.52800600	-1.22900200
C	-2.56491200	-4.00141500	0.05774800
C	1.03785200	0.15055300	1.78465400
H	0.54578400	1.13039200	1.71196700
H	1.23886500	-0.02190800	2.85653600
C	1.03787500	-0.15141500	-1.78445700
H	0.54558300	-1.13111200	-1.71147100
H	1.23883800	0.02072500	-2.85640500

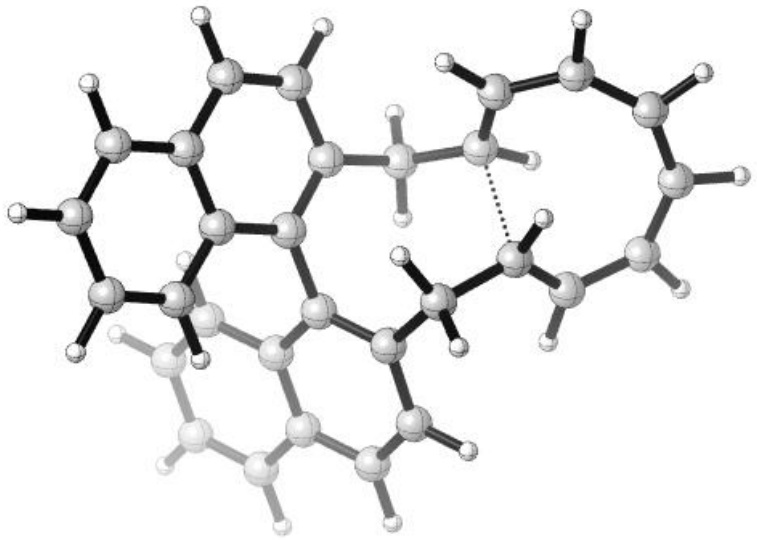

SBINAP_tetraene_8π2_TS
E(M062X/def2TZVP) = -1157.509113 Hartree
Free energy correction (M062X/def2SVP) = 0.401894 Hartree
G = -3037985.003

C	0.70907100	0.05508600	5.47818900
C	-0.70907100	-0.05508600	5.47818900
H	-1.08858400	-0.19919400	6.49547200
C	-1.74238000	0.01232300	4.54227000
C	1.74238000	-0.01232300	4.54227000
H	2.72492400	0.25946600	4.93833400
C	1.72146900	-0.40218100	3.19012600
C	-1.72146900	0.40218100	3.19012600
H	-2.61261500	0.19850200	2.58869600
C	0.60081800	-0.95925200	2.59959700
H	-0.12668100	-1.37702700	3.29479500
C	-0.60081800	0.95925200	2.59959700
H	1.08858400	0.19919400	6.49547200
H	-2.72492400	-0.25946600	4.93833400
H	2.61261500	-0.19850200	2.58869600
C	-1.34838400	0.91975900	0.15077300
C	-0.74152200	0.09892500	-0.78426200
C	-3.53173000	0.50933000	-0.85001600
C	-1.53403400	-0.56874800	-1.77801400
C	-2.75628700	1.12593400	0.09527600
C	-2.94351200	-0.36062800	-1.80747900

C	-0.95897800	-1.44562000	-2.74152200
H	-3.21340000	1.80094000	0.82264000
H	-4.80504000	-0.85042000	-2.80259300
H	-4.60955000	0.68050900	-0.88404400
C	-1.74238000	-2.07220700	-3.68086700
H	0.11792300	-1.61846200	-2.72469200
H	-1.28302900	-2.74171300	-4.40952600
C	-3.14195800	-1.85826900	-3.71053900
H	-3.75186200	-2.36149900	-4.46210200
C	-3.72654800	-1.02144600	-2.79241300
C	1.34838400	-0.91975900	0.15077300
C	0.74152200	-0.09892500	-0.78426200
C	3.53173000	-0.50933000	-0.85001600
C	1.53403400	0.56874800	-1.77801400
C	2.75628700	-1.12593400	0.09527600
C	2.94351200	0.36062800	-1.80747900
C	0.95897800	1.44562000	-2.74152200
H	3.21340000	-1.80094000	0.82264000
H	4.80504000	0.85042000	-2.80259300
H	4.60955000	-0.68050900	-0.88404400
C	1.74238000	2.07220700	-3.68086700
H	-0.11792300	1.61846200	-2.72469200
H	1.28302900	2.74171300	-4.40952600
C	3.14195800	1.85826900	-3.71053900
H	3.75186200	2.36149900	-4.46210200
C	3.72654800	1.02144600	-2.79241300
H	0.12668100	1.37702700	3.29479500
C	0.55427100	-1.60673100	1.23235200
H	-0.49667600	-1.70566900	0.92798700
H	0.93451000	-2.63659400	1.35420100
C	-0.55427100	1.60673100	1.23235200
H	-0.93451000	2.63659400	1.35420100
H	0.49667600	1.70566900	0.92798700

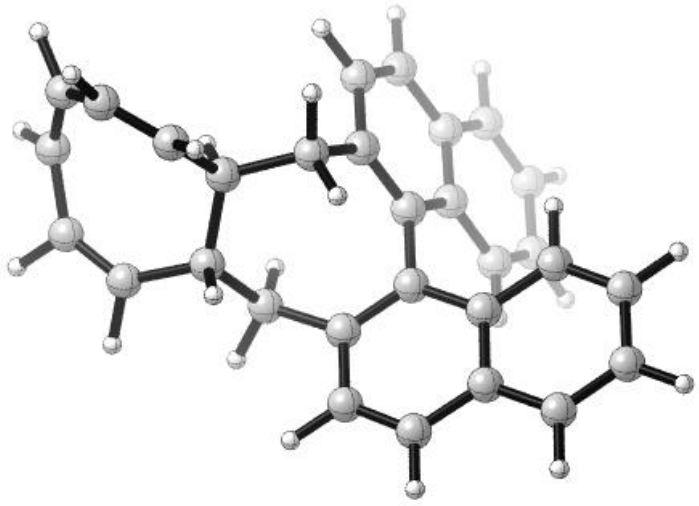

SBINAP_cyclooctatriene1_GS

E(M062X/def2TZVP) = -1157.546635 Hartree
Free energy correction (M062X/def2SVP) = 0.402889 Hartree
G = -3038080.91

C	0.37952800	0.93189600	-1.02683900
C	-0.71937400	0.70315000	-0.21738200
C	-0.06785300	3.32759100	-1.01429300
C	-1.51828800	1.80322200	0.24503300
C	0.69291800	2.26449100	-1.41962900
C	-1.19229600	3.12721700	-0.16819500
C	-2.62295400	1.62349400	1.12555100
H	1.56023700	2.42760200	-2.06406900
H	-1.72484300	5.22384600	-0.04627300
H	0.18021500	4.34268000	-1.33097700
C	-3.36976700	2.69642900	1.54965800
H	-2.87136100	0.61752900	1.46566700
H	-4.21140500	2.53659700	2.22517900
C	-3.05383300	4.00867200	1.12130200
H	-3.65591400	4.85139800	1.46397200
C	-1.98596600	4.21612500	0.28371500
C	-0.13877900	-1.35860600	1.03509400
C	-1.03012800	-0.68831800	0.21548000
C	-1.55941200	-3.33951000	1.01628200
C	-2.21476700	-1.34878800	-0.25667100
C	-0.42410200	-2.69670500	1.43028900
C	-2.48419200	-2.68505800	0.15803500
C	-3.13031000	-0.72127100	-1.14890700
H	0.28350600	-3.20946700	2.08670200
H	-3.85344400	-4.35935700	0.02823200
H	-1.76856600	-4.36236400	1.33609200
C	-4.25648200	-1.37878200	-1.58264200
H	-2.92586000	0.29419700	-1.49003600
H	-4.94434300	-0.88011900	-2.26704800
C	-4.53040100	-2.69986500	-1.15239800
H	-5.42928600	-3.20943900	-1.50231800
C	-3.65966800	-3.33714900	-0.30359800
C	2.57611600	-0.32633900	-0.63410100
H	2.90431200	0.68350500	-0.33689400
C	3.65108800	-0.94728100	-1.48417800
H	3.32531000	-1.76030300	-2.14397900
C	4.92601200	-0.54041300	-1.55116100
H	5.58574200	-0.99291500	-2.29824400
C	5.49908000	0.50373900	-0.70350000
H	6.15623100	1.23297800	-1.18782900
C	4.72192400	-0.35254600	1.56360400
H	5.33241500	-0.47562600	2.46622800
C	5.33817300	0.60352700	0.63033000
C	2.39206200	-1.14371600	0.65594000
H	2.24035300	-2.19997500	0.36445600

C	3.60321700	-1.09879100	1.55569700
H	3.48584300	-1.74320400	2.43498100
H	5.86915900	1.42271500	1.12627800
C	1.15662900	-0.74547700	1.51128700
H	1.33448300	-1.09946600	2.53823700
H	1.09013500	0.35056700	1.56405300
C	1.29680800	-0.17282700	-1.49446600
H	1.62093500	0.07494800	-2.51657000
H	0.76624700	-1.13498500	-1.55186300

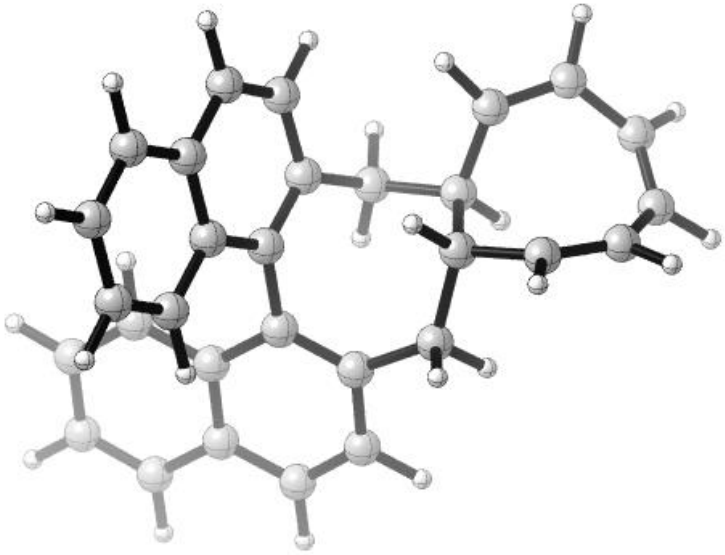

SBINAP_cyclooctatriene2_GS
E(M062X/def2TZVP) = -1157.536390 Hartree
Free energy correction (M062X/def2SVP) = 0.402462 Hartree
G = -3038055.128

C	-0.06544500	-1.62307800	0.82702200
C	-0.94670000	-0.80380800	0.14344100
C	-1.67986300	-3.46203000	0.76370500
C	-2.21533100	-1.32662600	-0.30505000
C	-0.46346300	-2.96061800	1.13127900
C	-2.58944400	-2.66049200	0.02419600
C	-3.11924800	-0.55932700	-1.09570500
H	0.23615700	-3.59266900	1.68265300
H	-4.10908600	-4.19487500	-0.13523000
H	-1.95966200	-4.48651600	1.01733300
C	-4.32366600	-1.08053500	-1.50516600
H	-2.84740100	0.45491000	-1.38680000
H	-4.99533200	-0.47193000	-2.11237200
C	-4.69872500	-2.39832100	-1.15176600
H	-5.65935900	-2.79794400	-1.47968300
C	-3.84348900	-3.17082700	-0.40606200
C	0.34460400	0.86259600	-1.19132900
C	-0.62219200	0.60606100	-0.23140400
C	-0.20661100	3.23677800	-1.15300900

C	-1.36680300	1.68612700	0.34858300
C	0.52011700	2.19296200	-1.66389700
C	-1.15104600	3.01611000	-0.11585100
C	-2.31691100	1.47970100	1.38990900
H	1.24242500	2.37417400	-2.46253900
H	-1.71555400	5.09865200	0.08926600
H	-0.06640300	4.25061800	-1.53333000
C	-3.01099200	2.53432700	1.93109400
H	-2.48457900	0.46705400	1.75914900
H	-3.73016200	2.35555500	2.73175800
C	-2.80054200	3.85394900	1.45972800
H	-3.36121400	4.68181800	1.89602100
C	-1.89020600	4.08619200	0.45938100
C	2.20626900	-0.13751800	0.78546500
H	1.71168500	0.83704900	0.91961700
C	2.54036200	-0.30223200	-0.70734000
H	2.99464700	-1.29751300	-0.83818800
C	3.54227100	0.73092900	-1.15825600
H	3.13403600	1.69482900	-1.47819200
C	3.41946600	-0.13277500	1.68969100
H	3.18600500	0.23045400	2.69718100
C	4.65487700	-0.64213500	1.54937800
H	5.25486600	-0.64495500	2.46770100
C	4.86159300	0.53245400	-1.28323300
H	5.47107100	1.30817200	-1.75802300
C	5.55365400	-0.66835600	-0.81690700
H	6.29583300	-1.12076900	-1.48216600
C	5.39763200	-1.20296800	0.40952400
H	6.02117600	-2.06849000	0.65797100
C	1.28808400	-0.22411300	-1.63393400
H	0.77516600	-1.19375600	-1.64165800
H	1.63680800	-0.03380100	-2.65969800
C	1.30001800	-1.24316200	1.37724900
H	1.15471900	-1.00105900	2.44524100
H	1.90452500	-2.16458500	1.37955600

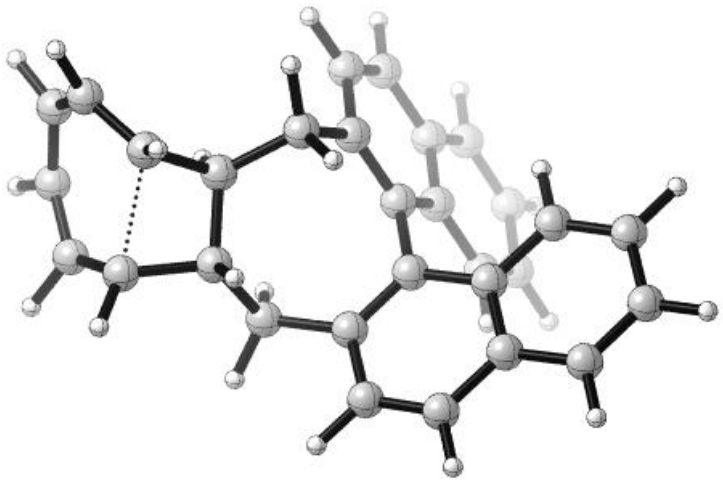

SBINAP_cyclooctatriene1_6π_TS
E(M062X/def2TZVP) = -1157.505308 Hartree
Free energy correction (M062X/def2SVP) = 0.402348 Hartree
G = -3037973.82

C	-0.41162500	0.88573100	1.16578700
C	0.59547900	0.67801200	0.23882600
C	-0.01635100	3.29240200	1.11048600
C	1.31950700	1.79812200	-0.29948700
C	-0.70659100	2.21328700	1.59107500
C	1.01240800	3.11583700	0.14642900
C	2.33999700	1.64050700	-1.28051500
H	-1.50663800	2.35863300	2.32062000
H	1.48418800	5.22310500	-0.02704100
H	-0.24992100	4.30157900	1.45582400
C	3.01719100	2.72850000	-1.77732000
H	2.57939500	0.63956800	-1.64117000
H	3.79373400	2.58454800	-2.53000200
C	2.71519500	4.03498800	-1.32311700
H	3.26168100	4.88961200	-1.72444400
C	1.73226600	4.22087200	-0.38283500
C	0.21384700	-1.41951600	-1.09920400
C	0.98532100	-0.69624000	-0.20467000
C	1.84135600	-3.23860500	-1.08439000
C	2.21382900	-1.24995000	0.29735900
C	0.66481500	-2.70070600	-1.53057600
C	2.64577300	-2.53135600	-0.15110400
C	3.02289600	-0.56116200	1.24600400
H	0.04814700	-3.25630900	-2.24092400
H	4.17786900	-4.05704700	-0.01324400
H	2.17462500	-4.21747300	-1.43520200
C	4.19287500	-1.11297000	1.71017300
H	2.70091900	0.41593500	1.60770900
H	4.79582000	-0.56858900	2.43842400
C	4.62254100	-2.38259600	1.25376000
H	5.55424300	-2.80819700	1.62910800
C	3.86209800	-3.07456500	0.34402700
C	-2.44839500	-0.43287000	0.65673500
H	-2.72020000	0.55368600	0.25211400
C	-3.72654500	-1.09194200	1.14819000
H	-3.56775700	-1.99777700	1.74703700
C	-4.86654400	-0.31971400	1.41938200
H	-5.50088300	-0.55775100	2.27840800
C	-5.29272700	0.65150000	0.52469300
H	-6.07106800	1.35573700	0.82904400
C	-4.47796300	-0.55481700	-1.48174900
H	-4.91367400	-0.77206700	-2.46521200
C	-5.02871300	0.56353600	-0.85824600
C	-2.19776300	-1.37011400	-0.49568900

H	-1.87959400	-2.33807700	-0.07080100
C	-3.64181100	-1.56419400	-0.94694300
H	-3.80651500	-2.54088600	-1.42628300
H	-5.57976700	1.25715500	-1.49850000
C	-1.15573700	-0.96948000	-1.55342600
H	-1.39918000	-1.45918100	-2.50872200
H	-1.19887300	0.11821500	-1.71794100
C	-1.30872900	-0.22401300	1.66543100
H	-1.73371900	0.06672400	2.63786600
H	-0.75025100	-1.16204500	1.80882300

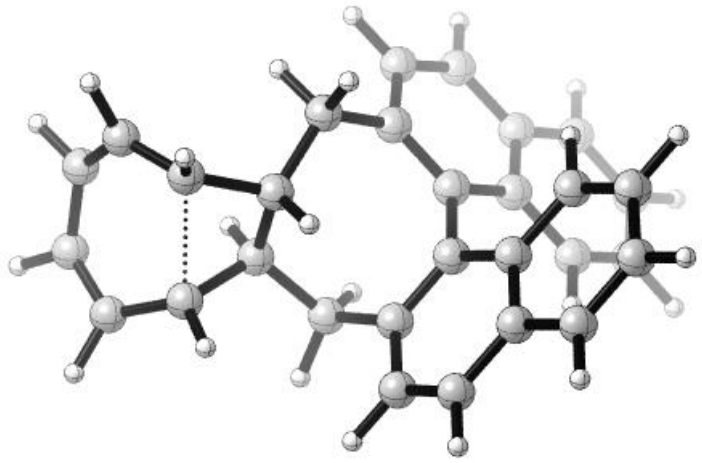

SBINAP_cyclooctatriene2_6π_TS
E(M062X/def2TZVP) = -1157.501379 Hartree
Free energy correction (M062X/def2SVP) = 0.401246 Hartree
G = -3037966.399

C	-0.11564000	1.30580800	1.11271700
C	0.81133800	0.76080400	0.23668700
C	1.05943000	3.45050300	1.05795700
C	1.88762300	1.56986000	-0.27077800
C	0.03262700	2.66740100	1.50997000
C	2.01592600	2.92445800	0.15077100
C	2.84254800	1.06344900	-1.19967900
H	-0.70305300	3.08658500	2.19949500
H	3.16399500	4.75443000	-0.01174900
H	1.15015900	4.48952800	1.38107200
C	3.86373900	1.85542800	-1.66738300
H	2.75584400	0.03229700	-1.54315400
H	4.58266300	1.44578200	-2.37844000
C	3.99101500	3.19837400	-1.23716600
H	4.80722300	3.81539700	-1.61559300
C	3.08330900	3.71882700	-0.34878800
C	-0.17651000	-0.99725600	-1.23665000
C	0.73165200	-0.65430500	-0.24618100
C	0.65207900	-3.28586100	-1.24860000
C	1.62587200	-1.63810000	0.28429000
C	-0.20180900	-2.32757700	-1.73340700

C	1.58229100	-2.97003600	-0.22363200
C	2.56316200	-1.33423600	1.31365700
H	-0.91778200	-2.57963700	-2.51907500
H	2.42703700	-4.96234300	-0.09379100
H	0.62672800	-4.30395100	-1.64257600
C	3.40673900	-2.30027800	1.80509700
H	2.60104800	-0.31815400	1.70953600
H	4.11681000	-2.04941400	2.59448900
C	3.36329900	-3.62248400	1.29600000
H	4.04007100	-4.37934600	1.69504200
C	2.47066900	-3.94677000	0.30537800
C	-2.08775900	-0.36665500	0.78216400
H	-1.58853900	-1.34321500	0.71837900
C	-2.37165600	0.09344600	-0.63167900
H	-2.75215600	1.12545000	-0.61515800
C	-3.53744700	-0.84613700	-0.90472500
H	-3.23118700	-1.85999100	-1.19490500
C	-3.51330900	-0.66508400	1.24512200
H	-3.55969100	-1.47940100	1.98263100
C	-4.52577600	0.29801600	1.43755300
H	-5.01647700	0.28581900	2.41929200
C	-4.74952000	-0.35984400	-1.40753800
H	-5.30612600	-0.93206700	-2.15579700
C	-5.34481800	0.76754300	-0.85256100
H	-6.18046000	1.24383400	-1.37160600
C	-5.16493800	1.11358800	0.50018100
H	-5.84399700	1.87364900	0.89564100
C	-1.22048900	-0.00304600	-1.66857700
H	-1.64438600	-0.28784100	-2.64335600
H	-0.76027800	0.98687800	-1.79051300
C	-1.28468500	0.54781000	1.71818200
H	-1.97601300	1.29626100	2.13326200
H	-0.92522200	-0.04642600	2.57658200

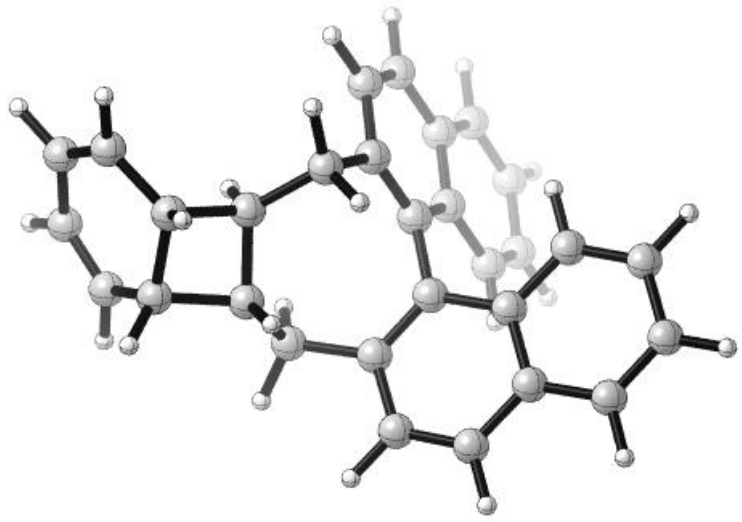

SBINAP_BOD1_GS

E(M062X/def2TZVP) = -1157.544087 Hartree
Free energy correction (M062X/def2SVP) = 0.404040 Hartree
G = -3038071.19

C	-0.36600200	0.90481500	1.23450600
C	0.58956600	0.67449600	0.25792200
C	0.09110000	3.30153600	1.16954800
C	1.31447200	1.78019100	-0.31048300
C	-0.60198700	2.23764300	1.67920600
C	1.06317600	3.10376600	0.15303500
C	2.28503600	1.60215400	-1.33819400
H	-1.35965200	2.40067800	2.44893500
H	1.57658300	5.19973200	-0.03753100
H	-0.09797600	4.31423400	1.53145400
C	2.96330300	2.67533500	-1.86469600
H	2.48489800	0.59736600	-1.71179300
H	3.70005800	2.51485300	-2.65319700
C	2.71442500	3.98749800	-1.39490500
H	3.26131600	4.83013500	-1.82028000
C	1.78286200	4.19330000	-0.40789900
C	0.20951100	-1.42035700	-1.11261400
C	0.96399100	-0.70276600	-0.19789900
C	1.86397400	-3.21621500	-1.12333600
C	2.19689900	-1.25197200	0.30151700
C	0.68338800	-2.68523400	-1.56681500
C	2.64971500	-2.51867500	-0.16777400
C	2.99262300	-0.57072600	1.26727900
H	0.07935100	-3.23524600	-2.29201100
H	4.19912900	-4.02807000	-0.04741100
H	2.21348000	-4.18258200	-1.49253600
C	4.16568200	-1.11703300	1.73013500
H	2.65793900	0.39609300	1.64447900
H	4.75690100	-0.57817800	2.47200300
C	4.61408200	-2.37303800	1.25467300
H	5.54806900	-2.79429000	1.62922400
C	3.86885100	-3.05655600	0.32637700
C	-2.38363200	-0.38535200	0.70734400
H	-2.61501000	0.59235700	0.25251900
C	-3.75892500	-1.06980800	0.93962100
C	-4.90104900	-0.18610300	1.33724100
C	-4.35514200	-0.52383900	-1.47034700
C	-2.14741600	-1.38207400	-0.43136200
H	-1.80054400	-2.32995200	0.01382600
C	-3.68964700	-1.51315500	-0.55735500
C	-5.54181600	0.53647500	0.40621800
C	-5.19739900	0.41883400	-1.01907500
H	-5.67969100	1.09874500	-1.72422700
H	-6.34968700	1.21430900	0.68856100
H	-3.65210800	-1.93732700	1.60730000

H	-4.03808500	-2.53098900	-0.80028000
H	-5.18522800	-0.11626700	2.38982300
H	-4.16982200	-0.61977700	-2.54441700
C	-1.17740800	-0.99848500	-1.54919300
H	-1.43640900	-1.52046300	-2.48295300
H	-1.23521800	0.08378900	-1.74300000
C	-1.28902200	-0.17738700	1.75256300
H	-1.72789800	0.14767700	2.70787900
H	-0.74965300	-1.12042000	1.93220400

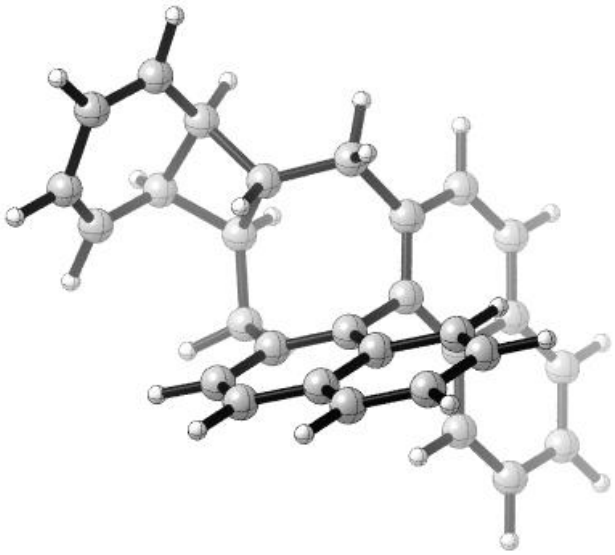

SBINAP_BOD2_GS
E(M062X/def2TZVP) = -1157.544016 Hartree
Free energy correction (M062X/def2SVP) = 0.403040 Hartree
G = -3038073.632

C	0.51078800	0.52946000	-1.27308900
C	-0.42984400	0.63161300	-0.25955000
C	0.80727700	2.94446100	-1.28352900
C	-0.77987100	1.91277600	0.27437800
C	1.12856100	1.70507900	-1.77551400
C	-0.15208300	3.08255800	-0.24605700
C	-1.73928000	2.06270700	1.31703800
H	1.87739900	1.60620900	-2.56422400
H	-0.01192000	5.24206500	-0.12163200
H	1.28800800	3.84111100	-1.68005000
C	-2.05389500	3.30552100	1.81033600
H	-2.22331300	1.17197500	1.72097000
H	-2.79063300	3.40133600	2.60931900
C	-1.42936200	4.46668100	1.29029500
H	-1.68914900	5.44739600	1.69133500
C	-0.50043700	4.35453400	0.28616100
C	-0.49817600	-1.40853600	1.21174100
C	-1.10588100	-0.59664300	0.26524900
C	-2.43595900	-2.89270500	1.21880100

C	-2.41063900	-0.92254600	-0.23515100
C	-1.18708200	-2.56381400	1.67657600
C	-3.08258400	-2.08224800	0.24944800
C	-3.06657300	-0.12062000	-1.21359200
H	-0.69824600	-3.19625000	2.42073500
H	-4.87643500	-3.29290500	0.13373400
H	-2.94738200	-3.78293200	1.59060900
C	-4.31662900	-0.45433300	-1.67591700
H	-2.56164300	0.76800000	-1.59483500
H	-4.80210200	0.17302000	-2.42493800
C	-4.98214900	-1.60634800	-1.18907700
H	-5.97476900	-1.85885900	-1.56467700
C	-4.37562000	-2.40085700	-0.24845300
C	1.74752100	-1.60272400	-0.69721800
H	1.30584100	-2.60042100	-0.54903800
C	1.96150100	-0.95195000	0.68306000
C	4.87663700	0.14525900	-0.76726600
C	3.29124300	-1.78251300	-0.78813200
C	4.47142300	-0.94814100	1.38506500
C	3.32711800	-1.68934900	0.76467100
C	5.16425900	-0.05743200	0.66077400
C	4.02862100	-0.64796600	-1.44054700
H	3.19094500	-2.68369300	1.21637900
H	5.40939800	0.94027000	-1.29307200
H	3.61122600	-2.73579500	-1.24103800
H	5.97166300	0.52093600	1.11377300
H	3.89852600	-0.50750900	-2.51794600
H	4.70914900	-1.11574800	2.43820500
H	2.18804400	0.11216600	0.52769000
C	0.88279200	-1.11169200	1.76321200
H	1.16140400	-1.93225900	2.44195900
H	0.83667500	-0.19861500	2.37827400
C	0.94011600	-0.83129300	-1.76617600
H	1.53110200	-0.72007800	-2.68647500
H	0.04544400	-1.41305000	-2.03026100

7.4 References

[1] I. Dissanayake, J. D. Hart, E. C. Becroft, C. J. Sumby, C. G. Newton, *J. Am. Chem. Soc.* **2020**, *142*, 13328–13333.

[2] A. Manaprasertsak, S. Tharamak, C. Schedl, A. Roller, M. Widhalm, *Molecules* **2019**, *24*, 3844.

[3] C. Cruché, W. Neiderer, S. K. Collins, *ACS Catal.*. **2021**, *11*, 8829–8836.

[4] B. Xu, J. A. Gartman, U. K. Tambar, *Tetrahedron* **2017**, *73*, 4150–4159.

[5] T. N. T. Nguyen, N. O. Thiel, F. Pape, J. F. Teichert, *Org. Lett.* **2016**, *18*, 2455–2458.

[6] M.-H. Yang, D. L. Orsi, R. A. Altman, *Angew. Chem. Int. Ed.* **2015**, *54*, 2361–2365.

[7] K. D. Reichl, N. L. Dunn, N. J. Fastuca, A. T. Radosevich, *J. Am. Chem. Soc.* **2015**, *137*, 5292–5295.

[8] G. Cheng, G. A. Mirafzal, L. K. Woo, *Organometallics* **2003**, *22*, 1468–1474.

[9] T. H. West, D. S. B. Daniels, A. M. Z. Slawin, A. D. Smith, *J. Am. Chem. Soc.* **2014**, *136*, 4476–4479.

[10] R. W. Murray, M. Singh, N. P. Rath, *Tetrahedron* **1999**, *55*, 4539–4558.

[11] N. Amirah Saad, S. Mohammad, M. Hafizi Abu Bakar, M. Tasyriq Che Omar, M. Litaudon, K. Awang, M. Nurul Azmi, *J. Braz. Chem. Soc.* **2022**, DOI 10.21577/0103-5053.20220067.

[12] M. Azmi, C. Gény, A. Leverrier, M. Litaudon, V. Dumontet, N. Birlirakis, F. Guéritte, K. Leong, S. Halim, K. Mohamad, K. Awang, *Molecules* **2014**, *19*, 1732–1747.

[13] B. Lenta, J. Chouna, P. Nkeng-Efouet, N. Sewald, *Biomolecules* **2015**, *5*, 910–942.

[14] H. D. Patel, T. Fallon, *Org. Lett.* **2022**, *24*, 2276–2281.

[15] R. D. Dennington II, T. A. Keith, J. M. Millam, **2016**.

[16] Y. Zhao, D. G. Truhlar, *Theor. Chem. Acc.* **2008**, *120*, 215–241.

[17] Y. Zhao, N. E. Schultz, D. G. Truhlar, *J. Chem. Theory. Comput.* **2006**, *2*, 364–382.

[18] Y. Zhao, D. G. Truhlar, *J. Chem. Phys.* **2006**, *125*, 194101.

[19] F. Weigend, R. Ahlrichs, *Phys. Chem. Chem. Phys.* **2005**, *7*, 3297.

[20] D. Rappoport, F. Furche, *J. Chem. Phys.* **2010**, *133*, 134105.